Proceedings of the Third

International Mobile Satellite Conference

IMSC '93

June 16-18, 1993
Pasadena, California

NASA
National Aeronautics and
Space Administration

I✦I
Government of Canada
Department of Communications

JPL
Jet Propulsion Laboratory
California Institute of Technology

CRC
COMMUNICATIONS
RESEARCH
CENTRE

Mobile SatCom:
Communications
for People
on the Move

Co-Sponsored by
The National Aeronautics and Space Administration/
Jet Propulsion Laboratory
and
The Department of Communications, Canada/
Communications Research Centre

Compiled by
Dr. Robert Kwan, Technical Co-Chair, JPL
Jack Rigley, Technical Co-Chair, CRC

Edited by
Randy Cassingham, JPL

Contents

Abstract

Satellite-based mobile communications systems provide voice and data communications to users over a vast geographic area. The users may communicate via mobile or hand-held terminals, which may also provide access to terrestrial cellular communications services. While the first and second International Mobile Satellite Conferences (Pasadena, 1988 and Ottawa, 1990) mostly concentrated on technical advances, this Third IMSC also focuses on the increasing worldwide commercial activities in Mobile Satellite Services. Because of the large service areas provided by such systems — up to and including global coverage — it is important to consider political and regulatory issues in addition to technical and user requirements issues.

The approximately 100 papers included here cover sessions in 11 areas: the direct broadcast of audio programming from satellites; spacecraft technology; regulatory and policy considerations; hybrid networks for personal and mobile applications; advanced system concepts and analysis; user requirements and applications; current and planned systems; propagation; mobile terminal technology; modulation, coding and multiple access; and mobile antenna technology. Representatives from about 20 countries are expected to attend IMSC '93.
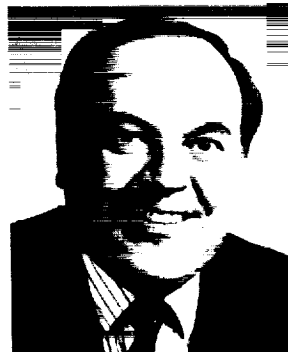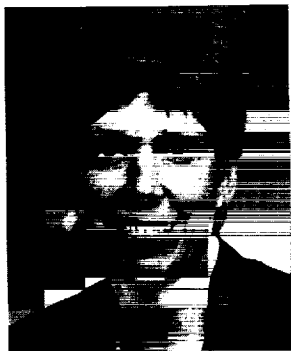
IMSC '93 Organizing Committee

Gregory M. Reck, NASA
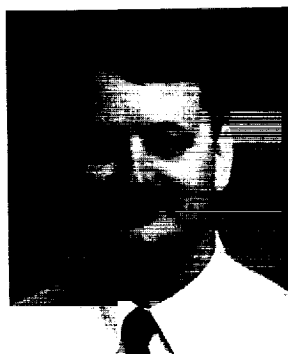Conference Co-Chair

Robert W. Huck, DOC
Conference Co-Chair

Valerie Gray, JPL
Conference Organizer

D.H.M. Reekie, CRC
Conference Advisor

Randy Cassingham
Conference Proceedings Editor and Records Manager

Message From the IMSC '93 Technical Co-Chairs

Robert Kwan
Jet Propulsion Laboratory

Jack Rigley
Communications Research Centre

Mobile satellite (MSAT) communications emerged as a viable telecommunications industry in the past fifteen years. With the introduction of Inmarsat's maritime service about fourteen years ago, a worldwide mobile satellite industry was created. Since that time, many international research and development organizations have undertaken the development of land mobile satellite technology.

In the early 1980s, the Department of Communications, Canada/Communications Research Centre (DOC/CRC) and the United States' National Aeronautics and Space Administration/Jet Propulsion Laboratory (NASA/JPL) independently established MSAT programs to develop enabling, high-risk technologies. At the same time, an initiative was undertaken to foster the development of a North American Mobile Satellite Service (MSS). Since 1983, DOC and NASA have cooperated in promoting and accelerating the commercial introduction of an MSS; this cooperation is best exemplified in our co-sponsorship of the 1990 International Mobile Satellite Conference in Ottawa, and today's Conference— IMSC '93—in Pasadena.

In recent years, mobile satellite services have evolved on a regional as well as a global scale. Australia already has land mobile capability, and the North American MSS is scheduled to be operational soon. Japan has been conducting mobile satellite experiments with L- and S-band satellites. Also, Europe, led by the European Space Agency, is currently examining a variety of options for a European MSS. With the intention of serving the growing global mobile communications market, myriad U.S. applicants have recently emerged proposing both "big" and "little" low-Earth orbiting satellite networks. In addition, Inmarsat has initiated studies on implementing global personal communications services.

As the MSS industry matures, the emphasis is shifting from terminal mobility to people mobility. This personal communications market is, and will be, served by both terrestrial and space-based network services. Cost, as well as the issues of service features and quality, will dictate the user's choice of affordable personal communications services. This service affordability may be achieved through system interoperability and optimal use of various network resources. Our IMSC '93 program has been designed to explore the technical, regulatory and market issues associated with this important trend.

We welcome you to IMSC '93, and wish you a pleasant stay in the beautiful city of Pasadena while you enjoy professional and intellectual interaction with your colleagues.
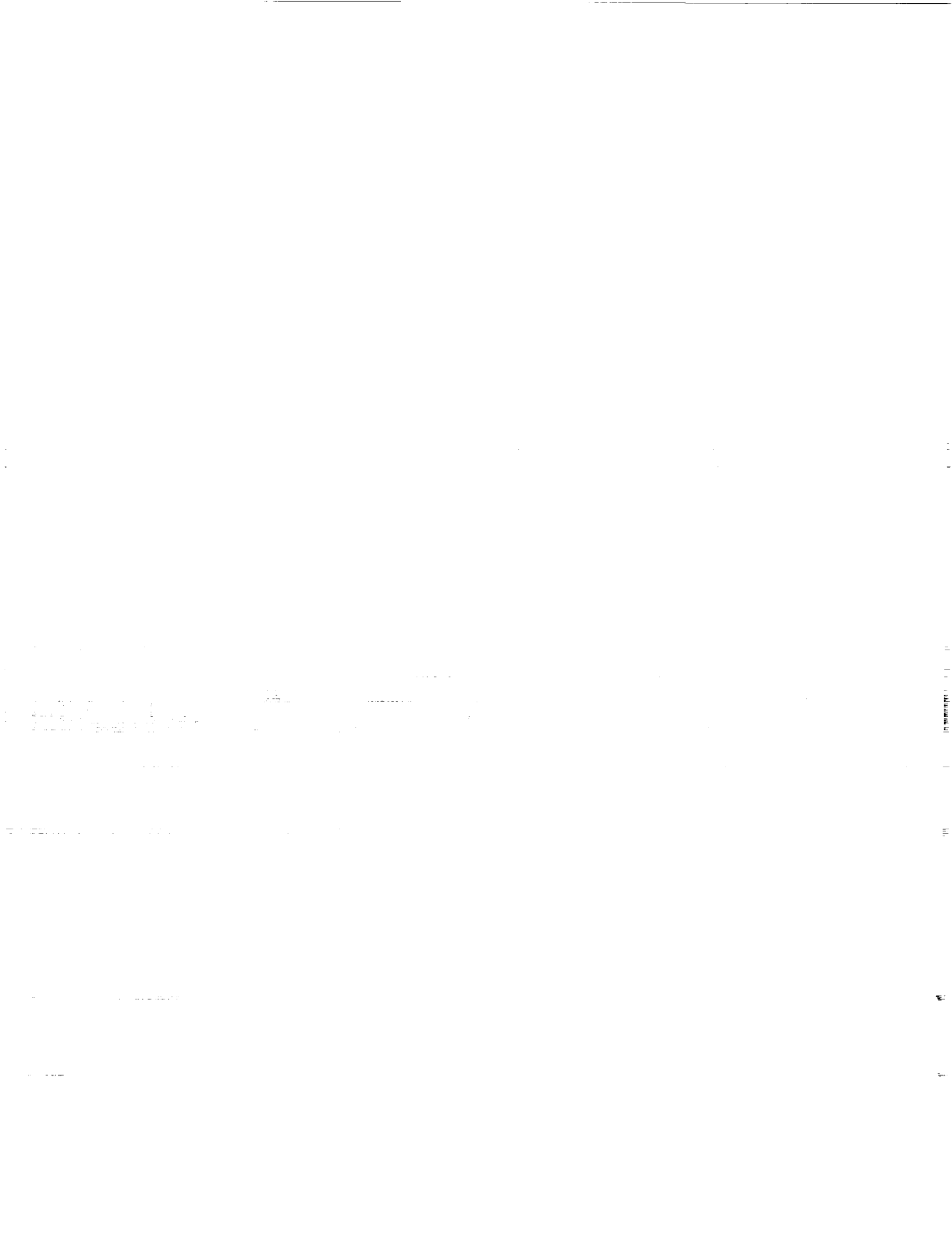
Session 1
Direct Broadcast Satellite/Audio

Session Chair—*Don Messer,* Voice of America, U.S.A.
Session Organizer—*Nasser Golshan,* Jet Propulsion Laboratory, U.S.A.

Worldwide Survey of Direct-to-Listener Digital Audio Delivery Systems Development Since WARC-92

D. Messer
Voice of America
Phone: 202-619-3012
Fax: 202-619-3594

ABSTRACT

Each country was allocated frequency band(s) for direct-to-listener digital audio broadcasting at WARC-92. These allocations were near 1500, 2300, and 2600 MHz. In addition, some countries are encouraging the development of digital audio broadcasting services for terrestrial delivery only in the VHF bands (at frequencies from roughly 50 to 300 MHz) and in the medium-wave broadcasting band (AM band) (from roughly 0.5 to 1.7 MHz).

The development activity increase has been explosive. This article summarizes current development, as of February 1993, as it is known to the author. The information given includes the following characteristics, as appropriate, for each planned system: coverage areas, audio quality, number of audio channels, delivery via satellite/terrestrial/or both, carrier frequency bands, modulation methods, source coding, and channel coding[1]. Most proponents claim that they will be operational in 3 or 4 years.

I. WHAT IS DBS-RADIO AND DIGITAL AUDIO BROADCASTING (DAB)?

DBS-Radio, that is direct-to-listener reception from a satellite, is a concept that incorporates the idea of reception into mobile, outdoor portable, and indoor portable (table top) receivers, as well as receivers with fixed directional outdoor antennas. What distinguishes it from DBS-TV is that the receiver/antenna system is supposed to work without an unobstructed direct line-of-sight to the satellite from the receiver's antenna. Most planned systems using this concept are being designed for all environments—rural, suburban, and urban reception. Some systems concentrate on mobile reception; most consider indoor reception to "table top" radios to be of equal or greater importance.

This collection of requirements forced a search for frequency allocations somewhere between 500 and 3000 MHz for satellite delivery. A simple tradeoff analysis shows that lower frequencies require spacecraft downlink antennas that are too large and higher frequencies require power levels per broadcast channel that are too high. Thus, after much preliminary work during the 1980's, DBS-Radio got to be an agenda item for WARC-92, with the proviso that if there were to be any frequency allocations, they would be above 500 MHz and below 3000 MHz.

Digital Audio Broadcasting (DAB) refers to any modern digital source coding, modulation and signal processing technique that will permit high quality audio to be broadcast and received with the audio quality preserved for the listener after RF propagation and decoding. The term encompasses any delivery method, terrestrial, satellite, and "hybrid"[2], and any reasonable frequency band allocated to broadcasting, from the AM band up to S-band.

The radio broadcasting industry in the USA is interested in digital audio for local terrestrial broadcasting to enhance audio quality and coverage under the existing licensing arrangements and overall structure of the use of roughly 11,000 radio stations. These broadcasters are nearly unanimous in their aversion to the introduction of satellite delivery of DAB, with its wide area coverage possibilities.

---

[1]   Any errors in up-to-date system descriptions are solely the responsibility of the author.

[2]   "Hybrid" refers to a satellite system design where in urban situations it may be necessary to "boost" the received satellite signal at one or more low power terrestrial transceiver sites for reception by the consumer receivers; also called "gap fillers".

II. THERE IS SUBSTANTIAL DBS-RADIO AND DAB ACTIVITY NOW ON A WORLDWIDE BASIS

During the 1980's, there was not much interest in the introduction of DAB services, either via terrestrial or satellite delivery. Two groups, one in the USA and one in Europe, largely within the confines of CCIR activities, studied the possibility of developing feasible broadcasting services. The activity was mostly centered on satellite delivery. Through these pioneering studies and a few WARCs, by 1988 it appeared that at least the developing nations had some interest in encouraging the introduction of BSS(Sound)[aka DBS-Radio]. The literature on the topic at that time concentrated on the value of providing "compact disk" quality audio into cars and other moving vehicles.

A European consortium, spearheaded by the CCETT laboratory in France and the IRT laboratory in Germany, with support from consumer manufacturers, the European Broadcasting Union and many European governments, moved from paper studies to the development of hardware. By the autumn of 1988, in time for WARC-88 in Geneva, this consortium, named Eureka 147, was able to demonstrate "CD" quality audio into a van driving around Geneva. The transmitter was located on a nearby mountain top. Demonstrations, experiments, and pilot broadcasting operations have continued with this system by French, German, British, and Canadian organizations.

During the period from 1988 until WARC-92 convened in February 1992, a few organizations noted the need, on a worldwide basis, for audio quality channels with less than "CD" reception quality as the goal. The Voice of America, with support from NASA, was among this small group. Partly as a result of this view, and with speeches made around the world at symposia, regional meetings preparing for WARC-92, etc., developing nations also became interested in DBS-Radio. It is not difficult to see how a large developing nation could use satellite delivery to its advantage. Therefore, when WARC-92 convened, just about every nation in attendance was in favor of allocating some spectrum for BSS(Sound) somewhere between 500 and 3000 MHz.

The development of an acceptable revision of the Table of Allocations to accommodate this new service was extremely difficult. The Conference nearly was torn apart on this issue. As is well-known, this part of the spectrum is heavily used, and is also coveted by other new services. The final compromise was to allocate three frequency bands. Each nation accepted one or more of these bands, sometimes with conditions limiting the use until 2007.

There are some spectrum management nuances related to the introduction of the service on a co-primary basis and the need to coordinate with neighboring nations, but the essence of the result is the following:

- 40 MHz in L-band (1452-1492 MHz)
- 50 MHz in S-band (2310-2360 MHz)
- 120MHz in S-band (2535-2655 MHz).

Roughly 1/2 the world's population lives in nations that chose the L-band allocation and the other half preferred one of the S-band allocations. The USA added a footnote that flat out prohibits the use of the L-band allocation; former Soviet Union Republics added a very restrictive footnote on the use of L-band, but not as strong as the USA one; most European nations, while choosing L-band, restrict its use to secondary status until 2007. For broadcasting, this is tantamount to prohibiting its use. Other than the USA and the USSR, the other nations that have a footnote allocation for one or both of the S-band allocations did not add any restrictive use of L-band. Thus, the Table of Allocations appears as an L-band allocation worldwide, with very important footnotes dealing with S-band preference, and with restrictions on the use of L-band. [A map depicting these allocations appears in J. Hollansworth's paper in this proceedings.]

A Planning Conference is supposed to be convened in 1998 or earlier. In the meantime, the upper 25 MHz of each of the 3 bands noted above can be used for operational broadcasting systems. Existing co-primary services are to be protected via standard ITU coordination procedures.

Spurred on by the activity leading to WARC-92, which was primarily about satellite delivery, and hence the use of frequencies above 500 MHz, interest developed about 2 years ago to use modern digital techniques for purely terrestrial radio broadcasting in the existing radio broadcasting bands (FM & AM).

The European Eureka 147 system is being tested for such a service, primarily for initial use at VHF just above 200 MHz. The European plan would be eventually to vacate the existing FM broadcasting in the 88.5-108 MHz band, but in the interim to use the higher VHF frequencies. This may take a long time. The Eureka 147 system requires a full 1.5 MHz spectral block within which 6 "CD" quality programs are broadcast via hundreds of subcarriers. Each program has its subcarriers spread across the entire 1.5 MHz. The subcarriers of the 6

programs are interleaved in frequency. With this concept it is not feasible to retain the current structure of local broadcasting, e.g. individual transmitter towers and different coverage patterns.

The situation in the USA is quite different. Four organizations are now engaged in source coding/transmitter/receiver development with the goal of moving digital services directly into the FM band, without disturbing the existing FM broadcasts. All of these are to be tested during the next 12 months through a testing program being designed and administered by the Electronic Industries Association (EIA).

The EIA will also be testing the satellite delivery receiver development sponsored by the Voice of America and being developed at the Jet Propulsion Laboratory. The field testing will be done at S-band using a TDRS satellite. Finally, the EIA will be testing the Eureka 147 system at L-band.

In summary, the interest in DAB has burgeoned since WARC-92. This is manifest in part by the amount of development work underway.

III. SUMMARY OF KNOWN ACTIVITIES AS OF FEBRUARY 1993

Largely through the use of two tables, the developmental activities known to the author are summarized in this section. One table deals with delivery systems; the other with receiver systems.

Delivery Systems

Table I, entitled DBS-Radio Systems, summarizes the different systems either under development or where some interest has been expressed or that were under development and were abandoned recently. With one dormant exception, all had a satellite component.

With respect to the satellite downlink, EIRP's range from approximately 45 dBW to over 50 dBW. Beam sizes vary from tens of thousands of square miles to millions of square miles at the 1/2 power points. Digital Satellite Broadcasting Corp. plans to use the extremely narrow beams to cover the highly populated areas of the USA; Afrispace plans to cover the 12 million square miles of Africa plus most of the middle-east with only 3 beams.

Note in Table I that the first 6 entries are all for coverage of the USA by satellite. Therefore, these will be using the planned USA band (2310-2360 MHz).

Neither Japanese nor Australian activities appear in the table. Both nations have expressed considerable interest in BSS(Sound). Australia was a leading proponent at WARC-92. The author expects in the not too distant future these two nations will introduce more details. Japan plans to introduce satellite DAB in the upper S-band, but there doesn't seem to be any urgency. Australia could well follow Canada's approach, and use L-band for both satellite and terrestrial delivery some time in the future.

Digital Receivers

Table II, entitled Digital Receivers, summarizes digital receiver development, including 3 that have been abandoned recently.

These range from systems still under early stages of development, such as the JPL one, to one that has been under test and evaluation for the past 5 years—Eureka 147. The Eureka consortium includes 3 major European consumer electronic manufacturers—Thomson, Philips, and Grundig. They are working on consumer packaging, and plan to be in production in 1995.

As noted earlier, the Eureka 147 system requires a 1.5 MHz frequency block to operate. This need is based on a fundamental decision regarding propagation effects for mobile receivers that was made many years ago. The designers believe that this level of frequency diversity is needed to combat frequency fading and related multipath effects. There is some evidence from recent Canadian measurements that this is the case. More precisely, it can be said that a channel coding and modulation mechanism such as that used by Eureka 147 has its mobile performance degraded if the block bandwidth is less than 1.5 MHz.

All the USA developers, including the JPL, are designing with the thought that this spread of what is effectively a 200 kHz or less program channel is not needed. It is anticipated that techniques such as adaptive equalization will permit the use of typical broadcast channels. In the JPL case, these could be as small as 50 kHz to accommodate the digital equivalent of monophonic FM. "CD" quality would require 4 times this channel bandwidth.

Entry #4 in the Table, Project Acorn, is unique in the sense that the FM and digital signals are simulcast

from the same transmitter antenna. The digital signal's power is roughly 30 dB less than the FM signal. It "rides" the instantaneous FM signal, shifted somewhat in frequency, with a multiplicity of subcarriers similar to that of Eureka 147, but not spread over such a large band. This is an example of what is called an "in-band/on-channel" system. Fixed installation tests with direct line-of-sight have been conducted. These show that the digital signal can be extracted from the much higher power FM signal at the receiver, and that the digital signal does not appear to distort FM reception. Mobile tests are expected soon.

The other USA "in-band" systems would use spectrum in the FM band that are unused in a local area.

Lastly, Project Acorn has been working on a digital variant of its technique to be used in the AM band. Some successful tests have been run, again with fixed installations and direct line-of-sight.

IV. CONCLUSIONS

1. Explosiveness

Tables I and II, which may be a little out-of-date and possibly incomplete, serve to show the large amount of recent activity on DAB, using both satellite and terrestrial delivery mechanisms. This is either a slow revolution or a fast evolution!

2. Remaining Barriers

Before 1992, any use of satellites for digital radio was blocked—no frequency allocations. Since this barrier was effectively removed, the current chief barrier is financing. This is clearly true for the satellite delivery systems. All serious proponents are faced with a high capital investment requirement.

Although financing as a barrier is less important for the development of purely terrestrial systems, it should be borne in mind that the radio broadcasting industry is not wealthy at the individual station level. There is substantial inertia to change.

Regulatory procedures are time-consuming. Nevertheless, the author feels that sooner or later there will be one or more licenses in the USA for satellite delivery. And there will be satellite delivery available in other parts of the world, obviously not globally all at once.

3. Standardization

The Electronic Industries Association's testing program is an important spur to getting things done in the USA. In about one year we should know what works well, etc. among the systems that will be tested, primarily for local broadcasting use.

The Europeans and Canadians are asking for standardization to be made as soon as possible. They propose the Eureka 147 system to be the standard. Based on recent CCIR meetings on digital audio, in particular positions of the delegates from the USA and Japan, it is unlikely that any serious efforts on standardization will begin until the EIA test results are known.

TABLE I — DBS-RADIO SYSTEMS

SYSTEM AND ORGANIZATION	DELIVERY			PLANNED USE FREQ. BAND				COVERAGE		COMMENTS
	SAT.	TERR.	BOTH	AM	FM	L	S	U.S.	ELSEWHERE	
1. Satellite CD Radio	X						X	X		2 sats, same 30 channels to all of U.S. on diff. freqs. U.S.; CD only; subscription service, primarily for mobile reception; FCC Public Notice under way.
2. American Mobile Sat. Corp.	X						X	X		2 sats, includes spot beams for Alaska, Hawaii, Puerto Rico; FCC filing in Dec.'92; both CD and "FM" qual. dig.
3. Digital Sat. Bdcstg. Corp.	X						X	X		2 sats; broad coverage of U.S. plus 31 very small beams for major U.S. markets; 20m. sat. antenna; subscrip. and open bdcstg; Dec.92 FCC filing.
4. Primosphere (Q Prime)	X						X	X		2 sats; 23 near CD & 6 talk channels; open bdcstg; FCC filing in Dec.'92.
5. Loral Aerospace Holdings	X						X	X		1 sat for lower 48 states; CD qual.; Dec'92 FCC filing.
6. Echosphere (Sky___?)	X						X	X		[no info.]
7. Inmarsat										[Nothing specific; only know it is interested.]
8. Odyssey (TRW)										[Nothing specific; only know it is interested.]
9. Afrispace;Worldspace	X					X			X	Has FCC license to experiment on a non-interference basis into Africa; has a Trinidad/Tobago applic. for Caribbean system; currently, low power, lightsat method for line of sight coverage with very large beams, e.g. 1/3 of Africa per beam
10. Radiosat International	X					X	X	X	X	Global system with 3 or 4 sats; very narrow beams; primary customers are international broadcasters; no filings with anyone.
11. Radiosat (G. Noreen)	X					X		X		Defunct; was going to use 1 to 2 MHz of mobile sat. spectrum to broadcast into vehicles in the U.S.
12. Strother Communic.		X				X		X		Dormant; wanted to test DAB terrestrially; got FCC experimental licenses for a few cities.
13. Eureka 147 (EBU)			X		X	X		X	X	Originally, both sat and terr for Europe, then Canada, then the world; deemphasis of sat in Europe, but Australia, Canada interested in sat as well as terr; well along with successful experiments.
14. Canadian Bdcstg Corp			X			X		X		Complete revision of radio broadcasting over to L-band; use of Eureka 147; very successful terr. experiments; system requires "blocks" of 6 CD channels using same transmitter, hence not acceptable to local U.S. broadcasters; nevertheless to be tested by the EIA in upcoming U.S. tests; satellite interest 8 to 10 years from now; terrestrial operations as soon as possible.
15. Brazil & Mexico			X			X			X	Mexico following Canada's lead; Brazil more interested in going straight to satellite delivery for all of South America.
16. Indostar (Indonesia)	X					X			X	Combined satellite, with S-band for community TV; has sent Advance Notice to the IFRB; a small number of "mono FM" channels to broadcast into the Indonesian islands.

TABLE II — DIGITAL RECEIVERS

SYSTEM AND ORGANIZATION	CD	AUDIO QUALITY LEVELS			FREQ BAND				SOURCE CODING	COMMENTS
		"FM STEREO"	"FM MONO"	"AM"	AM	FM	L	S		
1. Eureka 147 (EBU)	x	x	x	x		x	x		Musicam	At prototype production model stage; orig. just "CD quality", but now can handle various audio quality levels; versatile for terr. coverage shaping through the use of "active echoes" (coverage extenders and gap fillers); cannot be used for indiv. 200 kHz channels, a major drawback for U.S. local broadcasters; EBU pushing hard to make this a worldwide standard now.
2. Sat CD Radio/Stanford Telecom	x						x	x	(Open)	Archival, no more work going on; was to be a Eureka 147 competitor, using frequency hopping for frequency diversity rather than subcarriers spaced over 2 MHz or so.
3. JPL (VOA/NASA)	x	x	x	x		x	x	x	(Open) AT&T	Breadboard devt. under VOA sponsorship; for sat. deliv., although could be used in FM band since channels are no more than 200 kHz wide; uses a modular concept, with fixed and port. having the simplest design, and mobile complexities added for car use; to be tested at S-band during the EIA testing period this year.
4. Proj. Acorn (USA Digital) Gannett, Westinghouse, CBS	x				x	x			Musicam	The "In-band/on-channel" system favored by the NAB; tests so far successful on line of sight over the air simul. brdcsting of FM and dig.; use low powered dig. signal superimposed on the analog signal.
5. Lincom	x					x			?	Defunct; was to be an "in-band/adjacent channel" system.
6. American Digital Radio	x					x			?	Defunct; was to be an "in-band/adjacent channel" system.
7. German/French & U.S.cable feeds	x									Just to note that cable feed systems in the U.S. and Europe exist using C-band and Ku-band feeds.
8. General Instrument	x					x			Dolby?	Entering EIA testing with a claim to modify its cable delivery system for broadcasting locally; no details yet.
9. AT&T	x					x			PAC (AT&T)	Entering the EIA testing with its high quality 128 kbps stereo source coder and a channel coding system, which is not well defined, for use with 200 kHz broadcast channels.
10. AT&T and Amati	x					x			PAC (AT&T)	Entering the EIA testing with the same source coder as in #9, but with a different channel coder, even less well defined.

ESA Personal Communications and Digital Audio Broadcasting Systems Based on non-Geostationary Satellites

P. Lo Galbo, J. Benedicto, R. Viola

European Space Research and Technology Centre
European Space Agency
P.O. Box 299, 2200 AG Noordwijk, The Netherlands
Fax: 31-1719-84598, Telephone 31-1719-83142

Abstract

Personal Communications and Digital Audio Broadcasting are two new services that the European Space Agency (ESA) is investigating for future European and Global Mobile Satellite systems. ESA is active in promoting these services in their various mission options including non-geostationary and geostationary satellite systems. This paper describes a Medium Altitude Global Satellite System (MAGSS) for global personal communications at L and S-band, and a Multiregional Highly inclined Elliptical Orbit (M-HEO) system for multiregional digital audio broadcasting at L-band. Both systems are being investigated by ESA in the context of future programmes, such as Archimedes, which are intended to demonstrate the new services and to develop the technology for future non-geostationary mobile communication and broadcasting satellites.

1 Introduction

Following the conclusions of WARC'92 Conference, satellite personal communications will have a primary allocation in L-band (1.61-1.6265) for mobile-to-satellite links and in S-band (2.4835-2.50) for satellite-to-mobile links. Another important conclusion was the recognition of viability and market value of direct satellite radio broadcasting (DBS-R) and the assignment of a worldwide frequency allocation around 1.5 Ghz to DBS-R. As it will be detailed in the following paragraphs, one of the main technical challenges of these new services is represented by the fact that the geostationary orbit is less suited for a large penetration of personal communications and radio broadcasting services. ESA has been looking with increasingly interest to the exploitation of new orbit alternatives such as the circular Low Earth Orbit (LEO), the Intermediate Circular Orbit (ICO) and the Multiregional Highly inclined Elliptical Orbits (M-HEO). The utilization of these orbits poses challenging technological problems. The Agency's experimental programme called Archimedes has the purpose of exploring those challenges by flying one(or more) experimental satellite(s) by the year 1998 that will be representative of a future personal communication and sound broadcasting mission. This paper summarizes the definition studies that should lead to the formulation of two reference missions, personal and sound broadcasting, that will represent the basis for future technical trade-offs in the Archimedes context. In particular two systems will be presented in detail: the MAGSS-14 reference system utilizing ICO orbits around 10,000 Km of altitude for personal communications and the M-HEO(8) system utilizing 8-hours multiregional highly inclined elliptical orbit for direct radio broadcasting.

2 Satellite Personal Communication Systems

2.1 Service definition

Current or planned mobile satellite systems at Global or regional scale make use of Geostationary satellites operating at L-band.

These systems will support the traditional maritime services, and the more recently started aeronautical services. In addition, new land-mobile voice-data services will be introduced for users equipped with relatively small user terminals. These terminals can be either installed on vehicles or transported in a briefcase, or even deployed as a quasi-permanent installation in remote locations.

Contemporaneously to the development of the mobile satellite services, the terrestrial mobile systems have also experienced in the past few years a very rapid progression towards a commercial implementation of paging, messaging and telephony services using very compact lightweight (hand-held) transceivers. Progress has been possible mainly due to the technology development in the field of commercial low-power integrated digital and microwave circuits.

A clear inherent drawback of terrestrial digital cellular systems is the limited coverage, which will be restricted to the largest cities of the industrialized World and the interconnecting road and railway networks.

To offer full roaming capability is the goal of the future Universal Personal Telecommunication systems (UPTs). Such systems can only be implemented by complementing and interconnecting the Terrestrial Cellular Systems with one (Global) or several (regional) overlay Satellite Personal Communication systems, therefore extending the service also to rural and remote areas.

In the context of the above scenario, a number of Satellite Personal Communication systems have been proposed, namely Iridium, Odyssey, Globalstar, El-

lipso and Constellation, and others are currently being defined, like Project 21 from INMARSAT, and Archimedes from ESA.

The main technical difficulty associated with those new satellite systems stems from the portability required to the satellite user terminal, which has eventually to be integrated within a terrestrial cellular phone. This imposes very severe restrictions to the RF transmit power and the gain of the terminal antenna, which translates into low EIRP and G/T values. Such constraints are difficult to meet with systems using satellites in the Geostationary orbit (GEO) unless very large deployable antennas and complex repeaters are installed on-board [1]. This prompted some of the system proponents to study alternative satellite constellations using Intermediate (Medium) (ICO) or Low (LEO) Earth Circular Orbits which, although leading to satellites smaller than their GEO counterparts, require a much larger number of them. Also highly inclined elliptical orbits (HEO) have been proposed (Archimedes and Ellipso) as a cost-effective solution to deploy capacity region by region.

ESA is currently studying the aspects of such satellite communication systems, based on GEO, ICO, LEO or HEO satellite constellations. The non-geo system adopted as a reference, i.e. the Medium Altitude Global Satellite System (MAGSS), will be described hereafter.

2.2 MAGSS system implementation

2.2.1 User Terminal design

In the design of a mobile terminal for personal communications the primary requirements are to reduce its size and cost (hence complexity) to the minimum, to tailor the terminal design to the different user requirements in terms of mobility and degree of cooperation, and to offer a service compatible with those provided by the terrestrial systems. As described in Table 1, three types of satellite terminals are being envisaged: a Hand-Held (HH) terminal which can fit in a jacket pocket, a Portable (PT) terminal which can be either transported in a hand-bag or briefcase or installed in a semipermanent location, and a Vehicle-mounted (VH) terminal. A description of the technical features of those types of terminals is given in Tab. 2. Whereas the PT and VH terminals can be considered a miniaturised version of current portable and vehicle-mounted land terminal designs (operating with GEO satellites), the HH terminal represents a significant technological challenge, in particular concerning the antenna design and the miniaturisation of the RF front-end and the efficiency of HPA. Several antenna designs are currently being evaluated, all providing very low gain (0 to 3 dBi) in order to minimise the pointing requirements. The HH terminal is equipped with a low power transmitter (below 500 mW) in order to reduce the radiation exposure to the user and the size of batteries required.

2.2.2 Satellite constellation

The MAGSS system employs a best single-visibility Rosette [2] constellation for a number of 14 satellites. The MAGSS constellation has been selected among others because it provides the possibility to start providing World-wide services deploying only 7 satellites, achieving a minimum angle of elevation close to 10 degrees

and better than 30 degrees for more than 70% of the time.

The fully replenished constellation of 14 satellites achieves then a Global minimum angle of elevation of 28.5 degrees and better than 40 degrees for more than 90% of the time. The MAGSS constellation parameters are 10,354 Km of altitude, circular 6-hour orbits, and 56 degrees of orbit plane inclination, to maximise the coverage over the regions located between 30 and 60 degrees of latitude. A snapshot of the MAGSS constellation showing satellite coverage for a minimum angle of elevation of 28.5° is shown in Fig. 1.

2.2.3 Payload design and satellite capacity

In accordance with the WARC'92 frequency allocations, the MAGSS payload operates at 1.6 GHz and 2.5 GHz for the up and down mobile links respectively. The feeder links have been sized at Ka-band, although due to the complexity and cost of this option, the use of lower frequency bands (Ku and C-band) is being investigated. Fig. 2 shows a typical 37-beam spot beam coverage of the African and European regions from one of the MAGSS-14 satellites. Each spot beam has an edge-of-coverage gain of 24.5 dBi and is generated by Tx and Rx phased-array antennas. The payload transmits 300 Watts RF power at S-band , resulting into a total EIRP of 48 dBW. The total payload mass, including the Ka-band feeder-link transponder is estimated in 320 Kg, and the payload DC power consumption is 1200 Watts. The above payload would lead to a total satellite capacity of 930 duplex voice circuits ($2.4 Kbit/s$) to HH-type terminals or the equivalent of 4650 to PT-type terminals, assuming a required link quality target of 39 dBHz C/No. Representative link budgets are given for illustration in Tab. 3. Such satellite capacity can be demonstrated to be compatible with the provision of World-wide personal communication services to approximately 1 million users equipped with hand-held satellite phones.

3 M-HEO: Multiregional Highly Inclined Orbit in the context of the Archimedes programme

Systems based on circular orbits have the advantage to provide global coverage at the expenses of a fairly large constellation of satellites. An alternative approach which reduces drastically the constellation size is based on the use of highly elliptical orbits (HEO).

HEO systems have been used with success since 1966 in the former-USSR for community TV reception and emergency communications. More than 100 satellites have been launched in elliptical , Molniya, 12 hours orbit.

HEO constellations are well suited for regional or multiregional services. A satellite in HEO lies in a plane which inclined approximately 63° with respect to the equatorial plane. This gives the satellite the advantage of being viewed at very high elevation angles in northern (or southern regions). This distinctive advantage compensates for the higher slant-range in comparison with LEO or ICO systems, and makes the use of HEO satellites well suited for personal communication services and radio broadcasting in northern latitudes. In

10

fact it allows high signal availability without penalizing the system economy by imposing large link margins. The other advantage of HEO satellites is that when low-gain user-receiver antenna are used, as in case of personal receivers, in northern latitudes higher gain can be achieved (2-3 dB's more) compared with geostationary satellites.

In a HEO constellation the satellites are not stationary and are therefore used in the orbital arc around the apogee where they present a quasi-geostationary behaviour. The number of service areas is equal to the number of the apogee points on the Earth ground track. HEO orbits with more than one coverage area are called multi-regional orbits [3]. The number of service areas is given by the least common multiple between the orbital period (expressed in hours) and 24, divided by the orbital period.

The number of satellites for a given constellation is given instead by the number of service areas multiplied by the orbital period and divided by the selected duration of the active arc.

ESA has originally studied the Tundra and Molniya orbits for coverage of Europe with high elevation angles, recently the attention has been focused on M-HEO(8) and M-HEO(16) orbit. M-HEO orbits offers the possibility to promote a wide international cooperation which implies economies of scale in the system development and in sharing of the deployment costs.

The M-HEO(8) system is particularly interesting and suited for services such as personal communications and sound broadcasting, in fact it can offer:

- high availability and continuous 24 hours service tailored to cover the three most important market areas of the world, i.e. Europe, Far East and North America.

- A minimum number of satellites for continuous coverage of these three service areas

- The apogee at 26000 km allows power savings in comparison with other HEO alternatives or geostationary satellites. The lower apogee altitude offers also a considerable advantage over the other HEOs in terms of orbit mass that can be delivered by a given launcher.

In the framework of the Archimedes project, ESA is willing to pursue of utilization of HEO constellations for multiregional personal and sound broadcasting services. In the Archimedes programme ESA intends to target the development of an experimental satellite to demonstrate the viability of later operational systems. The M-HEO constellation for personal communications intends to reach the same service objectives of the MAGSS-14 system but on regional basis. Therefore this application will not be described further. The M-HEO system for sound broadcasting will instead be discussed in detail in the next paragraph.

3.1 The M-HEO system for Digital Audio Broadcasting

The feasibility of DBS-R is based on the possibility of receiving the satellite signal anywhere using small table-top radio, personal walkman-type and mobile receivers.

Blockage of the satellite line of sight and multipath effects would degrade DBS-R services to a non-acceptable level. This is translated into the requirements of high elevation angles and high received power flux density over wide areas. The importance of satellite elevation angles has been demonstrated in the frame of several field measurement campaigns at L and S-band. This problem is of particular relevance in all northerly regions of the earth. A geostationary orbit-based service shall include propagation margins in excess of 10 dB to serve those regions, this implies a design solution based on high-powered spacecraft with a large and complicated antenna system resulting in an high (unacceptable) cost for the telecommunication service.

In the basic configuration the M-HEO(8) system is composed by a constellation of 6 satellites in 8 hours elliptical orbits. The six-satellite M-HEO(8) system enables the users to receive the radio signals from satellites always visible with high elevation angles. The coverage area of the M-HEO(8) system includes all continental Europe where the minimum guaranteed elevation angle 100 % of the time is of more than 45 degrees. The other coverage areas are Japan, China, Asian CIS and Canada, USA, Mexico, where elevation angles better than 40 degrees 100 % of the time are guaranteed. Fig. 3 illustrates the minimum elevation angles in the three service areas.

The M-HEO(8) system in its baseline configuration provides integrated digital broadcasting services with possibility of user interaction such as:

- News and basic radiotext

- Bi-lingual News and stereo music, basic radiotext

- Multilingual News and HI-FI stereo music, full colour radiotex

- Multilingual News and CD stereo music, enhanced radiotex or television for pocket receivers

- Paging and Messaging services

- Interactive services providing users with a low bit rate response channel. The maximum bit rate is around 50 b/s.

- Navigation services integrated with meteorological data broadcasting.

In order to deliver the necessary power flux density to provide these services to small receivers, multi-beam antenna coverage of the three service areas is necessary. The M-HEO(8) coverage foresees the use of a reconfigurable antenna system providing in each service area a five beam coverage, i.e. four spot and a global beam. The four spot beams are arranged in the three service zones in order to match linguistic and geographical constraints. Each spot-beam provides 28 dBi of directivity at the 3 dB contour. The global beam is intended to provide 20 dBi gain at the 3 dB contour. The spot-beam coverage is illustrated in Fig. 4 for Europe.

The transponders are intended to provide a flexible share of resources according to the market and user population needs. The transponder can be configured to provide a given distribution of services with different quality and power level. It is fundamental that

11

the selected modulation and multiplexing technique allows such flexible allocation of bandwidth and power resources. Approximately 1000 W of DC power are allocated for the payload.

In order to simplify the satellite design there is no frequency reuse in a given service area, but in order to minimize the overall frequency requirements of the system, frequency is re-used in different regions. The overall down-link frequency requirement is in the order of 10 Mhz for operations in the three service areas. Note that thanks to the high elevation angles frequency coordination is simplified both with respect to geostationary satellites and terrestrial radio links.

Up-link of radio programmes takes place in a ground station equipped with 5 meter tracking antennas. Each satellite is tracked independently. A single up-link location above 58° can address the European, Far Eastern and North-American loops at the same time with a minimum satellite look-up angle of 5° degrees. Given that the up-link antennas never cross the geostationary arc, C-band can be used without problem of coordination with respect to GEO satellites.

The sound broadcasting service is intended for a diversity of users in the three service areas. Users are e-quipped with terminals that can be subdivided in three main classes:

- Type 1: $G/T = -12dB/K$ table-top radios e-quipped with directional antennas with adjustable elevation and azimuth.

- Type 2: $G/T = -15dB/K$ mobile receivers installed in cars, recreational vehicles with medium gain antenna with onmiazimuthal pattern.

- Type 3: $G/T = -19dB/K$ personal "walkman-type" receivers with low gain antenna with onmi-azimuthal pattern.

Table 4 derived from [4] provides an example of link budgets. In reference [4] an extensive investigation of the link performances of the M-HEO(8) sound broadcasting mission. Results are obtained for a mobile receiver, details on the channel modelling can be found in ref. [4]. In ref. [4] the COFDM signal has been optimized for the use on non-linear satellite channel. For the link budget of Tab. 4 a COFDM system with 280 carriers, symbol time 156.25 microsec, guard time 10 microsec and rate 1/2 convolutional coding, has been selected. In the example of Tab. 4 a maximum bit rate has been selected to 128 Kbit/s per carrier but lower data rates can be also multiplexed.

4 Conclusions

This paper has reviewed the user requirements and system implementation of future mobile satellite systems for personal communications and digital audio broadcasting, using the new frequency bands recently allocated by WARC'92.

The MAGSS-14 system has been described as a way to provide World-wide roaming capability to users equipped with dual terrestrial-satellite hand-held phones. The MAGSS system presented is based on 14 satellites in intermediate circular orbit, which shows to be a compromise between the satellite complexity required by equivalent Geo satellites, and the large number of satellites required by LEO constellations.

MAGSS-14 satellites have been sized to serve up to 1 Million users World-wide equipped with a hand-held terminal offering a range of voice, data, messaging and paging services, complementary to terrestrial cellular radio services.

In the context of the ESA Archimedes program, satellite systems utilizing elliptical orbits are being investigated to provide personal communications and sound broadcasting services.

Multiregional Highly Elliptical Orbits (M-HEO(8)) open-up a new market application of digital audio broadcasting with ancillary data and navigation services in the 3 key business areas of the world, i.e. Europe, North America and Far-East. Satellite radio broadcasting is attractive for users demanding international high quality radio services. Broadcasters have also shown a keen interest in satellite broadcasting and appreciate the high availability and quality that HEO systems can deliver but of course funding a full constellation goes beyond their possibilities. Manufacturers are also interested in satellite radio but are clearly waiting for concrete implementation plans for the space segment. As a result of this widespread interest it is evident that the R&D and initial build-up of an HEO constellation for satellite radio has to be provided via public initiative. ESA intends to promote this new challenging opportunity for satellite communications by flying the experimental Archimedes mission in order to substantially support this fascinating technical endeavor.

References

[1] J. Benedicto et al., *"Geostationary Payload Concepts for Personal Satellite Communications"*, In the IMSC-93 Proceedings.

[2] J. Benedicto, J. Fortuny, P. Rastrilla, *"MAGSS-14: A Medium Altitude Global Mobile Satellite System for Personal Communication at L-band"*, ESA Journal, 92/2, February 1992

[3] G. Solari, R. Viola *"M-HEO: Multiregional HEO satellite system for optimal coverage of the northern hemisphere,"* IAF-92-0425, IAF-World Space Conference 1992, Washington, 1-4 Sept. 1992

[4] C. Elia, R. De Gaudenzi, et al. *"Analysis of Transmission Schemes for Satellite Digital Audio Broadcasting, "*, To be presented at Globecom 93.
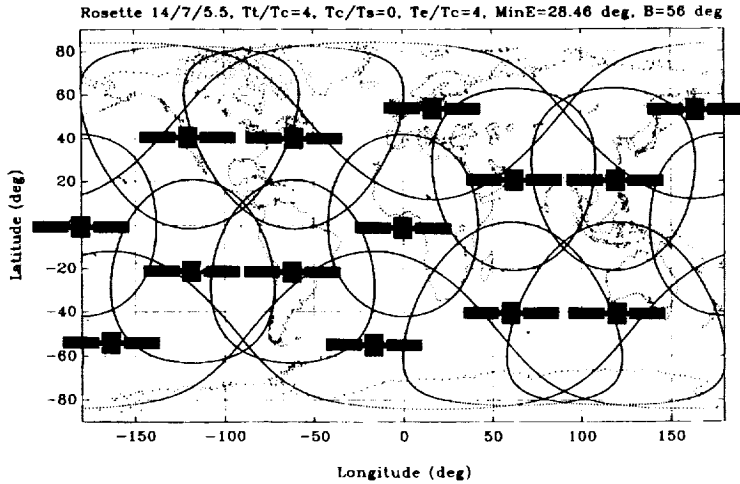
Fig. 1   MAGSS-14 Constellation (contours at 28.5″)
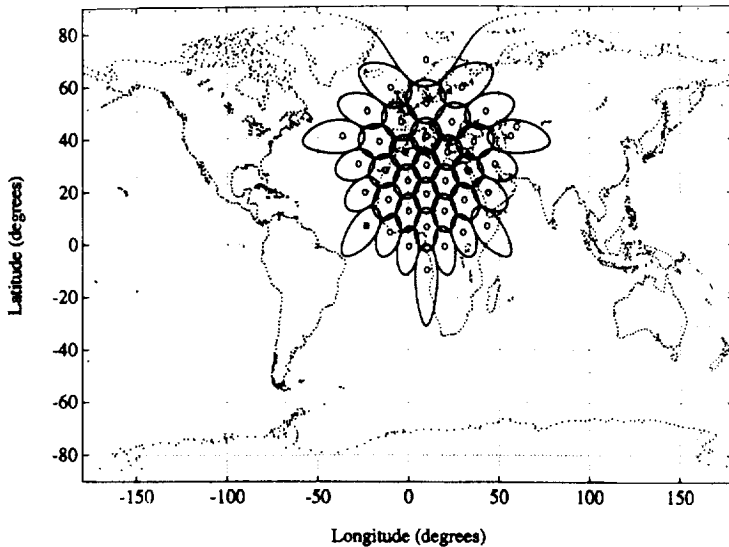
Fig. 2   MAGSS-14 Typical Spot Beam Coverage

	hand-held	portable	vehicle
size	pocket	laptop	antenna + set
antenna gain	0 ~ 3dBi	+7dBi	+4dBi
Tx RF power	< 500mW	1W	2W
EIRP [dBW]	-3 ~ 0	+7	+7
G/T [dB/K]	-24 ~ -21	-17	-20

Tab. 2   User terminal characteristics

MOBILE-TO-SATELLITE LINK (1.6GHz)	
elevation (deg)	30
mobile RF power (W)	0.5
mobile antenna gain (dBi)	0
mobile EIRP (dBW)	-3
path loss EOC (dB)	178.5
atmospheric loss (dB)	0.2
interference loss (dB)	1.0
multipath loss (dB)	1.0
satellite antenna diameter (m)	2.5
repeater noise temperature (dBK)	28
satellite G/T (dB/K)	-4.0
up-link C/No (dBHz)	40.9
overall C/No (dBHz)	40.5
required C/No (dBHz)	39
margin (dB)	1.5

SATELLITE-TO-MOBILE LINK (2.5 GHz)	
elevation (deg)	30
satellite antenna diameter (m)	1.6
satellite antenna gain (dBi)	24.5
TX power S-band (Watts)	300
Total satellite EIRP (dBW)	47.8
voice activation factor (dB)	4
number of duplex voice circuits	930
effective satellite EIRP per circuit (dBW)	22.1
path loss EOC (dB)	182.4
atmospheric loss(dB)	0.2
interference loss (dB)	1.0
multipath loss (dB)	1.0
mobile G/T (dB/K)	-25
down-link C/No (dBHz)	41.1
overall C/No (dBHz)	40.7
required C/No (dBHz)	39
margin (dB)	1.7

USER	MOBILITY	TERMINAL	CO-OPE RATION
Traveller	open/shadow	HH dual mode	High
Mobile	mobile chn.	VH dual mode	Low
Government	mob./outdoor	HH, VH	High
Remote Telephony	outdoor	HH, portable PT or VH	High
Recreational	land/sea	HH	Low
Data Collection	outdoor	semi-fixed PT	High

Tab. 1   User categories and services

Tab. 3   MAGSS-14 Sample Link-Budgets

13
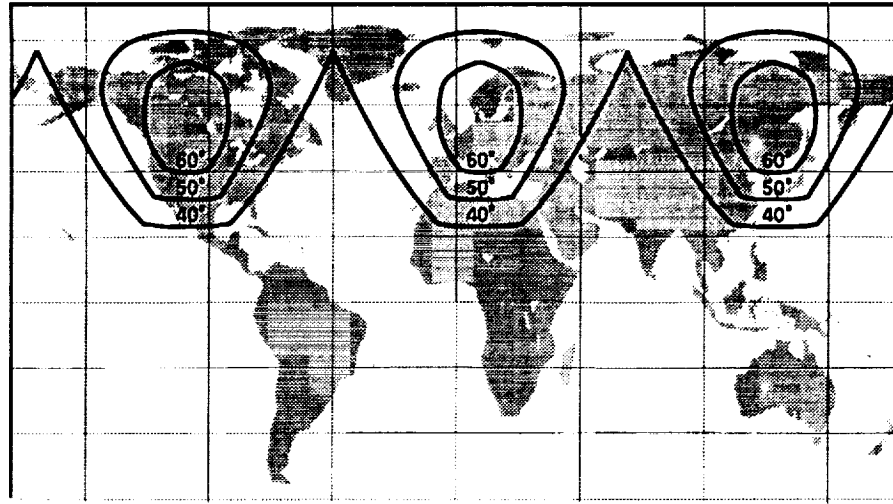
Fig. 3   M-HEO(8) Minimum Isoelevation Contours 24/24 hours
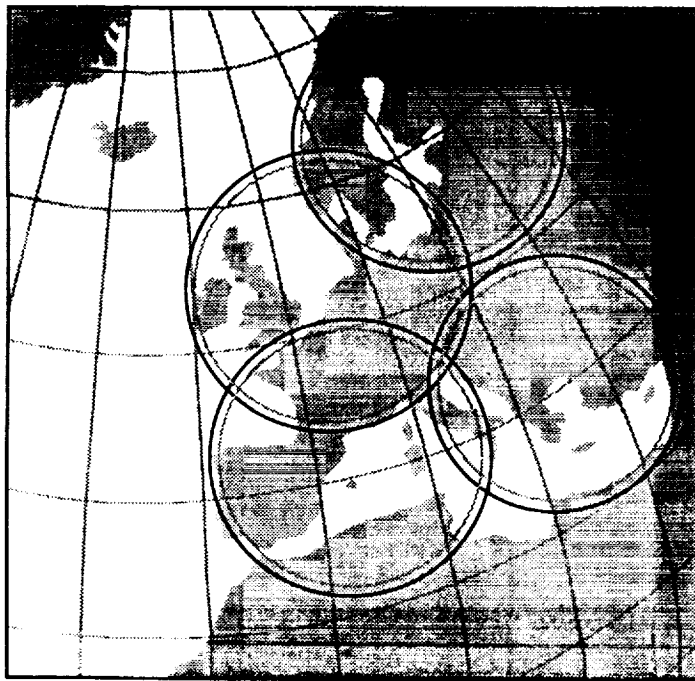
■ 27 dBi
▨ 28 dBi

Fig. 4   M-HEO(8) (-3 dB isogain at apogee)
Contours (Europe)

Table 4: Link budget for a M-HEO(8) mobile users (suburban) [4]

Frequency	L-band	L-band
Receiver Type	2	3
Modulation scheme	COFDM	COFDM
Coding rate	$r = 1/2$	$r = 1/2$
Bit rate (Kb/s)	128	128
Average Line of Sight Attenuation (dB)	2.5	2.5
Carrier-to-Multipath ratio (dB)	12	10
Estimated service availability (%) (suburban, elevation $\geq 60°$)	98	98
Required $\overline{E}_b/N_0$ (dB) (@ BER=10^{-3})	7.1	7.2
Receiver G/T (incl. point. loss)	-16	-21
Implementation Losses (dB)	1	1
Number of DAB programmes	14	14
Nonlinear distortion losses + satellite OBO (dB)	1.8	1.8
Occupied (99%) bandwidth (MHz)	1.9	1.9
EIRP per programme (dBW)	37.2	42.1

14

Direct Broadcast Satellite-RADIO, SPACE-SEGMENT/RECEIVER TRADEOFFS

Nasser Golshan
Jet Propulsion Laboratory
California Institute of Technology
Phone (818)354-0459
Fax   (818)393-4643

Abstract

This paper looks at the balance between receiver complexity and the required satellite EIRP for Direct Broadcast Satellite-Radio (DBS-R) service. In general the required receiver complexity and cost can be reduced at the expense of higher space-segment cost by allowing a higher satellite EIRP. The tradeoff outcome is sensitive to the total number of anticipated receivers in a given service area, the number of audio programs, and the required audio quality. An understanding of optimum choice of satellite EIRP for DBS-R under various service requirements is a critical issue at this time when CCIR is soliciting input in preparation for the ITU planning conference for the service.

I. INTRODUCTION

There has been considerable international effort in the areas of system studies, system development and regulatory work for a Broadcast Satellite Service Sound. An important successful international milestone was the 1992 World Administrative Radio Conference (WARC-92) allocation of L- and S-band spectrum for this service [1]. The Federal Communications Commission (FCC) is actively perusing the regulatory issues for the commercial introduction of this service in the S-Band (2.310-2.360 GHz) allocated at WARC-92 for the U.S. Several companies have filed applications before the FCC to provide this type of service [2].

This paper looks at the balance between receiver complexity and the required satellite EIRP for DBS-R service. In general the required receiver sensitivity and cost can be reduced at the expense of higher space-segment cost by allowing a higher satellite EIRP. The findings of a completed System Tradeoff Study [3] and an ongoing DBS-R Receiver Development Task [4] are used to quantify the tradeoffs between the space-segment and the consumer receiver complexity as the satellite EIRP is varied. A number of other parameters (the anticipated number of receivers in the service area, audio quality, and the number of broadcast programs) are treated as running variables.

II. THE BASELINE DBS-R SYSTEM

The baseline system is based on the findings of the Systems Tradeoffs Study Task [3]. The Task covered a technical study with related tradeoff analysis to identify and define viable system options for satellite broadcasting of radio and its reception by consumer type digital radios. A range of capacity, coverage, and audio quality requirements were considered for both portable and mobile reception in rural, suburban, and urban areas. Important system issues considered include: state of the art digital audio coding, propagation considerations for mobile and indoor portable reception, power and bandwidth efficient channel coding and modulation techniques, anti multipath signaling and diversity techniques, and finally space-segment technology and cost for DBS-R.

II.1 DIGITAL BIT RATE AND Audio QUALITY FOR DBS-R

Based on the status of audio coding technology, the following grades of audio quality and corresponding bit rates have been identified [3] for DBS-R applications: (AM quality, 16-32-kbps), (Monophonic FM quality, 48-64-kbps), (Stereophonic FM quality, 64-96-kbps), (audio quality near to

stereophonic CD quality, 96-128-kbps), (audio quality approaching stereophonic CD quality, 128-160-kbps), and (stereophonic CD quality, 160-192-kbps).

II.2. TYPICAL DBS-R LINK BUDGETS

Table 1 gives typical DBS-R link budgets for mobile and indoor portable reception of one near-CD quality audio program at a frequency of 2.35 GHz using a radiated RF power of 40.5 Watts over a 3-degree spot-beam resulting in an EIRP of 50.8 dBW. The mobile link margin of 6.6 dB is appropriate for mobile reception in rural and suburban areas, mobile reception in urban areas would require either terrestrial boosters or higher EIRP spot-beams. The portable link margin of 12.9 dB is sufficient for indoor reception in most houses. To avoid prohibitive link margins for portable reception inside buildings with large penetration loss (more than the 12.9 dB link margin), the following measures can be taken: attach an antenna to the inside or outside of a window, use higher gain antennas for table-top radios, or place the radio in a location of a signal peak of the indoor standing waves.

The mobile link budget is based on a mobile receiver with a G/T of -19.0 dB/K and a near coherent demodulator with soft Viterbi decoding combined with extensive time interleaving to mitigate intermittent signal blockage due to roadside objects. The portable reception link budget is based on a table-top portable receiver with a G/T value of -14.7 dB/K. The development of prototype receivers with such performance objectives is the subject of a companion paper at this conference [4]. In general the required receiver sensitivity and cost can be reduced at the expense of higher space-segment cost by allowing a higher satellite EIRP. Such a tradeoff would make sense if the additional space-segment investment prorated over the number of receivers is more than offset by the savings in the cost of the receiver. First we will look at the variation of the space-segment cost as function of satellite EIRP.

III. SPACE-SEGMENT COST TRADEOFFS VERSUS RECEIVER COMPLEXITY AS A FUNCTION OF SATELLITE EIRP VARIATION FOR TYPICAL S-BAND DBS-R SYSTEMS

The variation of satellite size and cost for DBS-R services has been already reported [3]. Figure 1 shows the space-segment investment as a function of the required down-link RF power for an S-Band DBS-R system with 3-degree spot-beams.

The baseline per program satellite RF power requirement for broadcasting one 128-kbps digital audio program over one 3-degree spot-beam has been given in table 1 as 40.5 Watts for a nominal EIRP of 50.8 dBW. Down-link RF power requirements for other digital audio rates can be estimated by noting that the needed RF power is proportional to the digital audio rate. The total RF power can be then estimated by summing the power requirement for each channel. Finally the total RF power can be used in conjunction with Figure 1 to estimate the space-segment investment.

Figure 2 shows the variation of space-segment investment (prorated over the number of receivers) as a function of the per channel EIRP. The numbers of program channels and receivers are treated as running parameters covering a range of 30-150 near-CD-quality channels and 2-20 million (M) receivers. As expected, the prorated space-segment cost is inversely proportional to the number of receivers. For the baseline EIRP, the prorated investment cost varies from $70 to $7 as the number of receivers goes from 2 M to 20 M if the total number of program channels is 30. The space-segment investment increases with the number of program channels. As an example, when the number of program channels is increased to 70 from the earlier example of 30 channels, the prorated (over the number of receivers) space-segment investment ranges from $17 (20 M receivers) to $170 (2 M receivers).

The variation of prorated space-segment investment as a function of EIRP also follows the same trends as the absolute costs discussed above with respect to the number of program channels and the number of receivers. For example the per-receiver increase in the space-segment investment for a 3 dB increase in the EIRP over the baseline system is typically $6.2 (20 M receivers, 30 channels), $62 (2 M receivers, 30 channels), $17 (20 M receivers, 90 channels), and $170 (2 M receivers, 90 channels).

Next we examine how a 3 dB increase in satellite EIRP over the baseline design can be used to lower the cost of the receiver. First let us identify those parts of the baseline receiver design where potential cost savings are likely to be realized if the satellite EIRP is increased say by 3 dB:

1. In the baseline design, the mobile receiver's front end has a G/T of -19 dB/K, with an antenna gain of 4.5 dBi and a total system noise temperature of 224 K (-23.5 dBK). A 3 dB increase in satellite EIRP will allow a lower cost front end with a G/T of -22 dB/K (for example an antenna gain of 3 dBi and system noise temperature of 317 K).

2. In the baseline design, the table-top portable receiver's front end has a G/T of -14.7 dB/K, with an antenna gain of 12 dBi and a total system noise temperature of 470 K (-26.7 dBK). A 3 dB increase in satellite EIRP will allow a lower cost front end with a G/T of -17.7 dB/K (for example an antenna gain of 10 dBi and system noise temperature of 589 K).

3. The signal processing portions of the receiver can be simplified at the expense of higher Eb/No requirements, for example:

   3.a. the near coherent demodulator can be changed to differential detection for the mobile receiver,

   3.b. soft decision decoding can be changed to hard decision decoding to save on de-interleaver memory.

Of the possible options to decrease receiver cost at the expense of higher satellite EIRP, items 1 and 2 above, namely lowering the G/T values of the front ends of the mobile and portable receivers, are the most promising candidates. The actual cost differential in the manufacture of each simpler receiver is estimated to be in the rough range of $10-$40; a better estimate can be obtained after the ongoing DBS-R receiver development Task [4] has been completed.

Finally we would like to compare the saving in the receiver cost versus the increase in space-segment cost when the satellite EIRP is increased from the baseline value. The outcome of the comparison depends strongly on the number of receivers and the number of program channels. For a system with 20 M receivers and 30 near-CD-quality channels, the per-receiver premium of $6.2 in the space-segment investment is more than offset in the lower per receiver manufacturing cost of $10-$40 for a 3 dB increase in the satellite EIRP.

On the other hand, for a system with 2 M receivers and 90 near-CD-quality channels, the per-receiver increase of $170 in the space-segment investment cannot be justified by lowering the per receiver manufacturing cost by $10-$40 for a 3 dB increase in the satellite EIRP. For this particular case, it may even make sense to build a receiver with higher sensitivity to reduce the satellite EIRP. It would probably cost $10-$40 to increase the receiver sensitivity about 2 dB beyond the baseline design. It would be technically very difficult to improve the performance of the mobile receiver much more than 2 dB beyond the baseline design unless a lower rate channel code is used instead of the rate 1/2 constraint 7 length convolutional code used in the link budget calculations. The ongoing work in the DBS-R Receiver Development Task [4] indicates that rate 1/3 constraint length 7 convolutional code outperforms the similar rate 1/2 by a couple of dB's in mobile channels with extensive intermittent short signal blockages. Hence, it is expected that a mobile receiver with a rate 1/3 code will require a smaller link margin than one with a rate 1/2 (at the expense of roughly 50% more bandwidth). It is anticipated that both code rates will be implemented in the prototype DBS-R receiver [4] and field tested. The results, when available, can be used to provide a tradeoff between space-segment cost versus spectrum requirements for the two code rates.

As a third example we look at a DBS-R system with 20 M receivers and 90 CD-quality channels. The per-receiver premium of $17 in the space-segment investment is in the same range as the $10-$40 estimate in cost savings in production of each receiver for a 3 dB increase in the satellite EIRP. On the basis of this rough tradeoff, the baseline EIRP will be near optimum for this case; a finer tradeoff can be made only when the DBS-R Receiver Development Task has been completed.

For some applications, space-segment costs cannot be compared in par with receiver manufacturing costs. If the two categories of costs need to be differently weighted, the comparisons made above should be modified accordingly, although the separate cost trades for receiver and space-segment as a function of satellite EIRP would still be valid.

Finally one should note that the quantitative results given above are valid only for S-Band DBS-R.

A separate but similar tradeoff analysis would be required for L-Band DBS-R.

SUMMARY AND CONCLUSIONS

An understanding of optimum choice of satellite EIRP for DBS-R under various service requirements is a critical issue at this time when CCIR is soliciting input in preparation for the ITU planning conference for the service.

In summary the per channel EIRP for optimum balance between space-segment investment and receiver manufacturing cost depends on the number of receivers and the number of program channels. The following findings are tentative and will be updated when the DBS-R Receiver Task has been completed:

. For a typical S-Band DBS-R system with 90 near-CD-quality channels and 20 M receivers, the baseline EIRP of 50.8 dBW per 3-degree spot-beam appears to be near optimum.

. If the number of receivers is significantly less than above, say around 2 M, then it would be advantageous to increase the receiver sensitivity to reduce the satellite EIRP. However it would be very difficult to increase the receiver sensitivity beyond around 2 dB from the baseline design without reducing the channel coding rate (and hence the spectrum efficiency of the system).

. If the number of program channels is reduced say from 90 to 30 near-CD-quality channels, with a large number of receivers, say 20 M, then it would make sense to increase the per channel EIRP to allow a lower G/T for receiver front-end to reduce receiver cost. The increase in satellite EIRP should be limited to roughly 3 dB over the baseline design, as the cost savings in receiver manufacturing will hit diminishing returns beyond 3 dB increase in the per channel EIRP.

Acknowledgment

REFERENCES

1. ITU, "Final Acts of the World Administrative Radio Conference (WARC-92)", Malaga-Torremolinos, Spain, 1992.

2. Marcus, D.J., "Five More Companies Seek Audio Satellite Licenses from FCC", Space News, January 4-10, 1993, p. 7.

3. N. Golshan, "Direct Broadcast Satellite-Radio Systems Tradeoffs Study, Final Report", JPL D-9550 (internal document), Jet Propulsion Laboratory, Pasadena, CA, March 92.

4. A. Vaisnys, D. Bell, J. Gevargiz, N. Golshan, "Direct Broadcast Satellite-Radio, Receiver Development", Proceedings of the Third International Mobile Satellite Conference, Pasadena, Ca, June 1993 (this proceedings).

TABLE 1. DBS-R LINK BUDGET FOR MOBILE AND INDOOR TABLE-TOP PORTABLE RECEPTION AT A FREQUENCY OF 2.35 GHz
For broadcasting one audio program over one 3-degree spot-beam with coverage of about one million square miles
QPSK modulation, R=1/2, Conv. code, soft decoding
Coherent demodulation for portable reception, near coherent demodulation for mobile reception

| AUDIO LINK BUDGET (DOWN-LINK)	Mobile Mean Value	Portable Mean Value	Units	Comments
Digital audio quality (stereophonic)	Near-CD	Near-CD		1
Audio bit rate	128.00	128.00	kbps	
Transmitter power per program	40.50	40.50	watts	
Frequency	2.35	2.35	GHz	
Satellite antenna diameter	2.98	2.98	m	
Satellite antenna gain	34.71	34.71	dBi	
Satellite antenna beamwidth	3.00	3.00	deg	
EIRP	50.79	50.79	dBW	
Satellite Elevation angle	30.00	30.00	deg	
Slant Range	38687	38687	Km	
Free space loss	191.61	191.61	dB	
Atmospheric losses	0.25	0.25	dB	
Pointing loss	0.5	0.5	dB	
Receiver noise temperature	224	470	K	
Receiver Antenna gain	4.5	12	dBi	
Receiver G/T	-19.00	-14.72	dB/K	
C/No	68.03	72.31	dBHz	
Eb/No available (beam center)	16.95	21.24	dB	
Theoretical Eb/No for BER=1.0E-4	3.30	3.30	dB	
Degradation mobile channel	2.00	0.00	dB	
Receiver implementation loss	1.50	1.50	dB	
Interference degradation	0.50	0.50	dB	
Receiver Eb/No Requirement	7.30	5.30	dB	
AVAILABLE LINK MARGIN, LINE OF SIGHT, Beam Center	9.65	15.94	dB	
AVAILABLE LINK MARGIN, LINE OF SIGHT, Beam Edge	6.65	12.94	dB	2 & 3

COMMENT 1.   Higher audio quality may become possible at this bit rate due to ongoing work by industry
COMMENT 2.   Direct mobile reception will be feasible in rural and suburban areas
COMMENT 3.   Direct indoor table-top portable reception will be feasible in most houses

Figure 1.   Space-segment investment as a function of radiated downlink RF power

Frequency = 2.35 GHz

Each step represents the addition of one more satellite

Radiated downlink RF power, Watts
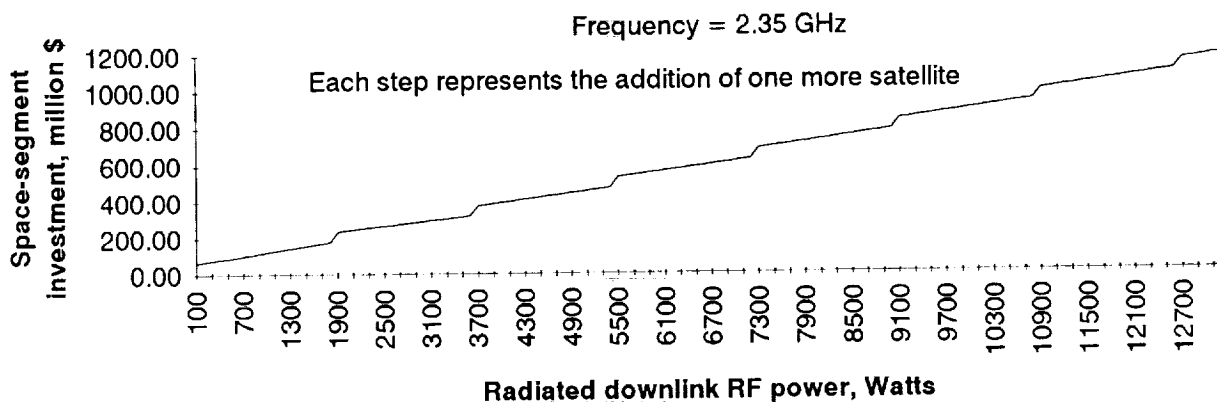
Figure 2. Space-segment investment as a function of per channel EIRP.
(Number of program channels, C, and number of receivers, R, are running
parameters). Frequency = 2.35 GHz
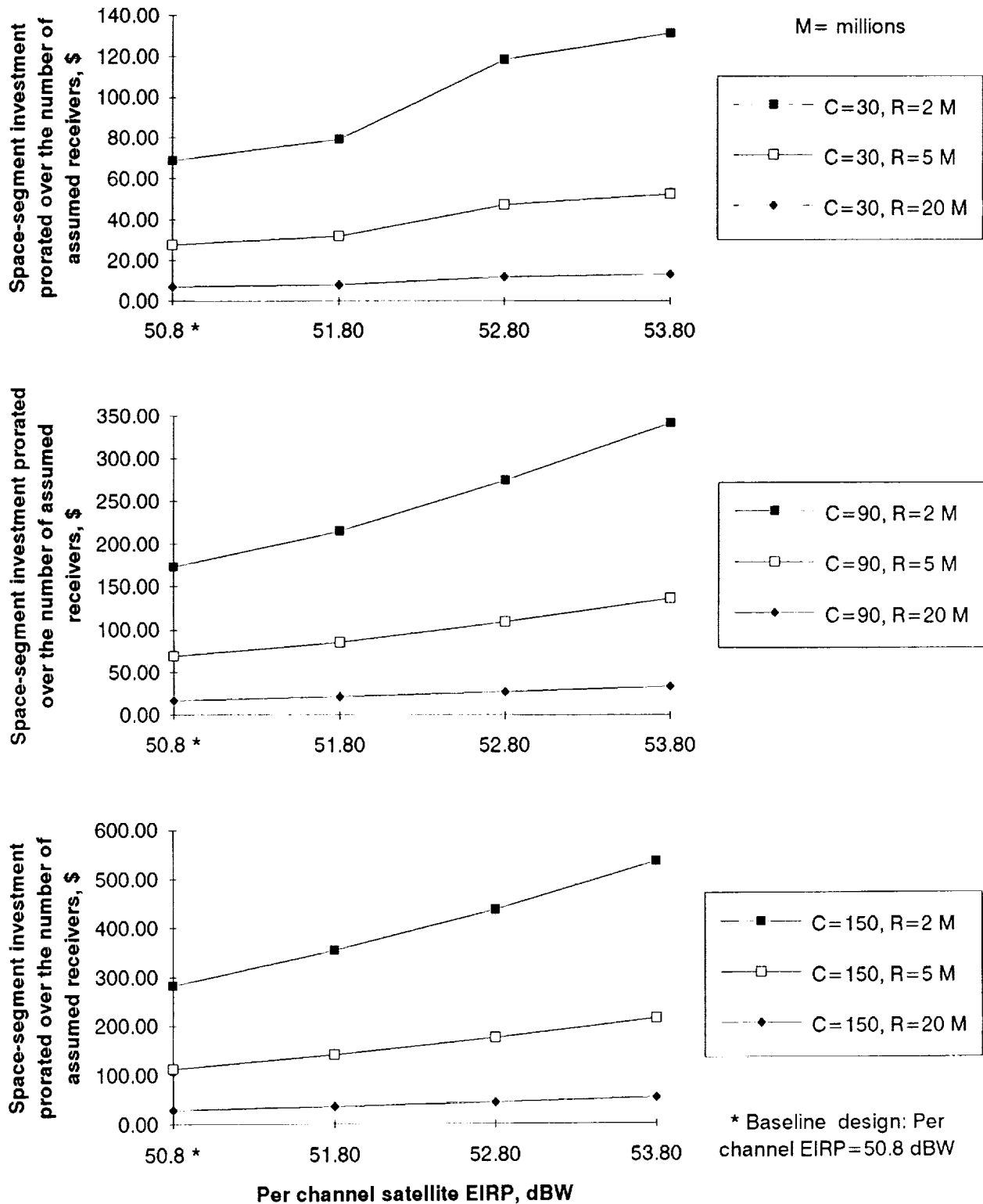
DIRECT BROADCAST SATELLITE-RADIO, RECEIVER DEVELOPMENT

A. Vaisnys, D. Bell, J. Gevargiz, N. Golshan
Jet Propulsion Laboratory,
California Institute of Technology,
Phone (818)354-6219
Fax (818)393-4643

ABSTRACT

This paper reports on the status of the ongoing Direct Broadcast Satellite-Radio (DBS-R) Receiver Development Task being performed at the Jet Propulsion Laboratory, California Institute of Technology (JPL). This work is sponsored by the Voice of America/ U.S. Information Agency through an agreement with NASA.

The objective of this Task is to develop, build, test, and demonstrate a prototype receiver that is compatible with reception of digital audio programs broadcast via satellites. The receiver is being designed to operate under a range of reception conditions, including fixed, portable, and mobile, as well as over a sufficiently wide range of bit rates to accommodate broadcasting systems with different cost/audio quality objectives.

While the requirements on the receiver are complex, the eventual goal of the design effort is to make the design compatible with low cost production as a consumer product. One solution may be a basic low cost core design suitable for a majority of reception conditions, with optional enhancements for reception in especially difficult environments.

Some of the receiver design parameters have been established through analysis, laboratory tests, and a prototype satellite experiment accomplished in late 1991. Many of the necessary design trades will be made during the current simulation effort, while a few of the key design options will be incorporated into the prototype for evaluation during the planned satellite field trials.

BACKGROUND

The DBS-R receiver design effort started as part of a joint NASA/VOA study of digital audio broadcasting via satellite. The motivators for the study were the recognition that the technology for digital audio broadcasting (DAB) via satellite was sufficiently close to maturity to be considered for various domestic and international broadcasting applications, as well as the requirement to help the United States delegation become technically prepared for the 1992 World Administrative Radio Conference (WARC).

The 1992 WARC allocated frequencies for sound Broadcasting Satellite Service (sound), (BSS(sound)) and Complementary Terrestrial Broadcasting in the L-band (1452-1492 MHz), and in two parts of the S-band (2310-2360 MHz) and (2535-2655 MHz). In the United States, satellite sound broadcasting will be implemented in the 2310-2360 MHz band.

The receiver development work will lead to a better definition of satellite sound broadcasting parameters such as signal structure and error protection requirements, margin requirements, and viable service options. The goal of this effort is to stimulate commercialization of satellite sound broadcasting in the U.S. through the transfer of technology to U.S. Industry.

THE PROPAGATION/RECEPTION ENVIRONMENT

Each of the environments that the receiver has to operate in, fixed, portable, and

mobile, influences the signal design or receiver operation in its own unique way. The signal must be designed for operation under the worst conditions, which usually occur during mobile reception.

The receiver enhancements that can be added to improve performance depend on the reception environment. For mobile reception, enhancements such as the use of channel state information for decoding, and channel equalization will be most useful. For indoor reception, on the other hand, the problems of large values of signal attenuation and frequency selective fading can be eased by enhancements such as more directive antennas and antenna diversity.

Mobile Reception Environment

The mobile propagation environment is characterized by very deep fades caused by blockage of the satellite signal by objects such as trees, buildings and other obstacles. The fades are usually so deep that the signal falls below any practical value of link margin.

Coding and time interleaving are the traditional methods used to combat this effect. The proper choice of coding complexity and interleaving depth are very important. Analysis results show that rate 1/3 rather than rate 1/2 convolutional coding results in better performance under severe blockage conditions, but requires more bandwidth. Longer time interleaving also protects against signal drop out, but requires more memory in the receiver and increases acquisition and re-acquisition times. The use of channel state information in decoding provides transparent performance improvement and is an example of a cost/performance trade that can be made in a mobile receiver.

Indoor Reception Environment

Away from building openings such as windows, the satellite signal suffers significant attenuation, dependent on the type of material used in the structure. Indoor propagation measurements conducted by the NASA Propagation Program also determined that there can be standing waves with very deep nulls. These nulls can be tens or more MHz wide, so that frequency diversity is not a good solution.

The proposed solutions to indoor reception problems are to use higher gain antennas to overcome the excess building attenuation, and antenna diversity to overcome the standing wave nulls. These are examples of enhancements to the receiver that can be added for indoor reception, but are not needed under other reception conditions.

DESIGN GOALS AND SOLUTIONS

A block diagram of the proposed receiver is shown in Figure 1, with the optional enhancements shown shaded. The receiver consists of an RF portion and a QPSK demodulator. The interface between the two sections is an A to D converter, thus the demodulator will be fully digital.

The functions of the receiver are to receive the satellite signal, demodulate, establish bit and frame synchronization, deinterleave, and decode the convolutionally encoded data.

The receiver will interface with a range of external audio decoders, depending on the type of audio service to be demonstrated. The receiver will support a range of data rates which will, as a minimum, encompass the following:

- AM Quality Digital Audio at 16-32 kbps,
- Monophonic FM Quality Digital Audio at 48-64 kbps,
- Stereo FM Quality Digital Audio at 64-96 kbps,
- Stereo CD Quality Digital Audio at 128-196 kbps.

Even lower data rates or combinations of different data rate programs will be supported by

time multiplexing the separate channels into a single data stream.

It is planned to implement several signal processing options into the prototype receiver for evaluation under field trial conditions, unless they can be eliminated during the simulation phase. These options are

- Variable interleaver length
- Rate 1/2 and 1/3 convolutional coding
- Coherent and pseudo-coherent demodulation

While it is possible to predict to a great extent the performance differences, in terms of bit error rate, of the above options, the impact on audio quality in a complex environment such as mobile reception is not so easy to evaluate under simulated conditions. For this reason these options will remain to be evaluated in the field.

Since the choice of coherent and pseudo-coherent demodulation does not affect signal design, both demodulation techniques can be built into a receiver which may have to operate over a range of reception conditions.

TEST AND EXPERIMENT RESULTS

JPL experience with mobile reception of satellite signals goes back many years with work in the Mobile Satellite area, as well as the 1991 field trials of low rate audio broadcasting with the INMARSAT MARECS B satellite. This work provided a large data base on the propagation characteristics of the mobile channel, which is very useful in simulation and testing of the receiver.

The MARECS B tests used a JPL developed modem operating at 16 kbps and 20 kbps, and a commercial audio codec. One of the goals of the experiment was to evaluate the effects of time interleaving over the range of zero to one second. The effect on bit error rate was as predicted analytically, but was more difficult to assess qualitatively. The problem was

that the modem and audio codec operated independently, and sync loss and reacquisition occurred independently in the two units. Thus overall performance in a difficult reception environment was not as good as it could have been [1].

SIMULATION AND PROTOTYPE IMPLEMENTATION

The receiver is currently being simulated on a Sun workstation, using Comdisco Systems SPW simulation software. Both symbol rate and sample rate simulations are being accomplished. The simulation platform is capable of generating realistic signal characteristics by modeling the signal amplitude and phase on actual field measurements of satellite signals. This is especially important in obtaining a faithful reproduction of the mobile reception environment.

Figure 2 illustrates a simplified block diagram of the DBSR receiver's QPSK demodulator. The simulation algorithm used for determining the performance of the symbol synchronizer and Costas loop is implemented at the symbol rate to avoid excessive simulation time. Therefore, each simulation cycle corresponds to one symbol increment instead of a sample increment. This approach significantly reduces the computation time as compared to simulating the system at the sample rate.

Both analytical and simulation tools are used to obtain the performance of the QPSK demodulator. The outputs of the integrate-and-dump filters are derived analytically, whereas simulation is used for obtaining the outputs of the loop filters, numerically controlled oscillator, update filter, and phase detector. In this figure, the analytical and simulation blocks are denoted by dark-blocks and clear-blocks, respectively. The results of the symbol rate simulation are bit-error-rate, acquisition time and tracking performance, for various receiver parameters [2].

The DBS-R digital receiver will be implemented using Field Programmable Gate Arrays (FPGA) or Application Specific Integrated Circuits (ASIC). This implementation will be accomplished using various Computer Aided Tools. These tools generate a software code representing the digital receiver that can be used for programming a FPGA or ASIC target chip. This process flow is shown in Figure 3.

From Figure 3, SPW is first used to implement the DBS-R receiver using the actual sampling frequency; this is referred to as sample level simulation. At this level, the analytical blocks shown in Figure 2 are implemented using their gate level representation. The sample level simulation is further extended to the hardware level implementation. At this level, the number of binary bits is specified for every component of the receiver; this is referred to as hardware level simulation. The results of the hardware simulation are used for generating the source code for programming the desired target (FPGA or ASIC). For the prototype receiver, the FPGA target was chosen over ASIC as the most rapid and economical approach. Therefore, new ideas and design changes can be implemented by simply reprogramming the receiver's FPGAs.

PROPOSED SATELLITE EXPERIMENT

After the receiver prototype is built, it is proposed to run a series of field trials with the TDRS satellite. This satellite has a 2 degree beam which can be steered around the United States and has enough power and link margin at S-band (around 2100 MHz) to support a link up to 256 kilobits. This will allow a comprehensive evaluation of receiver performance under both outdoor mobile and indoor reception conditions. It will allow a qualitative assessment of the impact of the design options that will still be open.

SUMMARY AND CONCLUSIONS

The DBS-R receiver is undergoing the final stages of the design process at JPL. Using field measured satellite signal propagation data in the simulation will allow the receiver design to be evaluated under realistic conditions. Digitally compressed audio data will be fed to the receiver mixed with noise and modified by the expected signal impairments. The recovered data will be played back in real time through the audio decompression system for a qualitative assessment of performance with various receiver design options.

While a great part of the design process will be accomplished via simulation, a satellite field trial is planned with a prototype receiver for a final assessment of receiver performance and the completion of any remaining design trades.

REFERENCES

[1]   A. Vaisnys, B. Abbe, M. Motamedi, "*A Direct Broadcast Satellite Audio Experiment,*" the 14th International Communication Satellite System Conference, Washington, DC, March 22-26, 1992, pp. 1411-1417.

[2]   J. Gevargiz, "*Performance Analysis of an all Digital BPSK Demodulator,*" Submitted to the 1993 IEEE Global Telecommunication Conference.
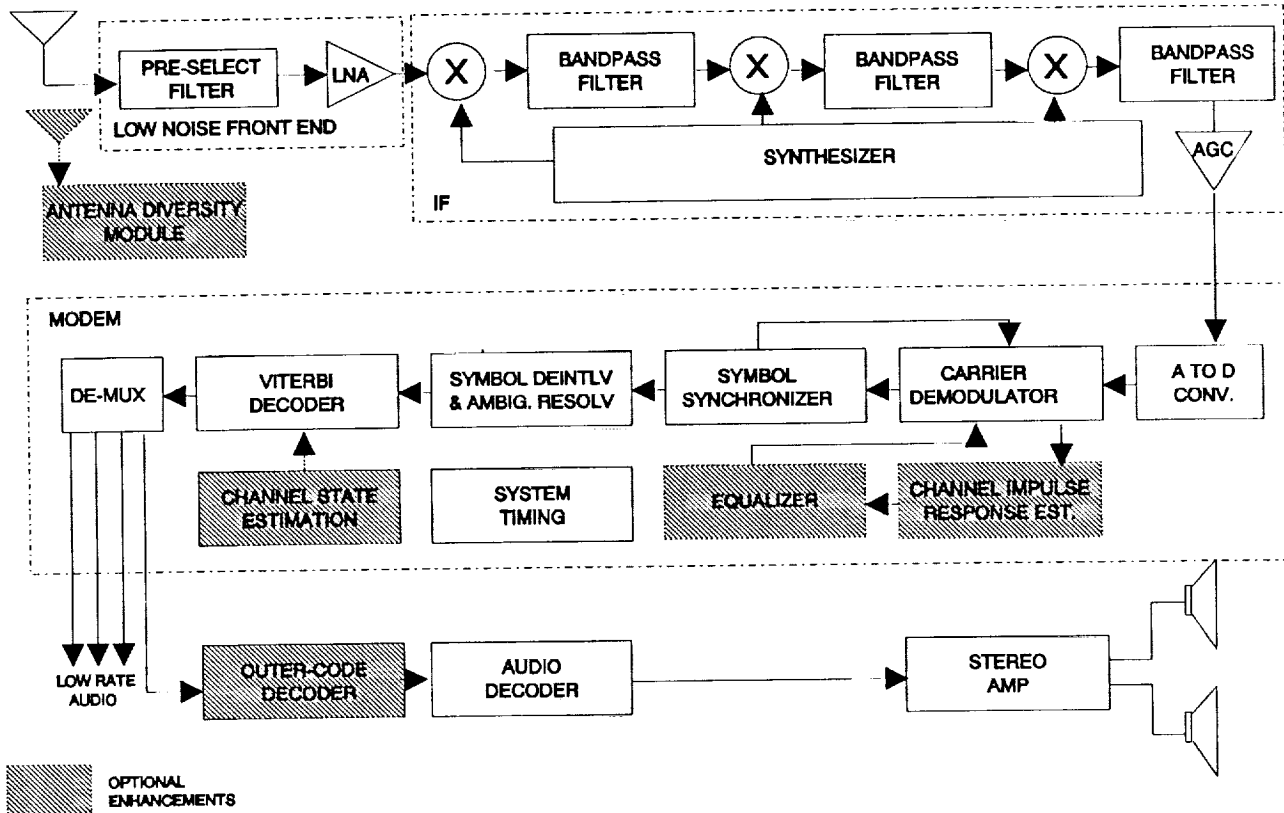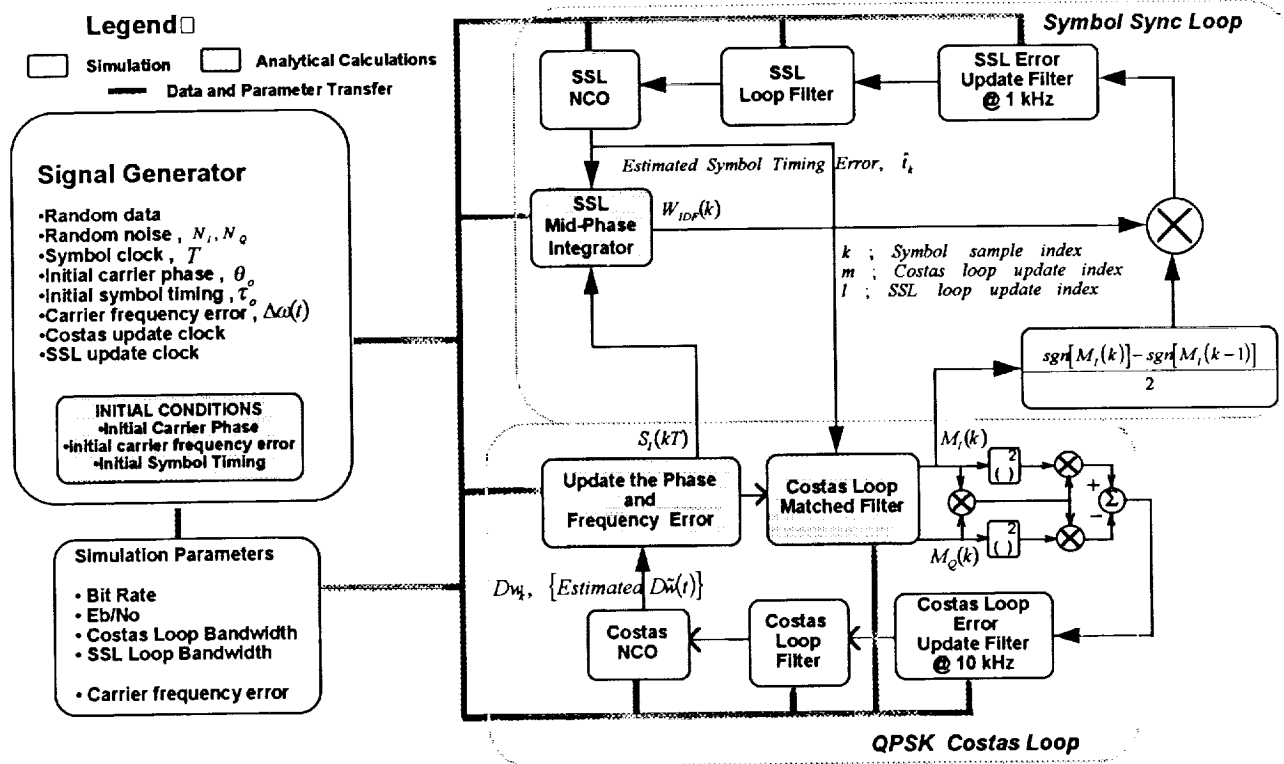
Figure 1. DBS Receiver Block Diagram

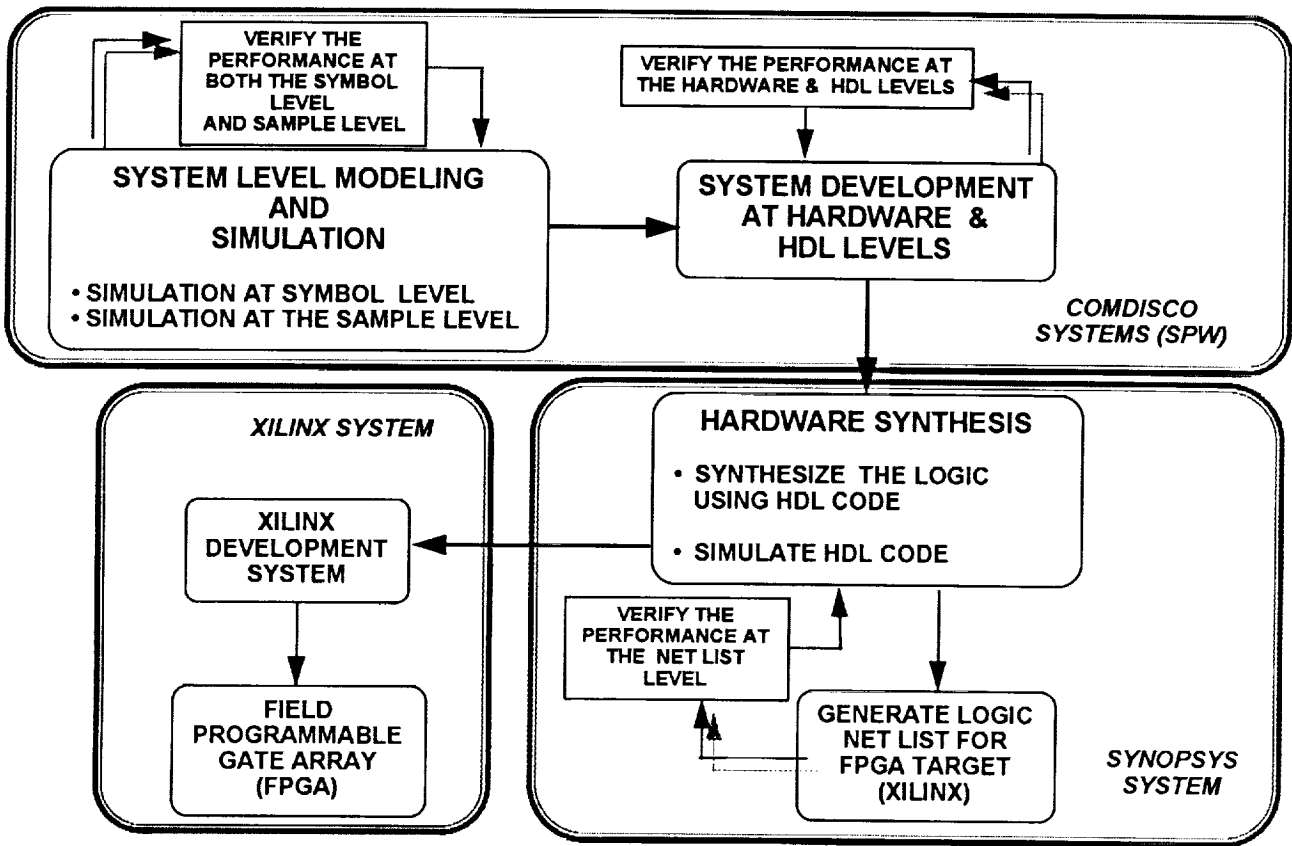Figure 2. SPW Implementation of the QPSK Demodulator

Figure 3. Flow Diagram of Simulation to FPGA Implementation

Utilizing a TDRS Satellite for Direct Broadcast Satellite-Radio Propagation Experiments and Demonstrations

James E. Hollansworth
National Aeronautics and Space Administration
21000 Brookpark Road
Cleveland, OH 44135, USA
(216) 433-3458
(216) 433-8705

ABSTRACT

The NASA/VOA Direct Broadcast Satellite - Radio (DBS-R) Program will be using a NASA Tracking Data Relay Satellite (TDRS) satellite at 62° West longitude to conduct live satellite S-band propagation experiments and demonstrations of satellite sound broadcasting over the next two years (1993-1994) (See Figure 1). The NASA/VOA DBS-R program has applied intensive effort to garner domestic and international support for the DBS-R concept. An S-band DBS-R allocation was achieved for Region 2 at WARC-92 held in Spain. With this allocation, the DBS-R program now needs to conduct S-band propagation experiments and systems demonstrations that will assist in the development of planning approaches for the use of Broadcast Satellite Service (Sound) frequency bands prior to the planning conference called for by WARC-92. These activities will also support receiver concept development applied to qualities ranging from AM to Monophonic FM, Stereophonic FM, Monophonic CD, and Stereophonic CD quality.

INTRODUCTION

The Direct Broadcast Satellite - Radio (DBS-R) Program is a joint effort between The National Aeronautics and Space Administration (NASA) and the United States Information Agency/Voice of America (USIA/VOA). In May, 1990, an interagency agreement established a detailed, multi-year technical effort with joint management and funding by both agencies. The agreement established a program designed to provide service and technology definition and development contributing to commercial implementation of a direct-to-listener satellite sound broadcasting service, thereby benefiting the U.S. satellite communications industry. NASA's Lewis Research Center (LeRC) was assigned program management responsibilities within NASA for the effort, while specific task areas were carried out by LeRC and the Jet Propulsion Laboratory (JPL). LeRC and JPL efforts for the DBS-R Program are conducted under the auspices of NASA's Office of Advanced Concepts and Technology [1].

A DBS-R service has been under discussion domestically since at least 1967, and internationally since at least 1971. Evolution of digital and mobile satellite communications technologies has enhanced the potential quality and availability of a DBS-R service well beyond original expectations. By its nature, a DBS-R satellite system can be very flexible in its antenna coverage area-from approximately 100,000 square mile coverage area using a 1° spot beam to 1,000,000 square mile coverage area using a 3° spot beam-depending upon the desired broadcast area to be reached with the necessary power flux density [2].

DBS-R will also be able to offer audio signals with various levels of sound quality-ranging from robust AM quality, through monophonic FM quality, stereophonic FM quality, monophonic CD quality and stereophonic CD quality. DBS-R digital audio signals will be able to reach a variety of radio receiver types (fixed, portable, and mobile) in various environments (indoor/outdoor, rural, urban, and suburban). Studies have shown that DBS-R systems can provide an economical cost per broadcast-channel-hour for wide-area coverage [2]. As the potential quality and availability of a direct-to-listener satellite radio service have evolved, so has recognition of the desirability of such a service. As a consequence, the 1992 World Administrative Radio Conference (WARC) established new frequency allocations for the Broadcast Satellite Service (BSS) (Sound).

DBS-R offers listeners and service originators many benefits not previously available in the audio broadcast medium. Satellites can broadcast on a single channel to a national, regional, or continental audience. Wider coverage presents new opportunities for audience access to a variety of types of programming. Such programming might include educational, cultural, national, or target audience-oriented broadcasts which may not be economically attractive to offer in any other way. Commercial radio broadcasting has not seen a more dramatic possibility for change since the introduction of FM stereo broadcasting.

THE DBS-R PROGRAM

The DBS-R Program is managed within the Communications Systems Branch of the Space Electronics Division at NASA's Lewis Research Center (LeRC), and the Voice of America's Office of Engineering. Two specific areas of the DBS-R program that need significant effort and study are propagation at S-band and targeted demonstrations.

1992 WORLD ADMINISTRATIVE RADIO CONFERENCE ACTIVITIES

The International Telecommunications Union, an organization within the United Nations, convenes periodic Administrative Radio Conferences to construct agreements among member nations on the use of radio frequency spectrum. The World Administrative Radio Conference for dealing with Frequency Allocations in certain parts of the Spectrum, was held February 3 - March 2, 1992, to consider frequency allocations for the Broadcast Satellite Service (Sound) in the 500-3000 MHz portion of the spectrum [3 and 4].

NASA and VOA made extensive contributions to the U.S. Conference preparations conducted by the Department of State, the Federal Communications Commissions (FCC) and the National Telecommunications and Information Administration (NTIA), particularly by providing numerous U.S. inputs on the subject of the BSS (Sound) to the International Radio Consultative Committee (CCIR).

WARC-92 established multiple frequency allocations for the BSS (Sound), within which DBS-R systems may be implemented. These allocations vary by nation (See Exhibit 1). The U.S. will use the 2310-2360 MHz band. The band 1452-1492 MHz was allocated to this service for a majority of nations throughout the world. However, in some nations, this allocation is secondary to other existing allocations until the year 2007. The band 2535-2655 MHz was allocated to BSS (Sound) for a number of nations in Eastern Europe, Commonwealth of Independent States, and Asia. The WARC also recommended that a future WARC be held prior to 1998, in order to plan the use of frequency bands allocated to the BSS (Sound) service (Ref. 3&4).

PROPAGATION STUDIES AND MEASUREMENTS

NASA conducts propagation research through JPL with investigative support currently performed by the University of Texas-Austin. Prior to WARC-92, the University of Texas-Austin conducted extensive propagation studies relevant to DBS-R in the frequency range 800 MHz to 1800 MHz.

The goal of these studies was to provide propagation data models to the United States WARC-92 Delegation and disburse the data to other countries that were interested in DBS-R. Additionally, the data was made available to satellite system engineers to assist in the design of DBS-R systems.

The research has shown that attenuation varies depending on the environment the receiver is in.

Indoors

During this phase of the propagation studies representative types of buildings were studied to determine what effect they had on the simulated satellite signal(s). These studies indicated that receivers located indoors in a building could experience impaired reception depending upon location. By moving the receiver or antenna only tens of centimeters the reception quality would improve from impaired to acceptable or better. More importantly, this research demonstrated that direct indoor reception of a digital audio signal transmitted by satellite is feasible with receiver antenna gain.

Outdoors/Mobile

During this phase of the propagation study representative measurements were made under varying environmental conditions from a sunny clear day to cloudy, rainy, and foggy days. Locations varied from the desert environment of Texas, to the mountains and seacoast of the pacific northwest to the middle west (St Louis, MO) and east coast (Connecticut and Washington, D.C.). The research indicated that outdoor mobile reception of a DBS-R satellite service was feasible.

Results of these studies contributed significantly to characterizing the indoor/outdoor/ mobile DBS-R reception environment and have formed the basis for several U.S. contributions to the CCIR, CITEL and other such organizations.

Our link budget calculation and experiments indicate that a relatively high powered satellite would be required. Ideally, the satellite should have at least an EIRP of 50 to 60 dBW which will allow sufficient link margins.

Propagation Studies Post WARC-92.

WARC-92 concluded with the United States Allocation for DBS-R at S-band (2310-2360 MHz). The allocation is in the process of being approved by the Federal Communications Commission. It is necessary that new propagation studies be conducted at

S-band. The specific purpose of studies would be to develop the propagation characteristics for S-band.

NASA currently has available, on a scheduled basis a TDRS satellite located at 62° West longitude (see Figure 1). Currently, the satellite in this "spare" position is the latest TDRS launched by NASA in mid January 1993. From this location elevation angles range from 10° for the extreme northwest corner of CONUS to better than 40° for southeast CONUS (See Figure 2). The TDRS satellite provides single-access service to low-earth orbiting spacecraft at both S-band and Ku-band via two steerable 4.9 meter antennas. (It also provides S-band multiple access service via an S-band helical phased array.) The two S-band single access (SSA) forward links (one per 4.9 m antenna) are normally used to transmit command data from the ground to LEO spacecraft at rates up to 300 kbps. The plan is that one of these forward links be used to serve as a satellite downlink to a DBS-R receiver in the 2020.435-2123.315 MHz frequency band which is near the 2310-2360 MHz DAB allocation. (These are the 3-dB band edges. In this range, the TDRS SSA forward link carrier frequency is user selectable over the 2030.435-2113.315 MHz region with a 20 MHz maximum allowable channel bandwidth which is limited by the forward processor hardware onboard the TDRS). Utilizing the TDRS in this fashion will provide a peak transmit EIRP of 46.5 dBW (26W S-band TWT transmitting through a 4.9 meter, 42% efficiency antenna with 4.4 dB line loss). This is nearly 63 times the EIRP of the INMARSAT's MARECS-B satellite used in the initial L-band experiments with an EIRP of 28.6 dBw. With TDRS, link margins for indoor portable reception of DBS-R are estimated to range from 10.77 dB (for reception of 192 kbps CD-quality audio at 20° elevation) to 18.95 dB (for reception of 32 kbps AM quality audio at 40° elevation) (See Tables 2-4). This assumes an indoor receiver with a G/T of -14.7 dB/K and 10^{-4} BER performance using QPSK modulation with rate 1/2, K=7 convolutional coding. For mobile reception using an omni-directional antenna with a receiver G/T of -19 dB/K, link margins range from 4.47 dB (reception of 192 kbps at 20° elevation) to 12.65 dB (reception of 32 kbps at 40° elevation) (See Tables 5-7). These margins are substantially larger than those of the earlier experiments.

It is NASA's intention to utilize the TDRS capabilities, in conjunction with the ongoing propagation studies at JPL and the University of Texas, to better understand the S-band propagation characteristics. While the results will not be at the authorized DBS-R allocation frequencies extrapolation of the data can be made to accurately reflect the signal characteristics at the U.S. authorization and the upper S-band (2535-2655 MHz) allocation. Recognizing these

facts we are currently in the process of developing a very extensive S-band propagation study.

Lewis Research Center in coordination with JPL has developed an initial TDRS S-Band propagation measurement plan that will address the following: (1) all or most of the issues that were addressed in the initial propagation plan and discussed earlier in this paper; (2) using as much of the existing equipment from the previous L-band experiments but shifting to the new S-band capability will allow us to accomplish most of the items in 1 plus the following: (a) mobile measurements of amplitude and phase in urban, suburban, and rural environments, and (b) probe spatial signal structure in buildings, in vehicles, behind trees, with linear positioner; and (3) using an airplane-campaign tested delay-spread receiver and new S-band front-end.

FUTURE DEMONSTRATIONS

It is the intention of NASA and the VOA to conduct various demonstrations during the period 1993 through 1994. The purpose of these demonstrations would be to demonstrate DBS-R receiver technology, to evaluate propagation and multipath effects and to educate observers regarding the capabilities of a DBS-R service. Satellite demonstrations of a DBS-R type service will help significantly in the development of planning approaches for the use of BSS (Sound) frequency bands prior to the future planning conference.

The first of these demonstrations is in conjunction with the Electronic Industries Association (EIA), Consumer Electronics Group, Digital Audio Radio Subcommittee which "will organize and initiate a fair and impartial analysis, testing and standards - setting program to determine which DAR technical system will best serve the consumer electronics industry and consumers." The EIA is planning to have demonstrations and testing of proponent systems in the July through December 1993 timeframe. This time schedule is paced by the fact that the CCIR plans to make its recommendations in 1994.

Additional demonstrations will be planned around significant events which will have positive influence for DBS-R. At this point details concerning where and when such demonstrations should be conducted are still being evaluated.

CONCLUSIONS

The relatively high downlink EIRP of TDRS's Single Access S-band beam (46.3 dBW) is quite sufficient for our proposed propagation experiments and demonstrations for most if not all of our DBS-R concepts and innovations that have been or will be

identified by the NASA/VOA DBS-R program team as critical for viable commercialization of this new and dynamic service.

ACKNOWLEDGEMENT

The author would like to extend a special thanks to the following individuals for their help and assistance. Mr. Faramaz Davarian and Mr. Nasser Golshan of JPL, and Mr. Rodney L. Spence of LeRC.

REFERENCES

[1] J. E. Hollansworth, *Direct Broadcast Satellite - Radio Program*, NASA Technical Memorandum 105910, October 1992.

[2] N. Golshan, *Direct Broadcast Satellite - Radio Program*, Final Report, JPL Internal Document D-9550, March 1992.

[3] *Final Acts of the World Administrative Radio Conference, WARC-92*, International [2] N. Golshan, *Direct Broadcast Satellite - Radio: Systems Tradeoffs Study*, Final Report, JPL Internal Document D-9550, March 1992.
Telecommunication Union, Geneva, Switzerland, 1992.

[4] *Introduction of the Broadcasting-Satellite Service (Sound) Systems and Complementary Terrestrial Broadcasting in the Bands Allocated to These Services within the Range 1-3 GHz. Resolution COM4/W*, Final Acts of the World Administrative Radio Conference, WARC-92, International Telecommunication Union, Geneva, Switzerland, 1992.

Table 1. DBS-R Broadcast of 192 kbps Stereo CD Quality Digital Audio Channel using TDRS 4.9-meter SSA Antenna (Ku-band feederlink is via 18.3-meter (60') terminal at White Sands,NM; portable receiver with 13 dBi gain)

GENERAL SYSTEM PARAMETERS	
Satellite Altitude (km)	35784.00 (GEO S/C Altitude)
Uplink Frequency (GHz)	14.70 (K-band Uplink to TDRS SGL Antenna)
Downlink Frequency (GHz)	2.05 (S-band Forward Link from TDRS SSA Antenna)
Required Value of Eb/No (dB)	3.30 (10-4 BER using QPSK and R=1/2,K=7 Conv. Coding)
Information Bit Rate (bps) per Channel	192000 (Stereo CD Quality Digital Audio)

TRANSMIT TERMINAL PARAMETERS	
Antenna Diameter (m)	18.30 (60 foot White Sands Ground Terminal)
Transmit Antenna Efficiency	0.50
HPA Xmit Power/Channel (after backoff)	5.00
Xmit Feed Loss (dB)	-2.00
Elevation Angle to Satellite (deg)	40.00 (TDRS Satellite located at 62 deg W)
Antenna Gain (dBi)	65.99
Antenna HPBW (deg)	0.08
Transmit Terminal Peak EIRP (dBW)	70.98

SATELLITE PARAMETERS	
Uplink Antenna Diameter (m)	2.00 (TDRS 2-meter SGL Antenna)
Uplink Antenna Efficiency	0.42
Uplink System Noise Temp (K)	4000.00
Uplink Antenna HPBW (deg)	0.72
Uplink Antenna Gain (dBi)	46.01
Satellite Receive G/T (dB/K)	9.99
Downlink Antenna Diameter (m)	4.90 (TDRS 4.9-meter S-band Single Access Antenna)
Downlink Antenna Efficiency	0.42
Xponder Power/Channel (after backoff)	26.00 (26 W S-band TWT)
Downlink Antenna Feed Loss (dB)	-4.40
Downlink Antenna HPBW (deg)	2.12
Downlink Antenna Gain (dBi)	36.68
Satellite Transmit Peak EIRP (dBW)	46.43

RECEIVE TERMINAL PARAMETERS	
Antenna Diameter (m)	0.30 (S-band indoor table-top portable receiver)
Receive Antenna Efficiency	0.50
System Noise Temp (K)	625.00
Elevation Angle to Satellite (deg)	40.00
Antenna Gain (dBi)	13.31
Antenna HPBW (deg)	28.04
Receive Terminal G/T (dB/K)	-14.65

LINK PARAMETER	UPLINK			DOWNLINK		
	numeric	dB	dB	numeric	dB	dB
Transmit Power/Channel (W)	5.00	6.99		26.0000	14.15	
Xmit Line Loss (dB)		-2.00			-4.40	
Xmit Ant Diameter (m)	18.30			4.90		
Xmit Ant Efficiency	0.50			0.42		
Xmit Ant Gain		65.99			36.68	
Peak Xmit EIRP (dBW)			70.98			46.43
Slant Range (km)	37778.30			37778.30		
Free-Space Path Loss (dB)			-207.34			-190.23
Atmospheric Loss (dB)			-0.50			-0.25
Rain Loss (dB) (99.9% availability)			-1.40			-0.05
Xmit Ant Pointing Loss (dB)			-0.10			-0.50
Recv Ant Pointing Loss (dB)			-0.50			-0.05
Other Losses (EOC,Pol,Interfer) (dB)			0.00			-3.00
Power Flux-Density (dBW/m^2)		-93.46			-116.41	
Recv Ant Diameter (m)	2.00			0.30		
Recv Ant Efficiency	0.42			0.50		
Recv Ant Gain		46.01			13.31	
Total System Noise Temp (K)	4000.00	36.02		625.00	27.96	
Recv G/T (dB/K)		9.99			-14.65	
Boltzmann Constant (dBW/K-Hz)		-228.60			-228.60	
Information Data Rate/Channel (bps)	192000	52.83		192000	52.83	
Up/Down Link Eb/No (dB)			46.89			13.47

Overall Eb/No (dB)	13.47
MODEM Implementation Loss (dB)	-2.00
Required Eb/No (dB)	3.30
Link Margin (dB)	8.17

TABLE 2 DBS-R LINK BUDGETS FOR INDOOR PORTABLE RECEPTION USING TDRS S-BAND DOWNLINK (SATELLITE ELEVATION ANGLE OF 40°, RECEIVER G/T OF -14.7 dB/K)

DIGITAL AUDIO QUALITY	AM	MONO-FM	STEREO FM	NEAR-CD	ALMOST CDCD-QUALITY	
DIGITAL AUDIO BIT RATE (kbps)	32.00	48.00	96.00	128.00	160.00	192.00
TDRS S-band SA Downlink Freq (GHz)	2.05	2.05	2.05	2.05	2.05	2.05
TDRS S-band SA Antenna Diameter (m)	4.90	4.90	4.90	4.90	4.90	4.90
TDRS S-band SA Antenna Efficiency	0.42	0.42	0.42	0.42	0.42	0.42
TDRS S-band SA Antenna HPBW (deg)	2.12	2.12	2.12	2.12	2.12	2.12
TDRS S-band SA Downlink Power (W)	26.00	26.00	26.00	26.00	26.00	26.00
TDRS S-band SA Downlink Power (dBW)	14.15	14.15	14.15	14.15	14.15	14.15
TDRS S-band SA Downlink Ant Gain (dBi)	36.68	36.68	36.68	36.68	36.68	36.68
TDRS S-band SA Downlink Feed Loss (dB)	-4.40	-4.40	-4.40	-4.40	-4.40	-4.40
TDRS S-band SA Downlink EIRP (dBW)	46.43	46.43	46.43	46.43	46.43	46.43
Satellite Elevation Angle (deg)	40.00	40.00	40.00	40.00	40.00	40.00
Slant Range (km)	37778.30	37778.30	37778.30	37778.30	37778.30	37778.30
Free-Space Path Loss (dB)	-190.23	-190.23	-190.23	-190.23	-190.23	-190.23
Atmospheric Losses (dB)	-0.25	-0.25	-0.25	-0.25	-0.25	-0.25
Rain Attenuation (50 mm/hr rain rate)	-0.05	-0.05	-0.05	-0.05	-0.05	-0.05
Pointing Loss (dB)	-0.50	-0.50	-0.50	-0.50	-0.50	-0.50
G/T of Indoor Portable Recvr (dB/K)	-14.70	-14.70	-14.70	-14.70	-14.70	-14.70
Boltzmann Constant (dBW/K-Hz)	-228.60	-228.60	-228.60	-228.60	-228.60	-228.60
Received C/No (dB-Hz)	69.30	69.30	69.30	69.30	69.30	69.30
Data Rate (dB-bps)	45.05	46.81	49.82	51.07	52.04	52.83
Available Downlink Eb/No (dB)	24.25	22.49	19.48	18.23	17.26	16.47
Theoretical Eb/No for 10-4 BER (dB) (QPSK with R=1/2,K=7 Conv. Coding)	3.30	3.30	3.30	3.30	3.30	3.30
Receiver Implementation Loss (dB)	1.50	1.50	1.50	1.50	1.50	1.50
Interference Degradation (dB)	0.50	0.50	0.50	0.50	0.50	0.50
Total Receiver Eb/No Requirement (dB)	5.30	5.30	5.30	5.30	5.30	5.30
Link Margin (dB) at beam center (dB)	18.95	17.19	14.18	12.93	11.96	11.17
Link Margin at 3-dB edge of coverage	15.95	14.19	11.18	9.93	8.96	8.17

COMMENTS:
INDOOR TABLE-TOP CD-QUALITY RECEPTION WILL BE FEASIBLE IN MOST SINGLE FAMILY HOUSES
INDOOR TABLE-TOP FM-QUALITY RECEPTION WILL BE FEASIBLE IN MOST BUILDINGS

DIGITAL AUDIO QUALITY	AM	MONO-FM	STEREO FM	NEAR-CD	ALMOST CD	CD-QUALITY
DIGITAL AUDIO BIT RATE (kbps)	32.00	48.00	96.00	128.00	160.00	192.00
TDRS S-band SA Downlink Freq (GHz)	2.05	2.05	2.05	2.05	2.05	2.05
TDRS S-band SA Antenna Diameter (m)	4.90	4.90	4.90	4.90	4.90	4.90
TDRS S-band SA Antenna Efficiency	0.42	0.42	0.42	0.42	0.42	0.42
TDRS S-band SA Antenna HPBW (deg)	2.12	2.12	2.12	2.12	2.12	2.12
TDRS S-band SA Downlink Power (W)	26.00	26.00	26.00	26.00	26.00	26.00
TDRS S-band SA Downlink Power (dBW)	14.15	14.15	14.15	14.15	14.15	14.15
TDRS S-band SA Downlink Ant Gain (dBi)	36.68	36.68	36.68	36.68	36.68	36.68
TDRS S-band SA Downlink Feed Loss (dB)	-4.40	-4.40	-4.40	-4.40	-4.40	-4.40
TDRS S-band SA Downlink EIRP (dBW)	46.43	46.43	46.43	46.43	46.43	46.43
Satellite Elevation Angle (deg)	30.00	30.00	30.00	30.00	30.00	30.00
Slant Range (km)	38609.69	38609.69	38609.69	38609.69	38609.69	38609.69
Free-Space Path Loss (dB)	-190.42	-190.42	-190.42	-190.42	-190.42	-190.42
Atmospheric Losses (dB)	-0.25	-0.25	-0.25	-0.25	-0.25	-0.25
Rain Attenuation (50 mm/hr rain rate)	-0.05	-0.05	-0.05	-0.05	-0.05	-0.05
Pointing Loss (dB)	-0.50	-0.50	-0.50	-0.50	-0.50	-0.50
G/T of Indoor Portable Recvr (dB/K)	-14.70	-14.70	-14.70	-14.70	-14.70	-14.70
Boltzmann Constant (dBW/K-Hz)	-228.60	-228.60	-228.60	-228.60	-228.60	-228.60
Received C/No (dB-Hz)	69.11	69.11	69.11	69.11	69.11	69.11
Data Rate (dB-bps)	45.05	46.81	49.82	51.07	52.04	52.83
Available Downlink Eb/No (dB)	24.06	22.30	19.29	18.04	17.07	16.28
Theoretical Eb/No for 10-4 BER (dB)	3.30	3.30	3.30	3.30	3.30	3.30
(QPSK with R=1/2,K=7 Conv. Coding)						
Receiver Implementation Loss (dB)	1.50	1.50	1.50	1.50	1.50	1.50
Interference Degradation (dB)	0.50	0.50	0.50	0.50	0.50	0.50
Total Receiver Eb/No Requirement (dB)	5.30	5.30	5.30	5.30	5.30	5.30
Link Margin (dB) at beam center (dB)	18.76	17.00	13.99	12.74	11.77	10.98
Link Margin at 3-dB edge of coverage	15.76	14.00	10.99	9.74	8.77	7.98

COMMENTS:
INDOOR TABLE-TOP CD-QUALITY RECEPTION WILL BE FEASIBLE IN MOST SINGLE FAMILY HOUSES
INDOOR TABLE-TOP FM-QUALITY RECEPTION WILL BE FEASIBLE IN MOST BUILDINGS

DIGITAL AUDIO QUALITY	AM	MONO-FM	STEREO FM	NEAR-CD	ALMOST CD	CD-QUALITY
DIGITAL AUDIO BIT RATE (kbps)	32.00	48.00	96.00	128.00	160.00	192.00
TDRS S-band SA Downlink Freq (GHz)	2.05	2.05	2.05	2.05	2.05	2.05
TDRS S-band SA Antenna Diameter (m)	4.90	4.90	4.90	4.90	4.90	4.90
TDRS S-band SA Antenna Efficiency	0.42	0.42	0.42	0.42	0.42	0.42
TDRS S-band SA Antenna HPBW (deg)	2.12	2.12	2.12	2.12	2.12	2.12
TDRS S-band SA Downlink Power (W)	26.00	26.00	26.00	26.00	26.00	26.00
TDRS S-band SA Downlink Power (dBW)	14.15	14.15	14.15	14.15	14.15	14.15
TDRS S-band SA Downlink Ant Gain (dBi)	36.68	36.68	36.68	36.68	36.68	36.68
TDRS S-band SA Downlink Feed Loss (dB)	-4.40	-4.40	-4.40	-4.40	-4.40	-4.40
TDRS S-band SA Downlink EIRP (dBW)	46.43	46.43	46.43	46.43	46.43	46.43
Satellite Elevation Angle (deg)	20.00	20.00	20.00	20.00	20.00	20.00
Slant Range (km)	39552.52	39552.52	39552.52	39552.52	39552.52	39552.52
Free-Space Path Loss (dB)	-190.63	-190.63	-190.63	-190.63	-190.63	-190.63
Atmospheric Losses (dB)	-0.25	-0.25	-0.25	-0.25	-0.25	-0.25
Rain Attenuation (50 mm/hr rain rate)	-0.05	-0.05	-0.05	-0.05	-0.05	-0.05
Pointing Loss (dB)	-0.50	-0.50	-0.50	-0.50	-0.50	-0.50
G/T of Indoor Portable Recvr (dB/K)	-14.70	-14.70	-14.70	-14.70	-14.70	-14.70
Boltzmann Constant (dBW/K-Hz)	-228.60	-228.60	-228.60	-228.60	-228.60	-228.60
Received C/No (dB-Hz)	68.90	68.90	68.90	68.90	68.90	68.90
Data Rate (dB-bps)	45.05	46.81	49.82	51.07	52.04	52.83
Available Downlink Eb/No (dB)	23.85	22.09	19.08	17.83	16.86	16.07
Theoretical Eb/No for 10-4 BER (dB)	3.30	3.30	3.30	3.30	3.30	3.30
(QPSK with R=1/2,K=7 Conv. Coding)						
Receiver Implementation Loss (dB)	1.50	1.50	1.50	1.50	1.50	1.50
Interference Degradation (dB)	0.50	0.50	0.50	0.50	0.50	0.50
Total Receiver Eb/No Requirement (dB)	5.30	5.30	5.30	5.30	5.30	5.30
Link Margin (dB) at beam center (dB)	18.55	16.79	13.78	12.53	11.56	10.77
Link Margin at 3-dB edge of coverage	15.55	13.79	10.78	9.53	8.56	7.77

COMMENTS:
INDOOR TABLE-TOP CD-QUALITY RECEPTION WILL BE FEASIBLE IN MOST SINGLE FAMILY HOUSES
INDOOR TABLE-TOP FM-QUALITY RECEPTION WILL BE FEASIBLE IN MOST BUILDINGS

DIGITAL AUDIO QUALITY	AM	MONO-FM	STEREO FM	NEAR-CD	ALMOST CD	CD-QUALITY
DIGITAL AUDIO BIT RATE (kbps)	32.00	48.00	96.00	128.00	160.00	192.00
TDRS S-band SA Downlink Freq (GHz)	2.05	2.05	2.05	2.05	2.05	2.05
TDRS S-band SA Antenna Diameter (m)	4.90	4.90	4.90	4.90	4.90	4.90
TDRS S-band SA Antenna Efficiency	0.42	0.42	0.42	0.42	0.42	0.42
TDRS S-band SA Antenna HPBW (deg)	2.12	2.12	2.12	2.12	2.12	2.12
TDRS S-band SA Downlink Power (W)	26.00	26.00	26.00	26.00	26.00	26.00
TDRS S-band SA Downlink Power (dBW)	14.15	14.15	14.15	14.15	14.15	14.15
TDRS S-band SA Downlink Ant Gain (dBi)	36.68	36.68	36.68	36.68	36.68	36.68
TDRS S-band SA Downlink Feed Loss (dB)	-4.40	-4.40	-4.40	-4.40	-4.40	-4.40
TDRS S-band SA Downlink EIRP (dBW)	46.43	46.43	46.43	46.43	46.43	46.43
Satellite Elevation Angle (deg)	40.00	40.00	40.00	40.00	40.00	40.00
Slant Range (km)	37778.30	37778.30	37778.30	37778.30	37778.30	37778.30
Free-Space Path Loss (dB)	-190.23	-190.23	-190.23	-190.23	-190.23	-190.23
Atmospheric Losses (dB)	-0.25	-0.25	-0.25	-0.25	-0.25	-0.25
Rain Attenuation (50 mm/hr rain rate)	-0.05	-0.05	-0.05	-0.05	-0.05	-0.05
Pointing Loss (dB)	-0.50	-0.50	-0.50	-0.50	-0.50	-0.50
G/T of Mobile Recvr (dB/K)	-19.00	-19.00	-19.00	-19.00	-19.00	-19.00
Boltzmann Constant (dBW/K-Hz)	-228.60	-228.60	-228.60	-228.60	-228.60	-228.60
Received C/No (dB-Hz)	65.00	65.00	65.00	65.00	65.00	65.00
Data Rate (dB-bps)	45.05	46.81	49.82	51.07	52.04	52.83
Available Downlink Eb/No (dB)	19.95	18.19	15.18	13.93	12.96	12.17
Theoretical Eb/No for 10-4 BER (dB)	3.30	3.30	3.30	3.30	3.30	3.30
(QPSK with R=1/2,K=7 Conv. Coding)						
Mobile Channel Fade Loss (dB)	2.00	2.00	2.00	2.00	2.00	2.00
Receiver Implementation Loss (dB)	1.50	1.50	1.50	1.50	1.50	1.50
Interference Degradation (dB)	0.50	0.50	0.50	0.50	0.50	0.50
Total Receiver Eb/No Requirement (dB)	7.30	7.30	7.30	7.30	7.30	7.30
Link Margin (dB) at beam center (dB)	12.65	10.89	7.88	6.63	5.66	4.87
Link Margin at 3-dB edge of coverage	9.65	7.89	4.88	3.63	2.66	1.87

31

TABLE 6. DBS-R LINK BUDGETS FOR MOBILE RECEPTION USING TDRS S-BAND DOWNLINK
(SATELLITE ELEVATION ANGLE OF 30°, MOBILE RECEIVER G/T OF -19.8 dB/K)

DIGITAL AUDIO QUALITY DIGITAL AUDIO BIT RATE (kbps)	AM 32.00	MONO-FM 48.00	STEREO FM 96.00	NEAR-CD 128.00	ALMOST CDCD-QUALITY 160.00	CDCD-QUALITY 192.00
TDRS S-band SA Downlink Freq (GHz)	2.05	2.05	2.05	2.05	2.05	2.05
TDRS S-band SA Antenna Diameter (m)	4.90	4.90	4.90	4.90	4.90	4.90
TDRS S-band SA Antenna Efficiency	0.42	0.42	0.42	0.42	0.42	0.42
TDRS S-band SA Antenna HPBW (deg)	2.12	2.12	2.12	2.12	2.12	2.12
TDRS S-band SA Downlink Power (W)	26.00	26.00	26.00	26.00	26.00	26.00
TDRS S-band SA Downlink Power (dBW)	14.15	14.15	14.15	14.15	14.15	14.15
TDRS S-band SA Downlink Ant Gain (dBi)	36.66	36.66	36.66	36.66	36.66	36.66
TDRS S-band SA Downlink Feed Loss (dB)	-4.40	-4.40	-4.40	-4.40	-4.40	-4.40
TDRS S-band SA Downlink EIRP (dBW)	46.43	46.43	46.43	46.43	46.43	46.43
Satellite Elevation Angle (deg)	30.00	30.00	30.00	30.00	30.00	30.00
Slant Range (km)	38609.60	38609.60	38609.60	38609.60	38609.60	38609.60
Free-Space Path Loss (dB)	-190.42	-190.42	-190.42	-190.42	-190.42	-190.42
Atmospheric Losses (dB)	-0.25	-0.25	-0.25	-0.25	-0.25	-0.25
Rain Attenuation (50 mm/hr min ren)	-0.05	-0.05	-0.05	-0.05	-0.05	-0.05
Pointing Loss (dB)	-0.50	-0.50	-0.50	-0.50	-0.50	-0.50
G/T of Mobile Recvr (dB/K)	-19.80	-19.80	-19.80	-19.80	-19.80	-19.80
Boltzmann Constant (dBW/K-Hz)	-228.60	-228.60	-228.60	-228.60	-228.60	-228.60
Received C/No (dB-Hz)	64.81	64.81	64.81	64.81	64.81	64.81
Data Rate (dB-bps)	45.05	46.81	49.82	51.07	52.04	52.83
Available Downlink Eb/No (dB)	19.76	18.00	14.99	13.74	12.77	11.98
Theoretical Eb/No for 10-4 BER (dB) (QPSK with R=1/2,K=7 Conv. Coding)	3.30	3.30	3.30	3.30	3.30	3.30
Mobile Channel Fade Loss (dB)	2.00	2.00	2.00	2.00	2.00	2.00
Receiver Implementation Loss (dB)	1.50	1.50	1.50	1.50	1.50	1.50
Interference Degradation (dB)	0.50	0.50	0.50	0.50	0.50	0.50
Total Receiver Eb/No Requirement (dB)	7.30	7.30	7.30	7.30	7.30	7.30
Link Margin (dB) at beam center (dB)	12.46	10.70	7.60	6.44	5.47	4.68
Link Margin at 3-dB edge of coverage	9.46	7.70	4.60	3.44	2.47	1.68

TABLE 7. DBS-R LINK BUDGETS FOR MOBILE RECEPTION USING TDRS S-BAND DOWNLINK
(SATELLITE ELEVATION ANGLE OF 20°, MOBILE RECEIVER G/T OF -19.8 dB/K)

| DIGITAL AUDIO QUALITY DIGITAL AUDIO BIT RATE (kbps)	AM 32.00	MONO-FM 48.00	STEREO FM 96.00	NEAR-CD 128.00	ALMOST CDCD-QUALITY 160.00	CDCD-QUALITY 192.00
TDRS S-band SA Downlink Freq (GHz)	2.05	2.05	2.05	2.05	2.05	2.05
TDRS S-band SA Antenna Diameter (m)	4.90	4.90	4.90	4.90	4.90	4.90
TDRS S-band SA Antenna Efficiency	0.42	0.42	0.42	0.42	0.42	0.42
TDRS S-band SA Antenna HPBW (deg)	2.12	2.12	2.12	2.12	2.12	2.12
TDRS S-band SA Downlink Power (W)	26.00	26.00	26.00	26.00	26.00	26.00
TDRS S-band SA Downlink Power (dBW)	14.15	14.15	14.15	14.15	14.15	14.15
TDRS S-band SA Downlink Ant Gain (dBi)	36.66	36.66	36.66	36.66	36.66	36.66
TDRS S-band SA Downlink Feed Loss (dB)	-4.40	-4.40	-4.40	-4.40	-4.40	-4.40
TDRS S-band SA Downlink EIRP (dBW)	46.43	46.43	46.43	46.43	46.43	46.43
Satellite Elevation Angle (deg)	20.00	20.00	20.00	20.00	20.00	20.00
Slant Range (km)	39552.52	39552.52	39552.52	39552.52	39552.52	39552.52
Free-Space Path Loss (dB)	-190.63	-190.63	-190.63	-190.63	-190.63	-190.63
Atmospheric Losses (dB)	-0.25	-0.25	-0.25	-0.25	-0.25	-0.25
Rain Attenuation (50 mm/hr min ren)	-0.05	-0.05	-0.05	-0.05	-0.05	-0.05
Pointing Loss (dB)	-0.50	-0.50	-0.50	-0.50	-0.50	-0.50
G/T of Mobile Recvr (dB/K)	-19.80	-19.80	-19.80	-19.80	-19.80	-19.80
Boltzmann Constant (dBW/K-Hz)	-228.60	-228.60	-228.60	-228.60	-228.60	-228.60
Received C/No (dB-Hz)	64.60	64.60	64.60	64.60	64.60	64.60
Data Rate (dB-bps)	45.05	46.81	49.82	51.07	52.04	52.83
Available Downlink Eb/No (dB)	19.55	17.79	14.78	13.53	12.56	11.77
Theoretical Eb/No for 10-4 BER (dB) (QPSK with R=1/2,K=7 Conv. Coding)	3.30	3.30	3.30	3.30	3.30	3.30
Mobile Channel Fade Loss (dB)	2.00	2.00	2.00	2.00	2.00	2.00
Receiver Implementation Loss (dB)	1.50	1.50	1.50	1.50	1.50	1.50
Interference Degradation (dB)	0.50	0.50	0.50	0.50	0.50	0.50
Total Receiver Eb/No Requirement (dB)	7.30	7.30	7.30	7.30	7.30	7.30
Link Margin (dB) at beam center (dB)	12.25	10.49	7.48	6.23	5.26	4.47
Link Margin at 3-dB edge of coverage	9.25	7.49	4.48	3.23	2.26	1.47
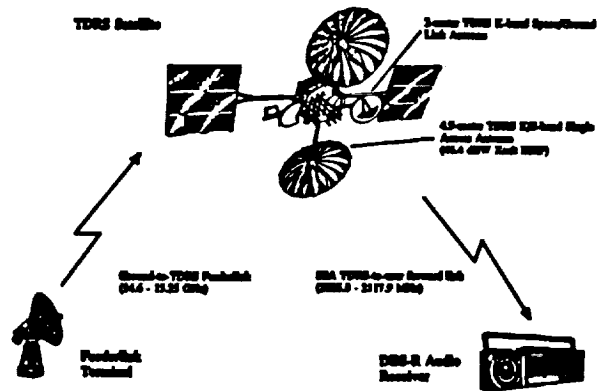
Figure 1. Schematic of DBS-R/TDRS Demonstration
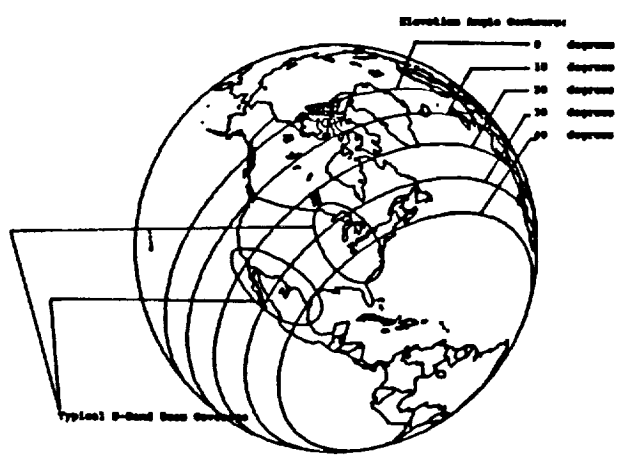
Figure 2. TDRS-1 Elevation Angle Contours From North America (Satellite at 62° West Longitude)

FREQUENCIES ALLOCATED BY WARC-92
TO BROADCASTING SATELLITE SERVICE (BSS) (SOUND) (DAB) BY COUNTRY

2310-2360MHZ USA ONLY
BSS(S) prohibited in USA in 1452-1492MHZ
POP=252M

1452-1492MHZ
NOT UNTIL 2007
POP=551M

Exhibit 1

Aeronautical Audio Broadcasting via Satellite

Forrest F. Tzeng
COMSAT Laboratories
22300 Comsat Drive
Clarksburg, MD 20871-9475, U.S.A.
Tel: (301)428-4659 Fax: (301)428-4534

ABSTRACT

A system design for aeronautical audio broadcasting, with C-band uplink and L-band downlink, via Inmarsat space segments is presented. Near-transparent-quality compression of 5-kHz bandwidth audio at 20.5 kbit/s is achieved based on a hybrid technique employing linear predictive modeling and transform-domain residual quantization. Concatenated Reed-Solomon/convolutional codes with quadrature phase shift keying are selected for bandwidth and power efficiency. RF bandwidth at 25 kHz per channel, and a decoded bit error rate at 10^{-6} with E_b/N_o at 3.75 dB, are obtained. An interleaver, scrambler, modem synchronization, and frame format were designed, and frequency-division multiple access was selected over code-division multiple access. A link budget computation based on a worst-case scenario indicates sufficient system power margins. Transponder occupancy analysis for 72 audio channels demonstrates ample remaining capacity to accommodate emerging aeronautical services.

INTRODUCTION

The field of mobile satellite communications has experienced rapid growth in recent years. Compared to the maritime and land mobile segments, the aeronautical segment of mobile satellite systems is relatively new. However, many new aeronautical services have emerged, and this trend is expected to continue. Some examples include air phone, in-flight news, in-flight customs clearance, and aeronautical facsimile (aero fax).

In this study, schemes were designed for low-rate audio coding, coded modulation, and digital transmission architecture to support live audio program broadcasting to commercial aircraft via the Inmarsat space segments. Due to the bandwidth and power limitations of the Inmarsat segments, the audio programs targeted for the current application include talk shows, sports coverage, news, commentaries, and weather, as well as intermission music. Consequently, a monaural audio signal of 5-kHz bandwidth (AM-quality audio) was selected. The information source also includes a subband broadcast data channel with a data rate range from 300 to 2,400 bit/s.

Several system design constraints were considered. These included use of the existing Inmarsat-Aero aircraft earth station (AES) antenna subsystem to minimize customer cost, simple and low-cost airborne subsystem (re-

ceiver) hardware, and applicability to both the Inmarsat-2 and Inmarsat-3 space segments. In addition, the RF bandwidth per audio channel had to be a multiple of 2.5 kHz to be consistent with the Inmarsat systems.

This paper describes a low-rate audio coding scheme that achieves near-transparent-quality compression of 5-kHz bandwidth audio at 20.5 kbit/s. Error protection strategies for compressed audio and data are also presented. Candidate coded modulation schemes are compared in terms of their power and bandwidth efficiency, and designs for an interleaver, scrambler, modem synchronization, and frame format are discussed. Multiple-access techniques are then compared, and link budget computation and transponder occupancy analysis results are presented.

AUDIO COMPRESSION AND ERROR PROTECTION

Audio Compression

The technique for adaptive predictive coding with transform-domain quantization (APC-TQ) [1] presented here combines time-domain linear prediction modeling and transform-domain quantization of the prediction residual signal. The APC-TQ technique is efficient in exploiting the nonuniform power spectral distribution that exists in audio signals. It also permits the direct implementation of auditory noise-masking techniques based on auditory characteristics, to maximize the perceived quality of the reconstructed audio.

The audio signal is band-limited to 5 kHz and sampled at a rate of 10.24 kHz. A frame size of 256 samples is used. The power spectrum model for each frame of audio samples is a product of two terms: a short-term model which represents coarse or envelope spectral variations, and a long-term model which represents fine or harmonic spectral variations. The resulting power spectrum model is used to determine the bit allocation for residual quantization.

Short-term prediction is accomplished by predicting each sample based on a weighted sum of a few samples immediately preceding it. A fifth-order linear predictive model is computed using the autocorrelation method [2]. The five filter coefficients are converted into line spectrum frequencies (LSFs) [3] and scalarly quantized using 24 bits overall (with 5, 5, 5, 5, and 4 bits for the five LSFs, respectively). The LSFs were found to have good

properties for quantization. In addition, they allow easy channel error concealment in terms of guaranteed filter stability and minimum filter distortion when in error.

Long-term prediction consists of estimating the optimum long-term prediction delay (i.e., pitch) and predicting each sample from a weighted sum of the three samples located around the delay. The delay is estimated by computing the autocorrelation function of the short-term prediction error signal over the delay range from 20 to 256 samples. The optimum delay is indicated by the location of the peak of the autocorrelation function, and the delay value is coded using 8 bits. The long-term prediction parameters are selected from a code book of 128 parameter sets [4], based on the criterion of minimizing the long-term prediction error power over the analysis frame.

The residual signal after short- and long-term prediction is quantized next. The 256 samples of the residual signal are transformed using a discrete cosine transform (DCT), and are quantized using a total of 465 bits. These bits are nonuniformly allocated based on the power spectral estimate obtained using the short- and long-term prediction parameters. Scalar Max quantizers [5] optimized for zero-mean, univariate Gaussian distribution are employed. A scaling parameter is determined in order to scale the DCT coefficients to unit variance. The parameter is then quantized logarithmically using 8 bits.

At the decoder, the short-term and long-term predictor parameters are decoded and used to determine the bit allocation. Based on this allocation, the transform coefficients are decoded and inverse DCT is applied to obtain the quantized version of the residual signal. This signal excites the cascade of long- and short-term synthesis filters to reconstruct the audio signal. At 20.5 kbit/s, a near-transparent-quality coded 5-kHz audio signal was reconstructed.

Error Protection

For aeronautical broadcast applications, the uplink C-band channel (ground earth station [GES] to satellite) and the downlink L-band channel (satellite to aeronautical earth station [AES]) can be modeled as an additive white Gaussian noise (AWGN) channel and a Rician channel (with a Rice factor of $K = 10$) [6], respectively. For broadcast audio, the transmission time delay is not as critical as for conversational speech. Therefore, an interleaver with an appropriate interleaving length can be used so that the multipath Rician fading downlink channel effectively becomes AWGN.

The use of convolutional codes is a proven technique for error correction under AWGN channel conditions. In this study, an inner-layer convolutional code was selected for both the audio signal and broadcast data. A target decoded bit error rate (BER) of 10^{-3} was selected for this inner-layer error protection scheme. The decoded BER is used as a basis for comparing the power and bandwidth

efficiency of several candidate coding and modulation schemes, as described below. Both the audio and data information were further protected by using an additional outer-layer error protection scheme to lower the overall decoded BER to less than 10^{-6}. At this BER, the subjective degradation to the audio is imperceptible.

Two approaches were considered for the design of the outer-layer error protection. The first approach treats audio and data separately and uses a Reed-Solomon (RS) code as the outer code to form a concatenated code with the inner convolutional code to protect data. Audio is protected using an unequal-error-protection (UEP) method. In UEP, the more sensitive bits of audio are given a higher level of error protection, while less-sensitive bits are given a lower level or even no error protection. The second approach treats audio and data as a single entity, and both are protected using an outer RS code, as in the first approach for data.

To attempt the first approach, a UEP scheme was devised which included (23, 12) Golay codes, (7, 4) Hamming codes, and parity checks as component codes, augmented by several judiciously designed error detection and error concealment techniques. This scheme provided sufficient protection for most bits of the short-term filter coefficients, pitch, long-term filter coefficients, and scaling parameter. However, there were no bits available to protect the remaining bits.

Work with the second approach for outer-layer error protection revealed that it was more efficient. Given the available redundancy, the concatenated code achieves the desired decoded BER of 10^{-6} for both audio and data at a very reasonable energy-per-bit to noise-power density ratio, E_b/N_o. This approach also allows a simpler decoder design, since only one RS decoder and one outer interleav-er are necessary. An RS(255, 229) code over a Galois field GF(256) was finally selected. This code can correct 13 symbol (byte) errors. Figure 1 is a block diagram of the overall transmission system.

CODING AND MODULATION

Coded Modulation

In selecting an appropriate inner-layer coded modulation scheme, only quadrature phase shift keying (QPSK), its variants, and octal phase shift keying (OPSK) were considered. These are well-known, proven techniques for satellite communications. Quadrature amplitude modulation schemes are not suitable for non-linear channel operations, while continuous-phase frequency shift keying and its variants, such as multi-h codes, are complicated, and their performance does not justify use in this application.

Several candidate coded modulation schemes were examined (Table 1). For separate coding and modulation schemes, rate 1/2, 2/3, 3/4, and 5/6 coded QPSK were considered. For combined coding and modulation
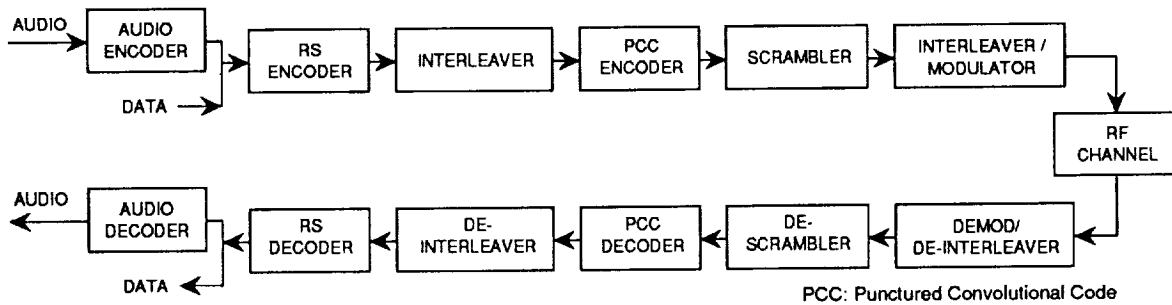
Figure 1. Digital Transmission System Block Diagram

Table 1. Candidate Coded Modulation Schemes

CODED MODULATION	E_b/N_0 (dB) @ 10^{-3}	RF BANDWIDTH (kHz)
1/2 QPSK	3	37.5
2/3 QPSK	3.5	30
3/4 QPSK	4	25
5/6 QPSK	4.6	25
2/3 OPSK (TCM)	5	20
5/6 OPSK (TCM)	5.7	17.5
2/3 D-OPSK (TCM)	8.4	20

schemes, rate 2/3 coded OPSK, differential OPSK (D-OPSK), and rate 5/6 coded OPSK were considered.

For the power estimates, an inner-layer decoded BER of 10^{-3} was assumed. For separate coding and modulation schemes, all convolutional codes were assumed to have a constraint length of 6 with 3-bit soft decision. In trellis-coded modulation (TCM) schemes, 16-state codes were assumed. The higher-rate convolutional codes (rate 2/3, 3/4, and 5/6) used in separate coding and modulation schemes were realized by using punctured convolutional codes [7] based on the rate 1/2 optimum code [8], to reduce decoding complexity.

The RF bandwidth estimates assumed a 35-percent rolloff factor for a square-root, raised-cosine shaping filter, and a 1.375-kHz guard band (0.6875 kHz at each side) for each carrier. The guard band value was selected based on the maximum AES receiver frequency error specified in the Inmarsat-Aero "System Definition Manual" (SDM) [9]. Also, a data rate of 1 kbit/s was added for modem synchronization and framing redundancies. These bits are used as preambles, unique words (UWs), audio channel ID information (for broadcast channel scanning), and flush bits. The computed bandwidth requirements were converted into multiples of 2.5 kHz to meet system requirements.

Based on the power and bandwidth requirements shown, two candidate coded modulation schemes were considered: rate 2/3 coded OPSK (TCM) and rate 3/4 coded QPSK. Rate 2/3 coded OPSK is more bandwidth-efficient, while rate 3/4 coded QPSK is more power-efficient. Rate 3/4 coded QPSK was selected, since it requires 1 dB less power, and the aeronautical

downlink is power-limited. Also, with increased bandwidth, carrier power can be increased without changing the power density. This is an important factor in frequency planning.

Interleaving and Synchronization

Two block interleavers were employed. The inner interleaver decorrelates burst errors created by the RF fading channel, while the outer interleaver decorrelates burst errors at the Viterbi decoder output. For the RF fading channel, the maximum fade duration had been shown to be about 20 ms [6], which corresponds to about 680 bits. For the rate 3/4 Viterbi decoder, the maximum burst length is less than 35 bits [10].

For inner interleaving, the number of rows (NR) was selected to be 775 bits, in order to exceed the maximum fade duration. The number of columns (NC) can theoretically be selected to be equal to the Viterbi decoding length, which is about six times the constraint length. However, in practice a larger NC must be used, especially for higher-rate codes such as the rate 3/4 code selected for this application [10]. An NC of 88 bits was used. The selection of these two particular values for NR and NC was based on the frame format described in the next subsection.

For the outer interleaver, NR was selected to be 25 bits and NC was selected as the RS code length, which is 255 bytes (2,040 bits). The 25-bit NR was selected for two reasons. First, it was desired not to introduce too much interleaving delay. Second, for consistency with the Inmarsat-Aero SDM, a frame size of 500 ms was selected. Given this frame size, it was decided that 51 kbit/s was a good value for both the outer interleaver size (2,040 × 25) and the incoming data rate (25.5 kbit/s × 2 s).

In terms of synchronization, the modem needs to be robust at a low carrier-to-noise power density ratio, C/N_o, in the presence of L-band Doppler shifts varying between ±2 kHz. In addition, multipath fading is prevalent at elevation angles below 10°, and signal can be blocked by the aircraft tail structure. Because coherent detection is used for power efficiency, reliable carrier frequency/ phase acquisition and tracking with a minimum of cycle slips is required. A channel scanning capability is also

desired so that a receiver can scan each of the available aeronautical channels.

The channel rate after rate 3/4 convolutional encoding, excluding framing bits, is 34 kbit/s. To simplify equipment design and implementation, the channel rate is required to be a submultiple of a 5.04-MHz master clock, for compatibility with other Inmarsat-Aero channel unit bit rates. A channel rate of 35 kbit/s meets this requirement and allows 3-percent capacity for framing overhead bits.

The bit rate of the system is approximately 67 percent faster than the 21-kbit/s Inmarsat-Aero standard channel. However, this is an advantage in terms of carrier synchronization and tracking, because frequency variations are a smaller percentage of the bit rate. The maximum AES received frequency error is specified as ±346 Hz, plus the AES Doppler shift of ±2 kHz, for a total uncertainty of ±2,346 Hz. Since this is less than 7 percent of the channel rate, conventional carrier tracking methods such as a Costas loop or decision-directed carrier tracking loop can be used. Symbol timing tracking is also straightforward, and a conventional symbol transition detector can be employed. As specified in the SDM, a scrambler is used for energy dispersal and to assist in symbol synchronization.

Frame Format

The channel frame format is shown in Figure 2. To maintain system compatibility with the Inmarsat-Aero SDM, the frame duration is chosen to be 500 ms. Each frame contains its own preamble and an 88-bit UW, which is identical to that used on the current Inmarsat-C channel. The preamble consists of 160 bits of unmodulated carrier for carrier synchronization, followed by a 160-bit alternating 0101 pattern for clock synchronization. The occurrence of these bits in every frame permits rapid acquisition and reacquisition after a fade or tail blockage. Each frame also contains a 16-bit station ID

field, which allows a receiver to perform station verification in order to facilitate rapid channel scanning.

The inner and outer forward error correction (FEC) interleavers were both chosen to have a time span of 2 s. Thus, a 2-s superframe structure was defined consisting of four 500-ms frames. A different 88-bit UW, denoted UW', is employed to mark the first frame of a superframe. A 12-bit frame counter field, denoted FC, immediately follows the UW and consists of a 4-bit frame counter repeated three times for bit error immunity.

Figure 3 is a block diagram of the procedure used to pack the program audio and secondary data channel bits into 500-ms frames. The program audio channel has an information rate of 20.5 kbit/s, and the data channel is assumed to have an information rate of 2,400 bit/s. If lower data channel rates are desired, the data field will have to be packed with enough dummy bits to achieve a 2,400-bit/s rate. To assemble a frame, 2 s of program audio (41,000 bits) and 2 s of secondary data (4,800 bits) are buffered in memory. It is assumed that the actual frame assembly is much faster than real time, so that the total transmitter delay is not much greater than 2 s. While the data are being processed, the next superframe is being buffered in memory for subsequent frame assembly.

TRANSMISSION SYSTEM ARCHITECTURE

Multiple Access

Due to the circuit-switched nature of broadcast audio programs, time-division multiple access (TDMA) was not considered. However, frequency-division multiple access (FDMA) and code-division multiple access (CDMA) methods were carefully compared.

CDMA possesses several advantages, including the possibility of overlay on top of narrowband users; system flexibility through the use of programmable codes; multipath rejection and interference suppression capabilities; and graceful degradation with an increased number of

(a) Superframe Structure (four 500-ms frames)

(b) Frame Structure
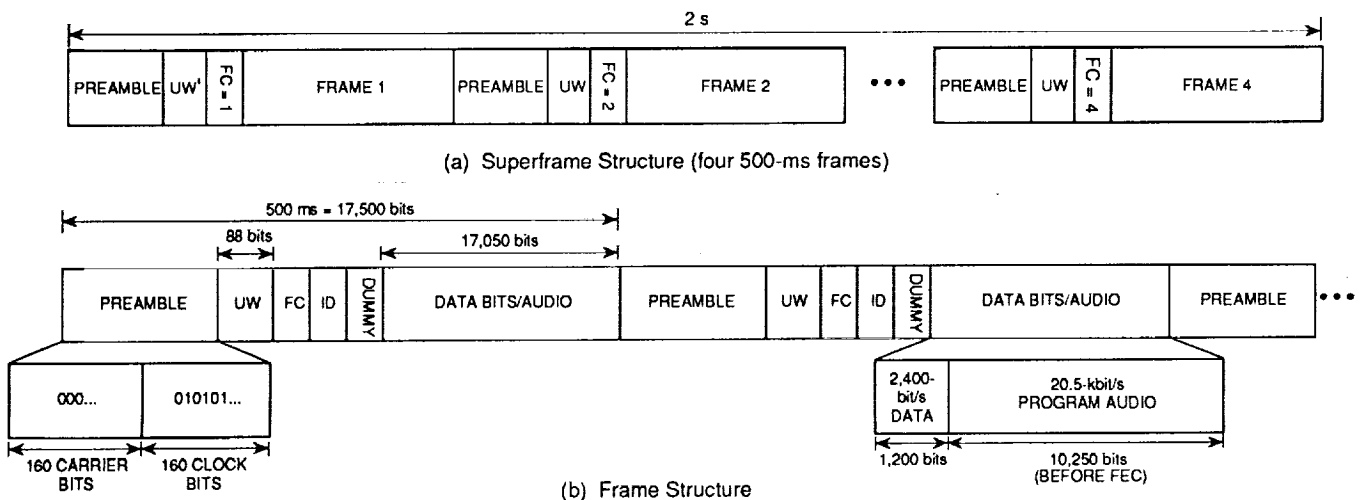
Figure 2. Frame Format

36

Figure 3. Frame Assembly

Flow (top row):
2,400-bit/s DATA → / 20.5-kbit/s PROGRAM AUDIO → **BUFFER 2 s OF DATA/AUDIO** —45,800 bits→ **RS ENCODE (255, 229)** —51,000 bits→ **INTERLEAVE 2,040 x 25** —51,000 bits→ **APPEND 6 FLUSH ('0') BITS** —51,006 bits→ **RATE 3/4 CONVOLUTIONAL ENCODE** —68,008 bits→ **APPEND 192 DUMMY ('0') BITS** —68,200 Bits→

(second row): **INTERLEAVE 88 x 775** (68,200 bits) → **SEPARATE INTO 4 500-ms FRAMES** (4 x 17,050 bits) →

17,500 bits → **INSERT 450 OVERHEAD BITS FOR FRAME 1**
17,500 bits → **INSERT 450 OVERHEAD BITS FOR FRAME 2**
17,500 bits → **INSERT 450 OVERHEAD BITS FOR FRAME 3**
17,500 bits → **INSERT 450 OVERHEAD BITS FOR FRAME 4**

→ **MUX** → 35-kbit/s CHANNEL DATA TO MODULATOR

active broadcast co-channels. However, the small channelized transponder bandwidth available (1.4 MHz maximum for Inmarsat-2, as described later), coupled with the high channel data rate, makes the processing gain very small for a direct-sequence CDMA system. Although a frequency-hopping CDMA system does not require contiguous bandwidth, the necessary frequency synthesizers would increase aircraft receiver complexity and cost. This consideration also applies to direct-sequence CDMA systems, which require additional circuits for code acquisition and tracking.

In view of the above considerations, FDMA/SCPC (single channel per carrier) was selected. Its implementation is relatively simple and is compatible with most of the existing Inmarsat traffic. Since the aero broadcasting system is downlink-limited, the intermodulation interference in an FDMA system does not critically limit system performance. However, it is still advisable to reduce intermodulation interference. This can be achieved by using an optimized frequency plan, examples of which are given in References 11 and 12.

Link Budget

A link budget (Table 2) was prepared for Inmarsat-2 satellite links. An elevation angle of 5° (a worst-case scenario) was assumed for AES, with a system margin of 3 dB. The concatenated RS/punctured convolutional code was simulated in software, and it was determined that an E_b/N_o of about 3.75 dB is required in order to achieve the desired decoded BER of 10^{-6}.

The link analysis further assumes that there is no adjacent satellite interference or co-channel interference involved. The adjacent channel interference effect is also assumed to be offset by the pulse-shaping filter and the guard bands. Note that this analysis is based on

Table 2. Link Budget Analysis

PARAMETER	VALUE
Uplink (GES to Satellite)	
Frequency	6.44 GHz
GES Elevation	5°
GES Tx EIRP	65 dBW
Path Loss (incl. atmos. loss)	201.3 dB
Satellite Rx G/T	-14 dB/K
Uplink C/N_o	75.3 dB-Hz
Satellite	
Satellite Gain	161.3 dB
Satellite C/IM_o	67.0 dB-Hz
Downlink (Satellite to AES)	
Frequency	1.545 GHz
AES Elevation	5°
Satellite Tx EIRP	25 dBW
Path Loss (incl. atmos. loss)	188.9 dB
AES Rx G/T	-13 dB/K
Downlink C/N_o	51.7 dB-Hz
Link Performance	
Overall C/N_o	51.6 dB-Hz
Required E_b/N_o at 10^{-6}	3.75 dB
Data Rate (22.9 kbit/s)	43.6 dB
Miscellaneous Loss (modem loss and random losses)	1.25 dB
Link C/N_o Requirement	48.6 dB-Hz
System Margin	3.0 dB

Inmarsat-2 satellite specifications. For Inmarsat-3 satellites, the link budget could show significantly better power capacity. In addition, if the flight route is such that the elevation angle is significantly greater than 5°, the 3-dB link margin could be achieved with a lower GES transmit effective isotropically radiated power (EIRP).

Aero-Band Occupancy

For initial system operation, it is assumed that three channels will be provided for each Inmarsat signatory in the Atlantic Ocean Region (AOR) East, AOR West, Pacific Ocean Region (POR), and Indian Ocean Region (IOR). There are six signatories in each region, for a total of 72 planned channels.

For the Inmarsat-3 space segment, the uplink C-band has a 29-MHz bandwidth (6,425 to 6,454 MHz), from which the aeronautical portion is allocated a 10-MHz bandwidth (6,440 to 6,450 MHz). The downlink L-band has a 34-MHz bandwidth (1,525 to 1,559 MHz), from which the aeronautical portion is also allocated a 10-MHz bandwidth (1,545 to 1,555 MHz). However, each of the two 10-MHz bands is divided into three bands of 3, 3, and 4 MHz, respectively, separated by some guard bands (1.2 and 1.4 MHz, 1.2 and 1.4 MHz, 2.3 and 1.3 MHz, respectively). Thus, the actual usable bandwidth is only 8.8 MHz.

For the Inmarsat-2 space segment, the uplink aeronautical C-band is allocated a 3-MHz bandwidth (6,440 to 6,443 MHz), and the downlink aeronautical L-band is also allocated a 3-MHz bandwidth (1,545 to 1,548 MHz). Each of these two bands is divided into two bands of 1.2 and 1.4 MHz, separated by a guard band. Consequently, the actual usable bandwidth is 2.6 MHz.

The aero-band occupancy percentage, m, was defined as the ratio of the total bandwidth required to support the 72 audio broadcast channels vs the total usable bandwidth allocated for aeronautical services. For the selected coded modulation scheme, the required RF bandwidth is 25 kHz for each audio channel. The corresponding occupancy percentage is then $m = 69.2$ percent for Inmarsat-2, and $m = 20.5$ percent for Inmarsat-3. These percentages are reasonable for high-data-rate audio programs, especially for Inmarsat-3 satellites. Thus, there should be ample system capacity remaining to accommodate many emerging aeronautical services.

CONCLUSIONS

A system design to support aeronautical broadcast of audio programs via the Inmarsat-2 and -3 space segments has been presented. Near-transparent-quality compression of 5-kHz bandwidth audio at 20.5 kbit/s were described. Candidate error protection strategies and coded modulation schemes were carefully compared to achieve robust performance with bandwidth and power efficiency. Designs for an interleaver, scrambler, modem synchronization, and frame format were presented, and the considerations used in selecting FDMA for multiple access were discussed. Results of the link budget computation and transponder occupancy analysis were also presented.

The designed system currently supports the transmission of AM broadcast-quality audio programs to commer-cial aircraft equipped with high-gain AES antenna sub-systems. With rapid advances in audio compression technology, higher quality broadcast audio programs such as near-FM audio could be supported in the near future, using the same transmission system described here. The system might also be capable of supporting the transmission of AM-quality audio programs to aircraft equipped with low-gain omnidirectional AES antenna subsystems. By using Inmarsat-3 spot beams, near-FM-quality audio broadcasts to aircraft with low-gain AES antennas might also be achievable.

ACKNOWLEDGMENTS

REFERENCES

[1] B. R. U. Bhaskar, "Adaptive Prediction With Transform Domain Quantization for Low Rate Audio Coding," IEEE ASSP Workshop on Applications of Signal Processing to Audio and Acoustics, New Paltz, NY, *Proc.* (unpaginated), October 1991.

[2] L. R. Rabiner and R. W. Schafer, *Digital Processing of Speech Signals*, Englewood Cliffs, NJ: Prentice-Hall, 1978.

[3] G. Kang and L. Fransen, "Application of Line-Spectrum Pairs to Low-Bit-Rate Speech Encoders," IEEE International Conference on Acoustics, Speech, and Signal Processing, Tampa, FL, *Proc.*, pp. 244–247, March 1985.

[4] Y. Linde, A. Buzo, and R. Gray, "An Algorithm for Vector Quantizer Design," *IEEE Transactions on Communications*, Vol. COM-28, No. 1, pp. 84–95, January 1980.

[5] J. Max, "Quantizing for Minimum Distortion," *IRE Transactions on Information Theory*, Vol. IT-6, pp. 7–12, March 1960.

[6] W. Sandrin *et al.*, "Aeronautical Satellite Data Link Study," *COMSAT Technical Review*, Vol. 15, No. 1, pp. 1–38, Spring 1985.

[7] Y. Yasuda, K. Kashiki, and Y. Hirata, "High-Rate Punctured Convolutional Codes for Soft Decision Viterbi Decoding," *IEEE Transactions on Communications*, Vol. COM-32, No. 3, pp. 315–319, March 1984.

[8] G. Clark, Jr., and J. Cain, *Error-Correction Coding for Digital Communications*, New York: Plenum Press, 1981.

[9] Inmarsat, "Aeronautical System Definition Manual," 1992.

[10] Y. Yasuda *et al.*, "Development of a Variable-Rate Viterbi Decoder and Its Performance Characteristics," 6th International Conference on Digital Satellite Communications, Phoenix, AZ, *Proc.*, pp. XII.24–XII.31, September 1983.

[11] T. Mizuike and Y. Ito, "Optimization of Frequency Assignment," *IEEE Transactions on Communications*, Vol. 37, No. 10, pp. 1031–1041, October 1989.

[12] H. Okinaka, Y. Yasuda, and Y. Hirata, "Intermodulation Interference-Minimum Frequency Assignment for Satellite SCPC Systems," *IEEE Transactions on Communications*, Vol. COM-32, No. 4, pp. 462–468, April 1984.

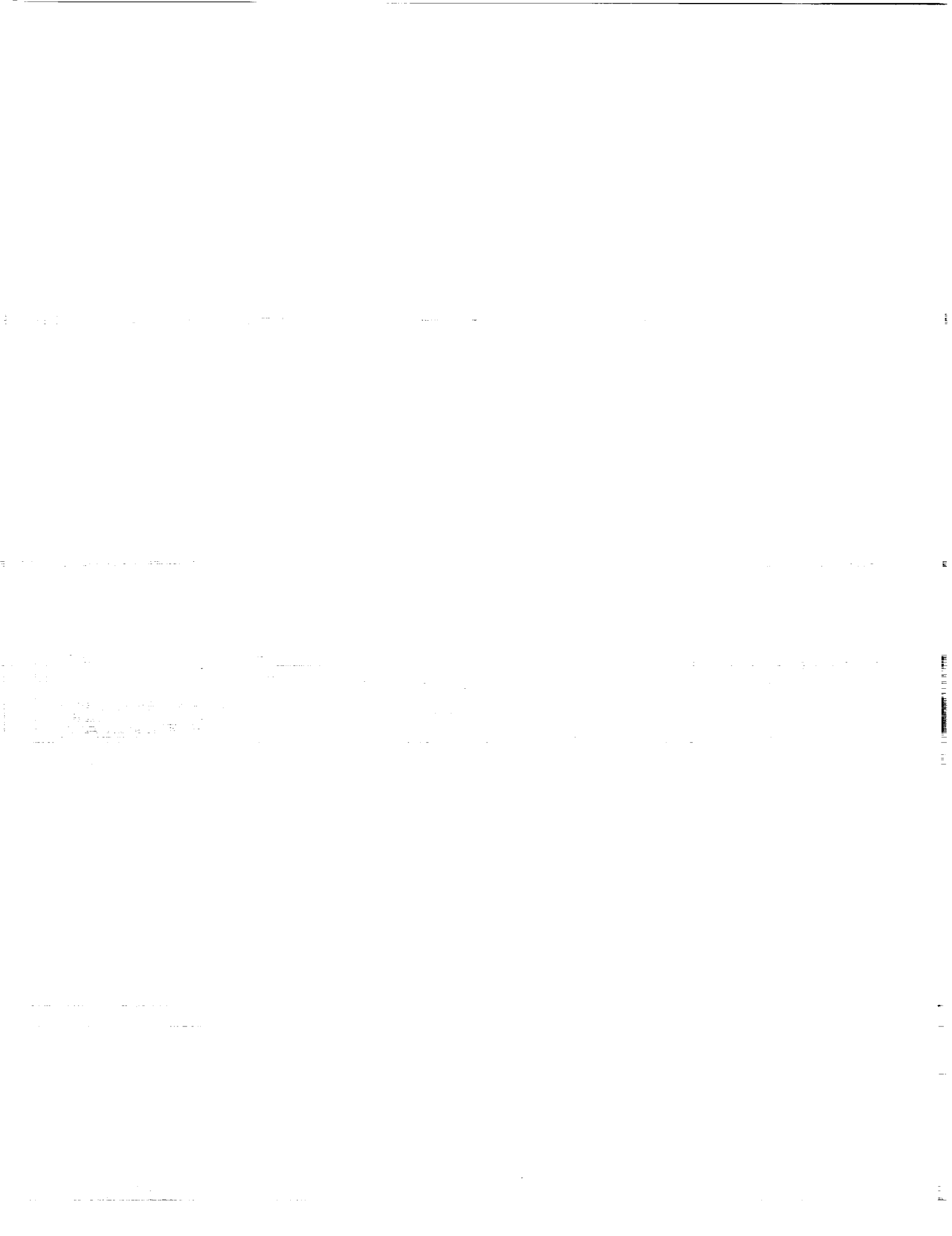# Session 2
Spacecraft Technology

Session Chair—*Shuichi Samejima,* Nippon Telephone and Telegraph, Japan
Session Organizer—*Alan Maclatchy,* Communications Research Centre, Canada

The MSAT Spacecraft of
Telesat Mobile Inc.

E. Bertenyi
Telesat Canada
1601 Telesat Court
Gloucester, Ontario, K1B 5P4, Canada
Phone 613 748-0123; Fax 613 748-8782

Abstract (full paper will be provided at the Conference)

This paper describes the MSAT spacecraft of the Canadian mobile satellite operator, Telesat Mobile Inc. (TMI). When launched in 1994, the large geostationary MSAT spacecraft which is currently under construction by Hughes Aircraft Co. and Spar Aerospace Ltd. will enable TMI to provide mobile and transportable communications services to its customers even in the most remote parts of the North American continent.

The main elements of TMI's mobile satellite system (described in a companion paper) are the space segment and the ground segment. TMI's space segment will employ one of two nearly identical satellites, one of which will be owned and operated by TMI, the other by the U.S. mobile satellite operator, American Mobile Satellite Corporation (AMSC). The two companies are participating in a joint spacecraft procurement in order to reduce the nonrecurring costs and to ensure system compatibility between the two systems; and they have also agreed to provide in-orbit backup to each other in the event of a catastrophic satellite failure.

The paper reviews the program status, performance requirements, main parameters and configuration of the MSAT spacecraft. The major features of the communications subsystem are discussed in some detail, and a brief summary is presented of the spacecraft service module.

Key technology items include the L-band RF power amplifier, which must operate with a high DC to RF power efficiency and generate low intermodulation when loaded with multi-carrier signals; and the large diameter deployable L-band antenna. The development status and expected performance of these spacecraft components is examined.

Adaptive Digital Beamforming for a
CDMA Mobile Communications Payload

Samuel G. Muñoz-García and Javier Benedicto Ruiz
ESA/ESTEC
Communication Satellites Dept., Radio-Frequency Systems Division
Postbus 299, 2200 AG Noordwijk, The Netherlands

Abstract (full paper will be provided at the Conference)

In recent years, Spread-Spectrum Code Division Multiple Access (CDMA) has become a very popular access scheme for mobile communications due to a variety of reasons: excellent performance in multipath environments, high scope for frequency reuse, graceful degradation near saturation, etc. In this way, a CDMA system can support simultaneous digital communication among a large community of relatively uncoordinated users sharing a given frequency band.

Nevertheless, there are also important problems associated with the use of CDMA. First, in a conventional CDMA scheme, the signature sequences of asynchronous users are not orthogonal and, as the number of active users increases, the self-noise generated by the mutual interference between users considerably degrades the performance, particularly in the return link. Furthermore, when there is a large disparity in received powers — due to differences in slant range or atmospheric attenuation — the non-zero cross-correlation between the signals gives rise to the so-called *near-far* problem. This leads to an inefficient utilization of the satellite resources and, consequently, to a drastic reduction in capacity.

Several techniques have been proposed to overcome this problem, such as Synchronized CDMA — in which the signature sequences of the different users are quasi-orthogonal — and power control. At the expense of increased network complexity and user coordination, these techniques enable the system capacity to be restored by equitably sharing the satellite resources among the users.

In this paper, an alternative solution is presented based upon the use of time-reference adaptive digital beamforming on board the satellite. This technique enables a high number of independently steered beams to be generated from a single phased array antenna, which automatically track the desired user signal and null the unwanted interference sources. In order to use a time-reference adaptive antenna in a communications system, the main challenge is to obtain a reference signal highly correlated with the desired user signal and uncorrelated with the interferences. CDMA lends itself very easily to the generation of such a reference signal, thanks to the a priori knowledge of the user's signature sequence.

First, the integration of an adaptive antenna in an asynchronous CDMA system will be analyzed. The adaptive antenna system can provide increased interference rejection — much higher than that afforded by the code alone — and, since CDMA is mainly interference

limited, any reduction in interference converts directly and linearly into an increase in capacity. Analyses and computer simulations will be presented that show how an asynchronous CDMA system incorporating adaptive beamforming can provide at least as much capacity as a synchronous system.

More importantly, the proposed concept allows the near-far effect to be mitigated without requiring a tight coordination of the users in terms of transmitted power control or network synchronization. The system is extremely robust to the near-far effect because the signals reaching the satellite from directions other than that of the desired user — which are likely to have different power levels — are adaptively canceled by the antenna.

Finally, a payload architecture will be presented that illustrates the practical implementation of this concept. This digital payload architecture demonstrates that with the advent of high performance CMOS digital processing, the on-board implementation of complex DSP techniques — in particular Digital Beamforming — has become possible, being most attractive for Mobile Satellite Communications.

Electrical Performance of Wire Mesh for
Spacecraft Deployable Reflector Antennas

Greg Turner
Harris Corporation, Government Aerospace Systems Division
PO Box 94000, Melbourne, FL, 32902

Abstract (full paper will be provided at the Conference)

Mobile satellite communications systems require large, high gain antennas at the spacecraft to minimize the antenna gain and power requirements for mobile user elements. The use of a deployable reflector antenna for these applications provides a lightweight system that can be compactly stowed prior to deployment on orbit. The mesh surface material is a critical component in the deployable reflector antenna design. The mesh is required to provide the desired electrical performance as well as the mechanical properties that are necessary to deploy and maintain the reflector surface on orbit.

Of particular interest in multi-channel communications applications is the generation of Passive InterModulation (PIM) products at the reflector surface that can result in interference in the receive band. Wire mesh has been specifically identified by some as having a high potential for PIM generation based solely on the existence of nonpermanent metal to metal contacts at the junctions that are inherent in the mesh design. There are a number of other factors, however, that reduce the likelihood of PIM occurring at the mesh reflector surface. Experimental data presented in this paper demonstrate that mesh PIM generation is not significant for typical applications.

This paper describes PIM and reflectivity performance of wire mesh composed of gold plated molybdenum wire in a tricot knit. This type of mesh has been successfully used for the deployable Single Access Antennas of the Tracking and Data Relay Satellite System.
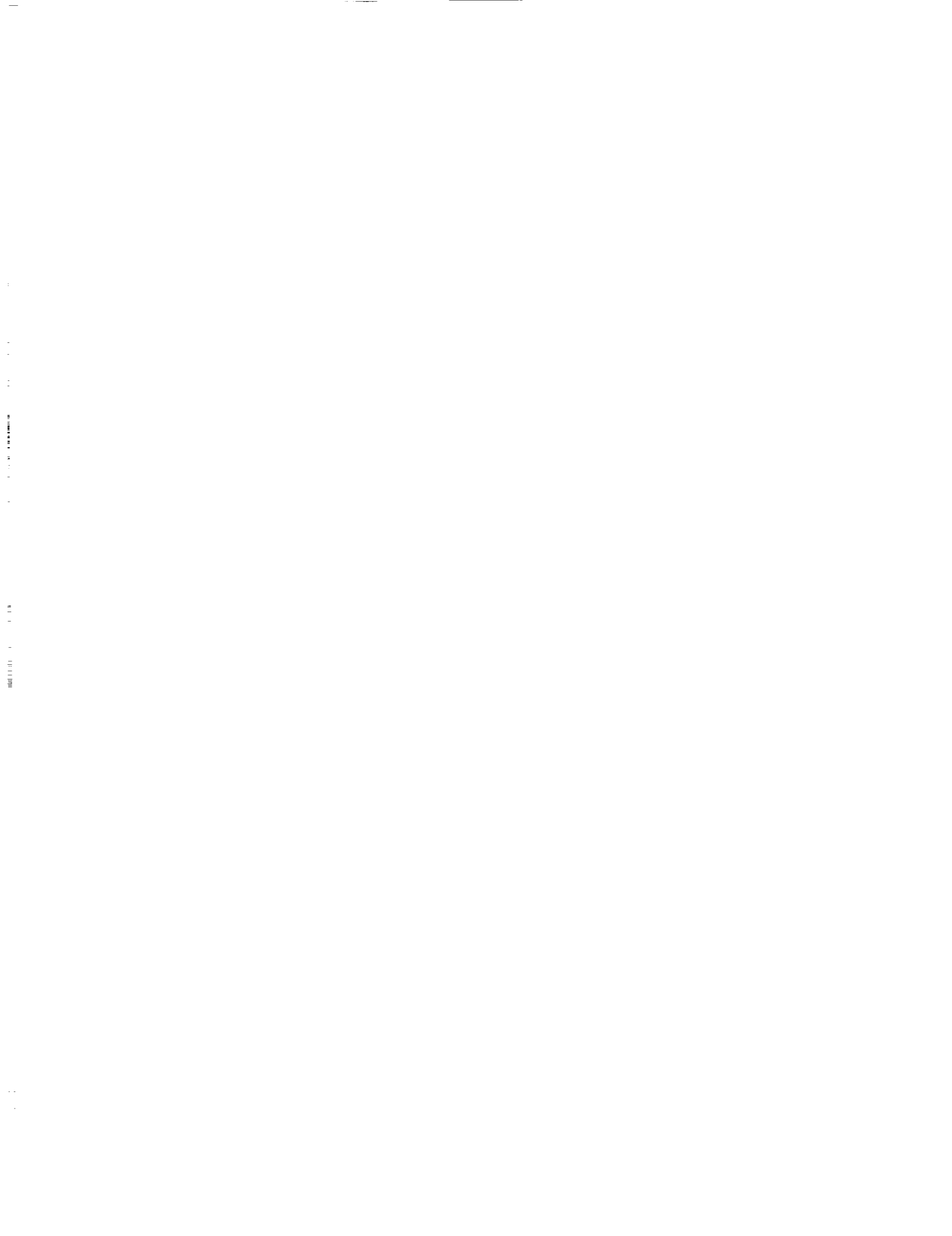
Adaptive Array Antenna for Satellite Cellular and Direct Broadcast Communications*

Charles R. Horton and Kenneth Abend
GORCA SYSTEMS INCORPORATED (GSI)
P.O.Box 2325
Cherry Hill, New Jersey
08034-0181 U.S.A.
Phone: 609-272-8200
Fax: 609-273-8288
email: knabend@gorca.com

ABSTRACT

Adaptive phased-array antennas provide cost-effective implementation of large, light weight apertures with high directivity and precise beamshape control. Adaptive self-calibration allows for relaxation of all mechanical tolerances across the aperture and electrical component tolerances, providing high performance with a low-cost, light-weight array, even in the presence of large physical distortions. Beam-shape is programmable and adaptable to changes in technical and operational requirements. Adaptive digital beam-forming eliminates uplink contention by allowing a single electronically steerable antenna to service a large number of receivers with beams which adaptively focus on one source while eliminating interference from others. A large, adaptively calibrated and fully programmable aperture can also provide precise beam shape control for power-efficient direct broadcast from space.

This paper describes advanced adaptive digital beamforming technologies for: (1) electronic compensation of aperture distortion, (2) multiple receiver adaptive space-time processing, and (3) downlink beam-shape control. Cost considerations for space-based array applications are also discussed.

SATELLITE ANTENNA DESIGN

High density RF communications traffic requires satellite antennas with high gain, precise beam pointing, and electronic speed and steering agility. If this is to be supplied with a large phased array antenna, problems of size, weight, cost, and performance arise. As uplink traffic becomes more intense or diverse, the need for multiple receivers and adaptive interference suppression adds to the cost.

Conventional approaches to maintaining antenna gain, suppressing interference, and controlling beam shape are dependent upon maintaining very stringent tolerances across the aperture. Even if rigidity and precise control is provided during manufacture, once the satellite is deployed it will be subject to (1) distortion of the structure after repositioning, (2) thermal distortion across the array, and (3) potential revised beam requirements due to changing business plans. The risk is of reduced operational performance due to gain degradation, increased sidelobe interference for uplink signals, and high sidelobe energy spillover for downlink traffic and for direct broadcast.

As an alternative to using sophisticated structural components and/or auxiliary subsystems to measure and correct for deformations and other sources of error, a class of self-calibrating adaptive digital beamforming techniques has been developed by GSI. These procedures compensate for aggregate errors without regard to their source: structural deformations, mutual coupling, solid state module phase errors, RF delay errors, and propagation anomalies. These procedures complement adaptive interference cancellation approaches. The cost savings due to reduced reliance on tight electrical and mechanical tolerances is greater than the cost of the digital

---

beamforming needed for multiple beam formation and adaptive interference suppression. The gain control achievable for direct broadcast saves prime power. The procedures may permit the antenna structure to be non-rigid and deformable resulting in a major weight reduction and consequently a reduced launch cost with improved performance. Advantages and benefits of adaptive processing are listed below.

TABLE 1. ADAPTIVE ARRAY ADVANTAGES
Antenna Array
• 30% to 40% reduction in mass
• complex RF components replaced by solid state electronics with firmware algorithms
• 100:1 easing of mechanical tolerances
• adaptive response provides immediate recovery from mechanical, electrical and RF disturbances
• design approach takes advantages of technology advancements in MMIC, VLSI, etc.
• low cost assembly and test due to relaxed mechanical requirements, ability to correct for errors, etc.
Satellite
• 10:1 reduction in system pointing requirement and "fine" attitude control, due to adaptive calibration of antenna and beam steering capability
• up to 50% reduction in satellite mass, some of which can be applied to increased on-orbit life
• significant reduction in solar array and battery power, due to more effective use of RF power
• conventional attitude control components could be replaced by attitude and position sensing using the array electronics
• self-calibrating features provide immunity to thermal or other mechanical distortions
• immunity to contentious uplinks due to antenna nulling
• low cost integration and test, and accelerated schedules
• significant reduction in cost of launch services
Communications Applications
• lower uplink RF power, or higher G/T margin, due to more precise beamshaping
• higher effective downlink EIRP due to precise spot beams
• software beamforming allows operational flexibility to meet changing requirements, traffic diversity, business plans, etc.
• very large number of users accommodated
• digital beam steering and software beam shaping provides instantaneous response to changing requirements
• very large aperture systems can be developed which could otherwise not be built

ADAPTIVE DIGITAL BEAMFORMING

We consider a phased array antenna consisting of transmit/receive modules with a receiver and A/D converter behind each. By sampling the aperture we obtain complete software control over transmit and receive beam formation. This includes the ability to (a) adaptively determine sets of weights that compensate for mechanical, electrical, and environmental errors, (b) adaptively home in on a transmitted signal while simultaneously suppressing contending signals, (c) digitally form multiple simultaneous receive beams, and (d) design and revise the transmitter footprint for broadcast operation.

Digital beamforming weights an array so as to (1) sense a desired signal and (2) attenuate interference. The received signal at each array element is assumed to have been heterodyned, filtered, sampled, and digitized so that $e_n(t)$ is a complex number representing the in-phase and quadrature components of the wavefront at the nth array element at time t. The beamforming concept is illustrated in Figure 1.

A beam is formed in the digital processor as a linear combination,

$$y = \sum_{n=1}^{N} w_n^* e_n = \mathbf{w}^h \mathbf{e} , \quad (1)$$

where $\mathbf{w}^h = (w_1^*, w_2^*, ..., w_N^*)$ is a vector of complex weights to be applied to the components, $e_1, e_2, ..., e_N$, of the received data vector, $\mathbf{e}$. The weights are obtained as the conjugate transpose (h) of the optimum weight vector,

$$\mathbf{w} = \alpha \mathbf{R}^{-1} \mathbf{s} , \quad (2)$$

where s is a low-sidelobe "steering vector" that would be used if interference were spatially homogeneous ($\mathbf{R} = \sigma^2 \mathbf{I}$) such as thermal noise. The directionality of the interference is accounted for in the NxN correlation matrix, $\mathbf{R}$, whose ij^{th} element is the correlation between the interference wavefront at elements i and j,

$$\mathbf{R} = E\{ \mathbf{e} \, \mathbf{e}^h \}.$$

Note that many beams may be formed simultaneously by choosing a different steering vector for each.

48

FIGURE 1. BEAMFORMING

Figure text:

$y(\theta)$ is the complex signal output

Σ

Digital Beamformer

w_1^*
w_2^*
w_3^*
w_N^*

Adaptive Weight Estimation

e_N
e_3
e_2
e_1

$w(\theta) = \alpha R^{-1} s(\theta)$

e_1 e_2 e_3 e_N Antenna Modules

steering direction of array

θ

array normal

communications terminal

Earth

$y = \Sigma \, w_n^* \, e_n$

where

e_n is the complex signal received by the nth antenna element

W_n is a complex weight developed by the signal processor

R is the spatial covariance matrix

$s = s(\theta)$ = low sidelobe array steering vector

Beamforming is said to be *adaptive* if the weight vector is computed on the basis of received signals (as opposed to being specified a priori). We note that there are two parts to adaptive beamforming. One relates to using received signal data to estimate the steering vector, **s**. The other relates to using received interference data to estimate R^{-1}.

Estimating **s** is called self calibration, self cohering, or adaptive focusing. Estimating R^{-1} is called adaptive nulling or interference cancellation. GSI is in the forefront of both aspects of adaptive beamforming. We will discuss the self-calibration aspect first.

ELECTRONIC COMPENSATION FOR APERTURE DISTORTION

Table 2 summarizes a number of adaptive self calibration algorithms that were developed

for radar applications. They involve the use of a variety of phase synchronizing sources to furnish the calibration pilot signal and they have been successfully applied to the calibration of real apertures, synthetic apertures, and inverse synthetic apertures. When used to establish a phase reference across a synthetic aperture they are equivalent

TABLE 2. SELF-COHERING TECHNIQUES

Dominant Scatterer
- Minimum Variance Algorithm - Steinberg (U of P)
- Multiple Scatterer Algorithm (MSA) - Attia (GSI)
- MSA with Subarray Processing - Attia/Kang (GSI/UofP)
- Phase Gradient Autofocus Algorithm - Jakowitz (Sandia)

Spatial Correlation
- Spatial Correlation Algorithm (SCA) - Attia (GSI)
- Multiple Lag SCA - Subbaram (GSI)
- Shear Averaging - Feinup (ERIM)
- Iterative SCA - Attia (GSI)

Phase History Reconstruction
- Image Plane Differential Phase Smoothing - Kupiec (MITLL)
- Aperture Plane Differential Phase Smoothing - Stockburger

Energy Constraint Method - Tsao/Subbaram (GSI)

49

to motion compensation or auto-focus techniques for SAR or ISAR imaging.

The key concept is that signals from the earth are received by individual array elements and combined in order to establish a phase reference that compensates for all errors. Correction for mechanical shape distortion is illustrated in Figure 2.

The simplest algorithms use the wave-front at the aperture from a strong signal as a phase synchronizing source for all array elements. Other algorithms use multiple sources, estimate parameters of an aperture distortion model, or adapt in an iterative manner. The spatial correlation algorithm correlates the signals received at adjacent array elements and introduces a time shift determined by the time of the correlation peak as well as a phase correction. This allows for correction of large distortions without ambiguity.

SPACE-TIME PROCESSING

Since the aperture samples the wavefront in both space and time, the signals can be simultaneously processed in both domains to separate signals according to angle of arrival and spectral content. In Figure 1, Equation (1) is applied in the spatial domain to implement a process called beamforming. In general, Equations (1) and (2) refer to to linear space-time processing. The temporal counterpart of beamforming is filtering and the temporal counterpart of self calibration is channel equalization. In the special case where $w=s=E\{e|signal\}$, the spatial weights represent a matched field steering vector and the temporal weights represent a white-noise matched filter for the signal.

With reference to Equation (1) and Figure 1, the formation of multiple beams to service multiple ground stations while eliminating uplink contention is relatively straight forward. The N dimensional data vector, e, is processed in an on-board digital processor to produce a set of K linear combinations of N complex numbers: y_1, y_2, ..., y_K. Each output
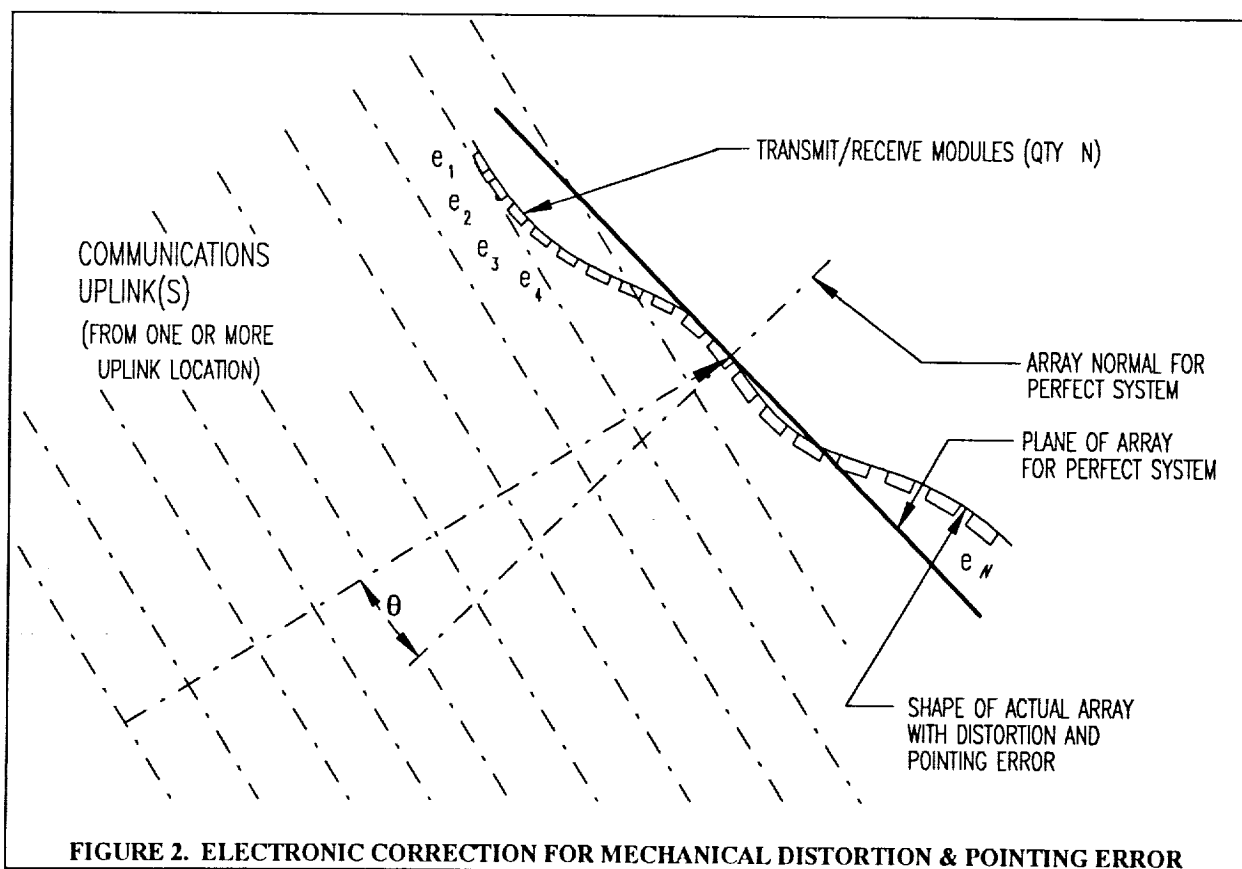
FIGURE 2. ELECTRONIC CORRECTION FOR MECHANICAL DISTORTION & POINTING ERROR

represents the signal received from one ground station. If θ_d represents the location of a particular ground station, then y_d is formed using Equation (1) with $w=w(\theta_d)$. In applying Equation (2) to obtain this weight vector, each component of the steering vector is given the same phase as the phase of that same component of a data vector, $e(\theta_d)$, that would be received from that station. The NxN correlation matrix could even be pre-computed as a diagonally loaded version of the rank K-1 matrix whose mn^{th} component is

$$\sum_{\substack{k=1 \\ k \ne d}}^{K} e_m(\theta_k) e_n^*(\theta_k).$$

The resulting y_d supplies a receiver with one signal while nulling all other signals.

DOWNLINK BEAMSHAPE CONTROL

For a properly calibrated array, the aperture illumination function, $f(x,y)$, and the azimuth-elevation far-field pattern, $F(u,v)$, are related by a two dimensional Fourier transform. The larger the aperture, the finer the control on where power is directed. At an altitude of h, the diffraction limited resolution (or pixel diameter) on the ground is at least $h\lambda/D$, where λ is the rf wavelength and D is the aperture diameter.

The desired intensity distribution $|F(u,v)|^2$, is specified as 1 for values of $u=\sin\theta$ and $v=\cos\phi$ corresponding to the location of cities that must be reached in a direct broadcast application. A criterion can be devised such as minimizing the average power outside of a given region. We specify F as 0 for values of (u,v) outside of the coverage region and as 1 for the location of target cities, and we find the least squares solution of the set of equations for f.[1] If the set of equations

---

[1]Acually, if only the power density $|F|^2$ is specified, then only the the spatial autocorrelation function of the aperture illumination is constrained.
$$<f(x+a,y+b)f^*(x,y)> = R(a,b)$$
where R and $|F|^2$ are a Fourier transform pair.

is underdetermined, the minimum norm solution for f is the desirable one because the norm of f represents the required transmitter power. Thus, if the array is well formed or properly calibrated, open-loop beamshaping by computer is relatively straight forward.

As described earlier, the problem of calibrating a large *receiver* array, using signals transmitted from the ground, has a reasonably precise solution. Data is collected at each element and processed so that the signals add coherently. The crucial question is whether it is possible to use the receive calibration corrections to correct errors in the transmitted wavefront.

This problem turns out to be more difficult. The signals transmitted from all array elements must be synchronized so that they add coherently in the target region. If errors exist in the transmitter chain, a closed loop procedure is required. Transmitter time or phase synchronization requires the return of a transponding signal from the target on the earth so that the two way propagation can be measured. While phased array receiver calibration is relatively well established [1,2], retrodirective transmitter calibration is a relatively new technology. However, GSI personnel have established feasibility in a ground based demonstration [3]. While further development is still needed, the potential payoff for adaptive transmitter self calibration is enormous.

COST CONSIDERATIONS

Many advanced array systems have been proposed and studied for space applications and less advanced array systems have been developed and built. Space-based applications include both remote sensing and communications, but the degree to which array technology has been actually deployed has been limited due to cost considerations.

The cost drivers include cost of electronics, due to the large number of array element modules; structural cost of arrays and space-

craft, to meet launch loads and minimize thermally-induced distortion or pointing error when on-orbit; the high cost of integration and test, for both payload and satellite; and launch cost, driven by the increased mass of the array structure and the spacecraft which are needed to meet system performance objectives.

The cost of electronics is being addressed via MMIC technology advancements, efficient signal processing electronics, design innovations and manufacturing efficiencies achievable with a large number of array modules. However, the other cost drivers have not been sufficiently addressed to make many advanced array concepts economically viable. As an example, a typical application of array technology to achieve power efficient satellite communications [to achieve very small spot beams which can be dynamically moved to match communications traffic requirements] results in a very large, complex satellite which also results in high launch costs.

The design concepts presented herein address these other cost drivers. The array structure can be built using very low cost, low mass designs since stiffness and distortion requirements are minimal. The allowable satellite and array pointing errors can be greatly relaxed, further simplifying other satellite subsystems and satellite operations, and significantly reducing over-all on-orbit mass. The costs of integration and test are minimized since alignment and component precision issues largely disappear. Finally, the launch costs are greatly reduced due to the large reduction in lift-off mass. A typical communications satellite constellation could be deployed with a net savings of tens of millions of dollars.

SUMMARY AND CONCLUSIONS

The performance obtainable by space-based array systems for communications and other applications is well known; however, the implementation of array technologies into operational systems has been limited due to the high cost of arrays, satellites and launch services. The adaptive array design approach described herein applies advanced signal processing technology originally developed for radar systems to next generation communications satellites. All of the advantages of array systems, for communications or remote sensing applications, are retained while making it possible to develop and deploy operational systems at affordable cost.

REFERENCES
[1] Steinberg, *Microwave Imaging with Large Antenna Arrays.* New York: Wiley, 1983.
[2] B.D. Steinberg and H. Subbaram, *Microwave Imaging Techniques.* New York: Wiley, 1991.
[3] E.H. Attia and K. Abend, "An Experimental Demonstration of a Distributed Array Radar," *IEEE AP-S International Symposium Digest,* pp. 1720-1723, London, Ontario, June 1991.

GORCA Systems, Inc. [GSI], an aerospace engineering company based in Cherry Hill, NJ, has made innovative contributions to the aerospace industry in the fields of commercial space, government, civil, and DoD space systems, advanced signal processing and remote sensing systems technologies and applications. GSI has also developed several spin-off technologies for commercial products. Phone:609-273-8200.

Dr. Kenneth Abend is Director of GSI's Advanced Signal Processing Laboratory. He is an expert on adaptive space-time processing and coherent imaging with distorted apertures. He has thirty five years experience in research, development, and analysis of advanced digital systems and techniques as applied to radar, sonar, communications, and pattern recognition.

Charles R. Horton, President of GSI, has a diverse background which includes technical and management contributions to NASA, DoD and commercial space systems and specialized components [both space and ground segments]. His background also includes development of advanced consumer electronics products.

SAW Based Systems for Mobile Communications Satellites

R.C. Peach, N. Miller and M. Lee
COM DEV Ltd.
155 Sheldon Drive
Cambridge, Ontario
N1R 7H6
(519) 622-2300
(519) 622-1691

ABSTRACT

Modern mobile communications satellites, such as INMARSAT 3, EMS and ARTEMIS, use advanced on-board processing to make efficient use of the available L-band spectrum. In all of these cases, high performance surface acoustic wave (SAW) devices are used. SAW filters can provide high selectivity (100-200 kHz transition widths), combined with flat amplitude and linear phase characteristics; their simple construction and radiation hardness also makes them especially suitable for space applications.

This paper gives an overview of the architectures used in the above systems, describing the technologies employed, and the use of bandwidth switchable SAW filtering (BSSF). The tradeoffs to be considered when specifying a SAW based system are analyzed, using both theoretical and experimental data. Empirical rules for estimating SAW filter performance are given. Achievable performance is illustrated using data from the INMARSAT 3 engineering model (EM) processors.

1.0 INTRODUCTION

All L-band mobile communication systems must operate within 34 MHz spectrum allocations (1525-1559 MHz forward link, 1626.5-1660.5 MHz return link), and must be able to service low gain mobile terminals. To cope with these limitations, systems such as INMARSAT 3, EMS and ARTEMIS use multiple spot beams, frequency re-use, and flexible frequency allocation between beams.

These systems require complex on-board processors, which use combinations of splitters, amplifiers, SAW filters and switch matrices to route traffic to the appropriate beams. Of these processors, which are currently under development at COM DEV, INMARSAT is by far the most sophisticated, though ARTEMIS has the most selective filters. The INMARSAT system also makes limited use of a technique called bandwidth switchable SAW filtering

(BSSF), or seamless combining, which allows a significant recovery of guard band spectrum [1] [2]. The principle of this method is to use banks of contiguous filters with the special property that adjacent filters, when operated simultaneously, add to form a continuous response without distortion in the crossover (guard band) region. Therefore, when a group of adjacent filters are allocated to a single beam, the entire band covered by the filters is usable, without any loss to intermediate guard bands.

An overview of SAW based processor architectures is given in section 2.0 of this paper, and the tradeoffs associated with the SAW filters are discussed in Section 3.0.

2.0 SYSTEM ARCHITECTURES

Figure 1 shows a simplified schematic of the INMARSAT 3 forward processor, proposed by Matra Marconi Space (MMS) and built by COM DEV, while Figure 2 shows an exploded view of its physical realization. The return processor is essentially similar, except for the reversal of the signal paths, and the addition of programmable gain in the individual filter channels.

The key parameters for the INMARSAT 3 processor are:

- Channel bandwidths from 4.5 to 0.45 MHz
- 20 dB Noise Figure
- Intermodulation products <-45 dBc
- 35 dB Nominal gain
- 40 dB of programmable gain
- Maximum mass 35 Kg (total of forward and return processors)
- Maximum power consumption 100 W (total of forward and return processors)
- High spectral efficiency (200 kHz guard bands, BSSF)

Dual redundant right and left circularly polarized (RHCP and LHCP) L-band input signals are split between a total of 15 filter modules, where they are down converted to a 160 MHz IF. Each filter module contains SAW filterbanks to channelize the spectrum, followed by GaAs FET switch matrices which allow any filter output to be routed to any one of eight output beams. The signals are upconverted to the final L-band frequency before leaving the filter modules, and are then combined in the eight output modules (one per beam). The mechanical arrangement is forced by the signal splitting and combining requirements. The input, output and LO distribution modules are housed in the horizontal stack, and interface with the filter modules in the vertical stack by blind mate connectors; this allows full connectivity between any input or output module and any filter module. Telecommand and telemetry is handled by the control module, which is placed on top of the vertical (filter) modules; control signals are routed to the horizontal modules via an additional housing on the side of the processor. To minimize mass, all module housings are machined from magnesium.

The input modules are among the simplest in the system. They contain redundant thin film GaAs input amplifiers and eight way power dividers implemented with cascaded Wilkinson splitters on high dielectric soft substrates. The output modules perform an inverse function, but are considerably more complex. In addition to combiners and amplifiers, they contain programmable gain blocks implemented with GaAs FET switches and controlled by an ASIC; interdigital bandpass filters are used to remove mixer spurious.

The filter modules, shown schematically in Figure 3, are the key elements in the system, as these provide all the frequency selectivity and signal routing. Three main types of filter module are employed, which differ in the frequency and bandwidth of their SAW filters, though a guard bandwidth of 200 kHz is used throughout. Each non-redundant module has a specific LO frequency that determines its position in the 34 MHz frequency band. Redundant modules can use any LO frequency, and can therefore substitute for any module of similar type. The implementation of the INMARSAT frequency plan with only three module types is another example of the use of BSSF. Because of the contiguous combining, a given filter bank can realize several channelization schemes, allowing greater standardization of module types, and hence greater reliability.

For reasons discussed in Section 3.0, the SAW Filters must operate at a relatively low IF; 160 MHz was chosen as a compromise between minimizing operating frequency and minimizing fractional bandwidth. After down conversion, the IF signals are amplified by discrete bipolar amplifiers optimized for low power consumption. The signals are then applied to the inputs of the two SAW filterbanks, each of which may contain up to three channels. Each filterbank output is them amplified by discrete amplifiers and fed into a 3x9 switch matrix, which allows any channel to be switched to any beam, or to be terminated if not in use. The switch matrix uses surface mount construction, and is built from custom hybridized units each containing three single pole double throw (SPDT) GaAs FET switches and a three way resistive power combiner. Isolation between channels is typically 60 dB. An ASIC controls the switch matrix operation. After routing through the switch matrix, each of the eight outputs is upconverted to L-Band. The up conversion frequency is offset from the down conversion frequency to minimize spurious signals.

The LO frequencies are generated externally to the processor and are distributed by the LO module. This uses combinations of power splitters and GaAs FET switches to route the LO signals to the appropriate filter modules. However, the distribution requirements are extremely complex, and the LO module is correspondingly complex.

The EMS system is far simpler in concept than INMARSAT, though similar technologies are used. It is being built by COM DEV and AME Space for Alenia Spazio as a supplementary payload for ITALSAT 2. The schematic of the EMS forward processor is shown in Figure 4. A Ku band uplink is employed, rather than the C-band uplink used for INMARSAT. Three 4 MHz wide slots are selected and down converted to an IF of approximately 145 MHz, where they are channelized by a non-contiguous bank of SAW filters with 250 kHz transition widths. The outputs are then upconverted to the L-band channels 1530-1534 MHz, 1540-1544 MHz and 1555-1559 MHz, using different LOs for each filter.

The EMS return processor replaces each 4 MHz filter with a bank of four 900 kHz filters, each with independent programmable gain. Selective use of these subchannels allows coordination with other systems using the same frequency bands. The return filters have centre frequency separations of 1 MHz and transition widths of 200 kHz; BSSF is not employed. This frequency plan produces overlap between filters, and hence a reduction in the usable filter bandwidth when adjacent filters are operated simultaneously. The ARTEMIS system is very similar to EMS, but the return

filter transition width is reduced to 100 kHz to avoid overlap. No attempt is made to recover these remaining 100 kHz guard bands using BSSF, but his would be a logical extension for future systems.

3.0 SAW FILTER TECHNOLOGY FOR ON-BOARD PROCESSING

SAW filters are particularly well suited to the high selectivity, linear phase requirements in on-board processing. However their characteristics are very different from those of classical filters, and this often causes confusion when systems are specified. This section discusses the tradeoffs and limitations associated with this class of SAW filter, based on both theoretical and empirical data.

Reference [1] discusses the basic properties of SAW filters for mobile communication systems, including BSSF. The SAW transversal filters used in INMARSAT, EMS and ARTEMIS, all use in-line transducer structures [1]. The transducers contain numerous interdigitated electrodes (typically 3000 to 9000), formed by photolithography in a thin (1000-2000A) aluminium film deposited on the polished surface of a piezoelectric crystal; ST-X quartz is used for these systems on account of its temperature stability. Each transducer has an ideal frequency response similar to that of a finite impulse response (FIR) digital filter; the electrodes serve as the taps, and their weights are controlled by varying the overlaps (apodization). The SAW propagation time between electrodes is equivalent to the sampling time.

The transfer functions of SAW transversal (or FIR) filters have no poles in the finite s plane, only zeros. They are usually also of very high order compared to classical filters (10000 electrodes in a transducer is not uncommon). Design techniques are therefore quite different, and are usually based on optimization techniques. Of these, linear programming [1] offers unrivalled flexibility. Current programs based on linear programming can design both filters and filterbanks with arbitrarily specified amplitude and phase responses. The most common requirement is for linear phase, flat amplitude characteristics, both for the individual and the combined filter responses.

For SAW filters, impulse response length is the most appropriate measure of filter complexity. For a linear phase design, a simple empirical rule can be used to predict the impulse response length [3].

$$\log (\delta_p \delta_s) = -1.05 - 1.45 \text{ BT} \qquad (1)$$

where B = transition bandwidth from passband to stopband edge.

T = impulse response length

$20\log((1+\delta_p)/(1-\delta_p))$ = Passband ripple (dB)

$20\log(\delta_s)$ = Stopband level (dB)

In the great majority of designs T is 2-3 times the reciprocal of B. It should also be noted that T is determined by the transition width, and is virtually independent of absolute bandwidth; it is also independent of centre frequency. The physical size of the filter can be obtained by multiplying T by the SAW velocity. However, the final size is significantly greater than this estimate for two reasons: first, the response must be factored between the two transducers in a non-optimal way, and second, a reasonable separation must be allowed between transducers to avoid electromagnetic coupling.

The choice of factorization is forced by practical considerations. For an in-line transducer structure the allowable weighting pattern on one transducer is restricted so that each electrode covers either all or none of the aperture (withdrawal weighting). Without this, the overall response would not, even to first order, be the product of the individual transducer responses, and this defeats all existing synthesis procedures. Empirically, it is well established that individual transducers rarely provide more than 35 dB of close-in rejection. To achieve higher rejections than this both transducers must contribute significantly to the out of band response. The withdrawal weighted transducer is therefore chosen to have reasonable out of band rejection and a reasonably regular passband response. The apodized transducer can then be designed to satisfy the overall specification. The design is then optimized to correct for second order effects, such as SAW diffraction and circuit loading, but corrections are applied to the apodized transducer alone, the other transducer is left fixed; this procedure is most effective if the length of the withdrawal weighted transducer is minimized. These design constraints are incompatible with fully optimal factorization, and some length penalty must be accepted. In addition, the requirements of BSSF and of correcting for second order effects also produce a length penalty.

For INMARSAT 3 the specified transition bandwidth is 200 kHz for all filters. However, a design value of 170 kHz was used, allowing 10 kHz margin for temperature drift and ± 10 kHz for manufacturing tolerances. With design passband ripples and stopband

levels of 0.2 dB and 50 dB respectively, equation (1) predicts an impulse response length of 13.70µs, equivalent to 4.34 cm for quartz (SAW velocity 3159 m/s). The actual length is approximately 7.1 cm, including 0.9 cm spacing between transducers. The net effect of all the above constraints is therefore to increase the total transducer length by about 40% from the estimate given by equation (1).

A 100 kHz transition width is specified for the ARTEMIS return filters, and a 75 kHz value has been used in the design. Combined with a 0.25 dB passband ripple and a 50 dB stopband level, equation (1) gives a predicted impulse duration of 30.3µs (9.56 cm on quartz). The length of the final design is 12.6 cm including 1 cm transducer separation. The net transducer length is therefore 21% greater than the ideal limit. This difference between the ARTEMIS and INMARSAT filters reflects the absence of BSSF constraints, and the use of a more sophisticated factorization procedure for the ARTEMIS designs. A reasonable practical estimate of overall filter length can therefore be obtained by taking the value of T from equation (1), increasing this by 30%, multiplying by the SAW velocity, and adding the transducer separation (0.5-1.0 cm) and an allowance for packaging (0.5-1 cm).

Manufacturing sensitivity is a critical factor in determining the minimum transition bandwidth and maximum operating frequency of a SAW filter. Photolithographic capabilities will allow operation at 1 GHz and above, but the achievable filter performance is severely degraded, and high selectivity, high precision filters are restricted to comparatively low frequencies. The major limiting factors are:

* Metallization uniformity
* Electrode linewidth control
* Photomask aberrations
* Substrate uniformity
* Substrate mounting stresses

All of these produce similar effects, which may be modelled as a variation in SAW propagation velocity. If such velocity errors are random, and average out over a short distance scale, they are comparatively harmless. However, the above effects usually produce troublesome long range variations.

For a given effective velocity error, the filter distortion is directly proportional to centre frequency. If the peak to peak velocity variations are similar for different filter lengths, then the distortion is also inversely proportional to the transition bandwidth. In addition, the velocity

perturbation caused by the metallisation increases in proportion to frequency. Unfortunately, there is no precise model available for assessing all tradeoffs; however, the following empirical formulas give a reasonable estimate of the achievable P-P passband ripples for an individual high selectivity quartz filter:

$$\text{P-P amplitude ripple=Design ripple} + 15tF^2/B \text{ dB} \quad (2)$$

$$\text{P-P phase ripple=Design ripple} + 250tF^2/B \text{ deg} \quad (3)$$

where t = metallization thickness (m) (typically 1e-7 to 2e-7 m)
F = centre frequency (MHz)
B = transition bandwidth (MHz)

The centre frequency should therefore be kept as low as possible, compatible with the fractional bandwidth constraints for the material; for filters with transition widths less than 200 kHz, 200 MHz is a reasonable upper limit.

So far, the effect of shape factor (ratio of bandwidth at stopband edges to bandwidth at passband edges) has not been considered; it does not directly affect device size but it does have a slight effect on passband ripple and out of band rejection. A low shape factor (very square response) is more difficult to realize with a withdrawal weighted transducer, and the overall filter rejection is reduced as a result. For shape factors of 1.2 or greater, close in rejections of 50 dB and far out rejections of 60 dB are achievable. For shape factors of 1.1, these values are reduced to 45 dB and 50 dB respectively. Achievable rejection is also weakly dependent on centre frequency.

4.0 EXPERIMENTAL SYSTEM PERFORMANCE

Figure 6 shows the combined response of two L-band channels measured on the INMARSAT EM forward processor shown in Figure 5. The individual filters have bandwidths of 0.75 MHz and 2.11 MHz, and together with a 0.54 MHz device form a contiguous set of three filters; including the guard band they give a total bandwidth of 3.06 MHz. Figure 7 shows the response of the 2.11 MHz filter combined with its other neighbouring filter to give a net bandwidth of 2.85 MHz. This demonstrates that BSSF can provide characteristics that are virtually indistinguishable from those of individual filters. In the above measurements the unused channels were switched to other outputs (beams); the absence of any residual responses

demonstrates the low levels of leakage in the SAW package, the switch matrix, and the splitter driving the output mixers.

Figures 8 and 9 show the combined in-band amplitude and phase responses of the three filters. The overall amplitude ripple is approximately 0.5 dB P-P. Although not observable in this case, some crossover distortion usually arises, and the ripple in the crossovers is often a few tenths of a dB worse than in other regions. The phase ripple clearly shows the transitions between the individual filters. This ripple could be improved by further alignment; but this is not justified as the phase requirements are comparatively non-critical. The filters are all made in matched sets and little change is observed in passband characteristics over the operating temperature range (-15 to 75°C).

5.0 CONCLUSIONS

The development of the INMARSAT and EMS systems has clearly demonstrated the feasibility of using SAW based on-board processors for spectrum allocation and routing. It has also provided a great deal of valuable information about the tradeoffs associated with the various technologies, particularly the SAW filters.

The greatest technical challenges have not been associated with individual components, but rather with the integration of so many technologies into a complete system. Other difficulties have only become fully evident during system level testing. Particularly notable in this regard is the control of spurious signals. The large number of signals and LOs going into the processors, and the large number of leakage paths and non-linear components, make spurious generation a major problem; work is still in progress to isolate and suppress unwanted signals.

ACKNOWLEDGEMENTS

The authors would like to acknowledge the invaluable contributions of P. Kenyon, R. Kovac, B. Van Osch and A. Veenstra to this work.

6.0 REFERENCES

[1] R. Peach & A. Malarky, "Enhanced Efficiency using Bandwidth switchable SAW Filtering for Mobile Satellite Communications Systems", *Proc. IMSC*, pp394-402, 1990.

[2] O. Andreassen, "A SAW Filter Bank for Telecommunications applications", *Microwave and RF Engineering*, pp43-48, Jan/Feb 1990.

[3] D.P. Morgan, "Surface-Wave Devices for Signal Processing", *Amsterdam: Elsevier*, 1985.
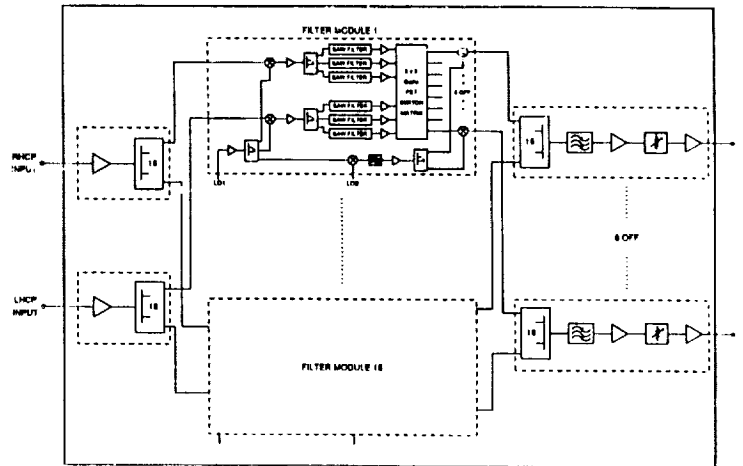
Figure 1. Simplified schematic of INMARSAT 3 forward processor
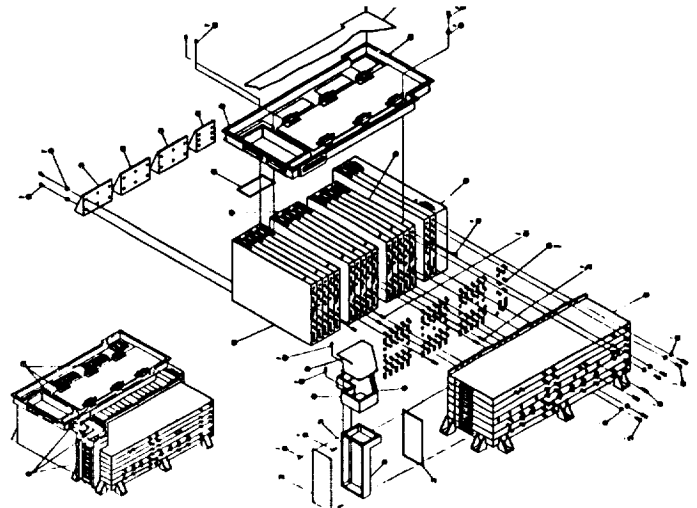
Figure 2. INMARSAT 3 forward processor construction
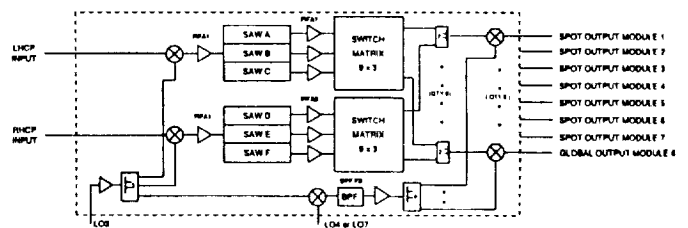
Figure 3. Simplified schematic of INMARSAT filter module
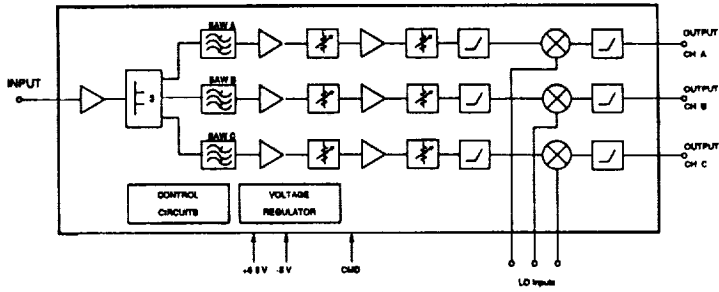
Figure 4: Schematic of EMS filter module

Figure 5. INMARSAT 3 EM forward processor

Figure 6. Combined frequency response of channels D and E
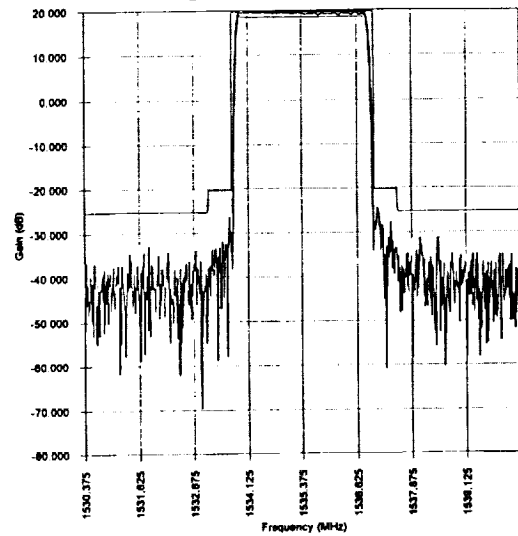
Figure 7. Combined frequency response of channels E and F

Figure 8. Combined amplitude response of channels D, E and F
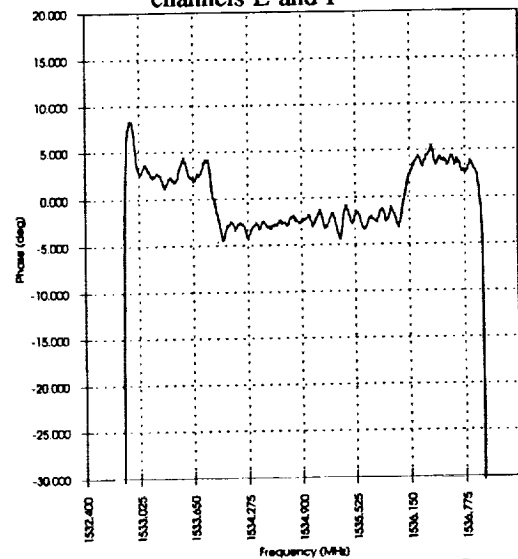
Figure 9. Combined phase response of channels D, E and F

Broadband Linearisation of High-Efficiency Power Amplifiers

Peter B. Kenington, Kieran J. Parsons and David W. Bennett
Centre for Communications Research
University of Bristol, Bristol, BS8 1TR, UK.
Tel: +44 272 303255
Fax: +44 272 255265

Abstract

A feedforward-based amplifier linearisation technique is presented which is capable of yielding significant improvements in both linearity and power efficiency over conventional amplifier classes (e.g. class-A or class-AB). Theoretical and practical results are presented showing that class-C stages may be used for both the main and error amplifiers yielding practical efficiencies well in excess of 30%, with theoretical efficiencies of much greater than 40% being possible. The levels of linearity which may be achieved with such a system are well in excess of those which are required for most satellite systems, however if greater linearity is required, the technique may be used in addition to conventional pre-distortion techniques.

Introduction

Recent advances in solid state power amplifier design have led to smaller and more efficient designs appearing on the market. Such systems have made use of improved semiconductor technology and marginal improvements in classical design techniques in order to yield adequate linearity at the highest possible efficiency.

Efficiency is the key factor in all of these systems, no matter what frequency band they are required to operate in. A relatively modest improvement in efficiency can lead to significant weight savings in the spacecraft and these savings multiply due to a form of 'positive feedback': Any efficiency improvement leads directly to a reduction in the power supply requirements for the amplifier and also to a reduction in the size and amount of heat-sinking required. These in turn mean that a smaller area of solar panels is required and a smaller and hence lighter support structure is necessary. It also leads to a significant reduction in the required size of the back-up batteries and hence their charging circuitry. All of these factors lead to a reduction in the overall spacecraft size and weight and hence to a significant reduction in launch costs.

The fundamental problem with the techniques used at present is that the linearity requirement leads to a compromise in the maximum efficiency obtainable, and further improvements in semiconductor technology will only yield marginal improvements in efficiency.

Broadband Linearisation

This paper describes a technique for linearising a highly non-linear, and hence efficient, amplifier over a broad bandwidth. Potential efficiencies in the range 40-60% are possible using this technique with IMD performance of between 30 and 50dB (or more). It can be used in conjunction with simple linearisation schemes currently in operation, such as 3rd-order predistortion, but will provide a reduction of all orders of distortion if required. The technique is based on an adaptive form of feedforward which overcomes the classical disadvantages of this technique, in terms of its inability to monitor and correct its own performance. Significant simulation work has been
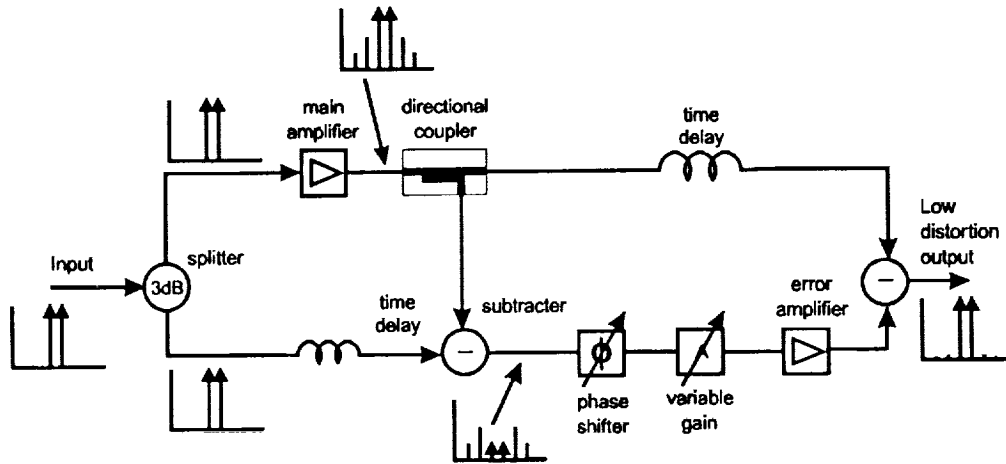
Figure 1: Simplified block diagram of a feedforward amplifier system.

performed on the system, yielding a detailed understanding of its operation, and demonstration systems have been built at VHF and UHF/SHF.

The system is based on the feedforward approach to amplifier linearisation shown in Figure 1 above. A two-tone test is shown for the purposes of illustration, however, any number of signals can be amplified simultaneously, with the only limitation being imposed by the overall peak envelope power (PEP) rating of the main amplifier.

The operation of a feedforward system may be summarised as follows (with reference to Figure 1). The input signal is split to form a main signal path (top) and a reference path (bottom). The signals in the main path are amplified by the main amplifier and a small portion of the output signal coupled off and subtracted from the reference path. The resulting signal contains predominantly the distortion information of the main amplifier and hence constitutes an error signal. This error signal is appropriately weighted in gain and phase and then amplified to the required level before being fed in anti-phase to the output coupler where it cancels the

distortion from the main amplifier. The resulting signal is therefore a linearly amplified version of the input signal; the bulk of the distortion from the main amplifier having been removed by the feedforward process.

Efficiency of a Feedforward Amplifier

The theoretical efficiency of a feedforward amplifier has been derived in the reference [1], and hence will not be reproduced here. However, the result of that derivation will be used in order to demonstrate the optimal coupling factors and peak theoretical efficiencies obtainable from a feedforward system. An extension to the derivation has also been performed and this incorporates the effects of loss in the delay element in the main (top) signal path, since this element can have a major effect on the efficiency obtainable from the system. Full details of this extension will be given in the literature [2] and only the results will be presented here.
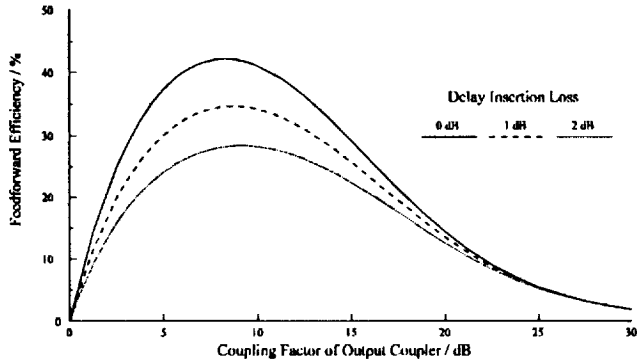
Figure 2: Feedforward efficiency characteristic using class-C main and error amplifiers and incorporating the effects of main path delay insertion loss.

Figure 2 shows the theoretical efficiencies which can be obtained from a feedforward system comprising of class-C main and error amplifiers and a main path delay element with varying degrees of loss. The class-C amplifiers are both assumed to have a DC to RF conversion efficiency of 60%. It can be seen that at an output coupling factor of a little under 10dB, the peak efficiency for a perfect system (no delay loss) is around 42%. As the delay loss increases, this efficiency is degraded until it reaches approximately 27% for a delay loss of 2dB. Note that the loss in the error coupler will be negligible due to its high value (30dB typically), and that the loss in the output coupler is already included in the derivation.

The variation of efficiency of the feedforward amplifier with the insertion loss of the delay element is shown in Figure 3, for values of insertion loss up to 3dB. This again demonstrates the marked effect of this loss on the overall efficiency of a feedforward system.

It is important therefore to attempt to minimise the delay loss in the feedforward system in order to maximise its efficiency and approach the 42% ideal. This can be achieved in a number of ways. If the delay is formed utilising coaxial cable, which may be the case at low frequencies, then the use of low-loss cables will obviously be of benefit. Alternatively, the delay may be etched onto a low-loss, high dielectric constant substrate. This also has the advantage of minimising the size of the delay element.

At higher frequencies the delay may be achieved in waveguide, although this may be bulky.

A much better approach would be to reduce the value of the delay element, and hence its loss, or eliminate it altogether.

Elimination of the main path delay in a feedforward system

A further derivation has been performed to assess the effects, both in terms of efficiency and overall distortion cancellation, of the reduction or removal of the main path delay element. This derivation will
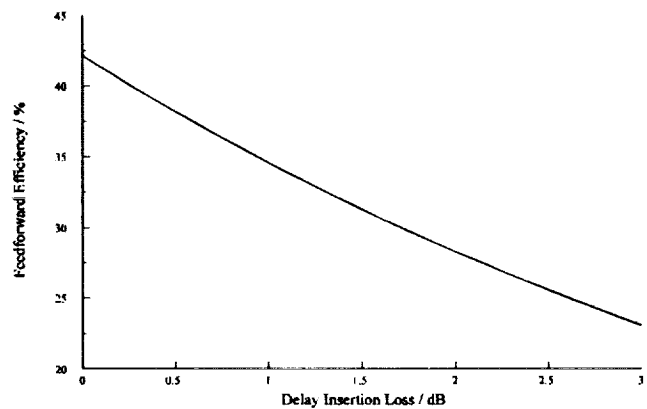
Figure 3: Maximum feedforward efficiency using class-C main and error amplifiers with main path delay insertion loss. This figure assumes that the optimum value of output coupling factor is being used.

be published in the literature [3] and so, again, only the significant results will be presented here.

Reduction (in value and hence size) of the delay element will result in a reduction in its insertion loss and also in an (unwanted) reduction in the level of distortion cancellation which can be achieved. However, if this reduction in cancellation is acceptable, i.e. it still allows the required specification to be met, then the reduction in loss can

61
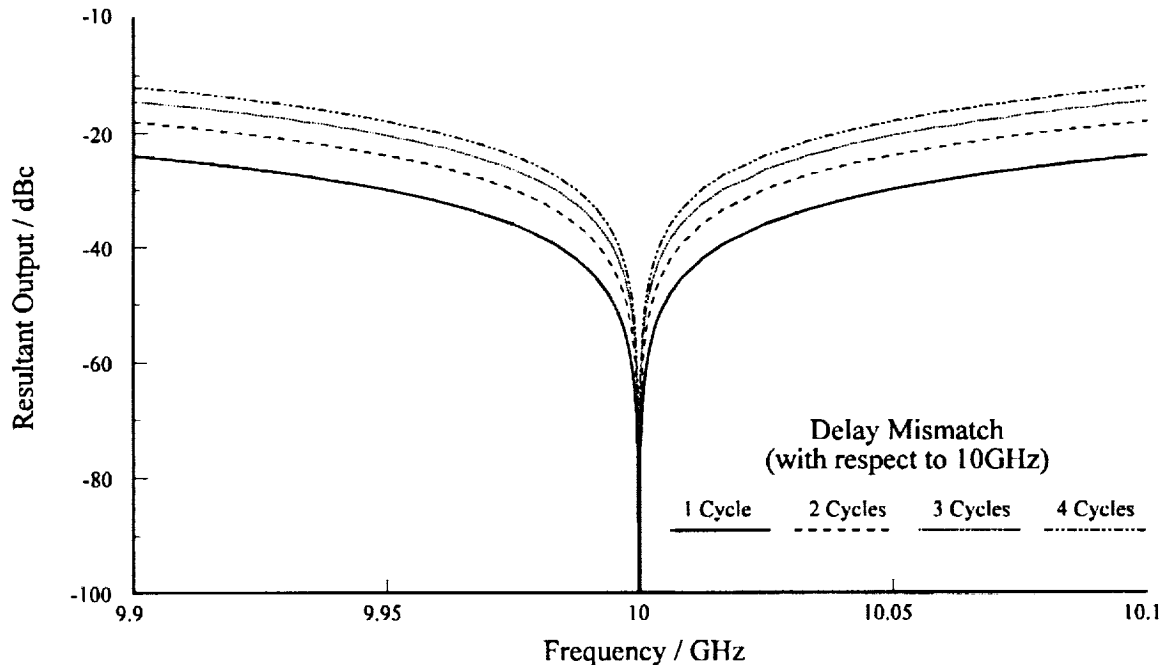
Figure 4: Distortion suppression which can be achieved across a 200MHz bandwidth at 10GHz with one cycle of delay mismatch.

be exploited as an improvement in overall efficiency of the linearised amplifier.

The level of cancellation which can be achieved across a 200MHz span at 10GHz is shown in Figure 4. Since the system is assumed to be set up on the centre frequency, perfect cancellation is achieved at this frequency. However, greater than 20dB of cancellation is achieved across the whole 200MHz span.

This translates in practice to a third-order intermodulation level of less than 35dB with respect to the tones in a two-tone test, when considering a class-C main amplifier with an intermodulation level of -15dB before compensation.

Decreasing the delay further, to a total of three cycles, will still yield a performance level equating to that of a good class-A amplifier (-30dB IMD products), for the above scenario. This amount of delay reduction should at least halve the loss in the delay element, if not completely eliminating it altogether.

Practical Results

A 'proof of concept' system has been built to verify the above theoretical results. A mid-VHF frequency band was chosen due to the relative ease of

fabricating class-C amplifiers at this frequency and the ready availability of couplers etc. at a reasonable cost. The results, in terms of percentage bandwidths etc., are scaleable to any frequency, although efficiencies will generally decrease above a few GHz and losses in couplers and delay lines will increase. The theoretical characteristics can be modified by inserting the required practical values (for a particular frequency band) in the empirical relationships derived in references [2] and [3].

The open-loop (uncompensated) response of the class-C main amplifier is shown in Figure 5. The spacing of the two tones is 50kHz and the third-order IMP is around 15dB below the level of the tones. Figure 6 shows the response of the complete feedforward system, utilising the main amplifier whose response is shown in Figure 5. Five cycles of delay mismatch are present in the main path of this system and this is

Centre Freq: 221 MHz   Span: 2 MHz

Res. B/W: 1 kHz   Video B/W: 1 kHz   Sweep: 6 s
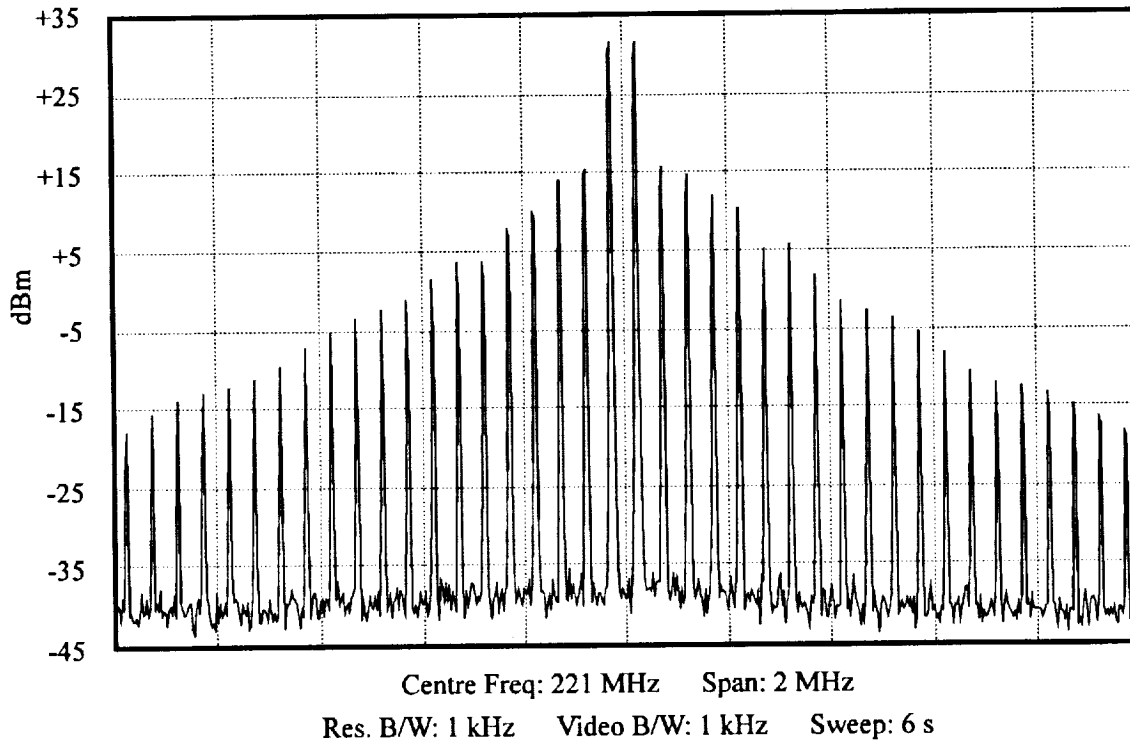
Figure 5: Open loop (uncompensated) spectrum of the VHF class-C main amplifier.

achieved by completely removing the main path delay, and hence completely eliminating its loss.

It can be seen that the linearity performance of this complete system is still very good and comparable with that of a good class-A amplifier. The largest third-order IMP is now almost 32dB down on the tones, an improvement of over 16dB.

The efficiency of this complete, practical system is around 33%, an improvement over the 27% efficiency which is achievable with the correct main path delay value.

Incorporation of Pre-distortion

The main amplifier in a feedforward system can incorporate RF or IF pre-distortion in order to initially improve its linearity, before further improvement by use of the feedforward system.

The use of pre-distortion will generally only eliminate low-order distortion and this is unacceptable in some circumstances. The use of feedforward will, in general, eliminate all orders of distortion by the same amount and hence can be used to improve upon the performance of a purely pre-distorted system.

The use of pre-distortion in conjunction with feedforward also benefits the feedforward technique as it allows significantly higher efficiencies to be achieved. It is also possible to use class-A error amplifiers, to obtain an improved distortion performance, without significantly affecting overall efficiency, since the power required from such amplifiers is now small. Overall efficiencies of up to 60% are achievable using this technique (in conjunction with class-C amplifiers) and pave the way for true high-efficiency satellite amplification.
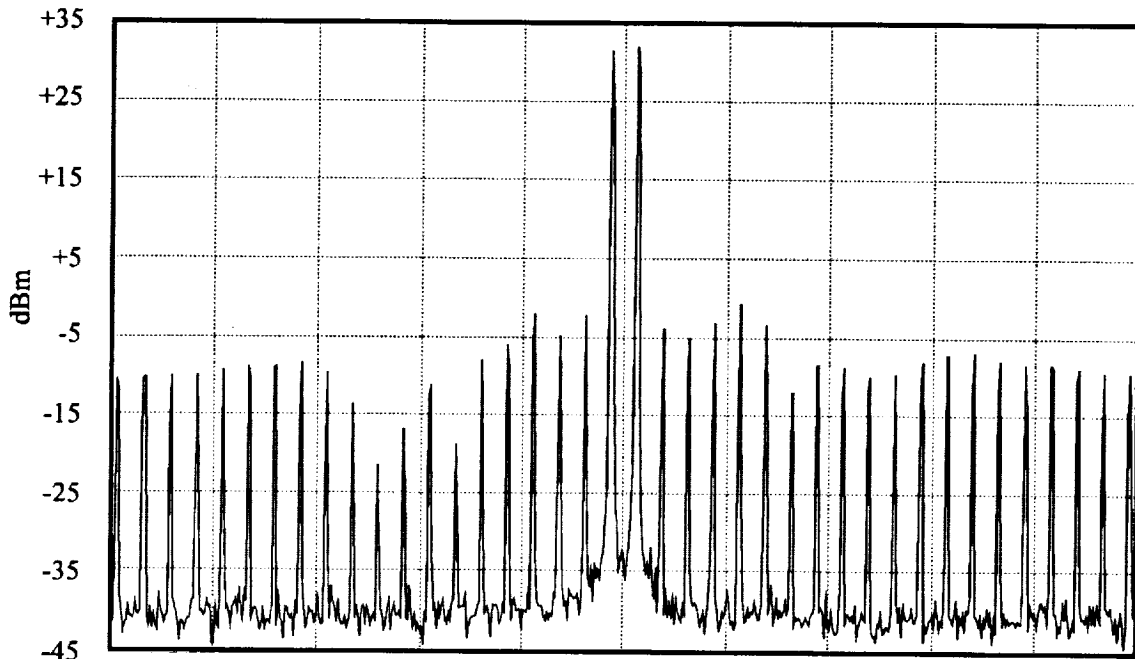
Centre Freq: 221 MHz   Span: 2 MHz
Res. B/W: 1 kHz   Video B/W: 1 kHz   Sweep: 6 s

Figure 6: Linearised output from the VHF class-C feedforward system.

Conclusions

This paper has suggested the use of the feedforward amplifier linearisation technique for use in fabricating highly-efficient satellite amplifiers. Theoretical efficiencies in excess of 40% are possible purely by the use of feedforward, with efficiencies approaching 60% being possible with a combination of adaptive pre-distortion and feedforward.

The problems of loss in the main path delay have been highlighted and potential solutions suggested which yield practical efficiencies significantly better than those possible with current techniques.

Finally, the complete removal of the main path delay has been highlighted as a method of improving efficiency in some circumstances.

Acknowledgements

References

[1] P.B. Kenington, "Efficiency of feedforward amplifiers", IEE Proceedings-G, Vol. 139, pp. 591-593, October 1992.

[2] K.J. Parsons and P.B. Kenington, "Efficiency of a feedforward amplifier with delay loss", submitted for publication to IEE proceedings.

[3] K.J. Parsons and P.B. Kenington, "The effect of delay mismatch on a feedforward amplifier", submitted for publication to IEE proceedings.

Session 3
Regulatory and Policy Issues

Session Chair—To Be Announced
Session Organizer—*Robert Bowen,* Communications Research Centre, Canada

U.S. Domestic and International Regulatory Issues

Lon C. Levin, Dennis C. Nash
American Mobile Satellite Corporation
1150 Connecticut Avenue, N.W., 4th Floor
Washington, D.C. 20036 U.S.A.
Phone: 202-331-5858
FAX: 202-331-5861

ABSTRACT

This paper will review the U.S. domestic and international regulatory and policy milestones since 1982, when NASA filed its petition with the Federal Communications Commission (FCC) to establish the U.S. domestic Mobile Satellite Service (MSS).

In 1985, the FCC proposed to establish MSS services and allocate spectrum for such service. In 1986, the FCC allocated L-band spectrum for MSS. In 1987, at the Mobile World Administrative Radio Conference (MOB WARC-87), despite U.S., Canadian, and Mexican efforts, the WARC did not adopt a multi-service, generic MSS allocation. In 1989, the FCC licensed the first MSS system. After two decisions by the U.S. Court of Appeals, the FCC's licensing actions remain intact.

The FCC also has permitted Comsat to provide international aeronautical and land MSS via the Inmarsat system. Inmarsat, however, may not serve the domestic U.S. market.

In 1991, the FCC accepted applications for MSS systems, most of which were non-geostationary proposals, for operation in the Radiodetermination Satellite Service (RDSS) bands, and the VHF and UHF bands. In 1992, the FCC proposed rules for non-geostationary MSS systems and applied a negotiated rulemaking procedure to each.

Also in 1992, the U.S. position for flexibility in existing MSS bands and for additional worldwide MSS allocations was adopted in large part at the 1992 World Administrative Radio Conference (WARC-92).

INTRODUCTION

There is increasing demand for versatile and ubiquitous mobile communication services. MSS is expected to help satisfy these communication needs in the future. MSS is designed to compliment existing terrestrial services by extending service coverage areas via satellite, thereby providing nationwide mobile service. The first of these systems is the AMSC system, which received its license in May 1989. AMSC's first satellite is scheduled to be launched in 1994. The FCC is currently in the process of developing the regulatory structure for other mobile satellite systems, particularly those that propose to use a non-geostationary platform.

This paper will first present an overview of the U.S. regulatory process. It will then provide a discussion of the licensing and allocation proceedings that led to the licensing of AMSC in 1989. It will review the U.S. policy limiting Inmarsat to international MSS services only with regard to North America. MSS activity at the International Telecommunication Union (ITU) will also be reviewed. Finally, other domestic MSS related proceedings will be discussed.

OVERVIEW OF THE U.S. REGULATORY PROCESS

Domestic Process

The FCC is responsible for the allocation of spectrum to the private sector, as well as for the licensing of private entities seeking to use the allocated spectrum.

Generally, the spectrum allocation process is initiated with the filing of a Petition for Rulemaking by an entity seeking to have spectrum allocated for a new service. The FCC places the petition on public notice, thereby triggering a comment period within which the public may provide its views on the proposal. If there is sufficient support for the petition, the FCC will then issue a Notice of Proposed Rulemaking (NPRM), which presents the desired allocation as well as provides tentative ideas on the technical and operational parameters for the use of that spectrum. The NPRM invites public comment on the proposal. After assessing the comments, the FCC issues an order establishing a specific allocation. The FCC order is subject to petitions for reconsideration, to which the FCC must respond. The FCC's decisions are ultimately subject to review by the U.S. Court of Appeals.

The next process involves the licensing of users of the newly allocated spectrum, and the formulation of rules within which the licensees must operate. The FCC follows a path similar to an allocation proceeding, first releasing an NPRM, soliciting comments, and finally issuing an order.

Before actual rules are established, the FCC may invite applications for the provision of the new service. This enables the FCC and the public to review concrete proposals for the use of the spectrum. Petitions to deny and comments are filed on the individual applications. Once all of the relevant information is gathered, the FCC issues its order.

An FCC order typically establishes financial, technical, and operational standards, in addition to strict construction and implementation milestones for the provision of the new service. The order is subject to petitions for reconsideration and review by the U.S. Court of Appeals.

A recent development in administrative procedure is the negotiated rulemaking. Under this procedure, the FCC requests interested parties, including applicants, to meet under the auspices of the FCC in order to develop mutually acceptable proposals for technical and operational rules that will be used as a basis for the FCC's rules. The underlying theory of this process is that the applicants, as well as other interested parties, can negotiate to establish the rules that are in their best interest.

International Process

ITU decisions have considerable impact on the domestic regulatory process. In particular, the allocations established at a WARC provide the underlying parameters under which a domestic allocation may be made. Typically, the FCC will allocate spectrum consistent with a particular WARC allocation, which are incorporated in the ITU's Radio Regulations. The FCC also takes note of technical and operational standards recommended by the ITU.

THE AMSC PROCEEDING

In 1982, NASA filed a petition for rulemaking to establish a MSS system by allocating spectrum to MSS and selecting one

or more licensees. In 1985, in response to the NASA Petition, the FCC issued an NPRM proposing to use UHF and L-band frequencies for mobile links and proposing a regulatory structure for the new service. The FCC also invited applications.

Twelve applications were filed in response to the NPRM. In 1986, the FCC allocated 28 MHz of the L-band for use by MSS systems for all mobile satellite services. The MOB WARC-87, however, did not adopt U.S. proposals to make the L-band more flexible but, instead, left standing the existing service-specific allocations.

In 1987, the FCC issued rules and regulations regarding the regulatory structure within which the MSS industry would develop. Given the limited amount of spectrum available, the FCC determined that only one licensee would be viable. The FCC, therefore, ordered all qualified applicants to form a single consortium. It also required that each applicant put $5 million in escrow for use by the consortium. In response to the FCC's order, eight of the twelve applicants formed a consortium in 1988.

In 1989, the FCC issued a license to the consortium and reaffirmed its allocation and regulatory structure orders. Of particular note, the FCC found that its generic allocation was consistent with the service specific allocations of the ITU; because the AMSC system is required to provide aeronautical safety services on a priority and preemptive basis within the allocated bands, the FCC held that AMSC's operations would be consistent with the ITU's Radio Regulations requiring aeronautical safety services (AMS(R)S) to operate on a primary basis in the bands.

AMSC Proceedings After 1989 License Decision

In 1991, the U.S. Court of Appeals upheld the FCC's MSS allocation rulings, finding that the FCC acted in a rational manner in determining that a generic MSS system that provides AMS(R)S on a priority and preemptive access basis is consistent with the international Radio Regulations. The Court, however, reversed the FCC's award of an MSS license to a mandatory consortium.

The Court stated that in order for the FCC to impose a mandatory consortium, it had to first find authority in the Communications Act enabling it to avoid a comparative hearing among mutually exclusive applicants. If such authority existed, then the FCC must articulate compelling circumstances that would justify selecting competing applicants by means other than through a comparative hearing.

In response to the Court's 1991 decision, in 1992, the FCC reaffirmed AMSC's status as the MSS licensee. In so doing, the FCC found that the necessary statutory authority exists under its rulemaking powers to establish a mandatory consortium and that the need to have a licensee participate in the ongoing international spectrum coordination process provided compelling circumstances sufficient to justify a mandatory consortium. The FCC's decision was challenged again in the Court of Appeals, but the Court, in 1993, dismissed the challengers for lack of standing, thereby leaving the FCC's decision intact.

THE AMSC LICENSE

AMSC is authorized to construct, launch, and operate the U.S. domestic mobile satellite system consisting of three satellites using L-

band frequencies for mobile links and Ku-band frequencies for feeder links. The orbital locations assigned to AMSC are 101° W.L. for the central satellite, 62° W.L. for the eastern satellite, and 139° W.L. for the western satellite.

The FCC allocated 28 MHz of L-band spectrum in the bands 1545-1559 MHz and 1646.5-1660.5 MHz for use by the U.S. mobile satellite service system. The FCC concluded that the efficiencies inherent in a single system would assure that aviation safety services would be made available soon. Accordingly, the FCC authorized AMSC to be both the MSS and AMS(R)S licensee.

Rather than adopt a rigid spectrum segmentation plan, the FCC devised an allocation structure that permits all mobile satellite services to be provided across 27 MHz of the allocation, while assuring that AMS(R)S traffic can enjoy additional protection relative to other services. Due to sharing constraints with Radio Astronomy, the remaining 1 MHz is limited to aviation safety and certain one-way services.

The FCC allocated 200 MHz of Ku-band for feeder link use to each of the three satellites. The central satellite at 101° W.L. was allocated 200 MHz of the 11/13 GHz band. The satellites located at 62° W.L. and 139° W.L. were allocated 200 MHz of the 12/14 GHz band.

AMSC will provide space segment on a common carrier basis, providing access to carriers and end users. AMSC's ground segment will be authorized separately. Earth stations accessing the system will be licensed separately. Typically, mobile units will be authorized under blanket licenses.

Services And Coverage Areas

AMSC is licensed to provide the full range of land, maritime, and aeronautical services, including two-way voice, dispatch, and mobile data. Fixed and transportable services may be provided where few alternatives exist. AMSC is authorized to provide service to the U.S. domestic market including all 50 states, Puerto Rico, the Virgin Islands, and U.S. coastal areas up to 200 miles offshore.

In recognition of the need for the AMSC and Telesat Mobile, Inc. (TMI) systems to be capable of mutual back-up and restoration, the FCC authorized AMSC to construct its satellites to cover Canada. AMSC may also construct its satellites to cover Mexico. Authority to operate in Canada and Mexico, as well as the Caribbean, must be obtained by separate application.

Aeronautical Matters

By its authorization, AMSC is required to accord priority and real-time preemptive access to AMS(R)S communications throughout the entire assigned bandwidth. AMSC also must develop arrangements for "hand-off" of aeronautical traffic to other MSS systems, such as the Canadian and Inmarsat systems.

The FCC expects that aeronautical mobile terminals will have certain unique characteristics to meet aviation safety operational requirements. Aeronautical mobile terminals must be type accepted and licensed under the FCC's rules governing aviation communications. The FCC expects the Federal Aviation Administration (FAA), which is the U.S. entity responsible for aviation safety, to be involved in the development of standards and practices in order to assure that aviation safety

70

satellite services will be of the highest integrity.

MSS EXPANSION BAND RULEMAKING

In 1990, the FCC adopted a NPRM, proposing to reallocate the bands 1530-1544 MHz and 1626.5-1645.5 MHz for domestic generic MSS. These bands are currently allocated domestically to maritime MSS. The FCC proposed that maritime safety services be afforded real-time preemptive priority in the MSS expansion band. AMSC's application seeking permanent authority to operate on these bands for domestic service has been held in abeyance pending completion of the rulemaking.

INTERIM SERVICE

In 1992, the FCC decided that AMSC may provide interim MSS via Inmarsat facilities. The FCC authorized AMSC to operate up to 30,000 mobile terminals. AMSC currently uses the Marisat satellite to provide data service. The FCC stated that others may use the Inmarsat system on an interim basis to provide U.S. domestic service on the condition that those services transition to the AMSC satellite system shortly after its deployment.

USE OF INMARSAT IN THE UNITED STATES

In 1989, the FCC established policies for the provision of international aeronautical services in the U.S. via the Inmarsat system. The FCC determined that Comsat, the U.S. signatory to Inmarsat, will be the sole U.S. provider of Inmarsat space segment for aeronautical services. In addition, the FCC decided that aeronautical services, provided via Inmarsat to aircraft over the U.S., could be offered on a permanent basis only to aircraft in international flight. The FCC defines international flights as those between the U.S.

and foreign points, and those flying over the U.S. between two foreign points. Inmarsat may not provide domestic land mobile service in the U.S. The FCC, however, has permitted Comsat to use Inmarsat facilities to provide international land mobile service outside of North America.

WARC 92

In February 1992, WARC-92 convened in Torremolinos, Spain. Two significant developments occurred at WARC-92. First, the international service limitations imposed upon a significant portion of the existing L-band spectrum were relaxed for the United States, Canada, Mexico, Australia, Brazil, Malaysia, and Argentina. Second, over 100 MHz of additional spectrum between 1-3 GHz were allocated to mobile satellite service for future use on a Region 2 (North and South American) as well as a global basis. To date, this new spectrum has not been allocated to MSS by the FCC, although portions of it are the subject of a number of proceedings.

OTHER SATELLITE-BASED MOBILE SERVICES

In 1986, the Geostar Corporation and two other applicants were authorized to construct, launch, and operate dedicated RDSS systems. Geostar also obtained authority to provide interim RDSS until its dedicated satellites became fully operational. In 1991, however, the Geostar venture ceased operations.

The FCC has licensed other satellite-based mobile communications service providers. In February 1989, Qualcomm, Inc. received authority to operate mobile terminals to provide messaging and tracking services using existing fixed satellite Ku-band space segment.

Soon after WARC-92, the FCC initiated

proceedings to implement additional MSS systems in spectrum allocated at WARC-92. A negotiated rulemaking process has been imposed on each proceeding. The FCC has concluded the allocation process for the data only low earth orbit (LEO) systems, permitting operation in the VHF and UHF bands, and is currently in the midst of the final portion of the licensing process for these "Little LEOs".

For MSS systems proposing operations in frequencies in the RDSS bands, the FCC completed the negotiated rulemaking phase in the first quarter of 1993 and is currently considering allocation and licensing proposals.

The FCC is considering MSS allocations in the 2 GHz bands as well as proposals to share portions of the 1675-1710 band with meteorological satellite operations.

International Organizations to Enable World-wide Mobile Satellite Services

Richard L. Anglin, Jr.
Anglin & Giaccherini
Attorneys at Law
8601 Falmouth Avenue, Suite 309
Playa del Rey, California 90293-8694
+1 310 306 5986
+1 310 306 7959 Fax

ABSTRACT

Numbers of systems exist or have been proposed to provide world-wide mobile satellite services ("MSS"). Developers of these systems have formulated institutional structures they consider most appropriate for profitable delivery of these services. MSS systems provide niche services and complement traditional telecommunications networks; they are not integrated into world-wide networks. To be successful, MSS system operators must be able to provide an integrated suite of services to support the increasing globalization, interconnectivity and mobility of business.

The critical issue to enabling "universal roaming" is securing authority to provide MSS in all of the nations of the world. Such authority must be secured in the context of evolving trends in international telecommunications, and must specifically address issues of standardization, regulation and organization. Today, only one existing organization has such world-wide authority. The question is how proponents of new MSS systems and services can gain similar authority. Securing the appropriate authorizations requires that these new organizations reflect the objectives of the nations in which services are to be delivered.

INTRODUCTION

An earlier paper addressed some of the institutional, political and cultural issues related to the provision of world-wide MSS. It postulated an international organizational form responsive to the criteria to be met to enable "universal roaming." [1] That paper argued that such an international organization must simultaneously respond to traditional business incentives, as well as respect the national sovereignty and objectives of the countries within which services are to be delivered.

The earlier paper proposed an international organization with two parallel elements. One was a traditional commercial corporation which would build, launch and operate MSS systems. The second was a parliament of delegates from each served nation whose main function was to franchise the distributors of MSS services, thereby responding to the unique needs of each country to be served. That paper, however, did not address how to evolve from the existing, proposed and as yet unannounced MSS systems to world-wide system(s) which provide truly universal service.

"Universal roaming" in the context in which it is generally used today means having a single telephone number by which a user may be reached independent of geographic location. Services implicit in this context are

narrowband voice and data. Over time, however, "universal roaming" will undoubtedly come to mean bandwidth on demand for a variety of services, both mobile-to-mobile and mobile-to-networks. Further, the user will have available a single, light weight terminal easily capable of establishing the most efficient connection for the type of service demanded, independent of carrier or MSS system.

This paper continues the earlier discussion and examines additional institutional, political and cultural issues related to the world-wide provision of MSS.

THE WORLD OF MSS TODAY

A number of MSS systems exist or are proposed to provide a variety of services; most are focused on niche markets. Likewise, system operators and proponents have adopted or espouse a variety of organizational forms for delivery of these services world-wide, and on a regional basis.

Global Systems

Inmarsat

The International Maritime Satellite Organization ("INMARSAT") is today the only operational world-wide MSS provider. It provides maritime and land mobile narrowband voice and data services via a number of satellites in geosynchronous orbit ("GEO") to terminals as small as suitcases. It is experimenting with the provision of aeronautical services, and plans to introduce handheld services in the near future.

INMARSAT is a "not for profit" consortium of member states ("parties") created by treaty. Services are provided in the member nations by designated "signatories" to the treaty, usually the nation's Post, Telephone and Telegraph ("PTT"). Revenues are shared between INMARSAT and the signatories based on each's equity

interest and revenue generated. Because of its structure, INMARSAT has "landing rights," the right to provide services, in virtually every country in the world.

Marathon

Russia has provided MSS, termed "Volna," using cross-strapped transponders on its GEO Gorizont satellites. It has established a new program called "Marathon" for the provision of commercial MSS, to include voice, telegraph, facsimile and high quality data channels.

The Marathon system will comprise now being developed Arkos satellites in GEO, three or four, and Mayak satellites, two to four, in a highly elliptical Molniya orbit.

Marathon, a commercially based inter-governmental organization, plans to make its spare capacity available on an undetermined basis to organizations outside the Commonwealth of Independent States ("CIS").

The Big LEOs

Motorola ("Iridium"), TRW ("Odyssey"), Loral/Qualcomm ("GlobalStar"), Ellipsat ("Ellipso") and Constellation Communications, Inc. ("Aries") all plan low earth orbit ("LEO") constellations to provide narrowband voice and data services to handheld user terminals world-wide. Several of these system proponents have offered equity participation in themselves to PTTs and private organizations throughout the world in return for cash investment and the right to provide services in the investor nation. They have argued that by investing in the service provider, a nation becomes a participant in the delivery of services and gains a claim to dividends from profitable operation of the system in proportion to the amount of investment and the amount of traffic generated by the investor nation. It is not clear, however, that any of these proponents have

secured landing rights in most nations of the world, much less world-wide.

The Little LEOs

Orbcomm, StarSys and VITA have proposed LEO constellations to provide data and messaging services world-wide. Several of these organizations have successfully negotiated contracts with in-country local entities to provide services in numbers of nations. As with the Big LEOs, world-wide landing rights have not been secured. In this case the world-wide MSS operator is acting as a wholesaler of capacity to traditional national service providers.

National and Regional MSS Systems

AMSC and TMI

American Mobile Satellite Corporation ("AMSC") in the United States and Telesat Mobile, Inc. ("TMI") in Canada have jointly designed regional MSS systems for North America. AMSC and TMI are both investor owned private companies that plan to offer narrowband voice and data services directly to users with fixed and mobile terminals.

Other Systems

Several proposals and systems other than those identified here have been advanced for national and regional MSS systems, including Australia's Optus and Mexico's L-band payload on Solidaridad. For the most part the system proponents are established national and regional telecommunications service providers seeking to expand their franchises through the provision of MSS. While sometimes proposing dedicated organizations to provide MSS, they are based on existing national and regional institutional relationships with their concomitant operating authority.

INTERNATIONAL TRENDS IN TELECOMMUNICATIONS

While MSS systems present unique issues which must be addressed, they are and will continue to be influenced by evolving international trends in the delivery of telecommunications services.

Businesses rely extensively on telecommunications services to coordinate operations in increasingly disperse geographic locations. Businesses demand new, sophisticated, reliable, world-wide services; they seek global interconnectivity, interoperability, and mobility. Further, as businesses focus on their core activities, they increasingly consider ownership and control of telecommunications networks as non-strategic, and look to global carriers to provide a full complement of services and to guarantee service level, quality and price.

Technologies and services are converging to create intelligent value-added networks offering varieties of services. Bandwidth, formerly a limiting factor, is becoming a commodity.

As a consequence, competition has become globalized as established system operators look for techniques and relationships to enable them to continue to serve their existing clients' needs world-wide. Traditional operating companies are being restructured in response to deregulation. The investment required to both modernize traditional telecommunications networks and to extend their reach into newly emerging centers of economic activity is fostering innovative regional arrangements among national service providers.

Today's MSS systems, existing and proposed, provide niche services to complement traditional telecommunications networks; they are not integrated into these world-wide networks. However, excellence in a niche market alone is insufficient for long-term survival. The niche operator has no direct control over the elements determining

the overall quality and reliability of end-to-end world-wide MSS. Thus, for long-term success MSS operators must establish relationships with other telecommunications service providers to provide an integrated suite of services.

CHALLENGES TO WORLD-WIDE MSS SYSTEM OPERATORS

With the exception of INMARSAT, MSS system operators are today not organized to provide world-wide services. To reach the objective of world-wide MSS, system operators face three sets of challenges: standardization, regulation and organization.

Standardization

International standardization has been a significant catalyst in the development of world-wide telecommunications systems. Standardization has fostered market competition while helping focus research and development on enhanced services and capabilities. A lack of standards leads to inefficiency in the delivery of telecommunications services and fragmented markets, both of which impact operators' ability to finance systems.

Timing in the formulation of standards is of critical importance because of the enormous cost of research and development. Manufacturers want to take early advantage of the availability of new services to establish a market share for their products. If standards are delayed, manufacturers are often forced to adapt their early products to conform to standards which evolve later, a cost which no one wants to bear.

Global compatibility of systems enhances customer choice of equipment, services, and suppliers; fosters greater competition among manufacturers and service providers; ensures larger production runs of terminal equipment which results in lower costs from economies of scale.

Established operators such as INMARSAT have defined their markets and services, and competitive manufacturers have responded to INMARSAT's de facto standards which are global. AMSC and TMI have jointly defined standards for their regional MSS systems. The other system advocates have proposed a variety of technical approaches to the provision of their services, all with implicit standards. While these "proprietary" standards serve the interests of their proponents, they do not facilitate global interoperability or interconnectivity.

Regulation

Regulation of MSS operators must be examined in the context of the dynamic tension between the pace of technological change and the need for stability of regulatory scheme.

International MSS spectrum issues were addressed at the 1992 World Administrative Radio Conference ("WARC"). Virtually all system operators and proponents argue that inadequate spectrum has been allocated to MSS. Nonetheless, very little of the allocated spectrum is in use today, and, consequently, regulators world-wide have little actual market data against which to judge the adequacy of the allocated spectrum. Further, technological advances may diminish the perceived need for additional spectrum.

Regulation by national authorities is, perhaps, the most significant challenge to world-wide MSS providers. In most nations the telecommunications service provider is the government-owned PTT. Even when it does not hold a full monopoly, the PTT controls its nation's radio frequencies, thus also controlling its competitors' operations. This structure defines the conditions under which an operator can provide MSS in the nation.

More progressive nations are taking steps to privatize their telecommunications systems, or otherwise allow some form of domestic competition. In spite of this trend,

most governments maintain a high degree of control over telecommunications service providers and vigorously protect their national enterprises. MSS providers must regard these privatized enterprises as national entities similar to the PTT. To be authorized to provide services in a particular nation, MSS providers must make favorable arrangements with each government, its PTT and any other entities designated by the government. If they do not, they will not be allowed to provide services in that nation.

Organization

Deregulation of national telecommunications system operators inherently favors new entrants and the introduction of innovative services, first in international and then in national markets, an advantage to be exploited by would be world-wide MSS service providers.

It has been suggested that the world-wide provision of MSS is truly a new kind of business that needs a new way of doing business. Because MSS systems are literally able to reach almost everyone in the world, their operators must have authority to serve their subscribers in every country to provide "universal roaming." To be successful, the world-wide MSS system operators must overcome each country's differing politics, culture and customs to structure relationships with each country to allow provision of services there.

Traditional multinational companies reflect the goals and culture of their founders and operators. They are tied to their countries of origin. Shareholders and managers of these companies are economically incentivized, and fear loss of control. They do not necessarily successfully accommodate national needs. Consortia are more like governments; they provide an effective forum for addressing multiple and often divergent objectives and cultures, but are operationally bureaucratic and cumbersome.

The organization of existing international telecommunications service providers and operators has followed the traditional theory of manufacturing and is based on economies of scale and/or scope. These theories advocate horizontal integration of organization, that is, large organizations with world-wide operations.

However, there are costs associated with the use of market mechanisms to develop these organizations: search costs to find appropriate strategic partners; costs to formulate, negotiate and formalize the institutional structure of the organization to be created; for monitoring and supervising the delivery of services and the functioning of the new organization; for adapting the organization to new technologic and market challenges. These transaction costs are mainly arguments for vertical integration of MSS service providers. [2]

It can be argued that world-wide MSS providers should be organized to take advantage of the strengths of small organizations: agility, easier access to management, high quality services, and the ability to offer customized business applications. World-wide MSS system operators require organizations which efficiently and cost effectively deliver services, and simultaneously respond to the individual requirements of the countries in which the services are provided.

INTERNATIONAL ORGANIZATIONS TO ENABLE WORLDWIDE MOBILE SATELLITE SERVICES

The question is how to evolve organizations to provide world-wide MSS that meet the above objectives. Arguably, the issue of spectrum is resolved for the foreseeable future. In addition, issues of standardization may be resolved by default via established operators such as INMARSAT, soon to be operators such as AMSC and TMI, and the negotiated rulemakings currently being

sponsored by the Federal Communications Commission ("FCC") for both Big LEO and Little LEO proponents. Therefore, the question remaining is one of organization, including the relationship between the service provider and the various nations in which services are to be offered.

The issue is fundamentally one of economics. The U.S. Department of Commerce estimates that MSS revenues will reach $300 million by 1993. "Revenues are projected to soar by the mid-1990s with the introduction of even more sophisticated services and the launch of satellites dedicated solely to mobile communications." [3] The Department of Commerce further estimated that in 1992 there were thirteen million MSS users world-wide.

Notwithstanding the glowing projections for world-wide MSS, it is doubtful that the total market can support the existing and currently proposed systems. And, there are even more systems on the drawing board.

The question is how to efficiently select the systems and operators to provide world-wide MSS that will be successful. Free market advocates argue that the most efficient decision process is the market, and that competing system proponents should get their systems financed, secure landing rights throughout the world, build and launch systems, deliver services, and thereby demonstrate economic success.

However, economic theory demonstrates that competition works well with private goods such as manufactured products, but that a pure market economy has difficulty with public goods such as infrastructure and with goods that have external effects such as MSS.

There are numbers of approaches to addressing this question, each with its own advantages and disadvantages.

First, the charters of existing international and regional telecommunications service providers can be expanded to encompass world-wide MSS services. The most logical existing organization for this expanded world-wide charter is INMARSAT. Regionally, existing satellite system operators may wish to extend their franchises through appropriate agreements.

Second, a joint venture could be created between INMARSAT and one or more of the system proponents to provide the full spectrum of services proposed to be offered. It is reasonable to assume that all of the system proponents have approached INMARSAT about such relationships.

Third, a new treaty organization could be created specifically to provide world-wide MSS. Not likely.

Fourth, an independent international authority such as the International Telecommunications Union ("ITU") could be given the authority to determine standards for world-wide MSS. Once the standards were established, with full participation by system proponents, then all operators wishing to provide service could negotiate their best deals to gain access to as much of the world's population as possible.

REFERENCES

[1]   Richard L. Anglin, Jr., "Alternative Legal Regimes to Enable Universal Telecommunications Roaming," presented to the *International Institute of Space Law ("IISL"), International Aeronautical Federation ("IAF"), World Space Congress*, September 1, 1992, Washington, D.C.

[2]   See, Prof. Dr. Klaus Spremann, "What is the Optimal Number of Competing Telecom Companies?" *Business Guide to Switzerland*, no. 1, pp. 11-13, February/March 1993.

[3]   U.S. Department of Commerce, *1993 U.S. Industrial Outlook*, U.S. Government Printing Office, 1993.

Use of Negotiated Rulemaking in Developing Technical Rules
for Low-Earth Orbit Mobile Satellite Systems

Leslie A. Taylor
Leslie Taylor Associates
6800 Carlynn Court
Bethesda, MD 20817-4302
301 229 9341
fax 301 229 3148

ABSTRACT

Technical innovations have converged with the exploding market demand for mobile telecommunications to create the impetus for low-earth orbit (LEO) communications satellite systems. The so-called "Little LEOs" propose use of VHF and UHF spectrum to provide position - location and data messaging services. The so-called "Big LEOs" propose to utilize the RDSS bands to provide voice and data services. In the United States, several applications have been filed with the U.S. Federal Communications Commission (FCC) to construct and operate these mobile satellite systems. To enable the prompt introduction of such new technology services, the FCC is using innovative approaches to process the applications.

Traditionally, when the FCC is faced with "mutually exclusive" applications, e.g., a grant of one would preclude a grant of the others, it uses selection mechanisms such as comparative hearings or lotteries. In the case of the LEO systems, the FCC has sought to avoid these time-consuming approaches by using negotiated rulemakings. The FCC's objective is to enable the multiple applicants and other interested parties to agree on technical and service rules which will enable the grant of all

qualified applications. With regard to the VHF/UHF systems, the Advisory Committee submitted a consensus report to the FCC. The process for the systems operating in the bands above 1 GHz involved more parties and more issues but still provided the FCC useful technical information to guide the adoption of rules for the new mobile satellite service.

INTRODUCTION

Miniaturization has enabled the space industry to build smaller satellites with more efficient power. The shrinking of satellites is accompanied by a decrease in costs, both for building the satellite and launching it. This has brought about a revolution in designing communications satellite systems, and has enabled entrepreneurs to consider deploying satellite systems to deliver mobile voice and/or data communications. Nine companies have applied to the FCC for authority to construct and operate constellations of non-geostationary satellite systems to provide mobile voice, data and position-location services.

The FCC instituted a new regulatory procedure to enable these systems to be licensed and placed into service promptly. This procedure is called Negotiated Rulemaking.

BELOW 1 GHz APPLICATIONS: THE LITTLE LEOS

In February 1990, ORBCOMM, a subsidiary of Orbital Sciences Corporation, filed an application to build, launch and operate a constellation of small satellites in low earth orbit to provide low cost, position determination and messaging services to millions of consumers in the United States and abroad. It represented the first private, global satellite system designed to provide direct access to the satellite for the user. Orbcomm's 24 satellites are projected to weigh just 330 pounds, with a per satellite cost of $8.6 million. To keep costs down, Orbcomm proposed the use of UHF and VHF frequencies to enable terminals to be built with currently available radio components.

LEOs below 1 GHz

**ORBCOMM
STARSYS
VITA**

Other applications for "Little LEO" service were filed by STARSYS, Inc., an affiliate of North American CLS, Inc., Volunteers in Technical Assistance VITA), and Leosat Corporation. North American CLS provides services and equipment to North American users of the French/U.S. Argos satellite system. VITA sought authorization to use three small satellites for a packet-switched network, for its non-profit disaster and medical relief service in developing countries. Leosat proposed serving the automotive market primarily. The FCC consolidated these proposals, and their associated rulemaking petitions, for purposes of spectrum allocation,

development of technical and service rules, and application processing.

The applicants petitioned for frequencies used primarily in the United States by the Department of Defense and for various fixed and mobile services around the world. After gaining the support of the United States government, the applicants, particularly ORBCOMM, marshalled support for the new mobile satellite service from countries throughout the world, and gained the needed spectrum allocations at the 1992 World Administrative Radio Conference. The bands allocated are 137-138 MHz, 148-150.05 MHz, 400.15-401 MHz and 399.9-400.05 MHz.

ABOVE 1 GHz APPLICATIONS: THE BIG LEOS

Motorola Satellite Corp., in June, 1990, announced its plans to launch and operate a LEO satellite network to provide mobile voice communications to virtually any point on earth. The Iridium™ system is essentially a cellular network with the microwave repeating towers, consisting originally of 77 satellites, orbiting 413 nautical miles above the ground. Motorola has since reduced the number of satellites to 66.

Ellipsat Corp., a small entrepreneurial firm (Fairchild is now an investor), in November 1990, filed an FCC application to launch six small satellites into elliptical orbit, to provide voice as well as position location service. In addition to being the first U.S. commercial system to propose use of elliptical orbits, Ellipsat was the first of the LEO applicants to request the RDSS frequencies for its system.

The RDSS frequencies -- 1610-1626.5 MHz (Earth-to-space) and 2483.5-2500 MHz (space-to-Earth)-- had been allocated for position location services at the 1987 World Administrative Radio Conference on Mobile Services.

In December 1990, Motorola filed for its system with the FCC, also proposing to use the RDSS frequencies for the Iridium™ system. The FCC then established a "cut-off date," requiring comments on the Motorola and Ellipsat application, as well as any other applications proposing to use the RDSS frequencies, to be filed by June 3, 1991. Four entities filed applications on June 3, 1991: (1) including Loral Qualcomm Satellite Services (LQSS) for its 48 satellite Globalstar™ system; (2) TRW Inc. for a medium earth orbit, 12 satellite system, Odyssey^sm; (3) Constellation Communications, for a 48 satellite system, Aries; and (4) the American Mobile Satellite Corp., AMSC, for use of the 1616.5-1626.5 MHz band for its geosynchronous mobile satellite system.

LEOs above 1 GHz

Motorola
Loral Qualcomm
TRW
Constellation
Ellipsat

The United States, with the support of these entities, was able to obtain a primary allocation in the 1610-1626.5 MHz and 2483.5-2500 MHz band, and a secondary allocation in the 1613.8-1626.5 MHz (space-to-Earth) to accommodate Motorola's desire to operate bidirectionally in the upper part of the L-band.

The FCC, in August, 1992, proposed adopting the spectrum allocations in the United States. In its Notice of Proposed Rulemaking (NPRM), ET Docket No. 92-28, FCC 92-358, the Commission sought comment on numerous technical aspects regarding operation of systems in these bands and noted the need for a separate proceeding to address MSS service rules and licensing, as well as the possibility of adopting a limitation on the type of access method to be used to maximize sharing possibilities.

The NPRM highlighted the many technical issues that would have to be addressed, if not resolved, before the Commission could proceed to process the pending applications. Not the least of these was Motorola's proposed bidirectional operation, which vastly complicates, if not precludes sharing spectrum with any other communications system, including other MSS systems. Another thorny issue concerns the extent to which compatible operations could be attained by the four CDMA systems, as well as compatibility with the FDD-TDD system proposed by Motorola.

FCC PROCESSING METHODS FOR MUTUALLY EXCLUSIVE APPLICATIONS

In the case of applications for the same spectrum which are "mutually exclusive," that is, the grant of one would result in a de facto denial of the other, Section 309 of the Communications Act requires a hearing. This right was affirmed by the U.S. Supreme Court in the case of Ashbacker v. United States, 326 U.S. 327 (1945) which states that, "where two bona fide applications are mutually exclusive the grant of one without a hearing to both" is improper." Hearings for radio licenses have been used extensively, although they are expensive and time-consuming. In some cases, radio license hearings have taken up to 10 years.

Wherever possible, the FCC has sought to use various mechanisms to avoid the hearing requirement of the Communications Act. The FCC has obtained authority from the Congress to conduct lotteries and has used this mechanism, in place of hearings, to

grant licenses for such services as cellular, paging and multipoint distribution service. In the case of the domestic-fixed satellite service, the Commission has established threshold financial qualifications which have enabled it to eliminate sufficient applicants for orbital locations to avoid comparative hearings. The use of so-called threshold qualifications have been permitted by the Courts.

FCC Processing Methods

- **Comparative Hearings**
- **Lotteries**
- **Pioneer's Preference**

Most recently, the Commission has developed a "Pioneer's Preference," which it is attempting to utilize as a threshold qualification to aid in the processing of multiple applications. See, Pioneer's Preference Order, 6 FCC Rcd 3488 (1991), recon. granted in part, denied in part, 7 FCC Rcd 1808 (1992), further recon., FCC 93-116, released March 8, 1993. The Pioneer's Preference allows an applicant that demonstrates that it "has developed an innovative proposal that leads to the establishment of a service not currently provided or an enhancement of an existing service" will be placed on a pioneer's preference track, and will not be subject to competing applications. Thus, if otherwise qualified, the applicants will receive a license. Other applicants will compete for the remaining licenses on a separate track. The Commission has stated that a preference will not be granted unless there is sufficient spectrum "to permit at least one additional license to be granted for the same geographic area." Further Reconsideration, Footnote 4.

While noble in intent, the Pioneer's Preference is based on the subjective judgment of the FCC as to what is "innovative." As the financial stakes are high in numerous new communications services, such as PCS, disappointed applicants have already taken the Commission to Court. This author believes that ultimately, the use of the Pioneer's Preference will be determined inconsistent with rights of applicants to comparative consideration.

The next approach to expediting the processing of applications for new communications services is likely to be the auctioning of spectrum. The Congress, in making available spectrum currently allocated for use by the U.S. government, is expected to establish an auction mechanism for commercial use to expedite the use of the spectrum as well as to provide revenue for the federal government. There is a possibility that the Congress may also authorize the FCC to use auctions for spectrum other than that which will be made available from spectrum allocated to the government. In particular, the Congress is considering the applicability of auctions to aware licenses for the provision of Personal Communications Services (PCS).

In the meantime, the FCC is attempting to use new alternative dispute resolution mechanisms to develop technical rules for new services which will enable it to grant all qualified applications. This approach will allow the marketplace, rather than the government, to determine which systems will succeed, and which will fail.

NEGOTIATED RULEMAKING PROCEEDINGS

The FCC's authority to use a negotiating committee mechanism is contained in the Federal Advisory Committee Act (FACA), 5 U.S.C. App. 2, and the Negotiated

Rulemaking Act of 1990 (NRA), Public Law 101-648, November 28, 1990. By law, the committee consists of representatives of the parties whose interests will be significantly affected by the outcome of the rules.

The goal of the Committee is to reach consensus on the language and substance of appropriate rules. If a consensus is reached, it is used as the basis of the FCC's proposals. If a consensus is not reached, majority and minority input can still be used by the FCC in developing regulations. The Commission can use a negotiated rulemaking (NRM) process if it determines that there is a "reasonable likelihood" that the committee can be adequately staffed with interested persons able to negotiate in good faith, and that there is a reasonable possibility of consensus.

In setting up an advisory committee, the FCC can identifies specific issues it wishes addressed, suggests limits as to the number of participants, and nominates a facilitator to serve as chair of the committee. The facilitator is a neutral party, without direct interest in the rules being discussed, helps the meetings proceed and manages the record and minute keeping.

While consensus is the goal, the FCC recognizes that such will not always be possible. Accommodation is made for such an eventuality, with the FCC leaving up to the committee the definition of consensus. If necessary, majority and minority reports can be submitted. Records of the meetings are placed in the public record and meetings are open to the public.

USE OF NEGOTIATED RULEMAKING FOR LEOS BELOW 1 GHz

In October 1991, the FCC issued a Notice of Proposed Rule Making, proposing allocation of the requested UHF/VHF frequencies to the "little LEOs." In February 1992, the FCC tentatively awarded a pioneer's preference award to VITA. Leosat's application was dismissed as improperly filed.

Prior to the commencement of the NRM, Orbcomm, Starsys and VITA met and agreed on a proposed set of rules, which were submitted to the FCC. The joint comments stated that all three systems could operate compatibly in the spectrum available. In addition, rules were agreed to concerning application requirements, license qualifications and technical conditions.

With this favorable environment, the NRM was convened, consisting of the applicants, existing users of the frequencies, potential band users and adjacent band users. The parties met for approximately six weeks and issued a report on September 16, 1992, reflecting the unanimous agreement of all the parties. This report formed the basis for the Notice of Proposed Rulemaking issued by the FCC in February 1993.

By all accounts, this first FCC negotiated rulemaking procedure worked to the advantage of the applicants, the FCC and the public interest. The affected parties quickly reached agreement, expediting FCC action on the service and technical rules and enabling the Commission to move forward on the processing of the applications.

USE OF NEGOTIATED RULEMAKING FOR LEOS ABOVE 1 GHz

The "Big LEO" regulatory situation is more complex than that of the "Little LEOS." This is in part due to the number of parties (five "Big LEO" applicants plus AMSC in contrast to two commercial "Little LEO" applicants and one non-profit applicant).

In addition, in the Big LEO proceeding, Motorola has repeatedly emphasized its requirement for sole use of the spectrum it seeks (1616-1626.5 MHz on a bidirectional basis) as well as its unwillingness to revise

any aspect of its system design.

Having already tentatively concluded not to award a Pioneer's Preference to any of the Big LEO applicants, in August 1992, the FCC proposed the establishment of a negotiated rulemaking to settle the outstanding technical and operational rules for the Big LEO systems. Most importantly, the Commission was seeking a mechanism by which it could grant all of the applications and would not have to make the hard choices between the Motorola proposal to band segment, which would leave virtually unusable spectrum in the lower L-band to the other applicants, and the full band sharing approach which would require major system changes by Motorola.

The FCC identified two primary issues to be addressed by the NRM: (a) what technical rules should be adopted for the service "to maximize the sharing of the spectrum and the capacity for multiple entry;" and (b) what technical rules should be adopted in order for the service to co-exist with other services.

The NRM began its work on January 13, 1993 and concluded on April 5, 1993. The Committee consisted of the applicants, including AMSC, potential future applicant Celsat, various federal agencies such as NASA, DOD and the FAA, and representatives of the aviation industry, including ARINC and manufacturers of GLONASS and GPS receivers.

The main issues addressed by the committee, in addition to the fundamental question of sharing the available spectrum, were sharing with radioastronomy, GLONASS and other primary users of the band.

As this paper was being written, it appeared that a majority report -- supporting total band sharing -- and a minority report proposing band segmentation, is the most likely outcome. This result would place the toughest decision

back in the lap of the FCC.

Despite the inability of the negotiation to unanimously resolve the most difficult issues, consensus as to methods of sharing with radioastronomy, GLONASS and other services appears likely. These parts of the report, as well as the tremendous amount of technical material and analysis presented, constitute valuable inputs to the Commission as well as the participants. This input will ease the Commission's enormous task of resolving this complex, but extremely important proceeding.

Negotiated Rulemaking

- **less adversarial**
- **technical focus**
- **consensus input to FCC**
- **speeds process**

The participants had the opportunity to work together on complex interference and sharing issues. This experience should reduce the controversy over proposed rules that the FCC issues, provide a useful foundation for actual system coordinations, and provide a basis for revising system technical characteristics to enable the MSS systems to operate compatibly with other users of the spectrum.

CONCLUSION

The FCC has now concluded two negotiated rulemakings. Both involved the development of rules for new mobile satellite systems. While a complete consensus was not achieved in both cases, the process appears to have reduced costs, and expedited FCC rulemaking and licensing actions with resultant benefit to the users of these new communications services.

THE PROVISION OF SPECTRUM
FOR FEEDER LINKS OF NON-GEOSTATIONARY
MOBILE SATELLITES

Robert R. Bowen
Department of Communications, Canada
300 Slater St., Ottawa, Ontario
K1A 0C8, Canada
Telephone 613-998-3974
FAX 613-952-1231

ABSTRACT

The possibility of sharing spectrum in the 30/20 GHz band between geostationary fixed-satellite systems and feeder-links of low-earth orbit (LEO) mobile-satellite systems is addressed, taking into account that ITU Radio Regulation 2613 would be a factor in such sharing. Interference into each network in both the uplink at 30 GHz and the downlink at 20 GHz is considered. It is determined that if sharing were to take place the mobile-satellite may have to cease transmission often for intervals up to 10 seconds, may have to use high-gain tracking antennas on its spacecraft, and may find it an advantage to use code-division multiple access. An alternate solution suggested is to designate a band 50 to 100 MHz wide at 28 and 18 GHz to be used primarily for feeder links to LEO systems.

INTRODUCTION

Recently a number of organizations have indicated the intention to implement non-geostationary (non-GSO) mobile satellites in the frequency range 1 to 3 GHz. Some of these systems would be located in low earth orbit (LEO) circular highly inclined orbits in the order of 1000 kilometres high, others in similar but higher orbits in the order of 10,000 kilometres high, and yet others in highly elliptical orbits with an apogee higher than geostationary altitude. The technical characteristics of these systems such as satellite EIRP and G/T, modulation and access technique, earth terminal characteristics, etc. may vary widely, according to the information provided by their proponents. Their common thread, from the perspective of this paper, is their need for feeder links to gateway stations in fixed-satellite bands above 3 GHz. This paper addresses that need for spectrum and orbit resources in the fixed-satellite service for feeder links for these non-GSO mobile satellites.

BACKGROUND

The satellite systems considered here are collectively known as "Big-LEO" mobile-satellite systems, even though some of them may be at higher altitudes than LEO or may be in elliptical orbits. A common characteristic in their need for feeder links is that spectrum in the frequency range 1 to 3 GHz is very much at a premium, even after the decisions of the 1992 World Administrative Radio Conference (WARC-92), and that by their very nature the systems are world-wide as distinct to national as many geostationary systems are. These two factors imply a need to implement the feeder links in a fixed-satellite band above 3 GHz that is accessible on a world-wide basis.

The problem that arises at this point is that Big-LEO feeder link systems do not share the spectrum very well with more conventional geostationary (GSO) fixed satellite (FSS) systems. At regular short periods of time the satellites are at the same angle as seen from a GSO/FSS system's earth station, and at different regular instants of time as seen from a LEO/MSS system's gateway or feeder-link earth station. At those instants of time one network may cause harmful interference into the other. It is this potential problem, and what to do about it, that is addressed in this paper.

Most GSO fixed-satellite networks to date are implemented in the 6/4 GHz bands or the 14/11 GHz bands on a world-wide basis, or in the 14/12 GHz bands for domestic systems in the Americas. The GSO in these bands is

heavily used. To avoid the need to coordinate LEO/MSS feeder-link systems with these GSO systems, the trend is to concentrate on use of the 30/20 GHz bands for those LEO/MSS feeder-link systems, in bands that are not currently in wide-spread use. The problem with this approach is that the 30/20 GHz bands are being considered by fixed-satellite operators as the next band to be used, both because of its attractive technical characteristics for some applications and because lower bands are becoming congested in some areas. The situation from a LEO/MSS perspective is made more complex because of Radio Regulation 2614 of the International Telecommunications Union (ITU), as modified recently at WARC-92, which gives GSO/FSS systems a very strong advantage in any coordination discussions with any non-GSO system, including a feeder-link system of a LEO/MSS network. For this reason, a LEO/MSS operator may be making a very expensive mistake in assuming that prior notification of a LEO/MSS network would avoid the need to accommodate GSO/FSS networks at a later date.

The approach suggested here is that, instead, a way of accommodating both must be found before such coordination difficulties arise, either by finding ways to share the same bands or agreeing to use different bands.

THE POTENTIAL PROBLEM

Let us suppose that a LEO/MSS feeder-link system and a GSO/FSS system are using the same frequency bands within the range 27.5 to 30 GHz in the Earth-to-space direction (the uplink), and within the range 17.7 to 20.2 GHz in the space-to-Earth direction (the downlink). As seen from the Earth the FSS satellite is fixed, and the LEO/MSS satellite is rapidly moving. Eventually, for a short period of time, the two satellites and the LEO/MSS earth station will be in approximately a straight line, and at other short periods of time the two satellites and the GSO/FSS earth station will be in a straight line. At these instants there may be harmful interference between the two networks, either in the uplink or in the downlink, or both, depending on the technical characteristics of the two networks. (See Figures 1 to 4.)

The problem can thus be broken down into its four components:

1. interference in the uplink from the GSO satellite into the LEO satellite;

2. interference in the uplink from the LEO satellite into the GSO satellite;

3. interference in the downlink from the GSO satellite into the LEO satellite; and

4. interference in the downlink from the LEO satellite into the GSO satellite.

If the two types of satellite networks are to share the same spectrum in the uplink or in the downlink, or in both directions, their characteristics must be such that they can share with widely varying characteristics of the other type of network, because each network may have to share the band with a number of networks of the other type. This observation applies particularly to a LEO/MSS network, which may have to share the spectrum at different instants with a large number of GSO/FSS networks in different parts of the world. This is based on the high frequency-reuse factor of the GSO by GSO/FSS networks, and an eventual high GSO/FSS satellite population in these bands, as there currently is in the lower 6/4 GHz and 14/11 or 14 12 GHz bands.

ANALYSIS APPROACH

Two approaches were considered in doing the necessary analysis of the above potential problem. One approach considered was to analyze in detail the sharing between particular GSO/FSS networks and particular LEO/MSS networks to determine the carrier-to-interference levels, technical constraints, etc for each pair of GSO and LEO networks. There were several problems in adopting that approach. One problem would have been the need to follow detailed changes in the design of both types of network, a difficult task in itself. A second problem would have been that despite the large amount of work required, the results would be dated by any future changes to either

network. The third problem, perhaps the most serious, would have been that the approach would not necessarily lead to general conclusions regarding use of the 30/20 GHz bands by the two types of networks.

A second approach, the one adopted here, was to analyze the sharing possibility without making any more assumptions about either the GSO or the LEO network than necessary, and when necessary use appropriate CCIR Recommendations to model the networks. The objective of the analysis is not to estimate precisely the magnitudes of the interferences between the networks, but rather to determine whether sharing between the GSO and LEO networks is easy, whether measures can and should be taken to permit sharing, or whether sharing is impossible and so separate frequency bands will be necessary for the two classes of network.

Because of the existence of ITU Regulation 2614, it is assumed in this analysis that if sharing of the same frequency band is to take place between a GSO/FSS system and a LEO/MSS system it is the latter that must adapt its characteristics to make the sharing possible.

ANALYSIS

In carrying out an analysis of the compatibility of the two classes of network, as discussed above, each of the four modes of interference are considered in turn, and constraints put on the relationship between system parameters at each stage. An inconsistency between these various constraints would indicate an inability to share the band.

In each of the four interference modes one can use the link equations

$$C = EIRP_d - FSL_d + G(\phi)_d \qquad ...(1)$$

$$I = EIRP_i - FSL_i + G(\phi)_i \qquad ...(2)$$

where
* EIRP is signal effective isotropic radiated power,
* FSL is free-space loss of the signal
* L_r is rain loss of the signal
* $G(\phi)$ is antenna gain at an angle

* ϕ off boresight
* C is the received strength of the desired signal
* I is the received strength of the interfering signal
* d refers to the desired signal, and
* i refers to the interfering signal.

These are rather simple versions of the well-known satellite link equation, not taking account of implementation margins, antenna losses, rain margins, etc. However, "ball-park" results are sought here, not fine-tuning of a result.

Uplink Interference from a LEO System into a GSO System

It is assumed here that the GSO/FSS system is carrying QPSK traffic with forward error correction, requiring a carrier to interference plus noise ratio C/(I+N) of about 10 dB. If CCIR Recommendation 523 is to hold, I should be about 12 dB below N, and so C/I should be about 22 dB. If we consider the transient worst case of the LEO earth station pointing toward the GSO satellite, in the same direction as the LEO satellite momentarily, as in Figure 1, ϕ is zero in (1) and (2). This requires a boundary condition of

$$EIRP_{gso,up} - EIRP_{leo,up} > 22 \text{ dB.} \qquad ...(3)$$

A variation of the LEO system's operation, if it could not or did not wish to meet the constraint of (3), would be to cease transmissions during the time that it was pointing towards the GSO satellite. If one assumes

* that the LEO earth station antenna diameter was 2 meters, a fairly large antenna with a diameter-to-wavelength ratio of 200 at 30 GHz,

* that transmission is interrupted while the GSO satellite is in the LEO earth station antenna's main beam,

* the LEO satellite is at an altitude of about 1,000 km,

* the earth station elevation angle

87

is 30°, a fairly high angle in Canada when pointing towards the GSO, and

* the earth-station-antenna model of Appendix 28 of the Radio Regulations applies

then the LEO earth station would have to cease operation for periods in the order of 6 to 10 seconds, and by so doing would be able to increase the LEO earth station by about 17 dB over that specified by equation (3).

Uplink Interference from a GSO System into a LEO System

The EIRP of a LEO earth station can be considerably lower than that of an earth station of a GSO/FSS system, if the space station antenna gains in the two systems are similar. This is because of the lower altitude and so smaller free-space-loss in the LEO system's transmission path. If the LEO slant range in the direction of the GSO at an elevation angle of 30° was 2,000 km., the difference in EIRP may be in the order of 12.5 dB. (If such were the case, 12.5 dB of the 22 dB of Equation (3) could be met in this way.)

The lower value of the LEO system's EIRP presents a problem, however, in terms of the C/I in the LEO system during the transient condition that the LEO and GSO satellites and a GSO earth station are in a straight line. (See Figure 2.) If the LEO system's modulation and access are say QPSK and TDMA, it would need a C/I during these transient conditions (lasting 6 to 10 seconds) of at least 15 dB. With an EIRP differential of about -12 dB, there is a need to improve the LEO's interference immunity by in the order of 27 dB. One way to meet that objective would be to place the LEO gateway stations in remote locations and have a LEO satellite antenna discrimination {G(0) - G(ϕ)} in the order of 27 dB. This would require both high-gain tracking antennas on the LEO satellite and LEO/MSS gateway stations in remote locations, both at considerable cost.

If the LEO system's access technique were CDMA these constraints could be relaxed. If that system had a CDMA bandwidth improvement factor of say 30 dB, and carried 100 messages simultaneously, its transient C/I could be as low as -12 dB, the EIRP differential due to the range difference. There would still be the need to meet the constraint in equation (3), but if CDMA were used uplink interference into the LEO system may not be a problem.

Downlink Interference from a LEO System into a GSO System

In this case the interference would be from the LEO satellite into the GSO/FSS receiving earth station. The earth stations of the GSO/FSS system may be quite small, requiring large GSO satellite EIRP's, or they may be in the order of 2 to 4 meters in diameter, similar to those of the LEO gateway stations. Thus similar power-flux-densities (pfd's) on the Earth's surface must be expected from the two systems. However, in the transient situation in which the two satellites and the GSO receiving earth station are in a straight line (see Figure 3) the GSO/FSS system would require a C/I of about 22 dB, the same as that considered for uplink interference into the GSO system. The only measures available to the LEO system operator to meet this constraint is to place its receiving gateway stations at remote locations and use large tracking satellite antennas to not illuminate areas where GSO earth stations might be, or to cease transmission from the satellite when the LEO satellite is in the path between the GSO satellite and its earth station, or some combination of these two techniques. The problem with the latter technique is that there may be a very large number of GSO earth stations, particularly in the top 500 MHz of the 30/20 GHz band where there is no need to share with terrestrial networks.

Downlink Interference from a GSO System into a LEO System

As discussed above, the pfd's of the two systems are expected to be similar, or the pfd of the GSO system might be higher if a large number of earth terminals with small receiving antennas were used. This would not be a problem for a LEO system that employed

CDMA, but a LEO system that used TDMA or FDMA would have to interrupt operation when its satellite, its earth station, and the GSO satellite were in a straight line as indicated in Figure 4. These interruptions would be in the 6 to 10 second range, the same as that experienced to combat uplink interference.

DISCUSSION

As indicated in the above analysis of the four interference modes, simultaneous use of a block of spectrum by a GSO/FSS system and a LEO/MSS feeder-link system would be quite difficult. Given the existence of ITU Regulation 2613, it would result in severe constraints being imposed on the LEO/MSS system designer and its operator. These include placement of LEO gateway stations at remote locations with associated backhaul costs, regular interruption of the operation of the LEO feeder-link system for intervals as long as 10 seconds, and the inclusion of high-gain tracking antennas on LEO/MSS spacecraft. The use of CDMA rather than TDMA or FDMA would ease some of the problems, particularly those into the LEO system, but would not solve the problems of interference into the GSO system and so the other constraints may have to be implemented whatever access scheme is used.

A technique that may be applicable in higher latitudes for LEO/MSS systems with inter-satellite links between the satellites is to recognize that the location of the LEO satellite may cause an interference problem, and at that point in time switch operations to a different satellite rather than interrupting the user traffic for up to 10 seconds. However, that would be a complex that could only be implemented by some MSS operators, ie. those with inter-satellite links in their networks.

There is an alternative regulatory solution that should be considered, given the fairly serious sharing problems with potentially expensive solutions discussed briefly above: that is the designation of a separate relatively small band in both the uplink and downlink directions in the 30/20 GHz frequency range that

would be used for LEO/MSS systems. In those bands Regulation 2613 would not apply, and GSO system operators would be encouraged to not use the bands. The sharing of the band by different LEO/MSS systems has not been analyzed here, but it is believed that this sharing problem is easier to solve than one in which GSO/FSS systems have to be taken into account.

Initial consideration of this possibility indicates that bands in the order of 50 MHz to 100 MHz in width would be adequate for the LEO/MSS feeder-link application. These bandwidths are only 2% to 4% of the 2.5 GHz wide 30/20 GHz FSS bands, and their designation could avoid a very difficult sharing problem with large associated costs. Frequency bands at 18 GHz and 28 GHz are being considered in Canada for this purpose.

Because a LEO/MSS system is by its very nature a global system, agreement on the use of frequencies for its feeder links would have to be reached on a world-wide basis. If sharing with GSO/FSS systems were contemplated the sharing consultations would be complex because sharing would be necessary between a LEO/MSS system and many GSO/FSS systems. In contrast, if the LEO/MSS systems were to use a separate designated band, this band would have to be agreed globally through action of the ITU. Because LEO/MSS systems are currently being designed and feeder-link frequencies for those systems chosen, and because these frequencies cannot easily be changed once they are chosen, the subject requires urgent attention.

In summary, it is concluded that LEO/MSS feeder-link systems could not be easily coordinated with GSO/FSS systems in the same frequency band. Further, it would be very difficult to design and operate a LEO/MSS feeder-link system such that interference into both the LEO/MSS system and the GSO/FSS system are at acceptable levels. Because of ITU Regulation 2613, the onus is on the LEO/MSS operator to ensure that such interference does not occur. **The designation of uplink and downlink fixed-satellite bands for LEO/MSS feeder links in the 30/20 GHz frequency range is seen as the basis for solution of this potential problem.**

DIAGRAMS OF INTERFERENCE CONDITIONS
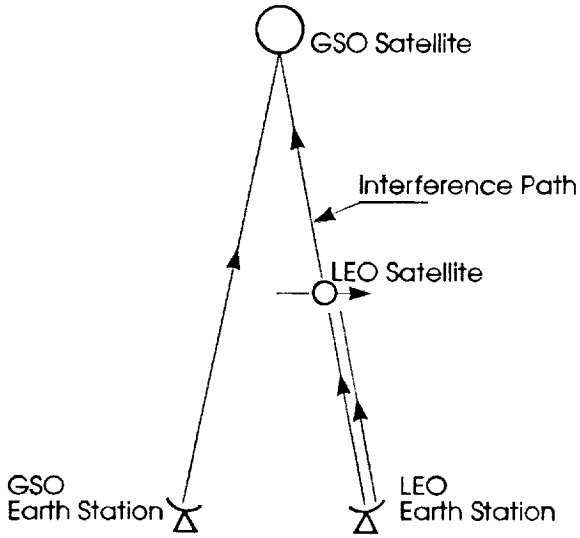
Figure 1
Uplink LEO Interference into GSO
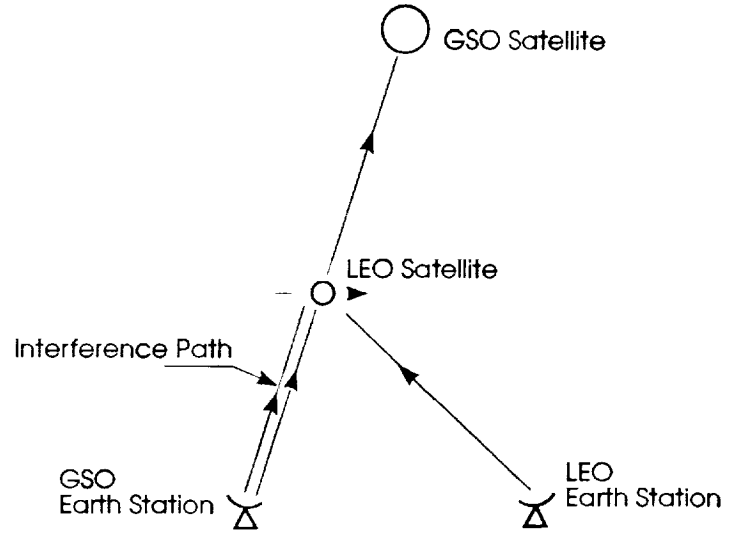
Figure 2
Uplink GSO Interference into LEO
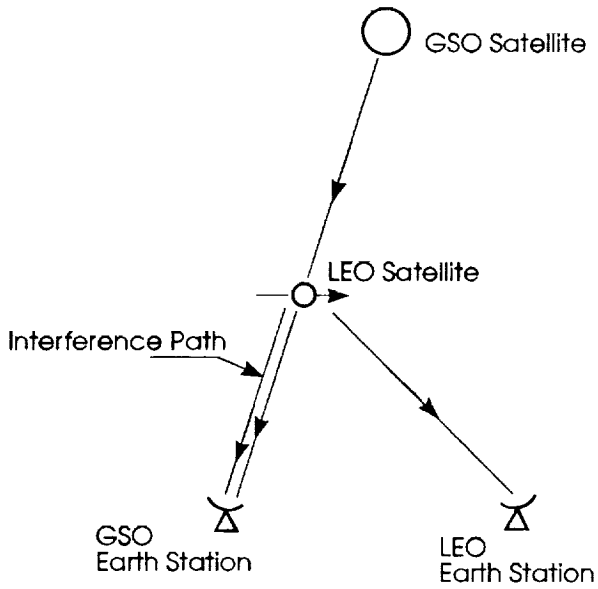
Figure 3
Downlink LEO Interference into GSO
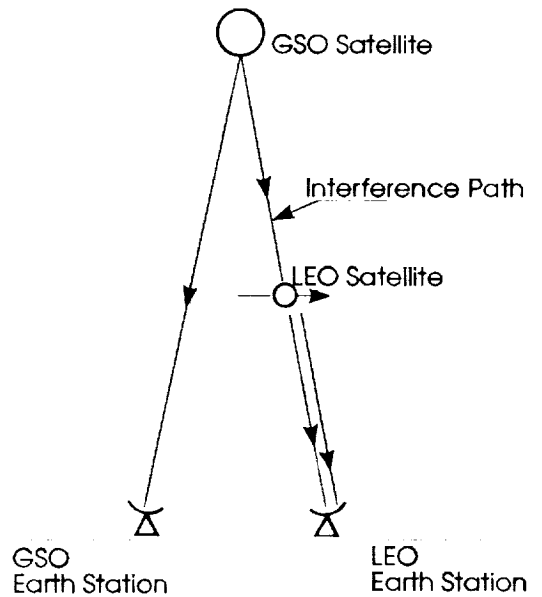
Figure 4
Downlink GSO Interference into LEO

The possibilities for mobile and fixed services in the 20/30 GHz frequency bands

C.D. Hughes
European Space Agency
ESTEC
P.O. Box 299
2200 AG NOORDWIJK
The Netherlands
telephone: +31 1719 83148
fax: +31 1719 84598

With the wide range of services now offered by satellite communications and broadcasting and the increasing trend towards small terminal systems, the traditional distinctions between fixed and mobile services are becoming less important. In the future mobile, portable and fixed services may well operate side by side in a hybrid manner. This trend is already apparent in Europe where extensive use is being made of the fixed service frequency allocations for broadcasting and for mobile services. Similarly many ostensibly mobile terminals are serving fixed installations.

Although the immediate future of mobile satellite communications continues to lie in the L-band frequency allocations, in the longer term the 20/30 GHz frequency allocations, offer the possibility of a new beginning where the advantages of hybrid systems can be included in the overall system designs at the outset.

The paper takes account of the experience gained using 20/30 GHz within the Olympus Utilisation programme and the likely demands for future services to highlight the most promising avenues for future system development.

This paper will be distributed at the Conference, or contact the author at the address above.

Use of the 30/20 GHz Band
by Multipurpose Satellite Systems

Stephen McNeil[1], Vassilios Mimis[2], Vishnu Sahay[1] and Robert Bowen[1]

[1]Department of Communications
300 Slater Street,
Ottawa, Ontario,
K1A 0C8
Canada
Telephone 613 990-4692
Facsimile 613 952-5108

[2]Communications Research Centre
P.O. Box 11490, Station H
Ottawa, Ontario
K2H 8S2
Canada
Telephone 613 991-1715
Facsimile 613 990-0316

ABSTRACT

The World Administrative Radio Conference (WARC) held in 1992 allocated the bands 19.7-20.2 GHz and 29.5-30.0 GHz to both the Mobile Satellite Service (MSS) and the Fixed Satellite Service (FSS) on a co-primary basis. An economic and flexible solution for the provision of both services is to place both payloads on one spacecraft. This paper describes some of the proposed applications of such a hybrid satellite network. It also examines the facility for spectrum sharing between the various applications and discusses the impact on coordination. The paper concludes that the coordination process would not be more onerous than traditional FSS inter-satellite coordination.

INTRODUCTION

WARC-92 addressed the spectral requirements of a new generation of multi-purpose satellites (MPS) operating in the bands 29.5-30 GHz and 19.7-20.2 GHz (Ka band). These satellites would provide both fixed-satellite and mobile-satellite services from the same spacecraft. WARC-92 decided that the mobile-satellite applications of these systems should have equal status from the radio regulatory perspective with the fixed-satellite applications in the aforementioned bands in Region 2 (the Americas).

The Canadian Department of Communications (DOC), in conjunction with the Communications Research Centre, has studied the technical and economical feasibility of a Ka band satellite offering fixed and personal communication capabilities. A pre-commercial payload is planned to be launched in 1997, followed by a fully operational commercial system in the 2005 - 2010 time frame.

This paper assesses the spectrum sharing capabilities between two such MPS satellites and its impact on the geostationary orbit resource. MPS satellites provide both fixed and mobile applications, and thus should provide a fair representation of the expected spectrum/orbit sharing environment.

THE CANADIAN MULTI-PURPOSE SATELLITE PROGRAM

The Canadian system will accommodate a wide variety of communications offerings, ranging from personal communications using relay terminals operating at a 2.4 kbps rate, vehicular mobile and portable terminals operating at a 144 kbps (2B+D) rate, aeronautical terminals carrying voice, data, or video information at 144 kbps or higher rates, and fixed terminals operating up to 1.544 Mbps (T1 rate). The smaller lower-capacity terminals of this menu will operate through one of 52 beams 0.6° in diameter in a beam hopping mode of operation controlled by the on-board network controller. The higher-capacity terminals with larger antennas and usable bandwidths will operate through a four-beam satellite antenna covering Canada. At the core of the satellite is a demodulator and modulator for each beam and a base-band digital switch to re-route traffic based on information in the message or carrier type. This regenerative on-board processing (OBP) essentially de-couples the uplink noise from the downlink and permits different types of modulation and access schemes between the uplinks and downlinks.

The option of a wide band, single beam, point to multipoint application may also be available. It would use a conventional repeater amplifier.

Services and Applications

Market viability studies have identified a large number of potential applications which could take advantage of the characteristics of Ka band satellite communications. These studies identified four major application groups to be supported by the Ka band payload applications and fall into one of the following broad categories:

- Single user relay services
- Narrowband multimedia applications
- Multiuser multimedia applications
- Point to multipoint application

Single User Relay Service

This service is designed to provide full connectivity with a terrestrial Personal Communications Network (PCN) and therefore it will offer the user single channel voice and messaging capabilities. As currently planned, the system will consist of a fixed or portable Ka band repeater terminal which provides satellite access to a mobile hand-held terminal.

Narrowband Multimedia Applications

The Narrowband Multimedia network services are based on the provision of a basic-rate Integrated Services Digital Network (ISDN) service anywhere within the satellite service area. Satellite access is provided via a portable terminal to either the public or a private network. The range of services to be provided via the family of multimedia terminals is equivalent to those in the basic ISDN environment. This includes one or two voice connections, low speed packet data, higher speed file transfer and video transmission at rates up to 144 kbps. A variety of terminals to support these fixed, mobile and aeronautical mobile applications will be made available.

Multi-user Multimedia Services

The Multi-user Multimedia (MUMM) service will support multimedia applications and a multi-user population within the same locale. The MUMM terminal will provide the link between the satellite and a number of users operating within a microcell which may be an office building or an industrial campus. Data rates up to primary rate ISDN are envisaged. A full range of voice, data, image and video applications will be supported.

Point to Multipoint Application

A point to multipoint capability may be available through a single wide band channel capable of transmitting a high bit rate. This application would be used in conjunction with a single wide coverage beam. On-board processing would not be used with this application due to the high bit rates.

APPLICATION LINK BUDGETS

Five link budgets are given in Table 1. Four of the budgets are currently proposed for the MPS. A fifth budget (Conventional - 1.544 Mbps) was derived based on the characteristics of the MPS but the satellite was assumed to be a simple repeater or bent pipe satellite.

All the link budgets assume 1/2 rate forward error correction (FEC), Viterbi soft decision decoding and a constraint length of 7. Other salient features of each of the example link budgets are described below.

Single User Relay (SUR)

This is used for personal voice and messaging communications. The antenna is a 5x5 cm microstrip patch antenna. The data rate is 2.4 kbps and high gain, 0.6° satellite spot beams are employed. Coherent MSK and differential BPSK are used on the uplink and downlink respectively.

Fixed Multimedia (FMM)

This application uses 20-30 cm parabolic antennas and can transmit up to 256 kbps (144 kbps for ISDN applications). It will also be served by high gain spot beams. Coherent QPSK is used for both up and downlinks.

Multi-User Multimedia (MUMM)

A 90-120 cm parabolic antenna in conjunction with medium sized satellite beams (G/T = 2.2 dB/K) are utilized. The link is capable of providing primary rate 1.544 Mbps (T1 rate) service. Coherent QPSK is used on both links.

Conventional

This link budget is not proposed for the MPS commercial satellite but is provided for comparative purposes. It has the all the same system characteristics as the MUMM application except the satellite is assumed to be a bent pipe. It was derived such that the faded C/N would result in the same bit error rate

(BER) as the faded C/N of the MUMM; approximately 10^{-7} BER.

High Definition Television (HDTV)

A digital wide band HDTV application could be implemented in the future. Its inclusion in this study is to see the effect of sharing with the narrowband applications. Coherent QPSK is also used for both links.

ORBITAL SEPARATION CALCULATIONS

The basic C/I equations used are given below.

$$(C/I)_D = (EIRP_w - D_w + G_w(0)) - (EIRP_i - D_i + G_w(\Theta)) + Q$$

$$(C/I)_U = (EIRP_w - D_w) - (EIRP_i - G_i(0) + G_i(\Theta) - D_w) + Q$$

where:

$(C/I)_D$ - downlink carrier to interference ratio (dB)
$EIRP_w$ - effective isotropic radiated power of the wanted transmitter (dBW)
D_w - wanted satellite discrimination (dB)
$G_w(0)$ - maximum gain of the wanted receiving earth station (dBi)
$EIRP_i$ - effective isotropic radiated power of the interfering transmitter (dBW)
D_i - interfering satellite discrimination (dB)
$G_w(\Theta)$ - gain of the wanted receiving earth station in the direction Θ (dBi)
$(C/I)_U$ - uplink carrier to interference ratio (dB)
$G_i(0)$ - maximum gain of the interfering earth station (dBi)
$G_i(\Theta)$ - gain of the interfering earth station in the direction of Θ (dBi)
Q - bandwidth factor = $10 \log (B_i/B_w)$ (dB)
B_i - bandwidth of the interfering signal (Hz)
B_w - bandwidth of the wanted signal (Hz)

Given the link budgets contained in Table 1 along with their C/I criteria, orbital separation requirements (Θ) between various applications can be calculated.

Assumptions

Co-coverage and co-frequency are assumed in all cases.
The C/I criterion used in all cases is found by allowing a 6% increase in the total noise power of the system. This corresponds to a C/I criterion of 12.2 dB above the C/N. All calculations were performed assuming clear air conditions.

Depending on the antenna size, the earth station antenna rolloff characteristics were assumed to be either:

$29 - 25 \log \Theta$ for $D/\lambda \geq 100$
or $49 - 10 \log(D/\lambda) - 25 \log \Theta$ for $D/\lambda < 100$

where:

Θ - antenna off-axis angle
D - antenna diameter or length
λ - wavelength

Studies recently performed within Canada have shown that a small rectangular microstrip patch antenna can be designed to meet the $49 - 10 \log (D/\lambda) - 25 \log \Theta$ sidelobe rolloff requirement.

Finally, the victim earth station was assumed to be 2 dB down from its own boresight and at the boresight of the interfering satellite beam.

RESULTS

The results of the orbital separation angle calculations are given in Tables 2 and 3. Separate angles are given for the uplink and downlink due to the regenerative on-board processing assumed. Links using regenerative OBP cannot be combined into a single separation angle using the same method used for bent pipe links. In practice, the angles could be 'combined' to reduce the overall separation, but as there is no accepted criterion or method for this, they are presented separately here.

For the uplink angles, the maximum number of narrowband carriers allowed to interfere into a wider band application was limited to the number of narrowband carriers actually planned for operational use. For example, consider the case of the SUR (2.4 kbps) interfering into HDTV. Over 5,000 of these narrowband channels could fit inside the HDTV's noise bandwidth. However since only 16 channels x 52 beams = 832 channels could be in use at any one time, only 832 carriers were allowed to interfere. Taking this same approach for the downlink only allows one interferer per wideband channel due to the proposed MPS frequency plan which only contains one downlink carrier per hopped beam. However this does not allow for generalization to other satellite systems where there could be several simultaneous interferers. To improve this, Table 4 is provided which allows a maximum of 10 interferers. Only the SUR interfering case is given as this is the only case with significant increases in separation angles with the increased number of interferers.

Generally the angles are in the same range as conventional FSS/FSS separation angles except for the lower rate applications (SUR, FMM). These applications cause larger separation angles due

95

primarily to the following:

- smaller earth station antennas compared to, for example, Ku band antennas, even after frequency scaling;
- high powered narrow bandwidth downlink transmissions;
- low powered uplink transmissions.

Some of the carrier combinations result in 0° separations (eg. SUR into MUMM). This is because even when the interferer is directly in the victim's mainbeam, the victim's C/I criterion is met. Note that this does not mean that 0° is required overall since the opposite interference mode (eg. MUMM into SUR) is always non-zero.

It should also be noted that some of the small non-zero angles are outside the applicable limits of the antenna rolloff equations and those angles would change somewhat (usually slightly larger).

Finally, the SUR/SUR interference on the downlink resulted in 96.9° separation. This is well beyond the valid range of the assumed antenna template and indicates that there is no off-axis angle which would yield the required discrimination from the SUR antenna.

Uplink

Generally the uplink separation angles are smaller than the downlink angles. One might expect that due to the very low uplink power of some of the applications, the EIRP differential between these and higher powered carriers would cause extremely large separation requirements. However, in most cases, this power deficit is offset by the superior discrimination of the larger antennas associated with the higher powered applications.

Downlink

The large angles found are due to the high powered narrow bandwidth applications; especially the SUR. The SUR (2.4 kbps) has the highest downlink EIRP of all the applications and yet also has the narrowest bandwidth. The high EIRP is required to overcome the low receive G/T of the relay terminal.

The angles become larger when there are multiple SUR interferers as shown in Table 4. The assumed number of 10 SUR interferers is arbitrary but the actual number will be limited to TWTA capability. Nonetheless, Table 4 is useful as it shows that different satellite frequency plans result in larger orbital separation requirements.

DISCUSSION

The majority of carrier combinations result in fairly small orbital separations and are comparable or slightly larger than the current situation in other bands. The lower rate, small antenna applications will require extra attention, but solutions for sharing are available. We will focus on the SUR for discussion purposes.

It can be seen that SUR shares better with the wider band applications. With the two satellite examples used here, the SUR can use the same frequencies as any of the wider band applications. For other satellite configurations, the SUR may be forced to share with an application such as digital television. It is interesting to note that the narrowband SUR shares well with the HDTV service which is the opposite of what might be expected.

It is important to keep in mind that the results are from one typical example of Ka band satellite systems. A wide range of different parameters are possible which could result in larger separation requirements. In the extreme case, where a large number of narrowband SUR carriers were in the same radio frequency channel as the wideband application, large orbital separations would be required. However, for most carrier combinations, traditional coordination arrangements would still exist at Ka band.

Overall, it would seem that the coordination process for Ka band satellites will not be much more involved than coordination in conventional bands. The addition of new applications using narrowband signals does add an extra element, but reasonable solutions exist to share the spectrum while conserving the orbit.

Despite the abundant spectrum at Ka band, as more systems migrate to the higher band more emphasis will have to be placed on designing systems which are more amenable to spectrum sharing with other satellites. Traditional methods such as frequency re-use and cross-polarization will eventually have to be employed.

CONCLUSION

This paper has described the applications proposed for a Canadian Ka band multi-purpose satellite and examined the spectrum sharing potential between such systems. For the types of traffic expected, co-frequency sharing with modest orbital separations is possible with care taken in the selection of carrier frequencies.

Table 1. Application Link Budgets

APPLICATION		SUR	FMM	MUMM	Conventional	HDTV
DESCRIPTION		2.4 kbps	256 kbps	1.544 Mbps	1.544 Mbps	30 Mbps
MODULATION		MSK/BPSK	QPSK	QPSK	QPSK	QPSK
UPLINK						
Frequency	(GHz)	30.0	30.0	30.0	30.0	30.0
Antenna Diameter	(m)	0.05	0.30	1.20	1.20	3.00
Antenna Gain	(dBi)	20.8	37.3	49.7	49.7	57.3
Antenna Rolloff Coefficient	(dB)	49	49	29	29	29
EIRP	(dBW)	15.0	39.2	61.2	63.0	79.8
Propagation Loss	(dB)	213.9	213.9	213.9	213.9	213.9
Availibility	(%)	95.50	99.50	99.50	99.50	99.30
Rain Fade	(dB)	2.0	6.0	6.0	6.0	5.1
Atmospheric Loss	(dB)	2.1	0.8	0.8	0.8	0.8
Satellite G/T	(dB/K)	16.7	16.7	2.2	2.2	-0.1
Additional Losses	(dB)	3.0	3.0	1.5	1.5	1.5
Data Rate	(Mbps)	0.0024	0.2560	1.5360	1.5360	30.0000
Noise Bandwidth	(MHz)	0.0062	0.4400	2.2440	2.2440	36.0000
Allocated Bandwidth	(MHz)	0.0070	0.5000	2.6000	2.6000	54.0000
Clear Sky C/N	(dB)	3.3	10.4	12.3	14.1	16.5
Clear Sky C/I Criterion	(dB)	15.5	22.5	24.5	26.3	28.7
DOWNLINK						
Frequency	(GHz)	20.0	20.0	20.0	20.0	20.0
EIRP	(dBW)	56.2	55.3	45.6	49.4	44.9
Propagation Loss	(dB)	210.4	210.4	210.4	210.4	210.4
Availability	(dB)	99.50	99.50	99.50	99.50	99.40
Rain Fade	(%)	6.6	4.6	4.4	4.4	4.0
Atmospheric Loss	(dB)	2.5	1.0	1.0	1.0	1.0
Antenna Diameter	(m)	0.05	0.30	1.20	1.20	3.00
Antenna Gain	(dBi)	18.9	33.7	46.2	46.2	53.7
Antenna Rolloff Coefficient	(dB)	49	49	49	49	29
Earth Station G/T	(dB/K)	-7.0	7.9	22.1	22.1	28.0
Additional Losses	(dB)	3.0	3.0	1.5	1.5	1.5
Data Rate	(Mbps)	0.0480	4.0960	12.2880	12.2880	30.0000
Noise Bandwidth	(MHz)	0.1350	6.8400	16.6800	16.6800	36.0000
Allocated Bandwidth	(MHz)	0.1550	7.9000	19.0000	19.0000	54.0000
Clear Sky C/N	(dB)	10.6	9.0	11.2	15.0	13.0
Clear Sky C/I Criterion	(dB)	22.8	21.2	23.4	27.2	25.2
COMPOSITE						
Availability	(%)	95.02	99.00	99.00	99.00	98.70

Notes:

1 - Forward error correction, rate 1/2, Viterbi soft decision decoding, constraint length of 7.

2 - SUR link is from/to Halifax; all others are from/to Ottawa.

3 - Antenna sidelobe rolloff is 29 - 25 log θ or 49 - 10 log(D/λ) - 25 log θ

97

Table 2. Uplink Separation Angles

Interferer ---> Victim	SUR 2.4 kbps	FMM 256 kbps	MUMM 1.544 Mbps	Conventional 1.544 Mbps	HDTV 30 Mbps
SUR 2.4 kbps	35.3°	6.4°	5.0°	5.9°	4.5°
FMM 256 kbps	22.0°	7.2°	5.6°	6.6°	5.1°
MUMM 1.544 Mbps	0.0°	2.1°	1.7°	2.0°	1.5°
Conventional 1.544 Mbps	0.0°	2.1°	1.7°	2.0°	1.5°
HDTV 30 Mbps	0.0°	1.7°	1.3°	1.5°	1.2°

Table 3. Downlink Separation Angles

Interferer ---> Victim	SUR 2.4 kbps	FMM 256 kbps	MUMM 1.544 Mbps	Conventional 1.544 Mbps	HDTV 30 Mbps
SUR 2.4 kbps	96.9°	18.6°	0.0°	0.0°	0.0°
FMM 256 kbps	11.4°	10.4°	3.0°	4.2°	2.1°
MUMM 1.544 Mbps	6.2°	5.7°	2.3°	3.3°	1.6°
Conventional 1.544 Mbps	6.2°	5.7°	2.3°	3.3°	1.6°
HDTV 30 Mbps	3.6°	3.3°	1.3°	1.9°	1.3°

Table 4. Downlink Separation Angles with Multiple Interferers

Interferer ---> Victim	SUR 2.4 kbps
SUR 2.4 kbps	96.9° (1)
FMM 256 kbps	28.5° (10)
MUMM 1.544 Mbps	15.5° (10)
Conventional 1.544 Mbps	15.5° (10)
HDTV 30 Mbps	9.0° (10)

Note:
    Numbers in brackets refer to the number of assumed interferers.

Session 4
Hybrid Networks for Personal and Mobile Satellite Applications

Session Chair—*Deborah Pinck*, Jet Propulsion Laboratory, U.S.A.
Session Organizer—*Deborah Pinck*, Jet Propulsion Laboratory, U.S.A.

(continued)

100.

Transparent Data Service with Multiple Wireless Access

Richard A. Dean

Department of Defense

Ft. Meade, MD 20755

(301) 688-0293

Allen H. Levesque

GTE Government Systems

Waltham, MA 02254

(617) 466-3729

ABSTRACT

The rapid introduction of digital wireless networks is an important part of the emerging digital communications scene. The introduction of Digital Cellular, LEO and GEO Satellites, and Personal Communications Services poses both a challenge and an opportunity for the data user. On the one hand wireless access will introduce significant new portable data services such as personal notebooks, paging, E-mail, and fax that will put the information age in the user's pocket. On the other hand the challenge of creating a seamless and transparent environment for the user in multiple access environments and across multiple network connections is formidable.

This paper presents a summary of the issues associated with developing techniques and standards that can support transparent and seamless data services. The introduction of data services into the radio world represents a unique mix of RF channel problems, data protocol issues, and network issues. These problems require that experts from each of these disciplines fuse the individual technologies to support these services.

INTRODUCTION

Multimedia wireless Data represents more than just a combination of radio, network and data technologies of which it is composed. These disciplines have evolved in largely independent communities and their fusion is neither obvious nor direct. Each has been spawned with separate technologies and in separate markets. It is only recently that combinations of these disciplines have been merged. Fig. 1 shows how the overlaps of these areas have combined in new techniques and markets.

Cellular telephones, for example, combine the Network switching and Radio technologies for voice applications, while ISDN combines Network switch-

ing and Data technologies. The integration of all three disciplines into Multimedia Wireless Data services combines the challenge of operating in the harsh radio environment with the sophisticated protocols required for data, and with the seamless services, switching, and transparency required of modern networks.
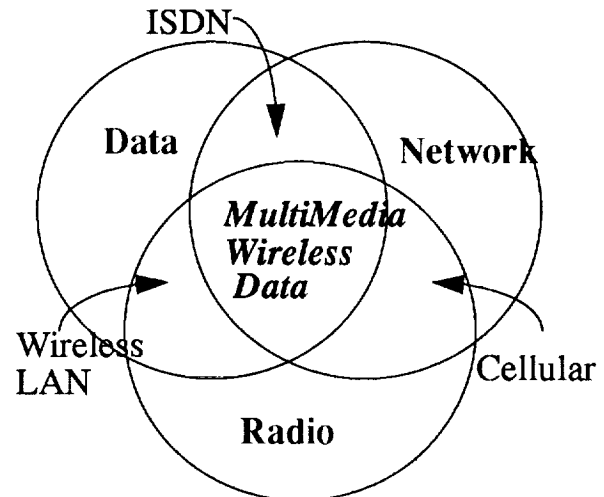
Figure 1. Technologies and Applications

The fusion of these disciplines is particularly challenging in light of the variety of access mechanisms that are possible, as with Cellular, Satellite, and Wireless LAN, each with a separate set of strategies, standards, and problems. The successful integration of these technologies have typically been viewed under the umbrella of Personal Communications Services and Networks (PCS & PCN). While market forecasts for PCS are euphoric, the technical coordination and management problems facing PCS are formidable. Essential to real progress in addressing these problems are first a clear strategy for accomplishing these technical challenges and, second, much greater cooperation among the independent communities of interest. The potential for PCS applications appears un-

bounded. It offers the possibility for creating a new infrastructure for the Information Age with improved services, convenience, and productivity.

PROBLEM DEFINITION

Besides the historical differences that divide these communities, Cellular Radio, Land Mobile Radio, Mobile Satellite, and Wireless LANs are separated by the perception of a fractured market which may lead in turn to a fractured solution. This highly fractured approach persists today in spite of a high degree of commonality in the architectures, services, and issues. Figure 2 shows an architectural view of these mobile services served by a common public network. They differ in the radio channel and associated protocol but share common services, control, and network interworking features.
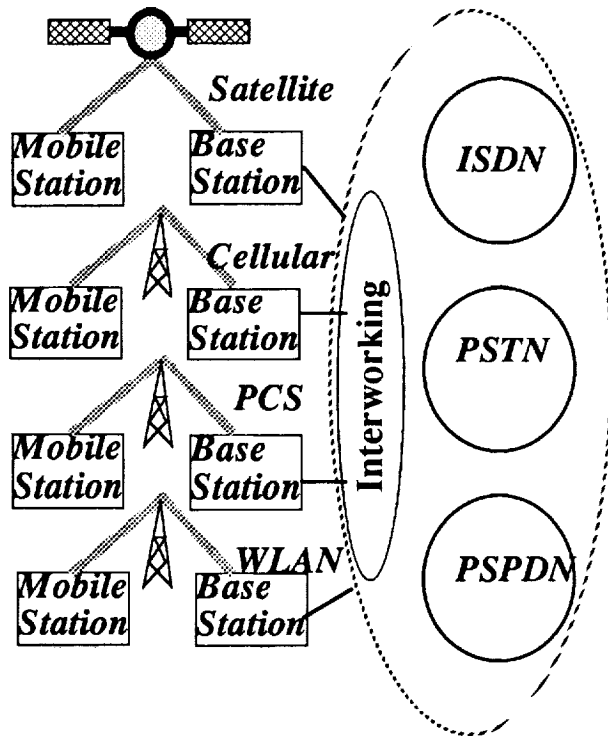
Figure 2 Strategic View of Wireless Networks

These networks and services evolved from independent markets. Their integration with the Public Network has been as ad hoc extensions rather than as part of integrated services. This is true for voice services and is especially true for data services such as G3 Fax. The myriad of approaches taken, for example, by Inmarsat, GSM European Cellular, and TIA North American Digital Cellular

defines different mobile fax terminals for each network. Clearly a better strategy and more coordination is required.

STRATEGY

The hope for Future Interoperable Wireless Data Services lies in creating a virtual open system within the emerging wired and wireless networks. A strategy for such an open system solution lies in use of a layered strategy such as defined by ISO layering model (OSI). While this structure applies in general, its specific application to interoperable wireless data leads to a natural strategy.
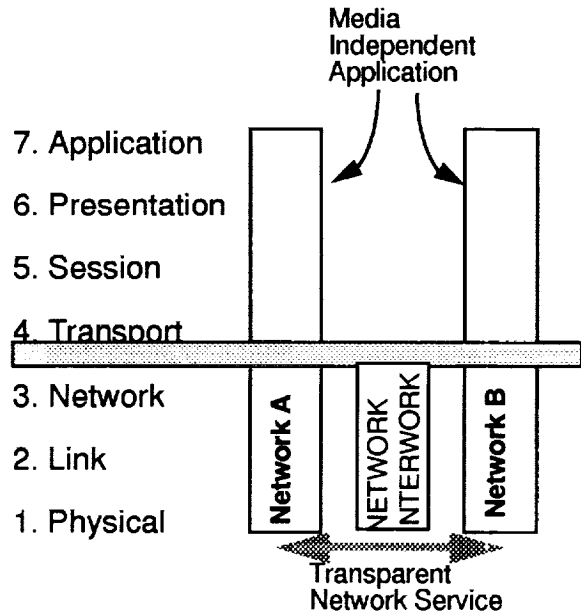
Figure 3. Layered Strategy

If the OSI model is organized generally by the application (layer 4-7) and the network (layer 1-3) as shown in Figure 3 then a general strategy for interoperability can be organized as follows:

Develop common sets of user applications that are media independent.

Develop network services that are application independent.

Develop Intelligent Network Services that invoke necessary network interworking to support transparent, seamless connections.

The first strategy simply organizes the applications into a manageable set of standard protocols.The PSTN G3 FAX, for example, is made media inde-

102

pendent under TIA 592 by isolating the T4 compression protocol and a piece of the T30 wireline controller. The US Government's secure telephone (STU-III) has likewise been segmented into a media independent protocol for multiple media applications.

The second strategy develops transparent and interoperable networks services and signalling. This is accomplished by access- independent call control, identity validation, registration, and mobility management. Such an approach is recommended by the Joint Experts Meeting of ANSI T1 and TIA TR45 in reference 1 and summarized below in Table 1. Such an approach allows services to be independent of access technologies such as CDMA and TDMA on a given network. It also allows services to be independent of the wireless access network such as satellite or cellular.

Table 1: Media Independence

Access Independent	Access Dependent
Application Protocol	Multiplex Scheme
Call Control	Radio Resource Mgmt
Identity Validation	Radio Link Protocol
Registration/Location	
Flow Control	
Maintenance & Config	

Inherent in such a strategy is transparency to the user and the application by provision of common physical, link and network layers or by automatic interworking capability. This strategy isolates the application from the variety of access RF technologies that will evolve due to competition within markets and the differences among wireless channels.

Figure 4 shows how layering might be accomplished with a G3 Fax connection between the PSTN and a Cellular network. A combination of common applications, common services, network interworking and intelligent networks create a virtual open system for this service.

The Intelligent Network plays a potentially significant role in making operation transparent. The Intelligent Network can support a transparency of service to the user across multiple wireless networks by customizing the connection and inserting the necessary interworking. Operation within the Intelligent Network can incorporate the following phases and functions.

Access Phase - Identify the User/Terminal

    <User Identity Established>
    <Terminal Identity Established>
    <User Services Established>
    <Terminal Services Established>

Connection Phase - Customize Network Service
    <User Dialed Number>
    <Examine User/Terminal Services>
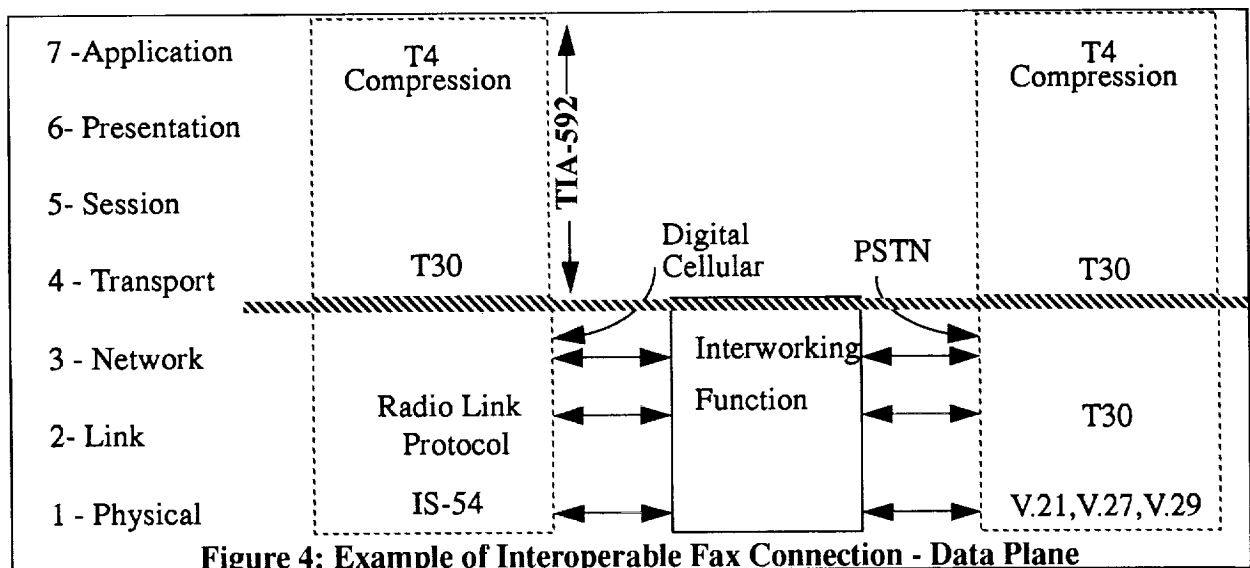
Figure 4: Example of Interoperable Fax Connection - Data Plane

<Examine Destination Network Services>

<Select Service Compatible Option>

Transmission Phase - Support Transparent Service

<Establish Necessary Interworking>

<Clear To Send>

<Data Transmission>

Earlier publications [4] have suggested use of IN services for wireless network mobility subscriber mobility. The above sequence expands that role to support service compatibility, service options, and interworking.

EXAMPLE: TR45.3 DIGITAL CELLULAR

This is not the first paper to suggest strategies for future wireless networks. Most network designers begin with such goals. For this reason it is perhaps more appropriate to search out good example to build upon. The European GSM and North American Digital Cellular TR45.3 are two such examples where this problem has been addressed [2]. Several significant approaches have been demonstrated in TR45.3 in reference [3] and are summarized below.

Layered Approach

A layered network model has been developed in TR45.3 to represent each network element needed to support a specific service. The notion of segmenting the network features into layers separates out the network's unique protocols and identifies a means by

which compatibility can be obtained by different manufacturers. The TR45.3 architecture defines the necessary entities for connection to the PSTN using a layered methodology as illustrated in Fig. 5. It represents the lower three layers of the Open Systems Interconnection model, the Physical, Link, and Network Layers. The reference model was adopted at the outset to clearly define the protocols to be supported by the different network elements. Where applicable common accepted data standards and procedures were specified and adapted to the cellular network environment. Figure 5 illustrates the Data Plane protocols used for G3 interoperable Fax service from a Cellular Mobile Terminal Equipment (TE) through the Base Station (BS)/Mobile Switch(MSC) and Interworking Function (IWF). Note how the layering allows clear visibility of the protocols and interfaces necessary at each element in the connection. Note also that the only variation one might expect between a cellular connection and a satellite connection would be in the Radio Link protocol (RLP) unique to that network.

Standard Services

Standard sets of bearer services are necessary across the variety of wireless access networks if transparent teleservices are to be provided. Bearer services would typically be synchronous, asynchronous or packet services necessary to support a broad base of teleservices across multiple networks. Rates

Figure 5. Layered Standards and Interfaces - Data Plane
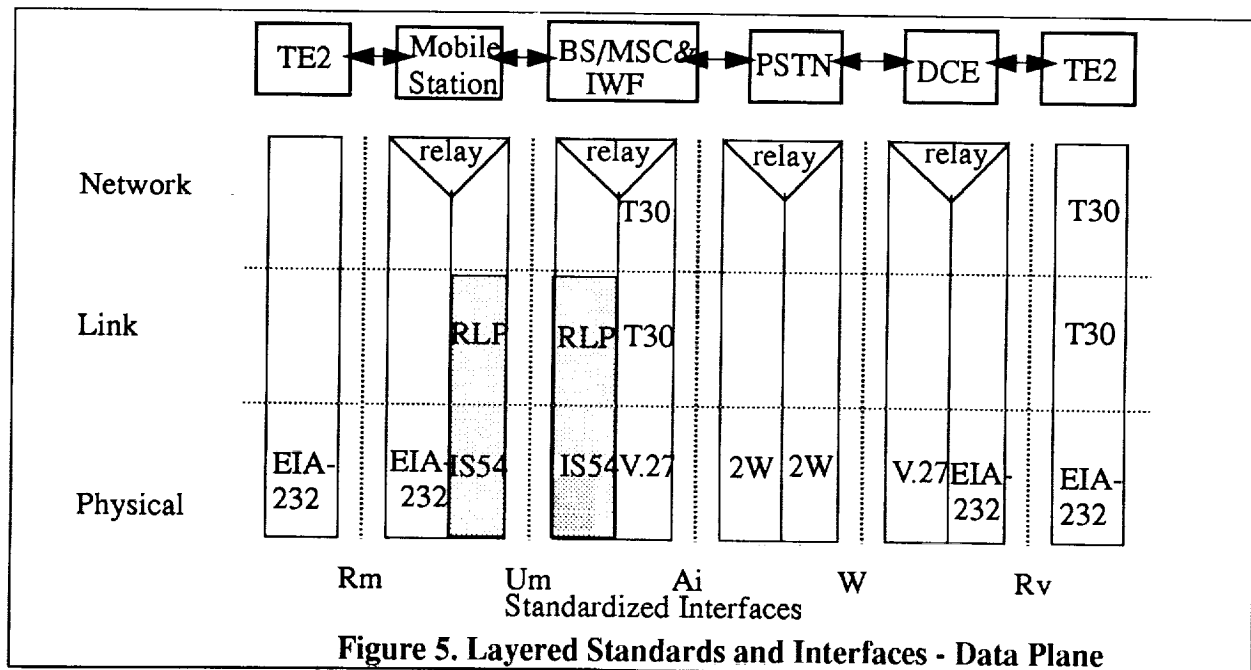
from 2.4 up to 28.8 kbps for traditional wireline data, and up to 64kbps for ISDN service are being considered. Custom services such as the G3 Fax and STU-III are also accommodated. A minimum subset of these however can clearly be accommodated across all media.

Network Interworking

Consistent with supporting teleservices identified above is the incorporation of necessary network interworking. Transparent interworking is the most important, and perhaps the most difficult part of the solution. It is at this point that all possible services connect with all possible networks. In general there are a common set of services and connections that simplify this problem. Figure 5 shows a TR45.3 example of Interworking for G3 Fax with the PSTN. The IWF supports a translation of data on the radio link protocol into a V.27 wireline modem with the necessary T30 control signalling to generate G3 compatible service on the PSTN. Other examples of interworking would be use of commonly available V series modems for synchronous service or a Hayes compatible control scheme for asynchronous data. Connections to X.25 Packet networks would require packet assembly-disassembly (PAD) functions. ISDN connections would require V.110 or V.120 rate adaption. The Government's STU-III can be accommodated with a 4.8 kbps synchronous bearer service and an IWF that includes V.21, V.26 and V.32 echo cancelling modems.

Standard Signaling Interfaces and Protocols

Uniformity of signaling, interfaces and protocols across wireless data networks supports common

hardware, services and interoperability. This is perhaps the biggest concern users have about the explosion of wireless technologies. TR45.3 has made a judicious selection of commonly used standards for interfaces and signalling as shown in Fig. 5 and summarized in Table 2.

Table 2: TR45.3 Interfaces & Protocols

Function	Standard	
Mobile Station	Rm	Sm (ISDN)
Signaling	EIA/TIA 602	Q.931. V.120
Rate	.3,2.4,4.8,..38.4	64kbps B Chan
Interface	EIA/TIA 232E	I.430
IWF Modems	V.21,V.22,V.22bis, V.32,V.32bis V.42, V.fast,Bell 103, Bell 212a	

Radio Access Independence

The TR45.3 Data Services have accomplished a large degree of access independence in their designs to date. This is largely a result of a layered approach and represents a major advantage for future applications. Figure 5 shows how the Radio Link Protocol and the IS54 TDMA physical layer are isolated from the other components in the network. This isolation will enable support of the same architecture, protocol and functional elements in the TR45 CDMA solution. It can also be emulated for satellite and PCS networks to support uniformity of products and user services.
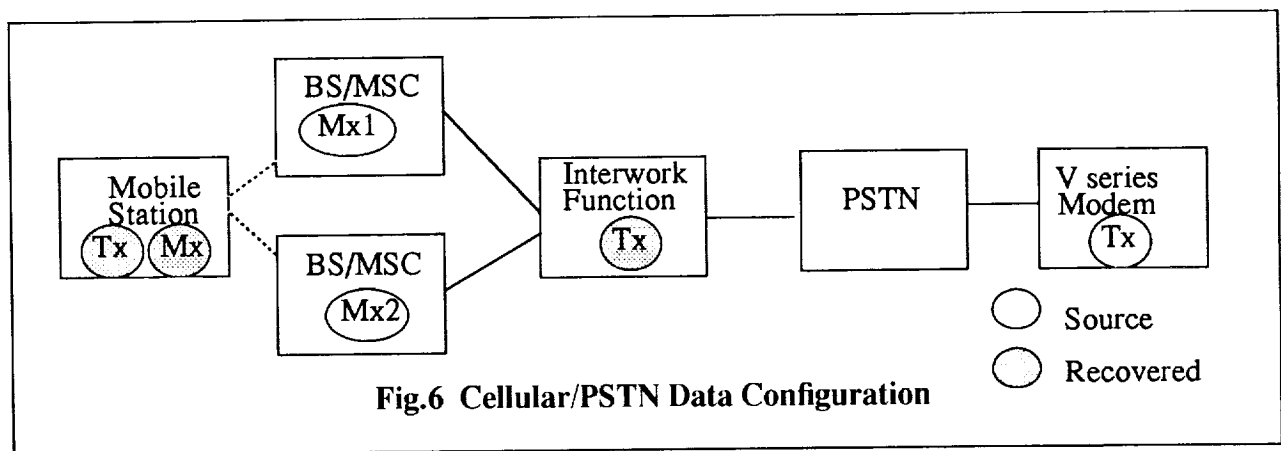
Fig.6 Cellular/PSTN Data Configuration

105

Timing and Synchronization

Data service for the wireless user connected across the Public Switched Telephone network presents several timing issues that must be resolved. The two significant issues to be addressed are Frame Sync and Bit Sync. Frame sync addresses the need to accommodate timing operation across a handoff. Bit sync addresses the need to accommodate clock mismatches across the network connection. Figure 6 highlights the different clocks in the system which leads to the sync problem in the internetwork connection. The PSTN V series modem transmit clock is shown as Tx and is the data rate of the PSTN source based on that PSTN modem's internal clock. This timing source is tracked by the Interworking Function modem which develops an estimate of this clock using a phase lock loop. This clock is further promulgated across the Cellular channel and appears again in the mobile as a reconstituted Tx. Figure 6 also shows the Digital Cellular synthesized clock Mx. This clock is generated at the MSC and is reconstructed at the mobile station. In general for an agreed upon data rate Mx and Tx are equal to the nominal rate of the data service (E.G. 4.8 kHz). In practice however the data rates of both clocks will differ from the nominal rate and will have some drift. Furthermore, the Mx clock cannot phase lock with the PSTN modem clock as it is locked to the rest of the cellular TDMA system. For PSTN modems the worst case clock accuracy is 1×10^{-4} while the Digital Cellular clock is assumed to be 1×10^{-6} or better. The differences in these clocks results in different transmission rates across the network. This difference can result in a slip in bit sync when there is either too much or too little data at the interface. These differences must be accommodated by the network if the service is to be usable. TR45.3 is currently considering the use of an elastic buffer at the IWF to address this problem. This introduces a modest delay into the connection but isolates the timing problem from the radio link protocol, a clear advantage.

The case shown reflects the situation with the transmission from the PTSN to the Cellular mobile station. Transmission from the mobile station to the PSTN modem represents a very different case. Here the MSC/BS clock can be used to drive both the mobile station and the Interworking function. Furthermore the PTSN modem receiver will track the MSC clock. Hence there is no real issue with bit synchronization in this direction. The bit sync problem as presented here will be common to all mobile networks independent of access scheme.

Frame Sync problems occur in Digital Cellular Networks primarily during handoffs between cell sites that have independent timing references. In general a gap in transmission can occur and the signal will reappear in some random phase alignment. Solutions to the frame sync problem are limited for the TDMA system as the overall timing of the Digital Cellular system is performed independently by each Base Station. The remaining practical solution under consideration in TR45.3 is to maintain frame sync across the handoff by inserting a frame counter in each frame so that added and deleted frame can be accounted for in the alignment of the data stream at the BS/MSC or the Interworking function. A modulo 2^n counter with n ranging from 4 to 8 can accomplish this task. If this scheme is accomplished, the net effect of handoff would be the insertion of burst errors in that data stream when frames are lost but bit sync is maintained.

Conclusions

The standardization of wireless data services represents significant challenges but the potential exists for a smooth path for a broad range of services and markets. Technical solutions lie in a fusion of existing network, radio, and data technologies. A strategy for such a fusion across the multiple wireless networks will require a clear technical strategy as outlined in this paper and, perhaps more importantly, cooperation among the currently insular cellular, satellite, network, and data communities.

References

1.*Report of the Joint Experts Meeting on PCS Air Interface Standards*, ANSI T1P1, TIA TR45, Nov. 1992

2.*Interoperable Wireless Data*, D Weissman, A. Levesque, R. Dean, IEEE Communications Magazine, Feb., 1993

3. *Stage 2 Service Description - Circuit Mode Data Services*, TIA TR45.3.2.5/92.12.15.03, Dec. 1992.

4. *Intelligent Network Concepts in Mobile Communications*, B. Jabbari, IEEE Communications Magazine, Feb. 1992.

Internetworking Satellite and Local Exchange Networks for Personal Communications Applications

Richard S. Wolff
Bellcore
445 South Street, Room 2M-293
Morristown, NJ 07962-1910
(201) 829-4537
(201) 829-5888 (fax)
rsw@thumper.bellcore.com

Deborah Pinck
Jet Propulsion Laboratory, California Institute of Technology
4800 Oak Grove Drive, Mail Stop 161-241
Pasadena, CA 91109
(818) 354-8041
(818) 393-4643 (fax)
pinck@zorba.jpl.nasa.gov

ABSTRACT

The demand for personal communications services has shown unprecedented growth, and the next decade and beyond promise an era in which the needs for ubiquitous, transparent and personalized access to information will continue to expand in both scale and scope. The exchange of personalized information is growing from two-way voice to include data communications, electronic messaging and information services, image transfer, video, and interactive multimedia. The emergence of new land-based and satellite-based wireless networks illustrates the expanding scale and trend toward globalization and the need to establish new local exchange and exchange access services to meet the communications needs of people on the move. An important issue is to identify the roles that satellite networking can play in meeting these new communications needs. The unique capabilities of satellites, in providing coverage to large geographic areas, reaching widely dispersed users, for position location determination, and in offering broadcast and multicast services, can complement and extend the capabilities of terrestrial networks. As an initial step in exploring the opportunities afforded by the merger of satellite-based and land-based networks, we are undertaking several experiments, utilizing the NASA ACTS satellite and the public switched local exchange network, to demonstrate the use of satellites in the delivery of personal communications services.

1. INTRODUCTION

The 90's and beyond will be an era of explosive growth in the demand for nomadic, ubiquitous and personal information exchange. This includes such fields as voice communications, data communications, image and video communications, multimedia, information services, position location services, and interactive communications to name but a few. Today's terrestrial networks are well on their way to supporting these applications. Currently, many different, and in some cases conflicting, and non-interoperable telecommunications networks are being deployed or planned. This is the case for both satellite networks as well as for terrestrial networks. Satellite system providers are designing LEO and GEO networks; terrestrial system providers are planning micro-cellular PCNs using low-power hand-held wireless "communicators"; wireless data network providers are deploying wide-area high-power packet radio networks; paging network providers are moving toward nation-wide alphanumeric messaging capabilities; cellular network providers are evolving towards digital and integrated voice/data services.

The unique strengths of satellites, such as large coverage areas, flexible network re-configuration, one-to-many communications and line-of-sight global networking, can be exploited to make satellites a critical element in achieving world-wide personal communications. Various satellite networks are now emerging, and it is important to insure their compatibility with each other and their interoperability with terrestrial networks. This effort should include a

wide range of stakeholders including satellite and terrestrial wireless network providers, local exchange and interexchange carriers, terminal, computer and satellite equipment manufacturers and information service providers, and their associated research and long range planning organizations. An important issue is to identify the roles that satellite networking can play in meeting these new communications needs. The unique capabilities of satellites, in providing coverage to large geographic areas, reaching widely dispersed users, for position location determination, and in offering broadcast and multicast services, can complement and extend the capabilities of terrestrial networks.

As an initial step in exploring the opportunities afforded by the merger of satellite-based and land-based networks, we are undertaking several experiments to demonstrate the joint use of satellites and terrestrial networks in the delivery of personal communications services. These experiments utilize the complementary capabilities of the local exchange network and the NASA ACTS satellite, and fall into the following domains: satellite-based two-way messaging, satellite-based delivery of personalized information services, satellite-based messaging for call control and delivery, and satellite-based subscriber location updates.

In these experiments, the NASA JPL ACTS Mobile Terminal (AMT) is being used to provide the nomadic end user with connectivity to the ACTS, and the local exchange network is being interfaced to the ACTS ground station gateway. These experiments will provide a better understanding of the interfaces needed to provide a seamless merger of satellite and land-based networks and will assist in identifying exchange and exchange access services to meet the emerging demand for personal communications. Furthermore, ways in which satellite technology can be utilized by local exchange network providers in facilitating the delivery of access services will be explored.

2. EXPERIMENT DEFINITION

The experiments involve the integration of several communications systems: the local exchange network, including Bellcore prototype personal communications applications software, the NASA ACTS satellite, the NASA ACTS earth station, and the JPL ACTS Mobile Terminal (AMT) interfaced to commercial terminal equipment utilizing Bellcore prototype application software. The following subsections provide an overview of these systems.

2.1 Personal Communications Applications Software

Bellcore has created prototype applications software that enables personalized information delivery. Two prototypes are being used in these experiments: Personal Telephone Management [1] (PTM) and Simple Information Filtering Tool [2] (SIFT).

The PTM prototype serves as an "intelligent agent" for end users, or clients, and assists in the screening and direction of telephone calls. With PTM, calls to a client are first screened, using the client's preferences contained in a personal profile, and then directed to the current location of the client. The client can, in real time, screen and re-direct calls, exchanging messages with the PTM. The prototype software runs on an experimental platform that interfaces to the local exchange network and to the NASA ACTS gateway.

The SIFT prototype uses client preferences, together with knowledge of the current location of the client, to screen, prioritize, summarize and deliver computer readable electronic messages. Designed to deliver information to people on the move, SIFT can forward a wide range of information in a form that can be read on conventional computer monitors and on the liquid crystal displays of portable or palm-top computers. This information can include the telephone numbers of callers, electronic mail, news summaries, weather reports, stock prices, etc. An easily modifiable client profile is used by SIFT to examine all incoming messages and to establish the priority of the information in relation to the current context of the client. The SIFT prototype can select from a variety of options including storing messages in electronic files, faxing them to preselected numbers, forwarding them to client colleagues, and converting them into speech for storage in an answering machine or voice mailbox.

2.2 The ACTS Satellite

The Advanced Communications Technology Satellite (ACTS) is an experimental K/Ka-band satellite that is being developed by GE under contract to NASA. It is scheduled to be launched in early July 1993 and will be placed in geostationary orbit at 100 degrees west longitude. In addition to its K/Ka-band operation, the ACTS has a multibeam antenna (MBA), a baseband processor (BBP) and a microwave switch matrix (MSM).

The MBA consists of an uplink receive antenna and a downlink transmit antenna. Basic antenna design is an offset-fed cassegrain configuration which has a

subreflector in between the feed and the main reflector. The receive antenna uses a 3.3 meter main reflector to produce "spot" beams that are approximately 110 miles in diameter. The MBA produces three basic types of spot beams. First, there are 3 pairs of "fixed" spot beams to provide coverage for users in Cleveland, Atlanta, and Tampa. Second, there are two pairs of "hopping" spot beams that can be scanned "continuously" over two large sectors in the United States. Third, there are two pairs of "scanning" beams that can be moved continuously over two large sectors in the United States.

The ACTS can be operated with either the BBP or the MSM in the transponder path. In the BBP-mode, the received uplink signal gets demodulated, decoded, baseband-processed, coded, and modulated by the BBP. In the MSM-mode, the received uplink signal gets routed by the MSM at an intermediate frequency and the signal experiences no baseband regeneration. For these experiments, only the MSM mode will be exercised. The MSM has four input ports and four output ports in a cross-bar architecture. Its sole mission is to dynamically connect any one of the four receivers to any one of the four transmitters.

2.3 NASA and JPL Ground Station Equipment

The NASA ground station at Lewis Research Center will be used as the satellite/terrestrial network gateway (S/T NG) to the public switched telephone network (PSTN) and the Bellcore equipment described above. This ground station, termed the HBR-LET, interfaces with the MSM mode of operation of ACTS. On the uplink portion of the HBR-LET, a two stage upconverter converts the signal to the 29 GHz to 30 GHz range. The uplink power is provided by a traveling wave tube amplifier (TWTA) which has a saturated power output of 85 Watts. The receiver portion of the HBR-LET consists of a four stage low noise amplifier at the front end. This is followed by a MMIC mixer and amplifier that converts the received signal from the 19 GHz to 20 GHz frequency range down to the 3 GHz to 4 GHz frequency range, where it is converted to baseband.

The JPL-provided fixed terminal equipment will interface at baseband with communications gateway facilities that will exchange messages with the Bellcore personal telephone management platform, which will be located at Bellcore facilities in New Jersey.

The JPL ACTS Terminal (AMT), including a global positioning system (GPS) receiver, has been mounted in an experiment van and will serve as the mobile

element for these experiments. The terminal controller (TC) controls the operation of the AMT. It contains the algorithms that translate the communications protocol into the operational procedures and interfaces among the terminal subsystems. For example, it executes the timing and handshake procedures for the interaction among the speech coder, modem, user interface, and any external device (i.e. data source or data sink) during link setup, relinquishment, or data rate change. The TC also has control over the operation of the IF and RF electronics. The TC, in addition, is responsible for providing the user with a system monitoring capability and supports an interface to the Data Acquisition System (DAS). Finally, the TC will support the test functions required during experimentation, such as bit stream generation, correlation, and bit error counting. In this experiment, the audio interface will be used as an "order wire" to support coordination and management of the experiment activities. Real-time, two-way voice over the satellite link is not part of the personal applications being examined.

The DAS will perform continuous measurements and recordings of a wide variety of propagation, communications link, and terminal parameters (e.g., pilot and data signal conditions, noise levels, antenna direction, etc.). The DAS will also provide real-time displays of these parameters. For this experiment, the DAS will be used to log and time stamp all messages exchanged between the TC and the user baseband terminal equipment.

2.4 User Terminal Equipment and Application Software

The experiments will utilize end user terminal baseband terminal equipment consisting of portable personal computers, telephone hand sets, and display and other input/output devices selected to emulate the functionality of future end user personal application appliances. This equipment will be designed to interface to the AMT. The Bellcore user terminal has been designed to interface with a GPS receiver located in the AMT or attached directly to the user terminal. The data collection capabilities and monitoring functions of the DAS will be used in conjunction with the Bellcore equipment to carry out the experiments.

Bellcore has created prototype application software that runs in the user terminal baseband equipment to provide user/network signaling and user information transfer. The software makes use of standard IP datagram protocols for communication with the personal telephone management platform. This software has been designed to interwork with the

AMT and with the GPS receiver.

3. EXPERIMENT PLANS

There are two different configurations for the Satellite/PCS experiments. In configuration 1, the user equipment is physically connected to the AMT equipment in the experimental van. There are four separate application scenarios for this configuration, each of which is described further in the remainder of this section. In configuration 2, the user equipment is remotely connected to the AMT via a local area terrestrial wireless network. The same four application scenarios as with configuration 1 will be tested. The attached figures provide high-level overviews of the proposed experimental setup. Figures 1 and 2 show configurations 1 and 2, respectively.

3.1 Satellite-based Two-Way Messaging

The objective here is to use satellite connectivity to send and receive electronic mail messages to nomadic end users equipped with portable computers. These computers would be capable of communicating directly with the satellite for data services. Prototype electronic mail sorting, filtering and routing software (SIFT) will be used to route high priority messages to a hybrid satellite terrestrial network gateway. Prototype application software will be used for the end user interface to the e-mail.

This experiment is shown in Figures 1 and 2 starting with the e-mail icon on the lower left. E-mail is sent to the nomadic user via the PSTN and the Bellcore software. High-priority messages are then forwarded to the satellite/terrestrial network gateway and transmitted up to ACTS. ACTS then forwards the message to the nomadic end user via the AMT (either directly or via a local area terrestrial radio link).

The experiment is designed to support the following application scenario. E-mail is sent to User A who is not in the office. The e-mail goes through the SIFT software which uses User A's personal profile to discover that this is high priority mail and must be forwarded to User A immediately. SIFT then checks the location data base to determine how to route the message to User A. If User A cannot be reached via a terrestrial network, SIFT then sends the mail to the S/T NG for transmission through the satellite to User A. When User A turns on the satellite-equipped PC, it identifies itself to the satellite and this information (user name, location, etc.) is stored in a location database at the S/T NG. Thus, when the mail for User A comes into the gateway, the gateway consults the location data base and determines where to send it. It

sends the message through the satellite directly to User A who can now access the message.

If User A now wishes to originate a message the same scenario occurs in reverse. The e-mail is sent via the satellite to the S/T NG for routing to the PTM. The message is then sent to SIFT for transmission to the recipient.

3.2 Satellite-based Delivery of Personalized Information Services

The objective here is to use satellite connectivity to deliver personalized information (e.g., headline news, financial data, weather reports, etc.) to nomadic end users equipped with portable computers. These computers would be capable of communicating directly with the satellite for data services. Prototype personal message summarizing, sorting and prioritizing software will be used to interface between information data bases and the hybrid satellite-terrestrial delivery networks. Prototype application software will be used for the end user interface to the personalized messages.

This experiment is shown in Figures 1 and 2 starting with the database icon in the center (bottom). Personalized database information is sent to the nomadic user via the PSTN and the SIFT software. It is then forwarded to the satellite/terrestrial network gateway and transmitted up to ACTS. ACTS then forwards the message to the nomadic end user via the AMT (either directly or via a local terrestrial wireless link).

The experiment is designed to support the following application scenario. This is a one-way information service initiated by User A. When the end user's satellite-equipped PC is turned on, its identity and location are sent (via satellite) to the location database at the S/T NG. User A maintains a personal profile of requests for the latest headline news, weather reports, stock quotes, etc. The profile is used by the SIFT software to filter and prioritize information received from appropriate data bases. Personal messages containing the data are then forwarded to the S/T NG for transmission to User A. The S/T NG consults the location data base to find User A and then sends the information to User A's satellite-equipped PC, enabling the end user to access the information.

3.3 Satellite-based Messaging For Call Delivery

The objective here is to use two-way satellite-based messaging to alert nomadic end users of incoming telephone calls. The message is received on a personal computer capable of communicating directly with the

satellite. Prototype call management and screening software, PTM, will be used to screen incoming calls to the end user's home location and send messages to the satellite network alerting a nomadic end user of incoming calls (name of caller and number). The end user responds via the satellite by returning a message regarding preferred call disposition, which is then processed by the PTM software. Call dispositions include routing the incoming call over the terrestrial public switched network to the current location of the end user, deflecting the call to another number, sending a text message to the caller (PTM converts to voice), etc.

This experiment is shown in Figures 1 and 2 starting with the caller icon on the lower right. A call comes in for the nomadic user via the PSTN and the PTM software. High-priority messages are then forwarded to the satellite/terrestrial network gateway and transmitted up to ACTS. ACTS then forwards the message to the nomadic end user via the AMT (either directly or via a local area terrestrial wireless link).

The experiment is designed to support the following application scenario. User A is called when he is not at his home location. The PTM software takes the call and queries a personal profile to find that User A is currently reachable only via the satellite network (i.e., User A is in a region that is not served by a terrestrial network). The PTM software then forwards information about the call (such as name of caller and number) to the S/T NG for transmission to User A. The S/T NG locates the user by consulting the location data base and passes the information along to User A in the form of a brief message. User A can then decide how to handle the call. The call handling information is then sent, via the satellite, back to the S/T NG for transmission to the PTM. The PTM can then take appropriate action to complete the call.

3.4 Satellite-based User Locating

The objective here is to use satellite connectivity plus GPS location capability to locate nomadic end users, update network data bases, and route calls and/or messages to their current location.

This application scenario is similar to several described above. However, in this case, the location of the nomadic end user A is not known to the terrestrial network. When a message (call or electronic message) is to be sent to User A, the terrestrial network queries the S/T NG for location information. A global paging message is sent out via the satellite, and User A's terminal responds with location data derived from the GPS receiver. This data is returned to

the terrestrial network location database, and the scenario continues as described above. This use of the GPS location capability has great potential in complementing terrestrial network functionality (e.g., subscriber registration) necessary to provide ubiquitous personal communications services.

4. SUMMARY

The ACTS satellite launch is scheduled for summer, 1993, and the user experiments, as described above, are planned for summer, 1994. Effort is now under way to interface the system elements and test the applications software. Independent tests of the subsystems have been carried out, including extensive use of the SIFT and PTM prototypes in terrestrial personal communications applications experiments.

These experiments will provide a better understanding of the interfaces needed to provide a seamless merger of satellite and land-based networks and will assist in identifying exchange and exchange access services to meet the emerging demand for personal communications.

REFERENCES

[1] W. S. Gifford and D. L. Turock, "The Electronic Receptionist: A Knowledge-Based Approach to Personal Communications", *ACM Conference on Computers and Human Interaction*, Monterey, CA, May, 1992.

[2] D. L. Turock and R. S. Wolff, "Making Telecommunications Nomadic", *Bellcore Exchange Magazine*, January, 1993, pp. 3-7.

* Bellcore software includes 1) SIFT software, 2) personal message summarizing, sorting and prioritizing
software, and 3) call management and screening software

Figure 1 Experimental Setup - Configuration 1

* Bellcore software includes 1) SIFT software, 2) personal message summarizing, sorting and prioritizing
software, and 3) call management and screening software
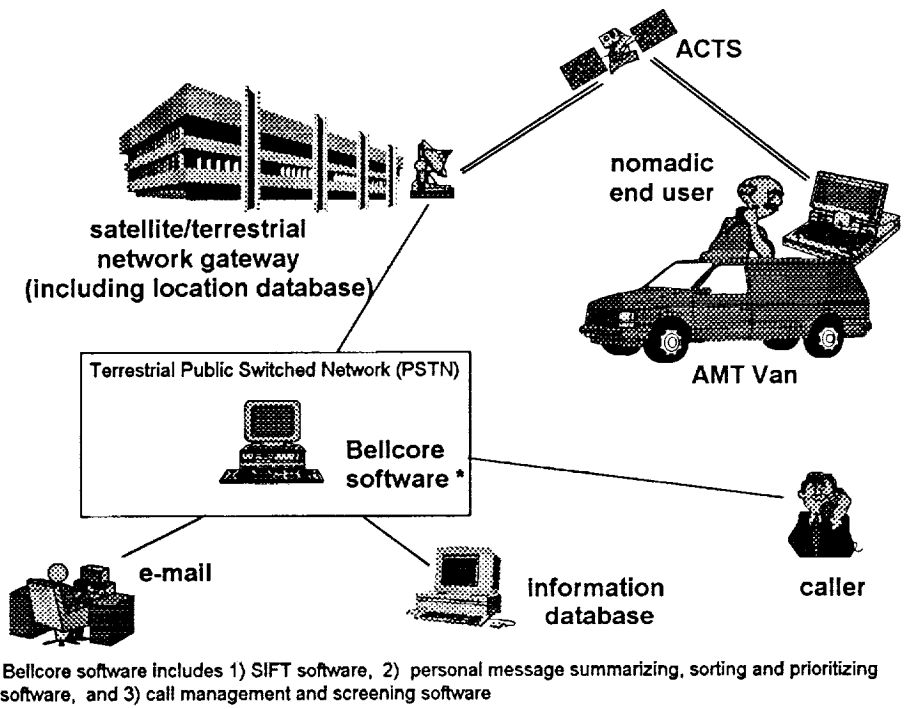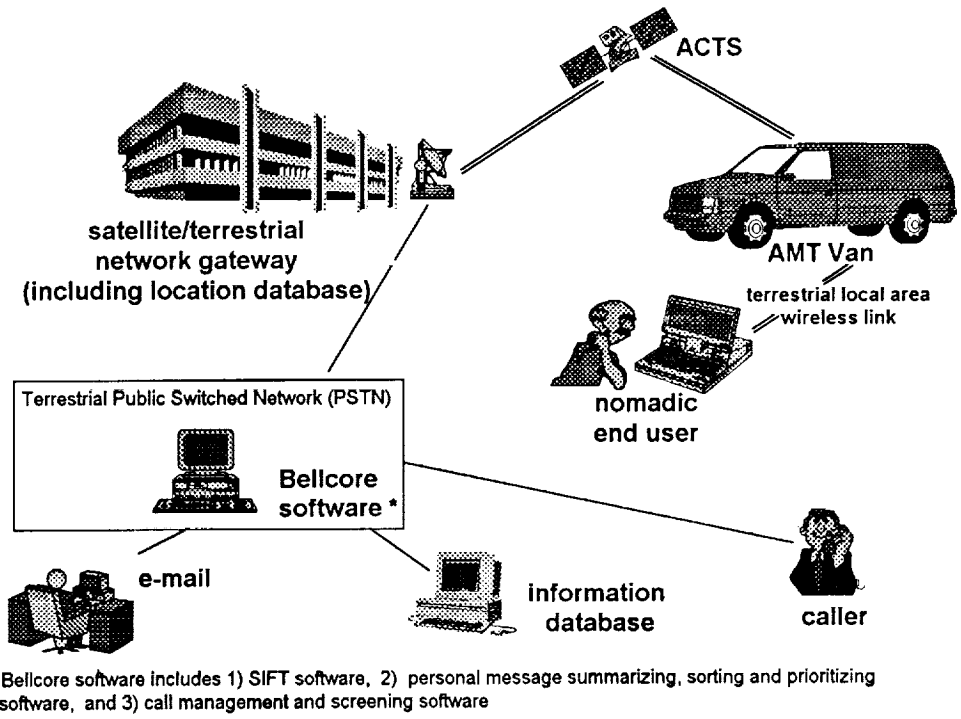
Figure 2 Experimental Setup - Configuration 2

Power Attenuation Characteristics As Switch-Over Criterion In Personal Satellite Mobile Communications

Jonathan P. Castro, Member, IEEE
Telecommunications Laboratory, Swiss Federal Institute of Technology,
CH-1015 Lausanne, Switzerland
Tel. +41 21 693 47 31
Fax +41 21 693 46 60

ABSTRACT

A third generation mobile system intends to support communications in all environments (i.e., outdoors, indoors at home or office and when moving). This system will integrate services that are now available in architectures such as cellular, cordless, mobile data networks, paging, including satellite services to rural areas. One way through which service integration will be made possible is by supporting a hierarchical cellular structure based on umbrella cells, macro cells, micro and pico cells. In this type of structure, satellites are part of the giant umbrella cells allowing continuous global coverage, the other cells belong to cities, neighborhoods, and buildings respectively. This does not necessarily imply that network operation of terrestrial and satellite segments interconnect to enable roaming and spectrum sharing. However, the cell concept does imply hand-off between different cell types, which may involve change of frequency. Within this prospective, the present work uses power attenuation characteristics to determine a dynamic criterion that allows smooth transition from space to terrestrial networks. The analysis includes a hybrid channel that combines Rician, Raleigh and Log Normal fading characteristics.

INTRODUCTION

Presently, when hand-off between terrestrial and space networks is intended, the satellite network must be part of the overall network. This means that the satellite ground infrastructure has to be interconnected with the mobile station centers and the public land mobile networks. Such interconnection would be rather complex and perhaps difficult to coordinate due to limits of national boundaries. Thus, an ideal alternative to combined coverage is an automatic scheme selection and re-selection of cells and beams while the mobile terminal is idle. The criterion is based on the fact that a mobile equipment performs initial measurements of the radio environment, then selects a network according to a programmed list of allowed networks before it indicates service availability. An important limit used to classify the network list is the power level at the receiver, which in part depends on the transmission effects influenced by shadowing and fading.

Signalization

The signal of the active link from or to the mobile terminal (MT) in a land mobile satellite system (LMSS) is continuously monitored. Thus, whenever signal degradation occurs a handover procedure is initiated towards a stronger alternative link. For integrated mobile systems, handover support would imply that the fixed network has access to both the terrestrial and satellite ground infrastructure (i.e., the satellite fixed earth stations (FES) must be directly linked to the terrestrial mobile services switching center (MSC). Considering the GSM[1] as an example, it implies that the FESs and MSCs are connected at the same level under the GSM Mobile application Part of the CCITT Signaling System No. 7. This type of connection requires close adaptation of the FES to the GSM standard to behave like the terrestrial MSC when performing handover. Furthermore, if satellite infrastructures with numerous FESs, are distributed around many countries, the interconnection of FESs with terrestrial MSCs will overlap with some Public Land Mobile Networks (PLMN) and introduce additional complications. Thus, we believe that the close internetworking of many different mobile networks into a single system, will not only be difficult to implement but will also be hard to

---

[1] Group Space Mobil, European Terrestrial mobile system.

administrate due to its complexity [1]. The question is then, how do we offer universal mobile communications without passing through a complicated design and complex system management. The following sections attempt to bring into consideration some alternatives.

POWER CHARACTERIZATION

Received power in experimental channel recordings was already illustrated in [2], nonetheless for completeness we outline a summary below. Signal attenuation in old cities with narrow streets like Munich [3], has high-frequency fading process superimposed on a low-frequency shadowing process, where relatively good and bad channel periods with an approximated mean of 15 dB are clearly distinguished. Similar observations could be made from recordings [4] in Australia. Open areas such as intercity highways, farm lands or spread suburban areas with open fields, essentially do not have obstacles on the direct line-of-sight path. Hence the received signal power has only small level variations due to multipath fading. However, there may still be total shadowing caused by bridges, trees or sporadic high mountains. In regions with vast open fields attenuation will depend primarily on the type of frequency transmission, more than on the shadowing obstacles. If transmission frequency is high (> 10 GHz), the received power level will have degradation due to atmospheric effects (i.e., rain). Nonetheless, the attenuation will not exceed 30 dB, and the mean (approximately 12 dB) remains close to the values in urban areas.

Network Selection

The MT selects a PLMN while it is idle. Hence real-time for fixed inter network interaction is not critical. Once on, the MT measures its ratio environment and indicates the available service automatically from a programmed list of allowed networks, (i.e., the Home PLMN and the ones under roaming agreements). As the MT operates over large and mixed areas, the environmental properties change and the received signal has varying statistical character. This means that the received power level cannot be represented by a model with uniform or constant parameters.

Furthermore, this implies that the channel is non stationary. Although statistical channel characteristics vary significantly over extended regions, propagation experiments show that they remain constant when areas have invariable environmental attributes. Hence, an all purpose land mobile satellite channel can be modeled as a non stationary system represented by M stationary channel models. A finite-state Markov model [4], [6] can integrate the Rician, Rayleigh and Log normal models.

Transmission Scenarios

In the context of universal personal communications, a MT will cross different environmental areas in random sequence but with probable characterization as summarized earlier. The signal propagation scenarios during a transmission event could be then classified in four independent states with the following received signal distributions:

S1	Sky-Path	High Rician dist.
S2	Clear-Path	Low " "
S3	Shadowed Path	Log normal dist.
S4	Diffused Path	Rayleigh dist.

Realistically, from the usage side, S1 corresponds to conditions when the user is traveling through the airspace, while S2 refers to transmissions in flat rural or desert areas and seas with almost uniform surfaces. S3 relates to suburban or semitropical regions with scattered high-ways and spread trees. Finally, S4 indicates communications in urban areas. It should be realized that S1 does not necessary imply 100 % signal reception, since the propagation phenomenon is subject to atmospheric effect.

State Analysis

Mathematically, the four states follow a discrete Markov chain [5], where the process has state transitions at times t_n, n = 1,2,3. . (possible into the same state). The discrete time $\{X_n\}$ (i.e., x_n for x(t)) starts in a initial state, say i when t = t_1 (x_1 =i), and makes a state transition at the next time step which is t = t_2 (x_2 = j, etc). The one-step transition probabilities are assumed to be independent of n, thus P_{ij} is the set of events for the transition

probabilities. The transition probabilities of P_{ij} for the 4 states is then expressed by a square matrix P,

$$P = \begin{bmatrix} 1-3P_1 & P_1 & P_1 & P_1 \\ P_2 & 1-3P_2 & P_2 & P_2 \\ P_3 & P_3 & 1-3P_3 & P_3 \\ P_4 & P_4 & P_4 & 1-3P_4 \end{bmatrix} \quad (1)$$

where

$$P_1 = P_{12} = P_{13} = P_{14}; \quad P_2 = P_{21} = P_{23} = P_{24}$$
$$P_3 = P_{31} = P_{32} = P_{34}; \quad P_4 = P_{41} = P_{42} = P_{43}$$

and $\quad E[i] = \dfrac{1}{3P_j} \qquad i = j = 1,2,3,4.$ (2)

To calculate the four steady state conditions, we define the probability that the Markov chain $\{X_n\}$ is in the state j at the nth step by

$$\pi_j^{(n)} = P[X_n = j], \quad (3)$$

then assume that the chain has stationary probability distribution $\pi = (\pi_1, \pi_2,...)$ satisfying the matrix equation $\pi = \pi P$, where each $\pi_j \geq 0$ and $\sum_i \pi_i = 1$. The matrix equation $\pi = \pi P$ can then be expressed as the set of equations by

$$\pi_j = \sum_i \pi_i P_{ij} \qquad j = 1,2,... \quad (4)$$

From equation (2) πj is defined by

$$\pi_j = \frac{E_i}{\sum_{i=1}^{n} E_i} \qquad j = i = n = 1,2,3,4. \quad (5)$$

The steady state probability vector is thus

$$\pi_j = [\pi_1, \pi_2, \pi_3, \pi_4]. \quad (6)$$

State Probability boundaries

The environmental states identified previously by the probability density functions, p.d.f (i.e., Rician, Log normal, and Rayleigh) depend very much on the propagation conditions defined by a parameter k, which is the ratio of power in the direct component and power in the diffuse component. k assumes that the propagation medium can be characterized by the combination of a direct path and a number of fading weak paths. The parameter k is referred to as the Rice parameter. As k --> ∞ all power is in the direct component, implying that reception is via a direct carrier line-of-sight (l.o.s) transmission from the satellite, and that the diffuse component is negligible. This condition would correspond to S1 in our model. As k --> 0, the received power is all diffuse and the received signal distribution has a Rayleigh density. Therefore, as the parameter k increases, the mobile channel passes from Rayleigh channel to a Rice channel and vice versa. This means it goes from S1 to S4.

Practically, the values for the Rice parameter depend on the reflective terrain in the vicinity of the MT, which is strongly influenced by the elevation angle of the MT-satellite l.o.s. Generally k increases significantly as the satellite is observed at higher angles, where more of the horizontal multipath is rejected. In like manner a dense collection of reflectors, as in metropolitan areas tends to produce lower values of k. Rural environment is more benign, while maritime areas involve primarily long-range sea reflections whose severity is strongly dependent on the ocean wave structure. During periods of shadowing due to trees, foliage, and terrain the Rice parameter is reduced by 3 to 10 decibels from average values and the channel state passes to S3.

NETWORK SELECTION

The selection criterion, as discussed in the introduction, is based on the power level of the received signal. Such a faded signal at any given time instant t is

$$R(t) = m(t)*\{R_{dir}(t) + R_{spec}(t)\} + R_{diff}(t), \quad (7)$$

where m(t) is the long-term signal fading with Log normal distribution. For S1 and S2 the received power is

115

$$R_{S1}(t) \equiv R_{S2}(t) = R_{dir}(t), \qquad (8)$$

assuming m(t) = 1 and neglecting the specular reflection $R_{spec}(t)$ since it is taken care by the antenna. The signal power for S3 is expressed as

$$R_{S3}(t) = m(t) * R_{dir}(t) + R_{diff}(t). \qquad (9)$$

Finally, for S4 the signal at the receiver comes mainly from the diffused power, thus

$$R_{S4}(t) = R_{diff}(t). \qquad (10)$$

The complex characteristics of the different received signal patterns just described and the spectral analysis were already presented in detail in [3], [4], [7], therefore they will not be repeated here. The fluctuation of the power level signal over a given threshold is the level-crossing rate (LCR), which influences directly the performance of the overall system. Whenever a signal goes below a threshold, the transmission quality is not warranted because there is a presence of fading implying errors [7]. Thus, using the LCR of a received signal we may calculate the BER and compare it to an expected performance. If the BER does not match a required level indicating an preassigned region, network switching process occurs. During this process the MT selects a strong terrestrial signal, sends a log-in-request and awaits log-in confirmation based on roaming agreements. While under the terrestrial coverage the MT receives periodical acknowledge-requests, if the MT does not reply, the terrestrial system sends a log-out confirmation to logout the MT, which in turn begins to listen to the satellite signal again after leaving the terrestrial link.

Switching Process

The network switching occurrences is obtained from the performance of the received signal or the conditional bit error rate (BER) probability, P_i (i = S1, S2...) which in the case of a BPSK modulation is given by

$$P_i = \frac{1}{2} erfc\left(\sqrt{\frac{E_b}{N_o}}\right) \approx Q\left(\sqrt{\frac{E_b}{N_o}}\right) \qquad (11)$$

where E_b is the signal energy per bit and N_o is the noise energy density. If we express P_i in terms of signal-to-noise ratio, S may be defined as the average power, R as the bit rate, N as the product of N_o and the signal bandwidth W; and the new P_i is

$$P_i = Q\left(\sqrt{\frac{2S}{N}\left(\frac{W}{R}\right)}\right). \qquad (12)$$

To relate the LCR to the P_i probability we first obtain N_{ro} as the number of times the received signal crosses a given threshold over a determined time period. We then calculate the normalized LCR, which from [7] is defined as

$$N_r(r_b) = \frac{v}{c} f_c \sqrt{\frac{\pi}{2(1+\rho)}} f_r(r), \qquad (13)$$

where r_b is the fading threshold, v is the vehicle speed, c is the speed of light, f_c is the transmission frequency, ρ is the correlation coefficient and f_r is the p.d.f of the signal according to the environmental state. From the ratio of N_{ro} and N_r we determine the average signal strength, S, as

$$\frac{N_{ro}}{N_r} = S \exp^{(-S_\bullet^2)}. \qquad (14)$$

The channel bandwidth, W, required to pass a M-ary PSK signal is given by

$$W = \frac{2R}{\log_2 M}. \qquad (15)$$

Thus, when the P_i probability of the received signal does not meet a service threshold quality level, the MT begins a network switching procedure (i.e., it will look a stronger signal in an alternative network).

A more dynamic way to begin the network switching process would be to measure the fading time. Because it is well understood that whenever long fading periods exist, the transmission quality will decrease due to high density of errors. originated by persisting shadowing or blocking. Thus from the

normalized LCR on equation (13), The average duration of a fade $t_f(r_b)$ relative to r_b, is equal to the probability that a transmitted signal remains below r_b divided by the number of times per unit time the signal is below r_b. That is

$$\bar{t_f} = \frac{1}{N_r(r_b)} \int_0^{r_b} f_r(r)dr = \frac{F_r(r_b)}{N_r(r_b)} \qquad (16)$$

where

$$F_r(r_b) = \int_0^{r_b} f_r(r)dr \qquad (17)$$

is the cumulative probability density function.

System Error Performance

The average bit error probability in the ith receiver state mainly due to fading attenuation as a result of shadowing or blockage is given [4] by

$$P_{si} = \int_0^{\infty} P_i f_r(r)dr , \qquad (18)$$

where f_r (r) is the probability distribution of fading attenuation in each ith state. The average BER at the output of the demodulator for the M state Markov channel model is then

$$P_{BER} = \sum_{i=1}^{M} P_{s2} \pi_i . \qquad (19)$$

EXPERIMENTAL OBSERVATIONS

The received signal power from a channel recording [3] in an area with narrow streets in the old city of Munich, shows on Figure. 4a relatively good and bad channel periods with a mean power level of 15 dB, however the bad periods are predominant for at least 34 s until a crossroad permits an obstructed view of the satellite from 928 - 932 s; but at 933 it falls again to a bad period. By contrast the received signal power from recordings on a highway, shows in Figure 4b. only small variations due to multipath fading. Although at 684 s there is total shadowing due to the blocking of a bridge, it does not last more than 2 s. All other shadowing events in this figure remain within acceptable fade margins. In the context of this study, the observation of Figure 4 indicates that the MT passes from state S3 to state S4 at

point 894, and it will probably remain in this state until it changes of environment. This may imply for example that network switching would begin when the deep fade duration exceeds 2 seconds. Of course the fade duration time would no be the only criteria for network switching, nevertheless it appears to be the most visible and measurable factor.
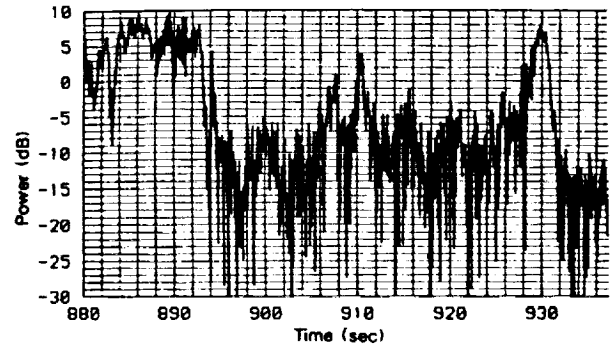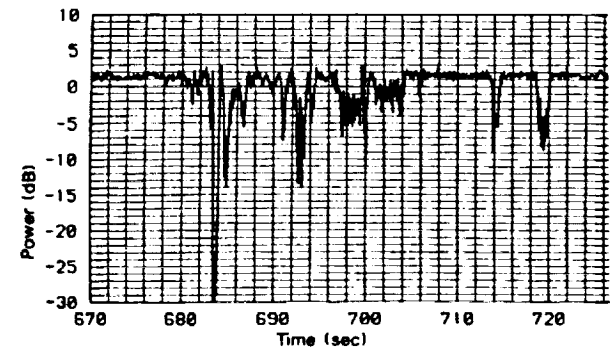
Figure 4. Received signal power level. 0 dB = mean received power. (a) City, cylindrical slot toroidal antenna with 6 dBi nominal gain, v = 10 km/h, 24 degree satellite elevation; (b) Highway, all conditions the same but v = 60 km/h [3].

Other statistical observations on the same recordings, show that in the city environments the received signal power is more than 10 dB below the unfaded satellite link at a 60 % probability , while it is only 8.5 % in the highways. This leads to deep fading periods longer than 0.1 s with 26 % probability in the city, and only 6 % in the highway [3]. Based on these type of percentages of the received power levels we can calculate the steady state probabilities of the four state model described in the preceding sections.

From preliminary simulations using the fade average technique, we can see in Figure

117

5a. that the average fading time in urban areas is logically higher than in rural or highway environments. The point to see in the plots is the magnitude of the difference between the fading periods once a link has lost the direct l.o.s with the MT, which is the case in the urban connection.
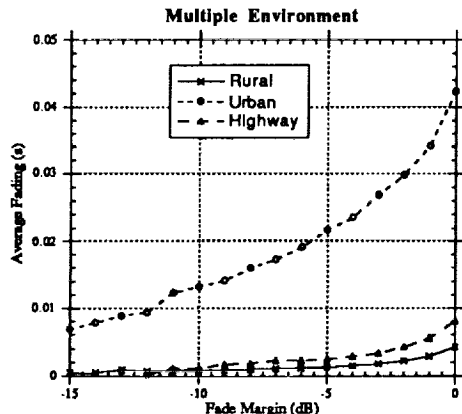
(a)
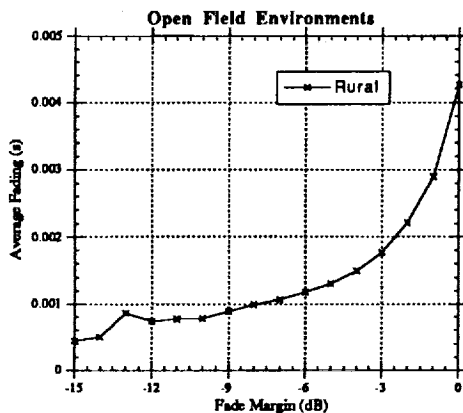
(b)

Figure 5. Average Fading. (a) Urban: v = 10 km/h, r_b = -15 dB, f_c = 1.6 GHz, k = 0 dB, Date rate = 4.5 kb/s, Highway: v = 60 km/h, k = 10 dB; (b) Rural: v = 120 km/h.

From the fading time illustrated in Figure 5b, we can observe thresholds that would lead to the initiation of the network switching mechanism. Yet again, this would not be the only factor to begin hand over; however it will be the predominant one.

CONCLUSIONS

In this paper we have discussed the complexity of an architectural level integration on mobile systems. Therefore, we have concluded that a service-level integration could be more practical, cost effective and more manageable if the MT selects a PLMN while it is idle where real-time for fixed inter network interaction is not critical. To support a universal MT that facilitates the selection and reselection of networks (i.e., the transition from satellite to terrestrial services or vice versa), we introduced a four state dual mode receiver along with the most probable mathematical analysis. In the study we also illustrated that fade duration would be a good dynamic alternative of network switching to that of calculating the BER probability. Future studies will include further characterization of experimental data and more simulation analysis to quantify state transition thresholds to adequately predict network switching.

REFERENCES

[1] Dzung D., "Link Selection and Handover Procedures in Mobile Communication Systems." ABB Corporate Research Communications Group, Int. Rept., Nov. 1990.
[2] J.P. Castro, "Cell selection and Reselection in Universal Satellite Mobile Communications," COST 227 TD(93)07 doc., Bradford, UK, Febr. 1993.
[3] Lutz E. et al., "The Land Mobile Satellite Communications Channel- Recording, Statistics and Channel Model," IEEE Trans. on Veh. Tech., vol. 40, no. 2, pp. 375-385, May 1990.
[4] Vucetic B. and Du J., "Channel Modeling and Simulation in Satellite Mobile Communication Systems," IEEE Journal on Select. Areas in Comm., vol. 10, no. 8, pp. 1209-1218, Oct. 1992.
[5] A.O. Allen, "*Probability, Statistics, and Queueing Theory with Computer Science Applications*," Academic Press, 2nd Ed. pp. 219, 1990.
[6] McCullough R. H., "The binary generative channel," Bell Syst. Tech. J., pp. 1713-1735, Oct. 1968.
[7] Castro J. P., "Statistical Observations of Data Transmission Over Land Mobile Satellite Channels," IEEE Journal on Select. Areas in Comm., vol. 10, no. 8, pp. 1227-1235, Oct. 1992.

Integration of Mobile Satellite and Cellular Systems

Elliott H. Drucker
President, Drucker Associates
12124 N.E. 144th Street
Kirkland, Washington 98034 USA
Tel: (206) 820-3411   Fax: (206) 820-3411

Dr. Polly Estabrook, Deborah Pinck, Dr. Laura Ekroot
Jet Propulsion Laboratory, California Institute of Technology
4800 Oak Grove Drive
Pasadena, California 91109 USA
Tel: (818) 354-2275, (818) 354-8041, (818) 393-1330   Fax: (818) 393-4643

ABSTRACT

By integrating the ground based infrastructure component of a mobile satellite system with the infrastructure systems of terrestrial 800 MHz cellular service providers, a seamless network of universal coverage can be established. Users equipped for both cellular and satellite service can take advantage of a number of features made possible by such integration, including seamless handoff and universal roaming.

To provide maximum benefit at lowest possible cost, the means by which these systems are integrated must be carefully considered. Mobile satellite hub stations must be configured to efficiently interface with cellular Mobile Telephone Switching Offices (MTSOs), and cost effective mobile units that provide both cellular and satellite capability must be developed.

INTRODUCTION

Commercial cellular systems have been in operation in North America for over ten years. Coverage has extended beyond urban centers to rural areas, with more territory falling under cellular coverage each year. Nonetheless, there are still vast stretches of land without cellular coverage in North America, and in many parts of the world cellular is limited to the largest cities.

A number of satellite systems have been proposed to provide mobile telephone service to remote areas of land as well as to ocean and airborne traffic. Because each of these is to a certain extent limited in capacity, it makes sense to use cellular, where it is available, for mobile traffic and to limit the use of mobile satellites to other locations. Current technology allows for very small, lightweight, and inexpensive cellular mobile terminals, so that adding cellular capability to a mobile satellite terminal should not pose a significant penalty. Integration of the cellular and satellite infrastructure systems will provide to the suitably equipped user the ability to operate without coverage boundaries, and to roam anywhere while receiving and making calls in a truly seamless network.

MOBILE TERMINAL ARCHITECTURE

To operate in both satellite and cellular systems, a mobile terminal must, of course, include radio equipment compatible with both. While some mobile unit baseband processing functionality, such as speech codecs, may be common for the two systems, the antenna and radio frequen-

cy (RF) portions will likely be so dissimilar as to require separate mobile hardware. This requirement suggests an architecture for dual mode satellite/cellular mobile terminals as shown in Figure 1.

A single handset/control unit, along with suitable system operating protocols, allows for a single user interface, both in terms of hardware and functionality. From the user's standpoint, operating procedures in satellite and cellular systems can be identical.

A common controller manages the interface to both the satellite and cellular transceivers and houses common functional components such as, possibly, the crystal frequency standard, baseband processing, repertory dialing memory, etc.

The cellular transceiver may operate using one or more of the North American or international analog or digital cellular standards. For reasons examined below, the cellular transceiver must be capable of operating in the cellular "idle" mode even while the satellite transceiver is in conversation mode.

The mobile satellite transceiver must be capable of "idle" mode operation even while the cellular transceiver is in conversation mode. It must also be capable of determining at any time the presence or absence of suitable satellite coverage.

INFRASTRUCTURE INTEGRATION

Calls to and from mobile satellite terminals are interconnected to the public switched telephone network (PSTN) at one or more satellite hub stations (SHS). Calls to and from cellular mobile terminals are interconnected to the PSTN at a mobile telephone switching office (MTSO). To support seamless handoff to and from cellular, the SHS must be connected to the MTSO by dedicated voice trunks. This is because the PSTN does not support rerouting of calls in progress. A call that originates on cellular, through an MTSO, will have to continue to be interconnected to the PSTN through that MTSO even after it is handed off to the satellite system.

To provide the connectivity required for satellite/cellular handoff, the SHS may appear to the cellular system either as an MTSO or as a cell site.

Hub Station as MTSO

Figure 2 illustrates the connection of an SHS as an MTSO. Connection to various MTSOs serving areas subtended by the satellite service is by IS-41 handoff links. "IS-41" refers to the industry standard that governs intersystem operation, including MTSO-to-MTSO handoff, for North American cellular systems.

Using this configuration, calls originated through the SHS would be handed off to cellular through the use of a voice trunk on the dedicated handoff link connecting the SHS to the "target" MTSO. Similarly, calls originated through an MTSO would be handed off to satellite service using a voice trunk on the handoff link connecting that MTSO to the SHS.

Hub Station as Cell Site

Figure 3 suggests an alternative interconnection between SHS and MTSO. Here, the link is the same used to connect cell sites to the MTSO. In North American systems, there is currently no standardization for this link, so details of the connection would be proprietary to the manufacturer of the cellular system.

While Figure 3 shows direct interconnection between the SHS and the PSTN, the MTSO could provide such interconnection for calls originated on the satellite system, just as it does for cellular calls. In addition, this configuration would allow the MTSO to perform switching and subscriber data base maintenance functions for the SHS. Such an arrangement could significantly reduce the cost of a hub station.

Hub Station Distribution

In cellular, intersystem handoffs generally occur between MTSOs serving adjacent areas, since it

is the movement of a mobile between such areas that precipitates the handoff in the first place. Thus, to fully support intersystem handoff, each MTSO needs handoff links only to adjacent MTSOs, typically a manageable number.

If the mobile satellite system to be integrated with cellular makes use of a single, centrally located hub station, then this SHS would require handoff links to each of the potentially hundreds of participating MTSOs in the national cellular network, as illustrated in Figure 4. The impracticality of this arrangement could be mitigated somewhat through tandem switching of intersystem links. However no protocols currently exist for such tandeming, and the adjacency limitation on MTSO-to-MTSO handoff described above limits its potential economic advantage.

The mobile satellite system may employ multiple, regionally distributed hub stations, as suggested in Figure 5. Such distribution may be a requirement of the satellite system architecture or may be by design in order to optimize integration with cellular. At any rate, each such regional SHS would have to maintain handoff links only to the MTSOs that service the same areas as the SHS. While the number of such links may still be large, especially if the number of regional SHSs is small, the average length of the required link will be greatly reduced compared with the single, centrally located SHS configuration.

In some mobile satellite systems it may be practical to use a large number of small, low capacity hub stations, perhaps modeled after VSAT terminals, for PSTN interface and cellular integration. In such a system, each participating MTSO could be equipped with its own SHS, most likely connected to the MTSO as a cell site. Such an arrangement is illustrated in Figure 6.

While the "SHS per MTSO" configuration is architecturally attractive for handling handoffs between satellite and cellular systems, it raises a number of difficulties as well. Primary among these is positional ambiguity. A call originated on the satellite system must be interconnected through one of perhaps dozens of SHSs within

the service area of the geostationary satellite's beam or the low earth orbit satellite's coverage footprint. To allow for subsequent handoff of the call to cellular, the SHS selected for the point of interconnect must be the one nearest to the position of the mobile unit being served. However, barring the addition of positioning capability such as GPS or LORAN, neither the mobile unit or the infrastructure equipment can make this determination.

INTERSYSTEM CALL PROCESSING

Registration and Call Delivery

In the cellular system, seamless roaming requires that incoming calls for a roaming mobile be automatically forwarded, or "delivered" from the mobile's home system to the system on which it is currently operating. The call delivery system relies on the mobile's manual or autonomous registration upon entering a "foreign" system. When a mobile so registers, its home system is alerted through an administrative data network to set up call forwarding to a temporary directory number that routes the mobile's incoming calls, via the PSTN, to the appropriate MTSO.

Integration of mobile satellite service into the cellular network creates some added complexity for call delivery. A roaming mobile may be intermittently in cellular coverage while traveling at the fringe of a system's service boundary, and simultaneously be in continuous satellite coverage. It is in just such situations that integration of satellite and cellular systems provides maximum advantage. However, frequent registration, and subsequent frequent changing of call delivery target numbers as a mobile moves in and out of cellular coverage, is impractical.

One possible approach to addressing this problem is "hierarchical call delivery". In this scheme, the roaming satellite/cellular mobile registers as usual on the cellular system with the exception that the registration message is expanded to include identification of current satellite coverage, if any, and an indication of

121

whether the user wishes calls to be delivered to the satellite system if the mobile is not currently in cellular coverage. If the mobile is outside of cellular coverage for a predetermined time, it registers on the satellite system. When a call to the satellite/cellular mobile is received by its home system, it is forwarded first to the system (cellular or satellite) on which it last registered. If the target is a cellular system, and if the mobile's registration included a satellite coverage indication, then the call could be forwarded again to the satellite service if it fails to respond to a page on the cellular system.

Satellite/Cellular Handoff

Handoff of calls in progress between satellite and cellular is required to extract maximum benefit from integration of the two systems. When a mobile operating on cellular reaches the limit of coverage, the call is dropped - a situation that need not occur if the call could be handed off to a mobile satellite system. On the other hand, when a mobile originates or receives a call while momentarily in a cellular coverage "hole" there is no need for the entire call to be conducted over scarce and expensive satellite channels if a handoff to cellular could be initiated upon leaving the coverage hole.

Coverage and propagation characteristics of the satellite and cellular systems are quite dissimilar. Therefore, handoff from cellular to satellite will require a different protocol than handoff from satellite to cellular, and both will necessarily be different from conventional cellular handoff.

Protocols for satellite/cellular handoffs can take advantage of the practical requirement for separate cellular and satellite transceivers in the mobile unit, as suggested in Figure 1. Thus, while engaged in conversation mode on one system, the mobile unit can scan for, monitor, and communicate on the control channels of the other.

Cellular to Satellite Handoff

In conventional cellular handoff, the system must determine the location of the mobile relative to coverages of the surrounding cells in order to determine the correct "target" cell. When a mobile is to be handed off from cellular to the mobile satellite system, no such location process is required, because the coverage of even the most tightly constrained satellite coverage beam will be vastly larger than, and totally subtend, even the largest cell. What is required, however, is a determination that, at the time of the handoff, the mobile is within satellite coverage and not, for instance, shadowed by overhead structure or terrain. A handoff from poor cellular coverage to satellite could substantially improve the quality of a call. On the other hand, if the mobile is parked under an overpass at that moment, such a handoff could result in an unnecessary dropped call.

One way to ensure that the mobile is receiving satellite coverage prior to a handoff is to query the mobile using the data messaging feature of cellular voice channels. The mobile would then respond with a data message that indicated the quality of its current reception of the satellite's control channel. Based upon this information, the cellular system could make a determination as to whether a handoff to satellite is warranted.

Satellite to Cellular Handoff

Two characteristics make satellite to cellular handoff unique. First of all, to conserve scarce satellite channels, such a handoff will ideally occur when the mobile enters or reenters adequate cellular coverage. Second, there is no practical way that the satellite system can by itself determine which of potentially hundreds of subtended cells should be the handoff target. To address these characteristics, satellite to cellular handoff most likely will be initiated by the mobile unit, possibly as follows.

122

While engaged in conversation on the satellite system, a mobile unit will scan for cellular control channels using its cellular transceiver. When a channel is received with suitable signal level as indicated by a predetermined formula, the mobile unit will send a message on that cellular control channel requesting a handoff from the satellite system. Using an administrative data link, the cellular system will forward the request to the serving satellite system, which will, in turn, set up the handoff to the MTSO and cell defined by the mobile's control channel transmission.

CONCLUSION

The integration of mobile satellite and cellular systems appears to provide advantages to the mobile user. Such integration will require appropriate configuration of a dual mode mobile unit, the integration of satellite and cellular infrastructure systems, and the development of protocols to handle intersystem call processing. This paper, in suggesting possible (but not necessarily optimal) approaches to each requirement, indicates that full satellite/cellular integration is practical.
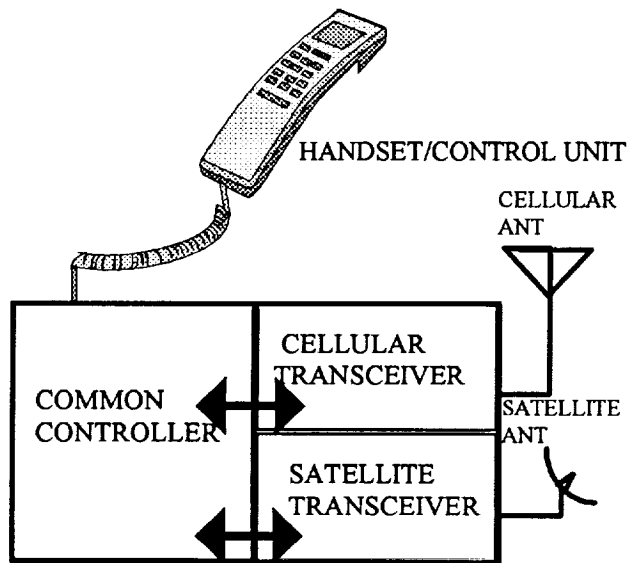
Figure 1. Satellite/Cellular mobile architecture
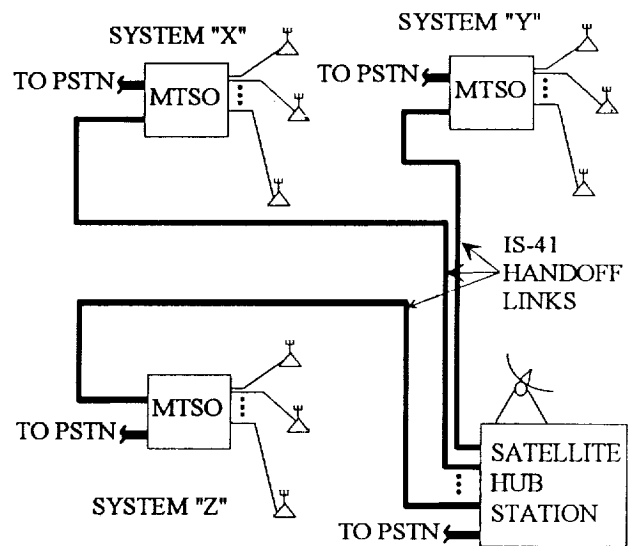
Figure 2: SHS connected to cellular as MTSO
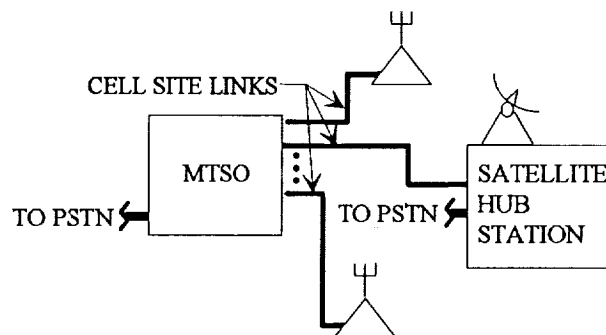
Figure 3: SHS connected to cellular as cell site

123
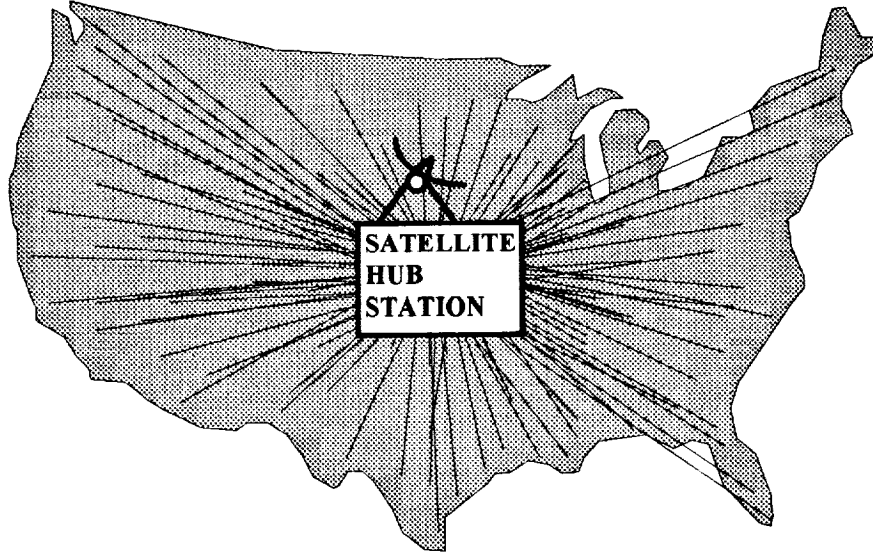
Figure 4: IS-41 links from single, centrally located SHS
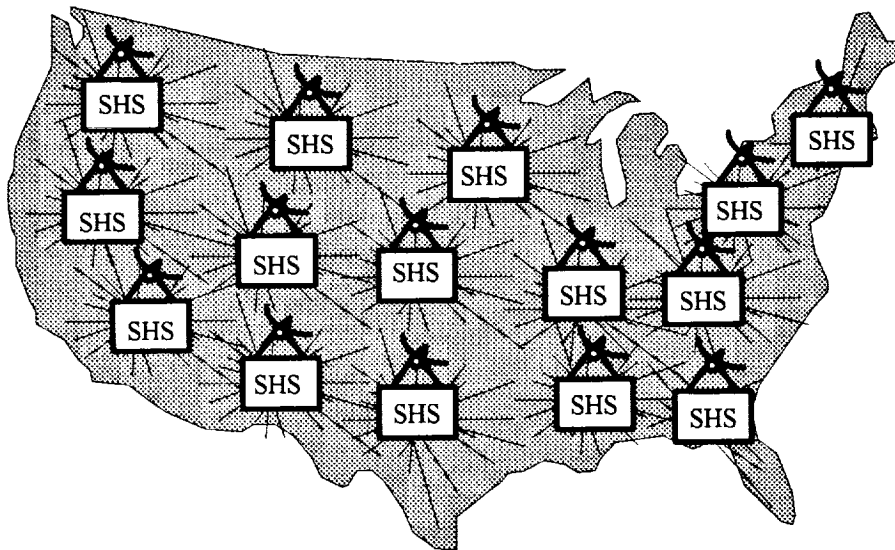
Figure 5: IS-41 links from regional satellite hub stations
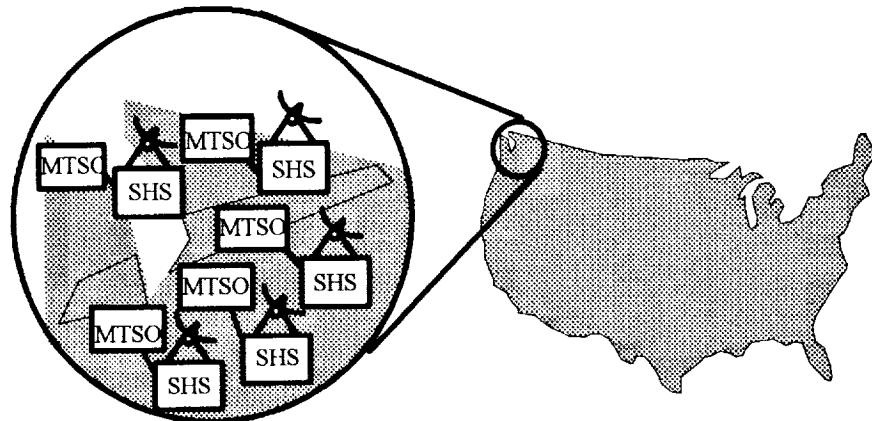
Figure 6: Satellite hub station at each MTSO

Interworking Evolution of Mobile Satellite and Terrestrial Networks

R. Matyas, P. Kelleher, P. Moller
MPR Teltech Limited
Suite 2000, 320 Queen Street, Ottawa
Canada K1R 5A3
Telephone: 613-563-1572
Facsimile: 613-563-0585

T. Jones
Inmarsat
40 Melton Street, London
England NW1 2EQ
Telephone: 44-71-728-1393
Facsimile: 44-71-728-1625

ABSTRACT

There is considerable interest among mobile satellite service providers in interworking with terrestrial networks to provide a universal global network. With such interworking, subscribers may be provided a common set of services such as those planned for the Public Switched Telephone Network (PSTN), the Integrated Services Digital Network (ISDN), and future Intelligent Networks (IN's).

This paper first reviews issues in satellite interworking. Next the status and interworking plans of terrestrial mobile communications service providers are examined with early examples of mobile satellite interworking including a discussion of the anticipated evolution towards full interworking between mobile satellite and both fixed and mobile terrestrial networks.

INTRODUCTION

Mobile Satellite Services (MSS) were first introduced in 1979 by Inmarsat and its member signatories to provide communications to ships at sea. These services have been systematically extended to include land and air applications. Service is now provided worldwide through satellites in each of four ocean regions. Australia is the first to have a domestic full service system with the launch of AUSSAT B1 in 1992. North America will be the first to have a regional telecommunications system (MSAT) with deployment scheduled for 1994 (messaging-only systems are now in operation by TMI in Canada, and AMSC and Qualcomm in the U.S.). These current generation systems are all based on the use of conventional geostationary satellites. Systems using a number of non-geostationary satellites are being proposed (Inmarsat P, Odyssey, Aries, Ellipsat, Iridium, Globalstar) that will provide communications to hand-held terminals around the turn of the century.

Fundamental to all of these systems is a desire to interwork with the existing terrestrial fixed and (in some cases) mobile networks. Interworking is the capability of separate networks to provide transparency for a common set of services and features. Of interest are those to be made available in the PSTN, the ISDN and the IN e.g. Universal Personal Telecommunications (UPT).

Furthermore, while the current focus in mobile networks is on providing terminal mobility there is an interest to eventually provide personal mobility as is being proposed for the UPT service. Terminal mobility refers to the capability of the network to keep track of and communicate with the user's terminal while that terminal is in motion. Personal mobility will remove the association of the user and a specific piece of equipment. The following discusses the evolution of the terrestrial and satellite networks to provide an overview of the trends towards global interworking. The focus in this paper is on network structure, access and management and service attributes, not on specific transmission technologies used.

ISSUES IN INTERWORKING

Interworking requires that the networks recognize, coordinate and route inter-network calls. In addition, bilateral agreements are needed between terrestrial and satellite service providers for billing and funds transfer.

A key issue in interworking a mobile satellite system with a terrestrial system is mobility management. A typical satellite system will consist of a single coverage beam, a population of mobile terminals (MT's), a Network Control Station (NCS) and a gateway (GW). The NCS is responsible for intra-satellite system control including satellite channel allocation and network management. The GW is the interface to the PSTN. The next level of system complexity is one where the satellite has several spot beams. Here the PSTN interface can be (1) one GW that can communicate with the MT's in all the beams or (2) a network of GW's distributed among the spot beams.

The latter case serves to reduce the terrestrial backhaul component of the overall connection when the GW selected is the one closest to the PSTN subscriber. The next level of complexity is a system that uses several spot beam satellites to provide, at its fullest capability, worldwide continuous coverage. Here, in each satellite's coverage area GW's located in several countries will provide access to the PSTN via international trunks.

The two inter-network call types, MT-originated (MTO) and PSTN-originated (PSTN-O), differ in their interworking requirements. For a MT-O call, the MT will signal the NCS (or a desired GW if the NCS function is devolved to GW's) to establish a call. While the NCS performs mobility management within its network, in this case there is no need for mobility management between the satellite and terrestrial systems. The GW will in turn coordinate call set-up with the PSTN based on the destination subscriber's phone number. For a PSTN-O call, it is necessary to (1) indicate to the PSTN that the call is being made to the satellite network and (2) to establish the location of the MT in order to establish the appropriate GW access and routing between the PSTN and that GW.

Subscriber mobility management between the networks is facilitated by (1) a unique code that identifies a database containing the mobile's location, (2) inter-network signalling, and (3) subscriber databases. In a mobile environment these databases will include the subscriber's service profiles as well as location registers. With a satellite network unique access arrangement, the calling party need not know himself the location of the mobile destination; the networks will know that the call is to the satellite system and will coordinate the appropriate routing.

While cellular and satellite mobile systems can operate autonomously, there is considerable interest in providing an inter-network roaming capability between such networks. Mobile roaming permits a subscriber to be serviced by one or more network providers. The mobile network in which a subscriber is normally registered is known as the "home" system whereas other networks are the "visited" systems. Subscriber roaming requires that a mobile network (1) detect the presence and determine the current location in the network of a roaming subscriber, (2) authenticate his identity, and (3) obtain his home service feature set. These functions require the deployment of location registers (databases) and the use of inter-network common channel signalling.

Efforts are being directed towards providing inter-cellular/MSS roaming by providing the subscriber with a dual mode terminal. The normal mode of operation is through the cellular system with access to the satellite system when the subscriber is beyond cellular coverage. Ultimately one terminal could provide universal ubiquitous access to the networks as described below.

TERRESTRIAL NETWORK EVOLUTION

The evolution of the fixed public, mobile terrestrial and mobile satellite networks is described in terms of network architecture, services and access. Figure 1 depicts an overview of their evolution. Coarse time frames are provided.

Fixed Network Evolution

The fixed public network has evolved from one providing Plain Old Telephone Service (POTS) to one of sophisticated features, flexibility and bandwidth. The ISDN is being implemented in many countries as an architecture which will support integrated voice, data and image services through standard interfaces over twisted-pair telephone wire to a subscriber's wall jack. Telephony enhancements include features such as call forwarding, calling line identification, among others. Two levels of service are planned: a Basic Rate (BRI) Service will provide two 64 kbps and one 16 kbps channels while Primary Rate (PRI) Service will provide 23 and 30 channels depending on the country. ISDN planners are now developing broadband networks with subscriber interfaces ranging from 32-138 Mbps.

The IN is an infrastructure that allows enhanced services (e.g. 800, automatic calling card, and Private Virtual Network services) to be deployed quickly and widely without requiring modifications to be made to every switch in the network. A typical IN structure is shown in Figure 2. A subscriber's special call request is intercepted by the IN switch which sends a query to the database for the information needed by the switch to complete the call. The operating support system administers network and customer information residing in the database. The Advanced IN (AIN) will allow rapid and customized development of new sophisticated services.

The UPT service will provide ubiquitous personal mobility within and across multiple types of networks. This is accomplished through the use of a unique personal telecommunications (PT) number that identifies a user rather than a piece of equipment. Prior coordination is required between visited and home service providers to extend UPT to roaming subscribers.

Terrestrial Mobile Evolution

First Generation Systems

First generation cellular radio systems are based on analog radio transmission technology. As shown in Figure 3 a typical analog system consists of four elements : (1) the Mobile (or portable) Terminal (MT), (2) the Base Station (BS), (3) Mobile Switching Centre

(MSC) and (4) element connectivity. The MT provides access to the BS via the radio interface. The BS under MSC control manages all MT activity within its assigned cell area. The BS allocates radio channels, performs signalling and performs BS maintenance functions.The MSC is the central switching and control element for all calls between the PSTN and the BS's, as well as for MT to MT calls. The MSC monitors MT status as relayed by the BS's (e.g. on/off hook), controls MT handoff between adjacent cells in conjunction with BS's, reacts to network maintenance indications and collects customer billing data.

Unlike the European analog systems which employed differing standards, the Advanced Mobile Phone Service (AMPS) was adopted as a single analog standard in North America. A high market penetration was achieved in North America to the point where systems are now capacity-limited.

Second Generation Systems

The second generation cellular systems currently being deployed employ digital technologies in the core and radio access portions of the network (see Figure 3). In addition to more efficient use of the spectrum based on the use of digital voice compression, these new systems are characterized by distributed network intelligence, the implementation of databases, and the standardisation of network interfaces. The strategic location of intelligence (e.g. databases) allows for the centralization of relevant subscriber information for intra- and inter-network access supporting for example national/international roaming. The deployment of digital capabilities in the cellular core network together with common channel signalling between MSC's in different networks allows for the real time exchange of routing information pertaining to the location of visiting subscribers thereby providing an automatic roaming feature based on the use of one directory number (DN) without the need for a separate roamer number. An MT is assigned a DN by a cellular service provider. Blocks of DN's are allocated to an MSC and because the MSC is associated with the PSTN exchange with which it interfaces, the DN's are used by the PSTN for cellular call routing. The digital MSC can also provide PSTN services such as Call Waiting, Call Forwarding, and Voice Messaging.

Second generation systems include location register functions which provide (1) stable information on subscribers normally registered in an area, (2) dynamic information on subscribers visiting an area, and (3) data for MT/subscriber authentication when service is requested in an area. The MSC has access to the location registers for information on the current location of its own and visiting subscribers. Common channel signalling techniques support call control and associated service features.

Second generation systems will support both telephony and data services. Out-of-band MT signalling will facilitate (1) cell-to-cell handoff which assures non-disruptive data service, and (2) ISDN-type features such as Calling Line Identification, and Completion of Calls to Busy Subscribers.

The evolution to digital is expected to be slow in North America into the mid 90's as many analog terminals are already in service. This will result in a dual analog/digital mode service as a transition strategy (per TIA specification IS.54).

In Europe and in some parts of Asia the diversity of first generation standards is to be replaced by the second generation Global System for Mobile (GSM) telecommunications TDMA standard. In North America similar systems are being implemented using the TIA IS.41 series of specifications. A major area of contention for digital cellular has been the method of air access with TDMA endorsed and being tested by some carriers and CDMA by others.

Third Generation Systems

Research activities are underway to merge cellular, cordless and paging technologies in a third generation system which will be available about the year 2000 when second generation systems are expected to reach full capacity. The intent will be to provide subscribers with universal wireless access from most locations to all current and advanced service features including POTS, personal mobility, and in microcellular coverage areas, data services up to PRI-ISDN.

Third generation systems are in the relatively early stages of definition. Important areas to be addressed include a network architecture with standard physical and protocol interfaces, equipment specifications which ensure interworking compatibility with different service providers, a common spectrally efficient air interface to support all types of wireless terminals and sophisticated techniques for subscriber mobility management in pico, micro and macro cell environments. The expected substantial signalling and control traffic may necessitate the development of higher capacity and faster packet protocols and associated networks.

Personal Communications Services (PCS) encompass wireless services including second generation cordless telephone in personal communications networks (PCN). The first generation cordless services were restricted to telepoint public environment systems and in the home. PCN's are systems based on the IN architecture and permit two-way calling, handoff between cells , and support of ubiquitous coverage. PCN technology is broadly similar to that in cellular

networks. However, the cells will operate in higher RF bands and be smaller. This will improve communications quality and increase network capacity. Also, the handsets are expected to be smaller and less expensive. PCS embodies the concept of a portable telephone and a unique telephone number. On the road the portable unit would operate like a cellular phone. At home or at the office the unit would be a cordless handset operating with the office PBX or the home telephone connection.

The ITU-defined future public land mobile telecommunications systems (FPLMTS) is a concept incorporating terrestrial- and satellite-delivered PCS services (see Figure 4). This will provide voice and non-voice services including personal communications with regional and international roaming. The World Administrative Radio Conference (WARC92) identified the spectral bands of 1885-2025 and 2110-2200 MHz for worldwide implementation of FPLMTS. A co-primary allocation of the bands 1980-2010 and 2170-2200 MHz was made to MSS allowing for a possible satellite component of FPLMTS. The latter provides a unique opportunity for a common satellite/ terrestrial mobile radio.

In 1988 the Commission of the European Communities launched its Research on Advanced Communications for Europe (RACE) program focused on creating the third generation Universal Mobile Telecommunications System (UMTS) by the turn of the century. UMTS will provide the functionality of cellular, cordless and paging services ubiquitously with a smart card ability which can be used to direct calls to a message system, screen calls, or answer more than one line. The UMTS recognizes the need for a unified standard at least in Europe. This is a parallel activity to that of the CCIR for FPLMTS. UMTS would include voice, video, data services and support BRI-ISDN and possibly higher rates in special environments. UMTS would use IN concepts. System functions such as location registration and handover could be handled by service control functions which offer the flexibility of service provisioning and tailoring. Elsewhere, the Wireless Information Network Laboratory (WINLAB) at Rutgers University is presently performing research into switching architectures and transmission techniques for third generation wireless networking. In Japan, NTT is performing research into an infrastructure which will support mobile-ISDN, IN and UPT services. This network is called the Intelligent Digital Mobile Communications Network (IDMN).

MOBILE SATELLITE NETWORKS

The current generation of mobile satellite systems include those presently in operation worldwide by Inmarsat and domestically in Australia as well as the regional MSAT to be launched in 1994 North America. Inmarsat operates a number of systems including Inmarsat A for high quality voice and data, Inmarsat C for store and forward data and Aeronautical for aeronautical voice and data. Inmarsat B is being phased in as a digital replacement for the original A system. Inmarsat M which will share a common access control and signalling system with B but will provide a lower cost alternative by using lower speed voice compression and lower rate data (facsimile optional) to smaller mobile and transportable earth stations. These systems all interface to the public networks through GW's called Land Earth Stations or Coast Earth Stations. The Inmarsat 1 and (the more powerful) 2 satellites use global beams whereas the Inmarsat 3 satellites (circa 1995) will operate through spot beams.

In Inmarsat M the MT may establish service by requesting a channel from an LES in its current ocean region. The selection of the LES and the implicit PSTN connection are made by the MT operator. A call from the fixed network is automatically routed to the international gateway in the originating country, and then routed to the LES supporting the dialled country code. Mobility is provided within whole continental regions, and global mobility is being studied. Inmarsat is investigating the possible use of a single network access code which would allow access from the public network without prior knowledge of the MT's location. This could require the establishment of location registers and call routing procedures for the desired MT. Interworking of M with cellular systems is being studied.

The Australian system which is called **mobilsat** is the first domestic system to provide voice/fax/data and packet switched messaging services. The AUSSAT B1 satellite provides a single national beam. A full duplex public telephony service provides connections to the PSTN and the ISDN via a gateway. Private network telephony, data and special services (e.g. emergency, position reporting) will be offered through shared or private base stations. A **mobilsat** Special Network will also be able to be interconnected to other mobile radio networks. This will be made using the customer's PABX as a common connection between the networks. An adaptor unit will be needed between the radio network and the PABX.

A form of interworking will be implemented in the MSAT system (US portion) where MT's will be required to operate in a dual cellular/satellite mode (referred to as Mobile Telephone Cellular Roaming Service). A subscriber's MT will give first preference to operation as a cellular radio, opting for operation within the MSAT system only when out of cellular coverage. Calls can originate either from the PSTN or the MT;

MT to MT calls are also allowed.

Inmarsat is in the process of defining its Inmarsat P system for hand-held terminals. P represents a natural evolution from the M, C and satellite paging systems being implemented worldwide.

With the capability of MSS systems to be deployed more rapidly at the global level than terrestrial systems, Inmarsat has adopted an interworking philosophy that is independent of the specific satellite network technology used. The intent is to have Inmarsat P as compliant as possible with the applicable CCIR FPLMTS interworking recommendations in the timescale for introduction. Should these recommendations accommodate from the outset the different technologies and parameter ranges, e.g.

transmission delay, satellites with/without (i) on-board processing, (ii) inter-satellite links, (iii) in-call satellite-to-satellite hand-off, then the likelihood of a mutually beneficial evolution of terrestrial and satellite networks will be greatly enhanced.

SUMMARY

This paper has summarized the evolution of the terrestrial fixed/mobile and satellite mobile networks. Most significant is the trend towards a service convergence whereby the subscriber will, through a compact handset, be provided ubiquitous and universal access to the fixed and mobile networks.
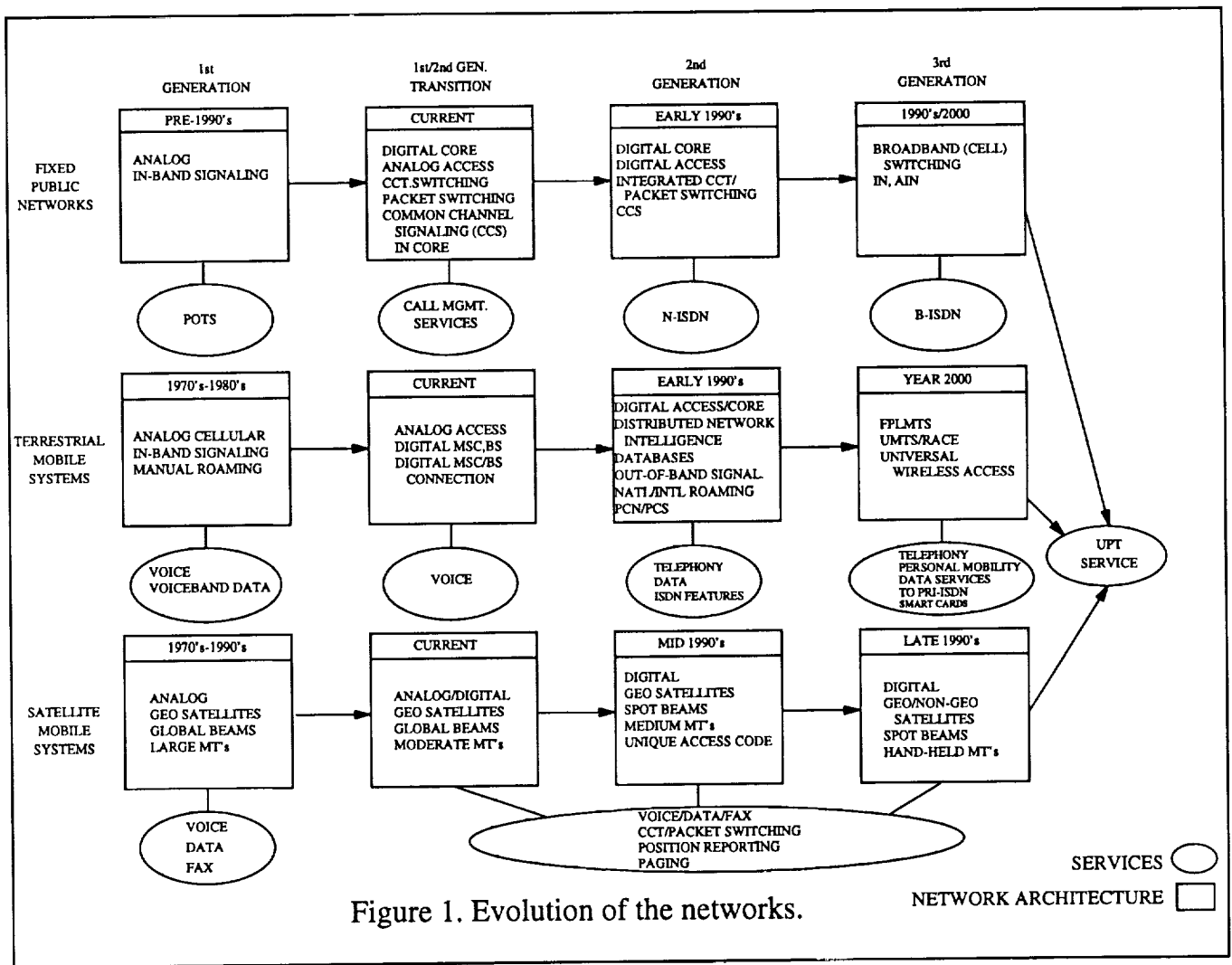
Figure 1. Evolution of the networks.

129

Figure 2. Intelligent network (IN) architecture.

MT/PT = MOBILE/PERSONAL TERMINAL   PSTN = PUBLIC SWITCHED TELEPHONE NETWORK
BS = BASE STATION   HLR = HOME VISITOR REGISTER
MSC = MOBILE SWITCHING CENTRE   VLR = VISITOR LOCATION REGISTER

Figure 3. Typical first and second generation cellular systems.

Figure 4. An example of a FPLMTS network.

130
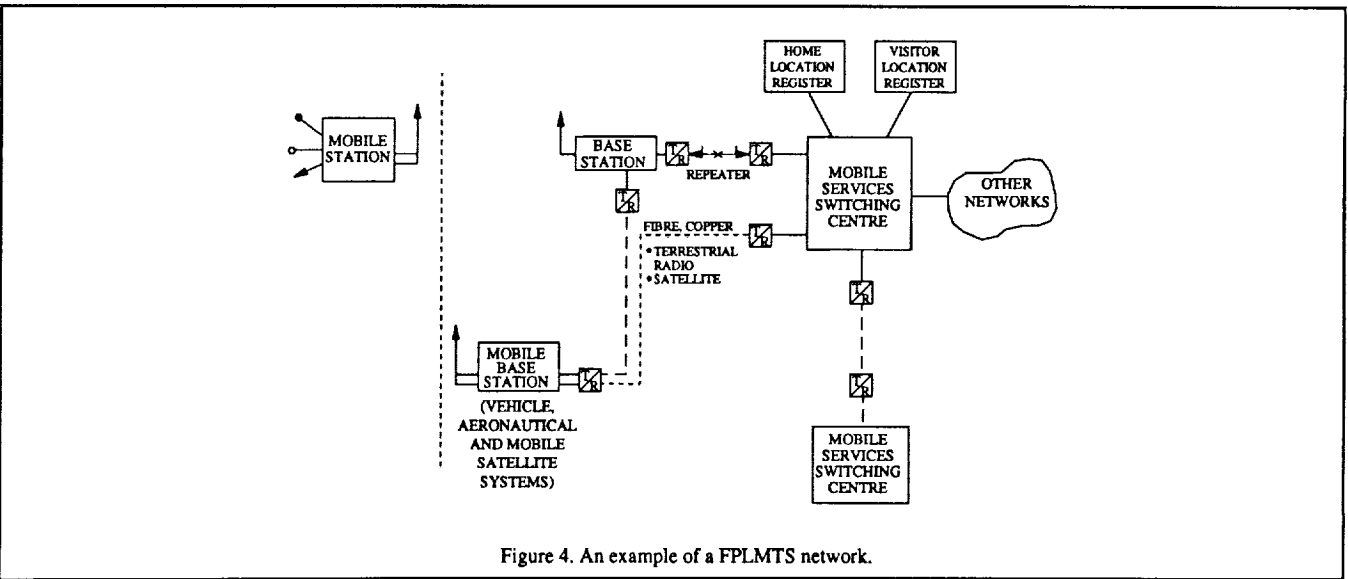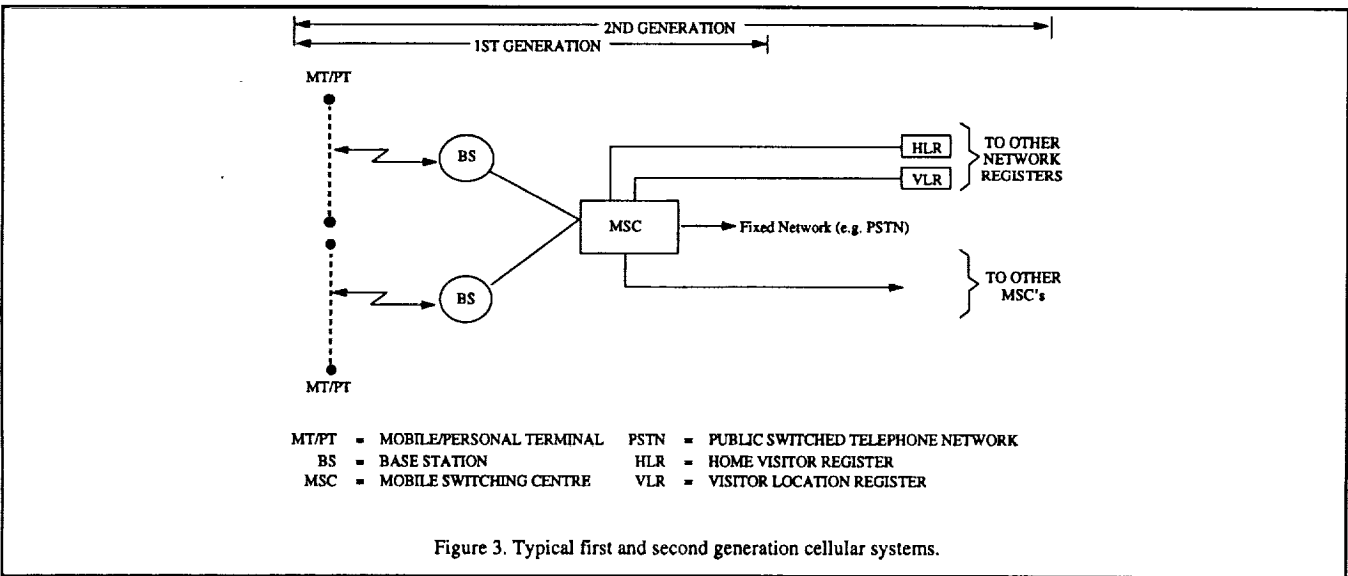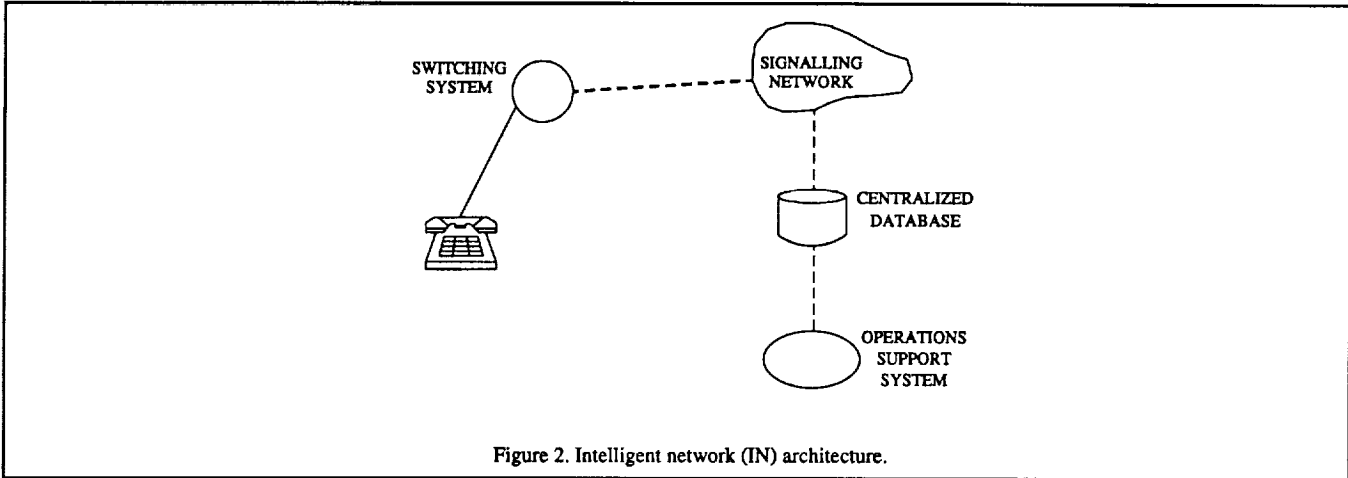
Interworking and Integration of the Inmarsat Standard-M with the Pan-European GSM System

R. Tafazolli and Professor B.G. Evans

Centre for Satellite Engineering Research (CSER)
University of Surrey
Guildford
Surrey GU2 5XH
England
Tel: +44- 483- 509834
Fax: +44- 483- 34139

Introduction

The market demand on mobile telephone communications has been increasing since the introduction of the cellular mobile telephone systems about twelve years ago. In Europe, projections indicate a demand of about 17 million subscribers for a fully deployed Pan-European system. The Pan-European GSM system is to harmonise the growth of the terrestrial mobile system. Studies conducted by the European Space Agency (ESA) indicate that even with 60-70% of the area being covered by the GSM, a significant traffic demand (voice and data) will still exist for areas not covered by the terrestrial systems.

This demand could be satisfied by a land mobile satellite system. The satellite system is therefore seen in a complementary role rather than in competition with the terrestrial system in an integrated telecommunication network. One possible scenario may be that initially the satellite system provides services to the rural areas together with areas still not covered by the GSM system. This service area is then gradually diminished as the terrestrial system expands until an optimum point is reached where the systems co-exist optimally.

The objective of this paper is to investigate the possibility of integration of a space based system, in this case Inmarsat Standard-M, with the GSM (Global System for Mobile communication). One very important advantage of incorporating GSM services in Standard-M is that it will be feasible to extend the GSM services economically worldwide, not only to land mobiles but also to aeronautical and maritime mobiles.

The GSM System

The idea of a Pan-European mobile communication system was originated in 1981 and it is to replace the many different analogue mobile telephone networks which exist throughout Europe. Roaming will be permitted within all the countries deploying the system.

The GSM offers digital voice channel together with several supplementary services and will be ISDN compatible. Very importantly the system has been structured to permit evolving technology to be incorporated.

The system adopts a TDMA structure and makes use of the CCITT Signalling System Number 7. Extensive use is also made of the other CCITT, CEPT and ISO (for layers 1,2 and 3 - the physical , data link and network layers) standards.

The main building blocks of the GSM network are shown in figure 1.

The Mobile Switching Centre (MSC) acts mainly as an ISDN exchange and represents the interface between the fixed network and mobile network. Each MSC has many Base Stations (BS) under its control, typically three. The MSC also controls mobile specific functions such as handover. In general, each MSC will have two associated location registers. Home Location Register (HLR) is used to store permanent and temporary information related to the mobile subscriber or related to the position of the MSs in each instant. Visitor Location Register (VLR) contains all kinds of information both permanent and temporary needed to handle the MSs in the area where it is roaming.

A Base Station provides radio coverage of geographical zone containing one or several cells. It provides the radio channels for both subscriber services and associated network

signalling. It is directly connected to the MSC associated with its coverage area. The Mobile Station enables subscribers to access the GSM network at any point within the service area. Various types are available of different transmission power levels- the higher powers being vehicle mounted rather than handheld.

GSM services and subscribers access

In this section, services which are supported in GSM and customer access to them will be described.

Tele/Data and Supplementary Services[1]
Teleservices

The teleservices provide complete capability for two customers to communicate with one another. The following generic teleservices are offered.

a) Speech transmission
b) Emergency call
c) Short message transmission (telegrams up to 256 characters)
d) Message handling service
e) Videotex
f) Teletex
g) Facsimile transmission group 3,4

Bearer Services

The bearer service provides a "transport-service" which enables customers to interchange data according to their specified application. The GSM services are:
a) Audio restricted 3.1 KHz
b) Data circuit duplex asynchronous 300-9600 bits/sec
c) Data circuit duplex synchronous 1200-9600 bits/sec
d) PAD access circuit asynchronous 300-9600 bits/sec
e) Data packet duplex synchronous 2400-9600 bits/sec
f) Alternate speech/unrestricted digital
g) 12.6 kbits/sec unrestricted digital
h) ISDN terminal support

Supplementary Services
a) Call forwarding
b) Call barring
c) Call waiting
d) Call hold
e) Three party service
f) Advice of charge. This is intended to pro-

vide sufficient information to a MS for an estimate to be made of the call charge incurred.

Customer access [1], [2]
Mobile stations with have different access capabilities. For example, a small compact handheld unit is unlikely to offer all services in the early 1990s. Therefore, GSM has developed a structured approach which allows for maximum evolution of products. This process is shown in figure 2. The figure shows that the MS consists of a Mobile Termination (MT) unit and terminal equipment. The function of the MT unit is to offer standard interfaces to the customer and to transfer the data on these interfaces over the radio interface (Um). For example, customers will be able to directly connect their ISDN terminal via the standard ISDN "S" interface to the MS. The ISDN terminal presents a 64 kbps data stream to the mobile termination and the composite effect of the rate adaptation in the ISDN terminal and mobile termination unit is to produce a flow of controlled data stream compatible with the capacity of the digital radio channel. Figure 2 also indicates the alternative which is being specified so that customers with non-ISDN terminals can either directly connect to the standard "S" interface or to a "R" type interface.

There are three types of MT:
MT0: includes functions belonging to MT, with support of no terminal interfaces.
MT1: includes functions belonging to MT, with an interface that complies with the GSM recommended subset of ISDN user-network interface.
MT2: includes functions belonging to MT, with an interface that complies with non-ISDN interface eg., CCITT X or V series interface.

The MT plus a TE/(TE+TA) constitutes the mobile station.

Inmarsat Standard-M Land Mobile System [3]
The Inmarsat Standard-M which will start commercial service by 1993, provides a digital communications service between the public switched terrestrial networks and mobile users on land or sea. Standard-M supports medium quality telephony, facsimile and 2400 bits/sec. Links to and from mobile installations are established via Inmarsat

geostationary satellites and the associated ground segment. Near global coverage provided between latitudes 75° north and south of the Equator.

The major elements of Standard-M system are shown in figure 3 and are described briefly as follows:

The Space Segment capacity is provided by Inmarsat's first generation (i.e, intelsat-V Maritime communications sub-system satellites) and subsequent generation space segment (Inmarsat-3).

Standard-M Mobile Earth Station (MES), which interface with the space segments at L-band (1.5/1.6 GHz) for communication with LESs.

Land Earth Stations interface with the space segment at C-band (4/6 GHz) and L-bands and with the terrestrial networks for communications with MESs.

Network Coordination Stations (NCS), located at the designated (co-located) LESs, which interface with the space segment at C-band and L-band for the purpose of signalling with MESs and LESs, and for overall network control and monitoring functions.

Standard-M services and customer access

This section describes the services which are recommended for Standard-M system. This, in no way, means that these are the only services which Standard-M system is capable of supporting.

Telephony Services are provided through 6.4 Kbits/sec full duplex.

CCITT Group-3 Facsimile Service is provided in accordance with the transmission standard CCITT Rec.T4 regarding Group-3 facsimile service.

2.4 Kbits/sec full duplex baseband data services (with optional fall back mode capability of operating 1.2 Kbits/sec) are supported. Figure 4 shows the customer access to data services. The recommended interface requirement between an MES (DCE) and its data terminal equipment (DTE) is the CCITT V.24, V.28 and ISO 2110 (equivalent to EIA specification RS-232C).

The recommended auto-calling and auto-answering protocol at the MES V.24 interface is the CCITT Rec.V.25 bis. Modem Interface Unit (MIU) is a logical block allowing a fixed Hayes compatible modem to interface with the LES and a DTE to interface with the MES. MIUs are useful on MESs to allow selection to off-the shelf modems and DTEs by the end users (using

"multi-numbering scheme").

The primary function of the MIU at the LES is to interface with the terrestrial modems, and to convert the analogue baseband voice and data format originated from fixed-user voice band modems to the Standard-M 2.4Kbits/sec SCPC satellite data channel format. The recommended protocol between the LES MIU and the terrestrial fixed-user's data modem is the CCITT Rec. V.22 bis.

Interworking between Inmarsat Standard-M and GSM Systems

The main purpose of this section is to prepare the ground for integration of GSM and Standard-M systems which is to be the subject of the next section. Before considering integration an understanding of the concept of interworking and how it can be achieved is necessary. The interworking in this chapter is described on the ability of GSM network to interwork with non-ISDN networks.

The concept of Bearer services was developed for the ISDN and has been extended to the GSM. Here an attempt will be made to interwork GSM Bearer services and hence its Teleservices with Inmarsat Standard-M network within the limitations of the two systems. Three areas of interworking were identified and thoroughly investigated:

1. Service interworking

Service interworking is required when the teleservices at the calling and called terminals are different (e.g. Teletex interworking with Facsimile).

2. Signalling interworking

For network interworking, signalling requirements have to be defined. Existing call control signalling procedures e.g SS#7, is used in the GSM while a subset of SS#5 is used in Standard-M.

3. Supplementary service interworking

From the network interworking, the following can be deduced:

1. Additional signalling messages "bearer capability" are required to be transmitted between MESs and LESs to support GSM services. Such messages will be needed to indicate things like service nature (i.e simple or duplex), service type (i.e short message service) etc. These signals can be accommodated since both MESs and LESs will be equipped with software expansion capabilities to accommodate new signalling codes for future Inmarsat service offer-

ings[3]. Hence this can be utilised to support new signalling messages required for GSM services.

2. Signalling conversion is required to convert the forward and the backward signals of SS#7 (ISUP) messages and information elements of Standard-M signalling system (subset of SS#5).

3. Appropriate interfaces at the MSSC are required to support GSM services within Standard-M network e.g X.30 and X.31 to support packet data services.

4. The MSSC must support all of GSM supplementary services.

5. Additional interworking functions (IWFs) will be required to support various GSM services. The IWFs will be in the following form:

i) Echo control devices at the MSSCs
ii) Modem pools and network based rate adaptation (i.e to allow for no more than 2400 bits/sec and no less than 1200 bits/sec user data rate) at LESs.
iii) Functions to select the appropriate modem and rate adaptation for each requested service.
iv) Appropriate interfaces at the MSSC (ISDN switch) to support data services with other specialised networks e.g X.32 access, to interface with packet networks including GSM.

6. To support short message services, provision must be made for a use of service centre, which acts as a store and forward centre for short messages. This centre can either be located at each LES or the GSM PLMN centre can be shared with the home LES.

Integration of Standard-M and GSM Terminals

In this section, the possibility of proposing a single terminal to access both networks will be looked at. The achievable level of integration will be determined by the amount of similarities between the two systems.

The two systems are very different at all the three lower layers of OSI model, thus there is no point in trying to integrate the Mobile Termination unit (MT) in GSM and the Mobile Earth Station (MES) in Standard-M into a single terminal. Hence customer interfaces at both the MT and MES were examined in order see how the GSM services can be supported in a dual-mode terminal. The dual-

mode terminals for both non-ISDN and ISDN services are shown in figures 5 and 6 respectively. In ISDN compatible terminal, the GSM Mobile Termination 1 (MT1) was considered, as MT1 is designed to support ISDN user interface, i.e "S" reference point, allowing TE1 to be connected directly to MT1. As Standard-M MES is designed to support non-ISDN terminals, some modifications were required to enable the MES to support ISDN terminals.

Integration of Standard-M and GSM Networks

The important elements of the two separate networks which monitor the mobile position and thus allow calls to be forwarded to the mobiles are the HLR in the GSM and NCS in the Standard-M system. The gateway between the two networks must therefore be a link between these two elements so that information can be exchanged as to the mobile location within the whole network. This is shown in figure 7. The GSM Directory Number (DN) is incorporated in the Integrated Network for the following reasons:

1. The GSM is designed to provide flexible and economic call set up procedures by incorporating network elements such as HLR, VLR and Mobile Network identity such as MSRN.

2. The main purpose of this integration is to allow Standard-M to complement the GSM by providing similar services as the GSM in the rural/maritime areas. Thus it is essential to harmonise the user access methods by adopting the GSM numbering scheme.

To reach this integrated scenario, careful steps were also taken to minimise the propagation delays due to satellite links and the terrestrial tails, by extensive use of the terrestrial elements. This also resulted in the following advantages:

i) Avoided many changes in the space segment due to the need to transmit many signalling messages to support roaming in the integrated network.

ii) Efficient utilization of the space segment radio resources i.e roaming can be supported with very little use of the satellite radio channels.

Summary

In this paper two main areas were examined in order to achieve maximum possible level of synergy between the Inmarsat Standard-M and the GSM systems.
In the interworking, signalling, supplementary services and network issues were addressed and many additional network interfaces were proposed. These solutions were aimed at incorporation of GSM services in Standard-M system as much as possible.
The network integration was obtained through detailed comparisons of the two systems in accordance with OSI/RM model. This resulted in the suggestion of a dual-mode terminal with fully defined user-machine interfaces to access both GSM and the "enhanced" Standard-M services.

References

[1] Mallinder B.J.T., 1988 "The GSM digital cellular system", GSM noyan permanent, CEPT, Paris.

[2] 1990, "GSM PLMN Access Reference Configuration", GSM Recommendation 04.02.

[3] 1988, "INMARSAT-M System Definition Manual", Issue 3.0, Module 1, INMARSAT Satellite Organisation- London.

[4] Alverche, M., And Branes, D., 1988, "Overview of the GSM Services and Facilities", Digital Cellular Radio Conference, Hagen, Germany.

Architectures and Protocols for an Integrated Satellite-Terrestrial Mobile System

E. Del Re°, F. Delli Priscoli^, P. Iannucci°, R. Menolascino°, F. Settimo°
° Università di Firenze; Dipartimento di Ingegneria Elettronica
Via S. Marta, 3; 50139 Firenze, Italy - Phone: +39 55 4796285 - Fax: +39 55 494569
^ Università di Roma "La Sapienza"; Dipartimento di Informatica e Sistemistica
Via Eudossiana, 18; 00184 Roma, Italy - Phone +39 6 44585325 - Fax +39 6 44585367
° CSELT, Centro Studi e Laboratori Telecomunicazioni
Via G. Reiss Romoli, 274; 10148 Torino, Italy - Phone: +39 11 2285036 - Fax: +39 11 2285582

ABSTRACT

This paper aims to depict some basic concepts related to the definition of an integrated system for mobile communications, consisting of a satellite network and a terrestrial cellular network. In particular three aspects are discussed:
- architecture definition for the satellite network;
- assignment strategy of the satellite channels;
- definition of "internetworking procedures" between cellular and satellite network, according to the selected architecture and the satellite channel assignment strategy.

INTRODUCTION

Essentially, there are two ways to implement an integrated satellite-terrestrial mobile system [1]:
1) considering the satellite network as a natural extension and a completion of the terrestrial one, reusing (as far as possible) in the satellite network the same procedures and protocols defined for the cellular one;
2) accepting that the satellite link may be based on specific procedures and techniques, assuming that the integration is obtained only by information interchange at the network side.

In this paper the first viewpoint is considered [2][3] and, to be concrete, architectures and protocols for the satellite network are described with reference to the cellular standard "Global System for Mobile communications (GSM)". An integrated system based on this standard seems possible but problems related to the complete reuse of the GSM protocols on the satellite network have been found. These results could be taken into account to define the future standards for mobile communication systems.

SYSTEM ARCHITECTURE

The reference payload is a geostationary satellite whose feeder link (i.e. the link from/to the "Fixed Earth Stations (FESs)" to/from the satellite) has a global coverage and whose mobile link (i.e. the link from/to the "Mobile Stations (MSs)" to/from the satellite) has a spot-beam coverage.

Basic issues of the satellite system configuration are the number of FESs, the FES-spot connection (i.e. the spots each FES can communicate with), the criteria for the FES-MS association. On these subjects the following issues must be considered:
- a static FES-MS association is proposed. The FES-MS association specifies the FES a certain MS is allowed to communicate with via satellite. Static means that the MS is semipermanently associated to the same FES as long as it roams in a certain spot; conversely, dynamic means that this association can be varied on a real time basis. As it is hereinafter explained, a dynamic FES-MS association permits the "selective landing" and the "alternative routing", but it does not result GSM-compatible.

Selective landing means that, in order to shorten the terrestrial tails, the connection between a MS and a fixed-user takes place through the FES closest to the fixed-user (i.e. the FES is selected on a call-by-call basis on the ground of the fixed-user location).

Alternative routing means that a call routed

through a congested FES (or "Base Station System (BSS)") can be rerouted through a different FES (i.e. the FES is selected on a call-by-call basis on the ground of the traffic situation).

In order to permit the selective landing in case of fixed-user originated calls, a stand-by MS should be tuned on the "Broadcast Control CHannel (BCCH)" carrier transmitted by the FES closest to the fixed-user, but, obviously, this is not possible since the MS can not be aware of the fixed-user which is going to call it.

Likewise, in order to permit the alternative routing in case of fixed-user originated calls, a stand-by MS should be tuned on the BCCH carrier transmitted by the "alternative" FES, but, obviously, this is not possible since the MS can not be aware either of the status of congestion of the serving cell or of the identity of the alternative FES.

- Since selective landing is not GSM compatible, in theory, increasing the number of FESs does not yield any benefit in terms of reduction of the average length of the terrestrial tails. In practice, such tails can be remarkably reduced by planning to associate each MS to the FES closest to the area where the fixed-users, which the MS is expected to communicate more frequently with, are located (e.g. the FES closest to the MS headquarter).

- Since alternative routing is not GSM compatible, by increasing the number of FESs per spot, the overall system efficiency decreases due to the partition of the GSM carriers among the FESs. Once the satellite capacity is known, the offered traffic in function of the number of FESs can be easily calculated by applying the Erlang-B formula. In case the above-mentioned efficiency decrease becomes unacceptable, a proper real time reservation mechanism of the carriers should be implemented (e.g. a demand-assignment mechanism with a network control station in charge of carrier assignment). However such a solution entails a remarkable increase in the satellite system complexity.

- As far as the FES-to-spot connection is concerned, the possible solutions range from the simple connection (each FES is allowed to communicate only with a spot, i.e., in general, the spot where the FES is placed), to the full connection (each FES is allowed to communicate with all the spots). Obviously, the full connection solution is more flexible. However, it imposes more stringent requirements on the on-board processor (e.g. a greater number of filters) and/or more complex frequency plans. Moreover, in the full connection solution, each FES must transmit at least a GSM carrier (the BCCH carrier) in every spot and this could be inefficient. The full connection solution can be either "static" or "dynamic". Dynamic means that each FES, in the framework of the GSM carriers assigned to it, can vary, on a real time basis, its carriers-to-spot assignment, in order to cope with contingent traffic situations; static means that each FES can vary the above-mentioned assignment only on a rearrangement basis. Periodic or continuous reconfiguration might be obtained with an on-board switching (controlled via telecomand) of carriers from/to the global beam to/from spot beams. The dynamic solution is more efficient but it requires that the on-board processor and/or the frequency plans are reconfigurable on a real time basis.

- It is more than likely that administrative requirements and/or political matters impose that a certain "Public Land Mobile Network (PLMN)" (and/or a certain country) is provided with its own FES. If this is the case, the MSs registered in a certain PLMN can be conveniently associated to a FES belonging to this PLMN (at least in case this is permitted by the FES-spot connection); so doing, in case of infra-PLMN calls, the passage through external PLMN is avoided.

In conclusion, it is proposed a satellite system configuration in which the number of FESs is kept to a minimum compatible with the above-mentioned administrative/political requirements. In the reasonable hypothesis that the number of GSM channels supported by the satellite system is remarkably higher than the number of FESs, statistical considerations suggest that the efficiency decrease caused by the semipermanent partition of the GSM carriers among the FESs, can be tolerated, thus avoiding the implementation of a complex real time carrier reservation mechanism. The most convenient FES-spot connection can be decided FES by FES depending on the payload characteristics and on the expected traffic between the FES and the spots. As to the static FES-MS association, a suitable criterion is to associate a certain MS to a FES belonging to the PLMN where the MS is registered. In the framework of the FESs belonging to the above PLMN, it is convenient to associate the MS to the FES closest

to the MS headquarter. Finally, in case the PLMN where the MS is registered has no FESs (or is not connected with one or more spots), the MS can be profitably associated to the FES (belonging to a different PLMN) closest to the MS headquarter.

CHANNEL ASSIGNMENT STRATEGY

Basically, in an integrated system, the assignment of satellite channels for a communication can be of two types:
1) at the same priority level as terrestrial cellular ones; in that case the choice between satellite and terrestrial resources can be based on link quality parameters (e.g. received signal power);
2) at a lower priority level, recognizing the specific features of the satellite resources (more limited, more costly but able to serve a wide area); in that case the choice between satellite and terrestrial channels should be based on traffic management criteria (e.g. satellite resources are chosen only if the terrestrial ones are not available for whatever reason).

The first approach considers the satellite system as an extension of the GSM network and satellite beams as GSM cells, not only from the architectural viewpoint but also from the operative one: this means that traffic channels, disregarding cellular or satellite, are allocated according to level and quality of the received signal. It has been already shown [4] that this choice leads to a poor network efficiency.

The second choice recognizes that it is unfair to compare satellite and GSM channels on the ground of signal quality and dangerous to allocate a satellite channel when free GSM channels exist in the terrestrial network. This straightforward *selective call set-up procedure* is suggested: *always try to allocate first GSM traffic channels; in case of a blocking state, switch to a satellite channel.*

The proposed strategy discriminates channel types on the base of network criteria (the occupancy state), not simply radio, so that satellite channels represent an overflow for the GSM ones, that remain the primary channels.

Application scenarios

An integrated traffic management strategy overcomes the classical satellite roles of:

- complementing the GSM network in uncovered areas;
- supplying purely additional channels in common areas;

The fixed traffic channel capacity scheme of the GSM system is a severe limitation when the nominal average traffic figures are variable; this may occur on a periodical basis (traffic overloads in specific cells) or because of the customers growth. Cellular networks, are highly vulnerable to such changes while satellite channels, used as overflow resources, can easily absorb the cellular traffic peaks. This feature allows a looser GSM channel dimensioning and avoids periodic reconfigurations.

The customers growth increases the average offered traffic. In this evolutionary process, the satellite can become a powerful planning support for the GSM network, since investments can be postponed. The advantages will be more consistent, if appropriate traffic handling procedures are developed.

An application example

A quantitative comparison between the GSM channel assignment strategy and that proposed in the previous section has been performed on a limited size example where *urban, suburban* and *rural* propagation conditions for the GSM network have been reproduced. *Marginal traffic* due to mobile customers roaming outside the GSM coverage but still in the satellite spot beam has been assumed too so that some customers can access only and directly the satellite channels with the same GSM service quality. The "wrong" selection of a satellite channel in the common coverage areas, due to a better received signal, is taken into account in a probabilistic way.

The limited available space suggests to summarize verbally the results. The *System Blocking Probability*, (i.e. the probability that a call is rejected because no traffic channel can be allocated) has been recognized as the most suitable parameter to quantify how the user perceives the quality of service. If overflow to the pool of satellite channels is allowed, local blocking states on GSM cells do not necessarily mean call rejection, as would be for a traffic handling strategy with no overflow. In the simulated example, overflow ensured a reduction of the

139

blocking probability of about 30% with respect to the nominal value.

A second performance figure, the *GSM Network blocking probability*, represents the probability that a call, originating in the GSM network, is rejected. As expected, the nominal blocking probability on GSM cells is reduced by the presence of a supporting satellite system; furthermore, it has been noted that with the overflow capability an increase of the satellite capacity produces, in percentage, a higher decrease of the GSM network blocking probability.

The benefits achieved on both System and GSM Network blocking probabilities are compensated by an increase of the *Satellite Blocking Probability*: this is perceived by mobile customers roaming in marginal areas and those that are better served by a satellite channel in common areas. Such probability is simply expressed by the fraction of calls that access directly the satellite network and are blocked. A partition of the satellite channels that only allows a preassigned amount of channels to host overflow traffic should mitigate this drawback. Dimensioning can be such to optimize the traffic globally handled by the network.

Handover

In cellular networks, handover prevents from forced call disconnections due to signal degradation in the passage between adjacent cells. In the integrated satellite/GSM environment, handover can be extended to the passage from different networks. Two possibilities (GSM-to-satellite and satellite-to-GSM) exist.

GSM-to-satellite handovers can occur when a mobile is leaving the GSM coverage and a satellite traffic channel offers an acceptable quality; hence, they are an extension of GSM handovers. Call continuity is maintained and service quality is increased but they are not traffic management tools.

Satellite-to-GSM handovers, on the contrary, aim at enhancing the overall network efficiency by maximizing satellite channels availability. The function is closely related to the selective call set-up procedure and consists in:
checking the occupancy state of the GSM channels that could be allocated to a satellite conversation; if at least one free channel exists in a suitable

GSM cell, the satellite call is handed over to the GSM network.

INTERNETWORKING PROCEDURES

As described in the previous section, traffic interchange between satellite and cellular network may be obtained with the selective call set-up or with the handovers. To define these procedures, it is to be noted that the GSM is already in the development phase and therefore solutions for an integrated system requiring any modification to the existing protocols of the terrestrial network are not reasonable. Modifications, if required, should be confined in the mobile terminal and/or in the ground infrastructure of the satellite subsystem.

Selective call set-up procedure

This definition refers to the MS possibility of establishing a communication through the satellite link when a traffic overload arises in the terrestrial network.

In a cellular network, a set-up procedure to/from a mobile terminal requires some preliminary operations, carried out by the terminal and the network. When an integrated system is considered and a selective call set-up is needed the following aspects have to be pointed out:
- when an MS is not engaged in any type of communication it selects the most suitable cell for communicating over the radio path. In all the considered architectures the spot beams are considered as "macrocells" and the cell search should concern even the satellite band. The frequency band distinction can be exploited to implement the priority selection criterion between terrestrial and satellite network: first the MS searches for a suitable cell in terrestrial PLMNs; in the areas covered only by the satellite system, the selection of terrestrial cells fails due to link quality measurements and the MS switches automatically to the satellite band. If a particular FES-MS association is preferred, it is necessary for the mobile terminal to check first the BCCH of "its own" FES, when it switches to the satellite band: this means that it must keep information about these carriers in its memory.
- The smallest area unit used in GSM for locating the MS is the "location area (LA)": it is composed by one or more "Base Station (BA)"

140

areas and is identified in a PLMN by a LA identification, which is a parameter broadcasted on the BCCH. A location updating procedure is performed by the MS when it selects a cell with a LA identification different from the one previously received. In an integrated system, we can assign a LA identification to every spot beam, to every FES or to the whole satellite network, according to the adopted architecture. In any case when an MS selects the satellite resources it must perform a location updating.

- When a mobile terminal communicates with the network it has to synchronize its burst transmissions so that they are properly received by the base station in the reserved slots. The synchronization problem of an MS has two aspects:

- initial synchronization, at the access phase to the network;
- adaptive correction of the synchronization, during a communication.

The latter aspect may have in the satellite system the same solution as in the GSM. On the contrary, a notably different solution must be used in the first case. In the GSM the *access burst* is received by the BS within the assigned timeslot even if the MS is at the cell boundary. A different situation occurs in the satellite network because of the long propagation delay and the quite large delay variation coming from the position of the MS within the spot beam: due to uncertainty of the receiving instant of an access burst, it is necessary to reserve a carrier to the access in every spot beam. Moreover, to allow FES to evaluate the propagation delay, the MS must send the access burst only at the beginning of specified timeslots.

On the satellite link, as a consequence of the synchronization, the MS performs the transmission of a burst, in a frame, at an instant which does not depend on the instant of reception: then, the timeslot of transmission may overlap to the timeslot of reception. Therefore, unlike a GSM terminal, the MS for the integrated system must have a duplexer.

After these considerations, we can define a procedure for a selective call set-up. We suppose that the MS has selected a GSM cell and that the set-up is not completed owing to a blocking state in this cell. It is suitable to distinguish two cases:
1) *mobile terminating call*: the mobile is the called MS, that is the traffic overload occurs in the

"call destination" cell. A procedure for trying an alternative routing through the satellite network is not advisable as, to implement it, modifications should be taken into account in the terrestrial network. As a matter of fact:
- the "Mobile Switching Centre (MSC" that receives the message of *assignment failure* is a GSM MSC and in this system an alternative routing is not provided;
- as previously reported, the MS waits for the *paging* message only on the proper channel of the selected cell. A procedure for a second set-up requires that the MS is registred as located in two LAs, one of which belonging to the satellite network. So, the mobile should perform a location updating for each network and listen to two *paging channels*. This integrated system should work in such a way that the call is first routed through the terrestrial network. A procedure for implementing this set-up type should be more complex than one of the GSM and, in any case, different.
2) *mobile originating call*: the MS has selected a GSM cell and it is the calling terminal, that is the traffic overload arises in the "originating call" cell. When the MS infers that it is not possible to establish the call in the GSM, it tries selecting a beam and, if this attempt is successful, it performs a location updating. Now it can repeat the set-up. The long time required to complete the procedure might be reduced if the MS avoids the first useless attempt. Unfortunately in the GSM, no parameter can be broadcasted on the BCCH to communicate to the MSs the traffic overflow.

GSM-to-satellite handover

Handover from cell to spot beam is a feature not simple to be implemented with GSM contraints.

In the GSM, the mobile, when performing the handover tunes to the "new" BS and transmits an access burst, at the beginning of a slot indicated by the "old" BS. This burst is sufficiently short, so that it is received in the assigned timeslot, even if the MS is at the boundary of the new cell. In a GSM-to-satellite handover, owing to the notable delay involved on the satellite link, it is necesssary for the mobile to have an additional timing indicator, in order that the burst is received by the FES in the assigned timeslot: the MS must know the precise delay, from a defined instant, of the

141

transmission of the access burst. This information should be communicated by the BS and therefore modification to the GSM network would be necessary.

Satellite-to-GSM handover

Satellite-to-GSM handover is one of the most interesting traffic management tool for the integrated system, as it permits to reduce occupancy of the satellite resources.

The criteria that are possible to adopt to start a satellite-to-GSM handover procedure may be different: for example it may be established that this procedure has to be carried out only when the satellite occupancy degree is over a certain fixed value.

To hand over a call from the satellite to the cellular network, it is up to the mobile to allow the satellite network to identify its position inside the beam: this may be achieved with the message *measurement report*, sent periodically by the MS. In it the identity of at least one cell, among those reported by the mobile, must be indicated with its complete identifier, that is broadcasted on the BCCH and allows to distinguish the cell inside the whole network. Obviously, it is suitable that cell specified by the MS is the one from which the received signal strength is the highest, since, presumably, the mobile is there.

Recall that, in the GSM, the neighboring cell BCCH frequencies to be monitored are communicated to the mobile through a well defined list, transmitted by the serving cell. Analogously, when the mobile communicates through the satellite, in this list the FES should indicate the frequencies that are BCCH carriers in the area where the MS is at this time. In other words, the FES should adapt the transmitted list according to the position of the mobile in the beam. This requires the mobile knows the GSM cell where it is immediately before the set-up. This condition excludes a handover from satellite to GSM, when the set-up occurs outside the GSM coverage. Instead the mobile may precise the cell when it accesses the satellite owing to the traffic overload in the terrestrial network.

Other problems may be due to the MSCs of the terrestrial network. Note that a "terrestrial" MSC overlaps to the neighboring MSC areas only with the boundary cells of its coverage area. So an

inter-MSC handover should occurs only between boundary cells of two MSCs. This fact might be taken into account in the implementation of the terrestrial network. Instead, in order to hand over the calls from the satellite to the GSM, all the cells inside a terrestrial MSC area should be considered boundary cells with respect to the area covered by the satellite MSC. The exploitation of this feature depends on the national implementation of the GSM.

CONCLUSIONS

An integrated system based on the GSM procedures allows to increase the efficiency of the cellular network and seems actually feasible. Some drawbacks related to the reuse of the GSM protocols have been highlighted. The design of a fully integrated system, for the next generation of a Personal Communication System, should take into account these drawbacks and define the architecture and protocols in such a way that the satellite network more naturally fits into the overall network.

ACKNOWLEDGEMENT

REFERENCES

[1] A. Arcidiacono, "Integration between terrestrial-based and satellite-based land mobile communications systems," *International Mobile Satellite Conference*, Ottawa, June 1990
[2] E. Del Re, "Satellite systems integrated with the terrestrial cellular network for mobile commmunications," *ESA STR-228*, August 1989.
[3] E. Del Re, "A satellite mobile system integrated with the terrestrial cellular network," *IEEE ICC '89*, Boston, MA, June 11-14, 1989.
[4] F. Delli Priscoli, E. Del Re, R. Menolascino, I. Mistretta, F. Settimo, "Issues for the integration of satellite and terrestrial cellular networks for mobile communications," *Workshop on Advanced Network and Technology Concepts for Mobile, Micro and Personal Communications*, JPL, Pasadena, September 1991.

142

HANDOVER PROCEDURES IN INTEGRATED SATELLITE AND TERRESTRIAL MOBILE SYSTEMS

G.E. Corazza*   M. Ruggieri°   F. Santucci°   F. Vatalaro*

*Universita' di Roma "Tor Vergata" - Dpt. Ingegneria Elettronica
Via della Ricerca Scientifica, 00133 ROMA - ITALY
tel.: +39-6-72594453; fax: +39-6-2020519

°Universita' di L'Aquila - Dpt. Ingegneria Elettrica
67040 Poggio di Roio - L'AQUILA
tel.: +39-862-432556; fax: +39-862-432543

ABSTRACT

The integration of satellite and terrestrial mobile systems is investigated in terms of the strategies for handover across the integrated cellular coverage. The handover procedure is subdivided into an inizialization phase, where the need for issuing a handover request must be identified, and an execution phase, where the request must be satisfied, if possible, according to a certain channel assignment strategy. A modeling approach that allows the design of the parameters that influence the performance of the overall handover procedure is presented, along with a few numerical results.

1. INTRODUCTION

Future mobile telecommunication networks should provide the user with the highest possible degree of mobility and service quality. This objective implies, in particular, the development of a seamless coverage achieved through the combination of different systems fully transparent to the user. In fact, no single system can be the optimal solution to a global coverage.

A promising configuration for future mobile network architectures is the integration of terrestrial cellular with satellite multispot systems [1-3]. The satellite system provides an overlay of large cells on the terrestrial cellular layout, and would be mostly utilized when users are in open areas (rural or suburban), while the terrestrial system would serve most of the large traffic generated in urban areas. In order for this architecture to be attractive from the user point of view, a single terminal with dual-mode capability is needed for a transparent connection to either system.

The peculiarity of an integrated system is the need to efficiently select the access medium (terrestrial or satellite) offering the best performance at any instant for every user. Therefore, an increase in network intelligence is the price paid for the agility provided to the user. In particular, a procedure for active user handling (handover) during the transition between cells belonging to the two systems must be added to the ones required in conventional cellular systems. In terrestrial cellular systems, in fact, handovers are needed when the channel quality belonging to a mobile user active call becomes unacceptably low, and the active call should be entrusted to a new base station (intercell handover) or simply to a new channel (intracell handover) [4-8]. In satellite cellular systems, intercell handover may happen between two spots belonging to the same satellite, or even to different satellites in the case of a multi-satellite system. In addition, in an integrated satellite and terrestrial mobile system the necessity for inter-system handover arises, for example, when the active user approaches the borders of the area serviced by the terrestrial system.

Reliability of handover procedures impacts heavily on the successful exploitation of an integrated system. A crucial point in the assessment of the procedure is the role played by the user terminal in handover decisions. In Network Controlled HandOver strategies (NCHO), for instance, the choice of the handover starting time and the target Base Station (BS) is performed by the Mobile Switching Center (MSC). When the decisions are taken at BS/MSC level, but the user terminal cooperates in the research of alternative base stations to the present one, it is a Mobile Assisted HandOver (MAHO). The maximum decentralization degree is reached when the mobile terminal itself takes the handover decision (Mobile Controlled HandOver, MCHO) [5]. The mentioned strategies result in different handover duration and features. Some key characteristics related to the above strategies are summarized in Table 1.

Given a handover strategy, the procedure for handing over the active call from one server to the other can be subdivided into two distinct steps:
- handover initialization: channel monitoring and recognition of handover necessity;
- handover execution: new resource assignment, if available.

HANDOVER STRATEGY	INTER-SYSTEM HANDOVER	INTERCELL HANDOVER	INTRACELL HANDOVER	TERMINAL COMPLEXITY	NETWORK SIGNALING
NCHO	critical	allowed	critical	low	usual
MAHO	allowed	allowed	allowed	fair	usual
MCHO	allowed	allowed	allowed	high	heavier

Table 1

The initialization phase must prevent an unnecessary request from being flagged, while, at the same time, be prompt in issuing the necessary ones. The time spent in trying to take the proper decision has a fundamental impact on the probability of successful handover. The handover execution phase depends on channel assignment strategies and on techniques aimed at reducing the probability of forced termination. In the present study, a procedure for inter-system handover inizialization and execution is analyzed.

2. INTER-SYSTEM HO INIZIALIZATION

Suppose the chosen strategy for handover is MAHO. The most appropriate quantity to be measured should be identified. The Bit Error Rate (BER) experienced in the demodulation of the received digital signals is the most reliable measure of quality, particularly in the presence of interference, when power level measurements may lead to misleading results. Therefore, it would be desirable that the Mobile Station (MS) periodically monitored the BER's pertaining to the signals coming from the serving Base Station (BS) and from all other adjacent or overlaying BS's. Unfortunately, BER measurements are not always feasible: due to the statistical nature of errors, a sufficient number of them must be detected before an estimate of reasonable accuracy can be made. This fact may introduce a significant delay in the measurement, especially in the case of low bit rates.

An istantaneous estimate of quality can be extracted by measuring the received signal-to-(interference plus noise) power ratio, SINR. However, in deciding in favor of an inter-system HO, the measured SINR's in the two channels cannot be directly compared unless both systems employ identical modulation and coding formats (which is often unreasonable due to the extremely different channel characteristics). A possible solution would be to set a minimum acceptable value for SINR in the two systems, and then compare the relative difference of the measured values to the respective minimum values. The comparison is meaningful only when the slopes of the BER vs. E_b/N_0 curves in the two systems are, at least, similar.

The simplest approach is to rely solely on power level measurements performed by the MS periodically, even though it should be evident that the lack of important information may lead to incorrect handover requests. As before, the comparison between the measured levels in the two systems should be carried out on the basis of the distance from a minimum acceptable level, assuming similar performance curves slopes.

2.1 The Modeling Approach

The model for an inter-system HO can be formalized as follows: suppose, for simplicity, that the MS sees only one BS in the terrestrial system, TBS (Terrestrial Base Station), and one in the satellite system, SBS (Satellite Base Station). If the MS is logged onto the terrestrial system, assume it is moving out of the serving cell following a straight line at a constant velocity. The terrestrial cell is overlaid by a cell in the satellite system controlled by the SBS. If the MS is logged onto the satellite system, assume it is moving toward a cell in the terrestrial system following a straight line at a constant velocity. Let $y_T(i)$ and $y_S(i)$ be the current estimate at $t = t_i$ of measured levels of the signals received from TBS and from SBS, respectively. Ignoring any co-channel interference, these estimates can be written as:

$$(1) \quad y_x(i) = P_x - L_x(i) - A_x(i), \quad x = T, S,$$

where P_T is the power transmitted from TBS, $L_T(i)$ and $A_T(i)$ are the free-space loss and shadowing contribution in the terrestrial path at $t = t_i$, P_S is the power transmitted from the satellite, $L_S(i)$ and $A_S(i)$ are the free-space loss and shadowing contribution in the down-link path at $t = t_i$. All quantities are expressed in dB. A_T(dB) and A_S(dB) are supposed to be quasi-stationary zero-mean Gaussian random processes. The stationarity is maintained as long as the environment in which the MS is moving does not change significantly. In (1) the effects of Rayleigh and Rice fading are neglected, assuming that the level estimates are obtained through proper filtering. However, the same filtering is not able to eliminate the effects of A_T and A_S, due to the much lower pitch

144

of shadow fading. Therefore it is advisable not to compare instantaneous quantities but rather averaged quantities:

$$(2) \quad \overline{y_T}(i) = \frac{1}{N} \sum_{n=0}^{N-1} y_T(i-n) \quad ,$$

$$(3) \quad \overline{y_S}(i) = \frac{1}{M} \sum_{m=0}^{M-1} y_S(i-m) \quad .$$

The number of averaging intervals can be different in the two systems since channel propagation conditions are usually different. Let ξ_T and ξ_S be the minimum acceptable levels for the power received from TBS and SBS respectively. Assuming the BER vs. E_b/N_0 curves in the two systems have similar slopes, the decision statistics can be based on the relative average levels:

$$(4) \quad \delta_x(i) = \overline{y_x}(i) - \xi_x \quad , \qquad x = T, S$$

The autocorrelation function of the two shadowing processes is supposed to be exponentially distributed [4]:

$$(5) \quad E\{A_x(i)A_x(i+n)\} = \sigma_{A_x}^2 \gamma_x^{|n|}, \quad x = T, S \quad ,$$

where $\sigma_{A_T}^2$ and $\sigma_{A_S}^2$ are the variances of the shadowing processes in the terrestrial and satellite links, while $\gamma_T < 1$, and $\gamma_S < 1$, are the parameters which determine the decaying rate of the correlation. The variance of the estimated relative level from TBS is:

$$(6) \quad \sigma_T^2 = \mathrm{Var}\{\delta_T\} = \frac{\sigma_{A_T}^2}{N}\left[1 + 2\sum_{n=1}^{N-1}\left(1 - \frac{n}{N}\right)\gamma_T^n\right] \quad ,$$

and a similar expression for $\sigma_S^2 = \mathrm{Var}\{\delta_S\}$. The variance in the estimates is usually large enough for an unnecessary handover to occur, that is a handover followed by a handover back to the former system. In order to decrease the probability of unnecessary handovers, P_U, a hysteresis cycle is introduced in the handover inizialization procedure. Letting $\Delta(i) = \delta_T(i) - \delta_S(i)$, the rules for issuing a handover request can be expressed as:

$$(7) \quad HO(i) \{TBS \rightarrow SBS\} : \Delta(i) < -H_T \quad .$$

$$(8) \quad HO(i) \{SBS \rightarrow TBS\} : \Delta(i) > H_S \quad .$$

where H_T and H_S are the hysteresis margins. The decision statistics is given by the distribution of the variable $\Delta(i) \sim N [\mu(i), \sigma^2]$, where $\mu(i) = E\{\delta_T(i)\} - E\{\delta_S(i)\}$ and $\sigma^2 = \sigma_T^2 + \sigma_S^2$.
An approximate evaluation of the probability of unnecessary HO can be obtained as:

$$P_U(TBS \rightarrow SBS) = \mathrm{Prob}\{\Delta(i) < -H_T, \Delta(i+k) > H_S\}$$
$$(9)$$
$$\cong Q\left(\frac{H_T + \mu(i)}{\sigma}\right) \cdot Q\left(\frac{H_S - \mu(i+k)}{\sigma}\right) \quad ,$$

$$\text{where } Q(x) \overset{\Delta}{=} \frac{1}{\sqrt{2\pi}} \int_x^\infty \exp\left(-\frac{t^2}{2}\right) dt \quad .$$

An expression similar to (9) holds for $P_U(SBS \rightarrow TBS)$. The larger the values for H_T and H_S, the longer will be the delay in issuing a handover request, D, which is comprised of two contributions [8]: the first is due to the averaging of measured levels, while the second is the effect of the hysteresis cycle. For a given MS speed, evaluation of D depends on the slope of $E\{\delta_T(i)\}$ and $E\{\delta_S(i)\}$ as a function of i. As far as the terrestrial link is concerned, the slope can be derived from [9]. In the case of the satellite link, a distinction must be made between systems employing geostationary (GEO) satellites and those with constellation of small satellites on low-Earth orbits (LEO). In the first case, for all practical purposes the path loss slope can be assumed to be almost zero. The situation changes drastically when the satellite is on a LEO: the relative angular velocity of the spacecraft w.r.t. Earth renders the slope much steeper. Only the case of a GEO orbit is considered here. The delay in issuing the handover request TBS -> SBS can be estimated through the following equation:

$$(10) \quad D_T = \frac{T_{av}}{2} + \frac{R}{v}\left(10^{H_T/K} - 1\right) \quad ,$$

where T_{av} is the averaging time, v is the MS velocity, R is the distance of the MS from the TBS at the overlay borderline, $K = 45 - 6.6 \log(h_B)$, h_B is the TBS antenna height. A similar expression holds for SBS -> TBS handover.

3. INTER-SYSTEM HO EXECUTION

In order to analyze inter-system handover execution, some assumptions are needed about network architecture. The satellite system is supposed to be integrated with a GSM-like (or DCS-like) terrestrial system [10]. The satellite system shares the fixed facilities of the terrestrial network. Since the switching facilities are located on ground, transparent satellites are considered. The Home Location Register (HLR) can be unique for both systems in the service area. The home of a user is located in the satellite system if and only if it belongs to an area not covered by the terrestrial system. On the other hand, a dedicated Visitor Location Register (VLR) is assumed for each system.
Suppose, as before, a simplified situation with only one TBS and one SBS in visibility. A flow diagram of the TBS->SBS handover procedure

(including initialization and excecution) is shown in Fig.1, while the main signaling flow is shown in Fig.2. While it is connected to a TBS during an active call, the dual-mode MS monitors the Broadcast Control Channels (BCCH) coming from both TBS and SBS. If MAHO is adopted, the measurements results are sent to the TBS on the Slow Associated Control Channel (SACCH) to assist the handover decision process performed at TBS/MSC level. Monitoring continues until the necessity for a handover is recognized. The handover request is issued to the Satellite MSC (S-MSC), which grants one of its available channels. The handover execution message is forwarded, through a Fast Associated Control Channel (FACCH), to the MS, which starts transmitting on the assigned satellite channel. Handover indication to the T-MSC includes characteristics of the granted channel and the relative commands. It is evident that the delay introduced by the satellite hop must be properly taken into account, since it may generate a time interval during which no message blocks are received from both the MS and the fixed network side.

As pointed out in the introduction, the handover failure rate is affected by the delay in the handover inizialization process. However, it also depends on the availability of free channels to be assigned to handover requests which, in turn, is tightly related to the selected channel assignment strategy. *Fixed* and *dynamic* criteria refer to the free channel selection among a pre-assigned permanent channel set of each cell or among all the available channels, respectively. An intermediate solution (*flexible*) adds to the pre-assigned permanent channels a set of emergency channels, which are distributed to the cells on either a scheduled or a predictive basis. Further, borrowing strategies are possible where the free channel can be also searched in the neighbouring cells, provided it does not interfere with the active calls [6].

In the present study the channel assignment strategy is supposed to be basic fixed, as this choice seems reasonable in an integrated satellite and terrestrial environment. However, the fixed assignment could be effectively modified in the cells where inter-system handovers more often take place. In particular, a subset of the pre-assigned permanent channels of each satellite and terrestrial cell covering the border area could be permanently devoted to satisfying inter-system handover requests.

Guard channels or queueing of handover requests have been proposed to keep the probability of handover failure low [6,7]. In particular, queueing of handover requests seems an interesting method of giving priority to handover requests with respect to new call attempts. The MS, after recognizing the need for handover, is usually able to communicate on the old channel with acceptable quality for a certain time interval, waiting for the new channel. Note that in Fig.1 the queueing alternative is considered.
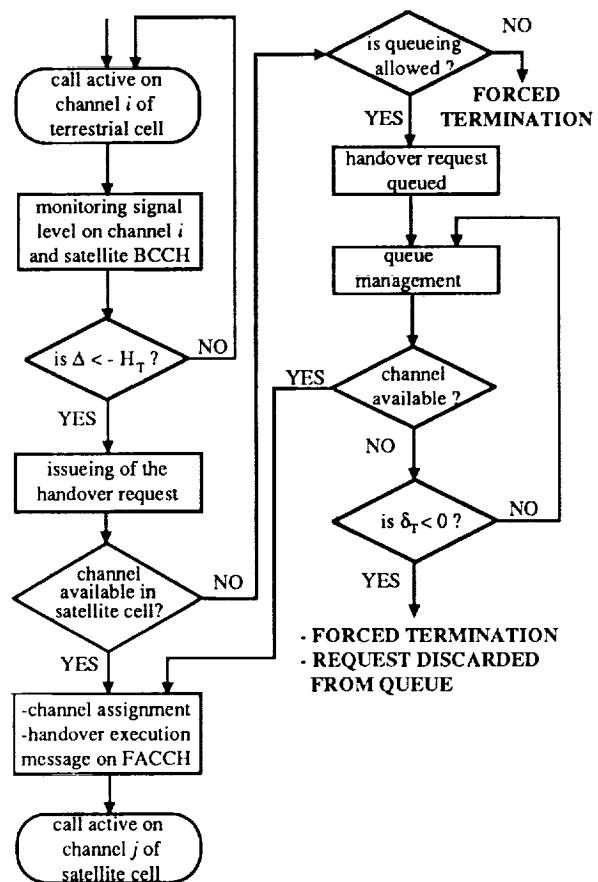
Fig. 1 - Terrestrial-to-satellite inter-system handover procedure flow-diagram
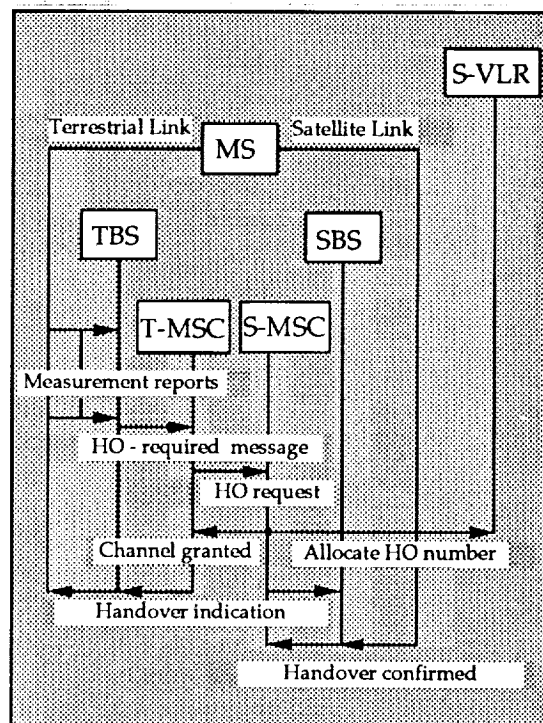
Fig. 2 - Handover signaling flow

146

4. NUMERICAL RESULTS

On the basis of the previously developed model, a numerical analysis is carried out. Fig.3 shows the standard deviations σ_T (continuous line) and σ_S (dotted line) as a function of the number of averaging intervals. The following values are assumed for the shadowing model parameters: $\sigma_{A_T} = 6.5$ dB, $\gamma_T = 0.8$, $\sigma_{A_S} = 5.5$ dB, $\gamma_S = 0.7$. Choosing N = 37 and M = 16, it turns out $\sigma_T \cong \sigma_S \cong 3$ dB. In this case, hysteresis margins can be equal.

The probability of unnecessary handover is plotted in Fig.4 versus the common value of hysteresis margin, assuming $\mu(i) \cong \mu(i + k)$. The benefit of inserting the hysteresis cycle is evident.

The delay in issuing the handover request is shown as a function of the hysteresis margin in Fig.5, supposing the sampling interval is 250 msec, R = 3000 m, v = 13 m/s, and for two values of the number of averaging intervals in the terrestrial link measurement N (N = 40, continuous line; N = 200, dotted line).

As far as the execution of inter-system handover is concerned, a queueing algorithm based on FIFO (First In First Out) discipline has been simulated for a satellite cell provided with 200 channels (110 s mean occupancy time), for a 15% handover traffic over the total offered traffic. The simulation results are reported in Fig.6, in terms of probability of handover failure versus the *residual handover margin*, here defined as the difference between the signal level at the time instant when the handover request is issued and ξ_T. As the advantages of queueing increase with this margin, it clearly results that the optimization of the handover procedure must involve both the inizialization and the execution processes.
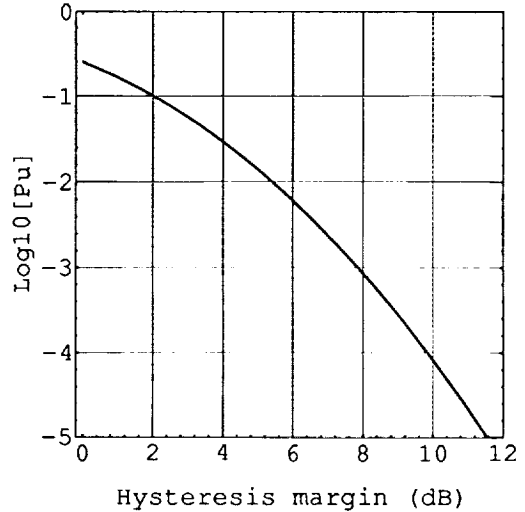
Fig.4 - Probability of unnecessary handover as a function of the common value of hysteresis margin $H_T = H_S$
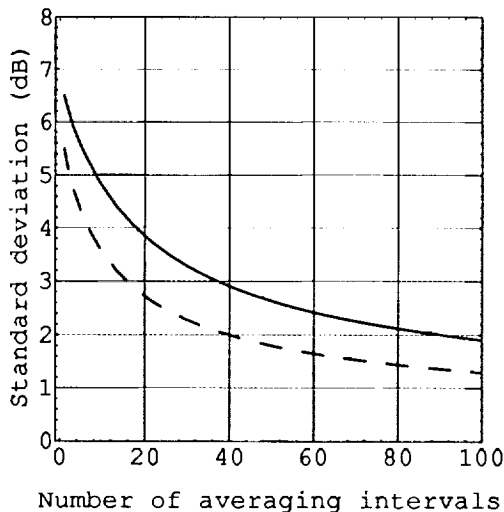
Fig.3 - Standard deviation in the power level measurement (continuous line: σ_T; dotted line: σ_S)
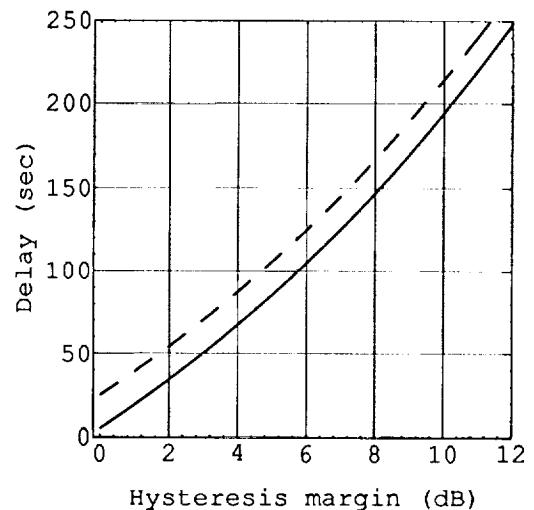
Fig.5 - Delay in the initialization phase of a TBS -> SBS handover (continuous line: N = 40; dotted line: N = 200)
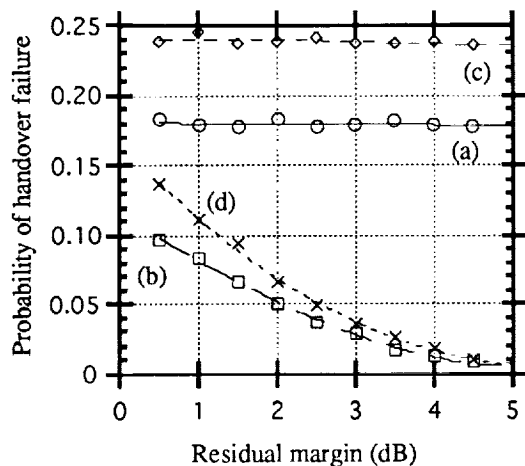
Fig.6 - Probability of handover failure offered traffic: (a),(b) 250 E; (c),(d) 300 E queue: (a),(c) unqueued ; (b),(d) FIFO

5. CONCLUSIONS

A key aspect in the integration of satellite and terrestrial mobile systems is the effectiveness and the reliability of inter-system handover procedures. Difficulty arises in trying to estimate the relative quality of two systems employing different modulation and coding formats. The criticity of the comparison and the user terminal complexity could be lowered if the satellite and the terrestrial systems were as similar as possible.

The optimum handover procedure should minimize the probability of unnecessary handover, on one side, and the probability of handover failure, on the other. The compromise between these two contrasting objectives must be carried out on the basis of a model that includes the overall handover procedure. The paper has proposed and analyzed a complete inter-system handover model, consisting of both the inizialization and execution phases.

REFERENCES

[1] G.E.Corazza, M.Ruggieri, F.Valdoni, F.Vatalaro: "System and Technology Aspects for EHF Cellular Communications", *Acta Astronautica*, vol.26, n.8-10, pp. 715-721, 1992 .

[2] C.Caini, G.E.Corazza, G.Falciasecca, M.Ruggieri, F.Vatalaro: "A Spectrum and Power Efficient EHF Mobile Satellite System to be Integrated with Terrestrial Cellular Systems", *IEEE JSAC*, vol.10 n.8, October 1992, pp. 115-1325.

[3] E.Del Re, "An Integrated Satellite-Cellular Land Mobile System for Europe", *8ᵉ ICDSC*, pp. 461-466, Guadeloupe, April 1989.

[4] M.Gudmunson, "Analysis of Handover Algorithms", *41st IEEE VTS Conf.*, St. Louis, May 1991, pp. 537-542.

[5] O.Grimlund, B.Gudmunson, "Handoff Strategies in Microcellular Systems", *41st IEEE VTS Conf.*, St. Louis, May 1991, pp. 505-510.

[6] S.Tekinay, B.Jabbari, "Handover and Channel Assignment in Mobile Cellular Networks", *IEEE Comm. Mag.*, Nov. 1991, pp. 42-46.

[7] P.O.Gaasvik, M.Cornefjord, V.Svensson, "Different Methods of Giving Priority to Handoff Traffic in a Mobile Telephone System with Directed Retry", *41st IEEE VTS Conf.*, St. Louis, May 1991, pp.549-553.

[8] A.Murase, I.C.Symington, E.Green, "Handover Criterion for Macro and Microcellular Systems", *41st IEEE VTS Conf.*, St. Louis, May 1991, pp. 524-530.

[9] M.Hata, "Empirical Formula for Propagation Loss in Land Mobile Radio Services", *IEEE Trans. Veich. Tech.*, Vol. VT-29, No. 3, August 1980, pp. 317-325.

[10] CEPT Study Group on Mobiles, "GSM Recommendations", CCH/GSM/PN, February 1988.

MSAT and Cellular Hybrid Networking

Patrick W. Baranowsky II
Westinghouse Electric Corporation
P.O. Box 1693 MS 8419
Baltimore, MD 21203, USA
(410) 765-0037 (work)
(410) 765-1330 (fax)

ABSTRACT

Westinghouse Electric Corporation is developing both the Communications Ground Segment and the Series 1000 Mobile Phone for American Mobile Satellite Corporation's (AMSC's) Mobile Satellite (MSAT) system. The success of the voice services portion of this system depends, to some extent, upon the interoperability of the cellular network and the satellite communication circuit switched communication channels. This paper will describe the set of user-selectable cellular interoperable modes (cellular first/satellite second, etc.) provided by the Mobile Phone and described how they are implemented with the ground segment. Topics including roaming registration and cellular-to-satellite "seamless" call handoff will be discussed, along with the relevant Interim Standard IS-41 Revision B Cellular Radiotelecommunications Intersystem Operations and IS-553 Mobile Station - Land Station Compatibility Specification.

INTRODUCTION

According to Frost and Sullivan International, in 1996 terminal sales for mobile satellite communications are expected to increase to $1 billion, with annual service revenues surpassing more than $472 million [1]. This will occur because we live in an information starved society that needs a means of seamless communications for land, sea, and air. Our current terrestrial cellular network covers significant portions of the United States and, although Inmarsat covers most of the planet, cost for terminals and service are excessive for many applications. For example, the least expensive Inmarsat voice terminal is the $15 thousand Standard M terminal with a $5.50 per minute phone rate [2].

The solution to this dilemma is a system that will provide both cellular and satellite coverage with user-selectable priority modes to determine which system has communications priority and under what circumstances, if any, a handoff to the backup system will occur. This is accomplished with a mobile phone tranceiver that contains both MSAT and cellular interactive equipment. The mobile must allow mode programming from the user handset and be capable of monitoring the status of either network. Then, the mobile phone can process status to generate registrations on the appropriate network or seamless call handoffs between networks.

This paper will discuss the details of MSAT and cellular interoperability by describing the five Series 1000 Mobile Phone modes of operation. The cellular only and MSAT only modes first must be described in enough detail to be referenced by the three hybrid modes. The hybrid modes, including MSAT Priority with Cellular Backup, Cellular Priority with MSAT Backup, and Cellular Home Location Register (HLR) Priority with MSAT Backup, will explain how similarity and flexibility between the MSAT and cellular networks allow an intricate scheme of priority allocation and handoff.

CELLULAR ONLY MODE

For day to day mobile voice communications in urban or suburban environments, cellular communications may be the network of choice. Cellular coverage is complete in most metropolitan areas and offers the most cost effective interface to the Public Switched Telephone Network (PSTN). In addition, a terrestrial network such as cellular eliminates the propagation delay associated with satellite communication (.25 seconds for a geostationary satellite). Thus, an individual confined to a metropolitan environment and performing voice communications may chance the dropped calls associated with cell to cell handoff and select the
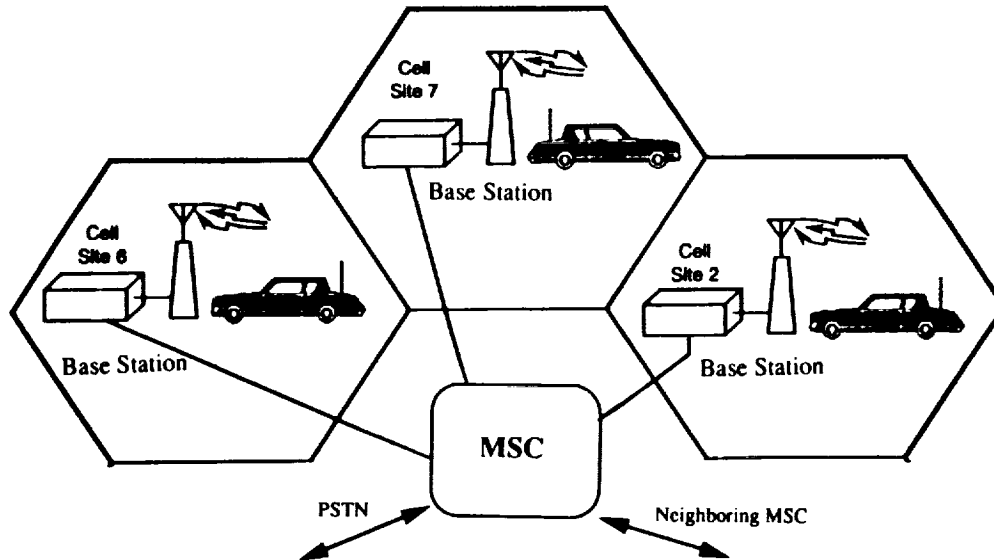
Figure 1: Cellular Network

cellular only mode.

The cellular network consists of a network of switches connected to the PSTN. These switches mimic the operation of PSTN End Office (EO) switches where calls routed throughout the PSTN are terminated and connected to the users. In the cellular network, all calls between a PSTN subscriber and a cellular mobile phone are still routed through the PSTN. The added feature is that the call terminates at a cellular Mobile Switching Center (MSC) which controls and connects directly to a network of cells encompassing and defining the MSC's region of coverage (Figure 1). Adjacent regions of cells are controlled by different MSC's. These cells contain base stations that provide the microwave links to the cellular mobile phone and T-1 trunks to shuttle this information to the MSC.

Upon mobile power-up, the cellular phone scans the preassigned control channels and locks onto the strongest channel which connects to the MSC through the control channel's base station. If the mobile phone is registered in the MSC's Home Location Register (HLR) database, all necessary information is already present to allow subscribed features like call waiting or conference calling to be implemented. If the mobile phone registers as a roamer in a visiting MSC, the visiting MSC requests permission for registration from the home MSC. Then, the mobile's status will be contained in the visiting MSC's Visitor Location Register (VLR) database. All PSTN calls, which are automatically routed to the home MSC, now will be forwarded to this visiting MSC.

Upon reply to a paging request or in response to a call initiation, the serving MSC will allocate a free voice channel from the mobile phone's resident cell.

The forward and reverse voice channels contain enough bandwidth (20 kHz each) to allow transmission of voice and either status control data or Supervisory Audio Tones (SAT) and signalling tones.

As a mobile phone engaged in a conversation travels between cells, a seamless handoff process is required (Figure 2). Once the SAT tones transponded by the mobile phone are received by the MSC with less power than a predetermined handoff threshold, the MSC sends a Measurement_Request_Invoke message to the target (neighboring) MSC using an IS-41 data link. This command includes information regarding the serving cell and channel of the mobile phone. The target MSC then commands all cells within proximity to the mobile's cell to read and report the received SAT power level. The target MSC assimilates the readings and responds with a Measurement_Request_Return_Result message to submit the signal quality of a potential target cell. The serving MSC then determines that the target MSC contained the cell with the strongest reception, so it sends the target MSC a Facilities_Directive_Invoke message to indicate the source and destination cells and the mobile phone's identification. The serving MSC also uses this opportunity to allocate the specific voice trunk channel between the two MSC's to establish a connection between the PSTN and target MSC through the serving MSC. The target MSC responds with a Facilities_Directive_Return_Result message which includes an allocated voice channel for the mobile phone and requests SAT. The serving MSC relays this status information to the mobile on the control portion of its voice channel. The mobile then acknowledges with a signalling tone and retunes to the new channel.

150

The target cell began sending SAT on the new voice channel after transmission of the Facilities_Directive_Return_Result message, so the mobile phone tunes to this SAT and transponds it back to the target cell to indicate a successful handoff. This causes the target MSC to send a Mobile_On_Channel_Invoke message over the IS-41 link to the serving MSC. Upon reception of this message, the serving MSC switches the PSTN connection from the serving cell to the target MSC. The target MSC then allows full voice communication through the target cell to the mobile phone. Communications will occur on this cellular voice channel until the next handoff or until an on hook is noticed by a loss of SAT.
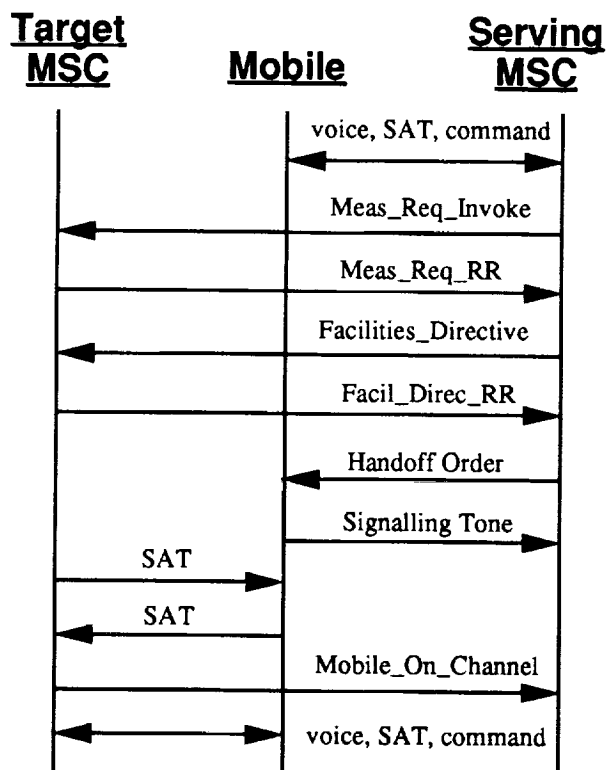
Figure 2: Cellular Call Handoff

MSAT ONLY MODE

Many applications for MSAT, including marine, airborne, rural, fax, and data communications, are difficult for cellular communications. In these circumstances, MSAT is the most consistent and possibly the only means of mobile communications to the PSTN. To avoid the added processing of hybrid modes, a user may choose to use the MSAT, only. He or she may not even purchase the optional cellular hardware.

The MSAT network consists of a Feederlink

Earth Station (FES) that supplies all communication channels to the mobile phones via a geostationary satellite and allows communications to the PSTN through a Gateway Switch (GWS) that operates similar to an MSC. All allocations are controlled by a Network Control Center (NCC) that performs all processing and maintains all control channels (Figure 3). As the system expands, more satellites and FES's may be added.
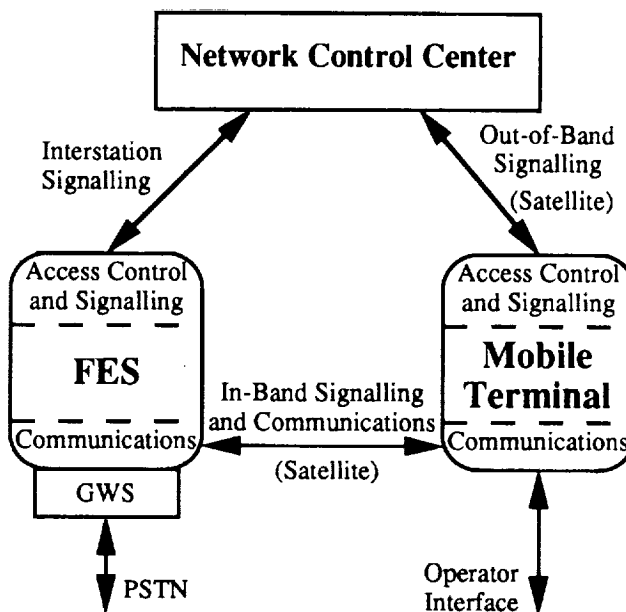
Figure 3. MSAT System Architecture

Upon power-up the mobile phone must find a control channel by first checking its previously assigned satellite beam, and if inaccessible, checking other beams. Before the mobile may access the system, it must read and update all system information from the control channel which includes congestion and configuration information. The mobile phone stores control channel and beam information in its non-volatile memory, and if a new channel is required, the mobile must perform a log-on procedure which tells the NCC who the mobile phone's identity and configuration.

At this point, the mobile phone is ready to make or receive phone calls. The structure of the MSAT system is similar to the cellular system because both contain separate control and voice channels with roaming information passed over the control channels and in-call information multiplexed over the voice channels. The main difference is that MSAT's voice channels cover thousands of square miles with beam overlap eliminating the need for a live-call handoff. Also, voice channels use Time Division Multiplexing (TDM) for control data and replace the SAT tone with a periodically required TDM unique word.

151
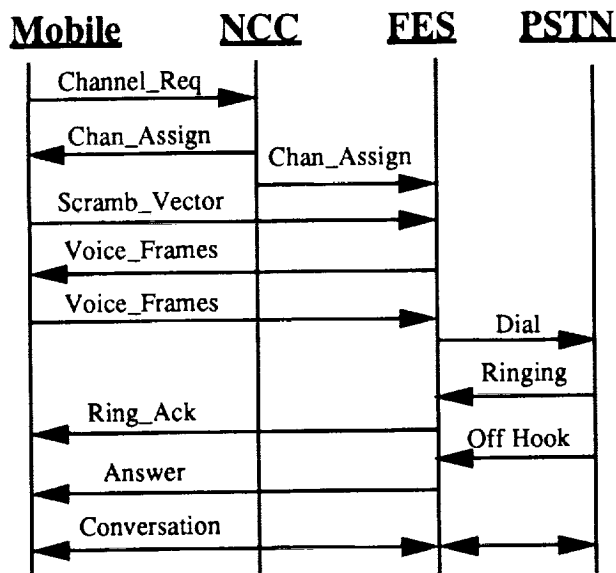
Figure 4: Mobile to PSTN Call Setup

When the mobile phone initiates a call (Figure 4), the called digits are sent with the mobile's identification to the NCC to request a voice channel. The NCC validates the identification number and assigns the voice channel for the mobile phone and the FES completes the call set up. The mobile phone then sends its security key and scrambling vector to the FES to verify database continuity and avoid fraudulent access. The FES and mobile then exchange voice frames containing off hook supervisory information causing the mobile to switch to voice mode. At this point, the FES dials the number through the PSTN and receives a response from the PSTN including ringing, busy, or operator recordings. The FES sends the response to the mobile phone which is passed to the user since the mobile phone is in voice mode. An off hook response from the PSTN to the FES causes the FES to change state to 'In Conversation' and requests a similar response from the mobile by sending an 'answer' unique word on the command portion of the voice frame. Conversation continues between the mobile phone and FES to the PSTN until a call release is issued by either party.

When a PSTN call is routed to the FES (Figure 5), the FES rings back the caller and requests a channel from the NCC which validates the mobile phones's identification number and determines its control channel. The NCC then verifies the mobile phone's availability by sending a call announcement to the mobile phone. The NCC validates the mobile based on its response and assigns the voice channel to both the mobile phone and the FES. The mobile phone retunes to the voice channel and sends its scrambling vector and access security key to the FES to be verified and allow

secure, non-fraudulent communications. The mobile phone then switches to voice mode and conveys the ringing tone from the FES voice frames to the user. The mobile phone acknowledges the receipt of ringing to the FES, and once the user answers the phone, voice frames are sent to the FES with an 'off hook' unique word causing the FES to establish a voice connection between the two users. Conversation continues until a call release is issued by either party.
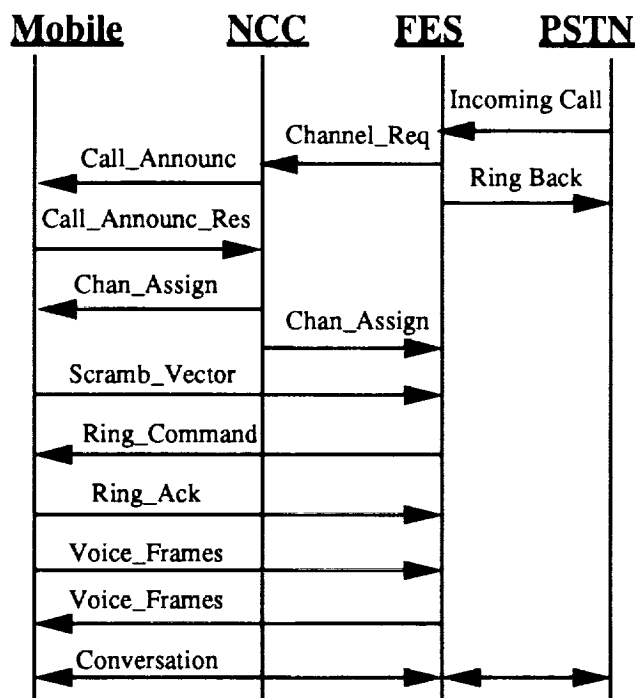
Figure 5: PSTN to Mobile Call Setup

When either the mobile phone determines that the user has hung up or the FES determines that the PSTN user has hung up, an 'on hook' unique word is sent on the voice control channel to request a call termination.

MSAT PRIORITY, CELLULAR BACKUP MODE

If a user is predominantly in a rural environment but occasionally visits urban areas, MSAT would be the preferred means of coverage but cellular would provide a potential redundancy. A user also may prefer the consistency of satellite coverage and only want cellular coverage as a backup to assure continuous communications availability. Every cell to cell handoff in the cellular network introduces a slight risk of dropping the call, so a user may prefer the consistency of a single satellite beam spanning thousands of square miles. If the user travels through a city where large buildings block the mobile phone's view of the satellite,

152

satellite coverage may temporarily wane and the cellular backup can be used.

Once the mobile phone is powered up, it attempts to operate in MSAT as described earlier. If all attempts to obtain a control channel fail or the MSAT refuses service based on the mobile's status or erroneous operation, the mobile phone automatically switches to cellular operation. If the mobile phone attempts to make a phone call and cannot obtain a voice channel, it will automatically switch to cellular mode and attempt the same phone call over the cellular network. Finally, if the mobile phone is roaming and notices loss of access to the control channel, it will attempt to find a new control channel, and if none exist, it will register on the cellular network. Once in the cellular system, the mobile phone will continually monitor the MSAT control signals and will periodically attempt to re-register on MSAT if a control channel is present.

Registration and re-registration is possible between these two systems because the GWS appears to be another MSC to the cellular network. When using MSAT, the HLR thinks that the mobile phone is in a VLR. When communications is lost with the satellite, the cellular transceiver attempts an autonomous registration which is received by the resident MSC and sent to the HLR. The HLR previously registered the mobile phone with the VLR in the GWS. Then, the HLR updates the database with the location of the resident MSC to allow all phone calls to be routed to this MSC rather than the GWS. The HLR treats the whole operation as if a cellular mobile just traveled from the coverage of one MSC to another. When the satellite coverage returns, the cellular portion of the mobile phone stops operating and the mobile phone registers with MSAT. This causes the GWS to send a registration notification to the HLR to re-register the mobile phone with the VLR of the GWS. This process also appears to be a cellular autonomous registration to the HLR. At this point all calls will be rerouted to the GWS from the HLR.

If a mobile phone roams into cellular coverage and then initiates a phone call, the MSC will determine network coverage. If the cellular call begins to fade, a seamless in-call handoff back to MSAT may be initiated. The details and occurrences of this seamless handoff are covered in the next mode and in figure 6.

While the satellite portion of the mobile phone is registered on the MSAT, the cellular portion of the mobile phone cannot independently register on an available MSC. This would cause the HLR to believe a mobile phone is fraudulently accessing the cellular network. From the HLR's point of view, the mobile phone is registered in one VLR (the GWS) and another mobile phone is trying to use the same mobile

identification to register on another MSC. At this point, the home MSC would cancel both registrations. Without being able to register in the cellular network while being registered on MSAT, handoff from MSAT to cellular is impossible because the cellular network has no idea where the mobile phone is located or with which cell to establish registration. Consequently, MSAT to cellular in-call seamless handoffs are impossible without significantly changing the operation of the cellular network. To avoid this, once a call is in progress on the satellite, no seamless handoffs to the cellular network will be allowed. Instead, if satellite coverage wanes during a phone call, the call will be dropped and then the mobile phone will autonomously register on the cellular network.

CELLULAR PRIORITY, MSAT BACKUP MODE

Of the three hybrid modes, this mode should be the most common. This mode allows a cellular user to fortify communications capabilities by allowing regular cellular operation with a satellite fall-back if cellular coverage degrades. This mode allows roaming analysis and registration similar to the methods of MSAT Priority with Cellular Backup, but this mode also allows seamless call handoff from cellular to MSAT during a phone call as cellular coverage wanes. Thus, the user, who is typically covered by cellular coverage but wants redundancy to patch the gaps in the cellular network, can maintain continuous communications coverage.

As mentioned previously, this mode allows a roaming mobile phone to analyze its coverage, and when the coverage degrades, switch to the other system. This uses the same principles as the satellite priority mode except the cellular service has priority, so if cellular coverage wanes and the mobile phone reverts to MSAT, the cellular coverage must be periodically tested to determine the ability to re-register. The process of registering on cellular is the same as with the satellite priority mode. The only difference is that the mobile phone will attempt registration on an MSC before resorting to a GWS.

The new concept introduced by this mode is the seamless call handoff. Since internal MSC cells have coverage overlap, any situation extensive enough to cause a cellular call to be dropped would not allow a seamless handoff to MSAT; whereas, the MSC's border cells present a situation where a mobile phone gradually leaves coverage. Consequently, the MSC is equipped with provisions, including inert cellular handoff channels, to provide seamless handoff from these border cells when cellular coverage is waning and another cell cannot receive the handoff. These inert channels are cross referenced with each border cell such

that the channels are considered acceptable by the MSC but are used by cells distant enough from the serving cell to avoid any possible contention during the handoff process.

Mobile   NCC   FES   MSC
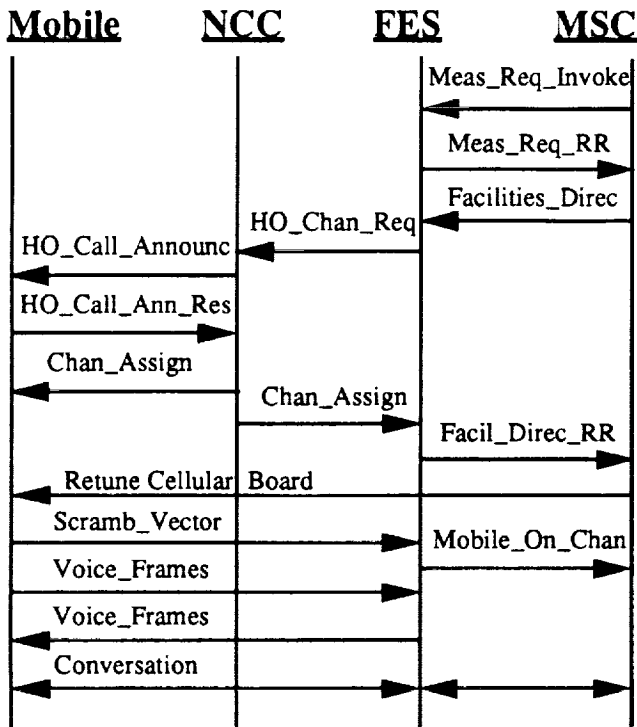
Figure 6: Cellular to MSAT Handoff

The ladder diagram (Figure 6) indicates that the cellular to MSAT handoff is a combination of MSC to MSC handoff (Figure 2) and PSTN to mobile call setup (Figure 5). This process succeeds in convincing the mobile that it is receiving a new phone call on the MSAT while convincing the serving MSC that it is handing off to a stronger target MSC. All can be accomplished with a single phone number shared between the cellular and MSAT networks.

Consistent with IS-41, the serving MSC begins searching other cells and neighboring MSC's whenever SAT degrades below a threshold. All MSC's will be fitted with software to petition the GWS whenever the border cells attempt handoff. The GWS will return the minimum value allowed by an MSC without deeming a call as lost, thus giving the adjacent MSC's top priority. If this nominal value is strongest, the mobile phone and MSAT perform call setup to assign a satellite voice channel. When the FES receives its channel, it sends a Facilities_Directive_Return_Result to the serving MSC to request the cellular portion of the mobile to change channels. This new cellular channel is inert but accommodates transparency with the MSC. Upon verifying the scrambling vector information, the FES

requests activation of the voice trunk from the serving MSC to the GWS to allow connectivity from the MSAT voice channel to the PSTN through the MSC. After the FES and mobile phone exchange voice frames, they both switch to voice mode and allow conversation. The handoff is complete.

CELLULAR HLR PRIORITY, MSAT BACKUP MODE

This mode is similar to Cellular Priority with MSAT Backup except roaming in a visiting MSC is avoided. The mobile phone will monitor its location, and if it is roaming and notices a pending registration on a visiting MSC, the mobile phone will cease cellular activity and register on the MSAT. Consequently, the user will minimize cellular roaming charges and still enjoy continuous coverage. The mobile phone will periodically sample the cellular network to determine whether it has returned to the home MSC. If so, cellular registration will be reinitiated.

If the mobile phone leaves the HLR during a phone call, the HLR will petition to handoff to a VLR as well as MSAT. This is similar to the regular cellular priority mode to minimize call disruption. If registered in the VLR upon completion of the call, service immediately will be transferred to MSAT. Thus, this mode has unique roaming functions, but operates similar to the standard cellular priority mode during a call.

CONCLUSIONS

The current communications market has dynamic needs which are satisfied only partially by any given communications system. To better match society's communications needs with networks of varying cost, topology, features, and performance, hybrid networking is the obvious solution. By introducing interoperability to networking, the users will reap the benefits of diversity. MSAT was developed with cellular interoperability considerations lending toward an integrated system of national connectivity, inexpensive urban voice communications, and high speed data communications.

REFERENCES

[1] "Mobile Satellite Service is Expected to Take Off During the Next Four Years", Radio Communications Report, Volume 11, Number 19, October 12, 1992.

[2] D. Meluso, "SATCOM for Sailboats: New Standards for Voice and Data Transmission", Sail, Vol. 23, no. 9, pp. 88-97, September 1992.

Session 5
Advanced System Concepts and Analysis—I

Session Chair—*Jai Singh*, Inmarsat, England
Session Organizer—*Arvydas Vaisnys*, Jet Propulsion Laboratory, U.S.A.

(continued)

/5 6

TRENDS IN MOBILE SATELLITE COMMUNICATION

Klaus G. Johannsen, Mike W. Bowles,
Samuel Milliken, Alan R. Cherrette, and Gregory C. Busche

Hughes Aircraft Company
PO Box 92919
Los Angeles, California 90009
(310) 364-7936; Fax (310) 364-7186

ABSTRACT

Ever since the U.S. Federal Communication Commission opened the discussion on spectrum usage for personal handheld communication, the community of satellite manufacturers has been searching for an economically viable and technically feasible satellite mobile communication system. Hughes Aircraft Company and others have joined in providing proposals for such systems, ranging from low to medium to geosynchronous orbits. These proposals make it clear that the trend in mobile satellite communication is toward more sophisticated satellites with a large number of spot beams and onboard processing, providing worldwide interconnectivity. Recent Hughes studies indicate that from a cost standpoint the geosynchronous satellite (GEOS) is most economical, followed by the medium earth orbit satellite (MEOS) and then by the low earth orbit satellite (LEOS). From a system performance standpoint, this evaluation may be in reverse order, depending on how the public will react to speech delay and collision.

This paper discusses the trends and various mobile satellite constellations in satellite communication under investigation. It considers the effect of orbital altitude and modulation/multiple access on the link and spacecraft design.

MOBILE SATELLITE ARCHITECTURE

The architecture of a mobile satellite is complex and its design varies strongly with orbit altitude. In general, it consists of

1) Multibeam mobile band antennas

2) Feeder link antennas

3) Crosslink antennas

4) Transponder, including processor for
    a) Signal routing
    b) Regeneration
    c) Storage and reformatting

The complexity is partly due to the large number of beams and the associated frequency translation and power amplification equipment, and, partly, to signal routing and dynamic bandwidth and power allocation. As traffic varies and power has to be appropriately allocated, beam bandwidth and beam power limitations have to be overcome by special techniques. Because of the complexity of the mobile satellites, new technologies have to be applied to save power and weight. These technologies are mostly in existence. However, a great deal of design effort still has to be spent on the realization. This is particularly true for onboard processors, active arrays, and the associated beamforming networks (BFNs). Active arrays are ideally suited for mobile applications because of their built-in redundancy and power sharing features. The problem of diplexing and passive intermodulation generation has to be addressed and the question of whether to use one or two mobile link antennas must be answered.

The choice for a mobile satellite system cannot be made without considering connectivity and circuit establishment. Worldwide connectivity can be accomplished by satellite crosslinks or terrestrial links between gateway stations. The circuit connection should be chosen to minimize path delay. For most connections, it seems that the GEOS has an advantage over LEOS and MEOS in that circuits need not be rapidly handed over from one beam to the next or one satellite to the other. However, studies indicate that even though MEOS and LEOS require more feeder link stations for identical total channel capacity, the total ground system cost for all scenarios remains the same because the money is in the ground circuit switching equipment, which remains constant.

SYSTEM CONSIDERATIONS

Orbit Altitude

The choice of altitude or the size of the spacecraft antenna is greatly influenced by the fact that uplink power levels of the mobile

handheld unit should be low, only a fraction of a watt, to avoid any health hazard and to keep battery packs small. If the ground coverage area is kept constant, then, with increasing altitude, the satellite antenna beamwidth must be reduced or the satellite antenna gain and size must be increased. Under these conditions, the ratio of gain over space loss is constant and received signal levels and transmitted power levels remain the same for all altitudes. The choice of altitude is also influenced by the fact that the earth is surrounded by two radiation belts, one electron belt at around 2,000 km and one proton belt stretching from about 1,000 to 30,000 km with a maximum at 6,000 km and saddle dip minimum at 13,000 km. A LEO has the advantage of low intensity radiation and small signal delay, but the disadvantage of frequent eclipse cycles and a large number of satellites. Also, the ground acquisition is more complex because beam coverages are quickly changing.

A MEOS, during a 6 to 8 hour orbit, sees a great part of the earth; therefore, only 8 to 12 satellites are required, and the altitude is pretty much on the declining radiation intensity versus altitude slope of the proton radiation belt. Still, because the satellites need a shield against proton radiation, they will be relatively heavier. Also, because the satellites are moving, each satellite beam has to be designed for maximum beam traffic.

In the case of GEO, three satellites are sufficient. However, for small levels of uplink power and for a sufficiently high number of channels and downlink carrier effective isotropic radiated power (EIRP), big satellite antennas with narrow (and therefore many) spot beams are required. For mobile to mobile traffic it is necessary to demodulate and route the signal inside the satellite. The large delay does not permit a dual hop operation.

Number of Satellites Versus Altitude

Table 1 gives the number of satellites as a function of altitude and orbit inclination at $10°$ground station elevation angle. The total number is coarsely calculated for the number of satellites required in one orbital plane, which depends on user elevation. From the resulting geocentric earth angle $2L$, one can obtain the minimum number of required spacecraft per orbit plane (π/L) and the minimum number of total satellites for ideal area coverage.

The approximate total number of satellites for given inclination is

$$N_i \cong \frac{2(1+0.57\sin i)}{1-\sqrt{1-\sin^2 L}}.$$

Traffic

Traffic is routed from gateway to the mobile user or from the mobile user to another mobile user. Connections are worldwide, i.e., a mobile user should be able to communicate with another mobile user half way around the earth. For LEOS, this feature requires satellite to satellite links; for MEOS, this requires a tolerable double hop; and for GEOS, a satellite crosslink or a double hop, the delay of which may be objectionable.

Signal Delay

Figure 1 shows the expected signal delay for LEO, MEO, and GEO. The signal delay consists of coding, path, and processing delay. For LEOS, the processing delay may exceed the path delay, because the signal is routed through several satellites. In case of GEO, the path delay is significant, and, for global interconnectivity, the path delay is equivalent to a dual hop delay, whether the signal is routed by terrestrial or intersatellite interconnections. Figure 2 shows the effect of signal delay on the user. There it seems that global interconnectivity from mobile to mobile user (LEOS and MEOS) is admissible; In the case of GEOS for 80% of the population, it is intolerable.Therefore, for GEOS, global interconnectivity is admissible only from mobile to fixed user, i.e., by satellite/terrestrial connection.But mobile to mobile connections within a single satellite coverage are still possible.

Frequency Spectrum

There are several frequency spectra in L-band and S-band designated to mobile communication. In addition, for communication to and from gateway stations, there are feeder link frequency bands of the fixed satellite services required. The available LMSS bandwidth at 1.5/1.6 GHz must be shared among all the mobile satellite operators. This need can be met by allocating sections of the band to each operator, where the allocation may change from region to region. Mobile satellites require a dynamic allocation of bandwidth to each beam. For GEOS, the allocation of bandwidth per system can be geographically fixed but may change with time of day or just with time. Because of necessary frequency coordination, the multiple access method for mobile to mobile band traffic is most conveniently chosen to be

158

frequency division multiple access (FDMA) or time division multiple access (TDMA/FDMA) as it permits allocation of small lumps of bandwidth. Because of the spectral density requirement, the L-S-band with 1.6 GHz up and 2.4 GHz down is reserved for multiple access/modulation systems, which have low spectral densities like TDMA or code division multiple access (CDMA).

Modulation and Multiple Access

Several types of voice coding, forward error correction, modulation, and multiple access systems are under investigation. The spectral channel packing density for FDMA is 5 kHz and for TDMA is 30 to 80 kHz per channel. With CDMA, the packing density is about 40 channels per MHz, i.e. ,40 CDMA channels can be superimposed in a 1 MHz band. While the normal mode of satellite operation uses a dual frequency band for up and downlink transmission, a novel approach uses time division duplexing (TDD), where the transmission to and from the mobile users takes place in a single frequency band (Iridium). It means that all network uplink transmission packets have to arrive at the spacecraft at the same time and that the total network must be synchronized.

With TDMA, where the transmissions are already synchronized, this is just another time constraint. It may require additional storage at the mobile earth station beyond what is required for TDMA burst transmission. If the transmission format is maintained, TDD will double spacecraft and ground terminal peak power and signal bandwidth, although average power will remain constant. The benefit of TDD is that only a single mobile satellite antenna may be used for both transmission and reception and that any intermodulation will not get into the satellite receive band.

Frequency Reuse

To have low power levels at the mobile transmit terminal, to provide many simultaneous transmissions to many distributed users, and to enable reuse of the mobile frequency spectrum, the mobile satellites are equipped with multibeam antennas. The antenna gain and number of beams is dictated by the link, i.e., uplink EIRP, number of channels, signal processing gain, and required E/N_0 for given error rate. Frequency reuse makes it possible to use the narrow mobile bandwidth many times over. For FDMA, four or seven separate frequencies are generally considered practical, i.e., the operating frequency can be repeated in the fifth or eighth beam. For CDMA, depending on spectrum bandwidth, every third beam or, ultimately, every beam may reuse the same frequency. If every beam uses the same frequency, the mobile unit at the third beam 3 dB crossover point will witness a threefold interference.

The frequency reuse factor with optimum beam stacking determines how far two beams, carrying the same frequencies, must be apart. With four distinctive frequencies, the beams of equal frequency are two beamwidths apart; with seven different frequency bands, corresponding beams are 2.5 beamwidth apart. The more frequency bands, the farther beams of the same frequency will be separated and the higher the beam isolation will be (Figure 3).

Bandwidth per Beam

To take advantage of frequency reuse, the available bandwidth must be divided by the number of frequencies. Assuming an antenna with K beams, frequency reuse 1/4, the L-band bandwidth can be reused K/4 times, i.e., each beam will carry one-fourth of the bandwidth. Assuming that out of the total 12 MHz land mobile band only 4 MHz is allocated for a given satellite, each beam will have 1 MHz, and the total L-band bandwidth will be K x 4/4 = K MHz. Assuming 5 kHz carrier spacing, each beam could provide room for 10 ^{6}/5 x 10^3= 200 channels. From a power point of view, only N carriers can be supported. Therefore, for FDMA only, a feeder link and downlink bandwidth in excess of N x 5 kHz has to be made available. Because several feeder link stations are uplinking simultaneously, there must be a packaging of carrier spectrum from C- or Ku-band to the mobile band and vice versa. However, the large amount of mobile bandwidth, made available by frequency reuse, can be put to advantage for stagger tuned transmissions and for easing coordination with other operators.

Assuming enough power is available, the beam capacity is 200 channels due to bandwidth limit. For beams with heavy traffic, however, bandwidth can be borrowed from adjacent beams and therefore the traffic of the congested beams can be increased, provided that traffic in the adjacent beams and available beam power permits it. In other mobile bands, e.g. 1.610 to 1.6265 GHz up, 2.4835 to 2.5 GHz down, more bandwidth may be available for LMSS bandwidth usage.

Flexible Power Allocation

Ideally, all beam amplifiers should amplify all signals. This process is automatically achieved in a phased array. If a reflector antenna is used, the beam amplifiers can be embraced by a hybrid matrix, or a selected number of beams may be embraced by partial matrices. Another approach is to use constant efficiency amplifiers. It can be shown that with a dynamic range of 6 dB most beam power requirements can be satisfied before bandwidth limitations occur.

Antenna Types and Sizes

The antenna size depends on the spacecraft altitude. For GEOS and 100 beams, the antenna diameter is about 5 to 7 meters; for MEOS and 60 beams, the diameter is about 2 meters; and for LEOS, the antenna can still be smaller. The antennas may be active arrays or passive reflectors. The active arrays, which have antenna elements and associated active elements in excess of the number of beams, have two distinct advantages, namely, they do not require redundant units or redundancy switches;rather, they are able to distribute power and provide it where needed. Signals are amplified by all the amplifiers, not only by a single devoted amplifier. If there is high traffic in a particular beam, as many carriers can be made available to this beam as the traffic necessitates and as bandwidth permits. Figure 4 shows various antenna concepts like dual reflector, active array, and single transmit/receive Cassegrain. The active array antenna, when evaluated on a system basis, proves to be most promising, provided it can be realized and deployed.

Satellite Crosslinks and Feeder Links

Satellite crosslinks simplify signal routing and reduce path delay. Crosslinks for LEOS and MEOS must be in the forward/aft direction and sideways to satellites in other orbit planes. Satellite crosslink frequency will be in Ka-band. The beamwidth of the crosslink antenna should be wide enough to hit the target satellite with some pointing uncertainty. To communicate with satellites that travel in the same direction, (seamless transmission), the number of orbital planes must be 3, 5, 7, etc. and connections are between alternating planes. While the GEOS feeder link requires only a fixed antenna, MEOS and GEOS may need tracking antennas to point at other gateway stations. Signals connected via crosslinks to other target areas or to a gateway station are routed within the satellite by the onboard processor.

Satellite Processor

A processor is necessary for feeder link to mobile beam routing, feeder link spectrum compaction and decompaction, and demodulation/remodulation for TDD. For very low mobile EIRP of O.5 watt, the GEO mobile to mobile link cannot be closed because of uplink noise limitation, unless the uplink noise is removed from the transmission by regeneration.

The processor can be of transparent or regenerative type and may take over the beamforming functions for matrixed amplifier antennas or phased arrays. A transparent processor would perform variable bandwidth switching and routing and, if necessary, mobile to mobile signal switching. A regenerative processor would also demodulate, remodulate, and store information for TDD operations and reformat up and downlink modulation. The processor makeup depends on the modulation/multiple access method used and on whether FDD or TDD is used, transmission is transparent or regenerative, beam to beam signal routing is done aboard the satellite or on the ground, or the processor has beamforming capability.

Mobile Signal Path

The workings of the mobile link become clear when following the signal path. In case of a TDMA/FDMA feeder link, the voice channel is sampled, A/D converted, and combined with other TDMA carriers in an FDM format. A particular gateway station may transmit a certain portion, a multitude of TDMA carriers out of the total number of carriers. Other gateway stations will occupy their share of the available feeder link spectrum. At the mobile satellite, the feeder link band, consisting of M interleaved carrier sub-bands, which go to a particular beam (b_n), where M is the number of contributing gateway stations, is received, filtered, and translated by the processor. The total feeder link spectrum is decompacted to a multilayered spectrum. For easy processing, it is advantageous if the feeder link provides grouping of carriers for the beam spectra, in which case, a single variable bandwidth filter can filter out the group of carriers addressed to a certain beam.

The beam spectrum is translated to the mobile link frequency (b_n), after which the signal

undergoes beamforming and amplification and is fed to the antenna feed network. Beamforming may, however, be performed at any point in the signal path, provided phase tracking is maintained through to the transmit antenna. Finally, the signal is transmitted in the form of TDMA/FDM and is received by the mobile user. The mobile receiver automatically locks up to the correct carrier frequency and to the correct burst time slot.

On return, the signal emanating from the mobile user is a time burst, which, when combined with time bursts of other stations, forms the TDMA data stream. The receive narrow beam antenna receives the TDMA carrier and other TDMA carriers originating from the same beam area and downconverts the signal to the IF frequency, where they are filtered and processed. The onboard processor frequency shifts the signals and fits them into a feeder link spectrum, which is the sum of all beam spectra, for downlink transmission. The receiving gateway station retrieves the signal. By regenerative processing, a single TDM carrier may be used in the downlink.

A certain number of frequencies and/or time slots can be made available for mobile to mobile traffic, beam to beam switching, and demodulation/remodulation. The router provides feeder link spectrum decompaction, mobile to mobile routing, de/remodulation, and return feeder link spectrum compaction.

For MEOS, the processor will only provide spectrum compaction/decompaction. Signal aboard the satellite routing is optional.

Link Performance

The transmission system employs voice activation and power control. The uplink noise claims part of the downlink EIRP. Its addition to the downlink noise has minimal effect on the mobile to feeder link traffic because the feeder link goes into a large earth station antenna, but it may bring the C/N link below threshold in the mobile to mobile traffic case, requiring either the G/T ratio to be increased or the mobile to mobile carriers to be demodulated.

SPACECRAFT CONFIGURATION

MEOS and GEOS configurations are three axis stabilized. The orientation of the spacecraft depends on the angle of the orbit toward the sun. When the sun is less than 23° from the orbit plane, the spacecraft flies orbit normal, i.e., the roll axis is in direction of flight, the yaw axis is in line with the earth center, and the pitch axis is perpendicular to the orbit plane. The solar wings

are in line with the pitch axis. In case of inclined orbiting MEOS, when the sun is more than 23° from the orbit, the spacecraft flies in the nadir orientation. While the earth goes around the sun and the seasons change, the yaw axis must rotate (which is another good reason why mobile satellites are circularly polarized).

The considered payload power is in the 2 to 4 kW range. For eclipse operation, it is assumed that the traffic is reduced to a fraction of daylight traffic. The payload mass, depending on configuration, is up to 1000 kg. Spacecraft designed for geosynchronous operation require some changes when they are applied to medium earth orbit:

1) Provide reaction wheel control (instead of momentum wheel control)

2) Provide yaw altitude reference

3) Modify earth sensor for MEO operation

4) Provide storage for telemetry and command

5) Increase electronic unit shielding

6) Provide thicker solar cell covers

7) Reduce allowable battery depth of discharge

CONCLUSION

The trend in mobile satellite communication at this time appears to go towards more sophisticated satellites with a large number of beams and onboard processing providing worldwide interconnectivity. The economic factor will play an important part in choosing between the LEO, MEO and GEO future mobile satellite system solutions. Ulitmately the best service provider at a reasonable system cost may win this competition.

REFERENCES

1) "Attractive Features of Advanced GSO MSS (TRITIUM)", Drs. G. Hyrcenko, K. Johannsen and F. Joyce, Commsphere December 1991, Herzilya, Israel.

2) "Economic and Technical Considerations of a GSO Global MSS (TRITIUM)", Dr. G. Hrycenko, Dr. K. Johannsen, P. Louie and W. Lukas, Pacific Telecom conference, Honolulu 1992.

3) MAGSS-14: "A Medium-Altitude Global Mobile Satellite System for Personal Communications", J. Benedicto et al, ESA Journal 1992.

Table 1. Number of Satellites Versus Altitude at 10° Elevation

Altitude, km	Inclination, deg	Distance to Satellite, R, km	Earth Centered Half Cone Angle, L, deg	No. of Satellites per Orbital Plane, 360/2L	No. of Satellites for Ideal Area Coverage $\dfrac{2}{1-\sqrt{1-\sin^2 L}}$	Approximate Total $\dfrac{2(1+0.57\sin I)}{1-\sqrt{1-\sin^2 L}}$	No. of Satellites per Plane X No. of Planes	Approx Min No. of Satellites
500	90		14.16	12.7	65.55	102.9	13 × 8	104
770 (iridium)	90	2101	16.85	10.68	46.62	73.19	11 × 7	77
1389 (global star)	52		26.05	6.9	19.68	28.5	6 × 5	30
6371 (1 R_E)	90		50.50	3.56	5.15	8.89	4 × 3	12
10,360 (6 hr)	90	14406	58.00	3.10	4.25	6.31	4 × 2	8
12,742 (2 R_E)	90	16953	60.86	2.95	3.89	6.11	4 × 2	8
13,900 (8 hr)	90	18181	62.04	2.90	3.76	5.58	4 × 2	8
15,500	90		62.94	2.85	3.66	5.74	4 × 2	8
20,000	90		66.02	2.72	3.35	5.28	3 × 2	6
25,800 (12 hr)	90		68.76	2.61	3.14	4.92	3 × 2	6
35,788 (24 hr)	0	40586	71.45	2.52	2.93	3	3 × 1	3
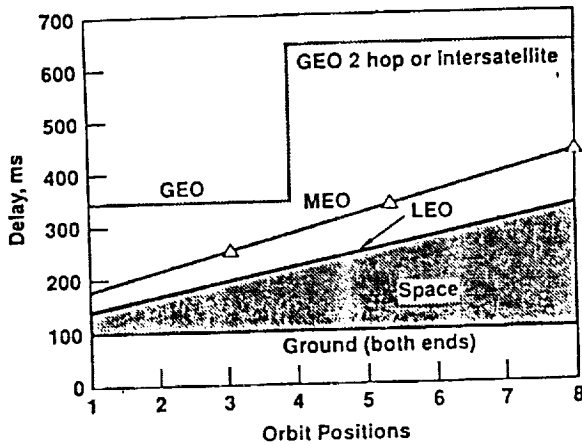
Figure 1. Path Delay Comparison
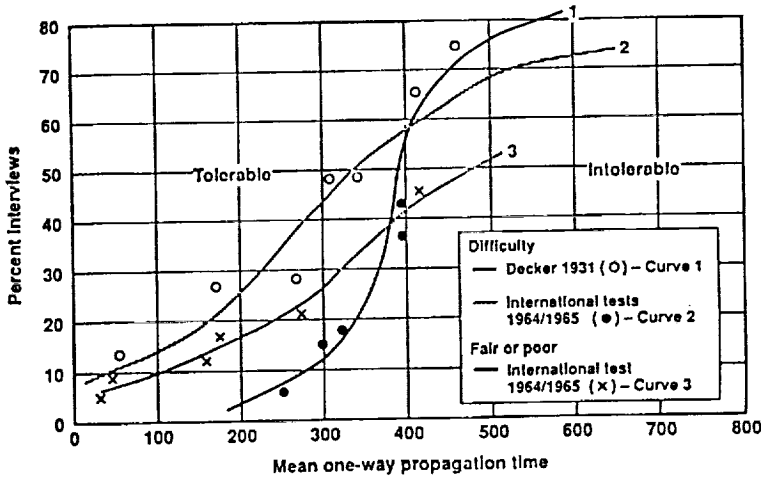
Figure 2. Effect of Signal Delay on Speech Quality
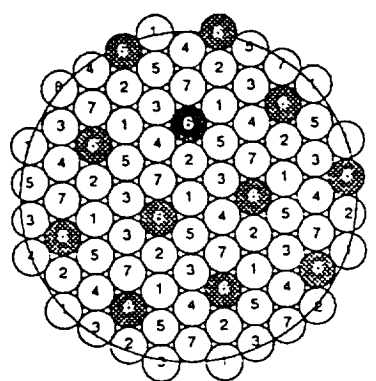
FREQUENCY REUSE PLAN – 7 FREQUENCIES

	REFLECTOR, 6 m DIAMETER
WORST CASE TOTAL ISOLATION, dB	18.8
WORST CASE INTERBEAM ISOLATION, dB	25.9

Figure 3. Reflector Isolation
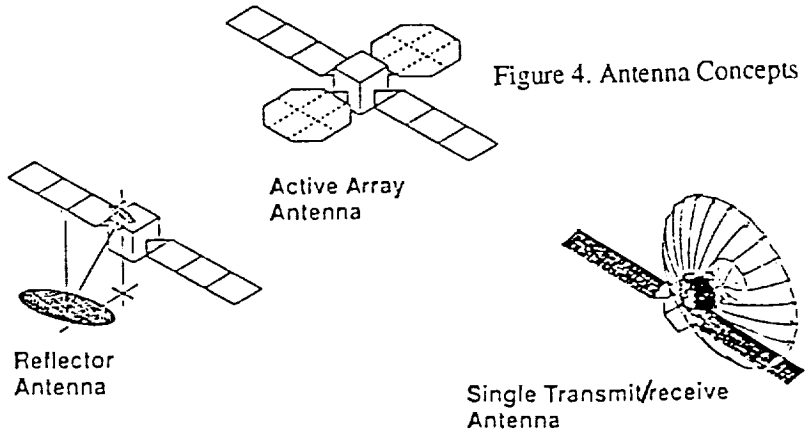
Figure 4. Antenna Concepts

Active Array Antenna

Reflector Antenna

Single Transmit/receive Antenna

162

Optimizing Space Constellations for Mobile Satellite Systems.

Roussel T., Taisant J-P.
France Telecom
38-40 Avenue du G^{al} Leclerc
92131 Issy-les-Moulineaux Cédex
France
Tel: (+33).16.1.45.29.62.98.
Fax: (+33).16.1.45.29.45.34.

ABSTRACT

Designing a mobile satellite system entails many complex trade-offs between a great number of parameters including: capacity, complexity of the payload, constellation geometry, number of satellites, quality of coverage ...

This paper aims at defining a methodology which tries to split the variables to give rapidly some first results.

The major input considered is the traffic assumption which would be offered by the system.

A first key step is the choice of the best Rider or Walker constellation geometries - with different numbers of satellites - to insure a good quality of coverage over a selected service area.

Another aspect to be addressed is the possible altitude location of the constellation, since it is limited by many constraints. The altitude ranges that seem appropriate considering the spatial environment, the launch and orbit keeping policy and the feasibility of the antenna allowing sufficient frequency reuse are briefly analysed.

To support these first considerations, some "reference constellations" with similar coverage quality are chosen. The in-orbit capacity needed to support the assumed traffic is computed versus altitude.

Finally, the exact number of satellite is determined. It comes as an optimum between a small number of satellites offering a high (and costly) power margin in bad propagation situation and a great number of less powerful satellites granting the same quality of service.

INTRODUCTION

The market recorded a few years ago a large increase of interest in mobile communications.

The first systems were analogic terrestrial systems with low capacity and low coverage area.

Maritime mobile communications provided by Inmarsat satellites on geostationnary orbits offered global coverage but with low capacity requiring powerful terminals.

Today, with the progress of technologies and the expansion of cellular digital systems, the terrestrial systems can provide large capacity with real handset terminals but the problem of large coverage is still remaining. A solution could be to use satellites to complete the cellular coverage for large regions having a low traffic density. The geostationnary orbit shows some limitations for such missions (big antennas, large propagation delays ...); others solutions based on low earth orbit (LEO) or intermediate circular orbit (ICO) are proposed.

However, the choice of such constellation parameters (number of satellites, altitude, inclination angle ...) is difficult because depending on a lot of interleaved variables.

The scope of our study is to propose a simple first optimization method which takes into account the major constraints for a decoupled choice of each of the constellation parameters.

TRAFFIC ASSUMPTION

Several hypothesis sustain the analysis:
- The service is a mobile satellite voice telecommunication service compatible with handset terminals.
- The quality shall be nearly the same than for cellular voice systems in term of availability, the terminal will weight less than 600g, and have an autonomy of approximatively 1 hour in active mode and around 10 hours in sleeping mode.
- The bandwith available is nearly 10 MHz in L band for the mobile return link and nearly 10 MHz in S band for the mobile forward link.

The number of subscriber and their repartition has an important impact on this optimization. As an example, the calculation is

conducted here on the basis of the inputs stated in the FCC filings [1].

SATELLITE CONSTELLATIONS

The technical litterature describes a great number of satellite constellations, with elliptical or circular orbits, polar or inclined, different ways to dispose the satellites into planes ...

In term of quality of coverage, the studies

The method leads to an optimization of each of these 3 points separately in order to minimise the cost of the mission for the service required. For a first approach of this problem, only the most important constraints are taken into account for the optimization of each parameter (figure 1). Further comparisons around these solutions would of course be needed to validate and refine the results.

The first study is on the constellation geometry which is chosen to provide the best
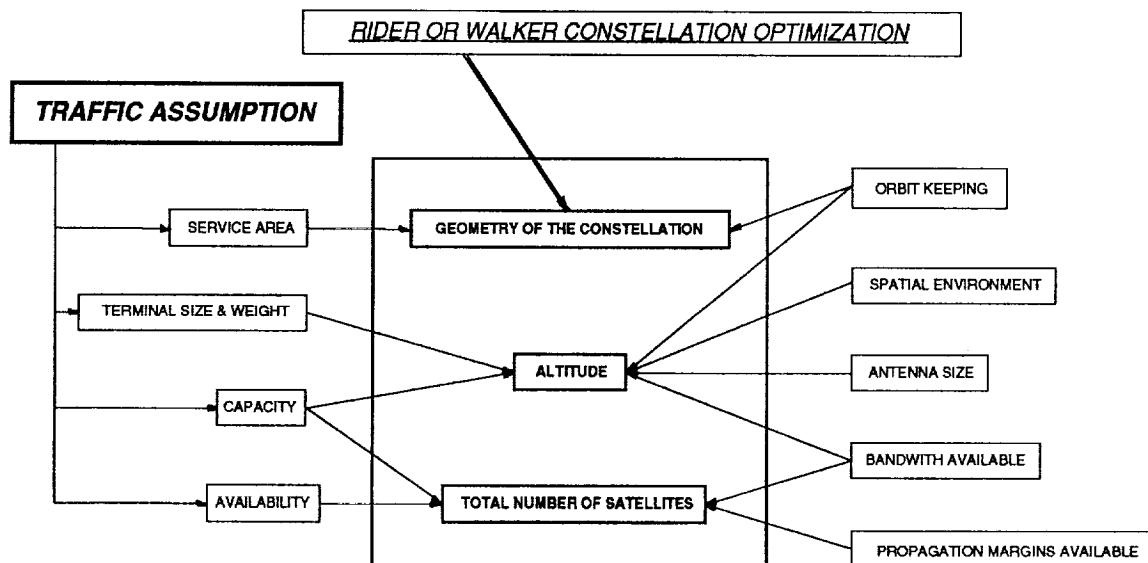
figure 1: Constellation optimization methodology

of Rider [2], Beste, Walker [3], Luders or Ballard [4] show different kinds of polar or inclinated circular orbits which give the best results for a worldwide coverage. The satellites are homogeneously distributed between several planes equally inclinated.

The High Inclinated Orbit (HIO) with elliptical orbit is a good solution for regional coverage, the satellite stay during long periods on the provided region, however in our case, the problem of such orbit is the same than for geostationnary orbit, the distance between the mobile and the satellite beeing too important.

A constellation can be described with a few parameters. These parameters have been regrouped in 3 major points:
- The number of satellites.
- The orbit altitude (or the period).
- The geometry of the constellation which correspond to the repartition of the satellites into planes, the location of this planes around the world, inclination angle and the phasing angle between 2 satellites belonging to adjacent planes.

quality of coverage for the desired regions. Then, the altitude and number of satellites are analysed.

OPTIMIZATION

Geometry of the Constellation

The constellations which are taken into account are the polar Rider constellations and the Walker or Ballard constellations.

Polar Rider Constellations

The best polar constellations for a large range of number of satellites, global or zonal coverage and for single or multiple visibility have already been identified by Rider.

For such constellations the coverage becomes better as latitude increase. There is no way to favour some medium latitude.

For single visibility and global coverage the Rider constellations are the best ones already

164

C-3

identified for a number of satellites greater than 15.

Walker Constellations

The other kind of constellations studied are the inclinated regular Walker [3] or Ballard [4] constellations. They are identified to provide worldwide coverage with single or multiple visibility levels.

For single visibility, the Walker constellations are better than Rider ones when the number of satellites is equal or less than 15.

However, this is not the only interest for Walker constellations. In fact the coverage of the entire world is not always a priority for a mobile telecommunication system. The coverage of high populated land masses could be sufficient. In such a case, "Walker-like" constellations can favour the of satellites per planes shall not exceed 4 times the number of planes and vice versa: too many planes will be very costly to be launched and too many satellites per plane create overlaps incompatible with the optimization.

Several thousand of constellations have been analysed.

Optimized Geometry

In accordance with the service area, we will focused on "Walker-like" constellations inclined around 50°. Four quality criterias are defined to perform the best constellations in relation with the assumed traffic distribution:
- The maximum and average values of D - the distance between a location on the earth and the nearest sub-satellite point - for latitudes between 0° and 25°.
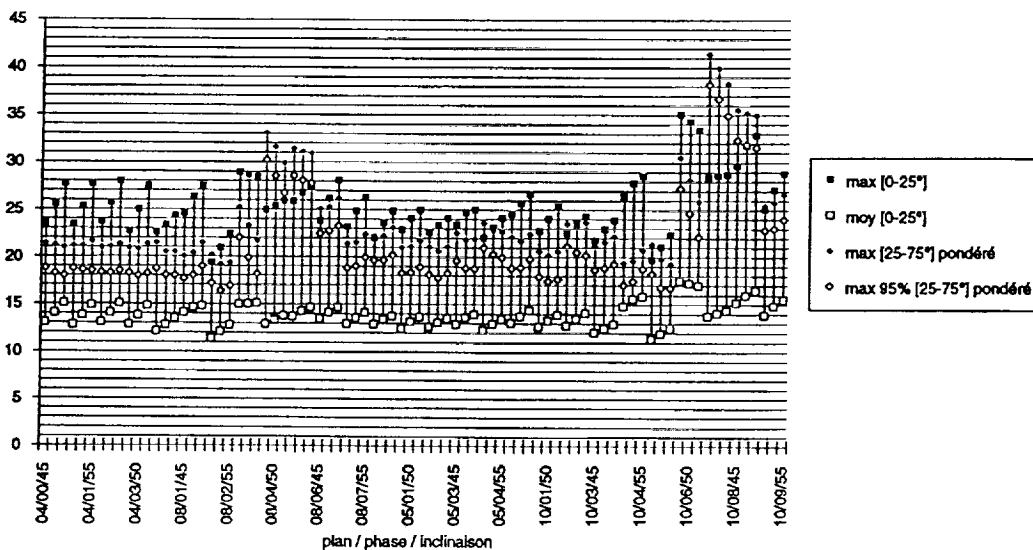
figure 2: 40 satellites geometry quality comparison for 45°, 50° and 55° inclination angles

latitude where the majority of the subscriber occur.

To analyse the quality of coverage for these constellations, large computations have been initiated. The time and space distribution of D, the distance between a location on the earth and the nearest sub-satellite point is calculated for each latitude and for a number of satellites varying from 5 to 99 (for a given altitude, this distribution directly corresponds to the elevation angle distribution).

For a number of satellite lower than 13, all the factorisation of the number of planes versus the number of satellite per planes with every possible phase number [3] and every inclination angle between 30° and 90° are computed.

For larger number of satellites, the number

- The maximum and the 95% values - over time and space - of D for latitudes between 25° and 70° weighted by the percentage of the traffic density on these latitudes.

In accordance with these coefficient values, for some different numbers of satellites, the best constellation geometries are identified.

An exemple of 40 satellites comparison is given in figure 2

Altitude

The choice of the altitude is the result of a very difficult trade-off due to the number of

165

constraints and implications. But several options can be put aside.

First, the ranges of altitude acceptable for spatial environment and orbit keeping policy reasons must be identified.

Then, the in-orbit capacity is compared for several constellations at different altitudes on the basis of similar coverage quality.

A further point must be assessed: the feasability of the satellite antennas, having the size and the number of beams needed for the capacity estimation.

The best altitude are identified and the launch policy is later approached for these different altitudes.

Spatial environment & orbit keeping

Electronics and solar arrays are affected by the ionizing radiations.

Different kind of radiations occur with more or less intensity depending on altitude and inclination angle [5]. Solar radiations correspond to proton or heavy ions radiations. Galactic radiations are composed of heavy ions.

The terrestrial magnetic field interfere with the magnetic field created by these radiations and trap the particle around the earth. These regions of trapped particle are defined as the Van Allen belts. The location of these belts fluctuate with time depending on solar activity.

3 kinds of phenomena occur in the presense of ionizing radiations:
- Background noise proportional to the radiation flow in the equipments
- Defaults on the material structure due to the quantities of radiations received for a long time. The solars array performances decrease with these quantities. If a maximum loss of a 25% of the capacity is accepted over 10 years, Si cell utilisation exclude altitude ranging between 1500 and 10.000 km on 50° inclinated orbits.
- Single event (SE) which are aleatory phenomena appearing sometimes during the crossing of only one high ionizing particle. The SE can be destructive (SEL) or can only involve a temporary loss of informations (SEU). The occurence of SE on electronics depend on their level of integration and their technologies. The Linear Energy Transfert (LET) depending on the material (1Mev/mm for Si) and the critical value L_s of the LET define the component sensibility to SE. No SE occur when the LET is lower than L_s but this lead to low integration levels; in the opposite, high integrated component levels with low L_s lead to SE occurence when the particles encountered are sufficiently energetic. A lot of studies have been made on several

components by CNES and ESA laboratories using CREME or NOVICE softwares to compute the LET and L_s values. On 50° inclinated orbits it is recommended to avoid the range of altitude between 2000 and 3200 km and above 12.000 km.

Another problem must be assessed: the orbit keeping policy, since the constellation net tends to get distorted with time.

The satellite trajectory is affected by several factors. The principal one is the earth gravitation, then the flattening of the earth at the poles, the atmospheric rubbing, the moon and solar attraction and the solar radiation pressure [7].

These constraints lead to change the orbit parameters. There is a decrease in altitude, fluctuations on inclination angle, an orbit ascension node drift and fluctuations on the true anomaly.

In the case of satellites constellations only the relative location between satellites is important. The ascension node drift and the inclination angle fluctuations are the same for all the satellites in the first order of magnitude. On the contrary, the true anomaly fluctuate differently for different satellites. However this correction doesn't depend much on the orbit altitude.

The decrease of altitude is related to atmospheric rubbing and solar radiation pressure. It depends on the initial altitude orbit, and in a second order of the inclination angle.

h (km)	770	860	1300	1600
Dh (km) atmos. rubbing	140	37	2	1
Dh (km) solar radiation	4.6	4.7	5.2	5.4
ergol consum. (kg)	9.2	4.2	0.7	0.8

figure 3

Figure 3 shows the altitude decrease for a 320 kg satellite with 7 m^2 section on 6 years life.

In term of orbit keeping, the altitude will be kept above 750 km with preference for altitudes greater than 1000 km.

These first studies on the altitude determination identify two ranges of altitude:
- Between 750 km and 2000 km (or 1000 km and 1500 km prefered).
- Between 10.000 and 12.000 km.

In orbit capacity

In the ranges of altitudes already identified, some of the best constellations found with the criteria defined in the " traffic assumption "

166

paragraph, are considered in order to provide equal quality coverage. This leads to select:

A - 99 satellites, 770 km altitude (99/11/1/53).
B - 63 satellites, 1000 km altitude (63/9/1/53).
C - 40 satellites, 1400 km altitude (40/8/2/52).
D - 27 satellites, 2000 km altitude (27/9/5/50).
E - 8 satellites, 10.000 km altitude (8/4/2/50).

These results display an important decrease of the required capacity as the altitude increases.
The choice of the higher altitudes should be the better one; however, for altitude near 10.000 km the number of channels required on a single satellite can be critical.
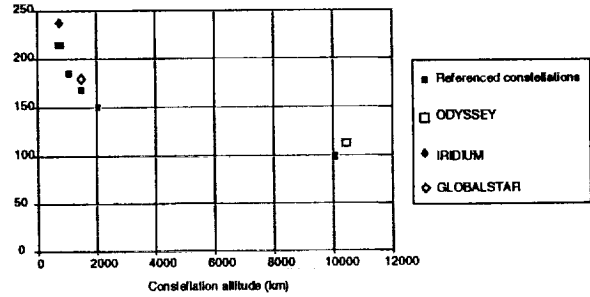
figure 5: Relative capacity in orbit to carry 90% of the traffic

figure 4: Satellite capacity (in number of channels) versus the percentage of traffic carried

An Iridium-like constellation (which provides lower quality of coverage) a Globalstar-like and an Odyssey-like constellation (which both provide better quality coverage) are also considered.

A model computes the satellites load versus time. For a mobile, the usefull satellite is the satellite which is in view with the highest elevation angle. The model takes into account the subscriber breakdown into several earth regions. A daily variation traffic curve is considered in the model. The satellite capacities needed to carry x% of the traffic are shown for the different constellations in figure 4.

The capacity required to be launched for each constellation is computed and compared to the reference constellation E. Results are shown in figure 5 for 90% of the call request provided.

Antenna size

The choise of the altitude depends also on the satellite feasability.

The mobile system makes the coverage with several spot beams. The number of spot beams needed depends on the maximum capacity that a beam should be able to support and on the total bandwith available. The size of these spot beams needs to be small enough to increase the satellite gain and then minimise the power consumption at both the satellite and the mobile terminal. A 1000 km diameter is assumed.

Circular beams allow a 7 cell frequency reuse pattern over an hexagonal structure.

The antenna size is calculated versus the altitude for the 1000 km diameter spot beams.

167

Calculation are carried to comfirm that the traffic can be supported by these values.

The antenna diameters found for the various altitudes are given in figure 6. These results point out that a 10.000 km altitude is related with an achievable antenna size and complexity.
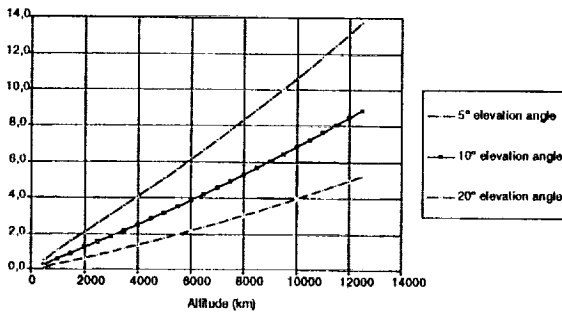
figure 6: L Band antenna size (m) versus the altitude

Altitude Conclusions

Two ranges of adequate altitudes are identified; between 750 and 2000 km and between 10.000 and 12.000 km.

As far as the LEOs are concerned, the prefered altitudes are the higher ones: they minimise the number of satellites to be launched and the in-orbit capacity. In fact, if the required number of channels were much larger, the choice of lower altitudes could be jpreferable. In the case studied here, an altitude around 1500 km is selected to minimise the radiation effect problems: constellation C is a good candidate.

A further study would be required to refine the launch strategy. Considering the launchers available in the late 90ies (including Atlas, Ariane 4 and 5) multiple launches could be used for the LEO C constellation targetting 1 or 2 planes per launch. Dual launches could be used for the ICO E constellation. The satellite design will have to comply with the fairing of volume and the mass performances of the launchers.

Number of satellites

The number of satellites, for a given altitude, influences the quality of the coverage.

Using a simulation model, the average propagation margins necessary on the satellite and on the mobile terminal is computed for some different qualities of coverage through the combination of the elevation angle distribution between the mobiles and the satellite and the differents margins corresponding to these elevation angles.

The different margins are evaluated for each elevation angles through a Lutz propagation

model [7]. They are computed for different availability, different Bit Error Rate (BER), different surroundings, different interleaving and different coding rates assumption.

The choice of the number of satellites correspond to a quality of coverage optimizing the average power margin versus the satellite sizing.

CONCLUSION

This paper describes a method to select satellite constellations responding to particular traffic assumption and service quality. Many elements like multiple access, modulation, hand-over technique ..., influence the final performances. However, they mostly stand as possible ways to improve the first approach based on traffic distribution over latitudes, constellation geometry, altitude, capacity and propagation margins.

In the case studied here, Walker constellations inclinated at 50° are prefered. Two altitudes are favorable: around 1500 km or around 10.000 km. The number of satellites will depend of the optimization between the average power margin and the satellite sizing.

A final choice between these 2 alternatives will be based on the comparison of their cost implied to manufacture and launch the 2 systems.

References

[1] Motorola, TRW, Loral-Qualcomm fillings before the FCC for MSS.
[2] W.S. Adams and L. Rider, Circular Polar Constellations Providing Continuous Single or Multiple Coverage Above a Specified Latitude, The Journal of the Astronauticals Sciences, Vol. 35, No 2, April-June 1987, pp.155-192.
[3] J.G. Walker, Continuous Whole-Earth Coverage by Circular Orbit Satellite Patterns, Royal Aircraft Establishment, Tech. Report 77044, September 1977.
[4] A.H. Ballard, Rosette Constellations of Earth Satellites, IEEE Trans on Aero. and Elect. Sys., AES-16, No 5, September 1980, pp 656-673.
[5] RADECS 89, Radiations: Effets sur les Composants et Systèmes, Montpellier, 11-14 Septembre 1989.
[6] D. Vienne, Les Perturbations d'Orbite: les Courses, leur Représentation, Cours de Technologie Spatiale: "Le Mouvement du Véhicule Spatial en Orbite", CNES,1980.
[7] E. Lutz, The Land Mobile Satellite Communication Channel-Recording, Statistics and hannel Model, IEEE Trans. on Veh. Tech., vol 40, No 2, May 1991, pp 375-385.

Geostationary Payload Concepts for Personal Satellite Communications

J. Benedicto, P. Rinous, I. Roberts,
A. Roederer, I. Stojkovic
European Space Agency - ESTEC
Keplerlaan 1, P.O. Box 299
2200 AG Noordwijk
The Netherlands
Tel. +31-1719-86555
Fax. +31-1719-84596

ABSTRACT

This paper reviews candidate satellite payload architectures for systems providing world-wide communication services to mobile users equipped with hand-held terminals based on large geostationary satellites.

There are a number of problems related to the payload architecture, on-board routing and beamforming, and the design of the S-band Tx and L-band Rx antenna and front ends. A number of solutions are outlined, based on trade-offs with respect to the most significant performance parameters such as capacity, G/T, flexibility of routing traffic to beams and re-configuration of the spot-beam coverage, and payload mass and power.

Candidate antenna and front-end configurations were studied, in particular direct radiating arrays, arrays magnified by a reflector and active focused reflectors with overlapping feed clusters for both transmit (multimatrix) and receive (beam synthesis).

Regarding the on-board routing and beamforming sub-systems, analogue techniques based on banks of SAW filters, FET or CMOS switches and cross-bar fixed and variable beamforming are compared with a hybrid analogue/ digital approach based on Chirp Fourier Transform (CFT) demultiplexer combined with digital beamforming or a fully digital processor implementation, also based on CFT demultiplexing.

INTRODUCTION

Land-mobile satellite communications is evolving towards providing compatibility with the services offered by terrestrial cellular personal communication systems, and complementing them in low population density areas where terrestrial coverage cannot be provided economically.

Offering the user world-wide roaming capability (as is intended in an FPLMTS context) requires integrating terrestrial and satellite networks and a user terminal capable of operating within both of them (frequently referred to as "dual-mode terminal"). This requires the development of satellite user terminals adapted to each application, such as vehicle-mounted terminals (VH), portable laptop terminals (PT), and pocket size hand-held telephones (HH). Existing L-band VH and PT terminals (for instance INMARSAT-M) are compatible with the current INMARSAT-II spacecraft and other satellites now in construction such as MSAT, INMARSAT-III, the EMS payload on ITALSAT-F2 and the LLM payload onboard ESA's satellite ARTEMIS. Satellite HH terminals have not been developed so far.

At its last conference (WARC'92) the ITU allocated new frequency bands to the mobile satellite service, from 1613.8-1626.5MHz (Earth-to-space) and 2483.5-2500MHz (space-to-Earth). These new allocations were primarily implemented for future satellite systems for HH voice communication, based on non-GSO satellites (so-called big LEOs) like the IRIDIUM, GLOBALSTAR, ODYSSEY, ELLIPSO and CONSTELLATION systems. The technical choice (non-GSO satellites) made for those systems is based on the belief that providing good quality voice and data communication services to HH terminals is far beyond the easy reach of GSO satellites. Nevertheless, some studies [1] have shown that although GSO satellites for HH communications are very large and complex, they could be implemented before the end of this century.

ESA is actively pursuing system studies and technology developments by different technical solutions based on GSO, Medium Earth Orbit (MEO) [2], Low Earth Orbit (LEO) and Highly inclined Elliptical Orbits (HEO) [3].

This paper summarises the results of internal studies performed to size a GSO payload for HH communication. Section 1 outlines the system background, section 2 describes the payload architectures studied and associated technologies, section 3 describes satellite mobile link antennas based on large unfurlable reflectors and deployable phased arrays and section 4 gives the overall payload configuration and system budgets for the selected option.

1. SYSTEM BACKGROUND

The satellite system considered here is for land-mobile personal communication, in particular to users equipped with HH terminals, using the recently allocated frequency bands in the L and S-bands.

Table 1. User categories and services			
USER	MOBILITY	TERMINAL	CO-OPE RATION
Traveller	open/shadow	HH dual mode	High
Mobile	mobile chn.	VH dual mode	Low
Government	mob./outdoor	HH, VH	High
Remote Telephony	outdoor	HH, portable PT or VH	High
Recreational	land/sea	HH	Low
Data Collection	outdoor	semi-fixed	High

A definition of the user categories and telecommunication services to be provided is given in Table 1. A variety of user terminals have been conceived (Table 2) to match the different user needs for mobility and transportability. Two parameters are of paramount importance when designing the mobile terminal for a given user application: the antenna (gain and profile) and the transmitted RF power. The antenna radiation pattern (and gain) has to be adapted to the problems of user mobility and hence possible degree of co-operation in pointing towards the satellite. The antenna profile and size is crucial to the terminal integration in a vehicle, suitcase, or for an ergonomic hand-held design. The transmitted RF power will have an effect on the DC power demand and therefore the size of the batteries required (transportability). In addition to that are the short and long term safety aspects for the user related to the biological effects of the radiated fields, especially for a HH-type terminal.

Table 2. User terminal types			
	hand-held	portable	vehicle
size	pocket	laptop	antenna + set
antenna gain	0 ~ 3dBi	+7dBi	+4dBi
Tx RF power	< 500mW	1W	2W
EIRP [dBW]	-3 ~ 0	+7	+7
G/T [dB/K]	-24 ~ -21	-17	-20

The most relevant system parameters are summarised in Table 3. The satellite has been sized to provide the equivalent of 5000 voice (2.4Kb/s coding rate) circuits to HH terminals over the land masses and coastal waters of the geographical areas from which the satellite is seen with more than 10° of elevation angle.

Table 3. System parameters	
Orbital position	GSO, 20° East
Coverage of land masses only	
Min. elevation for coverage	10°
Launch date	year 1998 - 2000
Lifetime (with 85% reliability)	10 years
Mobile frequencies, downlink	2483.5MHz - 2500.0MHz
Mobile frequencies, uplink	1613.8MHz - 1626.5MHz
Frequency re-use	2.5 (average)
Satellite throughput	5000 voice circuits
Voice activation	40%, both ways
Access	FDMA, 4KHz channels
Required link quality, C/No	39dBHz
Reference Terminal G/T (HH)	-24dB/K
Reference Terminal EIRP (HH)	-3dBW
Satellite EIRP (S-band)	62.6dBW
Satellite G/T (L-band)	+6.1dB/K

The forward and return link budgets are summarised in Table 4. The antenna coverages have been optimised for a satellite located at 20° East (over the European/African region). The margins in the link with the mobile users assume line-of-sight communication with C/M better than 5dB (Ricean channel).

Table 4. Mobile link budgets	
Forward down link (2.5GHz)	
EIRP/channel	29.6dBW
Satellite Tx antenna gain (*)	33.0dBi
Satellite power/channel	-4.4dBW
Number of activated channels	2000
Satellite EIRP (total)	62.6dBW
Path loss	-192.5dB
Atmospheric loss	-0.15dB
CCI interference loss	-1.0dB
C/M loss	-1.0dB
HH terminal G/T	-24.0dB/K
Received C/No	39.5dBHz
Overall forward link C/No	39.0dBHz
Margin (ref. 39dBHz)	0.0dB
Return up link (1.6265GHz)	
HH terminal EIRP	-3.0dBW
Path loss	-188.8dB
Atmospheric loss	-0.1dB
C/M loss	-1.0dB
CCI interference loss	-1.0dB
Satellite Rx antenna gain (*)	34.0dBi
Satellite system temperature	27.9dBK
Satellite G/T (at L-band)	+6.1dB/K
Received C/No at satellite	40.7dBHz
Overall return link C/No	40.2dBHz
Margin (ref. 39dBHz)	+1.2dB
(*) *includes Tx and Rx losses*	

2. REPEATER ARCHITECTURES

The repeater includes the feeder link interface sub-system, the payload processor and the Tx and Rx mobile link sub-systems. The payload processor performs routing, switching and beamforming. The primary driver for the processor is the large number of beams for the required coverage. This has a major impact on both channelisation and beamforming, but the advantages in on-board power saving, increased frequency re-use potential and improved satellite G/T are significant for this application. Other design drivers which have to be considered are: 1) large number of feeds (having an impact on switching and beamforming); 2) frequency re-use flexibility (easily implemented in a digital processor, but requires local oscillator tunability in an analogue one); 3) total capacity; 4) traffic routing flexibility; 5) fine channelisation for granularity, to reduce beam blocking probability; 6) possibility to rearrange the frequency plan in orbit; and last, but not least, 7) reliability (bearing in mind the fact that massive and complex processors lead to massive redundancy requirements). Three generic types of payload processors were considered and a detailed trade-off between them was performed.

SAW + Analogue BFN

This is a fully transparent processor based on group demultiplexing by SAW filter banks. The beamforming enables a limited number of spot beams to be generated giving contiguous coverage. This is a well known design used in many existing systems e.g. INMARSAT III, EMS and LLM payload on ARTEMIS. The main advantages of such a design are, besides the mentioned transparent group demultiplexing, power and bandwidth flexibility and the ability to handle any type of modulation, whereas the limitations are on matching traffic to beams (due to filtering granularity) and frequency re-use.

CFT + Analogue BFN

This payload processor is characterised by time domain analogue demultiplexing (which is enabled by the Chirp Fourier Transform), possibly enhanced by additional fine digital channelisation (if very narrow bandwidths, below 100KHz, are required), followed by an analogue beamforming network. The main features of all CFT based repeaters are low granularity, which can go down to very small channel groups (in case of FDMA) or to individual carriers (in case of a TDMA access scheme), simple and flexible L and S-band in-orbit frequency plan re-arrangement and the possibility to have a compressed feeder spectrum without the need to map the feeder to mobile spectrum.

CFT + Digital BFN

This processor is based on SS-FDMA concept of transponder channel switching, but is easily adapted for use with TDMA or CDMA access schemes, due to its transparent nature. The routing function is performed in principal on a channel-by-channel or carrier-by-carrier basis, using a demultiplexer implemented in hybrid CFT technology enhanced by digital demultiplexing [4]. In many cases, however, the ultimate channelisation down to single user circuit is not needed and significant reductions in processing load can be achieved by demultiplexing down to small groups of channels (typically 20 to 30 circuits), without noticeably degrading the overall performance. The coverage is achieved by a large number of narrowband repositionable overlapped beams. Beamforming is digital narrowband i.e. performed on a limited number of channels or carriers. There is a possibility to perform individual channel processing including on-board level control to save downlink RF power and active interference suppression to maximise frequency re-use. Total control of feed element signals enables beam re-configuration in case of failure or misalignment.

Accurate user location for beam pointing is a necessity, if the advantages of beam repositioning are to be utilised. Digital beamforming lends itself well to direction finding algorithms, which can be implemented in the return processor for this purpose. Other networking implications following from this design approach are mobile to mobile link service, adaptability to variations of traffic distribution and transparency for introduction of new services.

In summary, the main advantages are maximised routing flexibility, best frequency re-use capability, high RF power efficiency (due to near-peak antenna gain and possible power control), compact feeder link and, of major importance for service to hand-held terminals, peak satellite G/T. The single most significant disadvantage is that a processor of this type has not been flown before whilst it is based on technology which still needs to be developed to space standard.

Mobile and Feeder Link Subsystems

Due to the high incidence of components involved in mobile antenna feed element chains, significant advantages in payload mass and DC power consumption can be expected from their improvements. In particular integration and miniaturisation is needed for low-loss output combiners (semi-active antenna) and bandpass filters, very low noise figure L-band LNAs integrated with bandpass filters, and high efficiency medium-power S-band SSPAs.

The feeder link sub-system is not described in detail, because of its commonalty with previous designs. An

estimate of mass and DC power requirement for this sub-system is, nevertheless, presented in Table 5.

3. S/C ANTENNA DESIGN

The spacecraft multibeam antennas are required to provide reconfigurable coverage of land masses from several positions on the geosynchronous orbit and to accommodate changes in traffic to beams, with maximum DC to RF efficiency. Over 33dB gain is required in both the forward and return links, with 20dB sidelobe isolation for frequency re-use. It is further assumed that the same beam footprints are used for the up and down links.

Direct Radiating Arrays

Active arrays can provide the required flexibility. The use of separate transmit and receive antennas is conceptually simpler than the re-use of the same aperture, but implies complex deployment. For the same aperture, either interleaved or co-located (dual frequency) elements are possible. A configuration with separate antennas, 8m×2.7m at L-band for receive and 5.1m×1.7m at S-band for transmit, each with 192 subarrays of electromagnetically coupled annular slots, has been evaluated. The beams are elliptical and, even with optimum sub-arraying, sidelobe control requires a power inefficient excitation taper or use of different amplifiers. Beamforming is complex since all elements are involved for each beam.

Reflector Antennas

Multifeed reflector antennas are the other alternative. In the receive mode, where amplitude control at feed level has no power efficiency impact, focusing reflector antennas using *beam synthesis* [5] lead to the smallest feed and reflector sizes. Each beam is formed by optimal weighting of pre-amplified signals from only some of the feeds.

For transmit, amplifiers must operate close to nominal power for optimum DC to RF efficiency.

Active focusing reflector antennas, with overlapping feed clusters, and one power amplifier at each feed require complex power switching to cope with changes in beam loading. Imaging antennas [6] where a feed array is magnified by one or two reflectors, suffer from reflector oversizing and require inefficient feed illumination tapering for sidelobe control.

One preferred option is *semi-active multimatrix* antennas [7,8], as used for the INMARSAT III series, which provide the required performance with optimum power efficiency, together with minimum reflector and feed sizes. The same feeds are shared between several beams and are powered from identical amplifiers via Butler-like matrices, which direct the power towards the selected outputs depending on their input phase law.

A design with 35λ by 49λ (4.2m×5.8m at S-band) offset reflector (F/D=0.5) and a 128 element feed array
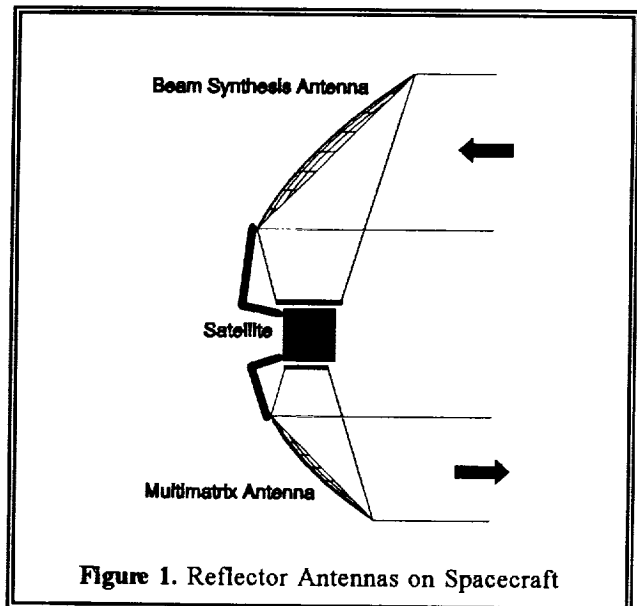
Figure 1. Reflector Antennas on Spacecraft

placed on the satellite wall (Figure 1) fed via 16 8×8 hybrid matrices (Figure 2) has been analysed for global coverage. As only land mass and 10° elevation coverage is required, the number of feeds and matrices is reduced accordingly, but not shown.
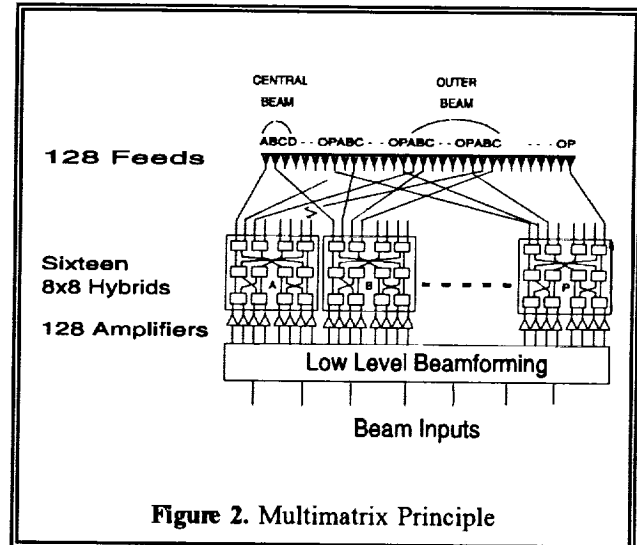
Figure 2. Multimatrix Principle

Since thousands of channels are transmitted into around 85 beams for land coverage, optimised complex excitations (with a limited dynamic range to simplify beamforming) can be used, as each amplifier contributes to many beams and, therefore, its power is averaged. With a 10dB range, central beams use 3 to 7 feeds and outer ones up to 16. The cross-over levels between beams vary from -3dB (centre) to -1.3dB (edge). Computed contours of typical beams over the Earth's surface with these excitations are shown in Figure 3 for the antennas of Figure 1. A scaled version of this antenna (6.5m×9m),

operating in the beam synthesis mode, is proposed for the receive function.

Figure 3. Selected Optimised 35dBi Directivity Contours
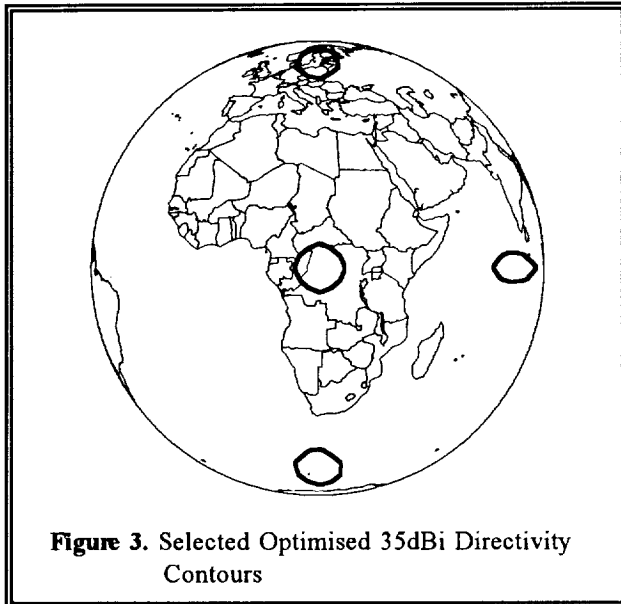
With digital beamforming it is envisaged to generate a large number of repositionable beams crossing over around 1dB.

4. CANDIDATE PAYLOAD

Previously performed trade-offs led to the conclusion that in the case of payloads with a large number of beams (as is inevitably the case for global personal communications) in conjunction with the requirement to use many feeds per beam, narrowband digital beamforming combined with CFT or all-digital multiplexing has a significant mass advantage over other techniques based on a SAW filter banks and analogue beamforming. Therefore, the candidate payload is based on the repeater design with digital beamforming and CFT processing. The preferred antenna option is beam synthesis on receive and the semi-active multimatrix on transmit, because it avoids the use of different amplifiers in the transmit mode and implies a minimum number of feeds per beam.

Figure 4 shows a basic block diagram of the candidate payload, while the main payload budgets are shown in Table 5. It should be noted that the RF power has been calculated for the most disadvantaged users - those in the beams with lowest peak gain at the edge of coverage. For users closer to the centre of the satellite coverage (i.e. near the sub-satellite point) there is a power advantage resulting from the lower path loss (approximately 1dB) and higher peak antenna gain. The actual benefit in total RF power requirement is directly dependant on the distribution of the users within the satellite coverage and has not been evaluated in this paper.

Table 5. Payload budgets		
	Mass [Kg]	**Power [W]**
C-band sub-system	12.2	306.0
receiver	*1.6*	*6.0*
HPA	*5.9*	*300.0*
output MUX	*1.8*	
receive antenna	*1.1*	
transmit antenna	*1.8*	
power supply unit	25.0	250.0
FWD and RTN processors	107.1	381.0
S-band SSPA (η=33%)	84.0	2744.0
low noise amplifiers (L-band)	33.4	211.0
S-band Tx antenna	95.0	
L-band Rx antenna	120.0	
TTC interface unit	4.0	
cables	43.8	
harness	30.0	
T o t a l	**554**	**3890**

It has been assumed for the mass budgets that most of the critical elements (all feeder link components, mobile link SSPAs and LNAs, and digital circuitry) are 2 for 1 redundant, the notable exception being the feed element chains within the processors (DACs and the analogue output components, including the CFTs). As the antennas are essentially focus fed, graceful degradation is not acceptable. A satisfactory reliability estimate was obtained by securing 3 additional redundant chains for every group of 11 chains (14 for 11 redundancy).

The assumed digital technology is radiation hardened CMOS ($0.8\mu m$), which is the selected option for a 1998-2000 launch.

Although FDMA access scheme has been taken for this example, this type of payload design is well suited for narrowband TDMA and would lead to similar, if not lower, mass and power figures, due to the fact that the processing load would be slightly lower in this case.

CONCLUSIONS

ESA is actively pursuing different space segment options for the provision of voice and data communications to users equipped with mobile, portable and hand-held terminals, at L and S-bands.

In particular a Geostationary (GSO) satellite option is attractive (compared to MEO or LEO satellite constellations), because of the low (3 to 4) number of satellites involved, the technological heritage and the relative simplicity of the ground segment and network management.

This paper has described possible GSO payload architectures, including L and S-band antennas and repeater sub-systems. For the mobile link antennas, direct

173
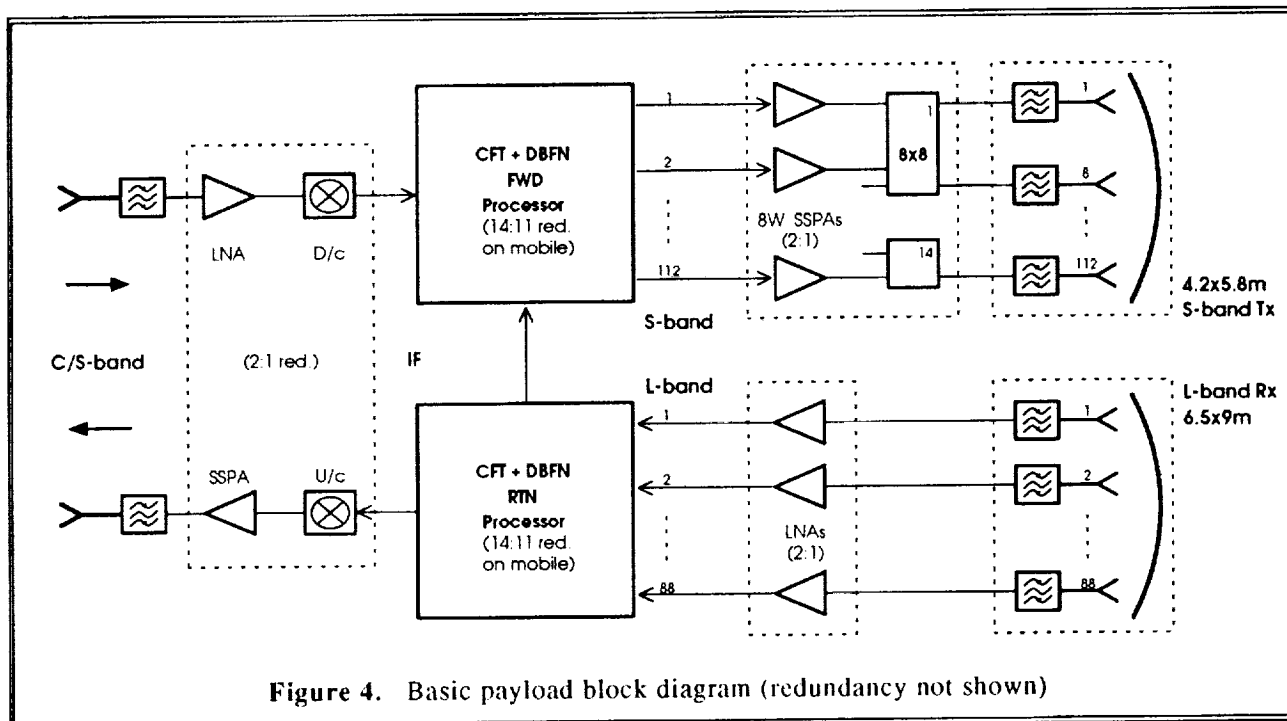
Figure 4. Basic payload block diagram (redundancy not shown)

radiating arrays and focusing multifeed reflector antennas have been evaluated. Concerning the payload processor, which performs the routing, switching and beamforming functions, analogue and digital implementations involving SAW filters, CFTs and digital beamforming technologies have been evaluated and compared.

Finally, a candidate payload is described and its total mass and DC power consumption are calculated for a total capacity of 5000 duplex voice circuits.

Key technologies that are required to be developed to space qualification are CFT-based channel transmultiplexing, digital beamforming, high efficiency medium-power S-band SSPAs, highly integrated very low-noise L-band LNAs and large (6 to 10 metres) unfurlable L and S-band antennas.

REFERENCES

[1] A. Zaghloul, F. Assal, B. Hutchinson, E. Jurkiewicz, *Satellite Communications to Hand-Held Terminals from Geostationary Orbit*, 9th International Conference on Digital Satellite Communications, Copenhagen, May 1992.
[2] J. Benedicto, J. Fortuny, P. Rastrilla, *MAGSS-14: A Medium-Altitude Global Mobile Satellite System for Personal Communications at L-band*, ESA Journal 92, Vol.16.
[3] G. Solari, R. Viola, *M-HEO: The Optimal Satellite System for the Most Highly Populated Regions of the Northern Hemisphere*, ESA Bulletin, May 1992, No. 70.
[4] A. Craig et al., *Applicability of Different On-Board Routing and Processing Techniques Applied to a Mobile Satellite System*, 3rd International Mobile Satellite Conference and Exhibition, Pasadena, June 1993.
[5] Le Normand et al., *A versatile array fed reflector antenna*, 1988 IEEE AP-S International Symposium Digest.
[6] R. Lo Forti, T. Jones, A. Roederer, *Performance evaluation of a near field fed double curvature reflector*, 1990 IEEE AP-S International Symposium Digest.
[7] S. Stirland, J. Joshi, A. Roederer, R.Graham, *Active and semi-active reflector antennas*, ESA Workshop on Advanced Beamforming Networks for Space, 1991.
[8] A. Roederer, *Semi-active satellite antennas*, invited paper, Proc. JINA '92.

A System Architecture for an Advanced Canadian Wideband Mobile Satellite System

P. Takats, M. Keelty, and H. Moody
Spar Aerospace Limited
21025 TransCanada Highway,
Ste-Anne-de-Bellevue, Quebec
H9X 3R2, Canada
Tel: (514) 457-2150
Fax: (514) 457-2724

ABSTRACT

In this paper, the system architecture for an advanced Canadian ka-band geostationary mobile satellite system is described, utilizing hopping spot beams to support a 256 kbps wideband service for both N-ISDN and packet-switched interconnectivity to small briefcase-size portable and mobile terminals.

An assessment is given of the technical feasibility of the satellite payload and terminal design in the post year 2000 timeframe. The satellite payload includes regeneration and on-board switching to permit single hop interconnectivity between mobile terminals. The mobile terminal requires antenna tracking and platform stabilization to ensure acquisition of the satellite signal.

The potential user applications targeted for this wideband service includes: home-office, multimedia, desk-top (PC) videoconferencing, digital audio broadcasting, single and multi-user personal communications.

INTRODUCTION

Both the development of experimental ka band satellite systems, such as Olympus and ACTS [1], and the conceptual studies of advanced future systems [2] has produced designs that offer satellite services to support a variety of user applications. These range from narrowband (handheld) personal communications to wideband B-ISDN trunking and supercomputer linkup. Coupled with this is the study of new payload and terminal technologies such as on-board processing, multiple spot beam antennas, and intelligent terminals to enhance the utilization of the ka-band.

The successfull application of all this technology is however critically dependent on the market forces for the various different communications services that will, or perhaps more correctly, that are foreseen to exist in the post 2000 timeframe. Consideration must be given to the implementation, by that time, of both the LEO type narrowband personal systems, and the possible widespread deployment of the terrestrial B-ISDN fibre optic network. It is perceived that a commercial opportunity may exist, in between these two applications, for an advanced wideband mobile satellite communications service, although the expansion of cellular bandwidths cannot be dismissed. The use of the ka-band, however, is in any case an advantage to satellite systems for "above the clouds" applications such as an aeronautical service.

In this paper, one possible conceptual approach to the design of such a wideband mobile satellite system is presented. It begins with a discussion of the overall system architecture followed by sections on both payload and terminal design. Some aspects of these designs, in particular the mobile terminal are currently only at a preliminary stage. The concepts reported here are part of a continuing overall study effort for the Canadian Department of Communications, carried out by a Spar led team of Canadian aerospace industry to develop an advanced ka band satellite mission.

SYSTEM ARCHITECTURE

The overall architecture of the advanced mobile satcom system comprises ka band service links and a ku band backhaul and private business network. The services supported on the ka band system include the single-user land mobile, fixed or portable USAT, and an aeronautical service. The performance and key link parameters for these are given in Table 1. The ka band system utilizes a 0.5 degree and a 2.3 degree hopping spot beam coverage for the land mobile and

aeronautical services respectively, while the ku band backhaul/business network operates with four fixed beams. The land mobile and fixed services are contrained to Canadian coverage only, and the aeronautical service is extended to all of North America including Mexico for continuity of transborder service.

Table 1. Service Parameters

Services	Avail %	BER	Info Rates (kbps)	# DL TX	# Beams
Single-User Mobile	99	10⁶	16-256	7	84
Fixed/Portable USAT	99.5	10⁶	16-E1		
Aeronautical	99.9	10⁶	16-E1	1	12
Fixed ku VSAT	99.9	10⁷	E1	4	4

The payload is a baseband regenerative type, providing the advantages of signal regeneration and full single-hop interworking of services and interconnectivity of terminals. An MF-TDMA primary uplink access supports information rates in increments of 16 kbps upto to the maximum carrier transmission rates. In addition, a key objective of this on-board processing design is to permit the greatest flexibility of bandwidth usage approaching that of a bent-pipe transponder in some respects. As such, the system will allow operation of various terminal sizes with different transmission rates required to support narrow (16 kbps) to wideband (T1, E1) source traffic.

The sizing of the conceptual design presented here, is based on market studies for the post 2000 timeframe previously carried out by others. The terminal populations for each service is given in Table 2 below. The aeronautical population is by user, and essentially only considers Canadian air traffic. The trunk rate indicated represents the average information rate utilized by a terminal with a 5% grade of service and a traffic intensity of .01 Erlangs/user.

Table 2. Service Populations

Services	Trunk Rate (kbps)	#Trunks/ hop(fix) beam	Pop./hop (fix) beam	Tot Pop.
Single-User Mobile Fixed/Portable USAT	64	16	1154	8078
Aeronautical	64	16	1154	1154
Fixed ku VSAT (@ 0.02 Erlangs/T and Pb=.01%)	E1	8	156	624

Single-User Mobile Service

This service, as its name indicates, is envisaged to support a single land mobile user with information rates upto 256 kbps. It also supports fixed/portable (but stationary during use) USAT applications that can operate at higher rates with larger terminals than is possible with mobiles which require antenna tracking and mobile power supplies.

The coverage for this service, comprising 84 spot beams which are organized in groups of 12 and served by 7 hopping TDM downlink carriers, is shown in Figure 1. The link budgets are given in Table 3 with notes regarding link parameters and assumptions. The budget also includes a 1 dB allowance for an adjacent satellite interference case produced by a "same satellite system" spaced about 8 degrees away. The system supports both mobile-to-base and mobile-to-mobile communications.

Table 3. Land Mobile Link Budget

Link Parameters		Forward: Base-to-Mobile		Return: Mobile-to-Base	
Description	Units	Uplink	Downlink	Uplink	Downlink
Frequency	GHz	14.0	20.0	30.0	12.0
TX Antenna Diameter	m	1.8	2.4	0.3x0.1	1.0
TX Antenna Gain[1]	dBi	46.2	43.3	34.0	29.5
Transmit Power	dBW	7.9	15.0	9.6	14.2
No. of Spots[2]	Spots	4	84	84	4
EIRP	dBW	54.1	58.3	43.6	43.7
Space Loss (39500 km)	dB	207.3	210.4	213.9	206.0
RX Antenna Diameter	m	1.0	0.3x0.1	1.6	1.8
RX Antenna Gain	dBi	31.0	32.0	44.7	44.9
G/T	dB/K	2.2	6.2	16.6	20.7
Transmission Rate[3]	kbps	1870.0	1500.0	364.0	13900.0
C/No Thermal	dB-Hz	77.6	81.2	74.9	84.9
Off-axis angle[4]	deg.	2.0	8.0	8.0	2.0
Adjacent Sat Interference	dB	83.4	87.0	80.8	91.2
C/No Unfaded	dB-Hz	76.6	80.2	73.9	84.0
Sat Pointing Loss	dB	0.2	0.5	0.5	0.2
Atmos Loss	dB	0.2	1.0	0.8	0.2
Ground Pointing Loss	dB	0.2	1.0	1.0	0.2
Multipath Loss[5]	dB	0.0	3.0	3.0	0.0
Availability	%	99.95	99.5	99.5	99.95
Ottawa Rain Fade[6]	dB	5.1	3.1	3.0	3.8
Polarization Loss	dB	0.1	0.5	0.5	0.1
System Margin	dB	1.0	1.0	1.0	1.0
Faded C/No	dB-Hz	69.7	70.0	64.1	78.5
Faded Eb/No	dB-Hz	7.0	8.3	8.5	7.0
Demod Impl. Margin	dB	1.5	1.5	1.5	1.5
Non-linearity degrad[7]	dB	0.0	0.0	0.2	0.0
Ideal Eb/No[8]	dB-Hz	5.5	6.8	6.8	5.5
BER faded		8.8x10⁻⁴	6.4x10⁻⁴	6.4x10⁻⁴	8.8x10⁻⁴
Maximum BER faded Overall Availability	%	6.4 x 10⁻⁴ 99.45		6.4x10⁻⁴ 99.45	
		Two-way: Mobile-to-Mobile 6.4x10⁻⁴ 99.0			

Notes:

1. Mobile TX gain is reduced by 1.0 dB for radome and rotary coupler and satellite gain is reduced by 1.5 dB for RF filter/coupling. Mobile antenna is 30 x 10cm microstrip patch array. Ka band satellite antenna is focus fed reflector with single horn per spot beam.
2. For ku band, 4 fixed beams and for ka band, 84 spots in hopping beam groups of 12.
3. RF transmission rate for a four phase modulation with rate 1/2 FEC convolutional coding and overhead for burst synchronization, symbol timing, and routing headers.
4. Off-axis angle is the adjacent satellite separation.
5. Multipath loss includes fading and shadowing in a mobile environment.
6. Rain fading for the Ottawa location, with a 3 dB uplink countermeasure gain using adaptive forward error correction (AFEC) and 1/2 information rate reduction.
7. Non-linearity degradation for mobile uplink using an offset continuous phase modulation (OQPSK, MSK) operated with a class C saturated impatt device.
8. Ideal Eb/No includes Viterbi soft decision decoding and differential detection for mobile terminals, and coherent for fixed base station terminals.
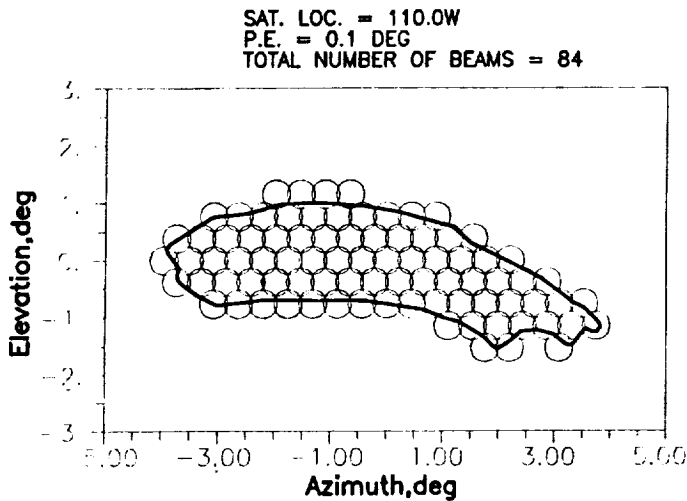
Figure 1. Land Mobile Coverage
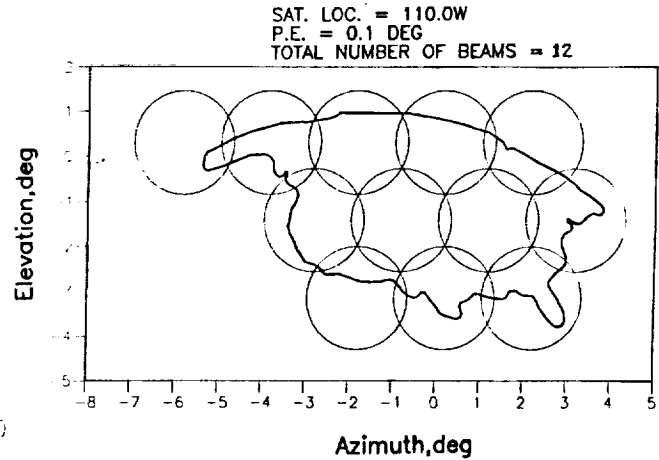
Figure 2. Aeronautical Coverage

The terminal is envisaged as essentially a vehicular unit that can either be directly used inside the vehicle or serve as a relay unit by being remotely accessed via a user to terminal air interface. The terminal consists of a 30 cm x 10 cm microstrip patch that mechanically tracks the satellite in azimuth, and transmits 10 w of RF power. Further details are discussed in the terminal design section below.

Aeronautical Service

The aeronautical service is essentially an airborne version of the land mobile service with some key differences as follows. The terminal requires doppler compensation due to aircraft motion and greater tracking capability in both elevation and azimuth. Since this service is offered to an inherently multi-user form of transportation, a higher time multipled multi-user source information rate is expected.

The coverage for this service, comprising 12 spot beams, served as a group of 12 by one hopping TDM downlink carrier, is shown in Figure 2. As noted previously, an all North American coverage is assumed. The link budgets are given in Table 4 along with notes regarding additional or different items to the land mobile service. The key differences include no allowances for rain fade, multipath, or atmospheric losses. This effectively permits the use of an aeronautical terminal, similar in size to the land mobile, but operating with 12 larger spot beams compared to the 84 spots required to support land mobile.

Table 4. Aeronautical Link Budget

Link Parameters		Forward: Base-to-Mobile		Return: Mobile-to-Base	
Description	Units	Uplink	Downlink	Uplink	Downlink
Frequency	GHz	14.0	20.0	30.0	12.0
TX Antenna Diameter	m	1.8	1.0	0.3	1.0
TX Antenna Gain[1]	dBi	46.2	32.9	37.3	29.5
Transmit Power	dBW	7.9	15.0	10.5	14.2
No. of Spots[2]	Spots	4	12	12	4
EIRP	dBW	54.1	47.9	47.8	43.7
Space Loss (39500 km)	dB	207.3	210.4	213.9	206.0
RX Antenna Diameter	m	1.0	0.3	1.0	1.8
RX Antenna Gain	dBi	31.0	33.7	34.4	44.9
G/T	dB/K	2.2	7.8	5.8	20.7
Transmission Rate	kbps	1870.0	1500.0	364.0	13900.0
C/No Thermal	dB-Hz	77.6	74.0	68.1	84.9
Off-axis angle	deg.	2.0	8.0	8.0	2.0
Adjacent Sat Interference	dB	83.4	79.8	73.9	91.2
C/No Unfaded	dB-Hz	76.6	73.0	67.1	84.0
Set Pointing Loss	dB	0.2	0.2	0.2	0.2
Atmos Loss	dB	0.2	0.0	0.0	0.2
Ground Pointing Loss	dB	0.2	0.5	0.5	0.2
Multipath Loss[3]	dB	0.0	0.0	0.0	0.0
Availability	%	99.95	100.0	100.0	99.95
Ottawa Rain Fade[4]	dB	5.1	0.0	0.0	3.8
Polarization Loss	dB	0.1	0.5	0.5	0.1
System Margin	dB	1.0	1.0	1.0	1.0
Faded C/No	dB-Hz	69.7	70.8	64.9	78.5
Faded Eb/No	dB-Hz	7.0	9.0	9.0	7.0
Demod Impl. Margin	dB	1.5	1.5	1.5	1.5
Non-linearity degrad	dB	0.0	0.0	0.2	0.0
Ideal Eb/No	dB-Hz	5.5	7.5	7.6	5.5
BER faded		8.8×10^{-4}	6.1×10^{-4}	8.9×10^{-7}	8.8×10^{-8}
Maximum BER faded Overall Availability	%	8.8×10^{-8} 99.95		8.9×10^{-7} 99.95	

Notes:

1. Mobile TX gain is reduced by 1.0 dB for radome and rotary coupler and satellite gain is reduced by 1.5 dB for RF filter/coupling. Mobile antenna is 30 cm microstrip patch array. Ka band satellite antenna is focus fed reflector with single horn per spot beam.
2. For ku band, 4 fixed beams and for ka band, 12 spots in one hopping beam group of 12.
3. Multipath loss is assumed zero for aeronautical service due to antenna directivity.
4. Rain fading assumed zero for operation above clouds at cruising altitude.

PAYLOAD DESIGN

The overall payload design consists of four main subsystems: the 84 and 12 beam ka band, the 4 beam ku band, and the On-Board Processing (OBP) systems. The OBP ties all subsystems together through a TST type of switch fabric that provides packet-switched interconnectivity of user traffic segmented into satellite data packets with self-routing headers.

As shown in the block diagram of the ka band payload in Figure 3, the other elements of the payload include single horn per spot beam antennas with a low noise receiver per horn. The uplink is, however, not hopped, so a filter/switch matrix maps the uplink carrier usage of a group of 12 spots corresponding to a hopping downlink group. In this way the uplink MF-TDMA bandwidth is shared over 12 spot beams to match the equivalent TDM downlink capacity which is hopped over 12 spot beam positions comprising the downlink group. The signal received from a group is bulk demultiplexed, demodulated and decoded by a Multi-Carrier Demodulator (MCD). This output enters the space switch through a T (Time or memory) stage port. The overall switch is a 6 x 6, which includes 2 ka band ports, one for each system, and four ku band ports.

The RF power subsystem approach selected for this conceptual design utilizes saturated TWTAs feeding dedicated downlink carriers per hopping beam group. An alternate approach, which is the subject of on-going studies, utilizes a hybrid matrix power system with linear SSPAs.

Table 5. Payload Mass and Power Estimate

Subsystem	Mass (kg)	Power (Watts)
84 Beam Ka Band	143	1250
12 Beam Ka Band	40	185
4 Beam Ku Band	75	130
OBP Switch	29	213
Total	287	1778

The key determining system-level factor in the evaluation of these two approaches is the degree of flexibility that is likely to be required in matching the satellite RF power to the instantaneous traffic distribution. The latter approach is inherently flexible in achieving this but currently has the significant technological disadvantage of the low DC power efficiency (10 %) of linear ka band SSPAs.

For the TWTA approach a DC power efficiency of about 40 % is achievable [3]. The critical aspect for this approach, however, is the selection of the spot beams comprising a hopping downlink group. The selection of the spots for a particular group are not necessarily physically contiguous, in fact the main criteria for spot selection is to ensure that the overall network traffic is as evenly distributed over the downlink TDM carriers, thereby maximizing the power utilization of the satellite. Mass and power estimates for this payload approach are given in Table 5 above. This payload size can be accomodated on a GE5000 bus for example.
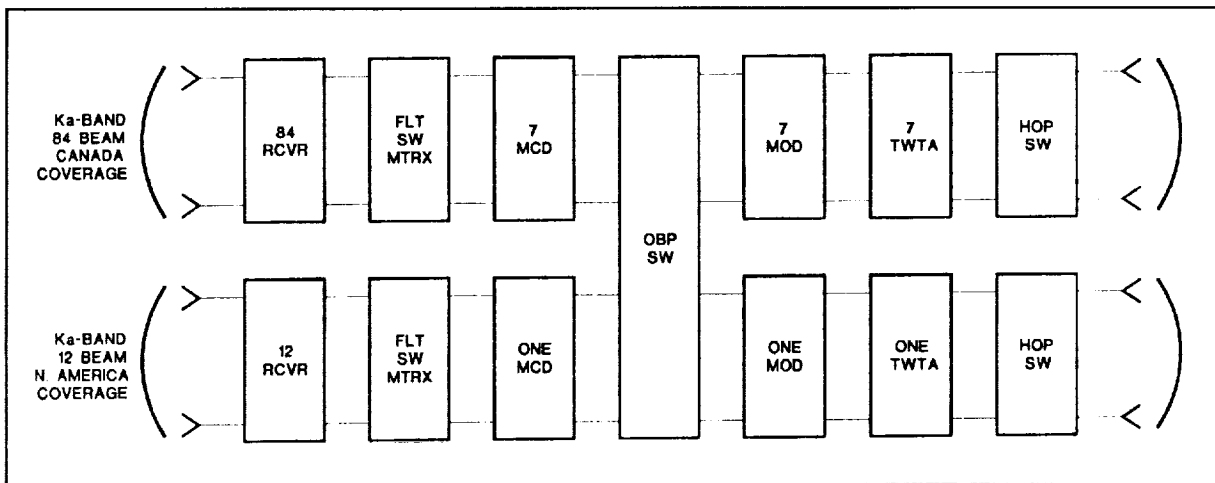
Figure 3. Ka-band OBP Payload

TERMINAL DESIGN

Earth Terminal Types

The focus of terminal design has been on mobile types, both vehicular and aeronautical. However the mobile satellite can support services to fixed terminals such as home office, multimedia and larger terminals for business applications. The former type are downgradable to the latter in terms of antenna tracking and acquisition capabilities and upgradable in terms of antenna size and terrestrial interface capabilities.

The key areas in the terminal design are:

- selection of antenna types
- selection of acquisition and tracking approach
- frequency control
- flexibility of terrestrial interface
- low cost approach

Antenna Design

The use of reflector type or microstrip patches are most attractive for mobile and small fixed terminals, although other approaches are possible - such as the use of dielectric lenses and slot arrays. Reflector types are compact and have high efficiency but have high cost. Microstrip arrays are adopted for the mobile application because of low cost and tolerable efficiency.

The best approach to signal acquisition and tracking is to employ patches with a relatively large beamwidth in elevation so that only the azimuth need be scanned and tracked [4].

A patch with dimensions 30 cm. by 10 cm. produces sufficient gain (about 34 dB) and elevation beamwidth (10 deg.) for the mobile application. A 10 deg. beamwidth in elevation is sufficient to allow for vehicle pitch, but a manually-adjustable elevation setting is used to adapt the antenna orientation to a particular geographical area. Separate patches are required for 30 GHz transmit and 20 GHz receive signals.

For azimuth signal acquisition a DC stepping motor is used to slowly scan until the FFT in the electronics package has detected a downlink signal. A dither approach to antenna tracking combined with vehicle motion sensors is then employed. In the probe approach to beam scanning, each spot is visited every 24 msec., equivalent to less than a meter distance travelled by the vehicle. The dither applied to the antenna moves it alternatively to either side of the estimated line of sight to the satellite and measures the signal strength of the probe signal, thus determining the pointing error's size and polarity. The 3.5 degree beamwidth at 20 Ghz imposes a tight requirement for pointing accuracy and tracking which may limit the degree of motion instability which can be tolerated. This is being further studied. A completely electronic approach to scanning using phased arrays is judged to be cost ineffective - a complete transmit/receive array may cost up to $4000.0 if the cost of phase shifters is included [5].

Terminal Architecture

The block diagram of the terminal is shown in Figure 4. This depicts the mobile version; for the fixed version the antenna controller and motion sensors are not present. The terrestrial interfaces are modular and
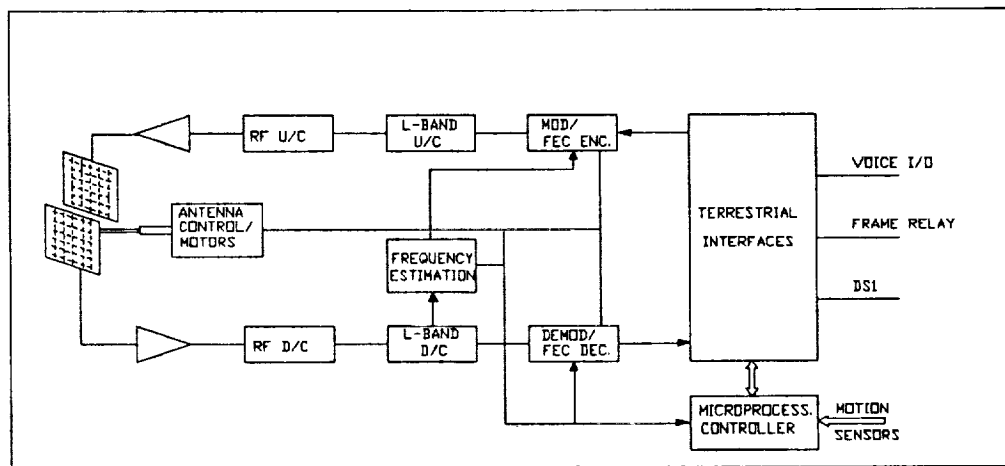
Figure 4. Terminal Architecture

179

adaptable to a variety of traffic types; voice and modest rate video for multimedia applications (up to 256 kbps), up to 2.048 Mbps for larger fixed antennas.

The transmit data stream is rate-1/2 encoded (this coding is removed in the satellite and the downlink is re-coded. A continuous phase modulation (MSK ,OQPSK) is used to reduce sidelobe regeneration and distortion due to saturation non-linearities. The uplink is transported in a TDMA frame. The transmitter is a maximum 10 watt Impatt device operated as a class C amplifier to maximize the DC power efficiency.

Should the quality of the downlink signal degrade due to a rain fade which is larger that the allocated margin, the receiver can decide to signal the corresponding transmitter to reduce itsdata rate by a factor of 1/2, and add an extra level of coding. This level of coding passes through the regenerating transponder without processing.

The downlink signal is in TDM form and is received with a G/T of approximately 7.9 dB (in the absence of rain). A two stage downconverter is used to process the signal to the IF level. Since the downlink signal is not continuous, but may consist only of a probe that is brief in duration, a special frequency estimator is used to minimize acquisition time. This consists of a FFT spectral estimator package. The estimator continually acquires multipoint DFT representations of the signal. It includes software to assess the DFT data and to estimate frequency errors. Frequency changes are expected to occur at a slow rate compared to that of the software execution.

All elements of the terminal are expected to be amenable to year 2000 volume production techniques. For example 1 watt 30 GHz SSPAs (11% efficiency) were available 5 years ago and it is expected that low cost 10 watt units will be available in less that 10 years.

CONCLUSION

This paper has presented an overview description of conceptual studies focusing on a particular approach to the system architecture of an advanced ka band mobile satellite system. The motivation for this approach is to suggest an architecture that 1) might reasonably be achieved in the immediate post 2000 timeframe involving a minimum of new development items, and 2) provides a satellite service that could effectively handle user applications requiring wideband mobile services.

The utilization of a saturated TWTA power system onboard the satellite and mechanical tracking of the terminal antennas are considered less challenging and

costly, at least in the immediate future, than the hybrid matrix approach and electronic steering of the terminal antenna. Significant development items, including the OBP switch and antenna systems, however, do remain to be fully achieved and demonstrated.

The overall feasibility of such a system that provides a wideband mobile service, particulary land mobile, does in general critically depend on the technical requirements for the aquisition and tracking of a relatively high gain terminal antenna. Through experiments such as the ACTS land mobile terminal, the feasibility and development of these type of terminals in a ka band propagation environment can be tested and demonstrated.

However, in addition to the significant technical work that needs to be done, further effort is required to identify and estimate the market potential for one or a range of user applications that could be commercially successfull using an advanced ka band satellite system.

ACKNOWLEDGEMENT

REFERENCES

[1] D.L. Wright and J.R. Balombin, "ACTS System Capability and Performance", AIAA 14th International Communications Satellite Systems Conference, Washington, DC, March 22-26, 1992.

[2] M.K. Sue, K. Dessousky, B. Levitt, and W. Rafferty, "A Satellite-Based Personal Communications Service for the 21st Century", International Mobile Satellite Conference, Ottawa, 1990.

[3] W.F Cashman, "ACTS Multibeam Communications Package: Description and Performance Characterization", AIAA 14th International Communications Satellite Systems Conference, Washington, DC, March 22-26, 1992

[4] K. Dessousky and T.Jedrey, "The ACTS Mobile Terminal (AMT)", AIAA 14th International Communications Satellite Systems Conference, Washington, DC, March 22-26, 1992

[5] Spar Aerospace Limited, "DOC Advanced Satcom Mission System Concept and Hardware Definition Program", Volume 6, Sept. 1992.

Applicability of Different Onboard Routing and Processing Techniques to Mobile Satellite Systems

A D Craig, P C Marston,
British Aerospace Space Systems Ltd
Gunnels Wood Road
Stevenage, Hertfordshire SG1 2AS
England
Tel: (+44) - 438-73-6228
Fax: (+44) - 439-73-6637

A Vernucci
Space Engineering
Via dei Berio 91
00155 Roma, Italy
Tel: (+39) -6-22595-203
Fax: (+39) -6-2280739

P M Bakken
Frobe Radio A/S
Prof Brochs gt
7030 Trondheim
Norway
Tel: (+47)-754-0347
Fax: (+47)-754-0447

J Benedicto
European Space Technology Centre
Postbus 299
2200 AG Noordwijk
The Netherlands
Tel: (31)-1719-86555
Fax: (31)-1719-17400

ABSTRACT

The paper summarises a study contract recently undertaken for ESA [1]. The study compared the effectiveness of several processing architectures applied to multiple beam, geostationary global and European regional missions. The paper discusses architectures based on transparent SS-FDMA analogue, transparent DSP and regenerative processing. Quantitative comparisons are presented and general conclusions are given with respect to suitability of the architectures to different mission requirements.

INTRODUCTION

As mobile systems develop towards a mass market with smaller mobile Earth stations (MES) a key requirement is for high gain spot beams to limit onboard and MES power and to provide scope for frequency reuse (FR). Associated with this is a need for channel to beam routing to accommodate a non-uniform and variable traffic distribution. The objective was to compare onboard processing and routing architectures, based on different approaches for future multibeam GEO missions and to identify regimes where the different approaches are most applicable.

In a generic sense all architectures comprise the Feeder Link (FL) antenna and Rx/Tx system, the Mobile Link (ML) antenna and Rx/Tx system (L-band) and the forward link (FWL) and return link (RTL) processors. The following options were studied:

A. Transparent SS-FDMA with processing of transponder channels comprising groups of user accesses. Implementation is analogue and divides between filter plus switch and Chirp Fourier Transform (CFT) options.

B. Transparent digital signal processing (DSP) characterised by channelisation to individual or small groups of FDMA user accesses with routing by either beam switching or beam steering.

C. Regenerative with channel demodulation and independent optimisation of FL and ML access and transmission characteristics.

Comparisons were made for integral Land-Aero-Maritime Global (LAMG) and Land Mobile Regional (LMR) missions.

Candidate architectures were defined for each option. An internal tradeoff for each option was based on a range of performance and implementation parameters leading to a number of preferred architectures. The preferred architectures were then compared using spread sheet models based on key system budgets and parametric implementation models.

The tradeoff is complex involving many criteria which will have different importance for different missions. These include payload mass and power, spectral efficiency, erlang efficiency

and flexibility to changing traffic, flexibility to vary channel characteristics (data rate, modulation), and to change frequency plan, flexibility to exchange channel power and bandwidth, system security against unauthorised access, associated ground segment and control requirements and development risks and timescales. The options display strengths and weakness with respect to these criteria; a key objective was to define regimes where the different options are preferred.

ASSUMPTIONS AND COMMON FEATURES

Various coverage concepts may be considered for the ML. A global beam has a simple antenna and good traffic flexibility but gain is low and there is no FR. Fixed contiguous spot beams provide high gain and FR but require a large antenna and routing capability. Alternatively larger numbers of overlapped spot beams (fixed or agile) may be used each supporting a single or limited group of users close to the beam peak; such an approach also provides higher spatial FR because of the localisation of users to the beam peak allows closer co-frequency beams. Antenna models were defined based on a focus fed multimatrix approach for contiguous beams and phased array (direct or imaging) for highly overlapped beams.

The LAMG mission assumes a global public service with a limited number of gateway stations within a single FL beam and 9 contiguous beams (or equivalent sized overlapped beams) on the ML (MES G/T = -12dBK). FDMA/FDM access is assumed with 9.6kbit/s channels taken as representative but with emphasis on service flexibility. Traffic distribution is assumed to be highly non-uniform.

The LMR mission combines public and private (VSAT) European services with a single beam FL and an ML with up to 12 contiguous beams (or equivalent size overlapped beams) (MES G/T = -12dB/K). Access is FDMA or CDMA.

Propagation characteristics on the ML are important particularly for land mobile services with shadowing and multipath losses which are dependent on environment, elevation and MES antenna pattern. Shadowing effectively excludes an urban service at European latitudes. For LMR shadowing and multipath margins of 5dB and 2dB were assumed. An average environmental link margin of 2.5dB was assumed for the LAMG mission (due to mixture of services).

Channel Level Control (LC) emerged as a key issue with respect to system optimisation in view of the large variations in link performance (in particular for land mobile). Without LC, margins must cover worst case conditions leading to excessive power requirements. Ideally individual channels would be dynamically controlled according to instantaneous link conditions. Various schemes involving ground or onboard LC were studied including those using the correlation between mobile uplink and downlink in order to save power on the critical mobile downlink.

Spectral efficiency is a key issue for the ML. Factors affecting it are channel and erlang efficiency and FR. FR is limited by antenna isolation, traffic distribution and control issues. The overlapped beam approach offers an advantage in this respect. Onboard Active Interference Suppression (AIS) aimed at nulling specific interferers is possible within some architectures.

Erlang efficiency drops if fixed channels are used in fixed spot beams. Methods of recovering erlang efficiency and traffic flexibility involve the use of beam overlaps, frequency addressing with multiple FL bands mapping to a common ML band in different beams, channel to beam switching, Variable Bandwidth and Centre Frequency (VBVCF) filters and agile beam steering.

OPTION A. ANALOGUE SS-FDMA

A transparent transponder is assumed with channels wide compared to individual accesses but narrow compared to the total bandwidth. Routing to beams is by analogue means (as Inmarsat 3).

Filter and Switch Matrix Architectures

Key requirements are for sufficient granularity in channelisation and beam switching and to maintain spectral efficiency on the ML.

Orthogonal FL polarisations may be used to give contiguous usage of the ML by feeding SAW filters adjacent in frequency from opposite FL polarisations. All signals have the same frequency translation. A disadvantage is the 100 percent overhead needed in FL bandwidth. Architectures were considered with typically 8 switchable filters (for each service in the case of LAMG) covering a band of typically 7MHz. If all filters have the same bandwidth a high level of granularity is implied which will limit traffic flexibility. A finer granularity and more flexibility is obtained if the filters are made different (for example with a binary relationship between bandwidths); this however implies that the traffic to a beam may be split between disjoint bands.

Alternatively FL bands, separated by guard bands, may be translated by different frequencies to provide contiguous bands on the ML maintaining ML spectral efficiency without the overhead in FL bandwidth. The disadvantage is in the number of synthesisers required to provide the translations.

VBVCF Architectures

A VBVCF filter makes it possible to reallocate the spectrum by filter tuning instead of switching. The bandwidth and centre frequencies are set by synthesisers. The maximum flexibility occurs when the VBVCF filters are considered to have 3 free variables, namely FL frequency, ML frequency and bandwidth. It is possible to have guardbands only for the FL with contiguous band usage for the ML to minimise spectrum. ESA sponsors SAW filter, VBVCF SAW filter bank and miniaturised switch development.

Fourier Transform Architectures

The architecture uses CFT technology and its inverse (ICFT). The 2 transform devices combine to provide an identity transform. The transform domain signal may be manipulated in the time domain by gating (multiplication by a periodic function) to shape the effective filter function between the input and output. The multiplier waveform may be read from a digital memory and changed by telecommand providing a high degree of traffic flexibility. Developments on CFT technology have been supported by ESA [2]. Expected performance is a guardband width of 100kHz over a processed band of 30MHz.

All the above options can be implemented with technology that exists or is in an advanced stage of development. The CFT architecture was selected for comparison with Options B and C following an internal tradeoff for Option A was based on performance, mass and power and technology risk. The approach offers a fine level of granularity and avoids mobile bandwidth fragmentation. Developments are required with respect to high precision SAW devices, chirp generators and mounting technology but no technical barrier to their implementation is known. The CFT approach showed comparable mass and power to filter based alternatives LMR but showed an advantage LAMG where one CFT processor provides flexibility and bandwidth for all 3 services. Figure 1 shows the FWL processor configuration applied to LAMG; the time domain processor (TDP) provides the gating waveforms.
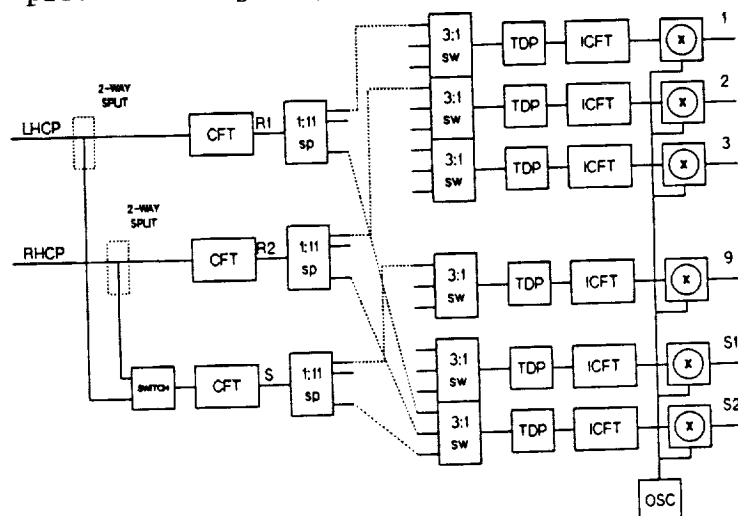
Figure 1.

Option A CFT forward link configuration.

183

OPTION B. TRANSPARENT DSP

The architecture features digital processing of FDMA channels based on either contiguous or highly overlapped beams.

The contiguous beam case assumes a small number of beams formed by a multimatrix antenna (traffic independent power handling). The processor interfaces at a beam port level giving relatively low processor mass and power due to the small number of ports. Total channelisation gives full routing flexibility. Individual channels have LC applied. This may be used to maintain FWL and RTL HPA drive, compensate for static downlink variations and for dynamic variation on the mobile downlink on the basis of observation of the return uplink power. Dynamic LC can in principle compensate for MES shadowing and gain variations but is limited by delay and multipath errors. Small numbers of channels are multiplexed into beam switching groups.

The overlapped beam case assumes a large number of beams (up to one per channel). Each beam is steerable (generated by a Phased Array (PA) using digital beamforming) providing near to peak gain to individual MESs thereby reducing power requirements both on-board and at the MES. The processor interfaces on a PA element basis.

Individual channels may have LC and AIS applied. Routing of individual or small groups of channels is by beam steering; a tradeoff exists between the number of independently steered beams and edge of coverage gain loss between beams. Overlapped beams allow higher FR because the use of beam peaks allows co-frequency beams to be closer whilst meeting isolation requirements. Figure 2 shows an example of a FWL architecture for the overlapped beam case.

The processor utilises a mixture of analogue and digital technology. A coarse level of channel demultiplexing and multiplexing involves a bank of fixed filters or a SAW CFT (or ICFT) device. The CFT approach is particularly advantageous when the total ML bandwidth is large and/or the

spectrum is fragmented. Where small bandwidths are envisaged demultiplexing and multiplexing may be performed entirely digitally. The key digital processing functions are fine channel demultiplexing and multiplexing, beamforming, LC and AIS.

AIS is based on complex weighting and addition of co-frequency beam outputs; weighting control may come from an onboard directional based adaptive algorithm. An additional DSP function which lends itself to inclusion in such architectures is source location using super-resolution processing of the array covariance matrix. Mobile terminal location is required prior to beam steering.

The processors have been assessed assuming projected parameters for rad hard 0.8μm CMOS technology (typically 80000 useable gates with 3μW/gate/MHz dissipation). The mass and power has been estimated based on optimised partitioning between ASICs, realistic constraints on individual ASICs and PCBs and on realistic packaging assumptions.

The major potential advantages of Option B are reduced onboard power due to onboard channel LC, the use of near peak gain (overlapped case), increased G/T, increased FR using overlapped beams and AIS and high traffic flexibility from agile beams. These must be traded against complexity, mass and power of the processing.

The RF power savings can be balanced against the power and mass of the processor. Where the RF power is large, as in LAMG, RF power savings are
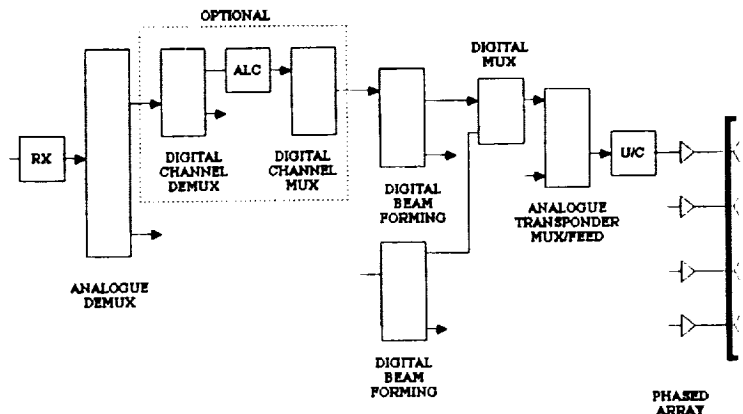
Figure 2. Option B overlapped beam forward link architecture.

large justifying the increased
processor mass and power. Where RF
power is modest, as in LMR, the RF
power savings are accordingly smaller
for the overlapped beam approach; in
this case the contiguous beam
architecture is preferred because of a
reduced processor overhead.

OPTION C. REGENERATIVE

Architectures are characterised by
baseband processing and feature onboard
regeneration, baseband channel to beam
routing/switching, signal reformatting,
onboard network control functions, etc.

The architectures considered for the
LMR mission were a fixed beam CDMA and
a hybrid FDMA approach based on agile
overlapped beams (as Option B) with a
regenerative front end. An FDMA
approach was considered for the LAMG
mission.

LMR CDMA Architecture

This architecture is described in a
companion paper at this conference [3]
and will only be outlined here. The
FWL is characterised by TDMA access and
regeneration of synchronous CDMA by
onboard multi-carrier modulators (MCM)
for the mobile downlink. Synchronous
CDMA has nominal zero self noise,
advantages in terms of spectral
efficiency on both FL and ML, onboard
power and FES complexity. The less
critical RTL is assumed to adopt a
transparent approach as in Option A or
B.

LMR FDMA Architecture

The FWL is characterised by TDMA,
onboard regeneration, buffering and
reformatting, FDM MCMs and digital
beamforming to provide multiple agile
beams to routing flexibility. The
architecture is therefore as a hybrid
between a regenerative and overlapped
beam Option B architecture. The RTL
assumes a non-regenerative Option B
approach. Performance is comparable
despite the cross noise generated by
non-synchronous codes operating in
adjacent beams. The approach has

to the overlapped beam Option B
architecture with the benefit of peak
gain and high ML spectral efficiency.
The essential difference is that the FL
demux/mux section of Option B is
replaced by the regenerative section in
Option C.

LAMG FDMA Architecture

The LAMG mission is characterised by
the requirement to flexibly accommodate
a range of services characterised by
different transmission parameters. A
regenerative architecture which
provides such flexibility was studied
characterised by a dual C-band and
Ku-band TDMA FL with onboard
regeneration, baseband processing and
FDMA ML. Both FWL and RTL are
regenerative in this case.

OVERALL TRADEOFF

Preferred architectures have been
defined for each mission within each of
the options. Quantitative comparisons
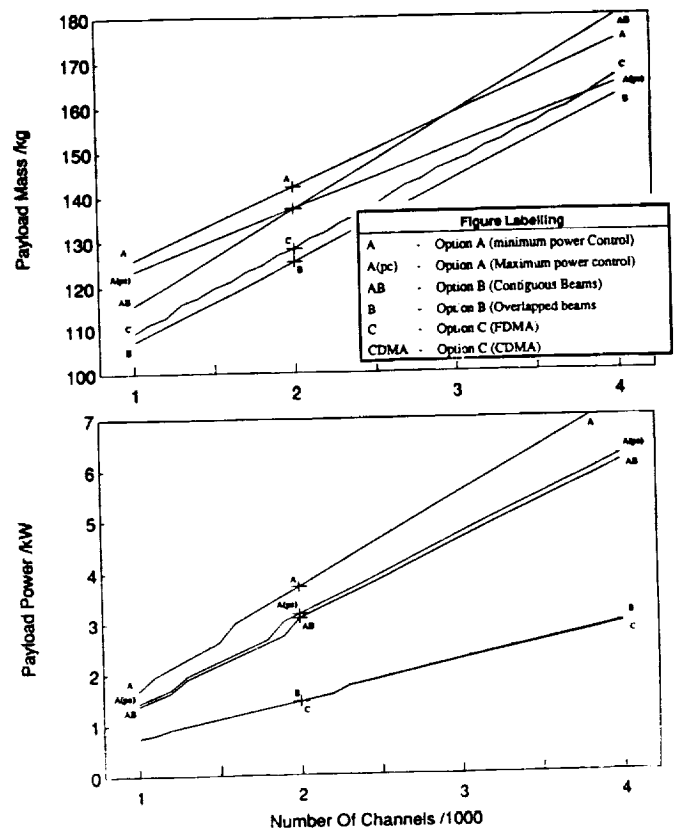
Figure 3. Payload tradeoff for LAMG mission.

185
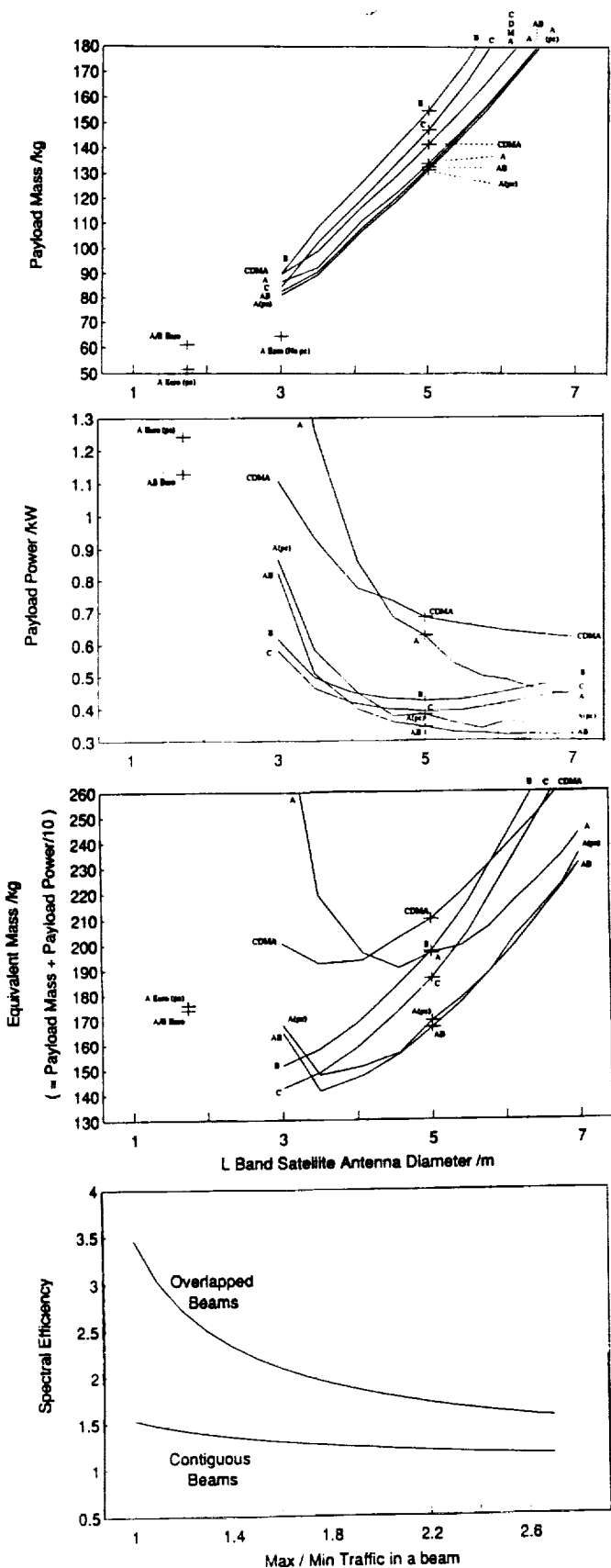
Figure 4. Payload tradeoff for LMR mission

were then made using spread sheet models. The minimisation of payload mass and power represents a complex tradeoff between antenna, power and processor subsystems depending strongly on RF power requirement.

Quantitative results showing payload mass and power versus channel capacity are shown in Figure 3 for LAMG (constrained to 9 beams). Option B (overlapped) provides the minimum mass and power; this is due to the large RF power savings resulting from the high ML gain. Option C has similar mass and power because it also assumes overlapped beams. The contiguous beam options are less efficient. Option A depends strongly on LC strategy.

The LMR mission has 2 major variables, namely capacity and antenna diameter (determining size and number of beams for the contiguous options). Figure 4 shows mass and power versus diameter (in the range up to 12 contiguous beams) for 2000 channels. The contiguous beam options are preferred because they involve lower processor mass and power and the RF power advantage of overlapped beams is low because total RF power is low. Figure 4 also shows total payload equivalent mass (10W/kg equivalence); the minimum for the contiguous beam cases as at approximately 3.5m representing a tradeoff between the effects of decreasing RF power and increasing processor and antenna equivalent mass. Also shown in Figure 4 is a comparison between spectral efficiency where overlapped beam approaches are preferred.

REFERENCES

[1]   Final Report of 'Study of Applicability of Different Onboard Routing and Processing Techniques to a Mobile Satellite System' ESA Contract 8972/90/NL/RE, British Aerospace, Space Engineering and Frobe Radio (1992).

[2]   ESA contract 9107/90/NL with SINTEF DELAB and FROBE RADIO, "Mounting of SAW devices" (On-going).

[3]   A Vernucci and A D Craig 'A European Mobile Satellite System Concept Exploiting CDMA and OBP' (presented at this conference).

A European Mobile Satellite System Concept Exploiting CDMA and OBP

A. Vernucci
Space Engineering
via dei Berio, 91
00155 Rome, Italy
Tel: (+39)-6-22595-203
Fax: (+39)-6-2280739

A.D. Craig
British Aerospace Space Systems
Gunnels Wood Rd
Stevenage Hertfordshire SG1 2AS, England
Tel: (+44)-438-73-6228
Fax: (+44)-438-73-6637

ABSTRACT

This paper describes a novel Land Mobile Satellite System (LMSS) concept applicable to networks allowing access to a large number of gateway stations ("Hubs"), utilising low-cost Very Small Aperture Terminals (VSATs).

Efficient operation of the Forward-Link (FL) repeater can be achieved by adopting a *synchronous* Code Division Multiple Access (CDMA) technique, whereby inter-code interference (*self-noise*) is virtually eliminated by synchronizing orthogonal codes. However, with a transparent FL repeater, the requirements imposed by the highly decentralized ground segment can lead to significant efficiency losses. The adoption of a FL On-Board Processing (OBP) repeater is proposed as a means of largely recovering this efficiency impairment.

The paper describes the network architecture, the system design and performance, the OBP functions and impact on implementation.

The proposed concept, applicable to a future generation of the European LMSS, was developed in the context of a European Space Agency (ESA) study contract.

INTRODUCTION

Among the LMSS concepts currently being evaluated by European space communications organizations, considerable interest is being paid to the possibility of sharing a K_u-band VSAT as the Hub of a **private** *mobile-service* network and as the Hub or User Terminal of a *business-service* network (use of multi-purpose or colocated satellites is assumed). The mobile-service sub-network will also allow access to **public** Hubs, interfaced to the terrestrial network, for which the low-cost constraint could be somewhat relaxed.

As widely discussed in the literature [1] [2] [3] [4], CDMA can improve the LMSS spectral efficiency; in particular the so called *synchronous* version of CDMA can result in even higher efficiency. The actual CDMA system capacity advantage is larger when the number of mobile-link beams is high and if voice activation and low-rate FEC encoding are adopted.

In contrast to the FL, the adoption of synchronous CDMA for the Return-Link (RL) is considered to be questionable, due to the difficulty of maintaining mobile terminal synchronization in the harsh LMSS propagation environment, and recourse is likely to be made to the more traditional *asynchronous* version.

Although the expected symmetrical FL / RL capacity requirements may lead to questioning of the utilization of different techniques for the two links, for a non band-limited system the higher synchronous CDMA spectral efficiency can be easily translated into a reduction of the RF power-per-channel requirement for the FL repeater. This is evident from fig. 1, showing a comparison between asynchronous and synchronous CDMA for the network configuration which will be illustrated later. For a nominal repeater capacity of 3,200 channels, corresponding to the power-limited capacity of the RL re-
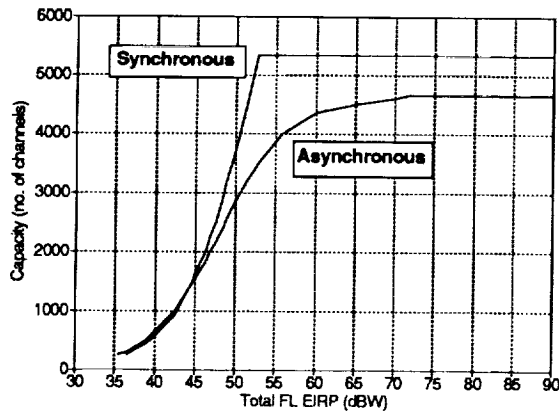
Fig. 1 EIRP requirements comparison

peater operated with asynchronous CDMA, a power saving of about 3 dB can be gained.

The above led to the definition of a LMSS concept, consistent with a highly decentralized ground segment, and making use of synchronous CDMA on FL and asynchronous CDMA on RL as a means to combine high spectral efficiency with savings in FL on-board RF power.

The concept was developed with reference to a geostationary satellite featuring a 6-beam L-band mobile link and a single Euro-beam K_u-band feeder link. This configuration is representative of a possible LLM follow-on payload, LLM being the LMSS subsystem to be flown aboard the European ARTEMIS satellite. A bandwidth of 7 MHz and an L-band EIRP of 49 dBW were assumed to be available. The peak antenna gain is in excess of 36 dB.

The available 7-MHz bandwidth is subdivided into 1-MHz segments, thus supporting 7 distinct CDMA accesses. The same 7-MHz band is re-used in each of the 6 beams, exploiting the CDMA interference rejection properties, thus leading to a total of 42 "CDMA modules". This approach was selected to provide compatibility with the first-generation European LMSS payload (EMS) and for gradual bandwidth utilisation, proportionally to traffic demand.

RATIONALE FOR USE OF OBP

Synchronous CDMA implies that Hubs should be designed to support both a clock and a carrier frequency loop so as to not impair the codes cross-correlation properties. The transmit

chip phase has to be controlled within a fraction of a chip (typically less than 100 ns), while the transmit carrier frequency must be maintained within a fraction of a symbol period (roughly ±500 Hz for a K_u-band up-link)

Another and more important problem concerns overhead, in terms of RF power, deriving from the need for FL Pilot Carriers (PCs). With CDMA, the Hub has to transmit a spread, although unmodulated, PC synchronous, at both *clock* and *carrier phase* level, with its traffic codes. The PC must be transmitted at a level at least 5 dB higher than the traffic codes, in order to allow dependable carrier recovery at the coherent mobile terminal demodulator and to maintain robust receive code synchronization.

Each Hub has to transmit its own PC, due to the practical impossibility for Hubs to synchronize their traffic codes, at *carrier phase* level, to a unique PC which could conceivably be transmitted by a Network Coordinating Station (NCS). If the number of Hubs is large, the PCs overhead also becomes large, thus significantly impairing the overall system efficiency.

This problem becomes particularly important for the system under consideration, featuring multiple L-band beams and bandwidth segmentation into CDMA modules, as the total number of PCs needs to be further multiplied by 42.

Fig. 2 shows how the PC overhead degrades capacity, for a variable number of Hubs. Fig. 2 also includes the extra overhead due to the need for each Hub to transmit a Signalling Carrier (SC) per CDMA module.
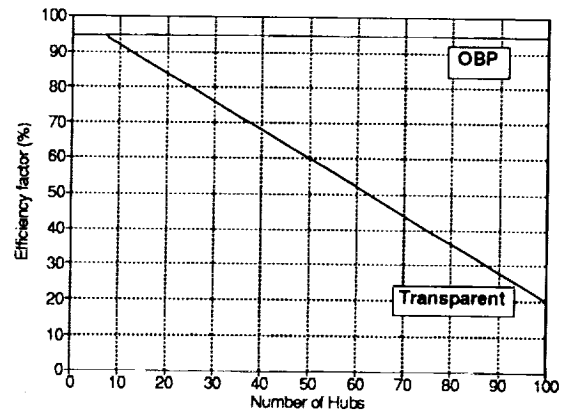
Fig. 2 System efficiency vs number of Hubs

188

As a final issue, the high CDMA capacity is achieved at the expense of a large feeder-link bandwidth. It can be easily seen that, to be able to independently address the 7 1-MHz CDMA modules in each of the 6 beams, a total feeder-link of 42 MHz is required (32 MHz would be required with FDMA to accommodate 3,200 channels with 10 KHz spacing).

An OBP repeater, featuring on-board generation of CDMA codes, offers an attractive solution to all the above problems, in that:
- the Hub access technique can be selected such as to simplify Hubs;
- a single PC for each CDMA module can be generated on-board, this clearly being coherent with the on-board generated traffic codes;
- the feeder-link bandwidth can be reduced by using a band-efficient access technique.

With OBP on the FL, the overall PC overhead becomes virtually independent of the number of Hubs and equal to a well affordable 5.3% (minimum), corresponding to a 0.23 dB loss.

In addition, the FL OBP repeater allows the efficient call routing (in Erlang terms) to spots, as on-board resources form a pool common to all spots, with sharing on a call-by-call basis.

The RL repeater was instead assumed to be transparent for the following main reasons:
- the RL topology (many-to-one) offers little room for gaining Erlang advantages;
- the complexity of implementing a large bank of on-board CDMA demodulators;
- moderate advantages to be gained, in terms of absolute power, e.g. by routing all up-link traffic in a single TDM down-link stream.

Nevertheless, RL OBP could still be considered attractive for reducing the down-link bandwidth requirement, for simplifying the Hub receive side, for allowing direct mobile-to-mobile calls (no double-hop via hub station) and to achieve some link performance improvements.

L-BAND DOWN-LINK DESIGN

The 7 CDMA modules of a spot beam all utilize the same family of preferentially-phased Gold codes; this configuration results in virtually no *self-noise* both because the selected

codes are nearly orthogonal and because of the frequency-staggering arrangement. However, because the same codes are also used on the co-frequency CDMA modules of the other spots, some interference is generated (*cross-noise*).

Should the "other" spots codes be in phase with the "wanted" beam codes, cross-noise would be only limited by antenna discrimination, reducing to an unacceptable 0 dB at spot beam cross-overs. For this reason, it is proposed that codes operating on the other beams be shifted with respect to each other by $1/6^{th}$ of the code length, thus taking advantage of an additional isolation factor.

This is feasible because of the good Gold codes self-correlation properties, resulting in a cross-noise nearly equivalent to that of random codes. This would have not been the case if Walsh functions had been selected, because these require an additional level of spreading to avoid interference peaks among codes operating in different spots.

The selected CDMA access operating parameters are shown in tab. 1.

Tab. 1 L-band down-link parameters

Vocoder rate	4,800 bps
FEC	convolutional, rate 2/3
Coded rate	7,200 sps
Chip rate	914.4 Kchip/s
Processing gain	127 apparent, 190.5 effective
Modulation	BPSK with coherent demodulation
Spreading	BPSK
Number of codes	127 per CDMA module

The use of a power-flexible antenna design (e.g. MultiMatrix Amplifier or Imaging Phased Array), allowing dynamic sharing of available on-board RF power among spots to match the current traffic level in each spot, is required to support the inherent system tolerance to traffic imbalance across spots. The availability of 7 CDMA modules gives a spot the capability of supporting a peak of 889 channels, i.e. 67% more than the average capacity in balanced traffic conditions.

Ku-BAND UP-LINK DESIGN

The preferred choice for Hub access is dual-rate TDMA (separate access channels for each rate). This results in the:
- minimization in number of modems both on-board and at Hubs;
- possibility of tailoring the access rate on the total Hub traffic and cost constraints (low-rate for private Hubs and high-rate for public Hubs);
- possibility of still supporting an adequate total private traffic level, by means a frequency-staggered multi-channel TDMA arrangement;
- fairly high flexibility to reassign capacity to Hubs. In particular, the proposed modular frame allows the reallocation of capacity blocks without having to upset the burst time plan.

The main TDMA access parameters are presented in tab. 2.

Tab. 2 Ku-band up-link parameters

	Private Hubs	Public Hubs
TDM access rate	3.072 Mbps	24.576 Mbps
Number of up-link carriers	16	1
Total access capacity	2,304 channels	2,304 channels
Max. Hub capacity (per TDMA carrier)	144 channels	2,304 channels
Frame elementary module	4 channels	6 channels
Frame efficiency	33.8 %	67.5 %
Antenna diameter	2.5 m	3.5 m
RF power	13 W (1 carrier)	50 W

The following is noted:
- the capacity of each access (2,304 channels) exceeds by 44% half of the repeater capacity thus leaving flexibility in accepting different private / public traffic sharings;
- re-allocations of capacity blocks need not be performed on a call-by-call basis, because of the fairly small block size;
- the fairly low frame efficiency results from the simple burst synchronization schemes; for private Hubs it was assumed that the TX start-of-frame (SOF) will be derived by adding a fixed delay to the RX SOF, while for public Hubs the delay will be adjusted on the basis of the current satellite position (open-loop control);

- interleaving and FEC coding are performed on a per-channel basis by Hubs, thus relieving the OBP from this task. A coding gain close to the soft-decision one can be attained, the up-link BER performance (10^{-4} @ 99.5% of time) being much better than that of the down-link;
- scrambling is performed at bundle level, assuming the presence of a de-scrambler following the on-board demodulator;
- voice activity will be detected at Hubs, inserting appropriate flags in their bursts, to allow OBP to suppress idle CDMA codes. Also a signalling channel is embedded in up-link bursts;
- no Reference Burst (RB) shall be transmitted from ground, due to the availability of a RB transmitted by the OBP into the RL down-link.

THE FL OBP REPEATER

Fig. 3 shows a payload functional diagram, with the FL OBP section being shown in more detail than that of the transparent RL.

A single TDMA demodulator is used for the 24.576 Mbps stream, while a Multi-Carrier Demodulator operates on the 16 3.072 Mbps streams. Frame Processors perform frame and clock alignment and multiplexing, thus generating two identical 17.023 Mbps streams.

An inherently non-blocking T-stage switch routes, on a call-by-call basis, incoming time slots to any of the 42 914.4 kbps output streams. The T-stage effectively performs space switching and concentration functions, by terminating unused up-link slots.

Each of the 42 streams, supporting 127 channels, is fed to a distinct CDMA Multi-Carrier Modulator, which modulates and spreads 127 channels and generates a PC and a Signalling Carrier, all with common hardware.

The 42 CDMA bundles are then associated in 6 groups of 7 bundles, each group being fed to a different spot via IF and RF devices.

The RL is basically transparent apart from the on-board signalling and RB carrier generator. Signalling information is generated by the On-board Network Controller (ONC). This carrier is frequency multiplexed with up-link signals converted at IF.
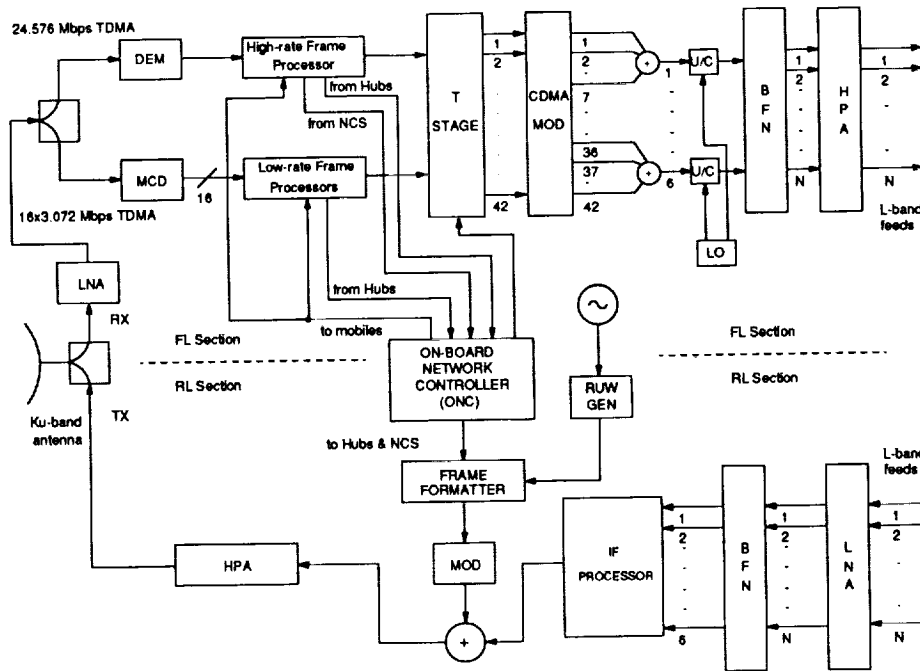
Fig. 3 Payload functional diagram

The ONC manages call handling protocols, by exchanging signalling with Hubs and mobile terminals (mobile signalling is processed at Hubs, the RL repeater being transparent).

SYSTEM ASSESSMENT

With the available 49 dBW EIRP, the overall L-band spectral efficiency of the proposed system is about 2.2 bps/Hz when the traffic is uniformly distributed over the 6 spots. This is considerably higher than that achievable with asynchronous CDMA (1.8 bps/Hz) or with conventional FDMA (0.95 bps/Hz) under the same network, payload and traffic assumptions.

The FDMA system capacity would be band-limited, so that a higher code rate (3/4) has been assumed for this comparison case. In this way the FDMA and the synchronous CDMA approaches would both have the same on-board FL RF power-per-channel requirement of about 19 mW (the cross-noise degradation in CDMA almost equals the lower coding gain in FDMA).

The effect of uneven traffic distributions was assessed by means of event-driven computer simulations, the main results of which are summarized in fig. 4. It is evident how synchro-nous CDMA possesses an inherently higher tolerance of traffic imbalance across spots than asynchronous CDMA, up to the point where all the available 127 codes are used (this condition is indicated by a dashed curve). If desired, this limit could be pushed further by selecting a different code length and modulation / coding parameters.

It is important to remark that the proposed CDMA system shows an inherent flexibility with regard to traffic patterns, in that uneven distributions can be accommodated without having to reconfigure the FL payload, as would be the case with a traditional FDMA repeater.
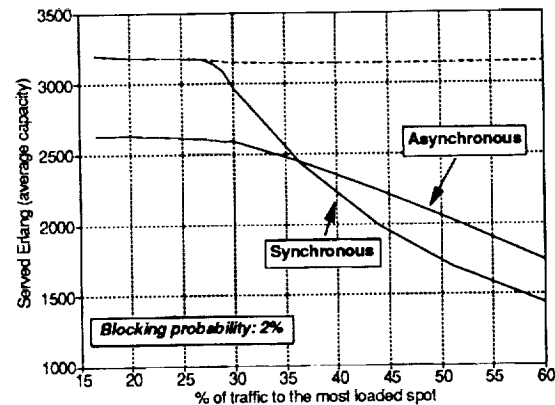
Fig. 4 System capacity vs traffic imbalance

As far as implementation aspects are concerned, a detailed payload modeling activity was performed to derive mass & power estimates and to determine the most suitable implementation technology.

The results of this analysis are shown in tab. 3, which indicates the mass and power of the FL and RL processors as percentage of the overall payload.

Tab. 3 Relative processors mass and power

	Mass (%)	Power (%)
Forward processor	9.7	10.8
Return processor	4.1	2.0
Total	**13.8**	**12.8**

It is evident that the FL OBP processor takes about 10% of the overall mass & power resources. In judging this figure, one has to also take into account that, even if OBP is not endorsed, an analogue processor would anyway be required to route channels to spots, thus reducing the proper OBP overhead to a few percent of the overall payload.

From the technology standpoint, a total count of 202 ICs was estimated, assuming the use of a 0.8 μm rad-hard CMOS fabrication process.

CONCLUSIONS

This paper demonstrates that the capacity of a regional Land Mobile Satellite System can be significantly improved by adopting a synchronous CDMA technique in the Forward Link, assuming that the system operates in the power-limited region, this being a typical condition for LMSSs.

The use of an On-Board Processor generating the CDMA codes on-board was shown to be able to further enhance the capacity of a system operating in conjunction with a highly de-centralized ground segment, featuring a large number of gateway stations (Hubs). OBP also yields the remarkable advantage of simplifying the Hub design and hence of limiting their cost.

The proposed system has been designed with particular care as to its adaptability to support uneven traffic distributions across the L-band spots, such as to make it able to operate efficiently under different traffic distribution patterns. The main technique used to achieve this is that of oversizing the internal payload paths, taking care to not cause adverse impacts on processor mass and power budgets.

As a result the FL processor only takes about 10% of the overall payload resources, a fraction of which would anyway have been used if an analogue processor were to be selected, in conjunction with a transparent repeater, to be able to route the up-link channels to the six down-link spots.

The implementation of the processor was assessed and considered to be well within the today's technology status.

ACKNOWLEDGMENTS

REFERENCES

[1] S. Arenaccio et al "Performance, implementation & network management techniques for a European CDMA-based LMSS", GLOBECOM 90

[2] Report of "Study of applicability of different routing and processing techniques to a mobile satellite system", ESTEC contract 8972/90 - British Aerospace, Space Engineering and Frobe Radio (1992)

[3] R. De Gaudenzi, R. Viola "High-efficiency voice-activated CDMA mobile communications system based upon master code synchronization", GLOBECOM 89

[4] A.J. Viterbi "Spread Spectrum communications - Myths and realities", IEEE Communications Magazine, May 1979

Study of LEO-SAT Microwave Link for Broad-Band Mobile Satellite Communication System

Masayuki Fujise, Wataru Chujo, Isamu Chiba, Yoji Furuhama

Kazuaki Kawabata* and Yoshihiko Konishi**

ATR Optical and Radio Communications Research Laboratories

2-2, Hikaridai, Seika-cho, Kyoto

619-02, Japan

Tel +81-7749-5-1511

Fax +81-7749-5-1508

* Toshiba Corporation ** Mitsubishi Electric Corporation

INTRODUCTION

In the field of mobile satellite communications, a system based on low-earth-orbit satellites (LEO-SATs) such as the Iridium system has been proposed[1]-[3]. The LEO-SAT system is able to offer mobile telecommunication services in high-latitude areas. Rain degradation, fading and shadowing are also expected to be decreased when the system is operated at a high elevation angle. Furthermore, the propagation delay generated in the LEO-SAT system is less pronounced than that in the geostationary orbit satellite (GEO-SAT) system and, in voice services, the effect of the delay is almost negligible. We proposed a concept of a broad-band mobile satellite communication system with LEO-SATs and Optical ISL[4]. In that system, a fixed L-band (1.6/1.5GHz) multibeam is used to offer narrow band service to the mobile terminals in the entire area covered by a LEO-SAT and steerable Ka-band (30/20GHz) spot beams are used for the wide band service.

In this paper, we present results of a study of LEO-SAT microwave link between a satellite and a mobile terminal for a broad-band mobile satellite communication system. First, the results of link budget calculations are presented and, the antennas mounted on satellites are shown.

For a future mobile antenna technology, we also show digital beamforming (DBF) techniques. DBF, together with modulation and/or demodulation, is becoming a key technique for mobile antennas with advanced functions such as antenna pattern calibration, correction, and radio interference suppression[5]. In this paper, efficient DBF techniques for transmitting and receiving are presented. Furthermore, an adaptive array antenna system suitable for this LEO-SAT is presented[6].

SYSTEM CONCEPT AND LINK BUDGET

Table 1 outlines the system. The transmission quality of each link is expressed in terms of the bit error rate.

193

When the satellite altitude is 765 km and the minimum elevation angle is 30 degrees, the number of satellites in this system is 200, because 10 orbital planes are required to cover the entire earth. In this system, it is assumed that the aperture diameter of the mobile antenna is 50 mm and the transmission power of the mobile antenna is 1W for both L-band and Ka-band system.

Table 2 and Table 3 show the results of link budget calculations. In the calculations, the QPSK modulation scheme where BT=1.0 and half-rate punctured coding/Viterbi decoding FEC whose constraint length is 7 are assumed. As for the transmission quality, a bit error rate (BER) of better than 1×10^{-7} and the average annual time of 1% are also assumed. In this calculation, the user terminal antenna size for L-band and Ka-band links are set 50 mm.

SATELLITE ANTENNAS

L-band Multibeam Antenna

In our proposed system[4], a fixed L-band (1.6/1.5 GHz) multibeam is used to offer N-ISDN (64kbit/s) service to the mobile terminals in the entire area covered by a LEO-SAT. Two types of active array antennas are proposed for this system.

A. Low sidelobe multiple planar-array antennas

First, low sidelobe multiple planar-array antennas are presented. The antenna system is composed of 5 planar-array antennas with different broadside directions. One is a circular aperture array antenna, and the others are rectangular aperture array antennas. The constitution of them are presented in Fig.1 and Fig.2. This antenna system radiates 37 beams. In this system, the number of users is assumed to be 185. The beam coverages of each array antenna are shown in Fig.3. Because this multibeam antenna radiates low sidelobe pattern, then frequency is reusable. When the isolation level is above 30dB, the relation between allocated frequencies and beams is shown in Fig.4. In this system, 13 frequencies are needed.

B. Small size conformal-array antenna

In this LEO-SAT system, some tens satellites are needed. As the antenna size must be as small as possible, so a small size conformal-array antenna is proposed. Fig.5 shows the constitution of the conformal-array antenna fit into this LEO-SAT system. In this system, the number of users is assumed to be 9. The beam coverages of this conformal-array antenna are presented in Fig.6. The weight of this conformal-array is about 30% of the low sidelobe planar-array antenna. But the more frequencies are needed in this antenna than the low sidelobe planar-array antenna.

Ka-band Antenna

For a high bit rate users, the Ka-band(30.0/20.0 GHz) beams are used. In the present technology, due to the limitation of power consumptions and the efficiency of the high power amplifier or low noise amplifier, the expected maximum bit-rate of Ka-band is 15.5 Mbit/s. For this frequency

band, a reflector antenna is proposed. The antenna configuration is presented in Fig.7.

The antennas mounted on the satellite is shown in Fig.8.

FUTURE MOBILE ANTENNA

Digital Beam Forming Technique

For a future mobile antenna technology, we show the digital beam forming (DBF) techniques[5]. The DBF can be applied to both L-band and Ka-band system. In this paper, the L-band DBF system is presented.

The basic block diagram of a digital beamformer for transmitting is shown in Fig.9, where digital PSK modulation is assumed. The configuration of the transmitting DBF antenna implemented by using multi-DSPs is shown in Fig.10.

The block diagram of a digital beamformer for receiving is shown in Fig.11, where digital PSK demodulation is assumed. The configuration of the receiving DBF antenna implemented by using multi-DSPs is shown in Fig.12.

Adaptive array antenna system

In a LEO-SAT system, the main beam should be directed to the direction of desired signal and nulls should be formed in the direction of interference signals. Then, the adaptive array antenna is useful as the mobile antenna. We propose a beam space CMA (BSCMA) adaptive array antenna. The constitution of the BSCMA is shown in Fig.13. In the BSCMA adaptive array, first, multiple

beams are formed in the multibeam former, then the beams with receiving signals over a sufficient power are selected. The weights for these selected beams are optimized in an adaptive loop. The BSCMA is useful for a mobile satellite communication array antenna that consists of more than ten element antennas, because the number of interferences that need to be considered is smaller than the number of elements.

CONCLUSION

We have calculated the transmission parameters for mobile/satellite links in a mobile satellite communication system that offers not only narrow band service but also broad band service to users. Then, we have shown two types of satellite on-board phased array antennas for L-band fixed multibeam and we have also mentioned a reflector antenna for Ka-band steerable spot beam. Furthermore, we have discussed the digital beam forming and adaptive array for the mobile users antenna.

REFERENCES
[1] R.L.Leopold: "Low-earth-orbit global cellular communications network," Mobile Satellite Communication System Conference, Adelaide, Australlia, Aug.1990.
[2] R.A.Summers and R.J.Lepkowski: "ARIES: global communication through a constellation of low earth orbit satellites," Collection of Tech. Papers, AIAA 14th Int. Com. Sat. Sys. Conf, pp.628-638, Mar. 1992.
[3] D. Castiel: "The ellipso system: elliptical low orbits for mobile communications and other optimum system elements," Collection of Tech.

Papers, AIAA 14th Int. Com. Sat. Sys. Conf, pp.642-649, Mar. 1992.

[4] M.Fujise, M.Nohara, K.Uehara and W.Chujo: "Broadband mobile satellite communication system by LEO-SATs and optical ISLs," GLOBECOM'92, Conference record Vol.1, pp437-442, Orlando, 1992.

[5] Y.Ohtaki, W.Chujo, K.Uehara and M.Fujise: "Implementation of a digital beamforming antenna for mobile satellite communications utilizing multi-digital signal processors," International Symposium Antennas and Propagation, Sappro, Japan, Sept 1992.

[6] I.Chiba, W.Chujo and M.Fujise: "Beam Space Constant Modulus Algorithm Adaptive Array Antennas," to be presented at ICAP'1993.

Table 1 Features of the LEO-SAT system

Service Capability	Low-rate Channel (~64kbit/s) High-rate Channel (~15Mbit/s) Demand Assignment
Transmission Quality (BER)	1 x 10-7 (99% of the Year)
Minimum Elevation Angle	30°
User Type Small-class Large-class	Car, Boat, Handheld Terminal, etc. Bus, Large Ship, Airplane, etc.
Satellite Orbit	Low Earth Orbit (765km in Height)
Number of Satellites	20/Orbit Plane x 10 Orbital Planes
Link Configurations -Mobile/Satellite Low-rate Channel High-rate Channel -Inter-satellite -Feeder Link	L-band Fixed Multi-beam Ka-band Steerable Multi-spot Beam Optical Link TBD

Table 2 Mobile/satellite link budget (uplink)

Frequency	1.64GHz	30.0GHz
Transmission Rate	64kbps	15.0Mbps
Required Eb/No	7.5dB	7.5dB
Uplink C/No	55.6dB-Hz	89.4dB-Hz
EIRP of Mobile Antenna	0.0dBW	20.9dBW
Free-space Path Loss	159.3dB	184.5dB
Rain Degradation	0.0dB	5.3dB
Boltzman Coefficient	-228.6BW/K-Hz	-228.6dBW/K-Hz
Satellite G/T	-13.7dB/K	19.6dB/K

Table 3 Mobile/satellite link budget (downlink)

Frequency	1.54GHz	20.0GHz
Transmission Rate	64kbps	15Mbps
Required Eb/No	7.5dB	7.5dB
Downlink C/No	55.6dB-Hz	89.4dB-Hz
G/T of Mobile Antenna	-26.5 dB/K	-8.5dB/K
Free-space Path Loss	158.7dB	181.0dB
Rain Degradation	0.0dB	2.8dB
Boltzman Coefficient	-228.6dBW/K-Hz	-228.6dBW/K-Hz
Satellite EIRP/ch	12.2dBW	43.0dBW
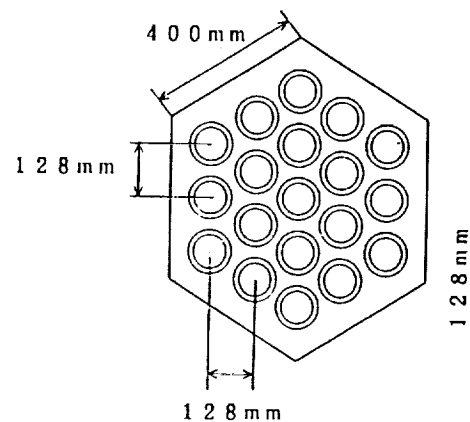
Figure1. Constitution of the low sidelobe planar-array antenna (Circular aperture array).
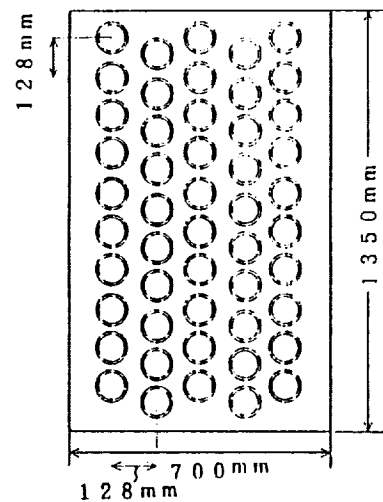
Figure2. Constitution of the low sidelobe planar-array antenna (rectangular aperture array).

196
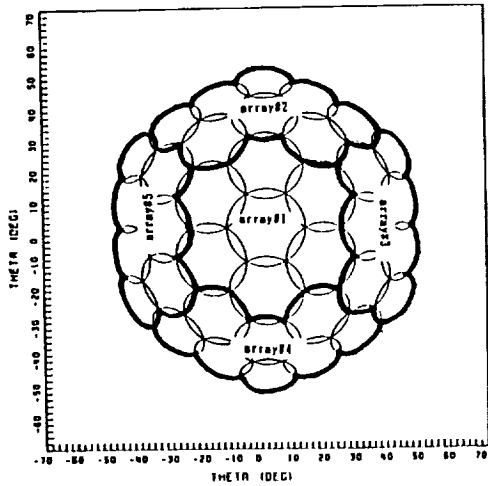
Figure3. Beam coverage of the low
sidelobe planar array antenna.
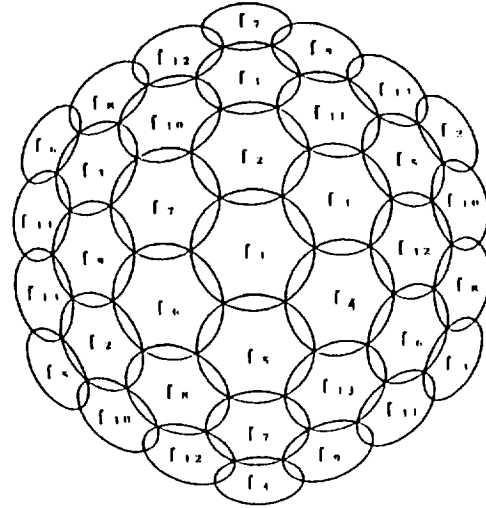
Figure4. The relation between frequencies
and beams.
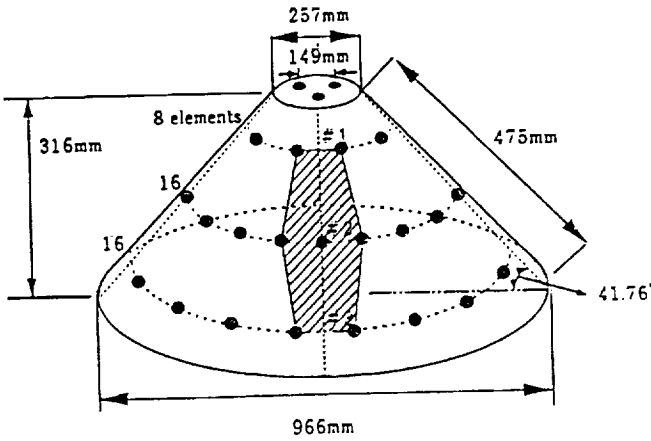
Figure5. Constitution of the small size
conformal array antenna.

Central beam
$\theta = 25.6°$
Gain=8.3dBi

Outer beam
8 beams
$\theta = 50.64°$
Gain=11.7dBi
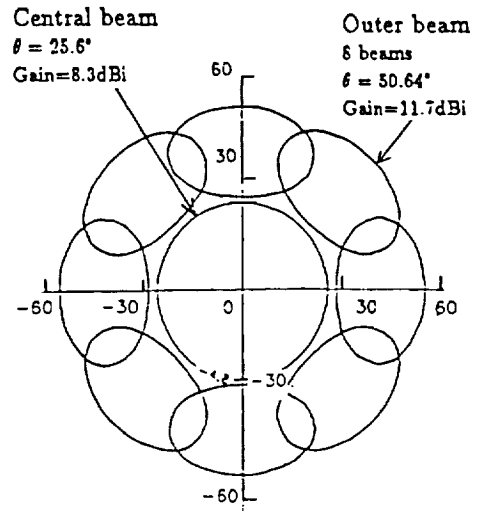
Figure6. Beam coverage of the conformal
array antenna.
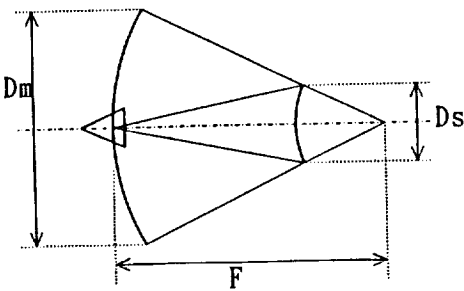
Cassegrain antenna

Dm = 1200 mm
F   = 720 mm
Ds = 288 mm

Figure7. Constitution of the Ka-band
antenna.
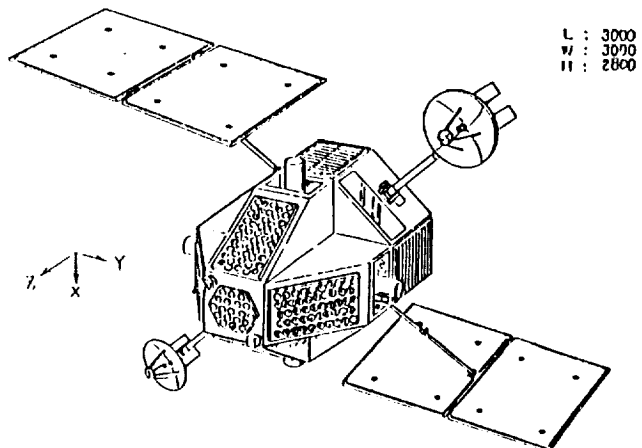
Figure8. Configuration of the antennas
mounted on the LEO-SAT.

197
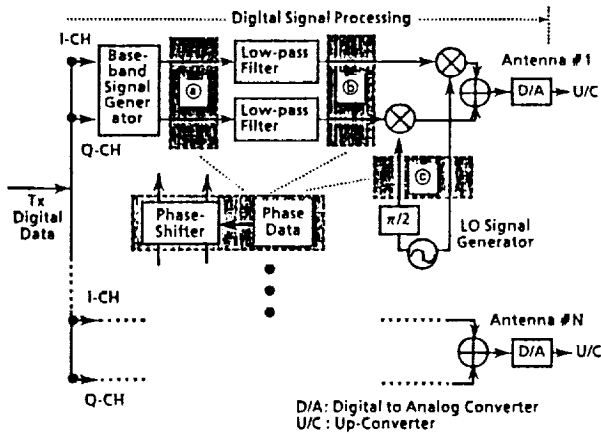
Figure9. Basic block diagram of
a transmitting DBF processor.
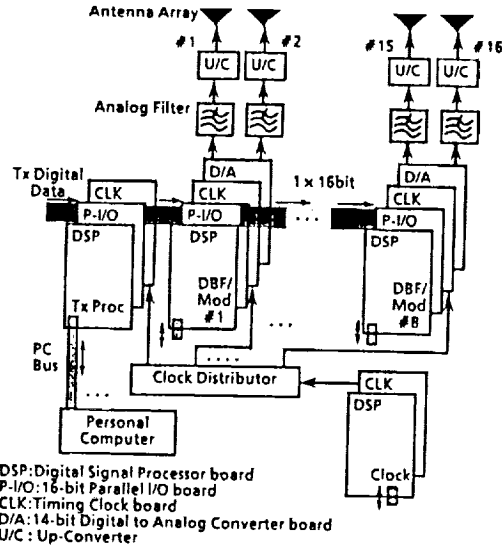
Figure10. Configuration of
a transmitting DBF antenna.
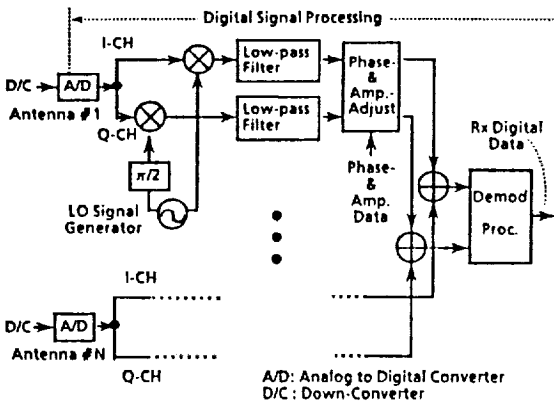
Figure11. Block diagram of
a receiving DBF processor.
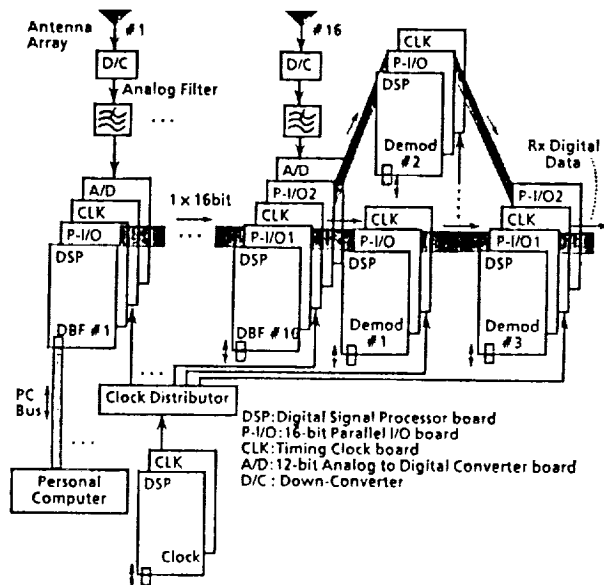
Figure12. Configuration of
a receiving DBF antenna.
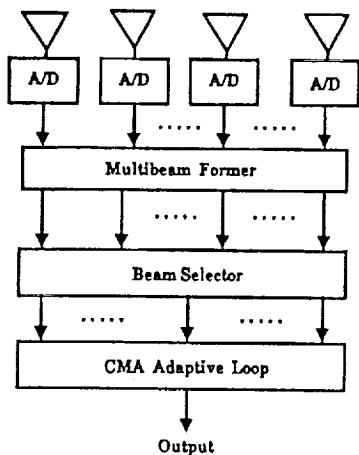
Figure13. Consitution of
the BSCMA.

198

ROCSAT-1 Telecommunication Experiments

J.F. Chang[*] R.R. Taur[†], T.H. Chu, H.S. Li[‡] Y.T. Su[§]
Y.W. Kiang[¶] S.L. Su[||] M.P. Shih, H.D. Lin[**] C.D. Chung[††]

March 8, 1993

Abstract

This paper addresses a telecommunication payload project approved by the R.O.C. NSPO's ROCSAT-1 space program. This project will enable several innovative experiments via the low-earth-orbit satellite ROCSAT-1, including multipath fading channel characterization, ionospheric scintillation measurement, real-time voice communications, and CDMA data communications. A unified L/S-band transponder payload is proposed for conducting these experiments in an efficient way. The results of these experiments would provide the evolving mobile communication communities with fruitful information.

1 Introduction

Due to the increasing demands of universal personal communications services, there has recently emerged the idea of using multiple low-earth-orbiting (LEO) satellites to provide additional mobile voice and data communications services, supplementing the evolving terrestrial mobile communication services. To carry out this idea, several projects, for examples, Iridium, Odysseys, and Globalstar, have been proposed by Motorola, TRW, and Loral ([1], [2]), respectively.

[*] J. F. Chang is with National Central University, Taiwan, R.O.C., Tel # : 011-886-35-4267113, Fax # : 011-886-35-425-4028.

[†] R.T. Taur is with LMSC Co., Inc..

[‡] T.H. Chu and H.S. Li are with National Taiwan University.

[§] Y.T. Su is with National Chiao-Tung University.

[¶] Y.W. Kiang is with National Taiwan University.

[||] S.L. Su is with National Cheng-Kung University.

[**] M.P. Shih and H.D. Lin are with Telecommunication Laboratories, Taiwan, R.O.C..

[††] C.D. Chung is with National Central University.

The operating quality of these proposed communication systems will be the primary subject for communications through highly dynamic environments, precisely the multipath fading channel resulting from the surface scattering effect. Since the relative speed between LEO satellites and ground terminals is extremely high and fast time-varying, a highly nonstationary fading channel that is fairly different from any existing multipath fading channel model, is expected. Due to the unique environment in Taiwan, fade characteristics can be quite different from that of other major cities in the world (for example, Chicago).

Recently, a long range space program, proposed by the National Space Program Office (NSPO) of the Republic of China (R.O.C.), has been approved by the Executive Yuan of the R.O.C. government. Within the program, the NSPO schedules to launch in 1997 her first (low-earth-orbiting) satellite, ROCSAT-1, with a designed life of about four years to perform several science and telecommunications experiments. A mixture of circular and elliptic orbits at 35° inclination have been suggested to accomplish the mission. On board ROCSAT-1, a telecommunication payload has been allocated to perform several ROCSAT-1 Telecommunication Experiments ([3], [4]). The major intent of this telecommunication payload is to evaluate the aforementioned cellular LEO satellite projects and to acquire adequate channel characteristic information for a better system design in Taiwan. Toward these ends, we have proposed four experiments, namely Fading Channel Characterization, Ionospheric Scintillation Measurement, Real-Time Voice Communications, and CDMA Data Communications. The purposes of the proposed experiments are:

1. To characterize the multipath fading chan-

nels of the L- and S- band LEO-satellite-based cellular voice and data communication systems. The fade characteristics may be unique for various specific environments in Taiwan.

2. To measure the L- and S- band ionospheric scintillation in Taiwan area simultaneously, and to further define the density and size distributions of the irregularities that are responsible for the scintillation.

3. To evaluate the end-to-end LEO personal CDMA space communication system performance by measuring the bit error rate (BER) and voice quality. Various vocoder techniques and rates will be employed for the experiments. Compatibility with terrestrial cellular CDMA systems will also be evaluated.

4. To perform the LEO CDMA space telecommunication using on-board store and forward processor. Global data collection, paging, and message broadcasting experiments will be conducted.

This payload project is currently under feasibility study. We shall give more details on the proposed experiments and the conceptual design of the proposed payload in what follow.

2 Experiment Description

2.1 Fading Channel Characterization

The measurement system is based on a spread spectrum communication technique. The approach is to transmit pseudo-noise (PN) sequence modulated S- and L- band carriers from a LEO satellite and observe channels' complex impulse response by despreading the received signals with a local PN replica. Basically, this system follows the approach proposed by [5] for cellular land mobile channel measurement. The high dynamics LEO environment, however, calls for extra efforts to remove the Doppler frequency and differential Doppler that are embedded in the received signal but undesirable to the channel characterization. For this reason a dual-channel architecture (synchronous and measurement channels)

for the ground measurement system is necessitated. The synchronous channel receives downlink beacon signal by use of a L-band tracking antenna with 26 dBi gain. It is responsible for tracking the variations of those variables induced by the satellite orbit dynamic (i.e., Doppler, differential Doppler, jerk, code Doppler) and acquiring the transmitted test signal (i.e., carrier frequency and PN code phase). This information is needed so that the "clean" channel responses free of orbit dynamic effects at desired delays can be obtained at the measurement channel.

Experiments will be conducted for various ground environment modes, including (1) suburban and rural, (2) vegetation, (3) marine, (4) hilly, and (5) metropolitan. These selected environments contain both typical mobile communication environments and special geographic features and terrains in Taiwan. The PN code rate will be 10 Mcps which yields a multipath resolution of 100 ns. For a code length of 8191 chips, the duration of the measured delay profiles is equal to 0.8191 ms. Table 1 gives the S-band power budget for the multipath resolution, in which the fade margin is fixed at least 15 dB. The EIRP at 10 degree elevation angle on the ground is 10 dBW for both S- and L- band measurement signals. The expected outputs of the whole experiment will include (i) an exhaustive collection of power delay profiles as well as delay Doppler power profiles for typical geographical features and terrains, (ii) the corresponding statistical description of path delays, amplitudes, and phases for all the significant paths, and (iii) relevant statistical quantities, such as rms delay and Doppler spreads, -3 dB and -7 dB profile widths, etc.. The outputs will provide communication system engineers with a thorough statistical description of a typical mobile LEO-satellite multipath channel.

2.2 Ionospheric Scintillation Measurement

Taiwan is in the equatorial anomaly crest region where the ionosphere quite often exhibits rather irregular behavior and GHz scintillation has been observed. Since the LEO satellite can scan a large area of about several thousands of kilometers wide and provide more spatial information than the geostationary satellite, our experiment is meaningful and will contribute significantly to the global morphology of ionospheric

scintillations.

L- and S- band beacon signals with EIRP of 3 dBW at EOL will be transmitted downlink simultaneously. Both amplitudes and phases will be sampled with a rate of 1000 samples/second, and recorded at the receiver. This is accomplished by using the S-band beacon as a reference to calibrate the phase of the L-band beacon. In order to maximize the link availability, circular polarization with axial rate lower than 5 dB is utilized. Dynamic range for amplitude is 16 dB with a resolution of 0.5 dB. The resolution for phase measurement is 5°. With the recorded data, we shall obtain useful physical quantities, such as correlation at the different frequencies, time instants, and positions, scintillation index, frequency power spectra for the log-amplitude and the phase, etc.. By using the Rytov solution of scintillation theory, several physical parameters of the ionospheric irregularities, such as turbulence strength, spectral index, etc., can then be derived. These results will be of much importance in understanding the structure and dynamics of the F-region nighttime irregularities. Moreover, they can also be correlatively compared with the VHF radar data, the total electron content data, in-situ measurements on board ROCSAT-1, and the spread-F data, to give us a deeper understanding of the ionosphere in Taiwan area.

2.3 Real-Time Voice Communications

The experiment system consists of a L-band transmitter, bentpipe transponder, and S-band receiver (as shown in Fig. 1). The programmable data pattern is used for BER measurement and error statistics analysis, while the voice input is also allowed for demonstration and evaluation of voice quality. Both standard and improved CELP (Code Exited Linear Predict Code) techniques at data rates of 9600, 4800, and 2400 bps are adopted in vocoder realization. A (2,1,7) convolutional code and corresponding soft-decision Viterbi decoder are employed for a 5 dB of BER improvement. The encoded symbol rate is fixed by 19.2 Kbps; henceforth, repetition codes of different code rates are employed prior to convolutional encoding. To reduce burst error effect, a block interleaver is used to span the encoded sequence over 30 ms. The interleaved sequence is then modulated by the DS/BPSK modulator. The PN period is programmable (rang-

ing from R6 to R13) at two chip rates 1.23 and 4.92 Mcps for evaluation of the underlined multipath fading effect. In order to resolve severe Doppler effects due to ROCSAT-1 motion, a pre-compensation/post-correction approach is adopted, which requires a tracking antenna of gain 26 dB at the receiver. The power budget for this experiment is given in Table 2. It is shown that 13 dBW of transmission power is needed to maintain a BER of 10^{-4}.

2.4 CDMA Data Communications

Three sub-experiments will be conducted, namely global data collection, global paging, and store-and-forward message transmission. CDMA scheme will be adopted as the access scheme.

The data collection experiment consists of a small number (8 to 12) of transmit only remote terminals and a receive only Hub terminal, for the collection of meteorological, oceanographic, hydrological, flood control, and seismic data. Though the basic packet data rate of 4.8 Kbps is assumed and the sampling rate will be no more than 20 Hz, a wide range of channel, data formatting and burst architecture, burst ranges, and access techniques will be possible for testing.

The global paging is a receive only experiment. It is intended to answer several important unsolved issues for future satellite handheld personal communications, such as phase noise effects, polarization effects, polarization or antenna diversity (inside buildings), interleaving, and FEC coding for low bit-rate transmission and reception. Since the paging signal is expected to be low bit rate to provide additional link margin for building penetration, this experiment will use S band small antenna to verify the reception phenomena at various floor levels and depths within a building, inside a moving vehicle, with the receiver carried on the person or inside a briefcase.

Since a LEO satellite is in a view for only a few minutes, store-and-forward message transmission will exercise an important feature for LEO satellite commuincations. A remote terminal may send a non-real-time message to the satellite stored and re-transmitted when the satellite passing through the receiving terminal. CDMA technology will be used for message transmission and acquisition. The proposed store-and-forward message experiment will be used to evaluate the feasibility and integrity of such a communication

system. Statistics on the message integrity, in terms of bit error rate, packet error rate and miss and false acquisition probabilities, will be obtained for various reception conditions.

3 Payload Description

A unified L/S-band transponder payload with components that have been flown on other satellite programs or are available in flight qualifiable form is proposed for this project. This payload consists of L/S-band antennas, an L/S-band bentpipe transponder, an L-band transmitter, and a baseband store-and-forward CDMA processor. Since ROCSAT-1 is a 1000 lbs class satellite with only about 400 W of total electrical power available for six different payloads, this payload will utilize a compact L- to S- band transponder with about 43 W of DC power consumption within Taiwan area, and about 8 kg of weight. The nominal DC voltage from satellite bus is 28 V. In order to minimize payload weight and power, mechanical tracking antenna is not recommended. Shaped antenna pattern to compensate for the free path loss difference within the coverage area is used instead. The spacecraft antenna will have beamwidth of about 120°.

The proposed payload is a space-qualified solid-state transmitter/receiver with L-band uplink and L- and S- band downlink, whose conceptual design is illustrated in Fig. 2. This payload is designed to provide the flexibility of dual mode operation at L- and S- bands. In one mode, the bypass switches may be exercised to make the payload as a transponder for transmission of real-time voice. In the other mode, it serves as either a store-and-forward CDMA regenerative transponder or a PN sequence transmitter. In both modes, the L- and S- band coherent beacon signals are always transmitted for scintillation measurement experiment. The payload is operated by an onboard computer unit interfaced to the satellite command and data handling subsystem, which also records the payload housekeeping data.

4 Conclusion

A L/S-band transponder payload has been proposed for the R.O.C. NSPO's ROCSAT-1 program, and will enable the following innovative experiments via the LEO satellite:

- Multipath fading channel characterization

- Ionospheric scintillation measurement

- Real-time voice communications

- CDMA data communications (store-and-forward message transmission, global data collection, and global paging)

These proposed experiments would promote a broad based participations by the scientific and technical communities as well as local industries in the R.O.C.. They would also stimulate and enhance the earth terminal technology readiness in Taiwan for competition in the emerging market place of digital wireless and personal communications. In particular, the measured LEO multipath fading channel characteristic and evaluation of the LEO personal CDMA space systems would provide the evolving mobile communication communities with fruitful information.

References

[1] Global Personal Communications Satellite Services, Motorola Inc. and Lockheed Missiles and Space Company, Nov. 1991.

[2] P.A. Monte and M. Louie, "GLOBALSTAR: A new mobile communications system" NASA publication No. 3132, pp. 1-9, Nov. 12-14, 1991.

[3] "Communications and Scintillation Experiments," NSPO ROCSAT-1 payload proposed by National Taiwan University and Lockheed Missiles and Space Company, July 1992.

[4] "L/S-Band Personal Communications Payload," NSPO ROCSAT-1 payload proposed by Telecommunication Laboratories and COMSAT Laboratories.

[5] D.C. Cox, "Delay-Doppler characteristics of multipath propagation at 910 MHz in a suburban mobile radio environment," *IEEE Trans. Antennas Propagat.*, vol. AP-20, pp. 625-635, Sept. 1972.

```
            (S-band, EOL budget)                    NOMINAL  TOL +/-
            ===============================
    * 1  PAYLOAD SGL EIRP, DBW (5W, 3dB)              10.00    0.00
    * 2  POINTING LOSS, DB                             0.00
    * 3  PATH LOSS, DB                               166.42
         3a  RANGE, KM                              2000.00
         3b  FREQUENCY, GHZ                             2.50
      4  ATMOSPHERIC LOSS, DB                          0.50
      5  POLARIZATION LOSS, DB                         1.00
      6  RAIN ATTENUATION, DB                          0.00
    * 7  SCINTILLATION LOSS, DB                        0.00
      8  SGL RECEIVED POWER, DBWI                   -157.92
    ............................................................
    * 9  RECEIVER G/T, DB/K (0dB, 200K, omni)        -23.01    0.00
     10  UNBUDGETED RECEIVE LOSS, DB                   0.00
     11  BOLTZMANN'S CONSTANT, DBW/HZ-k             -228.60
     12  SGL P/No, DB-HZ                              47.67
     13  PAYLOAD RETURN BANDWIDTH, MHZ               10.00
     14  REFERENCE BANDWIDTH, DB-HZ                  70.00
    *15  SIGNAL SUPPRESSION, DB                        0.00
     16  SGL P/N (TOTAL), DB                         -22.33    0.00
    ............................................................
     17  C/N AT GROUND, DB                           -22.33
     18  C/No AT GROUND, DB-HZ                        47.67
    *19  TDL DWELL TIME, DB [(2**13 -1)*Tc]          -30.87
     20  MATCHED FILTER OUTPUT C/N, DB               16.80    0.00
    ............................................................
     21  REQUIRED C/N, DB                            15.00
    *22  IMPLEMENTATION LOSS, DB                       2.00
    *23  OTHER SYSTEM LOSSES, DB                       0.00
     24  TOTAL REQUIRED C/N, DB                      17.00
     25  MARGIN AGAINST REQUIREMENT, DB              -0.20
     26  MARGIN TOLERANCE, +,-                       -0.20
```

Table 1. Power budget for channel characterization experiment.

```
                          UP-LINK
    ========================================================
            Transmit Power (20 W)              13 dBW
                    Antenna Gain                0 dB
                           EIRP                13 dBW
                          Range             2000 Km
                      Frequency              1.6 GHz
               Free Space Loss             -162.5 dB
          Atmospheric Attenuation            -0.5 dB
            Total Propagation Loss          -163.0 dB
          Receiver's Antenna Gain              3 dBi
               Polarization Loss             -1 dB
                        RF Loss              -1 dB
            Received Carrier Power          -149 dB
      Receiver's Noise Temp (400 K)          26 dBK
                Noise Density (No)         -202.6 dB
                    Received C/No            53.6 dB
                Bandwidth (5 MHz)             67 dB
                    Received C/N            -13.4 dB
    ========================================================

                         DOWN-LINK
    ========================================================
      Transmit Power (0.1 W, Signal only)    -10 dBW
      *** Assume 5W full power output ***
                    Antenna Gain              3 dBi
                           EIRP              -7 dBW
                          Range             2000 Km
                      Frequency              2.5 GHz
               Free Space Loss             -166.4 dB
          Atmospheric Attenuation            -0.5 dB
            Total Propagation Loss          -166.9 dB
     Receiver's Antenna Gain (1m dish)        26 dBi
               Polarization Loss             -1 dB
                        RF Loss              -1 dB
            Received Carrier Power         -149.9 dB
      Receiver's Noise Temp (100 K)          20 dBK
                Noise Density (No)         -208.6 dB
            Received C/No (Downlink)         58.7 dB
    ------------------------------------------------------
     Total received C/No (uplink + downlink)  52.4 dB
                    Data rate (9.6K)          40 dB
                   Receiver's Eb/No          12.4 dB
              Required Eb/No (10E-4)          8.5 dB
                      Coding Gain             5 dB
                  Implementation loss         2 dB
                          Margin             6.9 dB
    ========================================================
```

Table 2. Power budget for real-time voice communications.
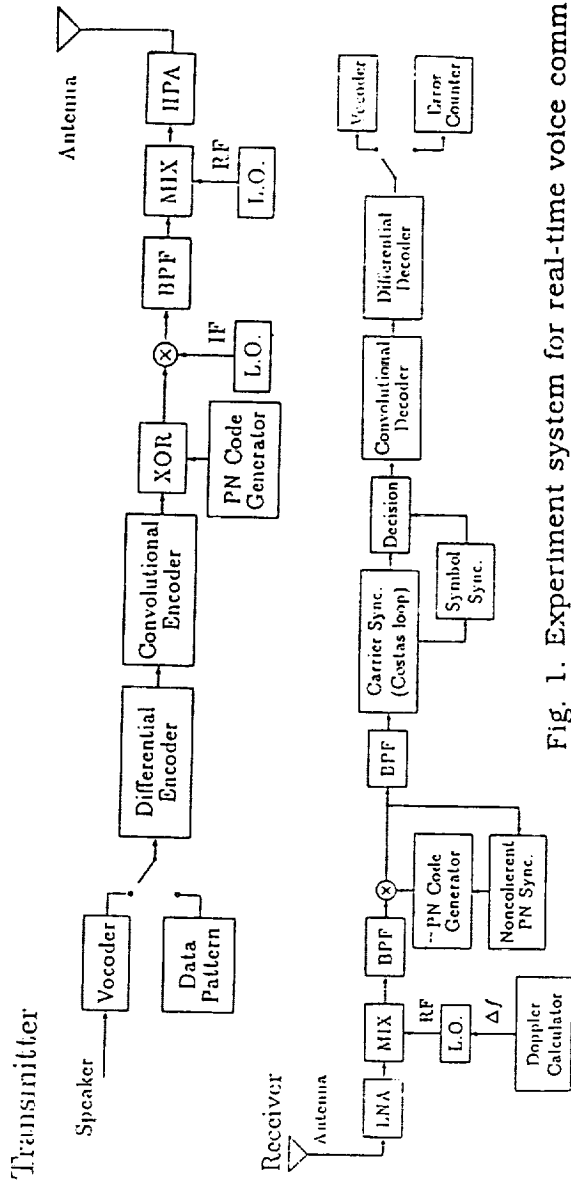
Fig. 1. Experiment system for real-time voice communications.
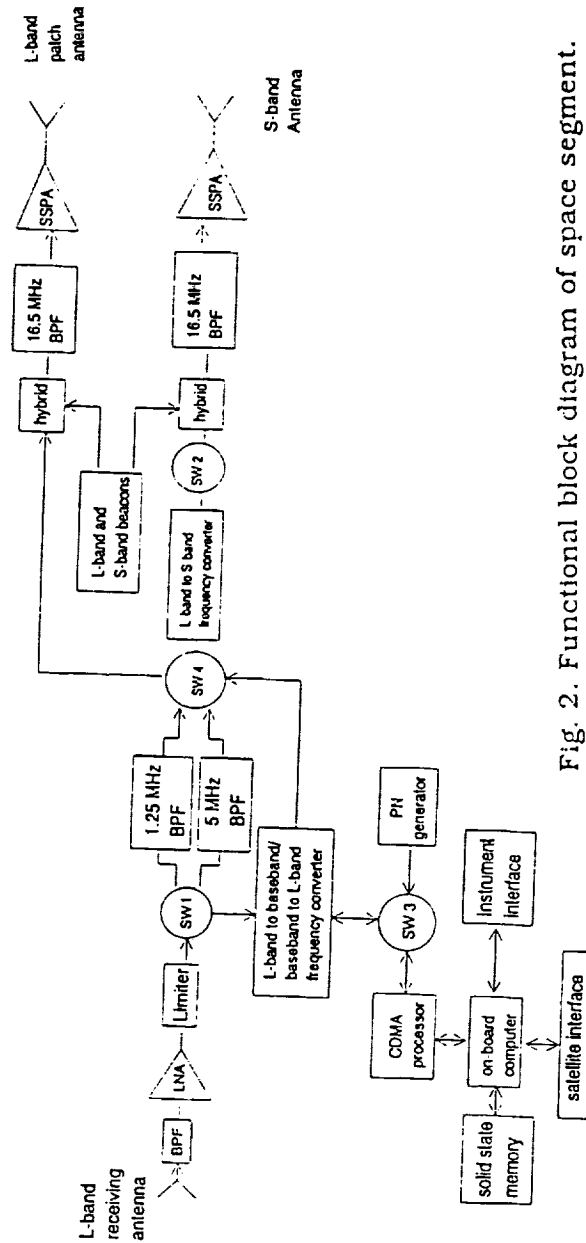
Fig. 2. Functional block diagram of space segment.

204

ACTS BROADBAND AERONAUTICAL EXPERIMENT

Brian S. Abbe, Thomas C. Jedrey, Dr. Polly Estabrook, Martin J. Agan
Jet Propulsion Laboratory
California Institute of Technology
M.S. 238-420
4800 Oak Grove Drive
Pasadena, California 91109
Phone: (818) 354-3887 FAX: (818) 354-6825

ABSTRACT

In the last decade, the demand for reliable data, voice, and video satellite communication links between aircraft and ground to improve air traffic control, airline management, and to meet the growing demand for passenger communications has increased significantly. It is expected that in the near future, the spectrum required for aeronautical communication services will grow significantly beyond that currently available at L-band. In anticipation of this, JPL is developing an experimental broadband aeronautical satellite communications system that will utilize NASA's Advanced Communications Technology Satellite (ACTS) as a satellite of opportunity and the technology developed under JPL's ACTS Mobile Terminal (AMT) Task to evaluate the feasibility of using K/Ka-band for these applications. The application of K/Ka-band for aeronautical satellite communications at cruise altitudes is particularly promising for several reasons: (1) the minimal amount of signal attenuation due to rain; (2) the reduced drag due to the smaller K/Ka-band antennas (as compared to the current L-band systems); and (3) the large amount of available bandwidth. The increased bandwidth available at these frequencies is expected to lead to significantly improved passenger communications - including full-duplex compressed video and multiple channel voice. A description of the proposed broadband experimental system will be presented including: (1) applications of K/Ka-band aeronautical satellite technology to U.S. industry; (2) the experiment objectives; (3) the experiment set-up; (4) experimental equipment description; and (5) industrial participation in the experiment and the benefits.

APPLICATIONS

There is presently a demand for high quality, reliable, voice and data satellite communication links between aircraft and ground to improve air traffic management services and to meet the growing demand for passenger communication services. The former are of importance as they should result in increased passenger and crew safety and should reduce flight time and operational costs by optimizing the aircraft's flight path. The latter are likely to be of concern to the airline companies in order to maintain customer satisfaction and allegiance.

Since 1991, Inmarsat has provided a single channel packet data link at 600 bps, nominally, and a single channel voice, data, or FAX link at 9.6 kbps using several antenna designs. Both channels are established at L-band using Inmarsat I and II satellites. The American Mobile Satellite Corporation (AMSC) will also be providing these services as well. Furthermore, both Inmarsat and AMSC have recently begun offering or plan to offer multiple voice and data channel services.

As these systems become implemented and more widely used at L-band, and the benefits provided by their operation are realized, it is likely that the communication role envisaged for aeronautical satellite communications will grow. Concepts such as providing passengers with an "office in the sky," e.g., voice, data, FAX, and compressed video teleconferencing, or real-time news and sports broadcast will expand. Air crew services such as real-time transmission of weather maps or compressed video transmission from the cockpit or cabin for security may become attainable. Additional demand for the planned telecommunication services mentioned above as well as for these new services will motivate a need for more spectrum than is likely to be available at L-band. The application of K/Ka-band for aeronautical satellite communications could be used to enhance the mobile satellite capabilities at L-band as these demands increase [1].

In addition to these commercially oriented needs, recent events in the Middle East (Persian Gulf War) and other potential hotspots around the world have suggested that the development of this type of technology would be extremely beneficial to our nation's military efforts. For these needs, the emphasis would be on providing compressed video imaging from an aircraft back to a fixed terminal, as opposed to the commercial emphasis of a broadcast application (compressed video imaging from a fixed terminal to the aircraft).

EXPERIMENT CONFIGURATION

The ACTS Broadband Aeronautical Experiment has been designed to not only prove the feasibility of K/Ka-band aeronautical mobile satellite communications, but to design the overall system in a manner that would allow for easy technology transfer to U.S. industry. The aeronautical system configuration consists of a fixed (ground-based) terminal, ACTS, and an aircraft terminal as shown in Figure 1. The fixed terminal consists of a communications terminal mated to the High Burst Rate Link Evaluation Terminal (HBR-LET) RF hardware including the 4.7 m antenna. The aircraft terminal's architecture will be similar to that of the ACTS Mobile Terminal [2]. In the forward direction (fixed station-to-aircraft) the fixed terminal will transmit a data and a pilot signal to ACTS. ACTS will then transmit these signals to the aircraft terminal while operating in the Microwave Switch Matrix (MSM) mode of operation (a bent pipe mode). The signal in the forward link will be at a maximum data rate of 384 kbps. On the return link (aircraft-to-fixed station) the signal transmitted from the aircraft terminal will consist of a data signal with a maximum data rate of 112 kbps.

Two transponders will be utilized on ACTS for this experiment. One transponder will be used to support the fixed station-to-aircraft forward link signals and the other the aircraft-to-fixed station return link. The first transponder will be configured with the 30 GHz Cleveland fixed beam for the uplink and a 20 GHz spot or steerable beam for the downlink to the aircraft. The second transponder will be configured with a 30 GHz spot or steerable beam for the uplink and the 20 GHz Cleveland fixed beam for the downlink.

EXPERIMENT OBJECTIVES

The primary objectives for the ACTS Broadband Aeronautical Experiment are to:

(1) Characterize and demonstrate the performance of the aircraft/ACTS/AMT K/Ka-band communications link for high data rate aeronautical applications. This includes the characterization of full-duplex compressed video, and multiple channel voice and data links.

(2) Evaluate and assess the performance of current video compression algorithms in an aeronautical satellite communications link.

(3) Characterize the propagation effects of the K/Ka-band channel for aeronautical communications during take-off, cruise, and landing phases of aircraft flight.

(4) Evaluate and analyze aeronautical satellite communication system concepts common to both L-band and K/Ka-band communication systems.

(5) Provide the systems groundwork for an eventual commercial K/Ka-band aeronautical satellite communication system.

The experimental system performance will be evaluated both quantitatively and qualitatively. Qualitatively, the principal criterion will be the ability to maintain a full-duplex video, or multiple channel voice or data link while the aircraft is in the cruise phase of flight, as well as during take-off and landing. Quantitatively, the link performance is a direct function of the bit error rate (BER). The BER in turn is a function of the received signal to noise ratio and its stability, frequency offsets including Doppler and Doppler rate, and other effects on the link such as phase noise, aircraft shadowing, and possibly multipath. The quantitative evaluation of system performance will therefore be presented in terms of two criteria: (1) the ability to maintain a minimum given received signal level, which is dependent on the performance of the aircraft antenna system in the aeronautical environment as well as the scanning (or steerable) beam characteristics of ACTS, and (2) the BER performance versus received bit signal energy to noise density ratio, E_b/N_o with the different channel disturbances as parameters. The quantitative assessment will include a comparison between theoretical results (analysis and simulation), laboratory measured results, and experimental results for various channel conditions encountered.

The required BER for video codecs is typically between 10^{-5} and 10^{-6}, higher than is normally required for voice communications (BER of approximately 10^{-3}). When operating at higher BER's, most video codecs will have serious audio distortion and intermittent video "tiling" effects. Therefore, in order to select a suitable video codec, a tradeoff between required BER for distortionless operation and data rate versus the available link margin will be performed. Currently, there are many commercial video compression products available. These products employ a variety of video compression techniques, implemented in a combination of hardware and software. Ideally, several video codecs will be tested in this experiment, as none have been designed for transmission over a channel with time-varying characteristics such as the aeronautical satellite channel.

The aeronautical environment is characterized by: (1) large variations in the elevation angle to the satellite in the aircraft frame of reference; and (2) blockage of the line-of-sight to the satellite by the

aircraft structure. Both effects are due to aircraft banking and changes in attitude angle during flight. An in-depth study of these effects will help in future designs of aeronautical satellite communication systems. Among the system parameters that will be most directly affected by these characterizations are the antenna scanning angle, the antenna beamwidth, and the antenna placement on the aircraft. Measurements will be made to characterize the propagation effects due to clouds, possible aircraft blockage, rain attenuation on both the uplink and the downlink, and other environmental conditions during take-off, cruise, and landing phases of flight. These measurements will be based on various transmitted and received beacon and pilot signals. An attempt will be made to categorize and separate the sources of channel degradation (cloud effects, aircraft obstruction, rain effects, etc.). Cumulative fade distributions will be computed for the different channel conditions encountered, and the associated terminal performance identified.

Several general aeronautical system (common to both L-band and K/Ka-band aeronautical satellite communications systems) concepts will be studied during this experiment including: (1) compressed video transmission and reception techniques; (2) multiple cabin and cockpit channels with call priority assignments; and (3) the aeronautical satellite link connection with the aeronautical telecommunications network. A thorough study of these system parameters will greatly enhance future aeronautical satellite system design and performance. A study of the compressed video transmission and reception techniques will assess the performance of the video compression units over the K/Ka-band mobile satellite communications channel. These units will further be categorized by the subject of the video transmission (Can the video compression unit handle video teleconferencing? How does the unit handle rapid motion?, etc.). Another system concept that will be looked at is the multiple channel system with priority assignment. For this set-up, several data or voice link lines will be established, with the highest priority being given to the aircraft cockpit, and the lesser priority being given to passenger communications. Finally, recommendations for the design of the aeronautical satellite communications equipment will be accomplished in a manner such as to ease the integration of the equipment with the Aeronautical Telecommunications Network (ATN).

From the data collected from this experiment, and the ensuing analysis, recommendations about the design of a practical and cost efficient commercial K/Ka-band aeronautical satellite communications system will be developed. These recommendations will not only include specifications for the aeronautical and ground communications terminal,

but also for the satellite design. Specifications for the performance of the terminal subsystems (e.g., modem and video compression unit) will also be included in the recommendations. Some of the system specifications will include typical Doppler offsets that a commercial system should be expected to handle, typical scanning angles of the antenna subsystem due to the banking motion of the aircraft, as well as the overall performance of the various video compression units in the presence of a K/Ka-band mobile satellite communications channel.

EXPERIMENT EQUIPMENT

The necessary equipment for this experiment includes an aeronautical mobile terminal, a fixed terminal, an aircraft, and ACTS. The aeronautical terminal and fixed terminal architectures are similar to that of the AMT for the land-mobile experiments as described in [3]. There are, however, several distinct differences between the two terminal developments: (1) the development of an aeronautical antenna that can track in elevation, as well as in azimuth; (2) the development of a higher rate modem (up to 384 kbps as opposed to up to 64 kbps) than for the land-mobile experiments; and (3) the use of a (several) video compression unit(s) in addition to a speech codec. A more complete description of this equipment can be found in [2]. A detailed description of ACTS can be found in [4].

LINK BUDGETS

The forward (data only) and return link budgets for the experimental configuration are presented in Table 1. ACTS' west scan sector beam is used to link to the aircraft; the EIRP and G/T of the edge of beam contours are taken to be 59.00 dBW and 15.00 dB/°K, respectively. The accuracy of these values is +/-1.00 dB. ACTS' Cleveland fixed beam is used for communications with the fixed terminal. The EIRP and G/T at the center of the beam are 69.50 dBW and 21.25 dB/°K, respectively. The aeronautical terminal G/T assumed is -5.00 dB/°K. The modulation scheme assumed is BPSK with a rate 1/2, constraint length 7, convolutional code, with soft-decision Viterbi decoding. A BER of 10^{-6} is assumed to be achieved at an E_b/N_o of 4.5 dB. A loss of 3.00 dB due to modem implementation, phase noise, and frequency offset effects are assumed. On the forward link both data and pilot signals (equal power) are transmitted (the link budget is shown strictly for the data channel). The total fixed terminal EIRP is 68.00 dBW. The resulting forward (at 384 kbps) and return link performance margins (at 112 kbps) are 3.29 dB and 2.89 dB, respectively.

EXPERIMENT RESULTS AND BENEFITS

The development and execution of this experiment will be accomplished in conjunction with U.S. industrial participation. A broadband aeronautical working group is being formed to assist with this effort. Members of this working group will come from a wide variety of interests in U.S. industry including: (1) aircraft manufacturers, (2) airline carriers, (3) satellite service providers, (4) aeronautical avionics manufacturers, (5) video compression companies, (6) broadcasters, (7) other government agencies, and (8) government regulators. Input from these groups during the development of the experiment will shape the experiment in a way that will provide for an efficient transfer of the technology and system concepts to a commercial venture. Their input will include: assistance with the experiment conceptual development, equipment development, use and operation of an aircraft, and overall experiment execution. Active participation by U.S. industry in this experiment will help to stimulate the commercialization of this service. It is anticipated that a commercially operated system that would provide compressed video broadcasts for passengers could be in service as early as the turn of the century.

SUMMARY

The ACTS Broadband Aeronautical Experiment will help verify that K/Ka-band mobile satellite technology could be useful in meeting increased demands for aeronautical mobile satellite communication services. The minimal amount of signal attenuation due to rain during the cruise phase of flight, the reduced drag due to the smaller K/Ka-band antennas (as compared to the current L-band systems), and the large amount of available bandwidth make the development of a K/Ka-band aeronautical mobile satellite system a logical choice for such non-critical passenger services as live video broadcasts of news and sports events, voice, FAX, data, etc. and other needs. Planned active industrial participation in this experiment will allow for the conclusions, technology, and system concepts to be easily transferred to U.S. industry to develop a commercial K/Ka-band aeronautical mobile satellite communications system.

REFERENCES

[1]   Nguyen, T., et al., "ACTS Aeronautical Experiments," AIAA Conference 1992, ppg. 1769-1781.

[2]   Abbe, B.S., et al, "ACTS Broadband Aeronautical Experiment," ACTS Conference 1992.

[3]   Agan, M.J., et al., "The ACTS Mobile Terminal: Poised for ACTS Launch," IMSC, June 1993.

[4]   Wright, D. and Balombin, J., "ACTS System Capability and Performance," AIAA Conference 1992, ppg. 1135 - 1145.

K-BAND DATA (19.914 GHz +/- 150 MHz)
AND PILOT (19.914 GHz +/- 150 MHz)

Ka-BAND DATA (29.634
GHz +/- 150 MHz)

ACTS

Ka-BAND DATA (29.634 GHz +/- 150 MHz)
AND PILOT (29.634 GHz +/- 150 MHz)

K-BAND DATA 19.194
GHz +/- 150 MHz)

HBR-LET
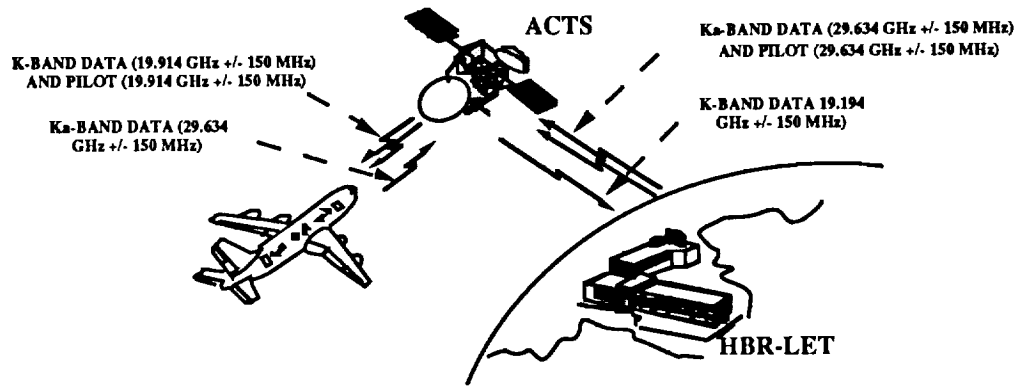
Figure 1 ACTS Broadband Aeronautical Experiment Set-Up

209

Table 1 Broadband Aeronautical Experiment Link Budgets

PARAMETER	FORWARD LINK	RETURN LINK
Transmitter Parameters		
EIRP, dBW	65.000	34.000
Pointing Loss, dB	-0.800	-0.500
Radome Loss, dB	0.000	-0.200
Path Parameters		
Space Loss, dB	-213.480	-213.340
Frequency, GHz	29.634	29.634
Range, km	38000.000	37408.000
Atmospheric Attenuation, dB	-0.360	-0.360
Receiver Parameters		
Polarization Loss, dB	-0.130	-0.850
G/T, dB/K	21.250	15.700
Pointing Loss, dB	-0.220	-0.320
Bandwidth, MHz	900.000	900.000
Received C/N_o, dB-Hz	99.860	62.780
Transponder SNR_{IN}, dB	10.320	-26.770
Effective Hard Limiter Suppression, dB	-5.000	-1.050
Effective Hard Limiter SNR_{OUT}, dB	5.320	-27.820

Transmitter Parameters		
EIRP, dBW	55.200	24.180
Pointing Loss, dB	-0.320	-0.220
Path Parameters		
Space Loss, dB	-209.890	-210.030
Frequency, GHz	19.914	19.914
Range, km	37408.000	38000.000
Atmospheric Attenuation, dB	-0.500	-0.500
Receiver Parameters		
Polarization Loss, dB	-0.850	-0.130
Radome Loss, dB	-0.100	
G/T, dB/K	-5.000	27.000
Pointing Loss, dB	-0.500	-0.500
Downlink C/N_o, dB-Hz	66.640	68.400
Overall C/N_o, dB-Hz	66.640	60.880
Required E_b/N_o (AWGN), dB	4.500	4.500
Modem Implementation Loss, dB	1.000	1.000
Loss Due to Frequency Offsets, dB	1.000	1.000
Required E_b/N_o, dB	6.500	6.500
Loss Due to ACTS Phase Noise, dB	1.000	1.000
Data Rate, kbps	384.00	112.000
Performance Margin, dB	**3.290**	**2.890**

210

Session 6
User Requirements and Applications

Session Chair—*Deanna Robinson*, Pacific Advanced Communications
Consortium, University of Oregon, U.S.A.
Session Organizer—*John Sydor*, Communications Research Centre, Canada

(continued)

211

The FAA Satellite Communications Program

Karen L. Burcham
Federal Aviation Administration
800 Independence Avenue NW, Washington DC 20591
Telephone (202) 267-7676
Fax (202) 267-5793

ABSTRACT

The Federal Aviation Administration is developing satellite communications capabilities to enhance air traffic services, first in oceanic and remote regions, and later for United States domestic services. The program includes four projects which develop technical standards, assure adequate system performance, support implementation, and provide for research and development for selected areas of U.S. domestic satellite communications.

The continuing focus is the application of automated data communications, which is already permitting enhanced and regular position reporting. Voice developments, necessary for non-routine communications, are also included among the necessary activities to improve ATC communications.

OBJECTIVES

The FAA Satellite Communications Program Plan objective is to provide for and facilitate operational use of Aeronautical Mobile Satellite (Route) Service (AMS(R)S) communications, where (R) stands for "Route" denoting the safety service, to meet civil aviation needs in oceanic and offshore areas, and possibly in U.S. domestic airspace as well. The FAA Plan concentrates on implementing the concept developed by the International Civil Aviation Organization's "Future Air Navigation Systems" (FANS) committee during recent years, at first for oceanic regions.

In the interest of improved air traffic management, the Program assists in developing national/international AMS(R)S standards, ensuring adequate system performance, supporting implementation, and providing research and development for U.S. domestic satellite communications. The general connectivity of the system is illustrated in Figure 1.

PROJECT AREA DESCRIPTIONS

There are four defined projects in the FAA Satellite Communications Program. The first three develop satcom capabilities and provide for operations in oceanic and remote regions where the FAA has current responsibility: the first developing data, the second developing voice, and the third supporting operations; and the fourth area will develop selected U.S. domestic applications.

Project 1: Oceanic/Remote Data

The development of satellite data communications for aircraft entails the generation of agreed-upon standards that permit aircraft flightworthiness and operational certification, and bring assured interoperability between aircraft and controllers by means of various service providers.

MOPS

Minimum Operational Performance Standards (MOPS) are developed jointly by the supplier/user industry and the FAA in an AMSS Special Committee (SC-165) provided for by RTCA, Inc. (formerly the Radio Technical Commission on Aeronautics). This independent body reacts to needs to define architectures, standards for signals and interfaces, and recommended tests that will bring uniformity and
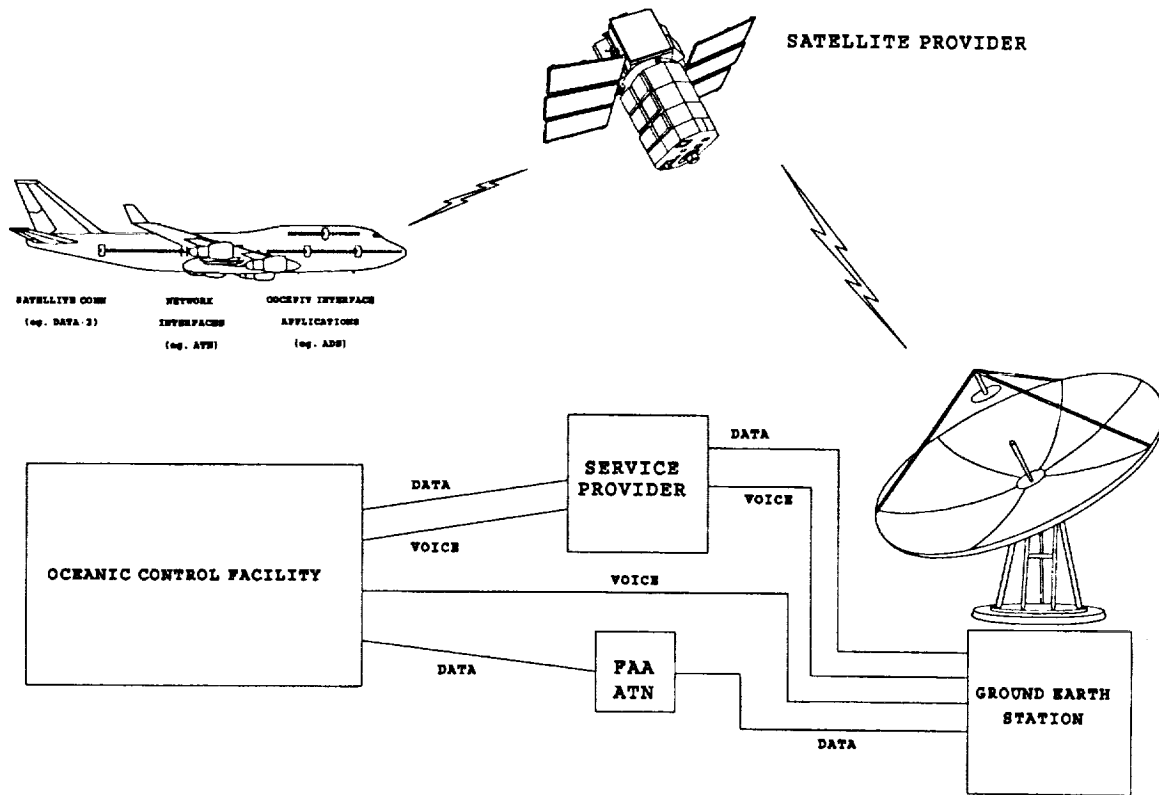
Figure 1. FAA Oceanic Air Traffic Control Operational Concept

interoperability for avionics used in aeronautical safety services.

While the MOPS focuses on describing only the Aeronautical Earth Station (AES) and its air-ground protocols, the committee also has developed a System Guidance document which permits understanding of end-to-end, pilot-to-controller service performance.

While not mandatory, the MOPS serves several purposes. It provides a published guide for manufacturers, operators, and users to implement the AMSS system in a coordinated way. Based on signal-in-space rather than on equipment design, the MOPS gives considerable freedom to design and innovation, while the standardization of signal characteristics provides for competitiveness and coordinated operations.

The MOPS also is a basis for manufacturers' acquisition of an FAA Technical Standards Order (TSO), which constitutes an FAA technical approval for equipment installation. It can assist as a basis for the installing facility's acquisition of Type Certification, which authorizes actual air traffic service applications.

The AMSS MOPS recently has been completed and is available through the RTCA. The next stage--modifications from knowledge gained during manufacturing, installation, and operation--is under way. The next MOPS edition is expected to be available early in 1994. FAA Program Plan support to this effort is focused within the Satellite Communications Program on oceanic and remote regions.

Needs of the Federal Communications Commission (FCC) to assure efficient and effective use of the radio spectrum

214

and non-interference were also supported by SC-165 in developing necessary changes to the Code of Federal Regulations, Part 87.

SARPs

Standards and Recommended Practices (SARPs), developed by member states' Civil Aviation Authorities within the International Civil Aviation Organization (ICAO), ultimately become treaty-level agreements among the member states that assure universal interoperability for international flight safety services. They define generally the AMS(R)S signal-in-space characteristics and protocols necessary for AES operation with its Ground Earth Station (GES).

Since 1989, the FAA has been a principal participant and architect in the development and validation of the AMSS SARPs. Similarly to the MOPS, these standards closely follow the system architecture defined in the Inmarsat System Definition Manual (SDM), but focus on describing signal characteristics rather than the specifics of design.

Under the International Telecommunications Union (ITU) Radio Regulations, the AMS(R)S designation denotes services which are afforded additional protection against interference. Similarly to the need to adapt FCC Rules to properly include aeronautical mobile satellite communications, the SARPs Working Group is supporting the efforts to establish non-interference and other performance standards for mobile satellite communications within the ITU's International Radio Consultative Committee (CCIR).

The AMSS SARPs are in the final stages of completion. They are expected to be validated through tests and modelling presently under way, and are scheduled to be presented to the ICAO Air Navigation Council for approval in mid-1994.

Following a circulation and agreement period to permit member-nation acceptance and aircraft implementations, the SARPs will facilitate worldwide AMSS operations. They should enable the realization of concepts held for many years, wherein air traffic operations would reap the full benefits of the integrity and timeliness of satellite services.

Oceanic Performance Analysis

Simulations are being developed and validated using projected AMSS traffic to ascertain effects on system performance and responsiveness. The outcome should permit estimates of operational capability, and should uncover areas where specific approaches could be implemented to enhance AMSS safety services. When complete in October 1993, the simulation model will be coordinated with developments in the Oceanic Development Facility (discussed below).

Develop SARPs-Compliant Capability

This project activity will acquire an AES and install and test it in an FAA-owned Boeing 727 aircraft at the FAA Technical Center (FAATC) near Atlantic City, NJ.

The AES interface with aircraft avionics, and through the satellite through the GES to end users, will employ the ISO 8208 standard as defined in both MOPS and SARPs. "Data-3," an Inmarsat definition, describes such an AES that can operate within the full Open Systems Interconnect (OSI) protocols. Use of this standardized protocol enables end-to-end interconnectivity advantages of the Aeronautical Telecommunications Network (ATN), now under design.

The principal objective of this project element is to validate the SARPs requirements by demonstrating and testing an in-flight AES using the SARPs-defined, ISO 8208 data protocol as the avionics interface. However,

because no Data-3 or SARPs-compliant AES will be available to meet the ICAO approval schedule, the present AES will be augmented by external software to emulate the additional SARPs-defined capabilities.

The AES installation on the FAA aircraft will then be able to operate as a complete ATN- and SARPs-compliant user terminal. The tests are scheduled for late 1993.

Optimize for Periodic Reporting

In the late '80s, ICAO Future Air Navigation Systems (FANS) study reports defined the need for an integrated Communications, Navigation, and Surveillance (CNS) capability to enhance safety services using satellites.

Within this capability is the requirement for periodic position reporting to controllers using aircraft-derived information, called Automatic Dependent Surveillance (ADS). Over oceanic and remote areas where conventional communications means are unreliable, satellite communications can be used instead for this purpose.

The use of existing signal architectures for regularly-spaced, short data messages is inefficient. Over the past few years, several schemes have been proposed for more efficient use of the communications channel to improve spectrum effectiveness and reporting timeliness.

Presently, simulations are being developed; and now, proceeding in coordination with Inmarsat, the completion of new reporting protocols for inclusion in the SARPs and implementations is scheduled for September 1993.

In its ultimate form, the Global Navigation Satellite System (GNSS), which will include both the US Global Positioning System (GPS) and the CIS Global Orbital Navigation Satellite System (GLONASS), will supply aircraft position information that is relayed from the aircraft through AMSS satellites, and through the ground network to air traffic controllers.

Equip FAA Aircraft for Trials

Development of worldwide standards for safety services expected to be useful for decades requires thorough testing in order to be assured that the requirements are correct, thorough, and unambiguous. The FAATC Boeing 727, now equipped for tests using a low-gain antenna and an early AES, will have installed a high-gain antenna and other capabilities to provide an effective AMS(R)S testbed.

A direct interface from the Comsat earth station at Southbury, CT, to the FAATC will be in operation to permit the real-time interaction necessary for these tests.

Project 2: Oceanic/Remote Voice

While ordinary and routine information is transmitted by voice in today's aeronautical communications, the use of data message services is becoming more pervasive. Although this trend will continue for AMS(R)S routine services, voice communications will still be very important. There are non-routine and emergency situations when controller and aircraft crew need direct and rapid access. The FAA is now developing a policy that will clarify the user selection of data or voice transmissions under various circumstances.

The Program Plan focus in this project area is on development of satellite voice capability for oceanic and remote regions. Aircraft that are fitted for AMS(R)S voice will enjoy the benefits of greatly improved reliability and connectivity with controllers anywhere in the satellite coverage areas.

Three activities are relevant, as follows.

216

Revise MOPS for Voice

The current MOPS (RTCA/DO-210) covers very minimally the voice circuit-mode services, relying on the Inmarsat SDM to support call setup and release definition of protocols and interfaces. The specific standards for these are now under accelerated development in SC-165, with the goal for completion early in 1994.

Controller Voice Architecture

Requirements are under development to provide the necessary interfaces for air traffic controllers to integrate AMS(R)S voice, to be used for non-routine needs, with routine data services.

Conduct Voice Trials

Northwest Airlines has installed an AES in a Boeing 747-400 equipped for aircrew and passenger use of satellite voice services. The airline, with Aeronautical Radio, Inc. (ARINC), and the FAA have drawn a joint test plan for using the system for AMS(R)S during Northwest's regular service in the Pacific area.

This trial of end-to-end AMS(R)S voice will be conducted first through connections from the aircraft's flight deck to the ARINC Comm Center, and patched through to the FAATC; and later, with direct connection from the aircraft to the FAATC. The trials are expected to begin in the second quarter of 1993 and will extend for six months.

Project 3: Oceanic/Remote Operations

This part of the Program Plan supports FAA elements that comprise a Satellite Operational Implementation Team. The Team was formed to treat several interrelated satellite programs that are in various stages of development. Its mission is to assure implementation of AMS(R)S for improved air traffic services according to a coordinated and scheduled plan. The target for completion of implementation for the oceanic area is late 1996.

Define Requirements

Initial activities in this project area include definition of requirements in support of an overall Satellite Operational Implementation Plan, now in draft form and scheduled to be completed by late 1993.

Conduct Engineering Trials

The FAA aircraft will continue to be used to collect data on AMS(R)S trials in the North Atlantic area. For a period from 1993 through 1995, trials will be run in coordination with the United Kingdom's Civil Aviation Authority.

Starting in 1994, the trials will operate with a full end-to-end ATN capability using AMS(R)S to handle Automatic Dependent Surveillance (ADS, or periodic position reports) and other messages. This will be the first exercise of the fully SARPs-compliant capabilities of these three systems.

Results will be integrated for analysis with data resulting from the continuing Pacific Engineering Trials. This activity, which began in 1992 prior to an ATN capability, provided ADS reports using an interim AES-equipped United Airlines aircraft in commercial service.

Integrate Oceanic Systems End-To-End

The next step in this project area will be to integrate AMS(R)S into the FAA's Oceanic Development Facility (ODF). This facility is under construction at the FAATC, and will serve as a principal test bed for all FAA oceanic communications and surveillance operations. Discussions have begun on schedule and goals, working with the oceanic program to ensure end-to-end function and performance. The final step will include the passage of

AMS(R)S directly between the Air Route Traffic Control Centers (ARTCCs) and the aircraft.

Project 4: Domestic Service Applications

The U.S. domestic applications project for AMS(R)S communications will focus first on the use of satellite communications in selected areas where it now is difficult to contact aircraft. Also within this area are investigations of satellite alternatives that could bring service advantages to the FAA such as reduced cost and improved availability.

Domestic/Offshore Helicopter Test

This project area will provide for the conduct of U.S. domestic area tests using an FAA helicopter with a loaned, interim AMSC AES and Marisat satellite capacity currently under lease to the American Mobile Satellite Corporation (AMSC). The test's three phases, scheduled from late 1992 through mid-1995, will move from Loran-C position reports to the use of the Global Positioning Satellite (GPS) capabilities reported through the AMSC's spot-beam satellite. Analyses of the results should support further developments in the FAA's domestic and offshore services.

In a second part of this project, the Jet Propulsion Laboratory (JPL) is under contract to the FAA to develop and test a low-cost, light-weight AES for helicopter use. The terminal should also be adaptable for use by fixed-wing aircraft.

Develop Applications and Equipment

This future planning project will investigate low-cost satellite communications alternatives for future domestic use, and will identify candidate systems for research. Coordinated work with the FAA's System Engineering service will identify where future needs are not yet being actively planned for.

Investigations will include use of the AMSC/TMI and next-generation Inmarsat satellite systems, possibilities for using future Low-Earth Orbit (LEO) and Medium-Earth Orbit (MEO), and store-and-forward terminals such as the "Aero-C" Inmarsat terminal.

Future R&D:

This project area will support selection, analyses, and testing of candidate systems; and provide for engineering trials and necessary revisions of the RTCA MOPS and ICAO SARPs. After surveying potential improvements to AMS(R)S, viable candidate architectures will be identified for further investigation and inclusion in planning.

CONCLUSION

The FAA Program Plan for satellite communications provides a basis for developing operational services to enhance air traffic control. It is an integral part of many ongoing improvements to the air traffic control system. Moving first from today's high-frequency radio to use of satellite communications through a service provider, the final step is envisioned to be direct AMS(R)S between flight deck and controller.

The Plan supports standards development; provides for coordinated domestic and international plans, tests and trials leading to integration with other automated FAA systems; and surveys and prepares for future improvement possibilities.

Availability of benefits should be accelerated by this activity for aircraft users equipped to these standards and interfacing with the ATN. The FAA R&D and operational activities to complete standards and integrate satellite communications will enable users to enjoy a level of communications integrity and availability not available by any other means.

218

CANADIAN AERONAUTICAL MOBILE DATA TRIALS

Allister Pedersen
Communications Research Centre (CRC)
Department of Communications, Canada
P.O. Box 11490, Stn. H
Ottawa, Ontario, Canada K2H 8S2
Phone: (613) 998-2011 Fax: (613) 990-0316

Andrea Pearson
Telesat Mobile Inc. (TMI)
1145 Hunt Club Road
Ottawa, Ontario, Canada K1V 0Y3
Phone: (613) 736-6728 Fax: (613) 736-4548

ABSTRACT

This paper describes a series of aeronautical mobile data trials conducted on small aircraft (helicopters and fixed wing) utilizing a low-speed store-and-forward mobile data service.

The paper outlines the user requirements for aeronautical mobile satellite communications. "Flight following" and improved wide-area dispatch communications were identified as high priority requirements.

A "proof-of-concept" trial in a Cessna Skymaster aircraft is described. This trial identified certain development work as essential to the introduction of commercial service including antenna development, power supply modifications and doppler software modifications. Other improvements were also proposed.

The initial aeronautical mobile data service available for pre-operational (Beta) trials is outlined. Pre-operational field trials commenced in October 1992 and consisted of installations on a Gralen Communications Inc. Cessna 177 and an Aerospatiale Astar 350 series light single engine helicopter.

The paper concludes with a discussion of desirable near term mobile data service developments, commercial benefits, current safety benefits and potential future applications for improved safety.

INTRODUCTION

Wide-area mobile communications services will improve significantly in North America with the introduction of MSAT services in late 1994 or early 1995.[1] In advance of the launch of MSAT; Telesat Mobile Inc. (TMI), with support from the Canadian Department of Communications Research Centre (CRC), has been introducing mobile satellite services using leased satellite capacity.

The initial service offering is a low-speed store-and-forward packet-switched mobile data service (MDS) via leased capacity through the INMARSAT II Atlantic Ocean Region West satellite and the Teleglobe Canada ground station located in Weir Quebec.[2] For more than 2 years the mobile data service has been used for Wide Area Fleet Management (WAFM) by various trucking companies, other land mobile fleets, marine fleets and portable users with

battery-powered briefcases. The MDS also serves SCADA (Supervisory Control and Data Acquisition) applications such as monitoring of remote natural gas compressor stations. The development of an aeronautical mobile data service known as AeroKIT™ was of considerable interest to prospective commercial and government users.

USER REQUIREMENTS

The user requirements for aeronautical mobile satellite communications were first discussed with potential MSAT aeronautical end-users in a series of meetings initiated by CRC in 1983/84. Although there is interest in the full range of MSAT voice, data and fax services; "flight following" and improved wide-area dispatch communications were identified as high priority requirements by Canadian aircraft operators.

While most commercial passenger flights in Canada are served by existing terrestrial VHF radio services, a significant number of aircraft operate in rural, remote and rugged areas well beyond coverage of terrestrial VHF radio dispatch systems and also beyond Transport Canada radar and VHF air traffic control coverage. HF systems are used to the extent possible but congestion, interference and varying propagation conditions may preclude any use of HF in the Canadian North for several weeks at a time.

There is therefore an urgent requirement for reliable, wide-area, cost-effective, truly mobile communications for small general aviation aircraft including helicopters. In the simplest terms the aviation community wants reliable communications for conventional dispatch purposes and "flight following". The Ontario Ministry of Natural Resources requires pilots to maintain a "flight watch" by having aircraft communicate their positions once every 30 minutes to their regional dispatcher.

The potential end-user community for this aeronautical mobile data service includes aircraft involved in search and rescue, forest-fire fighting, wildlife surveys, power line monitoring, air ambulance medevacs, resource development, airborne fishery surveillance and policing.

The Canadian market could include civilian and military aircraft, commercial passenger jets operating on routes in northern Canada, charter aircraft and various other general aviation aircraft.

PROOF OF CONCEPT TRIAL

Under the MSAT Field Trials Program, CRC provided a CAL Corp. land mobile data terminal to avionics specialists Gralen Communications Inc. and TMI for a "proof-of-concept" trial. Working with Telesat Mobile, Gralen Communications installed the 12V land-mobile data terminal and a prototype aeronautical mobile antenna in a Cessna 337 Skymaster.

The aeronautical mobile data trial was relatively straightforward to implement with end-to-end commercial services already in place for land, marine and SCADA applications. Successful 2-way mobile data communications, including GPS position reporting, were demonstrated as illustrated in the system concept (figure 1). The dispatch centre for the proof-of-concept trial was co-located in Ottawa at the TMI hub.

This proof-of-concept trial, while very successful, resulted in certain work being identified as essential to the introduction of commercial service. The proposed work plan included antenna development, power supply modifications, doppler software modifications, appropriate physical packaging for the transceiver and work on the existing land mobile dispatch centre. Other improvements also proposed included a cockpit dash-mounted emergency message switch and a dash-mounted "message waiting lamp".

TMI AEROKIT SERVICE-BETA TRIALS

The proof-of-concept trial and subsequent development effort resulted in a pre-operational AeroKIT™ service appropriate for Beta trial customers. While still under development the service already offers an effective wide-area aeronautical fleet management service that consists of 2-way store-and-forward messaging and flight following with the ability to constantly monitor aircraft position.

CAL Aeronautical Data Radio

As shown in Figure 2, the mobile installation includes a CAL Corp. ADT 200-A aeronautical transceiver, antenna, and LNA (Low Noise Amplifier); a Gandalf keyboard display terminal and a GPS antenna. The overall weight is 9.0 kg. The transceiver contains a GPS receiver card, operates from 28 V and is mounted in a standard ATR box that is 19 cm wide, 32 cm deep and 21 cm high. A doppler software modification allows the radio to be used on aircraft operating at speeds up to 1400 km/hr.

The data terminal consists of a standard QWERTY keyboard, numeric keypad and several special function keys for sending an emergency message or selecting menu items from the backlit 4X40 character liquid crystal display. The data terminal, which can be stored when not in use, is supplemented with a dash-mounted emergency message button and a dash-mounted "message waiting" lamp. An optional dash-mounted switch can be used to manually send takeoff/landing messages when they are not sent as a keyboard-entered coded message or when they cannot automatically be transmitted as they are in aircraft with retractable gear.

The LNA (13 cm W X 15 cm D X 4 cm H) is mounted inside near the transceiver antenna (16 cm diameter X 4 cm high). The transceiver antenna can also act as a GPS antenna although it has a null at the zenith. The GPS antenna is 9 cm in diameter and 1 cm high.

AeroKIT FLAG Dispatch Centre

The AeroKIT™ FLAG™ (Fleet Location and Graphics) dispatch centre (Figure 3) consists of an IBM-compatible PC, Unix operating system, messaging monitor, colour graphics monitor, keyboard, mouse, uninterruptible power supply and 2400 bps modem. The modem provides a permanent virtual circuit between the dispatch centre and the TMI hub via the datapac public packet-switched network. The FLAG™ dispatch centre developed by Ultimateast Data Communications of St. John's Newfoundland was already in use for various INMARSAT, AMSC and TMI mobile customers including the Canadian Coast Guard and Department of Fisheries and Oceans.

While the FLAG™ dispatch centre can display geographical maps of any dispatch area of interest in the world, a geographic display of North America is being used for the aeronautical data trials. The graphics screen displays on the map overlay the geographical position of all aircraft based on GPS position reports transmitted automatically from aircraft in the end-users own fleet. GPS worst-case accuracies are 100 metres horizontally and 156 metres vertically. The FLAG™ dispatch centre allows a dispatcher the capability to increase map detail by zooming in on any rectangular area chosen.

Other standard overlays include reference points such as city names, boundaries, roadways and road names and latitude/longitude grids (1 or 5 degree increments). A screen draw function allows the dispatcher to use the mouse as a white pencil to enter temporary information on the screen. Many other hardware and software options are available with FLAG™ dispatch centres.

End-to-end AeroKIT™ Service

The AeroKIT™ Beta trial service provides a 2-way dispatch and flight-following capability between a dispatch centre and a fleet of aircraft.

As with other mobiles using the TMI mobile data service, pilots can manually send/receive 3 types of messages to/from a dispatch centre using 3 different priorities. Messages can also be saved, retrieved and revised as required by either the pilot or dispatcher.

Flight Following

A very important feature of the service is that the mobile radio logs on to the satellite system automatically when the aircraft is powered up without any action by the pilot. Aircraft position reports are automatically transmitted at intervals prescribed by the dispatcher which can be as frequent as once every 3.75 minutes as configured for the Beta trials. A takeoff message, comprising all the information in the position report, can also be transmitted automatically for aircraft with an interface to the squat switch (wheels up/down indicator). For helicopters, float planes and other aircraft without retractable gear the automatic takeoff/landing messages can be sent manually using a dash-mounted switch, the keyboard or automatically using another interface such as a torque sensor to trigger the message. The foregoing embodies a reliable, automatic, highly accurate flight following capability that allows a pilot to concentrate on flying.

Cockpit Messaging

The Gandalf terminal can be used by the cockpit crew to send pre-programmed coded messages. With only 3 or 4 keystrokes a pilot can scroll through a list of coded messages, choose the appropriate message, and then transmit it. By default the message is sent as a routine message although the coded message can be sent priority or sent as an emergency coded message. Emergency messages overwrite the status line on the dispatch screen with a flashing message. Sample coded messages being used in the Beta trials include:
-out of chocks
-in chocks

-send destination weather
-send alternate weather
-arrived at destination
-15 (30, or 60) minutes to arrival

In a similar manner, crew can also select a variety of fill-in-the-blanks form messages such as the following; flight plan, freight information and revised ETA. Free-form text messages, up to 128 characters in length, can also be sent to the dispatch centre.

Position Reports

Regularly scheduled GPS position reports, and supplementary GPS position reports automatically sent along with the chocks messages, takeoff/landing messages and emergency messages all contain the following information:
-date and time (UTC)
-latitude/longitude
-horizontal velocity
-vertical velocity
-altitude
-bearing relative to true North
-GPS reliability report

Emergency Messaging

Transmission of an emergency message, by pressing the dash-mounted emergency button or the "E" and "TX" keys, receives special treatment. The emergency message is broken into 2 messages. Emergency message 1, which is transmitted twice for increased reliability, provides the position in latitude/longitude, reliability of position report, and heading. After emergency message 1 is re-transmitted, emergency message number 2 is sent containing horizontal speed, altitude, vertical speed and date/time.

Dispatch Messaging/Monitoring

The dispatcher also has the capability to send coded and form messages as well as free-form

text messages up to 121 characters per message. Dispatchers can also retrieve the detailed position report of an aircraft by placing the mouse cursor over the desired aircraft on the screen. The most recent position report, along with its date/time, is displayed as well as the distance and direction from the nearest reference location based on a user-determined list of place names and associated coordinates.

The "Aircraft Proximity" feature displays the identification of all aircraft within a specified radius of a selected location in order of the closest aircraft. The "Fleet Stats" feature lists the location of all aircraft in the fleet. "View Trips" allows the dispatcher to display, on the geographic overlay, the historical position reports for any aircraft for a time period specified in hours, days, weeks or months. The "View Trips" function provides important information about any overdue aircraft.

BETA TRIALS

The first Beta trial involved the installation of the CAL ADT 200 in a 4-place high performance single engine Cessna 177 RG (Retractable Gear) for test and demo purposes. The aircraft, owned by Gralen Communications and used for travel to customer sites, successfully demonstrated the full range of services including automatic takeoff/landing messages. This Beta trial indicated more EMI work was required resulting in the subsequent use of improved cable shielding and connectors. This trial led to Transport Canada (DO 160C) and Communications Canada approvals for the implementation of end-user trials commencing in March '93.

A second temporary installation in an Aerospatiale Astar 350 series light single engine helicopter demonstrated no communications problems from the antenna rotor.

Gralen Communications Inc. will be installing the CAL ADT in an Ontario Ministry of Natural Resources DeHavilland Twin Otter used for resource management and occasionally by the Ontario Provincial Police. Hydro Quebec is participating in the Beta trial with an installation in an AS 350 helicopter used for high voltage power line distribution surveillance. (The results of these trials, implemented after submission of the paper, will be reported at the conference).

FUTURE DEVELOPMENT WORK

Future work will focus on the development of a more appropriate keyboard/display for cockpit applications. The requirement for additional graphics overlays for specific end-user applications is under discussion. Ontario MNR dispatchers would benefit from an overlay displaying Ontario lakes suitable for Canadair CL-215 water bomber access. Overlays displaying remote airstrips and fuel caches may also be desirable features for the MNR dispatch computer. Implementation of a dispatch software feature to initiate a dispatch centre alarm after a prescribed number of regularly scheduled position reports were missed would be desirable. This would be an important safety improvement for accidents where ELT (emergency locator transmitter) signals may not be detected for up to 2 hours, where ELTs don't operate at all because of extensive ELT damage or the ELT antenna is damaged or upside down.

CONCLUSIONS AND BENEFITS

A reliable wide-area fleet management and flight-following system has been demonstrated in small general aviation fixed and rotary wing aircraft. The system offers automatic position reporting and takeoff/landing messages.

Service benefits include more reliable flight following, improved safety, capability for realtime re-routing, more efficient cockpit and dispatch communications and more timely information for better management decisions and customer invoicing.

ACKNOWLEDGEMENTS

REFERENCES

[1] G.A. Johanson, N.G. Davies, W.R. Tisdale, "Implementation of a System to Provide Mobile Satellite Services in North America", *IMSC '93 Conference Proceedings,* June '93

[2] D.J. Sward, G.R.Egan, "Satellite Mobile Data Service for Canada", *IMSC '90 Conference Proceedings,* pp. A15-19 June '90
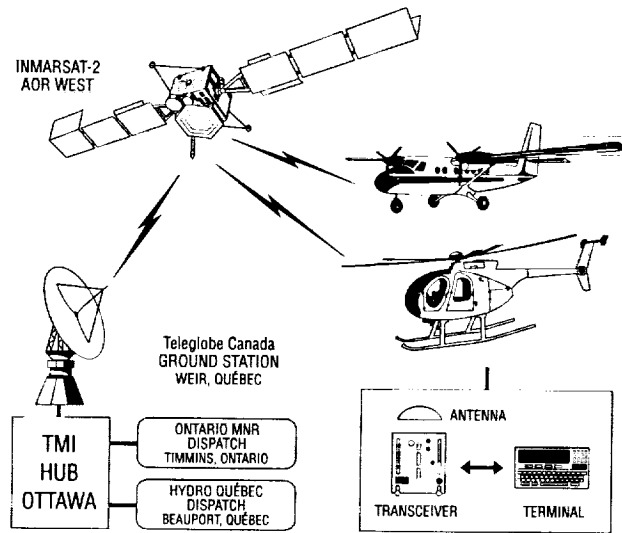
Figure 1 System Concept
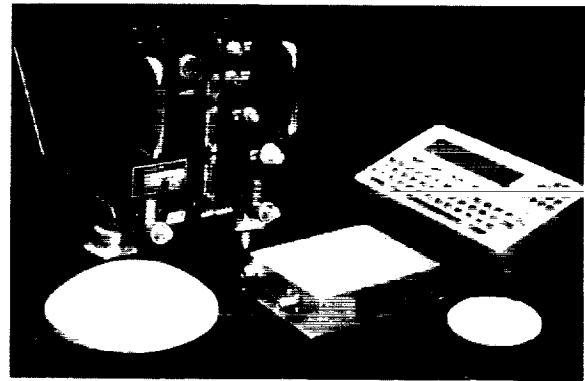
Figure 2 Aeronautical Data Radio
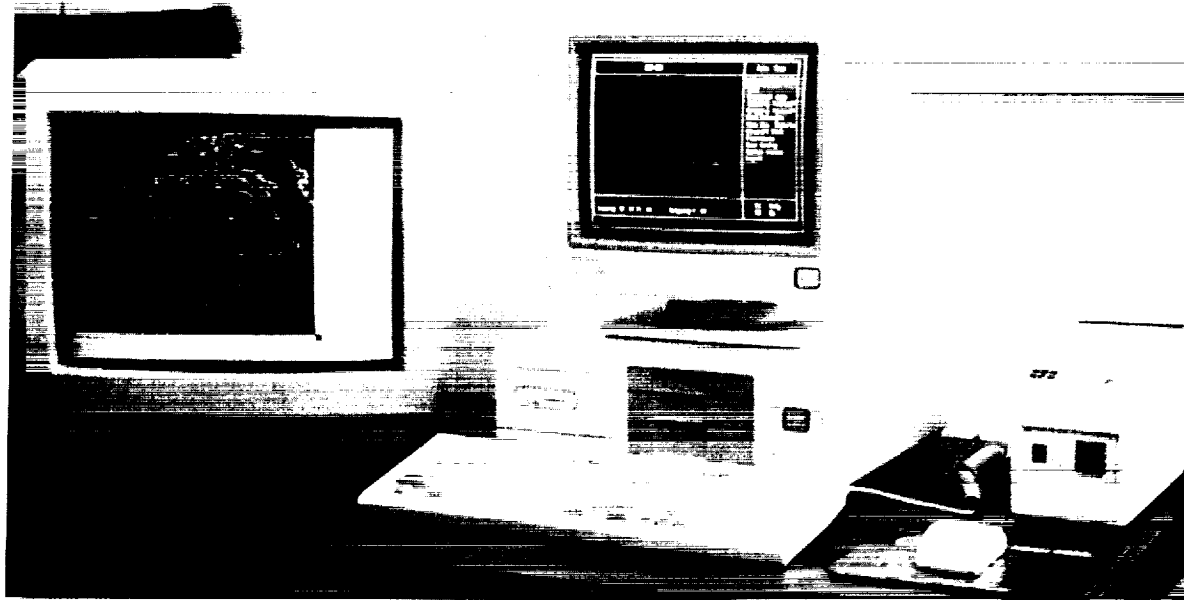
Figure 3 Dispatch Centre

ACTS MOBILE SATCOM EXPERIMENTS

Brian S. Abbe, Robert E. Frye, Thomas C. Jedrey
Jet Propulsion Laboratory
California Institute of Technology
M.S. 238-420
4800 Oak Grove Drive
Pasadena, California 91109
Phone: (818) 354-3887 FAX: (818) 354-6825

ABSTRACT

Over the last decade, the demand for reliable mobile satellite communications (satcom) for voice, data, and video applications has increased dramatically. As consumer demand grows, the current spectrum allocation at L-band could become saturated. For this reason, NASA and the Jet Propulsion Laboratory are developing the Advanced Communications Technology Satellite (ACTS) mobile terminal (AMT) and are evaluating the feasibility of K/Ka-band (20/30 GHz) mobile satcom to meet these growing needs. U.S. industry and government, acting as co-partners, will evaluate K/Ka-band mobile satcom and develop new technologies by conducting a series of applications-oriented experiments. The ACTS and the AMT testbed will be used to conduct these mobile satcom experiments. The goals of the ACTS Mobile Experiments Program and the individual experiment configurations and objectives are further presented.

ACTS MOBILE EXPERIMENTS PROGRAM

The ACTS Mobile Experiments Program focusses on just one part of the ACTS Experiments Program. Included in the latter of these two, are fixed terminal K/Ka-band experiments at T1 data rates (LBR-2 terminal experiments), fixed terminal K/Ka-band experiments at supercomputer data rates (600-800 Mbps, High Data Rate terminal experiments), mobile terminal experiments (2.4-384 kbps, AMT), and supervisory and control data application (SCADA) experiments (2.4 kbps, USAT's). The remainder of this paper will focus on the mobile terminal experiments. The goals of the AMT Experiments Program are as follows: (1) to prove the technologies and system concepts associated with the development of the AMT and ACTS for mobile satcom applications; (2) to characterize the K/Ka-band mobile satcom propagation channel for land-mobile and aeronautical-mobile purposes; (3) to seek out new applications for K/Ka-band mobile satcom; (4) to have U.S. industry and government participation in these experiments; and (5) to stimulate the commercialization of similar technological advances and satellite services. Approximately one dozen different experiments are

being developed between JPL and a variety of industrial/government partners to help the program to meet all of these goals. The basic ideas of some of these experiments are provided in Figure 1.

While the development of mobile satcom technology at L-band has reached a mature stage, there are many challenges that need to be overcome to allow K/Ka-band mobile satcom to become a reality. A detailed description of the terminal development is provided in [1], however, the main technological challenges of the AMT are: (1) to develop small, tracking, high-gain K/Ka-band vehicular antennas; (2) to overcome the large Doppler shifts and frequency uncertainties associated with K/Ka-band mobile satcom; (3) to design power efficient and robust modulation/demodulation techniques; and (4) to compensate for the high attenuation effects experienced with rain and other environmental conditions at K/Ka-band. The development of the AMT, and its use in these experiments will help to expedite solutions to these technical challenges.

Volumes of data characterizing the satellite propagation channel at L-, C-, X-, and even Ku-bands have been collected and thoroughly analyzed, however, very little information exists about the K/Ka-band satellite propagation channel. A limited amount of fixed site ground-based terminal propagation data exists from several propagation experiments that have been performed by Virginia Polytechnic Institute using the Olympus satellite. This data includes signal propagation and rain attenuation information for a fixed terminal in the immediate Blacksburg, Virginia area. No mobile satcom propagation data, or data that has rain attenuation statistics for any other part of the U.S. exists at this time. Performance of the AMT experiments throughout the country will go a long way toward characterizing the mobile satcom K/Ka-band channel, as well as to establish attenuation statistics throughout the U.S.

Some of the most exciting and potentially lucrative applications for K/Ka-band mobile satcom are in the satellite news gathering (SNG) and aeronautical broadcast areas. Mobile communications capabilities for SNG are often limited. In locations where a cellular system is available, mobile voice

communications are possible. In remote locations not covered by the cellular network, truly mobile communications are not always feasible. Typically, the SNG van will have to stop and set up fixed communications equipment to communicate with the broadcast station. This limits the response time for real-time and rapidly changing news events. For this type of application, mobile satcom would allow a quicker response to news events and the potential to provide a compressed video network feed to the SNG van while it is en route to these events.

Aeronautical point-to-multipoint mobile satcom capabilities, first proposed in late 1992, are limited to audio broadcasts of news and sporting events, and are not yet widely available on commercial aircraft. As this service is initiated and expands, it can be expected to include broadcast video transmissions as well. The bandwidths available and the small antenna sizes required to transmit and receive reasonably high data rates make K/Ka-band very suitable for this type of applications as well [2].

Another exciting new area for this technology is disaster and emergency medical service. More lives and property can be saved by providing rapidly deployed voice, data, and video communications to an area struck by a natural disaster such as an earthquake or forest fire.

In meeting all of the goals of this program, and developing new applications for mobile satcom technology, NASA and JPL have been actively seeking industrial and government participation in the development of these experiments. By conducting the program in this manner, JPL achieves several goals inherent to the program. U.S. industry decides what technologies are important, and the program provides the R&D to prove the high-risk technologies. The U.S. economy benefits with the development of new industrial capabilities and services. Approximately one dozen different experiments are being developed under the ACTS Mobile Experiments Program. A description of these experiments is provided in the following section.

ACTS MOBILE EXPERIMENTS

The ACTS Mobile experiments fall into two broad categories, land-mobile experiments and aeronautical-mobile experiments. The following sections provide a brief description of the experiments and the potential influence of the experiments on the U.S. marketplace.

Land-Mobile Experiments

The initial land-mobile experiment will be an internal NASA/JPL experiment during which the terminal and satellite technology are verified, and the land-mobile

satcom propagation channel is characterized. The experiment set-up is presented in Figure 2. The main objective of this experiment is to provide full-duplex voice, data, and low rate video communications at 2.4/4.8/9.6/64 kbps between a fixed terminal and a mobile terminal. For the first experiment, a small, mechanically-steered reflector antenna will be used. A second, follow-on land-mobile technology verification experiment has the same basic set-up and objectives, but, uses a small, mechanically-steered active array antenna. Such a system could provide additional capacity augmentation for current L-band satellite systems, as well as open up a whole new service with the video communications.

Following this experiment, a secure land-mobile experiment will be conducted in conjunction with the National Communications System (NCS). This experiment set-up is basically identical to the initial land-mobile experiments, however, to provide secure communications, a secure telephone unit (STU-III) is interfaced to the AMT. The main objective of this experiment is to provide secure full-duplex voice and data communications for national security and emergency disaster applications. A second follow-on secure experiment will involve an identical scenario, but substituting the small, mechanically-steered active array antenna for the reflector antenna.

Another of the land-mobile experiments involving disaster/emergency preparedness communications is the Emergency Medical Experiment. This experiment is being performed in conjunction with the EMSAT Corporation. During a typical paramedic call, communication is lost when the paramedic enters a building to handle a situation. For this experiment, the AMT will be interfaced to the base station of a portable transceiver. The paramedic will have the portable transceiver with him when he enters the building. The communications link will be initiated by the paramedic, to the AMT located outside, to the fixed station via ACTS, and finally through a land-line back to the hospital.

An experiment with a similar application to the Emergency Medical Experiment is the Telemedicine Experiment, to be performed in conjunction with the University of Washington Medical Center, located in Seattle, Washington. Many areas in rural America have extremely limited access to proper medical care and facilities. This experiment will provide medical imaging capabilities such as X-ray transmission from remote locations via ACTS and the AMT to the University of Washington Medical Center for diagnoses. The experiment set-up is provided in Figure 3. The operational data rates for this experiment are 2.4/4.8/9.6/64 kbps.

226

Currently on the ACTS/AMT Experiments docket are two separate SNG related experiments. The first experiment, performed in conjunction with IDB Communications, involves transmitting a remote live radio signal back to the broadcast station for retransmission. The second SNG experiment, performed in conjunction with NBC, involves a similar terminal configuration. Both of the experiments will improve current communications capabilities for remote, mobile SNG broadcasting, and will demonstrate low rate network video return feed.

Another experiment, performed in conjunction with CBS Radio, involves the transmission of high quality audio and music using a MUSICAM Perceptual Coder interfaced to the AMT. The initial experiment set-up tests the transmission of high quality mono audio at 64 kbps. Upon completion of this experiment, a second, more sophisticated experiment is performed that tests the transmission of high quality stereo audio at 128 kbps. The audio codec utilized in this experiment monitors the received signal quality, and varies the "degree of coding" necessary to maintain the link. In addition to code variation, the audio codec also adjusts the audio quality as required to maintain the link. The audio codec varies the bandwidth of the coded signal from 5 kHz to 20 kHz, and switches between stereo and mono audio, depending upon the link conditions.

A military experiment for the AMT is performed in conjunction with the Army-CECOM. This "Comm-on-the-Move" experiment outfits a HMMWV with the RF portion of the AMT, interfaced with a SINCGARS radio to provide mobile satcom, on the move, back to a fixed terminal. This experiment improves the current military communications capabilities.

A satellite/terrestrial personal communications network (PCN) experiment will be performed in conjunction with Bellcore. This experiment defines practical limitations of present personal satellite communications technology and develops hard data to direct the future course of technology development. Merging the current terrestrial-based equipment with the satellite-based equipment will further enhance the systems' capabilities. This experiment has two different configurations. The first set-up interfaces a hand-held personal computer to the AMT for the transmission and retrieval of data and E-Mail messages. The second configuration interfaces the AMT to a modified cellular radio system for wireless remote paging.

Aeronautical-Mobile Experiments

The initial aeronautical-mobile experiment is a NASA/JPL effort that verifies the terminal and satellite technologies. The aeronautical-mobile satcom propagation channel is characterized during the cruise phase of flight. The aeronautical mobile terminal equipment incorporates the land-mobile AMT equipment, with the exception of the land-mobile antennas. For this experiment, three separate electronically-steered phased array antennas are used. Due to the limited EIRP and G/T specifications on these antennas, the experiment is limited to voice and data transmission at a rate of 4.8 kbps.

The experiments with the most visibility and most potential profit are the broadband aeronautical experiments. A full description of these experiments is found in [2]. Two distinct groups are interested in applications of this type. Military organizations, such as the U.S. Air Force will transmit imaging from an aircraft back to a fixed station terminal for analysis. Commercial organizations, such as U.S. airlines, will provide passenger cabin broadcast video and return line "office-in-the-sky" capabilities such as voice and FAX transmissions. Initial link budget analyses show that terminal development for these experiments can support data rates up to 384 kbps on the forward link (fixed terminal to mobile terminal), and up to 112 kbps on the return link (mobile terminal to fixed terminal). The experiments set-up are shown in Figure 4.

For the commercial applications experiment, a broadband aeronautical working group is being formed to assist with the experiment and terminal development. The members of this working group come from a variety of interests in U.S. industry including aircraft manufacturers, airline carriers, satellite service providers, aeronautical avionics manufacturers, video compression companies, broadcasters. Active participation by U.S. industry in this experiment will help stimulate the commercialization of the service. A commercially operated system providing compressed video broadcasts for passengers could be in service as early as the turn of the century.

ACTS/AMT EXPERIMENTS SCHEDULE

The experiment period begins at the start of October, 1993, and is scheduled to run a two year period through the end of September, 1995. With the exception of the initial land-mobile experiment, two experiments will be in operation continuously for this two year period.

SUMMARY

The ACTS Mobile Experiments Program includes development of several mobile satcom technologies. The various experiments are joint efforts between U.S. industry and government. The experiments facilitate technological verification of the

227

terminal and satellite, the development of new satcom applications and commercial ventures, participation in the experiments by U.S. industry and government, and ultimately will stimulate the U.S. economy through the development of new industries.

REFERENCES

[1] Agan, M.J., et al., "Channel and Terminal Description of the ACTS Mobile Terminal," IMSC Conference 1993.

[2] Abbe, B.S., et al., "ACTS Broadband Aeronautical Experiment," IMSC Conference 1993.

ACTS MOBILE EXPERIMENTS
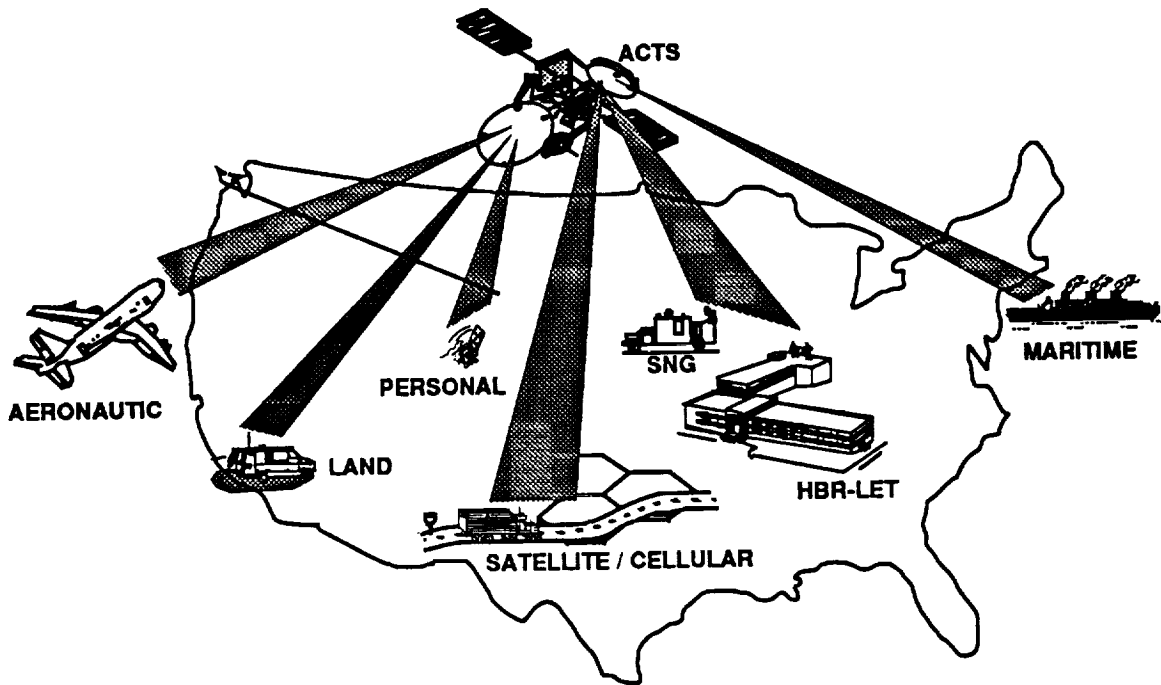
Figure 1 ACTS Mobile Experiments
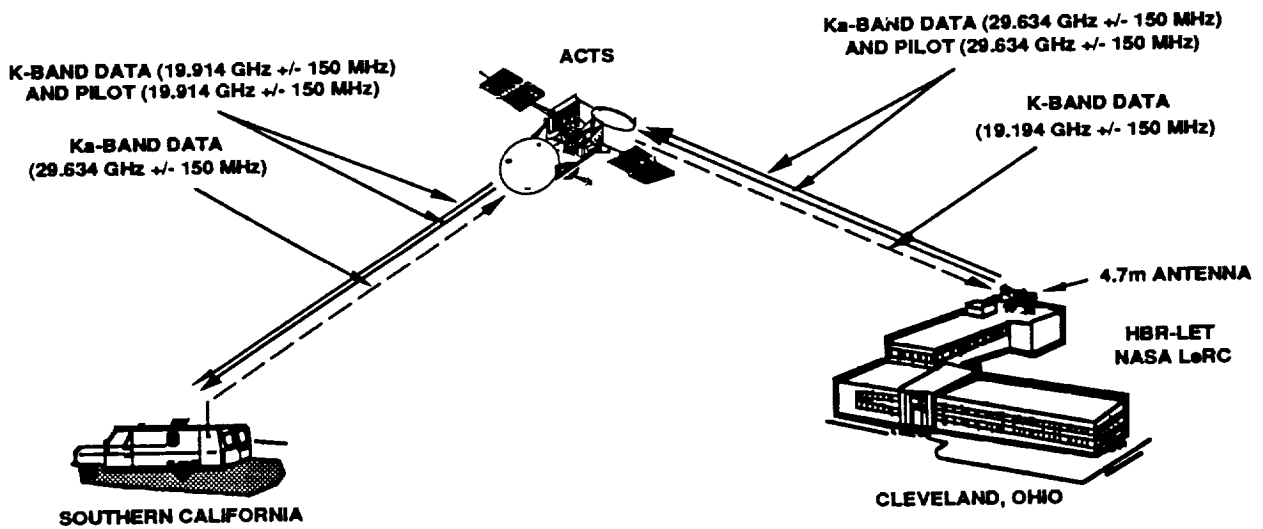
Figure 2 Land-Mobile Experiment Configuration
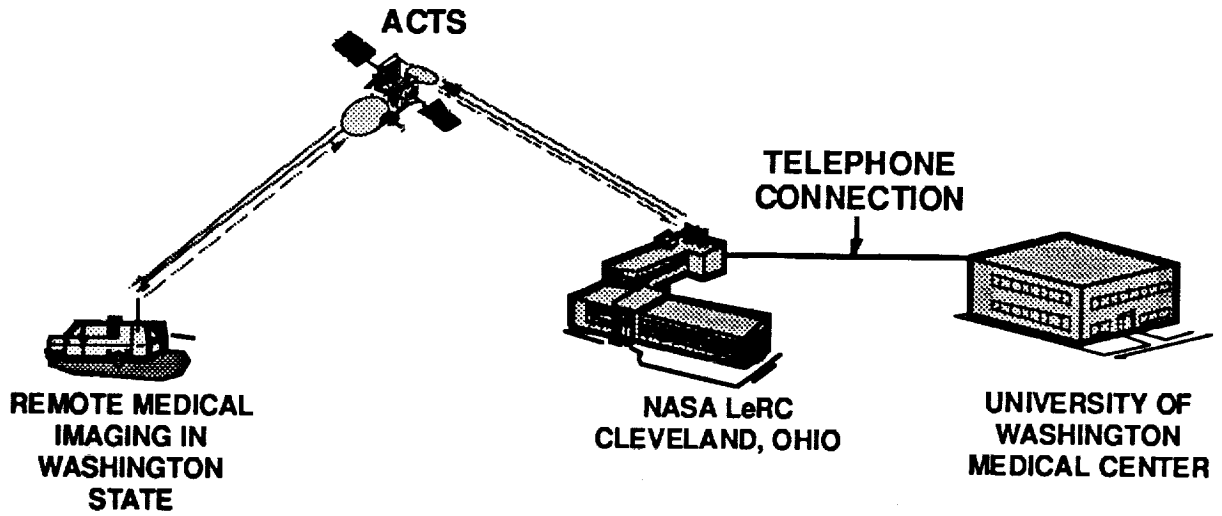
Figure 3 Telemedicine Experiment Configuration

K-BAND DATA (19.914 GHz +/- 150 MHz)
AND PILOT (19.914 GHz +/- 150 MHz)

Ka-BAND DATA (29.634 GHz +/- 150 MHz)

Ka-BAND DATA (29.634 GHz +/- 150 MHz)
AND PILOT (29.634 GHz +/- 150 MHz)

K-BAND DATA (19.194 GHz +/- 150 MHz)

HB R-LET
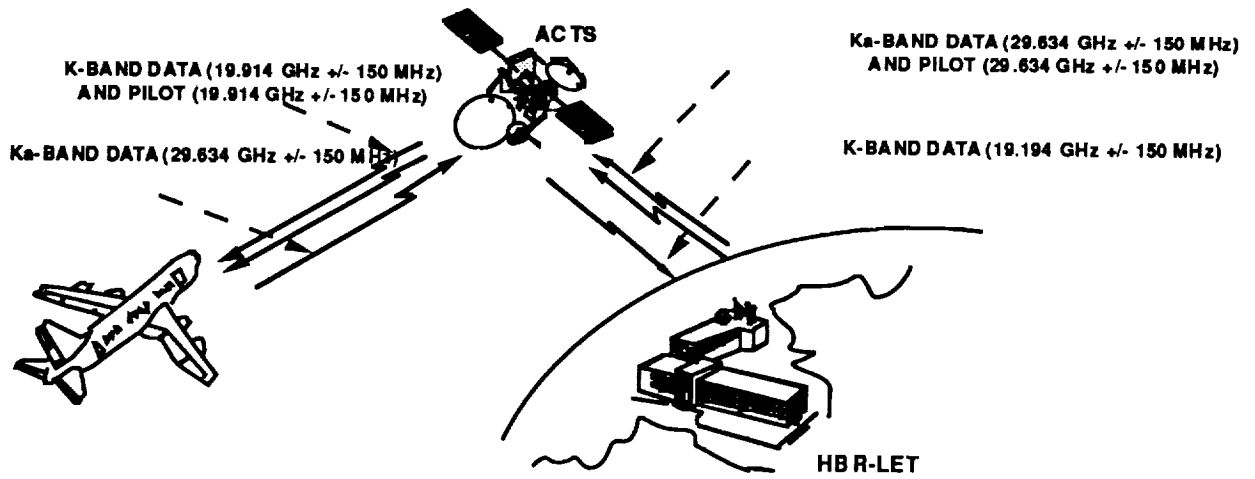
Figure 4 Broadband Aeronautical Experiment Configuration

Cockpit Weather Graphics Using Mobile Satellite Communications

Shashi Seth
ViGYAN, Inc.
Hampton, Virginia 23666

Telephone : (804) 865-6575
Fascimile : (804) 865-8177

ABSTRACT

Many new companies are pushing state-of-the-art technology to bring a revolution in the cockpits of General Aviation (GA) aircraft. The vision, according to Dr. Bruce Holmes - the Assistant Director for Aeronautics at National Aeronautics and Space Adminstration's (NASA) Langley Research Center, is to provide such an advanced flight control system that the motor and cognitive skills you use to drive a car would be very similar to the ones you would use to fly an airplane. We at ViGYAN, Inc., are currently developing a system called the **Pilot Weather Advisor (PWxA)**, which would be a part of such an advanced technology flight management system. The PWxA provides graphical depictions of weather information in the cockpit of aircraft in near real-time, through the use of broadcast satellite communications. The purpose of this system is to improve the safety and utility of GA aircraft operations. Considerable effort is being expended for research in the design of graphical weather systems, notably the works of Scanlon[1], and Dash [2]. The concept of providing pilots with graphical depictions of weather conditions, overlaid on geographical and navigational maps, is extremely powerful.

SYSTEM OVERVIEW

The PWxA works in three broad steps:

• Ground Processing System
• Satellite Communications System
• Airborne Processing System

Ground Processing System

To begin with the weather data is collected and analyzed at a central location. The analysis of the data includes extraction of relevant portions of the data, data compression, and encoding. This step is known as the Ground Processing. Next, the data are automatically transmitted to an earth station of a satellite communication system. These systems are illustrated in figure 1 below.
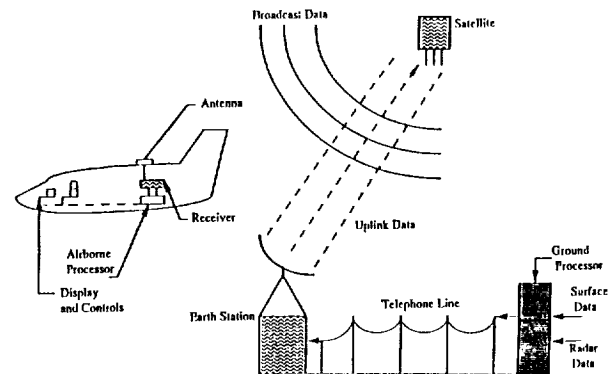
Figure 1. The Pilot Weather Advisor System Concept

Satellite Communications System

Data is received by the antenna and satellite communications receiver on board the aircraft, and transferred via a RS-232 interface to the airborne processing system on the aircraft. During Phase I [3] of this project, we used an Quallcom's OmniTRACS Mobile Communications System. This system consists of a mechanically steered antenna, and an OmniTRACS Communications Unit. The data was received using a Comstream Modem at 9600 bits per second (bps). We are currently working on an aerodynamic Ku-band microstrip antenna. The communication system has a low level of fault tolerance built into it, to detect and correct any faulty operations.

Airborne Processing System

The airborne system processes it into the required display formats, and stores these formats into a database on the airborne computer for later use. The control system allows the pilot to graphically display the information in a user friendly manner so that it does not distract him from his primary functions. The airborne system needs minimal interaction from the user, and is fairly fault tolerant. The PWxA is a broadcast receive-only system. All the information for the entire Continental United States (CONUS) is broadcast over the satellite system and received by all aircraft within the satellite's footprint. The on board processor selects the data needed to be displayed based on the pilots actions described below. No two-way interaction between the aircraft and the ground system is required.

The initial map that shows up on the screen is a CONUS map with about 60 surface sites. Surface Weather, Ground Based Weather Radar, and other products described below, are shown on this map at the pilots discretion. The pilot then inputs the following information:

1. The departure airport
2. The destination airport, and
3. An alternate airport

With these inputs, a suitably scaled trip map, just accommodating the route, can be displayed North-up with again about sixty (60) sites. The Global Positioning System (GPS) or LORAN interface supplies the position of the aircraft. The system utilizes this positional information to display the aircraft position on the CONUS, TRIP, or LOCAL map, whichever is selected. These maps are updated every minute to display the map in accordance with the current aircraft position.

Currently the plan is to update weather data at least four (4) times every hour, although the system does have the capability of updates every seven minutes. A looping function provides the historical trend of the weather on the map-type depictions in a forward time direction using a fast display technique. The display is always north-up, and a history of the aircraft track information is an option. All the maps are displayed using a map projection which renders great circles as nearly straight lines, and very

nearly shows areas in their true relative sizes.

The control system of the PWxA system is mostly menu driven with user control provided by function keys. Currently it is planned to provide for the display of three data sets:

Data Set 1 - Airport Category + Ground Weather Radar + Lightning + Alert Severe Weather Watch "Boxes"

Data Set 2 - Airport Weather + Ground Weather Radar + Lightning + Alert Severe Weather Watch "Boxes"

Data Set 3 - The TREND depiction of any one of the 550 sites for which surface observations are available.

The Airport Category symbol depicts the five Federal Aviation Agency (FAA) ceiling and visibility combinations which are representative of the VFR, MVFR, IFR, LIFR, or less than Category I IFR conditions. The Airport Weather symbol gives information about existing weather conditions such as liquid precipitation, or any obstructions to vision (eg. fog, haze, blowing snow), hazardous weather such as thunderstorms, tornado, hurricane, or any solid precipitation, or winds greater than 20 knots.

The TREND depiction compares the surface observations with the terminal forecast, hour by hour. This should be useful in determining whether the actual weather is developing according to the forecast.

FUTURE ENHANCEMENTS

The PWxA System as described here is designed to provide basic weather information to the enroute pilot for strategic planning purposes. The system could also be used pre-flight, to quickly obtain an overall view of the weather without having to read pages of alphanumerics. In the future, the depictions could be displayed directly on navigation moving maps to provide a powerful integrated weather/navigation flight management tool. As the NWS modernization program unfolds, we will be able to provide near real-time data such as winds and temperatures aloft, 3D radar products, automated pireps on

turbulence and icing etc. With slightly more computation power, we may even be able to provide trip profiles, by showing cross-sections of the trip with the winds, temperatures, and radar. Our satellite communications link could be stretched to update data 10 (ten) times an hour instead of 4 (four) times an hour. The limiting factor is not the PWxA system, but the weather acquisition and dissemination systems.

We have also begun considering how to use this information with an expert system to provide a continuous recommendation to the pilot for the course and altitudes he should fly, based on both the current observations and the forecast. We believe the forecasts have to get considerably better, and the Expert System formulation will have to get much more complex before such a system can provide reliable answers.

We have demonstrated the PWxA concept in flight in 1991 [4], on a Piper Malibu aircraft, as part of our Phase I work on a NASA Small Business Innovative Research (SBIR) contract. We are at present in Phase II of that contract, developing the operational prototype.

ACKNOWLEDGEMENTS

REFERENCES

[1] Charles H. Scanlon , "A Graphical Weather System Design for the NASA Transport Systems Research Vehicle B-737", NASA Technical Memorandum 104205, February 1992.

[2] Ernie R. Dash, Norman L. Crabill , "The Pilot's Automated Weather Support System Concept (PAWSS)", AIAA/FAA Joint Symposium on General Aviation Systems, Ocean City NJ, April 12 1990.

[3] W. Allen Kilgore , N.L. Crabill , S.T. Shipley, J. O'Neill , D. Stauffacher , I. Graffman, and S. Seth :"Pilot Weather Advisor, Final Report for SBIR Phase I, Contract No. NAS1-19250", September 1991.

[4] W. Allen Kilgore , N.L. Crabill , S.T. Shipley, J. O'Neill , D. Stauffacher , I. Graffman, and S. Seth : "Pilot Weather Advisor, 2nd Joint Symposium on General Aviation Systems", Wichita KS, March 16-17, 1992.

233
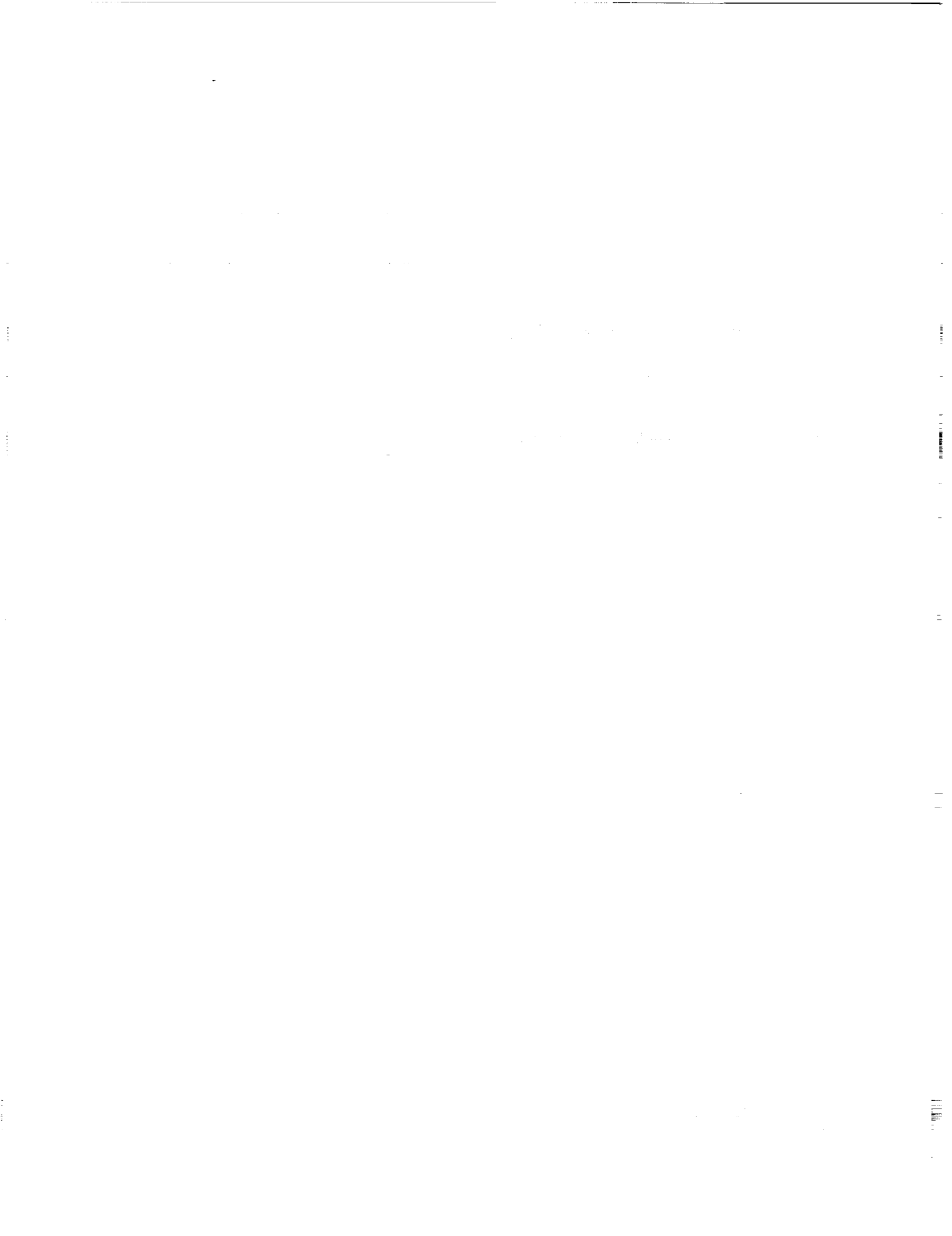
The AGRHYMET Data Communications Project

G. R. Mah
Hughes STX
EROS Data Center
Sioux Falls, SD 57198, USA

D. P. Salpini
USAID/Information Resource Management
1100 Wilson Boulevard
Arlington, VA 22209, USA

ABSTRACT

The U.S. Geological Survey (USGS) and the U.S. Agency for International Development (USAID) are providing technical assistance to the AGRHYMET program in West Africa. AGRHYMET staff use remote sensing technology to produce satellite image maps of the Sahel region of West Africa. These image maps may show vegetation greenness, sea surface temperatures, or processed weather satellite imagery. The image maps must be distributed from the AGRHYMET Regional Center in Niger to national AGRHYMET centers in the member countries of Burkina Faso, Cape Verde, Chad, Gambia, Guinea–Bissau, Mali, Mauritania, Niger, and Senegal. After consideration of a number of land– and space–based solutions for image map distribution, the best solution was determined to be use of International Maritime Satellite Organization (INMARSAT) land–based terminals. In April 1992, a field test and proof–of–concept demonstration using land–mobile terminals produced favorable results.

The USGS and USAID are setting up a wide area network using INMARSAT terminals to link the AGRHYMET sites for image data transfer. The system is in the procurement and installation phase and initial operating capability may be operational for the 1993 growing season, starting in May 1993.

INTRODUCTION

In the middle 1970's, the World Meteorological Organization, in cooperation with nine member nations in the Sahel region of western Africa, organized the AGRHYMET program to help the member nations increase agricultural crop production. [1] The role of AGRHYMET has since expanded to include supplying food production advice to government ministries, locust plague prediction and control, and assistance to the Famine Early Warning System program. To accomplish its mission the AGRHYMET program has set up the AGRHYMET regional center (ARC) in Niamey, Niger, and national AGRHYMET centers (NAC) in each of the member nations. A receiving station for satellite images from NOAA's Advanced Very High Resolution Radiometer (AVHRR) instrument was installed at the ARC by the French Government as part of its foreign aid program. The U.S. Agency for International Development (USAID), in cooperation with the U.S. Geological Survey's EROS Data Center (EDC), have set up a system to process the AVHRR data to make image maps that indicate the relative "greenness" of the area. Greenness maps are derived from the Normalized Difference Vegetation Index (NDVI) computed from AVHRR data. [2] They are distributed in hard copy format from the ARC to the NAC's via the mail system on 10–day intervals throughout the growing season. At present, the delivery of the greenness maps does not occur in a timely manner to support near–realtime assessment of crop production for policy decisions. It was proposed that a telecommunications system be installed to transfer the greenness maps electronically, in near–realtime.

REQUIREMENTS

The telecommunications system is required to provide a computer–to–computer communications link to transfer the greenness map data from the ARC to the NAC's and for the NAC's to transfer weather data back to the ARC. The system will operate primarily during the growing season and transfer data on 10–day intervals (decadal) between the

ARC and the NAC's. The system technical requirements are summarized as follows:

1. The system shall provide operational data transfer of greenness map image files ranging up to 4 MB from the ARC to a NAC. Other data sets and files may be added in the future as required.

2. Weather data ranging up to 500 KB shall be transferred from a NAC to the ARC.

3. The system shall be operational for the 1993 growing season and remain operational for 5 years.

4. Equipment installed at the ARC or a NAC shall be supported by ARC personnel for hardware and software maintenance and repair. The vendor will provide warranty service for the system's operational life of 5 years.

5. The transmission channel [or "telephone"] service shall be an operational system, using the same provider or service for the full 5 years of operation.

6. The system shall minimize the annual recurring costs of operation.

7. The system shall provide moderate growth capability to accommodate changing AGRHYMET requirements and services.

8. The system shall not require any special licensing or permits.

9. The system shall provide 99% availability during the growing season (i.e. – unaffected by storms, power outages, or fluctuations in local telephone service quality).

CANDIDATE SOLUTIONS

A number of techniques were examined, ranging from point–to–point digital radios to satellite communications systems, with a satellite system being the optimum choice. All ground–based systems were eliminated from consideration because of line–of–sight requirements or low data rate capacity. A diagram of a typical satellite–based system is shown in figure 1.

Figure 1. A Satellite–Based System

Among the satellite systems, most privately owned systems were eliminated due to lack of coverage over the Sahel or the uncertainty of continuing service for the 5 year project lifetime. This narrowed candidate systems to satellites operated by two international consortiums, INTELSAT (the International Telecommunications Satellite Consortium) and INMARSAT (the International Maritime Satellite Organization). Between the two systems, the INMARSAT approach was selected on the basis of being appropriate for AGRHYMET requirements, initial cost, recurring costs, and ease of operation and maintenance. A summary of the requirements criteria is shown in **table 1**.

INMARSAT System

The INMARSAT system consists of four satellites in geostationary orbits providing global coverage (figure 2). INMARSAT provides voice, fax, and data communications services between land–mobile, maritime, and fixed users. The proposed system will use land–based fixed terminals.

The system was originally set up to provide ship–to–shore radiotelephone service, but has since expanded to encompass large numbers of land–mobile users also. The system operates in a manner analogous to a long distance carrier, connecting to either a local phone system or an INMARSAT terminal. Access to the system is similar to a telephone system. A user dials the desired destination (phone number), and the system connects them.

236

System Configuration

Each site (both ARC and NAC) will use a fixed INMARSAT terminal with an external fixed dish antenna (1 to 2 m in diameter). The terminals will be linked to a dedicated personal computer (provided as part of the system) through FAX/modem. The terminal electronics unit, the personal computer, and an uninterruptible power supply will be located in the site computer room; while the antenna will be located outside the building (typically installed on the roof). The external antenna must be located within 15 m of the terminal electronics unit.

Table 1. Summary of Requirements Analysis

Requirement	INMARSAT	INTELSAT
Operational System	Yes	Yes, some terminal customization may be required
Duplex Link	Yes	Yes
Minimize Interaction Between Local PTT and System	COMSAT/Common Carrier pays fees	Transponder rental requires fees to each PTT, use of existing INTELSAT terminal in Niamey requires leased lines and coordination with PTT(s)
Minimize Licensing	License to enter country and possibly operator's permit, considered to be minimal requirements	Requires coordination with each country's PTT
Supportable by ARC Personnel	Vendor will train ARC personnel, provide spares and extended warranty, easily maintained	Vendor will train ARC personnel, provide spares and extended warranty, special skills required for maintenance and repair
System Life of 5 to 7 Years	Yes	Yes
Sahel Environmental Conditions	Terminals designed for operation in hostile environments	Can be modified to operate in Sahel environment
Initial Operation for 1993 Growing Season	Terminals available from stock	System development at vendor would take 3 to 6 months
Expandability/Growth	Yes, add terminals, add high data option for 56/64 KBPS link	Yes, add terminals, can increase data rate to width of channel, rent wider channel bandwidth to increase data rate
Easily Interface to Existing ARC/NAC Hardware	Yes, interface looks like phone line	Some specialized connection equipment may be required
Satellite Link Available for 5 to 7 Years	Yes, satellite links transparent to user	Yes, may be moved to another satellite as current satellite ages
Minimize Recurring Costs	Pay only 'phone' bill ($20k/yr)	Transponder rental, plus PTT fees

237

Figure 2. Global INMARSAT Satellite System Coverage

FIELD TEST DESCRIPTION AND RESULTS

A field test with two INMARSAT land–mobile satellite terminals was performed in April 1992. Data was relayed between the ARC in Niamey, Niger, and the NAC in Ougadougou, Burkina Faso, using an INMARSAT coast earthstation to turn the link around (double–bounce through the spacecraft). Transfer rates between 4.8 KBPS and 19.2 KBPS were measured, with the typical rate of 8 KBPS for a large file transfer. A greenness map test file of the West African coast was used, with a typical transmission time of 10 minutes (at an 8 KBPS data rate). Telebit modems were used, along with the MTEZ and Procomm Plus modem control software packages. Although both packages transferred data at acceptable rates, using the KERMIT utility in Procomm Plus yielded the highest sustained data transfer rates.

The system was also used to remotely log into EDC computer systems in the U.S. In most cases the system connected at rates between 2.4 KBPS and 19.2 KBPS, although some of the lower connection rates were imposed by the remote connection, not the INMARSAT link. Voice communication was also used extensively between both the West African sites and the U.S., although the main goal of the test was data transfers. The ARC site is shown in figure 3, and the NAC site is shown in figure 4.

Figure 3. ARC Site in Niamey
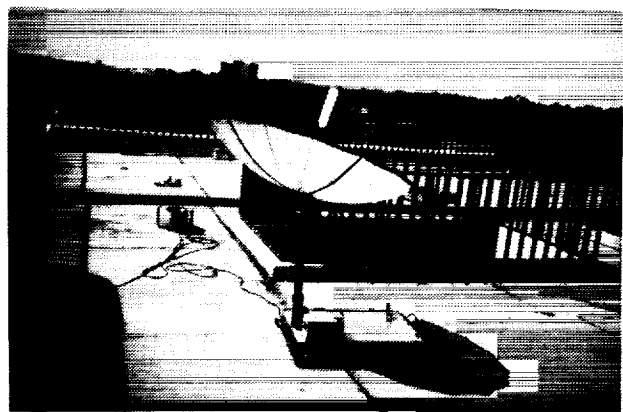
Figure 4. NAC Site in Ougadougou

238

As a proof of concept test, the INMARSAT system met all requirements. Further optimization of the selection of modems and software may yield higher sustained data rates than the 8 KBPS experienced. Moreover, the use of modems designed specifically for noisy links (i.e. – cellular telephony) may increase the total system throughput.
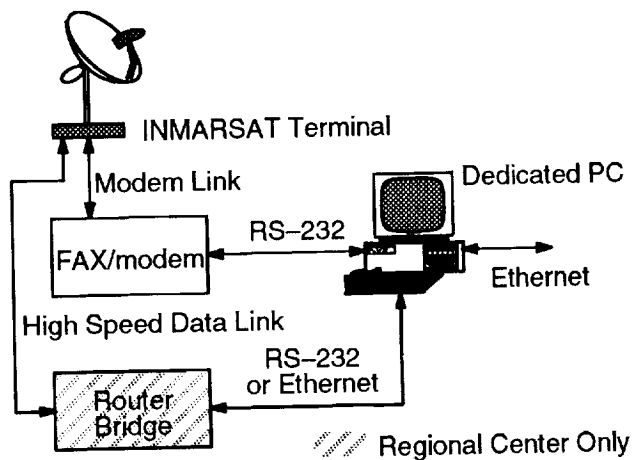
Figure 5. System Configuration

PHYSICAL CONFIGURATIONS

The configuration of the system is shown in figure 5. At the regional center the configuration consists of a INMARSAT terminal, a dedicated personal computer, a FAX/modem, a router/bridge, and an uninterruptible power supply for all the equipment. The national center sites consist of an IN-MARSAT terminal, a dedicated personal computer, a FAX/modem, and an uninterruptible power supply. Each computer will interface to the INMARSAT terminal through the FAX/modem using modem control (communications) software. The computers will also be equipped with an ethernet adapter to connect to the existing site local area network (LAN) using the LANtastic network operating system. Additionally, the computer at the regional center will have high-speed (DS0, X.25) capabilities using the bridge/router and the high-speed data option on the IN-MARSAT terminal.

OPERATIONAL AND SUPPORT REQUIREMENTS

Operational considerations fall into two categories: security and operational procedures. Physical security is required at each site. Physical separation of the terminal into two fixed sections will aid in security, but access to the external antenna, the termi-

nal electronics unit, and the dedicated computer must be restricted to authorized users. Operational procedures will be established to limit the number of people with access to the system, to require the use of a password to log onto the computer, and to set up the system in a manner that inhibits use in an undesired fashion (i.e. – use of voice capability from a data only installation).

Each site will require two or three people who are trained in routine operation of the system and simple troubleshooting procedures. Moreover, the ARC will require two to three people who are trained in operations, maintenance, and repair of the equipment. Training of ARC personnel will occur at the vendor's facility, and training of NAC personnel will occur at the NAC.

The skills required at the ARC will encompass two areas: operators and engineers. Operators will require training and expertise in using the equipment and in operational procedures. Engineers will require both knowledge of operations and equipment maintenance. A typical scenario at the ARC will have one operator per shift, with a backup person available as an alternate operator, and one engineer (possibly only on–call) per shift. The skills at the NAC's will be somewhat different. The operators will be trained in some of the routine equipment maintenance procedures as well as training to interface with ARC engineers for troubleshooting.

Since AGRHYMET is primarily supported by donor contributions, low recurring costs are important. An analysis of typical operating expenses is shown in table 2. The figures listed are based on nominal file sizes for each country and a 9.6 KBPS transfer rate.

CONCLUSIONS

USAID has funding to install a system of IN-MARSAT terminals to connect the ARC and the NAC's. The procurement process is underway, and initial operating capability is planned to support the 1993 growing season. Further uses of the system include remote diagnostics of the ARC computer systems from the EDC using the high–speed data link and support of field work using land–mobile terminals. Disaster relief efforts may also use land–mobile terminals as part of the AGRHYMET network.

Table 2. Recurring Cost Analysis

Country	NDVI File MB	Transfer Time min	Weather Data MB	Transfer Time min	Sea Surface Temp MB	Transfer Time min
Burkina Faso	0.40	5.56	0.20	2.78	n/a	n/a
Cape Verde	n/a	n/a	0.20	2.78	1.20	16.67
Chad	1.30	18.06	0.20	2.78	n/a	n/a
Gambia	0.03	0.42	0.20	2.78	1.20	16.67
Guinea Bissau	0.70	9.72	0.20	2.78	1.20	16.67
Mali	1.70	23.61	0.20	2.78	n/a	n/a
Mauritania	1.10	15.28	0.20	2.78	1.20	16.67
Niger	1.30	n/a	0.20	n/a	n/a	n/a
Senegal	0.20	2.78	0.20	2.78	1.20	16.67
Totals	6.73	75.42	1.80	22.22	6.00	83.34
Cost at $10/min		1508.45		444.48		1666.80
Cost at $6/min		905.07		266.69		1000.08

Total cost per decade (NDVI, weather, sea temp) =	3619.73	($10/min)
	2171.84	($6/min)
Total cost per decade (NDVI, weather only) =	1952.93	($10/min)
	1171.76	($6/min)
Total annual cost (13 decades, NDVI, weather data only) =	25388.14	($10/min)
	15232.89	($6/min)
Total annual cost (13 decades, NDVI, weather, sea temp) =	47056.54	($10/min)
	28233.93	($6/min)

Notes -

All links are double bounce ($10/min or $6/min in each direction)
Times are for compressed files (approximately 50% size reduction) at 9.6 KBPS
Sea surface temperature map is 8 bit pixels, 640x480 (VGA) resolution
Sea surface temperature maps are distributed weekly (twice per decade)
Sea surface temperature maps are shown as candidate new product

ACKNOWLEDGMENTS

REFERENCES

[1] Niamey Field Office, *The Center Scene*, Spring 1992, EROS Data Center, Sioux Falls, SD 57198, p. 4–6.

[2] Eidenshink, J. C., 1992: The 1990 Conterminus US AVHRR Data Set, *Photogrammetric Engineering and Remote Sensing*, Volume 58, Number 6, June 1992, 809–813.

240

Using Satellite Communications for a Mobile Computer Network

Douglas J. Wyman
Washington State Patrol
2803 156th S.E.
Bellevue, WA 98007 U.S.A.
(206) 455-7760
FAX (206) 438-7437

Patrol Car Automation

Law enforcement agencies are recognizing the requirement for Patrol Car Automation systems. Most currently available commercial systems for Patrol Car Automation are mobile data terminal systems that limit agencies to specific manufacturers of equipment. The currently available systems do not easily allow links to disparate information systems nor is the implementation of new processes or functions easily accommodated.

Mobile Computer Network

The Washington State Patrol (W.S.P.), in response to this need for Patrol Car Automation has developed a prototype Mobile Computer Network (MCN). The network uses "off the shelf" hardware to provide a file passing network environment for notebook computers in vehicles. This network links the officers with the W.S.P.'s information system, other Washington state agencies and the National Law Enforcement Telecommunications System. The system can provide direct links for messaging and inquiry between the Patrol cars, all other states and the Canadian Provinces.

Network Requirements

The W.S.P. troopers are responsible for a variety of administrative reports. There are also a number of software programs that assist the trooper in their tasks. This dictated the need for a system that incorporated a removable notebook computer. The current voice radio system has been at capacity for years; see Figure 1.
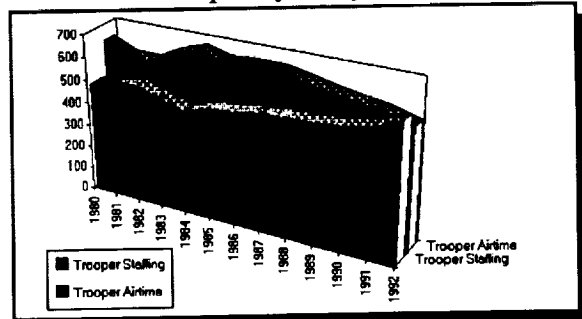
Figure 1 Trooper Airtime

The system will have to enhance the officer's effectiveness by reducing the amount of information the voice radio network is required to pass. The W.S.P. needs a system based on the existing microwave and UHF radio system for data communications but portions of the mobile network must be immune from terrestrial disasters due to the state's location on the Pacific earthquake zone and the threat of volcanic disturbance.

Network Design Overview

The Patrol's solution is the design of a Mobile Computer Network (MCN)

241

including Mobile Satellite Communications; see Figure 2.
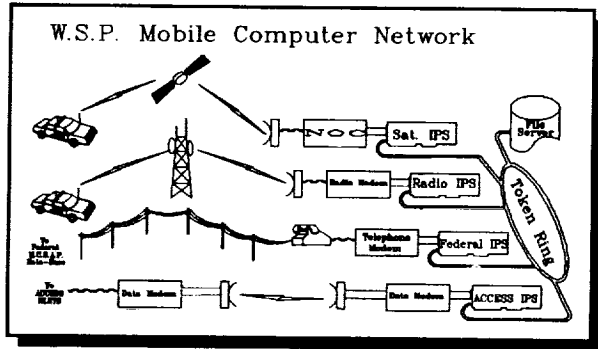
Figure 2 MCN Network

The network is designed around Imbedded Process Servers (IPS) which are single board I.B.M. compatible 80X86 computers linked on a token ring LAN. Each IPS operates in a client/server mode serving both network users and other IPS's. The mobile nodes on the network use background software that transfers all files deposited on the "network" directory back to the hub. These files carry a header designating destination, originator and other necessary information. The media location of the destination is transparent to the users. That destination can be on the UHF system, the physical LAN, the Patrol's SNA WAN or the satellite system.

MCN Mobile Network Software

The officer initializes the network software by loading two (2) background resident programs. The first is a short hardware specific program (HSP) that handles the placement on and retrieval from the communications media of the individual packets. This program has an Application Process Interface (API) that allows communication with other software. The second program loaded, called Radio Transfer (RXFER), is not hardware specific. It handles the presentation to the user and the operating system interface. RXFER is assigned a disk storage area as a network

"drive". It can be any drive or subdirectory. All files placed on this drive or directory are queued for transmission to the network hub. All files from the hub are placed in an inbox directory below the "network" directory. On initialization, RXFER insures the user is authorized network access and negotiates with the hardware program's API to establish packet sizes and inter-program communications areas of memory.

MCN Hub Operation

All IPS's have a network directory assigned in a table of directories. Each IPS monitors its directory for the presence of files. When a file is placed on its directory, an IPS will process the file in a manner prescribed by that IPS's process type and then delete the file. The file and directory method of process command permits sessionless server operation. The IPS controlling the UHF links to the officer monitors the radio data link. When data packets arrive, the system acknowledges each packet and, if necessary, reassembles packets into the complete transferred file. The completed file header is then examined for the destination address. The logical address is compared with a table of physical addresses. The file then is written to the directory indicated by the physical address. The individual packet acknowledgement synchronizes communication and insures completion and accuracy of file transmission.

Mobile Satellite Software

The integration of Mobile Satellite Communications into this network has both problems and benefits. The synchronous packet communications of the UHF system requires 2 messages for each packet. The near instantaneous transfer makes the

handshaking invisible to the user. The network software has timeout parameters for retransmission. The variable delays in transferring data packets over the mobile satellite make this method impractical. On the UHF system, the software has only the acknowledgement packet to guarantee that the packet transmitted has been received. In the mobile satellite system, once a packet is transferred from the mobile software to the satellite radio, accurate transmission is guaranteed by the satellite radio's firmware. this eliminates the need for an acknowledgement packet from the hub. One of our requirements is to have no hardware specific code in the RXFER program. This requires that the satellite specific HSP generate false acknowledgement packets. Since the addressing and modulation scheme of the mobile satellite radio system is inherently secure, the passing of sign-on packets with passwording and acknowledgement is unnecessary. The mobile satellite radio also offers a number of useful diagnostic functions. The HSP software examines packet requests and intercepts the specially encoded requests for diagnostic packets and returns packets with this information. It also mimics the sign on packet transfer sequences and all of the packet handshakes which the RXFER program requires for acceptance of this as normal network traffic.

Hub Satellite Software

At the hub, the use of the mobile satellite communications gives the added benefit of regular positioning information. The network's bindery of mobile node information is designed to make use of this information. At the hub end, a message accepted by the mobile satellite company's network operations center (NOC) may not be transmitted immediately to the mobile.

Parameters are set at the NOC to allow sufficient time for the mobile to be illuminated by the satellite, then to lock on and receive the packet. The NOC sets parameters for the amount of time to hold messages in queue before returning them as undelivered. Storage of messages at the MCN hub for extended periods awaiting either acknowledgement of receipt or an undeliverable message notice is required. Also required is a different method of triggering the mail store and forward function. In the UHF system, any loss of contact will transfer the mobile user's hub address into a mail directory. This is done because the user might have merely moved into an adjoining transmitter's coverage area. The user requires all undelivered messages to be immediately available to the new transmitter's IPC. The satellite system has only the one IPC and the timing of status transfer to mail depends on the size of the satellite IPC's message storage area and tables of message delivery status. On the UHF system, the HSP software is identical at each end. On the satellite mobile radio, the protocols required in the MCN hub to NOC communications are entirely different. The characteristics of mobile satellite radio required design changes from the traditional methods of mobile data transfer and modification in the expectations of the line trooper. These changes are not difficult and are eclipsed by the benefits of mobile satellite communications.

The Benefits of Patrol Car Automation

Currently, the W.S.P. prototype system offers the troopers all routine law enforcement query functions, a store and forward E-Mail function and outbound FAX from the car. Planned additions include image transmission, voice interface, heads-up display, ticket processing, driver's license

scanning, mobile docking ports and direct car to car interagency data communications. The benefits to the citizens of the state include the increase of stolen recoveries, quicker apprehension of wanted persons, reducing the delay for violators, greater recovery of fines and crime deterrence.

The Benefits of Satellite Mobile Computing

Incorporating satellite radio communications into the Mobile Computer Network has the benefit of providing a communications link that is virtually immune to terrestrial disaster. The Washington State Patrol intends to allocate sufficient satellite based mobiles to provide disaster backup links for the major public safety communications centers in the state. In the event that a disaster of any sort were to disable one or more of the public safety communications centers in the state, the assigned mobile would provide a link, for the communications center, to the National Law Enforcement Communications System (NLETS) and links to all units on the Mobile Computer Network. This backup would be provided not for the W.S.P. only, but for all public safety agencies in the state. The per officer cost of the terrestrial communications infrastructure makes mobile satellite communications the medium of choice for data communications in sparsely populated areas of the state.

National Law Enforcement Satellite

The Washington State Patrol has taken one of their MCN equipped cars to display at national conferences of law enforcement agencies. The use of satellite communications has sparked a great deal of interest in the national law enforcement community. The expense of establishing and maintaining a terrestrial communications infrastructure for the

disparate law enforcement agencies in the U.S.A. is sufficiently towering to inspire consideration of a mobile satellite communications network shared by law enforcement agencies nationwide; a system optimized for and dedicated to law enforcement.

244

DESIGN AND IMPLEMENTATION CONSIDERATIONS
OF A MSAT PACKET DATA NETWORK

Fouad G. Karam, Telesat Mobile Inc.
1145 Hunt Club Road, Ottawa, Ontario, Canada, K1V 0Y3
613-736-6728/Fax613-736-4548
Terry Hearn, Westinghouse Electric Corp.
410-993-1346/Fax410-765-9745
Doug Rohr, Westinghouse Canada
Arthur F. Guibord, Telesat Mobile inc.

ABSTRACT

The Mobile Data System, which is intended to provide for packet switched data services is currently under development. The system is based on a star network topology consisting of a centralized Data Hub (DH) serving a large number of mobile terminals. Through the Data Hub, end-to-end connections can be established between terrestrial users on public or private data networks and mobile users. The MDS network will be capable of offering a variety of services some of which are based on the standard X.25 network interface protocol, and others optimized for short messages and broadcast messages. A description of these services and the trade-offs in the DH design are presented in this paper.

1. INTRODUCTION

The mobile data services which are provided by TMI consist of two types :The basic services which are based on the standard X.25 network interface protocol, and the Reliable Transaction and the Unacknowledged data delivery services. These will be described briefly in Section 2 while Section 3 deals with presenting the logical and functional architecture of the Data Hub. This includes the protocol processing and associated interfaces, and the MDS network management which handles configuration, fault, accounting, performance and statistics.

During the initial stages of the development, several design trade studies were undertaken to establish the architecture of the central Data Hub. Results from these studies are presented in Section 4. The advantages of implementing the Data Hub as a number of distributed processors rather than a single processor are outlined. This paper also discusses how the chosen architecture provides for flexibility in system growth while meeting the overall availability and performance requirements.

In order to meet performance and system availability requirements, decisions had to be made with respect to computing platforms. As it will be demonstrated, fault tolerant computers are deployed for network and system management, while the real-time processing functions are handled by high throughput multi-processing systems operating in a real-time fashion.

Several failover and failure recovery scenarios will be analyzed and described in Section 5 of this paper. As it will be seen, the system designers ensured that equipment failure shall not cause an overall network failure.

2. OVERVIEW OF MOBILE DATA SERVICES

The Mobile Data System (MDS) provides for packet data transmission to mobile users. High efficiency and cost effectiveness are achieved by a large number of mobile users dynamically sharing the space segment. Data services provided by MDS fall into two categories: Basic, and Specialized. The basic service category within the MDS provides for the establishment of end-to-end virtual circuits

between DTEs attached to Mobile Terminals (MTs) and DTEs attached to the Data Hub (DH). The basic service category is composed of two distinct services: X.25 and asynchronous. The X.25 service is compliant with the 1988 version of the CCITT recommendation. The asynchronous service is based on CCITT recommendation X.3, X.28, and X.29. Figure 1 below shows the MDS basic services architecture.

2.1 Protocols and Their Characteristics

The motivation to support the Basic and the Specialized Services in a very efficient manner in order to minimize the utilization of the available L-band spectrum has led to the development of a number of protocols designed specifically for this purpose. The satellite protocols were designed to take advantage of the packet data transmission capability of the system. Whenever possible, MTs are assigned channel capacity by the Data Hub. This reduces the need for MTs to compete for capacity on a slotted Aloha random access channel and results in a more efficient use of spectrum. For instance, for any data transfer from the DH requiring an acknowledgement, the DH will allocate the necessary channel capacity, on a TDMA channel, to the MT in question. The system attempts to maximize the use of TDMA rather than slotted Aloha channels since these are much more efficient.

2.2 The MDS Satellite Protocols

A number of system requirements, that affected the choice and design of the satellite protocol architecture, are identified below; these are:

1. Support for a large number of MTs
2. Optimization of the satellite resources
3. Support for various types of user traffic varying from short messages to large file transfers
4. Flow and congestion control
5. The support of a priority scheme

6. Satellite protocol modularity and flexibility to allow for future growth.

2.3 Satellite Protocols Stack

The Basic and Specialized services are supported via internal MDS protocols operating between the DH and MTs. Figure 2 outlines the architecture for these protocols. The MDS Packet Layer Protocol (MPLP) provides procedures for the setup, maintenance and tear-down of virtual circuits between the DH and MTs. It is responsible for supporting the basic MDS services. The MDS Data Link Protocol (MDLP) provides for the reliable sequenced delivery of packets to the MPLP. Functionally, it is similar to LAP-B Multi-Link Procedure (MLP). The MDS Specialized Services Protocol (MSSP) provides for the multiplexing of application messages over the Reliable Transaction Service (RTS) and the Unacknowledged Data Service (UDS) supported by the MDS Transaction Protocol (MTP) and the MDS Unacknowledged Link Protocol (MULP) respectively. The MTP is used for transaction type data exchange, while the MULP provides for the transmission and reception of unacknowledged data packets to and from MTs.

The Channel Access and Control (CAC) defines a set of procedures for accessing the physical layer. The CAC is mainly responsible for allocating TDMA capacity as well as frame assembly and disassembly of data segments at the DH and the MT. The Bulletin Board (BB) provides for the dissemination of system information from the DH to all MTs. These are: channel definition, protocol parameters, and congestion avoidance indication.

Only the satellite protocols pertinent to user data transmission are discussed.

2.3.1 MDS Channel Access and Control

The MDS CAC specifies a set of procedures to access various MDS channels. The channel types supported in MDS are: (1)the outbound DH-D, TDM

246

channel with fixed frame size, each frame contains variable sized CAC segments, (2) Inbound MT-DT TDMA channel that carries variable sized bursts, each carrying variable sized segments on a reservation basis, (3) Inbound Slotted Aloha random access MT-DRr channel that carries fixed sized bursts, each containing fixed sized TDMA request segments, and (4) Inbound Slotted Aloha random access MT-Drd channel that carries fixed sized bursts, each containing one variable sized small data segment.

The CAC is highly efficient in use of the satellite capacity. It implements an eight-level priority scheme, a congestion control algorithm, as well as a load balancing algorithm over the outbound channels.

2.3.2 MDS Packet Layer Protocol (MPLP)

The MPLP functions as the network layer of the seven layer OSI stack. It is modelled after the ISO 8208 standard. The key features of MPLP are summarized below:

- MPLP supports the X.25 and Asynchronous data services. It also supports various X.25 features like the D, Q, and M bits, the negotiation of flow control parameters, the Fast Select and MDS User Identifier (MUI). All other X.25 optional facilities which are not acted upon by MPLP are conveyed transparently through the network for further treatment at the user side.

- MPLP supports the priority selection on an individual circuit basis. The MPLP user is able to signal one of eight priority level at call setup using the throughput class facility. MPLP conveys this information to the lower layers which will guaranty the corresponding priority of access for the duration of the call.

- MPLP is optimized over a satellite channel by modifying the use of layer 3 Receiver Ready (RR). A

specific procedure to deal with layer 3 RR generation is implemented in MPLP.

- MPLP provides for the authentication of every switched virtual circuit that is established between an MT and the DH; the MUI is used for this purpose.

- The MPLP does not support the Restart procedure. However, if a restart request is received from the user, MPLP clears all virtual circuits and resets all permanent connections.

2.3.3 MDS Data Link Protocol (MDLP)

MDLP is a highly efficient link layer protocol which optimizes the use of the satellite resources. The features of MDLP are summarized below:

- The MDLP, in contrast with LAP-B does not support layer 2 RR or RNR as a flow control mechanism. The protocol uses six Protocol Data Units (PDUs).

- MDLP does not require a link layer acknowledgement as in LAP-B. Acknowledgements are withheld until the window is closed or a link layer timer expiry occurs. An MDLP task at the DH or MT can request a selective repeat from its counterpart by forwarding, in a STAT_PDU frame, a bit map of the frames received and thus minimizing the activity over the spacelink.

- In order to satisfy the requirements of the CAC layer, MDLP supports the fragmentation and reassembly of MPLP packets. MDLP uses the "More" bit for this purpose.

- The maximum window size supported by MDLP is 15, allowing up to 15 outstanding frames to be unacknowledged.

247

- The MDLP at the DH makes use of the MDS TDMA capability. When the DH MDLP is expecting a link layer acknowledgement from the MT MDLP, the latter is explicitly solicited using the Poll bit. In such a case, TDMA request is made on behalf of the MT MDLP and the TDMA allocation is piggybacked on the MDLP frame.

2.3.4 MDS Transaction Protocol (MTP)

The MTP is optimized to support transaction type applications, and a single segment unacknowledged messaging capability. That is, when the data to be exchanged takes the form of a command-response, then MTP is the choice. The MTP is ideal for applications whose message data size does not exceed the maximum CAC segment size (max. 64 bytes).

The MTP is a highly efficient satellite protocol. The MTP user has the ability to specify the response length, the response delay, the number of message repeats to increase the probability of success over a noisy channel, and the delay between repeats.

2.3.5 MDS Unacknowledged Link Protocol (MULP)

MULP is primarily designed for use in applications such as broadcast or multicast of news, weather reports, and financial market information. The major features of the MULP are outlined below:

- MULP supports multiple simultaneous applications.
- MULP supports the fragmentation and reassembly of user messages which can be significantly large (up to 64 CAC data segments).
- Data integrity is guaranteed by MULP. Corrupted user messages are deleted and discarded.
- A MULP user is capable of specifying the number of times, his message is to be repeated. This parameter is highly important, to

overcome link errors and guaranty message delivery to the destination.

3. DH LOGICAL ARCHITECTURE

The Data Hub logical architecture is presented in Figure 3. It consists of four functional sub-systems:

- MDS Network Management Sub-system (MNMS)
- Satellite Network Access Controller Sub-system (SNACS)
- Data Channel Unit Sub-system (DCUS)
- Terrestrial Interface Sub-system (TIS)

The MNMS consists of an MNMS controller which provides the management functions of the system namely: MT, configuration, fault, performance, security, and accounting. Databases are stored and maintained locally by the MNMS. Also, a Man-Machine Interface (MMI) in the MNMS provides operator command and display facilities for control and monitoring of MDS operation.

The SNACS consists of a number of Satellite Protocol Processors (SPP) and a number of Network Access Processors (NAP-D). The SPP supports all the satellite protocols except MDLP, while the NAP performs the CAC and MDLP functions. It also supports the BB function used for the dissemination of system information to the MTs.

The DCUS consists of satellite interface channel equipment for MDS data channels. The following functions are provided: encoding, interleaving, scrambling and modulation of DH-D frames, and demodulation, descrambling, de-interleaving, and decoding of received IF signal into the inbound frames.

The TIS provides interface lines to public and private data networks. It also generates call records for basic services and forward them to the MNMS.

4.0 DH HARDWARE ARCHITECTURE

A number of trade studies were undertaken to define and develop a DH architecture. The studies examined trade-offs so

the target architecture meets the timing and sizing, reliability, availability, maintainability, and expansibility system requirements.

In order to evaluate different types of processors to perform the SNACS functions, a model to estimate CPU utilization was created. The model included system threads which represent basic and specialized protocol transactions between the MT and the PDN. These threads were then linked into MDS protocol transactions and a total CPU utilization was estimated.

The following architectures were evaluated as possible candidates for the MDS. (1)fault tolerant switching processors, (2)packet switches with open architecture, (3)VAX clusters, and (4) VMEBUS SPP and NAP-D. In this section the architecture of choice is presented. All others were rejected since they did not meet the acceptance criteria.

Figure 4 below shows the DH hardware architecture. The MNMS is based on a fault tolerant computing platform, while the TIS from Northern Telecom DPN-100 packet switch provides redundancy at various levels. Each of the SPP and NAP-D consists of two redundant VME chassis housing a number of Single Board Computers (SBC), which are based on the Motorola MC68040 microprocessor. The NAP-D and SPP communicate via a dual rail Ethernet LANs. The MNMS uses the same LANs to interface with the SNACS. The LAN protocol is TCP/IP. One LAN is designated for inbound traffic (MT to DH) and the other for outbound traffic (DH to MT). The TIS interfaces with the SNACS via a number of high speed X.25 V.35 circuits at 256 kbps each. The NAP-D communicates with the DCUS by means of redundant RS485/RS530 multidrop links running at 800 kbps.

5.0 SYSTEM FAILURE RECOVERY

The design goal for redundancy is to allow for a single component failure and to recover from the failure in a minimum time period by using the redundant component. The MNMS implements a redundancy manager which collects health information from DH components. This information is processed by a rules based knowledge system in order to choose the appropriate action for a given set of detected faults or errors. When the rules have indicated a failed component is required to be switched out of the system and a healthy standby component is available, the following actions are taken:

- the failed component is commanded to go OFF-LINE
- the standby component is updated with configuration data if required
- the standby component is commanded to go ON-LINE
- diagnostics are performed on the failed component
- equipment failures are replaced with Line Replaceable Units (LRUs)
- the failed component is placed in a STANDBY mode of operation.

The NAP-D cages will send health information to the MNMS on a periodic basis. Each NAP-D cage pair is configured in a warm standby mode of operation. Failure to report status to the MNMS, or receiving an unhealthy cage status, will cause a switchover to the standby NAP-D cage. This switchover will not cause active virtual circuits to clear.

The MDS channel units are full duplex units connected to the NAP-D by redundant multi-drop links. Each channel unit may be in the on-line, stand-by or off-line state as determined by the MNMS and the health of each unit. Standby DCUs have their operational code and are waiting for configuration and state transition data.

All SPP cages are in the on-line state. They "usually" carry user traffic on a full time basis. A processor card failure will cause all calls to be re-routed to another operational SPP card by virtue of the loadsharing feature implemented in the SPP software. The SPPs are sized to operate at 50% of their ultimate full load to allow for redundancy.
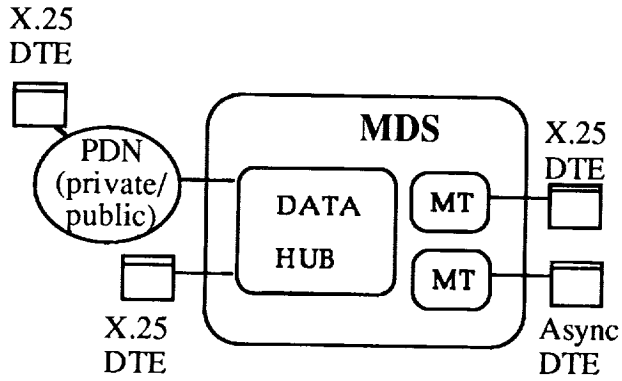
Figure 1: MDS Basic Services
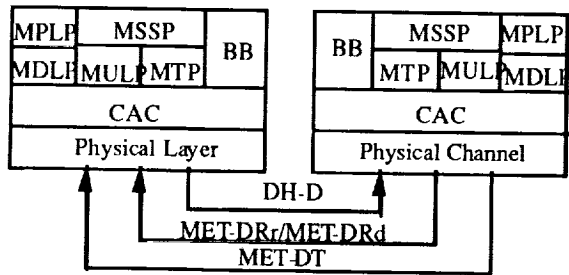
Figure 2: MDS Protocols Stack
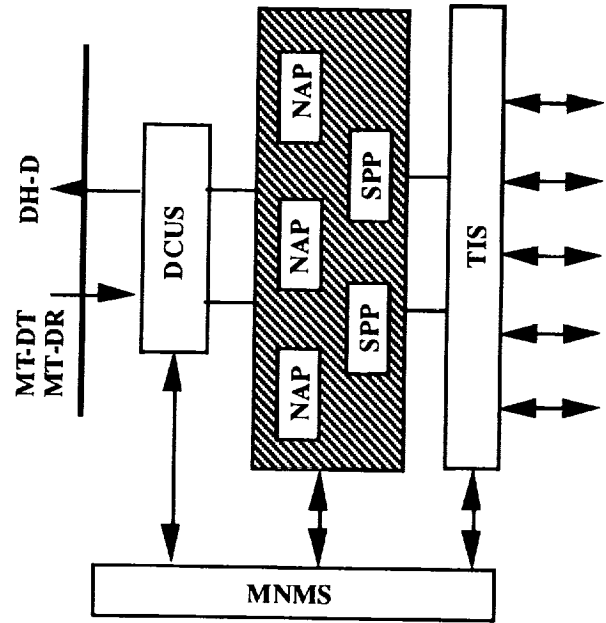
Figure 3: Data Hub Logical Architecture
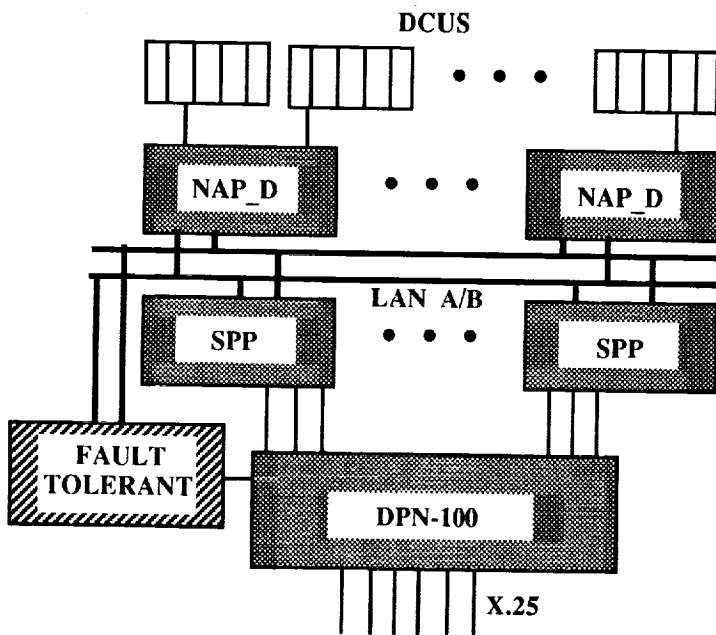
Figure 4: DH Block Diagram

EVOLUTION OF INMARSAT SYSTEMS AND APPLICATIONS

The Land Mobile Experience

Eugene Staffa and Ram Subramaniam
Inmarsat
40 Melton Street
London NW1 2EQ, England
Tel: +44 71 728 1000
Fax: +44 71 872 9538

ABSTRACT

Inmarsat has provided mobile satellite communication services for land mobile applications for well over a decade. Having started with the Inmarsat-A voice and telex system, Inmarsat is committed to the evolution of services towards a global personal, handheld satellite communicator. Over the years, users have benefited from the evolution of technologies, increased user friendliness and portability of terminals and ever decreasing cost of operations. This paper describes the various present systems, their characteristics and applications, and outlines their contributions in the evolution towards the personal global communicator.

INTRODUCTION

Since its inception in 1979, Inmarsat has beeen a major force in mobile communications. Inmarsat provides mobile satellite communications via geostationary satellites which, by virtue of their large area coverage and rapid interconnections via public switched networks, have played an important role in international communications. Inmarsat is the leading provider of emergency and disaster communications and of a variety of other mobile and transportable applications. Inmarsat land mobile services can thus be characterised as either providing an extension to public networks, or providing communications users with mobility. Table 1 provides the characteristics of the various systems.

Extending The Public Networks

Despite increasing investment in telecommunications infrastructure, there are many areas where Inmarsat is the only feasible solution for geographic, demographic or economic reasons. Inmarsat can serve the communication needs of international companies locating in areas of poor communications availability until the terrestrial networks catch up with demand. The alternative would be to postpone the decision to locate there - with the consequent loss of business opportunity, possibly millions of dollars worth of economic activity, and forgone job creation and contribution to the local economy. Inmarsat is today helping to develop the oil fields of Nigeria and Siberia, provide communications support for export control in southern Africa, and helps CIS and China in their transition to market economies, to mention only a few typical uses.

With the liberalization of the regulatory environment in many less developed countries, established businesses increasingly turn to Inmarsat as the means of securing a reliable telephone, fax or data link, essential to the conduct of their business, particularly outside the capital cities. In this way Inmarsat enables them to have the same high quality international communications that their competitors might enjoy elsewhere, contributing significantly to the expansion of global trade.

Over the past fifteen years, business demand for communications, particularly international direct dial access, has risen dramatically. The temporary or a transient use of Inmarsat-A system is serving to fill a void in countries such as smaller island communities in the Pacific or the Caribbean, or remote areas of Asia, Africa and Latin America.

Inmarsat has always been prominent in providing the UN and other international and national development organisations with means to manage their field operations and logistics in areas without terrestrial communications facilities. Inmarsat allows these agencies a more cost effective deployment of their resources in all parts of the world.

Mobility

Mobility in terms of mobile satcoms can mean a

vehicle mobile applications (i.e. terminals mounted on trucks, trailers, trains and utility vehicles), a transient, short-term temporary use by field teams operating away from base, or a transportable or portable use by individual users such as journalists or medical emergency or rescue personnel.

As the Inmarsat-A portable terminals decreased in size and cost, they have become the virtual backbone of the world emergency and disaster communications. They have been used by teams belonging not only to the UN agencies, but also to the Red Cross and other national and international organizations. They use Inmarsat for coordination or operations, supplies distribution management and they particularly appreciate the rapid deployment capability and reliability, often under extremely difficult circumstances. Their use has speeded up disaster relief to stricken areas and helped alleviate human suffering both in disasters and also in situations producing flows of refugees The current International Decade for Natural Disaster Reduction (IDNDR) will likely increase demand for mobile satcoms even further.

Similarly, the portability and simplicity of use has made Inmarsat-A communications tool of choice to hundreds of media teams all over the world to cover summits, scenes of natural disasters and wars. The Inmarsat-A portable terminal is an icon representing the mobile satellite industry that is recognisable to millions over the world.

INMARSAT-A

Inmarsat-A is an analog telephone and telex system. It operates on a single channel per carrier basis using frequency modulation and hence provides a linear channel supporting full duplex operation. In normal operation voice compandors are switched in to improve the subjective quality of the link. The summary of the technical characteristics are given in Table 1.

Network Configuration

The Inmarsat-A system comprises four independent communications networks (Satellite Ocean Regions), each network containing an opertional and spare satellite, mobile earth stations (MESs), a network coordination station (NCS) and land earth stations (LESs).

Land earth stations act as gateway between the PSTN and Inmarsat space segment. These are owned and operated by Signatories, who are also responsible for land line connections to the PSTN. Each LES has a parabolic antenna with a diameter in the range of 10-13m for transmission to and from the satellites. The uplink is at C-band and includes Automatic Frequency Compensation (AFC) System. Inmarsat-A NCS Services are provided at a designated Land Earth Station in each of the four satellite network regions. Each network co-ordination station is connected via terrestrial links to the Inmarsat Network Control Centre (NCC) in London. The NCS plays a key role in the network and is responsible for co-ordinating the access to communications channels between all LESs and MESs within the network, thereby ensuring full connectivity. The major NCS functions include SCPC call processing, monitoring of proper operation of signalling channels, database management and housekeeping, etc.

Inmarsat-A has been in service for more than 10 years and during these past years it has evolved both in the service it provides and the terminal design. In addition to the two primary services, voice and telex, a number of enhanced services have been added. The data and facsimile are two of the early services using the telephone channel. Full CCITT Group III operation is supported - the line speed (2400/4800/9600 bits/sec) being determined by the terrestrial connection.

High Speed Data

Recently, two new services were introduced - 56kbits/s - 64 kbit/s High Speed Data (HSD) and Duplex High Speed Data (DHSD). Currently available from several MES manufacturers are 56 or 64 kbit/s option kits, consisting of an additional digital encoder and modulator; the typical electrical interfaces for HSD are CCITT V.35 and RS-422. The HSD signal is sent to one of several LES that provide for automatic or semi-automatic interconnection to terrestrial switched digital networks, e.g. COMSAT, Eik or Goonhilly.

For Duplex High Speed Data (DHSD) operation, fully automatic, single number dialling has been adopted. The DHSD call starts as a duplex voice grade circuit, until the MES is switched to data mode. The development of HSD and DHSD services has provided the media community and oil/gas industry users with a means to transmit voluminous data files as well as still video pictures in more effective manner.

Another typical application is transmission of high quality voice (7.5 kHz), for example to provide **real time** broadcast quality to a news bureau. A G.722 audio codec and a transportable Inmarsat-A MES (available from several manufacturers or rental

agencies) are used by a news reporter to a news organization or bureau. It should be be noted that in the direction from the bureau to the reporter, a regular analogue voice channel is used as well.

For DHSD, typical additional real-time applications may be video-teleconferencing, or use the capacity for the provision of a multiplexed channel, offering a number of digitized voice, fax and data channels.

Terminal Evolution

Along with the service evolution, the land transportable terminal design have also evolved to provide smaller, lighter and easy to use terminals. At the start of service, the terminals were bulky, several hundred of thousands cubic centimetres, weighing more than 75 kg and consuming about 400 watts during the transmit. These terminals provided only voice and/or telex capability. In contrast, the contemporary transportable terminal could weigh as little as 23 kg including the foldable antenna. Inmarsat-As can be assembled in a few minutes and use simple antenna pointing system to enable correct orientation to the selected satellite. It would consume only about 280 watts during transmit.

INMARSAT-B

Inmarsat-B, which will start commercial service during this year, is the digital version of the Inmarsat-A system. It is also capable of operating with the spot beams of Inmarsat-3 satellites. Being an advanced digital system, there is scope for reduction in the space segment resource requirement, and therefore for a reduction in the end user charges. This fact will be particularly welcome by high volume users, as well as by new ones who will now see the economic hurdle to becoming an Inmarsat user considerably lowered. This, in turn, should give a renewed impetus to the use of satcoms by both the business community and by the international emergency and aid organisations.

The system provides voice, data, fax group calls and telex. Near toll quality voice is provided using 16 kbits/s voice codec algorithm. The G/T requirement of the terminal is the same as of Inmarsat-A (-4 dBK), hence the antenna requirements remain the same. One compact Inmarsat-B MES already available weighs 18 kg including a flat panel antenna. Its polymer packaging case is watertight when packed, and rain-proof when deployed, and can withstand a 30-inch drop on concrete. A DHSD facility is designed to be

standard: it can support up to 8 simultaneous telephone or up to 20 data channels. The summary of the technical characteristics is given in Table 1.

INMARSAT-C

The Inmarsat-C system was designed as a low cost, compact data messaging system for operation at sea and in a wide range of land mobile applications. The system has been in commercial operation since January 1991. The system operates on a packet transmission basis over the Inmarsat satellite which is able to interface to a range of terrestrial messaging systems including telex, X.25, voice band data and various electronic mailbox services. The summary of the system characteristics are given in Table 1.

The Inmarsat-C system provides Store and Forward Messaging, Data and Position Reporting, Polling and Enhanced Group Call services. The Store and Forward mode provides the user a reliable means of sending data or text messages between the mobile terminal and the fixed network subscriber via the satellite and either the public or private terrestrial services.

The data reporting protocol permits the user to send short messages of up to 32 bytes via a special channel. This service can operate on a "reserved" basis where the terminal sends a data report at pre-determined times or on an unreserved basis when it is sent at random. An acknowledgement of delivery is always provided. The polling service is used to initiate transmission of a data report from a mobile terminal. The polling signal defines how and when the terminal should respond and can address single or multiple terminals and optionally, it can also be limited to a defined geographical area. The Enhanced Group Call (EGC) service is a fundamental part of the Inmarsat-C system and provides the ability to broadcast messages to mobiles in a very flexible manner. The Land Mobile Alerting function is a special type of data reporting packet, used for alerting the LES and/or other service providers about an emergency (or a high priority message) via an Inmarsat-C terminal.

Inmarsat-C terminals for mobile applications are compact in size (4500 cm^3) weighing 3.5 kg, with a detachable antenna unit including HPA/LNA weighing about 2 kg. The antenna is omnidirectional and hence pointing to the satellite is not required.

The briefcase or portable terminals are lighter (4 kg) and smaller in size, with an integrated antenna. These terminals have directive high gain antennas to reduce the power consumption, hence it could operate

with batteries. No assembly is required, only simple antenna pointing to ensure correct orientation to the selected satellite. These terminals are the first generation of Inmarsat personal communication products.

The chief attractions of Inmarsat-C are its low cost terminals and the inexpensive communications charges, particularly for very short messages. Other very useful attributes are the public network interconnection and the ability to work with a variety of peripheral equipment via a digital interface. This powerful combination of user economics and engineering flexibility enables a virtually limitless range of applications.

Road Transport

One of the main successes for Inmarsat-C has been in the support of fleet management for the road transport industry. With this system, it is possible to set up closed user networks with any number of vehicles, as well as one or any number of individual users in an open network configuration. Fleet management is possible by continuous contact between the driver (and/or vehicle computer) and the dispatcher. Short data reports from vehicles, containing the position information determined by the integral GPS receiver, can be received and temporarily stored at the LES for delivery by a terrestrial link. They could be transmitted directly to a Inmarsat-C at the dispatcher's office, using a 'double hop'. This method, obviating the need for a terrestrial line altogether, can be very useful in cases where the terrestrial link is unavailable or unreliable.

Regular position reports can be displayed on a digital map in a dispatcher's office, together with a possible accompanying message. The ability to poll individual vehicles or entire fleets is seen by trucking operators as a most exciting feature - one that cannot be obtained over very large areas by terrestrial means. The satcom-based method of fleet management and control has saved many trucking companies thousands of dollars annually, making the investment in Inmarsat-C pay for itself in a very short time. There are several end-to-end solutions already on the market and 'one-stop-shops' for system implementation are now established on both sides of the Atlantic, e.g. in the Netherlands, the UK, Brazil and elsewhere.

Even simple two-way messaging can provide substantial benefits in the mobile environment. A very good example of this is the use of Inmarsat-C by a number of UN agencies, particularly by the UN High Commissioner for Refugees in Bosnia and elsewhere, substantially improving the logistics control and improving the emergency response capability. Other humanitarian agencies have used Inmarsat-C in support of their activities in food distribution in Russia and Africa.

Tracking of vehicles, trailers or cargo containers is another very good prospect for Inmarsat-C. It requires development of a securely mounted 'package' with a low-profile antenna and a reliable stand-alone power supply. The market for such device is estimated at several hundreds of thousands of units worldwide. Similarly to road transport, rail transport requires reliable data reporting and polling system, available over long distances and vast areas. Particularly in case of accidents in remote areas, satcoms are indispensable. Countries like China, Russia, Australia and others on all continents have tested Inmarsat-C for this purpose. The results are very encouraging and may lead to significant implementation schemes in the near future.

Electronic Office On The Move

Because of its worldwide reach and easy portability, Inmarsat-C is becoming a favourite with print journalists, aid workers and even the general business traveller. The most alluring feature of the system is the ability to send text files, even fairly large (up to 32 kbytes), composed on a PC attached to the Inmarsat-C transceiver, directly to a fax number, to another PC via PSTN or PSDN, and to send and retrieve messages from a mailbox set up at the LES or at any other appropriate point along the network. Recent advances in applications development also allow a direct connection to e-mail networks, enabling the Inmarsat-C user to become a remote or mobile X.400 user!

Rural, Remote and Backup Communications

Low investment cost as well as the ever expanding array of access modes and applications make Inmarsat-C an ideal system for all sorts of situations where voice contact is not required or is not necessary. Entry or retrieval of information in remote locations, whether by rural hospitals or by educational institutions or businesses, is a fast developing Inmarsat-C market. Several specific software applications are now under development in various parts of the world, for example to address rural banking requirements. An attractive applications area for Inmarsat-C networking is establishment of communications networks for dispersed communities, for example in Latin America, Africa and Asia.

254

SCADA

Remote sensors and control devices coupled with an Inmarsat-C transceiver allow Supervisory Control and Data Acquisition (SCADA). Large 'fleets' of SCADA terminals are envisaged for water management, pipeline and power lines monitoring, and remote industrial process control. In addition, applications for earthquake monitoring, hurricane or tropical storm warning, and flood reporting are being developed.

INMARSAT-M: A BREAKTHROUGH IN LOW COST MOBILE SATCOMS

In response to demand for smaller, lighter and cheaper mobile satcoms, Inmarsat has developed Inmarsat-M, the world's smallest, lightest and cheapest satcom voice terminal. This new digital standard, being made commercially available at this time, offers voice, fax group 3 and 2400 bits/s data facility. It will likely become a system of choice for tens of thousands of new users.

Inmarsat-M shares a common access control and signalling subsystem with the Inmarsat B system, thereby allowing significant economies of scale to be achieved in all ground segment components of the system.

The Inmarsat-M system provides duplex telephony employing an SCPC channel supporting a speech codec rate of 6.4 kb/sec (including FEC) in both forward and return directions, using an overall channel rate of 8 kbits/sec. Speech quality is adequate to allow connection to the public switched telephone network (PSTN).

For land application, there are primarily two types of terminals - one to serve the vehicle market and the other to the portable market. The vehicle mounted terminals have two units. The outdoor unit consists of the directional antenna, the HPA, the LNA and the diplexer(s). The indoor unit consists of the rest of the electronics. The high gain required to achieve the G/T of -12 dBK warrants a directional antenna with about 14 dBi gain, hence tracking is required. A 5-element cavity-backed spiral one dimensional array antenna with wide elevation and narrow azimuth beam was the first generation of antennas. These type of antennas are high profile and rather heavy. The evolution and technological development of antennas have produced an attractive low profile phased array antenna which can be mounted in place of the sun-roof of a car. Both of these antennas require mechanical steering in the zimuth

plane to track the satellite. An electronically steered adaptive monopole antenna would also achieve the required G/T with a reasonable profile and acceptable appearance for the vehicle mounted market.

'Portable' Users

The portable terminals are usually packaged in a briefcase type enclosure, with dimensions about 450x300x80mm. These have either detachable antenna or built-in antenna, under the cover of the case. In either case, patch arrays are used to obtain the gain required. Some design have folded antenna to achieve higher gain (about 18 dBi), in order to reduce the power consumption. This enables the terminal to operate with batteries for up to an hour without recharging.

This means that an independent satellite phone phone with an unlimited reach, is now available to the businessmen, explorers, surveyors, engineers, reporters, medical staff, security and government officials, with even greater ease than that offered by Inmarsat-A. As is the case with the existing Inmarsat-A and Inmarsat-C communications, productivity of people operating satcoms outside the available public networks is dramatically improved, reaping benefits many times in excess of the investment or operating costs of satcoms.

Thin Route Operations: Extension of Public Networks

Isolated land-locked or island communities can use Inmarsat-M as a cost-effective means of establishing a direct-dial telephone and fax service. The benefit of immediate and reliable communications is surely going to be felt not only in case of emergencies, but also in the conduct of business hitherto impossible due to lack of communications. In rural areas, communications availability is not always keeping up with demand. This is especially true for many farming regions, as well as for remote mining operations, logging, explorations and other temporary or transient activities.

Mobile Users

In Inmarsat-M, the mobile users - in trucks, cars, trains - can for the first time enjoy the benefits of satellite voice service. A low profile antenna enables Inmarsat-M installation not only on trucks, but also on a complete range of utility and even personal vehicles.

This creates a tremendous market opportunity even before further planned miniaturisation takes place. Similarly to Inmarsat-C, Inmarsat-M has been already trialled for the use by the railways, both on moving trains - for passenger use as well as the crew - and for the track maintenance teams and in case of emergencies. Inmarsat-M proved a very viable and cost-effective solution.

PAGING

Satellite paging is designed to complete the family of Inmarsat services, responding to several important user requirements: very low cost (around five hundred dollars); ability to work in the urban environment; offering a limited coverage even inside buildings (i.e. without the direct sight of a satellite); and, being receive only device, not requiring special licences or regulatory considerations. The messages can be broadcast in one or more ocean regions simultaneously, depending on the level of service subscribed to.

The service, with its pocket-sized alphanumeric receivers, will be a boon to international travellers, and is expected to be taken up by a whole range of vehicular users. Additionally, both Inmarsat-M and Inmarsat-C briefcase terminals can have an integrated pager for receiving alerts or short messages independently of whether actually turned on or logged in. The user can then call back when convenient.

WHAT THE FUTURE HOLDS

Inmarsat is continually striving towards goals of user friendliness, easy portability and lower cost. For Inmarsat-C, the work on the Applications Programming Interface (API) should go a long way towards complete modularity of various elements from LES to the MES and peripherals.

Inmarsat-M services and terminals may change further with introduction of more powerful Inmarsat-3 satellites in the 1995/6 timeframe. The spot beam capability of these satellites has opened up a wide range of possibilities of evolution of Inmarsat products such as smaller terminals (notebook size), and smaller, cheaper and more attractive antennas (e.g. vertical rod, disc and small horn) for vehicle mounted applications. On the service side, higher rate data and fax service, secure voice service, credit card facility and ISDN functions will all evolve in the coming years.

Inmarsat-C and Inmarsat-M are significant contributions towards small, easy to use personal satellite communications. But the ultimate goal to reach is a hand portable personal global communicator, so called Inmarsat-P. Development work on it is well underway for introduction around the end of the decade.

Table 1: Inmarsat systems technical characteristics

Characteristics	Inmarsat-A	Inmarsat-B	Inmarsat-C	Inmarsat-M
Typical antenna gain (dBi)	20	20	2	14
Typical antenna example	Parabolic Reflector	Dish/flat	Quadr. helix	Spiral/Lin. arr.
Typical antenna size	1.2 m dia	1 m dia	100 x 25 mm cyl	0.4m dia/length
MES figure of merit (dBK)	-4	-4	-23	-12
MES EIRP (dBW)	36	33	13	22
Voice coding rate (bit/s)	N/A	16k APC	NA	4.2 IMBE
User data rate (bit/s)	9.6k	9.6k	600	2.4k
Comm. channel rate/modulation	FM	24k/OQPSK	1200/BPSK	8k/OQPSK
Interleaving time (s)	N/A	N/A	8.64	N/A
Forward link satellite EIRP (dBW)	18	16	21.4	17
Channel spacing (kHz)	50	20	5	10
HSD/DHSD option	56/64 kbit/s	64 kbit/s	N/A	N/A
Scheduled service date	1982	1993	1991	1993

ACTS Advanced System Concepts and Experimentation

Mr. Brian S. Abbe
Jet Propulsion Laboratory, California Institute of Technology
4800 Oak Grove Drive, MS 238-420
Pasadena, CA 91109, USA
Phone: 818 354-3887
Fax: 818 354-6825

Mr. Noulie Theofylaktos
NASA/Lewis Research Center
21000 Brookpark Rd., MS 54-6
Cleveland, OH 44135, USA
Phone: 216 433-2702
Fax: 216 433-6371

Abstract (full paper will be provided at the Conference)

Over the course of the first two years of experimentation with the Advanced Communications Technology Satellite (ACTS), many different K/Ka-band applications-oriented experiments will be conducted and evaluated for their commercial viability. In addition, the technological developments and advanced systems concepts associated with the various terminals and the satellite itself will also be examined. Beyond these existing experiments and the current terminal developments, many other new and exciting experiment ideas and advanced system concepts exist. With the additional use of ACTS for the last two years of its lifetime, many of these ideas could be explored.

In the mobile satellite communications arena, a particular applications-oriented concept that has yet to be developed is a maritime-mobile experiment. Applications of K/Ka-band mobile satcom technologies to the pleasure cruise industry could provide similar communications services as those that are being developed for the broadband aeronautical experiments. A second applications-oriented experiment that could be of interest is the development of a hybrid satellite-cellular system experiment. In such an experimental system, a mobile K/Ka-band satellite service would extend the coverage of the already existing cellular network.

Many new system concepts and terminal developments could also be accomplished. The initial characterization of the K/Ka-band mobile satellite communications propagation channel and evaluation of the currently existing rain compensation algorithms (RCAs) could lead to a second generation RCA development that would improve the overall ACTS Mobile Terminal (AMT) performance. In addition, the development of an enhanced modem to be used with the AMT that utilizes CDMA spread spectrum would also improve the overall terminal efficiency and provide a greater commercial potential for K/Ka-band applications. Other techniques worthy of further exploration and evaluation include the development of new Doppler estimation algorithms and demodulation techniques such as pseudo-coherent demodulation. The possibility of exploring these new and exciting experiment and conceptual ideas, as well as many others, with an extended ACTS satellite lifetime, will be examined in this paper.

Session 7
Current and Planned Systems

Session Chair—*Chandra Kutzia,* Com Dev Ltd., Canada
Session Organizer—*Jack Rigley,* Communications Research Centre, Canada

(continued)

EUTELTRACS
The European Experience on Mobile Satellite Services

Jean-Noël Colcy, Rafael Steinhäuser
EUTELSAT
33 Av. du Maine, F75755 Paris Cedex 15
Phone: + 33 1 45384786, Fax: +33 1 45384798

ABSTRACT

EUTELTRACS is Europe's first commercially operated Mobile Satellite Service. Under the overall network operation of EUTELSAT, the European Telecommunications Satellite Organisation, EUTELTRACS provides an integrated message exchange and position reporting service.

This paper describes the EUTELTRACS system architecture, the message exchange and the position reporting services, including the result of recent analysis of message delivery time and positioning accuracy.

It also provides an overview of the commercial deployment, the regulatory situation for its operation within Europe and new applications outside its target market, the international road transportation.

SYSTEM ARCHITECTURE

The EUTELTRACS system is a mobile satellite system which provides customers in Europe with two-way data communications as well as vehicle position-fixing, such services being offered within the coverage of the EUTELSAT satellites (Figure 1).
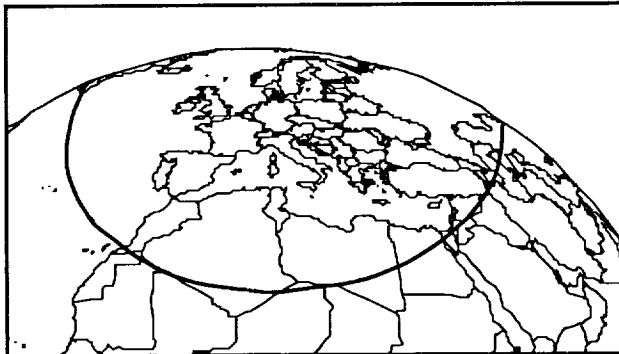
Figure 1 - EUTELTRACS Service Coverage

It is based on the same design as the OmniTRACS system [1] which has been operated by QUALCOMM on a commercial basis in the USA since November 1988.

Figure 2 highlights the components of the EUTEL-TRACS system. One can distinguish five basic elements in the system:

- the customer's terminal or dispatch centre, and its link to a Service Provider's Network Management Centre (SNMC), with which the customer is able to send and receive messages and also to access position information about his fleet of mobiles;

- the SNMC and its link to the Hub Station which processes and keeps a record of all transactions with the customers;
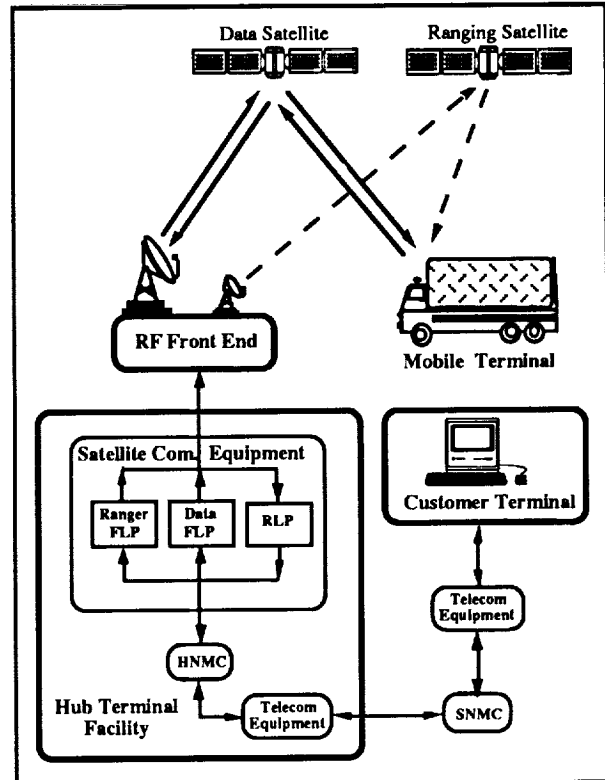
Figure 2 - EUTELTRACS Network Architecture

- the Hub Station, consisting of two antennas and associated RF frontends, and the Hub Terminal Facilities (HTF), whose main functions are to process, control and monitor the traffic flow (messages and position information) between SNMC's and the mobiles. In particular, the Hub Terminal Facilities provide all necessary functions in order to control satellite access in both directions (base to mobile and mobile to base);

- the EUTELSAT satellites, which are used to transmit the Forward Link carrier (transmitted by the primary Hub antenna to the mobiles), the Return Link carriers (transmitted by the mobiles to the Hub station) and the Ranging beacon (transmitted by the secondary Hub antenna to the mobiles). The Ranging signal is to support the localisation function (the signal is for localisation timing information only and contains no data modulation).

- the Mobile Communication Terminal (MCT), mounted on the vehicle, with which the vehicle driver can receive messages from his base and transmit messages back to it. The same Mobile Communications Terminal is used to perform the necessary measurements for the position reporting service.

MESSAGE EXCHANGE SERVICE

Satellite Transponders

The EUTELTRACS messaging system operates on the Data Satellite through two transponders on orthogonal polarisation.

The Forward Link is a "power" link, typically requiring a saturated transponder in order to maximise the power flux density on the earth's surface.

The Return Link is a bandwidth link requiring 36 MHz of bandwidth (to accommodate the messages generated by 45,000 MCT's), but little power due to the low EIRP radiated by the MCT's.

Forward Link

The Forward Link is composed by a Time Division Multiplex (TDM) stream transmitted by the Hub Station and received by the MCT's, on a single carrier communication link [2]. The Forward Link wave form is mixed with a chirp wave form to mitigate potential interference from nearby satellites and multipath fading. The Forward Link signal occupies a 2 MHz bandwidth due to the spreading wave form.

The data information is sent out at data rates of 4,960 bits/second (BPSK, rate 1/2 Golay encoded) called the 1X data rate or 14,880 bits/second (QPSK, rate 3/4 coded) called the 3X data rate. This results in a constant 9.92 ksymbol/s PSK wave form occupying 9.92 kHz of bandwidth. The choice in the actual data rate used for each individual MCT is done dynamically and depends on the reception environment of the mobile.

Return Link

The Return link (mobile to hub), is a low information data rate stream using a rate 1/3 convolutional encoder (K=9) in conjunction with Viterbi decoding. A powerful interleaving scheme reduces interference effects such as those FM/TV could create.

As shown in Figure 3, a combination of techniques [2] is involved to generate the MCT Return Link wave form. It combines a 32-ary FSK scheme, which encodes 5 coded symbols onto one FSK symbol, to a DSS (Direct Spreading Sequence) MSK modulation at 1 MHz rate. The resulting signal is then randomly frequency hopped over the whole Return link bandwidth to increase the resistance of the transmission to potential interference. The transmitting MCT and the receivers at the Hub use the same frequency hopping pseudorandom sequence, enabling the reception and demodulation of the data.

During message transmission on the Return Link, the MCT transmitter amplifier operates at half duty cycle so that antenna tracking maintains lock on the Forward Link downlink signal. Transmission is enabled 50% of the time

at 15.12 millisecond intervals. During the next 15.12 ms, the amplifier is disabled to perform antenna tracking on the Forward Link down link to maintain pointing, frequency tracking and time tracking tasks.

Each transmission interval contains either one 32-ary FSK symbol at 1X data rate (55 bit/s) or three 32-ary FSK symbols at 3X data rate (165 bit/s). The choice on the actual data rate used for each individual MCT is done dynamically depending on the transmit environment of the mobile. That choice is under control of the Hub Network Management Computer (HNMC) which monitors all Return Link signal levels, thus instructing the MCT's.
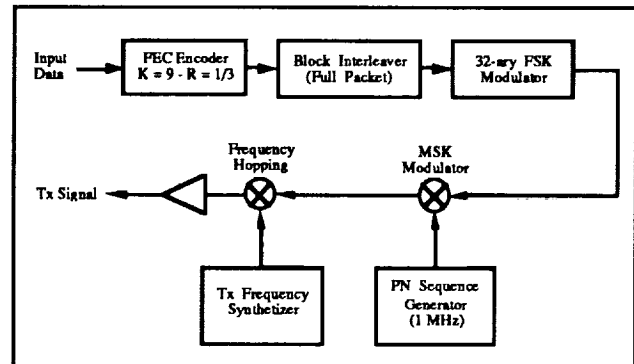
Figure 3 - Return Link Transmit Signal Generation

Acquisition of the Forward Link and set-up of the MCT through reception of special system packets is required before the MCT will attempt any transmit tasks. These packets are periodically broadcast for using the proper return frequency channel.

Data integrity

The messaging function uses a fully acknowledged store and forward protocol.

On the Forward Link, the mobile is required to acknowledge the successful reception of the packets by transmitting an acknowledgement packet on the Return Link. If no acknowledgement is received, the packet is retransmitted up to 12 times in one hour before being declared as not acknowledged. No new messages are transmitted to an MCT before completion of the previous message.

On the Return Link the packets transmitted from the MCT's are acknowledged by the HNMC. If no acknowledgement is received by the mobile the message is retransmitted for up to 50 times before aborting it.

On both links the acknowledgements are sent only if the FEC is able to reconstruct the packets without any error. This procedure ensures that the messages delivered to the mobiles or to the dispatch centre are completed and error free.

Messages Delivery Time

The performance of the system can be estimated measuring the delay time, including the queuing time before transmission, necessary to establish a full data exchange from the first transmission of a packets to the reception of

the acknowledgement. The distribution of the delay time can be interpreted in terms of number of attempts to establish a full transaction.

Four categories have been defined for the purpose of the analysis:
- data exchange which only needed 1 try (delay time between 20 to 30 sec);
- data exchange which only needed 2 or 3 tries (delay time between 2 min to 3 min);
- data exchange which needed up to 8 tries (delay time between 12 min to 20 min);
- data exchange which needed up to 12 tries (delay time < 1 hour);
- packets which never go through and are not delivered.

The distribution within the above categories depends upon the mobile environment. Three kinds of different environments were defined:
- environment without any blockage (i.e. fixed site, maritime or aeronautical applications, etc.);
- environment as encountered by a land mobile in motion in flat or hilly country, suburban area, etc. refered to as the nominal environment for land mobile applications;
- marginal environment (i.e. edge of coverage, elevation angle to the satellite lower than 10°, mountainous area, large city with skyscrapers, etc.).

Table 1 presents the performance as measured during test campaigns [3] performed with mobiles in motion:

	20 to 30 sec	2 to 3 min	12 to 20 min	< 1 hour	not deliver
No block.	99.2%	0.6%	0.2%	0%	0%
Nominal	85.6%	9.9%	4.5%	0%	0%
Marginal	73.3%	14.9%	8.1%	2.9%	0.8%

Table 1 - Message delivery time distribution

These results show that for land mobile applications more than 95% of the messages are delivered within three minutes. For other applications as fixed sites, aeronautical or maritime applications, a percentage of 99% of the messages is reached within a delivery time of half a minute.

In addition they prove that the communication is still possible in extreme cases such as urban areas or edge of coverage and low elevation angle to the satellite with only less than 1% of the messages which could not get through the system with the normal procedure. In that case, the customer gets an information of no delivery of his message and can require a further try via the Hub if so desired.

MOBILE POSITIONING SYSTEM

Method

The method calls for two separate satellites in geostationary orbit in order to derive timing information from the signals transmitted through the two satellites. A precise timing measurement of the round trip delay and the time difference between the two wave forms transmitted by the Hub station as measured at the MCT provide all the necessary information for the determination of the vehicle position by multilateration [4]. This method was chosen for the positioning system because of its consistency, reliability, economy and accuracy.

Normal messaging is performed through the primary satellite with Forward and Return Links. Round trip delay is measured for all message packets as part of the demodulation process. When a Return signal is detected, time alignment must be adjusted and maintained otherwise demodulation of the message will not occur and a retransmission will ensue.

The secondary Hub station uplinks a low power signal identical to the forward message signal (though not carrying any information) through the Ranging satellite. The period of the triangular spreading signal in this copy of the message wave forms is long enough in time so that position ambiguities do not arise through the coverage when the MCT antenna acquires and tracks alternately the two forward link signals from two different pointing directions. The antenna stops tracking the Primary down link signal, acquires and tracks the Ranger signal, and then returns to the Primary. After acquisition of the ranging signal, the MCT reports the derived time difference with any return message or acknowledgements of forward messages. This Position Report packet in this system contains time difference information rather than a true position.

Satellite positioning

In order for the Position Reporting System to locate vehicles on the earth, a reliable means of supporting that function with current and accurate satellite positions is necessary. Rather than obtain ephemerides from satellite controllers, satellite position determination is obtained through the reverse process of multilaterating the satellite from fixed terminals.

The ability to pinpoint the satellite in real time provides a robust positioning system which immediately follows any stationkeeping manoeuvres and quickly adjusts to backup satellite configuration in the unlikely event of a satellite failure. There is complete identity in hardware and software used by the Fixed Units and the mobile units. The main difference between them within the system is how the Hub Terminal views them.

Fixed unit geographical locations are important for the positioning accuracy, both for the satellite location and hence the MCT location. Fixed Units must be spread as far as possible within the service coverage and yet have an antenna gain high enough to satisfy the link budget requirements.

Altitude Model Data Base

The distance values from the MCT to the two satellites derived from the time measurements must be combined with the altitude information to estimate the MCT location. This altitude model is included in a numerical database of the Earth's shape which resides in the HTF computer. The distance from the centre of the earth based on the WGS84 ellipsoid. Altitudes above this are based on the USGS (United States Geological Survey) world data base, which includes recent satellite survey data. The grid spacing currently implemented for simplicity and memory

considerations is ten arc minutes, with a model height precision of 100 feet. Mobile positions within the grid spacing use linear interpolation to derive the mobile's altitude. Hence, in rough currently terrain, the altitude model will be in error by 1/2 the peak-to-peak roughness if mobiles travel typically in the valley floor.

Positioning Accuracy

The position error have been analysed in terms of two components:

- a position bias error between the measured average value given by the Position Reporting system and the real coordinates (estimated using high accuracy maps or, when not available, using a GPS receiver) mainly due to the inaccuracy of the altitude model database. This error express itself as a North / South bias in the position solution;
- a random error between the measurements for a given location, which can be described in terms of average error and maximum error with a given confidence level (usually 95%) and will depend on the angular separation between the two satellites, the timing accuracy of the different signals and the positioning accuracy of the 2 satellites used. As the angular separation along the geostationary orbital arc between two EUTELSAT satellites can at present range from 3° to 14.5°, this error express itself mainly as a East / West random error in the position solution. Figure 4 presents the random accuracy variation versus the satellites angular separation. These performances induced an operational limit of 6°.
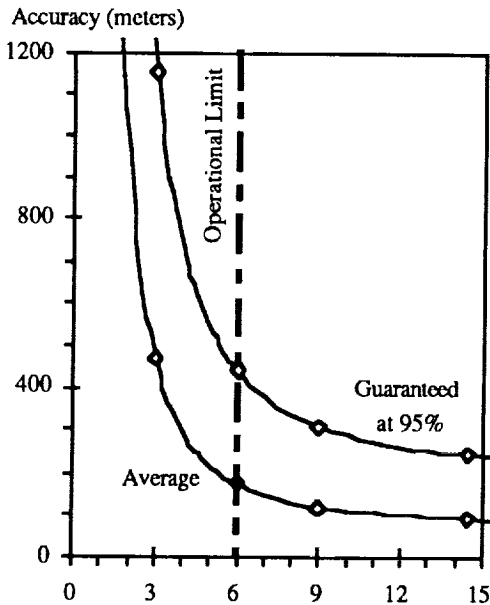
Figure 4 - Random Accuracy vs. Satellite Angular Separation

It should be noted that in the case of land mobile applications the Root Sum Square (RSS) applies with the two above errors, while in the case of maritime applications, only the random error has to be considered.

Tables 2 and 3 show the positioning performances of EUTELTRACS as recorded during recent field trials.

	Maritime	Flat	Hilly	Mount.
Aver.	n.a.	10m	40m	200m
Guar.	n.a.	20m	120m	420m

Table 2 - Bias Error versus Environment

	3°	6°	9°	14.5°
Aver.	460m	170m	120m	80m
Guar.	1150m	440m	320m	240m

Table 3 - Random Accuracy vs. Satellite angular Separation

To conclude, we can state that for instance using two satellites having 14.5° of angular separation, the positioning error of a maritime mobile is of around 80m as average value and 240m as guaranteed limit in 95% of the cases, and the position error of a land mobile travelling in hilly country is found equal to:

$$\sqrt{40^2 + 80^2} = 90m \text{ as average;}$$

$$\sqrt{120^2 + 240^2} = 270m \text{ limit in 95\% of the cases.}$$

COMMERCIAL DEPLOYMENT

The Service Provision

In terms of commercial deployment, EUTELTRACS operates via national or regional Service Providers, each connected to the central Hub station operated by EUTELSAT from a base just outside Paris. The enduser therefore has the dual advantage of being able to exploit pan-European products and services while at the same time dealing directly for everyday needs with a local and immediately accessible service management.

Overall responsibility for the EUTELTRACS service is consequently divided between three key parties: as network provider, EUTELSAT makes available the space segment, the satellite capacity, and the central hub facility. It also takes responsibility for monitoring and controlling the network during EUTELTRACS operations.

All aspects concerning system hardware and software and the mobile terminals themselves are handled by ALCATEL QUALCOMM, which also takes overall responsibility for marketing.

Finally, the individual regional Service Providers deal with the endusers and act as an interface between their customers and the network provider. Service Providers operate individual Service Network Management Centres (SNMC's) in their own region, from where they channel their customers' traffic to the Hub station; consequently, it is the Service Providers who invoice the endusers for the transactions, the equipment and software, and the installation, maintenance and training.

Advantages for the Road Transportation

For the vehicle fleet operator, EUTELTRACS is a valuable tool in the drive for increased efficiency, reduced

overheads, a sharper competitive edge, approved quality assurance, maximum security and tighter, Just-In-Time deliveries.

By coordinating fleet vehicle activities using the EU-TELTRACS system, less time is lost on the road, there is a significant decrease in empty kilometres and forward planning becomes more effective. Fuel and maintenance overheads have been shown to be reduced, delivery dates can be guaranteed with a far higher degree of accuracy and fleet flexibility is significantly increased.

The benefits of the system for the monitoring of critical deliveries and the provision of realtime information on the status of perishable loads are considerable, as are the facilities for tracking and relaying emergency alerts on hazardous goods and valuable loads.

Finally, as the manufacturing industry continues to strive for tighter margins and streamlined productivity by using the latest Just-In-Time production methods, transportation companies can use EUTELTRACS to redirect shipments or change pickup points at a moment's notice, thereby reducing delays and increasing transport flexibility.

Specific Benefits of Euteltracs

Unlike any existing or projected competitors in the land mobile communications field, EUTELTRACS offers endusers specific benefits that are tailormade to the needs of the European transportation industry:

- Fully integrated message exchange and position reporting system: There is no additional equipment or cost burden for position reporting;
- Low entry cost system: The development of a proven communications technology that can exploit capacity on non-dedicated satellites, accurate even when in inclined orbit, has resulted in a system that offers guaranteed availability, long-term reliability and a low cost-toefficiency ratio;
- A "one stop shopping" service: The enduser obtains the entire service from a single point of sale for subscription, transactions, terminals, software, installation, maintenance and financing;
- Full territorial coverage: The EUTELSAT satellites assure permanent Europeanwide access to the system even in mountain ranges and areas of low traffic density;
- It is designed for regional applications: Only a single Hub station is necessary, leading to optimised and rapid response network management;
- A proven system: The EUTELTRACS technology is well established and large numbers of terminals are already installed worldwide;
- Integrated computer communication: Messages are transmitted as computer-compatible data, enabling further processing at both ends of the data link;
- Fully harmonised system for land mobile applications: The modulation, coding and satellite access scheme, as well as all protocols used, are adapted to cope with the land mobile radioelectric and topographic environment conditions;
- Secure, closed-user-group system: There can be no "intruders" in the system.

Present Commercial Situation

At the present time nine Service Providers are offering the service to ten European countries. They will soon be joined by a Service Provider in Hungary, first country in central Europe to offer EUTELTRACS . Trials in Russia already started and a Service Provision in the course of 1993 is expected.

Nearly 2,000 EUTELTRACS terminals have been delivered to Service Providers for installation on vehicles. Present projections indicate that over 4,500 terminals will be operational by year end 1993. A similar uptake than the one of the US OnniTRACS service can be expected, where after 3 years nearly 40,000 terminals are in operation.

REGULATORY CONSIDERATIONS

Regulatory Overview

Each of the countries in Europe that comes within the EUTELTRACS service coverage area, has its own national regulations for the operation of radio equipment within its jurisdiction. In most cases, such regulations require the Mobile Service Operator to obtain an individual license for the use of the equipment concerned, on each and every occasion that he enters any country. Clearly, such a requirement is not compatible with the concept of a European wide mobile Satellite Communications Service.

CEPT Recommendation

As a first step towards resolving this situation, the CEPT, in October 1988, issued a recommendation that introduced the concept of the CEPT circulation card. This circulation card is intended to be accepted in lieu of a license for use of the designated equipment within any of the participating countries. In order to become a participant in the circulation card procedure, the Administrations of the countries concerned are required to provide a written "declaration", identifying the type of equipment involved and confirming that it may enter and/or operate within that country without the need to acquire a separate license of any kind.

To avoid the need for such a circulation card procedure in the longer term and particularly to eliminate the need for the mobile terminal operator to have to carry the associated documentation, the CEPT issued in February 1991 a further recommendation on transborder operation of EUTELTRACS terminals within Europe. This recommendation introduced a procedure that envisages unobstructed transborder operation on the basis of a European wide recognition of a properly authorised terminal carrying the appropriate logo and type approval certification number. Ultimately, this type approval will meet the European Telecommunications Standards Institute (ETSI) standard. Implementation of the requirements of this recommendation will require major changes in the regulatory regimes in most European countries and will therefore take time to achieve. In the meantime, the circulation card procedure is available as an interim solution.

265

EUTELSAT Regulatory Activities

In order to increase awareness of these CEPT Recommendations and to promote a speedy action in their implementation among the EUTELSAT member Administrations, the Eutelsat Executive Organ initiated a program of bilateral discussions with the respective administrations. Depending upon the circumstances of the individual administrations, these discussions were conducted by correspondence (letter / telex / facsimile), by telephone or by personal visits and meetings. Since the beginning of these efforts in April 1991, nearly 30 Administrations have signed the declaration to validate the circulation card for their countries. Some of these declarations were valid only until a specified date, while others had no time limitation. In some cases when the declarations expired they were renewed or extended; in other cases they have not been renewed.

Based on these declarations and the expiries, extensions and renewals, there are currently nearly 30 Administrations, including some in Eastern Europe, that are entitled to participate in the CEPT circulation card procedure. In all cases, the declarations authorise both the carriage and operation of the Euteltracs terminals within the countries concerned. In addition to the circulation card procedures, over 10 Administrations have so far implemented the necessary legislation, directives or instructions to permit transborder operation without the need for individual licences. In several cases this has been effected through a form of Administrative or Ministerial licence exemption under existing legislation. In other cases it has been achieved with new legislation that either grants licence exemption or establishes a General Class licence for operation of EUTELTRACS.

MOBILE SATELLITE DATA APPLICATIONS

EUTELTRACS is now also being introduced as a mobile satellite data service on a number of nonroad transport applications presented below.

Mobile Data Broadcasting

One of the main advantages of satellite communications is the ability to broadcast information to an infinite number of receivers on a large coverage zone in a very efficient manner. Thus, the EUTELTRACS network can be used to broadcast messages to a large group of vehicles. Due to its very fast forward link messaging feature, EUTELTRACS started early 1993 to broadcast every couple of seconds Differential Global Positioning System (DGPS) correction data, to achieve a positioning accuracy of approx. 3 meters. It should be noted that for this application the messages are sent through the network in priority mode, enabling the delivery to the mobiles within less than five seconds. Other messages like weather or road status information messages could be also broadcast.

Monitoring of Fishing Activities

In order to improve the control of fishing activities in European waters, the Commission of the European Communities (CEC) is in the process of discussing with the Member States the introduction of a Directive requesting that all major fishing boats be fitted with satellite communications terminals.

In the framework of this activity, the CEC is testing EUTELTRACS, a system that perfectly meets the need for position reporting of mobiles. In addition to the control function, the fishing companies could use EUTELTRACS to improve their fleet management.

Aeronautical Communications

Even if the position reporting service of EUTELTRACS cannot be used for aircraft (only mobiles on the surface of the earth can be located), the messaging service can become a valuable additional mean of communications on a frequency band different to the exhaustively used aircraft communications links. Due to the high speed of aircraft, communication means like EUTELTRACS are subject to a significant Doppler effect. This effect can be compensated by improving the stability of the local oscillator. In addition to this modification, a suitable antenna has to be mounted on aircraft.

Modified mobile units for aeronautical purposes are already being put into commercial operation.

Supervisory Control and Data Acquisition (SCADA)

EUTELTRACS solar powered terminals can be used on remote or isolated sites for monitoring and control of networks, for example pipelines. Terminals can report periodically, send alerts at special events, be interrogated by the base or used for remote control. The reliability of EUTELTRACS for SCADA applications is very high due to the fact that all terminals are fully controlled by the Hub facility (they can therefore be fully operated without attendance) and that in case of satellite failure, the terminals automatically search for the alternate satellite. Further advantages of EUTELTRACS terminals are their small size, easy installation and low cost.

REFERENCES

[1] *An overview of OmniTRACS: the First Operational TwoWay Mobile Kuband Satellite Communications System*, I. M. Jacobs (QUALCOMM, San Diego) Space Communications (Netherlands) Vol. 7, No. 1, December 1989

[2] *Modulation, Spread Spectrum and FEC Coding Techniques Used in the EUTELTRACS Land Mobile Satellite System*, L.A. Weaver, F.P. Antonio, A.J. Viterbi, I.M. Jacobs, K.S. Gilhousen (QUALCOMM Inc., San Diego) DSP 90 Politecnico di Torino 24/25 Sept. 1990

[3] *Land Mobile Communications in Kuband Result of a Test Campaign on EUTELSAT IF1*, J.N. Colcy and J. Dutronc (EUTELSAT, Paris). International Journal of Satellite Communications, Vol. 8, 4363 (1990)

[4] *The EUTELTRACS Position Reporting System Characteristics and Performance*, J.N.Colcy and J.Dutronc (EUTELSAT Paris), W. G. Ames (QUALCOMM Inc., San Diego), NAV 90 - The 1990 International Conference of The Royal Institute of Navigation, Warwick, UK

The ORBCOMM Data Communications System

David C. Schoen, Paul A. Locke
Orbital Communications Corporation
12500 Fair Lakes Circle
Fairfax, Virginia 22033
(703) 631-3600
(703) 631-3610 Fax

ABSTRACT

The ORBCOMM system is designed to provide low-cost, two-way data communications for mobile and remote users. The communications system is ideally configured for low data rate applications where communicating devices are geographically dispersed and two-way communications through terrestrial means is cumbersome and not cost effective.

The remote terminals use VHF frequencies which allow for the use of very small, low-cost terminals. ORBCOMM has entered into joint development agreements with several large manufacturers of both consumer and industrial electronics to design and build the remote terminals. Based on prototype work, the estimated retail cost of these units will range from $50 to $400 depending on the complexity of the design.

Starting in the fall of 1993, ORBCOMM will begin service with a demonstration network consisting of two operating satellites. By the end of 1994, a full operating network of 26 satellites, four Gateway Earth Stations, and a Network Control Center will be in place.

The full constellation will provide full coverage of the entire world with greater than 95% communications availability for the continental U.S.

This paper describes the ORBCOMM system, the technology used in its implementation, and its applications.

INTRODUCTION

There is a multitude of communications options open to industry and government organizations. However, most are either expensive or lack sufficient coverage of remote areas to be cost effectively used for low density communications needs in geographically remote locations. Industrial investments of billions of dollars have been made in VSATs, microwave communications systems and leased line services to provide the appropriate communications network for their Supervisory Control and Data Acquisition (SCADA) systems. These systems are cost effective for the high data rate, high volume communications needs of SCADA where continuous communications is required for legal and/or operational efficiency reasons.

Although the requirement for high data rate, high reliability

communications in many operations is unquestionable, there is also a need for cost effective communications for low data rate information. These communications requirements are characterized by short messages of approximately 100-200 bytes in length, sent on an infrequent basis. These communications are primarily non-time-critical messages which either increase the efficiency of the operation, enhance the overall safety and reliability of the operation, or improve the business functions within the operation. The communications link is usually to and from remote and geographically dispersed locations, where no existing infrastructure such as cleared land, power, etc. exists.

A good example of such a communications requirement is data collection and fail-safe control at interstitial points on a pipeline. The major control points along the pipeline, such as feed points, pump stations, and major valve outs, for the most part are under the control of SCADA or manual systems. However, there is a need for collecting data, such as pressures and temperatures, at intermediate locations. This type of information is important in implementing a fail-safe system for remote stretches of pipeline. In this application, data is monitored continuously and alarms are triggered if limits are exceeded. The communication requirement is small, roughly 100 bytes of data every half hour with very infrequent alarms sent to the dispatcher. Action is taken to isolate the problem by remotely or automatically commanding a gas actuated valve. Communications with these locations are critical to identify the problem area and take the appropriate action to correct the problem.

Low data throughput applications such as these make the cost of existing communications systems prohibitive to the implementation of distributed controls in remote areas. Microwave systems can cost as much as $300,000 to install in a single site. VSAT terminals at a remote location can cost $50,000. Ku-Band mobile satellite terminals could possibly be installed as fixed terminals at the cost of about $3,000 to $4,000. Such capital intensive investments make the cost per byte too high to justify the incremental benefit of fault isolation.

Finally, a very large application of remote communications is personal messaging to personnel in remote locations. The geographic extent of the many industries forces field crews to roam outside of the coverage of existing terrestrial based radio and cellular systems. Such lack of coverage results in poor communications with the crew and a reduction in operational efficiency. The existence of a low-cost messaging system for mobile users can help alleviate this specific problem.

This is only one example of an industrial requirements for low data throughput communications. Until recently these problems have been identified, but there has not been a solution which adequately and cost effectively satisfies these needs. The remainder of this paper will introduce and describe the ORBCOMM communications service based on low Earth orbiting (LEO) satellite technology and VHF operating frequencies. The unique combination of a dispersed network of LEO satellites and communications equipment operating at VHF frequencies will, for the first-time,

provide a low cost communications system with 100% geographic coverage of the Earth. With these two powerful attributes, the ORBCOMM data communications network promises to provide many operational benefits to mobile and remote users.

IMPLEMENTATION

The ORBCOMM system is being implemented specifically to provide a communication channel for short messages from vehicles or equipment which travel over wide areas or which are located in remote areas which cannot be economically served by existing technologies. The ORBCOMM system is being engineered to provide this service at low cost. All of the other existing or proposed systems lack one or more of the three key characteristics of the ORBCOMM system:

a) Ubiquity -- 100% geographic coverage is not planned by any terrestrial system;

b) Low Cost -- Until ORBCOMM, ubiquity required high first and recurring costs;

c) Messaging Proficiency -- Other systems provide messaging as an adjunct to their primary voice or positioning services.

As with other data communication systems, ORBCOMM consists of a set of message processors interconnected by digitally modulated radios. The ORBCOMM network consists of subscriber terminals (STs), the network control center (NCC), satellites and gateway earth stations (GES). The subscriber terminals are the point of origination and/or destination for all messages in the system. The NCC, via the Gateway stations, serves as the interconnection point between the fixed data networks and the population of subscriber terminals.

Subscriber terminals are very small message processing devices with integral RF modems used to access the ORBCOMM system. These devices are typically handheld or integrated into another communications or computing device. ORBCOMM subscriber terminals are the smallest, lightest and least expensive commercial satellite transceivers available. Subscriber terminals can be configured to support a variety of applications.

The most basic service is a low data rate (2400 bps uplink, 4800 bps downlink, low latency) data collection service for applications in monitoring remote equipment. Since the system has two-way communications capability, more sophisticated supervisory control applications are possible for monitoring remote systems and taking action when required. The full ORBCOMM service can provide personal and data messaging and position determination, allowing for inexpensive E-mail type communications with the home office or between mobile user terminals.

The Network Control Center (NCC) is the connection point between public and private data networks and the ORBCOMM network. The NCC serves as the message processing center, performing message switching for the entire U.S. ORBCOMM network. Remote equipment or personnel anywhere in the U.S. is accessed through a single connection to the NCC. The NCC sits at

the center of a star network of gateway earth stations. Collocated at this site are the additional service functions required for providing certain value added services, the satellite control center and the customer service and billing functions.

The ORBCOMM satellites are essentially message routing and queuing computers in low-Earth orbit, accessed by various radio links. The ground based elements of the ORBCOMM Network are interconnected by a constellation of low-Earth orbiting satellites. The satellites to be used to provide the initial service weight less then 100 pounds each and can be launched, eight at a time, on Pegasus XL launch vehicles. Despite the relatively low weight, each satellite: contains eight receivers and three transmitters; uses three axis, gravity-gradient assisted, magnetic attitude control system and has a capability of about 70 watts of orbit-average power. The satellites also contain GPS receivers, used to assist in the determination of the spacecraft orbit for the attitude control system and to provide satellite position and velocity information to subscriber terminals with position determination capability.

Service introduction plans envision various classes of satellites launched in a phased approach. The initial phases use very small lightweight satellites. Follow-on phases will use larger, more capable spacecraft, tailored in capacity as the size of the emerging market becomes more predictable.

The Gateway Earth Stations (GESs) interconnect the network control center computer to a satellite's computer so that messages can be passed between the STs

visible to that satellite and the NCC. Gateway Earth Stations pass data packets to and from the satellite computers to the message handling systems of the network control center. The initial ground segment configuration includes four GESs in the contiguous United States, located so as to maximize the amount of mutual visibility between the gateway sites and the subscriber terminal population. Each GES will be required to track only one spacecraft at a time. Multiple spacecraft coverage will be obtained through the diversity of sites.

The GES consist of medium gain (14 - 17 dBi) tracking antennas, RF and modem equipment, and communications hardware to send and receive packets to and from the Network Control Center. The gateways are fully redundant and designed for unattended operation.

ORBCOMM does not provide international service through it's satellite network. However, NCCs in other countries can be interconnected, via the public switched network, in order to provide international service.

VHF SPECTRUM CONSIDERATIONS

The VHF spectrum used by ORBCOMM was allocated at WARC-92 to the "Little LEO" systems.

The 137.0-138.0 MHz band, used for satellite to ST and GES communications, was identified as the most suitable downlink because it is allocated only to space services. Use of this band by space research and space operations has been declining in recent years because it is a relatively narrow allocation, unable to support the high data rate down links found on most modern spacecraft.

The use of relatively narrow band carriers for the ORBCOMM 137 MHz services suggests that sharing between LEO MSS systems would be quite practical. The required technique has been to coordinate access between the various narrow-band carriers of separate systems.

The 148.0-149.9 MHz band, used for ST and GES to satellite communications, was identified as the most suitable uplink because it had an existing allocation to space operations, was close enough in frequency to the downlink to allow a common antenna and did not appear to have any intractable coordination issues.

Current users of this band include a relative large number of terrestrial mobile systems. In order to operate in this band, the ORBCOMM satellites use a technique called the Dynamic Channel Activity Assignment System (DCAAS) to allow the subscriber terminals to communicate effectively in the presence of nearly co-channel uplink interference. This system allows uplink channel frequencies to be reassigned in response to measured and predicted statistical time variation of channel use by the interfering services.

The entire uplink band is scanned in 2.5 kHz intervals using a measurement filter identical to the modulation matched filter once per 5 seconds. The instantaneous power level in each slot is recorded. This power level is included in a weighted time average for that slot. The slots are then ranked from the lowest to highest power levels. In addition, the spacecraft receivers keep a record of the packet error rate on each channel in use in order that the dynamic channel allocation algorithm

can measure the quality of channels in use.

The DCAAS process, onboard each satellite, keeps a continuous rank ordering of channel slots from 'best' to 'worst'. The top 'N' channels on the list, with 'N' equal to the number of spacecraft subscriber receivers, are the ones used in current communication. This set of satellite receive frequencies is continuously relayed to the STs via an order wire channel.

COST INFORMATION

The ORBCOMM system is being engineered to allow subscriber terminal prices to range from $100 to $400 depending on the level of features included in the unit. Operation in the VHF frequency bands providing message communication only allows these price levels to be attained. Electronic components, subsystems and units designed and produced in volume for the VHF frequency band are already produces in high volume for a variety of other applications, such as push-to-talk radios and television sets. As a result, many of the components and the large scale integration processes required in the fabrication of ORBCOMM subscriber units are in use today in high volume manufacturing plants around the world. This will bring the benefits of economies of scale allowing consumer level pricing. This is not the case for the L-Band or Ku-Band components required for other satellite based systems. The many high quality, push-to-talk VHF radios available at prices ranging from $150 to $500 validate the low-price potential of the ORBCOMM equipment.

Service price will incorporate a

271

recurring monthly access charge and usage charges based on the level of messaging activity. Retail prices will typically be the equivalent of $0.25 to $1.00 per 100 byte message. Pricing alternatives will be offered including: peak and non-peak pricing, volume discounts, and sliding scale pricing.

IMPLEMNTATION SCHEDULE AND REGULATORY STATUS

The ORBCOMM system is being constructed according to a phased implementation schedule. Two spacecraft are to be launched in October 1993, providing "intermittent" service. At the time of the launch of these spacecraft, the full ground system will be in place. Intermittent service will be used to conduct "beta" tests and to serve markets for which 6-10 communications opportunities per day are a suitable first step. Throughout 1994, ORBCOMM will be launching additional spacecraft. Service with minimal delays will be available at the beginning of 1995.

ORBCOMM expects final regulatory approval by August of 1993. The first two spacecraft are being constructed and launched under authority of an experimental license, which also grants permission to conduct market trials for up to 1000 terminals. The FCC has given ORBCOMM permission to begin construction of the complete constellation prior to the granting of the full license.

BETA TESTING PROGRAM

With less than a year to go to start commercial service, active measures are being taken to obtain the input of the various industries in the development of the communications network through a

series of beta test programs. ORBCOMM is currently planning several beta tests with pipeline operators, marine equipment suppliers and other potential market leaders. The purpose of these tests is to develop and test the remote communications equipment as well as gain critical operating experience with the network. ORBCOMM is also developing a beta test program for a meter reading service for remote locations.

ORBCOMM is relying on industry participants to provide significant value added services to the industry. ORBCOMM realizes the crucial benefit of user input to the development of the network and is promoting active user involvement in every step of the development cycle.

SUMMARY

By focusing on low density communications between remote and mobile users in geographically dispersed locations, ORBCOMM will fill a communications need that is currently not met in any cost effective way. The combination of low Earth orbiting satellites and VHF operating frequencies provides a low cost communications service with 100% geographic coverage of the Earth. The low cost of the communications service will for the first time make access to remote locations for lower volume data communications economically feasible. ORBCOMM will begin service in 1994 with applications directly targeted at communications needs which until now have not been adequately addressed.

mobilesat® - A WORLD FIRST

Paul Cooper, Linda Crawley
Mobile Services

OPTUS COMMUNICATIONS
GPO Box 1512
Sydney Australia
Ph: 61-2-238 7751
Fax: 61-2-238 7803

ABSTRACT/INTRODUCTION

Mobilesat will be the worlds's first truly mobile satellite telephony service to be offered in the land mobile market. Essentially a car phone which will be offered as a fixed service at a later date, mobilesat will bring circuit switched voice communications to remote and rural areas of Australia. This paper will outline where mobilesat fits as part of Optus, Australia's new telecommunications carrier, and briefly discuss the mobilesat system, its market and the future of mobile communications in Australia.

OPTUS COMMUNICATIONS - The new telecommunications carrier in Australia.

Optus Communications is the new telecommunications carrier in Australia. Our business mission is to be a customer-focused leader in long distance and mobile communications services.

The name, Optus, is derived from the latin verb 'optare', meaning 'to choose'. This new competitive environment will change forever the range and price of communications services available to Australia.

Optus is 51% owned by Australian shareholders, and 49% by the international telecommunications companies: Cable and Wireless PLC and Bell South Inc. Optus is building a dynamic and innovative service-based company using leading edge technology and talented people resources.

Optus has a policy of stimulating local technology development and communications equipment manufacturing through strategic alliances and joint ventures. This will see new export opportunities arise for Australia's information technology and telecommunications industries.

The Optus network has three main components - fixed, mobile and satellite based. Mobilesat will provide mobile and fixed telephone services to rural and remote areas, enabling Optus to provide complete national mobile coverage and total network facilities to the Australian telecommunications market.

mobilesat® - THE SYSTEM

The mobilesat range of services will be deployed using the L-band capacity on the Optus B series satellites. These satellites are HS601 satellites built by the Hughes Aircraft Company and launched by the China Great Wall Corporation. The first satellite was launched successfully last August. The second is due to be launched in March 1994.

The KU band payload on the Optus B satellites will provide for the continuity of service for the broadcasting industry, business data services and remote direct-to-home TV services. Each satellite carries a single 150 watt L-Band transponder. This gives coverage over the Australian continent and 200 kilometres out to sea.

The ground segments of the system will consist of two Network Management Stations (NMS)

located on either side of the continent giving complete redundancy; public access gateway stations to provide access to the public switched telephone network, and mobile terminals (telephones).
(see fig 1)

Generic Service Features

The mobilesat service will provide full duplex high quality voice with a robust digital architecture to give toll quality performance in the mobile environment. Connection to an an auxiliary interface unit will provide circuit-switched data at 2400 bps, facsimile, packet-switched messaging and interconnect to Global Positioning System (GPS) information for position reporting.

Suppliers

The mobilesat system has been totally designed and developed in Australia. NEC Australia are providing the telephone terminals and the hardware component of the Network Management Stations; Computer Sciences of Australia are providing the software component of the ground segment NMS. The factory acceptance process will continue into the second half of 1993.

Westinghouse Electric Corporation has signed a memorandum of understanding with Optus regarding supply of mobilesat terminals in 1994.

Prototype mobilesat terminals are also being supplied by NEC Australia. These will be trialled by selected companies from our target market later this year, ensuring a smooth transition to the launch of commercial service in December.

MARKET ANALYSIS

The Australian continent covers an area of 7.6 million square kilometres with a small population (17.5 million at June 1992). This population is concentrated in urban areas around the coastal fringe. Despite the population concentration in the urban areas the Australian export economy revolves in the main, around

industries such as agriculture, mining, and tourism which are mostly located in the more remote regions of the country. Cellular services will provide coverage of up to 85% of the population but only 5% of the land area. This leaves many communities with little or no access to a reliable communications network. Mobilesat will fill this gap: it is targetted at providing services for the rural and remote areas of Australia, providing services similar to those enjoyed by their urban counterparts.

The system capacity in Australia for mobilesat telephones is expected to be about 50,000 users. This market has been segmented according to industry type and application into the following broad areas:

mining
utilities
emergency services
local government
state government
road transport
rail transport
the public market.

Market analysis forecasts show that the largest users of mobilesat will be the public sector, which includes small business in rural areas; together with Emergency Services and Public Utilities such as gas, water and electricity. This is closely followed by the Mining Industry.
(see fig 2)

Typical applications for mobilesat

Mining companies in Australia operate in a harsh environment. Field exploration crews operating in remote areas require a communications network which is reliable and secure. Market research indicates that mining companies would use mobilesat for control of operations, safety and simply to keep field crews in touch with head office or friends and family back home.

Data can be entered into a personal computer attached to a mobilesat terminal and transmitted to Head Office in a major town or city. Analysis time can be cut down considerably this way.

Safety is a major concern throughout the Australian Mining industry. In the event of accident or injury, an effective telecommunications system can mean the difference between life or death. Mobilesat has the added capability of call memory at the press of a button. This one-touch number can be programmed to call an emergency number or the mining base office.

Transport companies are also interested in using mobilesat to enhance efficiency of their operations. Mobilesat has been working with major transport organisations to develop the hardware and software components of the system and test them in the tough, long distance working conditions of the target markets.This involves an integration of the voice component of mobilesat with data and GPS. The integrated system is known as Transtracs. For example, in the latest trial two vehicles were equipped with a mobile satellite data terminal, GPS receiver and roof-top antenna to provide location and status reports to fleet head office.

At head office a map displayed text which included information such as vehicle ID and location, speed and direction. The text appeared in a 'window' against a map background showing the vehicle's geographic location.

Operational data and all ingoing and outgoing messages were automatically stored in a relational database which was then available for later reference to resolve delivery discrepancies or assist in report writing.

Connected to the mobilesat system to provide Australia-wide voice communications, Transtracs will support third party equipment in fleet vehicles such as electronic in-vehicle monitoring systems, driver input units and barcode readers, mobile fax and printers, and load monitoring for refrigerated or hazardous goods. This means that road, rail or coastal shipping fleet services will enjoy improved efficiency, timeliness and safety of their operations.

The most ubiquitous user of the mobilesat service, however, will be the average person who needs a phone on the road, for either pleasure or business. These customers will use mobilesat in the way their city cousins use cellular car phones, for communication convenience. Adding a fax or data port will make the mobile office achievable.

Pricing

Approximate pricing expectations for mobilesat are as follows: (prices in Australian dollars unless otherwise specified.)

Mobilesat telephony terminal	$7000.00
Auxiliary Interface Unit	$ 800.00
One time connection fee	$ 100.00
Monthly system access fee	$ 30.00
Voice charge per minute (distance independent)	$ 1.50
mobile to mobile calls per minute	$ 2.40
messaging service per month	$ 100.00

These figures compare to $1000 for a cellular telephone, $3000 for a hand-held cellular telephone, $3000-5000 for a HF radio and cellular call charges of $40.00 per month and long distance cellular charges at 60c per minute.

Prices for mobilesat equipment and airtime are also considerably less than our satellite competitors. For example, A$35-40,000 for an Inmarsat M terminal with airtime at US$5.40 per minute.

Competitive threats

Mobilesat enjoys the distinct advantages of satellite delivered systems over terrestrial two-way communications - voice quality, reliablity and coverage area. No repeater towers are necessary for coverage, and the cost of communicating over 500 or 5,000 kilometres is the same. Mobilesat also competes extremely

favourably on a cost basis with other proposed satellite systems and has an added advantage - the true mobility of an in-vehicle telephone. These superior aspects of the service position mobilesat as a world leader in land mobile communications from an economic and technological viewpoint.

THE FUTURE

Mobilesat, the Australian designed and soon to be implemented service, will be the first domestic mobile satellite service in the Pacific, as well as the world. This will provide to Australians a service capability currently not available and will provide rural and remote Australia with the advantages that cellular services have provided to the urban areas. Optus, via the mobilesat service and its other terrestrial and satellite infrastructure, looks forward to providing a level of customer service and total network coverage that will position it as the dominant telecommunications carrier in the Pacific region.
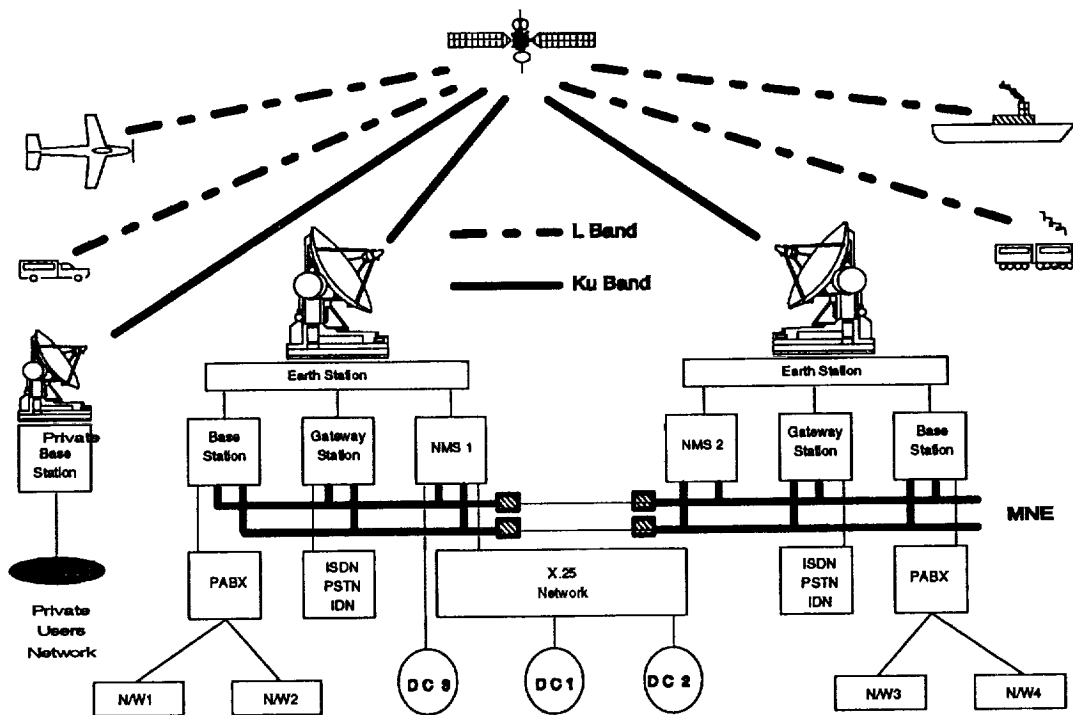
Figure 1
mobilesat® configuration

mobilesat ™

Market Projections

Forecast by Applications

Mining 15%   Public/Domestic 16%

Rail Transport 3%
Road
Transport 5%

Federal
Government 6%

Utilities 16%

State
Government 12%

Emergency
Services 16%

Local
Government 11%
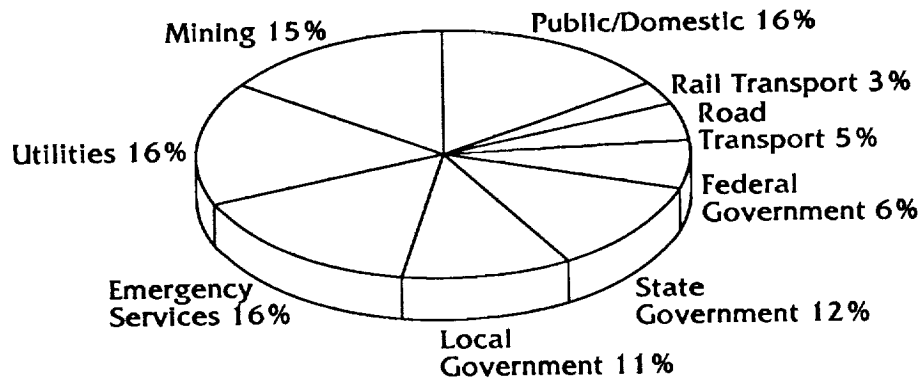
Figure 2
mobilesat® market projections

277

Implementation of a System to Provide Mobile Satellite Services in North America

Gary A. Johanson, Westinghouse Electric Corp.
P.O. Box 746, MS-8665, Baltimore, MD 21203, U.S.A.
410-765-9045/Fax410-765-9745
N. George Davies, Telesat Mobile, Inc.
613-736-6728/Fax 613-736-4548
William R. H. Tisdale, American Mobile Satellite Corp.
202-331-5858/Fax 202-331-5861

ABSTRACT

This paper describes the implementation of the ground network to support Mobile Satellite Services (MSS). The system is designed to take advantage of a powerful new satellite series and provides significant improvements in capacity and throughput over systems in service today. The system is described in terms of the services provided and the system architecture being implemented to deliver those services. The system operation is described including examples of a circuit switched and packet switched call placement. The physical architecture is presented showing the major hardware components and software functionality placement within the hardware.

SYSTEM DESCRIPTION

Services Provided

The technically compatible systems which AMSC and TMI are implementing, and which will enter service in mid-1994, will provide a full range of user services to subscribers throughout the continental United States and Canada, Alaska, Hawaii, the Caribbean Basin, plus offshore territorial waters to at least 200 n. miles. These services will be provided primarily to land vehicular mobile terminals (MTs), but the system will also accommodate transportable, maritime and aeronautical terminals.

The mobile telephone service terminal will support:

- Basic voice service interconnected to either public (PSTN) or private networks. Services will include a variety of advanced calling features.

- Circuit switched asynchronous data service at rates of 1200, 2400 and 4800 b/s.

- CCITT Group 3 facsimile service.

Multi-mode variants of mobile terminals will provide full interoperability with terrestrial cellular networks.

The Net Radio variant of the MT will support network broadcast and dispatch services in private systems.

The Mobile Data variant will provide packet-switched data service at 2250 to 5000 b/s interconnected with public (PSDN) and private data network applications.

Network Architecture

Overall System Architecture

The MSS System is comprised of five principal components:

- The MSS Satellite

- The Network Operations Center/Network Communications Controller (NOC/NCC)

- The Feederlink Earth Station (FES)

- The Mobile Terminal (MT)

- The Data Hub (DH)

The identical large geostationary MSS satellites [1] [2], one each owned by AMSC and TMI, will be described only briefly in this paper. The satellites provide the radio links between MTs which operate exclusively in the L-band, and the various fixed control and gateway stations, which utilize Ku-band. The satellite transponders provide the necessary frequency translation. The coverage area is served by six L-band beams and a single Ku-band beam. The current frequency plan supports division of the available L-band spectrum into approximately 1800 full duplex 6 KHz channels. The channels are aggregated in circuit pools from which they are demand assigned to support communication to individual subscribers. Frequency reuse is possible between the east and west beams.

The Communications Ground Segment [3], which is being developed by Westinghouse Electric Corporation under

joint contract to AMSC and TMI, is logically divided into two primary parts: the Network Control System (NCS) and the Communications System (CS). This is shown in Figure 1.
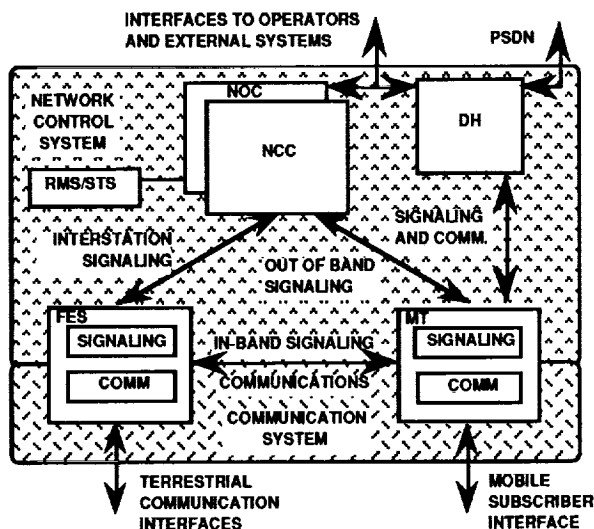
Figure 1. Logical Structure of the CGS

The NCS is comprised of the NOC/NCC, and parts of the FES(s) and MT(s), and performs the functions of system management and control. This includes commissioning and authentication of MTs, paging, call setup/teardown, initial signaling between system elements, channel assignment and congestion control. The NCS utilizes less than five percent of the satellite bandwidth for control/signaling channels, which function in a combination of random access, TDM and TDMA formats. The NCS span is designed to include all ground segment elements, all beams, and, in the future, multiple satellites.

The CS is comprised of elements of the FES(s) and MT(s), and provides connections between the MTs and other MTs or destinations in private networks or the PSTN/PSDN.

The signaling and communications links are digital, and the voice communications links employ voice activation.

Network Elements

The NOC provides the principal interfaces to the CGS for operators. It is designed to perform the functions of fault, accounting, configuration, performance and security management for the CGS. It accumulates information related to individual calls from other network elements to generate call billing and performance records for each call. The NOC has important interfaces with providers of Aeronautical Mobile Satellite (Route) Services (who have priority use of some portions of the L-band spectrum), with other independent users of the satellite, with AMSC and TMI counterpart NOCs, with Customer Management

Information Systems, and with the Satellite Operations Center. Its operations are largely non-real-time.

The NCC provides real-time control of the CGS system for circuit switched operations. It manages the access of users to the CGS and assigns satellite channels on a demand basis to provide communications links between FESs and MTs. The NCC manages out-of-band signaling channels which the MTs access to request communications channels and is capable of performing periodic performance verification tests of MTs using the CGS. The NCC is designed to establish a call connection within approximately three seconds and to support a maximum call establishment rate of 70 call attempts per second.

The FESs provide the interface between the CGS and terrestrial communications networks to permit communication between MTs and the PSTN, private networks and cellular systems. A FES consists of a number (up to 1500) of frequency agile channel units which are interconnected to a Ku-band earth station to support two-way communications with individual MTs. The FES interfaces to the PSTN through a Mobile Telephone Switch which implements various calling features and provides the capability to support roaming between the CGS and cellular systems by multi-mode MTs. Individual FESs will support up to 20 call attempts per second.

The CGS design supports inclusion of the NOC/NCC and FES function in a single integrated installation. Multiple FESs are also possible and may be remotely located.

The Mobile Terminals, which operate at L-band frequencies, are small, low cost units which can be easily installed on land vehicles. The MTs may also be adapted for the maritime and aeronautical environment. They are capable of accessing the signaling channels to the NCC and support single channel two-way communications with the FESs. MTs have an antenna with a gain of approximately 8 dB to provide a G/T of -16 dB/K and an EIRP of 12.5 dBW.

The Data Hub provides packet switched data services to mobile terminals by managing a number of packet data channels in each beam and the allocation of capacity to individual data MTs. The DH supports interactive data sessions, efficient query-response sessions, and data broadcast. The interface to the DH from terrestrial networks uses the X.25 protocol via a commercial packet switch. The user interface at the MT may be either via the X.25 or an asynchronous protocol. The DH supports a maximum data throughput rate of 6,000 32-byte packets per second and a call placement rate of up to 130 calls/second. A MT operating in the packet data network may interrupt the packet service to receive or place circuit switched calls.

280

Remote Monitoring Stations in each beam of the CGS monitor the use of the L-band spectrum and the quality and performance of the signaling channels. A System Test Station, located at the NOC/NCC, provides for testing of FES channel unit performance.

A simplified block diagram of the CGS system, including a non-collocated FES, is shown in Figure 2.
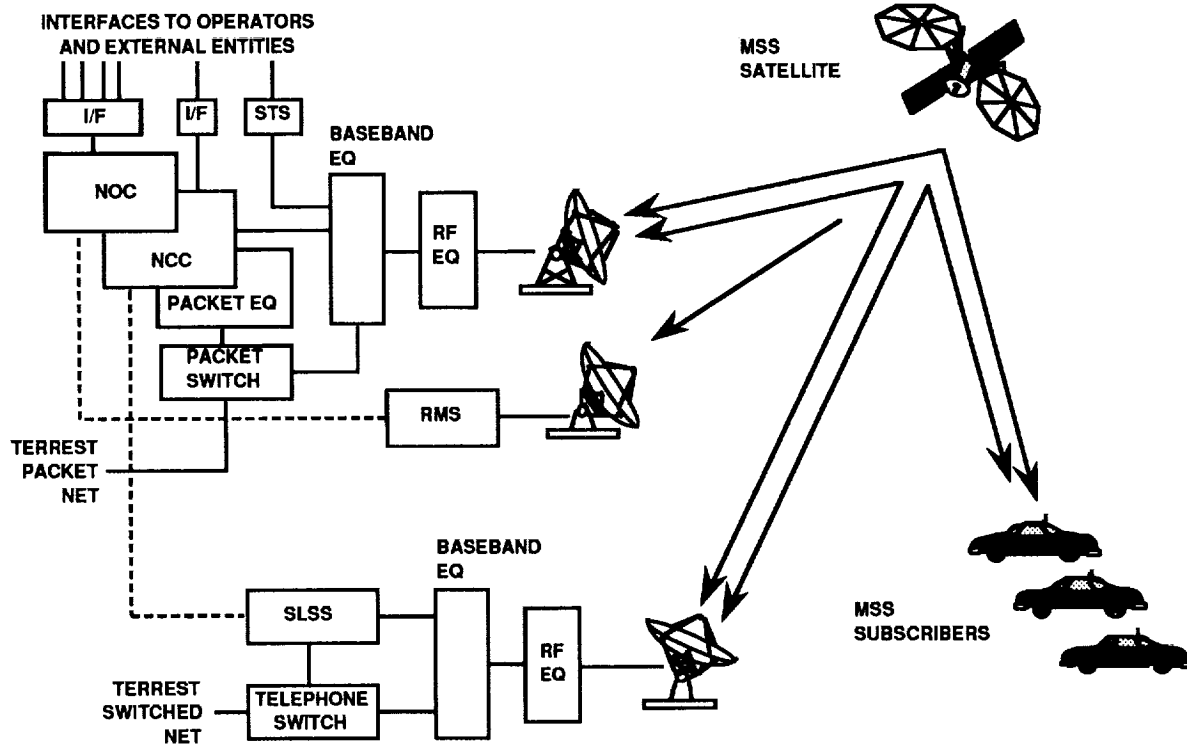
Figure 2. CGS System Architecture

SYSTEM OPERATION

Provision of Services

At the time of commissioning (the time at which a MT electronically "enters" the system) the MT is assigned a "set" of control channels [4]. These channels comprise the primary outbound (NCC or DH to MT) TDM channel, one or more inbound random access channels, and one or more inbound TDMA channels.

Following commissioning, all idle MTs continuously monitor the outbound TDM channel. This channel carries commands, pages, and responses to signals from individual mobiles by specific address, plus "bulletin board" information, which may be of significance to all mobiles.

The bulletin board consists of several numbered and time-stamped pages. A MT cannot operate within the system until it has acquired the latest update of the complete bulletin board.

The inbound random access (slotted aloha) channels are used only for MT initiated functions, such as requests for call placement, or network specific functions such as control channel changes. All subsequent MT signaling is transmitted on one of the inbound TDMA channels.

A variety of error detection and retransmission schemes are used to insure the integrity of signaling.

Circuit Switched Call Placement Scenarios

To place a mobile to land circuit switched call, the MT subscriber will enter the destination telephone number at his terminal and push a SEND key, in a manner similar to that used in cellular telephony today.

The MT will then transmit its electronic serial number (ESN) and the first 10 digits of the destination in a Signaling Unit in a single burst on a random access channel. On receipt, the NCC will check the validity of the information, and will respond to the MT with transmit and receive frequency channel assignments. The same information will also be sent to the serving FES. Both the MT and the FES will tune to these channels, and, through

281

an exchange of protocol, establish communication. Concurrent with this process, the FES will instruct the Gateway Switch to establish the necessary terrestrial connection. The call will then be cut through to the switch, which will provide standard call progress tones. Subsequent signaling (for example that required to perform tandem dialing or to activate advanced calling features) will be handled by 96-bit Signaling Units inserted into the communication stream.

Land-to-mobile calls are established in essentially the same manner. When the FES receives the MT bound call from the terrestrial network, it signals the NCC with the MT identification, and the NCC subsequently pages the mobile to establish the radio link.

Packet Switched Call Placement Scenarios

To place a mobile-to-land packet switched call, the MT subscriber will generate an X.25 call request using a PC or specialized interface unit. The call request message containing the X.121 address of the called party is transmitted to the DH via a random access data channel. The DH then attempts to complete the call via the interconnected Public Switched Data Network (PSDN). When the host on the PSDN responds with a call accept message, this is transmitted to the calling MT via TDM data channels. When a block of data is to be sent from the MT, the MT formulates a capacity request message and transmits this to the DH via a random access data channel. The DH responds by allocating a unit of capacity on the TDMA channel which can be extended by requests form the MT, piggy-backed on the data message, until the transmission of the block of data is completed. A block of data sent from the host on the PSDN is transferred to the MT by the DH in packets via the TDM channel. Reliable information transmission over the mobile satellite link takes place in packets of up to 64 data bytes under an ARQ protocol.

Land-to-mobile calls are placed as a result of a call request received by the DH from a host on the PSDN. The DH sends an X.25 call request to the MT and allocates capacity on the TDMA channels for its response. Once a connection is established, data messages are exchanged as described above.

Network Management

Architecture

Figure 2 shows the overall Network Architecture. The components that form the Network Management Architecture are primarily the Network Management System (NMS), the NOC, and the MDS Network Management System (MNMS). The NMS is the administrative system management function that is responsible for setting management policy and procedures. The NMS consists of three separate

functional areas: System Engineering (SE), Network Engineering (NE), and the Customer Management Information System (CMIS). SE is responsible for long range planning functions. Traffic analysis techniques are used to predict when the network should be expanded or reconfigured to meet long term growth requirements or changes in system utilization. NE is responsible for carrying out the decisions made within the SE organization and as such formulates tactical plans for meeting the daily needs of the Network. These tactical plans, such as the definition of circuit pools, satellite resource planning, frequency allocation usage, and network configuration, are electronically communicated to the NOC and the MNMS for implementation. The CMIS is the interface to the users of the communications services, the mobile terminal subscribers. Through this system, new customers are entered into the network or their user profiles are updated. It is also through the CMIS interface that the NOC and MNMS provide the billing data for call placed by subscribers.

The NOC is the heart of the network management process for circuit switched operations as is the MNMS for packet switched operations. The NOC and MNMS each have a director which controls and keeps status on the remainder of the elements. The director obtains status and alarms and provides control through the use of agents. An agent is located at each physically separate site and provides local control for all of the managed objects at that site. Each agent is responsible to the director for all alarming, event recognition, and the execution of network control or configuration commands. Standard network management protocols are used, although all objects are not required to use the same protocol. An example would be the concurrent use of Simple Network Management Protocol (SNMP) and Common Management Information Protocol (CMIP) at the same site to manage different objets. The NOC and MNMS provide centralized network management for Configuration, Accounting, Security, Faults, and Performance.

Call Billing

Each network element involved in processing real time call information collects information about that call. Two types of information are collected: billing information and performance information. Billing information is transferred to the NOC after each circuit switched call completion and to the MNMS after each packet switched call completion. The NOC and MNMS will hold that information in local storage until requested by CMIS. The data will then be transferred in batch mode. The CMIS may request individual call records at any time from the NOC or MNMS. That data is transferred immediately. Performance data is also transferred to the NOC or MNMS after each call. This data is transferred daily for analysis by the NE and SE functions. The results of this analysis are used to plan future operations, short term or long term.

Resource Management

The NOC and MNMS are responsible for the overall management of network resources. However, these elements do not manage the most important resources, satellite bandwidth and power, on a real time basis. That task is accomplished by the NCC for circuit switched calls and by the Data Hub for packet switched calls. These elements manage the real time assignment of satellite channels at the appropriate power to or between Mobile Terminals and from the terrestrial networks. Other network resources, not required for call assignment on a real time basis, are managed by the NOC and MNMS.

SYSTEM IMPLEMENTATION

Physical Architecture

A simplified block diagram of the physical implementation of the Communications Ground Segment Architecture is shown in Figure 3. This is a generalized architecture that would accomplish all system functions. At this time, the implementations for the initial TMI and AMSC sites are different in that they do not both support all of the possible system functions. The differences between the two site configurations will be explained after the general architecture is described.
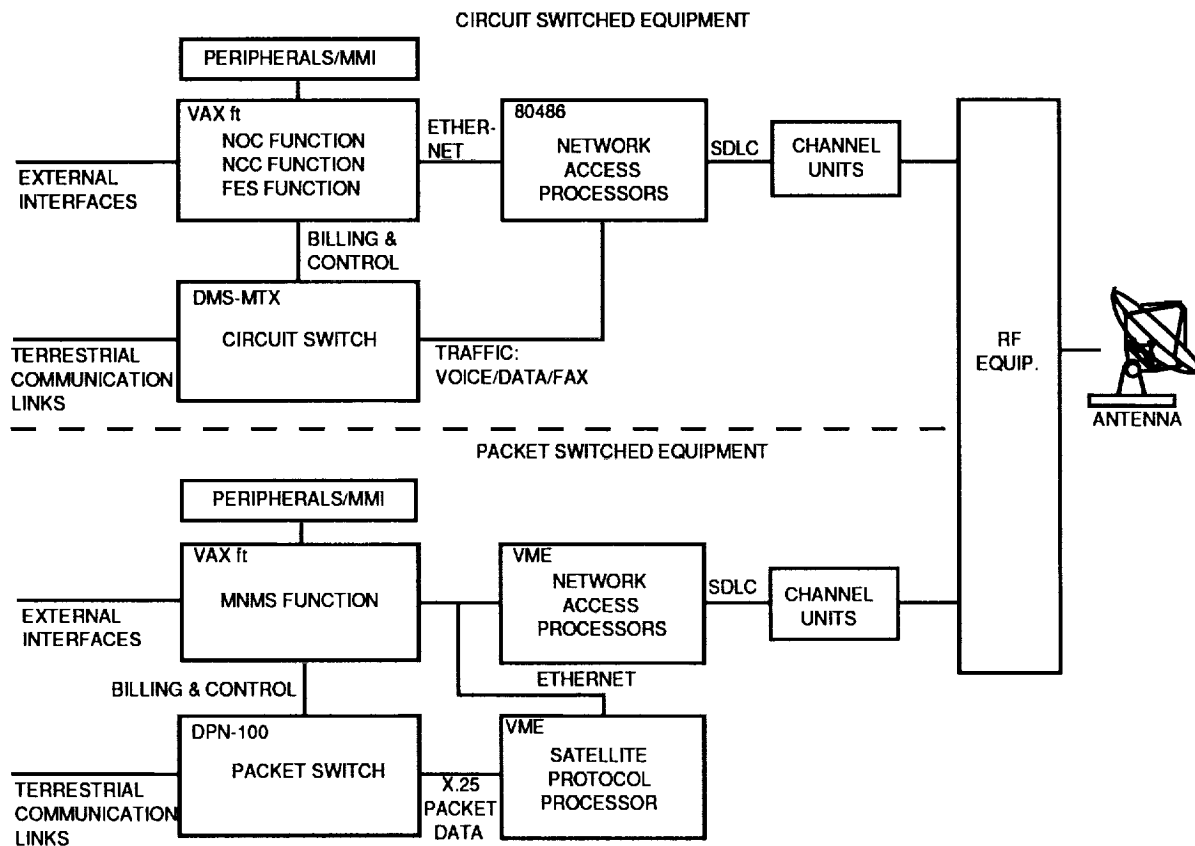
Figure 3. Hardware Implementation Diagram

The typical site may be divided into a circuit switched configuration comprising a NOC, NCC, and FES and a packet switched configuration containing a Data Hub. At a typical combined site installation, a single Radio Frequency (RF) subsystem, provided by Satellite Transmission Systems, is used.

The NOC, NCC, and FES functions are combined into a single fault tolerant computer platform, a Digital Equipment Corporation VAXft 810, plus several peripherals and communications devices. All functions

utilize operator terminals and mass storage. In addition, the NCC and FES make use of channel units from EF Data Corporation, that provide the conversion to/from digital baseband signals to modulated Intermediate Frequency (IF) signals. These signals are used to communicate to Mobile Terminals via the RF equipment which provides the conversion from IF to Ku-band. The FES element contains a switching element, a Northern Telecom DMS-MTX cellular switch. This switch provides the connection between the Mobile terminals and the terrestrial network for all circuit switched calls.

283

Communication between the VAX and its peripherals is via dual rail Ethernets while communications traffic to the terrestrial network is carried via T-1 telecommunication links.

The data hub architecture is implemented using a number of computing technologies. The Terrestrial interface is accomplished utilizing a Northern Telecom DPN-100 packet switch carrying X.25 traffic. The Satellite Protocol Processor and Network Access Processor are implemented via redundant VME based processing elements. The channel units and RF equipment are the same as in the circuit switched architecture (the channel units being defined for packet operation via a different software load). The MNMS function is implemented using a VAXft 810 as in the circuit switched architecture allowing both hardware and software commonality for the MNMS and NOC functions.

Non-collocated system elements and external interfaces are connected via the MSS Internetwork. This network employs various communications technologies depending on the amount and frequency of data traffic. Connectivity spans from low speed dialup modems to high speed dedicated circuits. As the system is expanded, the most time critical data transmissions will be to keep the off-line elements in hot standby mode, ready to take over operations in case of on-line element failure. Other Internetwork transactions include the addition of new customers, the resulting billing data, and transfer or control of resource information.

AMSC Site

The AMSC site incorporates full capability for Cellular Interoperability as well as Networked Radio operations. The installation will not initially include a data hub, so that support of packet data services will be a future capability.

TMI Site

The TMI site will contain a data hub and thus will directly support packet data services, as well as integrated voice/data services to Mobile Terminals capable of both packet and circuit switched operations. The TMI Site will also support Networked Radio Operations. Cellular Interoperability will be incorporated at a future time.

Mobile Terminal

Operational Modes and Configurations

MTs can be configured as circuit switched, packet switched, or both for integrated voice/data operation. When packet switched operation is one of the selections, all communications will be initiated through the data hub. Circuit switched calls will then be processed to the selected FES for termination to the terrestrial network.

Cellular Interoperability may be added as an option to circuit switched MTs. In addition, Networked Radio operation may be added. MTs that are required to provide position location information may be outfitted with a GPS option. Facsimile and circuit switched data communications may also be configured.

In addition to the mode selection available, various configurations may be provided depending on the vehicle type. Land Mobile, Fixed Site, Maritime, and Aeronautical configurations are available.

Cost and Availability

The initial production Mobile Terminals are scheduled to be available by mid-1994 in time for planned service introduction which is in late 1994 for AMSC and early 1995 for TMI. Two MT providers are planning on introducing MTs, Westinghouse and Mitsubishi.

The retail price for a circuit switched, land mobile, cellular interoperable MT with voice and circuit switched data capability is expected to be under US$2,000. A similar price is anticipated for a land mobile, packet switched MT with Global Positioning System position location capability.

REFERENCES

[1] D. Whalen and G. Churan, "The AMSC Space Segment", *14th International Communications Satellite Systems Conference*, pp 394-404, March 22-24, Washington, DC.

[2] E. Bertenyi, "The MSAT Spacecraft of TMI", *International Mobile Satellite Conference '93*, 16-18 June, 1993, Pasadena, CA

[3] J. Lunsford, R. Thorne, D. Gokhale, W. Garner, and G. Davies, "The AMSC/TMI Mobile Satellite Services (MSS) System Ground Segment Architecture, *14th International Communications Satellite Systems Conference*, pp 405-426

[4] L. White, A. Agarwal, B. Skerry, and W. Tisdale, "North American Mobile Satellite System Signaling Architecture", *14th International Communications Satellite Systems Conference*, pp 427-439

VAX and VAXft are trademarks of Digital Equipment Corporation. DMS-MTX and DPN-100 are trademarks of Northern Telecom.

The Iridium™ System
Personal Communications Anytime, Anyplace

John E. Hatlelid
Motorola, Inc.
1764 Old Meadow Lane, Suite 1
McLean, VA 22102 USA
(703) 893-5067
FAX (703) 760-0884

Larry Casey
Motorola, Inc.
2501 S. Price Road
Chandler, AZ 85248 USA
(602) 732-3393
FAX (602) 732-3046

ABSTRACT

The Iridium system is designed to provide handheld personal communications between diverse locations around the world at any time and without prior knowledge of the location of the personal units. This paper will provide an overview of the system, the services it provides, its operation, and an overview of the commercial practices and relatively high volume satellite production techniques which will make the system cost effective.

A constellation of 66 satellites will provide an orbiting, spherical-shell, infrastructure for this global calling capability. The satellites act as tall cellular towers and allow convenient operation for portable handheld telephones.[1] The system will provide a full range of services including voice, paging, data, geolocation, and fax capabilities.

Motorola is a world leader in the production of high volume, high quality, reliable, telecommunications hardware.[2] One of Iridium's goals is to apply these production techniques to high reliability space hardware. Concurrent engineering, high performance work teams, advanced manufacturing technologies, and improved assembly and test methods are some of the techniques that will keep the Iridium system cost effective.

Mobile, global, flexible personal communications are coming that will allow anyone to call or receive a call from/to anyplace at anytime. The Iridium system will provide communications where none exist today. This connectivity will allow increased information transfer, open new markets for various business endeavors, and in general increase productivity and development.

OVERVIEW

Motorola is leveraging its expertise as the leading U.S. manufacturer of cellular equipment and a leading world manufacturer of mobile communications radios in the design of the Iridium system. The system will provide a digitally switched telephone network and a global dial tone allowing the user to place a call to or be called by any other telephone in the world. A user will have the convenience to call a portable telephone number and talk directly to an individual--global roaming is designed into the system and you call the handheld phone of a person, not just the place where a fixed phone is located.[3]

A key feature of the system is the use of a constellation of low altitude satellites which will not have annoying voice delay. The low altitude satellites allow the use of low power, handheld telephones in this personal communication system. Earth gateways provide the interface to the public switched telephone networks and determine the routing as a call is placed. The system will have its own operational control system for command and control of the communications system and the constellation of satellites.

The Iridium system will provide the full range of communication services that are expected in a modern system. High quality voice using a pocketable handheld telephone is the driving requirement. The system will also have provisions for paging, data, messaging, fax, and geolocation.

System operation is similar to existing ground-based cellular. In fact the dual mode handset will have the capability to operate on both cellular and Iridium frequencies and with both communication architectures. When a call is dialed and sent, the system will first try to use a cellular channel from the local terrestrial system. Iridium will transmit to a satellite on an Iridium channel only if ground-based cellular is not available. The gateways will route the calls through the constellation in the most economical fashion and will use existing terrestrial infrastructure when necessary. As such the Iridium system will complement existing systems, not replace them.

SYSTEM DESCRIPTION

The Iridium system provides global, handheld personal communications. It is based on a cellular telephone concept and will use pocketable telephones for communications to or from anyplace at anytime without prior knowledge of the portable telephone's location. The three major system elements are the pocket size handset, the constellation of 66 spacecraft, and the ground infrastructure--the gateways and the system control facility, see Figure 1. The following sections provide additional detail.

Handset

The pocket size handset, see Figure 2, is designed with a dual mode capability--both ground-based cellular and Iridium calls can be placed. The user will specify when the phone is purchased which terrestrial capability is desired. The phone will have both modes built in and will attempt a call through ground-based cellular first. If a cellular circuit is available, it will be used. When cellular is not available, the call is routed through the satellites.

In addition to this voice capability, the handset will also be capable of sending or receiving paging, fax, and data messages. A standard port on the side of the unit will provide the data interface to a fax, printer, or other data unit. In addition, the system will continuously monitor the location and status of all subscriber units.

Not all users require a handheld unit. Other subscriber units will be available including solar powered telephone kiosks and pager-only units. The advantage of the solar powered kiosk is use in lesser developed areas without a hardwired telephone or power grid. The phone booth can connect anywhere, anytime even without terrestrial telephone or power lines. A basic level of telephone service could be provided in this fashion where service had never before been available or for emergency restoration of service after a disaster.

Spacecraft

Iridium spacecraft are another key element in the system's ability to provide handheld personal communications. They will create beams of coverage similar to the cells of a ground-based cellular system. In ground-based cellular, the ground antennas are at fixed locations and create fixed cells of coverage that a mobile user randomly moves through. The Iridium satellites act as antenna towers several hundred miles tall and create cells of coverage that move as a result of the orbital satellite's motion. Even a mobile Iridium user is relatively fixed with respect to satellite motion and cell to cell handoff of a user is deterministic based on the uniform motion of the satellites in their low earth orbits.

The satellites will also have cross links to route calls between satellites. Each satellite will support

up to four simultaneous cross links--one to each of the satellites immediately ahead of or behind it in its own orbital plane and also one to satellites to the left or right in adjacent orbital planes.

Ground Infrastructure

The ground infrastructure for the Iridium system include gateways and the system control facility. Gateways are in key locations worldwide as they contain the Iridium databases for billing purposes and will be used as the interconnect point into the public switched telephone network.

Since each satellite has crosslinks, a gateway does not have to be in view of every satellite. Yet, gateways will be involved in every call. They will first determine if the user of an Iridium handset is a valid user. Given that a valid user is attempting to make a call, gateways will also have the databases to determine the location of the called telephone. The gateway will then determine the call routing and will format a header with the information needed by the satellite switch to route the call. After the completion of the call, the gateway will develop billing information.

The system control facility will control the communication system and will also command and control the spacecraft. The configuration of the constellation of satellites will be controlled to provide the most efficient full-earth coverage. The system control facility will also read the state of health and configuration of the satellites and associated systems and subsystems. Anomalies will be detected and resolved in the control facility.

SERVICES

The Iridium system is designed to provide a quality personal communications service to users anywhere in the world. Digital transmissions will provide a full range of communication services including voice, paging, data, facsimile, and geolocation.

Voice

Ubiquitous, handheld, personal voice communications are the hallmark of the system. A user anywhere on the surface of the earth is assured that at least one satellite will always be in view and will be available to provide high quality voice service. Iridium satellites in low earth orbit are designed to allow high quality transmissions without the time delay of geosynchronous communication satellites. The system is designed with 16 dB link margin which allows communication in a variety of routine fading situations including from inside a vehicle and through foliage. [4]

Paging

Global paging is another quality service offered by the Iridium system. The handheld telephone can receive a page and separate pager-only units will be available for those users needing just paging.

Data

Transparent data service (at 2400 bits per second) is offered in the Iridium system. Different length messages are possible with one option being a short message to provide location and user status.

Fax

The system will communicate facsimile messages. The pocket size handset will have a data port built into it that will provide the interface to an external fax unit. The handset will be able to receive and store faxes in memory. The user can review the fax by scrolling through the information using a display screen on the handset. A hard copy of a fax can be printed by using the data port to connect to a fax or printer.

Geolocation

For the Iridium system to work, it must locate the user unit. The geometry of the system can provide location during routine standby operation. A Global Positioning System (GPS) chip can be built into special user units if more precise location is required.

OPERATION

The users of this system want a system that operates efficiently and provides high quality, reliable, personal communications. The Iridium

system is designed to provide just that--quality personal communications at anytime, anywhere in the world, with the system not needing prior knowledge of the user's location. The system has a robust design with global coverage that provides the convenience and capability that users demand.

Coverage

A global personal communication system requires continuous worldwide coverage. The Iridium system, with its constellation of 66 low altitude satellites, uses circular polar orbits of 420 nautical miles altitude. There will be six orbital planes with 11 satellites per plane. The constellation is designed to have at least one satellite in view of all locations on the surface of the earth at all times.

The system control facility will schedule cells to turn off as the satellites move through the northern and southern latitudes where the greatest overlap occurs. Each of the 66 satellites project a pattern of 48 cells--or a system total of 3168 cells. Only 2150 active cells are needed to cover the earth so at any given time about 70 percent of the cells are active.[4]

Convenience

The customer expects convenience in a personal communication system. Experience in the worldwide cellular industry has clearly shown the trend to small, light weight, handheld telephones. This subscriber unit driven system was designed having learned from those experiences. The Iridium system will diminish a lot of the limitations to personal communications by providing readily available, easily used, high quality communications where they have not existed before.

Capability

The Iridium system is the next logical step in personal wireless communications. Ground-based cellular systems have steadily grown as their convenience and capability have been accepted. Yet there are substantial geographic and financial problems in building a global ground-based system. A range of options were studied before the low altitude constellation option was picked for

Iridium. This option provides global coverage and allows robust connectivity to pocket size handsets. Higher altitude satellites, including geosynchronous, were considered but were not accepted since closing the link to a small handset is difficult in many situations and the round trip voice delay is a concern.

PRODUCTION EFFICIENCIES

The Iridium program must be a commercial success with a profit for the investors. Future revenues must cover the cost of operating the system and provide a return on the initial investment for system development. Motorola is studying the ways that this personal communications program can benefit from high volume commercial production techniques, not only in the subscriber units but also in the satellites, to make it more cost effective. Some of the areas for cost efficiencies include emphasis on high quality, statistical process control, advanced technologies, improved design and manufacturing methods, and also improvements in assembly and test.[2]

Motorola was one of the first winners of the Malcolm Baldridge National Quality Award. Emphasis on excellence is continuing through a quality program that strives for six sigma quality in all aspects of work--this equates to no more than 3.4 defects per million operations. All of the partners and suppliers must also meet these high quality standards.

Motorola is a world leader in the design and production of electronic components and wireless communication equipment. This lead is the result of working to stay up to date in producing electronic components as the technology continues to reduce the size of components. Motorola engineers can design and produce Application Specific Integrated Circuits (ASICs) and Multi Chip Modules (MCMs) approaching the limits of the state of the art. Proven techniques will be applied as appropriate to reduce the cost, size, weight, or risk of developing the necessary hardware.

Electronic circuit density has increased as the technology has progressed from components with

long leads to MCMs. Even MCMs transitioned to fine pitch leads with very close spacing, while the newer technology has now advanced to direct attachment without leads. These improvements have come with challenges in design and manufacturing. One approach is the use of advanced robotic assembly lines for the assembly and test of these devices. In addition, advanced simulation tools are needed for the design and analysis of these components. Motorola is using these capabilities in several existing programs including Space Station Freedom communication system work. Technology improvements continues to yield parts that are lighter, smaller, more reliable, and more repeatable in performance from unit to unit even directly off the assembly line. Technology reuse from adapting a previous design is used to speed production and improve reliability.

Reuse is emphasized throughout the design and production process. One area that has paid off is improvements in software that allow a design engineer to enter parameters in a data base and that data is tied to all of the design, analysis, and even production steps. This one time entry of data reduces the chance of a data entry error. This reduces errors and speeds up the equipment set up for the production process.

Concurrent engineering is being used to reduce total acquisition costs and improve reliability. The goal of concurrent engineering is to get all disciplines involved early in the design process to reduce future design changes by insuring that all considerations for manufacturing and testing the product are factored into the initial design. In this way a more complete design is developed that can be built with few changes and satisfy all requirements.

SUMMARY

Global handheld personal communication will greatly improve our ability to place or receive a call anywhere in the world at anytime. The Iridium system will provide this portable telephone capability with pocket size handsets. A constellation of low altitude satellites allows quality service with low power, handheld telephones. Global personal communications are coming with one person, one number service at anytime, anywhere in the world--the Iridium system is leading the way.

REFERENCES

[1] R. W. Kinzie, *Leo Systems and the Economy*, Satellite XII Conference, April 25, 1993.

[2] L. D. Casey and J. W. Locke, *Rendezvous Radar for Orbital Vehicles*, AIAA Space Programs and Technologies Conference, March 24-27, 1992.

[3] J. D. Adams, *Satellite Technology for Personal Communications*, National Communications Forum, October 13, 1992.

[4] R. J. Leopold, *The Iridium$^{TM/SM}$ Communications System*, Tuanz '92: Communications for Competitive Advantage Conference and Trade Exhibition, August 10-12, 1992.
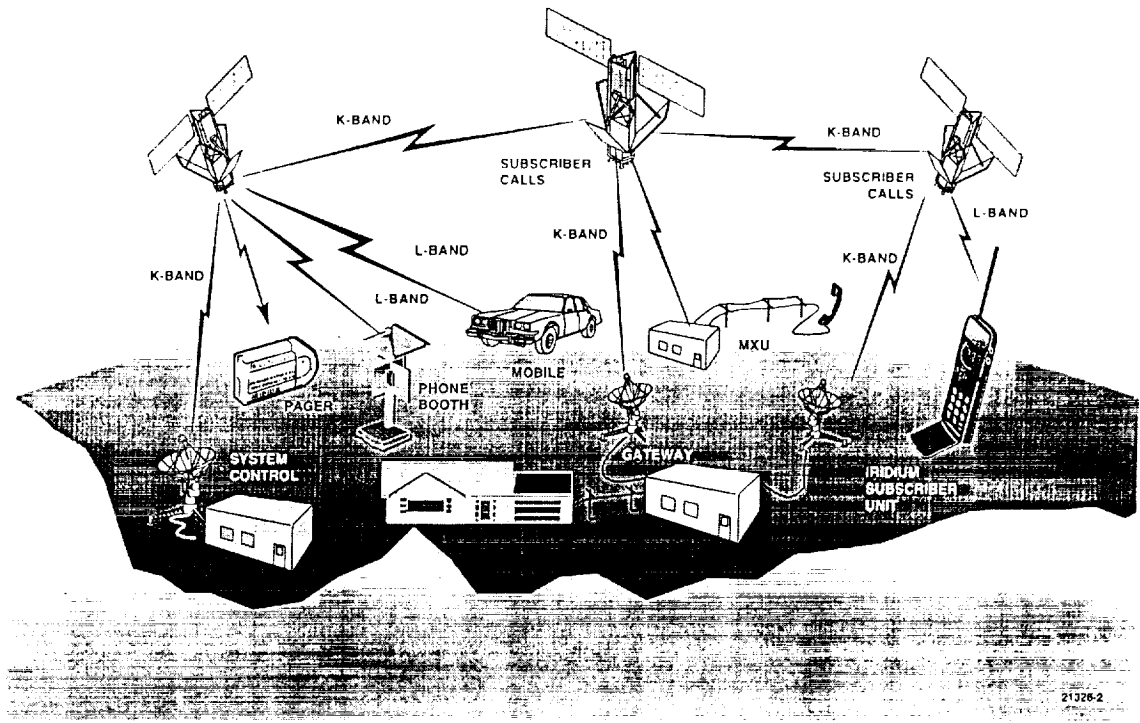
Figure 1. Iridium System Overview

Figure 2. Iridium Handset

THE GLOBALSTAR MOBILE SATELLITE SYSTEM FOR WORLDWIDE PERSONAL COMMUNICATIONS

Robert A. Wiedeman
Vice President of Engineering
Loral Qualcomm Satellite Services, Inc.
3875 Fabian Way, Palo Alto CA. 94303
(415)-852-6201

Andrew J. Viterbi
Vice Chairman
Qualcomm Incorporated
10555 Sorrento Valley Rd.
San Diego, CA. 92121-1167

1.0 INTRODUCTION

Loral Aerospace Corporation along with Qualcomm Inc. have developed a satellite system which offers global mobile voice and data services to and from handheld and mobile user terminals with omni-directional antennas. By combining the use of low-earth orbit (LEO) satellites with existing terrestrial communications systems and innovative, highly efficient spread spectrum techniques, the Globalstar system provides users with low-cost, reliable communications throughout the world. The Globalstar space segment consists of a constellation of 48 LEO satellites in circular orbits with 750 NM (1389 km) altitude. Figure 1 shows the global coverage. Each satellite communicates with the mobile users via the satellite-user links and with gateway stations.

The gateway stations handle the interface between the Globalstar network and the PSTN/PLMN systems. Globalstar transceivers are similar to currently proposed digital cellular telephones in size and have a serial number that will allow the end user to make and receive calls from or to that device anywhere in the world.

The Globalstar system is designed to operate as a complement to existing local, long-distance, public, private and specialized telecommunications networks. Service is primarily designed to serve the rural and thin route communications needs of consumers, government users, and private networks.

Due to the orbit selection and the use of CDMA spread spectrum technology the number of circuits over a region is increased due to multiple satellite coverage. Each satellite operates as a repeater in space, eliminating complex call setup procedures and on-board processing. Globalstar has been configured to link the mobile user to a terrestrial gateway through a single satellite so that the system requires no satellite crosslinks.

Globalstar offers services which are not currently available, such as world wide cellular roaming. Globalstar service offerings will meet the needs of the general public both domestically and globally where it is not cost effective to provide terrestrial based cellular services.

Signal availability and quality to the user is the most important factor in choosing a technology for MSS services. The user signal availability is determined by a large

number of factors which are statistically developed to determine what the user experiences during a MSS call. For example, a user which is stationary in a clear area will experience a certain propagation effect while another user using a hand held device while in a vehicle traveling under a heavily leafed tree canopy may experience a different value. The Globalstar user receive signal level and transmit power is adjusted to account for impairments. Rural and suburban propagation models have been developed by Vogel of the University of Texas [1] which show the probability of needing margin in certain conditions. These models when combined with multiple satellite availability (path diversity) and elevation angle statistics from the satellite constellation determine signal availability.

2.0 CDMA IS OPTIMUM FOR THIS SERVICE

Frequency Division Spread Spectrum CDMA (FD/SS/CDMA) provides optimum and flexible service quality to the end user. The FD/SS/CDMA modulation choice allows multiple signal paths from more than one satellite which mitigates fading and blocking.

The user is provided signals which are optimized for the subscriber's environment. Link margin is provided to each user independently as the gateway senses that it needs margin. User margin is provided in three independent ways. First, there is thermal margin built into each link to account for the inherent thermal noise from all sources. Second, a power control ability is built into the hardware which when activated boosts the power amplifier output by up to 10 dB in 0.5 dB steps both under the direction of sensing circuits in the user equipment and under control of the gateway that is handling the call. This provides a total "link by link margin"

of 11 dB. Third, the Globalstar system constellation provides additional mitigation of shadowing and blocking using path diversity. This path diversity is equivalent to having more margin on a link by link basis. When these margins are used with the suburban/rural model for fading, shadowing and blocking, the resulting availability is shown in Figure 2. The results show that significant improvement in availability is provided with path diversity.

For example, the user equipment in a rural/suburban environment which is experiencing a fade will first sense a degradation of the receive frame error rate. The unit will open loop increase its power to maintain quality and send a request to the gateway which increases the forward link power. On the return link the gateway measures the frame error rate and Eb/No and sends up/down power control commands to the user unit closed loop. At the same time the uplink signals are being received by a second or third satellite, since the Globalstar system provides multiple satellites in view of the user's omni-directional antenna. The signal level of these alternate paths is measured by the same gateway serving the user. The gateway software controls both the power sent to and transmitted by the user as well as the usage of the alternate signal paths. At a predetermined point, depending on the system loading, the alternate signal paths are combined by the gateway receivers improving the received signal from the user. The alternate paths are monitored for level and stability and according to preset thresholds the user is commanded to the best alternate path.

Link performance is assured by power control which maintains the service quality constant over a wide range of fading, shadowing and blocking environments. For satellite systems fading is Rician in nature and not typified by the Rayleigh

model. Globalstar link budgets provide adequate margins for Rician fading conditions while shadowing and blocking is provided by satellite diversity.

Users in severely degraded situations will obtain service in excess of that available from FDMA/TDMA systems. For example, a user may be in a situation where the power control and thermal margin of 11 dB has been exhausted and the user is in need of even more margin. Globalstar's system will sense this situation and the user transferred to another satellite which has a less degraded path.

With CDMA there is no "brick wall" in capacity or signal quality. The system operator has control of the user signals which are requesting services. The Globalstar system has been designed to provide maximum capacity under modeled conditions which represent average conditions expected for the market served. When circuit demand begins to peak the system control facilities adjusts the power distribution to maintain overall signal quality, individual signal links continue to power control as discussed above. When the system reaches maximum capacity at a certain quality, several options are available to the system operator. As examples, two of these options are discussed here. Unlike FDMA or TDMA systems where the capacity reaches the "brick wall" and no further users may be added to the system, the CDMA systems utilize graceful degradation to maintain flexibility. The operator may allow more subscribers to occupy the bandwidth, slightly degrading the overall signal quality from a Mean Opinion Score of 3.5 to 3 or less. Alternatively, the system operator can redistribute a portion or all of the users over more of the satellites in view, thus reducing the blocking and shadowing path diversity for the users which may need it. During these traffic peaking conditions some users may experience

some higher levels of noisy transmission and loss of signal quality for short periods of time.

The Globalstar system offers the system operator maximum flexibility in channel assignment. Since all frequencies are reused in all of the beams, the interaction between gateways is minimized. Since the frequency reuse factor is maximized and the traffic load is averaged over several satellites, the utilization of the satellite is maximized and system loading as discussed above can exceed 100%. The system, in addition, has excess circuits available for handoff and path diversity situations. By comparison, in FDMA and TDMA the frequencies must be assigned in blocks to certain beams and since there cannot be 100% frequency reuse, system efficiency is therefore reduced. Since the system efficiency is 100%, the maximum capacity to a region may be realized and the capacity to each country can be maximized.

With CDMA the ability to concentrate circuits in a small region is important for emergency and disaster communications. For these conditions only CDMA has the flexibility to allow maximum capacity in a small region. Combinations of demand assignment, decreased quality, and other CDMA techniques, can make thousands of circuits available compared to the "brick wall" limitation of FDMA/TDMA.

The spectrum utilization with CDMA systems is maximized. Multiple systems can share the bandwidth with few coordination factors. International sharing with other CDMA operators requires similar sharing coordinating. Since the system downlink Power Flux Density (PFD) around the world is limited and since operation of uplinks are limited by EIRP density and health hazard reasons, these parameters can be coordinated within reasonably small limits.

Considering the downlink sharing, the capacity of the spectrum is the addition of all systems operating with CDMA, less the inter-system interference. Essentially, this means that there are many more power sources (satellites) in view of the region that is being served. The degradation to each system is a percentage of its capacity due to sharing of the interference power between the systems. However, the coordinated result is greater than any single system alone. The usage of the spectrum by several CDMA systems is over twice that of a TDMA system.

The advantage of CDMA to various administrations around the world is the freedom from spectrum segmentation required for operation of a FDMA or TDMA system. Spectrum segmentation, if implemented, results in warehousing of spectrum. This means that if country A and country B are attempting to coordinate systems and one of these is an FDMA or TDMA system and the beams cover both countries, either all or in part, the portion segmented for the FDMA or TDMA system is unusable for the second country even if the first country doesn't bring its system into use. CDMA on the other hand prevents this warehousing. The full bandwidth is available to both countries. If one doesn't deploy, the other just experiences less interference in its system.

3.0 SYSTEM DESIGN FOR GLOBALSTAR OPTIMIZES THE USE OF CDMA

The advantage of Globalstar is that it uses simple and reliable satellites. Forty eight satellites are launched to provide maximum path diversity in the temperate zones and to handle peak traffic. If there are random failures of several satellites, the coverage of the system is not affected most of the time. Therefore, there is no need to have hot spare satellites on orbit, nor the need to launch individual replacement satellites on a crash schedule. FDMA and TDMA systems, since they must only have single satellite coverage of a user, must replace their failed satellites as they fail.

Globalstar has high elevation angles in the temperate zones of the world, for example the average elevation angle in CONUS is up to 55 degrees. The minimum elevation angle, occurring only infrequently and for a very short duration of time is 20 to 32 degrees depending on location. These high elevation angles and path diversity mitigate shadowing and blocking. Reliable path diversity is provided by 100% two satellite coverage in CONUS, three satellite coverage up to 90% of the time and four-satellite coverage up to 35% of the time.

Globalstar has the lowest path delay of any of the proposed LEO systems with the maximum path delay, including vocoder processing, of less than 100 ms. The maximum propagation path delay is 18 ms for the user-satellite-gateway link; the remainder is processing. Since there is no onboard processing or inter-satellite links, the processing is minimized and the overall path delay is reduced, providing excellent quality without the need for echo cancelers, etc.

The implementation method chosen by LQSS allows an easy extension of terrestrial cellular developments underway. Qualcomm Incorporated has developed a CDMA cellular telephone system which improves the spectrum efficiency over analog by a factor of about 15. This system is being deployed currently in several wireline cellular systems in the USA. LQSS plans to modify this system slightly, to account for increased path delay and effects of doppler, and utilize it for satellite delivered cellular telephony.

294

As such, this is the only LEO system proposed which has a heritage for its gateway and user equipment.

A key element in Qualcomm's terrestrial system implementation is the use of a Rake receiver which makes use of all available signal paths to insure that a quality signal is delivered to the user and the gateway. A Rake receiver makes use of the CDMA modulation to receive many signal paths simultaneously and coherently combine them to develop the highest signal input to the decoder. A multiple finger receiver is operated, with each receiver assigned to a particular signal path to decode. A separate receiver continuously searches for signal paths with the user's code. Once a path is found it is assigned to a receiver finger. Logic within the receiver reviews the signal levels emerging from these receivers and performs decisions on combining. It is unimportant whether these are direct paths or multipath signals, all signals received are available to be combined.

The benefits of the usage of two satellite coverage and the Qualcomm unique RAKE receiver design, combined with mitigation of fading and blocking of the hand held user equipment, are very important. Consider the case of a user which is shadowed by a propagation impairment. At the onset of shadowing the user would normally be utilizing a single satellite path to a gateway. The second and third satellite paths, although present would not be in use. As the shadowing increases the unit senses an increased frame error rate, makes an open loop power increase and requests power control, the gateway responds and begins closed loop control. The signal level remains constant at the shadowed satellite. The increased power level will be transmitted by the second and third satellites to the gateway and, depending on system operation be utilized (closed-loop) to optimize the user's power requirements. The need for excessive link margin is thus avoided.

4.0 SUMMARY

Globalstar will use a constellation of 48 satellites to provide continuous coverage of the areas of the world requiring mobile connectivity. The Globalstar system is designed to operate as a complement to existing local, long-distance, public, private and specialized telecommunications networks. Service is primarily designed to serve the rural and thin route communications needs of consumers, government users, and private networks. Frequency Division Spread Spectrum CDMA (FD/SS/CDMA) provides optimum and flexible service quality to the end user allowing multiple signal paths from more than one satellite which mitigates fading and blocking. Link margin is provided to each user independently as the gateway senses that it needs margin. Path diversity, guaranteed by multiple satellite coverage is equivalent to having more margin on a link by link basis. When these margins are used for mitigating fading, shadowing and blocking, the resulting availability is better than a TDMA system with higher margin but with no path diversity.

The Globalstar system offers the system operator maximum flexibility without the need for difficult synchronization, thereby allowing many gateways. Since CDMA maximizes frequency reuse, the traffic load is averaged over several satellites, the utilization of the satellite is maximized and system loading can exceed 100%. The spectrum utilization with CDMA systems is maximized. Multiple systems can share the bandwidth with few coordinating factors. International sharing with other CDMA operators requires similar sharing coordination. The advantage of CDMA to

various administrations around the world is the freedom from spectrum segmentation required for operation of a FDMA or TDMA system which reduces operational efficiency.

Reference [1]

NASA Reference Publication 1274, February 1992; Propagation Effects for Land Mobile Satellite System; Overview of Experimental and Modeling Results, Julius Goldhirsh and Wolfhard J. Vogel

ODYSSEY

Odyssey Personal Communications Satellite System

Christopher J. Spitzer, Odyssey Systems Engineer

TRW Space and Defense, Space & Electronics Group

TRW

3rd International Mobile Satellite Conference and Exhibition

Abstract

The spectacular growth of cellular telephone networks has proved the demand for personal communications. Large regions of the world are too sparsely populated to be economically served by terrestrial cellular communications. Since satellites are well suited to this application, TRW filed with the FCC on May 31, 1991 for the Odyssey construction permit. Odyssey will provide high quality wireless communication services worldwide from satellites. These services will include: voice, data, paging, and messaging. Odyssey will be an economical approach to providing communications. A constellation of 12 satellites will be orbited in three, 55° inclined planes at an altitude of 10,354 km to provide continuous coverage of designated regions. Two satellites will be visible anywhere in the world at all times. This dual visibility leads to high line-of-sight elevation angles, minimizing obstructions by terrain, trees and buildings. Each satellite generates a multibeam antenna pattern that divides its coverage area into a set of contiguous cells. The communications system employs spread spectrum CDMA on both the uplinks and downlinks. This signaling method permits band sharing with other systems and applications. Signal processing is accomplished on the ground at the satellite's "Gateway" stations. The "bent pipe" transponders accommodates different regional standards, as well as signaling changes over time. The low power Odyssey handset will be cellular compatible. Multipath fade protection is provided in the handset.

New Opportunity for Mobile Comm

Terrestrial-based mobile (cellular) communications have grown explosively over the past decade. There are nearly ten million cellular telephones in service within the United States in 1992. The use of radio-telephones is just the first stage in a move to wireless personal communications. Because part of the population is widely disbursed, it cannot be economically served by terrestrial wireless systems. Satellites are more ideally suited to provide service to the population in more remote regions. This includes potential subscribers who cannot be served at all and terrestrial users who have temporarily moved into regions where no service is provided. A new generation of satellites can provide economical access to individuals without the need for heavy, costly satellite Earth terminals. Decisions at the 1992 WARC have opened the way for worldwide satellite based mobile communications using designated frequencies in the S and L Bands.

For nearly 30 years satellites have been used to provide communications to broad areas of the world. Nearly all these satellites have been maintained in geostationary orbit so that the ground antennas could point to a fixed location. User terminals were either fixed ground stations with large disk antennas or large portable ("lugable") terminals which required a disk type antenna with the capability to point at GEO satellites.

The logical extension of satellite services to personal communications is the use of hand-held telephones. Improvements in microcircuits over the past decade have made possible the packaging of an entire satellite earth station into a hand-held telephone, with an omnidirectional antenna. The satellites no longer need to provide the stationary ground track of the GEO satellite. There are several difficulties related to the 35,860 km GEO altitude and equatorial orbit. The orbit is located so far from the earth that 270 milliseconds is required for a signal to propagate to the satellite and return. This causes confusion and inefficiency with interactive communications like voice transmission. Many voice users find the GEO-delay annoying, even when echo cancelers are employed. This great distance also results in signal attenuation. At high latitudes, geostationary satellites are observed at low elevation angles due to the zero-degree inclination of the orbit. Subscribers may experience signal blockage by terrain, vegetation, or buildings.

The new microcircuitry permits consideration of orbits nearer the Earth, reducing path loss and propagation delay, simplifying satellite design and reducing space segment cost. Careful orbit design will keep the elevation angles to the satellites can be kept well above the horizon at all latitudes. The question is: Which orbit is best to take advantage of this frequencies designated by the 1992 WARC for personal mobile communications?

Satellite Altitude & Constellation Selection

Selection of the orbit is a trade-off among the following among the following factors: number of satellites & launch flexibility; system reliability; spacecraft antenna size; spacecraft power; cost of each satellite and life cycle cost; satellite lifetime; terrestrial view angles / line-of-sight elevation angle; degree of Earth coverage; effect of Van Allen belt radiation; handset power; and propagation delay

These factors are interrelated and can only be assessed by synthesizing a fully optimized design (see figure 1). A trade off between design cases for two low Earth
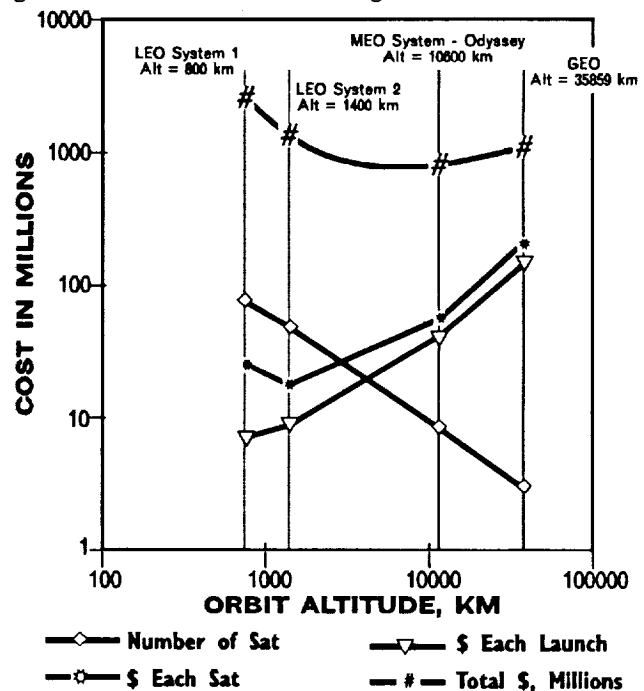
Figure 1: Satellite Cost Trades

orbits (LEO), Medium Earth Orbit (MEO), and GEO satellites was made. For each case the communications mission was to provide a comparable number of personal communications circuits to 0.5-Watt handsets. Each constellation was designed to provide continuous worldwide service with a terrestrial view angle of not less than 10 degrees. Each case was then assessed for total cost.

Geostationary satellite designs require only three or four satellites to provide service to the entire world, however require more than one hundred very narrow beams (produced by very large apertures), complex transponders, and large amounts of power to provide personal communications.

Since propagation losses drop with square of the distance, at lower altitudes satellite antennas can be smaller and transmission power can be reduced. Satellites can be smaller and less expensive in lower orbits since less power is required to close a communications link. The launching cost drops with altitude since the satellites are smaller and less energy is required. However the number of satellites increases rapidly as the orbit altitude drops as shown by the diagonal line in Figure 1. Very close to the Earth the slant range for transmission becomes the governing factor therefore the relative savings are mitigated by the need for a large number of satellites. For Low Earth Orbits nearly 70 satellites are required to provide continuous service. Close to the earth the satellite cost is dominated by slant range more than altitude.

The most significant feature of this trade is that the minimum total cost falls between geosynchronous and low earth orbit as shown by the curve at the top of this graph. The medium altitude orbit requires only twelve satellites to provide continuous global visibility.

Odyssey Orbit

The selected Odyssey constellation contains 12 satellites at an altitude of 10,354 km with four satellites in each of three orbit planes inclined at 55° (see figure 2). The indicated constellation provides continuous, global coverage with dual satellite visibility in some major regions. The Odyssey MEO provides several advantages beyond low
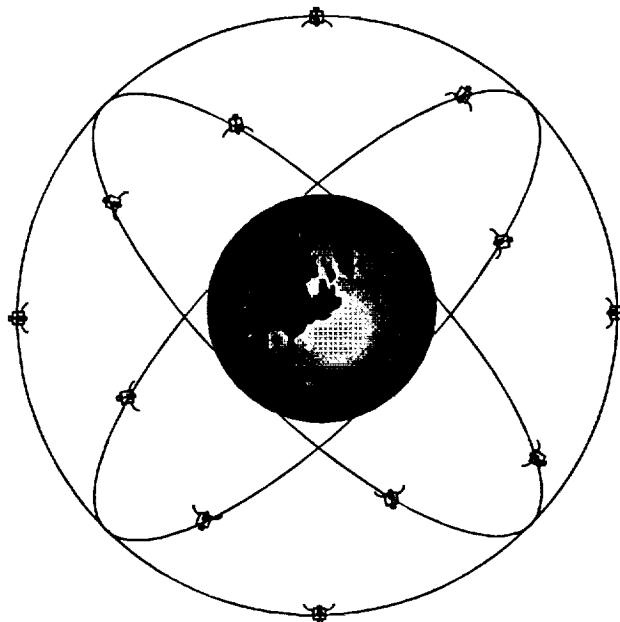
Figure 2: Odyssey Constellation

cost: the propagation time delay is reduced to only 68 to 83 milliseconds which is imperceptible in human conversations. The satellites in this constellation are designed for a 10 year on-orbit lifetime. LEO satellites have a typical lifetime of 5 to 7 years. Only nine satellites are required to ensure that one satellite is visible at all times. Consequently, continuous service to several regions can be started with only nine satellites. By adding only three satellites two or three satellites are visible at all times and service can be provided to most of the world's land mass. This relatively small constellation can be developed and launched in a short time. This will ensure that service can be provided in a short time to market.

Odyssey System Architecture

The Odyssey System is designed to fulfill the following requirements and criteria: minimum life cycle capital cost & low cost to end user; maximum time delay of 100 ms; minimum number of satellites; access to a low power handset; flexible Worldwide land mobile service; no satellite on-board processing; no satellite-to-satellite cross-links; frequency sharing by CDMA; reliable continuity of service; low risk of call dropout; clear, high quality voice circuits

The Odyssey system will provide economical, high quality, personal communication services from medium altitude orbit (MEO) satellites. Services include voice, data, and messaging/paging. Odyssey will provide a link between mobile subscribers and the public switched telephone network (PSTN) via dedicated ground stations (Figure 3). The satellite shall illuminate its assign region with a 19
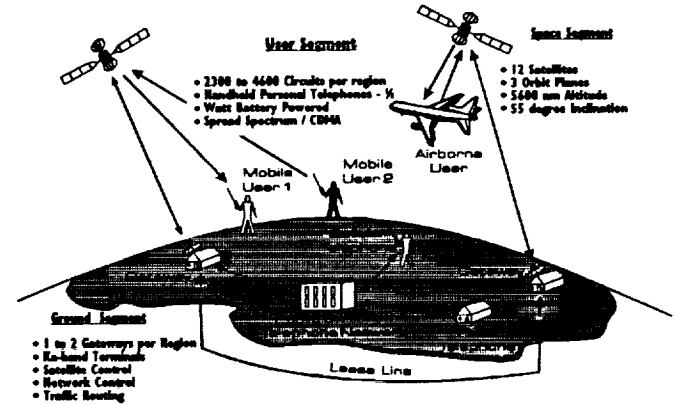
Figure 3: Odyssey System Overview

beam, 5-degree-beamwidth multibeam arrangement. A 37 beam arrangement is currently under study to improve the link margin to the user. Figure 4 shows this pattern covering CONUS. For intercontinental calls, the terrestrial toll network will be used.

Economical design is important so that the subscriber service charge can be priced in line with terrestrial service charges. Economy is achieved through low investment cost, a major consideration for all satellite programs because the production and launch of reliable satellite networks is a very expensive business. TRW achieves this with a small constellation of MEO satellites that provides continuous global coverage.

Call Setup with Odyssey

Priority is given to use of the terrestrial cellular services. When a call is placed the HPT first senses the presence or absence of cellular frequencies and attempts to

298

place a call through the local cellular network. If cellular service is not available or the call is blocked, then the call is routed through Odyssey. User circuits established through a particular satellite enter the PSTN at a ground station located within the region served by the satellite. Odyssey call setup is conducted via order wire to a master control station. A separate order wire channel is assigned to each satellite antenna beam. In making a circuit request, a user terminal transmits requests to overhead satellites. The user is assigned to the beam which provides the strongest signal to the base station, and is instructed to use a suitable power level and a particular spread spectrum code appropriate to that beam. The entire call setup procedure is transparent to the user.

In most cases, a user will remain within a given cell for the duration of a call, thus precluding the need for handover . There are two reasons for this. First, the cells are relatively large; the cell diameter is typically 800 km (497 mi). Second, the cell pattern will remain relatively fixed, since a satellite is continuously reoriented to maintain coverage of its assigned region. Consequently, the need to reassign frequency subbands and spread spectrum codes will occur quite infrequently. But capability will be provided to reassign a user to a different beam if necessary. In
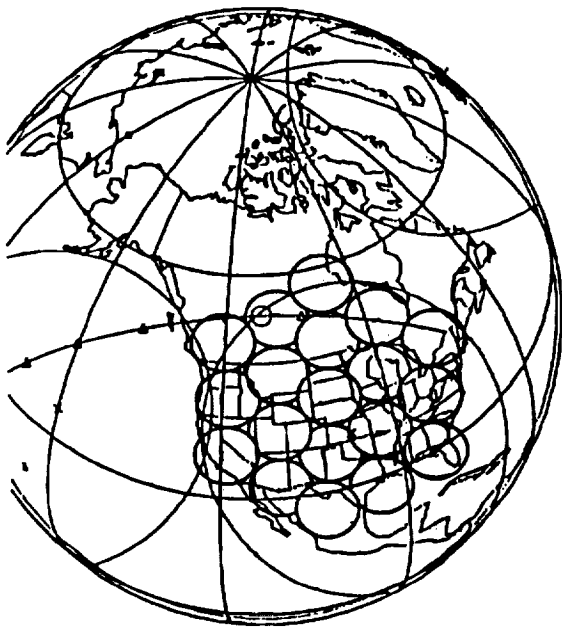
Figure 4: Odyssey Beam Pattern

the case of very long callers, circuit transfer to another satellite can be performed at the base station without the participation of the subscriber.

Satellite Lifetime

The "total cost of ownership" depends on all capital and operating expenditures over a fixed period. Cellular facilities are typically depreciated over a 7-year period, for example. Geostationary satellites are currently designed for lifetimes of ten to fourteen years. Experience has shown that the electronics designs and backup techniques support these durations. Lower altitude satellites, however, have experienced shorter lifetimes due to degradation by atmospheric deterioration such as exposure to ionized oxygen. Due to the "South Atlantic Anomaly", low altitude satellites

are also exposed to high levels of radiation from the Van Allen Belts. In some cases, less redundancy has been built into lower altitude satellites. Odyssey will be designed with full redundancy for 10 years on-orbit lifetime to reduce the cost of ownership.

Communications System Design Drivers

The Odyssey communication system design is driven by several key requirements of personal telephone users. Other driving requirements are manufacturability and reliability of the key system component form the user's point of view - the Handheld Personal Telephone (HPT). Cost effectiveness and capability to generate revenue are also drivers. These key requirements are:

- *Full duplex voice communication*
- *High quality voice encoding: a mean average score (MOS) of 3.5 or better*
- *24 hours communication system availability*
- *Communication capability covering all of the global land masses*
- *Low cost HPTs*
- *Dual mode compatibility with terrestrial cellular systems*
- *Battery capacity for 90 minute talk time duration*

- *Battery capacity for 24 hour standby mode*
- *HPT operation similar to terrestrial cellular*
- *Alphanumeric paging capability*
- *Meets health and safety standards*
- *Data transmission capability*

Frequency Plan

Frequencies for satellite based personal mobile communications were designated at the 1992 WARC. Uplink transmissions from user to satellite are conducted at L-band (1610 to 1626.5 MHz), while downlink transmissions are at S-band (2483.5 to 2500 MHz). The Odyssey signaling method will be spread spectrum (CDMA), which has been proven in numerous government applications. Spread spectrum permits sharing of the frequency spectrum by multiple service operators. In contrast, FDMA or TDMA signaling requires extensive frequency coordination between multiple operators. Spread spectrum also reduces the data rates and power for signal transmission compared to TDMA.

Transmissions between the ground station(s) and the satellites take place at Ka-band. Distinct subbands are reserved for the transmissions to and from each cell. In the return direction, for example, the composite signals received from the different cells are frequency-division-multiplexed (FDM) prior to translation from L-band to Ka-band. Conversely, in the forward direction, the satellite demultiplexes the FDM uplink transmission into its component subband signals following translation from Ka-band to S-band. The composite subband signals are then routed to the various downlink antenna feeds. The required Ka-band bandwidth in either direction is the product of the subband bandwidth and the number of cells in the satellite antenna pattern.

299

Handheld Personal Telephone (HPT) Design

The major Odyssey HPT design driver is simplicity and low cost. A user will perceive no apparent difference between HPT usage in the Odyssey system and today's terrestrial cellular system HPTs. The Odyssey user terminal will be a modified version of a cellular HPT, which can operate at either cellular or satellite frequencies. Odyssey HPTs will use antennas of a quadrifilar helix design.

The Odyssey HPT will transmit approximately 0.5 Watt average power. This transmit power level will be adequate for both voice and digital data transmission. The transmit power level provides an appropriate margin against loss due to rain, vegetation, path distance, etc. It is important to point out that since the Odyssey system operates with high elevation angles of greater than 30 degree, less margin is required for path loss parameters than with LEO systems which must operate at shallow elevation angles.

Odyssey HPTs will be compatible with terrestrial cellular signal formats. This will be achieved by the addition of microelectronic chips to existing HPT designs to produce interoperability with both cellular and Odyssey. The chip sets will be matched to the standards of various regions of the world. In Europe, the HPTs will be interoperable with GSM. In the U.S., the HPTs will work with the American Digital Standard (ADS), Advanced Mobile Phone Service (AMPS), or Odyssey. The Odyssey HPT will meet all of the communication system design driver requirements listed in the previous section.

Gateway Stations

The Gateway station shall provide the connection between the Odyssey satellite link and the PSTNs in each region. Most calls will be directed to the local PSTN. Long distance calls will be directed to the designated long distance PSTN in the Gateways region. The rare Odyssey to Odyssey calls will be routed to the appropriated Odyssey Gateway station through dedicated inter-Gateway leased lines.

The gateway also provides all of the signal processing for the Odyssey system.

Each gateway station will be equipped with four 10-ft tracking antennas which are separated by 30 km. Three of the antennas may be simultaneously communicating with as many satellites.

The fourth antenna will be available to acquire an additional satellite, so that handover of responsibility from one satellite to another can take place without a gap in communications. The fourth antenna can also serve a diversity function in the event of heavy rainfall, since rain cells are typically much less than 30 km in diameter.

Payload Design

Odyssey incorporates a conventional 19 channel architecture for both the forward and return links. Redundancy paths are not shown. In the return link each of the 19 receive beams will be fed to low noise amplifiers (LNA), upconverted to Ka-band, amplified by a high power amplifier or TWTA, and then directed to the Ka-band base station antenna.

The forward link will be the complement of the return link. The Ka-band signal will be received from the base station antenna, down converted, filtered, amplified and directed to the S-band antenna. No feed networks are required for antenna beam shaping. Each transmit channel will be connected to a power amplifier hybrid network to

allow for maximum loading of beams in high traffic areas. A simplified block diagram of the transponder is shown in Figure 5.
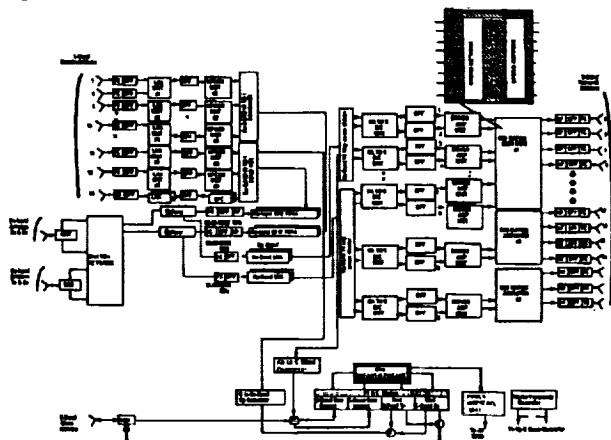
Figure 5: Odyssey Payload Block Diagram

All communication processing is performed on the ground, simplifying the design of the payload on the satellite. This "bent pipe" system also has the advantage of allowing different communication formats to be routed through the Odyssey satellite to accommodate various regional demands. The "bent pipe" design also gives the Odyssey system the capability of updating the communication formats with future developments in communication technology.

Spacecraft Design

The spacecraft platform will be derived from the TRW Advanced Bus development program (see figure 6). TRW has constructed a test bed to demonstrate the Advanced bus design. This new TRW Advanced Bus concept
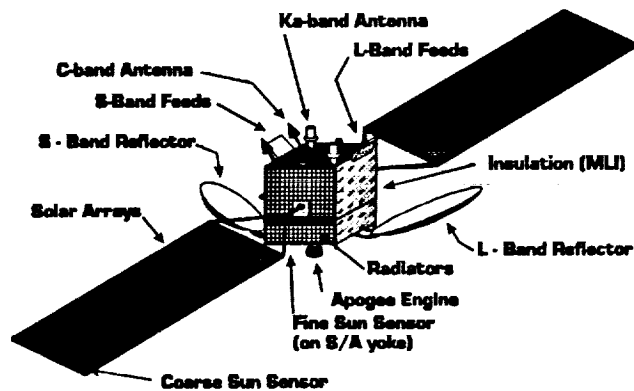
Figure 6: Odyssey Satellite

is successfully being used on several new satellite programs, including NASA's Total Ozone Mapping Satellite (TOMS). TRW is also drawing on its experience from building fleet spacecraft systems such as the U.S. Navy's FLTSATCOM (provides worldwide mobile fleet communications) and NASA's Tracking and Data Relay System (TDRS). Also TRW has been performing studies for NASA on upgrading the TDRS Satellites.

The L-band reflector is approximately 2.25 meters and the S-band reflector is 1.4 meters in diameter. Two Ka-band antennas are gimbal mounted on the Earth-facing panel. The spacecraft points the S and L-band antennas by body steering. Solar Arrays are kept pointed toward the sun

300

by use of single axis solar array drives. The satellites are launched two at a time on an Atlas II and Ariane 4.

The effects of the radiation environment have been analyzed for the Odyssey satellite. The Van Allen belts the major source of potentially damaging ionizing radiation. The selected Odyssey orbit puts the satellites between the outer and inner Van Allen Belts (Figure 7). Solar flares are another source of radiation. Flares are relatively more hazardous to geostationary satellites because the flares are deflected by the Earth's magnetic field. The Odyssey solar arrays, electronic components, and shielding have been
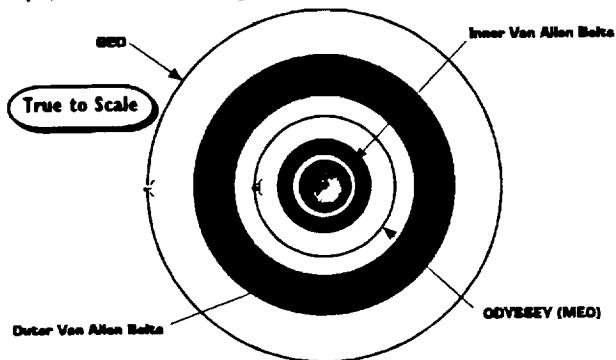
Figure 7: Orbit Position Relative to Van Allen Belts

selected and sized to tolerate the radiation environment for a 10 year mission. New TRW designs in solar arrays and electronic component assemblies has kept the weight of these components to a minimum.

Odyssey Constellation Landmass Coverage

Each satellite's multibeam antenna pattern divides its assigned coverage region into a set of contiguous cells. The total area visible to a satellite will have regions of significant population density, and regions with few subscribers. Consequently, the satellite antennas are designed to provide coverage to only a portion of the total area visible to the satellite. The antennas are fixed mounted to the satellite body. During the period that a satellite is assigned to a particular region, the satellite attitude is controlled so that the antennas remain pointed in the desired direction. Steering the antennas is a key feature of Odyssey which provides a unique benefit: telephone calls are never handed over from satellite to satellite and circuits are seldom passed from beam to beam. This avoids what can be a major communications synchronization problem for LEO satellites which frequently handover telephone calls from satellite to satellite.

Considerable study has been applied to the definition of the 9 service areas to cover the Earth (figure 8). At any time most of the satellites provide primary service to these regions. Additional satellites are used for the transi-

Figure 8: Odyssey Landmass coverage Areas

tion before a satellite moves on to the next assigned region. Traffic builds up on the approaching satellite while traffic wanes on the receding satellite. Cellular telephone calls typically last for only two to three minutes. Therefore, with coverage overlap of approximately 10 minutes, most calls will be completed before satellite coverage will be removed. Each satellite will be visible over any region for almost two hours, but will be only used during intervals that provide the highest elevation angles (typically 60 to 70 minutes). If responsibility for a region is shared among two or more satellites, multiple ground stations will be required. With the full constellation of 12 satellites, a minimum line-of-sight elevation angle of 30 degrees can be guaranteed to at least one of the satellites visible in every location more than 95% of the time. The satellite body steering of the S and L-band antennas provides considerable flexibility for defining service areas to match demand.

Capacity

The capacity of an individual satellite beam is governed by both thermal noise and "self noise" of the spread spectrum system. The capacity of each satellite is approximately 2300 voice circuits. Since the 12-satellite Odyssey constellation can provide dual satellite coverage of any region, the system capacity relative to a region like CONUS will be 4600 voice circuits.

With the basic constellation of 12 satellites, Odyssey will support 2.3 million subscribers worldwide. At least one voice circuit must be provided for each 100 subscribers to avoid call blockage during times of peak demand. Coverage could be expanded by increasing the number of satellites. Use of a synchronous waveform and orthogonal codes could further extend the number of voice channels. A combination of these methods could multiply the capacity by a factor of eight. These techniques could increase the theoretical Odyssey subscriber population to 18.4 million.

Elevation Angles

Perhaps the most important advantage of the Odyssey orbits is high view angles. Two Odyssey satellites will be visible anywhere in the world at all times. This dual coverage leads to high line-of-sight elevation angles, thereby minimizing obstructions by terrain, trees and buildings. Figure 9 shows the elevation angles for GEO, LEO, and Odyssey (MEO) satellites. Geostationary satellites provide
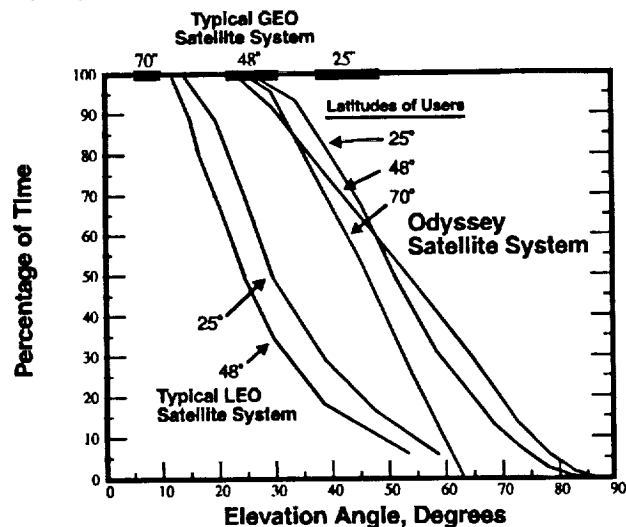
Figure 9: Percent of Time Highest Satellite is Greater than Elevation Angle

301

attractive view angles at latitudes near the equator, but very low view angles at high latitudes. This is illustrated at the top of Figure 9 for GEO. LEO satellites the influence of latitude and longitude is continuously varying since the satellites are moving relative to the Earth. Therefore LEO satellites would provide relatively low view angles most of the time as shown for the LEO system on the left side of Figure 9. But for the Medium Earth Orbit Odyssey the view angles average 45 to 55 degrees at all latitudes. With the full constellation, a minimum line-of-sight elevation angle of 30 (depending on user latitude) can be guaranteed to at least one satellite more than 95% of the time. This is a major benefit to the user since obstructions from trees, buildings and terrain can be avoided and less link margin is required in the communications link budget.

Demand for Mobile Comm Service

We also remember that communications is a service business. Provision of economical and quality service is essential. Service rates are an important factor which determines the success of any mobile satellite business. We get some insight into the economic elasticity of mobile communications service by looking at two segments: Cellular and INMARSAT. After 16 years INMARSAT has 18,000 subscribers paying an average rate of $7.50 per minute. Cellular, after 8 years, has 17.6 million subscribers paying an average service rate of $0.83 per minute. This suggests that decreasing prices by a factor of 10 increases demand by a factor of 1000. TRW has performed market surveys with 4300 participants. The data from this survey confirms the shape of this elasticity in the vicinity of the cellular prices. The survey also shows strong demand for a universal satellite based service. The Odyssey service cost is based on $0.65 per minute and a subscriber base of one to two million subscribers. At higher service rates we would expect a sharp drop in the number of subscribers, which may not sufficiently support a business of this magnitude

Basic Market Areas

TRW has defined four segments which we are continuing to examine for the Odyssey service. We are also in the process of quantifying the demand for each group. These groups are:

-   Corporate and government users who have a compelling need for continuous service over wide regions

-   The second group is business travelers, both national and international roamers who lack service because of technical or "political" incompatibilities

-   Residents of sparsely populated regions who will never receive cellular service because there are not enough subscribers to pay for the infrastructure

-   Citizens of nations which lack communications infrastructure and would benefit from wireless communications.

Odyssey would provide high priority service for premium customers who require reliable mobile communications via a small HPT. Subscribers can have a single telephone which roves with them and doesn't require SIMM cards or special access codes. Odyssey provides the advantage over cellular of access at any location within the Odyssey service regions, almost anywhere in the world. Cellular wireless service is only available in metropolitan regions. Areas where the population is less than 40 to 50 people per square mile cannot be economically supported by Cellular systems. Many different standards prevent use of a cellular telephone outside of the country of origin. In many parts of the world even wire line service is not available. Odyssey would provide communications service without concern for cellular incompatibility or lack of corresponding agreements. Odyssey is designed to provide high quality service. Odyssey employs large cells, up to 800 km (500 miles in diameter) over regions 4000 km across. Furthermore, calls are not switched or handed off to another satellite, minimizing the risk of call dropout. Odyssey requires virtually no handovers and subscribers will not experience processing delays or cease to function. Other systems may need to desynchronize frequently.

The best news for the subscriber is that the service rates would be competitive with cellular. From an communications operators perspective one of the strengths of the Odyssey system is the extraordinary flexibility for adjusting service regions. Odyssey can provide expanded capacity in areas where the demand is greatest.

Odyssey's Relationship With Telecoms

Odyssey will establish strategic service partnerships with several telephone companies in order to cooperate with operators in every country. Odyssey would be a natural extension of the existing infrastructure. Odyssey would provide access to many potential customers who are currently out of reach. Odyssey would expand the customer base and reduce total investment cost in many cases. The Odyssey business plan presumes that many telephone companies around the world would participate in the service, distribution, operations and investment. We anticipate that a private prospectus will be offered later this year.

Odyssey Schedule

The Odyssey program has been fashioned to be the "first to market" with personal communications by satellite. The pacing element is regulatory approvals from the FCC. All business arrangements will be contingent on the U.S. regulatory approval since the U.S. is potentially the largest market for mobile communications. The conventional Odyssey satellites are designed for a three year development time after FCC approval. The relatively small number of satellites would be dual launched in one year using two different launch vehicles for diversity.

Concluding Remarks

New frequency allocations for Mobile Satellite Service (MSS) were approved at WARC'92. Regulatory approval will open the way for a new era of universal personal communications by satellite. Economic viability of MSS, however, will depend on the most cost effective solutions to satellite architecture. The most notable benefits of Odyssey system will be:

-   *Low life cycle capital cost: fewer, simpler, longer life satellites & fewer base stations*

-   *Flexible, reconfigurable worldwide coverage*

-   *Continuous, reliable, uninterrupted service: higher view angles, no cell-to-cell handover*

-   *High quality voice transmission: digital spread spectrum with imperceptible delay*

-   *Subscriber convenience: inexpensive, easy to use, cellular compatible handset*

-   *Competitive service rates: spectrum sharing*

-   *Low space segment risk: Straightforward bent pipe transponder with proven hardware*

-   *Manageable satellite operations: fewer moving parts.*

Inmarsat's Personal Communicator System

Nick Hart, Hans-Chr. Haugli, Peter Poskett and K. Smith
Inmarsat
40 Melton Street
London, NW1 2EQ, England
Phone: 44 71 728 1330
Fax: 44 71 728 1625

New Address after May 1993:
99 City Road
London, EC1Y 1AX, England

Abstract (full paper will be provided at the Conference)

Inmarsat has been providing near global mobile satellite communications since 1982 and Inmarsat terminals are currently being used in more than 130 countries. The terminals have been reduced in size and cost over the years and new technology has enabled the recent introduction of briefcase sized personal telephony terminals (Inmarsat-M). This trend continues and we are likely to see Inmarsat handheld terminals by the end of the decade. These terminals are called Inmarsat-P and this paper focuses on the various elements required to support a high quality service to handheld terminals. The main system elements are:

- The handheld terminals
- The space segment with the associated orbits
- The gateways to terrestrial networks.

It is both likely and desirable that personal handheld satellite communications will be offered by more than one system provider and this competition will ensure strong emphasis on service quality and cost of ownership.

The handheld terminals also have to be attractive to a large number of potential users, and this means that the terminals must be small enough to fit in a pocket. Battery lifetime is another important consideration, and this coupled with radiation safety requirements limits the maximum radiated EIRP. The terminal G/T is mainly constrained by the gain of the omnidirectional antenna and the noise figure of the RF front end (including input losses).

Inmarsat has examined, with the support of industry, a number of Geosynchronous (GSO), Medium Earth Orbit (MEO) and Low Earth Orbit (LEO) satellite options for the provision of a handheld mobile satellite service. This paper describes the key satellite and orbit parameters and tradeoffs which affect the overall quality of service and the space segment costing. The paper also stresses not only the importance of using and sharing the available mobile frequency band allocations efficiently, but also the key considerations affecting the choice of feeder link bands.

The design of the gateways and the terrestrial network is critical to the overall viability of the service, and this paper also examines the key technical parameters associated with the Land Earth Stations (LES), which act as gateways into the Public Switched Telephone Network (PSTN). These not only include the design tradeoffs associated with the LES, but also the different terrestrial network interface options.

The paper concludes with a brief description of the satellite propagation conditions associated with the use of handheld terminals. It describes how the handheld results in a number of propagation impairments which are not common to the previous measurements associated with

vehicle mounted antennas. These measurements indicate that there is a complex tradeoff between link margin and the elevation angle to the satellite which has a significant impact on the space segment requirements and costing.

THE EUROPEAN MOBILE SYSTEM (EMS)

A. JONGEJANS, R. ROGARD
European Space Agency
Postbus 299
2200 AG NOORDWIJK
The Netherlands
TEL: 31 1719 83142
FAX: 31 1719 84598

I. MISTRETTA, F. ANANASSO
Telespazio S.p.a
Via Tiburtina, 965
00156 ROME
ITALY
TEL: 39 640793738
FAX: 39 640793624

Abstract : The European Space Agency is presently procuring an L band payload in order to promote a regional European L band system coping with the specific needs of the European market. The payload, and the two communications systems to be supported, are described below. The potential market for EMS in Europe is discussed.

1 - INTRODUCTION.

The European Space Agency has developed and launched elements of the first generation of Global L-band satellites in the early 80's (MARECS-A launched in 1981 and MARECS-B2 in 1984). From 1983 onwards, in the framework of the PROSAT programme, extensive theoretical and experimental work in the field of mobile satellite communications was carried out, resulting in the design of two Land Mobile Satellite Communication sytems and in the development of the EMS payload to be embarked on the ITALSAT-2 satellite due for launch by mid-1995.

2 - EMS PAYLOAD

The optimisation of the space segment is a key issue for a competitive land mobile voice service as the space segment cost is predominant.This leads to the requirement for efficient use of the radiated power from the correct orbital position over the useful coverage only. For Europe, an edge of coverage gain of about 26 dB can be achieved with a single beam from a 13 deg east orbital position. Another key element is the possibility to reuse the L-Band spectrum from this orbital position through the use of CDMA techniques. A Eurobeam for the feeder link at Ku band offers the possibility of having a VSAT station as Hub. The EMS payload consists of two transponders connecting the Fixed Earth Stations (FESs) at Ku-band with the Mobile Earth Stations (MESs) at L-band and vice versa. The main characteristics of the EMS payload are summarised below:

Feederlink	:	Ku-band
Mobile link	:	L-band
L-band	:	42.5 dBW
L-band G/T	:	-2 dB/K
Ku-band G/T	:	-1.4 dB/K
Useful bandwidth	:	12 MHz
Payload DC power	:	400 W
Payload Mass	:	60 kg

EMS characteristics

In order to facilitate coordination with other L-band satellite networks and to allow flexible handling of the payload capacity, the total useful bandwith has been divided into independent sub-bands. In the forward link the total useful bandwidth consists of three 4 MHz bands.In the return link, where the interference problems are most acute, each of the above three bands has been further divided into four channels each, of 1 Mhz, referred to as "virtual transponders". Each virtual transponder can be remotely and independently switched on or off and its gain adjusted. Channel filtering is achieved by using

SAW technology at an IF frequency of about 140 MHz.

Two separate offset L-band antennas are used for transmit and receive, reusing the ITALSAT F-2 Ka-band elliptical reflectors (projected aperture diameter: 2m) and dedicated L-band four "cup" feeds. RHC and LHC circular polarisations are provided. The typical coverage is shown in Figure 1. Assuming a nominal voice channel EIRP of 19 dBW, 600 channels can be served simultaneously (including voice activation factor).

3 - PROPOSED MOBILE SYSTEMs
(see Refs. 1 and 2)

Two baseline systems are foreseen to be operated via EMS:

A-The Low-data-rate PRODAT-2 system.

The PRODAT-2 system is the operationnal evolution of the experimental PRODAT system which has been successfully tested and demonstrated in Europe under the responsibility of the European Space Agency between mid-1987 and end 1992 (Ref 1).The main characteristics are very similar and the experience gained during the trial phase together with the evolution of the market has provided scope for optimisation of the system. The system is an open, centralised and modular system in which the fixed user is connected to the Hub via the public network, either directly or via national or regional concentrators (see Fig. 2). Link characteristics are given below:

> -Store and forward
> -Forward link:BPSK/TDM 1500 bit/s
> -Return link: CDMA/OQPSK 600bit/s
> -Adaptative block coding with ARQ
> -Omnidirectionnal mobile antenna
> -10 W RF power

PRODAT-2 main characteristics

-The basic communication functions are retained (Bi-directional messaging, broadcast, request/reply and polling). The public network access to the Hub is compatible with CCITT X400 recommendations in addition to conventionnal fax/telex links. Several other improvements have been implemented to cope better with users requirements. The PRODAT-2 system is now ready for demonstration, for which a pre-series of fully industrialised MES's (including a GPS card for position determination) are available. The two

manufacturers (FIAR-Italy and PESA-Spain) are ready to produce MES's at competitive prices.

B- The Mobile Satellite Business Network (MSBN) voice and data system

The present MSBN definition is the result of many detailed studies including market surveys, and in-depth technical evaluation. The basic MSBN concept represented in figure 3. shows that a fixed user has direct access to his fleet of mobiles through his own VSAT station installed on his premises and pointed towards EMS. The VSAT station operates at Ku-band and the mobile station at L-band. The MSBN system uses quasi-synchronised CDMA access techniques in both directions over the satellite link.(see Ref 3). The choice of CDMA eases the coordination with other satellite systems and is particularly suited to the PMR (Private Mobile Radio) concept where all the independant networks share a common bandwidth resource without the need for network coordination. The synchronisation of the transmissions in both directions allows a greater number of simultaneous users due to the drastic reduction in the self-noise level. Also,the mobile receiver acquisition is eased as a synchronisation signal is continuously transmitted providing chip, code and carrier synchronisation. In the basic configuration, a pair of channels (codes) are allocated to each business network in a star configuration, and those channels are shared between the MES's under the VSAT station control to handle up to about 125 trucks under average traffic conditions. It should be noted that the system allows for a modular growth of the communication capabilities of the VSAT station according to the growing needs of the transport company. On the other hand, a VSAT station may be shared by more than one company to reduce costs to smaller companies. The link characteristics of MSBN are given below:
> -L-band mobile link
> -Both link uses CDMA Quasi Synchronised
> -QPSK at 867 KChip/s
> -Voice at 6.4 Kbit/s
> -Data at 2.4 Kbit/s
> -Convolutional and block coding
> -Steered mobile antenna with 11 dB
> gain (see refs. 4 and 5)
> -10 W RF in transmit

MSBN main characteristics.

An experimental MSBN network is presently under procurement by the Agency, and one FES

manufactured by SAIT (Belgium) and 14 MES's from Fiar (Italy) and PESA (Spain) will be available for tests and demonstration by the end of 1993, using the Marecs-A satellite.

4 -SERVICES AND COMPETITION

Market surveys have revealed an urgent need in Europe for specialised mobile services for the business world, as distinct from public services offered by Public Telecommunications Operators (PTO's). In the international road-transport sector, for instance, the needs are particularly pressing. Companies that operate fleets of vehicles transporting goods across Europe are very anxious to maintain instant communications with their vehicles wherever they are.

With the opening of borders towards Central and Eastern Europe, the satellite now appears as the only practical way to provide mobile services to those countries on a significant scale.
The poor telecommunication infrastructure of eastern European countries also justifies the need for portable terminals either for data and/or voice services to help interactive businesses.

The actual mobile satellite services being introduced mainly by the PTO's in Europe are Inmarsat's standard-C and Eutelsat's Euteltracs. It is clear that even if the trans-border communication services offered are unique in Europe, their market penetration rate is rather slow. The reasons for this might be marketing, too high tarifs, inadequacy of performances vis-a-vis user requirements or simply an immature market.Both systems have a centralised approach imposing the use of public networks to connect the fixed user to the satellite system. The start of these services ahead of EMS is not considered as a handicap but rather a preparation of the market for satellite services. Other competition will come from the digital European cellular system GSM which is presently being introduced. The prices of mobile terminals will certainly be lower than satellite terminals due to the economies of scale, but the flexibility and the service prices can easily be challenged by a well-designed regional satellite system.

5 - ASSESSMENT OF POTENTIAL SUBSCRIBERS

Awareness of the addressable market and definition of the potential user profiles are fundamental if a successful and profitable Land Mobile Satellite System is to be implemented. A correct market segmentation

allows both the definition of systems/products/services that suit the various user requirements and the formulation of appropriate marketing messages directed to the various segments, aiming at differentiating the system/service/product with respect to the various competitors. A study performed by Telespazio for the Agency (see Ref. 6) has evaluated the potential subscribers to EMS, limiting the analysis to the addressable potential terrestrial user. The methodology persued included the following steps:

(a) Assessment of present population of the various user segments.
(b) Assessment of the future population (1995 to 2005)
(c) Assessment of the potential users (interested in mobile communication services irrespective of the telecommunication system, terrestrial or satellite).
(d) Assesment of the addressable users (interested in LMSS communication services).
(e) Assessment of the potential subscribers for EMS specifically.

Estimates of potential users interested in mobile communications services in Europe in 1995 and 2005 are given below:

Year	Potential Users (x1000)	
	1995	2005
Trucks [1]	2000	2687
Railways Passenger coaches Goods wagons	69 962	76 1231
Professional Travels	9000	9460
Data collection & Monitoring Appl.	840	1023
Car Rental [2]	34	46
Rescue Users	tbd	tbd
Buses [2]	92	107
Total	12997	14630

[1] Trucks >3t

[2] Only Italian users

The potential truck user include only those having capacities greater than 3 tons. For the other user groups, the entire future population of users has been assumed (data regarding rescue users were not available). It is worth noting that the end-user prices assumed in the baseline forecast for the voice and data service on EMS, have been determined on the basis of the end-user prices of terrestrial cellular systems with the addition of a price for the satellite services. The prices considered have been :

Terminal Prices ($) :
data	:2200
voice	:3500
End-User Prices ($)	:
Subscription charege	:32
Data charge	:0.28$kbit
Voice charge	:1$/min.

Finally, the potential EMS subscribers have been determined on the basis of service introduction time in the market and competition from other LMSS system.

The figure below shows the growth curves for EMS potential subscribers per basic service.

POTENTIAL SUBSCRIBERS OF EMS
Growth Rate

● Voice+Data ✦ Data ○ Paging ▲ Total Subscribers
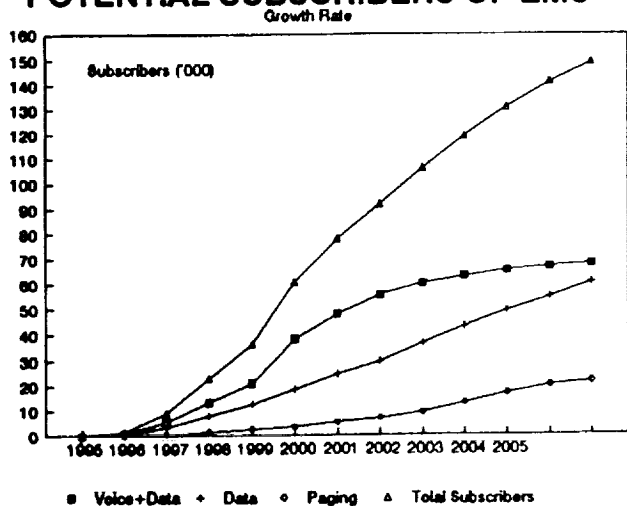
6 -IMPLEMENTATION SCENARIO

The deployment of any telecommunication system generally involves answering at least two major questions:
-How will the system be implemented ?
-How will the system be operated ?
Key points of the physical implementation of any LMSS are :
- Space segment. Identification of its characteristics and availability of the in-orbit capacity and backup capacity.

- Network deployment. Determination of various phases to make the system operative.

In order to prepare the market,an interim PRODAT-2 low data rate service will be provided using Marecs-A residual capacity. Then, the EMS payload embarked on Italsat F-2 will be available in orbit by mid-1995. Backup capacity will be provided by the LLM (L-band Land Mobile) payload to be embarked on ARTEMIS, with a launch in 1996.

As far as network deployment is concerned, it depends primarily on constraints dictated by the technical and marketing/commercial analysis. In particular, three main stages have been highlighted with reference to technical and operational considerations:

a) Test and demonstration of the system. This is aimed at validating the system from the both performance and operational capability standpoints.

b) Pilot project (Pre-operational phase). This is aimed at refining the system. In addition, it is directed primarily at promoting the system and validating it from an operational viewpoint.

c) Operational Phase. This phase is divided into two steps :

(1st) Private Network
(2nd) Public Network

The rationale for this choice is based on to both market analysis and operational considerations. A reasonable date for Public Service introduction might be 1996.

7 - CONCLUSIONS

The future European Mobile system making use of a piggy-backed payload on a fixed communication satellite has been presented and the various inherent elements described. The design selected has been carefully matched to the requirements of the main potential user groups that have been identified. The chosen options allow problems related to the coordination with other satellite systems to be overcome from an interference point of view. Moreover, the regional system described can compete with other mobile telecommunication services and can be profitable for the system operator. Even if modest in size, EMS also will open a new market for the European mobile and VSAT stations manufacturers and the associated value-added service providers.

REFERENCES

[1] Results of Field Trials Conducted in Europe with the PRODAT System
R. Rogard, A. Jongejans and C.Loisy
ESA Journal - 1989 Vol 13

[2] LMSS: From Low Date Rate to Voice Services.
R. Rogard
Proceeding 14th International Communication Satellite Systems Conference AIAA), Washington DC, March 92

[3] First Satellite Communication Trials using BLQS-CDMA.
M.L. de Mateo et al., also included in the proceedings of the IMSC'93.

[4] Microstrip Monopulse Antenna for Land Mobile Communications.
Q. Garcia et al., included in the Proceedings of the IMSC'93.

[5] Small Stearable Land Mobile Antenna - Final Report.
Estec contract: 8394/89/NL/PB
VTT Technical Research Centre of Finland.

[6] System Architecture and Market aspects of an European Land Mobile Satellite system via EMS.
F. Ananusso, I. Mistretta.
Proceeding 14th AIAA conference - March 92 Washington DC.
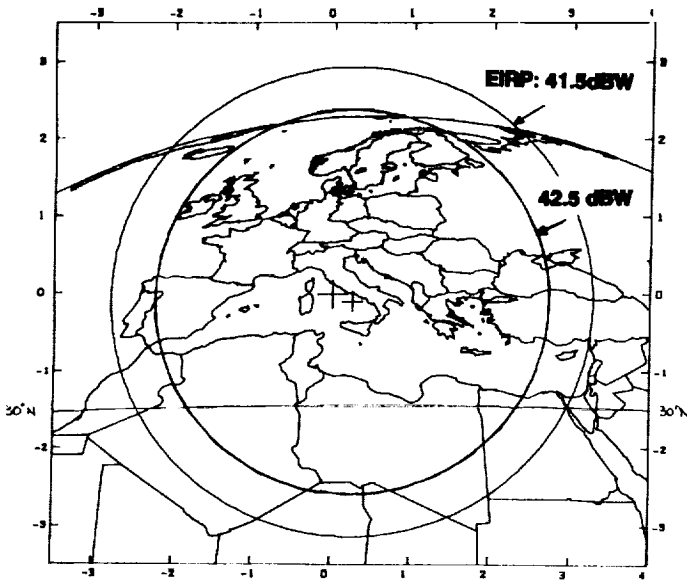
FIG.1: EMS TRANSMIT COVERAGE
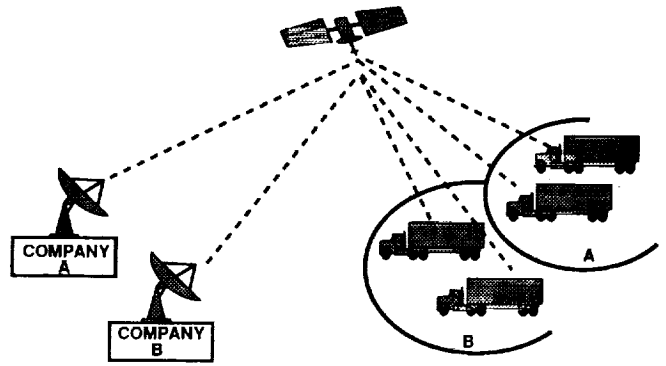
FIG 3: MSBN NETWORK
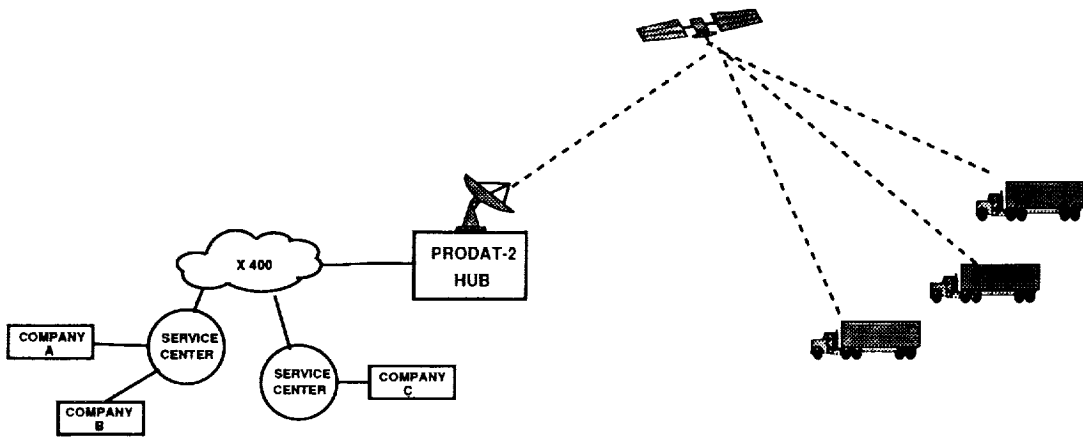
FIG:2 PRODAT2 NETWORK CONCEPT

FIG 4: PRODAT MOBILE STATIONS
OLD (LEFT) AND NEW (RIGHT)
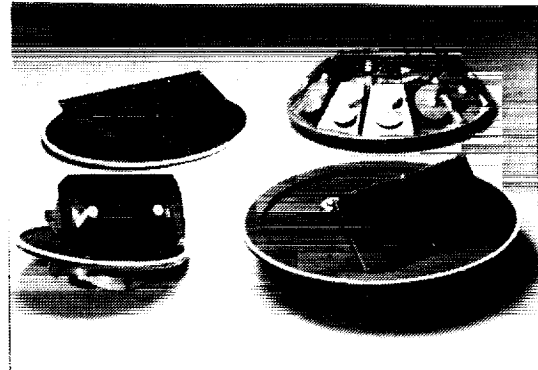
FIG 5: PROTOTYPE MOBILE ANTENNAS
DEVELOPPED FOR MSBN

310

Session 8
Propagation

Session Chair—*Barry G. Evans,* University of Surrey, England
Session Organizer—*David Rogers,* Communications Research Centre, Canada

(continued)

311

312

Land Mobile Satellite Propagation Measurements in Japan Using ETS-V Satellite

Noriaki Obara, Kenji Tanaka
Shin-ichi Yamamoto and Hiromitsu Wakana
Kashima Space Research Center,
Communications Research Laboratory,
Ministry of Posts and Telecommunications
893-1 Hirai, Kashima
Ibaraki 314, Japan
Phone: +81-299-84-4144
Fax: +81-299-84-4149

ABSTRACT

Propagation characteristics of land mobile satellite communications channels have been investigated actively in recent years [1], [2], [3]. Information of propagation characteristics associated with multipath fading and shadowing is required to design commercial land mobile satellite communications systems, including protocol and error correction method. CRL (Communications Research Laboratory) has carried out propagation measurements using the Engineering Test Satellite-V (ETS-V) at L band (1.5 GHz) through main roads in Japan by a medium gain antenna with an autotracking capability. This paper presents the propagation statistics obtained in this campaign.

INTRODUCTION

Expressways, by which almost all main cities are connected, play a very important role for land transportation in Japan. Since vegetative shadowing and blockage due to buildings are rare along expressways, satellite communication services such as voice, video and message transmission are suitable over wide areas in Japan. CRL carried out propagation measurements through main expressways and several ordinary roads, which totaled more than 4,000 km. This paper presents the propagation characteristics in this campaign, especially, sta-tistical characteristics of receiving signal power and non-fade/fade durations.

EXPERIMENTAL CONFIGURATION

A continuous wave (1.5 GHz band) transmitted from the geostationary ETS-V satellite was received by an electronically steerable 19-element phased array antenna with about 12 dBi antenna gain. This antenna is controlled by two vehicle's directional sensors: an optical fiber gyroscope and a geomagnetic sensor [4]. Since receiving signal power is sampled every 6.28 cm by pulses that are generated at the wheel axle of a test van, propagation characteristics are measured independently of the van's speed. Satellite elevation angles along these roads are about 40 to 50 degrees. Figure 1 shows experimental routes in this campaign and Table 1 shows typical examples of environmental conditions. Figure 2 shows the measurement van running on an expressway.

MEASUREMENT RESULTS

Based on a given threshold of a signal level, it can be determined whether a propagation channel is on a fade state (below the threshold) or a non-fade state (above the threshold). When the threshold is less than -5 dB, fade states are mainly caused by obstacles such as overpasses and guideposts along roads. Figure 3 shows examples of distributions of obstacles in expressways.

Receiving Signal Power

Figure 4 shows cumulative distributions of receiving signal power with respect to the line-of-sight level. Since every curves are straight in the range of about -2 to 2 dB, probability density distributions are Gaussian distributions in this range. This distribution corresponds to Rician distribution with high SN ratio (large Rice factor). Between about -4 dB and system noise level (about -25 dB), every curves have moderate inclinations and are fixed, especially in expressways data. In this range, the fades are mainly caused by shadowing and blockage. The propagation channel in expressways has a stronger tendency to be classified into two states (available or unavailable for communication) than in ordinary roads. Two states correspond to a line-of-sight condition and a blockage condition due to man-made structures such as overpasses and tunnels. Since most satellite links are power-limited, a large fade margin above 5 dB to combat shadowing and blockage is ineffective for providing acceptable services. When the fade margin is 5 dB, satellite communication services are available at least about 90 % of the total distance in expressways, even though including tunnels.

Non-fade/Fade Duration Distribution

Non-fade Duration Distribution

In Figure 5, cumulative distributions of non-fade durations for different threshold levels and measuring conditions are presented, respectively. The ordinate is Gaussian scale and shows the probability of non-fade duration exceeding the abscissa value. Characteristics of these measured curves are almost independent of the threshold level except the threshold of -3 dB, which include level fluctuation due to thermal noise and antenna tracking error under a line-of-sight condition, as shown in Figure 5 (a), and the probability density function (PDF) of non-fade durations in both ordinary roads and expressways can be rep-

resented by a combination of two log-normal distributions with different mean values and deviations [3], [5], as follows.

$$P.D.F.(\ln(x))$$

$$= w_0 \cdot \frac{1}{n_f} \cdot \frac{1}{\sqrt{2\pi}\sigma_0} \exp\left\{-\frac{(\ln(x)-\ln(m_0))^2}{2\sigma_0^2}\right\}$$

$$+ w_1 \cdot \frac{1}{\sqrt{2\pi}\sigma_1} \exp\left\{-\frac{(\ln(x)-\ln(m_1))^2}{2\sigma_1^2}\right\}$$

$$\text{for} \quad x \geq 6.28(cm) \tag{1}$$

where w_0 and w_1 are weight factors ($w_0+w_1=1$), m_0 and m_1 are mean values, and σ_0 and σ_1 are standard deviations of each log-normal distribution term. The factor n_f is normalizing factor for truncated log-normal distribution.

In ordinary roads, the probability of non-fade duration longer than 100 m is less than 10 % within all non-fade states, but in expressways, it exhibits 10~50 % probability, as shown in Figure 5 (b). Moreover, expressways data show that durations longer than 1 km exhibit 5 % probability on an average.

Fade Duration Distribution

Figure 6 shows cumulative distributions of fade durations for different threshold levels and measuring conditions. Characteristics of these curves are almost independent of the threshold level except -3 dB threshold level as shown in the non-fade duration case.

Since expressways have obstacles of two specific lengths in overpasses and tunnels, these curves have large inclination at durations of both about 10 m and 1 km, as shown in Figure 6 (a), (c). Therefore, the curves do not fit such simple model as that in non-fade durations. In ordinary roads, however, the PDF of fade durations can be approximated very well with the model of equation (1). Especially in rural and suburban areas that are mainly shad-

314

owed by trees, the PDF are almost straight lines in log-log scale, as shown in Figure 6 (b). Therefore, the PDF can be also represented by an exponential function,

$$P.D.F.(x) = a \cdot x^{-D} \qquad (2)$$

where a and D are constant values. To study complex structures in nature, the terminology "fractal" is recently used in many aspects of physical phenomena. This characteristics of fade duration correspond to fractal dimension of D.

Non-fade/Fade State Transition Frequency

For designing of communications protocol or error correction method, it is useful to know how frequently communications channels are interrupted. Table 2 shows frequency of transition from non-fade state to fade state per kilometer and a ratio of total durations of fade states to the total measuring distance. The transition frequencies on expressways are less than that on ordinary roads by about five times. Even if vehicle's speed on expressways is twice larger than that on ordinary roads, transition frequency per minute is less than that on ordinary roads by twice on an average.

CONCLUSIONS

Measured data show that propagation channels in expressways can be classified into two states. Two states correspond to a line-of-sight condition and a blockage condition due to overpasses and tunnels. When the fade margin is 5 dB, satellite communication services are available at least about 90 % of the total distance. Distributions of non-fade durations can be approximated by the combination of two log-normal distributions, and distributions of fade durations can be approximated by a simple exponential function, especially in rural areas. Expressways data also show that non-fade states exhibit durations of longer than 1 km at 5 % probability on an aver-

age. This value is larger than that on ordinary roads by about ten times. Moreover, non-fade/fade states transition frequency is about five times less than that on ordinary roads. Therefore, expressways in Japan are more suitable for land mobile satellite communications services.

REFERENCES

[1] W. J. Vogel, J. Goldhirsh and Y. Hase, "Land-Mobile-Satellite Propagation Measurements in Australia Using ETS-V and INMARSAT-Pacific," *The Johns Hopkins University/APL Tech. Report* SIR89U-037, 1989.

[2] A. Benarroch and L. Mercader, "LMSS Propagation Model Based on a European Experiment Using MARECS Satellite," *Electronics Letters.*, vol. 27, no. 4, pp. 298-300, 1991.

[3] Y. Matsumoto, R. Suzuki, K. Kondo and M. H. Khan, "Land Mobile Satellite Propagation Experiments in Kyoto City," *IEEE Transactions on Aerospace and Electronic Systems*, vol. 28, no. 3, pp. 718-727, July 1992.

[4] K. Tanaka, S. Yamamoto, H. Wakana, S. Ohmori, M. Matsunaga and M. Tsuchiya, "Antenna and Tracking System for Land Vehicles on Satellite Communications," *Vehicular Technology Society 42nd VTS Conference Frontiers of Technology*, Denver, USA, May 1992.

[5] N. Obara and H. Wakana, "Fade/Non-fade Duration Characteristics and a Model for Land Mobile Satellite Communications Channels," *Proceedings of IEEE Antenna and Propagation Symposium*, Chicago, USA, July 1992.

Total measuring distance

about 4,000 km
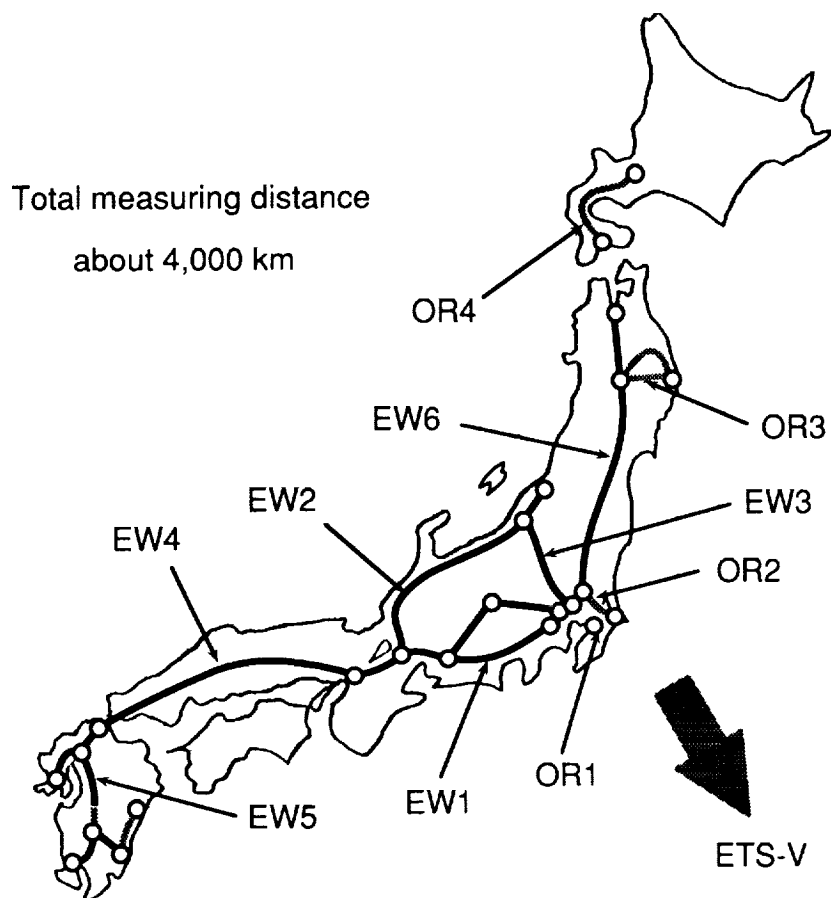
Figure 1. Experimental routes in this campaign.

Table 1. Typical examples of environmental conditions.

Data Name*	Route Name	Total Distance (km)	General Environmental Conditions
EW1	Toumei	400.7	Hilly terrain, infrequent shadowing by overpasses and guideposts.
EW2	Hokuriku	495.2	Mountainous terrain, infrequent shadowing by overpasses and tunnels.
EW3	Kan-etsu	254.3	Hilly terrain, infrequent shadowing by overpasses and tunnels.
EW4	Chugoku	566.1	Mountainous terrain, shadowing by overpasses, tunnels and trees.
EW5	Kyushu	331.2	Mountainous terrain, shadowing by overpasses, tunnels and trees.
EW6	Tohoku	681.0	Hilly terrain, infrequent shadowing by overpasses and guideposts.
OR1	Chiba City	25.7	Urban roads, frequent shadowing by buildings and overpasses.
OR2	Route 356 & 16	101.5	Suburban roads, infrequent shadowing by utility poles, guideposts and trees.
OR3	Route 106	108.7	Rural roads through hilly terrain, shadowing by trees and tunnels.
OR4	Route 5, 37 & 230	243.5	Rural roads including hilly terrain, shadowing by trees and tunnels.

Note: * "EW" is an expressway and "OR" is an ordinary road.

Figure 2. Measurement van running on an expressway.

Data: EW1   Data: EW2

- ▤ Overpass
- ▥ Guidepost
- ■ Tunnel
- ▨ Tree
- ☐ Others
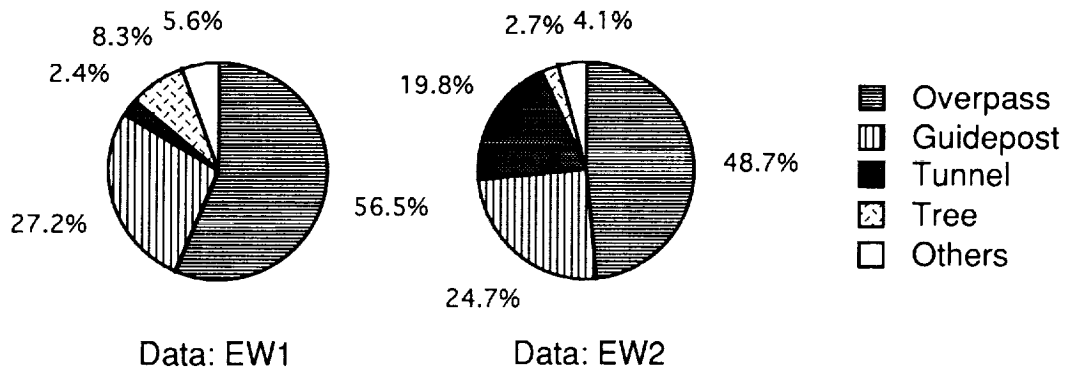
Figure 3. Distributions of obstacles in expressway.

Table 2. Ratio of total duration of fade states to the total measuring distance and transition frequency from non-fade state to fade state with -5 dB threshold level.

Data Name	Fade States Ratio (%)	Non-fade/Fade States Transition Frequency (counts/km)
EW1	3.35	3.33
EW2	13.60	0.97
EW3	8.82	1.86
EW4	8.76	18.10
EW5	10.02	10.74
EW6	2.88	2.37
OR1	21.46	62.01
OR2	1.70	23.34
OR3	11.48	57.32
OR4	5.14	25.54
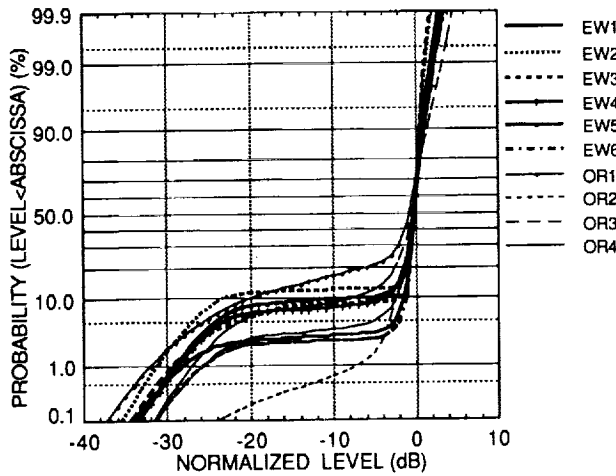
Figure 4. Cumulative distribution of receiving signal power.

Legend: EW1, EW2, EW3, EW4, EW5, EW6, OR1, OR2, OR3, OR4
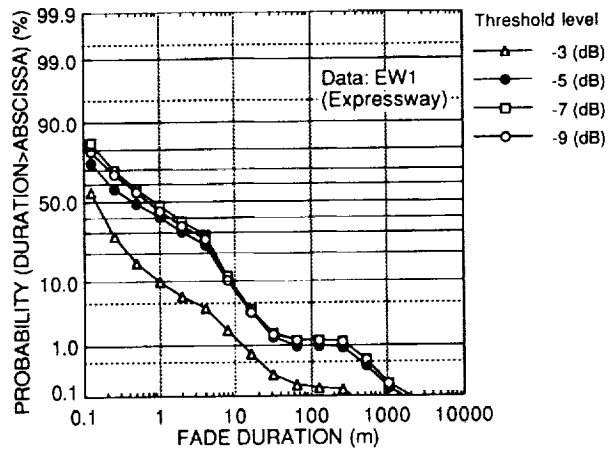
Figure 6 (a). Fade duration distribution of EW1 (expressway).

Data: EW1 (Expressway)

Threshold level: -3 (dB), -5 (dB), -7 (dB), -9 (dB)
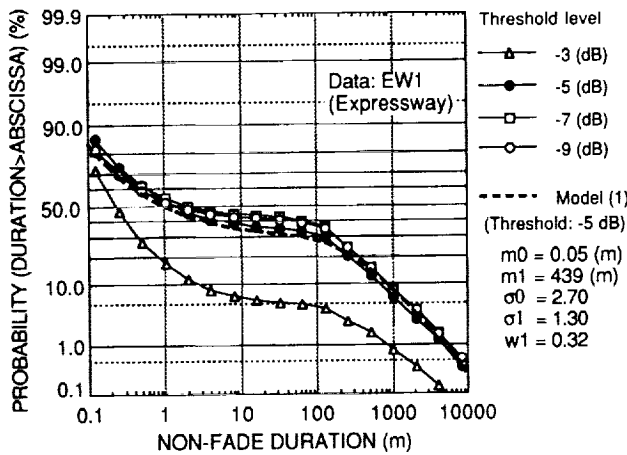
Figure 5 (a). Non-fade duration distribution of EW1 (expressway).

Data: EW1 (Expressway)

Threshold level: -3 (dB), -5 (dB), -7 (dB), -9 (dB)

Model (1) (Threshold: -5 dB)

$m_0 = 0.05$ (m)
$m_1 = 439$ (m)
$\sigma_0 = 2.70$
$\sigma_1 = 1.30$
$w_1 = 0.32$
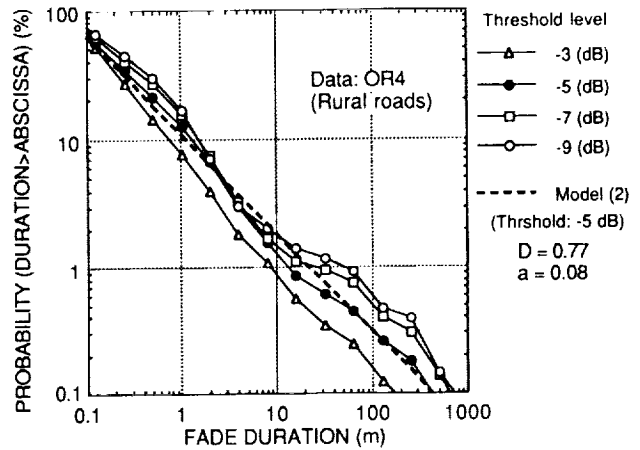
Figure 6 (b). Fade duration distribution of OR4 (rural roads).

Data: OR4 (Rural roads)

Threshold level: -3 (dB), -5 (dB), -7 (dB), -9 (dB)

Model (2) (Thrshold: -5 dB)

$D = 0.77$
$a = 0.08$
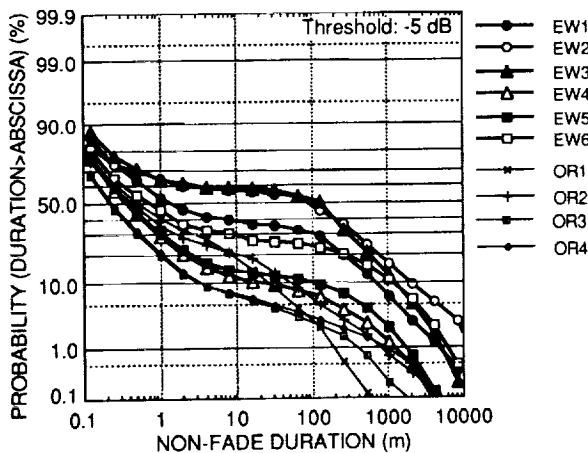
Figure 5 (b). Non-fade duration distribution for different measuring conditions.

Threshold: -5 dB

Legend: EW1, EW2, EW3, EW4, EW5, EW6, OR1, OR2, OR3, OR4
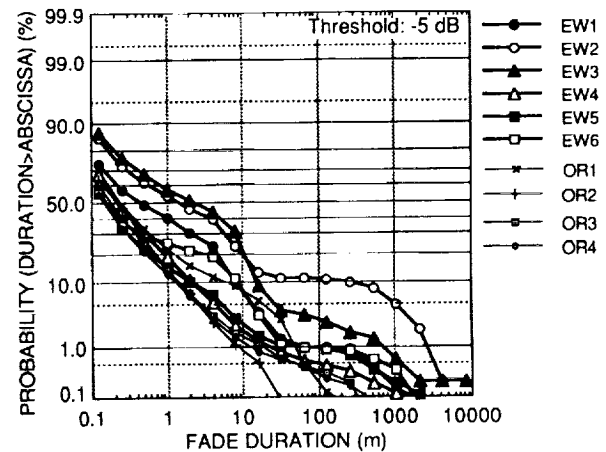
Figure 6 (c). Fade duration distribution for different measuring conditions.

Threshold: -5 dB

Legend: EW1, EW2, EW3, EW4, EW5, EW6, OR1, OR2, OR3, OR4

318

Measurements on the Satellite-Mobile Channel at L & S Bands

H. Smith, J.G. Gardiner, S.K. Barton
Department of Electronic and Electrical Engineering
University of Bradford
Richmond Rd.
Bradford
West Yorkshire
BD7 1DP
England
Tel: 44 274 384060
Fax: 44 274 391521

ABSTRACT

An experiment is described in which measurements are made on the satellite-mobile channel at L and S bands. A light aircraft carrying a c.w. beacon is flown at elevation angles of 40, 60 & 80 degrees to a mobile receiver. The signal strength at the mobile is recorded in open, urban, suburban & tree shadowed environments. This data is then analyzed to produce statistics for the channel with respect to frequency, elevation angle and environment. Results are presented together with a brief discussion, suggested interpretation and conclusion.

INTRODUCTION

Over the last decade in both Europe and the USA, interest in the development of a Land Mobile Satellite Service (LMSS) and in providing CD quality radio broadcasts from satellites, has given rise to a requirement for information on the satellite mobile channel at low microwave frequencies. In Europe, the use of satellites in Highly Elliptical Orbits (HEO's) has been proposed for these systems [1,2], as in these regions due to the low elevation angle of geostationary satellites, large margins are required to compensate for signal fluctuations caused by natural or man-made obstacles. It is assumed that a HEO satellite system will require much lower propagation margins, thus making a practical system possible. WARC'92 has allocated frequencies at about 1.5GHz (L-band) and 2.5GHz (S-band) for these services. The University of Bradford (UoB), the United Kingdom Radiocommunications Agency (UK-RA) and the European Space Agency (ESA), have for the last three years been collaborating on an comprehensive narrowband channel characterisation, involving measurement campaigns at 1.556GHz and 2.619GHz, in different physical environments using beacons at a range of elevation angles to the mobile.

EXPERIMENTAL DETAILS

A light aircraft fitted with a suitable c.w. beacon simulates the signal from the satellite. Since the propagation statistics are both elevation and environment dependent, the aircraft is flown over selected terrains at elevation angles to a ground mobile of 40, 60 and 80 degrees. The mobile receiver records the varying signal strength at the vehicles antenna in time synchronism with a vehicle speed signal and position/altitude information. The terrains were as follows:
Open rural
No obstructions to a line of sight path at any elevation angle, open flat countryside for a several hundred metres on each side of the

road.

Urban

The city of Bradford, UK. Many buildings close to the roadside of several stories. Short section of urban freeway.

Suburban

Buildings of one or two storeys, set back between 10 and 20 metres from the side of the road.

Tree shadowed

Mature deciduous trees of varying density and distance from the road. The statistics given are for a typical mix or "composite" cover.

EQUIPMENT

A c.w. transmitter was located in a Rallye 235E light aircraft. At L-band this unit consisted of a synthesiser operating at 1.556GHz and amplification to 0dBW. At S-band a 1.309GHz synthesiser was used together with a frequency doubler and again, amplification to 0dBW. An antenna having a gain of 2.8dB and a beamwidth of $\pm 45°$ of boresight was mounted under the tail of the aircraft pointing directly down.
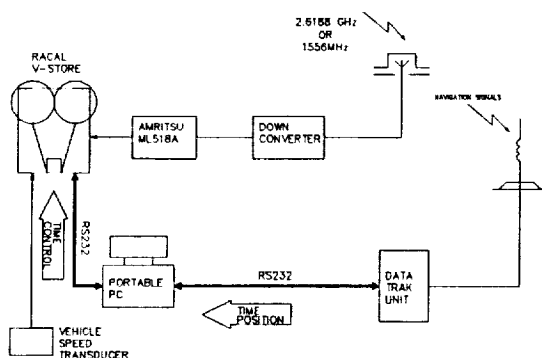
Figure 1- Mobile receiver system

The mobile receiver system was as shown in figure 1, it was identical for both frequencies except for the frequency downconverter unit which was appropriately configured to provide an intermediate frequency suitable for input into the commercial signal strength measurement receiver (Anritsu ML518A). The

output from the receiver was a unipolar voltage related to the received signal power, which was recorded on an FM tape recorder. The antenna on the mobile was identical to that on the aircraft but pointing vertically upwards. A unit was fitted to the mobile's transmission so that the vehicle speed could be recorded along with the signal envelope. Both the aircraft and the mobile were fitted with "DATATRAK" locator units, giving an output of position every 1.6s accurate to ± 35m.

ANALYSIS

In the laboratory, the aircraft altimeter recordings and navigational information from the aircraft and the mobile is used to determine areas in the signal strength recordings at which the required elevation angles occur. These portions of the tape are digitised (both signal strength and vehicle speed), and a statistical analysis is performed. The amplitude of the recorded signal is processed, generating a probability density function (pdf) from which a Cumulative Density Function (CDF) is produced (first order statistics). For the same data, the duration of fades occurring at various levels below the reference is determined, producing information on level crossing rates, average duration and distribution of fades (second order statistics). However, before the first and second order statistics are calculated a 20 wavelength sliding window is applied to the data (due to experimental conditions), and a 0dB reference for the data of 1.1dB below the 99% level of the CDF is chosen. For in depth documentation of the experimental system, errors, referencing and analysis, [3] should be consulted.

RESULTS

Only the CDF's for the four environments at both L and S-bands will be presented here in figures 2-5. An anticipated level of error for the curves is ± 0.7dB with an error in the

determination of elevation angle at a maximum of 2 degrees. Consideration of the curves leads to the following comments.

Open rural (figure 2)

In an open environment, received signal statistics show a general independence from elevation angle and frequency, indeed, the statistics say more about the characterisation experiment than the channel. It is thought that the small differences in the curves are due to residual multipath generated by the varying traffic density on each run.

Urban (figure 3)

The general form of the curves is as might be expected, in that they show that larger margins are required for a given availability at S-band than for L-band. The CDF for an angle of 80 degrees however, shows that for availabilities in excess of 80% - 90% larger margins are required at S-band, than might have been anticipated. It is thought that this is largely due to terrain culture close to the vehicle. During the measurements it was noticed that more significant signal perturbation occurred when passing under overhead road signs or utility poles at S-band than at L-band. Certainly for S-band, the first order statistics in urban areas do not present a favourable margin for any system, it is almost certain that in a practical system some form of repeater would be needed. The margin required at L-band is significantly smaller and it may be that this alone would justify the choice of a frequency of ≈ 1.5GHz as opposed to ≈ 2.6GHz for these systems.

Suburban (figure 4)

In the suburban areas results which are different in nature occur at L and S band, in that at S band the curves are similar for all elevation angles, indeed, the CDF's show agreement within the limits of experimental error up to 90% availability. The L band curves show a difference for each elevation angle. At present no explanation is offered for this behaviour.

Tree shadowed (figure 5)

If it is borne in mind that the L-band measurements were made with full dense foliage and the S-band with no foliage, the statistics show a significant worsening from L to S band. Outside of urban areas, tree shadowed routes pose a significant problem to these systems. Much difficulty was experienced in producing a set of curves which may be said to form representative statistics.

Open rural area data as "calibration"

It would be reasonable to expect that a back to back test on an ideal transmit/receive experimental system would result the generation of a "brick wall" CDF, ie. a change from no values occurring, to all values occurring, at point which was related to the signal level (ie. a dynamic range of fades of 0dB). In the case of the open rural area the actual dynamic range of the measurement was ≈ 2.6dB (1% of CDF to 99% of CDF) for most cases. It is therefore suggested that as a "first approximation" the S-band, 80 degree curve on figure 2 be used to calibrate all others. That is, for any given curve, in any given environment, at any given % of the cdf, the fade level to be considered is the fade level obtained from the relevant graph minus the equivalent fade level (for that given % of the CDF) from the 80 degree open rural area CDF. Table 1 of margins v availabilities has been developed using this idea and is therefore suggested as a guide for systems planning purposes. It should be noted however that these "margins v availability" apply strictly to the curves presented here and are not intended to be applied to cover all propagation effects.

CONCLUSIONS

In general, at both L and S bands, for a given environment, an increase in satellite to mobile elevation angle from 40 to 80 degrees is accompanied by an improvement in primary statistics. For a given elevation angle, as the environment in which the mobile finds itself changes from urban to suburban to open, so here too the improvements in received signal statistics mentioned above are also seen.

The results indicate that, for Northern Europe, propagation problems associated with geostationary satellites could be significantly reduced by using a satellites in a suitable high elevation orbit. The maximum benefit would be obtained by using L-band frequencies for the mobile links, with a satellite elevation angle from the mobile as near 90° as possible.

ACKNOWLEDGEMENTS

REFERENCES

[1] P. Dondl, "LOOPUS opens a new dimension in satellite communications" *Int. Jnl. Sat. Comms*, Vol 2, 1984

[2] D. Robson et al, "ARCHIMEDES for BSS(S)", *Report on ESA contract No.8642/89/F/RD(SC)*, November 1990

[3] H. Smith et al, "Characterisation of the Land Mobile Satellite (LMS) Channel L & S Bands: Narrowband measurements" *Report on European Space Agency AOP's 104433/114473*, February 1993

Table 1 - Suggested Margins v Availability

AREA	AVAIL (%)	MARGIN (dB)					
		L-BAND			S-BAND		
		ELEVATION (deg)					
		40	60	80	40	60	80
URBAN	99	13.1	10.7	8.1	17.3	15.4	13.0
	95	8.2	5.9	1.3	12.5	11.0	6.7
	90	5.5	3.8	0.9	10.1	8.7	4.3
	85	4.5	3.1	0.9	8.7	7.4	3.2
	80	4.0	2.7	0.8	7.6	6.3	2.7
	70	3.4	2.4	0.7	5.8	4.8	2.4
SUBURBAN	99	7.2	4.4	2.2	12.5	10.8	9.2
	95	4.5	2.5	1.4	6.7	6.0	6.3
	90	3.5	1.9	1.1	5.1	4.5	5.2
	85	3.0	1.7	1.0	4.4	3.9	4.7
	80	2.7	1.6	0.9	3.9	3.5	4.2
	70	2.3	1.4	0.8	3.3	3.0	3.6
TREE SHADOWED	99	11.3	7.7	4.1	12.6	10.5	9.0
	95	7.9	4.9	2.0	6.3	5.7	5.2
	90	5.9	3.4	1.5	4.7	4.2	3.8
	85	4.8	2.8	1.4	4.0	3.6	3.2
	80	4.0	2.5	1.3	3.6	3.3	2.8
	70	3.3	2.2	1.2	3.1	2.8	2.5

orlm

Figure 2 - Open rural area CDF's

urban

Figure 3 - Urban area CDF's
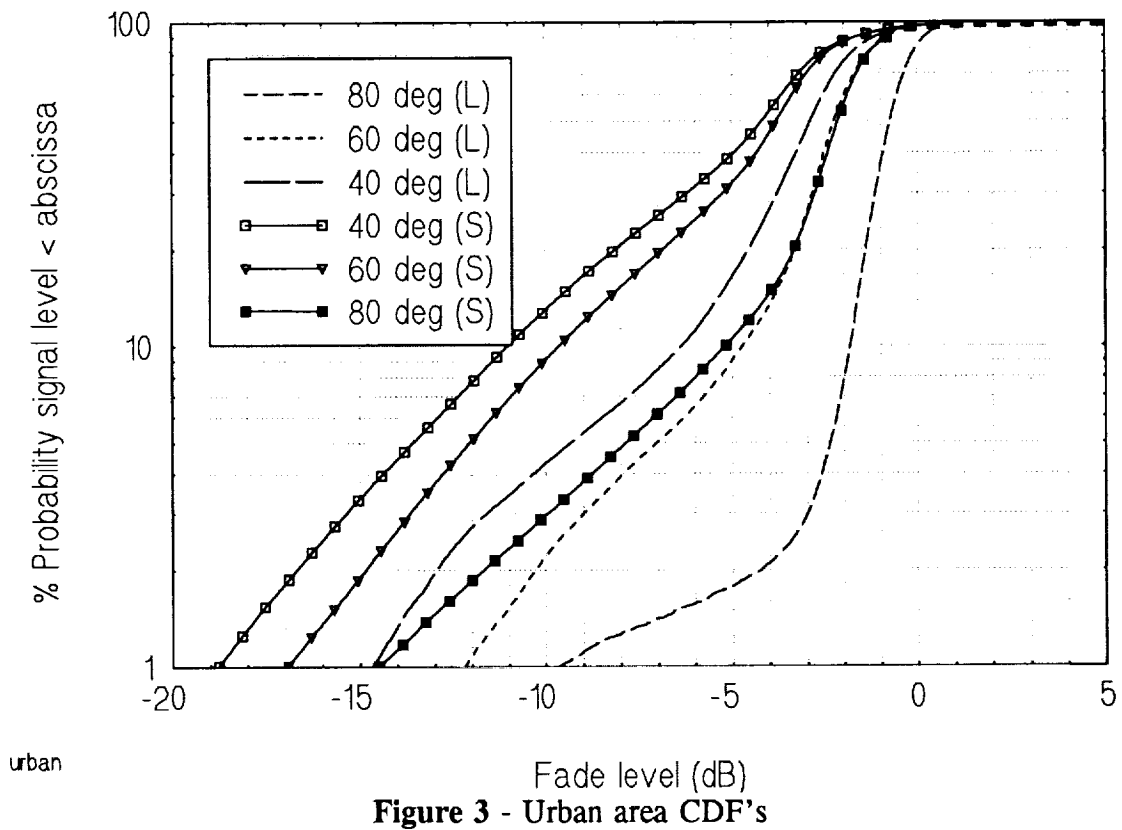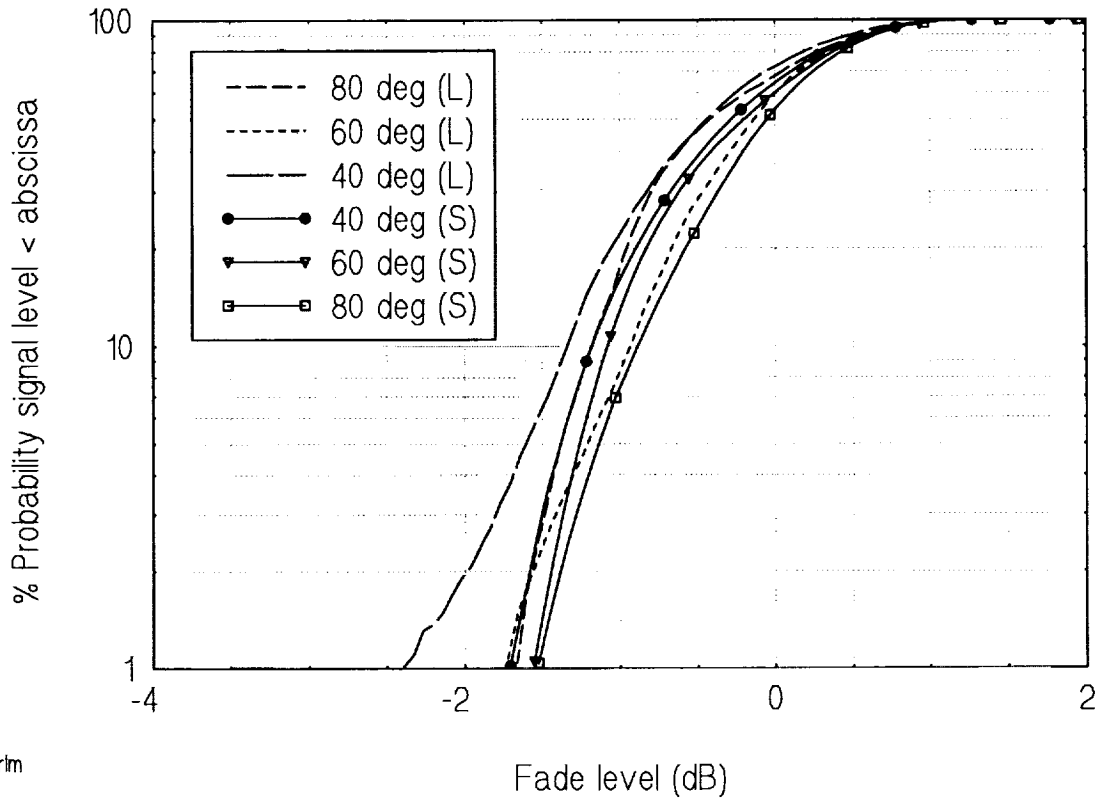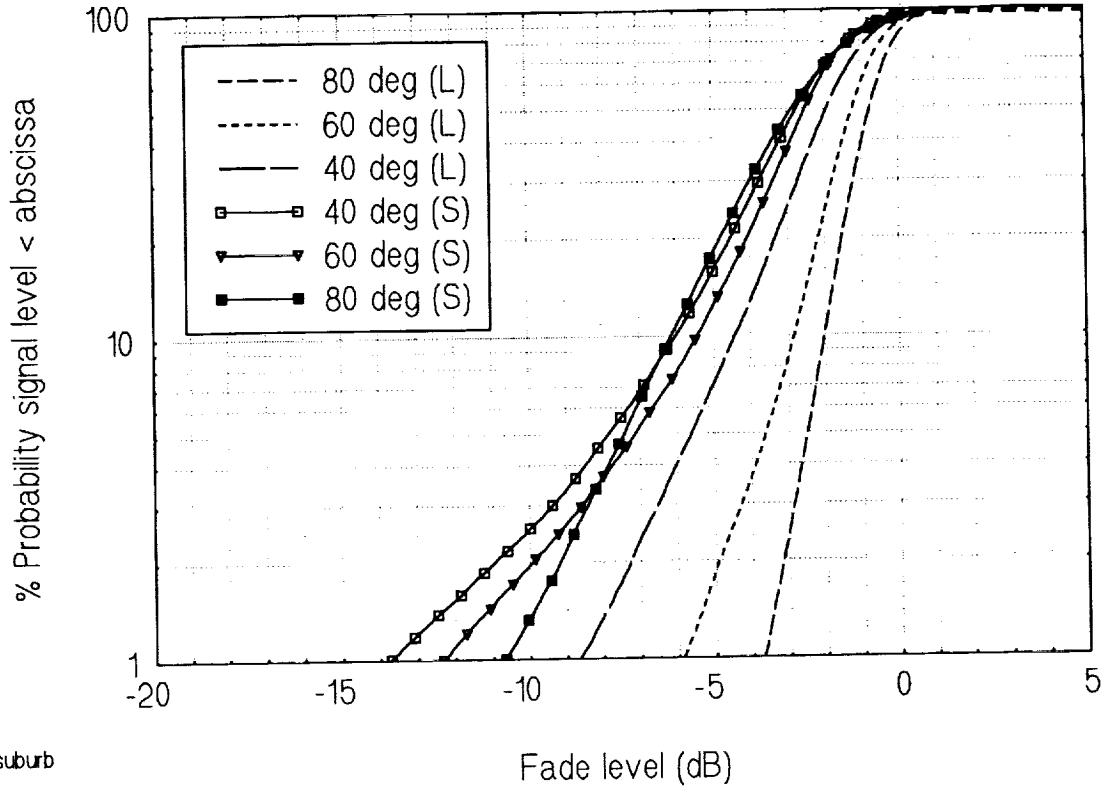
Figure 4 - Suburban area CDF's
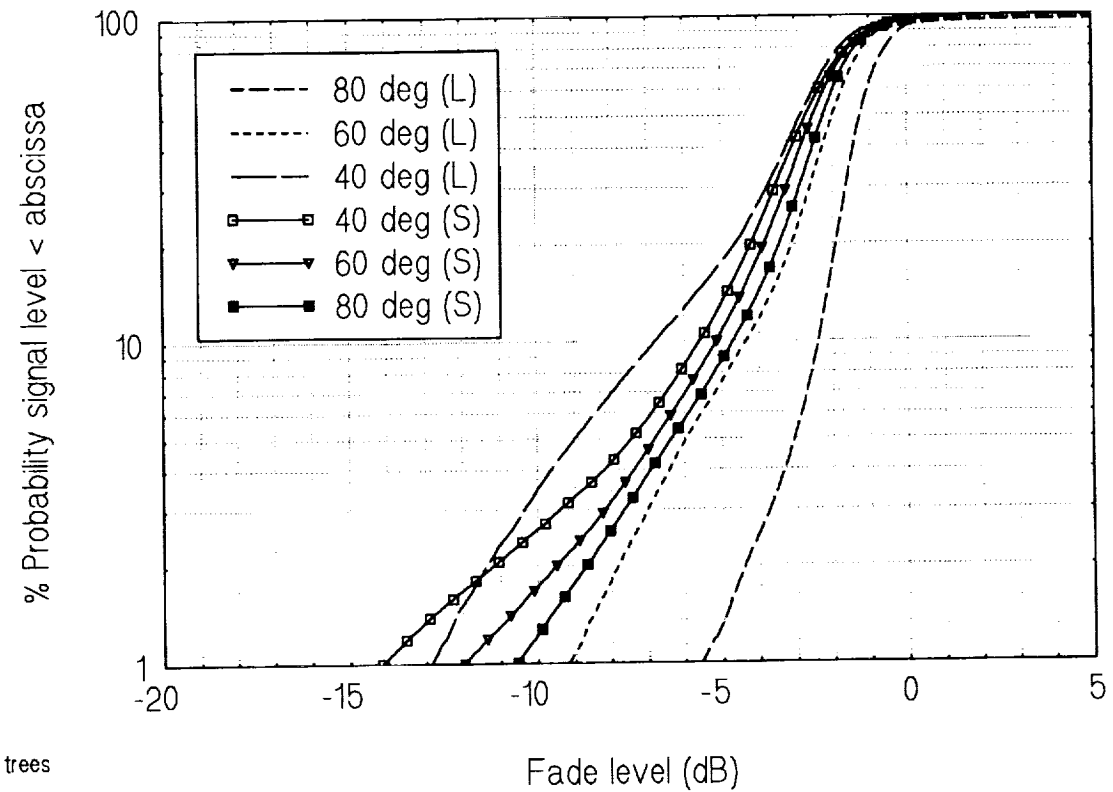
Figure 5 - Tree shadowed area CDF's

K-Band Mobile Propagation Measurements Using ACTS

Julius Goldhirsh[#], Wolfhard J. Vogel[*], Geoffrey W. Torrence[*]
[#]The Johns Hopkins University, Applied Physics Laboratory
Johns Hopkins Road, Laurel, Maryland, 20723-6099
Telephone: 301-953-5042, Fax:301-953-5548
[*]The University of Texas, Electrical Engineering Research Laboratory
10100 Burnet Road, Austin, Texas, 78758-4455
Telephone: 512-471-8608, Fax: 512 471 8609

ABSTRACT

An overview of two planned propagation campaigns employing land-mobile scenarios with ACTS is presented. The campaigns will be undertaken through a joint effort involving The Johns Hopkins University, Applied Physics Laboratory (APL), The University of Texas at Austin, Electrical Engineering Research Laboratory (EERL), and the NASA Lewis Research Center (NASA LeRC). Propagation campaigns are planned in Central Maryland in November 1993 (elevation angle $\approx 40°$) and in Fairbanks, Alaska in June 1994 (elevation angle $\approx 8°$) employing a computer controlled antenna tracking system located atop a van containing a receiver/data acquisition system. The antenna will track (in azimuth) downlink transmissions at 19.914 GHz from ACTS during the mobile propagation measurements. The major objectives of the campaigns are to measure the fade and multipath effects of trees and terrain at 20 GHz for rural and suburban scenarios and to extend existing models which were previously validated at UHF to S-Band.

BACKGROUND

Since 1983, EERL and APL have undertaken 13 land-mobile propagation campaigns involving transmitter platforms located on stratospheric balloon, remotely piloted aircraft, helicopters, and geostationary satellites. An overview of the first eleven experiments and other results are presented in NASA Reference Publication 1274 [1]. The earlier experiments were performed at UHF (870 MHz) and the latter ones at UHF and/or L-Band (1.5 GHz). In particular, fading and multipath effects due to trees and terrain were determined for rural and suburban areas. These effects were examined in open fields, along tree lined highways, and in mountainous terrain. The results were expressed in terms of distributions of fading, fade and non-fade durations, and space diversity. The fade distributions, for example, provide information as to the percentage of distance travelled such that different attenuation margin levels are exceeded. Such information provides criteria for establishing design fade margins for different driving scenarios. Empirical models were developed from which one is able to calculate the fade distributions for roadside tree scenarios for elevation angles ranging from 20° to 60° and frequencies ranging from UHF to S-Band.

GENERAL OBJECTIVES OF PLANNED TESTS

The objective of the planned tests is to execute systematic propagation

measurements at 20 GHz employing ACTS in Central Maryland and Fairbanks, Alaska. In Central Maryland the elevation angle is 39° and in Fairbanks, it is 8°. The rationale for making measurements in Central Maryland employing ACTS is to build on previous LMSS measurement experience and propagation results at UHF and L-Band [2, 3]. Measurements will be made along the same system of roads as previously examined. The Alaska campaign will enable exploration of fading effects for low angle measurements which include possible scintillations. Results at K-Band will represent a natural extension of previous ones at UHF and L-Band, where frequency scaling criteria will be explored at this new frequency and elevation angle. Empirical models developed and validated for UHF to S-Band will also be tested at K-Band [4].

GENERAL EXPERIMENTAL CONFIGURATION

We plan to provide a tone generator at 3.373 GHz at the input the High Burst Rate, Link Evaluation Terminal (HBR/LET) upconverter located at NASA LeRC. This will ultimately result in CW radiation at an uplink frequency of 29.634 GHz and downlink transmissions at frequency of 19.914 GHz. Transmissions at this latter frequency will be received by the mobile van located either in Central Maryland or Fairbanks Alaska. In Central Maryland, the east scan sector "Spot Beam 10" should provide a peak EIRP of at least 65 dBW. In Alaska we plan to use the steerable antenna which will provide an EIRP of approximately 55 dBW.

LINK PARAMETERS FOR THE LMSS CONFIGURATION

The link parameters are listed in Table 1 for both the Maryland and Alaska locations. A 15 cm diameter ($\approx 7°$ beamwidth) receiving antenna is planned for use on the van.

Assuming a 400 Hz receiver bandwidth, the carrier to noise ratios should be 58 dB in Maryland and 47 dB in Alaska. For an 10 dB carrier to noise ratio margin, fading effects covering 48 and 37 dB dynamic ranges are possible, respectively.

ANTENNA TRACKER SYSTEM

Shown in Figure 1 is a block diagram of the antenna tracker system. The antenna and the angular rate sensor (Block #1) rest on a rotary table driven by a step-motor system (Blocks #5–#7). When the vehicle under the rotary table turns, the rate sensor develops an output voltage proportional to the angular turn rate (i.e., $d\theta/dt$). This voltage is integrated (Block #2) giving another voltage signal proportional to the turning angle θ. This voltage signal is fed into a voltage-to-frequency converter (Block #4) (via a summing network (Block #3) to be described shortly) whose output gives a series of pulses at a frequency proportional to the turning angle. These pulses and a direction signal are, in turn, fed to the stepping motor driver (Block #5) such that the rotary table is driven in such a direction as to reduce the turning angle θ. When the error angle reduces to zero, no further pulses are injected into the stepping motor driver. If the rate sensor experienced no drift, the above tracking loop would keep the rotary table platform pointed in an approximate constant azimuth direction maintaining zero error angle.

Because the rate sensor has a slowly drifting offset voltage, the table would slowly rotate after about 30 seconds if no further controls were applied. An up/down counter (Block #8) and PC (Block #9) are used to derive the absolute table position with respect to a known reference position on the rotary table (employing a home-switch). The above mentioned drift offset is corrected

326

approximately once per second by comparing the average table direction with the average direction from a flux-gate compass mounted to the vehicle (Block #10) creating an offset voltage which is interfaced with the PC (Block #9). The resultant offset angle signal established by the PC (Block #9) is fed via a D/A interface to the summing circuitry (Block #3). The offset compensates for the rate sensor drift and when added to the "apparent turning angle" (Block #2) gives the "true turning angle," θ. The PC will also contain software which mitigate fluxgate compass errors caused by magnetic anomalies due to the vehicle and roadside structures.

The elevation of the antenna is established by locating the vehicle on a horizontal surface and peaking the received signal radiated from the satellite. It is expected that for the planned roads to be traveled, the elevation angle changes should be within $\pm 2°$ of the nominal pointing angle. Since the beamwidth is approximately $\pm 3.5°$ relative to the pointing axis, a deviation of $\pm 2°$ in elevation results in a received power loss of ± 1 dB assuming a Gaussian beam pattern.

MOBILE RECEIVER SYSTEM

The mobile receiver system is depicted in Figure 2 and shows a microwave spectrum analyzer and frequency synthesizer at the heart of the RF system. Other main functional components are the aforementioned antenna tracker system, a low noise frequency downconverter, an intermediate frequency stage with automatic frequency control (AFC), and a PC based data acquisition system. Ancillary sensors give vehicle speed and direction.

The 19.914 GHz vertically polarized ACTS pilot signal is focused by the antenna into the waveguide feed of the RF front end. There the 19.7–20.2 GHz low noise amplifier (LNA) determines the noise temperature of the

receiver (430 K). After amplification, the pilot signal is fed to the first mixer through a bandpass filter, which eliminates image sideband noise. The local oscillator is locked to the same high-stability frequency reference as the spectrum analyzer. The mixer output (1.7-2.2 GHz) is again amplified and fed to the IF system in the mobile van's interior. There the Tektronix 2756P spectrum analyzer in its non-sweeping mode is used as a tunable receiver with a 10 MHz IF output. Having a spectrum analyzer built into the receiver also affords convenient trouble shooting and signal acquisition. The 10 MHz signal is first converted to 455 kHz and finally to 10 kHz. At that frequency, a filter bank of 11 analog filters with 100 Hz spacing is used for AFC and keeps the satellite pilot signal centered in the receiver. The AFC has a 0.1 sec time constant. The 10 kHz signal is also fed to a quadrature detector, converted to base band, and low-pass filtered with a 200 Hz cutoff frequency. This results in a receiver noise bandwidth of 400 Hz. The in-phase and quadrature phase voltages are amplified and sampled by the PC based data acquisition system at a 1000 Hz rate. The resulting data are stored on the computer's hard disk, which has the capacity to hold over four hours of continuous data. The time, vehicle speed, and direction are stored once every second. The antenna pointing parameters are stored at a 5 Hz rate.

DOPPLER SHIFT CORRECTION

At a low elevation angle, the maximum Doppler shift will be about $\pm v/\lambda$, where v is the vehicle speed and λ is the wavelength. At 20 GHz, a maximum shift of ± 2000 Hz is expected assuming a top speed of about 65 mph. The AFC voltage will be corrected by an amount depending on the vehicle speed, direction, and the satellite elevation angle. The correction signal will be calculated by the computer. This will ensure that the pilot

signal always reappears within the $\pm$ 1000 Hz AFC capture range.

SAMPLING RATE AND BANDWIDTH

For L-Band measurements with azimuthally omni-directional antennas and low gain on the horizon, a signal bandwidth of 200 Hz was found to be sufficient to capture the dynamic behavior of the received signal amplitude and phase variations and provide enough fade margin while observing low power satellite beacons. As a rule of thumb, one should sample the standing wave field set up by the interference between the direct line-of-sight signal and the multipath components at an interval of about $\lambda/8$. This condition was satisfied at L-Band ($\lambda = 20$ cm) by the present system which achieved a spatial sampling interval of 2.5 cm at a speed of 55 mph. A similar argument can be made about signal variations due to shadowing by tree branches or utility poles. At 20 GHz ($\lambda = 1.5$ cm), an azimuthally omni-direction antenna should mandate proportionally wider bandwidths and higher sampling rates. Considering that the beamwidth of the antenna is relatively narrow ($\approx 7°$) however, the main Doppler effect is just a shift in frequency with limited spread. The AFC will compensate for the frequency shift. The current signal bandwidth of the receiver is about 200 Hz, but can easily be increased to 500 Hz if that proves necessary.

PLANNED CAMPAIGNS

As of this writing, the ACTS satellite is expected to become operational in October, 1993. The key periods and locations in which the campaigns will be executed are as follows:

1. **November, 1993 (Central Maryland):**
   Field measurements are planned in Central Maryland in November 1993. These measurements will be executed along a system of roads previously examined at UHF and L-Band where previous driving scenarios will be replicated [2, 3]. The system tests encompass fours hours per day during five contiguous days.

2. **June, 1994 (Fairbanks, Alaska):**
   Field measurements are planned in Fairbanks, Alaska during the early part of June. This month represents the most benign period for Alaska when trees are in full bloom. Four hours per day of measurements are planned during five contiguous days.

REFERENCES

[1] J. Goldhirsh and W. J. Vogel, "Propagation Effects for Land Mobile Satellite Systems: Overview of Experimental and Modeling Results," *NASA Reference Publication 1274*, February, 1992.
[2] J. Goldhirsh and W. J. Vogel, "Roadside Tree Attenuation Measurements at UHF for Land-Mobile Satellite Systems," *IEEE Trans. Antennas Propagat.*, vol. AP-35, pp. 589-596, May, 1987.
[3] J. Goldhirsh and W. J. Vogel, "Mobile Satellite System Fade Statistics for Shadowing and Multipath from Roadside Trees at UHF and L-band," *IEEE Trans. Antennas Propagat.* vol AP-37, no. 4, pp. 489-498, April, 1989.
[4] W. J. Vogel, J. Goldhirsh, and Y. Hase,"Land-Mobile-Satellite Fade Measurements in Australia," *Journal of Spacecraft and Rockets*, vol. 29, no. 1, pp. 123-128, January-February, 1992.

328

Table 1: Link parameters for the land-mobile ACTS configuration employing the microwave switch matrix mode and the steerable antenna.

PARAMETER	BOTH SITES	MARYLAND (Central)	ALASKA (Fairbanks)
Satellite:			
Longitude (°W)	100		
Downlink Frequency (GHz)	19.914		
Uplink Frequency (GHz)	29.634		
Polarization	Vertical		
Receiver Site Locations:			
Latitude (°)N		39.25	65.0
Longitude (°)W		77.0	147.7
Elevation (°)		38.7	7.9
Azimuth (°)		213.9	129.5
Receiver System Parameters			
Polarization	Vertical		
Antenna Efficiency	0.6		
Antenna Diameter (cm)	15		
Antenna Gain (dB)	28		
Beamwidth (°)	6.8		
System Temperature K (Nominal)	430		
Link Budget:			
EIRP (dBW)		65	56
Free Space Loss (dB)		−210.0	−210.6
Atmospheric Gas Loss (dB)		0.5	2.2
Radome Loss (dB)	0.5		
Mobile G/T (dB/K)	1.7		
Signal Power Received (dBW)		−118.0	−129.3
Noise Power (dBW/Hz)	−202.2		
Carrier/Noise (dB per Hz)		84.2	72.9
Carrier/Noise (dB; 400 Hz)		**58.2**	**46.9**

329
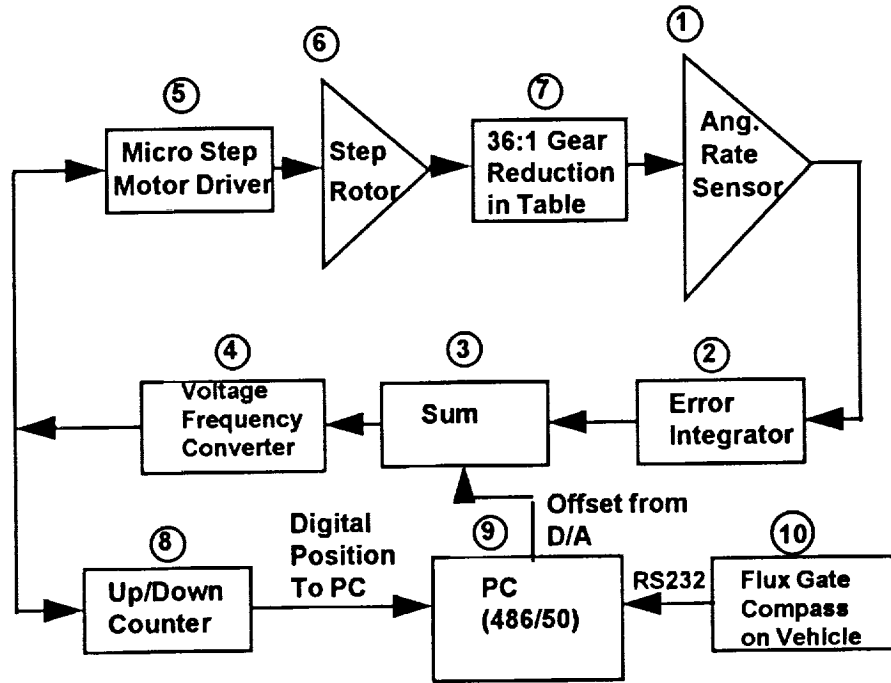
Figure 1: Block diagram of mobile antenna tracking system.
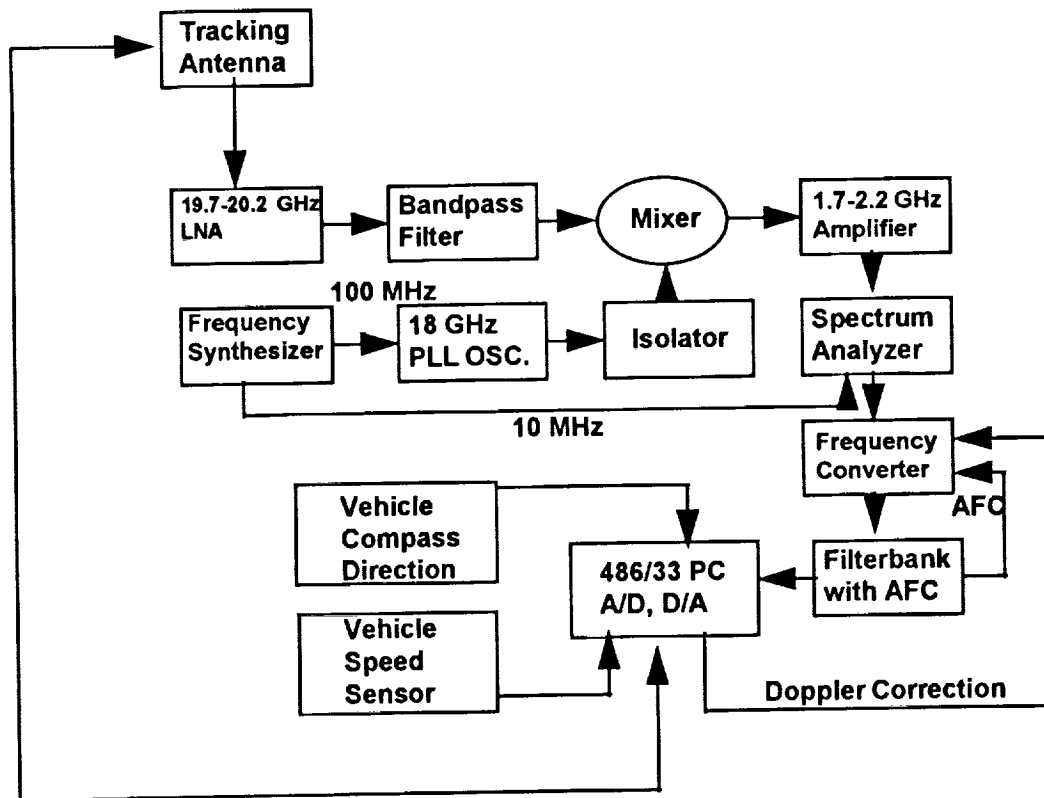
Figure 2: Block diagram of mobile receiver system.

Measurement of Multipath Delay Profile in Land Mobile Satellite Channels

**Tetsushi Ikegami, Yoshiya Arakaki, Hiromitsu Wakana
and *Ryutaro Suzuki**

Communications Research Laboratory
Ministry of Posts and Telecommunications
893-1 Hirai, Kashima, Ibaraki 314 Japan
Phone: +81-299-84-4120, Fax: +81-299-84-4149

*National Institute of Multimedia Education
Ministry of Education
2-12 Wakaba, Mihama, Chiba 261 Japan

ABSTRACT

Mobile satellite communication channel has been evaluated mainly with fading statistics of signal. When bandwidth of transmitting signal becomes wider, frequency selectivity of fading becomes significant factor of the channel. Channel characteristics, not only signal variation but multipath delay spread should be evaluated. A multipath measurement system is proposed and developed for mobile satellite applications. With this system and ETS-V satellite, multipath delay profiles are measured in various environments including Tokyo metropolis and Sapporo city at 1.5 GHz. Results show that the maximum excess delay is within $1\mu s$ and the maximum delay spread is $0.2\mu s$ at elevation angles of 40 to 47 degrees. In wideband signal transmission of about 1MHz and more, designers should consider the effect of selective fading due to the multipath of land mobile satellite channel.

INTRODUCTION

The evaluation of mobile satellite communication channels has focused on the fading statistics of level fluctuation. In the near fu- ture, the wideband signal will be used in CDMA, TDMA or mobile sound broadcasting systems. In the evaluation of wideband transmission, delay profile of channel should be measured, because multipath due to reflection off the structure around mobile earth station induces a frequency selectivity of the link, which results in wave form distortion or inter-symbol interference on the transmitting signal. In order to measure the multipath, we propose measuring system for mobile satellite channel and develop a prototype. This paper shows the proposed system and reports a preliminary results of measurement in Tokyo metropolis and Sapporo city.

BACKGROUND

There are some methods of multipath measurement in radio communication links[1][2]: the reception of a response to a transmitted narrow pulse signal, referred to as pulse method, the correlation of the transmitted PN-PSK-SS signal to reference PN sequence, which results in a similar response as in the pulse method, referred to as PN method.

In the pulse method, transmitting peak power must be high enough to obtain sufficient signal to noise ratio, however transponders

are generally operating at power-limited mode and link margin is usually not enough to use the pulse method. The PN method is popular in terrestrial land mobile channels, however high precision local oscillator must be used at both transmitter and receiver as a reference carrier to achieve quasi-coherent detection, because carrier recovery function does not work well in a typical Rayleigh fading condition.

As the satellite communication link has a frequency conversion function in an onboard transponder, the use of high precision local oscillator in earth station cannot compensate frequency difference between the transmitting and receiving earth stations. Therefore another method should be used in mobile satellite channels.

In mobile satellite communications, line-of-sight links are mainly used and a receiver can easily track the phase of a direct wave. Therefore it is sufficient to measure the level of multipath delay profile and phase fluctuations of the delayed multipath components relative to the direct wave. The proposed measuring system receives the transmitted PN-SS signal through a satellite, achieves quadrature coherent detection while synchronizing to the direct wave and gives the delay profile as complex correlation outputs.

SYSTEM DESCRIPTION

In this system the earth station transmits a PN-SS signal to a satellite, then a coherent matched filter (CMF) receiver[3] of a receiving earth station detects quadrature multipath delay profiles as complex correlation outputs while a carrier recovery loop tracks the direct wave from the satellite. The CMF is a kind of Costas loop coherent detector for the PN-SS signal and con-tains two correlators for PN code as arm filters of the Costas loop.

Figure 1 shows the principle of the measurement system. The received PN-SS signal is converted to complex baseband signals with the recovered carrier. Digital correlators correlate the baseband signals with the reference PN code and give a complex delay profile for one frame of PN code. The carrier recovery loop tracks the largest correlation peak which comes from the direct wave. Therefore correlators produce delay profiles having information of the phase relative to the direct wave even if there are frequency conversions in satellite links. Signal to noise ratio at the correlator output can be improved by recursive integrators which consist of adders, frame memories and weighting circuits.

The measurement system is developed based on a communication equipment[4][5]. The system description and block diagram are shown in Table 1 and Figure 2, respectively. Digital correlators in both I and Q arms operate asynchronous with PN clock at twice the PN clock to avoid the use of clock recovery circuit. The bandwidth of the transmitting signal is limited to 3 MHz which corresponds to the bandwidth of a transponder.

RESULTS

Measurements are performed at urban, suburban and mountainous areas using ETS-V(Engineering Test Satellite five) located at 150 degrees East[6]. The elevation angles to the satellite are relatively high and range from 40 to 47 degrees. This report shows the preliminary data of Shinjuku Tokyo where many tall buildings of up to 250 m in heights are risen, and Sapporo which is a typical large city in northern part of Japan.

C-5

As in Figure 3, Kashima base earth station transmits a PN-SS signal and the mobile earth station onboard a measuring van receive the left-handed circular polarized signal from the ETS-V at 1.5GHz. A receiving antenna used in the measurement is a quadrifilar helix antenna which has a gain 3 dBi and an omnidirectional beam. The received data are recorded on a digital data recorder.

Figure 4 and 5 show some examples of measured delay profiles at Shinjuku. In each figure, a broken line shows the reference profile where only direct wave exists. There are no output in Q-channel in principle if the received signal contains a direct wave only, whereas there are some level in Q-channels in Figure 4 and 5. This fact explains that the received signal consists of some delayed multipath components.

The mean excess delay d and the delay spread S which are the measure of multipath, are expressed in the following equations[2],

$$d = \int_0^\infty \tau E(\tau) d\tau \qquad (1)$$

$$S^2 = \int_0^\infty \tau^2 E(\tau) d\tau - d^2 \qquad (2)$$

where $E(\tau)$ is normalized power delay profile.

The delay spread is calculated in Equation (2) with the measured delay profiles, in these calculations the effect of band limitation to correlation function is considered. Table 2 and 3 summarize the measurements of the received signal level relative to the line-of-sight level and the delay spread in Shinjuku and Sapporo. Figure 6 and 7 are maps of the measuring points. So far, an excess delay of more than 1μs is not observed and maximum

delay spread is on the order of 0.2 μs.

The coherent bandwidth, which is a measure of frequency selectivity, is defined as the frequency separation at which correlation of two signals is 0.5. If the distribution of multipath delay follows exponential distribution, the coherence bandwidth Bc can be expressed with delay spread S as[2]

$$B_c = \frac{1}{2\pi S} \qquad (3).$$

For reference, the coherent bandwidths Bc are calculated with Eq. (3), which may not express the exact value of Bc of the channels. Calculated Bc are from 0.8 MHz to 4.0 MHz. More detailed analyses must be done on this point, however, design of wide band transmission link of approximately 1 MHz and more should consider the effect of multipath delay carefully.

CONCLUSION

A multipath measuring system for mobile satellite links is proposed and a prototype is developed. Field test measurements are performed using ETS-V satellite at 1.5 GHz. In land mobile satellite links at moderate elevation angles of around 45 degrees, there are no multipath components with an excess delay of more than 1 μs which is typical in terrestrial land mobile links. However, owing to the fact that the delay spread of around 0.2 μs is observed, it can be concluded that frequency selectivity should be considered in wide band system on the order of more than 1 MHz. Detailed analyses such as statistical properties of delay spread or coherence bandwidth are left as further study.

333

REFERENCES

[1] G. L. Turin, et al.,"A Statistical Model of Urban Multipath Propagation", IEEE Trans. VT-21, 1, pp.1-9, Feb. 1972.

[2] W. C. Y. Lee: "*Mobile Communications Engineering*", McGraw-Hill, 1982.

[3] N. Hamamoto et al.:"PN-SS equipment for satellite communications with data demodulation by matched filter", Trans. IEICE Japan, vol. J69-B, pp.1540-1547, Nov. 1986.

[4] T. Ikegami, et al.:"Experiments on a coherent matched filter receiver for spread spectrum mobile satellite communications", IEICE Trans., vol. E,5, pp.1130-1136, May 1991.

[5] T. Ikegami, et al.:"Field trials of a spread spectrum mobile satellite system using ETS-V satellite", IEEE GLOBECOM91, 38A4, Phoenix, Dec. 1991.

[6] T. Ikegami, et al.:"Land mobile communication experiments with ETS-V satellite", IEEE VTC87, pp.166-169, Tampa, June 1987.
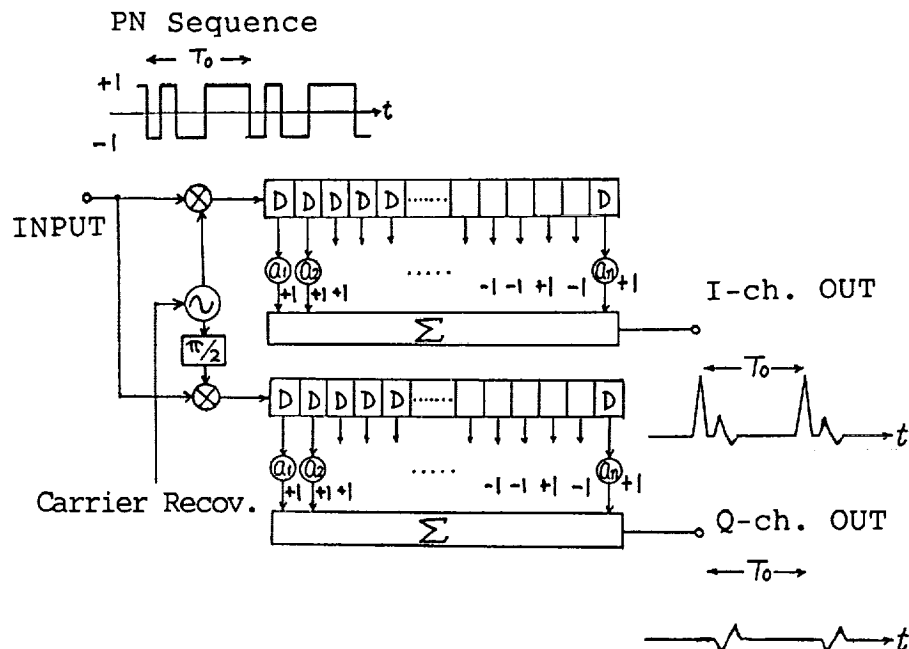
Fig. 1   Principle of multipath measurement

Table 1   Major specification of equipment

PN Code	M-sequence, Length 1023
PN Chip Rate	2.4552MHz
Modulation	BPSK
Demodulation	CMF, Coherent Detection
Matched Filter	8bits Digital Correlator, 2046stages
AFC Range	±10kHz
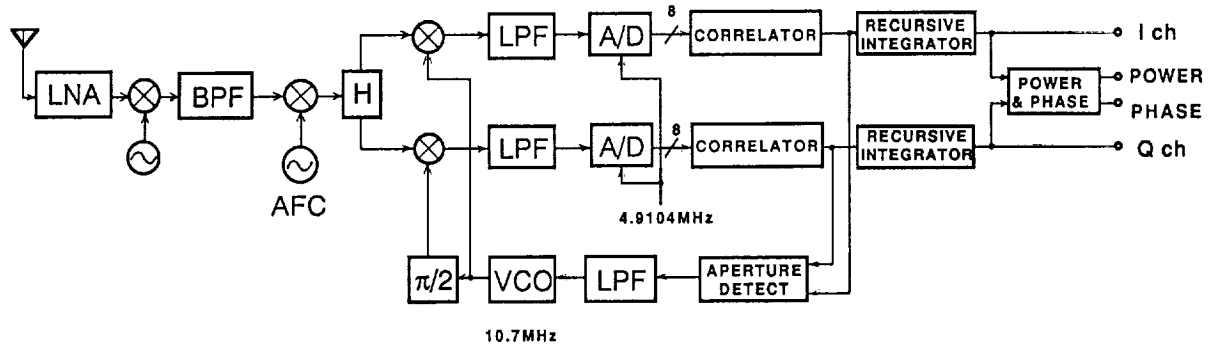
Fig. 2   Block diagram of receiver
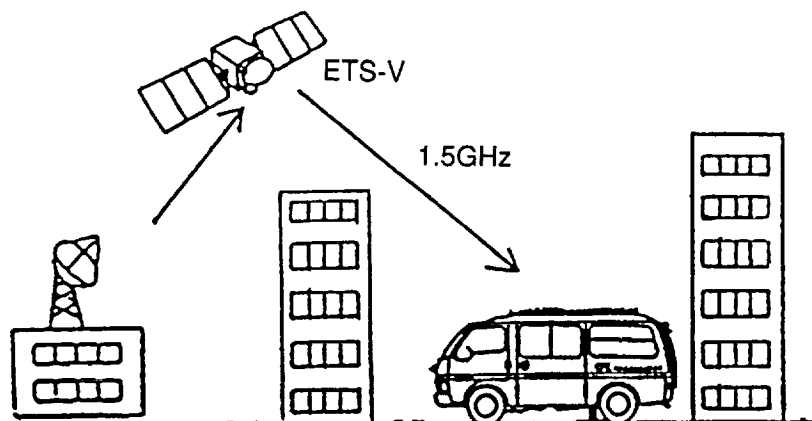
Fig.3 Configuration of experimental system
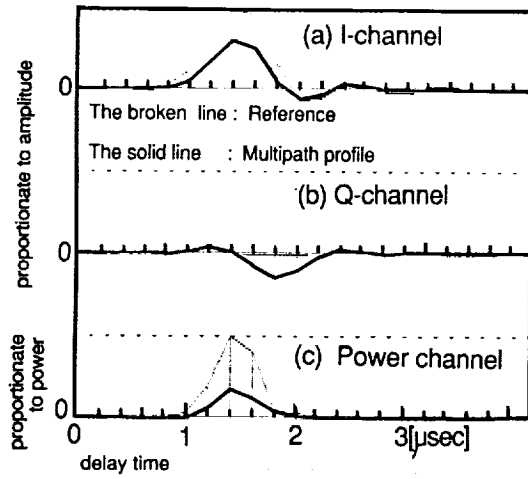
Fig.4 Multipath profile
Shinjuku data #12
(a) I-ch (b) Q-ch (c) Power-ch
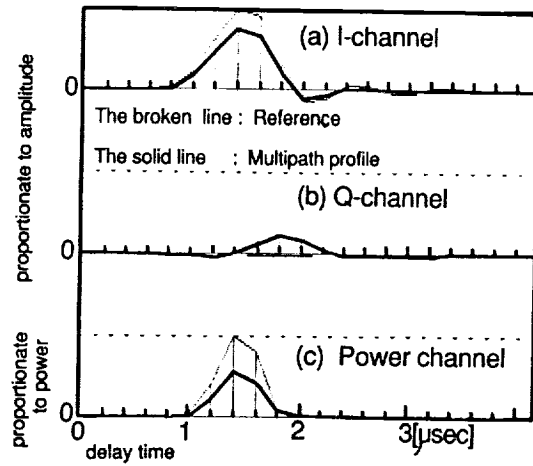
Fig.5 Multipath profile
Shinjuku data #19
(a) I-ch (b) Q-ch (c) Power-ch
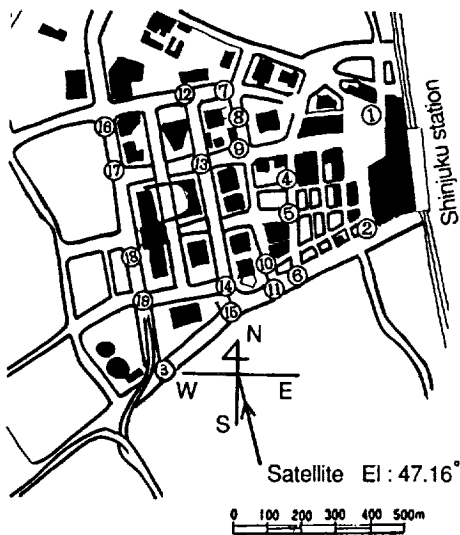
Fig.6 Point of measurement
(Shinjuku Tokyo) E 139.77° N 35.68°
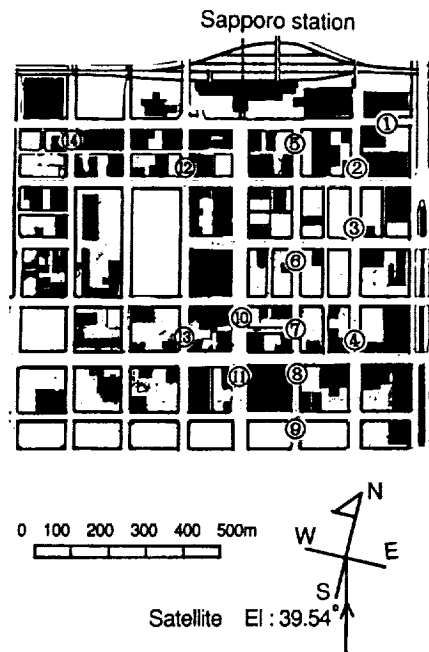
Fig.7 Point of measurement
(Sapporo Hokkaido) E 141.35° N 43.07°

Table.2 Shinjuku multipath data

Point	Received level [dB]	Delay spread [μ sec]
#1	− 2 . 6	0 . 0 6
#2	− 3 . 2	0 . 0 4
#3	− 1 . 9	0 . 0 7
#4	− 0 . 4	0 . 0 8
#5	− 1 . 6	0 . 0 4
#6	− 2 . 3	0 . 0 5
#7	0	0 . 0 5
#8	− 2 . 1	0 . 0 4
#9	− 2 . 0	0 . 0 5
#10	− 8 . 3	0 . 1 8
#11	− 1 . 9	0 . 0 5
#12	− 4 . 9	0 . 1 6
#13	− 1 . 7	0 . 1 0
#14	− 1 . 4	0 . 0 6
#15	− 2 . 0	0 . 0 6
#16	− 0 . 7	0 . 0 7
#17	− 1 . 7	0 . 0 4
#18	− 0 . 7	0 . 0 5
#19	− 2 . 7	0 . 1 1

Table.3 Sapporo multipath data

Point	Received level [dB]	Delay spread [μ sec]
#1	− 0 . 6	0 . 0 7
#2	− 1 . 3	0 . 0 8
#3	− 1 . 9	0 . 0 8
#4	− 2 . 3	0 . 1 9
#5	− 4 . 6	0 . 1 5
#6	− 3 . 2	0 . 1 5
#7	− 5 . 8	0 . 1 1
#8	− 3 . 9	0 . 1 9
#9	− 4 . 3	0 . 0 9
#10	− 1 1 . 0	0 . 1 2
#11	− 7 . 3	0 . 1 3
#12	+ 0 . 3	0 . 0 7
#13	− 3 . 6	0 . 1 6
#14	− 4 . 9	0 . 0 5

A Study of Satellite Motion-Induced Multipath Phenomena

R. M. Allnutt, A. Dissanayake, C. Zaks, and K. T. Lin

COMSAT Laboratories, 22300 COMSAT Dr
Clarksburg, Maryland 20871-9475, USA
Phone (301) 428-4411
FAX (301) 428-3686

Abstract

Experiments have been undertaken at COMSAT Laboratories to determine some of the propagation effects likely to be encountered by handheld satellite communications devices. L-band pilot tones aboard geosynchronous satellites at 15° and 40° elevations were used to examine diurnal signal variations measured by using a hemispherical antenna. It was found that the receiver with a hemispherical antenna suffered daily peak-to-peak signal level variations of up to 12 dB compared to only 2 to 3 dB for a receiver equipped with a directional antenna. These results were highly repeatable, and extensive tests were conducted to confirm the accuracy of the data. The results suggest that the diurnal variations were due to multipath effects caused by the motion of the satellite with respect to the receive antenna. Noting that the orbit inclinations of the satellites used in the experiment were only on the order of 2 to 3°, the results also suggest a potentially serious signal variation problem for low-gain antenna-based communications systems using low earth orbit satellites, since the satellite elevation angles relative to earth change far more rapidly.

Introduction

With the current and projected rise in the use of mobile communications systems, significant efforts are being invested in propagation studies at the frequencies concerned, particularly L-band. Many of these studies have involved taking signal propagation data from fast moving vehicles [1],[2]. However, little consideration has been given to signal propagation for stationary or slow-moving communications systems, principally the handheld variety. Handheld personal communications systems will be power-limited and restricted to small operating margins. Only limited blockage and multipath experiments have been used to develop preliminary fade margins and performance specifications. So far, effects induced by the satellite movement have been ignored. A few experiments have been conducted at COMSAT Laboratories to identify propagation phenomena that handheld satellite communications systems are likely to encounter.

This paper discusses one particular set of experiments which involved the diurnal variation of an L-band satellite signal received by an omnidirectional antenna. The results reported herein indicate that diurnal motion of the satellite, or its corollary, physical movement of the antenna, can cause signal variations in excess of 9 dB peak-to-peak for low-gain antennas under certain conditions. A preliminary finding is that close-in multipath effects may be the cause of the variations.

System Description

Two receivers were set up, one employing a 16-dB-gain dish antenna with a 25° half power beamwidth, and the other using a 3-dB-gain hemispherical Global Positioning System (GPS) antenna. A computer-controlled frequency tracking system was used to keep the receivers locked on the signal. The GPS-based receiver was slaved to the frequency of the dish-based system to avoid potential discrepancies during frequency tracking. The receivers were coupled to a 10-MHz crystal reference source for coherency, and their down-converters shared a common local oscillator to further maintain system coherency. The signal power was measured by a detector within a 65-Hz bandwidth to allow sufficient measurement range. The high resolution and linear outputs of the receivers were sampled at 100 Hz, but since storage space was limited, the data were recorded at a rate of 10 Hz. The receivers were automatically calibrated and re-centered on the signal after each minute of recording, as the signal center frequency drifted diurnally due to the Doppler effect. Concurrently,1 second averaging of the noise level at a frequency 1-kHz below the pilot's center frequency was made, and a record of the noise level was stored to allow accurate assesment of potential gain fluctuations along the receive chains. For more information on the receivers, see Reference 3.

Long-Term Signal Variations

The two antennas were positioned on a flat roof at the Laboratories, with the rest of the equipment in an air-conditioned room directly below the antennas. The signal source was a 1.537525-GHz pilot tone re-broadcast via a global coverage antenna on the INMARSAT-II F-4 satellite in geosynchronous orbit at 55.5° west with an elevation angle of 40°. The pilot EIRP at the satellite was about 10 dBW.

Figure 1 shows the variation in signal power over 24 hours obtained with the GPS antenna directed at zenith, and with the high-gain antenna lined up on the satellite. Both antennas had clear paths to the satellite, as they were mounted on a flat rooftop, about 2.5 m apart and 1.5 m above the surface. There are significant differences in the signatures of the two signal levels shown in Figure 1. The peak-to-peak signal variation experienced by the GPS-based receiver is nearly twice that observed for the high-gain antenna system. To obtain the results shown in in Figure. 2, the GPS antenna was lined up along the satellite look angle; the high-gain antenna was left unchanged. In this case the GPS antenna system experienced as much as 4 times greater peak-to-peak variations. Of equal significance is the rapidity signal variation measured by the GPS antenna; the signal changed by up to 7 dB within 1.5 hr, compared to less than 1 dB of change over the same time interval when measured by the high-gain antenna.

Measurements made over several days indicated that the signal level variations obtained were highly repeatable from day to day. Figure 3 shows data from 4 consecutive days. The time series for each day of data is progressively shifted by the difference between a sidereal day and a calendar day (approximately 4 min.). The correlation over 4 days on a sidereal basis is evident in the figure.

Extensive receiver checks were performed to eliminate the possibility of equipment effects which could contaminate the results. A stable signal source, offset a few Kilohertz from the satellite's pilot tone, was set up on the roof, and the response of the GPS-based system was tested over 12hours. The received signal remained within 0.5 Hz of the transmit frequency and experienced less than 0.1 dB power level variation. Noise level checks that were conducted over many days indicated the same order of stability. Investigations into weather patterns showed that even though there had been significant changes in the daily temperature cycles, no such changes were detected in the received signal levels from either antenna. It was also determined that there were no extraneous interfering signals. It became clear from these intensive investigations that the major variations in the observed signal-to-noise ratios were soley the result of changes in the received carrier level.

After ruling out all local effects, interfering signals, and equipment problems, the signal level variations were determined to be due to diurnal variations in the satellite position, satellite mutation effects and, to a lesser extent, changes in Doppler frequency. In an attempt to settle the location dependency of the effects, the GPS antenna was moved to atop a 10-ft pole at the very edge of the roof and directed toward the satellite. Figure 4 presents almost 24 hr. of measurement data. From this figure, it is evident that the signal variations are different from the previous ones and also greatly reduced; the total daily peak- to-peak variation recorded from the dish antenna and the GPS antenna are similar. Also, the effects were not diurnally repetitive. This could be attributed to the fact that there was a large car parking lot 40 ft directly below the GPS antenna. Some of the data were recorded over a weekend, when there were comparatively few cars were moving around. On regular working days the distribution and number of cars varies. This indicates that a constant reflective surface may not have existed during the measurement period, which could explain the dissimilarity in the daily signal traces. Therefore, it can be argued that the recorded signal level was fairly dependent on the reflective quality of its surrounding; hence, the signal level is probably location-dependent. This suggests that the daily observable variations in signal level recorded by the hemispherical antenna are due to multipath effects, which change over the course of a day because of the motion of the satellite with respect to the receive antenna.

To support the above argument, a similar experiment was conducted at yet another location. The receivers were moved to a flat, open grassy area on COMSAT grounds bordering a highway. Data could only be recorded during working hours, since the equipment could not be left unattended outside overnight. Approximately 6 hours of data were taken and as can be seen in Figure 5, the recorded data bears little resemblance to that measured on the roof. The changes in signal level at the GPS antenna were much smaller and smoother at the new location, but as before, the peak-to-peak variations were always greater than those measured by the dish antenna.

To independently confirm the validity of the results obtained using the INMARSAT-II F-4 , another pilot tone from a different satellite (INMARSAT-II at 15°W) was tested. The tone frequency was at 1.537528- GHz, with an elevation of approximately 15° and an azimuth of 110°. Measurements were made on the roof, and data were taken over several days (see Figure 6). While the long-term tre of the signal traces recorded by the dish and GPS antenna receivers were very similar, the peak-to-peak variations over the course of a day were significantly different; 4 dB for the dish and

over 10 dB for the GPS antenna. As noted before, changes in signal levels were again highly repeatable from day to day. Having almost identical signal behavior when using a second satellite source may again suggest that the signal level variations are due to changes in multipath characteristics caused by motion of the satellite relative to the earth stations. It was evident that the dish receiver was more affected than in previous measurement campaigns, possibly because of a partial interception of its lobe with the roof surface. This might suggest that the multipath was produced from an area directly in front of the antennas, probably the roof surface.

These independent sets of measurements, bearing remarkable similarity in terms of diurnal variation to the data sets made using the INMARSAT-II F-4 satellite, seem to support that there is a much larger diurnal variation in signal level received by a hemispherical antenna than by a narrowbeam antenna. It also could imply that the variation may be the result of closein multipath effects.

Another pilot tone at 1.5415 GHz aboard the MARECS B-2 at 15° west has also been measured, and showed variations similar in shape to those for the 15° elevation satellite discussed previously. Preliminary investigations of diurnal signal variations measured through a glass window from inside an office at COMSAT Laboratories have also shown similar results.

Conclusions

The satellite used for the measurements wasgeosynchronous orbit with an inclination of 2.2°. The elevation angle changes by less than ±2.2° over a sidereal day. The movement of the satellite with respect to earth is therefore slow, leading to correspondingly slow changes in multipath effects. By inference, if the signal had emanated from a low earth orbiting satellite, similar changes (but at a higher rate) would be experienced by the user, particularly when employing a low-gain antenna.

Increases in signal variations observed when a low-gain antenna was lined up along the satellite look angle suggest an increased contribution from reflected signal components of the antenna's surroundings, as a large part of the antenna pattern intercepted multipath-producing surfaces. The results from the measurements indicate a strong relationship between the physical orientation of the antenna, and the profile/texture of the surrounding surfaces, whether they were walls, flat areas, cement, or foliage.

It appears that the user of a handheld satellite communications terminal would have to be aware of its limitations in order to use it satisfactorily. Also, further propagation studies of the phenomena, including an investigation into the nature of the suspected multipath components, is prudent.

References

[1] ``Measurement and Modeling of Land Mobile Satellite Propagation at UHF and L-Band, Including the Results from the Dedicated Stratospheric Balloon Experiment of July 18, 1986," W.J. Vogel and U. Hong, A technical report submitted to the Jet Propulsion Laboratory under contract 956520, May 1987.

[2] ``Multiband Propagation Experiment for Narrowband Characterization of High Elevation Angle Land Mobile-Satellite Channels," G. Butt, B. G. Evans, and M. Richaria, Electronics Letters, July 16,1992, Vol. 28 No.15 pp. 1449-50

[3] ``Propagation Considerations on L-Band Handheld Communication Service Operations Via Satellite," R. M. Allnutt, A. W. Dissanayake, K. T. Lin, and C. Zaks, International Conference on Antennas and Propagation, Edinburgh, Scotland, April1993, Proc.
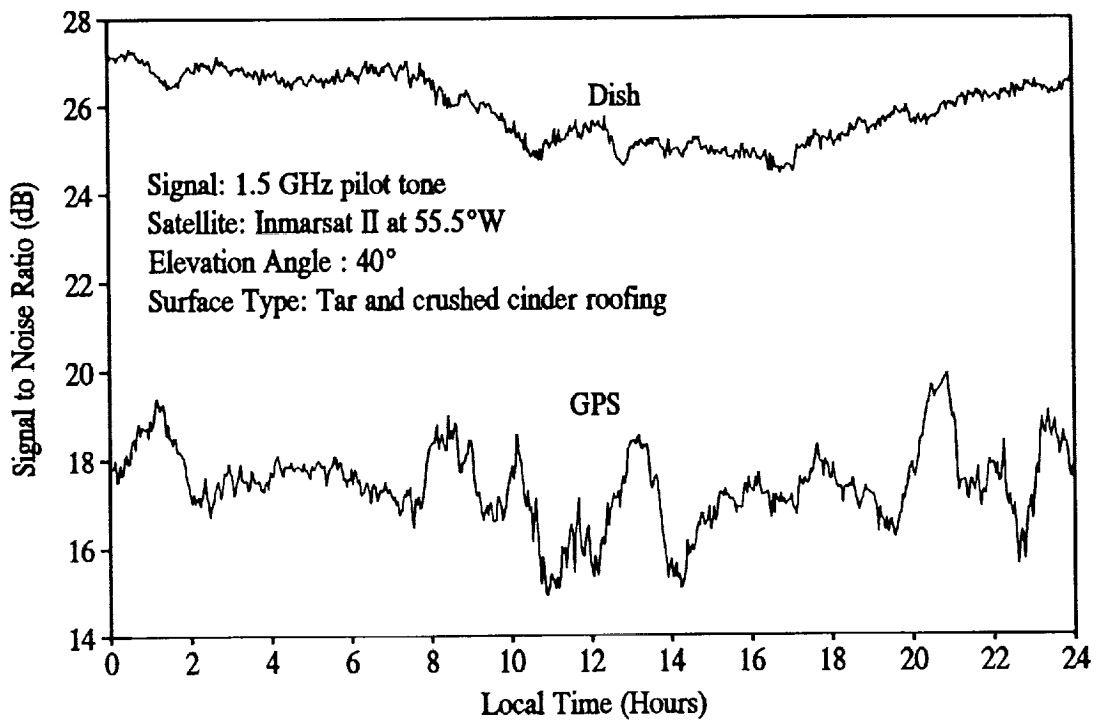
Figure 1. A Comparison of Received Satellite Signal Strength at 1.5 GHz Between Directional (Dish) and Hemispherical (GPS) antenna; 14 October 1992
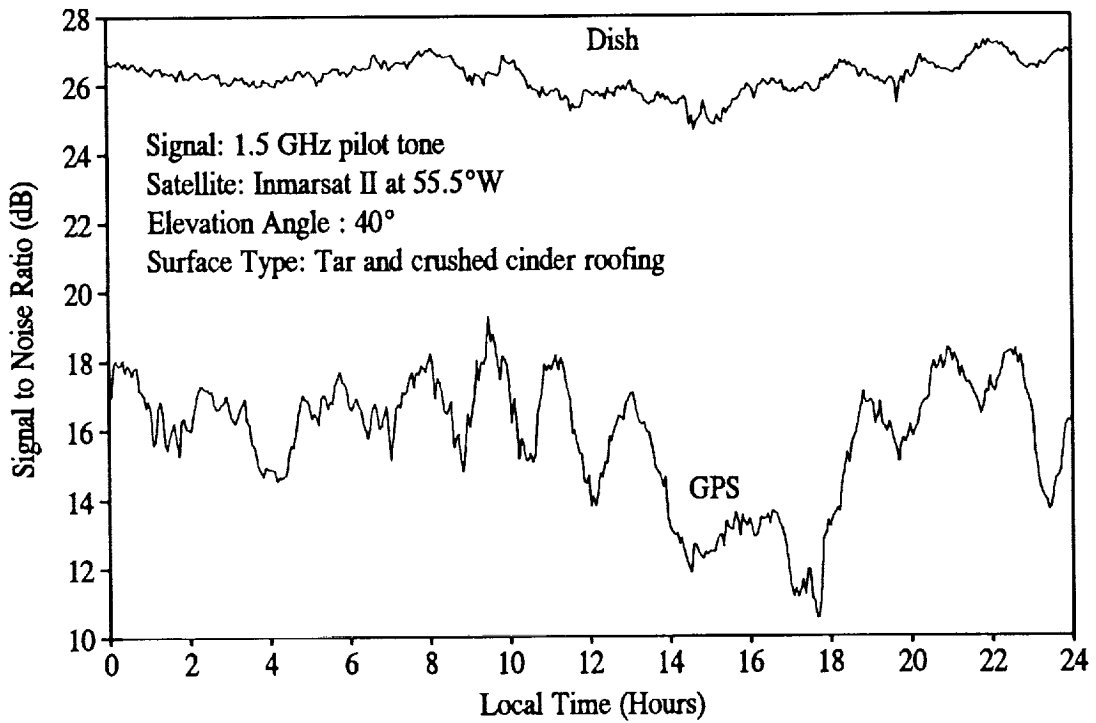
Figure 2. A Comparison of Received Satellite Signal Strength at 1.5 GHz Between Directional (Dish) and Hemispherical (GPS) antenna; 24 October 1992
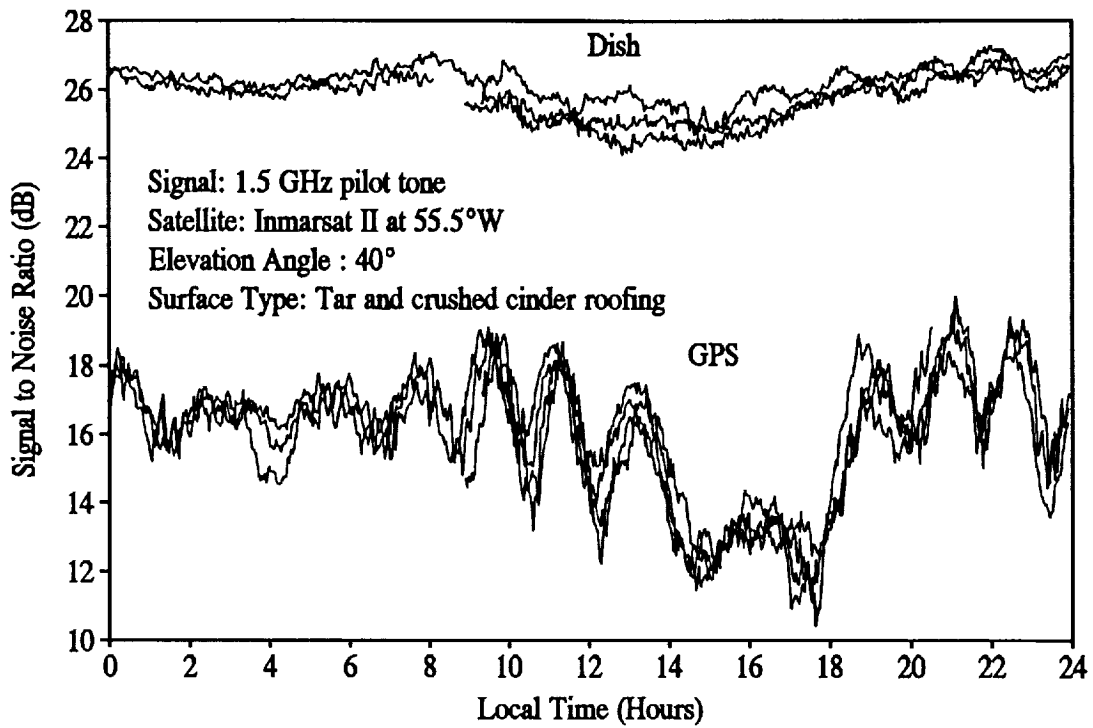
*Figure 3. A Comparison of 4 Days of Satellite Signal Strength Data Measured
(22 - 25 October 1992).*
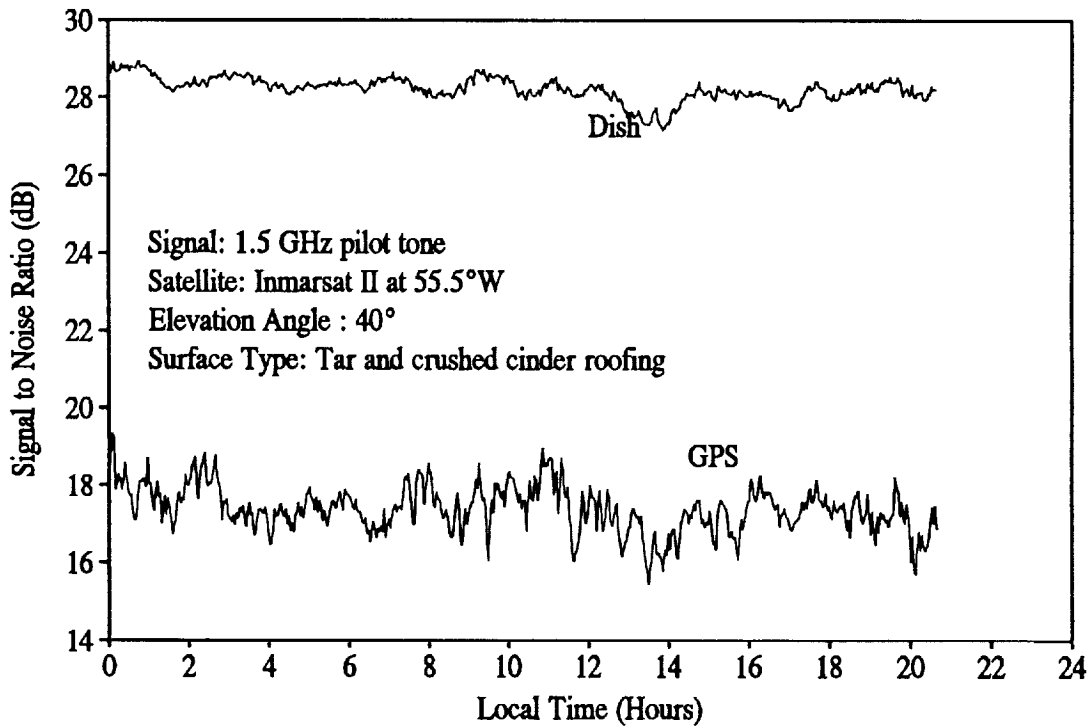
*Figure 4. A Comparison of Received Satellite Signal Strength at 1.5 GHz
Between Directional (Dish) and Hemispherical (GPS) antenna; 11 October 1992*
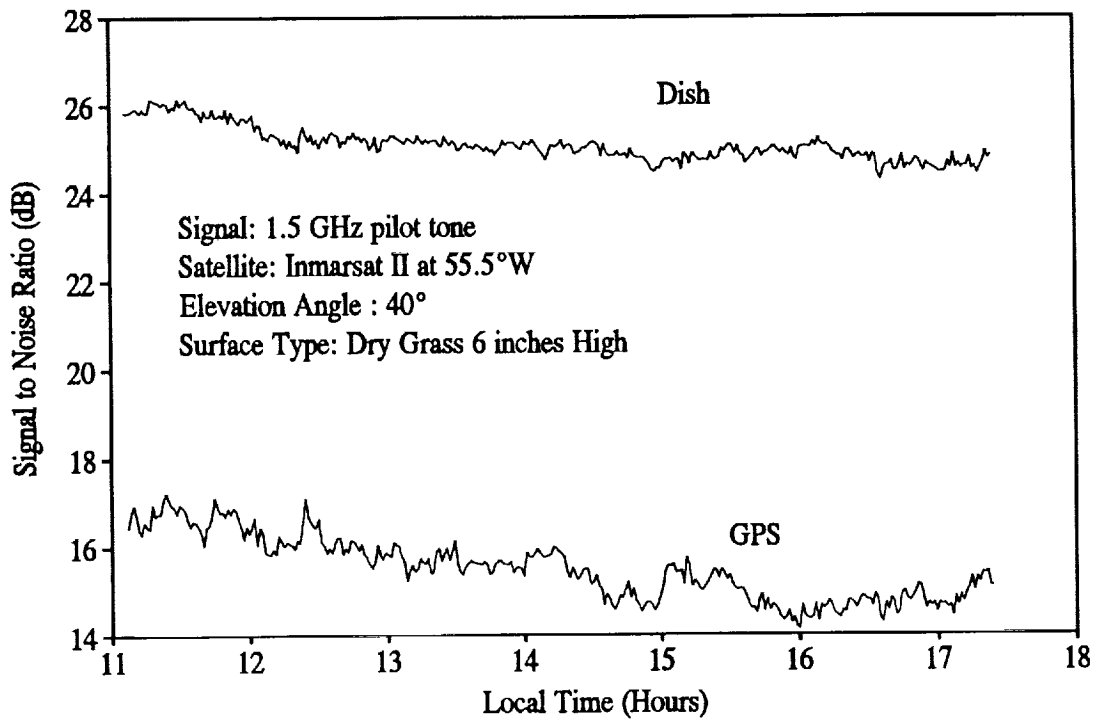
*Figure 5. A Comparison of Received Satellite Signal Strength on a Grass Surface
28 October 1992*
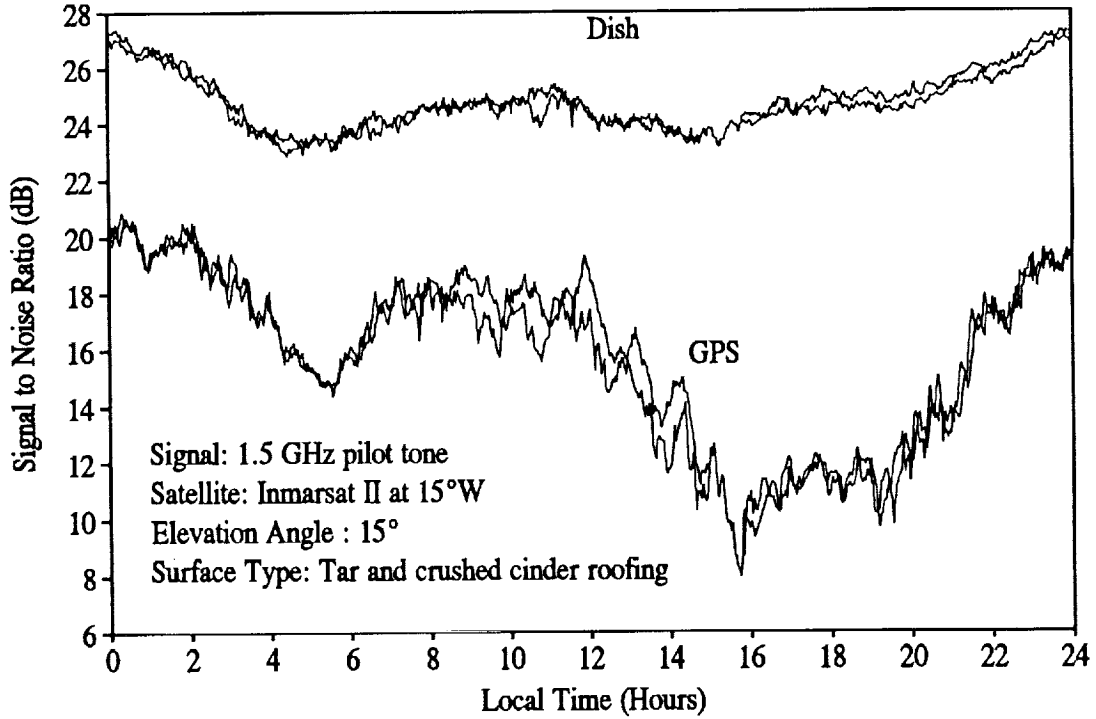
*Figure 6. A Comparison of Received Signal Strength from a Second Satellite
7-9 December 1992*

ELECTROMAGNETIC FIELD STRENGTH PREDICTION IN AN URBAN ENVIRONMENT: A USEFUL TOOL FOR THE PLANNING OF LMSS

G.A.J. van Dooren[1], M.H.A.J. Herben[1], G. Brussaard[1], M. Sforza[2], and J.P.V. Poiares Baptista[2]

[1] Eindhoven University of Technology, Telecommunications Division, PO Box 513, 5600 MB Eindhoven, The Netherlands, tel.:+31-40-473458, fax:+31-40-455197
[2] European Space Technology and Research Centre, Electromagnetics Division, PO Box 299, 2200 AG Noordwijk, The Netherlands, tel.:+31-1719-83298, fax: +31-1719-84999

ABSTRACT

In this paper a model for the prediction of the electromagnetic field strength in an urban environment is presented. The ray model, that is based on the Uniform Theory of Diffraction (UTD), includes effects of the non-perfect conductivity of the obstacles and their surface roughness. The urban environment is transformed into a list of standardized obstacles that have various shapes and material properties. The model is capable of accurately predicting the field strength in the urban environment by calculating different types of wave contributions such as reflected, edge and corner diffracted waves, and combinations hereof. Also antenna weight functions are introduced to simulate the spatial filtering by the mobile antenna. Communication channel parameters such as signal fading, time delay profiles, Doppler shifts and delay-Doppler spectra can be derived from the ray-tracing procedure using post-processing routines. The model has been tested against results from scaled measurements at 50 GHz and proves to be accurate.

INTRODUCTION

In the last decade, the market for personal telecommunications is growing rapidly. Therefore, paging channels, mobile, broadcast and portable services have more and more the interest of the planners of modern telecommunications systems. Especially Land Mobile Satellite Systems (LMSS) have a large and continuously increasing interest of system designers and radio wave propagation engineers. It is obvious that, for planning purposes, it is necessary to investigate whether a certain system will meet the required performance criteria *before the system is actually installed*. Therefore, a prediction tool from which information regarding the performance of the communications channel can be deduced, is required. Nowadays, most of the LMSS field prediction models are based on empirical regression fits to numerical measurement results [1, 2, 3] and fail for some particular urban environments. Further, the theoretical models available are often based on crude approximations and assumptions. So a more accurate predictive procedure should use a detailed description of the urban environment in order to analyse the channel characteristics for a number of well defined locations and configurations of the mobile receiver site.

In this paper we describe a deterministic model for field strength prediction in an urban environment, which facilitates the calculation of communication channel parameters such as fading, Doppler shift, and time delay spread. Different types of multipath wave-propagation phenomena, such as reflection, diffraction, and higher order combinations of reflection and/or diffraction, are considered. The model is based on the Uniform Theory of Diffraction (UTD) and includes the effects of the non-perfect conductivity of the obstacles and their surface roughness. Moreover, it permits the antenna characteristics of both the transmitter and receiver to be taken into account. Also, the problem of an object in the near-field of the antennas is addressed and predicted and measured results are compared. Objects with complex shapes are modelled by a number of standardized objects with suitable dimensions and material properties. Particular problems present in conventional prediction methods, such as shadowing and strong specular reflection, are solved by the new model. In this way, our model extends the region of validity of existing models, and improves the physical insight into the wave propagation processes. The major part of this research has been financed by the European Space agency (ESA).

ELECTROMAGNETIC WAVE MODELLING

The model used to describe the interaction of the incident electromagnetic (EM) wave with the objects in the urban environment is UTD [4], heuristically extended to include effects of non-perfect conductivity and surface roughness [5, 6, 7, 8]. UTD is a high-frequency asymptotic technique that assumes the different waves to propagate along straight lines (rays). This propagation can be mathematically described by:

$$\vec{E}^o = \vec{E}^i \cdot C \, A(s) \, e^{-jks} \qquad (1)$$

where $\vec{E}^{o,i}$ indicates the outgoing or incident field, C is a dyadic coefficient describing the physical interaction

of the wave and the object, A is a factor depicting the divergence of the outgoing wave, k is the wavenumber for free space and s is the distance from the observation point to the point on the object at which the interaction took place. The factor C depends on the material properties of the obstacle, the direction of propagation of the incident and outgoing wave, the wavelength and the shape of the obstacle edges and surfaces. Well-known dyadics C are those for LOS (direct) propagation, reflection and diffraction [4] and corner diffraction [9]. Some forms of the divergence factor A are:

$$A(s) = \begin{cases} 1 & \text{, for a plane wave} \\ s^{-1/2} & \text{, for a cylindrical wave} \\ s^{-1} & \text{, for a spherical wave} \end{cases} \quad (2)$$

In our field strength prediction model the following types of waves can be included:

- direct (LOS) wave;

- reflected wave;

- edge diffracted wave;

- reflected-diffracted wave;

- diffracted-reflected wave;

- corner-diffracted wave;

- double-diffracted wave (dd).

Some of the wave contributions are visualized in figure 1. If necessary, contributions of higher order can be taken into account.

Note that the reflection may take place at both the ground and at the obstacle. The reflection and diffraction points can be found using Fermats principle of stationary optical path length [4], yielding reflection points on some face of the obstacle and edge diffraction points at its edges.

Given the coordinates of the source (the satellite) and the observation point (the mobile receiver) and the description of the urban environment, the total field at the observation point can be described by:

$$\begin{aligned} \vec{E}^{obs} \propto \ & \vec{E}^{LOS} \varepsilon^{LOS} \\ & + \sum_l \vec{E}_l^{refl} \varepsilon_l^{refl} \\ & + \text{ other types of rays} \\ & + \sum_m \vec{E}_m^{dd} \varepsilon_m^{dd} \end{aligned} \quad (3)$$

where the functions ε account for possible blockage of the wave contributions by obstacles in the urban environment.

The received field at the observation point is obtained by first calculating the field strength relative to the free space value (i.e. the case where the field strength is

proportional to the distance between transmitter and receiver). Afterwards the absolute level of the free space value is determined using the well-known radio equation. According to this procedure, the ray-tracing analysis is used to calculate the explicit attenuation of the radio signal induced by the urban environment. This attenuation factor is called site shielding factor (SSF) and is also of interest for other applications [10, 11].

Some of the parameters of interest for the design of a LMSS are the field strength along a trajectory through the urban environment, the mean excess delay time and delay spread, the Doppler spectrum and the delay-Doppler spectrum [12]. These characteristics can be derived by performing a ray-tracing procedure for the environment under consideration and storing the following parameters for each ray and each observation point:

1. the type of ray (LOS, reflected, diffracted, etc.);

2. (complex) $\vec{E}$ vector;

3. direction of propagation;

4. absolute path length measured from source to observation point via the point of stationary phase, or a corner point of the obstacle.

The influence of the antenna receiving pattern of the mobile is simulated by introducing antenna weight functions (in amplitude, phase and polarization). This can be performed *after* the ray tracing for the individual wave contributions has been finished. So, this post-processing feature facilitates the analysis of for instance the antenna type and antenna orientation dependence. The received signal by the antenna is now given by:

$$\begin{aligned} E^{obs} = \ & \varepsilon^{LOS} G^{LOS} \vec{E}^{LOS} \cdot \hat{e}_{pol}^{LOS} \\ & + \sum_l \varepsilon_l^{refl} G_l^{refl} \vec{E}_l^{refl} \cdot \hat{e}_{pol}^{refl} \\ & + \text{ other types of rays} \\ & + \sum_m \varepsilon_m^{dd} G_m^{dd} \vec{E}_m^{dd} \cdot \hat{e}_{pol}^{dd} \end{aligned} \quad (4)$$

where the value of the (complex) antenna voltage patterns G are calculated using the angle between the direction of arrival of the particular ray and boresight direction, while the scalar product with $\hat{e}_{pol}$ accounts for the polarization discrimination.

The post-processor also permits the use of measured antenna patterns by reading the amplitude and phase of a measured antenna voltage pattern from a table. So, different post-processors can provide information on the field strength (co- and cross-polarization), the mean excess delay and delay spread (LOS and obstructed case), and the delay-Doppler spectrum from one and the same ray-tracing file. In this way, the time-consuming

ray-tracing analysis needs to be performed only once for a given observation line and environment.

Note that in some cases an obstacle will be located in the near-field of the antenna or vice-versa. In this particular case it is necessary to consider the combined problem of obstacle and antenna scattering [13]. For ground station reflector antennas this problem has been studied quite extensively and some of the results of this work demonstrate that (theoretically) the combined, near-field method is the only correct approach. For the present application, however, it is decided, both from a computational and a practical point of view, to perform a far-field analysis implying that the interactions of the EM wave with the obstacle and antenna are treated independently.

A time delay analysis is easily performed using the computed data saved for each ray and each observation point. Since each ray will have a different path length from source to observation point, the arrival of the individual waves causes a train of pulses with different amplitudes in the time domain. The same is true in the frequency domain for the Doppler spectrum: each wave will have a different direction of arrival and different amplitude, thereby giving rise to a train of spectral lines in the Doppler spectrum around the carrier frequency. A classification of the arriving waves with respect to the delay time and the Doppler shift will result in the delay-Doppler spectrum [12].

MODELLING OF URBAN ENVIRONMENT

Since in an urban environment a great variety of obstacle shapes and materials used may occur, there is a need for a flexible, standardized type of obstacle to model the environment.

It was found that therefore the so-called block-shaped obstacle, shown in figure 2, can effectively be used [13]. This obstacle is numerically specified by the (x,y,z) coordinates of its eight corner points. Figure 2 also shows some specific forms of the block-shaped obstacle.

Since it is allowed that some of the corner points (nearly) coalesce, the block-shaped obstacle can effectively be used as an element of a box of building-bricks. Because of this property it is suited to model modern buildings in urban environments (having rectangular shapes) as well as traditional houses in rural environments (having wedge type roof shapes). Also other shapes such as pyramids can easily be modelled and analysed. All combinations of blocks are permitted, and in this way very complex shapes can be built up. Each obstacle has its own material properties and surface roughness. Because of this standardization of obstacle types, only one ray-tracing algorithm is sufficient for the analysis.

The main advantage of the use of the block-type obstacle is the fact that simplifications are introduced

in the calculations of, for example, the reflected and diffracted field parameters. The block-type obstacle has the property that all its sides are straight and all its faces are plane. This implies that phase front of the wave reflected field from one of these planes has the same radii of curvature as that of the incident wave. Because of the straight edges there is no need for the calculation of the caustic distance used in UTD [4].

The modelling proposed has one main disadvantage: cylindrical shapes such as lamp posts and grain warehouses are less accurately modelled. This drawback can be circumvented by approximating a circular cylindrical shape by a combination of two (or more) polygonal cylinders as shown in figure 3. If this approximation appears to be too crude, a second standardized obstacle could be introduced, which possesses a elliptic cylindrical shape. Also this kind of obstacle can be analysed using a UTD theory for convex shapes [14]. It can be shown, however, that the replacement of a cylindrical obstacle by a block-shaped obstacle introduces only considerable changes in the received field *behind* the obstacle. In practice, where a large number of contributions will be received, an error in one of them will lead to just a small error in the whole.

The relevant parameters for the block-type obstacle can be derived semi-automatically from high-accuracy digital databases of rural and urban environments. Also an interface with a CAD package may be developed.

PRACTICAL VERIFICATION

Recently the model proposed has been experimentally verified for some scaled obstacles at a frequency of 50 GHz [10, 11, 15]. In all comparisons of measurements with theoretical predictions very good agreement has been obtained. Not only the field strength, but also the arrival times of the individual wave contributions were measured and compared to results predicted by the model [10]. From this comparison it was found that the individual rays propagate independently (as assumed in UTD) and that a strong polarization dependence of the signal amplitude exists for conductive block-shaped obstacles [11]. This polarization dependence appears to be due to slope diffraction at the side faces of the obstacle [13] and more or less disappears for less conductive materials [15]. Further, it was found that the corner diffraction contribution can, in some cases, not be neglected in the analysis, especially for low-elevation LMSS.

ANALYSIS OF TEST CASE

As an illustrative example, we have analysed the 'urban' environment shown in figure 4. The rectangular obstacles have dimensions 86m x 20m x 68m (width x thickness x height), and the pyramid is obtained from

345

the rectangular block-shaped obstacle by placing the corner points from the top face very close together. Therefore the base of the pyramid is also 86m x 20m and its height is 68m. The rectangular building corresponds to the dimensions of the building of Electrical Engineering at the campus of Eindhoven University of Technology. The left rectangular obstacle is assumed to be perfectly conductive and has a surface roughness of 0, the right rectangular obstacle has a relative permittivity ϵ_r of $2 - 0.1i$ and a surface roughness of $0.1m$, while the pyramid has $\epsilon_r = 3 - 0.2i$ and a surface roughness of $0.1m$. An observation line is defined by the starting point with coordinates $(100m, 75m, 5m)$ and the end point $(-25m, 75m, 5m)$. A total number of 1000 observation points on this line has been used. The satellite position is specified by the azimuth and elevation angles, each having a value of $25°$. The contributions included in the analysis were the direct, reflected, edge diffracted and corner diffracted waves and waves that encounter a combination of reflection and diffraction.

For this geometry we have deduced the field strength on the observation line defined for vertical polarisation at a frequency of 1 GHz and for isotropic transmitting and receiving antennas. This result is shown in figure 5. In this figure the regions of LOS propagation and of strong specular reflection are indicated.

Also the Doppler spectrum around the carrier-frequency of 1 GHz has been calculated for a speed of the mobile of 50 km/h along the trajectory indicated in figure 4. This result is shown in figure 6, where the maximum Doppler shift is 40 Hz. A total of 11500 spectral components are found along the trajectory defined, of which only 10% is plotted in figure 6.

The 3-dimensional delay-Doppler spectrum is shown in figure 7. From this spectrum information on the time delay profile and the Doppler spectrum can be found by using a projection of the data derived onto the time-axis and the Doppler frequency axis, respectively. From a separate time delay analysis it was found that in the LOS regions the mean excess delay time is $0.004\mu s$, while the delay spread is $0.014\mu s$ Further, the mean excess delay time in the obstructed regions is $0.08\mu s$, and the delay spread in these regions is $0.058\mu s$.

These results illustrate the potential of the model developed. The calculations were performed on a 486 computer taking 3 hours of CPU time, resulting in an average of $10s$ per observation point.

CONCLUSIONS

A deterministic model for the prediction of the field strength in urban environments has been described. The model, that is based on the Uniform Theory of Diffraction (UTD), includes effects of the non-perfect

conductivity of the obstacles and their surface roughness. It proves that the use of a flexible, standardized type of obstacle simplifies the ray-tracing algorithms necessary to find reflection and diffraction points. Further, the block-type obstacle proposed is able to (numerically) model frequently encountered shapes such as rectangular blocks (office towers) and wedges (rural rooftops).

The effects of the receiving antenna pattern can be included in a post-processor, which can calculate the field strength along an observation line, together with the Doppler spectrum, time delay profile and the delay-Doppler spectrum. From these parameters relevant information can be deduced for the planning and design of a LMSS.

The model predictions have been verified against scaled measurements at a frequency of 50 GHz. In all cases good agreement between measurements and theory has been obtained.

Besides for mobile communications systems, the model can also be used to analyse the performance indoor radio communications systems. Other fields of technology that may have an interest in the prediction model are (transhorizon) interference prediction, optimal placement of VSAT stations in urban environments, and coupling of interference from terrestrial systems into satellite systems.

References

[1] Y. Okumura, E. Ohmori, T. Kawano, and K. Fukuda, "Field strength prediction and its variability in VHF and UHF land-mobile radio service", *Rev. Elec. Commun. Lab.*, vol. 16, no. 5, pp. 825–873, 1968.

[2] D.O. Reudink, "Properties of mobile radio propagation above 400 MHz", *IEEE Trans. Veh. Technol.*, vol. VT-23, no. 11, pp. 143–159, 1974.

[3] D.C. Cox, "Multipath delay spread and path loss correlation for 910 MHz urban mobile radio propagation", *IEEE Trans. Veg. Technol.*, vol. VT-26, no. 11, pp. 340–344, 1977.

[4] R.G. Kouyoumjian and P.H. Pathak, "A uniform geometrical theory of diffraction for an edge in a perfectly conducting surface", *Proc. IEEE*, vol. 62, no. 11, pp. 1448–1462, 1974.

[5] R.J. Luebbers, "Propagation prediction for hilly terrain using GTD wedge diffraction", *IEEE Trans. Antennas Propag.*, vol. AP-32, no. 9, pp. 951–955, 1984.

[6] R.J. Luebbers, "Finite conductivity uniform GTD versus knife edge diffraction in prediction of propagation path loss", *IEEE Trans. Antennas Propag.*, vol. AP-32, no. 1, pp. 70–76, 1984.

[7] K.A. Chamberlin and R.J. Luebbers, "An evaluation of Longley-Rice and GTD propagation models", *IEEE Trans. Antennas Propag.*, vol. AP-30, no. 6, pp. 1093–1098, 1982.

[8] R.J. Luebbers, "A heuristic slope diffraction coefficient for rough lossy wedges", *IEEE Trans. Antennas Propag.*, vol. AP-37, no. 2, pp. 206–211, 1989.

[9] F.A. Sikta and W.D. Burnside and T.T. Chu and L.J. Peters JR, "First order equivalent current and corner diffraction scattering from flat plate structures", *IEEE Trans. Antennas Propag.*, vol. AP-31, no. 4, pp. 584–589, 1983.

[10] G.A.J. van Dooren, M.G.J.J. Klaassen, and M.H.A.J. Herben, "Measurement of diffracted electromagnetic fields behind a thin finite-width screen", *Elec. Lett.*, vol. 28, no. 19, pp.1845–1847, 1992.

[11] G.A.J. van Dooren and M.H.A.J. Herben, "Polarization-dependent site-shielding factor of a block-shaped obstacle", *Elec. Lett.*, vol. 29, no. 1, pp. 15–16, 1993.

[12] W.C. Jakes Jr. (editor), *Microwave mobile communications*, New York, John Wiley & sons, 1974.

[13] G.A.J. van Dooren, "Electromagnetic diffraction models for the shielding of single- and dual-reflector antennas by obstacles with simple shapes", IVO Technical Report (ISBN 90-5282-162-3), Eindhoven University of Technology, 1991.

[14] P.H. Pathak, W.D. Burnside, and R.J. Marhefka, "A uniform GTD analysis of the diffraction of electromagnetic waves by a smooth convex surface", *IEEE Trans. Antennas Propag.*, vol. AP-28, no. 5, pp. 631–642, 1980.

[15] G.A.J. van Dooren and M.H.A.J. Herben, "Field strength prediction behind non-perfectly conducting obstacles using UTD", *submitted for publication*, 1993.

Figure 2: General block-shaped obstacle and some specific obstacles.
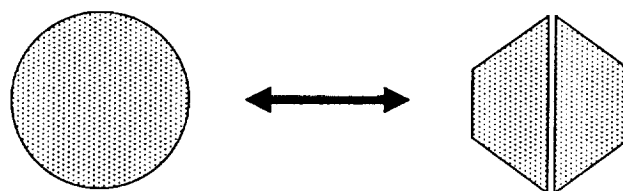
Figure 3: Approximation of a circular cylinder by a combination of polygonal cylinders (a cross section of both shapes is shown).

Figure 1: Wave contributions included in the theoretical analysis.
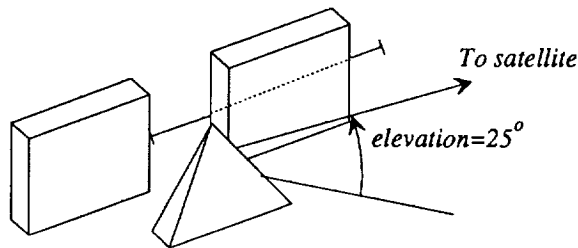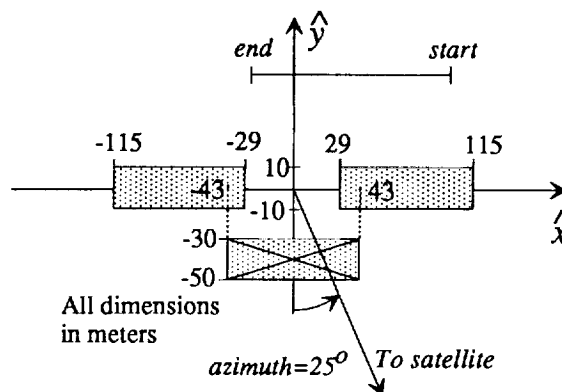
Figure 4: Geometrical setup of the testcase.

347
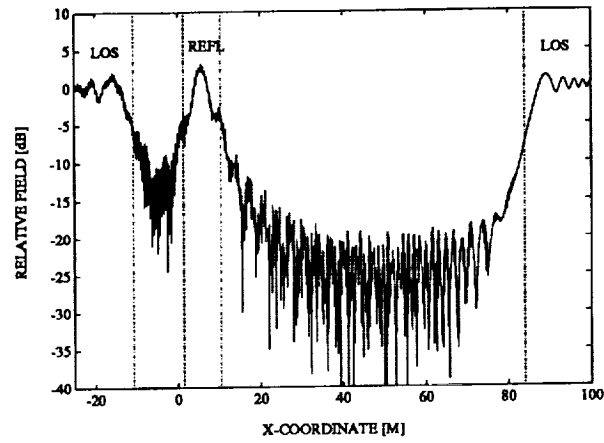
Figure 5: Calculated field strength along observation line indicated in figure 4.
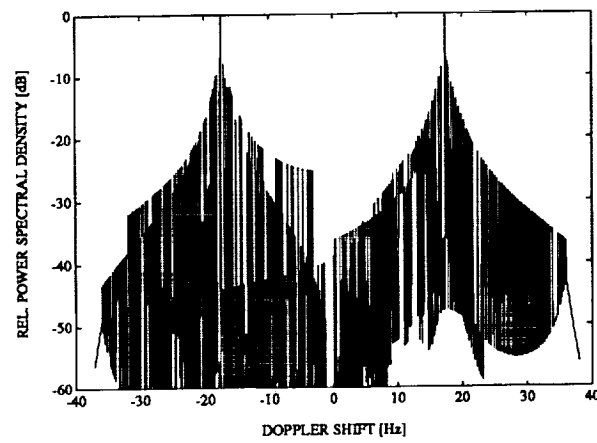
Figure 6: Calculated Doppler spectrum for observation line indicated in figure 4 at a speed of 50 km/h.
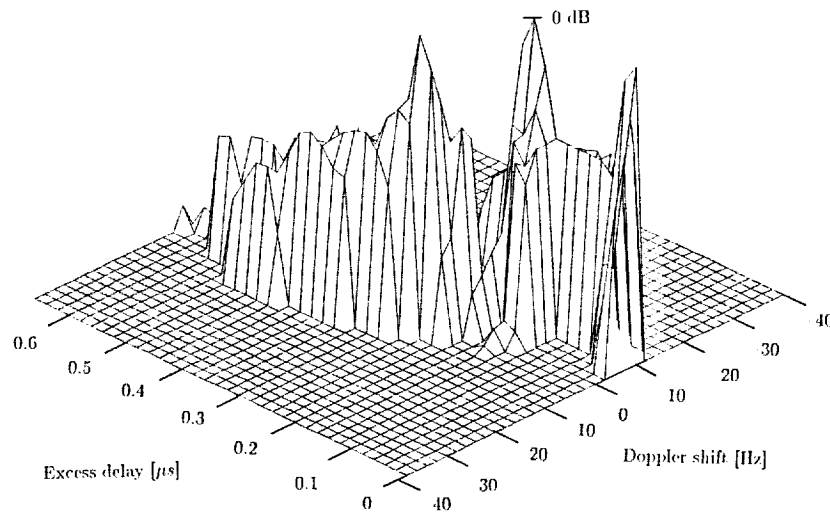
Figure 7: Calculated delay-Doppler spectrum for observation line indicated in figure 4 at a speed of 50 km/h.

348

Propagation Model for the Land Mobile Satellite Channel in Urban Environments

M. Sforza[1], G. Di Bernardo[2], R. Cioni[3]

ESA[1], Keplerlaan 1, 2200 AG Noordwijk, The Netherlands
Phone: +31 1719 83298, Telefax: +31 1719 84999
Space Engineering[2], Via dei Berio 91, 00155 Rome, Italy
Phone: +39 6 225951, Telefax: +39 6 2280739
Ingegneria dei Sistemi[3], Via Roma 50, 56126 Pisa, Italy
Phone: +39 50 502769, Telefax: +39 50 502470

1   Abstract

This paper presents the major characteristics of a simulation package capable of performing a complete narrow and wideband analysis of the mobile satellite communication channel in urban environments, for any given orbital configuration. For the RF frequency range the model has been designed to be applicable (1 up to 60 GHz), the wavelength-to-average urban geometrical dimension ratio has required the use of the Geometrical Theory of Diffraction (GTD) [1], extended to include effects of non-perfect conductivity and surface roughness. Taking advantage of the inherent capabilities of such a high frequency method, we are able to provide a complete description of the electromagnetic field at the mobile terminal. Using the information made available at the ray-tracer and GTD solver outputs, the Land Mobile Satellite (LMS) urban model can also give a detailed description of the communication channel in terms of power delay profiles, Doppler spectra, channel scattering functions and so forth. Statistical data, e.g. cumulative distribution functions, level crossing rates or distributions of fades are provided too. The user can access the simulation tool through a Design-CAD user-friendly interface by means of which he can effectively design his own urban layout and run consequently all the envisaged routines. The software is optimised in its execution time so that numerous runs can be achieved in a considerable short time.

2   Introduction

Urban areas will likely represent a significant market for the conventional mobile communication services and for the new concepts of personal communications through hand-held terminals. The propagation of an electromagnetic field in such environments is, on the other hand, a very complex phenomenon to simulate. To date the analyses of the link impairments and the estimation of their impact on the LMS system performance have been mainly based upon experimental data and empirical models, [2]-[4]. The development of a deterministic model not directly related to specific environmental urban scenarios and designed on canonical electromagnetic laws is therefore strongly needed.

Based on this sort of considerations and having in mind to develop a user-friendly prediction tool to be used not only by propagation engineers but also by LMS system planners, the

European Space Agency (ESA) decided to place a study contract with two Italian companies, Space Engineering and Ingegneria dei Sistemi (IDS), in 1992, [5]. The main features of the LMS prediction tool developed under this contract are hereafter described.

3 The LMS urban prediction tool

The GTD-based prediction tool for LMS systems in urban environments can be considered as the result of the interaction of several functional blocks, each of them properly designed in order to save computational time and increase modularity and transportability. The core of the simulation package is represented by the Ray Tracer and the GTD Solver codes. In addition we also have an Urban Area Modeler, an Electromagnetic (E.M.) Mesher and a Post Processor Unit. A functional block diagram of the package is reported in Fig. 1 while a detailed description at subsystem level is given in the following sections.

3.1 The Ray Tracer

In most of the existing GTD prediction packages (e.g. NEC-BSC) ray tracing and electromagnetic field computation are performed in the same logical step; the ray tracing parameters calculated at any observation point are not saved for further processing (e.g. at a different RF frequency) and this inevitably results in a great computational inefficiency particularly in complex environments such as urban areas. In our LMS prediction tool, the two operations are kept separate and are performed by two distinct modules. All the ray tracing parameters are saved in a file before actually starting the e.m. calculation. This software architecture implies a sensible reduction of the CPU time and is naturally suitable for optimization and upgradability.

The input parameters for the Ray Tracer are: the satellite position, the urban area model, the vehicle speed and path and the number of electromagnetic interactions to be considered. The model has in-built the opportunity to generate orbital configurations other than the conventional geostationary one; this feature is extremely important to simulate a large variety of LMS constellations, from Low to Medium and Helliptical Earth Orbiting multisatellite systems (LEO, MEO, HEO). The urban geometry of the vehicle path is given through a set of straight lines with a user-assigned speed for each of them. As for the number of the electromagnetic interactions, the LMS urban prediction tool has been to date designed to include up to the second order, i.e. double reflected or diffracted and all the different combinations with the direct and single scattered rays.
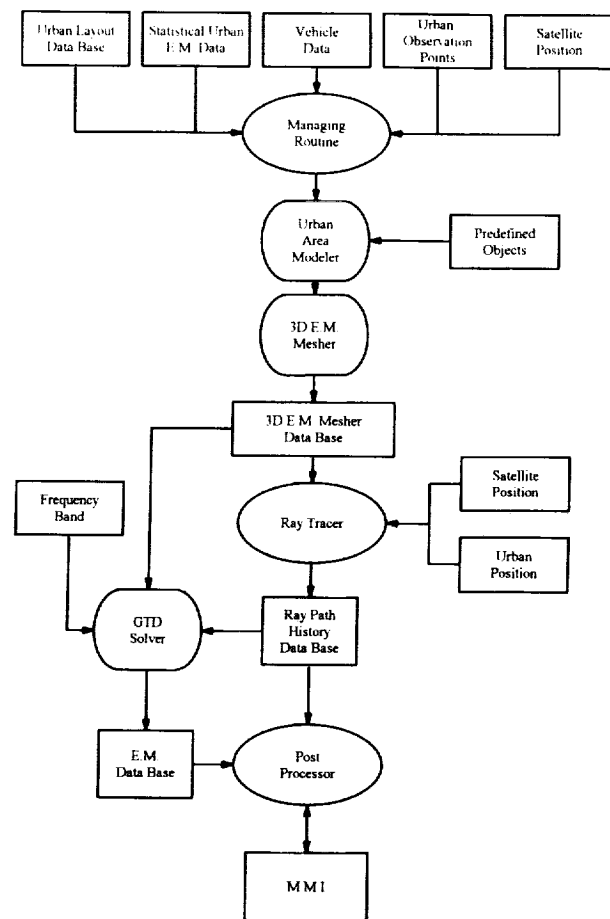
Fig. 1 LMS prediction tool block diagram

The software architecture has been anyhow conceived to be easily upgradable for any higher order of contributions.

In order to reduce the computational time, the Ray Tracer considers as *active* part of the user-defined urban layout the boolean combination of the portions contemporarily seen by the satellite and the mobile terminal. Once all the ray paths relevant to a certain observation point are computed, they are stored on a high capacity hard disk and the mobile position is updated. In Fig. 2 a sketch of the Ray Tracer active area for a typical urban area is reported where all the relevant rays (reflected, diffracted, etc.) are clearly visible.
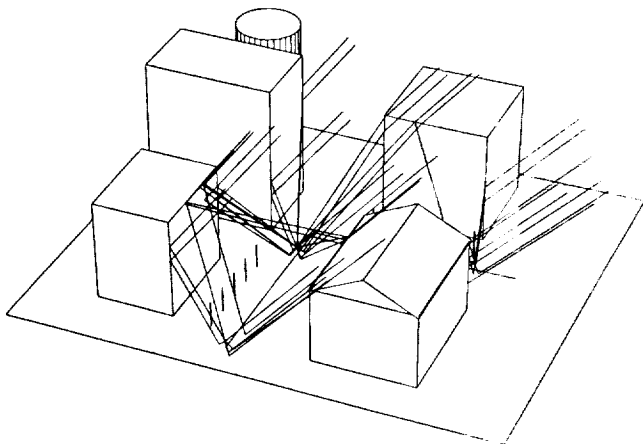
Fig. 2 Typical Ray Tracer output

3.2 The GTD solver

This unit performs the actual electromagnetic computations according to the uniform theory of diffraction and using, where applicable, the geometrical optics and the Fresnel coefficients for the reflection ray paths. The extension to non perfectly conductive materials and surface roughness is achieved through heuristic formulations and user-defined look-up tables for the complex reflection coefficients. The effect of leafage absorption is also modeled directly by the user introducing weight functions or empirical relations.

The input parameters for the GTD Solver are, for any given satellite position and observation point: the ray path history file, the e.m. urban model and auxiliary information, e.g. RF frequency. The direct, reflected, diffracted and refracted field components are then computed in amplitude and phase. This information is stored in a file and handed over to the Post Processor Unit.

3.3 The Urban Area Modeler and E.M. Mesher

The urban layout is characterised by a set of large and small objects representing urban parameters, such as buildings, tunnels, overpasses, trees, street lamps, phone booths, parked cars, etc. Through the Urban Area Modeler implemented in Design-CAD, the user is able to create a fully controlled urban environment placing building by building; it is envisaged, for future developments, also an automatic generation procedure based on a set of statistical parameters (urbanization factors). The urban layout previously considered for the computation of the active Ray Tracer area is reported in Fig. 3.
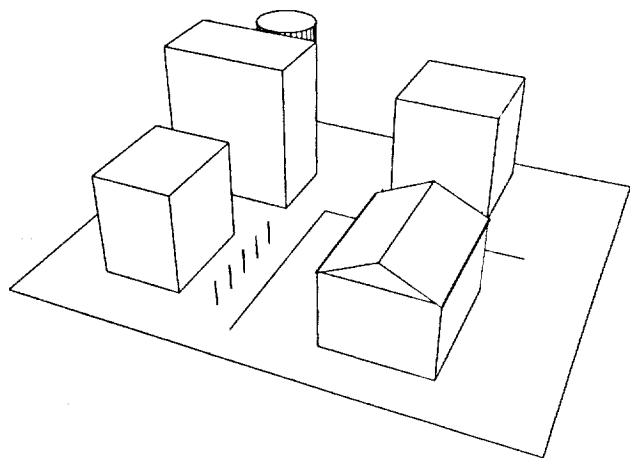
Fig. 3 Urban Modeler output

The Urban Modeler has also the possibility of accepting as input file the layouts of actual cities (Paris, London, Rome, etc.) if given in forms of digital terrain data bases.

Large objects are defined mainly by boxes and cylinders of predefined dimensions; more complex urban objects can be built using flat panels. Trees are characterised by a spherical leafage and a cylindrical trunk while other small objects (nearby vehicles, dust bins, phone booths, etc.) are accounted for with spheres of given radius, scattering isotropically. All the objects materials are defined with their complex permeability and permittivity.

The E.M. Mesher is the unit interfacing the urban layout modeler with the electromagnetic solver. It performs all the required verifications and manipulations on the CAD file, in ASCII format, and translates it into a solver acceptable input format. The objects' electromagnetic properties are included at this stage.

3.4 The Post Processor Unit

Under the supervision of a managing module interfacing the solver output database with the user control screen, the Post Processor Unit performs the following tasks: extraction of the time series of the received e.m. field, field weighting by the preselected mobile terminal antenna pattern, computation of the narrowband statistical functions and wideband channel parameters. It is important to stress that the user has the opportunity to select his mobile receive antenna within a large set of predefined radiation patterns; a computed weight function can also be user defined to take into account the effect of the vehicle roof. In Fig. 4, the time series for the test case presented in Fig. 3 is reported.

The set of statistical narrowband analyses available to the user includes Probability and Cumulative Distribution Functions (PDF and CDF), Average Fade Durations (AFD), Level Crossing Rates (LCR), Distribution of Fades

and Connections, Time-share of Fades and Connections.
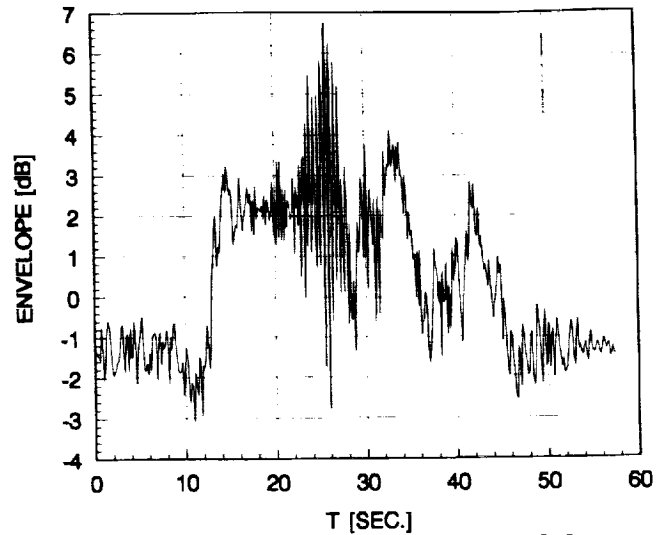
Fig. 4 Time series (segment A-B of the trajectory)

The list of wideband channel parameters is also quite exhaustive: Doppler and power delay profiles, channel scattering function, delay spread and coherence bandwidth. Through the use of these routines the LMS system engineer can effectively achieve a very detailed characterisation of the narrow and wideband channel, ([6]-[7]). Fig. 5 reports, on the base of the previous urban layout, the corresponding PDF and CDF; it is clearly visible the multipath effect due to the strong reflecting buildings (perfect conductivity) along the trajectory considered.

Fig. 5 PDF and CDF

352
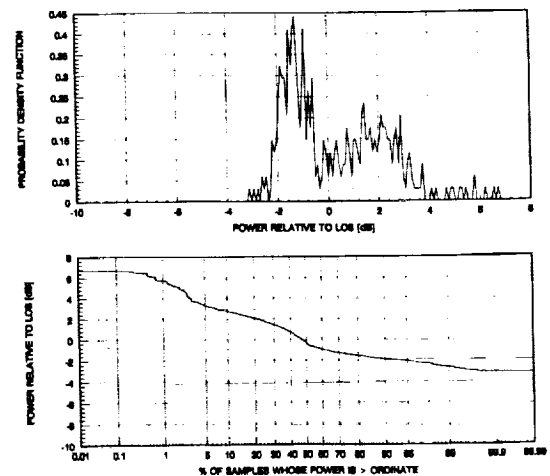
In Fig. 6, the scattering profile of the urban channel computed in several observation points along the selected trajectory is presented. It is very interesting to observe the mutual interaction between different ray contributions generated by the urban area elements.

through Microsoft Visual Basic. The user can visualize and interact with the Urban Modeler via a DesignCAD-3D tool, incorporating a large set of commands and macros.
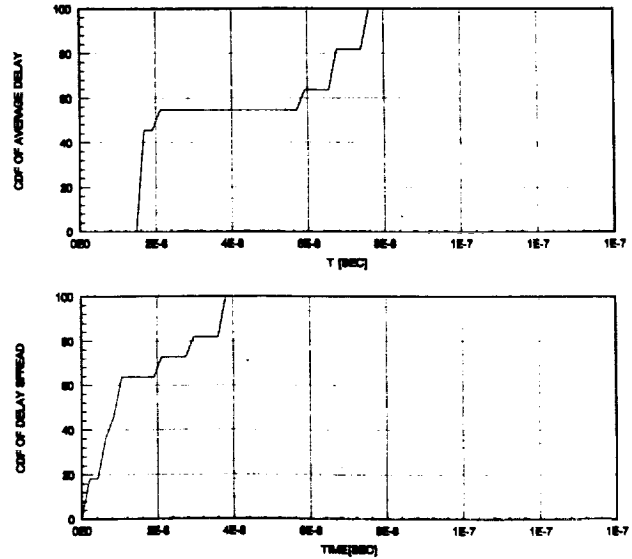
Fig. 7 Average Delay and Delay Spread CDFs

Fig. 6 The Scattering Channel Profile

Finally, the cumulative distribution functions of the average delay and delay spread are given in Fig. 7. The segmented shape of the curves is due to the limited number of observation points considered in our test case. It is fairly easy to notice that the maximum average delay is around 76 ns while the delay spread is always less than 40 ns.

4 The hardware and software platforms

The LMS prediction tool for urban environments has been presently designed to run on PCs with MS-DOS operating system. The requirements for the hardware platform are an 80486 processor, 8 Mbyte of memory and 200 Mbyte of hard disk, a VGA or better EGA graphic card. FORTRAN has been used to develop all the model units but the Man Machine Interface running under Windows environment

5 Conclusions

A brief summary and description of the main features of a GTD-based LMS prediction tool for urban environments has been presented in this paper. The model can be effectively used to simulate and estimate the behaviour of the narrow and wideband channel for any given mobile satellite system in built-up areas. The user can define his own urban layout through a Design-CAD tool inserting buildings, tunnels, phone booths, parked vehicles and many other typical urban items. The model itself is suitable for simulating moving vehicles at given speed as well as personal communication network users equipped with hand-held terminals. The set of wideband parameters and statistical functions available to the user, being a propagation engineer or an LMS system planner, is fairly comprehensive.

In the next future, the LMS prediction tool

will be upgraded insofar as higher orders of electromagnetic contributions and the transmitter located inside the urban layout will be taken into account and implemented. With proper but minor modifications of the Ray Tracer and the GTD solver and with the consequent update of the MMI, the model itself will be then able to estimate channel parameters also for in-building and cellular radio communication networks. In addition to the afore mentioned improvements, the LMS prediction tool will also undergo fairly extensive and comprehensive validation campaigns in the ESA Compact Antenna Test Range, on a scaled model of urban environment, and using actual experimental data.

Acknowledgements

6   References

[1] J.B. Keller, *Geometrical theory of diffraction*, J. Opt. Soc. of America, vol.52, pp.116-130, Feb. 1962.

[2] J. Goldhirsh and W.J. Vogel, *Propagation effects for Land Mobile Satellite Systems: overview of experimental and modeling results*, NASA Ref. Publ.1274, Feb 1992.

[3] J.D. Parsons, *The mobile radio propagation channel*, Pentech Press, London, 1992.

[4] S. Kozono and K. Watanabe, *Influence of environmental buildings on UHF land mobile propagation*, IEEE Trans. Comm, vol.25, pp.1133-1143, Oct. 1977.

[5] *Propagation model for the land mobile satellite radio channel in urban environments*, ESA contract 9788/92/NL/LC(SC), Final Report, Apr. 1993.

[6] W.C.Y. Lee, *Mobile communication engineering*, McGraw-Hill Book Co., New York, 1982.

[7] W.C. Jakes, *Microwave mobile communications*, John Wiley, New York, 1974.

A Prediction Model of Signal Degradation in LMSS for Urban Areas

Takashi Matsudo, Kenichi Minamisono,
Yoshio Karasawa and Takayasu Shiokawa
KDD R&D Laboratories
2-1-15 Ohara, Kamifukuoka-shi, Saitama
356, Japan
Tel: +81-492-66-7877
Fax: +81-492-66-7510

ABSTRACT

A prediction model of signal degradation in LMSS for urban areas is proposed. This model treats shadowing effects caused by buildings statistically and can predict a Cumulative Distribution Function (CDF) of signal diffraction losses in urban areas as a function of system parameters such as frequency and elevation angle, and environmental parameters such as number of building stories and so on. In order to examine the validity of the model, we compared the percentage of locations where diffraction losses were smaller than 6dB obtained by the CDF with satellite visibility measured by a radiometer. As a result, it was found that this proposed model is useful for estimating the feasibility of providing LMSS in urban areas.

INTRODUCTION

Recently, proposals for a Land Mobile Satellite Service (LMSS) using handheld terminals have been advanced. In urban areas, signal degradation in LMSS is anticipated to be very large because of heavy shadowing effects caused by buildings. However, quality of service is still expected to be good even if users with handheld terminals are in urban areas.

Some propagation models for LMSS have been proposed [1],[2], however, it has become ambiguous to define environmental parameters in these models. It is therefore difficult to apply the models to areas where the urban structure is different.

In Japan, prediction methods for visibility in urban areas have been developed [3],[4]. These methods have used urban structure statistics such as a Probability Density Function (PDF) of building stories and building width as a function of the number of building stories, but they can not estimate signal fading.

In this paper, we propose a new type of prediction model of signal degradation in LMSS

for urban areas. The proposed model treats shadowing effects caused by buildings statistically and can predict the Cumulative Distribution Function (CDF) of signal diffraction losses in urban areas as a function of system parameters such as frequency and elevation angle, environmental (urban structure) parameters such as number of building stories and width, and average road width.

LMSS PROPAGATION MODEL APPLICABLE TO URBAN AREAS

Basic Concept of Proposed Model

In general, the following propagation phenomena should be taken into account for propagation model in LMSS.

(1) Visibility of a direct wave from a satellite.
(2) Diffraction losses of a direct wave near and in shadow regions.
(3) Effects of multipath fading due to reflection from buildings and ground.

However, it seemed too complicated to consider the correlation between direct wave power affected by shadowing and average power of reflected waves, so the model proposed in this paper only takes the above items (1) and (2) into account as the first step in the development of the propagation model.

Generally, signal degradation caused by a single building can be calculated with fairly good accuracy by a knife-edge diffraction model [5]. In our proposed model, we apply this single knife-edge diffraction model to a number of buildings randomly distributed along a road.

The condition of buildings in an urban area is treated statistically as environmental parameters in our model. The parameters consist of the distribution of the number of building stories, building width as a function of building stories, and average number of buildings per km along a road. These parameters incorporated into the

model are easily obtained from a public data base.

The important character of our model is to be able to relate signal diffraction losses in dB caused by buildings with the environmental parameters. By using this model, we can calculate the CDF of signal diffraction losses in urban areas.

Proposed Model and Calculation of CDF

Table 1 shows environmental parameters used in this propagation model. These parameters can be obtained easily from a public data base.

To develop the LMSS propagation model for urban areas, it becomes important to decide how to deal with the conditions of buildings. In our model, we assume that a building of height z [story] has a width W(z)[m], and that the depth is the same as the width.

The PDF of building stories B(z) and the building width W(z) of height z [story] are given in the following equations [3],[4], respectively,:

$$B(z) = \begin{cases} \dfrac{1}{F-G} \exp\left(-\dfrac{z-G}{F-G} \right) & (z \geq G) \\ 0 & (z < G) \end{cases} \qquad (1)$$

$$W(z) = 55\{1.0 - 1.1\exp(-0.1z)\} \quad [m] \qquad (2)$$

where F and G represent an average building height in stories and a minimum building height in stories, respectively.

Figure 1 shows the model of a building used in our propagation model. We assume that an antenna is located at a distance x [m] from the building and that the antenna height is h_a [m]. The antenna receives a satellite signal diffracted by the building edge. Further, we assume that the shadow length L(z) exists at the antenna position x along a road.

At first, we will estimate the diffraction loss at the antenna position x and the shadow length L(z) as in Fig.1.

A diffraction loss caused by a building can be evaluated from a knife-edge model with fairly good accuracy, and a diffraction loss J(v) in dB is calculated by the following equations [5],:

$$J(v) = 6.9 + 20\log\left\{ \sqrt{(v - 0.1)^2 + 1} + v - 0.1 \right\}$$
$$(v > -0.7 \text{ for } J(v) > 0) \quad [dB] \qquad (3)$$

$$v = h\sqrt{\frac{2}{\lambda}\left(\frac{1}{d_1} + \frac{1}{d_2} \right)} \cong h\sqrt{\frac{2}{\lambda d_2}} \qquad (4)$$

$$d_2 = \sqrt{\left(h_s \cdot z - h_a\right)^2 + \left(x \cdot \mathrm{cosec}(\phi)\right)^2} \quad [m] \qquad (5)$$

where:
h = height of the building edge above the straight line joining the antenna position to the satellite [m]
d_1 = distance from the satellite to the building edge [m]
d_2 = distance from the antenna position to the building edge [m]
λ = signal wavelength [m]
h_s = building height per story [m/story]
ϕ = azimuth angle [degree].

The relation between the edge height h and the number of building stories z can be expressed by the following equations,:

$$h = \left\{\left(h_s \cdot z - h_a\right) - x \cdot \mathrm{cosec}(\phi) \cdot \tan(\theta)\right\} \cos(\theta)$$
$$[m] \qquad (6)$$

where:
θ = elevation angle [degree].

As is evident from Eq.(3) and (4), a diffraction loss J is defined as a function of the edge height h. By using Eq.(3)-(6), we can solve the edge height h at which a diffraction loss gives J [dB]. Once we calculate h as a function of J , we can obtain the edge length Le [m] as in Fig.1. At any position on the Le, a diffraction loss is equal to J(h).

To be exact, the edge length Le is not equal to the shadow length L(z) as in Fig.1, but we assume that both lengths are equal in order to simplify the calculation of the CDF of signal diffraction losses. This assumption may result in overestimation of the edge length when the azimuth angle ϕ is near 0° or 180°.

Then the shadow length L(z), in which the diffraction loss due to a building of z [story] is equal to J(h), is given by the following equations,:

$$L(z) = \begin{cases} W(z)\left(1 + \cot(\phi)\right) & [m] & (x \leq H_s) \\ W(z) + \cot(\phi)\left\{(h_s \cdot z - h_a)\cot(\theta)\sin(\phi) - x\right\} \\ & [m] & (H_s \leq x \leq H_e) \\ W(z) & [m] & (H_e \leq x) \end{cases}$$
$$(7)$$

356

where H_s [m] and H_e [m] are the distances between a building and shadow boundaries in a shadow cast by a building as shown in Fig.1.

In Eq.(7), if $H_e \leq x$, the antenna position x is located out of the shadow cast by a building. However, the diffraction losses are caused by the edge at the top of a building, so we assume that L(z) is equal to W(z) in $H_e \leq x$.

From the above discussion, it is evident that to calculate the CDF of signal diffraction losses is equivalent to summing up the shadow length L(z) along a road on which diffraction losses are larger than a given threshold value J_{thr}[dB].

Therefore, the total shadow length T per km on which diffraction losses are larger than J_{thr} can be estimated by integrating L(z) from z_{thr} to infinity as in Eq.(8),:

$$T = \int_{z_{thr}}^{\infty} D \cdot B(z) \cdot L(z) \ dz \qquad [m] \qquad (8)$$

where:

z_{thr} = number of stories of buildings which cause a diffraction loss J_{thr} at an antenna position x [story]

D = average number of buildings per km shown in Table1 [/km]. This is easily obtained from a public data base.

Finally, the CDF of signal diffraction losses J[dB] which are larger than a given threshold value J_{thr}[dB] can be obtained by Eq.(9),:

$$P(J \geq J_{thr}) = 100 \cdot \frac{T}{1000} \qquad [\%]. \qquad (9)$$

Here we summarize the procedure for estimating the CDF of signal diffraction losses.

Step1: Give the diffraction loss (threshold value) J_{thr} in dB.

Step2: Calculate the building height z_{thr} [story] at which the diffraction loss is J_{thr} [dB] (Eq.(3)-(6)).

Step3: Estimate shadow length L [m] as a function of height z [story] (Eq.(7)).

Step4: Estimate the total shadow length T [m] per km over which the diffraction losses are larger than J_{thr} [dB] (Eq.(1), (2), (8)).

Step5: Calculate CDF; $P(J \geq J_{thr})$ [%] (Eq.(9)).

Figure 2 shows one example of the cumulative distribution of signal fading calculated by the model presented here. A person with a handheld L-band terminal for LMSS is assumed to be on a sidewalk in an urban area. The environmental parameters are set at values for a typical urban area in Tokyo, Japan, and h_s is assumed to be 4 [m/story] [4]. Since buildings registered in original public data bases are higher than 4 stories or more (i.e. height $\geq$16m), a minimum number of stories G in Eq.(1) is set at 4 in the calculation. The definition of azimuth angles Az is shown in Fig.3. For example, L90 means 90° to the left of the direction of travel and R90 means 90° to the right of the direction of travel.

COMPARISON BETWEEN CALCULATED VALUES AND MEASURED DATA

An Outline of a Field Experiment

In order to examine the validity of this model, we carried out a field experiment in an urban area. In the experiment, satellite visibility (Line-Of-Sight(LOS) condition) was measured by measuring sky noise temperature T_n [K] with a radiometer as a function of azimuth and elevation angles.

If T_n is higher than a given threshold value T_{thr} [K], we understand that the LOS condition is lost. Since the boundary of the LOS condition gives a signal diffraction loss of 6dB, we compared satellite visibility measured by the radiometer with the percentage of locations where diffraction losses were smaller than 6dB estimated by this model.

The center frequency of the radiometer was 12GHz (bandwidth: 100MHz, time constant: 0.1sec) and a horn antenna (half-power beamwidth: about10°) was used. All experimental equipment was installed aboard a van.

Calibration of the measurement system for the determination of T_{thr} toward the direction of the shadow boundary was carried out at a site where there was only one building. As a result of the

357

measurement, a noise temperature of 176.6K was assigned to T_{thr}.

The experiment was carried out in one of the most built-up areas (Shinjyuku area in Tokyo) in Japan. The values of the environmental parameters are the same as the ones shown in Fig.2 except for x=10m, h_a=3m and R=29.1m.

The van was driven round a course, the length of one circuit being about 6.5 km. The antenna direction relative to the travel direction of the vehicle was maintained constant for the period of each experiment. The definition of azimuth angles Az in this experiment is shown in Fig.3.

Results

Figure 4 shows examples of measured noise temperatures for elevation angles El = 20°, 40° and 60° at Az=R90. Each dashed line means a noise temperature of T_{thr}. From this figure, we can clearly recognize that the visibility depends on elevation angles.

Figure 5 shows a comparison between calculated values expressed as lines and measured data expressed by symbols. For example, the line R90 means calculated values for Az=R90 in Fig.3, and the symbol MR90 means measured data for the same Az. The calculated values represent the percentage of locations where signal diffraction losses are smaller than 6dB estimated by the model presented here. The measured visibility is defined as the percentage ratio of the distance for which $T_n \leq T_{thr}$ to the length of one circuit (6.5 km).

As seen from this figure, the agreement between calculated values and measured data is excellent in predictions for cases having visibilities more than 50%. However, we can recognize some discrepancies between the calculated values and the measured data for cases having a measured visibility smaller than 50%. This discrepancy may be caused because buildings with a height of lower than 4 stories (i.e. height < 16m) are completely omitted in the calculation.

CONCLUSIONS

We proposed a new type of prediction model of signal degradation in LMSS for urban areas. Good agreement was confirmed between satellite visibility estimated by this model and that measured by experiments. Since we use environmental parameters easily obtained from a public data base, this model can be expected to be useful for estimating the feasibility of providing LMSS in urban areas in many countries.

In future, the effects of both direct wave degradation and multipath fading should be related to environmental parameters.

REFERENCES

[1] CCIR, "Factors affecting the choice of antennas for mobile stations of the land mobile-satellite service," *Rep.925-1*, vol.VIII, ITU,1990.
[2] E. Lutz et al.,"The Land Mobile Satellite Communication Channel-Recording, Statistics and Channel Model," *IEEE Trans.Vehicle.Tech.*, vol.40, no.2, pp.375-386, May 1991.
[3] E. Ogawa and A. Satoh, "Path visibility and reflected wave propagation characteristics in built-up areas," *IEICE Trans.* , vol.J69-B, no.9, pp.958-966, September 1986.
[4] Y. Ito, "Propagation characteristics for mobile reception of satellite broadcasting in urban areas," *IEICE Trans.* , vol.J73-B-II, no.7, pp.328-335, July 1990.
[5] CCIR, "Propagation data for land mobile-satellite systems for frequencies above 100MHz," *Rep.1009-1*, vol.V, ITU, 1990 including the contribution document to CCIR WP5B (Dec., 1991) from Japan (Doc. 5B/3-E).

Table 1. Environmental parameters used in the propagation model

parameters	notation	unit
building stories	z	[story]
building height per story	h_S	[m/story]
average number of buildings per km	D	[/km]
PDF of building stories	B(z)	
building width (as a function of z)	W(z)	[m]
average road width	R	[m]
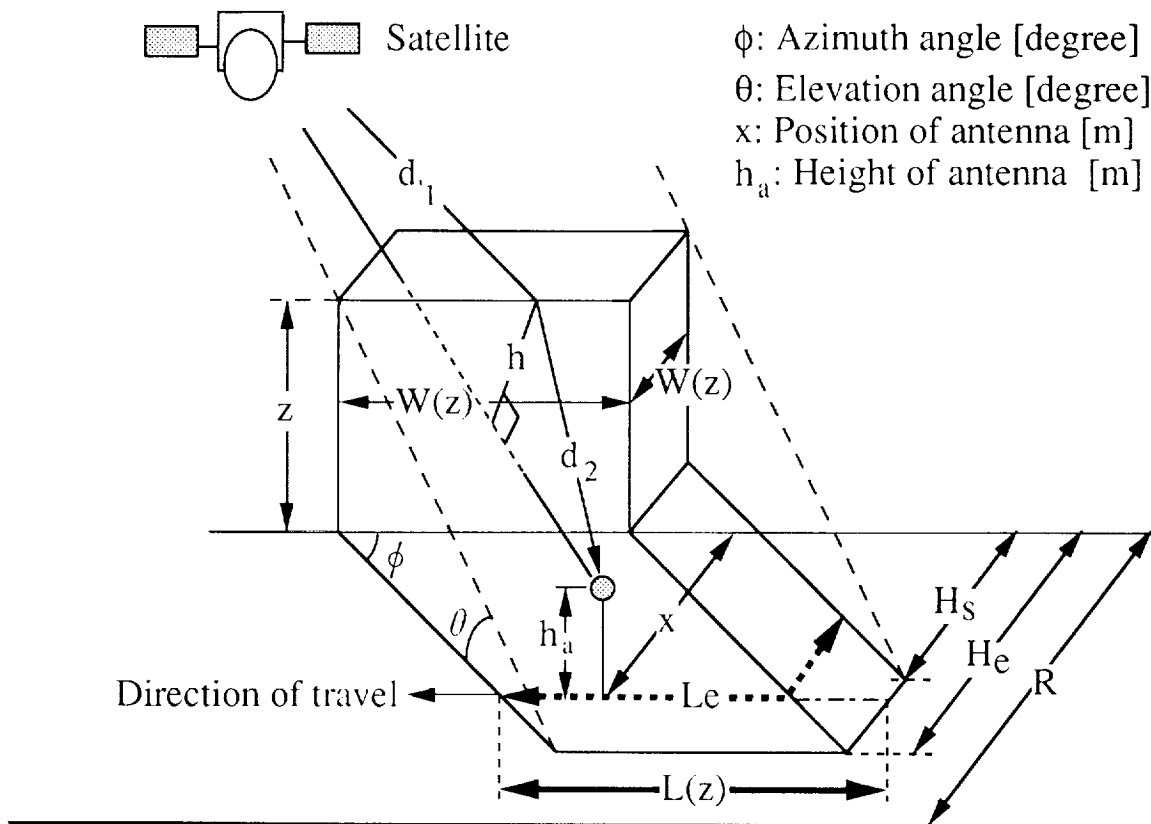
Figure 1. Model of a building for estimating signal diffraction losses.

Az=R90

Figure 2. One example of cumulative distribution of signal fading calculated by the proposed model.
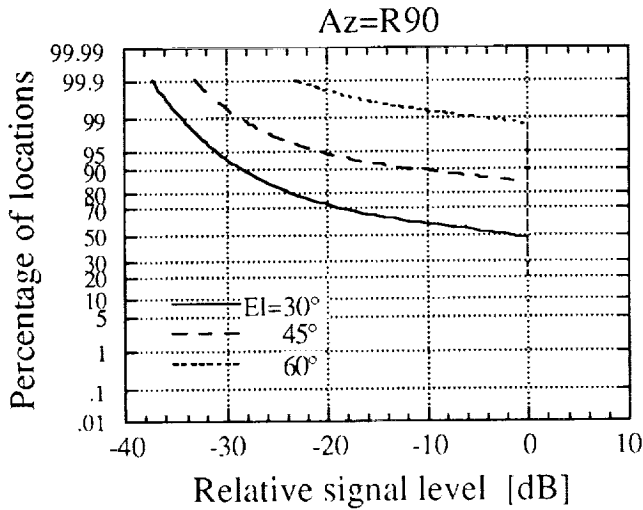
Minimum Stories [story]	: G	= 4.000
Mean Stories [story]	: F	= 5.800
Average Number of Buildings per km [/km]	: D	= 26.460
Azimuth Angle [degree]	: ϕ	= 90
Position of Antenna [m]	: x	= 2.000
Height of Antenna [m]	: h_a	= 1.500
Road Width [m]	: R	= 30.000
Frequency [GHz]		= 1.540
Wave Length [m]	: λ	= 0.195

(a) Elevation angle of 60°

(b) Elevation angle of 40°

(c) Elevation angle of 20°

Figure 4. Examples of measured noise temperatures for three elevation angles (Az=R90). Each dashed line means T_{thr} (176.6K).

Figure 3. Definition of azimuth angles. For example, L90 means 90° to the left of the direction of travel and R90 means to the right of the direction of travel.
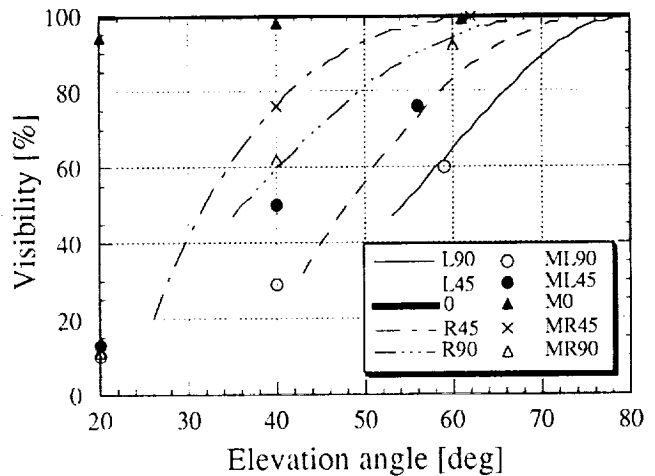
Figure 5. Comparison of visibility between measured values and calculated ones (the percentage of locations where signal diffraction losses are smaller than 6dB).

360

Global Coverage Mobile Satellite Systems: System Availability versus Channel Propagation Impairments

M. Sforza, S. Buonomo, J.P.V.Poiares Baptista

European Space Agency
Keplerlaan 1, 2200 AG Noordwijk, The Netherlands
Phone: +31 1719 83298
Telefax: +31 1719 84999

1   Abstract

Mobile Satellite Systems (MSS) in Highly Elliptical (HEO) and circular Earth orbits at Medium (MEO) and Low (LEO) altitudes have been intensively studied in the last few years as an effective means of providing global communication services. Such global coverage MSS networks are also expected to mitigate typical channel impairments usually encountered in geostationary Land Mobile Satellite (LMS) systems. In the design stages of these satellite networks, information regarding the mobile propagation channel is needed to assess the overall link availability versus elevation angle and environmental scenarios. For multisatellite LMS configurations, the mobile user on the Earth surface sees at any given time more than one satellite of the constellation. In our paper, it is shown that, under certain working assumptions regarding the statistics of the propagation channel, an improvement of the link availability may be achieved through the use of a multisatellite constellation. The analyses have been carried out using the European Space Agency (ESA) LMS propagation data base which presently covers a wide range of elevation angles and environmental scenarios.

2   Introduction

For a geostationary (GEO) LMS system, large implementation margins are usually required to compensate for signal blockage due to man-made or natural obstacles and for multipath effects. Unfortunately a consistent part of the potential users resides in locations around the world (Europe, North America, Commonwealth of Independent States, Australia and Japan) where the elevation angle is almost always below 30-40 degrees; under these conditions, as a satellite is power limited, we must accept a degradation in the quality of the communication link. Alternative satellite constellations in HEO and MEO configurations (MAGSS-14, M-HEO, [1]-[2]) have been recently studied, at the European Space Research and Technology Centre (ESTEC); these systems can provide a very large coverage (global for MAGSS-14), enhanced in the regions between 30° and 60°. An additional feature of MAGSS-14 and M-HEO is the multivisibility, i.e. the intrinsic possibility for the mobile (or hand-held) terminal to have in sight more than one satellite of the constellation; the user equipped with a smart receiver may therefore be able to select the one presenting the best propagation conditions. The number of the satellites simultaneously seen by the receive terminal depends on the location and varies within the day. For each of these satellite-mobile communication links we have different elevation angles and certainly different propagation statistics, these varying in a uniform environment only with the elevation angle. The objective of this paper is to estimate whether, statistically-wise, an improvement of the overall link availability can be achieved with respect to a GEO system. The analysis has been performed making use of a comprehensive propagation data base, owned by ESA. These experimental data and the corresponding empirical model currently cover a wide range of elevation angles and environments. In this paper, we have limited our effort to the analysis of tree-shadowed

environments only.

3 The channel model

Several experimental campaigns have been carried out in the last decade to collect narrowband data for the characterisation of the LMS propagation channel, ([3]). The European Space Agency has embarked in a number of projects to investigate these propagation impairments as a function of frequency (L- and S-bands), elevation angle and environments, ([4]-[6]). Recently ([7]), a modified version of the Empirical Roadside Shadowing model, originally developed by Vogel and Goldhirsh ([3]), has been elaborated and validated with the ESA LMS propagation data base. In our Modified ERS (MERS) model, the range of elevation angles spans from $20°$ to $80°$ and the Percentage of Optical Shadowing (POS) from 35% to 85%; the roadside trees were also of deciduous variety, as in the ERS model. The empirical expression, obtained in two different forms by curve fitting the measured cumulative fade distributions, is given, in dB, by:

$$F(Pr, \theta) = -A(\theta)ln(Pr) + B(\theta) \qquad (1)$$

$$F(Pr, \theta) = \alpha(Pr)\theta^2 + \beta(Pr)\theta + \gamma(Pr) \qquad (2)$$

where Pr is the percentage of the distance (and time, with a vehicle at constant speed) over which the fade is exceeded and θ is the elevation angle. With respect to the ERS model, we have extended and validated the equations (1) and (2) for values of Pr up to 30%. In terms more familiar to system engineers, Pr is an indication of the outage experienced in the channel given a certain fade margin on the link. The parameters A and B, in dB, only depend on the elevation angle:

$$A(\theta) = a_1\theta^2 + a_2\theta + a_3 \qquad (3)$$

with $a_1 = 1.117 \cdot 10^{-4}, a_2 = -0.0701, a_3 = 6.1304$

$$B(\theta) = b_1\theta^2 + b_2\theta + b_3 \qquad (4)$$

with $b_1 = 0.0032, b_2 = -0.6612, b_3 = 37.8581$.

The coefficients α, β and γ in equation (2) depend only on the outage probability Pr; they are reported in Table 1.

Pr (%)	$\alpha(Pr)$	$\beta(Pr)$	$\gamma(Pr)$
1	0.0038	-0.7147	38.7381
5	0.0021	-0.4605	26.4910
10	0.0026	-0.4603	23.1121
15	0.0030	-0.4815	21.4773
20	0.0033	-0.4851	20.0729
30	0.0032	-0.4533	17.4575

Table 1. MERS parameters, as in equation (2).

In Fig. 1, the parametrical curves obtained from the MERS model, equation (1), are plotted with the actual experimental data; the computed rms error is in this case 0.5 dB. For equation (2) the best fit to the experimental data was found to be practically the same. Equation (1) will be used for the computation of Pr for any of the satellites of the constellation visible to the mobile terminal at any given time, within a period of 24 hours.
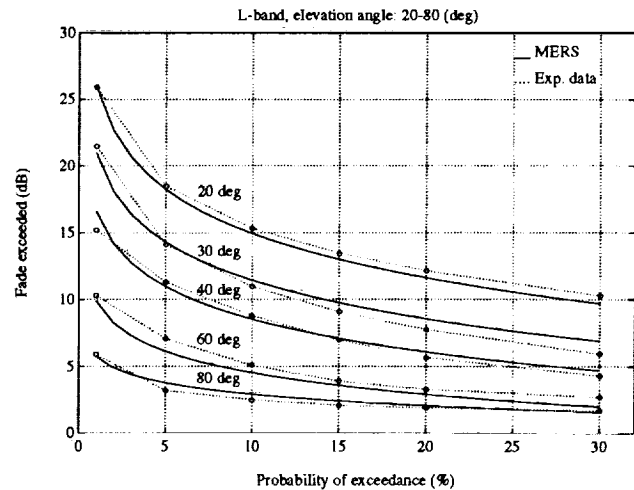
Fig. 1 MERS model vs. experimental data

4 Multivisibility

We will now apply the MERS model presented in the previous section to estimate whether an improvement in the overall link availability can be expected in a multisatellite LMS system with respect to a geostationary one. It has to be stressed that we are not considering here multivisibility as a true diversity scheme; we have limited our work only to optical and geometrical considerations. A true diversity technique would have a strong impact on

the coverage achievable by the multisatellite LMS, on its frequency plan and number of satellites, on the receiver design and so forth. The MAGSS-14 ([1]) mobile satellite constellation is hereafter taken into account; three European locations have been selected to test the applicability of the multivisibility concept, namely Rome, Noordwjik (ESTEC) and Stockholm. The mobile or hand-held terminals are assumed to roam, during the duration of a call (we have not considered for the time-being broadcasting services) in uniform wooded areas in the outskirts of the cities previously mentioned, where the MERS model is expected to be applicable. A short description of the main features of the LMS system under consideration will be now given.

MAGSS-14

Within the framework of its ARCHIMEDES project, ESA is examining the possibility of exploiting the potential advantages of multiregional or global coverage LMS systems for mobile, portable and hand-held terminals. The communication services currently investigated span from voice and data channels (up to 4.8 kbit/s) to high quality broadcasting. The orbital parameters of relevance for our application are reported in the following table. For other details on the MAGSS-14 overall objectives at system level, see references [1].

	MAGSS-14
No. of satellites	14
Orbital period (hours)	6
Apogee altitude (km)	10354
Perigee altitude (km)	10354
Inclination (degrees)	56

Table 2. MAGSS-14 orbital parameters

4.1 Overall link availability

The following assumptions on the channel statistics have been taken into account to estimate the overall link availability in case of multivisibility:

- the MERS channel model, within its range of applicability, is herein considered to compute fade margins and outage probabilities, (eq. 1);

- due to the intrinsic limitations of our empirical channel model, satellites seen from the termi-

nal location at elevation angles below 20° are disregarded;

- satellites at elevation angles higher than 80° present channel statistics identical to those at 80°;

- the wooded environments for the locations under test have all the same general physical characteristics;

- these physical characteristics and the associated channel statistics do not change in azimuth and during the day;

- longitude and latitude of the receive terminal remain constant during the duration of the call (3 minutes, as working assumption).

In figures 2 and 3 we have reported, as an example, the number of visible satellites and the elevation angles of the 14 satellites of the constellation during a 24 hours period at ESTEC, respectively.
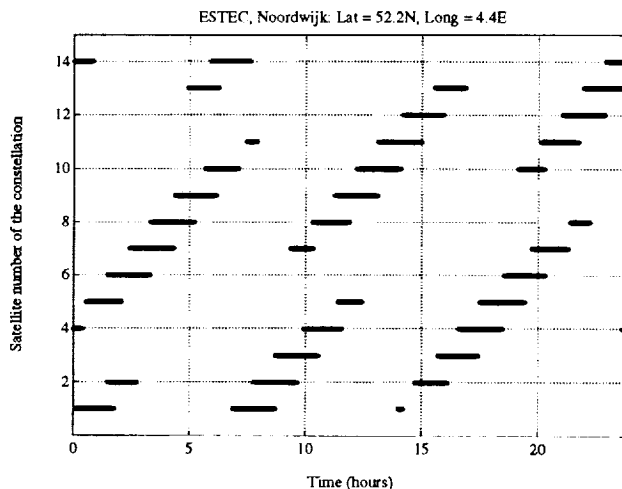
Fig. 2 Visible satellites at ESTEC

A sampling interval of 3 minutes has been used in the simulation. The maximum elevation angle during the day is instead presented in figure 4; it is fairly easy to recognise that the latter is the envelope of the curves in Fig. 3. The computation of the overall link availability in a situation of optical multivisibility requires further assumptions in addition to the ones previously quoted.

363
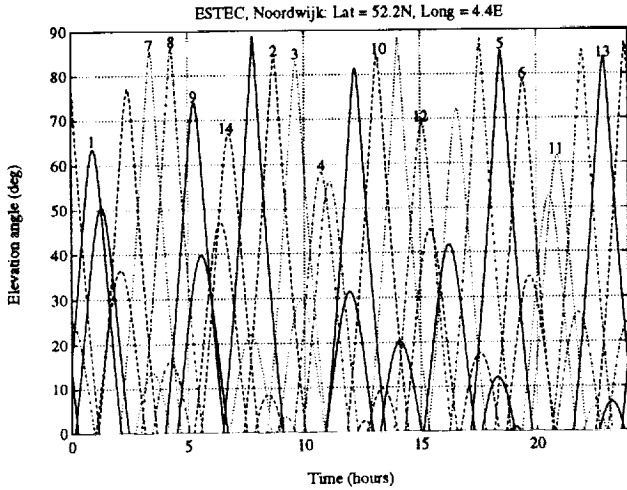
Fig. 3 Elevation angles of the visible satellites
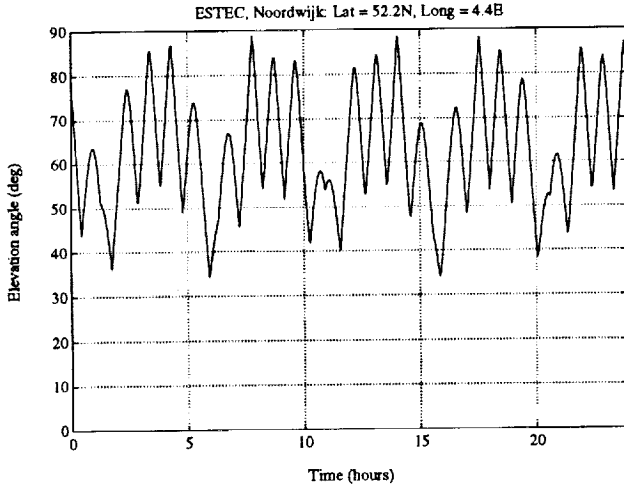
Fig. 4 Maximum elevation angle

With more than one visible satellite to the mobile or hand-held terminal at any given time, we can apply the MERS model to compute, for each of them, the probability of outage Pr, the elevation angle being the only changing parameter. From a probabilistic point of view, we might consider the multivisibility as the combination of events all characterised by the same distribution function. These events are, in the real world, correlated due to the environment surrounding the receive terminal and to the particular satellite constellation. We should therefore consider the joint probabilities to estimate the overall link availability. This implies, for any i-th sampling interval, that the multivisibility event can be characterised as:

$$
\begin{aligned}
S_{multi_i} &= \{S_{1,i}, S_{2,i}, ..., S_{k,i}, ...\} \\
&= \{S_{1,i} \cap S_{2,i} ... \cap S_{k,i} ...\}
\end{aligned}
\quad (5)
$$

where $S_{k,i}$ is the event associated to the k-th satellite visible (k changes with location and time) to the terminal, during the i-th sampling interval. The computation of the probability of the event S_{multi_i} requires, unless additional hypotheses are made, the knowledge of the conditional probabilities $Pr\{S_{1,i} \mid S_{2,i}, ..., S_{k,i}, ...\}$ and so forth. These are usually not available. We have then decided to estimate boundary conditions assuming, on one hand, uncorrelated events and, on the other, totally correlated; in the attempt to obtaining results as close as possible to actual operational situations, we have also calculated intermediate conditions making quite general working assumptions on the diversity philosophy, at system and receiver levels.

Case 1: channels uncorrelated
In practical terms, this means that the presence of vegetation does not play any effective role, probabilistically-wise, on the channel statistics of any visible satellite within a sampling interval. In such a case, we then have:

$$
Pr\{S_{multi_i}\} = \prod_k Pr\{S_{k,i}\}
\quad (6)
$$

This is clearly the best overall propagation channel we can consider in terms of highest link availability.

Case 2: channels totally correlated
However low the occurrence of such situation might be (e.g. a receive terminal completely surrounded by uniform vegetation with two satellites in visibility on the same orbital plane, during the sampling interval) we must consider it to determine the other boundary condition. In this case, the selection of one of the visible satellites during the call is assumed absolutely random:

$$
Pr\{S_{multi_i}\} = \frac{1}{k} \sum_k Pr\{S_{k,i}\}
\quad (7)
$$

Case 3: channels partly correlated
This is certainly a likely situation and the one which has probably a more direct impact in the implementation of a true diversity scheme. We will assume that the mobile or hand-held terminal is equipped with a receiver capable of selecting at call set-up and for its entire duration (3 minutes) the satellite at the highest elevation angle. In a way, we are trying to find a more realistic estimator possibly closer to an actual system implementation.

364

The average availability levels are summarised in Table 2 for the three margin figures considered, i.e. 3, 5 and 7 dB. In Figures 5, the overall link availabilities are reported for ESTEC, assuming a fixed margin of 7 dB; the call set-up is uniformly distributed during the 24 hours period. For the figures given in Table 2, the maximum rms error is 9%; such limited fluctuation of the availability figure around its average value confirms that the assumption of a call set-up randomly distributed in the 24 hours period is reasonable.
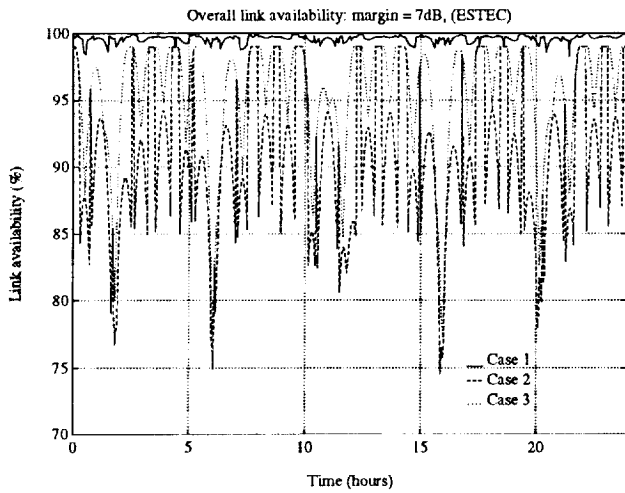
Fig. 5 Link availability for MAGSS-14, ESTEC

	Link availability (%)		
Location	Case 1	Case 2	Case 3
Stockholm, 3 dB	95	79	79
Stockholm, 5 dB	98	88	89
Stockholm, 7 dB	99	90	94
ESTEC, 3 dB	96	81	81
ESTEC, 5 dB	98	89	91
ESTEC, 7 dB	99	91	96
Rome, 3 dB	96	81	81
Rome, 5 dB	98	89	91
Rome, 7 dB	99	91	96

Table 2 Overall link availabilities, MAGSS-14

As expected, the case of channels totally uncorrelated and correlated provide the boundary conditions for the analysis whereas the intermediate situation of partial correlation (Case 3) well represents a possible operational scenario. In many sampling intervals, the latter overlaps with the bottom curve and this happens more frequently with low fade margins; this can be explained considering that in

some cases only two satellites are optically visible to the receive terminal. If for one of them, this depending upon the elevation angle, the available margin is not enough then Case 2 and 3 present the same availability figures. A direct comparison with a geostationary system has been attempted considering the same locations and a satellite at 10E. The results are plotted in the figures 6, 7 and 8.
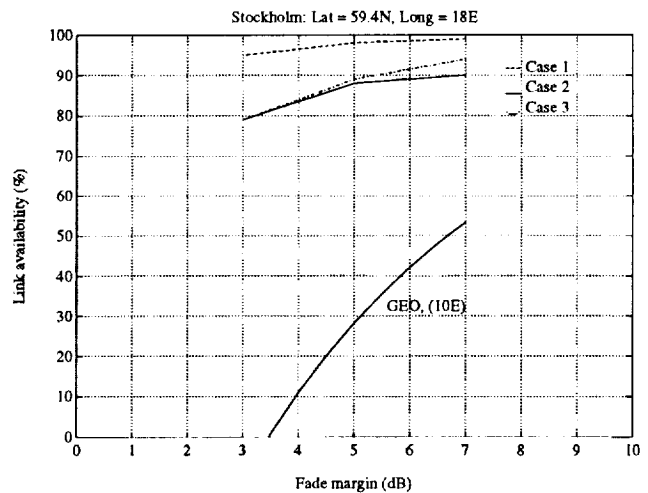
Fig. 6 Link availability (MAGSS-14 vs. GEO)

The results reported in the last three figures must be carefully interpreted. For the locations under investigation given a fixed margin on the satellite-mobile link, a multisatellite LMS system provides in general a much better link availability than a conventional geostationary. This improvement varies with the location considered and the available fade margin; the higher the latitude of the place the hand-held or mobile terminal dwells in, the higher the benefit introduced by a multisatellite constella-
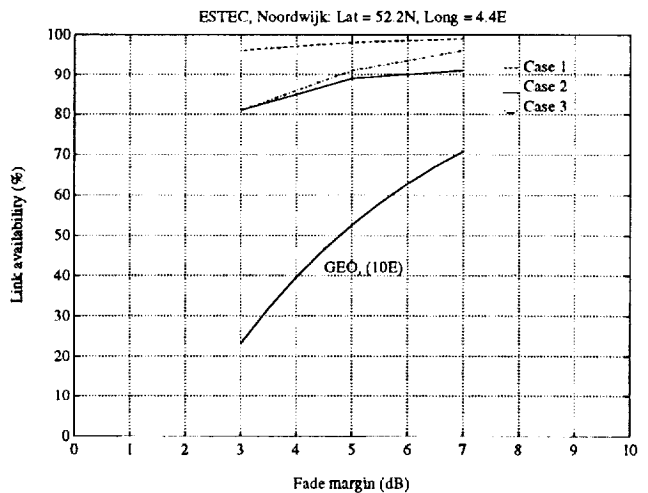
Fig. 7 Link availability (MAGSS-14 vs. GEO)

365
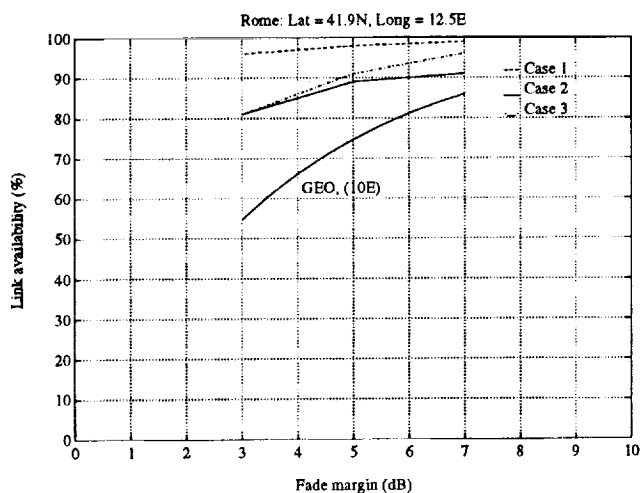
Fig. 8 *Link availability (MAGSS-14 vs. GEO)*

tion (in Stockholm we move from a 53% figure up to a minimum of 90% at 7 dB in multivisibility conditions). On the other hand, the higher the fade margin made available on the link, the lower the gap between multivisibility and geostationary systems.

It is instead debatable whether we can trade-off link availability with maximum allocated fade margin, that is RF power. Unless specific hypotheses on the system frequency plan and on the diversity technique implemented at receiver level are made, multivisibility in general deteriorates the interference environment in that it lowers the average C/M . Under this sort of considerations, we can not straightforwardly conclude from the previous curves that we can save power, having fixed a minimum goal for the link availability.

5   Conclusions

In this paper we have estimated, under certain assumptions on the channel statistics, that a non negligible improvement in the link availability can be expected for a multisatellite LMS constellation with respect to a conventional geostationary system. This improvement depends on the available fade margin and varies with the geographical location. The higher the latitude and the lower the available system fade margin, the higher the benefit coming from the use of a multisatellite constellation. It must be finally reminded that we have only considered geometrical not true multivisibility

hence these results should be interpreted in terms of probabilistic boundary conditions.

Acknowledgements

6   References

[1] J. Benedicto, J. Fortuny, P. Rastrilla, *MAGSS-14. A Medium Altitude Global Mobile Satellite System for Personal Communication at L-band*, ESA Journal, vol. 16, no. 2, pp. 117-133, 1992, The Netherlands.

[2] G. Solari, R. Viola, *M-HEO. The Optimal Satellite System for the Most Highly Populated Regions of the Northern Hemisphere*, ESA Bullettin, no. 70, pp. 81-88, May 1992, The Netherlands.

[3] J. Goldhirsh, W.J. Vogel, *Propagation Effects for Land Mobile Satellite Systems: Overview of Experimental and Modeling Results*, NASA Ref. Publication no. 1274, Febr. 1992.

[4] A. Jongejans et al., *PROSAT. Phase I Report*, ESA STR-216, May 1986.

[5] H. Smith, M. Sforza, B. Arbesser-Rastburg, *Propagation Measurements for Land Mobile Satellite Systems Using Highly Elliptical Orbits*, Proceed. 2nd Conf. on Satellite Comms, pp. 517-520, Liege, Belgium, 22-24 October 1991.

[6] M. Sforza, B. Arbesser-Rastburg, J.P.V. Baptista, *Propagation Aspects for the Planning of Land Mobile Satellite Systems*, Proceed. 14th AIAA Int. Communication Satellite Systems Conf., pp. 1448-1452, Washington, USA, March 22-24, 1992.

[7] M. Sforza. S. Buonomo, *Characterisation of the Propagation Channel for Non-geostationary LMS Systems at L- and S-bands: Narrowband Experimental Data and Channel Modelling*, Proceed. XVII NAPEX Conf., June 14-15 1993, Pasadena, California, USA.

Systems Implications of L-Band Fade Data Statistics for LEO Mobile Systems

Carrie L. Devieux
Motorola Satellite Communications
2501 So. Price Rd
Chandler AZ 85283 USA
Phone: 602-732-3109
Fax: 602-732 3046

Abstract

This paper examines and analyzes research data on the role of foliage attenuation in signal fading between a satellite transmitter and a terrestrial vehicle-mounted receiver. The frequency band of measurement, called L-Band, includes the region 1610.0 to 1626.5 MHz. Data from tests involving various combinations of foliage and vehicle movement conditions clearly show evidence of fast fading (in excess of 0.5 dB per millisecond) and fade depths as great or greater than 16 dB. As a result, the design of communications link power control that provides the level of accuracy necessary for power sensitive systems could be significantly impacted. Specific examples of this include the communications links that employ Code Division Multiple Access (CDMA) as a modulation technique.

INTRODUCTION

The research discussed in this paper focuses on the propagation of L-Band communication signals from satellites to ground-based, mobile receivers. More specifically, the test involved the collection and measurement of RF time-series data. The receiver was mounted on a vehicle traveling through wooded terrain. An aircraft-mounted transmitter provided a signal representative of a Low Earth Orbit (LEO) satellite for a portion of the test, while a geosynchronous satellite was used as a second signal source. Two runs were selected from the collected data as representative of the test results; Run 769: Moderately wooded area (vehicle receiver), simulated LEO satellite transmitter (aircraft). Run 343: Heavily wooded area (vehicle receiver), geostationary satellite transmitter. During run 769, the speed of the test vehicle varied between 10 and 20 miles per hour. In run 343, the test vehicle's speed was held constant at 25 miles per hour. Figures 1 through 5 show run 769 data, and Figures 6 through 10 show run 343 data. Measurements were performed by Dr. W. Vogel of the University of Texas.

Review of Fade Data

The fade data (figures 1, 2, 6, and 7) illustrates a slowly varying mean value of fade and a more rapidly varying deep fade component (10 to 20 dB). The figures also reveal a very fast component, which is generally accepted to be caused by scattering. Some researchers model this as a Rayleigh process whose mean is a Lognormal distribution. Other models have also been developed (references 1, 2 and 3).The timeseries of figures 1, 2, 6, and 7 provide a measure of fade rate (their rise and decay times), which is a function of vehicle speed as well as shadowing. This test measures rates of change that exceeded 0.5 dB per millisecond.

Fade Duration and Level Crossing Rate

Fade duration is the length of time that a received signal is under a specified threshold (i.e., a fade margin value -- relative to unobstructed line-of-sight). Thresholds of 4, 10, and 16 dB have been considered. Level Crossing Rate (LCR) is defined as the rate at which a fading waveform crosses a specified threshold (4, 10, or 16 dB) in one direction. The LCR is calculated as a distribution for the selected thresholds. Fade durations and LCRs are shown in figures 3, 5, 8, and 10, respectively.

CDMA CONSIDERATIONS

Power control is the single most important system requirement for Direct-Sequence Code Division Multiple Access (DS-CDMA). The power of each user accessing a cell must be controlled to ensure that resources are shared equitably among users and that the capacity is maximized (reference 4, page 305). Recent studies (5) indicate that CDMA capacity could be quite sensitive to power control accuracy. In fact, accuracy of 1 dB or better would be needed. System user capacity must be reduced to maintain the voice quality objective, for a given power control accuracy. The reverse link to a satellite receiver suffers a time varying attenuation when the line-of-sight from a mobile user transmitter is shadowed by tree foliage. The same applies in the forward direction (from the satellite to a ground-based mobile receiver). In both cases, the signal's rate of change is primarily related to the speed of the vehicle and the density of foliage. Satellite motion is of less significance. During a shadow period, the signal level reaching a receiver can easily vary 5 to 20 dB, thus decreasing the received $E_b/(N_o+I_o)$ with deleterious effects on voice quality. The following procedure can be used to compensate for shadowing. Transmit power could be adjusted dynamically with a closed-loop power control to compensate more precisely for a time varying fading due to foliage. Considering the up-link, if a user is traveling through a forested area, the received power level would be measured at the ground station gateway. A command signal would be sent to the subscriber unit in order to adjust its power to compensate for the up-link fade. Unfortunately, there is a time delay as a result of the round trip (user-satellite-user). In the case of a LEO satellite at 400 nautical miles altitude, the user-satellite-user delay is about 10 milliseconds for high grazing angles and 30 milliseconds for low grazing angles. The delay with a LEO at 800 nm altitude is 20 to 60 milliseconds. Medium earth orbit satellite (MEO) systems have higher delays (120 milliseconds) but less variation over the field-of-view. During the propagation delay time, the differential between the fade level and the corrective signal can reach several dB (perhaps 5 to 10), rendering power control ineffective. A fade event could even disappear entirely, leading to overcorrection. The above closed loop power control has to be used especially when the downlink frequency is different from the uplink (for example, L-band up/ S-band down) because the fades tend to be uncorrelated. If L-band is used on both the uplink and downlink, time-division duplexing (TDD) has to be used. Measurement of downlink fade can in principle be used to control uplink power. Suppose a fade measurement is made at time (t1). For a typical 60 millisecond TDD frame, the next uplink transmit burst will occur 30 milliseconds later. By that time the fading channel would have changed considerably. In any of these two cases the time delay will cause a power control error of several dB.

TEST RESULTS, RUN 769

Time-series Waveforms and Differential Variation of Fade Depths

Two fade regions were examined to obtain a more complete statistical description of fade variations for the recorded time-series. The first fade region was in the vicinity of the 5.0 dB absolute fade area, and the second was in the 10.0 dB area. The objective was to evaluate fade variation over an interval of (t) milliseconds for each of the regions. In figure 3, the results are presented as the probability that the fade variation over the interval exceeds a specified amount (dB). For example, the fade in the 5.0 dB area during an interval of 32 milliseconds varies by more than 2 dB for 50% of the time. At the 30% probability level, the fade variation is about 3.5 dB.

Fade Duration Statistics and Level Crossing Rates

Figure 4 illustrates the cumulative probability of exceeding a given fade duration. Typical durations of 10 to 30 milliseconds, 50% of the time are observed. This is consistent with deep short duration fades as exhibited by the parent time-series data waveforms. The level crossing rate is the number of times the fade time-series waveform crosses a stated threshold in a positive direction. Figure 5 shows the distribution of level crossings per second. At the 50% point, the LCR is about 2 per second for a 16 dB threshold, 6 per second for a 10 dB threshold, and 4 per second for a 4 dB threshold.

TEST RESULTS RUN 343

Samples of the time-series data for run 343 are illustrated in figures 6, 7. It should be noted that the fade slopes are greater than those of run 769, which is primarily due to the somewhat higher test vehicle speed used in run

343, as well as higher density foliage. Figure 8 shows the statistical fade changes for run 343. The differential fade variation is typically greater than 4.0 dB over a time interval of 32 milliseconds about 50% of the time. Likewise, it is about 8.0 dB for the same time interval, for 10% of the time. Fade duration statistics in figure 9 show durations typically between 5 and 7 milliseconds. Figure 10 illustrates the level crossing rates for run 343. At the 50% point, the LCR is 12 per second for a 16 dB threshold, 16 per second for a 10 dB threshold, and 18 per second for a 4 dB threshold.

CONCLUSIONS

The test results reveal it is highly unlikely that a 1 dB power control accuracy can be maintained when communicating in a tree-shadowed environment even using a closed-loop power control system. The fade situation is nominally severe for heavily wooded areas and degrades further as vehicle speed increases. Tree shadowing produces fast-varying shadowing. Any system design based on a slow-varying shadow model is grossly inadequate in self-interference-limited satellite CDMA systems. Further analysis and simulation is recommended to evaluate CDMA capacity and voice quality over a mobile LEO satellite link.

REFERENCES

1. J. Goldhirsh and W. J. Vogel, "Propagation Effects for Land Mobile Satellite Systems: Overview of Experimental and Modeling Results," NASA/JPL Reference Publication 1274, February 1992.
2. T. Hase, "Fade/Non-Fade Duration of Land Mobile Satellite Communications Link," IEEE GLOBECOM, 1990.
3. W. J. Vogel, J. Goldhirsh, and Y. Hase, "Land-Mobile Satellite Propagation Measurements in Australia using ETS-V and INMARSAT-Pacific," The Johns Hopkins

University/APL Technical Report, SIR89U-037, 1989.

4. K. S. Gilhousen, I. M. Jacobs, R. Padovani, A. J. Viterbi, L. A. Weaver, and C. E. Wheatley III. "On the Capacity of a Cellular CDMA System," IEEE Transactions on Vehicular Technology, May 1991.

5. E. Kudoh, and T. Matsumoto. "Effect of Transmitter Power Control Imperfections on Capacity of DS/CDMA Cellular Mobile Radios," IEEE, International Communications Conference (ICC-92), Chicago, June 1992.
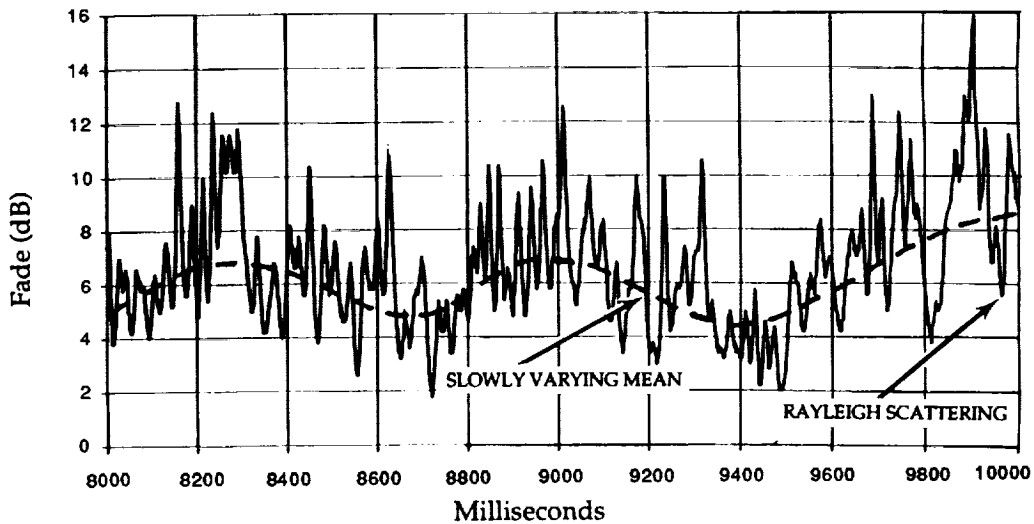
Figure 1. Run 769 Time-Series Waveform 8-10 Sec
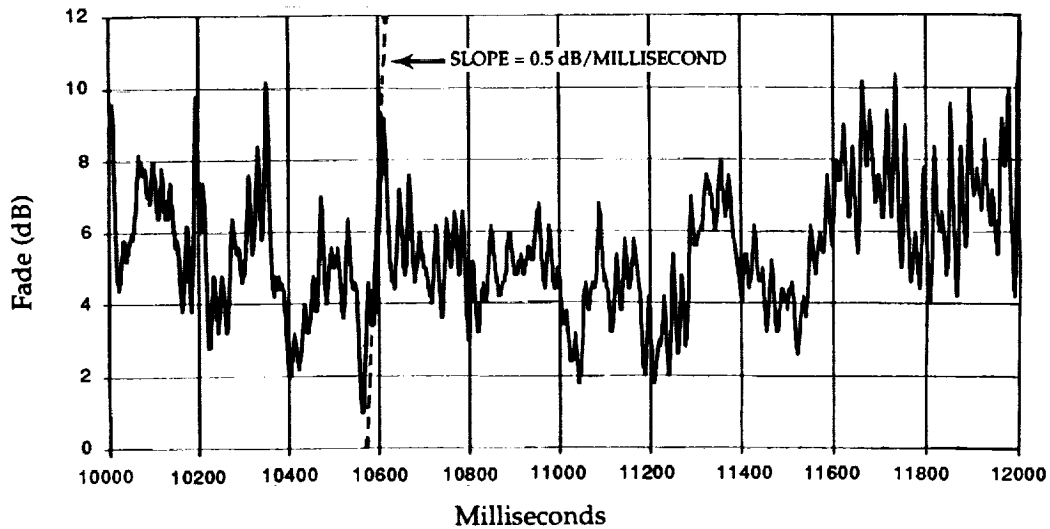
Figure 2. Run 769 Time-Series Waveform 10-12 Sec
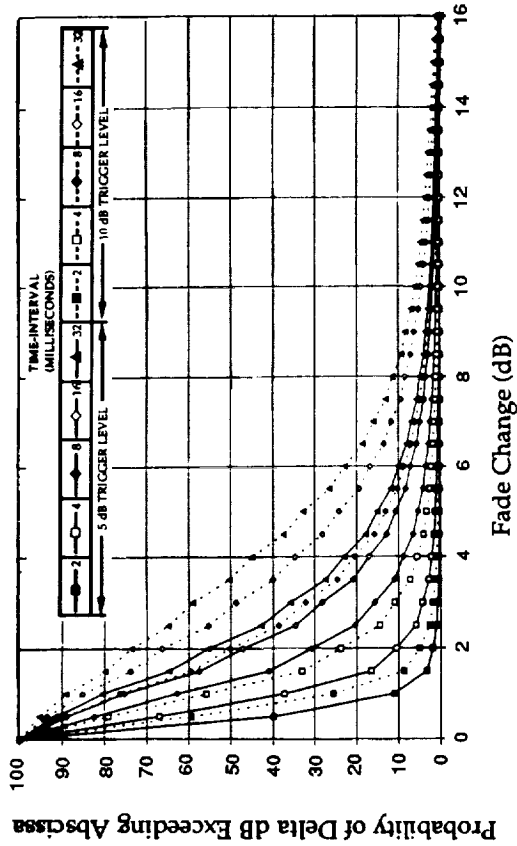
Figure 3. Run 769 Cumulative Probability Distribution of Fade
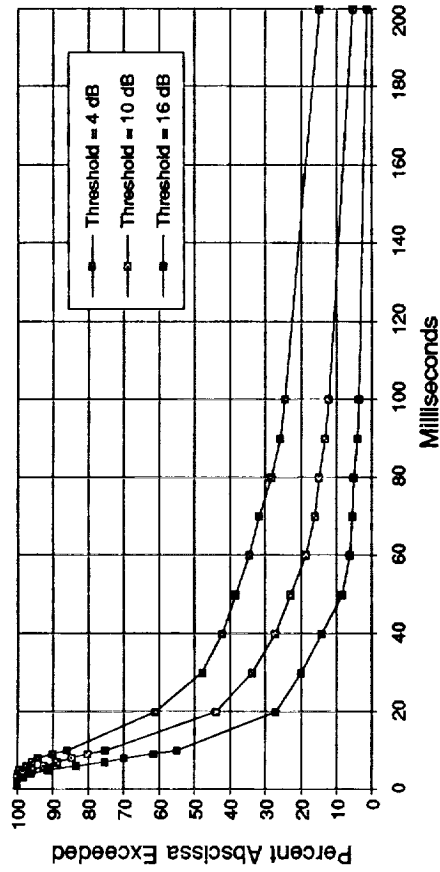
Figure 4. Run 769 Duration Statistics (10-20 MPH)
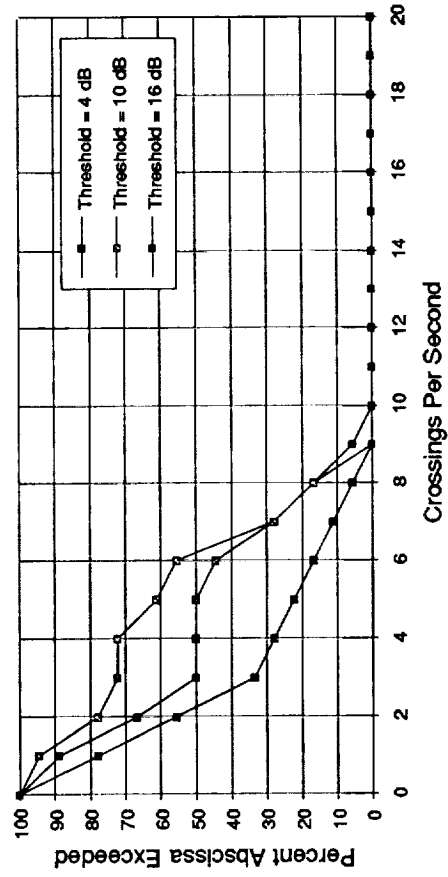
Figure 5. Run 769 Level Crossing Rate
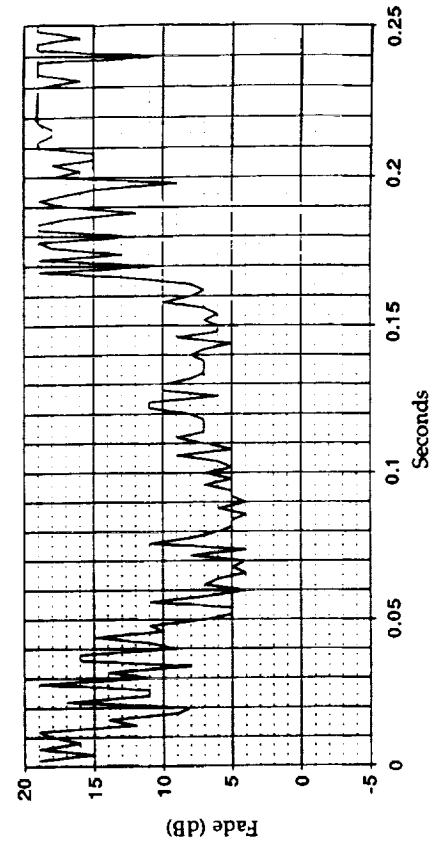
Figure 6. Run 343 Time-Series Waveform 0-25 Sec

371
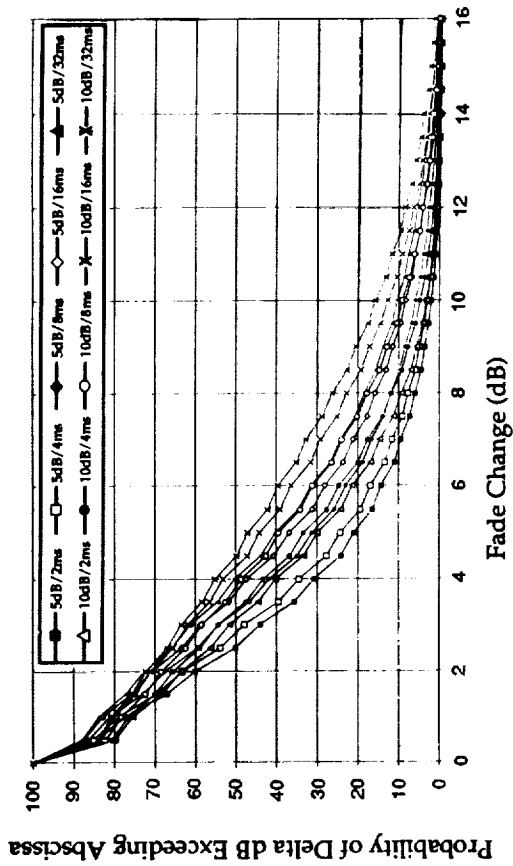
Figure 8. Run 343 Cumulative Probability Distribution of Fade Change

Figure 10. Run 343 Level Crossing Rate
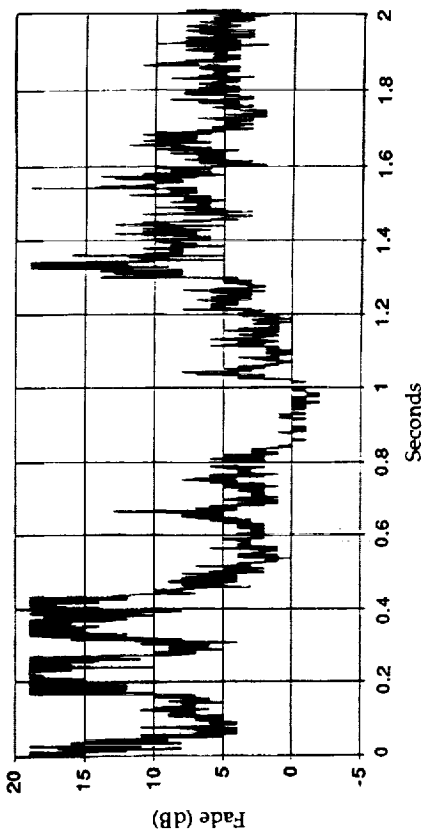
Figure 7. Run 343 Time-Series Waveform 0-2 Sec
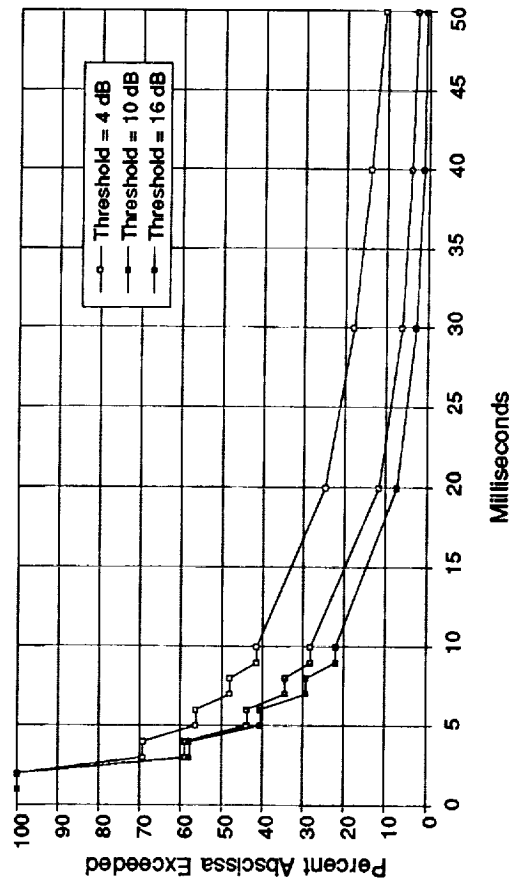
Figure 9. Run 343 Duration Statistics (25 MPH)

Session 9
Mobile Terminal Technology

Session Chair—Russell Fang, COMSAT, U.S.A.
Session Organizer—Martin Agan, Jet Propulsion Laboratory, U.S.A.

(continued)

The Westinghouse Series 1000 Mobile Phone: Technology and Applications

Brian Connelly

Westinghouse Electronic Systems
P.O.Box 746 MS 8419
Baltimore, MD 21203
Phone: 410-765-8814
Fax: 410-765-2386

ABSTRACT

Mobile satellite communications will be popularized by the North American MSAT system. The success of the overall system is dependent upon the quality of the mobile units. Westinghouse is designing our unit, the Series 1000 Mobile Phone, with the user in mind. The architecture and technology aim at providing optimum performance at a low per unit cost. The features and functions of the Series 1000 Mobile Phone have been defined by potential MSAT users. The latter portion of this paper deals with who those users may be.

I. INTRODUCTION

Westinghouse is designing a mobile satellite telephone, the Series 1000, for use with American Mobile Satellite Corporation's and Telesat Mobile Inc.'s mobile satellite (MSAT) service. The phone supports voice with a built in handset, facsimile with a standard telephone port, and data with an RS-232 port.

The Series 1000 Mobile Phone is the first generation of a line of Westinghouse mobile satellite communications products, and will be available in late 1994. Industry has been eagerly anticipating the MSAT system on which it is intended to operate, which is well documented in current literature [1-2].

II. THE WESTINGHOUSE APPROACH

Westinghouse has combined proprietary techniques with advanced technology to create a design that will render outstanding performance at a low per unit cost. Westinghouse is leveraging its capabilities in digital signal processing, microwave design, and software development to assure a mobile phone that is completely compatible with the MSAT ground network.

One of the major design challenges of the Series 1000 Mobile Phone is overcoming the stringent link margin requirements (Table I). The system does enjoy an unusually high satellite EIRP, but the Ricean fading characteristic of satellite channels presents complex design issues. Without a proper design, a prolonged fade can cause the satellite position to be lost, information to be dropped, fax machines to timeout, or the call to be disconnected. As such, the Series 1000 Mobile Phone design must incorporate fade mitigation and compensation techniques. At very low look angles, the problem is made more challenging by an increased number of obstructions. Look angles for a few representative cities are:

Acapulco	69°
Miami	52°
Los Angeles	46°
Chicago	39°
Boston	32°
Vancouver	29°
Quebec	28°
Honolulu	23°
Anchorage	9°

The most common obstruction will be trees. Because

Table I Series 1000 Mobile Phone Characteristics

Transmit Frequency	1626.5 - 1660.5 MHz
Receive Frequency	1525.0 - 1559.0 MHz
Modulation	QPSK
Channel Rate (Inbound)	6750 bps
Channel Rate (Outbound)	6750 bps
Voice Codec Rate	4200 bps
Antenna Polarization	RHCP
Channel Spacing	6.0 KHz
Channel Increments	0.5 KHz
FEC Encoding	
at 2400 bps information rate	Rate 1/2
at 4800 bps information rate	Rate 3/4
in packet-switched mode	Rate 1/3

Link Budget	Uplink	Downlink
Satellite EIRP		30.8 dBW
Satellite G/T	2.7 dB/K	
MP EIRP	12.5 dBW	
MP G/T		-16.0 dB/K
Path Loss	187.2 dB	187.7 dB
Other Losses	3.4 dB	4.8 dB
(C/No)	53.2 dBHz	50.9 dBHz
(C/No) threshold	47.3 dBHz	47.3 dBHz
Link Margin	5.9 dB	3.6 dB
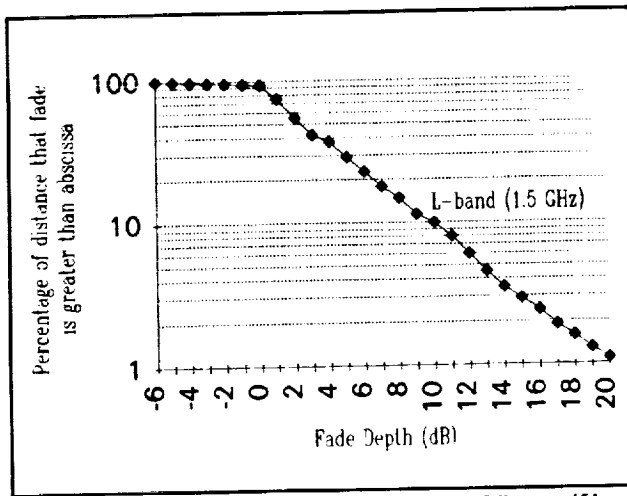
Figure 1 Cumulative fade distributions in heavy foliage at 45°

the Series 1000 Mobile Phone offers interoperability with the existing cellular network, more populous areas with building obstructions will be covered by the cellular system.

L-band propagation statistics have received some attention in recent years [9]. Most notably, the Applied Physics Laboratory of Johns Hopkins University has performed detailed measurements, at the MSAT frequencies, of fade statistics from roadside trees and mountainous terrain. An example of the kind of fade distribution with which the Series 1000 Mobile Phone must contend is shown in Figure 1. This data was collected from the Baltimore-Washington parkway in central Maryland during summer; thus the deciduous trees were in full bloom with maximum moisture. The elevation angle is 45°. The Series 1000 Mobile Phone is designed to handle fade depths of this magnitude.

The duration of the fades is another important statistic when considering the effects of signal propagation.

The major system functions of the Series 1000 Mobile Phone are shown in Figure 2. The configuration will change somewhat depending upon the application, but the basic building blocks remain the same.

Digital Signal Processing

The digital signal processing (DSP) subsystem performs the physical layer protocols of the Series 1000 Mobile Phone. Perhaps the most innovative design area, the DSP subsystem houses the following critical functions:

► Demodulator - Implemented on a single chip, it employs a proprietary optimization method to obtain soft decision bits from a QPSK modulated signal. It also performs carrier acquisition and tracking, symbol timing acquisition and tracking, and signal strength calculations used by the beam steering controller.

► Coding Sequence - This refers to a series of bit-manipulation techniques used for forward error correction and channel encryption. Convolutional encoding and Viterbi decoding are used. The signal is interleaved to prevent bursty errors, and it is scrambled for security.

► Voice Codec - An improved multi-band excitation (IMBE) algorithm developed by DVSI is used. It operates at 6400 bps with an information rate of 4200 bps. As this codec is also being used on the Inmarsat and Optus systems, it is quickly becoming an international defacto standard.
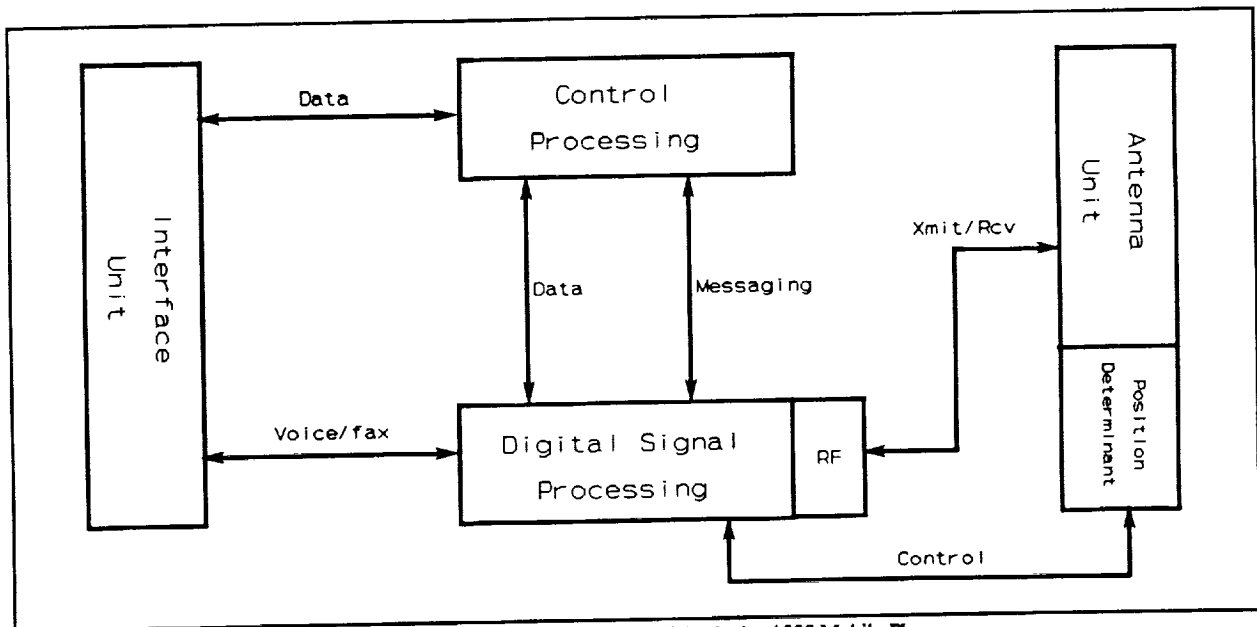
Figure 2 Functional Block Diagram of the Series 1000 Mobile Phone

376

► Noise Cancellation - Many applications, such as use inside trucks or hands-free operation, will require some form of noise cancellation. This is either an analog or digital process in which background noise is cancelled while the user is speaking. Additionally, noise may be suppressed while the user is silent. Noise suppression affords no increase in signal-to-noise ratio, but there is a perceived performance improvement.

► Fax Protocol - The MSAT system is unique in that it uses real time facsimile (fax) transmission over the satellite link with automatic repeat request (ARQ) functionality. The LAP-B ARQ adds the ability for error-free communications over the satellite link. The user may select whether or not they wish to use ARQ, in case they would prefer a shorter phone call with more errors in transmission. Real-time transmission offers some distinct advantages, including billing procedures identical to a regular voice call and confirmation of message delivery.

Control Processing

The control processing (CP) subsystem will perform all the upper layer, byte-level protocol functions. The link layer signalling protocol is used to communicate with the Group Controller (GC) for call management. Another set of protocols is used for network management and signalling. For the data mode, this includes X.25 and several MSAT-specific data communication protocols. Call setup and release protocols define the procedures for establishment and takedown of voice, data, and fax calls.

When the Series 1000 Mobile Phone is not engaged in a call, the CP subsystem will continuously monitor the GC bulletin board channel. This will provide network status information updates, incoming call indications, congestion control parameters, and other control messages. The CP will also respond to GC commands.

The algorithm to detect the crossover of beams is performed in the CP subsystem. Packet error rates are calculated for the beam the Series 1000 Mobile Phone is using and the signalling channels in other beams. Depending on the quality of the channels, the Series 1000 Mobile Phone decides when a switch of beams should occur and notifies the GC appropriately.

Antenna Unit

Several types of antennas are available for use with the Series 1000 Mobile Phone. For land vehicle applications, a phased array will be offered. This antenna is a flat plate about a foot in diameter. The gain of the antenna in the direction of the signal will not

drop below 9 dB. Because the phased array is aesthetically pleasing on smaller vehicles, it is expected to be the most popular antenna type.

The mechanical antenna configuration is less rugged, but in some ways preferred. Acquisition time for this antenna will be slower, about 6 seconds. But the mechanical antenna can dither at small intervals, and thus can maintain extremely accurate satellite tracking when used in conjunction with an angular position determinant.

A third alternative is an omni-directional mast antenna. In order to meet performance specifications the size of the mast needs to be about 3 feet. Nevertheless it will meet the needs of certain niche applications.

The frame formats on the MSAT voice channels call for large periods of time, as long as 0.48 seconds, with no signal being transmitted. For the directional antennas, this makes it extremely difficult to track the satellite based solely on signal strength. In half a second, a vehicle could potentially change its orientation by as much as 25-30 degrees. As such, it is desirable to use an angular position determinant to steer the antenna. Accelerometers and gyros may be used, but they are expensive and not well suited to a rugged environment. A compass or magnetometer would do the job more cost effectively, but they are subject to local magnetic perturbations. An angular rate sensor is another potential solution, with the drawback of long-term drift.

User Interface

The Series 1000 Mobile Phone is capable of more than just simple voice and data satellite transmission. It is also equipped with convenient user features and enhanced functionality.

The Westinghouse Series 1000 Mobile Phone offers complete interoperability with the existing cellular network, including the ability for live call hand-off. Thus, the MSAT system should be understood as complementary to the cellular industry. Cellular interoperability involves complex billing and licensing issues as well as intricate call hand-off procedures. A more thorough examination of this issue is detailed in [3].

Another feature available from Westinghouse Series phones is satellite trunked radio operation. Satellite trunked radio service provides a communication net that allows all suitably equipped mobile phones in a closed user group (CUG) to receive voice transmissions from all other mobile phones in the same CUG, and from the base station. Communications originate from mobile phones on a push-to-talk basis, and are re-transmitted at the base station so that other mobile phones in the net will be able to hear both sides of the conversation. The service is implemented on a single circuit-

377

switch channel shared by the all the CUG members. Satellite trunked radio will be particularly useful for small rural fleets.

For position location, a global positioning system (GPS) option can be added to the Series 1000 Mobile Phone. Position determination is necessary in fleet management, maritime, and aeronautical applications. The position determination system may also be located external to the Series 1000 Mobile Phone, as in the case of a vehicle already equipped with a position determinant.

Table II Features of the Series 1000 Mobile Phone

Alphanumeric Handset Display
PC Connectivity
Programmable from Keypad
Hands-Free Operation
Speed Dialling
Call Waiting
Call Hold
Call Transfer
Call Barring
Conference Calling
Call Forwarding
Voice Mail
Handheld Option
Horn Alert

Other features of the Series 1000 Mobile Phone pattern those already common in cellular and landline operation. The conveniences that the user has become familiar with at home will not have to be compromised with the Series 1000 Mobile Phone. A brief list of some of the important features is shown in Table II.

III. APPLICATIONS

The discriminating factor for the MSAT system lies in the ubiquitous nature of satellite coverage. As such, the MSAT market is concentrated in non-urban areas where cellular coverage is not available. Approximately 15 million people are in these areas, unserved by the cellular network. Satellite extension service will target government and business arenas, as well as the cellular consumer that is frequently moving in and out of coverage.

Seamless Voice

Many businesses require communications across a wide area not completely covered by cellular [5-7]. Building and construction crews, for example, require constant communications with a relatively transient team of people and machinery. These crews move in and out of cellular coverage based on the job, but a single Series 1000 Mobile Phone communications system would always meet their requirements.

Law enforcement and fire-fighting personnel in rural areas would find use for a Series 1000 Mobile Phone, and would have the added benefit of a secure link because of the scrambling inherent in the MSAT system. And when a search-and-rescue operation is required, or for disaster management, they have the advantage of instant connectivity at remote sites. Rescue teams will also be able to make use of the aeronautical capability of the Series 1000 Mobile Phone. Emergency medical personnel are able to obtain remote professional support, report breakdowns, and alert destination hospitals of their status.

Geological surveys are becoming increasingly important, especially if precious natural resources are involved. A satellite mobile system is useful in this scenario for monitoring the survey workers and coordinating supplies and assistance. Mining is another activity that requires coordination of men, materials, and machinery over vast areas. Efficiency and safety in mining and excavation are improved a great deal with constant reporting to a home facility.

The cellular network is growing at an astounding rate. But over long driving distances cellular communications can be sparse and inadequate. The MSAT system will always have a niche market because it offers not only unlimited range, but communication that is reliable and secure, as well as fax and data services.

Transportation and Fleet Management

Perhaps the most significant market demand for MSAT services is that of wide-area trucking. A Series 1000-based fleet management system may be used for:
- real-time schedule and routing updates,
- reporting cargo status for refrigeration units, high-value goods, or toxic materials,
- reporting vehicle performance for maintenance and spares planning,
- locating vehicles in distress,
- monitoring vehicle travel patterns for many vehicles over a large area,
- optimizing pickup strategy in order to maximize load capability and minimize fuel and mileage,
- and allowing two-way communication with drivers.

Larger fleets may wish to adapt their system with a specialized interface unit or software so that drivers would have an automated menu-driven system. If several fleet management centers are involved, the MSAT system may be combined with a VSAT system to yield a single consolidated network [8].

Fleet management, however, is not limited to the trucking industry. Oil companies have the added requirement of marine fleets and on- and off-shore drilling rigs. Also their pipelines, which require remote monitoring and control, are well suited to mobile data transmission.

The existing North American system for railcar location allows updates on a daily basis and is considered by most to be unsatisfactory. Improved terrestrial systems have been proposed, but are costly and inefficient. Satellite mobile services would provide a single system for passenger and freight applications.

Marine

The AMSC/TMI system will operate up to 200 nautical miles (370 km) off coastal waters. Inmarsat, an international mobile satellite system, currently operates in this region but is restricted from operating inland. Inmarsat data shows that 75% of all shipboard communications occur within the 200 nautical mile perimeter. Furthermore, there is significant commercial activity along the major rivers and Great Lakes involving cargo ships, tug boats, and barges.

Ships at sea are usually equipped with sophisticated navigation and position location tools, but shore-based fleet managers are divorced from this information because of inadequate communications links. Two-way communications is preferred in order to send a wide range of data to and from the ships. For example, charts and maps could be updated in real-time, weather and ice reconnaissance information could be relayed, and fishing productivity could be increased through coordinated tracking.

IV. CONCLUSION

The basic design of the Westinghouse Series 1000 Mobile Phone has been explained. The Series 1000 is a sophisticated design which affords a wide variety of interface options including voice, fax, data, GPS, cellular, and satellite trunked radio services. The market demand for this product is high, and several potential market areas have been discussed.

REFERENCES

[1] G. Johanson, N. Davies, W. Tisdale, "Implementation of a System to Provide Mobile Satellite Services in North America," *Third International Mobile Satellite Conference*, Pasadena, CA, June 1993.

[2] G. Davies, W. Garner, et al, "The AMSC/TMI Mobile Satellite Services (MSS) System Ground Segment Architecture," AIAA 14th International Communications Satellite Systems Conference, Washington, D.C., March 1992.

[3] P.W. Baranowsky, "MSAT and Cellular Hybrid Networking," *Third International Mobile Communications Conference*, Pasadena, CA, June 1993.

[4] Wozencraft & Jacobs, *Principles of Communication Engineering*, New York: Wiley, 1965.

[5] J.D. Kiesling, "Land Mobile Satellite Systems," *Proceedings of the IEEE*, Vol 78, No 7, July 1990.

[6] O. Lundberg, "The Future of Mobile Communications," *ITU's Telecom Conference*, Geneva, October 1987.

[7] A. Pedersen, "User Applications of Mobile Satellite Services," *Vehicle and Information Systems Conference*, 1989.

[8] K.M. Murthy and K.G. Gordon, "VSAT Networking Concepts and New Applications Development," *IEEE Communications Magazine*, May 1989.

[9] J. Goldhirsch and W. Vogel, "Mobile Satellite System Fade Statistics for Shadowing and Multipath from Roadside Trees at UHF and L-band," *IEEE Transactions on Antennas and Propagation*, Vol 37, No 4, April 1989.
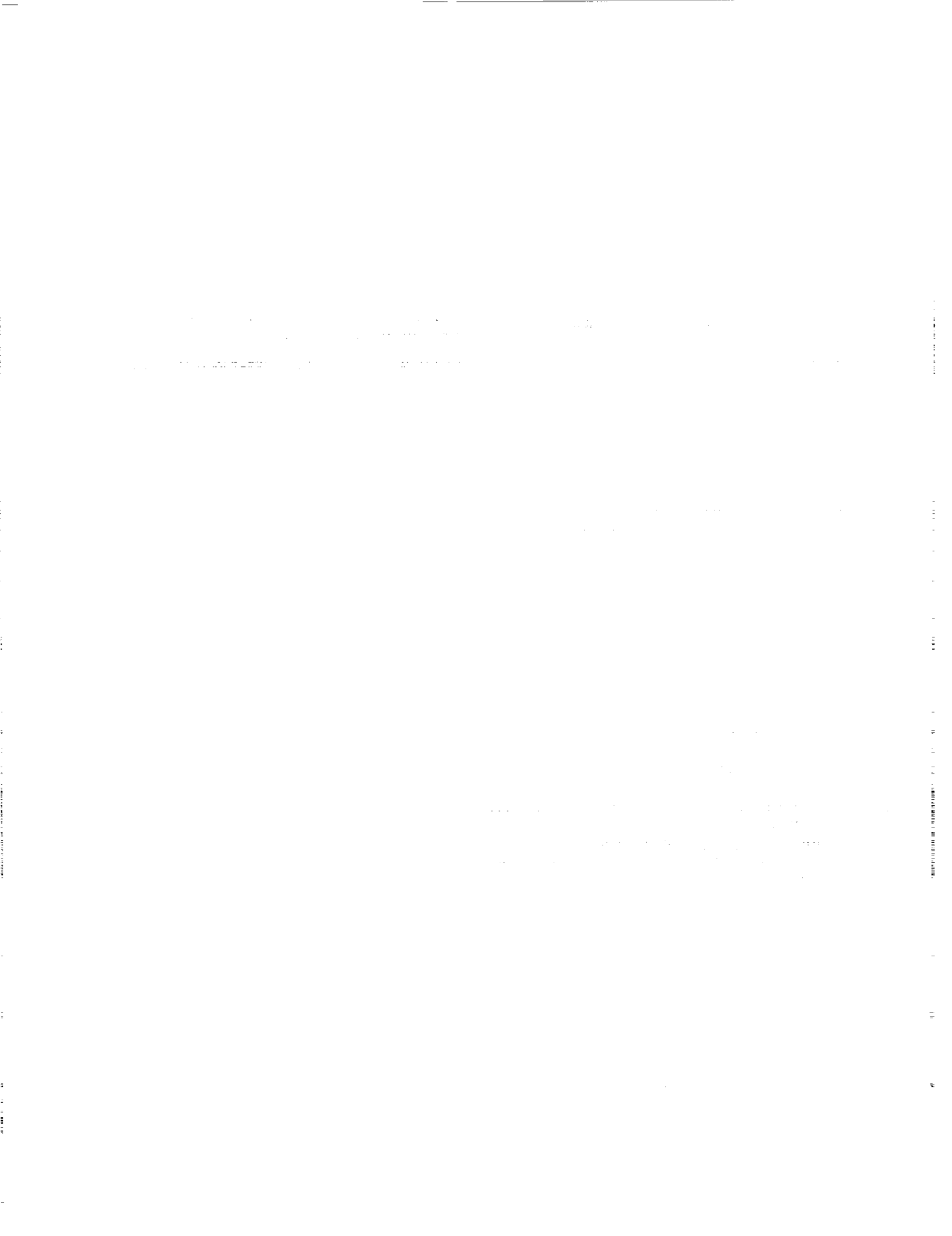
First Satellite Mobile Communication Trials Using BLQS-CDMA

Maria Lua de Mateo*   Simon Johns*

Michel Dothey**   Carl Van Himbeeck**   Ivan Deman**   Bruno Wery**

* European Space Agency
Keplerlaan 1
2200 AG Noordwijk
The Netherlands
Tel.: 31-1719-84582
Fax.: 31-1719-84596

** Sait Systems
Chaussee de Ruisbroek 66
B-1190 Brussels
Belgium
Tel.: 32-2-3705390
Fax.: 32-2-3322890

Abstract

In this paper, technical results obtained in the first MS-BN Land mobile technical trial are reported. *MSB-N* (Mobile Satellite Business Network) is a new programme undertaken by the European Space Agency (*ESA*), to promote mobile satellite communication in Europe, including in particular voice capability. The first phase of the MSBN system implementation plan is an experimental phase. Its purpose is to evaluate through field experiments the performance of the MS-BN system, prior to the finalisation of its specifications. Particularly, the objective is to verify in the field and possibly improve the performance of the novel satellite access technique *BLQS-CDMA* (Band Limited Quasi-Synchronous-Code Division Multiple Access) ([1]), proposed as baseline for the MSBN.

1. INTRODUCTION:

The first series of MSBN Land Mobile trials were successfully conducted in June/July 1992, and followed up by some additional tests in January 1993. The tests were carried out using the Marecs-A satellite, existing infrastructure (ESA Villafranca C-band station) and BLQS-CDMA prototype terminals (one mobile and one fixed), developed within the European Space Agency's Advanced System Technology Programme (ASTP) by SAIT Systems (B).

The objectives of the trial were the testing of the technical performance of the system (with particular reference to the new access scheme BLQS-CDMA described in [1]), and the implementation of user oriented tests and demonstrations.

Overall, this first Land mobile trial has been very successful. It has not only enabled the acquisition of a large amount of important technical information, but it has also raised the confidence of ESA in the general system performance, and proved the viability of the new system in providing good quality communications.

The paper is divided into six sections (this is Section 1):

Section 2 includes a general description of the MSBN system concept ([4]). In Section 3, the main trial objectives are outlined. The overall test set-up is described in Section 4, together with the different facilities/equipment involved in the trial. In Section 5, the technical results are reported, of particular importance is the return link synchronization. Overall conclusions are drawn in Section 6.

2. DEFINITION OF THE MSBN CONCEPT:

The basic MSBN concept represented in Figure 1 shows that a fixed user has direct access to his own mobile fleet through the satellite transponder. The FES (Fixed Earth Station) is a VSAT station which operates in the Ku-band frequencies, and

the MES (Mobile Earth Station) operates in the 1.5/1.6 Ghz frequency band (or L-band).

In the basic scenario, a pair of channels (one Forward Common Channel (FCC), and one Return Common Channel (RCC)) is permanently allocated to each network: a network consists of an FES and a set of MES's organized in a closed user group as a *star network*. The overall system is controlled by a Network Management Station (NMS) which has the capability to transmit and receive in both frequency bands (Ku and L-band).

The access technique is based on Code Division Multiple Access (CDMA). Therefore, several networks operate over the same frequency band (typically 1 Mhz), the various networks using a different set of codes. With the newly developed BLQS-CDMA scheme, both network terminal *synchronization*[1] and carrier frequency control[2] are required for optimum performance ([1]). This reduces intra-system interference (self-noise) with respect to conventional CDMA and simplifies the MES receiver design.
To achieve more easily synchronization, a common clock and frequency reference is broadcast by a master station (the NMS or alternatively one of the FES's) on a dedicated *pilot* signal, produced by direct sequence modulating a precise frequency reference. All signals transmitted by the FES's or MES's are synchronized with respect to this common reference signal.

Bandlimitation is achieved with Nyquist chip pulse shaping with no degradation compared to the unfiltered case.

In practice, BLQS-CDMA possesses all the intrinsic advantages of CDMA, but has an efficiency comparable to orthogonal transmission systems like FDMA and TDMA.

3. TRIAL OBJECTIVES:

As pointed out above, BLQS-CDMA relies on chip clock and carrier frequency synchronization for optimum performance. Chip clock synchronization is straightforward in the forward link (ie from the fixed station (FES) to the mobile one

---

[1] By synchronization event, we mean that all the transmitter code epochs and frequencies are quasi-aligned at the satellite transponder input. The error shall be less than $\pm$ 0.3 chips

[2] within a range of say $\pm 6.10^{-2} R_b$, R_b being the uncoded bit rate.

(MES)) while it is more problematic in the return link (ie from the MES to the FES). Due to this, one of the main objectives of the trial has been the verification of the return link synchronization.

In general, the key objectives of this first trial can be summarized as follows:

1. the verification of the *return link synchronization* algorithms of which two, one called "Dzung algorithm" ([3]) and the other called "Sait algorithm" ([2]), were implemented.

2. the verification of the global system performance in different environments (voice quality of the various vocoders, antenna tracking capability..)

3. the implementation of user oriented tests and demonstrations.

4. TRIAL CONFIGURATION:

4.1. Experiment Scenario:
A block diagram showing the configuration during the experiment is given in Figure 2.

The MSBN system is planned to be operational early 1995 and will use *EMS* (European Mobile Satellite). Due to the unavailability of EMS, the Marecs A-satellite was used instead, although the feeder links are at C-band (instead of Ku-band).

As shown in Figure 1, the following signals were transmitted/received:

- *The C-Band uplink signal*, transmitted from Villafranca (FES) to the MES terminal, was composed of two signals:

  1) *the Spread Spectrum (SS) pilot signal or FRC (Forward Reference Channel)* and,
  2) *the Spread Spectrum (SS) traffic signal or FCC (Forward Common Channel).*

The baseband data entering the FES SS modulator can be selected between the vocoder output (voice mode), or a random data generator (data mode). All the satellite tests were performed in voice mode, as these provided the greatest feedback of system performance.

- *The C-band received signal or RCC (Return Common Channel)*, transmitted from the

MES terminal to Villafranca (FES), consisted of *the MES Spread Spectrum (SS) signal,* which after down conversion was acquired and demodulated via the FES (SS) demodulator. Recovered baseband data was routed to the vocoder (voice mode), since, as already mentioned, all the satellite tests were performed in voice mode.

The maximum signal bandwidth was 1.2 Mhz.

4.2 Description of facilities/equipment involved in the experiment:

4.2.1 The Marecs-A satellite:

The Marecs-A is a geostationary satellite located 22.3 degrees East; its present inclination is $i \approx 5^o$.

In general, the geostationary orbit inaccuracies (ie satellite's inclination) induce a doppler shift on both the carrier and chip frequencies of the MES signal received by the FES. This doppler has to be accounted for within the return link synchronization process.

4.2.2 The Agency's Payload Monitoring Station at Villafranca:

Situated close to Madrid (Spain), this station is the dedicated Marecs-A TT&C and payload-monitoring station. The station is fully equipped for payload testing with sophisticated computer-driven test equipment, 12 m C-Band dish, 4 m L-band dish and L-band standard gain horn for precise EIRP measurements. The main parameters of the C-band facilities are:

- Max C-Band EIRP: <= 80 dBW (6.4 Ghz).

- C-Band G/T: 32.4 dB/K

As shown in Figure 1, the interface between the *fixed terminal (FES)* and the C-Band station in Villafranca (S) was at IF (70 Mhz).

4.2.3 Description of FES & MES equipment:

4.2.3.1 Main characteristics:

The newly developed (MES & FES) prototype terminals include fully digital multirate modems using the BLQS-CDMA access technique. BLQS-CDMA is a direct sequence modulated CDMA (D-S/QPSK) that makes use of quasi-synchronized signature sequences (*preferentially phased Gold codes*[3]) belonging to an almost orthogonal se-

---

[3] Gold codes all having mutual cross-correlation $R_{xy} = -1$ for $\Delta =$ two-sided maximum timing offset $= 0$.

quence set.

The modem flexibility permits operation in several modes, depending on the selected chip rate (from 150 Kchip/s to 1.2 Mchip/s), bit rate (from 2.4 Kbit/s to 19.2 Kbit/s) and, spreading factor (from 31 to 511). Convolutional coding (r=1/2, K=7) may be applied to further enhance the system efficiency.

Both voice and data transfer are possible. Nevertheless, as mentioned above, only the voice mode was tested during the satellite trial. The voice is digitized using the SVQ (Spectral Vector Quantization) voice coding technique. Three different speech coders (operating[1] at 6.4 Kbit/s (Inmarsat-compatible), 3.0 Kbit/s & 1.8 Kbit/s respectively) are implemented.

4.2.3.2 MES equipment in Trial Vehicle:

The mobile set-up can be described as follows: the antenna was mounted on the roof of the trial vehicle (Renault Espace), whilst the HPA/LNA (High power amplifier/Low noise amplifier) module, MES terminal (developed by SAIT and interfacing at IF= 70 Mhz with the HPA/LNA module), and other supporting equipment were installed inside the vehicle and powered by a 12 V battery module.

The antenna used for the trial was a mechanically steerable prototype, developed within the European Space Agency's Advanced System Technology Programme (ASTP). It has a tracking capability and a gain of about 10 dBi. An omnidirectional antenna was also used to perform some tests at the lowest bit rates. Finally, a GPS antenna was mounted on the roof rack of the vehicle to allow GPS data recording during the mobile trials.

All relevant information regarding the state of both the mobile and static terminals could be visualized in real time graphically during the experiment and/or recorded in a capture file on the PC for further post-processing (MMI facility).

5. PRESENTATION OF RESULTS:

5.1 Test routes:

Tests were first carried out *in a fixed set up* between Villafranca and Brussels to ensure the system was functioning correctly; following this, the vehicle was fitted with the mobile terminal and verification of the system was again undertaken. The system was then ready for satellite testing in

---

[1] including error protection.

		Sequence Length (chips/symbol)				
		31	63	127	255	511
Symbol	9.6		X(*)	X(*)		
Rate	4.8	X		X(*)	X(*) (Mode 1)	
(Ksymb	2.4			X	X(*)	X(*)
/s)	1.2					X(*)

Notes:
(1) Mode 1 is the nominal mode.
(2) X indicates the possible modes of operations.
(3) (*) indicates the modes tested during the trial.
(4) During the satellite tests, the highest vocoder rate was always used for any given symbol rate.

Table 1: Modes of Operation.

earnest.
Most of the *mobile tests* were carried out on a section of the Brussels/Paris motorway to the south of Brussels, the surroundings were much the same for the entire length of motorway used. That is to say the sides of the motorway were lined with a mixture of high trees and bushes with the occasional open area while the central reservation was mainly clear of obstructions.

5.2 Modes of Operation:

As already pointed out, different modes of operation are possible, depending on the selected chip rate (from 150 Kchip/s to 1.2 Mchip/s), bit rate (from 2.4 Kbit/s to 19.2 Kbit/s) and, spreading factor (from 31 to 511). Table 1 shows all the possible combinations (indicated by X in Table 1). The majority of tests were carried out using mode 1 (from now on called the "nominal mode"). However to establish correct operation of the other modes, additional tests were also performed (indicated by (*) in Table 1).

5.3 Result Discussions:

For each mode of operation, a set of parameters were recorded at both fixed & mobile sites. Since it is not practical to present all the analyzed results from the trial, only some representative statistics covering the main parameters are presented in this paper. All of them refer to the nominal mode.

5.3.1 Acquisition/Reacquisition times:

During the mobile tests, it was not possible to measure accurately the acquisition/reacquisition times, however they were observed to be very fast and proved to be crucial in maintaining communi-cations in a land mobile environment. Under Lab conditions, acquisiton was typically accomplished in less than 1 sec at Eb/No= 0.5 dB, whilst reacquisition times of less than 0.2 sec were achieved at Eb/No= 2dB and after a coasting time of 1 minute.

Generally, the tracking of the antenna performed extremely well even when the vehicle was turning at 30 deg/s. The angular sensor (added to the antenna during the January 93 tests) helped to a large extent to maintain correct antenna pointing during periods of blockage.

5.3.2 Performance of the RTN Link synchronization:

5.3.2.1 Definition of the RTN Link synchronization concept:

The goal of the RTN Link synchronization is to synchronize the code phase of the Return Common Channel (RCC) with the one of the locally generated reference at the FES (FRC). The RTN Link synchronization is accomplished in two phases: during the *acquisition phase*, both code phase and chip frequency errors are estimated by the FES and transmitted to the MES which adjusts its transmit code phase and chip frequency accordingly. During the *tracking phase*, the FES tracks the return link code phase error by comparing the code phase of the mobile terminal (RCC) with the code phase of the pilot (FRC) and commanding the necessary corrections in the MES. This operation is repeated at regular time intervals (To= 1 second).

Two different tracking algorithms, called "Dzung algorithm" and "Sait algorithm" respectively, were tested during the trial. The "Dzung algorithm" ([3]) can be described as "a phase correction based method", since the corrections sent by the FES to the MES represent code phase correction values. In contrast, the "SAIT algorithm" ([2]) is a "frequency correction based method". The FES compares now the chip frequency of the mobile terminal (MES) with the chip frequency of the pilot and uses the forward link to command the chip frequency corrections within the MES.

Both algorithms were tested during the satellite trials in both static and mobile conditions; all the mobile tests were carried out on the same section of the Brussels/Paris motorway to the south of Brussels, the surroundings were much the same

384

for the entire length of the motorway used. In all cases, speeds of up to 120 Km/h were reached and both hard acceleration and breaking conditions were tested. Each recording session lasted for a duration of 10 minutes. The results are presented below.

5.3.2.2 Results on RTN Link synchronization:

The results on the RTN Link synchronization are shown in Figure 3. Both "Dzung" and "Sait" algorithms show similar performances in a mobile environment: in both cases, the mean of the steady-state code phase error is < 0.02, and the standard deviation is not greater than ± 0.08 chips. Concerning the D-DLL's jitter[5], the values are slightly worse for the "Dzung algorithm" than for the "Sait algorithm"; this difference in performance may be due to the different code phase control procedures (discrete or continuous) each algorithm applies. The "Dzung algorithm" is based on code phase corrections: the D-DLL has to accept every second code phase jumps of $f(t).T_0$, where $f(t)$ is the residual[6] chip frequency deviation (in chips/s), and To (=1 sec) is the time correction interval. The D-DLL reacts to these jumps within a transient time that decreases with the D-DLL bandwidth.

On the contrary, the "Sait algorithm" is a method based on chip frequency corrections; this means that the code phase is updated continuously (ie Rb code phase corrections per second at the MES, where Rb is the bit rate), and the D-DLL smoothly tracks the code phase evolution without any transient.

5.3.3 Subjective voice quality:

The voice quality provided by each of the three vocoders implemented in the terminals (6.4, 3.0 & 1.8 Kbit/s) was evaluated during the trial. For all of them, both continuous transmission and voice activation were tested. The speech quality of the vocoder was, under favourable conditions, felt to be good at 6.4 Kbit/s and 3 Kbit/s, while at 1.8 Kbit/s, the quality degraded somewhat.

A demonstration was organized at ESTEC the last day of the trial, when more than 20 people attended experiencing with satisfaction the new system. People appreciated the fact that the voices

---

[5] Digital Delay Lock Loop of the FES traffic demodulator

[6] ie after the acquisition phase

of individuals could be recognized.

6. CONCLUSIONS:

During this first series of MSBN Land Mobile trials, the use of BLQS-CDMA for mobile applications has been positively demonstrated. The results obtained were very encouraging and will allow further enhancements of the system performance.

Main achievements can be summarized as follows: both 6.4 Kbit/s & 3.0 Kbit/s speech coders provided good voice quality (for the 1.8 Kbit/s, the quality was somewhat degraded), and was found to be insensitive to the vehicle speed. The initial acquisition and reacquisition after blockages was very fast (an estimation of the latter being in the order of those measured under lab conditions). Generally, the tracking of the antenna performed extremely well even when the vehicle was turning at 30 deg/s. The angular sensor (added to the antenna during the January 93 tests) helped to a large extent to maintain correct antenna pointing during periods of blockage. The return link synchronization was tested with a variety of doppler shifts and doppler rates and found to work quite well; in mobile conditions, code phase errors < 0.02 ± 0.08 chips were achieved.

References

[1] R. de Gaudenzi, C. Elia and R. Viola, "Bandlimited Quasi-Synchronous CDMA: A Novel Satellite Access Technique for Mobile and Personal Communication Systems", IEEE Journal on Selected Areas in Communications, vol. 10, n.2, February 92

[2] M. Dothey, C. Van Himbeeck, I. Deman, B. Wery, Final report on "Baseband Processor for Reconfigurable Mobile Terminals", ESTEC contract no. 8909/90/NL/RE.

[3] W.R. Braun, D. Dzung, P. Eglin, G. Mastner, P. Rauber, Final report on "Definition of the Mobile Network Synchronization Experiment", ESTEC Contract No. 8728/90/NL/RE, November 1990.

[4] A. Jongejans et al., "The European Mobile System", also included in the Proceedings of the IMSC'93.
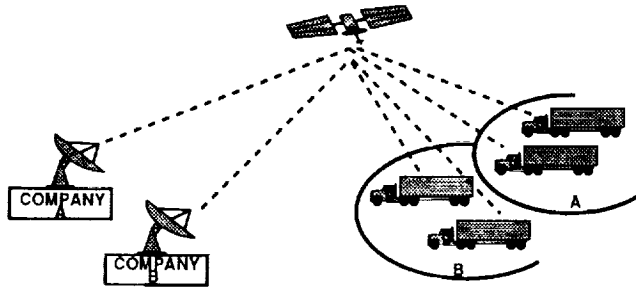
FIGURE 1: MOBILE SATELLITE BUSINESS NETWORK CONCEPT
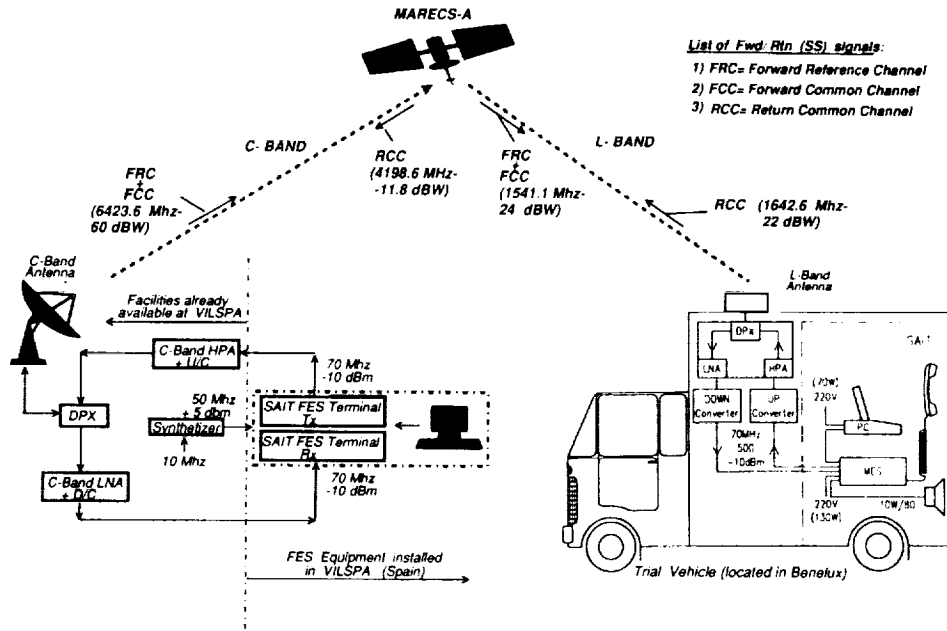
FIGURE 2: EXPERIMENT CONFIGURATION
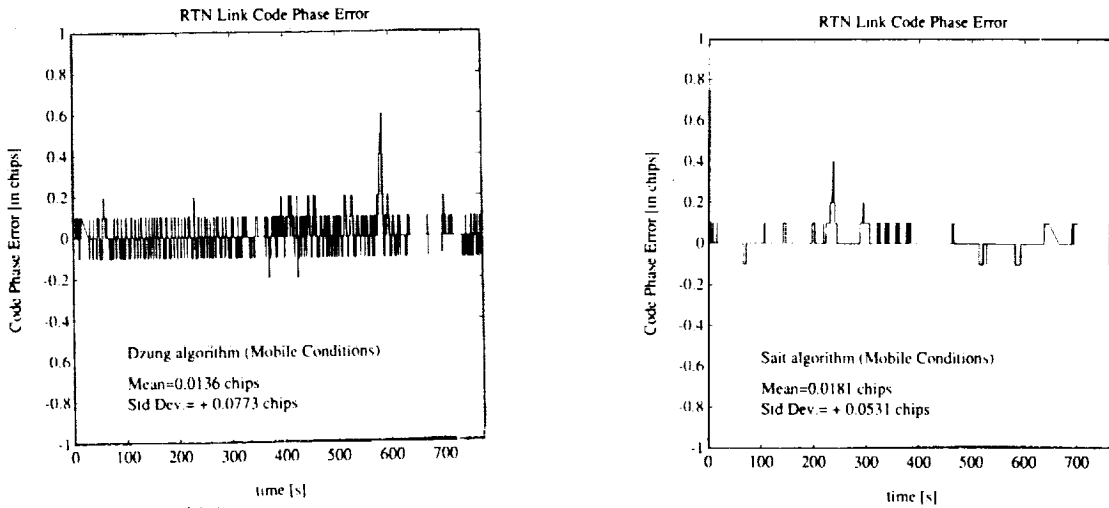
FIGURE 3: RTN LINK CODE PHASE ERROR IN TRACKING MODE.

CHANNEL AND TERMINAL DESCRIPTION OF THE ACTS MOBILE TERMINAL

B.S. Abbe, M.J. Agan, C.C. Girardey*, T.C. Jedrey

Jet Propulsion Laboratory, California Institute of Technology
4800 Oak Grove Drive
Mail Stop 238-420
Pasadena, California 91109
Phone: (818) 354- 3426 FAX: (818) 354-6825

ABSTRACT

The Advanced Communications Technology Satellite (ACTS) Mobile Terminal (AMT) is a proof-of-concept K/Ka-band mobile satellite communications terminal under development by NASA at the Jet Propulsion Laboratory. Currently the AMT is undergoing system integration and test in preparation for a July 1993 ACTS launch and the subsequent commencement of mobile experiments in the fall of 1993. The AMT objectives are presented, followed by a discussion of the AMT communications channel, and mobile terminal design and performance.

AMT OBJECTIVES

The AMT is a part of a larger ACTS program which has as its goal to pave the way for the next generation of communications satellite technology and services. The ACTS program is developing high risk technologies so as to reduce risk and thus stimulate commercial use by U.S. companies. The AMT is a mobile digital communications terminal that is being developed by the Jet Propulsion Laboratory (JPL) for NASA in an effort to advance the technology and system concepts necessary for a commercially viable mobile satellite communications system at K/Ka-band frequencies.

The AMT, as depicted in Figure 1, will demonstrate speech and data transmissions in the Ka-band mobile satellite communications channel. Ka-band is particularly promising for mobile communications because of the large amount of available spectrum and the amenability to small high gain antennas. The AMT is being developed as a mobile satellite communications platform by NASA to aid the development of aeronautical mobile, maritime mobile, land mobile, micro-terminal, and personal communications. Additionally, the AMT will be used to characterize the Ka-band mobile communications channel through a series of propagation experiments.

AMT SYSTEM ARCHITECTURE

The AMT will utilize the geosynchronous ACTS satellite in bent-pipe mode. The key ACTS technologies that the

---

* Visiting member of JPL technical staff from ESA-ESOC

AMT will exploit include high gain spot-beam antennas and a 30 GHz uplink and a 20 GHz downlink. ACTS is scheduled to be launched into geosynchronous equatorial orbit at 100° W in July 1993. It will carry a four year supply of expendables, and has been approved for a two-year experiment cycle starting in September 1993. Funding for two additional years of experiments is pending.

The AMT uses a frequency division multiple access (FDMA) architecture. The fixed station transmits an unmodulated pilot which is used by the mobile terminal for antenna tracking, as a frequency reference for Doppler precompensation and in measuring rain attenuation. The system can run at data rates of 2.4, 4.8, 9.6 and 64 kbps.

AMT COMMUNICATIONS CHANNEL

Rain Attenuation

One of the challenges of operating at 20 and 30 GHz is that these frequencies are susceptible to rain attenuation. In preparation for ACTS launch some propagation experiments at these frequencies have been performed by Virginia Polytechnic Institute and State University (VPI) using the European Space Agency's (ESA) Olympus satellite. The experience gained with Olympus has resulted in a valuable data base of 20/30 GHz propagation data.

VPI built fixed site ground-based terminals to receive the 12, 20 and 30 GHz Olympus beacons. Due to the respective locations of Olympus (19° West) and the ground-based receivers (VA), the beacons were visible at a 14° path elevation angle. VPI conducted measurement campaigns in 1990, 1991, and 1992, and has established statistics on signal attenuation, including rain attenuation. The statistics published to date are for the period January-May 1991 [2]. Yearly statistics are not available yet.

A comparison of the VPI empirical rain attenuation data has been made with the rain attenuation predicted by theory [3]. A statistical rain attenuation model (Manning's model) using the parameters of the Olympus satellite and the Blacksburg ground location was used to generate the theoretical attenuation statistics. The predicted statistics based on Manning's model are for an average year.

Although the comparison of both the predicted and empirical data sets can only be indicative, mainly because the statistics have been established for different lengths of time, the comparison is still a valuable attempt to validate Manning's model with actual data, as it is the only experimental data available to date.

Both sets of data, predicted and empirical data sets, are analyzed in detail in [2] and [3]. The worst month case statistics derived by VPI were obtained for March and May 1991. The data demonstrates that for 94% of a month time (worst month case), the rain attenuation did not exceed 3 dB at 30 GHz and 1dB at 20 GHz. 97% of the time the rain attenuation did not exceed 5 dB at 30 GHz and 2.5 dB at 20 GHz. 98% of the time the rain attenuation did not exceed 8 dB at 30 GHz and 3.6 dB at 20 GHz. These data points indicate how rapidly the attenuation level increases with the link availability. Manning's yearly model predicts attenuations that are lower by 3.5 dB and 1.6 dB respectively, for a link availability of 98%.

The empirical VPI data obtained for the five month period, January-May 1991, which intuitively shows less attenuation than the worst-month data, matches the yearly Manning model better. At lower attenuation levels (less than 5 dB) the empirically derived rain attenuation is more severe than predicted, and at larger attenuation levels, it is less severe.

ACTS is located at 100° West longitude; its ground-based terminals will operate at an elevation angle of at least 30°. Rain attenuation will therefore be less severe than for Olympus, due to the shorter propagation path through the atmosphere. The simulation based on Manning's model has been run for ACTS, at various locations representing the different climates and rain conditions in the US. The data demonstrates that, for a link availability of 98% of an average year, the attenuation will theoretically not exceed 1.2 dB at 30 GHz, and 1 dB at 20 GHz.

Shadowing

A mobile satellite system like the AMT is affected by shadowing and multipath propagation due to roadside obstacles and terrain conditions. The degree of shadowing depends on the intersecting path length with roadside obstacles. Many parameters affect the intersecting path, like path elevation angle, azimuth direction to the satellite, nature and geometry of the obstacle (tree, utility pole), obstacles set back from the road, lane and direction driven, size and type of road driven (rolling/flat, straight/road bends), etc. Also, the antenna pattern, the environment, rural/suburban, the season, and the frequency, affect the degree of shadowing.

No data is currently available on Ka-band shadowing effects. However, research and experiments on shadowing have been conducted at UHF(870 GHz) and L-band (1.5 GHz)[4]. These measurements have been used to quantify the influence of the system variables on the degree of shadowing and to assess the statistics of shadowing as a function of these variables.

Although the measurements have not been carried out at Ka-band, a few important conclusions can be drawn from the L-band data that are of importance for the AMT experiment. The statistics presented here were obtained at L-band, and as such, define the lower shadowing limit at Ka-band.

1) An increase/decrease of 20° in the path elevation angle (40° - 60°), will significantly reduce/increase respectively the degree of shadowing, by 7.5 dB at the 2% link outage probability level [4].

2) Driving on the lane which is the farther away from the roadside obstacle can reduce shadowing significantly. The farther away the vehicle is from the obstacle, the shorter will be the intersecting path with the obstacle, thereby reducing the degree of shadowing. Also, the wider the road is, the larger will be the improvement. The data analyzed here demonstrated at the 1% probability level, a 2.5 dB reduction on a wide road with trees, and a 4 dB reduction on a narrow road with utility poles [3].

3) Fades were calculated up to 10 to 15 dB and 1 to 8 dB at the 1% and 10% probabilities, respectively [4]. These results were obtained with a low-gain antenna system using ETS-V (elevation angle 51°). Fades for the "high gain antenna mode", were calculated up to 25 dB at the 1% probability level.

Doppler, frequency offset, and Doppler rate

A significant impairment to AMT communications is the frequency offset introduced by the various oscillator instabilities throughout the link and the Doppler and Doppler rate introduced by vehicle motion. Typical vehicular induced Doppler frequency offsets and Doppler rates can approach 3 kHz and 370 Hz/sec respectively if they are not compensated for. Oscillator instabilities can raise the total frequency offset to 10 kHz or greater depending on how often the system oscillators are calibrated.

Phase Noise

The phase noise of the AMT communications channel, though not an inherent problem of Ka-band communications, is a serious impairment that the AMT must overcome. The ACTS communication payload, having been designed for high rate transmissions, possesses very low phase noise (-108 dBc/Hz) at frequency offsets of 1 MHz. It has, however, a high phase noise specification closer to the carrier (-52 dBc/Hz at 1 kHz) which is problematic for low bit rate communications like the AMT. The AMT modulation scheme must be designed such to minimize the degradation due to this phase noise.

AMT DESIGN AND PERFORMANCE

A block diagram of the AMT is presented in Figure 2. Descriptions of each of the subsystems follow. A key feature of the AMT that is interwoven among several of the subsystems is the rain compensation algorithm (RCA) [6]. The basic premise of the RCA is that by lowering the data rate from 9.6 kbps to 4.8 or 2.4 kbps in the advent of a rain event, the link margin can be increased by approximately 3 dB and 6 dB, respectively. The RCA is a novel algorithm by which the AMT is able to dynamically adjust the data rate to help mitigate the effects of rain attenuation. The RCA utilizes pilot power measurements at the mobile terminal and satellite beacon power measurements at the fixed terminal to determine rain attenuation. The rain attenuation information is communicated to both terminals through the AMT communications protocol [7] and a conflict free decision as to whether the data rate should be lowered or raised is made.

The link budgets for both the forward and return links are presented in Table 1, and include actual measured subsystem performance to the extent possible. A photograph of the mobile terminal is shown in Figure 3.

Speech Codec

The speech codec converts input analog speech signals to a compressed digital representation at data rates of 2.4, 4.8 and 9.6 kbps, with monotonically improving voice quality. The 2.4 kbps compression algorithm is the government standard LPC-10, the 4.8 kbps algorithm is the proposed CELP government standard, and at 9.6 kbps an MRELP algorithm is adopted. Data rate switches are performed upon command from the TC based on RCA information or upon user command. Data rate switching is performed with no user intervention and "on-the-fly" to have minimal impact on the continuity of the link. Finally, the codec is capable of interfacing to the Public Switched Telephone Network (PSTN). For example, the user at the mobile terminal can place a call to a telephone anywhere in CONUS.

Terminal Controller

The terminal controller is the brain of the terminal. It contains the algorithms that translate the communications protocol into the operational procedures and interfaces among the terminal subsystems. For example, it executes the timing and handshake procedures for the interaction among the speech coder, modem, user interface, and any external device (data source or sink) during link setup, relinquishment, or data rate change. The TC also contains the RCA routines and is responsible for executing them. The TC also has control over the operation of the IF and RF electronics and maintains high-level control over the antenna platform. The TC in addition is responsible for providing the user with a system monitoring capability and supports an interface to the data acquisition system

(DAS). Finally, the TC will support the test functions required during experimentation, such as bit stream generation, correlation and bit error counting.

Modem

The baseline AMT modem will implement a simple but robust DPSK scheme with rate 1/2 convolutional coding and interleaving. The driver here is to minimize the impact of the phase noise of ACTS on the performance of the modulation scheme . The performance of the modem at a data rate of 9.6 kbps is a bit error rate (BER) of 10^{-3} at an E_b/N_o of 6.6 dB in AWGN with frequency offsets and including modem implementation losses. The modem has been designed to handle frequency offsets of +/- 10.0 kHz without additional degradation. Simulations have determined that up to 1.0 dB of degradation due to ACTS phase noise could be experienced. Alternate pseudo-coherent BPSK modulation schemes wherein link synchronization information is imbedded into the data channel were explored for possible Eb/No performance gains, but the performance was found to be seriously degraded in the presence of phase noise. In addition to the 2.4, 4.8 and 9.6 kbps rates the modem will be designed to handle up to 64 kbps for the demonstration of high quality digital audio and slow scan compressed video on the forward link. Essential to the modem design is a built-in robustness to deep, short-term shadowing. The modem will "free-wheel", i.e., not lose synchronization through a signal outage caused by road-side trees and will reacquire the data rapidly after such a drop-out.

IF Converter

The IF up/down converter translates between 3.373 and a lower 70 MHz IF at the output/input of the modem. A key function of the IF converter is pilot tracking and Doppler pre-compensation. The down-converted pilot is tracked in a phase-locked loop and used as a frequency reference in the mobile terminal. The tracked pilot is also processed in analog hardware and mixed with the up-converted data signal from the modem to pre-shift it to offset the Doppler on the return link. The IF converter provides the TC and antenna subsystem with pilot signal strength for RCA and antenna pointing operation respectively. Finally the pilot in-phase and quadrature components are provided to the DAS for link characterization.

RF Converter

Preceding (or following) the antenna the RF up (down) converter will convert an IF around 3.373 GHz to (from) 30 (20) GHz for transmit (receive) purposes. The choice of the 3.373 GHz IF band is dictated by compatibility with the fixed station RF hardware to be used at NASA LeRC during demonstration. For the passive reflector antenna, the RF up-converter will also provide the antenna with sufficient power on the transmit signal through the use of a TWTA.

389

Antennas

The vehicle antenna is a critical Ka-band technology item in the AMT. Two types of antennas are being developed. The first is a "passive" elliptical reflector-type antenna to be used in conjunction with a separate TWTA or a solid state power amplifier (SSPA), and the second is an "active" array antenna with MMIC HPA's and LNA's integrated onto the array. Both antennas have their distinct advantages. The reflector is simpler and less risky and when a transmit power of 1.5 W or less is required does not need the somewhat bulky TWTA. For higher data rate applications when a higher transmit power is required the reflector can be used with the TWTA. The active array, despite being more complex and risky to develop, exploits MMIC technology to overcome some of the losses in the Ka-band hardware. The integration of the amplifiers also leads to a smaller more conformal antenna assembly. The antenna will have a minimum EIRP of 22 dBW, G/T of -8 dB/K, and bandwidth of 300 MHz. Testing of the reflector antenna has found the actual minimum G/T to be -6 dB/K. The reflector will reside inside an ellipsoidal water-repelling radome of outside diameter 9" (at the base) and maximum height 3.5".

The antenna pointing system enables the antenna to track the satellite for all practical vehicle maneuvers. Either of the two antennas will be mated to a simple yet robust mechanical steering system. A scheme wherein the antenna will be smoothly dithered about its boresight by about a degree at a rate of 2 Hz will be used. The pilot signal strength measured through this dithering process will be used to compliment the inertial information derived from a simple turn rate sensor. The combination will maintain the antenna aimed at the satellite even if the satellite is shadowed for up to ten seconds. This mechanical pointing scheme is one of the benefits of migration to Ka-band. The considerably smaller mass and higher gain achievable relative to L-band make the mechanical dithering scheme feasible and obviate the need for additional RF components to support electronic pointing. The necessary processing will reside in the antenna controller.

Data Acquisition System

The DAS performs continuous measurement and recording of a wide array of propagation, communication link, and terminal parameters (e.g., pilot and data signal conditions, noise levels, antenna direction, vehicle velocity and heading, etc.). The DAS also provides real-time displays of these parameters to aid the experimenters in the field.

CONCLUSIONS

The ACTS mobile terminal is a proof-of-concept K/Ka-band mobile satellite communications terminal that has been developed by JPL for NASA. The terminal has been designed and the technology developed to explore the potential of a future commercial satellite system at these frequencies. They key technical challenges are to: 1) develop tracking, high-gain vehicular antennas, 2) design power efficient communications schemes, 3) compensate for high rain attenuation, 4) overcome high Doppler shifts and frequency uncertainties.

The AMT is currently undergoing system integration and test in preparation for a two year experimentation period starting in September 1993. U.S. industry has expressed significant interest in experimenting with the AMT as evidenced by the many planned experiments which are detailed in [8]. In addition a smaller derivative system is planned for broadband aeronautical experiments [9]. The goal of stimulating commercial use of K/Ka-band for mobile satellite communications is being achieved and hopefully the end result will be a commercial satellite system at these frequencies.

REFERENCES

[1] "ACTS Mobile Terminal Modem Functional Requirements Document", Document AMT-017, Rev 1.0, internal JPL document, November 20, 1991.

[2] VIRGINIA POLYTECHNIC INSTITUTE AND STATE UNIVERSITY, Bradley Department of Electrical Engineering, Blacksburg, Virginia 24061, "Communications and Propagation Experiments Using The Olympus Spacecraft - Analysis of Olympus Propagation Data for the Period January to May 1991", November 1992.

[3] C. Girardey, "The AMT Communication Channel", internal JPL document, AMT No. 48, 1993.

[4] J. Goldhirsh and W. J. Vogel, "Propagation Effects for Land Mobile Satellite Systems: Overview of Experimental and Modeling Results", NASA Reference Publication 1274, February 1992.

[5] Khaled Dessouky and Thomas Jedrey, JPL, "The ACTS Mobile Terminal", Proceedings 14th AIAA Conference, March 22-26, 1992, Washington, DC.

[6] E. H. Satorius, "Rain Compensation Algorithm for the ACTS Mobile Terminal System", JPL IOM no. AMT:331.5-92-094, internal document, Sept. 15, 1992.

[7] N. Lay and K Dessouky, "A Communication Protocol for Mobile Satellite Systems Affected by Rain Attenuation", IEEE J. Selected Areas in Commun., vol. 10, no. 6, August 1992.

[8] B. Abbe, et al., "AMTS/AMT Experiments", IMSC 1993.

[9] B. Abbe, et al., "ACTS Broadband Aeronautical Experiment", ACTS Conference 1992.
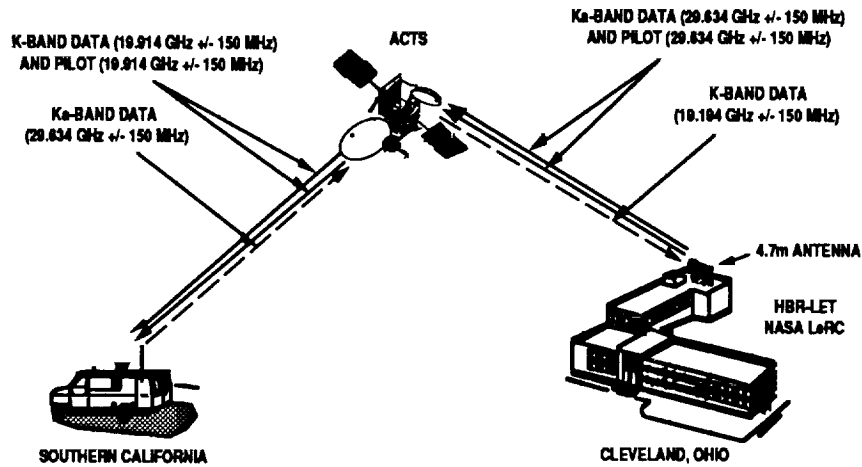
Figure 1 The AMT Experimental Setup
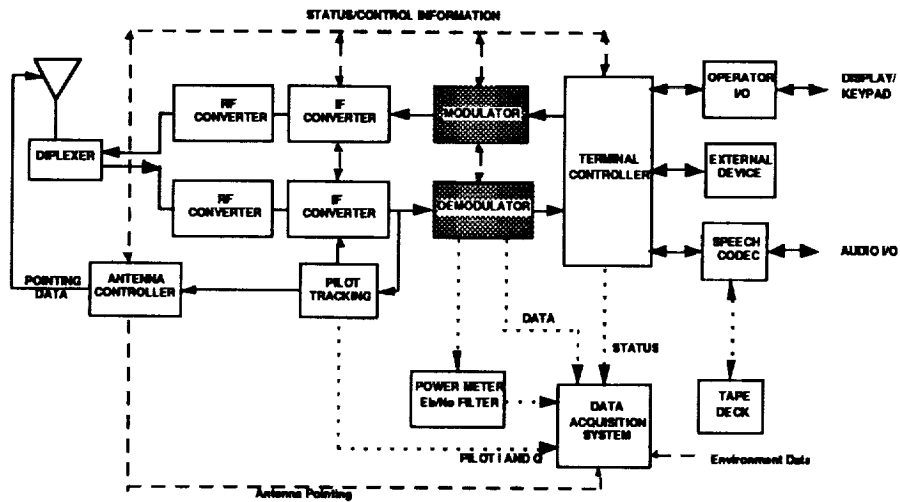
Figure 2 Block Diagram of the ACTS Mobile Terminal
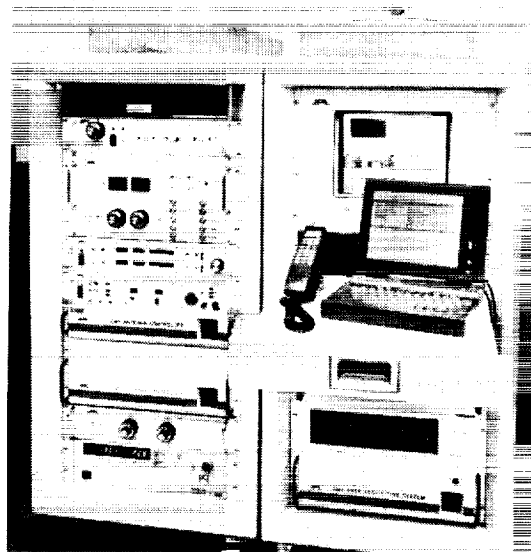
Figure 3 ACTS Mobile Terminal Photograph (Mobile Terminal)

Table 1 AMT Link Budgets

RETURN (AMT-TO-ACTS-TO-HUB) LINK BUDGET

UPLINK: AMT-TO-ACTS

TRANSMITTER PARAMETERS	
EIRP, DBW (NOMINAL)	22.00
POINTING LOSS, DB	-0.50
RADOME LOSS, DB	-0.40
PATH PARAMETERS	
SPACE LOSS, DB	-213.34
(FREQ., GHZ/MHZ	29.63
RANGE, KM)	37408.00
ATMOSPHERIC ATTN, DB	-0.44
RECEIVER PARAMETERS	
POLARIZATION LOSS, DB	-0.50
G/T, DB/K	19.56
POINTING LOSS, DB	-0.32
BANDWIDTH, MHZ	900.00
RECV'D C/N0, DB.HZ	54.66
TRANSPONDER SNR IN, DB	-34.88
LIM. SUPPRESSION	-1.05
TRANSPONDER SNR IN, DB	-35.93

DOWNLINK: ACTS-TO- HUB

TRANSMITTER PARAMETERS	
EIRP, DBW	30.06
POINTING LOSS, DB	-0.22
PATH PARAMETERS	
SPACE LOSS, DB	-210.03
(FREQ., GHZ/MHZ	19.91
RANGE, KM)	38000.00
ATMOSPHERIC ATTN, DB	-0.50
RECEIVER PARAMETERS	
POLARIZATION LOSS, DB	-0.13
ANT. DIRECTIVITY (MIN.), DBI	
SYSTEM TEMP., K	
G/T, DB/K	27.00
POINTING LOSS, DB	-0.50
DOWNLINK C/N0, DB.HZ	74.78
OVERALL C/N0, DB.HZ	53.58
REQ'D EB/N0 (AWGN--SIMULATION), DB	6.00
MODEM IMPLEMENT. LOSS, DB	0.60
REQUIRED EB/N0, DB	6.60
LOSS DUE TO ACTS PHASE NOISE, DB	1.00
FADE ALLOWANCE (OVERALL), DB	3.00
DATA RATE, BPS	9600.00
REQ'D EFFECTIVE C/N0, DB.HZ	50.42
HARDWARE PERFORMANCE MARGIN, DB	3.16

FORWARD (HUB-TO-ACTS-TO-AMT) LINK BUDGET

UPLINK: HUB-TO-ACTS

TRANSMITTER PARAMETERS	
EIRP, DBW	37.00
POINTING LOSS, DB	-0.80
PATH PARAMETERS	
SPACE LOSS, DB	-213.48
(FREQ., GHZ/MHZ	29.63
RANGE, KM)	38000.00
ATMOSPHERIC ATTN, DB	-0.36
RECEIVER PARAMETERS	
POLARIZATION LOSS, DB	-0.13
G/T, DB/K	21.25
POINTING LOSS, DB	-0.22
BANDWIDTH, MHZ	900.00
RECV'D C/N0, DB.HZ	71.86
TRANSPONDER SNR IN, DB	-17.68
EFF. LIM. SUPPRESSION, DB	-1.00
HARD LIM. EFF. SNR OUT, DB	-18.68

DOWNLINK: ACTS-TO-AMT

TRANSMITTER PARAMETERS	
EIRP, DBW	45.04
POINTING LOSS, DB	-0.32
PATH PARAMETERS	
SPACE LOSS, DB	-209.89
(FREQ., GHZ/MHZ	19.91
RANGE, KM)	37408.00
ATMOSPHERIC ATTN, DB	-0.32
RECEIVER PARAMETERS	
POLARIZATION LOSS, DB	-0.50
RADOME LOSS, DB	-0.20
ANT. DIRECTIVITY (MIN.), DBI	18.90
SYS. TEMP. (REF TO REFLECTOR), K @	320.00
G/T, DB/K	-6.15
POINTING LOSS, DB	-0.50
DOWNLINK C/N0, DB.HZ	55.76
OVERALL C/N0, DB.HZ	55.63
REQ'D EB/N0 (AWGN--SIMULATION), DB	6.00
MODEM IMPLEMENT. LOSS, DB	0.60
REQUIRED EB/N0, DB	6.60
LOSS DUE TO ACTS PHASE NOISE, DB	1.00
FADE ALLOWANCE (OVERALL), DB	3.00
DATA RATE, BPS	9600.00
REQ'D EFFECTIVE C/N0, DB.HZ	50.42
HARDWARE PERFORMANCE MARGIN, DB	5.21

Low Cost Coherent Demodulation for Mobile Satellite Terminals

Santanu Dutta and Steven J. Henely

Mobile Communication Satellite System
Rockwell International
400 Collins Road, NE
Cedar Rapids, Iowa 52498
(319) 395 8257

ABSTRACT

This paper describes some low cost approaches to coherent BPSK demodulation for mobile satellite receivers. The specific application is an Inmarsat-C Land Mobile Earth Station (LMES), but the techniques are applicable to any PSK demodulator. The techniques discussed include combined sampling and quadrature downconversion with a single A/D, and novel DSP algorithms for carrier acquisition offering both superior performance and economy of DSP resources. The DSP algorithms run at 5.7 MIPS and the entire DSP subsystem, built with commercially available parts, costs under $60 at quantity-10,000.

INTRODUCTION

Low cost mobile terminals are essential to the commercial success of many of the mobile satellite services (MSS) being launched today. This is because the services are based on the premise of a mass market, whose penetration will be critically dependent on the terminal cost. Driven by the desire to also minimize the space segment cost, some mobile satellite service providers, such as Inmarsat in its "C" standard, have opted for coherent rather than differential PSK modulation. Coherent demodulation is more complex than differential detection, the more popular approach, and tends to increase the terminal cost.

Modern PSK demodulators are almost invariably implemented by DSP. However, it is not widely recognized that, per today's pricing of programmable DSP chips, the cost of the DSP solution goes up quite rapidly with the processing speed (millions of instructions per second, or MIPS) and the on-chip memory. Floating point chips also extract a premium over fixed point devices. Table 1 shows the MIPS, internal memory and unit cost at quantity-10,000 for some popular programmable DSP chips.

It is clear from Table 1 that there is considerable incentive to engineer the DSP alogrithms for minimum MIPS and on-chip memory, while keeping the performance *acceptable*. In the present case, "acceptable performance" was that defined in the Inmarsat-C System Definition Manual (SDM).

Table 1. Comparison of Low Cost DSP Chips

Vendor	Product	Type	Cycle Speed (MHz)	On-Chip Prog. Mem.	On-Chip Data Mem.	Unit Cost @ qty 10K ($)
Analog Devices	ADSP-2105	16-bit Fixed Pt.	10.0	1K x 24 (RAM)	512 x 16 (RAM)	20.00
	ADSP-2101	16-bit Fixed Pt.	12.5	2K x 24 (RAM)	1K x 16 (RAM)	36.00
	ADSP-21010	32-bit Fl. Pt.	12.5	external	external	49.88
Texas Instr.	TMS320C25	16-bit Fixed Pt.	12.5	4K x 16 (ROM)	544 x 16 (RAM)	14.86
	TMS320C51	16-bit Fixed Pt.	28.5	8K x 16 (ROM)	1K x 16 (RAM) 1K x 16 (dual RAM)	28.89
	TMS320 C31-27	32-bit Fl. Pt.	13.5	4K x 32 (dual ROM) 2K x 32 (dual ROM)		40.00

Prices are for the Industrial temperature range (-25 C to +85 C), except for TMS320C51 and TMS320C31-27, which are currently not available in that temperature range
(The Industrial temperature range is preferred for land mobile services)

In this paper, the techniques discussed are (1) simultaneous bandpass sampling and quadrature downconversion using a single A/D, and (2) a novel DSP algorithm for carrier acquisition, with features suitable for MSS. Other DSP innovations are also featured in the Rockwell Inmarsat-C terminal but are not discussed here for lack of space and proprietary reasons.

Demodulator Hardware Architecture

Figure 1 shows functions performed in DSP in the Rockwell LMES.
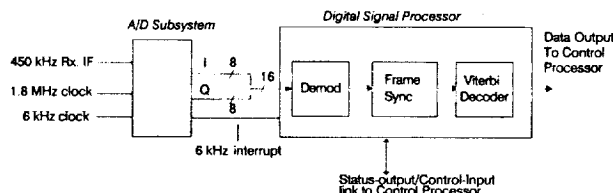
Figure 1. Demodulator Hardware Architecture

The received signal at the IF of 450 kHz is simulta-
neously sampled and quadrature downconverted to the
nominal frequency of 0 Hz by a single 8-bit A/D.
Thereafter, the complex samples are processed in the
DSP chip to perform the functions of carrier frequency
and phase estimation, symbol synchronization, BPSK
matched filtering, frame deinterleaving, UW detection
and tracking, erasure sensing and Viterbi decoding. Of
these, only carrier frequency and phase estimation are
discussed here.

INPUT SAMPLING/ DOWNCONVERSION

Subharmonic quadrature sampling was the tech-
nique used. This combined the processes of input sam-
pling and quadrature downconversion, leading to a sig-
nificant reduction or simplification of the signal condi-
tioning circuitry preceding the A/D. We first discuss
two conventional approaches and then describe the ap-
proach used.

Conventional Approach A

Probably the most conventional approach is to mul-
tiply (mix) the IF signal with two quadrature-phase lo-
cal oscillator (LO) signals at IF. The mixer outputs are
lowpass filtered and digitized by "slow" A/D converters.
Figure 2 shows a block diagram of this approach.
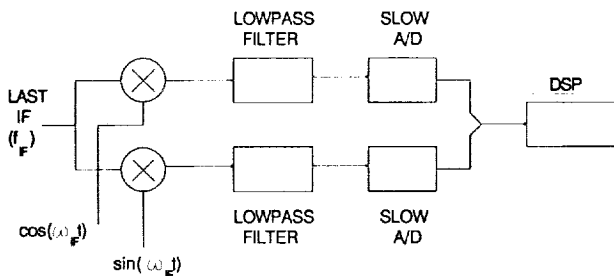
Figure 2. Conventional I/Q Downconversion and
Input Sampling

The required operating bandwidth of these A/D's is
the sampling rate, which, according to the Nyquist theo-
rem, is lower bounded by the width of the receiver's
stopband. In the present design, the stopband width is
approximately 6 kHz.

For ideal circuit components, this yields mathemati-
cally perfect I and Q samples. However, because of the
separate analog paths of the I and Q signals, the possi-
bility of gain and phase mismatch exists. Selecting com-
ponents with good match increases the terminal cost.
There is also the problem of DC bias if active mixers
are used. The two-path sampling approach also re-
quires many more discrete components than a single-
path approach, as used in Conventional Approach B
and the present implementation.

Conventional Approach B

Another approach common in today's digital wireless
modems is single-path sub-Nyquist sampling with the
complex downconversion in DSP. In this approach, the
input sampling rate has to be at least 2-times the IF
stopband width. After digital Hilbert transformation,
the sampling rate can be decimated to a frequency
equal to the stopband width.

Implemented Approach

The bandpass IF signal at 450 kHz was sampled by
pairs of pulses, with an intra-pair time separation of
$1/(4.IF) = 1/(1.8 \text{ MHz})$ and inter-pair separation of
$1/(6 \text{ kHz})$. Figure 3 explains the concept.
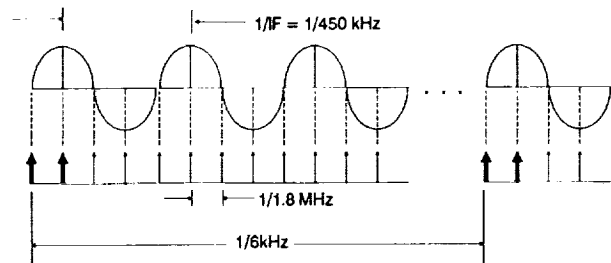
Figure 3. Concept: Combined I/Q Downconversion
and Input Sampling

The process may be thought of as sampling with the
complex sampling function, $(1+j1)\delta(t-nT)$. The 90-de-
gree phase shift between the sampling pulses in each
pair is achieved by time staggering. As in Conventional
Approach B, only a single A/D is required. Moreover,
the input rate is 6 kHz, unlike Conventional Approach
B, in which the rate would be 12 kHz. Figure 4 shows
the hardware block diagram.
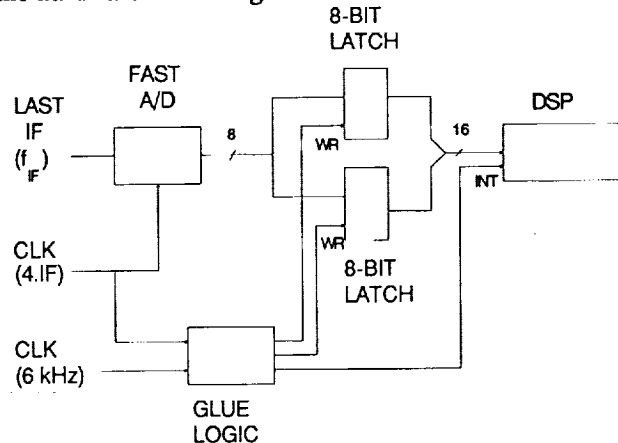
Figure 4. Hardware Block Diagram: Combined I/Q
Downconversion and Input Sampling

The economy of this approach, both in sampling cir-

cuitry and DSP code is obvious. Compared to Conventional Approach A, the advantages are in circuit matching requirements and low parts count. Compared to Conventional Approach B, it avoids the digital Hilbert transformer and runs at a lower input sampling rate.

Although economical in hardware and immune to mismatch errors, this approach does have its own imperfection. However, the imperfection is acceptable here because of the noisy input signal. The input samples are at perfect phase quadrature only at the nominal IF (450 kHz). If the band of interest (stopband) is small compared to the nominal IF, the phase error relative to quadrature, even at the band edge, is small. For example, in the present design, the stopband is approximately $+/-3$ kHz. The phase error for this frequency is $\theta = +/-0.6$ degrees. It can be shown that this creates a cochannel self-interference term that is at $20\log_{10}\{\sin(\theta)\}$ relative to the desired signal, i.e approximately -40 dBc. The fact that the modem operates in E_s/N_0 of typically 3.7 dB makes this level of self-interference quite acceptable.

The present approach also requires a faster A/D than the conventional approaches. In the present design, an operational bandwidth of 4.IF = 1.8 MHz is required, as opposed to a bandwidth of 6 kHz in Conventional Approach A and 12 kHz in Conventional Approach B respectively. However, low cost flash A/D's in the low MHz range are now available, making this approach a better choice from a cost standpoint. The cost of the A/D used, in quantity-10K, was $6.75.

CARRIER ACQUISITION ALGORITHMS

Demodulator Requirements

The detailed performance requirements are given in the SDM [1] and are not repeated here. However, the key challenges are highlighted.

Transmit Signal Characteristics
Modulation:	Unfiltered BPSK
Coding:	Rate-1/2 Convolutional
Symbol rate:	1200 bps

Fading Channel Characterisitics
Unfaded C/N$_0$:	34.0 dBHz
Fading Type:	Rician, C/M = 7 dB
Fading bw.:	0.7 Hz

Blocked Channel Characteristics
Unblocked C/N$_0$:	35.0 dBHz
Duration:	2.7 s
Period:	8.9 s

Doppler Characteristics
Max. Shift:	$+/-$ 850 Hz
Variation Rate:	$+/-$ 10 Hz/s

In [1], the performance requirements are specified in terms of the Packet Error Rate (PER) for the fading channel and the blocked channel separately. Performance specifications for different packet sizes and input

C/N$_0$ are provided; here we cite only those for the 128-byte packets and the above C/N$_0$ values for illustration.

Typical SDM Performance Requirements
PER(128) fading ch.:	8%
PER(128) blocked ch.:	10%

When the demodulator performance requirements are translated into carrier acquisition requirements, the following facts emerge:

(1)   The low prevailing C/N$_0$, while making the demodulation task difficult, makes it possible to use non-ideal processing techniques. This was exploited in the input sampling scheme.

(2)   Conventional phase locked loop techniques for carrier acquisition will not work because of the conflicting requirements of *large capture bandwidth* ($+/-$850 Hz) and *rapid acquisition* on the one hand, and *low phase noise* on the other. The capture range was actually set even higher, at $+/-$ 1300 Hz, to enable rapid frequency search on power up. During the latter phase, the receiver is hopped in 2.5-kHz steps. Rapid carrier acquisition is required so that (a) the initial frequency search time is short, and (b) not many bits are lost when the LMES emerges from a blockage or transmit mode (the communication is half-duplex).

Review of Carrier Recovery Techniques for BPSK Demodulation

The two major problems in BPSK demodulation are recovery of the carrier phase and symbol clock phase. In this paper, we discuss only the former.

Carrier recovery may be performed by either open loop or closed loop techniques. One popular open loop technique is to continuously operate an FFT in the background and use it to obtain a coarse frequency estimate; this is used to aid a closed loop carrier synchronizer. An alternative approach is described by Viterbi [2]. Both of these techniques are much more complex and demanding of DSP resources than the closed loop techniques. It was therefore decided to implement the present demodulator based on closed loop techniques alone.

A simple phase locked loop cannot be used because a BPSK signal has a suppressed carrier. However, modified phase locked loops are usable, such as the squaring loop and the Costas loop. Many text books, e.g. [3], provide extensive coverage of both techniques. The Costas loop has the advantage over the squaring loop that it is capable of wider bandwidth operation [ibid p.304]. Therefore, the Costas loop was chosen.

Cahn has analyzed the performance of the Costas loop and shown that, in most receive applications, there is a conflict between the required lock-time/capture-range and the acceptable level of phase noise [4]. This is explained below.

The capture range of a basic Type I phase locked loop (without a perfect integrator in the loop filter) is directly proportional to the loop resonance frequency, and hence also the loop bandwidth [3, p.364]. As the loop bandwidth determines the amount of phase noise in the loop's voltage controlled oscillator (VCO), it is clear that *large capture bandwidth and low phase noise are conflicting requirements for a Type I loop*.

In Type II loops (loop filter has a perfect integrator), the capture range is theoretically unbounded. In practical systems, it is bounded by the loop's dynamic range. Thus, *for Type II loops, the capture range and phase noise (loop bandwidth) are unrelated*.

We now examine the lock time. This is given by Gardner for Type II loops as [5, p. 76]

$$T_{acq} = 4.2(\Delta f)^2/B_n^3 \qquad (1)$$

where,

T_{acq}:	acquisition time
Δf:	frequency offset
B_n:	loop noise bandwidth

The expression for Type I loops is very similar [Spilker, p.364] and differs only in the multiplying constant. Irrespective of the type of loop, note that the lock time is inversely proportional to the cube of the loop bandwidth. This makes it difficult to simultaneously achieve rapid phase lock during carrier search, and low phase noise during carrier tracking.

Cahn proposed to overcome this problem by creating an outer frequency locked loop around the inner phase locked loop, as shown in Figure 5 (excluding the adaptive AFC gain control, which is the contribution of the present work).
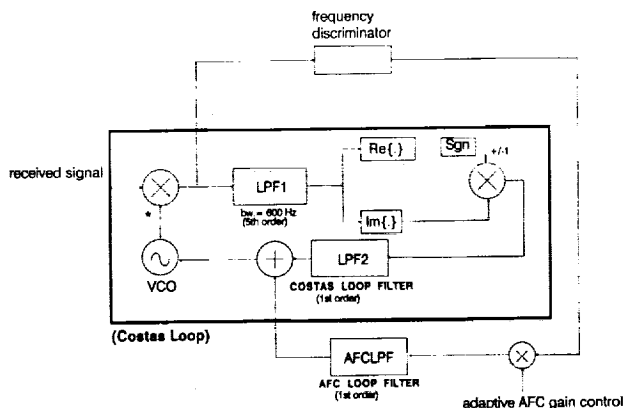
Figure 5. AFC-aided Costas Loop

The outer loop acts as an automatic frequency control (AFC) loop; this configuration is known as the "aided" phase locked (or Costas) loop. Both the outer

and the inner loops provide error signals to the VCO input. However, the AFC loop's contribution is proportional to the *frequency difference*, and not the *phase difference*, relative to the input carrier. This configuration increases the capture range and reduces the lock time because an AFC loop can perform the task of pulling in carriers with large offset much better than a phase locked loop. However, the AFC loop also contributes noise to the VCO's driving function. Therefore, the AFC loop bandwidth has to be limited so that its contribution to the VCO's phase noise is small compared to that of the phase locked loop. Cahn found an AFC loop bandwidth of 0.1 times the bandwidth of the phase locked loop to be a suitable choice.

New Carrier Recovery Scheme

Although Cahn's AFC loop solves the capture range problem and provides some help in reducing the lock time, the latter is still unacceptable per the present design goals, given below.

Carrier Recovery Design Goals

Loop Bandwidth:	60 Hz
(determine by phase noise	
and Doppler rate tracking)	
Capture Range:	+/- 1300 Hz
Mean Acquisition Time:	1 s

In the present demodulator, the lock time was further reduced over Cahn by making the AFC loop gain adaptive. The inner loop was a Type II Costas loop with 60-Hz loop bandwidth, a capture range of over 100 Hz and an acquisition time (for 100-Hz offset carriers) of approximately 0.8 s. The outer loop had a capture range of +/- 1300 Hz and an acquisition time of approximately 1.0 s. The adaptive AFC gain control scheme is described below.

The AFC gain scheme first investigated was:

IF(NOT.(inner loop lock)) THEN
    AFC GAIN = HIGH
ELSE
    AFC GAIN = LOW

Practical implementation of this scheme revealed a number of problems. It was found that, in order to achieve the target lock time of 1 s, the AFC loop gain had to be increased to a very high value. At this high AFC gain, the phase noise contributed by the AFC loop often prevented the inner loop from locking. Moreover, the AFC loop gain would undergo damped oscillation around its steady state value for an unacceptable length of time before the frequency uncertainty settled down to within the 100-Hz capture range of the inner loop. This meant that the decision to switch the AFC gain to a low value could not be based on a lock detector operating on the inner loop. The AFC loop would have to autonomously switch gain, based on some measurement of its own state.

Autonomous AFC Gain Switching

The key requirement is for the AFC loop to determine that it is sufficiently close to its steady state value. The time response of the AFC loop's error signal, e_{AFC}, to a step change in frequency, for large AFC gains, has the characteristic underdamped shape shown in Figure 6.
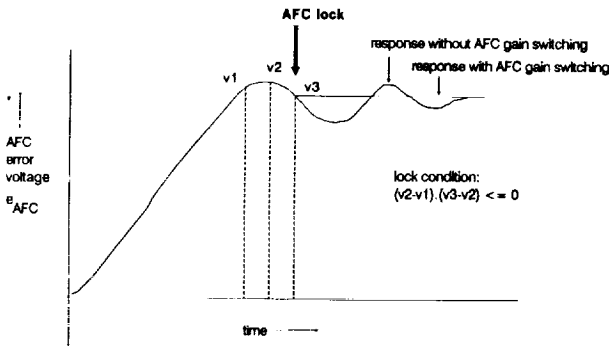
Figure 6. Typical AFC error signal response without noise (artist's impression)

It is clear that a change in sign of the derivative of e_{AFC} (noise assumed to be absent) indicates that e_{AFC} has just traversed its first peak. Usually, this point is sufficiently close to the steady state value. Thus, a change is sign of the first derivative of e_{AFC}, say e_{AFC}', may be taken as the signal to clamp down the AFC gain. Figure 6 shows this conceptually.

When noise is present, this approach is not fool-proof as noise can cause premature sign changes in e_{AFC}'. The following remedy was applied to this problem. e_{AFC} was filtered by a 1.6 Hz bandwidth filter before its derivative was taken. However, this measure, by itself, could not eliminate all occurrences of spurious AFC lock indication. Thus a waiting time of 0.8 s was introduced on each occurrence of AFC lock. During this time, the AFC gain would be clamped down to its LOW value. If, at the end of this period, the inner loop still indicated no lock, the AFC gain would be returned to its HIGH value. The waiting time was selected to be 0.8 s as this was the acquisition time of the inner loop.

Special Accommodation for Fading and Blocked Channels

Some customization of the above concepts were incorporated to further improve performance in fading and blocked channels. Instead of two AFC gains, three gain values were used -- HIGH, MEDIUM and LOW.

High AFC gain was used on "initial search" for the carrier. The "initial search" condition was defined to exist on power up and on changing the receiver's tuned frequency. If, after once acquiring the carrier, it was lost (presumably due to fading or blockage) then the MEDIUM gain was applied. The use of a medium gain

ensured rapid resynchronization when the carrier returned from a fade or blockage. As it had been gone only for a short period, the frequency could not have changed very much. If the inner loop remained continuously out of lock for more than 25 s, the "initial search" condition was declared to exist, on the assumption that significant frequency change might have occurred in the intervening period (due to Doppler or oscillator drift). The LOW gain was applied only when the inner loop was locked.

DEMODULATOR PERFORMANCE RESULTS

The "proof of the pudding" for the above techniques is in meeting the SDM PER requirements and the derived requirement of 1-s carrier acquisition time. Figures 7 and 8 show the PER performance of the Rockwell LMES demodulator in the SDM fading channel.
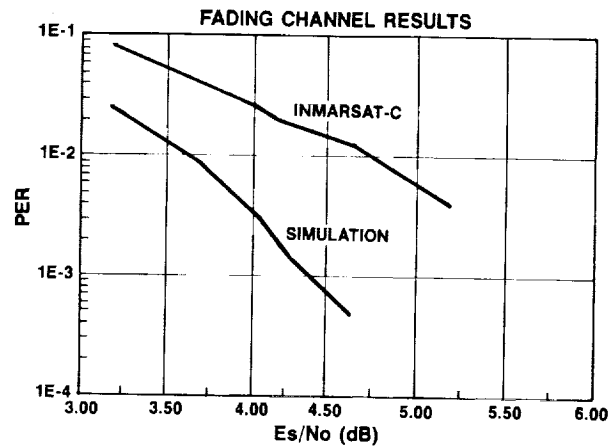
Figure 7. Fading Channel Performance
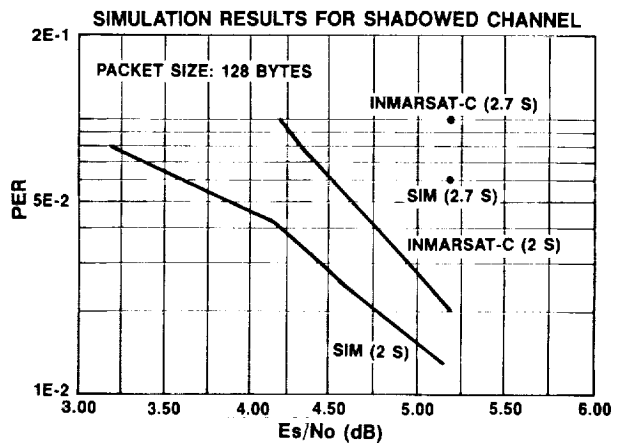
Figure 8. Blocked Channel Performance

It is clear that Inmarsat-C performance requirements are satisfied.

The statistics of the carrier acquisition time, for 850 Hz offset, in a fading channel with unfaded $C/N_0 = 34$ dBHz, is given below (simulation results).

Carrier Acquisition Statistics
Mean carrier acquisition time: 1.1 s
Median carrier acquisition time: 0.9 s
90-percentile carrier acquisition time: 1.8 s

Since the other major aim of the design was cost minimization, the outcome of that effort is noted below.

The processing speed requirement of the Demodulator part of the algorithm is 4.8 MIPS, while that for the entire DSP subsystem is 5.7 MIPS. The program code size is approximately 1.5K. The implementation was based on one Analog Devices ADSP 2101 chip, for which the quantity-10K unit price is approximately $38. If the program memory size could be reduced to under 1K, the ADSP 2105 chip could be used at the quantity-10K unit price of $20. This is considered feasible by additional innovations in code optimization and is planned for future product revisions.

The entire cost of the DSP subsystem, including external memory, A/D and other sampling circuit components, is under $60.

SUMMARY

When addressing a mass market, it is important to minimize product cost while keeping product performance above a defined level of acceptability. While the costs of DSP parts have been falling in general, a significant difference still exists between the "low-end" parts with modest MIPS and on-chip memory, and the higher end parts featuring greater DSP resources. In this paper, some novel input sampling techniques and DSP algorithms are presented which helped to realize an Inmarsat-C demodulator using low-end parts.

REFERENCES

[1]   *Inmarsat-C System Definition Manual (SDM), Release 2.0*, Inmarsat, London, September 1992.

[2]   Viterbi, A. J. and Viterbi, A. M., "Nonlinear Estimation of PSK-Modulated Carrier Phase with Application to Burst Digital Transmission," *IEEE Transactions on Information Theory*, Vol. IT-29, No. 4, pp. 543-551, July 1983.

[3]   Spilker, J. J. Jr. *Digital Communications by Satellite*, Prentice Hall, 1977, pp. 302-305.

[4]   Cahn, C. R., "Improving Frequency Acquisition of a Costas Loop," *IEEE Transactions on Communications*, Vol. COM-25, No. 12, pp. 1453-1459, December 1977.

[5]   Gardner, F. M., *Phaselock Techniques*, 2nd ed., John Wiley & Sons, 1979.

Direct Digital RF Synthesis and Modulation for MSAT Mobile Applications

Stewart Crozier, Ravi Datta, John Sydor
Department of Communications
Communications Research Centre
3701 Carling Avenue
P.O. Box 11490, Station "H"
Ottawa, Ontario, Canada K2H 8S2
Telephone: (613) 998-2388
Facsimile: (613) 990-6339

ABSTRACT

A practical method of performing direct digital RF synthesis using the Hilbert transform single sideband (SSB) technique is described. It is also shown that amplitude and phase modulation can be achieved directly at L-band with frequency stability and spurii performance exceeding stringent MSAT system requirements.

INTRODUCTION

Direct synthesis of RF modulation has always been a touchstone concept with radio terminal designers. It has always held the promise of hardware reduction with the achievant of superior performance. However, most direct synthesis achievements have been at frequencies substantially lower than those that will be used with planned mobile satellite and personal communications systems. For the current MSAT and INMARSAT mobile satellite systems, specifications for long term frequency stability, phase noise, spurious emissions, and channel control significantly exceed the capabilities of existing direct digital synthesizers, which are limited primarily by the speed and resolution of their digital to analog converters (DACs). In view of the current pace of DDS technology, even when the limitations of the DACs are overcome, achievement of MSAT performance objectives at L-Band by DDS technology will not materialize until after the launch and commissioning of MSAT. When such technology does materialize there is no guarantee that it will be available at a low enough cost to make its incorporation into terminals viable. Up to now conventional Phase-Lock loop technologies or combined Phase-locked loop/DDS hybrid technologies seem the most promising frequency synthesis schemes for narrow band L-Band signal processing.

In view of the current limitations of DDS technology, CRC along with private researchers [1] has developed a new RF digital modulation technique that does not rely on the extensive use of phase lock loops and mixer/filter upconversion stages. The technique is extremely versatile and can be implemented at low cost. Phase and amplitude modulation can be achieved directly at L-Band with frequency stability and spurii performance exceeding stringent mobile satellite system requirements. This new technique is based on a unique hybrid of technologies, all of which are mature and highly amenable to low cost mass production practices. As a consequence this technique holds the promise of being able to bypass the problems limiting the evolution of DDS as it is currently envisioned.

HILBERT TRANSFORM SSB GENERATION

Any modulating signal $f(t)$ can be upconverted to a higher frequency by using the Hilbert transform (phase shifted SSB) technique [2]. In order to do this both the modulating signal and the carrier frequency must be generated as quadrature components and mixed by balanced modulators (Fig.1). Each modulator outputs a double sideband signal, $f_{d1}(t)$ and $f_{d2}(t)$.

$$f_{d1}(t) = A\cos\omega_m t \cos\omega_c t$$

$$= \frac{A}{2} [\cos(\omega_c + \omega_m)t$$
$$+ \cos(\omega_c - \omega_m)t] \qquad (1)$$

$$f_{d2}(t) = A\sin\omega_m t \sin\omega_c t$$

$$= \frac{A}{2} [\cos(\omega_c - \omega_m)t$$
$$- \cos(\omega_m + \omega_c)t] \qquad (2)$$

By subtracting or adding the outputs of each modulator, we generate either the upper or lower sideband, i.e.:

$$F_o(t) = A\cos(\omega_m + \omega_c)t \qquad (3)$$

In (3) we see that our modulating signal is shifted up by the carrier frequency. By exercising coarse control at a high frequency with the carrier, and a fine control at the lower modulating frequency, it is possible to exercise a wide band, fine control at an offset from the carrier frequency.

One major problem with the design of Hilbert Transform SSB modulators is the preservation of the $\pi/2$ phase shift over a wide band of frequencies. Failure to do so results in the emergence of the cancelled sideband. A phase error of 1 degree will result in the cancellation of the undesired sideband by only 35 dB. Most mobile satellite specifications require sprurii emissions to be in excess of 65 dBC. A second serious problem that exists with the practical implementation of the Hilbert transformation is the leakage of the carrier through the balanced modulators. Low cost suppressed carrier balanced modulators in practice cannot reject the carrier by more than 25 dB. This is why in most practical SSB radios the modulated output is filtered by a highly selective filter prior to further up-conversion.

To overcome these inherent problems, yet take advantage of the frequency control capability demonstrated in (3), requires modification to the basic Hilbert transform circuit shown in Figure 1.

FEEDBACK CONTROLLED HILBERT TRANSFORM SYNTHESIZER

Figure 2 shows one approach that can be taken to mitigate the hardware limitations of the Hilbert transform circuit. What is shown is an SSB RF synthesizer that can produce outputs at L-Band which can be stepped in 1 Hz increments and have phase noise lower than -80 dBC at 1Khz from the carrier. Spurii content lower than -60 dBC is also achievable.

The circuit has a low frequency dual DDS synthesizer that generates quadrature outputs. For example, this circuit and its DACs may produce a signal from 0.1 to 1.1 MHz in 1 Hz steps. The DDS is driven by a 20 MHz crystal which is divided down within the DDS, hence the phase noise of the output of the DDS is that of its crystal reference (F_{ref}) improved by $20 \log (f_{ref}/f_{output})$ dB. However this improvement is limited by the noise floor of the DDS circuitry (-150 dBC). What limits the spectral purity of the device is the performance of the 12 bit digital to analog converters which have spurious deficiencies due to glitches, output settling, and nonlinearity; with glitches being the main contributor. Theoretically the digitized sine output of a 12 bit DAC will provide a broadband signal-to-spurious ratio of 72 dB.

The output of the quadrature DDS is sent to the Hilbert transform circuit and to the balance circuit, which will be discussed later. A second signal is injected into the Hilbert transformer circuit from a coarse step synthesizer. This can be as high as 1600 MHz, however, with our experimental circuits we use a phase lock loop synthesizer operating in the 50-400 MHz range. This synthesizer has 1 MHz step sizes and is a single loop device with a very wide loop filter (10-30 Khz wide). Consequently the microphonic and spurii problems are significantly mitigated with this synthesizer. Phase noise for this

device is of the order of -80 dBC at 1 kHz offset.

The combination of the DDS and the single loop PLL set the performance limits on the output RF signal. It is the last circuit, the balance circuit, which eliminates the most deleterious sources of signal degradation with the Hilbert transformer SSB synthesizer. Details regarding this circuit are covered in [1]. Within the balance circuit error signals are generated which are proportional to the carrier leakthrough and the phase and amplitude errors causing the undesired sideband signal.

Carrier leakthrough is determined by measuring the level of the DC signal that is generated by mixing the RF output of the modulator with the carrier signal generated by the PLL. If the RF output of the modulator contains the carrier signal then this will be detected by the mixing process. The resulting error signal is used to drive DC biasing circuits which change the DC offset bias on the balanced modulators within the Hilbert transform modulator circuit. By adjusting the DC bias it is possible to eliminate carrier feedthrough with the balanced modulators.

Suppressing the undesired sideband signal is a somewhat more complex process, but in essence involves further mixing of the DDS signals and RF output. The balance circuit produces a phase error control signal which is used to adjust the phase of the I and Q signals from the DDS. An amplitude error control signal is also generated to control the amplitude of one of the DDS signals.

Because of its feedback nature this hybrid synthesizer has a time delay on the order of 10 milliseconds between the time a frequency instruction is loaded into it and the time the required RF signal is synthesized. Figures 3 and 4 show the typical RF performance characteristics of the synthesizer

The ability to control the frequency and phase of the output signal to such a high degree of accuracy makes it possible to use the synthesizer as a signal modulator.

DIRECT MODULATION APPROACH

Figure 5 shows the block diagram of a direct RF modulator. The system consists of a microprocessor with FM and AM look-up tables, a feedback controlled Hilbert transform synthesizer, as described earlier, and an amplitude modulator.

The approach taken to generate an arbitrary modulation format is to take the desired complex baseband modulation signal and break it up into equivalent FM and AM signals. The FM signal is then generated by the DDS and translated directly to the RF frequency using the Hilbert transform SSB technique. The AM portion is applied to the FM signal directly at RF using a mixer.

Consider the complex baseband MPSK transmit signal given by

$$s(t) = \sum_k a_k\, h(t-kT) \qquad (4)$$

where

$$a_k = \exp(j2\pi m/M), \quad m=1..M \qquad (5)$$

represents the complex data symbols, M is the number of phases, and h(t) is the impulse response of the desired baseband transmit filter. For example, QPSK modulation with M=4 and a 60% roll-off root-raised-cosine (RRC) filter is specified for the MSAT communications channels. The equivalent FM and AM signals are given by

$$s_{FM}(t) = \frac{d}{dt}\, phase[s(t)] \qquad (6)$$

$$s_{AM}(t) = |s(t)| \qquad (7)$$

The bandwidth of the FM and AM signals is much wider than the bandwidth of the desired filter response, h(t). This implies that the

sampled versions of the FM and AM signals must have many samples per symbol period to ensure that a sufficient number of FM and AM sidelobes are properly characterized and that the undesired sampling images are suppressed to acceptable levels. It is difficult to compute the FM and AM signals in real time because of the high sampling rates involved and the calculations required to convert from cartesian to polar coordinates. A table lookup approach was used for this reason. It was found that 32 samples per symbol period is sufficient to force the FM images down more than 70 dB with no additional band-pass filtering required at the output of the DDS. This allows the DDS to be used for both FM modulation and channelization over several MHz of bandwidth. Using 32 samples per symbol period for the AM portion as well resulted in excellent performance. The AM sampling images fall off much slower than the FM images, but the AM images are easily suppressed at baseband using a simple low-pass filter at the output of the AM DAC.

The table lookup approach stores one symbol period of the FM and AM waveforms for all possible bit patterns of a given length. The table size is an exponential function of the length, L, of the desired impulse response, h(t). With differential encoding encorporated into the FM and AM tables, the FM and AM waveforms are independent of the phase of the first symbol spanned by h(t). This makes both tables M times smaller than one might initially expect, and differential encoding is free. The required table size in bits is given by

$$\text{table size} = B \, N \, M^{L-1} \quad \text{bits} \quad (8)$$

where B is the number of bits per sample and N is the number of samples per symbol. As an example, a good approximation for the 60% RRC filter has been found which easily meets the MSAT specs using a span of only L=5 symbol periods. With B=16, N=32, and M=4 for QPSK, the FM and AM tables are only 128 K bits each.

Figure 6 shows the reconstructed spectrum obtained with these parameters. The first sidelobe, at a frequency of 1 symbol rate, is due to the filter h(t) and is down 45 dB. The first image, at a frequency of 32 symbol rates, is mostly due to the unfiltered FM spectrum and is down about 75 dB.

CONCLUSIONS

A practical method of performing direct digital RF synthesis using the Hilbert transform SSB technique has been described. It was also shown that amplitude and phase modulation can be achieved directly at L-band with frequency stability and spurii performance exceeding stringent MSAT system requirements. Related research being conducted at CRC indicates that a direct RF down-converter/demodulator is also feasible.

References

[1]   U.S. Patent 5162763; K. Morris, *Single Sideband Modulator for Translating Baseband Signals to Radio Frequency in single stage*, November 10, 1992.

[2]   Single Sideband Issue, Proceedings of the I.R.E. Vol. 44, No. 12, Dec 1956, .
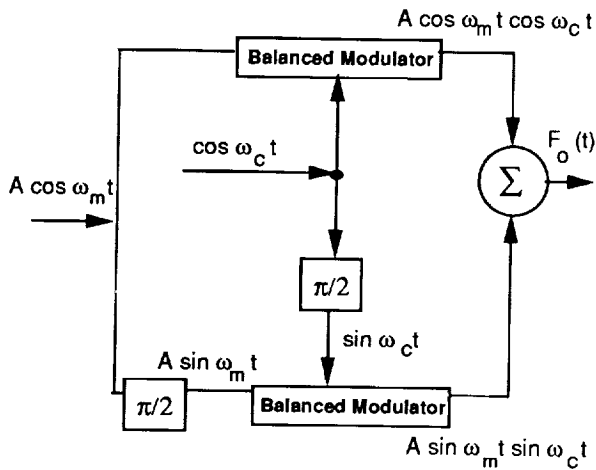
Figure 1 Hilbert Transform SSB Circuit
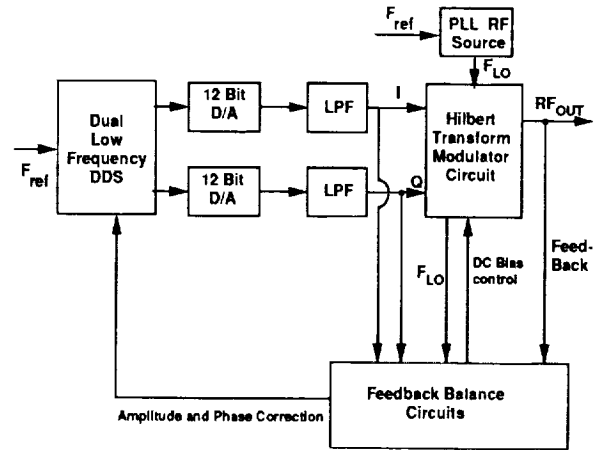
Figure 2
Hybrid DDS/PLL Hilbert Transform Synthesizer

MARKER
69.937 Ø MHz
-4.8Ø dBm

7Ø.ØØØ MHz
RES BW 3 kHz   VBW 1Ø kHz   SPAN 5ØØ kHz
                              SWP 15Ø msec
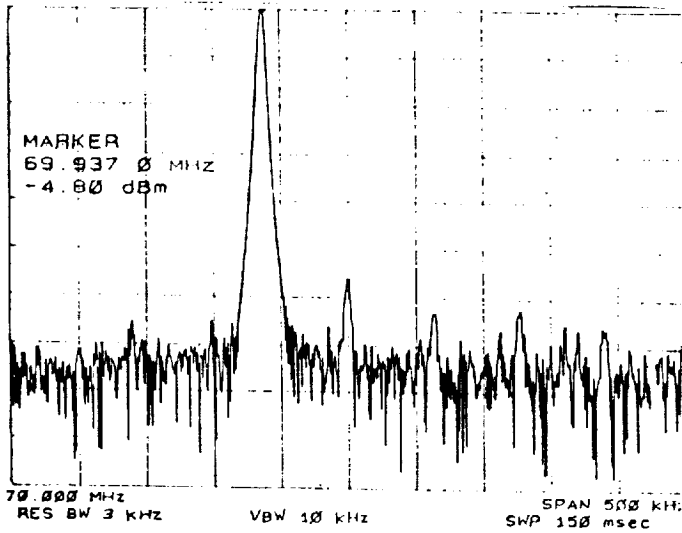
Figure 3
Synthesizer Output - Wide Band Width

MARKER
7Ø.Ø63 485 Ø MHz
-4.4Ø dBm

7Ø.Ø63 485 MHz
RES BW 1Ø Hz   VBW 3Ø Hz   SPAN 5ØØ Hz
                             SWP 15.Ø sec
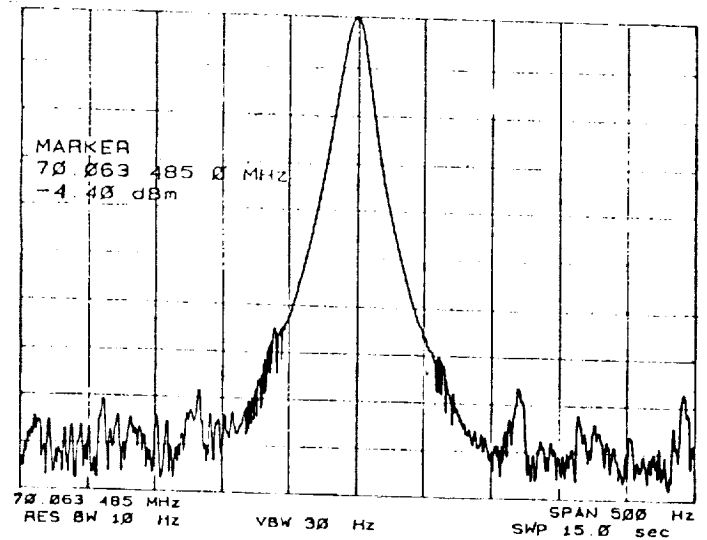
Figure 4 Synthsizer Output - Narrow Band Width
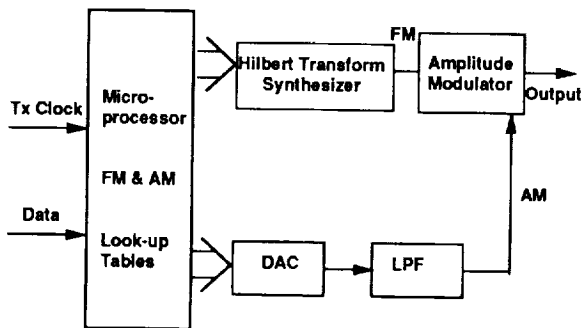
Figure 5
Block Diagram of Direct RF Modulator
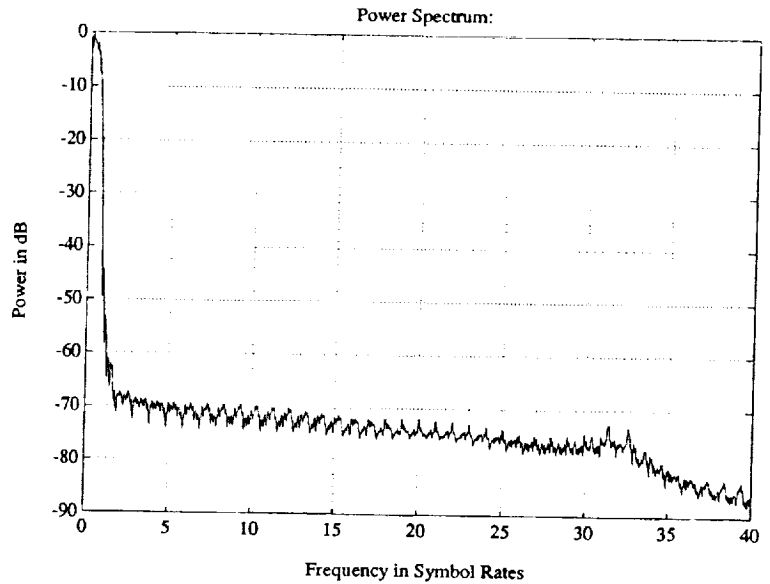
Figure 6
Power Spectrum of Reconstructured Signal

403
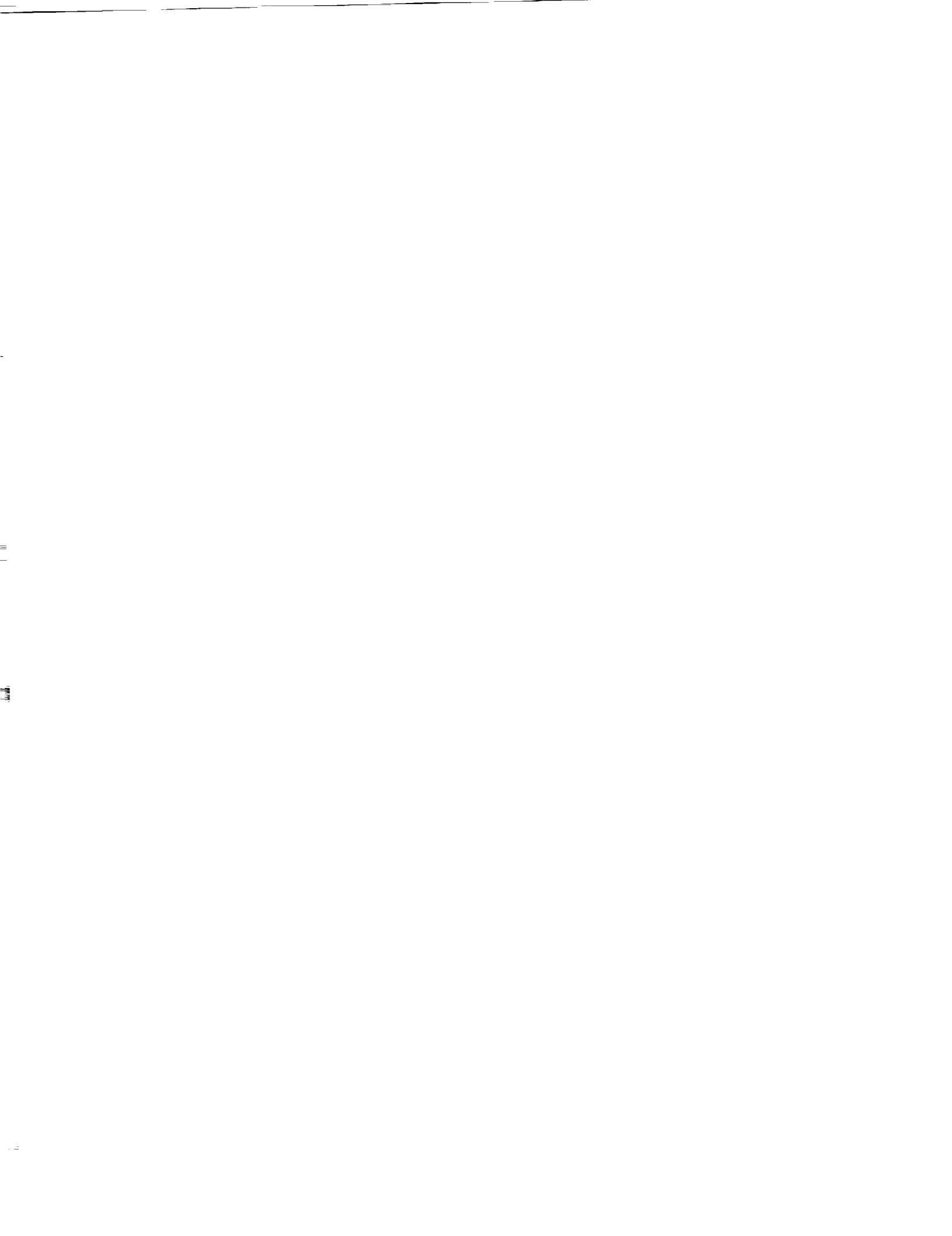
Asynchronous Timing and Doppler Recovery in DSP Based DPSK Modems for Fixed and Mobile Satellite Applications

B. Koblents, M. Belanger, D. Woods and P.J. McLane

Department of Electrical Engineering

Queen's University, Kingston, ON, K7L 3N6

Telephone: (613) 545-2937

Fax: (613) 545-6866

ABSTRACT

While conventional analog modems employ some kind of clock wave regenerator circuit for sychronous timing recovery, in sampled modem receivers timing is recovered asynchronously to the incoming data stream, with no adjustment being made to the input sampling rate. All timing corrections are accomplished by digital operations on the sampled data stream and timing recovery is asynchronous with the uncontrolled, input A/D system. A good timing error measurement algorithm is a zero crossing tracker proposed by Gardner. Digital, speech rate (2400 – 4800 bps) M-PSK modem receivers employing Gardner's zero crossing tracker were implemented and tested and found to achieve BER performance very close to theoretical values on the AWGN channel. Nyguist pulse shaped modem systems with excess bandwidth factors ranging from 100% to 60% were considered. We can show that for any symmetric M-PSK signal set Gardner's NDA algorithm is free of pattern jitter for any carrier phase offset for rectangular pulses and for Nyquist pulses having 100% excess bandwidth. Also, the Nyquist pulse shaped system is studied on the mobile satellite channel, where Doppler shifts and multipath fading degrade the $\pi/4-$DQPSK signal. Two simple modifications to Gardner's zero crossing tracker enable it to remain useful in the presence of multipath fading.[*]

I. INTRODUCTION

Within the last decade, low cost digital signal processing systems have become available. As these devices have become more powerful, it has become practical and desirable to implement fully digital modems with almost all the communications features implemented as realtime firmware. Timing recovery is a vital function of any modem, without which digital communication is impossible. We consider the timing recovery problem in a voice rate, fully digital modem which has been implemented as real time firmware on Second Generation Digital Signal Processors. The modem consists of a series of 4800 bps uncoded DQPSK modems employing Raised Cosine pulse shaping with excess bandwidth factors (α) ranging from 100% to 60%. Our modem employs asynchronous timing recovery, whereby the modem receiver recovers timing phase from the oversampled input signal, leaving it's input A/D converter free running. Such timing recovery techniques for digitally implemented modems are discussed in [1]. Zero crossing tracker timing error detectors of the type described by Gardner [1][2], are used to complete the timing recovery loops. The modem is experimentally tested on the AWGN channel, simulating the behaviour on a fixed satellite communications link. We show how to implement Gardner's algorithm for digital application and present the first experimental results on its performance. Additionally, the 4800 bps modem is modified to incorporate Doppler correction mechanisms and $\pi/4-$DQPSK modulation to enable it to operate on the mobile satellite channel with non-linear amplifiers. These modifications are also tested in the laboratory. The performance of the 4800 bps modem family on the mobile satellite fading channel is examined with the use of computer simulations. In particular, it is demonstrated that the zero crossing tracker timing error detectors can remain useful on the fading channel with simple modifications to their structure.

II. ASYNCHRONOUS TIMING RECOVERY

In traditional analog modems, timing recovery is accomplished by regenerating a local clock wave to be synchronous with the data clock, and uses this local clock wave to adjust the frequency and phase of the input A/D converters to be synchronous with the incoming data [1]. One example of this synchronous timing recovery is shown in Figure 1. In a fully digital implementation, on the other hand, the input sampling takes place at the A/D converter at the very front end of the system as shown in Figure 2 and the sampling rate can be asynchronous to the incoming data stream. This Figure shows our complete receiver which will be discussed in the sequel. In most cases, the input sampling rate is an integer multiple of the nominal symbol rate, but the receiver sampler is free running and never explicitly locked to the transmitter baud clock [1,3]. Timing correction is accomplished by aligning the decimator strobes shown in Figure 3, with the pulse peaks out of the matched filters.

In our implementation, the receiver samples are kept track of by a sample counter, which is incremented once per sampling period, in a modulo N fashion, with N being the number of samples per symbol. To align the data strobes with the matched filter pulse peaks, it is necessary to retard them by a sampling interval. That is accomplished by resetting the receiver sample counter to negative one instead of zero at the end of the symbol where the timing decision is made, resulting in the next symbol epoch being one sampling interval longer than nominal. This aligns the receiver decimator strobe with the transmitter data strobe. We refer to this as adding a sample and it represents a negative rate conversion. Dropping a sample, or moving one back in the sample count represents a positive rate change. What we have described is sample rate conversion in order to align the transmitter and receiver data rates. As in the previous section, the timing error correction in the pulse shaped modem is asynchronous. Two methods can be considered: the adding and dropping of samples, as discussed in the previous section, and a new method [1,3] based on polyphase filter interpolation between the samples of the receiver response. In the first case, as described in the previous section, the timing error is allowed to build, until the timing phase mismatch is approximately one sample period long, and then a sample period is either added or dropped from the timing epoch

following the decision. In systems with many samples per symbol, this is quite satisfactory. The adding or dropping of samples produces the required sample rate conversion to match transmitter and receiver data rate.

In systems with a more limited degree of oversampling, however, the timing offsets can grow to be quite significant fractions of a symbol period, and cause performance degradation [1]. Hence, a more precise way of controlling the timing error is desired. If a point on the response, in between the system sampling points were available, it would be desirable to move to this intermediate point instead. That kind of reasoning leads to timing correction by means of interpolation between sample points, which raises the effective sampling rate of the system, at least as far as the timing correction loop is concerned [1,3]. For a non-dispersive channel, a simple way to design such interpolators is given in [1]: simply design the receiver FIR matched, data filters to the desired oversampling rate, M, and then pick off M separate filters, by taking successive Mth taps out of the oversampled impulse response. In such a system the timing resolution is reduced to T_s/M where T_s is the received sampling period. In [1] this is termed filter coefficient interpolation.

Figures 3 and 4 represent DSP based results with and without filter coefficient interpolation based timing recovery. Note the increased timing resolution produced by filter coefficient interpolation. More details can be found in [4]. The case of a coherent BPSK voice rate modem was treated in [5].

III. EXPERIMENTS WITH RAISED COSINE PULSE SHAPED MODEMS

We will do our tests for the transmitter shown in Figure 5. Fading is introduced in the transmitter for our tests to be discussed later. For now we consider an AWGN channel.

In [2], Gardner introduces a non-decision aided (NDA) zero crossing tracker algorithm for Nyquist pulse shaped modems, which has the following form. The timing error measurement for the receiver in Figure 2 is given by

$$
\begin{aligned}
u(n) = x_I&\left(n - \frac{1}{2}\right)[x_I(n) - x_I(n-1)] \\
&+ x_Q\left(n - \frac{1}{2}\right)[x_Q(n) - x_Q(n-1)]
\end{aligned}
\tag{1}
$$

where $(x_I(n), x_Q(n))$ are the (inphase, quadrature) samples at symbol time n. This NDA variant of Gardner's

zero crossing tracker is shown in [4] to be free of self noise in the case of $\alpha = 100\%$ for any PSK data transition, and not just those with equal pulse heights [1]. Both variants of Gardner's zero crossing tracker can be adapted to operate with rectangular pulse shapes [4]. For $.6 \leq \alpha < 1$, intersymbol interference will occur on the mid-band samples in (1). This gives rise to timing jitter. The effect of this jitter is studied in [4] and it was found that excellent performance can be attained by smoothing $u(n)$ in (1) with a 50 Hz, first order, digital loop filter.

The MSAT signal standard will use Raised Cosine (RC) pulse shapes with $\alpha = 60\%$ and DQPSK modulation with conventional convolutional coding. As such, a family of 4800 bps modems has been developed with α ranging from 100% to 60%. Experimental performance testing has been carried out for the AWGN channel, that is for no fading in Figure 5. Figure 6 shows BER results for the 60% excess bandwidth case. Results for the 70%, 80%, 90% and 100% cases are similar [4] and are invariant with respect to excess bandwidth. In all cases, implementation losses are kept well under 1 dB. The timing synchronizer shows very good behaviour. Table 1 shows results for the worst case considered, with $\alpha = 0.6$, for three SNR's. It can be seen that at high SNR, there is an almost complete absence of jitter. More channel noise does induce some timing jitter, but even at an SNR corresponding to a BER on the order of 10^{-2}, the timing jitter is very low, with only 15 corrections in the wrong direction. We have also implemented the filter coefficient interpolation algorithm and similar performance was obtained.

IV. DOPPLER AND MOBILE FADING

The modems described so far have been developed for and tested experimentally on an additive white Gaussian noise channel which accurately describes only a stationary satellite link. On a mobile link, a clear line of sight to the satellite cannot be guaranteed, and some degree of multipath interference, or fading is inevitable. In addition, Doppler shifts of the carrier frequency occur as the vehicle on which the mobile unit is mounted accelerates, decelerates, or changes direction. A further complication arises when cheaper class C amplifiers are used with $\pi/4$-DQPSK modulation in order to save cost. Use of non-linear amplifiers leads to large amounts of spectral regrowth, and causes adjacent channel interference problems [7].

Doppler tracking techniques [5,6] have been incorporated into the RC pulse shaped modem described in the previous section. These techniques rely on rotating the received signal phasor to compensate for detected Doppler offsets. Since this rotation is carried out on the detected signal following the data filtering, it has no particular bearing on timing recovery, which has been demonstrated [4] to be immune to any phase offset if the NDA variant of the Gardner zero crossing tracker is used. Both closed- [5] and open-loop [6] algorithms have been studied. We have also included modification of the root-raised cosine pulse shaped transmitter portion of the modems to use $\pi/4$-DQPSK modulation which has been shown to minimize spectral regrowth [7].

The behaviour of the 4800 bps RC pulse shaped modem system on the multipath fading channel has been studied with the aid of computer simulations. The multipath fading model used in the simulations is Rician [8,9]. The fading was incorporated into the transmittor for testing as shown in Figure 5.

Simulation results on moderate fading channels with our original system configuration (DQPSK with open/closed Doppler tracking and ramp-varying Doppler factor corresponding to 40 Hz + /- 20Hz/sec.) are very poor: the timing recovery loop exhibits tremendous jitter, and does not provide any useful information, while the bit error rate is 50%. The cause of the jitter can be seen when the timing is frozen, and the mid-baud data filter outputs on the I and Q rails are plotted. As expected, it is found that there is severe distortion on the nominal zero crossing points when the fading is a constructive interference and gives a received signal well above the average level. On the other hand, a destructive deep fade, severely alleviates timing information. Hence the fading directly interferes with the operation of the zero crossing tracker timing error detector. Two separate modifications to the timing recovery loop have been implemented, both of which restore the functionality of the zero crossing detector making it useful on the fading channel. These modifications are based on deducing the presence of severe fading interference, either the constructive or destruction type, and the suppression of timing recovery while either type of fade is in progress. Since timing drift is a relatively slow phenomenon the receiver need not lose synchronization, unless the fade is of extremely long duration, which is so rare an event that it is impractical. Thus, we establish a window of signal ampli-

tude levels, centered about the mean signal level, in which timing error measurements will be computed from (1).

The first modification is to implement a zero-crossing threshold on the timing error signal in (1). If the nominal zero crossing point on either the I or Q rail is too large, timing corrections are not made. Timing is frozen until the zero crossing points are again within an acceptable range. After the thresholds are optimized, this modification yields the results shown in Figure 7, which are very close to those obtained with perfect timing, but are for timing jitter and a Doppler of 40 Hz. Figure 7 is for a Doppler shift of $B_d = 40$ Hz with a time variation of 20 Hz/sec. In both cases the time variation of the fading is due to a first-order Butterworth filter. The losses due to fading are larger for this filter than for higher order filters. For the Rayleigh ($K = 0$) case, the bound in equation (9.124) and Table 9.2 of [10] gives the BER floor as $4\pi B_d T$, for the first-order Butterworth filter and $.5(\pi B_d T)^2$ for the second order Butterworth case. Thus the first-order case has higher losses for the usual values of K.

The second modification involves continuously measuring the received signal power. An acceptable power level can be obtained by observing a fade-free signal. A severe fade either decreases the signal power as a result of destructive interference of multipath components, or increases it as a result of constructive interference. It is possible to implement an upper and lower signal envelope threshold defining an acceptable power range, and only perform timing measurement in (1) if the received signal power lies in that range. The average signal power depends on the K—factor, and the power thresholds have to be optimized over the expected range of operation, which in our case is for $K = 5$ dB to $K = 20$ dB. Again results very close to those given above for the timing error thresholding were obtained.

V. CONCLUSIONS

Fully digital, asynchronous timing recovery has been demonstrated to give excellent results in laboratory experiments on speech rate (2400 and 4800 bps) modems with RC pulse shaping. Gardner's zero crossing tracker timing error detector has been applied to RC pulse shaped speech rate modems with excellent results on the additive Gaussian noise and Rician fading channel. The NDA form of the zero crossing tracker has been found to be immune to pattern noise for any data phase transition, making it ideal

for timing error detection in M-PSK and M-DPSK systems with $M > 4$. In RC pulse shaped systems with α down to 60% ISI induced self noise is sufficiently controlled by loop filtering. In addition, the NDA timing error detector is immune to phase offsets.

REFERENCES

[1] F.M. Gardner, "Demodulator Reference Recovery Techniques Suited for Digital Implementation", ESA Contract 6847/86/NL/DG, Final Report, May 16, 1988.

[2] F.M. Gardner, "A BPSK/QPSK Timing Error Detector for Sampled Receivers", IEEE Trans. Comm., COM-34, pp.423–429, May 1986.

[3] M. Oerder and H. Meyer, "Digital Filter and Square Timing Recovery", IEEE Trans. Comm., Vol. COM-36, pp. 605–611, May 1988.

[4] B. Koblents, "Asynchronous Timing Recovery in M-PSK Data Modems", M.Sc. Thesis, Queen's University, Kingston, Ontario, Canada, July 1988.

[5] P.J. McLane, W. Choy, T. Tay, "Filter Coefficient Interpolated Timing Recovery in Sampled Coherent PSK Receivers", Globecom '92.

[6] M.K. Simon and D. Divsalar, "Doppler-Corrected Differential Detection of MPSK", IEEE Transactions on Communications, Vol. 37, pp. 99–110, February 1989.

[7] S.N. Crozier, "A Comparison of Three QPSK Type Modulation Schemes for Mobile Satellite SCPC Voice and Data Services", 16th Biennial Symposium on Communications, Kingston, Ontario, Canada, May 27–29, 1992.

[8] K.A. Norton, L.E. Voler, W.V. Mansfield, and P.J. Short, " The Probability Distribution of the Amplitude of a Constant Vector Plus a Rayleigh Distributed Vector", Proceedings of the IRE, Vol. 43, pp. 1354–1361, Oct. 1955.

[9] G.T. Irvine and P.J. McLane, "Symbol-Aided Plus Decision-Directed Reception for PSK/TCM Modulation on Shadowed Mobile Satellite Fading Channels", IEEE Journal on Selected Areas in Communication, Vol. 10, No. 8, pp. 1289–1299, October 1992.

[10] E. Biglieri, D. Divsalar, P.J. McLane and M. K. Simon, "Introduction to Trellis-Coded Modulation with Applications", Macmillan 1991.

2,097,152 SYMBOLS			
SNR, $2E_b/N_o$, dB	14.9	12.5	9.5
BER	1.2×10^{-5}	1.2×10^{-4}	1.2×10^{-2}
Forward Corrections	30	42	59
Backward Corrections	0	1	15
Net Number of Corrections	30	41	44

Table 1: Numbers of timing corrections at high, moderate and low SNR.
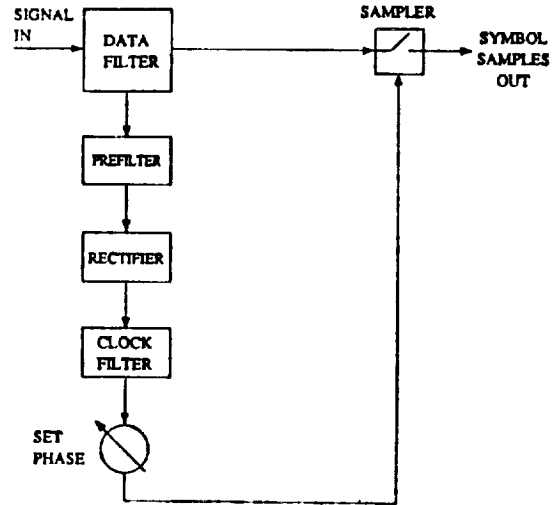
Figure 1: Feedforward clock recovery.
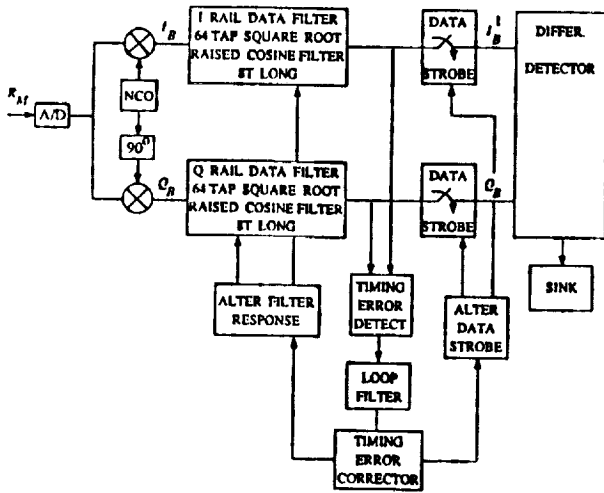
Figure 2: 4800 bps raised cosine pulse shaped modem receiver block diagram.
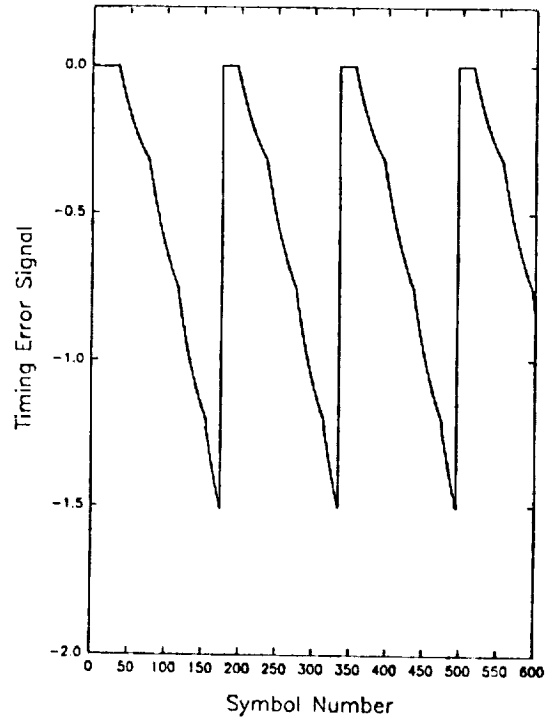
Figure 3: Timing error signal for simulated pulse shaped modem with timing correction by adding and dropping samples only. Timing drift: same as for Figure 4.

409
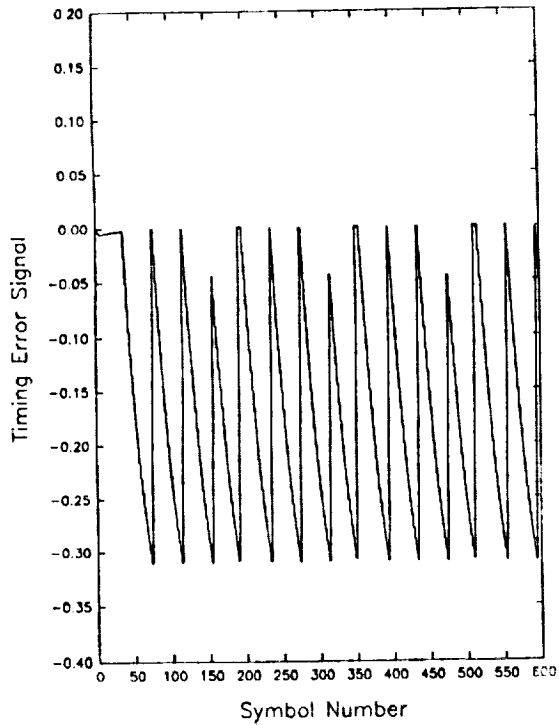
Figure 4: Timing error signal for simulated pulse shaped modem with coefficient interpolation timing recovery. Timing drift: transmitter filters permuted every 30 symbols, sample dropped every 120 symbols.

Figure 5: Block diagram of transmitter that includes fading for system testing.

BIT ERROR RATE PERFORMANCE
60% EXCESS BANDWIDTH, GARDNER'S NDA TIMING ALGORITHM

SNR (2Eb/No)

-- SERIES 1: THEORETICAL PERFORMANCE
-- SERIES 2: EXPERIMENTAL RESULTS
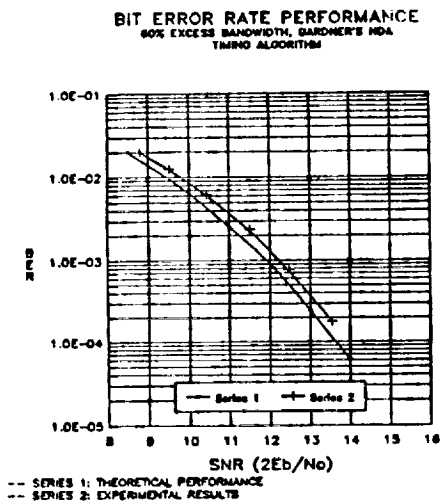
Figure 6: BER performance for 60% excess bandwidth, 4800 bps raised cosine pulse shaped DQPSK modem.

π/4−DQPSK
Rician Fast Fading Channel

o   AWGN Theoretical
●   K=13dB, perfect timing
▽   K=10dB, perfect timing
▼   K=10dB, with Doppler
□   K=5dB, perfect timing
■   K=5dB, with Doppler

SNR (2Eb/No)
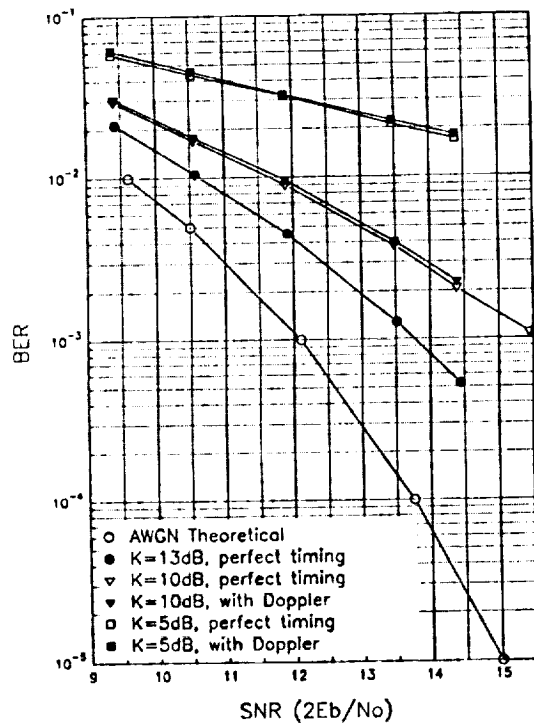
Figure 7: BER performance for a 40 Hz Rician Fast Fading channel with a first order Butterworth Doppler filter and with a time-varying 40 Hz Doppler offset.

410

Improved Frame Synchronization Schemes for Inmarsat-B/M SCPC and TDM Channels

Si-Ming Pan, Randy L. Hanson, Donald H. Madill, and Paul C. Chapman

SED Systems Inc.
P.O. Box 1464
Saskatoon, Saskatchewan, Canada S7K 3P7
Phone: 306-931-3425
Fax: 306-933-1486

ABSTRACT

This paper proposes faster, more robust frame synchronization schemes for various Inmarsat-B and Inmarsat-M communication and signalling channels. Equations are developed which permit frame sync strategies of the type specified by Inmarsat to be evaluated in terms of average true lock time, average false maintenance time, and average search time. Evaluation of the currently specified framing schemes shows that a significant performance improvement is obtained by optimizing the threshold parameters of the scheme. The optimization seeks a compromise between the conflicting requirements of maximizing true lock time and minimizing search time.

INTRODUCTION

Frame synchronization is essential for time division multiplexed digital transmission. Inmarsat-B/M SCPC communication channels use framing to demultiplex the voice, sub-band data, and dummy bits; to synchronize the descrambler and FEC decoder; and to provide frame boundary indications for the voice decoder [1][2]. Inmarsat-B/M TDM signalling channels use framing for similar purposes. Frame synchronization statistics are also used as a real-time measure of in-service error performance on both types of channels.

The main motivation for considering frame synchronization performance improvement on these channels is related to its effect on overall synchronization performance. The overall synchronization scheme comprises in order carrier, clock, and frame synchronization parts. Each part is a necessary but not sufficient condition for subsequent parts. Therefore, overall sync acquisition performance depends on performance of each of its parts. If the frame synchronization part is implemented separately from the other parts, then overall acquisition performance remains constant as frame sync performance is improved, and combined carrier and clock acquisition performance is correspondingly relaxed. The overall acquisition performance requirements together with the specified frame synchronization scheme for these Inmarsat-B/M channels imply performance requirements on combined carrier and clock acquisition which are difficult to achieve especially under high bit error rate channel conditions. Therefore, improved frame sync schemes could make it easier to achieve cost-effective implementation of an overall synchronization scheme for these channels. In addition, a better framing scheme may result in more accurate and more reliable in-service error monitoring.

The performance of a framing scheme is typically described by three random quantities. These are a) the true lock time, T_{LO}, which is the time between true declaration of sync and false declaration of sync loss due to channel errors; b) the false maintenance time, T_{MF}, which is the time during which a false framing codeword pattern is temporarily assumed to be correct; and c) the search time, T_{FT}, which is the time required to locate the true framing codeword.

The true lock time (T_{LO}) gives a measure of the robustness of the framing scheme to channel bit errors. Because of random or burst channel errors, framing schemes may incorrectly determine that synchronization has been lost and initiate a new search for syncwords. When this false out-of-sync declaration occurs, the information in the frame is lost until synchronization is reacquired. In order to increase the information throughput and the reliability of in-service channel BER monitoring, a longer true lock time is desirable.

The false maintenance time (T_{MF}) gives a measure of the detectability of the scheme. Frame synchronization may actually be lost due to a large slip, lightning, or microwave switching. When these true out-of-sync events occur, the framing scheme should detect the event and then start a new search as soon as possible. This detection will take a variable amount of time, since information bit

411

patterns may occasionally resemble the syncword pattern. A shorter false maintenance time is desirable.

The search time (T_{FT}) gives a measure of the speed of framing acquisition and reacquisition. A shorter search time is desirable.

The false maintenance time is in general a component of search time because incorrect acceptance of information bits as a frame boundary and then detection of the false acceptance can occur within the search process.

Other framing performance measures may be defined, but these are not directly relevant to the performance optimization with respect to threshold parameters discussed here. Optimization with respect to the number of consecutive syncword tests used to make search and lock decisions would involve other performance measures, such as the frequency of false detection, which is defined to be the probability of declaring an information bit pattern to be a syncword.

FRAME FORMATS AND FRAMING SCHEMES OF INMARSAT-B/M SCPC AND TDM CHANNELS

The frame format of the Inmarsat-B 24 kbps SCPC channel [1] is shown in Figure 1 (a), where the number of framing bits or syncword length is N=48 bits and the syncword repeats every frame length M=1920 bits, which corresponds to a frame duration T_M=80 ms. To obtain fast reacquisition for short interruptions by blocking and shadowing, the Inmarsat-M 8 kbps SCPC channel uses the N=24 bit unique word as the syncword in each M=480 bit subframe which corresponds to a subframe duration T_M=60 ms [2], as shown by Figure 1 (b). Figure 1 (c) illustrates the frame format of the Inmarsat-B/M 6 kbps TDM channel [1][2], where N=32 bits, M=1584 bits, and T_M=264 ms.

Frame sync strategies have been specified by Inmarsat for each of SCPC/B, SCPC/M, and TDM/B-M types of channels [1][2]. The framing scheme employed by Inmarsat for the 24 kbps SCPC/B channel is as follows:

(a) Frame synchronization loss shall be deemed to have occurred if "total frame pattern loss" has occurred in both of any two consecutive (exactly 80 ms apart) received framing bit patterns.

(b) Frame synchronization acquisition (or reacquisition) shall be deemed to have been achieved when two consecutive (exactly 80 ms apart) framing bit patterns are received without the occurrence of "partial
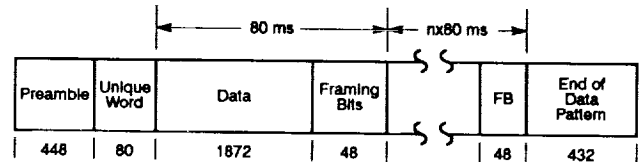
(a) 24 kbps Inmarsat-B SCPC Communications Channel
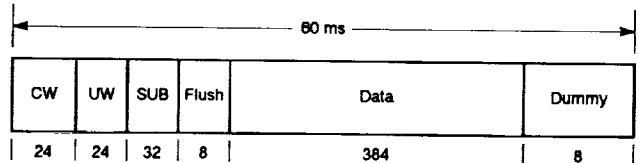
(b) 8 kbps Inmarsat-M SCPC Communications Channel
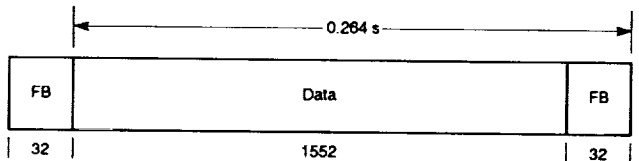
(c) 6 kbps Inmarsat-B/M TDM Signalling Channels

Figure 1. Frame Formats of Inmarsat SCPC and TDM Channels.

frame pattern loss" in the first of the framing bit patterns and without the occurrence of "total frame pattern loss" in the second of the framing bit patterns.

"Total frame pattern loss" and "partial frame pattern loss" are defined as the occurrence of more than 8 and 6 bit errors respectively in the 48 bit syncword.

If the error thresholds for "total frame pattern loss" and "partial frame pattern loss" are represented by e_m and e_s respectively, then setting e_m=8 and e_s=6 describes the SCPC/B framing scheme. Letting the number of consecutive pattern tests for frame sync acquisition and loss declaration be represented by α and β respectively, and then setting α=2 and β=2 further describes the Inmarsat-B SCPC channel framing scheme. Parameters e_m, e_s, α, and β are used to describe each framing scheme in this paper. The Inmarsat-specified values of these parameters for each framing scheme are given in Table 1.

The state transition diagram is commonly used to model a framing scheme [3][4]. For the framing scheme defined for the 24 kbps SCPC/B channel, the state transition diagram is given by Figure 2 (a). The framing scheme defined for the 8 kbps

412
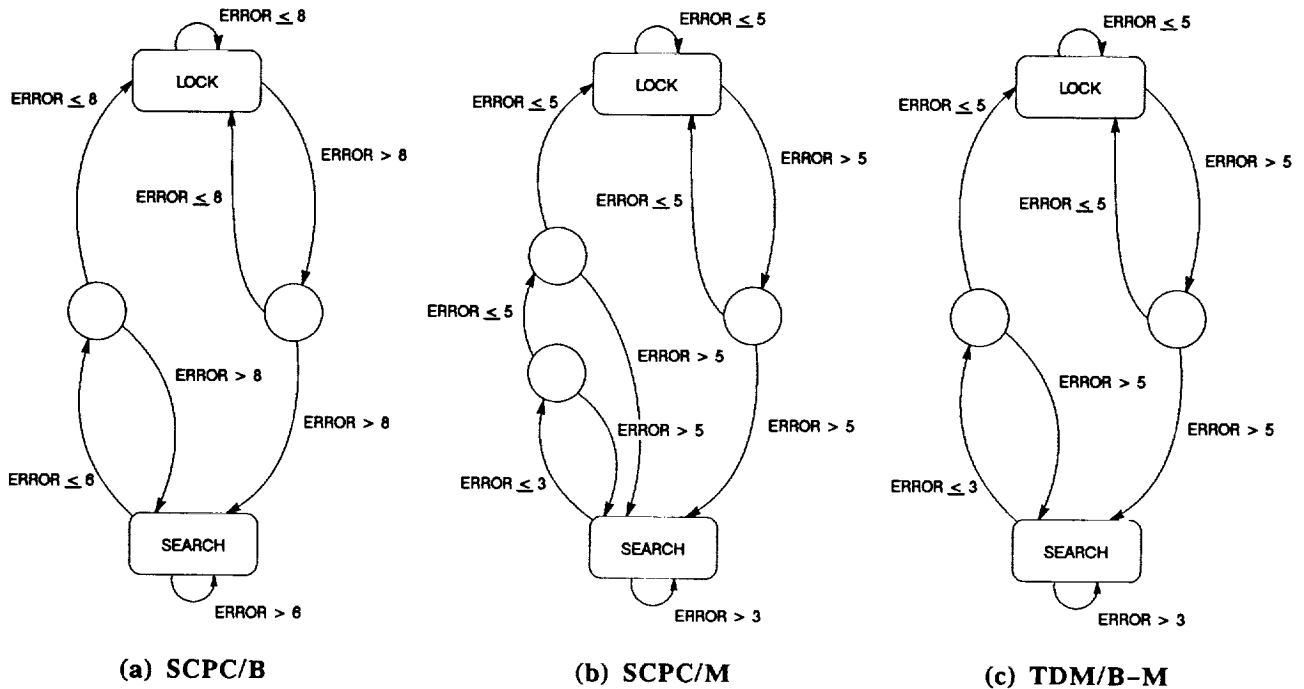
Figure 2. State Transition Models for Inmarsat-Specified Framing Schemes.

SCPC/M and 6 kbps TDM/B-M channel [1][2] is similarly obtained as shown by Figure 2 (b) and Figure 2 (c) respectively.

MEAN VALUES OF FRAMING PERFORMANCE MEASURES

The three performance measures—T_{LO}, T_{MF}, and T_{FT}—are random variables. Their expected values are used as the evaluation criteria upon which to determine an optimum scheme. Variance of these performance measures is not considered in the optimization. The probability distribution of these performance measures can be computed by using methods developed in [5].

To develop the mean of the true lock time $(\overline{T}_{LO})$ and the false maintenance time $(\overline{T}_{MF})$ for each of the three framing schemes, a general maintenance flow graph shown in Figure 3 is used. A substitute symbol p is used to represent transition probability P_{MF} for false maintenance and P_{MT} for true lock, where for given values of threshold e_m and channel error rate P_e:

$$P_{MF} = \sum_{x=0}^{e_m} \binom{N}{x} (0.5)^N \qquad (1)$$

$$P_{MT} = \sum_{x=0}^{e_m} \binom{N}{x} P_e^x (1 - P_e)^{N-x} \qquad (2)$$
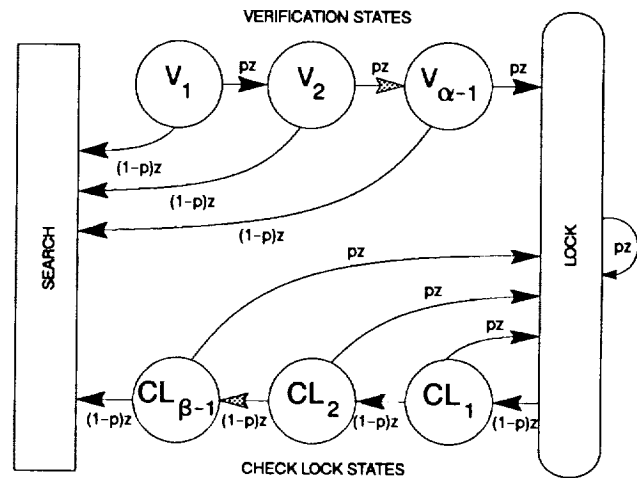
$p=P_{MF}$ for developing mean of T_{MF}
$p=P_{MT}$ for developing mean of T_{LO}

Figure 3. General Maintenance Flow Graph for Framing Schemes.

The transition delays, z, in the flow graph are equal to T_M, whose value depends on the frame format under study. In the general flow graph, $(\alpha-1)$ consecutive verifications lead to declaration of correct alignment, indicated by V_1, V_2,... $V(\alpha-1)$. Similarly, $(\beta-1)$ consecutive failed checks in the lock state are indicated by intermediate states CL_1, CL_2,...$CL(\beta-1)$.

413

If V1 is defined as the starting state and the search state is defined as the absorbing state in the general flow graph, then the mean of the false maintenance time is obtained by evaluating the first derivative of the generating function for the resulting specific flow graph at z=1. The generating function is developed by applying Mason's formula on the flow graph [3]. The mean of the false maintenance time is determined to be

$$T_{MF} = \left[\frac{1 - (P_{MF})^{\alpha - 2}}{(1 - P_{MF})} + \frac{(P_{MF})^{\alpha - 2}}{(1 - P_{MF})^{\beta}} \right] T_M \qquad (3)$$

By using a similar analysis, but defining the lock state as the starting state, the mean of the true lock time is developed as

$$T_{LO} = \left[\frac{1 - (1 - P_{MT})^{\beta}}{P_{MT}(1 - P_{MT})^{\beta}} \right] T_M \qquad (4)$$

The search process is very complex. The mean and probability distribution of the search time has been developed [5], and the results are used in this paper. Assuming the starting position of the search process is uniformly distributed among all bit positions in a frame, the average search time may be computed from the average maximum reframe time ($\overline{T}_{RF}$) and the bit time (T_b) as

$$T_{FT} = \frac{1}{2} \left[\overline{T}_{RF} + (1 - P_{AT}) \ \overline{T}_{RF} + T_b \right] \qquad (5)$$

The average maximum reframe time, which represents the worst case of the search starting position, is given [5] by

$$T_{RF} = \frac{T_M + (M - 1)P_{AF}\overline{T}_{MF}}{P_{AT}} \qquad (6)$$

where P_{AT} and P_{AF} are the transition probabilities for acquisition.

Assuming random information bits and sync-word patterns with sharply peaked autocorrelation, the transition probability P_{AF} and P_{AT} in (6) can be calculated by using

$$P_{AF} = \sum_{x=0}^{e_s} \binom{N}{x} (0.5)^N \qquad (7)$$

$$P_{AT} = \sum_{x=0}^{e_s} \binom{N}{x} P_e^x (1 - P_e)^{N-x} \qquad (8)$$

PERFORMANCE EVALUATION AND OPTIMIZATION

Based on equations (1) through (8), the mean values of three performance measures (T_{LO}, T_{MF}, and T_{FT}) for each of the previously defined Inmarsat framing schemes are evaluated at various channel error rates. The channel error rate P_e ranges between 0.01 and 0.04 for Inmarsat SCPC and TDM channels at specified values of C/No. The evaluation is carried out for an extended channel error rate range from 0.1 to 0.01 in order to take the effect of deep fading into account.

The shortest possible search time, the shortest possible false maintenance time, and the longest possible true lock time are desired for any framing system. To find an optimum framing scheme, these performance measures should be calculated for a range of scheme parameters (e_m, e_s, α, and β).

It has been found that better performance may be obtained by using schemes with threshold parameters (e_m, e_s) different from those specified by Inmarsat. Framing schemes with significantly improved performance relative to the specified schemes have been found for each of the 24 kbps SCPC/B, 8 kbps SCPC/M, and 6 kbps TDM types of channels. The parameters of these improved framing schemes are given in Table 1. The evaluated performance of these improved schemes is given in Tables 2, 3, and 4. The performance of the framing schemes currently specified by Inmarsat is shown for comparison.

As indicated in Tables 2, 3, and 4, the suggested framing schemes show improved framing performance for all three types of channels. Compared with the specified schemes, the average true lock times of the suggested schemes are much longer, while the average search times and reframe times are either somewhat shorter or remain the same. False maintenance times are essentially the same for both specified and suggested schemes.

For a channel with errors, the designer must seek a compromise between the conflicting objectives of maximizing true lock time and minimizing false maintenance time. The improvement obtained in the true lock time results from the fact that appropriately increasing e_m greatly increases the true lock time while the false maintenance time is only slightly increased. This does not significantly alter the search performance. The improvement in search performance is obtained by finding a best combination of the values of e_s and e_m.

The framing performance may be further improved by changing the values of α and β. This

414

Table 1 Framing Scheme Parameters

		e_m	e_s	α	β
24 kbps SCPC/B	specified	(8)	(6)	(2)	(2)
	suggested	12	7	2	2
8 kbps SCPC/M	specified	(5)	(3)	(3)	(2)
	suggested	6	2	3	2
6 kbps TDM/B-M	specified	(5)	(3)	(2)	(2)
	suggested	7	3	2	2

Table 2 Performance Comparison between Specified and Suggested Framing Schemes for 24 kbps SCPC/B (T_M=80 ms)

		$\overline{T}_{LO}$ (hr)	$\overline{T}_{FT}$ (ms)	$\overline{T}_{RF}$ (ms)	$\overline{T}_{MF}$ (ms)
Specified Scheme	Pe=0.01	$1.6 \cdot 10^{16}$	40.03	80.05	80.001
(e_m=8, e_s=6, α=2, β=2)	Pe=0.05	1816.2	40.24	80.24	80.001
	Pe=0.1	0.0664	49.14	89.15	80.001
Suggested Scheme	Pe=0.01	$2.5 \cdot 10^{17}$	40.03	80.05	80.17
(e_m=12, e_s=7, α=2, β=2)	Pe=0.05	$7.83 \cdot 10^{9}$	40.17	80.28	80.17
	Pe=0.1	704.3	44.02	80.30	80.17

Table 3 Performance Comparison between Specified and Suggested Framing Schemes for 8 kbps SCPC/M (T_M=60 ms)

		$\overline{T}_{LO}$ (hr)	$\overline{T}_{FT}$ (ms)	$\overline{T}_{RF}$ (ms)	$\overline{T}_{MF}$ (ms)
Specified Scheme	Pe=0.01	$1.8 \cdot 10^{12}$	40.10	82.19	60.008
(e_m=5, e_s=3, α=3, β=2)	Pe=0.05	1033.7	42.09	82.68	60.008
	Pe=0.1	0.302	48.74	89.83	60.008
Suggested Scheme	Pe=0.01	$4.2 \cdot 10^{15}$	32.00	63.99	60.065
(e_m=6, e_s=2, α=3, β=2)	Pe=0.05	85924.9	33.96	65.95	60.065
	Pe=0.1	5.886	49.44	81.44	60.065

Table 4 Performance Comparison between Specified and Suggested Framing Schemes for 6 kbps TDM/B/M (T_M=264 ms)

		$\overline{T}_{LO}$ (hr)	$\overline{T}_{FT}$ (ms)	$\overline{T}_{RF}$ (ms)	$\overline{T}_{MF}$ (ms)
Specified Scheme	Pe=0.01	$1.03 \cdot 10^{11}$	134.02	268.04	264.14
(e_m=5, e_s=3, α=2, β=2)	Pe=0.05	97.31	139.584	273.60	264.14
	Pe=0.1	0.0591	205.91	339.93	264.14
Suggested Scheme	Pe=0.01	$6.1 \cdot 10^{14}$	134.04	268.07	265.86
(e_m=7, e_s=3, α=2, β=2)	Pe=0.05	201088.0	139.590	273.63	265.86
	Pe=0.1	6.775	205.93	339.96	265.86

has not been done in this work. Changing the values of α and β will not only greatly affect the variance of the three performance measures, but also change the frequency of false detection. Frequency of false detection is nearly the same for Inmarsat–specified schemes as for the suggested improved schemes.

CONCLUSION

This paper has presented equations for performance measures that can be used to evaluate the framing performance of Inmarsat–B/M SCPC and TDM channels. Based on these equations, currently specified framing schemes have been evaluated and improved schemes have been proposed. These proposed schemes all show much longer average true lock times, very slightly longer average false maintenance times, and either nearly unchanged or shorter average search times. Thus, the proposed framing schemes would greatly improve the robustness of frame synchronization on these Inmarsat channels, especially for the case of high channel error rates. The significant reduction in false out–of–sync events not only increases information throughput but also reduces the frequency of false loss–of–synchronization alarms and therefore increases the reliability of real–time in-service channel BER monitoring. The proposed framing schemes also improve or leave unaffected the acquisition/reacquisition performance. Improved frame sync acquisition performance could

ease implementation of the overall synchronization scheme. The only price paid for these improvements is a very slight degradation in the detectability performance of the schemes. The impact of this small degradation is not significant. These frame sync performance improvements can be achieved simply by changing the values of the threshold parameters of the framing scheme. This change is easy to perform on existing frame sync implementations. Therefore, it is recommended that these proposed schemes replace those currently specified by Inmarsat.

REFERENCES

[1] *Inmarsat–B System Definition Manual*, Issue 3.0, November 1991.

[2] *Inmarsat–M System Definition Manual*, Issue 3.0, November 1991.

[3] R. W. Sittler, "System Analysis of Discrete Markov Process," *IRE Transactions on Circuit Theory*, vol. CT–3, no. 12, pp. 257–66, 1956.

[4] E. V. Jones and M. N. Al–Subagh, "Algorithm for Frame Alignment – Some Comparisons," *IEE Proceedings*, vol. 132, no. 7, pp. 525–36, 1985.

[5] D. E. Dodds, S. M. Pan, and A. G. Wacker, "Statistical Distribution of PCM Framing Times," *IEEE Transactions on Communications*, vol. COM–36, no. 11, pp. 1270–75, 1988.

Estimation of Frequency Offset In Mobile Satellite Modems

W.G. Cowley†, M. Rice and A.N. McLean
Digital Communications Group
University of South Australia
The Levels, Pooraka, South Australia 5095
fax +61-8-302 3873
†(Currently at the Communications Research Centre, Ottawa
and the University of Ottawa, Electrical Engineering Dept.)

Abstract

In mobilesat applications, frequency offset on the received signal must be estimated and removed prior to further modem processing. A straightforward method of estimating the carrier frequency offset is to raise the received MPSK signal to the M-th power, and then estimate the location of the peak spectral component. An analysis of the lower signal to noise threshold of this method is carried out for BPSK signals. Predicted thresholds are compared to simulation results. It is shown how the method can be extended to π/M MPSK signals. A real-time implementation of frequency offset estimation for the Australian mobile satellite system is described.

1 Introduction

Frequency uncertainty in mobile satellite applications arises from doppler offsets due to vehicle motion or local oscillator drift. As the symbol rate r_s is usually low, the frequency offset can be a substantial fraction of r_s and must be removed prior to receive filtering and carrier or timing synchronisation.

A number of previous approaches have used frequency offset detectors in a feedback loop to correct for frequency shifts e.g. [1]. Relatively little attention has been given to feedforward estimators which operate over a block of symbols. In burst mode applications where rapid acquisition is important, the feedforward form of estimation is desirable.

Estimation of the frequency offset during carrier only or preamble portions of the received signal is easier than when modulation is present. Most of this paper concerns the case when random BPSK or QPSK symbols are transmitted. Estimation of the frequency offset with carrier is examined in [2].

A relatively simple form of estimating the frequency offset involves stripping the modulation by raising the MPSK signal to the M-th power, and then es-

timating the location of the resulting spectral peak via the Fast Fourier Transform (FFT) algorithm. This will be called the FFT method. Other forms of nonlinearity may be used for removing the modulation (e.g. [3]), but only the M-th power operation is considered in this paper.

The frequency resolution of the FFT method is limited by the the duration of the received signal. However it is possible to improve the accuracy of locating a single spectral component by interpolating between the largest bins, or by evaluating the Discrete Fourier Transform iteratively to locate the spectral peak. In practice, small errors in the frequency estimate (e.g. less than 1% of r_s) may not matter since they can be removed during carrier phase recovery.

An interesting alternative to the FFT method has been reported in [4]. This technique effectively estimates the autocorrelation function of the M-th power signal at selected lags and uses this to efficiently estimate the spectral peak location.

Section 2 analyses the FFT method for BPSK, in order to predict the probability of failure. In section 3, simulated results are compared to the predicted results for BPSK. In addition simulations of QPSK are presented. In section 4 a modified version of the FFT method is described which can be used with π/M versions of MPSK. Finally, section 5 presents a summary of the real-time implementation of frequency estimation and signal detection strategies for preamble and message signals.

2 Threshold Analysis for the FFT Method

An important question concerning the FFT method of frequency offset estimation is when the technique is likely to fail due to a noise peak in the FFT being larger than the desired signal peak. In this case, since the offending noise peak may occur at any bin in the FFT
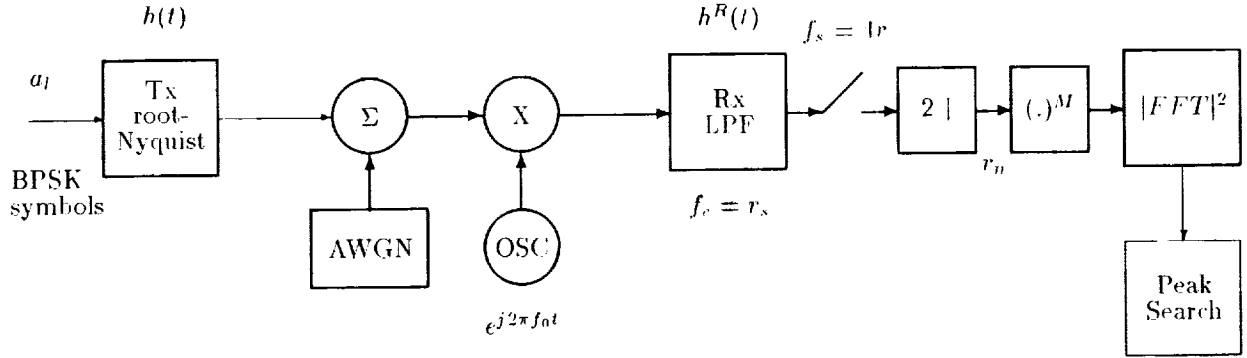
Figure 1: Baseband Signal Model for FFT Method of Frequency Offset Estimation

output, the resulting estimate is effectively a uniformly distributed random variable with no correlation to the actual offset. The probability of failure is primarily a function of the E_b/N_0, the number of symbols used, and the signal constellation size M. This failure threshold is analysed for BPSK signals in this section.

The signal model employed is shown in Figure 1. Thick lines indicate complex-valued quantities. Standard square-root raised-cosine transmit filtering is assumed, with transmit filter impulse response $h(t)$. At the receiver, frequency estimation must be carried out before normal receive filtering since the frequency offset may be a substantial fraction of the symbol rate. In this model an ideal filter with twice the normal bandwidth is used, i.e. $f_c = r_s$ Hz, prior to frequency estimation. It is assumed that the filtered signal is sampled and then decimated by a factor of 2, to two samples per symbol period T. This is the minimum possible sampling rate, and furthermore ensures that the noise samples are independent which makes the following analysis tractable. The use of 2 samples per T, allows a frequency offset f_o of up to $\pm r_s/4$, for example, for QPSK, or twice this amount for BPSK. The effect of not decimating the signal, and using 4 samples per T, is investigated by simulation in section 3 and found to be quite similar to the minimum sampling-rate case under discussion.

Received signal samples before the squarer can be expressed

$$r_n = s_n + w_n \tag{1}$$

with the signal component s_n

$$s_n = e^{j2\pi f_o n 2 T_s} \sum_k a_k h(\tau + n2T_s - kT) \tag{2}$$

where a_k is the k-th transmitted symbol $= \pm 1$, T_s is the initial sampling period $= T/4$ and τ is an arbitrary

time offset. The signal samples are taken without timing recovery or matched filtering and so contain significant InterSymbol Interference (ISI). The squared signal is a "noisy" complex exponential; this section assumes that the random components in s_n^2 are uncorrelated and small compared to the thermal noise terms. These assumptions appear to be justified at low signal to noise ratios. σ_S^2 will denote $E\{|s_n|^2\} = E_b/4$. The zero-mean complex-valued noise samples w_n have real and imaginary parts whose variance will be denoted σ_R^2 equal to $N_0/4$.

Consider now the power estimates from the Discrete Fourier Transform of N received samples raised to the M-th power i.e. $r_0^2, r_1^2 \cdots r_{N-1}^2$. Let

$$P_m = \left| \sum_{n=0}^{N-1} (s_n + w_n)^2 e^{-j2\pi nm/N} \right|^2 \tag{3}$$

for $m = 0, \cdots N - 1$ Let the bin containing the signal peak be at $m = m_S$; this value of P_m will be denoted P_S. The other bins contain independent noise power estimates. Any noise bin ($m \neq m_S$) will be denoted P_N.

To determine the mean value of the noise power estimates, from the last equation

$$E\{P_N\} = E\left\{ \sum_p \sum_q (s_p + w_p)^2 (s_q^* + w_q^*)^2 \right.$$
$$\left. e^{-j2\pi m(p-q)/N} \right\} \text{ for } m \neq m_S \tag{4}$$

where $*$ denotes complex conjugate. The only non-zero terms in this expression arise from one of the signal times noise components and the noise-only components.

418

The former term is

$$E\{\sum_p \sum_q 4s_p w_p s_q^* w_q^* \epsilon^{-j2\pi m(p-q)/N}\}$$

which, remembering that the noise samples are independent, simplifies to

$$\sum_p 4E\{|s_p|^2\}E\{|w_p|^2\} = 8N\sigma_S^2\sigma_R^2$$

and the latter term is

$$E\{\sum_p \sum_q w_p^2 w_q^{*2} \epsilon^{-j2\pi m(p-q)/N}\}$$

which simplifies to, using $E\{x^4\} = 3\sigma_x^4$ when x is $N(0, \sigma_x^2)$

$$\sum_p E\{|w_p|^4\} = 8N\sigma_R^4$$

The final result is

$$E\{P_N\} = 8N(\sigma_S^2\sigma_R^2 + \sigma_R^4) \qquad (5)$$

Space does not permit a full derivation of the mean and variances of P_S and P_N in this paper. Proceeding in a similar fashion to that illustrated above, the following results are obtained:

$$\sigma_{P_N} = E\{P_N\} \qquad (6)$$
$$E\{P_S\} = N^2\sigma_S^4 + E\{P_N\} \qquad (7)$$
$$\sigma_{P_S}^2 = \sigma_{P_N}^2 + 16N^3\sigma_R^2\sigma_S^4(\sigma_S^2 + \sigma_R^2) \qquad (8)$$

These results assume that terms of order N have been neglected from the variance expressions.

In order to compute the probability that $P_N > P_S$ we need to know the density functions of P_N and P_S. These distributions are not obvious due to the non-linear operation before the FFT. However it may be observed that (5) to (8) correspond exactly to the expressions for mean and variance of chi-square and non-central chi-square distributions (e.g. [5] (1.1.109) and (1.1.122)) each with 2 degrees of freedom. Using these distributions

$$p_{P_N}(p_N) = \frac{1}{2\sigma^2}e^{-p_N/2\sigma^2} \text{ for } p_N \geq 0 \qquad (9)$$

$$p_{P_S}(p_S) = \frac{1}{2\sigma^2}e^{-(s^2+p_S)/2\sigma^2}I_0(\sqrt{p_S}s/\sigma^2)$$
$$\text{for } p_S \geq 0 \qquad (10)$$

where $2\sigma^2 = E\{P_N\}$, $s^2 = N^2\sigma_S^4$ and $I_0()$ is the zero-th order modified Bessel function of the first kind.

Let p_F denote the fail probability when any $P_N > P_S$. Then

$$p_F = 1 - \text{prob}(\text{ all } P_N < P_S)$$
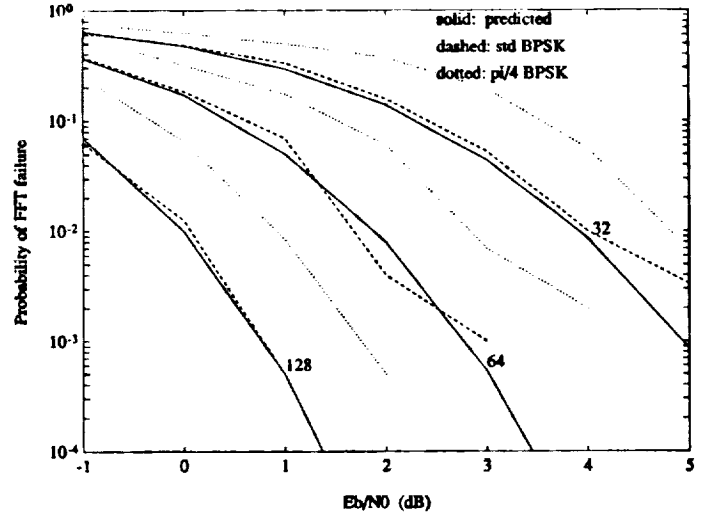
Figure 2: Failure Probability for BPSK Signals

For a given value p_S, of P_S, since the P_N are independent,

$$\text{prob}(\text{ all } P_N < p_S) = \left(\int_0^{p_S} p_N(p_N)dp_N\right)^{N-1}$$
$$= \left(1 - e^{-p_S/2\sigma^2}\right)^{N-1}$$

and so

$$p_F = 1 - \int_0^\infty \left(1 - e^{-p_S/2\sigma^2}\right)^{N-1} p_{P_S}(p_S)dp_S \qquad (11)$$

When (10) is substituted into (11), the failure probability may be integrated numerically.

From here it is easy to predict the variance of the resulting errors in the frequency estimate $\hat{f}_o$. Letting $\Delta f_o = \hat{f}_o - f_o$, as Δf_o is uniformly distributed, with either $|\Delta f_o| < f_s/2$ when the FFT fails, else $|\Delta f_o| < f_s/2N$, gives

$$\sigma_{\Delta f_o}^2 = \frac{1}{12}\left((\frac{f_s}{2})^2 p_F + (\frac{f_s}{2N})^2(1 - p_F)\right) \qquad (12)$$

where N is the FFT size.

3 Simulation Results for the FFT Method

The signal model in Figure 1 was simulated in order to check the predicted FFT thresholds derived in section 2. A normalised symbol rate of 1 symbol per second was used. The continuous-time signals in Figure 1 were simulated with 4 samples per T. The excess bandwidth parameter in the transmit filter was 40%.

During the simulations, packets of random bits were generated and a random frequency offset between

419
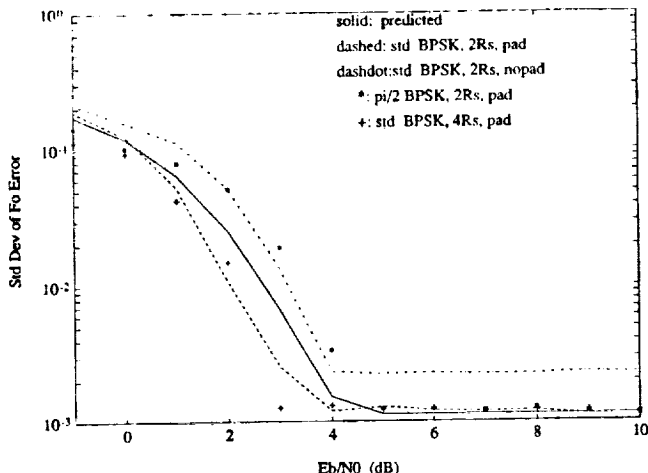
Figure 3: Frequency Accuracy for 64 BPSK Symbols

Figure 4: Frequency Accuracy for 64 QPSK Symbols

$\pm r_s/4$ was added. The FFT size was twice the number of symbols received, without any zero padding of the data samples and with the decimation shown in Figure 1. When the data was zero padded with an equal length of zeros, the FFT was four times the number of symbols. The zero padding gives improved performance since it reduces the signal loss caused by frequency offsets at non-integer multiples of the initial frequency resolution, and the frequency accuracy is improved. It could be argued that the effective number of independent noise bins in the FFT output is the same (N) with or without zero padding; this seems to be supported by simulation.

Figure 2 shows a plot of FFT failure probability for 32, 64 and 128 bit BPSK signals. The predicted values from (11) are plotted with solid lines. These simulations used twice oversampling (i.e. 2 samples per T) and zero padding. (Since the analysis effectively assumes bin-centred doppler frequencies, the use of zero padding is appropriate to remove most of the loss due to random frequency offsets.) The figure shows fairly good agreement between the predicted and measured results for BPSK. The lack of simulation results at low values of p_F reflects the difficulty in simulating rare FFT failures at high signal to noise ratios. Plots for $\pi/2$ BPSK are discussed in the next section.

In Figure 3 the standard deviation of the frequency error Δf_o is plotted for 64 bit BPSK signals and compared to the predicted value from section 2. In the evaluation of (12), N was doubled for comparison with simulations using zero padding. All the simulations show approximately similar thresholds in the vacinity of $E_b/N_0 = 4$ dB, below which the frequency error increases rapidly as the failure probability becomes significant. It can be seen that twice oversampling without padding gives slightly worse results, as expected.

Four times oversampling, with padding, has been included for comparison. In this case the noise samples are correlated and the noise spectrum is no longer flat, as it is for section 2. Notice that the final accuracy, above threshold, is the same as two samples per T with padding, as expected.
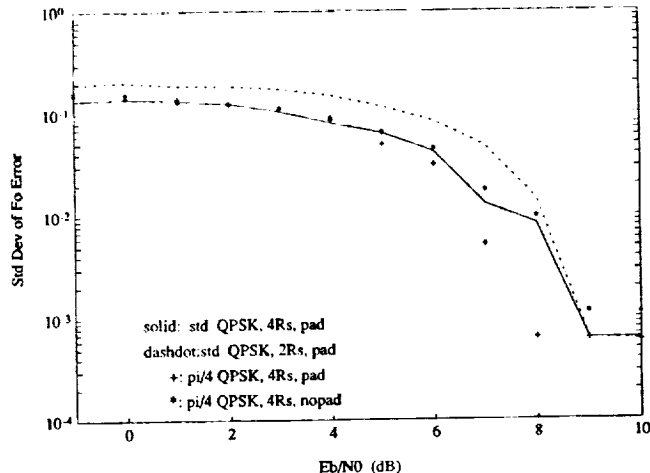
Figure 4 shows 64 symbol QPSK simulations of frequency accuracy using the FFT method. Again the vertical scale is relative to $r_s = 1$ symbol/sec. The threshold is significantly higher than the $M = 2$ case (almost 6 dB). Again the thresholds for $2r_s$ or $4r_s$ sample rates appear to be similar, and the advantages of padding can be seen.

Reliable frequency estimation below the thresholds shown in figures 3 and 4 could be obtained by using more symbols per FFT, or by combining results from separate FFTs (see section 5).

4 Frequency Estimation for π/M MPSK

Variants of MPSK modulation such as $\pi/2$ BPSK (or Aviation BSPK) and $\pi/4$ QPSK can readily be handled by the FFT method of frequency offset estimation. These modulation schemes are now used in some mobile satellite systems (e.g. [6]). They rotate alternate symbols by π/M radians which reduces the amplitude variations in the transmitted signal.

The effect of these symbol rotations can be appreciated as follows. Suppose that the receive signal has been ideally filtered and sampled at one sample per T with no ISI or thermal noise present. The sampled signal could be written

$$a_0, \; a_1 e^{j\pi/M} e^{j\delta}, \; a_2 e^{j2\delta}, \; a_3 e^{j\pi/M} e^{j3\delta}, \cdots$$

420
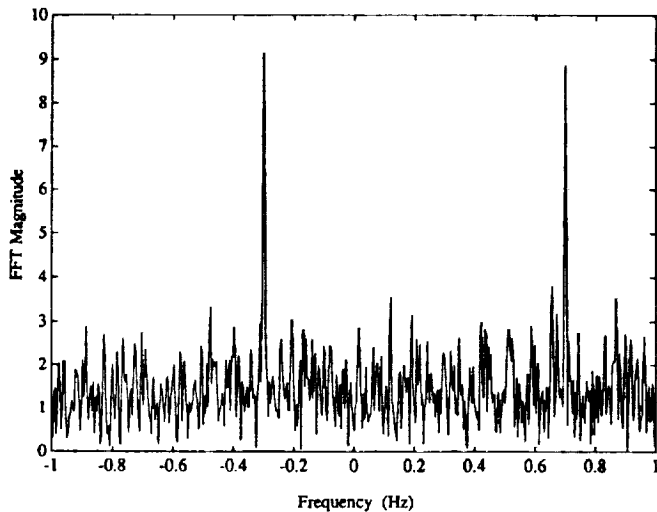
Figure 5: Sample Power Spectrum for $\pi/2$ BPSK

where $\delta = 2\pi f_o T$ represents the phase change per symbol period due to frequency shift. After the M-th power operation the samples become

$$a_0^M, \quad a_1^M e^{j\pi} e^{jM\delta}, \quad a_2^M e^{j2M\delta}, \quad a_3^M e^{j\pi} e^{j3M\delta}, \cdots$$

If $a_k \in e^{j2\pi/M}, k = 0, 1, \cdots M - 1$, then $a_k^M = 1$ so the previous sequence can be written

$$1, \quad -e^{jM\delta}, \quad e^{j2M\delta}, \quad -1e^{j3M\delta}, \quad \cdots$$

This represents a discrete-time complex exponential, whose frequency is M times the original f_o, which has been modulated by a sequence of alternating sign, $\cdots 1, -1, 1, -1 \cdots$, of period $r_s/2$. (The MPSK case would be the same except for the alternating signs.) The signal spectral component is therefore split into two discrete components, separated from Mf_o Hz by $\pm r_s/2$.

In the practical case with more than one sample per symbol period and ISI and/or noise, the effect in the frequency domain is similar. Figure 5 shows a typical spectral estimate from the FFT method for 128 bits of $\pi/2$ BPSK at $E_b/N_0 = 6$dB. The frequency offset was 10% of r_s; two components can therefore be seen at $0.2r_s \pm r_s/2$. It can be observed that the noise spectrum is flat as 2 samples per T were used in this simulation.

In order to estimate the frequency offset for π/M MPSK signals, the peak sum of FFT bins separated by r_s Hz can be located. This is a straightforward extension of the normal peak search method for MPSK. At this stage the analysis described in section 2 has not been extended to $\pi/2$ BPSK, although this should be possible. Some simulation results for π/M MPSK are shown in figures 2, 3 and 4. The higher failure probability in figure 2 might be expected due to the spectral peak splitting and consequent lower noise immunity.

The $\sigma_{\Delta f_o}$ thresholds are slightly higher for $\pi/2$ BPSK, although this appears to be reversed for $\pi/4$ QPSK with four times oversampling. Further simulations would be necessary for precise location of these thresholds since a very small number of FFT failures can significantly effect the shape of the frequency error in the threshold region.

5 Real-Time Implementation

A real time implementation of a frequency estimator was required for use in mobilesat(TM) mobile terminals. The mobile terminals are required to acquire phase acquisition of a 3300 symbols/sec $\pi/4$ QPSK voice activated carrier using a 40ms preamble, or else, assuming loss of the preamble, (due to blockages, fading etc.), within 180ms. In addition, initial acquisition must be obtained using a continuous transmission (during "Call Set Up" mode) within 120ms with a 500Hz frequency offset. These acquisition times are specified at E_b/N_0 of 6dB. Refer to [6] for details.

Two methods were developed to meet these specifications. These incorporated detection, frequency estimation, timing estimation and then phase estimation, in that order. In the case of the preamble, the signal was designed to have two discrete components. This allowed a very reliable and efficient PSD correlation method to be used for detection, frequency and timing estimation. To summarise, four times oversampled data was used, and an FFT length of 256 was chosen, giving a bin width of 51.6Hz. Detection was based on comparison of a peak to average bin correlation ratio with a threshold. A detection threshold was chosen by experiment. This gave 100% correct detects at values of E_b/N_0 down to 3dB. To obtain better resolution than the bin width, an interpolation method was used between bins. This gave a worst case RMS frequency estimate error was of about 6.7Hz, and typically less than 3Hz at 3dB. Running on a 50MHz DSP32C, this required a processing time of 855ms per estimate, and an update rate of every 8 symbols (2.4ms) was chosen. This resulted in measured total carrier acquisition times (ie including detection, frequency timing and phase recovery) of less than 27ms (typically about 26ms) at E_b/N_0 of 6dB. About 10ms of this is due to filtering and phase recovery delays.

In the case of the preambleless (i.e. random data) signal acquisition, the $M = 4$ FFT method was used. As with the preamble case, four samples per symbol period and a 256 length FFT was used without padding (i.e. 64 symbols). This gave an equivalent bin width of 12.8Hz (0.0039 relative to r_s), although using interpolation the frequency resolution could be made much less. Frequency errors of 10.3Hz maximum and 3.8Hz typically at Eb/No of 3dB were recorded, which were

421

considered acceptable given the lock range of the phase recovery technique.

The variance of the signal to noise ratio estimate was found to be too high to produce a reliable detection/rejection rule when compared with a detection threshold. To improve this, the FFT output was lowpass filtered to suppress spurious components from causing erroneous detections. In addition, hysteresis was built into the detection process, to prevent premature detection of signals i.e. before the FFT input buffer had sufficient samples of an unfaded signal to produce an accurate frequency estimate. These two enhancements allowed a trade-off between reliability and detection time to be made. This was done experimentally to meet the mobilesat specifications, and produce very reliable detection and estimation. Total processing delay per frequency estimate was 1050ms and an update rate of 8 symbols was chosen. The typical times for carrier acquisition were measured to be about 80ms at 6dB.

At lower values of E_b/N_0, the detection time was increased although the 120ms specification was still easily met at 3dB. Detection failure was set at about 1.5dB. Signals with lower E_b/N_0 are too noisy to be useful in the given application.

A crucial performance parameter in the random data frequency estimation technique was the input noise bandwidth. Due to the high tolerable frequency offsets ($<$ 1500Hz) the received signal was digitally filtered using a low pass filter with cut-off at 1.25 times the symbol rate (i.e. slightly larger than in sections 2 to 4). This was found to give good performance under all conditions, although improvements could be attained with tighter filtering.

6 Conclusions

A method of analysing the lower E_b/N_0 threshold for the M-th power method of frequency estimation for BPSK signals has been presented. Simulations show reasonable agreement with the predicted probability of the wrong FFT peak being chosen. The FFT method can be readily be adapted to π/M MPSK signals, with a small loss in performance for $\pi/2$ BPSK. Sample simulations for BPSK and QPSK signals give some idea of the effects of oversampling and zero padding on the FFT threshold. An implementation of the FFT method, and related processing, has been tested in real-time operation, and optimised on mobile satellite channels. This includes using the results of multiple transforms, rather than one large one, to produce reliable estimation and detection at the required operating point.

References
[1] T. Alberty , V. Hespelt and H. Gockler, "A Digital Multicarrier Demodulator with Fast Synchronisation for Mobile SCPC Satellite Communications", *Proc. ICDSC-8*

[2] D. Rife and R. R. Boorstyn, " Single-Tone Parameter Estimation from Discrete-Time Observations", *IEEE Trans. Inform. Theory*, Vol. IT-20, No. 5, Sept. 74.

[3] A. J. Viterbi and A. M. Viterbi, "Nonlinear Estimation of PSK-Modulated Carrier Phase with Applications to Burst Digital Transmission", *IEEE Trans. Inform. Theory*, Vol. IT-29, No. 4, July, 1983

[4] S. N. Crozier and K. W. Moreland "Performance of a Simple Delay-Multiply-Average Technique for Frequency Estimation", Proc. *Canadian Conf. on Elec. and Comp. Eng.*, Toronto, Sept. 1992

[5] J. G. Proakis, *"Digital Communications"*, 2nd Ed, McGraw-Hill, 1989

[6] "User Terminals for Accessing the Mobilesat Satellite Communications System", *Standards Australia*, AS 4080, 1992

Theoretical and Simulated Performance for a Novel Frequency Estimation Technique

N94-22808

Stewart N. Crozier

Communications Research Centre
3701 Carling Ave., P.O. Box 11490, Station H, Ottawa, Ontario
K2H 8S2. Canada
ph: 613-998-9262, fax: 613-990-0316

ABSTRACT

A low complexity, open-loop, discrete-time, delay-multiply-average (DMA) technique for estimating the frequency offset for digitally modulated MPSK signals is investigated. A nonlinearity is used to remove the MPSK modulation and generate the carrier component to be extracted. Theoretical and simulated performance results are presented and compared to the Cramer-Rao lower bound (CRLB) for the variance of the frequency estimation error. For all signal-to-noise ratios (SNRs) above threshold, it is shown that the CRLB can essentially be achieved with linear complexity.

INTRODUCTION

Most conventional burst transmission systems with frequency uncertainty provide a preamble of unmodulated carrier and/or a carrier modulated with a known symbol pattern, for initial frequency estimation and synchronization purposes. There are also many other applications where it is desirable to estimate the frequency error from a modulated signal with unknown data. In either case, it is desirable to have a fast, efficient, and accurate frequency estimation algorithm, both for initial acquisition and tracking purposes.

In this paper, a low complexity, open-loop, discrete-time, delay-multiply-average (DMA) approach to estimating the frequency offset for digitally modulated signals is investigated. M-ary phase shift keyed (MPSK) signaling formats are considered. An M-power-type nonlinearity can be used to generate a carrier component when the data symbols are unknown. The special case of pure carrier and/or known symbols is included by setting $M=1$. Performance is theoretically approximated and compared to the Cramer-Rao lower bound (CRLB) for the variance of the frequency estimation error. Simulated performance is also presented and compared to the theoretical approximations and bounds. It is shown that, when optimum delays are employed, performance is within about 0.5 dB of the CRLB for all signal-to-noise ratios (SNRs) above threshold. A simple extension to the DMA algorithm, which approximates true maximum-likelihood (ML) estimation, is also examined. With the ML

extension, the CRLB is essentially achieved for all SNRs above threshold.

Previously known open-loop techniques which provide performance close to the CRLB typically involve some form of fast Fourier transform (FFT) processing [1]. The complexity of FFT based algorithms is order $KL \log_2(KL)$ where K is the observation time in samples and L is the zero-stuffing factor required to obtain the desired frequency resolution using an FFT of size KL. Small L values of 2 or 4 are usually recommended when the FFT is used only for a coarse search [1]. To approach the CRLB, additional processing is required to perform a fine search for the peak of the likelihood function. The complexity of the DMA based algorithm presented in [2] is order KB where B is the number of DMA branches employed. The number of branches required depends on the desired threshold SNR, but can typically be made fewer than $\log_2(K)$ for many applications. For example, 3 branches were found to be sufficient for the MSAT application described in [3], with $K=100$. This paper presents a modified version of the basic DMA algorithm described in [2] and a simple ML extension. In addition to providing improved performance, the complexities of the new DMA algorithm and its ML extension are both of order K.

FREQUENCY ESTIMATION

Single Branch DMA Approach

Figure 1 shows an open-loop frequency phasor estimator, based on the DMA approach. The sampled (discrete) complex baseband received signal, $\{r_k\}$, is modeled as

$$r_k = A a_k \exp(j\omega k) + w_k$$
$$= A a_k W^k + w_k \tag{1}$$

where the complex phasor, W, is defined as
$$W = \exp(j\omega), \tag{2}$$

A is the signal's complex amplitude, a_k represents the MPSK modulation data symbols, given by
$$a_k = \exp(j2\pi m/M), \quad m \in \{0,...,M-1\}, \tag{3}$$

ω is the frequency offset measured in radians per sample or symbol period, T, and w_k is additive noise.
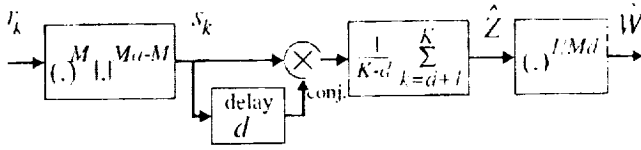
Fig. 1: Single branch DMA frequency estimator.

The sample SNR at the receiver input is defined as

$$\gamma = \frac{P_r}{P_w} = \frac{|A|^2}{E\left[|w_k|^2\right]} \tag{4}$$

where E[.] denotes the expected value operator. For mathematical convenience, and without any loss in generality, it is assumed that |A|=1, so that P_r=1 and P_w=1/γ.

The received signal is first passed through a generalized M-power-type nonlinearity to remove the MPSK modulation. The nonlinearity is generalized in the sense that the phase is multiplied by M but the amplitude can be raised to a different power, namely M_a. From (1), the signal at the output of the nonlinearity is given by

$$s_k = r_k^M |r_k|^{M_a - M} = A^{M_a} W^{kM} + n_k \tag{5}$$

This nonlinearity is equivalent to that introduced in [4] for carrier phase estimation. The noise term, n_k, is quite complicated in general. Although simulation results are presented for different values of M_a and M, the theoretical approximations are restricted to the case of M_a=M. With this restriction, n_k is given by

$$n_k = \sum_{m=1}^{M} \binom{M}{m} w_k^m A^{M-m} W^{k(M-m)} \tag{6}$$

The objective is to obtain an estimate of W, since this phasor contains the phase rotation over a single sample period due to the frequency offset, ω. Multiplying the received signal samples, $\{r_k\}$, by the sequence $\{W^{-k}\}$ would remove the frequency offset. An estimate of

$$Z = W^{Md} \tag{7}$$

is obtained first, and is given by

$$\hat{Z} = \frac{1}{K-d} \sum_{k=d+1}^{K} s_k s_{k-d}^* \tag{8}$$

where K is the number of samples used in the measurement, and d is the delay in sample periods. The estimate of W is then given by

$$\hat{W} = [\hat{Z}]^{1/Md} \tag{9}$$

In the absence of noise and possible phase ambiguities associated with multiple complex roots, it is clear that $\hat{Z} = Z$ and $\hat{W} = W$.

Multiple Branch DMA Approach

There is a fundamental phase ambiguity problem associated with all frequency estimators of this type. Without a previous estimate for guidance, the maximum resolvable frequency offset is less than $1/(2TMd)$ Hz. The larger the delay, the more potential phase ambiguities. The phase ambiguity problem results from not knowing which of the Md complex roots to choose. In most cases the ambiguity can be resolved by employing a ball-park estimate to guide the selection of the appropriate complex root. Given a previous estimate, obtained using delay d_{b-1}, a new estimate, using delay $d_b > d_{b-1}$, can be obtained as follows

$$\hat{W}_b = \hat{W}_{b-1} \left[\frac{\hat{Z}_b}{\hat{W}_{b-1}^{Md_b}} \right]^{1/Md_b} \tag{10}$$

If the delays are selected such that
$$d_b = p_b d_{b-1} \qquad , b = 2...B \tag{11}$$
where p_b is an integer greater than or equal to 2, then (10) is equivalent to

$$\hat{W}_b = \hat{W}_{b-1} \left[\frac{\hat{Z}_b}{\hat{Z}_{b-1}^{p_b}} \right]^{1/Md_b} \tag{12}$$

If the root operation in (10) or (12) always takes the principle root and the phase difference between the current and previous estimate is within π/Md_b, which is the maximum resolvable phase difference with delay d_b, then the overall result corresponds to the correct root and the phase ambiguity is resolved. If the previous phase error is too large to resolve the phase ambiguity, then the incorrect root which is closest to the previous estimate will be selected. Equations (10) and (12) are clearly equivalent to (9) if the appropriate root is selected.

The new DMA based algorithm is depicted in Figure 2. The approach is similar to that given in [2], in that multiple DMA branches are used to resolve potential phase ambiguities as the branch delays increase. The method shown for resolving phase ambiguities is that of (12). This method can be used because the delays are specifically chosen to be increasing powers of 2, resulting in p_b=2 for each branch. The major difference between the DMA approach of Figure 2 and the DMA approach of [2] is the rotate-add-decimate (RAD) operation, which is performed repeatedly on the signal, s_k, at the output of the nonlinearity.

To simplify the description of the technique, the observation time in samples is restricted to be
$$K = 3 \times 2^{B-2}, \qquad B \geq 2, \tag{13}$$
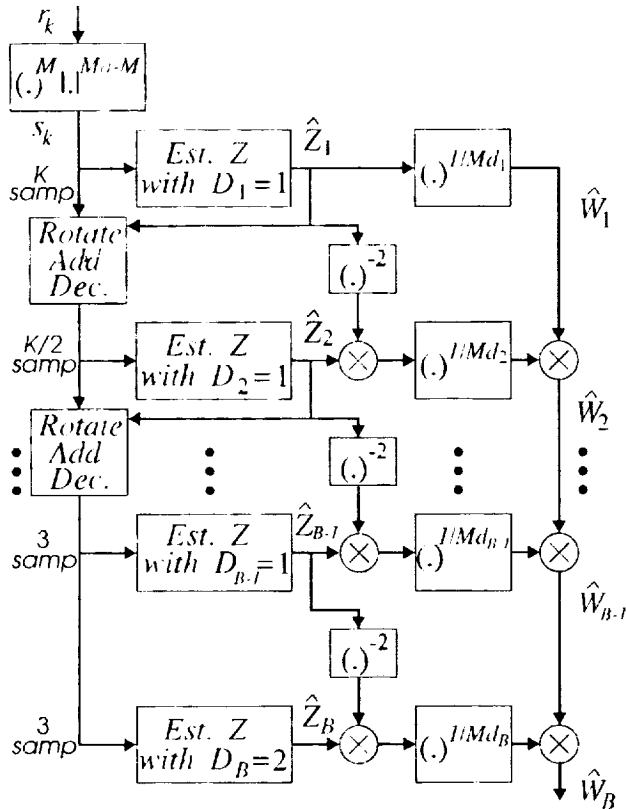
Fig. 2: Bank of B frequency estimators with rotate-add-decimate (RAD) processing.

where it is assumed that at least the bottom 2 branches shown in Figure 2 are employed. More general values of K can be accommodated, but the values of K given in (13) are the most convenient. The desired delays in original samples for the B branches are

$$d_b = 2^{b-1}, \qquad b = 1...B \tag{14}$$

The RAD operation always decimates by 2. Thus the corresponding delays in decimated samples for the B branches are given by

$$D_b = 1, \qquad b = 1...B-1$$
$$= 2, \qquad b = B \tag{15}$$

Only 3 samples are processed in the final 2 branches and the RAD operation is not used between the last 2 branches. This is why a delay of 2 samples is used in the final branch. In [2], it is shown that the optimum delay for the final branch is 2/3 the number of samples.

The idea behind the RAD operation is to pseudo-coherently combine sample pairs to improve the sample SNR by approximately 3 dB, while simultaneously lowering the complexity by reducing the number of samples to be processed later. The RAD operation performed after the b-th branch is given by

$$s_{k,b+1} = s_{2k-1,b} + \hat{z}_b^* s_{2k,b}, \ k = 1...K_{b+1}, \ b = 1...B-2 \tag{16}$$

where

$$\hat{z}_b = \hat{Z}_b / |\hat{Z}_b|, \qquad b = 1...B-2 \tag{17}$$

is the unit amplitude rotation factor applied after the b-th branch, and

$$K_b = 3 \times 2^{B-b-1}, \qquad b = 1...B-1$$
$$= 3, \qquad b = B \tag{18}$$

is the number of decimated samples used to estimate Z in the b-th branch. The RAD operation performed after the b-th branch requires only $K_b/2$ multiplies and adds. The RAD operation removes the estimated frequency error from the input signal in a pairwise fashion, enabling approximate coherent combining. The estimated frequency error is not completely removed, as this would require about $2K_b$ multiplies. The RAD operation also has an interesting frequency domain interpretation. It is equivalent to performing down-conversion, low-pass filtering with a 100% roll-off root-raised-cosine (RRC) filter, decimating-by-2, followed by upconversion or reintroduction of the frequency error. After decimation, the actual frequency error may lie within one of the aliased spectra. The processing used to select the correct root is equivalently selecting the appropriate aliased spectrum.

The majority of the processing is that required to compute the Z estimates for each branch. The total number of complex multiplies and adds is

$$\# mult = 3K - B - 4$$
$$\# adds = 3K - 2B - 4 \tag{19}$$

which indicates a complexity of only order K.

Maximum Likelihood Extension

Consider the pure tone case with $M_a=M=1$ so that $s_k=r_k$ as defined in (1) and (5). The additive noise is assumed to be white and Gaussian with $n_k=w_k$. The maximum likelihood (ML) frequency estimator finds the frequency $\hat{\omega}_{ML} = u$ which maximizes the function

$$f(u) = |S(u)|^2 = S(u) S^*(u) \tag{20}$$

where

$$S(u) = \sum_{k=1}^{K} s_k U^{-k} \tag{21}$$

is the Fourier transform of $\{s_k\}$ with U defined as

$$U = \exp(ju) \tag{22}$$

Newton's method can be used to find the maximum of $f(u)$ by finding the zero-crossing of the first derivative of $f(u)$, provided the initial guess is close to the peak of the main lobe of $f(u)$. A good initial guess is given by the frequency estimate $\hat{\omega}_B = phase(\hat{W}_B)$ from the final branch of the DMA based estimator of Figure 2. The simulation results show that there is little to be gained by using more than a single step of Newton's method. Thus, an approximate ML

425

extension to the DMA based frequency estimator of Figure 2 is given by

$$\hat{\omega}_{ML} \approx \hat{\omega}_B - \frac{f'(\hat{\omega}_B)}{f''(\hat{\omega}_B)}$$

(23)

The first and second derivatives of $f(u)$ are given by

$$f'(u) = 2\,\mathrm{Re}[S'(u)\,S^*(u)]$$

$$f''(u) = 2|S'(u)|^2 + 2\,\mathrm{Re}[S''(u)\,S^*(u)]$$

(24)

where the n-th derivative of $S(u)$ is given by

$$S^{(n)}(u) = \frac{d^n}{du^n}S(u) = \sum_{k=1}^{K}(-jk)^n\, s_k\, U^{-k}$$

(25)

Combining the above results to further simplify (23) gives

$$\hat{\omega}_{ML} \approx \hat{\omega}_B + \frac{\mathrm{Im}\left[S_0\, S_1^*\right]}{|S_1|^2 - \mathrm{Re}\left[S_0\, S_2^*\right]}$$

(26)

where the 3 sums, S_0, S_1 and S_2 are defined as

$$S_n = \sum_{k=1}^{K}k^n\, s_k\, \hat{w}_B^{-k}, \qquad n=0,1,2$$

(27)

with the definition that

$$\hat{w}_B = \hat{W}_B/|\hat{W}_B| = \exp(j\hat{\omega}_B)$$

(28)

With a few further minor manipulations to the sums in (27), it can be shown that the total number of multiplies and adds required to implement the ML extension is upper bounded by

$$\#\,mult = \#\,adds = 2.5K$$

(29)

Thus, the complexity of the ML extension is also order K. The ML extension can also be applied to one of the sets of K_b decimated samples. With this slight modification, the complexity of the ML extension can be reduced even further to that of a constant. It is shown in the next section that the performance penalty with this modification is very small.

THEORETICAL ANALYSIS

For the theoretical results which follow it is assumed that the noise samples, $\{w_k\}$, are Gaussian and uncorrelated, that $M_a=M$ in the nonlinearity, and that all potential phase ambiguities are correctly resolved. An approximation for the variance of the frequency estimator shown in Figure 1, measured in $(\mathrm{radians}/T)^2$, was derived in [2]. The approximation is most accurate for high SNRs and/or long observation times, when the true angular variance of $\hat{W}$ is small. The result is

$$V(K,d,N) = \frac{\min[d,K-d]N}{(K-d)^2 d^2 M^2} + \frac{N^2}{2(K-d)d^2 M^2} \quad (rad/T)^2$$

(30)

where

$$N = \sum_{m=1}^{M}\binom{M}{m}^2 m!\,\gamma^{-m}$$

(31)

is the power of the noise terms defined in (6).

The frequency estimate variance for each of the branches shown in Figure 2 can be approximated by

$$V_b' = (K_b/K)^2\, V(K_b, D_b, N_b), \qquad b=1...B$$

(32)

where K, D_b, and K_b are as defined in (13), (15), and (18), respectively. The scale factor in (32) is required to convert from decimated sample periods back to original sample periods, T, to preserve the units of $(\mathrm{radians}/T)^2$. The N_b term represents the effective noise power at the input to the b-th branch. For SNRs above threshold, the frequency estimation error remaining after each branch is typically well within the 3 dB bandwidth of the 100% roll-off RRC filter used in the following RAD operation. Since this filter cuts the noise power in half each time it is applied, a good approximation for N_b, for SNRs above threshold, is

$$N_b = (K_b/K)\,N, \qquad b=1...B$$

(33)

where K and K_b are again given by (13) and (18). For the final branch in Figure 2, the approximation becomes

$$V_B' = (K_B/K)^2\, V(K_B, D_B, N_B)$$

$$= (3/K)^2\, V(3, 2, 3N/K)$$

$$= \frac{27N}{4K^3 M^2}\left[1 + \frac{3N}{2K}\right] \quad (rad/T)^2$$

(34)

For high SNRs (or for all SNRs with $M=1$), N can be approximated by the first term in (31), which gives

$$N(\gamma \gg 1) \approx M^2 \gamma^{-1}$$

(35)

With this approximation

$$V_B(\gamma \gg 1) \approx \frac{27}{4K^3\gamma} \quad (rad/T)^2$$

(36)

Note that the variance at high SNRs is not a function of M. For low SNRs the extra noise terms become more significant and performance does depend on M. However, for the new DMA frequency estimator with RAD, the last noise term in (34) is reduced by an additional factor of K^{-1}, which is not present for the frequency estimator presented in [2]. At low SNRs, where large values of K are typically required, this improvement can be very significant.

The Cramer-Rao lower bound (CRLB) on the variance of any discrete-time frequency estimator is given by [2, 5]

$$\mathrm{CRLB}(K,\gamma) = \frac{6}{K(K^2-1)\gamma} \quad (rad/T)^2$$

(37)

Comparing this with (36), the degradation in dB relative to the CRLB for the frequency estimator of Figure 2, at high SNRs, is given by

$$\mathrm{Deg}(\gamma \gg 1) \approx 10\log\left(\frac{9(K^2-1)}{8K^2}\right) \quad \mathrm{dB}$$

(38)

For large observation times, $K \gg 1$, the degradation from the CRLB is approximately $10\log(9/8)=0.5$ dB. Note that there is no degradation from the CRLB with $K=3$. The

simulation results show that the performance of the new DMA frequency estimator with RAD remains very close to the CRLB for all SNRs above threshold.

The CRLB, as given in (37), applies to the original K received samples, $\{r_k\}$, and is valid for the MPSK signal model used with any value for M. For the pure carrier case, without a nonlinearity (i.e. $M_a=M=1$), a CRLB can also be derived for each set of K_b decimated samples at the input to the b-th branch of Figure 2. The result is

$$CRLB_b = (K_b/K)^2 \, CRLB(K_b,\gamma_b), \qquad b = 1...B \qquad (39)$$

where K and K_b are defined in (13) and (18). The scale factor in (39) is required to convert from decimated sample periods to original sample periods, T, to preserve the units of $(radians/T)^2$. The γ_b term represents the sample SNR at the input to the b-th branch. Using the same arguments as for (33), a good approximation for γ_b, for all SNRs above threshold, is

$$\gamma_b = (K/K_b)\,\gamma, \qquad b = 1...B \qquad (40)$$

where K and K_b are again given by (13) and (18). Simplifying (39) further gives

$$CRLB_b = \frac{6}{K\left(K^2-(K/K_b)^2\right)\gamma}, \qquad b=1...B \qquad (41)$$

The degradation in the CRLB, measured in dB for the b-th branch, where K_b decimated samples are used instead of the original K samples, is given by

$$Deg_b = 10\log\left[\frac{CRLB_b}{CRLB}\right]$$

$$= 10\log\left[\frac{K_b^2(1-K^{-2})}{K_b^2-1}\right] \, dB, \qquad b=1...B \qquad (42)$$

For $K\gg1$, the degradation is approximately given by

$$Deg_b(K \gg 1) \approx 10\log\left[\frac{K_b^2}{K_b^2-1}\right] \, dB, \quad b=1...B \qquad (43)$$

Representative examples of the degradations in the CRLB for $K_b=3$, 6 and 12 are 0.51, 0.12 and 0.03 dB, respectively. The degradation in the CRLB is clearly negligible for $K_b \geq 12$. Note that the ML extension described earlier can be applied to any set of K_b decimated samples (e.g. $K_b=12$), and not just to the initial set of K samples. Thus, for large values of K, the complexity of the ML extension can be reduced to a fixed constant, independent of K, with negligible degradation in performance. Thus, the complexity of the complete frequency estimator with the ML extension remains approximately $3K$.

EXAMPLE PERFORMANCE RESULTS

The simulated performance results are presented in terms of measured root-mean-squared (RMS) frequency error in (cycles/T) versus sample SNR, γ, in dB. An observation time of $K=48$ samples was used, and 5000 independent trials were simulated for each SNR. Figure 3 shows the results for the case of pure carrier with no nonlinearity ($M_a=M=1$). Three sets of simulation results are shown. The first set, with $d=1$, is for the single branch estimator of Figure 1 or the first branch in Figure 2. The second set, with $d_B=32$, is for the final branch of the new DMA estimator of Figure 2. The third set is for the ML extension applied to the original $K=48$ samples. The performance is essentially the same for a decimated set of 12 or more samples. Also shown, for comparison, are the corresponding theoretical approximations and the CRLB. It is observed that the theoretical approximations are quite accurate for all SNRs above threshold. With the ML extension, the CRLB is essentially achieved for all SNRs above threshold. The threshold SNR is observed to be about 0 dB for this case.
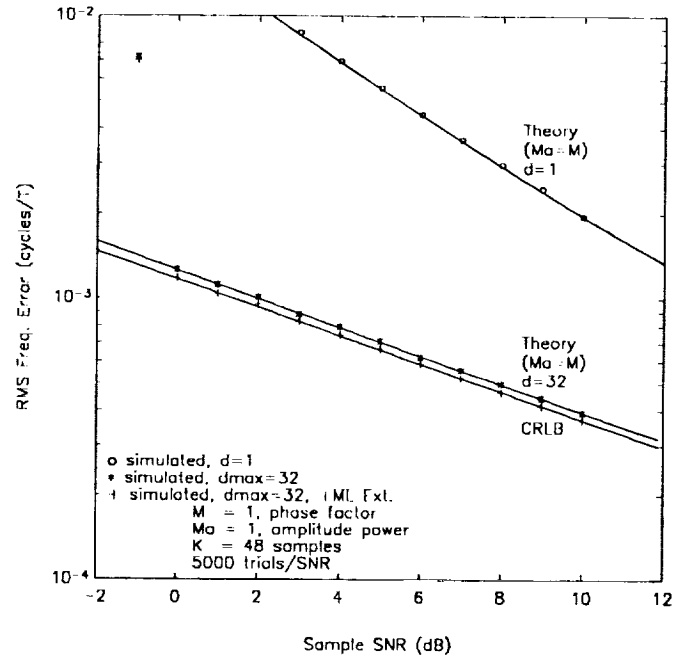
Figure 3: RMS frequency error versus sample SNR, γ, for pure carrier ($M_a=M=1$, dmax=d_B).

Figures 4 and 5 show simulation results for BPSK and QPSK signaling, respectively. For the simulated BPSK results in Figure 4, $M=2$ and $M_a=1$. For the simulated QPSK results in Figure 5, $M=4$ and $M_a=1$. Not shown are the simulation results with $M_a=M$, but they closely match

427

the theoretical approximations for all SNRs above threshold. The simulation results with $M_a=1$ are clearly better than the theoretical approximations with $M_a=M$. Note that the simulated performance of the DMA estimator with RAD remains within about 0.5 dB of the CRLB for all SNRs above threshold, and that the CRLB is essentially achieved with the ML extension. As expected, the threshold SNRs are much higher with $M>1$. Longer observation times are required to provide lower thresholds.
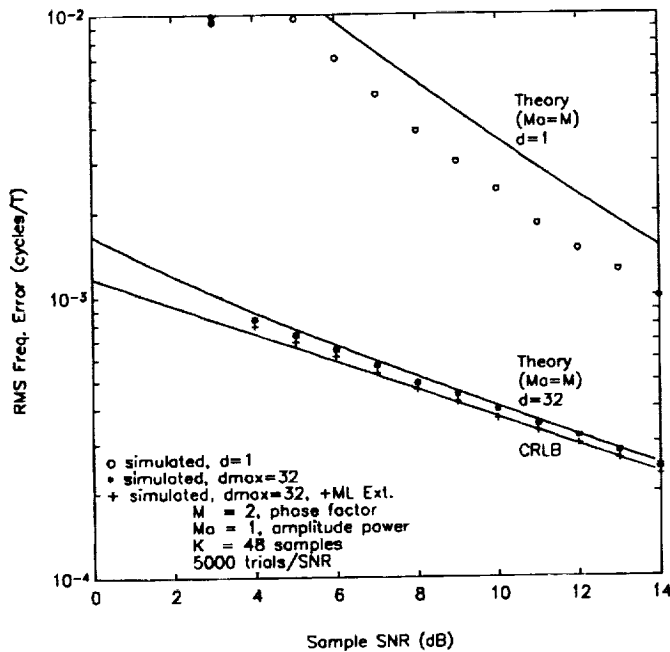
Figure 4: RMS frequency error versus sample SNR, γ, for BPSK signaling ($M=2$, $M_a=1$, dmax=d_B).

CONCLUSIONS

A low-complexity, open-loop, discrete-time, delay-multiply-average (DMA) approach to estimating the frequency offsets for MPSK modulated signals was investigated. A simple maximum likelihood (ML) extension was also considered. Theoretical and simulated performance results were presented and compared to the Cramer-Rao lower bound (CRLB) for the variance of the frequency estimation error. It was shown that the frequency estimate variance can be improved by orders of magnitude over that obtained with a delay of $d=1$. Without the ML extension, performance is typically within about 0.5 dB of the CRLB, for all SNRs above threshold. With the ML extension, the CRLB is essentially achieved. The complexity of the new DMA algorithm, with or without the ML extension, is approximately $3K$, where K is the observation time in samples.
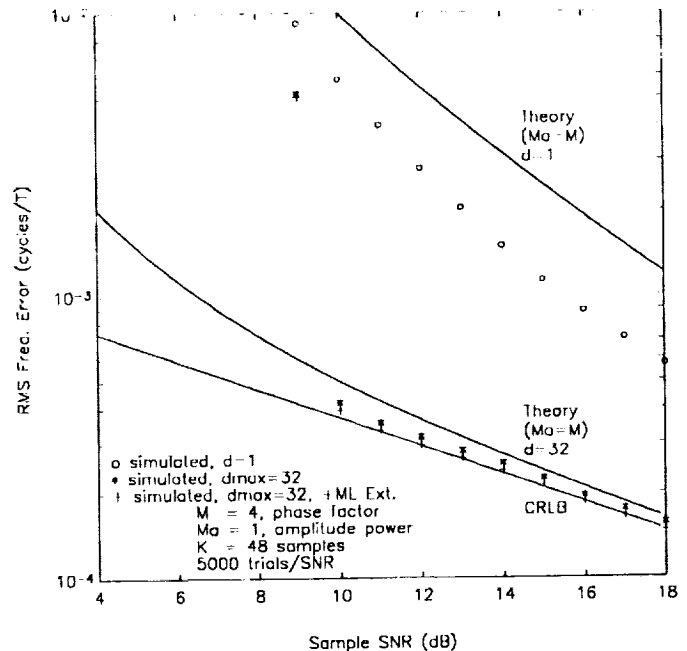
Figure 5: RMS frequency error versus sample SNR, γ, for QPSK signaling ($M=4$, $M_a=1$, dmax=d_B).

REFERENCES

[1] D. C. Rife, "Single-Tone Parameter Estimation from Discrete-Time Observations", IEEE Trans. on Information Theory, Vol. IT-20, No. 5, pp. 591-598, Sept. 1974.

[2] S. N. Crozier and K. W. Moreland, "Performance of a Simple Delay - Multiply - Average Technique for Frequency Estimation", Canadian Conference on Electrical and Computer Engineering, Toronto, Ontario, Canada, paper WM10.3, Sept. 13-16, 1992.

[3] R. J. Young and S. N. Crozier, "Implementation of a Simple Delay-Multiply-Average Technique for Frequency Estimation on a Fixed-Point DSP", Third International Symposium on Personal, Indoor and Mobile Radio Communications, Boston, Massachusetts, paper 2.6, pp. 59-63, Oct. 19-21, 1992.

[4] A. J. Viterbi and A. M. Viterbi, "Nonlinear Estimation of PSK-Modulated Carrier Phase with Applications to Burst Digital Transmission", IEEE Trans. on Information Theory, Vol. IT-29, No. 4, pp.543-51, July, 1983.

[5] A. D. Whalen, Detection of Signals in Noise, Academic Press Inc., 1971.

A PATTERN JITTER FREE AFC SCHEME
FOR MOBILE SATELLITE SYSTEMS

Shousei Yoshida
C&C Systems Research Laboratories, NEC Corporation
1-1, Miyazaki 4-chome, Miyamae-ku, Kawasaki 216, Japan
Phone +81-44-856-2122
Fax +81-44-856-2230

ABSTRACT

This paper describes a scheme for pattern jitter free automatic frequency control (AFC) with a wide frequency acquisition range. In this scheme, equalizing signals fed to the frequency discriminator allow pattern jitter free performance to be achieved for all roll-off factors. In order to define the acquisition range, frequency discrimination characteristics are analyzed on a newly derived frequency domain model. As a result, it is shown that a sufficiently wide acquisition range over a given system symbol rate can be achieved independent of symbol timing errors. Additionally, computer simulation demonstrates that frequency jitter performance improves in proportion to E_b/N_0 because pattern-dependent jitter is suppressed in the discriminator output. These results show significant promise for application to mobile satellite systems, which feature relatively low symbol rate transmission with an approximately 0.4-0.7 roll-off factor.

INTRODUCTION

In relatively low symbol rate transmission systems, such as mobile satellite systems, large carrier frequency offsets are induced by the frequency instability of a mobile terminal's oscillator and/or by the Doppler frequency shift. Such offsets may sometimes be as large as the symbol rate itself, and the automatic frequency control (AFC) loops [1], [2] commonly incorporated into satellite modems to eliminate frequency offsets prior to carrier phase recovery must have an acquisition range sufficient to handle the large offsets. Conventionally, such wide acquisition range is achieved by utilizing a continuous-wave (CW) pilot carrier. However, this results in poor frequency and power efficiency. Far better from this viewpoint would be the use of a modulated carrier.

When carrying out AFC with a band-limited MPSK modulated carrier, a single sample per a symbol period may be used for frequency discrimination. Then, the phase change for the modulated carrier over a full symbol contains the sum of the data symbol phase and the phase

shift induced by frequency offsets. Hence, in order to be free from pattern jitter, the modulation must be removed by some nonlinear process such as an Mth-power operation for a signal point, i.e. an ISI free point to be sampled at $T_b/2$, where T_b is the symbol period. By this removal, however, the frequency offsets become M-fold, and the acquisition range is reduced to be within $\pm 1/2MT_b$. Furthermore, the nonlinear process produces a loss in carrier-to-noise ratio (C/N), which results in a degradation of frequency jitter performance of the AFC.

A scheme involving the measurement of a phase shift induced by frequency offsets between two samples in a symbol period has been proposed [3]. In this scheme, a root raised-cosine filter with 100 percent excess bandwidth is employed on the transmitter side to shape the pulse in such a way as to produce two inter-symbol interference (ISI) free points over half a symbol, and these two ISI free samples are used for detecting frequency errors to attain pattern jitter free performance. The usage of this filter, however, increases transmission frequency bandwidth. In band-efficient communication systems, such as mobile satellite systems, a pattern jitter free AFC scheme with a wide acquisition range, which can be applied to systems with smaller roll-off factors, is urgently needed. This paper proposes an advanced AFC scheme, in which equalizing signals fed to the frequency discriminator allow pattern jitter free performance to be achieved for all roll-off factors.

PATTERN JITTER FREE AFC SCHEME

With regard to frequency discrimination methods, cross-product frequency discrimination (CPFD) is widely used, which is especially well suited to digital implementation [1], [2]. CPFD operates to detect frequency errors by using two successive samples obtained from a CW carrier. Specifically, it calculates the sine of a phase shift induced by frequency offsets during a sample period. When carrying out AFC with a modulated carrier, in order to avoid an undesirable reduction in the acquisition range, frequency discrimination without explicit modulation removal is preferred. CPFD using two samples per a symbol period is
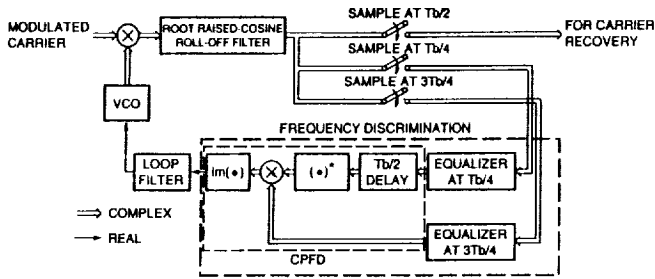
Figure 1. Proposed AFC scheme configuration.

Figure 2. Frequency discrimination block diagram.

Figure 3. Frequency acquisition characteristics.

a possible approach. Root raised-cosine filtering with 100 percent excess bandwidth yields two ISI free points spaced $T_b/2$ apart and placed symmetrically with reference to the midpoint of the symbol period. Using these samples at $T_b/4$ and $3T_b/4$ for CPFD, pattern jitter free performance can be achieved. Without said filtering, however, these two ISI free points cannot be expected to be obtained, and the CPFD output will include pattern-dependent jitter. In order to combat such pattern jitter, the author has introduced two T_b-spaced equalizers to cancel out the ISI on the two samples in the symbol period, where $T_b/4$ and $3T_b/4$ has been chosen as the two sample timings to simplify the demodulator structure.

The proposed AFC scheme configuration is shown in Figure 1. Frequency offsets in an MPSK modulated carrier are first eliminated by a VCO output, and the result is passed through a root raised-cosine RX filter. The band-limited signal is sampled with optimum symbol timing at $T_b/2$ for later carrier phase recovery, and is subsequently sampled at $T_b/4$ and $3T_b/4$ for frequency discrimination. Since ISI naturally exists on these samples at $T_b/4$ and $3T_b/4$, equalizers work so as to cancel out the ISI before frequency discrimination (see Figure 2 for QPSK). The equalized samples at $T_b/4$ and $3T_b/4$ are fed to the frequency discriminator, where frequency errors are detected based on CPFD. The errors are averaged by a loop filter, and are utilized to control the VCO. Thus, pattern jitter free performance is achieved at the cost of a relatively small increase in complexity.

Frequency acquisition characteristics obtained by computer simulation are shown in Figure 3. The simulation was implemented for QPSK modulation at a 3200 symbols/sec rate. An 11-stage PN sequence was chosen as the modulation pattern. The roll-off factor for the RX filter was 0.4. The number of taps for the RX filter and for each equalizer was 9. The loop bandwidth for the AFC was set to be $0.001/T_b$. In the proposed scheme, pattern-dependent jitter is less than that occurring in the case without equalizers.

As has been mentioned above, although pattern-dependent jitter in the proposed scheme is definitely suppressed, it is difficult to understand intuitively the operation involved in detecting frequency errors in the acquisition stage. Specifically, it is of great interest to determine the possible influence exerted on the frequency discrimination characteristics by
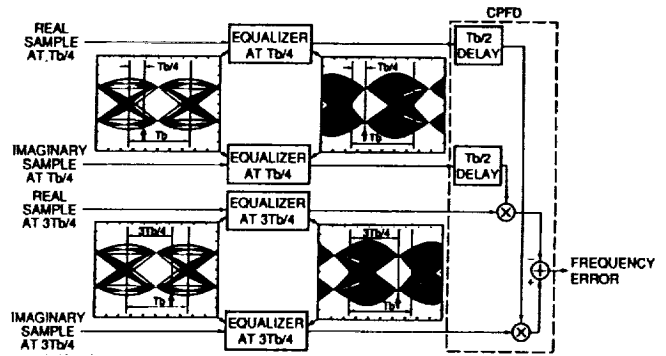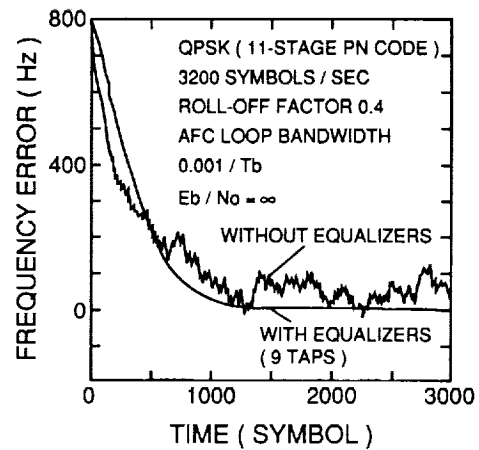
the two equalizers, which operate independently at $T_b/4$ and $3T_b/4$ sample timings. In an attempt to clarify the frequency error detecting operation, in the discussion which follows the author derives equalizer characteristics and attempts to define frequency discrimination characteristics analytically.

EQUALIZER CHARACTERISTICS

The equalizer spectrum characteristics can be derived from the spectrum characteristics of the channel filter. First, the impulse response $g(t)$ of a raised-cosine roll-off filter is sampled, where the sample period is T_b, and the sample timing difference from the midpoint of $g(t)$ is $\gamma T_b(-0.5 \leq \gamma < 0.5)$. The sampled signal $g_s(t)$ is expressed by

$$g_s(t) = g(t + \gamma T_b) \sum_{n=-\infty}^{\infty} \delta(t - nT_b)$$

$$= g(t + \gamma T_b) \frac{1}{T_b} \sum_{n=-\infty}^{\infty} e^{jn\omega_b t}$$

$$(\omega_b = 2\pi/T_b). \tag{1}$$

430
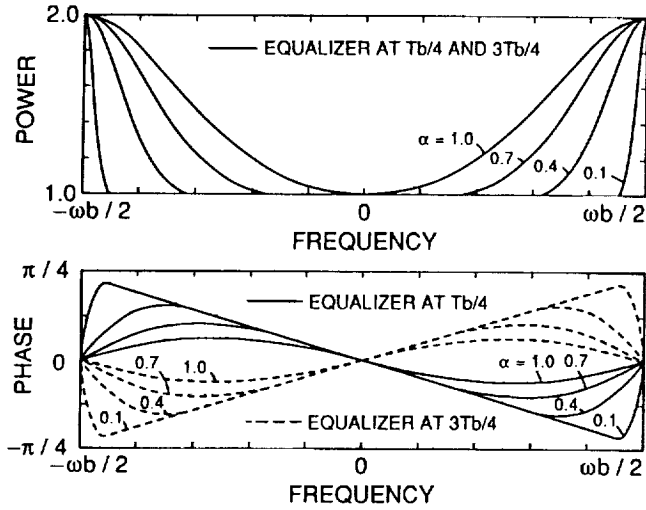
Figure 4. Equalizer spectra.

The Fourier transform $G_s(\omega)$ of $g_s(t)$ is written by

$$G_s(\omega) = \frac{1}{T_b} \sum_{n=-\infty}^{\infty} G(\omega - n\omega_b)e^{j(\omega - n\omega_b)\gamma T_b}. \qquad (2)$$

Here, since $G(\omega)$ represents the raised-cosine roll-off spectrum, aliasing effects cause overlaps only to adjacent spectra.

$$
\begin{aligned}
G_s(\omega) &= \frac{1}{T_b}[G(\omega)e^{j\omega\gamma T_b} + G(\omega + \omega_b)e^{j(\omega+\omega_b)\gamma T_b} \\
&\quad + G(\omega - \omega_b)e^{j(\omega-\omega_b)\gamma T_b}] \\
&\quad (-\omega_b/2 \le \omega < \omega_b/2). \qquad (3)
\end{aligned}
$$

Substituting the raised-cosine roll-off spectrum $G(\omega)$ into (3), $G_s(\omega)$ may be rewritten as follows.

$$
\begin{aligned}
G_s(\omega) &= \frac{1}{T_b}e^{j\omega\gamma T_b} \quad (0 \le \omega < (1 - \alpha)\omega_b/2) \\
&= \frac{1}{2T_b}\left\{ 1 - \sin\left[\frac{\pi(\omega - \omega_b/2)}{\alpha\omega_b}\right]\right\} e^{j\omega\gamma T_b} \\
&\quad + \frac{1}{2T_b}\left\{ 1 + \sin\left[\frac{\pi(\omega - \omega_b/2)}{\alpha\omega_b}\right]\right\} e^{j(\omega-\omega_b)\gamma T_b} \\
&\quad ((1 - \alpha)\omega_b/2 \le \omega < \omega_b/2) \\
G_s(\omega) &= G_s^*(\omega) \quad (-\omega_b/2 \le \omega < 0) \qquad (4)
\end{aligned}
$$

where α is the roll-off factor. The equalizer spectra are represented as $1/G_s(\omega)$. Figure 4 shows equalizer spectra at $T_b/4$ and $3T_b/4$, i.e. when $\gamma = 1/4$ and $-1/4$ in $1/G_s(\omega)$. Each equalizer works so as to zero-force both the amplitude distortion and the phase distortion of the folded spectrum $G_s(\omega)$ at around $\pm\omega_b/2$.

The impulse response $h_s(nT_b)$ of each equalizer, where n is an integer, is given by the inverse Fourier transform of $1/G_s(\omega)$.

$$h_s(nT_b) = \frac{1}{2\pi} \int_{-\omega_b/2}^{\omega_b/2} \frac{e^{j\omega n T_b}}{G_s(\omega)} d\omega. \qquad (5)$$
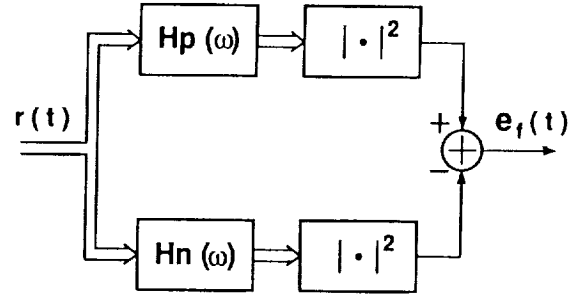
(a)
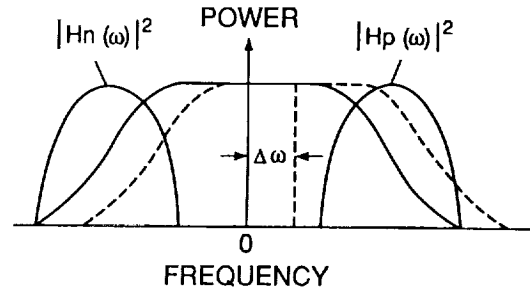
(b)

Figure 5. Differential power measurement frequency discrimination. (a) Block diagram. (b) Discrimination principle.

FREQUENCY DISCRIMINATION CHARACTERISTICS

In this section, in order to define the acquisition range for the proposed scheme, a new discrimination model is derived in the frequency domain, and it is used to analyze frequency discrimination characteristics.

Frequency Discrimination Model

It has previously shown that CPFD may be considered as equivalent to differential power measurement frequency discrimination (DPMFD) [4]. A DPMFD block diagram is given in Figure 5(a), and the discrimination principle is illustrated in Figure 5(b). In DPMFD, differential amounts of output power from two filters located respectively in positive and negative frequency bands are calculated as frequency errors. For CPFD which operates at a double symbol rate of $2/T_b$, the positive/negative filter spectra $H_p(\omega)$ and $H_n(\omega)$ may be expressed as follows.

$$H_p(\omega) = \frac{1}{2}\left[e^{-j\omega T_b/4} - je^{j\omega T_b/4}\right]$$

$$H_n(\omega) = \frac{1}{2}\left[e^{-j\omega T_b/4} + je^{j\omega T_b/4}\right]. \qquad (6)$$

431
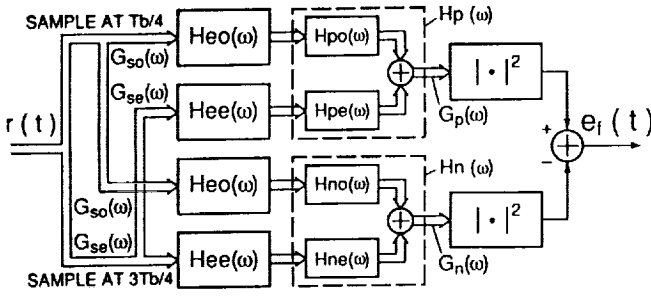
Figure 6. Frequency discrimination model.

Figure 7. Positive/negative filter output spectra.

In the proposed scheme, a sampled signal at $T_b/4$ and a sampled signal at $3T_b/4$ are fed to different T_b-spaced equalizers, which separately remove ISI at $T_b/4$ and $3T_b/4$. The results are input to the positive/negative filters in DPMFD. Here, since the positive/negative filters alternately receive the equalized signals at $T_b/4$ and $3T_b/4$, these filters are divided into two parts, i.e. one part for receiving an equalized signal at $T_b/4$ and another part for receiving an equalized signal at $3T_b/4$, and the two outputs are combined. Impulse responses $h_p(t)$ and $h_n(t)$ of the positive/negative filters are expressed by using impulse responses $h_{po}(t)$ and $h_{no}(t)$ at $T_b/4$, and impulse responses $h_{pe}(t)$ and $h_{ne}(t)$ at $3T_b/4$ as follows.

$$h_p(t) = h_{po}(t + T_b/4) + h_{pe}(t - T_b/4)$$
$$h_n(t) = h_{no}(t + T_b/4) + h_{ne}(t - T_b/4) \qquad (7)$$

where $h_{po}(t), h_{pe}(t), h_{no}(t)$ and $h_{ne}(t)$ are

$$h_{po}(t) = -j\delta(t)/2 \quad h_{pe}(t) = \delta(t)/2$$
$$h_{no}(t) = j\delta(t)/2 \quad h_{ne}(t) = \delta(t)/2. \qquad (8)$$

The frequency discrimination model is shown in Figure 6. The positive/negative filter output spectra $G_p(\omega)$ and $G_n(\omega)$ are calculated by the following equations.

$$G_p(\omega) = G_{so}(\omega)H_{eo}(\omega)H_{po}(\omega) + G_{se}(\omega)H_{ee}(\omega)H_{pe}(\omega)$$
$$G_n(\omega) = G_{so}(\omega)H_{eo}(\omega)H_{no}(\omega) + G_{se}(\omega)H_{ee}(\omega)H_{ne}(\omega) \qquad (9)$$

where $G_{so}(\omega)$ and $G_{se}(\omega)$ are sampled signal spectra for $G(\omega)$ at $T_b/4$ and $3T_b/4$. Here, $G(\omega)$ is given by $G_t(\omega - \Delta\omega)H_r(\omega)$, where $G_t(\omega)$ and $H_r(\omega)$ are the TX signal spectrum and the RX filter spectrum respectively. Both have raised-cosine roll-off characteristics. $\Delta\omega$ values are frequency offsets. Furthermore, $H_{po}(\omega)$, $H_{pe}(\omega)$, $H_{no}(\omega)$ and $H_{ne}(\omega)$ are Fourier transforms of $h_{po}(t), h_{pe}(t), h_{no}(t)$ and $h_{ne}(t)$.

$$H_{po}(\omega) = -j/2 \quad H_{pe}(\omega) = 1/2$$
$$H_{no}(\omega) = j/2 \quad H_{ne}(\omega) = 1/2. \qquad (10)$$

The $G_p(\omega)$ and $G_n(\omega)$ spectra for some $\Delta\omega$ values are computed as depicted in Figure 7.

Frequency Discrimination Characteristics

Frequency errors are defined as the power difference between $G_p(\omega)$ and $G_n(\omega)$, i.e.

$$e_f = \int_{-\omega_b/2}^{\omega_b/2} \mid G_p(\omega) \mid^2 d\omega - \int_{-\omega_b/2}^{\omega_b/2} \mid G_n(\omega) \mid^2 d\omega. \qquad (11)$$

Figure 8 shows frequency discrimination characteristics calculated using (11). It may be seen that a sufficiently wide acquisition range over a given system symbol rate can be achieved, and that the discrimination curves are dependent on roll-off factors. As the roll-off factor approximates 0.0, frequency error becomes smaller, gradually decreasing to zero. This is because the frequency range in which spectrum characteristics for $G_p(\omega)$ differ from those for $G_n(\omega)$ is reduced as the roll-off factor decreases (see Figure 7).

Frequency discrimination characteristics of the scheme using a CW carrier are shown together in Figure 8. The discrimination curves are represented as the product of sine function and root raised-cosine roll-off characteristics. Figure 8 also shows that the detection sensitivity, i.e. a differential coefficient at 0 Hz $\Delta\omega$ in the discrimination characteristics, of the proposed scheme is approximately half of that of the scheme using a CW carrier.

Frequency Discrimination Characteristics with Symbol Timing Errors

When the proposed scheme is implemented into mobile satellite modems, the symbol timing recovery influence in frequency acquisition should be discussed. For arbitrary

432
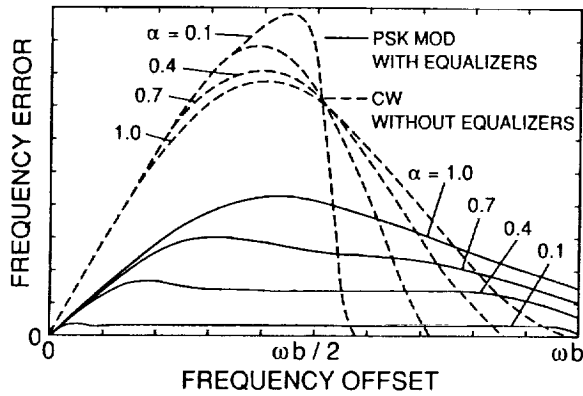
Figure 8. Frequency discrimination characteristics.
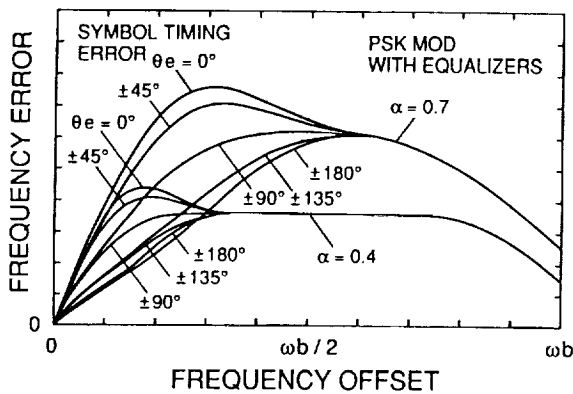
Figure 9. Frequency discrimination characteristics with symbol timing errors.

symbol timing errors $\theta_e (-180° \leq \theta_e \leq 180°)$, $G_{so}(\omega)$ and $G_{se}(\omega)$ represent sampled signal spectra for $G(\omega)$ at $(1/4 - \theta_e/360°)T_b$ and $(3/4 - \theta_e/360°)T_b$. Figure 9 shows frequency discrimination characteristics with symbol timing errors. Although the discrimination curves are dependent on symbol timing errors within a $\Delta\omega$ value of around $\omega_b/2$, the errors are still obtained with a wide frequency range. At more than $\Delta\omega$ value of $\omega_b/2$, the curves are made free from symbol timing errors. This is because there exist overlaps no longer in the folded spectra for the sampled signals at $(1/4 - \theta_e/360°)T_b$ and $(3/4 - \theta_e/360°)T_b$. In the proposed scheme, even if symbol timing is not recovered, frequency acquisition can be achieved with a wide acquisition range. After the symbol timing acquisition, pattern jitter free performance is attained.

SIMULATION RESULTS

The author has carried out a computer simulation to evaluate the proposed scheme for frequency jitter performance in the presence of Gaussian noise and for residual pattern jitter performance.
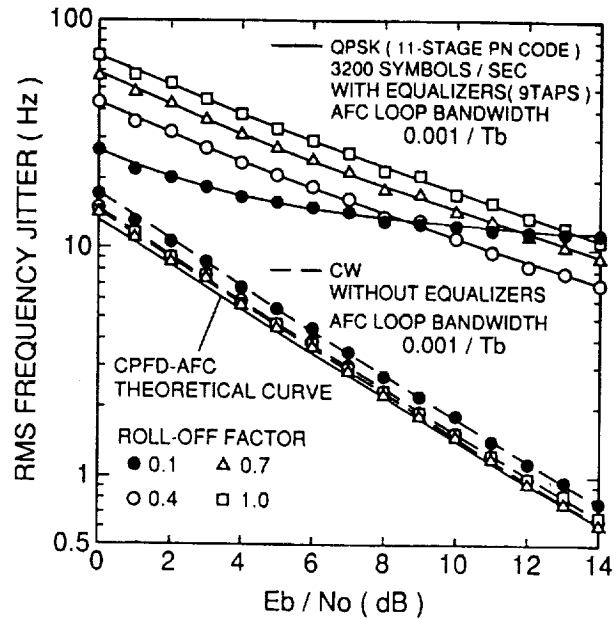
Figure 10. Frequency jitter performance in noise.

Frequency Jitter Performance in Noise

Figure 10 shows frequency jitter performance of the proposed scheme in the presence of noise. The simulation was implemented for QPSK modulation at a 3200 symbols/sec rate. An 11-stage PN sequence was chosen as the modulation pattern. The number of taps for the RX filter and for each equalizer was 9. The loop bandwidth for the AFC was set to be $0.001/T_b$. In the proposed scheme, frequency jitter performance improves in proportion to E_b/N_0, because pattern-dependent jitter is suppressed in the discriminator output. As the roll-off factor becomes smaller, the performance tends to be gradually degraded. In the case of too small a roll-off factor such as 0.1, residual pattern jitter due to imperfect equalization is dominant in the total frequency jitter performance.

The frequency jitter performance of the scheme using a CW carrier is shown together in Figure 10, in which the performance is independent of roll-off factors, and is consistent with the theoretical curve for CPFD-AFC [2]. The frequency jitter performance of the proposed scheme cannot be prevented from degrading as compared with that of the scheme using a CW carrier.

Residual Pattern Jitter Performance

Residual pattern jitter performance of the proposed scheme was evaluated with regard to the number of taps for the equalizers, as shown in Figure 11. Although residual pattern jitter performance may be dependent on the modulation pattern, an 11-stage PN sequence was used as an example in the simulation. The loop bandwidth for the AFC was set to be $0.001/T_b$. Consequently, as the number

433
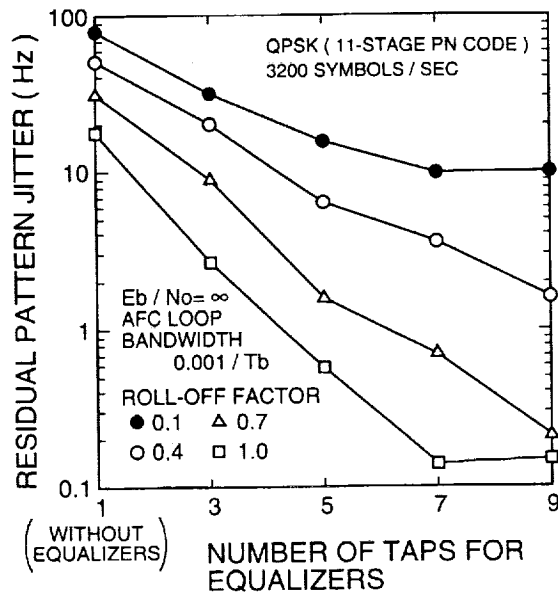
Figure 11. Residual pattern jitter performance.

of taps for the equalizers increases, residual pattern jitter performance improves. The improvement is greater for a larger roll-off factor, because impulse responses of the RX filter and of the equalizers with larger roll-off are shorter. By narrowing the AFC loop bandwidth, the performance may improve to some degree. This is, however, undesirable for suppressing pattern-dependent jitter, because the acquisition time increases. The number of taps for the equalizers should be designed to be as few as possible, if the pattern jitter is negligible in the total frequency jitter performance under operational E_b/N_0 conditions.

CONCLUSION

This paper has proposed a scheme for pattern jitter free AFC with a wide frequency acquisition range. In the proposed scheme, equalizing signals fed to the frequency discriminator allow pattern jitter free performance to be achieved for all roll-off factors. In order to define the acquisition range, frequency discrimination characteristics have been analyzed on a newly derived frequency domain model. As a result, it was shown that a sufficiently wide acquisition range over a given system symbol rate could be achieved independent of symbol timing errors.

Additionally, computer simulation has been carried out, which demonstrated that frequency jitter performance improved in proportion to E_b/N_0 owing to suppressing pattern-dependent jitter. These results showed significant promise for application to mobile satellite systems, which feature relatively low symbol rate transmission with an approximately 0.4-0.7 roll-off factor.

The author believes that applying the proposed concept to some other combination of the channel filters, e.g. a

TX filter with root raised-cosine roll-off, a brick-wall RX filter for frequency discrimination [3] and another RX filter with root raised-cosine roll-off for data detection, were also possible. Those results were not discussed in this paper.

ACKNOWLEDGMENTS

REFERENCES

[1] C. R. Cahn, "Improving Frequency Acquisition of a Costas Loop," IEEE Trans. Commun., vol. COM-25, pp.1453-1459, Dec. 1977
[2] F. D. Natali, "AFC Tracking Algorithms," IEEE Trans. Commun., vol. COM-32, pp.935-947, Aug. 1984
[3] M. K. Simon, D. Divsalar, "Doppler-Corrected Differential Detection of MPSK," IEEE Trans. Commun., vol. COM-37, pp.99-109, Feb. 1989
[4] T. Alberty, V. Hespelt, "A New Pattern Jitter Free Frequency Error Detector," IEEE Trans. Commun., vol. COM-37, pp.159-163, Feb. 1989

Session 10
Modulation, Coding and Multiple Access

Session Chair—*Michael Miller*, University of South Australia, Australia
Session Organizer—*Robert Kwan*, Jet Propulsion Laboratory, U.S.A.

(continued)

A CDMA SYNCHRONISATION SCHEME

C. Soprano

European Space Agency
Telecommunications Missions & Systems Department
Directorate of Telecommunication Programmes
ESTEC, P.O. Box 299, 2200 AG Noordwijk, The Netherlands
Phone +31-1719-83208
Fax +31-1719-84598

INTRODUCTION

CDMA (Code Division Multiple Access) is known to decrease inter-service interference in Satellite Communication Systems. Its performance is increased by chip quasi-synchronous operation which virtually eliminates the self-noise; however, the theory (ref.1) shows that the time error on the synchronisation has to be kept at less than one tenth of a chip which, for 1 Mchip/sec. spreading rate, corresponds to 10^{-7} sec. This, on the return-link, may only be achieved by means of a closed loop control system which, for mobile communication systems, has to be capable of autonomous operation. Until now some results have been reported (ref.2) on the feasibility of chip quasi-synchronous operation for mobile communication systems only including satellites on GEO (Geostationary Earth Orbit). In what follows the basic principles are exposed and results are presented showing how low chip synchronism error may be achieved by means of an autonomous control loop operating through satellites on any Earth orbit; the complete theory may be found in ref.3.

SYSTEM DESCRIPTION

An overall scenario is shown in fig.1. Each mobile terminal generates Transmit Time Epochs, which correspond to the epochs of transmission of the PN codes, i.e. to the beginning of each transmitted symbol on the Return-Link. The reception of these signals at the hub earth station generates Receive Time Epochs which are compared with a locally generated stream of Reference Time Epochs. The processing of the resulting Time Error results in a correction signal which will be transmitted on the Forward-Link to each mobile terminal. The above quantities may be represented as:

1) Transmit Epoch $\quad TX_i = T_i$

2) Receive Epoch $\quad RX_i = TX_i + \dfrac{D_o}{c} - \dfrac{1}{c}\int_0^{T_i} V_r(t)\,dt$

3) Reference Epoch $\quad REF_i = T_i$

4) Time Error $\quad E_i = -\dfrac{D_o}{c} + \dfrac{1}{c}\int_0^{T_i} v_r(t)\,dt$

In the above c is the velocity of light, Do is the length of the transmission path between Transmitter and Receiver at the time instant $t = 0$, Vr(t) is the total radial velocity of the transmitter with respect to the receiver. The quantity Ei refers to the error occurring to the time epoch transmitted at the time $t = i*T$; its actual time of occurrence is therefore $t = i*T + Tp$ in which Tp is the total propagation time at the time instant $t = i*t$. The temporal behaviour is shown in fig. 2 in which the sampling time interval Ts is defined; the error is supposed to be measured at each time instant

5) $Ti = To + i*Ts$

Assuming that the following conditions are met:

6) $\quad T_s \gg T_p \qquad \dfrac{1}{c}\int_{T_{i-1}}^{T_i} v_r\,dt \ll \dfrac{1}{F} \qquad \dfrac{D_o}{c} \ll T_s$

the quantity Ei' may be expressed as

7) $Ei' = (1/F)*[INT(RXi*F) - RXi*F + 0.5]$ {sec.}

in which INT(x) means "the first integer less than x". The conditions above imply that the sampling time interval is much greater than the propagation time and that the system behaves so smoothly that the magnitude of the difference between the Ei' belonging to two contiguous sampling times i*Ts and (i+1)*Ts is a small fraction of 1/F. The fulfillment of conditions (6) allows the system to behave as a linear delay-less sampled data control system which may be analyzed with the Z-transform formalism. The functional block diagram of the synchronisation system at the hub earth station is shown in fig.3. The initial acquisition of the received PN codes is assumed to be supported by fully parallel correlators. This because the initial time error

may take any value up to the time duration of one symbol and the corresponding values of the correction signals will not be compatible with the holding range of a DLL (Delay Lock Loop). The main requirements for the system are:

- the r.m.s. value of the time error has to be less than 0.1 chip (ref.1); this for 1 Mchip/sec. corresponds to $10^{(-7)}$sec.;
- the transmission of control signals must take a fraction as small as possible of the available transmission capacity; therefore, the control system will operate in a sampling mode of which the sampling period has to be as long as feasible;
- operation with "real life" inaccuracies induced by hardware such as clock frequency generator errors and achievable resolution of the correction signals;
- operation in presence of noise;
- operation in voice activation mode;
- resistance to the outages induced by the mobile satellite communication channel.

The synchronisation control loop

The feedback control loop will act, at the mobile terminal, on the transmission time of each symbol in order to achieve, at the control station, chip synchronisation between the received spread spectrum signal and a time reference locally generated. As the feedback control loop has to minimise the time error generated by the motion of the mobile terminal and of the satellite with respect to the hub station, a second order control loop has to be considered as a minimum. This is a loop in which the control signal is derived from a double integration of the error signal versus time. Its controller may look as shown in fig.4; fig.5 shows the equivalent mathematical model of the system. The controller generates a correction signal given by:

8) $CORR_i = A * C_i + B * C_i'$

9) $C_i = C_{(i-1)} + E_i$

10) $C_i' = C_{(i-1)}' + C_i$

E_i is the time error as defined in 4), A and B are coefficients independent from the time. The two expressions 9) and 10) are equivalent to:

11) $C_i' = 2*C_{(i-1)}' - C_{(i-2)}' + E_i$

The model of fig.5 assumes that only the controller, shown as C(z), affects the dynamic behaviour of the control loop. In the same model the quantity R(z) is the reference time and the quantity M(z) is the timing alteration corresponding to the motion of TX towards RX. For the case of constant velocity motion, by means of Z-transform the limit value of the time error may be found to be zero. However, this only holds at sampling time instants; during the time interval between sampling instants the system is left free to evolve and a substantial time error will develop. According to the complete analysis (ref.3), the time error shows a triangular behaviour versus time and its peak value may exceed the specified values; for the simple case of constant radial velocity the peak value of the time error is given by:

12) $E_{ipeak} = (V_{ro}/c)*T_s$

This may be corrected applying the correction all along the time interval Ts. This implements an interpolation between two consecutive values of the correction signal which is still given by

13) $CORR_i = A * C_i + B * C_j'$

14) $C_i = C_i + C_{i-1}$

15) $C_j' = C_{j-1}' + C_i$

but the term C_j' is updated at each transmitted symbol, i.e. at each time epoch TXj; the coefficient B has to be scaled down by a factor equal to F. A result of a computer run for this simple case is shown in fig.6. After an initial transient the time error shows the foreseen triangular shape; at the time instant T1 the control signal is switched to (13) and the error collapses to virtually zero. In the case of a system at constant radial acceleration the principle of interpolation of correction signal may be shown to reduce the error; besides, it also may be applied to control loops of higher order.

Operation in presence of noise

From fig.5 it will be seen that any correction signal is equal to the sum of the error signal proper plus a sample of noise. This affects the error signal generated in the next sample and so on, resulting in the variance of the time error plus noise being greater than the sum of the two. This could be seen by deriving the following from (1), (2), (3) and (13):

16) $E_i = \frac{1}{c}[\int_{T_{i-1}}^{T_i} V_r \, dt - \int_{T_{i-1}}^{T_{i-1}} V_r \, dt] + k E_{i-1} + k' E_{i-2}$

Assuming for simplicity that Vr(t) = Vro it will be:

17) $E_i = -N_i + k \cdot E_{i-1} + k' E_{i-2}$

in which Ni is the sample of noise at the sampling time t=i*Ts. This shows that, at any time, the noise appearing at the "error output" of the system is actually made of two components: the input thermal noise generated, at that time, by the receiver, and the response of the loop to the thermal noise generated in the past. The performance of the system in presence of noise is improved by taking as error sample the average on a number of consecutively received time epochs; the variance of the noise in the loop is reduced by a factor equal to the squared root of that number. Additional improvement is given by adaptive control of the noise bandwidth of the loop. This is needed by mobile terminals moving with high acceleration.

Voice Activated Operation

At each mobile terminal the transmission of the RF carrier is inhibited during the time intervals in which the user is silent. System synchronisation then may only be achieved during short and random transmission time intervals. This may result in an exceedingly low sampling rate and it leads to a "burst forcing" mode of operation by which, irrespective of the activity of the user, the mobile terminal is forced to transmit bursts with a minimum frequency. This frequency may be minimised by some computational capability at the mobile terminal. For each transmitted symbol the following may be shown to hold:

18) $E_j = E_{j-1} + \frac{1}{c} \int_{T_{j-1}}^{T_j} V_r(t) \, dt$

in which the quantity vr(t)/c is measurable as Doppler effect. Therefore, the mobile terminal, once synchronised, may execute Doppler measurements on the RF carrier of the Forward-Link and from these it can derive the correction quantities to be applied to the transmission timing. This is an open loop mode of operation; errors affecting Doppler measurements, due to hardware limitations, will cumulate and a large error transient will develop when the system is switched back to its closed loop mode of operation. Should this transient exceed 0.5 chips the synchronisation would be lost and the PN code would have to be reacquired. In this mode of operation the double integrator has to be continuously updated as if the system was in regular

closed loop operation; missing this updating, the same large transient as before will eventually develop. The needed updating of the double integrator may be derived from (11).

Resistance to transmission outages

Transmission outages given by mobile channels and occurring on the forward link may induce unrecoverable transmission errors on the control signal which will then be erased by the decoder. During a transmission outage occurring on the forward link and including consecutive correction signals the integrators may be left running on the last input value. This, in general, will result in an increased time error at the end of the outage itself; the eventual magnitude of the error is function of the radial acceleration to which the system has been subject during the outage. In the ideal case of a system at constant radial velocity the time error during a communication outage on the return link will only increase if the link is noisy; this because the last correction signal refers to an error measurement corrupted by noise. The random walk of the clock frequency generator during the outage may also give a contribution to the build-up of the error.

COMPUTER SIMULATION IMPLEMENTATION AND RESULTS

The system was modeled as shown in fig.7 in which M(t), S(t), N(t) represent the motion of the mobile terminal, the motion of the satellite, the thermal noise generated by the receive front end at the control earth station. The thermal noise is assumed to impress, on the time of occurrence of the receive time epochs, a Gaussian distributed time jitter. The dynamic behaviour of the PN code tracking device is accounted for as a linear second order low-pass filter (ref.4). The model is only valid if:

- all the de-spreaders are of the same type and have the same parameters,
- all the PN-code tracking devices operates in a linear region.

Output "1" represents the noise versus time in open loop conditions, output "2" represents the total time error versus time of the received time epochs. Clearly this model does not take into account transmission specific aspects but only deals with the control system. Several cases were actually implemented including a quasi geostationary earth orbit, i.e. a 24 hours period

439

circular orbit having 10 degrees inclination, 12 hours and 8 hours Molnya orbits as considered by the Agency for its ARCHIMEDES satellite system; also orbits proposed for future commercial systems were simulated, such as a 10000 Km altitude 6 hours period circular earth orbit and a 900 Km altitude circular earth orbit. The latter case needs a third order control loop. For brevity, only the results for the 10000 Km and for the 900 Km circular Earth orbits are presented, these cases being the most critical. The acquisition phase is shortened by means of variable sampling rate; for the six hours earth orbit it goes from 4 samples per second, during the initial acquisition phase, to 1 sample per second in steady state. This value was selected in view of the assumed dynamic of the mobile terminal; for reduced dynamic it could be increased. The effect of the resolution of the time control signal was taken into account by quantisation of the correction signal in steps of magnitude ranging from 1/64 to 1/8 of a chip. The acquisition phase is declared to be completed when the error Ei is found to be $<= 10^{(-7)}$; the system is declared to have gone out of track if at any Ti is

19) $ABS\{E(i)-E(i-1)\} >= 0.5*10^{-6}$

This to reflect the holding properties of a DLL, the presence of which is also taken into account by imposing that, at steady state, the magnitude of the difference between two time contiguous and quantised correction signals has not to exceed $0.25*10^{(-6)}$ sec. which corresponds to +/- 25% of a chip. With this the DLL always operates in its holding region. The used parameters give a 14 sec. acquisition time. To shorten the time taken by each run, the frequency F has been assumed to be 1 Ksymbol/sec.; the system however has been sized in view of the achievement of a time error not greater than $10^{(-7)}$ sec. as requested by the transmission of 8 Ksymbols/sec. with a spreading factor equal to 127. This is also equivalent to the 8 Ksymbols/sec. transmission with a spreading factor equal to 127 in which the interpolator output is taken every 8 symbols. Noise is averaged across 120 msec.

The 6 Hours Circular Earth Orbit

Fig.8 shows the time error resulting from the application to the mobile of an acceleration equal to 0.01 Km/(sec*) for 10 seconds, after which the mobile moves at constant speed equal to 360 Km/h. For simplicity the motion of the mobile is supposed to take place towards the satellite. The time error only develops during the accelerated phase of the motion of

the mobile terminal; due to the second order control loop, the error at constant velocity of the mobile terminal is very small, being very small the acceleration of the satellite. The effect of finite quantisation, from 1/64 to 1/8 of a chip, is shown in fig.9. Fig.10 shows the error resulting from the application of the same acceleration to a mobile constrained to move along a circular track having 1 Km radius. The control signal is quantised at 1/64 of a chip. The noise performance of the system is shown in figs.11 and 12 which refer to the two above cases with noise corresponding to operation at 5 dB Eb/No.

The 900 Km altitude Circular Earth Orbit

Results for this orbit are shown in fig.13.

CONCLUSIONS

A control loop has been analyzed and simulated for chip synchronisation in chip quasi-synchronous CDMA schemes including satellites on any earth orbit. The proposed system is based on a high order sampled control loop, a linear interpolator and an adaptive gain control; during steady state conditions, the mobile terminal may generate control signals and this decreases constraints on the periodicity of generation of control signal. The same control loop also may be used for burst synchronisation in a TDMA system, which is a much less critical case.

REFERENCES

1) R. de Gaudenzi and oth.: "Bandlimited Quasi Synchronous CDMA"; IEEE J-SAC Vol 10, No 2, Feb. '92.

2) M.L. de Mateo and oth.:"First Satellite Mobile Communications Trials using BLQS/CDMA", IMSC "93

3) C.Soprano: "Analysis and simulation results of a CDMA synchronisation system for mobile satellite communication systems including satellites on any earth orbit", ESA Journal, vol. 17, n.1, March 1993

4) R. de Gaudenzi and oth.: "A Digital Chip Timing Recovery Loop for Band-Limited Direct-Sequence Spread-Spectrum Signals", to appear on IEEE Transactions on Communications".
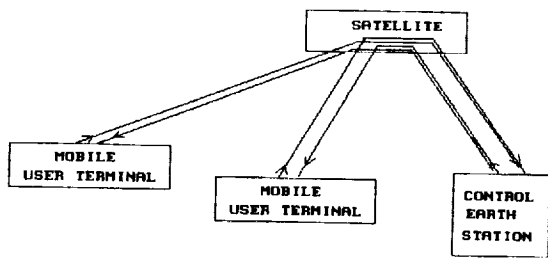
FIG.1 OVERALL SYSTEM ARCHITECTURE
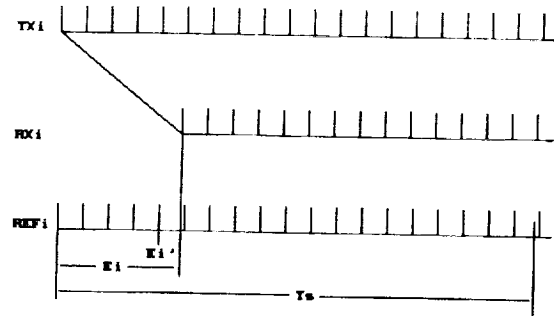
FIG.2 DEFINITION OF TIME ERROR
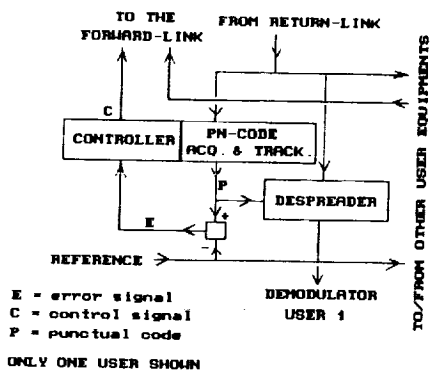
E = error signal
C = control signal
P = punctual code

ONLY ONE USER SHOWN

FIG.3 CONTROL EARTH STATION
FUNCTIONAL BLOCK DIAGRAMME
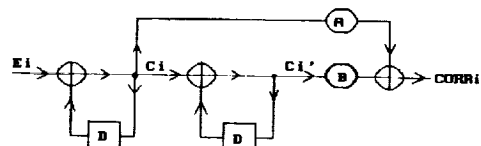
FIG 4 EXAMPLE SECOND ORDER CONTROLLER
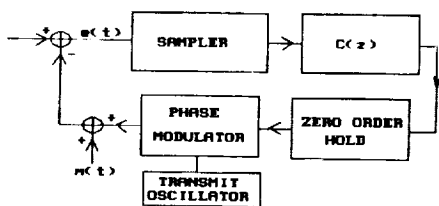
FIG.5 SECOND ORDER SAMPLED CONTROL SYSTEM
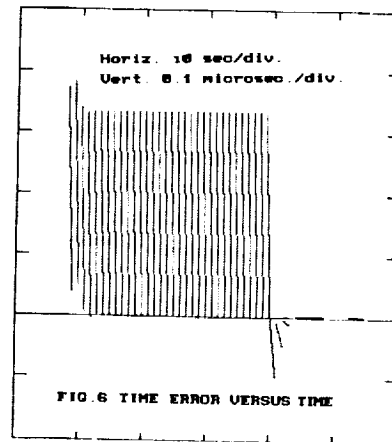
FIG.6 TIME ERROR VERSUS TIME
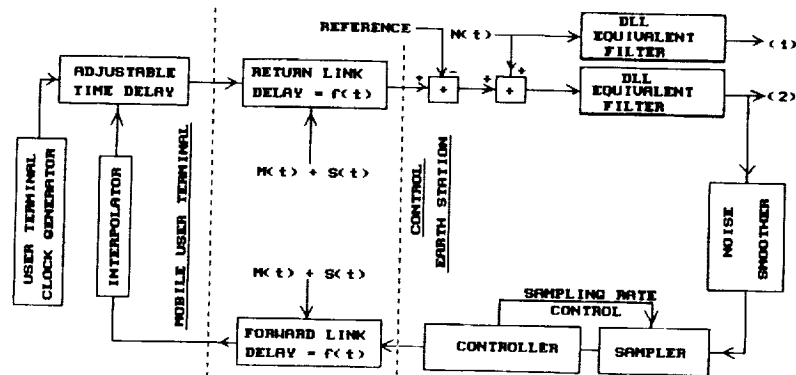
FIG.7 SYSTEM SIMULATION MODEL

441

Quant. = 0
No noise

Hor. 10 sec/div
Vert. 0.1 micrsec/div

FIG.8

Quant. = 1/8 chip

FIG.9

Hor. 10 sec/div
Vert. 0.1 microsec/div

Quant. = 1/64 chip
No noise

FIG.10

Eb/No = 5 dB
Hor. 10 sec/div
Vert. 0.1 microsec/div

Quant. = 1/64 chip

FIG.11

Eb/No = 5 dB
Hor. 10 sec/div
Vert. 0.1 microsec/div

Quant. = 1/64 chip

FIG. 12

No noise
Hor. 10 sec/div
Vert. 0.1 microsec/div

Quant. = 1/64 chip

FIG. 13

442
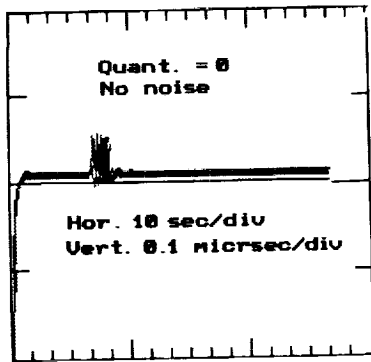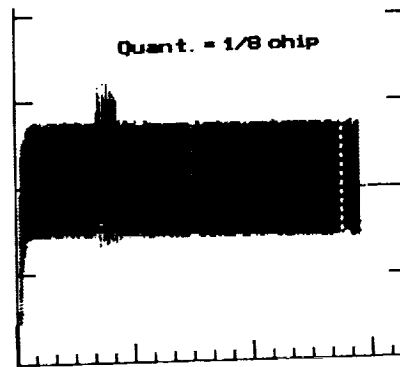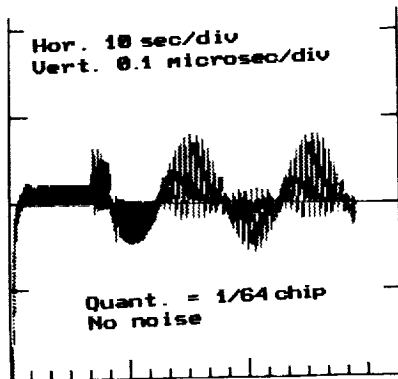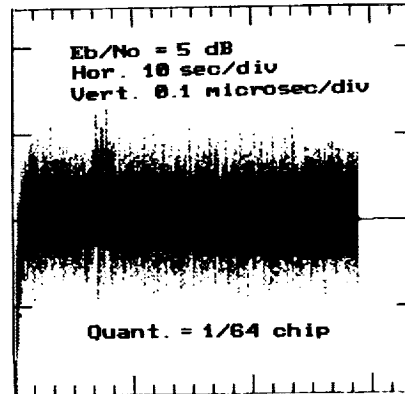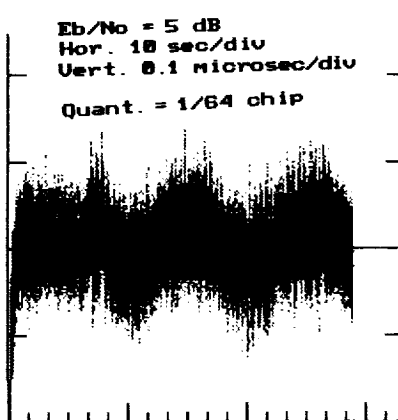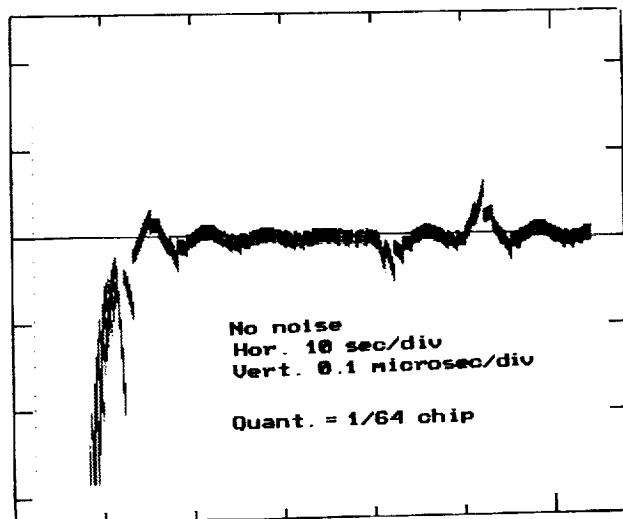
A Protocol for Satellite Access via Use of Spot-Beams

Stefan Ramseier, Anthony Ephremides
Center for Satellite and Hybrid Communication Networks
University of Maryland
A.V. Williams Building
College Park, MD. 20742, USA
Phone: +1 301 405 7900
Fax: +1 301 314 8586

ABSTRACT

In this paper, we develop a new protocol for multiple access to a GEO-satellite that utilizes an electronically-switched spot-beam. The emphasis is on an integrated voice/data protocol which takes advantage of the propagation latency, and which offers centralized control with excellent delay and throughput characteristics. The protocol also allows full exploitation of the advantages of a hopping beam satellite, such as smaller earth stations and frequency re-use.

INTRODUCTION

A protocol introduced in the early '80's, called Interleaved-Frame Flush-Out (IFFO) [1,2], provided for a reservations-based multiple-access to a geostationary satellite by means of time-division. The protocol had the properties of totally distributed control and of advantageous use of the propagation latency.

Recently, this protocol was modified to include voice and data service by means of the movable boundary idea, implemented in the time-domain, and of the isochronous slot assignment to voice calls [3].

In this paper, we consider the use of a hopping beam, and we show how the propagation latency and the periodic focus of each beam on subsets of users can be used to advantage in a similar way to that used in the structure of the IFFO protocols.

The main idea is to have a switch on board the satellite, such that the advantages offered by the hopping beam satellites, such as smaller earth stations and frequency re-use, can be fully exploited, while preserving the excellent delay and through-put characteristics of the original protocols, which use distributed control.

In the remainder of this paper, we first briefly describe the main features and characteristics of the IFFO protocol family, and we then proceed with the description of the model of our communication network with a single hopping beam satellite. Next, we present the new Hopping-Beam (Non-)Interleaved-Frame Fixed-Length (HB-IFFL & HB-NIFFL) protocols, and we outline a delay and throughput analysis. We further introduce an extension to Voice/Data applications, and we demonstrate the features of the new protocols with an example. We conclude this paper with a summary and an outlook to future research activities.

THE IFFL/NIFFL PROTOCOL FAMILY

The family of Interleaved-Frame Flush-Out (IFFO) protocols was introduced by Wieselthier and Ephremides in the early '80's [1,2]. They were mainly designed for totally distributed access control, taking advantage of the propagation latency, which is especially important for satellite links. The IFFO protocols are characterized by a frame length that adapts to bursty channel traffic, resulting in very high efficiency. In the Interleaved-Frame Fixed-Length (IFFL) and Non-Interleaved-Frame Fixed-Length (NIFFL), the frame length is kept constant, which is desirable for voice traffic. An overview of these protocols is given in [3]; in this paper, we concentrate on the fixed-length schemes applied to transparent satellites (bent-pipe).

We now briefly describe some characteristics which will be needed in the subsequent paragraphs: The IFFL/NIFFL protocols are characterized by fully distributed control and a frame

length which is equal to the round-trip delay R, where R is measured in terms of slot durations. The frame consists of a status slot (denoted USS in Fig. 2) and $R - 1$ traffic slots. The status slot is divided into M TDMA minislots, one for each earth station.

The reservation mechanism for the IFFL protocols works as follows: Each earth station transmits a reservation request in its minislot of frame k, based on the number of packets that arrived during frame $k - 1$. After the roundtrip delay R, i.e., at the beginning of frame $k+1$, each earth station receives the requests of all other stations, and the traffic slots are then allocated in a fully distributed manner, based on all reservation requests and an algorithm known to all users. Hence, the messages arrived at an earth station during frame $k-1$ can be transmitted in frame $k+1$. If there are more reservation requests than traffic slots, the so-called excess packets are delayed until frame $k+3$, at which point they are again subject to further delays if there is again a large backlog. It can be seen that there are two interleaved packet streams, the even-numbered frames being independent of the odd numbered frames.

A variant of the IFFL protocols, called Fixed-Contention IFFL (F-IFFL) allows the transmission of packets during unreserved slots in a Slotted-ALOHA fashion, which considerably increases throughput with respect to the Pure Reservation IFFL (PR-IFFL) described above.

The NIFFL protocols are similar to the IFFL protocols, with the difference that if any unreserved slots are present in frame $k + 2$, some or all of the excess packets of frame $k + 1$ can be transmitted, without postponing them to frame $k + 3$. In [3], the Voice/Data NIFFL (VD-NIFFL) protocols were introduced, using a reservation scheme for voice traffic and NIFFL for data.

SATELLITES WITH A SINGLE HOPPING BEAM

In our work, we focus on satellites with hopping beams. Such satellites offer many advantages, such as a higher received power on the ground due to the focusing beam antenna of the satellite, i.e., the transmitted power is no longer spread over the whole hemisphere, but concentrated on a circle with, say 150 miles in diameter. This allows frequency re-use, and, hence, many parallel communications channels.
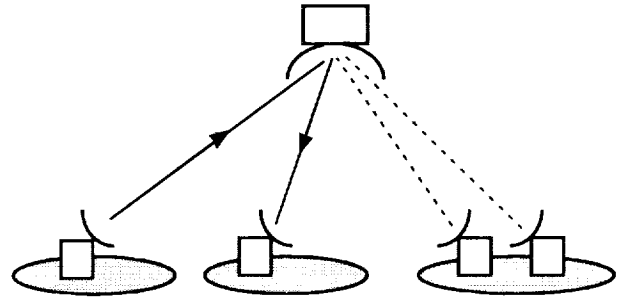
Figure 1: Network Configuration: There are a total of M earth stations in B footprints.

In this paper, we consider a communications network that consists of a satellite with a single hopping beam and M earth stations in B footprints (see Fig. 1), M_b stations in beam b:

$$M = \sum_{b=1}^{B} M_b. \qquad (1)$$

We assume that the switching time of the beam is small compared to the burst length (e.g. for the NASA ACTS satellite, the switching time is < 75 ns). We further assume that there is enough memory on-board the satellite to buffer traffic for one slot, that signal processing on board the satellite is very fast, and that the satellite knows which earth station is in which beam.

THE HB-IFFL PROTOCOL FAMILY

In this section, we will show how the IFFL/NIFFL protocols can be modified for use with a satellite with a single hopping beam. The main idea is to use a switch on board the satellite in a way that the access control is now centralized, although it seems to be distributed from the user's point of view.

The Hopping-Beam Interleaved-Frame Fixed-Length (HB-IFFL) protocols are, like the IFFL/NIFFL protocols, reservation-based time division multiple access (TDMA) control, where non-reserved contention slots may be accessed by each user. However, while for the IFFL/NIFFL schemes it was assumed that all earth stations can receive all the traffic transmitted by the satellite,

this no longer holds for the hopping beam satellite. We therefore have to find a way to transmit the outcome of the reservation process to all earth stations. This will be done by having a switch on board the satellite, which allocates reserved traffic slots to the earth stations, as will be explained in the sequel.

The uplink frame structure of the HB-IFFL protocols is depicted in Fig. 2. Each frame consists of an uplink status slot (USS) and $L_k - 1$ data slots, where L_k is the frame length. The uplink status slot is divided into M TDMA uplink slots, one slot for each station. The downlink frame structure is similar, with the difference that the downlink status slot (DSS) is divided into B downlink slots, one for each footprint.
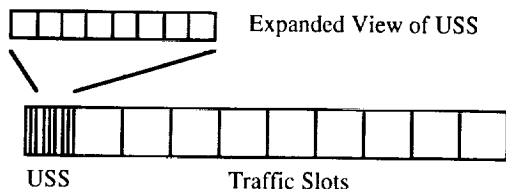
Figure 2: Uplink Frame Structure: There are $L_k - 1$ traffic slots and one Uplink Status Slot (USS), which is divided into M TDMA minislots.

The reservation mechanism works as follows (see Fig. 3): The satellite switches its uplink beam such that each of the M stations is covered during its minislot. In its minislot in frame k, each station transmits information about the packets that arrived in frame $k - 1$, i.e., the number of slots it wants to reserve for each receiving station in frame $k + 1$ (e.g. one packet for station 7 and three packets for station 9)[1].

The satellite receives the USS of frame k with a delay of R/2 slots and decodes it immediately. It then composes the beam/switching pattern for frame $k + 1$ and transmits it sequentially on all B beams. Hence, each minislot of the DSS contains the same information, namely the beam pattern, dwelling time and transmitting time for each station in frame $k + 1$.

Because the satellite has to receive the entire USS before it can compose and transmit the DSS,

the DSS is transmitted $R/2+1$ slots after the USS. The DSS then arrives at the earth stations after another $R/2$ slots, or $R + 1$ slots after the transmission of the USS. Hence, it is natural to select the frame length L_k to be greater than or equal $R + 1$ (instead of R, as for the IFFO protocols).

The R traffic slots of each frame are simply delayed by one slot at the satellite before they are transmitted on the downlink[2].

Upon reception of the DSS by the earth stations, each earth station knows if its reservation request has been granted, and it can start to transmit immediately in the traffic slots that were reserved for it.

Hence, with the "trick" of the on-board switch, the HB-IFFL protocols behave very much the same way as the original IFFL protocols, with a slightly increased frame length, however.

DELAY AND THROUGHPUT ANALYSIS

In this next section, we provide a brief throughput and delay analysis for some variants of HB-IFFL. We characterize these variants, we try to relate the analysis to that of the IFFL/NIFFL protocols where this is possible, and we point out the differences.

We assume that each of the M earth station has a buffer in which to store arriving packets, which are assumed to form a Bernoulli process with rate λ in every slot. The total arrival rate is, therefore, $M\lambda$ packets per slot, which is equal to the throughput rate under stable operation, since no packets are rejected.

PR-HB-IFFL

This Pure Reservation scheme is the one we described in the previous section. It is characterized by the fact that unreserved slots are not used for contention. An analysis similar to PR-IFFL, which is based on a Markov Chain representation, can be used [3], with frame length $R + 1$ instead of R, and delay $R + 1$ instead of R.

---

[1] This procedure is similar to IFFL/NIFFL, but here not only the number of packets, but also the destination address has to be transmitted

[2] An alternative would be to insert an empty slot *after* the USS. Then the satellite could simply repeat each incoming uplink slot on the downlink. The idle slot would then appear on the downlink at the end of the frame, i.e., *before* the DSS. However, this results in a reduced throughput.
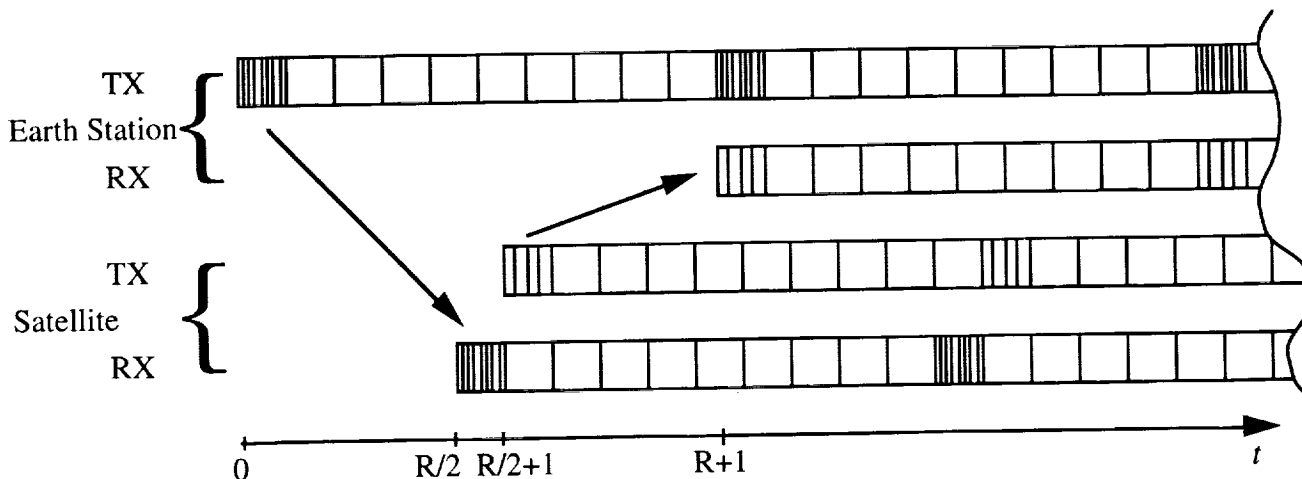
Figure 3: Sequence of Up- and Downlink Status Slots: At time 0, the USS of frame k is transmitted by the earth stations to the satellite, where it is received at $R/2$. The satellite transmits the DSS at $R/2 + 1$, and the earth stations receive it at $R + 1$.

F-HB-IFFL

This scheme is similar to PR-HB-IFFL, but unreserved slots can be used for contention in a predefined way, using some Slotted ALOHA mechanism. Note that due to the hopping beam, the F-IFFO analysis cannot be applied. We have to consider two possibilities of packet loss:

- Packets of the stations in the same footprint collide. The probability of this happening is smaller than for F-IFFL when there is more than one footprint.

- Packets are lost because the hopping antenna of the satellite is not listening to the right footprints at the right time.

Hence, it can be seen that to quantify the second item of the above list, we have to define the hopping pattern of the satellite during non-reserved slots, and the way each earth station transmits packets during these slots. We consider two different strategies:

1. During the unreserved slots, the satellite's beam hops in a manner unknown to the ground stations. The ground stations transmit their packets according to some algorithm (maybe more than once during a frame). A packet is only received by the satellite if it

is transmitted while the satellite is listening, and if there is no collision. The DSS will contain information about successfully received packets, such that all earth stations are informed about success of failure of their transmissions.

2. The satellite announces in the DSS what hopping pattern it will use during the unreserved slots (according to some algorithm, which may use information about excess packets). The ground stations transmit their packets according to some algorithm (e.g. with a given probability) while the satellite is listening. As mentioned before, the DSS will contain information about successfully received slots.

For a large number of beams, strategy (1) has a low probability of success because of the low probability that the satellite is listening to the right footprint. Hence, strategy (2), seems to be more promising. The algorithm for earth stations to transmit their packets has to be designed carefully, however, in order to reduce the probability of collisions. The exact analysis of delay and throughput is yet to be elaborated, but it can be said already that the advantage of F-HB-IFFL over PR-HB-IFFL will probably be smaller than of the corresponding IFFL schemes.

446

PR-HB-NIFFL

These Pure-Reservation Hopping-Beam Non-Interleaved-Frame Fixed-Length protocols are similar to PR-HB-IFFL, with the difference that if any unreserved slots are present in frame $k + 2$, some or all of the excess packets of frame $k+1$ can be transmitted, without postponing them to frame $k + 3$. Hence, the even- and odd-numbered frames are no longer interleaved. Because the satellite knows about the excess packets (it received the requests for the previous frames), it can adjust its hopping pattern an transmit this information on the DSS. Hence, the same delay and throughput analysis as for PR-NIFFL can be used, which is based on a first-order Markov chain [3], with the modification of the frame length and delay ($R + 1$ instead of R).

F-HB-NIFFL

This scheme is similar to PR-HB-NIFFL, but unreserved slots can be used for contention in a pre-defined way, using some Slotted ALOHA mechanism. As already mentioned for the interleaved version of this protocol, the F-IFFO analysis cannot be applied because of the hopping beam. The same comments as above apply, i.e., the delay and throughput analysis strongly depend on the contention algorithm used by the earth stations.

VOICE/DATA APPLICATIONS

The new protocols described in this paper can be extended to Voice/Data application much in the same way as originally suggested in [3]. These Voice/Data HB-NIFFL (VD-HB-NIFFL) protocols use a reservation scheme for voice traffic and HB-NIFFL for data. Once a voice call is accepted by the system, it is guaranteed access to one slot in each frame until completion. Each frame is divided into voice and data slots, where it is appropriate to define the maximum number of voice slots V_{max} such that $V_{max} \leq R$. Voice calls are accepted as long as the total number of calls does not exceed V_{max}, otherwise they are blocked. In the so-called fixed boundary implementation, data packets are transmitted in the data slots using one of the NIFFL protocols, whereas in the movable boundary implementation, data packets may also be transmitted during unused voice slots.

Performance parameters of the VD-HB-NIFFL protocols are the blocking probability of voice calls P_b and the packet delay for data. Assuming that voice calls arrive with poisson rate λ_V and that the call duration is exponentially distributed with parameter μ_V, the well-known Erlang formula can be used to compute P_b. For the data packets, the delay analysis for the movable boundary scheme is more complicated, because the number of packets which can be transmitted in a frame depends on the number of on-going voice calls. For a detailed analysis, the reader is referred to [3].

EXAMPLE

In this section, we quote an example from [3] to quantify the performance of the VD-HB-NIFFL protocols. Since we want to minimize both the call blocking probability P_b and the expected packet delay $E(D)$, we use a weighted sum as our performance measure:

$$E(D) + \alpha P_b, \qquad (2)$$

where α is the weighting factor. We assume that there are a total number of $M = 10$ users and that the roundtrip delay is $R = 11$ slots (which for a geostationary satellite and a data rate of 64 kbps corresponds to a voice data rate of about 5.8 kbps).

Fig. 4, which is taken from [3], shows the weighted performance index as a function of V_{max} for the fixed-boundary version and two values of α, i.e., 2 and 8, where delay is normalized with respect to the frame length $R + 1$. In each case, curves are plotted for a fixed value of data-packet throughput. Note that for throughput values of 0.48 and greater, the curves terminate at values of $V_{max} < 6$; in each of these cases the value of the throughput corresponds to a utilization of 0.96 for the corresponding value of V_{max}. Throughput values that correspond (for a specific value of V_{max}) to a utilization of 1.0 or greater result in infinite delay, and hence an infinite value of the weighted performance index.

SUMMARY AND OUTLOOK

It was shown that the IFFL/NIFFL protocols, which were designed for a transparent satellite [3],

447
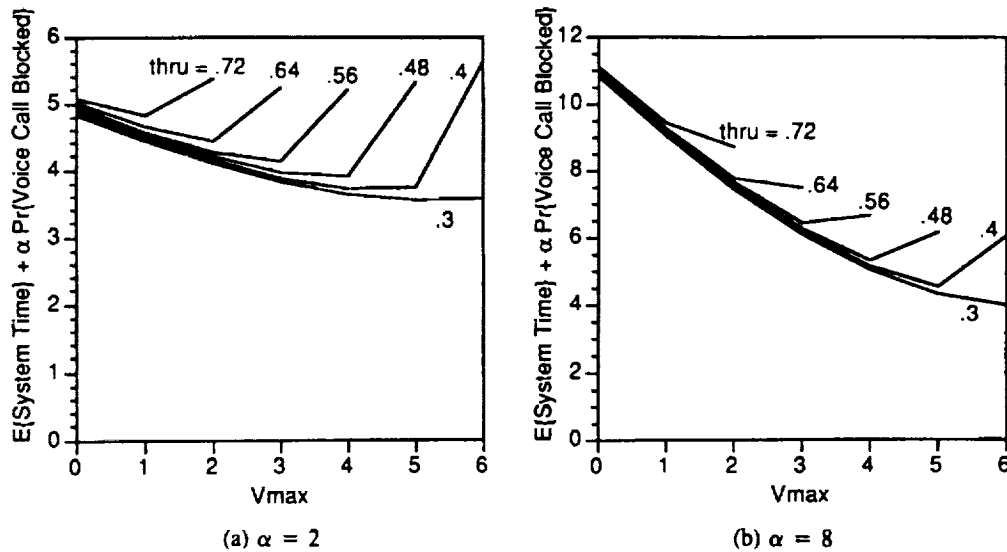
Figure 4: Weighted performance index for fixed-boundary PR-VD-HB-NIFFL (roundtrip delay $R=11$ slots, $M=10$ users..

can easily be adapted for satellites with a single hopping beam and an on-board switch. The excellent delay and throughput characteristics of the original protocols could be preserved, while allowing for making full use of the advantages offered by the hopping beam satellites, i.e., smaller earth stations and frequency re-use. Note that due to the on-board switching, delays of these protocols using centralized control are similar to protocols using fully distributed control, as opposed to traditional centralized control access schemes which involve a double hop over the satellite link, and, hence, double the delay.

We conclude this paper by listing some questions to be addressed in future work:

- What is the optimum strategy for earth stations to transmit excess packets during unreserved slots?

- How does distributed flow control on the ground improve system performance?

- Does on-board memory increase throughput? What about on-board flow control?

- What is the trade-off between call blocking probability, delay and buffer overflow ? Jordan and Varaija [4] showed that the blocking of some calls even when resources are available may result in a decrease of the overall blocking probability. Can this result be applied to the HB-NIFFL protocols?

- How can these protocols be applied to satellites with multiple hopping beams?

REFERENCES

[1] J.E. Wieselthier, "A New Class of Multi-Access for Packet Communication Over a Satellite Channel – The Interleaved Frame Flush-Out Protocols," *Ph.D. dissertation*, University of Maryland, March 1979

[2] J.E. Wieselthier, A. Ephremides, "A New Class of Protocols for Multiple Access in Satellite Networks," *IEEE Trans. Automatic Control*, Vol. AC-25, pp. 865–879, 1980

[3] J.E. Wieselthier and A. Ephremides, "A Study of Channel-Access Schemes for Integrated Voice/Data Radio Networks," *NRL Report 9359*, Nov. 1991

[4] S. Jordan and P. Varaiya, "Control of Multiple Service, Multiple Resource Communication Network," submitted to *IEEE Transactions on Communications*, Jan. 1991

A HIGH QUALITY VOICE CODER WITH INTEGRATED ECHO CANCELLER AND VOICE ACTIVITY DETECTOR FOR MOBILE SATELLITE APPLICATIONS

A.M.Kondoz, B.G.Evans

Centre for Satellite Engineering Research
University of Surrey, Guildford, Surrey, GU2 5XH, U.K.
Tel: (0483) 509131, Fax: (0483) 34139

ABSTRACT

In the last decade low bit rate speech coding research has received much attention resulting in newly developed good quality speech coders operating at as low as 4.8 Kb/s. Although speech quality at around 8 Kb/s is acceptable for a wide variety of applications, at 4.8 Kb/s more improvements in quality are necessary to make it acceptable to the majority of applications and users. In addition to the required low bit rate with acceptable speech quality, other facilities such as integrated digital echo cancellation and voice activity detection are now becoming necessary to provide a cost effective and compact solution. In this paper we describe a CELP speech coder with integrated echo canceller and a voice activity detector all of which have been implemented on a single DSP32C with 32 KBytes of SRAM. The quality of CELP coded speech has been improved significantly by a new codebook implementation which also simplifies the encoder/decoder complexity making room for the integration of a 64-tap echo canceller together with a voice activity detector.

1. INTRODUCTION

After the successful development of low bit rate speech coding in the last decade, we are now beginning to see its real time application in various systems ranging from simple digital speech storage to very complex cellular and satellite mobile telephony. For mobile satellite communication systems, resources such as power and bandwidth are very limited. These systems employ very small transceiver terminals requiring larger satellite power. This is particularly true for land mobile and personal communication satellite systems, for which only a few MHz of bandwidth have been allocated on a primary basis. For such services to be economical they must be very spectrally efficient. In order to be competitive and use modulation schemes that will not cause excessive distortion over the difficult satellite propagation channel, digital coding of speech at around 4.8 Kb/s or less is required.

Robustness to channel errors is an important perfor-

mance measure of a speech coding algorithm designed for mobile communication systems. Unlike most line communication systems, mobile communication systems have to withstand very high channel error rates. Speech coders are not expected to operate in these severe conditions without some form of forward error correction (FEC), but should be able to cope with residual errors of up to 2×10^{-2}. Hence, when designing a speech coder, its performance under channel errors should not be compromised for higher clean channel performance.

In addition to the speech quality under various channel conditions, the echo over long delay satellite systems should also be minimised. The disruption caused by echo in a system is proportional to the delay in that system, which becomes large if satellites are used. Also important is the use of the satellite cannel for other services when the speech channel is not active. By using a voice activity detector (VAD) for about 50 % of the time each speech channel can be used for other services thus doubling the usage of the allocated channel capacity. When there is no speech activity, the transmitter may also be turned off to conserve battery power and to reduce the interference to other users.

In the following sections we present a compact robust speech coder with integrated echo canceller and a VAD, implemented on a single DSP32C, which addresses and proposes solutions to the above problems.

2. CELP SPEECH CODING

At bit rates of 4.8 Kb/s CELP is the most widely reported speech coding algorithm. Although, CELP has been around for about a decade, it is only in the last few years that working implementations became available [1][2]. The processing stages of a CELP coder can be split into three blocks. The LPC analysis, long term prediction (LTP) analysis and the codebook search. It is the type of codebook excitation, computed every subframe which makes the difference between various CELP versions.

In the CELP using a standard codebook, it is assumed that the size of the codebook is large enough to cater for both voiced and unvoiced speech excitations.

However, at low bit rates, this assumption fails at the fast voiced onsets where, the LTP cannot built up fast enough to track the built up of voiced speech. Therefore, the speech quality deteriorates significantly as the bit rate is reduced by increasing the size of the subframe (vector). In addition during voiced regions where more than one main pitch excitation is necessary for good objective matching, the LTP predictor accuracy reduces very rapidly with the increase in the subframe size hence resulting in poor performance. In some versions, mixed codebooks are used, where, part of the codebook is similar to multi-pulse excitation, catering for the above cases. However, these approaches have preselected codebook structures which limits their performance. In the following a dynamic secondary excitation codebook is described where the excitation pulse positioning is made adaptive with the LTP lag (pitch) computed for the same subframe.

In pitch adaptive mixed excitation (PAME) the static codebook is split into two parts. The first part is made adaptive with respect to the LTP lag (pitch delay) as follows. The excitation buffer is filled with unit sample amplitudes, one every D samples starting from the first position. The rest of the vector elements are set to zero. During the search of the codebook, this vector is synthesised and its phase position is determined by shifting its synthetic response one sample at a time for $D-1$ times. Each phase position is then treated as a new excitation vector. In order to guard against pitch doubling errors in the LTP search, if the lag D is greater than $2D_{min}$ the same process is applied again by placing the excitation pulses every $D/2$ samples. The total number of excitation vectors that are searched is then found by adding all the phase positions considered. This is similar to regular pulse excitation with decimation factors of D and $D/2$. After selecting the best excitation vector from the adaptive section using C_a phase positions, the search continues in the fixed part of the codebook. Here, a further $C_f = C - C_a$ vectors are searched and the best performing vector index from the overall search process is transmitted to the receiver (C is the total number of allocated codebook indices). At the receiver, after decoding the LTP lag, the corresponding excitation vector is decoded.

By forcing the secondary excitation to have pitch structure, it is possible to match voiced onsets more accurately. This is because, firstly, the LTP memory builds up faster to track the incoming periodicity more accurately and secondly, the secondary excitation provides the required periodicity where the LTP fails. This of course depends on the accurate computation of the periodicity by the LTP in the first place. Many other adaptation schemes may be used to accurately place the secondary excitation pulses every pitch period. The LTP lag adaptation is useful because it does

not require extra computation or bits. If all the possible pitch and phase combinations were to be used then for a subframe size of 60 (60+1+2+...+30+29+...+20) 750 combinations would be needed, which reduces to (40+1+2+..+20) 250 possibilities for a subframe size of 40. Encoding and decoding processes of the codebook index in this algorithm can have three possibilities which are communicated to the receiver by the fixed subframe size and the decoded LTP lag D.

The fixed part of the codebook was implemented in the form of a single shift centre clipped overlapping codebook. Overlapping codebooks are useful in reducing the computation of the codebook search as well as requiring less storage. If $h_w(n)$ represents the weighted STP impulse response, the synthesised vector $\hat{s}_k(n)$ due to the kth excitation vector $x_k(n)$ of a single shift codebook is,

$$\hat{s}_k(n) = \sum_{i=0}^{n} h_w(i)x_k(n-i) \qquad (1)$$

Since, in a single shift codebook the difference between two consecutive vectors is only one sample at either end of the two vectors, the synthesised vector $\hat{s}_{k+1}$ can be computed in terms of $\hat{s}_k$ as,

$$\hat{s}_{k+1}(n) = x_{k+1}(0)h_w(n) + \hat{s}_k(n-1) \qquad (2)$$

The spectrum of STP and LTP inverse filtered speech is assumed to be flat. However, this is not strictly true. Therefore, the secondary excitation should be shaped accordingly to compensate for the model inaccuracies. Although, this is applicable to all secondary excitation types, it is more important in the pitch adaptive case where, placing a single pulse in time corresponds to a DC in frequency. To further improve the speech quality, therefore, adaptive shaping using the STP parameters can be applied to the secondary excitation. This shaping should be included in the AbS loop to make it most effective. A block diagram of a CELP encoder with pitch adaptive secondary excitation including adaptive shaping is shown in Figure 1. Although, the shaping process requires extra computation, if its impulse response, is computed together with the STP filter impulse response then during the search process, no additional computation is required. The only extra computation required both at the encoder and decoder is the implementation of shaping once every subframe, to produce the final output.

3. ECHO CANCELLATION

Echo in a telecommunication system is the delayed and distorted sound which is reflected back to the source. Echo is generated at the two-to-four wire converting hybrid transformer due to imperfect impedance matching. Here, we are only concerned with the electrical

echo for which the CCITT have a set of recommendations, G.165.

The source of electrical echo can be understood by considering a simplified block diagram of a connection between a pair of subscribers S1 and S2 shown in Figure 2. It can be seen from this block diagram that each subscriber has a two wire loop over which the received signal from the far end and the transmitted signal to the far end travel. The hybrid converts from 2 to 4 wire line working. The role of the hybrid is to direct the signal energy arriving from S1 and S2 to the upper and lower paths of the four wire circuit, respectively, without allowing any leakage back to the two sources over the opposite direction line pairs. Because of the impedance mismatching in the local loops however, some of the transmitted signal returns to its original source who hears a delayed version of his speech. This is called the talker echo, the subjective effect of which depends on the round trip delay around the loop. For short delays and reasonable attenuation (6 dB or more) the talker echo cannot be distinguished from the normal side tone of the telephone and hence does not cause problems. In applications such as satellites however, as a consequence of high altitude a round trip delay of 540 ms (270 ms each way) is possible, which makes the echo very disturbing and may in fact destroy conversation. When this is the case, it is essential to control or even to remove the echo.

A block diagram of an echo canceller for one direction of transmission is shown in Figure 3 where the far end signal is denoted by $y(i)$, the unwanted echo signal $r(i)$, and the near end talker signal $x(i)$. The near end talker signal and the echo are added together at the output of the hybrid. Since the far end signal is available as a reference for the echo canceller, the replica of the echo $\hat{r}(i)$ is estimated by matching the signals on both paths of the four wire section. This echo replica is then subtracted from the total of the returned echo and the near end signal as

$$u(i) = x(i) + r(i) - \hat{r}(i) \tag{3}$$

The difference between $r(i)$ the returned echo and $\hat{r}(i)$ the estimated echo should be as small as possible for good echo cancellation performance. The echo canceller produces the echo replica by using the far end reference signal in a transversal filter. If the impulse response of the filter is the same as the echo path response then the estimated echo and the returned echo become identical resulting in a perfect echo cancellation. Since the echo path response is not known in advance and may vary slowly with time, the coefficients of the transversal filter are adapted. In order to produce no distortion on the near end talker signal, the filter coefficients are only updated when there is no near end activity.

An echo canceller should in general satisfy the following fundamental requirements: Rapid convergence of the filter coefficients when turned on, very low echo when there is no near end speech, slow divergence when there is no far or near end speech and little divergence during times that both near and far end signals are present.

An echo canceller can be split into adaptive transversal filter, near end speech detection and residual error suppression parts. In a digital echo canceller both the reference and echo signals are available in digital form. Therefore the echo path impulse response can be represented in digital form denoting it by h_k to form

$$r(i) = \sum_{k=0}^{N-1} h_k y(i - k) \tag{4}$$

Assuming the system is linear and the echo path impulse response N is of finite length, then the echo canceller form the replica of the returned echo using

$$\hat{r}(i) = \sum_{k=0}^{N-1} a_k y(i - k) \tag{5}$$

When $a_k = h_k$, $k = 0, 1, ..., N - 1$ the returned and estimated echoes are identical resulting in no residual echo. The coefficients of the transversal filter are updated to match the slowly time varying echo path impulse response by minimising the mean squared residual error. When there is no near end speech $(x(i) = 0)$ the filter coefficients are updated in such a way that as a result the residual error tends to a minimum. The update of the coefficients at each iteration is controlled by a step size β,

$$a_k(i + 1) = a_k(i) + 2\beta e(i) y(i - k) \tag{6}$$

The convergence of the algorithm is determined by the stepsize β and the power of the far end signal $y(i)$. In general making β large speeds up the convergence, while a smaller β reduces the asymptotic cancellation error. The convergence time constant is inversely proportional to the power of $y(i)$, and that the algorithm converges very slowly for low signal levels. To overcome this situation, the loop gain is usually normalised by an estimate of the far end signal power.

$$2\beta = 2\beta(i) = \frac{\beta_1}{P_y(i)} \tag{7}$$

where β_1 is a compromise value of the step size constant and $P_y(i)$ is an estimate of the average power in $y(i)$ at time i. The far end signal power can be estimated by

$$P_y(i) = [L_y(i)]^2 \tag{8}$$

451

where

$$L_y(i+1) = (1-\rho)L_y(i) + \rho|y(i)| \qquad (9)$$

where a typical value of $\rho = 2^{-7}$. The above equation is only an estimate of the average signal level which is updated for every sample using the approximation for ease of implementation in real-time.

The quality of the echo canceller can be affected significantly if the near end speech is not detected accurately. This is because the filter coefficients will be adjusted wrongly and hence will distort the near end speech. Therefore the coefficients are only updated when there is no near end speech and kept fixed during near end activity to prevent divergence. The power estimate $\hat{s}(i)$ of the near end composite signal $s(i) = x(i) + r(i)$ is usually compared with the power estimate $\hat{y}(i)$ of far end signal $y(i)$ to decide if there is near end activity. The power estimates can be computed using

$$\hat{s}(i+1) = (1-\alpha)\hat{s}(i) + \alpha|s(i)| \qquad (10)$$

and

$$\hat{y}(i+1) = (1-\alpha)\hat{y}(i) + \alpha|y(i)| \qquad (11)$$

where a typical value for α is 1/32. Near end speech is declared when

$$\hat{s}(i) \geq MAX[\hat{y}(i), \hat{y}(i-1), \hat{y}(i-N)] \qquad (12)$$

In order to avoid continuous switching, every time near end speech is detected, it is assumed to last for some time (typically 600 samples).

The echo canceller performance can be improved by a residual echo suppresser. This can be done simply by comparing the returned signal power with a threshold relative to the far end signal and completely eliminating it if it falls below the threshold. Again the returned signal power is estimated using

$$L_u(i+1) = (1-\rho)L_u(i) + \rho|u(i)| \qquad (13)$$

Whenever, $L_u(i)/L_y(i) < 2^{-4}$ the residual echo suppresser is activated. In some applications however, it may be perceptually more acceptable to leave a very low level of random signal to indicate that the line is not dead. The above algorithm with 64 tap filter has been implemented with a multi rate CELP coder operating at 4.8, 6.4 and 8 Kb/s and found to satisfy the CCITT recommendations completely [3].

4. VOICE ACTIVITY DETECTION

Discontinuous transmission (DTX) may be used to allocate the channel to other uses when there is no speech to be transmitted. DTX transmission simply makes use of the fact that every speech channel is not active continuously. In a duplex line conversation each party is active only for less than 50% of the time. Even during activity there are times that sizeable gaps between words and expressions exist. Therefore, by using a voice activity detector (VAD) to indicate active times, the channel may be allocated to another call when it is not needed. The use of VAD to indicate activity on the line may also be used to transmit non-speech data during the speech pauses which is very attractive in multi-media services. Alternatively, in mobile communication systems, the transmitter may be turned off to reduce the co-channel interference and also conserve the batteries of the hand held portable mobile terminals. This has been adopted as part of the overall specification of new mobile systems such as GSM. The efficiency or the gain of such systems depends on the performance of the VAD algorithm which has to work in severe background noise environments typical in a vehicle mounted mobile. The basic assumptions that the principles of a VAD algorithm can be based on are as follows:

1. Speech is a nonstationary signal. Its spectral shape usually changes after short periods of time, e.g., 20 to 30 ms.

2. Background noise is usually stationary during much longer time periods and changes very slowly with time.

3. Speech signal level is usually higher than the background noise level (otherwise speech will be unintelligible).

Using the above assumptions a VAD algorithm can be designed to detect silence gaps as well as distinguishing background noise with and without speech. In systems where the background noise level is very low, a simple signal energy threshold can be used to detect the silence regions. However, in systems where large and varying background noise is present, a much more intelligent algorithm needs to be used. This is typical of mobile systems where the mobile terminal is placed in a moving vehicle. In these systems, the noise level is very high and changing making it impossible to distinguish speech with background noise and background noise alone by using a simple energy threshold function. Since the level of the background noise could be changing, the threshold should be made adaptive. However the threshold should be updated only when there is no speech. For this the spectral characteristics are checked to see if it is likely to be speech with frequently changing spectral shape or noise with fairly stationary frequency response. Since speech can be classified as voiced with very slowly changing strong pitch, the change in periodicity within the frame time may also be considered to reinforce the confidence about speech detection. The accuracy of the VAD decision can be improved if the CELP LPC parameters are quantised

using LSFs. The LSF parameters for stationary signals remain fairly constant and do not change very rapidly. Therefore, the change in the LSF parameters from one frame to the next may be used to indicate signal stationarity [4].

If nonspeech decision is indicated a further conditioning is applied to eliminate the possibility of cutting out speech mid-bursts. This is done by adding a hangover stage to the VAD output. Before making the final decision that speech is not present a number of nonspeech frames have to be detected consecutively. This is determined by the length of the hangover time which is in the order of 60 to 100 ms (or 3 to 5 frames). If after the hangover time the decision still indicates nonspeech then the output of the VAD is used to indicate this to the DTX controller.

5. ROBUSTNESS TO CHANNEL ERRORS

The channel error performance mainly depends on the way the parameters are quantised and error protected. The most error sensitive CELP parameters are the LPC coefficients, followed by the excitation vector gain, LTP lag and gain, and finally the codebook index. CELP is generally robust up to the error rates of 10^{-3} without any FEC. The error protection can be split into two parts, one is achieved without any redundancy which is called built-in protection and the other is implemented by using extra redundancy bits in the form of FEC. By using Line Spectrum transformation, the residual errors on the LPC parameters can be controlled. The monotonicity of the Line Spectral Frequencies (LSF) can be used for error detection and correction [5]. This scheme is very effective at bit error rates (BER) of up to 10^{-2}.

Since the optimum vector gain is quantised as an absolute value, when one or more gain values are corrupted, they produce very annoying background noise. This is especially annoying when the speech is silence and errors result in very large decoded gain values, which produce loud blasts. To reduce this problem an optimum gain control algorithm has been developed and used [5].

It is assumed that in the worst case, the ratio of any subframe gain magnitude $|g(i)|$, $i = 1, \ldots, Q$ to the mean gain magnitude $\bar{g}$ of the corresponding frame, is not greater than a factor α. The second assumption is that the residual error rate is low enough that only one gain term per frame is corrupted. Again, this is a reasonable assumption for a satellite channel, except perhaps, during periods of deep fading. In the design, it is assumed that these (rare) situations will be detected and coped with by employing lost frame reconstruction techniques. Thus, at the receiver, we wish to find any gain for which $|g(i)|/\bar{g} > \alpha$, and then adjust it to achieve the desired ratio. There are two related problems that first need to be solved.

1. Whenever gain control is invoked, we are assuming that there is at least a single gain term corrupted within the frame. Thus, the average gain $\bar{g}$ for the frame cannot simply be computed from the sum of the received gains. This problem can be overcome by computing separate sub-average gains, $\bar{g}(i)$ for Q clusters of gains. The ith cluster is composed of all the other subframe gains except $|g(i)|$. Thus,

$$\bar{g}(i) = \frac{1}{Q-1} \sum_{j=1}^{Q} |g(j)|, \ j \neq i = 1, \ldots, Q; \quad (14)$$

where $g(i)$ is the excluded gain and Q, is the number of excitation subframes per frame.

2. Since we now have Q sub-average gains, we have to determine which one to use in the corruption tests. Since we are only interested in *upwardly corrupted* gains, and taking into account the assumption that the variance of the gains is limited, we would expect the cluster of gains with the corrupted gain to have the highest variance. Therefore, the best sub-average to use is that of the cluster with the minimum variance, as this is more likely to be closest to the full average gain $\bar{g}$. The cluster variances $\sigma^2(i)$ are calculated as,

$$\sigma^2(i) = \frac{1}{Q-1} \sum_{j=1}^{Q} (\bar{g}(i) - |g(j)|)^2, \ j \neq i = 1, \ldots, Q \quad (15)$$

Let the cluster with the minimum variance be cluster I. Then if the test for *upward corruption*, $|g(I)| \leq \alpha \bar{g}(I)$ fails, $g'(I)$ the controlled gain is reset as: $g'(I) = \bar{g}(I) \times sign[g(I)]$.

The ratio α is very important in these tests. If it is set too high, then a significant proportion of corrupted gains will pass the test, resulting in a degraded performance with channel errors. On the other hand, setting α too low means some uncorrupted gains will be 'adjusted', leading to degradation in the clear channel speech quality of the coder. In practice, it is very difficult to strike a reasonable balance which is speaker independent. A more attractive alternative is to adopt an adaptive approach in which the test factor changes according to the gains being considered. Since the test is trying to determine the deviation of the suspect gain from the mean gain, the test can be changed into,

$$|g(I)| \leq \alpha' \sigma(I) + \bar{g}(I) \quad (16)$$

where α', the adaptive factor is given by,

$$\alpha' = MIN[\sigma(i)]/\sigma(I), \quad I \neq i = 1, \ldots, Q \quad (17)$$

Parameters	Number/Frame	Bits/Frame
STP(LSF)	10	37
LTP	4×1-tap	4×(7+5)=48
CB index	4	4×7=28
CB gain	4	4×5=20
Total	-	139

Table 1: Configuration of CELP at 4.43 Kb/s with 30ms frame

This produces the best performance, giving only a negligible reduction in clear channel $segSNR$, whilst detecting a high proportion (about 88%) of the corrupted gains.

Built in error control for the LSFs and excitation vector gains was found to be sufficient for a maximum residual error rate of 10^{-2}.

6. CODER PERFORMANCE

The CELP coder described in Table 1 has been implemented on a single DSP32C with 32 Kbytes of SRAM. Using the same DSP a 64-tap echo canceller together with a VAD and built in error control was integrated with the main CELP encoder/decoder. This resulted in a complete solution in one DSP enabling a very cost effective and compact implementation. Since the coder uses 133 bits of the available 144 every 30 ms frame, the remaining 11 bits were used for very robust synchronisation. Every frame a sync-pattern that differed from any possible data patterns at least in two bit positions was used, enabling very fast locking time and robust synchronisation under channel errors.

The speech quality of the coder was assessed using informal listening tests. In these tests the CELP coder defined in Table 1 scored a MOS of 3.5. Its higher bit rate version at 6.65 Kb/s again defined by the same table but with a 50 Hz frame rate scored a MOS of 3.9 and was found to be better than the full rate GSM coder. Both versions were also found to be transparent to channel errors of up to 2×10^{-3}. At 10^{-2} very slight degradation was noticed due to corrupted LTP lags.

The performance of the 64-tap echo canceller was tested against the CCITT G.165 and was found to satisfy it fully. This coder has been used in various VSAT terminals produced by different manufacturers and found to be very acceptable by the users.

7. REFERENCES

[1] M.R.Schroeder, B.S.Atal "Code-excited linear prediction (CELP): High quality speech at very low bit rates", Proc. of ICASSP-85, pp 937-940.

[2] M.R.Suddle, A.M.Kondoz, B.G.Evans "DSP Implementation of Low Bit Rate CELP Based Speech Coders", Proc. 6th Int. Conf. on Digital Processing of Signals in Communications, Loughborough, U.K., Sep-1991, pp 309-314.

[3] M.R.Suddle, A.M.Kondoz, B.G.Evans "A Single DSP Multi-Rate Voice Coder with Integrated Echo Canceller", 3rd Int. Workshop on Digital Processing Techniques Applied to Speech Applications", ESA/ESTEC, Netherland, 1992.

[4] H.G.Asjadi "Real-time Implementation of Low Bitrate Speech Coders for Satellite and Land Mobile Communications", PhD Thesis, University of Surrey, Guildford, U.K. 1990.

[5] S.A.Atungsiri "Joint Source and Channel Coding for Low Bit-rate Communication Systems", PhD Thesis, University of Surrey, Guildford, U.K. 1991.
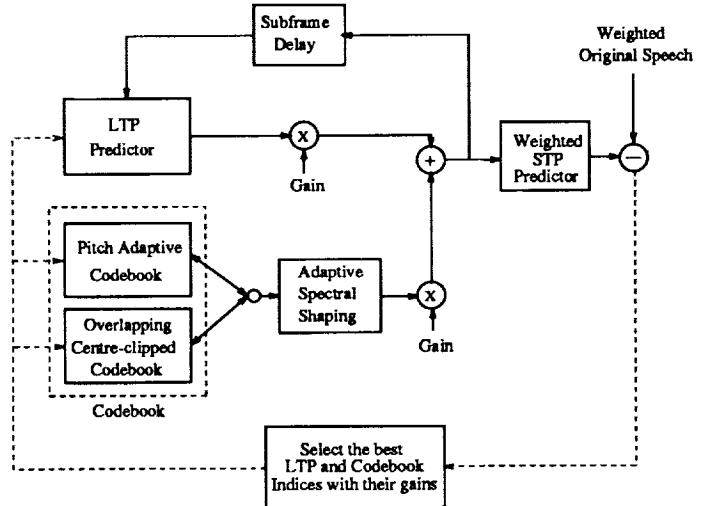
Figure 1: CELP with PAME excitation
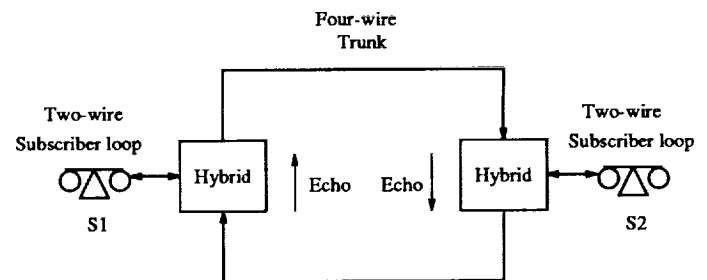
Figure 2: A duplex telphone line connection

$$u(i) = x(i) + r(i) - \hat{r}(i)$$
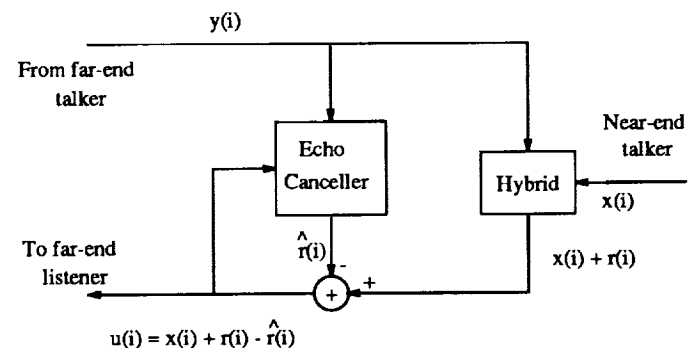
Figure 3: An Echo canceller set-up

454

Performance of the Unique-Word-Reverse-Modulation Type Demodulator for Mobile Satellite Communications

Tomohiro Dohi, Kazumasa Nitta, Takashi Ueda
NTT Mobile Communications Network Inc.
1-2356 Take, Yokosuka-shi, 238-03 Japan
Phone : +81 468 59 3462 Fax : +81 468 57 7909

ABSTRACT

This paper proposes a new type of coherent demodulator, the unique-word(UW)-reverse-modulation type demodulator, for burst signal controlled by voice operated transmitter (VOX) in mobile satellite communication channels. The demodulator has three individual circuits: a pre-detection signal combiner, a pre-detection UW detector and a UW-reverse-modulation type demodulator. The pre-detection signal combiner combines signal sequences received by two antennas and improves bit energy-to-noise power density ratio (E_b/N_0) 2.5 dB to yield 10^{-3} average bit error rate (BER) when carrier power-to-multipath power ratio (*CMR*) is 15 dB. The pre-detection UW detector improves UW detection probability when the frequency offset is large. The UW-reverse-modulation type demodulator realizes a maximum pull-in frequency of 3.9 kHz, the pull-in time is 2.4 seconds and frequency error is less than 20 Hz. The performances of this demodulator are confirmed through computer simulations and its effect is clarified in real-time experiments at a bit rate of 16.8 kbps using digital signal processor (DSP).

INTRODUCTION

Practical mobile satellite communication systems are being developed in many countries. In Japan, the characteristics of mobile satellite channels were obtained from a field test of experimental mobile satellite systems (EMSS) using the Engineering Test Satellite V (ETS-V)[1]. The results confirmed that the channels of the mobile satellite communication system are high *CMR* Rician fading channels. Meanwhile, since satellite communication channels are power-limited, forward error correction (FEC) must be employed to improve BER in low carrier power-to-noise power ratio (CNR) channels.

To improve the received E_b/N_0, signal combination should be powerful. Conventionally, two types of signal combination scheme are well-known. One is the post-detection signal combination scheme [2], and the other is the pre-detection signal combination scheme [3]. When the post-detection scheme is employed, each demodulator must operate stably before the received E_b/N_0 is improved. On the other hand, when the pre-detection scheme is employed, a demodulator can operate stably after the received E_b/N_0 is improved. Since the conventional pre-detection scheme is a feed-back type, its ability to track variations in channel state is inferior. Therefore, this paper proposes a pre-detection signal combination scheme with a feed-forward loop. Its tracking ability is very high.

In mobile satellite communication channels, rapid UW detection after shadowing is required. Since the received UW is used for demodulation in the proposed scheme, UW detection must be carried out ahead of demodulation. Furthermore, the range of pull-in frequency is expanded 30 times that of the conventional scheme, because the UW detector detects correlation value from the phase difference of received signals.

In mobile satellite communications, carrier frequency offset due to Doppler shift occurs when the mobile station moves at high speed. When the transmission rate is assumed to be 16.8 kbps, the frequency error must be less than several tens Hz to prevent carrier slip. To keep this frequency error, highly precise automatic frequency control (AFC) is required. This paper proposes a UW-reverse-modulation type demodulator including AFC circuit. In this demodulator, a reverse modulated signal sequence is used for estimating the carrier fre-
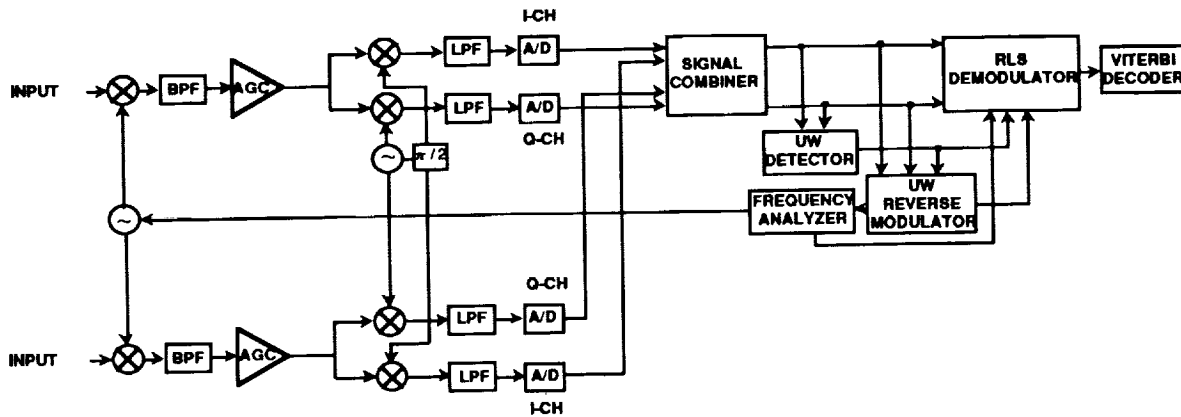
Figure 1   Configuration of the Receiver

quency offset by fast Fourier transformation (FFT). Consequently, short pull-in time (2.4 seconds), high precision (frequency error is 20 Hz) and wide pull-in range (about 4 kHz) are realized using this scheme.

In this paper, configuration and characteristics of the mobile terminal receiver are described in detail.

CONFIGURATION

Configuration of the receiver is shown in Figure 1. The receiver consists of RF/IF circuit, pre-detection signal combiner, pre-detection UW detector, UW-reverse-modulation type demodulator including AFC circuit and Viterbi decoder. The receiver has two RF/IF circuits. Both RF/IF circuits consist of a band pass filter (BPF), automatic gain control (AGC) circuit and low pass filters (LPF). The RF/IF circuit down-converts the received RF signal sequence into the IF band, and the IF signal sequence is down-converted into the baseband. In the signal combiner, each analog signal sequence is converted into a 12 bit digital signal sequence with identical timing. Each branch's signal sequence is combined to improve the received E_b/N_0. The combined signal is led to the UW detector. The UW detector consists of two correlators. These correlators are switched according to the degree of phase rotation. The frame is reconstructed in the UW detector and sent to the demodulator. The recursive least squares (RLS) algorithm is employed in the demodulator. In the AFC circuits, the reverse modulated signal sequence is used for estimating the carrier frequency offset by FFT. When the carrier frequency offset is larger than 1 kHz, the output from FFT is used as the control voltage of the voltage-controlled oscillator (VCO). On the other hand,

the output is multiplied by the received baseband signal sequence when the carrier frequency offset is less than 1 kHz. Consequently, carrier offset component is removed from received signal sequence used in the demodulator. The constraint length is 7 (k=7), the coding rate is 1/2 (R=1/2), and 4 bit soft decision is employed for Viterbi decoder. The signal combiner, UW detector, UW reverse-modulation-type demodulator including AFC circuit and Viterbi decoder were implemented on DSP.

PRE-DETECTION SIGNAL COMBINER

Configuration and Principle

In the pre-detection signal combiner, the received E_b/N_0 is theoretically improved 3 dB, because the direct wave's signal amplitude is combined and noise power is combined. Configuration of the pre-detection signal combiner is illustrated in Figure 2. Signal sequences are received by two antennas and converted into baseband analog signal sequences by quadrature detection in the RF/IF circuits which consist of frequency converters, BPFs and AGC amplifiers. These signal sequences are A/D converted with identical timing, and one signal sequence is multiplied by the other signal sequence's complex conjugate. Since this product is derived from A/D converted signals with identical timing, influence of modulation upon phase is removed from the product. The product means that noise and fading components are added to the phase difference of the 2 received direct waves at each branch. Noise and fading components is removed from the signal by averaging, and obtained phase difference is multiplied by one signal sequence and combined with the

456
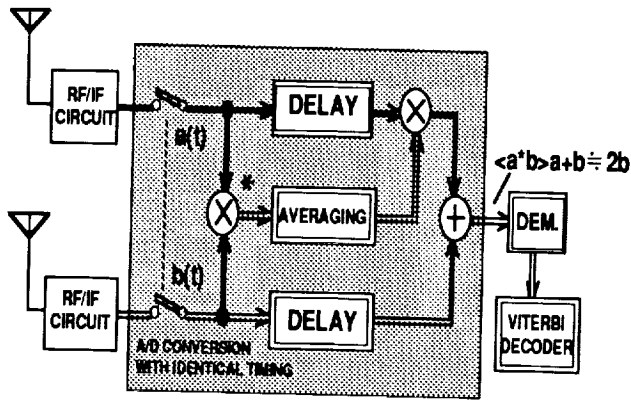
Figure 2   Configuration of Pre-detection Signal Combiner

Figure 3   Relation between the Number of Symbols and Combining Gain

other signal sequence. In this operation, it doesn't matter that the clock used for A/D conversion is not synchronized to the transmitted signal if the clock rate is faster than transmission symbol rate. Clock synchronization is established in the demodulator after combination.

The Number of Averaging Symbols

To achieve accurate phase combination, noise and fading component must be removed from the received signal by averaging. Required number of averaging symbols was clarified through computer simulations. In these simulations, it is assumed that CMR is 15 and 20 dB, and that E_b/N_0 is 0 dB. The relation between the number of averaging symbols and combination gain is shown in Figure 3. When CMR is 15 dB, the degradation of combination gain with 30 averaging symbols is less than 0.5 dB compared to the theoretical value (3 dB). When CMR is 20 dB, it is 0.3 dB. Therefore, 30 averaging symbols are enough to realize high combination gain. The improvement in BER performance with signal combination is confirmed through the real-time experiments described later.

UW DETECTOR

In the demodulator, UW detection must be carried out ahead of demodulation, because the received UW is used for demodulation. To realize compact and low cost mobile terminals, temperature-compensated crystal oscillators (TCXO) that do not utilize thermostatic ovens are required. TCXO stability is within 1 ppm. When transmission bit rate is assumed to be 16.8 kbps in the S-band (2.6 / 2.5 GHz), it is

required that frame synchronization must be kept when ΔfT (Δf: frequency offset) is less than 0.2. If frequency offset is small, the probability of UW detection with the conventional scheme is good. However, if frequency offset is large, the probability is degraded significantly. Therefore, a new UW detection scheme is required to satisfy this requirement of frame synchronization. Configuration of the proposed UW detector is illustrated in Figure 4. This detector has a phase rotation detector and selects one of two correlation detectors according to the degree of phase rotation. One correlation detector is a conventional type. In this detector, the input signal sequence is memorized in delay circuit with taps and multiplied by the complex conjugate of the UW pattern. The products are integrated, and each component of integration is squared and added. This yields the correlation value. In the other detector, the input signal sequence is detected differentially at first. Detected sequence is memorized in delay cir-
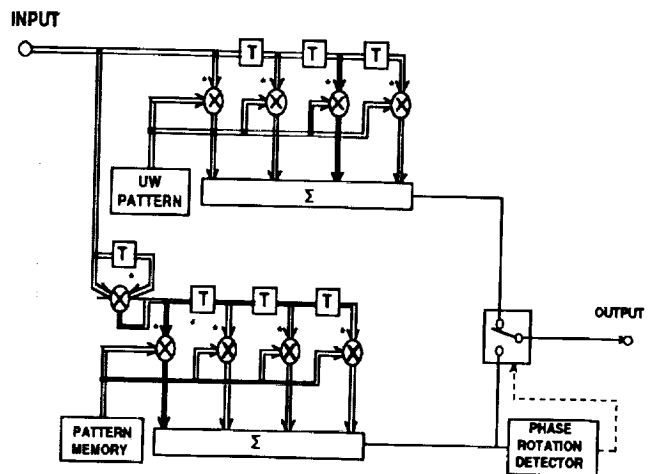
Figure 4   Configuration of UW Detector

457
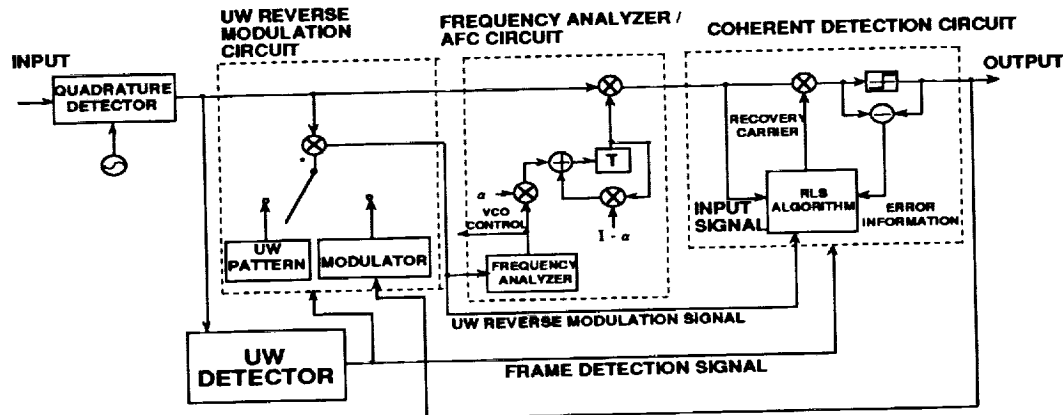
Figure 5 Configuration of UW-Reverse-Modulation Type Demodulator

cuits and multiplied by the complex conjugate of the difference of adjacent symbols in the UW pattern memorized in pattern memory. Remaining behavior are the same as those of conventional detector. Absolute ratio of real part to imaginary part of integration is used to detect the degree of phase rotation. When the degree of phase rotation is small, the real part is much larger than the imaginary part, and the conventional correlator is selected. When the real part is not much larger than the imaginary part, the new correlator is selected. Performance of the UW detector is described in the section on experimental results.

UW-REVERSE-MODULATION TYPE DEMODULATOR

Configuration and Principle

In the S-band, when TCXO stability is 1 ppm, maximum frequency offset is considered to be 2.6 kHz. When the mobile station moves at 100 km/h and the elevation angle is 40 degrees, the frequency offset caused by Doppler shift is 180 Hz. If the transmission rate is assumed to be 16.8 kbps, the frequency error must be less than 20 Hz to prevent carrier slip. On the other hand, since this demodulator is applied for burst signal controlled by VOX, rapid pull-in time is required. Under these conditions, frequency control by AFC is required to operate the receiver normally. As above-mentioned, the maximum pull-in frequency is assumed to be 3 kHz. Furthermore, it is assumed that frequency error is 20 Hz, and pull-in time is 3 seconds. The proposed UW-reverse-modulation type demodulator is shown in Figure 5. In the AFC circuit, the reverse modulated signal sequence is used for estimating frequency offset by applying FFT. The reverse modulated signal sequence consists of a UW reverse modulation signal sequence and a reverse modulated information signal sequence. Received baseband signal sequence is multiplied by the complex conjugate of the UW pattern. The product
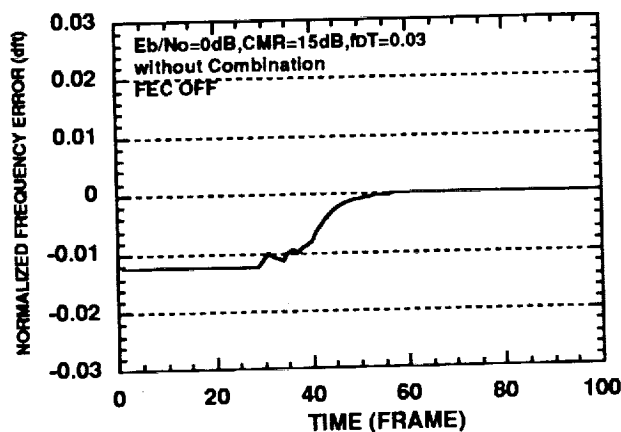
Figure 6 Pull-in Performance
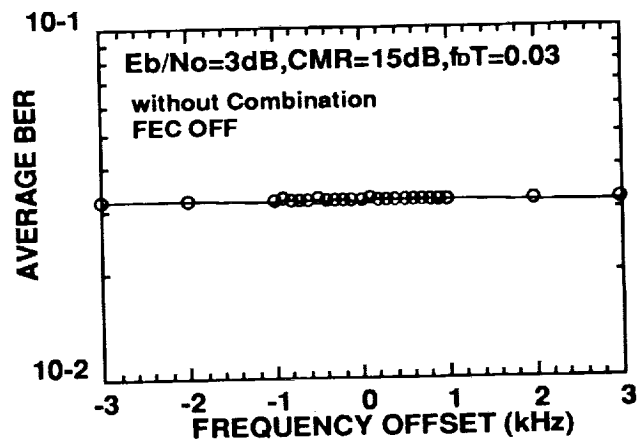
Figure 7 Pull-in Frequency Performance

458

sequence is the UW reverse modulation signal sequence. The information data sequence following the UW signal is modulated after demodulation. Received baseband signal sequence following the UW signal is multiplied by the complex conjugate of the modulated signal sequence. The product sequence is the reverse modulated information signal sequence. The result of estimating is used as the VCO control voltage when the carrier frequency offset is larger than 1 kHz. When carrier frequency offset is less than 1 kHz, after averaging the results of estimating, the result is multiplied by the received baseband signal sequence, and the carrier offset component is removed from the received signal sequence.

Characteristics of the proposed AFC

AFC performance was clarified through computer simulations. In these simulations, ideal frame and clock synchronization was assumed. It was assumed that the transmission bit rate is 16.8 kbps, UW length is 64 bit and information bit length is 608 bit. The relation between pull-in time and normalized frequency error (frequency error / transmission rate) is shown in Figure 6. In this figure, the horizontal axis indicates the number of frames, that is, time, and the vertical axis indicates the normalized frequency error after pull-in. Pull-in time is 60 frames (2.4 seconds), and this satisfies the requirement given above. Normalized frequency error after pull-in is 0, which definitely satisfies the requirement. The relation between frequency offset and average BER is shown in Figure 7. Average BER is not degraded if the frequency offset is less than 3.9 kHz. Average BER will be degraded due to the bandwidth limitation of the IF filter if experimentally measured.

EXPERIMENTAL RESULTS

The above-mentioned techniques were clarified in real-time experiments. Experimental parameters are shown in Table 1. According to results of the EMSS experiment, CMR was assumed to be 15 dB. Each frame consists of a 64 bit UW and 608 bit of information data. A 16.8 kbps, nine-stage pseudo noise (PN) sequence is the transmitted data. A five-stage PN sequence is the UW data. After a π/4-shift quadrature phase shift keying (QPSK) signal

(roll off factor $\alpha = 0.5$) is generated in the baseband, it is modulated and transmitted over a communication channel. Rician fading is generated by a fading simulator. RF/IF circuit is composed of analog devices. Signal combiner, UW detector, UW-reverse-modulation type demodulator including AFC and Viterbi decoding are implemented as DSP.

The average BER performances are shown in Figure 8. There are 4 kinds of average measured BER performances plotted in Figure 8. Solid curve indicates theoretical performance without FEC or signal combination. Points indicate measured values without the proposed techniques, measured values with FEC, measured values with signal combination and measured values with both FEC and signal combination. The degradation of average BER performance of the demodulator without signal combination or Viterbi decoding compared to the theoretical one is less than 0.5 dB. Therefore, it can be said that the demodulator is very precise. When using signal combination and Viterbi decoding, average BER performance is improved about 3 dB in terms of E_b/N_0 to yield BER = 10^{-3} compared with the one of using Viterbi decoding only.

Table 1 Experimental Parameters

Modulation	π/4-QPSK (α=0.5)
Demodulation	Coherent Detection
Frame Length	40ms
UW	64bit
Data	608bit
Bit Rate	16.8kb/s
FEC	k=7,R=1/2
	Convolutional Coding / Soft Decision Viterbi Decoding
CMR	15dB
foT	2.4×10⁻³
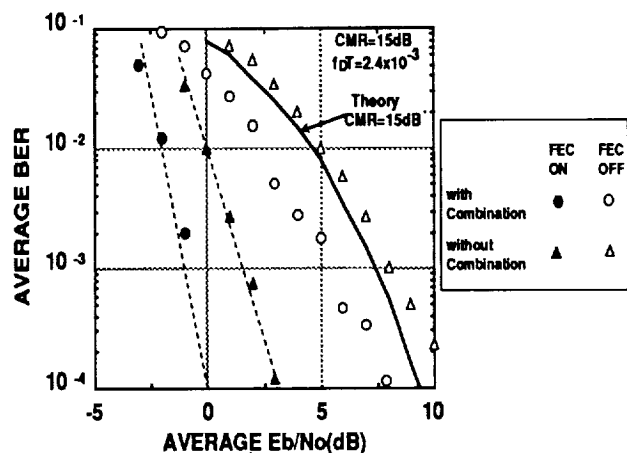
Figure 8 Average BER Performances

459

The relation between frequency offset and UW miss detection probability of the proposed UW detection scheme is shown in Figure 9. Since it is difficult to measure the UW miss detection probability when E_b/N_0 is assumed to be 0 dB, E_b/N_0 is assumed to be -3 dB and -2 dB. When the transmission bit rate is 16.8 kbps and absolute value of frequency offset is is more than 100 Hz, UW miss detection probability of the proposed scheme is superior. When absolute value of frequency offset is less than 100 Hz, UW miss detection probability of the conventional scheme is better than that of the proposed scheme. The conventional scheme is poor with large frequency offset. Consequently, when the threshold of selection is assumed to be 100 Hz, best UW detection performance is obtained.

The relation between frequency offset and average BER at 3 dB E_b/N_0 is shown in Figure 10. When the frequency offset is 2 kHz, BER performance degradation is only 40 % compared to the no frequency offset case. When the frequency offset is 3 kHz, BER performance degrades because of the IF filter.

CONCLUSION

Configuration and performances of a UW-reverse-modulation type demodulator for mobile satellite communication systems is presented. Pre-detection signal combiner combines two branch signal sequences ahead of detection to allow accurate behavior in the low *CNR* condition. Consequently, the received E_b/N_0 is improved 2.5 dB. Frame synchronization is established before demodulation to realize rapid synchronization. Proposed UW detector does not degrade UW detection probability even if the frequency offset is large. This new demodulator realizes a maximum pull-in frequency of 3.9 kHz, pull-in time is 2.4 seconds and frequency error is less than 20 Hz. Application of these techniques enables the receiver to operate normally in satellite communication channels.

ACKNOWLEDGEMENT

The authors wish to thank Mr. Kuramoto, Mr. Mishima, Mr. Murota and Mr. Hagiwara for their helpful guidance and encouragement.

REFERNCES

[1] T. Sakai and T. Dohi, "Bit Error Rate Characteristics on Mobile Satellite Communication
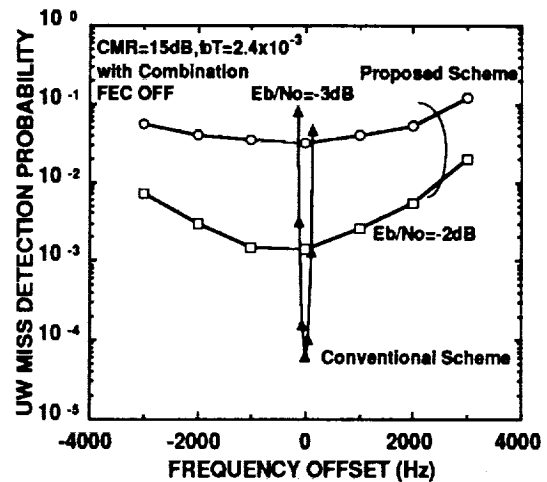
Figure 9 Relation between Frequency Offset and UW Miss Detection Probability
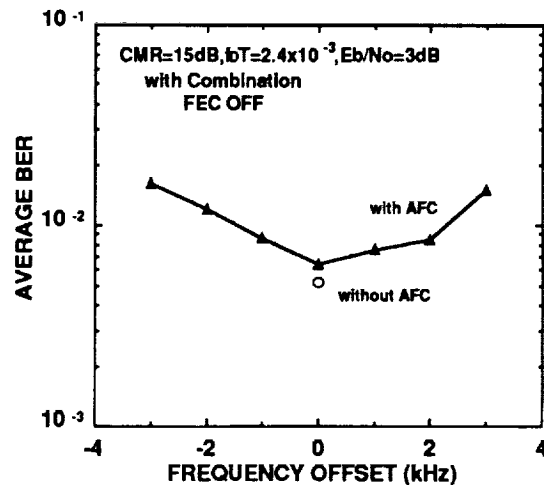
Figure 10 Pull-in Frequency Performance

Channels", *Trans. IEICE*, J72-B-II, pp. 285-289, July 1989.
[2] S. Hara and N. Morinaga, "Post-Detection Combining Diversity Improvement of 4-Phase DPSK System in Mobile Satellite Communications", *Trans. IEICE*, J72-B-II, pp. 304-309, July 1989.
[3] J. Granlund, "Topics in the Design of Antenna for Scatter", *Technical Report 135*, Lincoln Laboratory, MIT, November 1956.

460

DS-SSMA capacity for a mobile satellite system

Francesco Bartucca   Ezio Biglieri*

Dipartimento di Elettronica, Politecnico, Corso Duca degli Abruzzi 24, I-10129 Torino (Italy). Tel: +39 11 5644030, Fax: +39 11 5644099, e-mail: biglieri@polito.it

Abstract

We consider a cellular satellite system conceived to enhance the capabilities of the pan-European terrestrial system (GSM). This adopts EHF band and highly-inclined orbits. We present a preliminary assessment of system capacity based on asynchronous direct-sequence spread-spectrum multiple access (DS-SSMA). Performance is measured in terms of error probability achieved by K users simultaneously accessing the system with a given signal-to-noise ratio.

INTRODUCTION

A cellular satellite system has recently been proposed [3, 4, 12] which is conceived to enhance the capabilities of the pan-European terrestrial cellular system (GSM). Intended as an efficient complement to GSM, this new system adopts EHF band (specifically, 40/50 GHz), and highly-inclined orbits. Its main goals are: [3, 12] (i) To provide higher source data rates (64 kbit/s, and possibly $n \times 64$ kbit/s) in order to support ISDN-compatible teleservices. (ii) To expedite the diffusion of mobile services in Europe and expand their coverage to Eastern Europe, part of North Africa, and the Near East. (iii) To integrate maritime and aeronautical users into the terrestrial network. (iv) To offer private users a solution for implementation of mobile-radio closed networks with coverage radii up to a few hundred kilometers. (v) To allow implementation of networks of small, portable terminals in the perspective of a forthcoming worldwide personal communication system.

In this paper we present a preliminary assessment of system capacity based on asynchronous direct-sequence spread-spectrum multiple access (DS-SSMA). System performance is measured in terms of error probability achieved by K users simultaneously accessing the system with a given signal-to-noise ratio.

SYSTEM MODEL

In the model of an asynchronous DS-SSMA sys-

---

tem [13], K users transmit digital data over a common satellite channel with center frequency f_c. The signal transmitted by the kth user is

$$s_k(t) = \sqrt{2P}\, b_k(t) a_k(t) \cos(2\pi f_c t + \theta_k) \qquad (1)$$

where P denotes the common transmitted power, $b_k(t)$ is the data-bearing signal, $a_k(t)$ is a periodic waveform with period T and formed by N rectangular chips, each with duration $T_c = T/N$ and amplitude ± 1, and θ_k is the carrier phase. The signal $b_k(t)$ is a rectangular waveform taking on the value $b_{k,l}$ in the time interval $[lT, (l+1)T]$, where $b_{k,l}$ the lth source bit from user k, taking on values ± 1 with equal probabilities and independently of the other $b_{i,j}$.

The code sequence assigned to the kth user takes on value $a_k^{(j)}$ in the interval $[jT_c, (j+1)T_c]$ for a code word $a_k^{(0)}$, $a_k^{(1)}$,..., $a_k^{(N-1)}$ taking values ± 1. The signal bandwidth is proportional to $T_c^{-1} = N/T$, and hence N is the bandwidth-expansion factor.

The signal received by the kth user is

$$\sqrt{2P} \sum_{k=1}^{K} a_k(t - \tau_k) b_k(t - \tau_k) \cos(2\pi f_c t + \phi_k) + n_k(t)$$

where $n_k(t)$ is a white Gaussian noise process independent of the other random variables (RV) and whose two-sided power spectral density is $N_0/2$. The delay τ_k and the phase $\phi_k = \theta_k - 2\pi f_c \tau_k$ model asynchronous transmission. We assume that τ_k is uniformly distributed in $[0, T]$, ϕ_k is uniformly distributed in $[0, 2\pi]$, and τ_k, ϕ_k are independent of each other and of the other RVs in this model.

The kth-user receiver computes the correlation between the received signal and $a_k(t)\cos(2\pi f_c t)$ in the time interval $[0, T]$, and makes a decision on the value of $b_{k,0}$ based on the sign of this correlation. Consider receiver #1, and with no loss of generality assume $\tau_1 = \phi_1 = 0$. With $f_c \gg 1/T$, the correlator output is

$$Z_1 = \sqrt{\frac{P}{2}}\, T\, b_{1,0} + \sqrt{\frac{P}{2}}\, u + n, \qquad (2)$$

where the first term in the right-hand side is the useful signal, the second term is the interference from

the other users, and n is white Gaussian noise. The multiple-access interference RV u is defined as

$$u = \sum_{k=2}^{K} \left[b_{k,-1} R_{k,1}(\tau_k) + b_{k,0} \hat{R}_{k,1}(\tau_k) \right] \cos \phi_k =$$
$$= \sum_{k=2}^{K} w_k \cos \phi_k \qquad (3)$$

where $R_{k,1}$ and $\hat{R}_{k,1}$ are partial crosscorrelations

$$R_{k,1}(\tau) = \int_0^T a_k(t - \tau) a_1(t)\, dt$$
$$\hat{R}_{k,1}(\tau) = \int_\tau^T a_l(t - \tau) a_1(t)\, dt \qquad (4)$$

with $0 \leq \tau \leq T$.

The average error probability for user #1 can be evaluated by using the moments of this RV u.

Assume $b_{1,0} = 1$. Then the average error probability $P(E)$ is equal to $P(Z_1 < 0)$, and we have

$$P(E) = \int Q\left[\sqrt{\frac{2PT}{N_0}} \left(1 + \frac{u}{T}\right) \right] f_u(u)\, d \qquad (5)$$

where $PT/N_0 \triangleq E_b/N_0$ is the signal-to-Gaussian noise power ratio, and $E_b \triangleq PT$ is the energy per bit. The function $Q(x)$ is defined in the usual way:

$$Q(x) = \frac{1}{\sqrt{2\pi}} \int_x^\infty \exp(-t^2/2)\, dt. \qquad (6)$$

Once the moments of the RV Z_1 have been evaluated, several techniques are available to compute the error probability (5). Refs. [1, 2, 14] summarize some of them, based on series expansions or on Gauss quadrature rules. In the following we shall use a technique advocated in [13] and based on Gram-Charlier series.

Gram-Charlier expansion

Gram-Charlier series expand a probability density function (pdf) in terms of derivatives of a known pdf [5].

Following [13], define a RV x associated with multiple-access interference and Gaussian noise:

$$x = x_0 \left(\frac{T}{u} + \sqrt{\frac{2}{P}} \frac{u}{T} \right); \quad x_0 = \left(\frac{E[u^2]}{T^2} + \frac{N_0}{2PT} \right)^{-\frac{1}{2}},$$

where x_0 is a normalization factor for x. The average error probability is given by

$$P(E) = P(x < -x_0) = \int_{-\infty}^{-x_0} f_x(x)\, dx \qquad (7)$$

where $f_x(x)$ is the pdf of the RV x. This can be expanded in the form

$$f_x(x) = \frac{1}{\sqrt{2\pi}} \exp\left(-\frac{x^2}{2}\right) \sum_{n=0}^\infty c_n He_n(x) \qquad (8)$$

where $He_n(x)$ is the nth Hermite polynomial

$$He_n(x) = (-1)^n \exp\left(-\frac{x^2}{2}\right) \frac{d^n}{dx^n} \exp\left(-\frac{x^2}{2}\right). \qquad (9)$$

The coefficients c_n are obtained from the orthogonality relation of Hermite polynomials, and are given by $c_n = E_n/n!$, where $E_n = E[He_n(x)]$. The coefficients E_n are generalized moments, and can be written in terms of the central moments of x. Since the pdf of x is an even function, and $He_n(x)$ is odd when n is odd, E_n is zero for n odd. The generalized moments E_{2n} can be expressed in the form

$$E_{2n} = \sum_{n=0}^n h_{2n,2k} E[x^{2k}]$$

where $h_{2n,2k}$, the coefficients of the orthogonal polynomials $He_{2n}(x)$, can be computed using the recursion

$$h_{2n,2k} = -\frac{n(2n-1)}{n-k} h_{2n-2,2k}, \quad k = 0, \ldots, n-1$$
$$h_{2n,2n} = 1, \qquad\qquad\qquad \text{for all } n$$

The coefficients E_{2n} can be computed from [13]

$$E[x^{2k}] = x_0^{-2k} \sum_{i=0}^k \binom{2k}{2i} \frac{E[u^{2i}]}{T^{2i}} \frac{(2k-2i)!}{2^{k-i}(k-i)!} \left(\frac{N_0}{2PT} \right)^{k-i}$$

By substituting (8) into (7), and using the previous results, we obtain a series expansion for the average error probability:

$$P(E) = Q(x_0) - e^{-x_0^2/2} \sum_{n=1}^\infty \frac{E_{2n}}{(2n)!\sqrt{2\pi}} He_{2n-1}(-x_0). \qquad (10)$$

The first term is the error probability we would achieve in the presence of an additive Gaussian disturbance whose power spectral density is the sum of the multiple-access interference and of the Gaussian noise.

This technique provides satisfactory results when the number of users is large and the signal-to-Gaussian noise ratio is low [13]. In this situation, two to three terms in the summation are enough for a good approximation to error probability. The moments of the RV u can be computed as described in [14].

Gaussian assumption

When the number of users is large enough, the pdf of the multiple interference is often assumed to approximately Gaussian, with a variance equal to the sum

of the variances of the multiple-access interferers and of the Gaussian noise. The average error probability based on the Gaussian assumption can be expressed as

$$P(E) = Q\left[\left(\frac{N_0}{2E_b} + \frac{K-1}{3N}\right)^{-\frac{1}{2}}\right]. \quad (11)$$

Choosing the code sequences

A class of binary code sequences with good correlation properties is provided by the maximum-length sequences. Another choice is suggested by Pursley and Roefs [10]: among all the maximum-length sequences with period $N = 2^n - 1$, we retain only those whose correlation sidelobes have lower energies: these sequences are called AO/LSE (auto-optimal/least sidelobe energy). The main drawback with these sequences is the small number of them available for each value of N. Another possible choice is provided by Gold sequences [7].

NUMERICAL RESULTS

In this work we consider a pseudo-random sequence with length $N = 255$ generated by an 8-stage shift register whose feedback connections are described by the polynomial 453 (octal notation). We assume that each user is assigned a shifted version of the sequence, so that a maximum of 255 users can be accommodated by the system.

Fig. 1 shows the average error probability of the system versus the number of users for several values of signal-to-Gaussian noise ratio E_b/N_0. The curves are obtained through the Gram-Charlier expansion method described before. The asterisks denote the approximation obtained under the Gaussian assumption, and refer to the error probability curve lying above them. It can be seen that the Gaussian assumption provides accurate enough results when the number of users is very large, and hence for high $P(E)$ values. The curves were obtained by retaining three terms in summation (10), and taking moments of the RV u up to order six.

Fig. 2 reorganizes the results by showing the number of users that can access the system at the same time, as a function of the signal-to-Gaussian noise ratio for several values of error probability. We can see that, if an error probability less that 10^{-6} is sought, we need an E_b/N_0 of at least 20 dB for 25 simultaneous users. If each user transmits at a speed of 64000 bit/s and the processing gain is 255 (24 dB), the bandwidth used is $64000 \times 255 = 16.3$ MHz, that is, each user needs a bandwidth of about 650 KHz. Under these conditions CDMA multiple access offers no advantage with
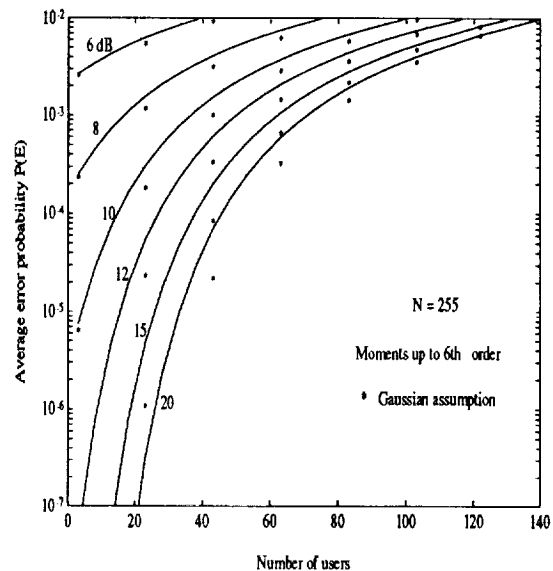
Figure 1: Average error probability P(E) versus the number of users for different values of the ratio E_b/N_0 for maximum-length sequences with $N = 255$.
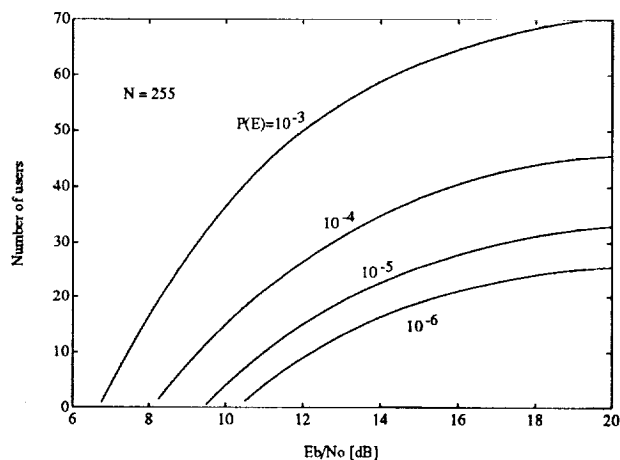
Figure 2: Number of simultaneous system users vs. E_b/N_0. The length of the code sequences is 255.

respect to FDMA, which would need about 128 KHz to transmit at 64 Kbit/s. Thus, SSMA would need an efficient coding scheme (which provides a suitable coding gain) to become attractive.

To increase the number of users that can access the system while keeping the same error performance we may think of using longer sequences, which will increase processing gain. The average error probability $P(E)$ obtained with a sequence of length 511 (feedback shift register with nine stages and generating polyno-

463

mial 1021) was computed. The corresponding values of system capacity vs. E_b/N_0 are shown in Fig. 3. We see that to achieve $K = 25$ and $P(E) = 10^{-6}$ as before, 13 dB are enough, with a savings of about 7 dB. The cost is a twofold increase in bandwidth occupancy.
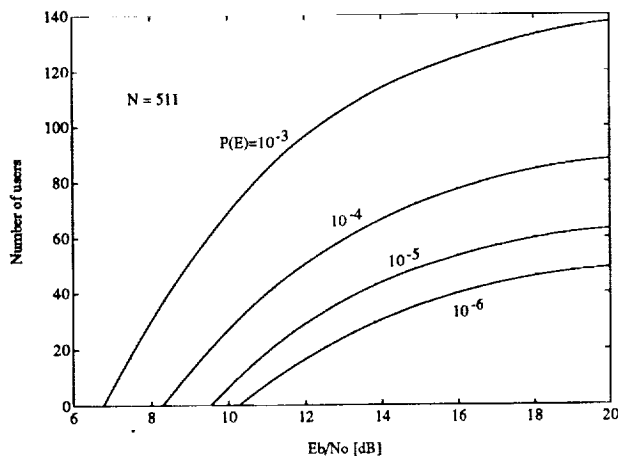
Figure 3: Number of users that can access the system with an assigned performance vs. E_b/N_0. The sequence length is 511.

Consideration of the satellite channel

We now consider some of the major factors that increase the capacity of an SSMA system [6], viz., voice activity, spatial discrimination provided by cross-polarization frequency reuse, and multi-beam antennas.

Voice activity. With a 35% voice activity factor, the number of users in Fig. 2 and Fig. 3 must be multiplied by $1/0.35 = 2.86$. Thus, when $N = 255$, for $P(E) = 10^{-6}$ and $E_b/N_0 = 20$ dB we have about 70 users, and the bandwidth is $650000 \times 0.35 = 227.5$ Kz per channel. With $N = 511$, for the same values of $P(E)$ and E_b/N_0 we have about 140 users, and the bandwidth per channel is about the same.

Cross-polarization frequency reuse. As for frequency reuse by cross-polarization, a quantitative analysis can be performed by using the computational techniques described before. Assume that K users access the system with each polarization. If X_{p} denotes the relative signal level with a given polarization, and received by a user transmitting with the opposite polarization, the total signal received by the kth user is

$$r_k(t) = \sqrt{2P} \sum_{k=1}^{K} A_k(t) + X_{\mathrm{p}} \sqrt{2P} \sum_{k=K+1}^{2K} A_k(t),$$

where

$$A_k(t) = a_k(t - \tau_k) b_k(t - \tau_k) \cos(2\pi f_c t + \phi_k).$$

The output of the kth-user correlator is

$$Z_1 = \sqrt{\frac{P}{2}} T b_{1,0} + \sqrt{\frac{P}{2}} u + X_{\mathrm{p}} \sqrt{\frac{P}{2}} u' + n \quad (12)$$

where the first term in the right-hand side is useful signal, the second the interference from the users with the same polarization, and the third the interference from the cross-polarized users. As usual, n is Gaussian noise. The RV u was defined in (3), while u' is defined as follows:

$$
\begin{aligned}
u' &= \sum_{k=K+1}^{2K} \left[b_{k,-1} R_{k,1}(\tau_k) + b_{k,0} \hat{R}_{k,1}(\tau_k) \right] \cos \phi_k \\
&= \sum_{k=K+1}^{2K} w_k \cos \phi_k
\end{aligned}
$$

$$(13)$$

The two RVs u and u' are independent, because b_k, τ_k, and ϕ_k are independent for each user. If we define the new RV $v = u + X_{\mathrm{p}} u'$, we obtain for error probability the same expression as (5), and hence to compute it we can use the same technique as before. To evaluate the moments of v we follow [8], and obtain

$$E[v^{2n}] = \sum_{p=0}^{n} \binom{2n}{2p} E[u^{2p}] X_{\mathrm{p}}^{2n-2p} E[u'^{2n-2p}] \quad (14)$$

where the moments of u and u' are calculated as above.

The error probability obtained with a cross-polarized channel attenuation equal to 6 dB, and sequence length 255 was computed. The corresponding values of capacity vs. E_b/N_0 are shown in Fig. 4. We can see that the capacity increase is about 85%, which could not be obtained by FDMA.

Fig. 5 shows capacity curves with sequence length 255, cross-polarization diversity, and a 35% voice activity factor.

If error-control coding is used, these curves move toward left by an amount equal to the coding gain.

Spatial discrimination Channel capacity can be further increased if multi-beam antennas are used, which allow a degree of frequency reuse. The amount of reuse depends on the maximum interference that can be tolerated among beams transmitting in the same bandwidth. A factor of frequency reuse equal to 2 or 3 seems reasonable, which implies increasing the capacity by a factor 2 or 3 if the interference is negligible.

464
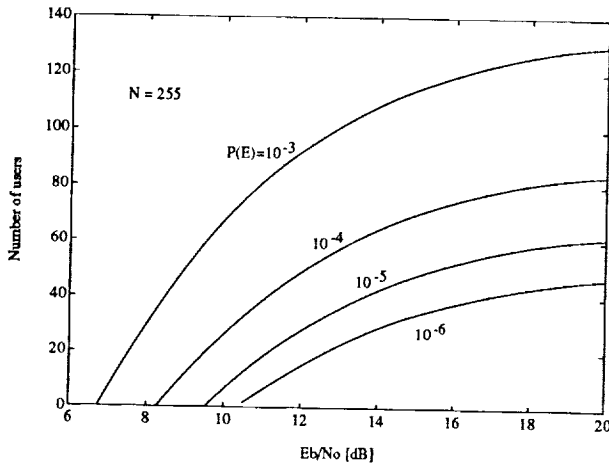
Figure 4: Number of users that can access the system with a given $P(E)$ for an attenuation of the cross-polarized channel equal to 6 dB.
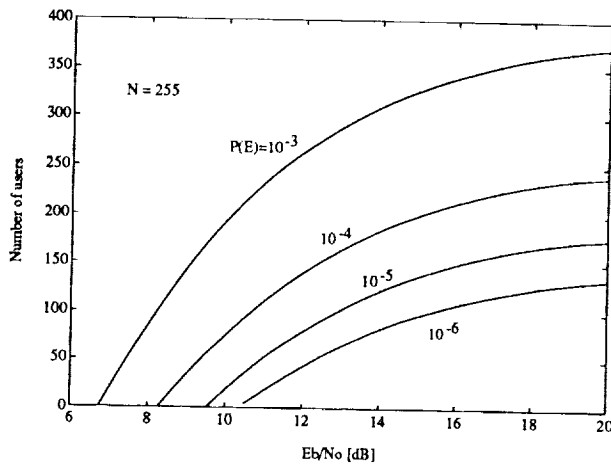
Figure 5: System capacity with single beam for several values of average error probability, an attenuation of the cross-polarized channel equal to 6 dB, and 35% voice activity factor vs. E_b/N_0.

SYSTEM CAPACITY

Consider now the satellite mobile radio system described in the Introduction. Assume 1000 channels with 40 beams, i.e., 25 channels per beam. From Fig. 6, obtained from Fig. 5 by zooming in the relevant region of E_b/N_0 and $P(E)$ values, we can see that for 25 users to access the system with $P(E) = 10^{-6}$ we need $E_b/N_0 \simeq 11,3$ dB. With code sequences of length $N = 511$, we need about 10.8 dB to achieve the same
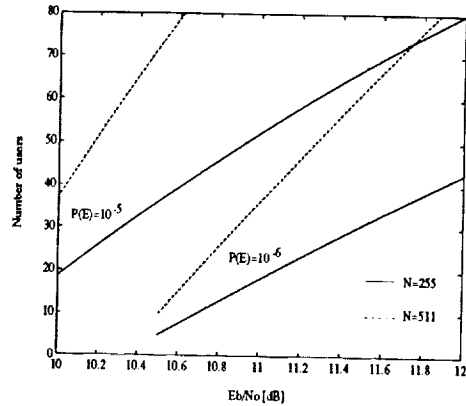
Figure 6: System capacity per beam for relevant values of $P(E)$ and E_b/N_0.

number of channels. By doubling the bandwidth, the achievable improvement is only 0.5 dB.

A note on synchronous SSMA

To achieve a more efficient use of the bandwidth with spread-spectrum modulation, multiple-access noise due to asynchronous transmission should be eliminated. This may be accomplished by making the users' spreading modulation *synchronous at the satellite*, thus providing channels that are ideally orthogonal. In synchronous design, the users' signal would have to be synchronized to a small fraction of a chip time to achieve the desired orthogonality and minimization of interference. In this system, timing control algorithms, their accuracy, and their impact on system design are be important issues that will not be dealt with here. In the following, capacity evaluations are extended to synchronous SSMA.

With a fully synchronous system the delays τ_k in the system model can be disregarded, and we assume $\tau_k = 0$ for $k = 1, 2, \ldots, K$. The signal received by the kth user is

$$r_k(t) = \sqrt{2P} \sum_{k=1}^{K} a_k(t) b_k(t) \cos(2\pi f_c t + \theta_k) + n_k(t)$$

$$(15)$$

and the output from the correlator is

$$Z_1 = \sqrt{\frac{P}{2}} b_{1,0} T + \sqrt{\frac{P}{2}} w + n \qquad (16)$$

where the RV w is defined as

$$w = \sum_{k=2}^{K} b_{k,0} R_{k,1}(0) \cos \theta_k \qquad (17)$$

465

with

$$R_{k,1}(0) = \int_0^T a_k(t)a_1(t)\,dt. \qquad (18)$$

Apart from a factor $1/T$, $R_{k,1}$ is the crosscorrelation between a pseudo-random sequence and its translated version, . It is well known that $R_{k,1}(0)$ takes values $-T/N = -T_c$, with N the sequence length. Thus, the RV w can be given the form

$$w = T\sum_{k=2}^{K} b_{k,0}\cos\theta_k \qquad (19)$$

and is the sum of $K-1$ independent RVs.

To evaluate error probability, we compute the moments of w and apply the Gram-Charlier expansion method as before. Fig. 7 compares the error probability of a system with 250 users and that of a channel with a single user and additive white Gaussian noise as the only disturbance. If an error probability 10^{-6} is desired, we need only to increase the signal-to-noise ratio by 0.2 dB with respect to the Gaussian channel. The spectral efficiency increases considerably, as we can allocate 250 users in the bandwidth $64000 \times 255 = 16,3$ MHz.
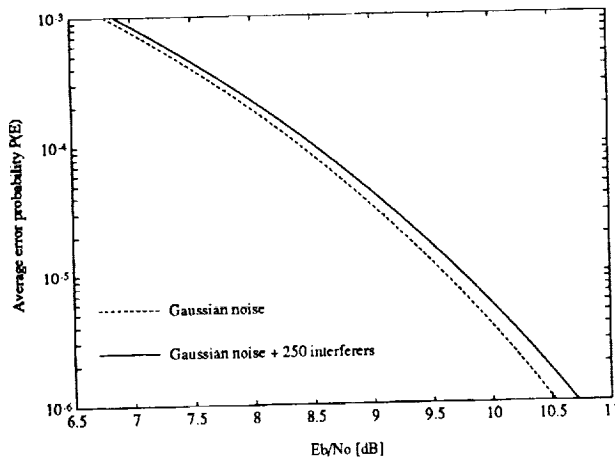
Figure 7: Average error probability vs. E_b/N_0 with synchronous transmission and sequence length 255.

References

[1] S. Benedetto, E. Biglieri, and V. Castellani, *Digital Transmission Theory*. Englewood Cliffs, New Jersey: Prentice-Hall Inc., 1987.

[2] S. Benedetto, E. Biglieri, A. Luvison, and V. Zingarelli, "Moment-based evaluation of digital transmission system performance," *IEE Proceedings-I*, Vol. 139, No. 3, pp. 258-266, June 1992.

[3] C. Caini, G. Falciasecca, F. Valdoni, and F. Vatalaro, "A cellular satellite system conceived to enhance capabilities of a terrestrial cellular system," *Global Satellite Communications Symposium*, Nanjing, China, 1991.

[4] G. Falciasecca, A. Paraboni, M. Ruggieri, F. Valdoni, and F. Vatalaro, "Feasibility of an EHF (40/50 GHz) mobile satellite system using highly inclined orbits," *Proc. IMSC'90*, Ottawa, pp. 131-135, June 1990.

[5] R. S. Freeman, "On Gram-Charlier approximation", *IEEE Trans. on Commun.*, Vol. COM-49, pp. 122-125, February 1981.

[6] K. S. Gilhousen, I. M. Jacobs, R. Padovani, and L. A. Weaver, Jr., "Increased capacity using CDMA for mobile satellite communications", *IEEE Journal on Selected Areas in Communications*, Vol. 8, N. 4, pp. 503-514, May 1990.

[7] R. Gold, "Optimal binary sequences for spread-spectrum multiplexing", *IEEE Trans. on Information Theory*, Vol. IT-13, pp. 619-621, Ottobre 1967.

[8] V. K. Prabhu, "Some considerations of error bounds in digital systems", *Bell System Technical Journal*, Vol. 50, pp. 3127-3151, 1971.

[9] M. B. Pursley, D. V. Sarwate, and W. Stark, "Error probability for direct sequence spread spectrum multiple-access communications - Part I: Upper and lower bounds", *IEEE Trans. on Commun.*, Vol. COM-30, pp. 975-984, May 1982.

[10] M. B. Pursley and H. F. A. Roefs, "Numerical evaluation of correlation parameters of optimal phases of binary shift-register sequences", *IEEE Trans. on Commun.*, Vol. COM-27, pp. 1597-1604, October 1979.

[11] M. B. Pursley, "Performance evaluation for phase coded SSMA communications - Part I: System analysis", *IEEE Trans. on Commun.*, Vol. COM-25, N. 8, pp. 795-799, August 1977.

[12] F. Valdoni, M. Ruggieri, F. Vatalaro, and A. Paraboni, "A new millimetre wave satellite system for land mobile communications," *European Transactions on Telecommunications*, Vol. I, N. 5, pp. 533-544, September-October 1990.

[13] K. T. Wu, "Bandwidth utilisation of direct sequence spread-spectrum system", *Proceedings of International Symposium on Communications*, Tainan, Taiwan, R.O.C., December 9-13, 1991.

[14] K. T. Wu, "Average error probability for DS-SSMA communication systems", *in Proc. of the 18th Annual Allerton Conference Commun., Control, Comput.*, pp. 359-368, October 1981.

SEPARABLE CONCATENATED CODES WITH ITERATIVE
MAP DECODING FOR RICIAN FADING CHANNELS

J.H. Lodge and R.J. Young
Communications Research Centre,
3701 Carling Ave., Ottawa, Canada. K2H 8S2
(tel) 613-998-2284, (fax) 613-990-6339

ABSTRACT

Very efficient signalling in radio channels requires the design of very powerful codes having special structure suitable for practical decoding schemes. In this paper, powerful codes are obtained by combining comparatively simple convolutional codes to form multi-tiered "separable" convolutional codes. The decoding of these codes, using separable symbol-by-symbol maximum *a posteriori* (MAP) "filters", is described. It is known that this approach yields impressive results in non-fading additive white Gaussian noise channels. Interleaving is an inherent part of the code construction and consequently these codes are well suited for fading channel communications. Here, simulation results for communications over Rician fading channels are presented to support this claim.

1. INTRODUCTION

In practice, very efficient signalling in radio channels requires more than the design of very powerful codes. It requires designing very powerful codes that have special structure so that practical decoding schemes can be used with excellent (but not necessarily truly optimal) results. Examples of two such approaches include the concatenation of convolutional and Reed-Solomon coding, and the use of very large constraint-length convolutional codes with reduced-state decoding. In this paper, an alternate approach is introduced. The initial simulation results are very encouraging.

The work discussed in this paper was motivated by concepts introduced in [1] for the decoding of concatenated convolutional codes. In that paper it is shown that symbol-by-symbol MAP decoding for the inner code allows soft decisions to be passed to the outer decoder, resulting in impressive performance. The inner decoding algorithm can be thought of as a type of nonlinear filter that accepts as its input a noisy signal. Then it makes use of the structure inherent in the inner code to produce a noisy output "decoded" signal (that is hopefully less corrupted in some sense than the original input signal). Here we apply a similar philosophy to the decoding of separable convolutional codes. A "separable code" is defined to be a concatenated code where component codes and interleaving are chosen and

combined in such a way that any codeword of the resulting composite code has the special property that it can be subdivided into valid codewords corresponding to any one of the component codes by appropriately grouping the output bits into code symbols [2][3].

The organization of this paper is as follows. In Section 2 some of the background behind the concept is summarized. We discuss the system model and MAP "filtering" for convolutional codes. Separable convolutional codes, and the use of separable MAP "filters" for decoding these codes, are described in Section 3. Simulation results for communication over Rician fading channels are presented in Section 4.

2. BACKGROUND

The symbol-by-symbol MAP algorithm can be used for codes that can be represented by a trellis of finite duration. For the system model shown in Figure 1, we provide a brief summary of the symbol-by-symbol MAP
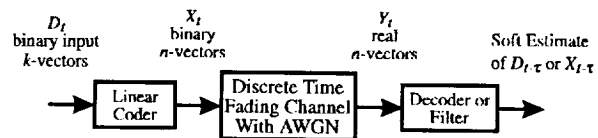
Figure 1. A block diagram of the system model.

algorithm as given in [4] and the appendix of [5]. The simple time-invariant 4-state trellis, shown in Figure 2, is used to illustrate the concepts. This trellis corresponds to a rate-1/3 convolutional code. In general, the trellis may be time-varying with the number of states, M_t, being a function of the time index t. It is assumed that at the start and the end of the time interval of interest, the coder is in the zero state. Any given input sequence $_iD_{i'}$ of binary (e.g., 0 or 1) k-vectors, that satisfies the above end conditions, will correspond to a particular path through the trellis that is described by a sequence of states

$$_{i-1}S_{i'} = \{S_{i-1} = 0, \ldots, S_t = m, \ldots, S_{i'} = 0\} \qquad (1)$$

where $S_t \in \{0, \ldots, M_t\text{-}1\}$.

$D_t[X_t]$

$0 [-1,-1,-1]$

$1 [1,1,1]$

$0 [1,1,-1]$

$1 [-1,-1,1]$

$0 [-1,1,-1]$

$0 [-1,1,1]$

$1 [-1,1,-1]$

t-2 t-1 t t+1

time
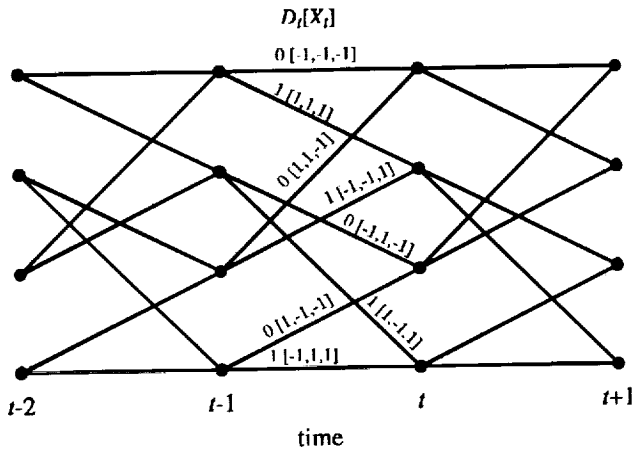
Figure 2. A trellis corresponding to a rate 1/3, 4 state convolutional code.

For each path through the trellis the coder produces a particular channel input sequence

$$_iX_{i'} = \{X_i, \ldots, X_t, \ldots, X_{i'}\}, \qquad (2)$$

where X_t is an n-vector denoted by

$$X_t = [x_{t_1}, \ldots, x_{t_n}] \qquad (3)$$

of binary (e.g., -1 or +1) elements. In the example trellis of Figure 2, $k=1$, $n=3$ and $M=4$ for all t. For notational convenience, the functional dependence of X_t on S_{t-1} and S_t is only shown when required. The corresponding channel output sequence is given by

$$_iY_{i'} = \{Y_i, \ldots, Y_t, \ldots, Y_{i'}\}, \qquad (4)$$

where Y_t is an n-vector denoted by

$$Y_t = [y_{t_1}, \ldots, y_{t_n}] \qquad (5)$$

with the real-valued elements having conditional probability density functions given by

$$p(y_{t_j} | x_{t_j}) = \left(2\pi\sigma^2\right)^{-1/2} \exp\left[-(y_{t_j} - G_{t_j} x_{t_j})^2 / 2\sigma^2\right] \qquad (6)$$

where G_{t_j} is the time-varying gain of the fading channel. Clearly this model is appropriate for antipodal signalling over a flat fading channel with additive thermal noise, typical of mobile satellite communications, under the assumption that the demodulator is able to accurately determine the gain and phase of the fading channel.

Now consider the problem of determining the *a posteriori* probabilities (APP) of the state transitions

$$p_t(m', m) = \Pr\{S_{t-1} = m'; S_t = m|_iY_{i'}\}$$
$$= \frac{p(S_{t-1} = m'; S_t = m;_iY_{i'})}{p(_iY_{i'})} \qquad (7)$$

Throughout the paper, we shall refer to probability densities such as the numerator in (7) as a "probability", with the understanding that dividing it by $p(_iY_{i'})$ makes it a true probability. Following [4], we use the joint probability

$$\sigma_t(m', m) = p(S_{t-1} = m'; S_t = m;_iY_{i'}), \qquad (8)$$

recognizing that $p_t(m',m)$ can be computed from $\sigma_t(m',m)$ by either dividing by the constant $p(_iY_{i'})$ or equivalently by the sum of all possible joint transition probabilities at the time t. It can be shown [4] that the above joint probabilities can be expressed as the product of three independent probabilities;

$$\sigma_t(m', m) = \alpha_{t-1}(m')\gamma_t(m', m)\beta_t(m), \qquad (9)$$

where

$$\gamma_t(m', m) = p(S_t = m; Y_t | S_{t-1} = m') \qquad (10)$$

$$\alpha_t(m) = \sum_{m'=0}^{M_{t-1}-1} \alpha_{t-1}(m')\gamma_t(m', m) \qquad (11)$$

$$\beta_t(m) = \sum_{m'=0}^{M_t-1} \beta_{t+1}(m')\gamma_{t+1}(m, m') \qquad (12)$$

Here we refer to $\gamma_t(m',m)$ as the branch probability and it is given by

$$\gamma_t(m', m) =$$

$$\Pr\{S_t = m|S_{t-1} = m'\}\prod_{j=1}^{n} p\left(y_{t_j} | x_{t_j}(m', m)\right) \qquad (13)$$

where the first term on the right-hand side is usually a straightforward function of the probability distribution of the input data and the coder structure. The second term on the right-hand side is a product of conditional symbol probability densities as given in equation (6). The branch probabilities account for the "present" n-vector of channel outputs, while the "past" channel outputs are accounted for by the forward recursion defined by equation (11), and the future channel outputs are accounted for by the backward recursion in equation (12).

Consider applying these techniques to obtain the *a posteriori* probabilities of the **coded** bits (i.e., the elements of X_t) rather than on the **information** bits (i.e., the elements of D_t). If the coded bits are assumed to be independent, with p_0 and p_1 being the probability that any given bit is a 0 or 1, respectively, then

$$p(x_{t_j} = 0;_iY_{i'}) = p(x_{t_j} = 0; y_{t_j}) = p(y_{t_j} | x_{t_j})p_0 \qquad (14)$$

However, the coded bits are not independent due to the structure imposed by the coder. Consequently, we would

like to use the MAP processing to determine the probabilities, $p(x_{t_j}=0; {}_iY_{i'}|C)$, where the conditioning on C refers to the knowledge of the coding structure. This can easily be done by defining the set of all transitions for which $x_{t_j}=0$;

$$A = \{(m',m): x_{t_j}(m',m) = 0\}, \qquad (15)$$

and then summing over the joint transition probabilities to obtain the joint probability

$$p(x_{t_j} = 0; {}_iY_{i'}|C) = \sum_{(m',m)\in A} \sigma_t(m',m). \qquad (16)$$

The noisy codeword enters the MAP "filter" as a vector of independent probabilities, and then is output from the filter with the probabilities (which are no longer independent) being refined according to the structure of the code. A similar procedure can be used for determining the probability that the information bit d_{t_j} is zero by replacing the set A by

$$A' = \{(m',m): d_{t_j}(m',m) = 0\}. \qquad (17)$$

In this paper, we distinguish between the terms "MAP filter" and "MAP decoder", with the former computing the *a posteriori* probabilities of the coded bits and the latter the *a posteriori* probabilities of the decoded bits. (Clearly for systematic codes, the *a posteriori* probabilities of the information bits are a subset of the probabilities for the coded bits.) If hard decisions are performed on the output of the MAP filter, the minimum average probability of coded bit error is achieved. However, the resulting word may not be a valid code word. A good choice for a valid codeword can be obtained by iterating the filtering operation until a valid code word is obtained. Of course, the assumption of independent probabilities by the MAP algorithm is erroneous when the algorithm is used iteratively.

3. SEPARABLE CONVOLUTIONAL CODES AND ITERATIVE MAP FILTERING

Recall that a separable code is defined to be a concatenated code where component codes and interleaving are chosen and combined in such a way that any codeword of the resulting composite code has the special property that it can be subdivided into valid codewords corresponding to any one of the component codes by appropriately grouping the output bits into code symbols. Next, we describe a technique that results in a very large powerful convolutional code by appropriately combining smaller component convolutional codes.

The first important observation is that convolutional encoders are linear and shift-invariant [6].

Therefore a sum of valid codewords, each with a different delay, is still a valid codeword. The second is that time-division interleaving can be implemented as is illustrated in Figure 3. Note that this structure does not destroy the shift-invariant property, unlike most interleaving schemes. Therefore this type of combined encoder/interleaver can be used as a building block for the type of composite code that is desired. This concept is illustrated in Figure 4 for a two-tier example code. Each tier contains a number of identical coders with inputs interconnected to the coder outputs of the previous tier. The interconnection must be done such that the codewords arriving from the previous tier are linearly combined through the current tier in such a way that the outputs can be subdivided into valid codewords for the previous tier. For example, in Figure 4, c_{11}, c_{12} and c_{13} are three valid codewords for code CE1. In general, these three codewords may not be identical to the two codewords generated by the first tier.

Here, we develop such an interconnection using a
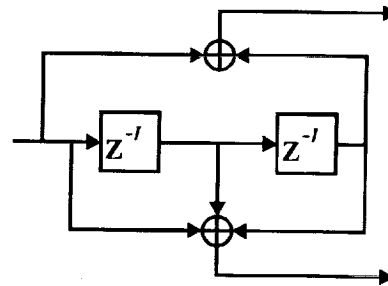
Figure 3. An example convolutional encoder including *I*-fold time division interleaving.
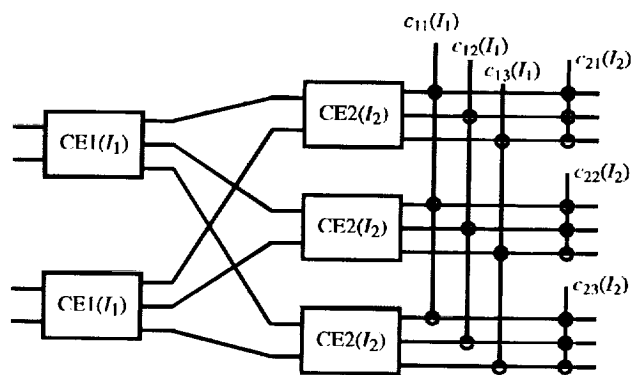
Figure 4. Two-tier coding with rate 2/3 component codes. $CE1(I_1)$ is an encoder with I_1-fold interleaving for code 1. $CE2(I_2)$ is an encoder with I_2-fold interleaving for code 2. c_{1q} is the qth valid codeword for code 1, with I_1-fold interleaving. c_{2q} is the qth valid codeword for code 2, with I_2-fold interleaving.

469

recursive approach. Starting with a rate k_1/n_1 convolutional coder at the first tier, we wish to add a second tier consisting of rate k_2/n_2 coders. In our interconnection there will be k_2 coders at tier 1 and n_1 coders at tier 2. The concatenation of tier 1 and tier 2 is treated as a supercoder of rate $k'_2/n'_2 = k_1k_2/n_1n_2$. To connect a third tier of rate k_3/n_3 coders we repeat the above process. There will be k_3 supercoders at tier 2 and n'_2 coders at tier 3 and after the interconnection this will produce a supercoder of rate $k'_3/n'_3 = k'_2k_3/n'_2n_3$. In general, interconnecting tier i to tier $i+1$ requires k_{i+1} supercoders at tier i and n'_i coders at tier $i+1$. This concatenation is treated as a supercoder of rate k'_ik_{i+1}/n'_in_{i+1} for subsequent interconnections. The final supercoder resulting from concatenating N tiers of convolutional coders has a rate

$$\frac{k'_N}{n'_N} = \frac{\prod_{i=1}^{N} k_i}{\prod_{i=1}^{N} n_i}. \tag{18}$$

The actual interconnection of tier i to tier $i+1$ is straightforward. If we denote the jth coder at stage i as $c_{i,j}$, then our interconnection strategy is to connect the mth output of supercoder $c_{i,j}$ to the jth input of coder $c_{i+1,m}$.

The individual codewords from the convolutional coders are dispersed as they propagate through subsequent tiers. In order to facilitate MAP filtering, we must be able to construct valid codewords from each tier. Let us denote the output sequence of n'_N bits as

$$\{b(0),b(1),b(2),\ldots,b(n'_N-1)\}.$$

Then, the mth code symbol from the ith tier is

$$\{b(m),b(m+p),b(m+2p),\ldots,b(m+(n_i-1)p)\}$$

where

$$p = \begin{cases} \prod_{j=i+1}^{N} n_j, & \text{for } i < N \\ 1, & \text{for } i = N \end{cases} \tag{19}$$

and

$$m = \left\{0,1,2,\ldots,\frac{n'_N}{n_i}-1\right\}. \tag{20}$$

Note that each of the component codewords (appropriately interleaved) is present at the output. The purpose of the interleaving is to make the distance of the composite code approximately proportional to the product of the distances of the component codes.

Usually, it is desirable to choose the interleaving factors for the tiers to be mutually prime.

In multidimensional signal processing, digital filtering is often performed using "separable" filters. That is, in order to avoid excessive computational requirements, one-dimensional filtering is performed sequentially in each of the N dimensions, rather than performing a single massive N-dimensional digital filter. In this paper, we investigate the analogous approach for the decoding of multi-tiered codes. That is, MAP filters will be used sequentially for each tier. Consider the two-tier case first. MAP filtering can be performed on the codewords corresponding to the first tier giving a new set of refined probabilities, taking into account only the structure of the first component code. These new probabilities are then further refined by MAP filtering the codewords corresponding to the second tier to complete a single filtering cycle. This process can be iterated any number of times. The extension to the cases with more than two tiers is obvious. In the multidimensional signal processing case, iterating the filtering does not make sense because the filters are linear. However, in the separable coding case, the filters are highly nonlinear and additional filtering cycles can significantly improve the performance. In the final cycle, decoding with the MAP algorithm (defined at the end of section 2) should be used in order to recover the information bits.

In processing a continuous stream of received bits, some form of block processing is necessary because receiver memory and delay are not unlimited. However, by nature, convolutional codes are not ideally suited to block processing. Our strategy is to overlay a two segment processing window onto the incoming stream. The first segment of the window identifies the portion of bits that will be decoded and the second segment acts as a view into the future for the processing. After each decoding process is completed, the window is moved forward to the position just past the last decoded bit. The forward and backward recursions of the MAP processing are performed over the entire window, however, the decoding phase does not output bits from the future segment.

There is memory that must be carried forward from one block to the next. This memory consists of the forward recursion probability vector for each cycle of each interleaved tier. The number of probability vectors carried forward is therefore given by

$$\text{\# of } \underline{\alpha}\text{'s} = N_c \sum_{i=1}^{N} I_i \tag{21}$$

where N_c is the number of cycles of MAP processing, N is the number of tiers and I_i is the interleaving factor at

the *i*th tier. The forward recursion probability vector is initialized at time 0 so that state 0 is probability 1, as given by

$$\alpha_0(i) = \begin{cases} 1, & i = 0 \\ 0, & i = 1, 2, ..., M - 1 \end{cases} \tag{22}$$

where M is the number of states in the trellis. At the start of processing each block, the backward probability vector at time t_e, corresponding to the end of the block, is initialized such that all state probabilities are equal, as given by

$$\beta_{t_e}(i) = \frac{1}{M}, \ i = 0, 1, ..., M - 1. \tag{23}$$

Obviously, these are not likely to be the true backward recursion probabilities at this time, however, we do not decode bits from this segment of the sequence. If the future block is chosen large enough, then by the time the recursion reaches the segment that will be decoded, the backward recursion probabilities should be close to their true value.

For convenience in the MAP processing, we restrict the number of bits in the present and future blocks to be a multiple of a fundamental block size. We define this fundamental block size, B, as

$$B = n'_N \prod_{i=1}^{N} I_i. \tag{24}$$

Then, the number of bits in the present block is PB and the number of bits in the future block is FB. In order to minimize decoding overhead, P should be chosen to be much larger than F. Also, F must be chosen to be large enough to allow the backward recursion probabilities to reach their true values by the time they reach the segment to be decoded.

4. SIMULATION RESULTS AND DISCUSSION

The performance of MAP processing of signals transmitted though Rician fading channels was investigated by software simulation. The 2-tier concatenation of 16 state, rate 2/3 systematic codes shown in Figure 4 was used with I_1 and I_2, the interleave

factors, being 15 and 16 respectively. The complete simulation model is shown in Figure 5. Random bits are encoded with the concatenated encoders and then passed to a 9×240 block interleaver. The concatenated encoders provide good code symbol interleaving but do not interleave the individual bits of the code symbol; the function of the block interleaver is to provide interleaving of the bits. The size of the interleaver was chosen to be equal to the fundamental block size of the simulation as described by equation (24). The output of the block interleaver is passed to the fading channel using antipodal signalling. The fading filter was designed with a 10% raised cosine frequency response and its 3 dB bandwidth was defined to be the fading bandwidth. For Rician fading channels, the k-factor is defined to be the ratio, in dB, of the average fading path power to the direct (ie., line-of-sight) path power. The output of the fading channel and the fading process itself are passed to individual block deinterleavers so that the fading process samples remain time aligned with the received signal samples. The received signal samples are then processed by the MAP algorithm which uses the channel information. The magnitude and phase of the fading process are removed from the received signal samples prior to the MAP processing. In addition, the knowledge of the time varying signal-to-noise ratio is used to correctly transform the samples to bit probabilities.

Bit error rate performance results were generated for an AWGN channel and Rician fading channels with fading bandwidths equal to 0.03 of the symbol rate and k-factors of -10 dB and -5 dB. For an assumed bit rate of 4800 bps and binary signalling, the above fading rate would be approximately 140 Hz. The simulation results can be seen in Figure 6. Interestingly, the strength and diversity of the code results in better performance with fading than without it, in low signal-to-noise conditions, due to the additional power in the fading bandwidth. While these results are quite encouraging, it should be noted that it is assumed here that the demodulator is capable of perfectly estimating the thermal noise spectral density, and the time-varying channel state (i.e.,
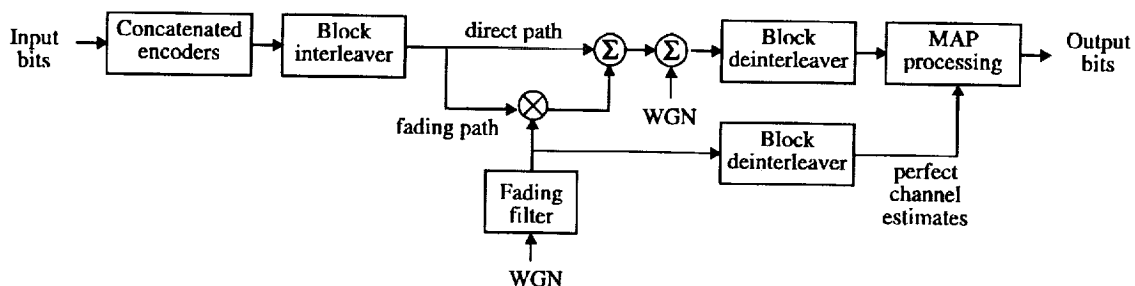
Figure 5. A block diagram of the simulation model.

471

magnitude and phase). Clearly, this is an optimistic assumption and consequently future work will be required to develop demodulators capable of providing the MAP decoders with the necessary inputs, and evaluating the resulting performance losses. One possible approach is to use reference symbols [7] to estimate the parameters of the fading channel. As a point of reference, Figure 7 shows the performance of the commonly used constraint length 7 rate 1/2 convolutional code, with ideal interleaving, perfect channel state information, and MAP decoding. Of course, this code can be decoded with much less delay and computational effort than the more powerful separable code.

As would be expected with such powerful coding techniques, the decoding process is quite computationally intensive. Therefore, the development of efficient implementation techniques is an important area for future work. For some codes, it is possible that simpler algorithms (e.g., [1]) can replace the MAP processing without severely degrading the performance.

While there still remain a number of areas for future work, the initial simulation results indicate that the iterative use of MAP "filters" for the decoding of separable convolutional codes can offer extremely power efficient transmission for those applications that can tolerate the large computational requirements, large block lengths, and long decoding delays that are typical of such powerful coding techniques.

REFERENCES

[1] J. Hagenauer and P. Hoeher, "A Viterbi algorithm with soft-decision outputs and its applications," Proc. GLOBECOM'89, Dallas, Texas, pp. 47.1.1-47.1.7, Nov. 1989.

[2] J.H. Lodge, P. Hoeher and J. Hagenauer, "The decoding of multidimensional codes using separable MAP "filters"," Proc. Queen's University 16th Biennial Symp. on Communications, pp.343-346, May 1992.

[3] J. Lodge, R. Young, P. Hoeher, and J. Hagenauer, "Separable MAP 'Filters' for the Decoding of Product and Concatenated Codes," IEEE International Conference on Communications ICC'93, Geneva, Switzerland, May 1993.

[4] L. Bahl, J. Cocke, F. Jelinek, and J. Raviv, "Optimal decoding of linear codes for minimizing symbol error rate," IEEE Trans. Inform. Theory, vol. IT-20, pp. 284-287, Mar. 1974.

[5] G.D. Forney, "The Viterbi algorithm," Proc. IEEE, vol. 61, pp. 268-278, Mar. 1973.

[6] G.D. Forney, "Convolutional codes I: Algebraic structure," IEEE Trans. Inform. Theory, vol. IT-16, pp. 720-738, Nov. 1970.

[7] M.L. Moher and J.H. Lodge, "TCMP - A modulation and coding strategy for Rician fading channels," IEEE J. Sel. Area. Comm., Vol. 7, pp. 1347-1355, December 1989.

Figure 6. The average bit error rate versus the energy-per-bit-to-noise-spectral-density ratio for a 2-tier concatenated code in Rician fading environments, with four cycles of MAP processing.
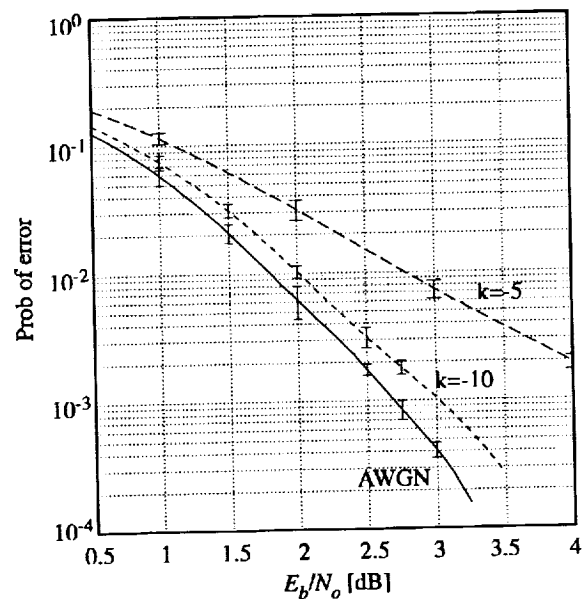
Figure 7. The average bit error rate versus the energy-per-bit-to-noise-spectral-density ratio for a single rate 1/2 code in Rician fading environments.

472

Diversity Reception for Advanced Multi-Satellite Networks : a CDMA Approach

E. Colzi*, R. De Gaudenzi *, C. Elia*, F. Giannetti **, R. Viola*

* European Space Agency
European Space Research and Technology Centre, RF System Division
P.O. Box 299, 2200 AG Noordwijk, The Netherlands

** University of Pisa
Dipartimento di Ingegneria della Informazione
Via Diotisalvi 2, 56126 Pisa, Italy

Abstract

Diversity reception for Synchronous CDMA (S-CDMA) is introduced and analyzed. A Gaussian co-channel synchronous and asynchronous interference approximation is derived to evaluate the effects on the system bit error rate. Numerical results are provided for a simple mobile communication system where the signals transmitted by two distinct satellite in visibility are coherently combined by a three fingers Rake receiver. A second example showing performance of an integrated ground / satellite single frequency network for digital audio broadcasting is presented. Results show the capacity advantage of utilizing S-CDMA in combination with diversity reception.

1 Introduction

In this paper we will analyze the viability of synchronized code division multiple access, in presence of multipath and fading channel. The presence of a number of signal replicas resolvable in time at the receiver side will be in general called 'multipath' with the understanding that this might be the result of either an intentional satellite diversity or caused by signal reflections.

In case of satellite and terrestrial communication systems utilizing portable receivers equipped with omnidirectional antenna, efficient techniques shall be employed to counteract the performance degradation due to the frequency selective nature of the channel. Multipath processing offers an significant improvement together with the following system advantages:

- *Diversity combining and satellite soft hand-over.* In case of multi-satellite networks, satellite diversity (Fig. 1) can be exploited, allowing to increase service availability and to reduce propagation margins.

- *Multipath combining.* Multipath propagation can create additional diversity condition. In some cases the local signal reflections can advantageously be used for improving the system performance.

To simplify the analysis, we consider in the following, the case of signals originated in the same physical location. This approximates well the case of satellite-to-mobile links and all broadcasting applications.

2 Multipath Effects: System Performance Evaluation

In ref. [1] it has been introduced a S-CDMA system that, while retaining distinctive advantages of CDMA, offers efficient utilization of power and bandwidth.

In fact, by using orthogonal code sets, the inter-user interference is drastically reduced. This implies that the system capacity is not limited by self-noise. Moreover S-CDMA can contain an embedded reference code ("master code") that simplifies the chip timing and carrier phase extraction at the receiver side, permitting coherent signal detection in mobile conditions. In summary, the main system features considered for further analysis are:

- A set of M independent data sources code division multiplexed. Preferentially phased Gold codes are utilized as spreading sequences The *master code* constitutes the reference for receiver synchronization and channel sounding.

- The communication channels are direct-sequence QPSK modulated (DS-QPSK). In general the I and Q spreading sequences are different. Transmitted signal bandwidth limitation is obtained by means of square-root raised-cosine Nyquist chip shaping.

The channel considered is a time-varying multipath channel with an impulse response referred to the nominal carrier angular frequency ω_0 of the type:

$$h_c(\tau; t) = \sum_{i=1}^{L} \beta_i(t)\delta(\tau - \tau_i)\exp j\left[\Delta\omega_i(\tau - \tau_i) + \theta_i(t)\right]$$

where L is the total number of paths and $\beta_i(t)$, $\Delta\omega_i(t)$, $\theta_i(t)$, $\tau_i(t)$ are the i-th path amplitude, frequency shift, phase and delay respectively. In general they can be modeled as stationary ergodic processes. We assume that the bandwidth of each process is much lower than the symbol rate in order to consider constant all the channel parameters in one symbol. The time dependence of these parameters will not be further reported in our notation for simplicity. To ease analytical derivations we also assume that $\tau_i = (i-1)T_C$, where T_C is

the signature code chip duration time. Therefore, only delays of multiple integer of the chip duration time are considered. By simulation it has been verified that the results are very much the same for the case of non integer chip delays.

In the following, we derive an approximate expression of the bit error rate (BER) for S-CDM systems in time-varying multipath channels.

Let us introduce the following notation

M	number of active DS-QPSK users
P	user signal power
$d_{p,k}^l$	k-th data bit; in-phase l-th user
$d_{q,k}^l$	k-th data bit; in-quadr. l-th user
$\underline{c}_p^l$	I signature seq. vector, l-th user
$\underline{c}_q^l$	Q signature seq. vector, l-th user
T_S	symbol duration time
$T_b = T_S/2$	bit duration time
$G_p = N/2$	processing gain
$n(t)$	AWGN one sided spect. density N_0
$|\cdot|_N \stackrel{\Delta}{=} \cdot \bmod N$	
$\{\cdot\}_N \stackrel{\Delta}{=} int\left\{\frac{\cdot}{N}\right\}$	

We also define

$$\underline{\underline{S}}_z \stackrel{\Delta}{=} \begin{bmatrix} \underline{c}_z^1 & \underline{c}_z^2 \cdots \underline{c}_z^M \end{bmatrix} \qquad z = p, q \qquad (1)$$

$$\begin{bmatrix} \underline{x}_{z,k} \end{bmatrix}^T \stackrel{\Delta}{=} \begin{bmatrix} d_{z,k}^1 & d_{z,k}^2 & \cdots & d_{z,k}^M \end{bmatrix} \qquad z = p, q \quad (2)$$

and the $(N \times N)$ shift matrices $\underline{\underline{U}}$ and $\underline{\underline{D}}$ such that: $U_{ij} = \delta_{i,j-1}$ and $\underline{\underline{D}} \stackrel{\Delta}{=} \underline{\underline{U}}^T$, where δ is the Kronecker delta.

To calculate the degradation introduced by multipath propagation, we assume coherent detection of the line of sight (LOS) signal. In other words, the receiver is synchronized in frequency, phase, and timing to the LOS signal, ignoring the presence of multipath. Fig. 2 illustrates the reference demodulator. We can collect the N samples per symbol at the output of the chip matched filter into a vector $\underline{y}$ of length N.

$$\begin{aligned}
\underline{y}_k &= \underline{y}_{p,k} + j\underline{y}_{q,k} = \sqrt{P}\left\{\underline{\underline{S}}_p \underline{x}_{p,k} + j\underline{\underline{S}}_q \underline{x}_{q,k}\right. \\
&\quad + \sum_{i=1}^L \beta_i \exp(j\phi_i)\left[\underline{\underline{D}}^{|i|_N}\left(\underline{\underline{S}}_p \underline{x}_{p,k-\{i\}_N} + j\underline{\underline{S}}_q \underline{x}_{q,k-\{i\}_N}\right)\right. \\
&\quad \left.\left. + \underline{\underline{U}}^{N-|i|_N}\left(\underline{\underline{S}}_p \underline{x}_{p,k-1-\{i\}_N} + j\underline{\underline{S}}_q \underline{x}_{q,k-1-\{i\}_N}\right)\right]\right\} + \underline{n}_k
\end{aligned}$$

In the above formula we have neglected the effect of interchip interference. This is justified by the fact that we use raised-cosine chip shaping and we have assumed perfectly synchronized spreading sequences at chip level. $\underline{n}_k$ is the vector of complex AWGN samples at the chip matched filter output. ϕ_i includes the channel phase rotation due to a frequency shift ($\phi_i = \Delta\omega_i t + \theta_i$). The use of $|\cdot|_N \stackrel{\Delta}{=} \cdot \bmod N$ and $\{\cdot\}_N \stackrel{\Delta}{=} int\left\{\frac{\cdot}{N}\right\}$ allows to take into account delays larger than $T_S = NT_C$

Since many independent users contribute to the total self-noise interference, the condition for the application of the central limit theorem is fulfilled. Therefore we can assume the interference as a Gaussian process.

Furthermore, assuming ϕ_i uniformly distributed in $[0, 2\pi)$, we can easily evaluate an approximate bit error probability through the use of the equivalent signal-to-noise ratio.

$$P_e^{l,p}(\underline{\beta}) \simeq Q\left(\sqrt{\frac{\frac{2E_b}{N_0}\beta_1^2}{\left\{1 + \beta_1^2 \frac{M-1}{2G_p^2}\frac{E_b}{N_0} + \left\{\sum_{j=2}^L \beta_j^2\right\}\frac{M}{G_p}\frac{E_b}{N_0}\right\}}}\right)$$

$$(3)$$

where $\underline{\beta} = (\beta_1, \beta_2, \ldots \beta_L)$. In the above formula we recognize at denominator the contribution of synchronous and asynchronous interference to the overall signal-to-noise ratio. The probability of error, once the system parameters are fixed, is only function of the vector of path amplitudes $\underline{\beta}$.

In some cases it is interesting to evaluate the average bit error probability

$$P_e^{l,p} = \int_0^{+\infty} \cdots \int_0^{+\infty} P_e^{l,p}(\beta_1, \beta_2, \cdots, \beta_L)\, p(\beta_1) \cdots p(\beta_L)\, d\beta_1 \cdots d\beta_L$$

$$(4)$$

We can find a similar expression for the in-quadrature branch. The total probability of error will be

$$P_e^l = \frac{1}{2}\left(P_e^{l,p} + P_e^{l,q}\right) \qquad (5)$$

Eqns. 3 and 4 have been successfully validated through extensive time-domain system computer simulation. Fig. 3 gives the results for different value of carrier-to-multipath ratio.

3 Study Case 1: Rake Receiver for Multi-satellite Reception

In this section we will examine the performance of a coherent Rake receiver [2]. Some quantitative results obtained from the theoretical analysis derived in the previous section are compared with time-domain simulation results. We consider a system using Gold codes with a code length N=63, 15 direct sequence QPSK users utilizing different I and Q codes.

To validate the analytical results we assume two channel models:

a) *The static channel*, in which some of the channel parameters, namely L, β_j, are fixed. This channel well approximates the case of very slowly variant channels. The static channel is representative of receiving two satellite in LOS visibility, neither with shadowing nor multipath, the two satellite having different received power levels (different relative C/M) due to different terminal antenna gain in each satellite direction and/or different slant range.

b) *The time-varying channel*, each satellite channel is modeled as a lognormal LOS signal plus a delayed multipath component with the same lognormal distribution. The fading processes representing the two satellite contributions are assumed to be independent. The lognormal LOS shadowing process standard deviation is set to a relatively high value (5 dB) to represent the case of a low elevation satellite link. The C/M for each satellite is set to 10 dB.

474

The assumptions for the channel model are summarized in Table 1. Fig. 4 shows the architecture of a K-path coherent Rake receiver. The K strongest received paths are individually demodulated by K independent receiver branches. The demodulator outputs are then weighted and coherently combined.

The weight determination is eased by assuming that all paths are statistically independent. The optimal weights are determined by maximizing the equivalent signal-to-noise ratio at the output of the combiner $\left(\left(\frac{E_b}{N_0}\right)_{eq}^{out}\right)$. It can be shown that for a K-path Rake receiver

$$\left(\frac{E_b}{N_{tot}}\right)_{eq}^{out} = \frac{E_b \gamma_S}{N_0 \gamma_0 + I_S \gamma_S + I_A \gamma_A} \quad (6)$$

where W_i is i-th branch weight,

$$I_A = \frac{M}{G_p} E_b \qquad I_S = \frac{M-1}{2G_p^2} E_b \quad (7)$$

and

$$\gamma_0 = \sum_{m=1}^{K} W_m^2 ; \gamma_S = \left[\sum_{m=1}^{K} \beta_m W_m\right]^2 ; \gamma_A = \left[\sum_{j=1}^{K} W_j^2 \left(\sum_{m=1;m\neq j}^{K} \beta_m^2\right)\right] \quad (8)$$

The weight values that maximize $\left(\left(\frac{E_b}{N_0}\right)_{eq}^{out}\right)$ result to be

$$W_i = \frac{\beta_i (N_0 + I_A \sum_{j=2}^{K} \beta_j^2)}{\beta_1 (N_0 + I_A \sum_{j=1,j\neq i}^{L} \beta_j^2)} \quad (9)$$

When estimation of N_o is difficult to perform , a sub-optimal solution is to set $W_i = \beta_i/\beta_1$. Fig. 5 shows the Rake receiver performance for the static channel. We notice, in this case, a performance improvement due to combining at low C/M (cfr. Fig. 3). In case of high C/M, the presence of a strong path produces such an increase of asynchronous interference on the other Rake branches to render almost useless the combining process.

A more noticeable gain is produced by the Rake when the time-varying channel is considered. Fig. 6 compares Rake and conventional receiver BER using the conditions defined in table 1. In these cases the Rake receiver in presence of a signal coming from two different satellite having independent fade distribution, provides a considerable gain due to its inherent diversity capability.

Channel	Sat-1		Sat-2	
	μ (dB)	σ (dB)	μ (dB)	σ (dB)
Static	0	0	0	0
T.v. one Sat	-3	5	—	—
T.v. two Sats	-3	5	-3	5

Study cases for the multi-satellite visibility
Table 1

4 Study Case 2: S-CDMA Based DAB System

A possible application of the S-CDMA and Rake demodulator is in a mixed, satellite and terrestrial Digital Audio Broadcasting System (DAB). In this case, the Rake receiver will greatly improve the system efficiency by exploiting the additional reception diversity offered terrestrial re-transmitters covering satellite shadowed areas. We will assume as system baseline the utilization of a constellation of satellites in Highly Elliptical Orbit [5]. With the selected type of orbit, elevation angle is better than 60° will be provided to the majority of mainland Europe. The geostationary orbit is also reported here as reference case. The overall system architecture, sketched in Fig. 7. Several coded Direct-Sequence Spread-Spectrum (DS-SS) signals carrying audio programs originated in different studios, are synchronously CDM multiplexed in the Feeder Link Station (FLS) modulator. Rate 3/4, $k = 7$ convolutional coding and direct sequence QPSK modulation has been finally selected as trade-off between power and bandwidth efficiency. Many FLS's up-link their DAB programs to the operational HEO satellites (or to the single GEO satellite). In case of multiple access in the satellite up-link, different CDM signals coming from various FLS are multiplexed in CDMA mode at the satellite transponder input. In this situation, in order to minimize the co-channel interference, all the FLS's sharing the same frequency band shall be synchronized in time and in frequency. The satellite acts as a transparent transponder and broadcasts the signals toward the earth where they are received by mobile, portable and fixed users at L-band. The terrestrial single frequency gap-filler network retransmits the DAB signals at the same satellite carrier frequency over highly shadowed (urban) areas. In our case the overall capacity results to be limited by the terrestrial SFN co-channel interference, hence the coding gain can be more relevant than the asymptotic spectral efficiency. Additional performance improvement in the multipath dominated urban environment is achieved by using the Rake receiver.

4.1 Channel Modeling

The fading model for the wideband satellite mobile channel, is a simple extension of the one discussed in [6]. Line-of-sight signal shadowing is modeled as a multiplicative lognormal process with mean μ_{LGN} and standard deviation σ_{LGN}. The instantaneous multipath results from the sum of several reflected rays, each of them characterized by a different amplitude, phase and delay with respect to the line-of-sight component [2]. It has been found that a single delayed ray model, with equivalent average power and Rayleigh fading superimposed, is sufficient for an accurate modeling of the multipath interference in the CDM system under study and that the associated delay is not critical when greater than $2 \div 3$ chips. For the cellular terrestrial network a regular structure has been assumed like in [6]. For symmetry reasons the user locations are referred only to a portion of the cell. A complete block diagram of the terrestrial channel is depicted in Fig. 8. We will assume that the envelope of each cell signal received at the mobile side will be affected by independent zero

Case	C/M (dB)	μ_{LGN} (dB)	σ_{LGN} (dB)	$[\overline{E_b}/N_0]_{req}$ (dB)
AWGN	∞	0	0	3.9
HEO/LGA	10	-3	2	6.7
HEO/HGA	12	-3	2	6.4
GEO/HGA	7	-6.5	3	12.3

mean lognormal process with 8 dB of standard deviation, and a path loss proportional to the inverse of the fourth power distance [6]. Another very important issue in modeling the UHF terrestrial urban channel is the time variant delay distribution characterization. For our particular network of terrestrial retransmitters broadcasting the same CDM multicarrier signal, we simply assume that all the signals multiplexed in CDM coming from the same cell carrier are chip and symbol synchronous[1], while any pairs of signals coming from different cell locations are chip asynchronous (i.e. the differential delay is assumed to be greater than one chip).

4.2 DAB System Performances

The basic modem design principle and detailed analysis is reported in References [1], [7].

In Table 2 simulation results for the satellite channel utilizing rate 3/4, $k = 7$ CCQO-QPSK-CDM system are summarized. The terrestrial system is complementary to the basic satellite broadcasting system as it is intended to provide good service quality in highly populated urban areas where, even using HEO, the line-of-sight signal is often lost. In this case, a Single Frequency Network (SFN) of cellular repeater transmitting at the same satellite carrier frequency can operate as gap-filler. The SFN simulator used consists of a regular 19 cells structure, where each cell transmits a CDM signal received at the user location with its relevant geometric path loss and lognormal shadowing. To keep the simulation time within acceptable limits, the coded symbols are PSK modulated but not spread by the Gold sequences. Effect of CDM self-noise is taken into account at the receiver side by injecting a non-stationary Gaussian noise level corresponding to the instantaneous interference level at the despreader output. Soft signal combining at the symbol matched filter output is suboptimally performed. Instantaneous signal rays amplitude is used by the equivalent self-noise generator to compute the self-noise level. Figure 9 show the the worst-case user location simulated BER of the terrestrial network versus the spectral efficiency, i.e. the channel loading, for the three fingers and single finger Rake receiver. Performance analysis in the coded case can not be easily performed because of the non-stationary noise samples statistics at the Viterbi decoder input due to signal and interference shadowing. It can be observed that, for a target worst-case BER of 10^{-3}, by using rate 3/4 CCQO-QPSK-CDM, one can achieve SFN spectral

efficiency of about 0.6 b/s/Hz, a value comparable to the satellite channel capacity. Rate 1/2 CCQO-QPSK-CDM does not provide any appreciable SFN efficiency improvement. The three fingers Rake receiver allows a considerable capacity gain both for the coded and the uncoded system, ant its performance results about two times better than the single finger Rake receiver.

5 Summary and Conclusions

In this paper we have analyzed the behaviour of S-CDMA in frequency-selective channels, providing an handy-to-use formula for evaluating the system bit error rate based on a Gaussian co-channel interference approximation. In the second part we have presented two study cases to illustrate potential adavnatges provided by the Rake receiver diversity exploitation on the receiver performance. Results of study case one show that when two satellites are constantly in visibility (static case) the interference situation worsens and a only a limited improvement can be achieved through combining. Different is the case with the user experiencing two satellites in visibility but with two independently shadowed channels. In this case the Rake receiver diversity exploitation is a clear premium in terms of capacity and service availability. The same conclusions apply to the case of a satellite DAB system with terrestrial gap-filler single frequency network. Once more consistent diversity gain is achievable on the terrestrial SFN where many independently faded signals with different delays are available at the demodulator input.

References

[1] R. De Gaudenzi, C. Elia, R. Viola, "Band-Limited Quasi-Synchronous CDMA: A Novel Satellite Access Technique for Mobile and Personal Communication Systems", IEEE J. on Sel. Areas in Comm., vol. 10, no. 2, Feb. 1992.

[2] G.L. Turin, "Introduction to Spread-Spectrum Antimultipath Techniques and their Applications to Urban Digital Radio", Proc. IEEE, vol. 68, pp. 328-353, March 1980.

[3] Z. Xie, R.T. Short, C.K. Rushforth, "A Family of Suboptimum Detectors for Coherent Multiuser Communications,"" J. Sel. Areas in Comm., vol. 8, pp. 683-690, May 1990

[4] C. Loo, "A Statistical Model for a Land Mobile Satellite Link," IEEE Trans. on Vehic. Techn., vol. 34, August 1985.

[5] P. Lo Galbo et al., "ESA Personal Communications and Digital Audio Broadcasting Systems Based on non-Geostationary Satellites", IMSC-93, session on DBS and Enhanced Services.

[6] K.S. Gilhousen, I.M. Jacobs, R. Padovani, L.A. Weaver, "Increased Capacity Using CDMA for Mobile Satellite Communications", IEEE J. on Sel. Areas in Comm., vol. 8, no. 4, May 1990.

[7] R. De Gaudenzi and F. Giannetti, "Analysis of an Advanced Satellite Digital Audio Broadcasting

---

[1]By simulation it has been shown that by synchronizing at chip/symbol level the cell signals, a doubling of the overall SFN capacity can be achieved.

Figure 1: Satellite diversity and gap transmitters for increased availability quality
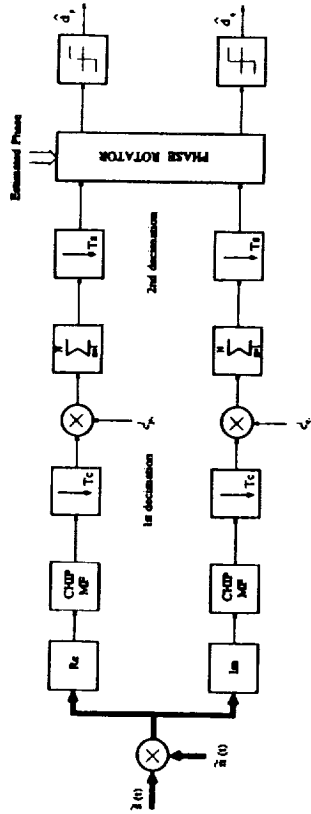
Figure 2: I-Q DS/QPSK demodulator block diagram
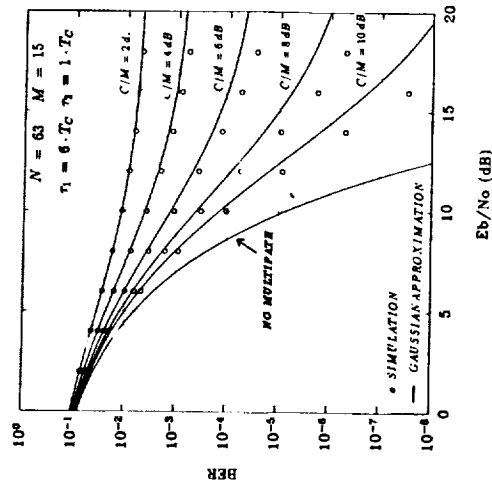
Figure 3: BER vs. E_b/N_0, static channel

Figure 4: K-paths Rake receiver block diagram

Figure 5: Rake performance in the static channel

Figure 7: S-CDMA DAB System Architecture

Figure 9: BER versus Spectral Efficiency (worst case)

Figure 6: Performance in the Multi-Satellite channel

Figure 8: Terrestrial Channel Block Diagram

System Services and Architecture of the TMI Satellite Mobile Data System

D. Gokhale, A. Agarwal
COMSAT Laboratories
22300 COMSAT Dr, Clarksburg, Md 20871
(301) 428 4220 (Tel)
(301) 428 7747 (Fax)

A. Guibord
Telesat Mobile Incorporated

ABSTRACT

The North American Mobile Satellite Service (MSS) system being developed by AMSC/TMI and scheduled to go into service in early 1995, will include the provision for real time packet switched services (Mobile Data Service - MDS) and circuit switched services (Mobile Telephony Service - MTS). These services will utilize geostationary satellites which provide access to Mobile Terminals (MTs) through L-band beams. The MDS system utilizes a star topology with a centralized Data Hub (DH), and will support a large number of mobile terminals. The DH, which accesses the satellite via a single Ku band beam, is responsible for satellite resource management, for providing mobile users with access to public and private data networks, and for comprehensive network management of the system. This paper describes the various MDS services available to the users, the ground segment elements involved in the provisioning of these services, and a summary description of the channel types , protocol architecture and network management capabilities provided within the system.

INTRODUCTION

The North American Mobile Satellite Service (MSS) system [1] being developed by AMSC/TMI and scheduled to go into service in early 1995, will include the provision for real time packet switched services (Mobile Data Service - MDS) and circuit switched services (Mobile Telephony Service - MTS) The MDS system uses packet switching techniques to provide for the dynamic sharing of satellite resources between a large number of mobile users. The architecture of the MDS system is similar to packet switched VSAT systems, wherein a centralized Data Hub (DH) communicates with a large number of remote units. In contrast to currently deployed land mobile data systems such as INMARSAT Standard C, which primarily support store and forward messaging, the MDS system provides a flexible architecture which is capable of supporting a wide variety of application types. Potential applications which can be supported

via this system include Remote Data Base Access and Entry, Fleet Management, Supervisory Control and Data Access (SCADA), and multicast data, as well as messaging. Potential customers of this system include transportation (trucking, taxicab) companies, field sales, field services, public services agencies (police, ambulance, fire), oil companies, utilities, as well as the general category of mobile professionals.

MDS GROUND SEGMENT ARCHITECTURE

The ground segment architecture of the MDS system is shown in Figure 1. The MDS ground segment elements consist of a Data Hub (DH), Mobile Terminals, and Remote Monitoring Stations. The MDS system can be configured to operate either in an integrated manner within the MSS system, or as a standalone system. In an integrated system, the DH interfaces with the MSS Network Operations Center (NOC) for allocation of system resources, and with the Network Control Center (NCC) for supporting circuit switched services to integrated voice data MTs. In an integrated system, the DH RF Equipment may be shared with the NCC or FeederLink Earth Station (FES) RF Equipment. In a standalone configuration, the MDS system operates with a pre-allocated set of resources from the NOC operated by the MSS service provider. A brief description of the MDS ground segment elements is provided next:

Data Hub Terminal Equipment (DH - TE) - The DH-TE provides packet switched communication services to MTs. On the terrestrial side the DH interfaces to public and private data networks as well as customer host computers. It provides for the dynamic assignment of MDS capacity to MTs on a demand basis. It also provides for the overall management and control of the MDS network. The DH interfaces with the Network Management System (NMS), which includes the Customer Management Information System (CMIS), to obtain customer configuration information and to provide network usage information. Network status and configuration

information are also communicated between the DH and Network/Systems Engineering functions within the NMS.

Mobile Terminal (MT) - The MT provides user access to the packet switched services provided by the MDS system. Four MT types are supported by the MDS: full duplex, half duplex, receive only, and integrated voice/data. The half duplex MT, which does not require an RF diplexer provides a low cost, limited feature, alternative to the basic full duplex MT. The receive only MT supports only unicast services and can be used for applications such as paging and multicast data reception. The integrated voice data MT (IVDM) combines the capabilities of a full duplex MDS MT, and a circuit switched MT.

Remote Monitor Station (RMS) - The RMS provides the capability to monitor the L Band RF spectrum and transmission performance in a specific L-band beam. An RMS is located in each L band beam and interfaces with the DH via a satellite or terrestrial link.

MDS SERVICES

In designing MDS services, two key requirements were taken into account - a) emphasis was placed on providing application independent core networking services and b) supporting service offerings that are compliant with international standards. Emphasis on the core networking services, which provide for basic packet switched circuit setup, data transfer and circuit takedown, allows the system to support user specific applications in a very flexible manner. Adherence to international standards makes it possible to use commercial off-the-shelf communications software for providing value added services and also reduces the cost associated with implementing the MDS ground segment. The standards compatible core networking services category is referred to as Basic Services in the MDS system. Since some MDS capabilities (such as multicast data, and TDMA bandwidth reservation) could not be optimally accessed via the core networking services, an additional service category referred to Specialized services is also supported by the MDS system.

As described earlier, the Basic services category provide for transparent communications services between data terminal equipment (DTE) connected to the mobile terminal and DTEs connected to the data hub. Two types of Basic Services are provided within the MDS system: X.25 and Asynchronous. The X.25 Service provides for the establishment of virtual circuits between an X.25 DTE attached to the MT and a fixed X.25 DTE connected to the DH. Figure 2 shows the X.25 Service architecture.

As shown in the figure, the DH can directly interface with the fixed DTE, or the interconnection can be via an intermediate public or private data network. This service is compliant with the 1988 and 1984 versions of the CCITT Recommendations X.25. The X.25 service provides a flexible mechanism for the deployment of value added services. An MDS service provider can easily provide such services by integrating off-the-shelf hardware and/or software such as protocol gateways (e.g SNA packet assemblers/disassemblers). A number of such X.25 gateway products are commercially available on the market from a large number of vendors. Applications such as store and forward messaging can also be easily supported via off-the-shelf communications software packages on personal computers and workstations.

The second service in the Basic Services category is the Asynchronous Service which provides for the interconnection of an asynchronous DTE connected to the MT with a packet mode DTE connected to the DH. The Asynchronous Service uses procedures compliant with the 1988 and 1984 versions of the CCITT recommendations X.3, X.28 and X.29 protocols. Figure 3 shows the Asynchronous Service architecture. As shown in the figure, the Asynchronous Service also provides the capability for the asynchronous DTE attached to the MT to communicate with a fixed asynchronous DTE through the use of an external Packet Assembler/Disassembler.

The primary advantage associated with the basic services: X.25 and Asynchronous is that they provide the flexibility to support value added services without any impact on the core MDS network. However a number of attributes associated with a landmobile system cannot be fully utilized by these services. To provide a mechanism for utilizing these attributes, the MDS system also supports two Specialized Service categories: Reliable Transaction Service (RTS) and Unacknowledged Data delivery Service (UDS). RTS provides the capability to efficiently complete a short transaction (request/response) between mobile and fixed users. This service is especially efficient when the fixed user connected to the DH originates the transaction request, since the DH can allocate space on the inbound reservation channel for the response. For applications (e.g cargo monitoring, location tracking) which require periodic polling, this service is much more efficient than using the X.25 service, since a) fewer messages are generated and b) a prioiri capacity can be assigned on the inbound channel.

The second specialized service is the Unacknowledged Data delivery Service (UDS) which provides the capability to transmit non-assured data. More importantly, UDS provides the capability of multicasting data to MT User Groups. Both the RTS

and UDS services are offered to end users via a specialized services access function within the DH and the MT. Message primitives and formats for applications to communicate with the specialized service access function have also been standardized in the MDS system.

In addition to packet data services, MDS also supports the provisioning of an integrated voice/data Service to MTs. This service allows a class of MTs termed Integrated Voice/Data MTs (IVDMs) to use the circuit switched system (MTS) for voice, stream data, and facsimile, and the packet switched system (MDS) for packet data services. The circuit switched service provisioning is supported via co-ordination between the DH and the Network Control Center (NCC) which allocates the satellite circuit resources for the mobile telephony service. The call setup signalling between the NCC and the telephony call control function at the MT is done over the MDS channels by utilizing the RTS Services. A FES selected by the NCC for completing the call provides the interconnection of the circuit with the public switched telephony network (PSTN).

MDS CHANNEL ARCHITECTURE

Four channel types (one outbound, three inbound) are defined at the physical layer to provide the connectivity between the MTs and the DH. The outbound (DH to MT direction) channel termed DH-D, operates as a Time Division Multiplex (TDM) channel with a data rate of 6750 bps using differentially encoded QPSK modulation and rate 3/4 convolutional coding. The frame structure utilized over the DH-D channel is shown in Figure 4. Fixed size frames which carry variable data segments are transmitted over this channel which operates at a nominal information rate of 5062 bps. The DH-D frame structure provides the common timing reference for the synchronization of inbound channel frames.

Three types of inbound channels: MT-DRr, MT-DRd, and MT-DT are used in the MDS system. These channels employ differentially encoded QPSK modulation at a transmission rate of 6750 bps. Data is coded using rate 1/3, constraint length K = 7 convolutional coding. The MT-DRd is a contention type channel (slotted aloha) which is used to transmit short packets for interactive applications. The MT-DRr is also a contention type channel, except that it is only used for making capacity requests for the MT-DT channel. The MT-DT channel is a reservation (assigned) channel, the access to which is controlled by the DH.

The frame structures for the three channels are shown in Figure 4. The MT-DRd and MT-DRr

channel framing consist of fixed size slots (108.15 msec, and 42.88 msec respectively). The transmission of data packets into these slots is done in accordance with the slotted Aloha scheme. The MT-DT channel uses variable length framing. The access to the MT-DT channel is done in a Time Division Multiple Access (TDMA) manner under the coordination of the DH. Two types of MT-DT frames (types A & B) are used. Type A frames which provide for two information fields, are used to support the piggybacking of requests for additional capacity on the TDMA channel. This technique enables the MT to pipeline data requests and have the capability to transfer data at rates close to the inbound channel information rate.

MDS PROTOCOL ARCHITECTURE

The internal protocols designed for the MDS system are required to provide sufficient functionality for supporting the Basic and Specialized service categories, while taking into account the unique characteristics associated with the land mobile environment,. Efficiency was an extremely important criteria in designing these protocols, given the high cost associated with the MSS satellite resources. Efficient recovery of errored packets due to the fading and shadowing conditions was another important requirement. Unlike typical VSAT systems, where the remote nodes are designed to be operational at all times, the design of the MDS protocols also needed to take into account the requirements for frequent resynchronization of the protocol state machines given the operational nature of the MTs.

The internal protocol architecture used within the MDS network is shown in figure 5. A layered protocol architecture consistent with the Open System Interconnect (OSI) model is used in designing the MDS protocols. The access to the MDS physical channels (DH-D, MT-DRd, MT-DRr, and MT-DT) is controlled by the Channel Access and Control (CAC) protocol. The CAC protocol provides different functionality at the MT and the DH. At the DH, the CAC protocol is responsible for formatting of packets within the DH-D frames, and for allocating TDMA capacity on the MET-DT channel, in response to requests from the MT or upper layer protocols at the DH. At the MT, the CAC controls access to the inbound channels. It implements the retransmission backoff algorithm for accessing the slotted Aloha (MT-DRr, and MT-DRd) channels. It is also responsible for monitoring the inbound packet queues and for requesting MT-DT channel capacity. The CAC provides for the prioritized processing of packets within the MDS network. It also implements algorithms for congestion control of the MT-DRd, MT-DRr, and MT-DT channels.

481

The Basic Service Categories (X.25 and Asynchronous) in the MDS system are supported by the MDS Packet Layer Protocol (MPLP) and MDS Data Link Protocol (MDLP). The MDS Packet Layer Protocol (MPLP) provides procedures for the setup, data transfer, and clearing of multiple virtual circuits between the MT and the DH. ISO 8208 which supports symmetric X.25 packet interconnection is used as the baseline protocol for MPLP. MPLP incorporates small enhancements to ISO 8208 for more efficient operation in the MDS environment. For instance, a strategy which reduces the number of Receiver Ready (RR) packets is incorporated into MPLP.

The MDS Data Link Protocol (MDLP) provides for the reliable sequenced delivery of packets. In terms of functionality, the MDLP is similar to the Link Access Protocol - Balanced (LAP-B) defined in CCITT Recommendation X.25. However, unlike LAP-B, MDLP incorporates a number of features that provide for efficient operation in the landmobile environment. These include a selective repeat error recovery scheme to recover from lost packets, and a rapid synchronization of the protocol state machine in response to frequent MT on/off conditions.

The MDS Specialized Services Protocol (MSSP) provide for the multiplexing of application messages over the reliable transaction and unacknowledged data delivery services provided by MDS Transaction Protocol (MTP) and MDS Unacknowledged Link Protocol (MULP), respectively. MTP supports transactions involving short messages between the MT and the DH and vice versa. MTP is especially efficient when the transactions are originated by fixed users, since capacity for the response can be allocated over the reservation channel (MT-DT). MULP provides for the transmission and reception of unacknowledged data packets to and from MTs. More importantly it provides for the multicasting of data from the DH to MT user groups.

Finally the Bulletin Board protocol (BBP) provides for the dissemination of system information from the DH to all MTs. The bulletin board pages are organized in a manner that reduces the system overhead, while providing for significant flexibility in making incremental changes and incorporation of additional system parameters.

MDS NETWORK MANAGEMENT ARCHITECTURE

The MDS system provides for a comprehensive set of network management procedures. All five functional areas specified within the OSI network management framework: Configuration, Fault, Performance, Security, and Accounting are covered within the system. Key items within each of these functional areas are briefly summarized below:

Configuration Management - Procedures are provided for automated commissioning of new MTs, performance verification of MTs, updating of MT parameters, system parameter distribution, and maintenance of several databases that contain network configuration information. Keeping in mind the mobility of the users as well as the evolving nature of the service, MDS provides for the dynamic reconfiguration of all system and MT specific parameters via automated system procedures (MT parameter update and bulletin board distribution).

Fault Management - The DH incorporates several procedures to detect network failures and implement appropriate restoral actions. Failure modes that are detected include malfunctioning channel units, failure of terrestrial links, failure of RF link, rain fade, and lack of connectivity with the NOC. The DH is also required to implement procedures for the detection of malfunctioning MTs.

Performance Management - The DH maintains, and makes available to the network operator, management information variables related to overall MDS performance. These include traffic loads, congestion indicators, error indicators, and protocol statistics. The MT is also required to maintain performance statistics for each internal MDS protocol layer (MPLP, MDLP, MTP, CAC, Physical). Messages have also been defined to transfer these statistics back to the DH and make them available to network and systems engineering personnel.

Security Management - Given the large potential for fraudulent access in a mobile environment, a number of access authentication procedures have been incorporated into the MDS system. At the simplest level, two separate terminal identification numbers are used when communicating with the MT. A Forward Terminal Identification Number (FTIN) is used for outbound messages from the DH to the MT, while a Reverse Terminal Identification Number (RTIN) is used for inbound messages. More sophisticated security mechanisms are also provided for access authentication, during virtual circuit setup, and via a periodic polled challenge issued by the DH. An

additional user facility has been defined within the X.25 call request and call accepted packets to carry the authentication information.

Accounting Management - The DH maintains accounting records for both the basic, as well as specialized services. The Basic Services records are collected by the off-the-shelf packet switch (Terrestrial Interface Subsystem). The accounting records are made available to the CMIS operated by the service provider, which is responsible for customer billing.

REFERENCES

[1] J. Lunsford, R. Thorne, D. Gokhale, W. Garner, G. Davies, "The AMSC/TMI Mobile Satellite Services (MSS) System Ground Segment Architecture", AIAA 14th International Communications Satellite Conference, Washington, D.C. March 1992
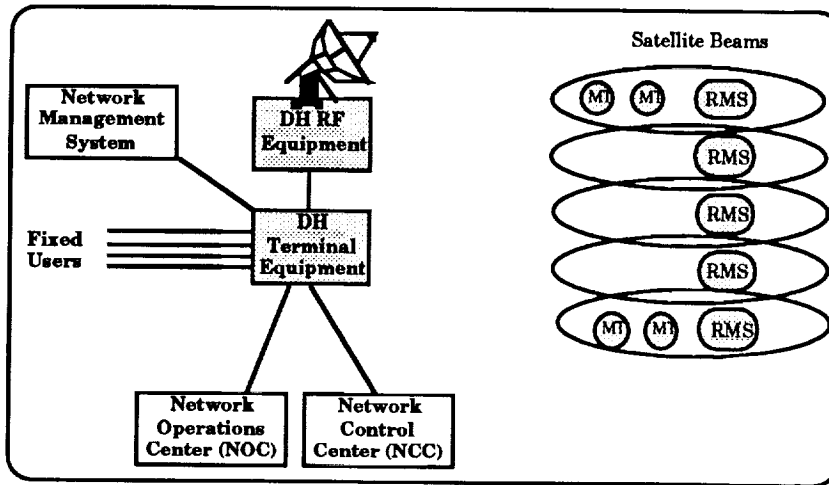
Figure 1. MDS Ground Segment Architecture
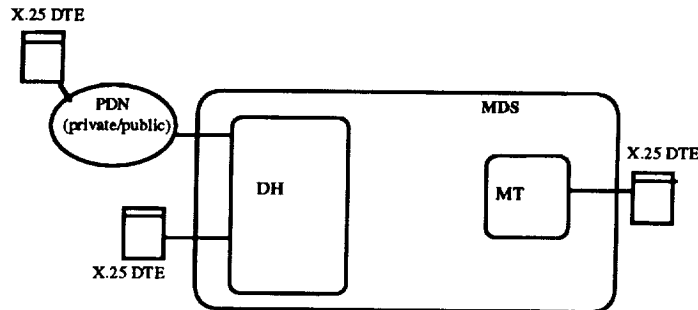
Figure 2. X.25 Service
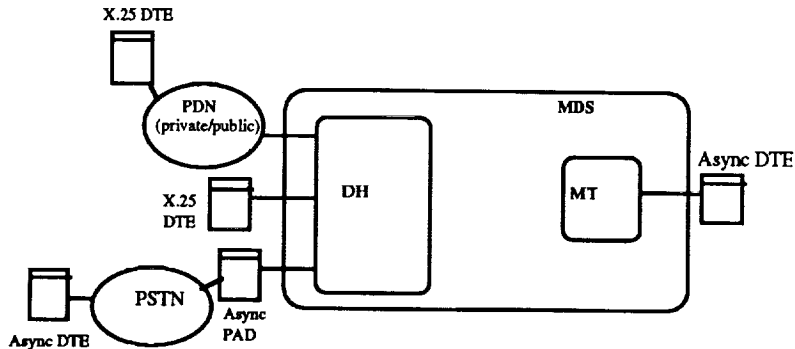
Figure 3. Asynchronous Data Service

483

DH-D

|← 1608 bits, 238.22 ms @ 6750 bps →|

UW	Coded Data	Flush

32 bits   196 bytes (after rate 3/4 FEC coding)   8 bits

MT-DRr

|← 298 bits, 42.88 ms @ 6750 bps →|

CW	Bit Timing	UW	Data	Flush

48 bits   32 bits   32 bits   21 -rate 1/3 coded bytes   18 bits

MT-DRd

|← 730 bits, 108.15 ms @ 6750 bps →|

CW	Bit Timing	UW'	Data	Flush

48 bits   32 bits   32 bits   75-rate 1/3 coded bytes   18 bits

MT-DT (Type-A)

|← <= 7552 bits, <= 1118.8 ms @ 6750 bps →|

CW	Bit Timing	UW	Fixed length data	Flush	Variable length data	Flush

48 bits   32 bits   32 bits   24 coded bytes   18 bits   24-900 coded bytes   18 bits

MT-DT (Type-B)

|← <= 7360 bits, <= 1090.4 ms @ 6750 bps →|

CW	Bit Timing	UW'	Variable length data	Flush

48 bits   32 bits   32 bits   48- 900 coded bytes   18 bits

Figure 4. MDS Channel Frame Formats
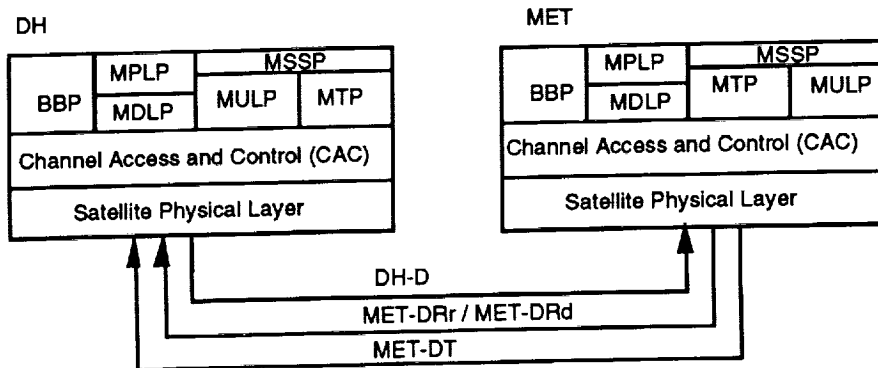
Figure 5. MDS Protocol Architecture

A COMPARISON BETWEEN COHERENT AND NONCOHERENT MOBILE SYSTEMS IN LARGE DOPPLER SHIFT, DELAY SPREAD AND C/I ENVIRONMENT

KAMILO FEHER

University of California, Davis; Davis, CA 95616
916-752-8127 or 916-752-0583; FAX 916-752-8428

ABSTRACT

The performance and implementation complexity of coherent and of noncoherent QPSK and GMSK modulation/demodulation techniques in a complex mobile satellite systems environment, including large Doppler shift, delay spread and low C/I, are compared. We demonstrate that for large $f_d T_b$ products, where f_d is the Doppler shift and T_b is the bit duration, noncoherent (discriminator detector or differential demodulation) systems have a lower BER floor than their coherent counterparts. For significant delay spreads, e.g., $\tau_{rms} > 0.4\ T_b$ and low C/I coherent systems outperform noncoherent systems. However, the synchronization time of coherent systems is longer than that of noncoherent systems.

Spectral efficiency overall capacity and related hardware complexity issues of these systems are also analyzed. We demonstrate that coherent systems have a simpler overall architecture (IF filter implementation-cost versus carrier recovery) and are more robust in an RF frequency drift environment. Additionally, the prediction tools, computer simulations and analysis of coherent systems is simpler. The threshold or capture effect in low C/I interference environment is critical for noncoherent discriminator based systems.

We conclude with a comparison of hardware architectures of coherent and of noncoherent systems, including recent trends in commercial VLSI technology and direct baseband to RF transmit, RF to baseband (0-IF) receiver implementation strategies.

MODEM/RADIO ARCHITECTURES

In Fig. 1 a Quadrature (QUAD) modulator, nonlinearly amplified (NLA) modulator radio architecture is illustrated. The Baseband Processor (BBP) could implement conventional QPSK [6] $\pi/4$-DQPSK [1, 7] or Gaussian MSK, GMSK functions [6, 8]. In the baseband to RF implementation, a slow Frequency Hopped Spread Spectrum-TDMA application is illustrated. The demodulation could be coherent or differential (discrimination detection) as illustrated in Fig. 2 and Fig. 3, from Ref. [1].

DEFINITIONS

QPSK   Conventional QPSK [6]

$\pi/4$-QPSK $\pi/4$-shifted QPSK - The standard modulation technique for IS-54-EIA standard [7] as well as for the Japanese digital cellular system.

GMSK   Gaussian filtered MSK [6] used in the DECT European standard [8] with noncoherent receivers and the GSM European system with coherent receivers.

F-QPSK   Feher's filtered QPSK [5, 6] for nonlinearly amplified systems. This modem/radio [2] doubles the capacity of European GMSK standard cellular/wireless systems.

PERFORMANCE

The $P(e) = f(E_b/N_o)$ performance in a Rayleigh faded channel is illustrated in Fig. 4. Note that the coherent F-QPSK system has a 7dB advantage over the noncoherent GMSK system filtered with $BT_b = 0.5$ [2]. The integrated out-of-band spectrum (ACI = adjacent channel interference), Fig. 5, indicates that F-QPSK is about 50% more spectrally efficient than GMSK. In Fig. 6 and Fig. 7 the performance in large Doppler $\log(f_D T)$ and large delay spread environment is illustrated. Coherent and differential $\pi/4$-QPSK results are presented, based on [9]. These illustrative sample results are

summarized in Table 1, based on Ref. [1]. In this Table, a comparison of coherent-noncoherent GMSK and F-QPSK systems is presented.

REFERENCES

[1]   K. Feher, *Cellular Digital Personal Communications*, (working title), A forthcoming book under contract with Prentice Hall, Inc., Englewood Cliffs, NJ, USA. Expected publication year: 1994.

[2]   P. Leung, K. Feher, "Low Cost F-QPSK Modem Radio Solutions for Doubling the Capacity of European Standard Cellular/PCS Systems," *Proc. of the Wireless Symposium and Exhibition*, San Jose, CA, Jan. 1993.

[3]   T. Le-Ngoc, S. Slimane, "IJF-OQPSK Modulation Schemes with MLSE Receivers for Portable/mobile Communications," *Proc. IEEE 42nd Veh. Tech. Conference*, pp. 676-680, Denver 1992.

[4]   Y. Guo, K. Feher, "Frequency Hopping F-QPSK for Power and Spectrally Efficient Cellular Systems," submitted to IEEE Vehicular Technology Conference, 1993.

[5]   K. Feher, "Filter: Nonlinear Digital," US Patent No. 4,339,724, issued July 13, 1982; Canada No. 1130871, August 31, 1982.

[6]   K. Feher, Ed., *Advanced Digital Communications Systems and Signal Processing Techniques,"* Prentice-Hall, Englewood Cliffs, NJ, 1987.

[7]   EIA IS-54 Dual-mode subscriber equipment - Network equipment compatibility specification, December 1989.

[8]   DECT Specification. Physical Layer, CI SPEC Part 1, Rev 06.0.

[9]   K. Feher, "Modems for Emerging Digital Cellular-Mobile Radio Systems," *IEEE Trans. on Vehicular Technology*, May 1991.
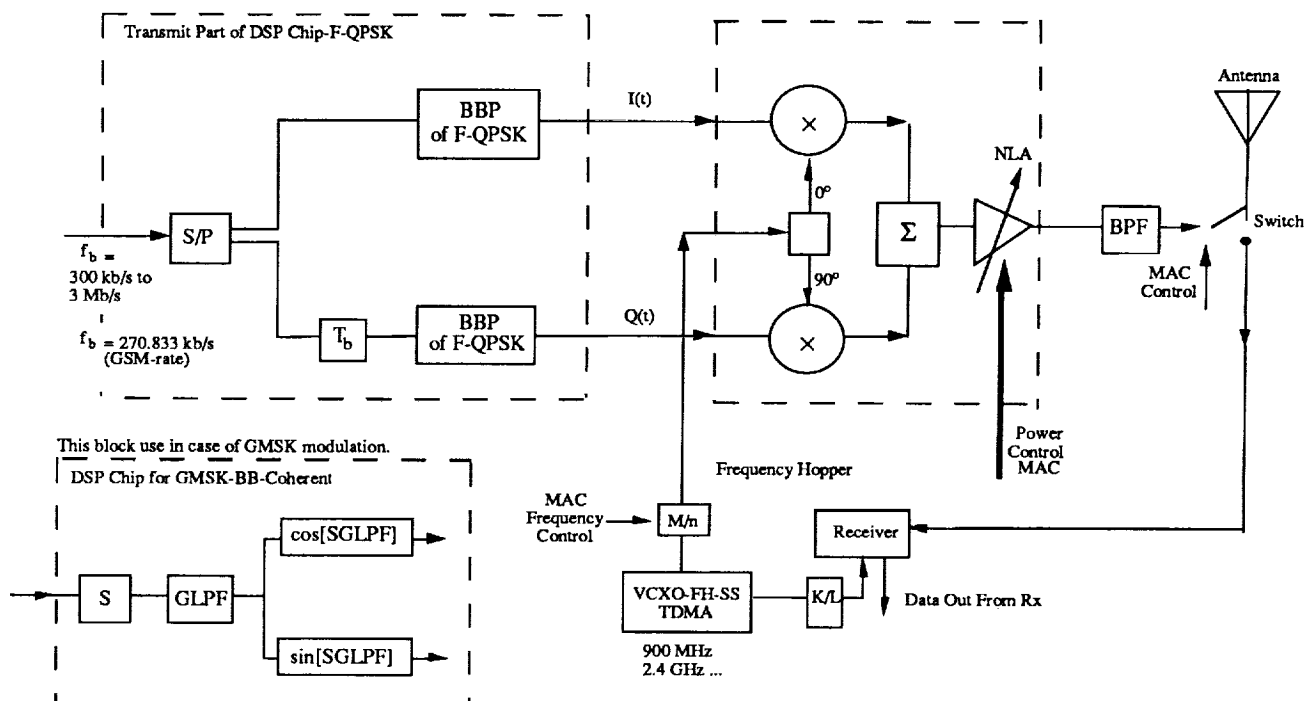
Fig. 1 Transmitter of a BB to RF radio for F-QPSK or GMSK nonlinear amplifier applications (slow frequency hopping-spread spectrum SFH-SS-TDMA) Ref. [1].
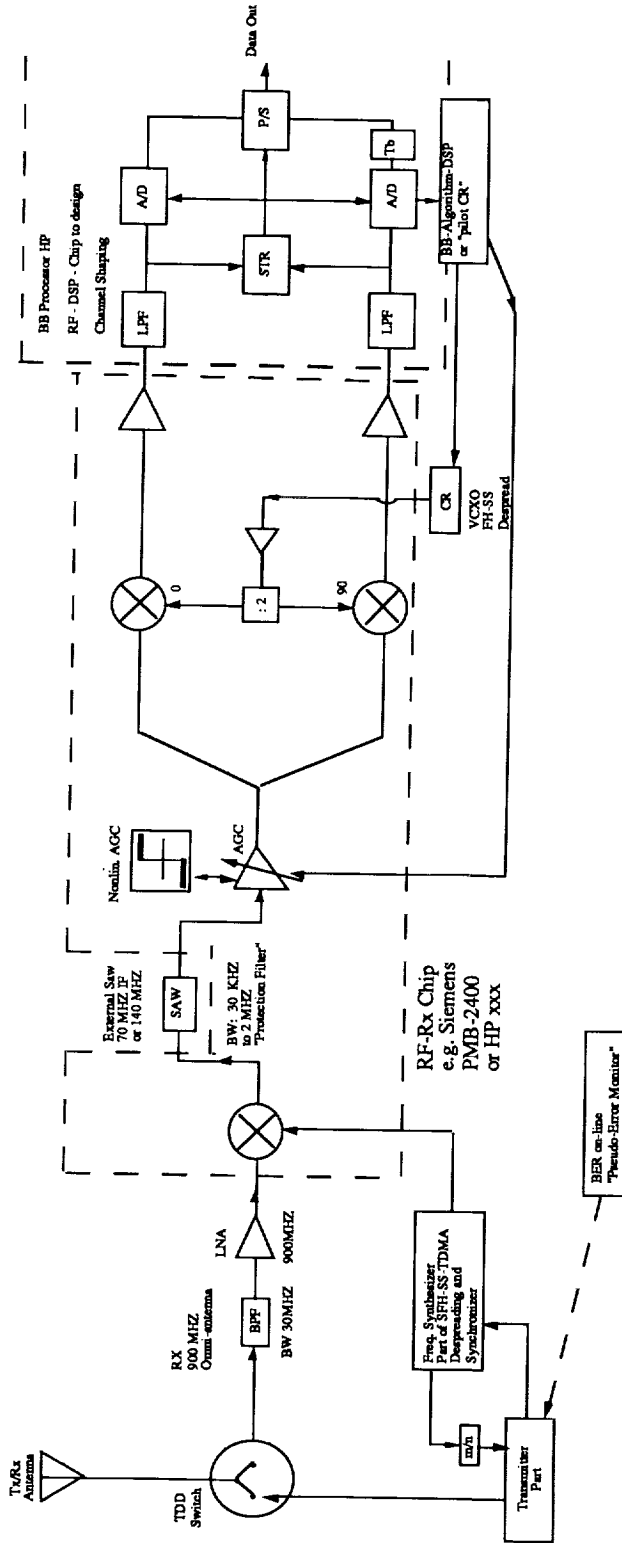
Fig. 2 Receiver with one IF stage for Coherent F-QPSK or GMSK systems (TDMA-TDD-SFH-SS) [Ref. 1].
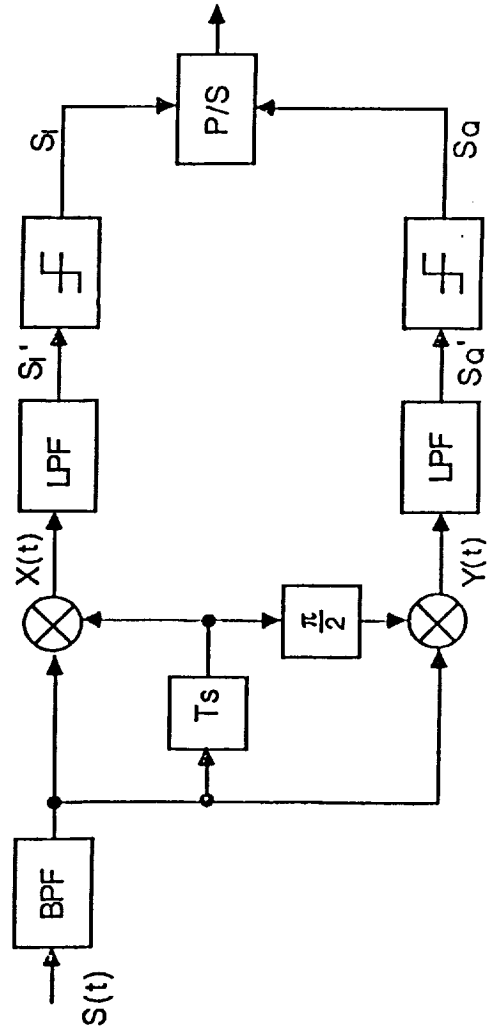
Fig. 3 Differential Demod of a QPSK modem.

487
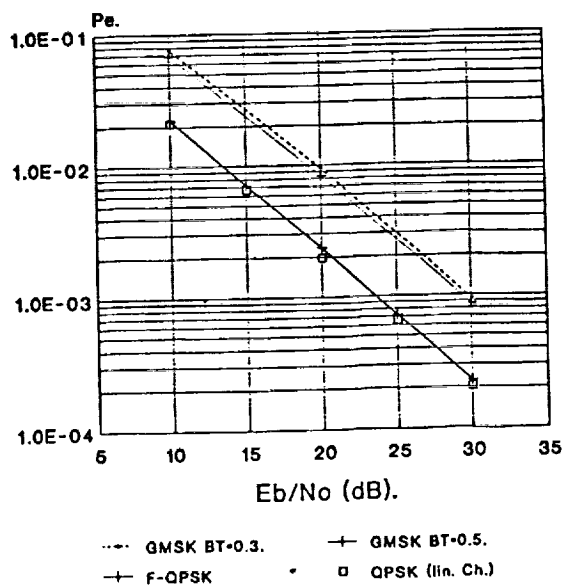
Fig. 4 BER of coherent F-QPSK and noncoherent GMSK BT=0.5 (DECT) in Rayleigh fading.
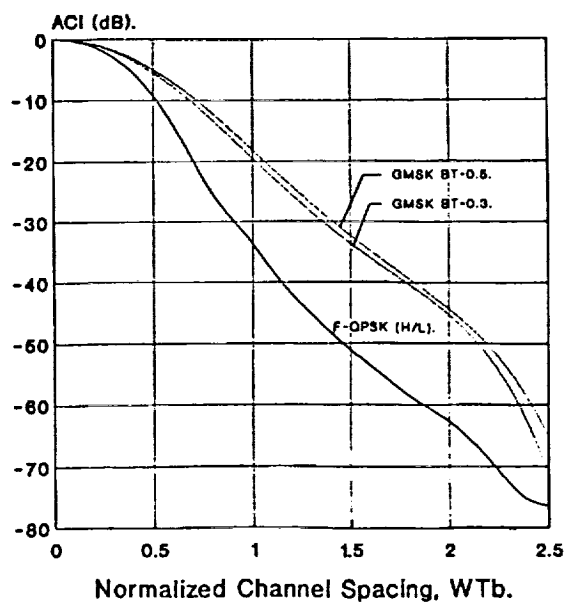
Fig. 5 ACI of F-QPSK and GMSK.
F-QPSK: Butterworth BPF (4 ord), BiTb=.55
GMSK: Gaussian BPF (4 ord), BiTb=0.6.
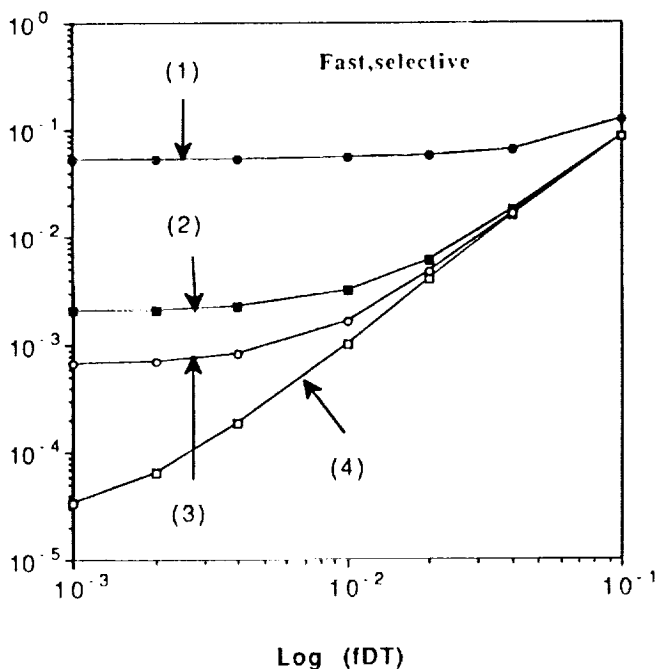
Fig. 6 P(e) vs. $f_D T$ of $\pi/4$-DQPSK in a frequency-selective fast fading channel. f_c=850 MHz, f_s=24 kBaud, α=0.2, C/I=∞ dB. (1) τ/T=0.1, C/D=10 dB, (2) τ/T=0.1, C/D=30 dB, (3) τ/T=0.5, C/D=10 dB, (4) τ/T=0.5, C/D=30 dB.
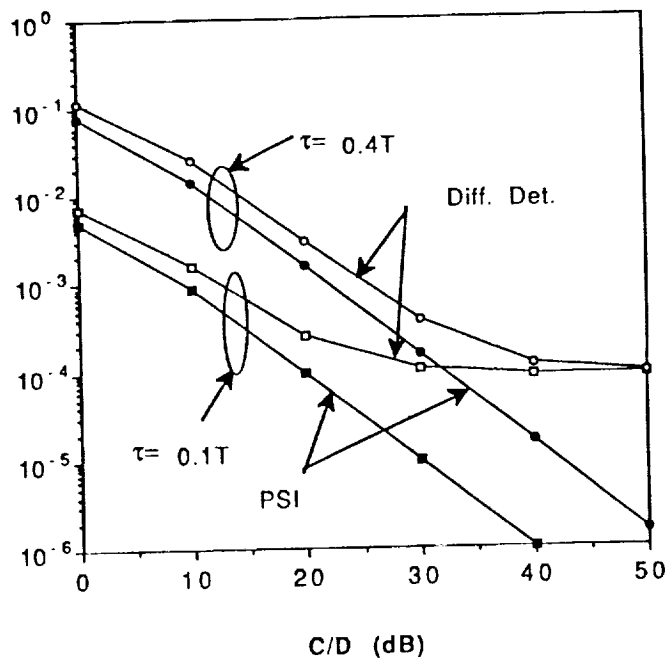
Fig. 7 Error-floors of the fade compensated $\pi/4$-QPSK and $\pi/4$-DQPSK in a frequency-selective fading channel as functions of C/D for τ=0.1T and 0.4T. The fading rate is assumed to be $f_D T$=3×10^{-3}.

488

Table 1 Coherent-Noncoherent GMSK and F-QPSK Comparison.   Ref. [1].

Maximal bit rate and delay spread τ_{rms} issues	COHERENT QPSK OR F-QPSK (or GMSK-similar, however worse performance.)	DIFFERENTIAL DQPSK (or DGMSK)
τ_{rms} "worst case" 1µs		
τ_{rms} = 200 ns		
BER = 10^{-2} floor due to τ_{rms}/T_s	τ_{rms}/T_s = 0.2	τ_{rms}/T_s = 0.15
$P_{(e)}$ = C/I degrad(addit) of 1dB due to τ_{rms}/T (4*more sensit. than for "floor"	τ_{rms}/T_s = 0.075 QPSK F-QPSK is higher abut 50%	τ_{rms}/T_s = 0.05
Maxim. bit rate f_b		
for 10^{-2} Error Floor 1µs[200ns]	600 kb/s [3 Mb/s]	300 kb/s [1.5 Mb/s]
for 1dB τ_{rms} caused degr. 1µs[200ns]	150 kb/s [750 kb/s]	75 kb/s [375 kb/s]
CAPACITY ISSUES BASED ON C/I = 3 dB (CCI advantage)	BER=10^{-2} C/I-15dB (Rayleigh)	BER=10^{-2} C/I=18dB
NORMALIZED RELAT. CAPACITY		
Based on k = 9 to k = 7 reuse	100%	70% (30% loss)
Based on WER and throughput	100%	20% (80% loss)
Spectral efficiency ACI and BPF versus LPF caused advantage, i.e., lower noise BW-coherent receiver (normalized to coherent)	100%	60%
Increased Bit Rate or Cell Coverage/Adaptive Equalization	Relatively simple/low cost DSP/SW adaptive equalizer could increase rate (coverage)	Very costly if at all feasible adaptive equalization technology (theory not well understood-requires original new research).

Table 1 (continued) Coherent-Noncoherent GMSK and F-QPSK Comparison.

	COHERENT QPSK	DIFFERENTIAL DQPSK
Bit rate (PHY) change, without loss of performance (within range)	Automatic SW (software controlled) in BBP	Very difficult could require change of IF-BPF
Spectral Efficiency for ACI=-20dB nonlinearly amplified radio	F-QPSK = 1.42 b/s/Hz GMSK = 0.94 b/s/Hz BT_b = 0.5 and 0.98 b/s/Hz for BT_b = 0.3	Approx. 0.7 b/s/Hz depending on BPF complexity
Synchronization Time (CR) (relative to no CR - differential loss of frame efficiency for 1000 or 10,000 bit word (packet)	50 bits:1000 = 5% (max 100 bits = max 10% 50 bits:10,000 = 0.5% max 100 bits for CR=max.1% - a disadvantage. Parallel CR and STR design could eliminate this drawback.	Potential of 1% to 10% packet/synch time advantage(?). However, could be lost due to BPF transient ringing. Synch. Time advantage could be lost due to DC comp. to sat. time requirement.
Threshold capture effect (discriminator-impulse noise)	No problem	Potential problem in the critical BER = 10^{-2} range with discriminator.
Tools (prediction)	Well known.	Much more involved as IF-BPF imperfect; impact of frequency tolerance GMSK BT_b = 0.3 very difficult.
RF-oscillator drifts include synthesizer - impact on BER - DC restoration.	Simple.	Very costly - potential danger like in DECT.
Additional down conversion/filters	Not required.	Very costly, extra stage could be required due to lower IF and BPF problems.
Carrier Recovery Requirements	Yes. Simple pilot in band and other Costas . . . well-known techniques. No Doppler problem. Low power solution. GSM, ADC other cellular have it.	No need for CR. Advantage
DC power-extra for CR	Could be marginally higher for demand alone.	Discriminator power requirement is smaller than coherent. However, DC battery power advantage could be lost due to LO or synthesizer-DC compensation requirement.
IC Chips-Trend	Most manufact. companies developing QUAD (coherent struct.)	Noncoherent discrim. today cheaper however overall radio extra IF, BPF, DC compensation not evident.
Overall Cost/DC Power estimate	About same as noncoherent receiver (total radio) with new technology.	About same.
RF Frequency 900MHz 1.9GHz, 2.4GHz Bit Rate Variation	Same architecture for both RF frequencies Flexible bit rate	Could require in some applications extra expensive IF stage (space/cost) does not lead to software driven bit rate change

Pseudo-Coherent Demodulation for Mobile Satellite Systems*

Dariush Divsalar and Marvin K. Simon

Jet Propulsion Laboratory
California Institute of Technology
M.S. 238-420
4800 Oak Grove Drive
Pasadena, California 91109
Phone: (818) 393-5138 FAX: (818) 354-6825

Abstract

This paper proposes three so-called pseudo-coherent demodulation schemes for use in land mobile satellite channels. The schemes are derived based on maximum-likelihood (ML) estimation and detection of an N-symbol observation of the received signal. Simulation results for all three demodulators are presented to allow comparison with the performance of differential PSK (DPSK), and ideal coherent demodulation for various system parameter sets of practical interest.

Introduction

A land mobile satellite channel can be characterized by AWGN, phase noise, frequency offsets due to local oscillator instabilities, Doppler and Doppler rate, Rician fading, and shadowing due to vegetation, terrain, and man-made buildings. The severity of these impairments varies for different applications depending on the satellite transponder, data rate, carrier frequency, type of antenna, and so on. For example, if a high gain antenna is used for the mobile, then Rician fading can be ignored. The modem designed to operate in such a channel must be robust in the face of frequent but rapid signal outages and must be able to reacquire the signal quickly. In the absence of a mid-band pilot, coherent demodulation is not an appropriate choice for this channel due to the long signal reacquisition time caused by the above mentioned impairments. Therefore, differentially coherent PSK (DPSK) can be selected as an alternate modulation scheme because of its simplicity and ability to recover quickly from the fade events. The bit error rate performance of uncoded DPSK is worse than that for coherent demodulation by about 1 dB in E_b/N_0. Convolutionally coded DPSK, however, requires about 3 dB higher E_b/N_0 than coherently demodulated PSK at a bit error rate of 10^{-3} in an AWGN channel assuming 3-bit soft quantization. To reduce this penalty, we consider pseudo-coherent demodulation which represents a compromise between the two extremes of coherent and differentially coherent demodulation.

This paper proposes three so-called pseudo-coherent demodulation schemes. The schemes are derived based on maximum-likelihood (ML) estimation and detection of an N-symbol observation of the received signal. Typical values of N range from 5 to 15 symbols. The first scheme is based on ML estimation of carrier phase assuming that the unknown frequency offset is perfectly compensated by a frequency estimator *prior* to the phase estimation process. The second scheme is based on direct ML estimation of a time varying phase caused by the presence of the frequency offset. This scheme does not require a separate frequency estimator as in the first scheme. Last of all, a scheme is proposed which is a hybrid of a simple open loop frequency estimator and the ML estimate of carrier phase *conditioned* on perfect knowledge of the frequency offset. Due to the time-varying phase, both the second and third demodulators are equipped with a 180 degree phase jump detector to resolve the periodic 180 degree phase ambiguities that occur. Simulation results for all three demodulators are presented to allow comparison with the performance of DPSK for various system parameter sets of practical interest.

Derivation of a pseudo coherent demodulation scheme in the absence of frequency offset

Consider the transmission of a BPSK modulated signal over AWGN channel with unknown carrier phase. For simplicity we use the complex envelope signal representation. The transmitted signal in the interval $kT \le t < (k+1)T$ is

$$s(t) = \sqrt{2P}e^{j\phi_k} \tag{1}$$

where P denotes the constant signal power, T denotes the PSK symbol duration and ϕ_k the transmitted phase which takes on one of two values 0 and π. The corresponding received signal in this same interval is

$$r(t) = \sqrt{2P}e^{j\phi_k}e^{j\theta} + n(t) \tag{2}$$

where $n(t)$ is a zero mean complex Gaussian noise with two-sided power spectral density $2N_0$ and θ is an arbitrary carrier phase introduced by the channel. In (2) we have assumed that the received signal is down-converted to baseband by a frequency reference signal

$\exp(j2\pi \hat{f}_c t)$, where $\hat{f}_c$ is the estimate of the received carrier frequency f_c and is provided by a Doppler frequency estimator. If we assume perfect frequency estimation i.e. $\hat{f}_c = f_c$, then at the output of the integrate-and-dump (I&D) filter we obtain

$$r_k = \sqrt{2P}e^{j(\phi_k + \theta)} + n_k \qquad kT \le t < (k+1)T$$
$$(3)$$

where n_k is a sample of zero mean complex Gaussian noise with variance $\sigma_n^2 = N_0 / T$ per dimension.

Consider now a received sequence $\mathbf{r} = (r_{k-1}, ..., r_{k-N})$ of length N and assume that the carrier phase θ is constant over the length of this sequence. Then the likelihood function is

$$p(\mathbf{r}|\boldsymbol{\phi}, \theta) = (\frac{1}{2\pi\sigma_n^2})^N e^{-\frac{1}{2\sigma_n^2}\sum_{i=1}^{N}|r_{k-i} - \sqrt{2P}e^{j(\phi_{k-i}+\theta)}|^2}$$
$$(4)$$

where vector $\boldsymbol{\phi} = (\phi_{K-1}, ..., \phi_{K-N})$ is the transmitted phase sequence. Equation (5) can be written as

$$p(\mathbf{r}|\boldsymbol{\phi}, \theta) = Fe^{\alpha\sum_{i=1}^{N}\text{Re}\{r_{k-i}e^{-j(\phi_{k-i}+\theta)}\}}$$
$$(5)$$

where

$$F = (\frac{1}{2\pi\sigma_n^2})^N e^{-\frac{1}{2\sigma_n^2}\sum_{i=1}^{N}|r_{k-i}|^2 - \frac{NP}{\sigma_n^2}}$$
$$(6)$$

which is independent of the data, and

$$\alpha = \frac{\sqrt{2P}}{\sigma_n^2}$$
$$(7)$$

We would like to obtain the maximum-likelihood estimation of the carrier phase θ given the observation $\mathbf{r} = (r_{k-1}, ..., r_{k-N})$. Thus, $\hat{\theta}_{ML}$ should satisfy

$$\ln p(\mathbf{r}|\hat{\theta}_{ML}) = \max_{\theta} \ln p(\mathbf{r}|\theta)$$
$$(8)$$

$$p(\mathbf{r}|\theta) = E\{p(\mathbf{r}|\boldsymbol{\phi}, \theta)\}$$

But
$$= F\prod_{i=1}^{N}\left(\frac{1}{2}\sum_{\phi_{k-i}} e^{\alpha\text{Re}\{r_{k-i}e^{-j(\phi_{k-i}+\theta)}\}}\right)$$
$$(9)$$

$$= F\prod_{i=1}^{N}\cosh\left(\alpha\text{Re}\{r_{k-i}e^{-j\theta}\}\right)$$

or

$$\ln p(\mathbf{r}|\theta) = \ln F + \sum_{i=1}^{N}\ln\cosh\left(\alpha\text{Re}\{r_{k-i}e^{-j\theta}\}\right)$$
$$(10)$$

Then, the solution to

$$\frac{\partial \ln p(r|\theta)}{\partial \theta}\bigg|_{\theta=\hat{\theta}_{ML}} = 0 \qquad (11)$$

results in $\hat{\theta}_{ML}$. Using (11) in (12) we obtain

$$\frac{\partial \ln p(\mathbf{r}|\theta)}{\partial \theta} = -\alpha\sum_{i=1}^{N}\tanh(\alpha\text{Re}\{r_{k-i}e^{-j\theta}\})$$
$$\bullet (\text{Re}\{jr_{k-i}e^{-j\theta}\}) = 0$$
$$(12)$$

For small signal to noise ratio we have the approximation

$$\tanh x \approx x \qquad (13)$$

Therefore, $\hat{\theta}_{ML}$ should satisfy

$$\sum_{i=1}^{N}\text{Re}\{r_{k-i}e^{-j\hat{\theta}_{ML}}\}\text{Re}\{jr_{k-i}e^{-j\hat{\theta}_{ML}}\} = 0$$
$$(14)$$

which results in the maximum-likelihood estimate of phase

$$e^{j\hat{\theta}_{ML}} = \left(\frac{\sum_{i=1}^{N}r_{k-i}^2}{\left|\sum_{i=1}^{N}r_{k-i}^2\right|}\right)^{\frac{1}{2}}$$
$$(15)$$

The structure of the demodulator corresponding to (15) is shown in Fig. 1.
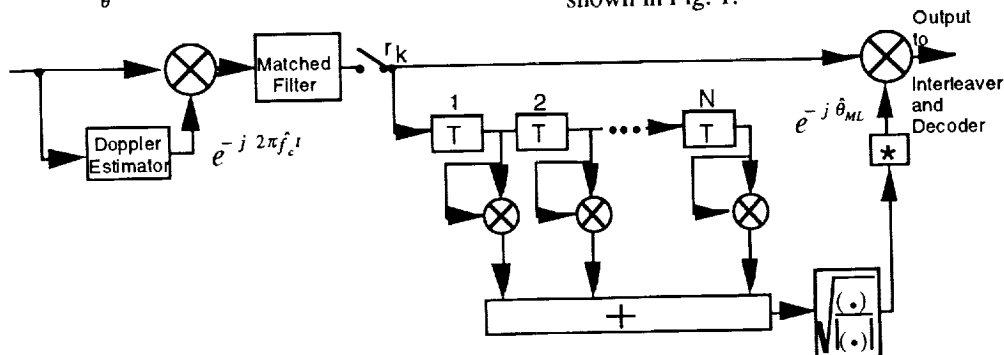
Figure 1. Pseudo-Coherent Demodulator (Scheme 1)

This scheme can be shown to be equivalent to a similar scheme proposed in [1] if the nonlinearity used in [1] is a squaring device. However, the authors of [1] did not specifically show that their structure is based on maximum-likelihood estimation.

We now present the relative bit error performances of a communication system employing the proposed demodulation scheme with respect to comparable systems using DPSK and ideal coherent demodulation. To do this we consider the three systems illustrated in Figs. 2, 3, and 4 respectively. In all three cases, the transmitter uses a constraint length $K=7$, rate $r=1/2$ convolutional encoder with an interleaving size of 4x32 symbols. A Viterbi decoder with infinite bit quantization input and decoder buffer size of 32 bits has been used at the receiver.
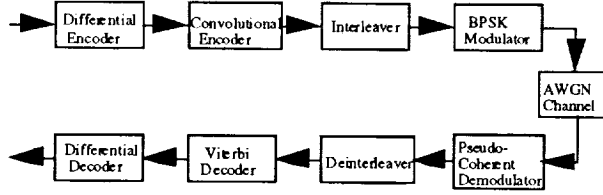
Figure 2. System 1, with Pseudo Coherent Demodulation.
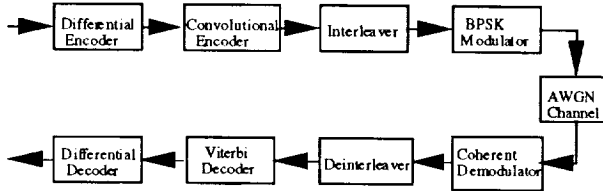
Figure 3. System 2, with Coherent Demodulation.
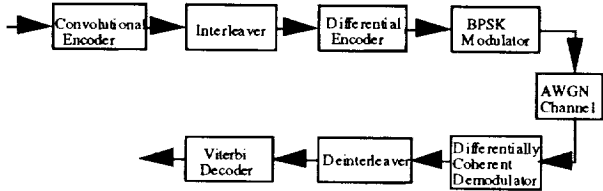
Figure 4. System 3, with Differentially Coherent Demodulation (DPSK).

Simulation results for the bit error performance of the three systems are shown in Figure 5. As can be seen from this figure, the proposed pseudo-coherent demodulator requires 2.40 dB less E_b/N_0 than the DPSK demodulator, and 0.85 dB more E_b/N_0 than an ideal coherent demodulator at a bit error rate of 10^{-3}. In obtaining the simulation results, perfect Doppler frequency tracking was assumed.
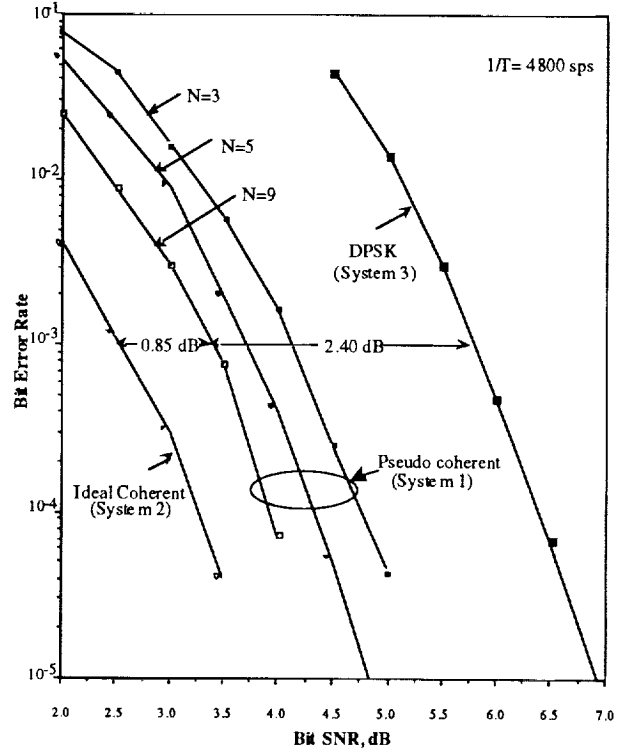
Figure 5. Simulation Results

Derivation of a pseudo coherent demodulation scheme in the presence of frequency offset

Let θ_k be the unknown time-varying carrier phase (due to frequency offset) at time $t = kT$. Then, θ_k can be written as

$$\theta_k = \theta_0 + 2\pi f kT \qquad (16)$$

where θ_0 is the initial carrier phase and f is the frequency offset. Similarly, the phase at time $t = (k-i)T$ is related to the phase at time $t = kT$ by

$$\theta_{k-i} = \theta_k - 2\pi f iT \qquad (17)$$

We are interested in finding the maximum-likelihood estimate of θ_k by observing N past received samples $r_{k-1}, r_{k-2}, \ldots, r_{k-N}$ denoted by the vector $\mathbf{r}$, i.e.

$$p(\mathbf{r}|\hat{\theta}_{k,ML}) = \max_{\theta_k} p(\mathbf{r}|\theta_k) \qquad (18)$$

To obtain $p(\mathbf{r}|\theta_k)$, we first find

$$p(\mathbf{r}|\boldsymbol{\phi},\theta_k,f) = Fe^{\alpha \sum_{i=1}^{N} \operatorname{Re}\left\{ r_{k-i} e^{-j(\phi_{k-i} + \theta_k - 2\pi f iT)} \right\}} \qquad (19)$$

where F and α are given by (6) and (7) and $\boldsymbol{\phi} = (\phi_{k-1}, \ldots, \phi_{k-N})$ is a vector of BPSK phases, each

493

taking values 0 or π. Next, we compute $p(\mathbf{r}|\theta_k, f)$ by averaging (20) over the binary-valued equiprobable data phases producing

$$p(\mathbf{r}|\theta_k, f) = E\left\{p(\mathbf{r}|\underline{\phi}, \theta_k, f)\right\}$$

$$= F\prod_{i=1}^{N} \cosh\left(\alpha \operatorname{Re}\left\{R_{k-i}e^{-j\theta_k}\right\}\right)$$

(20)

where $R_{k-i} \overset{\Delta}{=} r_{k-i} \, e^{j2\pi f iT}$. Finally, we compute $p(\mathbf{r}|\theta_k)$ by averaging (20) over the frequency shift f assuming as its density function a uniform distribution between $-f_{max}$ and f_{max} where f_{max} corresponds to the maximum expected (Doppler) frequency shift. The result of this averaging gives

$$p(\mathbf{r}|\theta_k) = E\left\{p(\mathbf{r}|\theta_k, f)\right\}$$

$$= \frac{F}{2f_{max}}\int_{-f_{max}}^{f_{max}} \prod_{i=1}^{N} \cosh\left(\alpha \operatorname{Re}\left\{R_{k-i}e^{-j\theta_k}\right\}\right) df$$

(21)

To obtain $\hat{\theta}_{k,ML}$ we need to determine the solution to

$$\left.\frac{\partial p(\mathbf{r}|\theta_k)}{\partial \theta_k}\right|_{\theta_k = \hat{\theta}_{k,ML}} = 0$$

(22)

Using small signal-to-noise ratio (SNR) approximations for sinh(.) and cosh(.), we obtain the final result as

$$e^{j\hat{\theta}_{k,ML}} = \left(\frac{\sum_{i=1}^{N} r_{k-i}^2 \operatorname{sinc}(4f_{max}iT)}{\left|\sum_{i=1}^{N} r_{k-i}^2 \operatorname{sinc}(4f_{max}iT)\right|}\right)^{\frac{1}{2}}$$

(23)

where $\operatorname{sinc}(x) = \sin(\pi x)/\pi x$.

The structure of the demodulator corresponding to (23) is shown in Fig. 6. Due to time-varying phase and the structure of the ML estimator, the demodulator is equipped with a 180 degree phase jump detector to resolve the periodic 180 degree phase ambiguities. Without a 180 degree phase jump detector, the differential decoder fails at the end of each 180 degree phase jump period. The phase jump detector compares the present and the previous phase estimates for detection. The bottom portion of Fig. 6 shows the phase jump detector.

Simulation results for the bit error rate of the pseudo-coherent demodulator using scheme 1 and scheme 2 are compared and the results are shown in Fig. 7. Scheme 1 is the best in the absence of frequency error, but it is very sensitive even to very small frequency offsets. Scheme 1 will fail for frequency offsets even as small as 1 Hz. Therefore, in practice, it is preferable to use scheme 2 even though there is a small penalty due to using a phase jump detector.
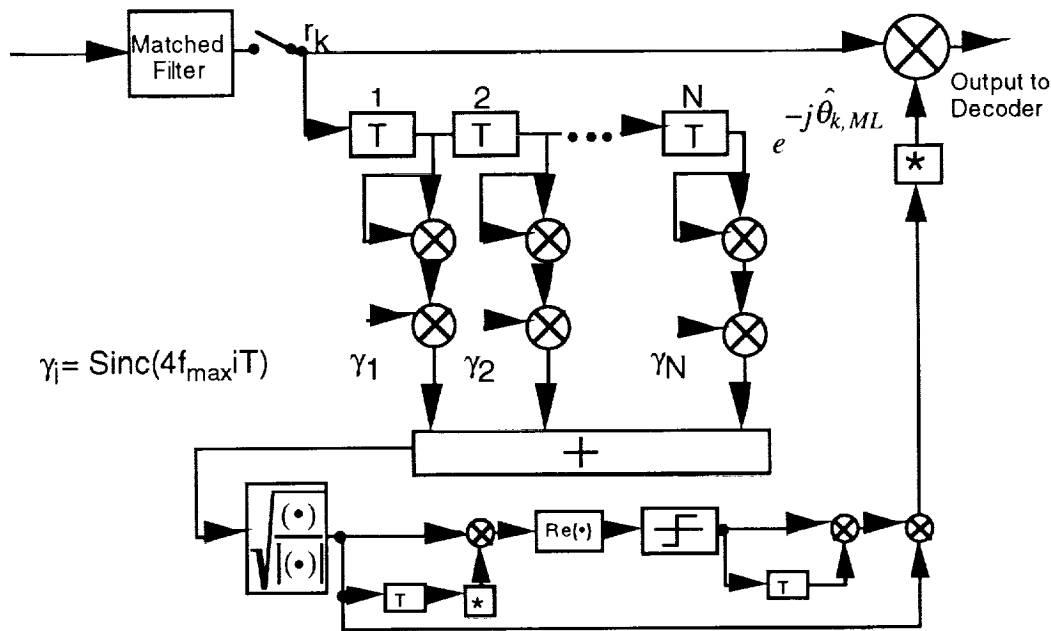
Figure 6. Pseudo-Coherent Demodulator (Scheme 2)

494
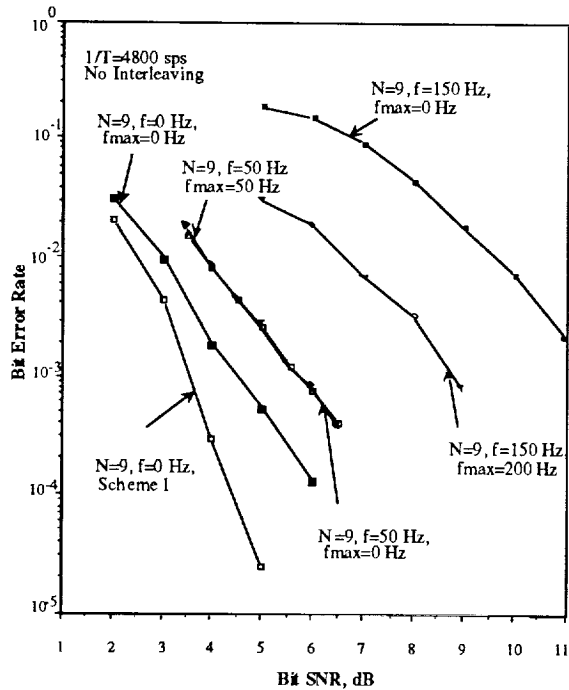
Figure 7. Simulation results.

A pseudo-coherent demodulation scheme with an open loop frequency estimator

The third proposed pseudo-coherent demodulation scheme uses a simple open loop frequency estimator together with the ML estimate of the carrier phase conditioned on perfect knowledge of the frequency offset. Due to time-varying phase and the structure of the ML estimator, the demodulator is again equipped with a 180 degree phase jump detector to resolve the periodic 180 degree phase ambiguities. The structure of the demodulator is shown in Fig. 8. A typical sample function of the phase estimate in the presence and absence of noise is shown in Fig. 9. Simulation results have been obtained to compare the bit error probability of this scheme with DPSK for various cases of practical interest. These results are illustrated in Fig. 10.
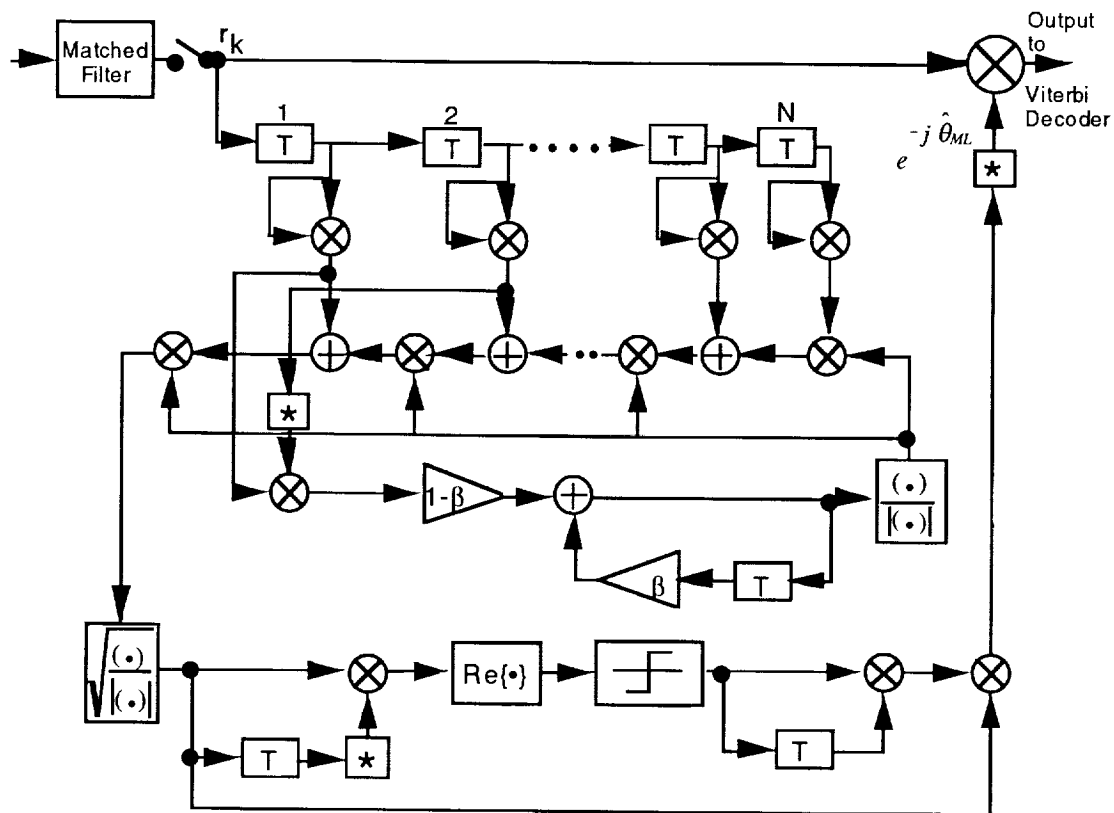
Figure 8. Pseudo coherent Demodulator (Scheme 3)
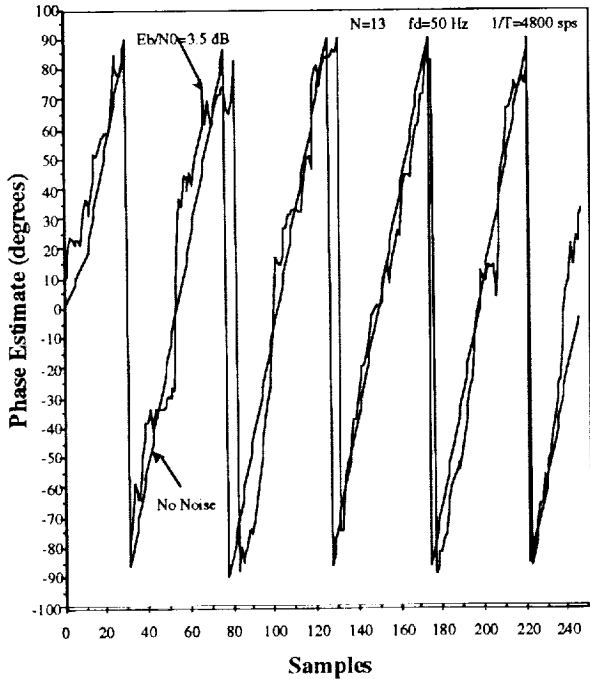
Figure 9. Sample function of phase estimate
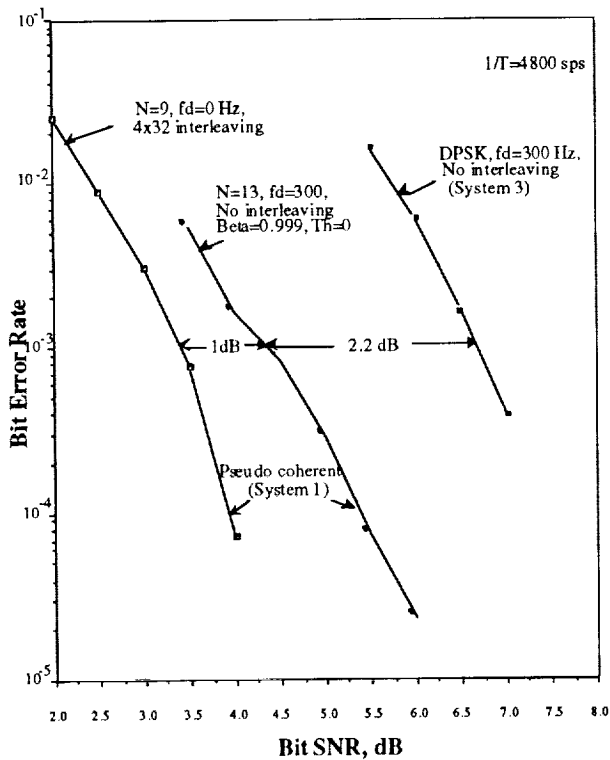
Figure 10. Simulation results

Conclusion

In this paper, three pseudo-coherent demodulation schemes were proposed. The schemes were derived based on maximum-likelihood (ML) estimation and detection of an N-symbol observation of the received signal. Simulation results for all three demodulators were presented to allow comparison with the performance of differential PSK (DPSK) and ideal coherent demodulation for various system parameter sets of practical interest.

Scheme 1 can be used if there is an external frequency estimator with very small frequency error variance. Scheme 2 can be used if the frequency offset is small, or the receiver is equipped with an external frequency estimator. Scheme 3 can be used if the frequency offset is large and no external frequency estimator is used.

Acknowledgment

References
[1] A. J. Viterbi and A. M. Viterbi, "Nonlinear Estimation of PSK Modulated Carrier Phase with Application to Burst Digital Transmission," IEEE Trans. on Inform. Theory, Vol. IT-29, No. 4, pp. 543-551. July 1983.

496

Session 11
Advanced System Concepts and Analysis—II

Session Chair—*Ed Ashford*, European Space Agency, The Netherlands
Session Organizer—*Jack Rigley*, Communications Research Centre, Canada

Transmission Over EHF Mobile Satellite Channels *

W. Zhuang[†], J.-Y. Chouinard, A. Yongaçoğlu
Department of Electrical Engineering, University of Ottawa
161 Louis-Pasteur, Ontario, Canada K1N 6N5
Tel.: +1 613 564-8159, Fax: +1 613 564-6882

Abstract

Land mobile satellite communications at Ka-band (30/20 *GHz*) are attracting an increasing interest among the researchers because of the frequency band availability and the possibility of small earth station designs. However, communications at the Ka-band pose significant challenges in the system designs due to severe channel impairments. Because only very limited experimental data for mobile applications at Ka-band is available, this paper study the channel characteristics based on experimental data at L-band (1.6/1.5 *GHz*) [1]-[3] and the use of frequency scaling [4]. The land mobile satellite communication channel at Ka-band is modelled as lognormal-Rayleigh fading channel. The first and second-order statistics of the fading channel are studied. The performance of a coherent BPSK system over the fading channel at L-band and Ka-band is evaluated theoretically and validated by computer simulations. Conclusions on the communication channel characteristics and system performance at L-band and Ka-band are presented.

1. Introduction

Land mobile satellite (LMS) services at L-band frequencies have been investigated and developed throughout 1980s; system concepts and corresponding technologies are being transferred to the land mobile satellite communication industry [5]. In order to be viable, future LMS telecommunication systems, such as personal communication systems, will have to provide a large number of users with diversified services, while being

cost-effective. However, increased use of L-band frequencies leads to the important problem of radio spectrum congestion: because of the availability of large bandwidths, Ka-band is attracting more and more attention in the land mobile satellite research field. Furthermore, at Ka-band, the user equipment (e.g. portable transceivers) can be significantly smaller and eventually less expensive than the equipment used at L-band. It is therefore expected that LMS systems operating in the Ka-band will provide the service users with larger information capacities, a wider variety of services, and this at a low cost. Unfortunately, the Ka-band LMS channel is subjected to severe propagation impairments such as rain attenuation, scintillation, as well as large Doppler frequency shifts, all of which must be taken into account while designing personal satellite communication systems.

The objective of this paper is to model and analyze the EHF land mobile satellite channel, and to evaluate the performance of a coherent BPSK system in the channel. Here, we consider the 30/20 *GHz* Ka-band channel with up links at 30 *GHz* and down links at 20 *GHz*. Being the critical link, only the down link propagation channel is discussed. The remainder of this paper is organized as follows. The first-order statistical description of the LMS channel is discussed in Section 2. Section 3 presents the second-order statistics of the fading channel at Ka-band, which are compared with those at L-band. An upper bound of the bit error rate of a coherent BPSK system over the fading channel is derived theoretically in Section 4, and is validated by computer simulations for the cases of light, average and heavy shadowings. Finally, Section 5 concludes the present work.

[†]Currently with TR Labs, Edmonton, Canada.

2. First-Order Statistics of the LMS Channel

It is well known [1], [6] that a land mobile radio channel can be modelled as a Rayleigh fading channel with its local mean, the line-of-sight (LOS) component, following a lognormal statistical distribution. The channel corrupts the transmitted signaling waveform by introducing a multiplicative gain $r(t)$ and phase shift $\theta(t)$, which can be expressed as

$$R(t) = r(t) \cdot \exp[j\theta(t)] = \qquad (1)$$

$$z(t) \cdot \exp[j\phi_L(t)] + g(t) \cdot \exp[j\phi_M(t)] \quad (2)$$

where the LOS and multipath phases ($\phi_L(t)$ and $\phi_M(t)$) are uniformly distributed between 0 and 2π. $z(t)$ is a lognormally distributed random process representing the amplitude of the LOS signal, $g(t)$ is the envelope of the multipath component and is Rayleigh distributed. The probability density function (PDF) of the lognormally distributed LOS component is [7]

$$p(z) = \frac{1}{\sqrt{2\pi d_0} z} \exp[-\frac{(\ln z - \mu)^2}{2d_0}] \qquad (3)$$

where μ and $\sqrt{d_0}$ are the mean value and standard deviation of the normally distributed random process $ln[z(t)]$. The PDF of the received signal envelope $r(t)$ is [1]

$$p(r) = \frac{r}{b_0\sqrt{2\pi d_0}} \int_0^\infty \frac{1}{z} \cdot$$
$$\exp[-\frac{(\ln z - \mu)^2}{2d_0} - \frac{r^2 + z^2}{2b_0}] I_0(\frac{rz}{b_0}) dz \quad (4)$$

where b_0 is the power of the multipath signal.

In Table 1, the parameters of the L-band (1.5 GHz) mobile satellite channel are displayed [1]-[3]. The calculations are based on measurement carried on in Ottawa, Canada. For the experiment, the INMARSAT's MARECS A satellite was used. The elevation angle from Ottawa to the satellite was about 20°. So far, the assessment of the LMS model has been carried out only at UHF and L-band. Due to lack of sufficient experimental LMS data at Ka-band, a comprehensive prediction of the relevant fading parameters cannot be done. However, from the mechanism of the LMS modelling at L-band, it is reasonable to assume that the LMS model is suitable

to be used for the channel at Ka-band with the model parameters being appropriately scaled. In this paper, we concentrate our analysis on the frequency non-selective fading channel.

Table 1: L-band channel model parameters.

L-band (1.5 GHz) channel	b_0	μ	$\sqrt{d_0}$
light shadowing	0.158	0.115	0.115
average shadowing	0.126	-0.115	0.161
heavy shadowing	0.0631	-3.91	0.806

The effect of multipath fading and shadowing on the LMS system performance depends on the system operation environments. In open and tree-shadowed areas, multipath fading results from both specular reflection and diffuse scattering from the terrain surrounding the mobile earth station. With the increase of the RF frequency, the amplitude of the reflection coefficient and the ground conductivity also increase; therefore, more scattering at Ka-band may come from small obstacles or terrain irregularities than those at L-band [8]. On the other hand, the mobile antenna radiation patterns at Ka-band are expected to be narrow enough to eliminate the problem to a great extent. As a result, in first approximation, it may be considered that multipath fading does not impair system performance at Ka-band more than that at L-band [4]. In the following discussion, the power of multipath component at Ka-band is taken to be the same as that at L-band.

With the RF frequency 30/20 GHz of Ka-band, the shadowing on the LOS component may come even from the leaves and the small branches of the trees whose dimensions are comparable with the wavelength (1.0-1.5 cm). Therefore, the LMS systems at Ka-band are expected to suffer more attenuation and diffusion due to shadowing in comparison with those at L-band. To the authors knowledge, very limited experimental data at Ka-band for mobile applications is available at the present time in the open literature and existing frequency scaling methods are not of straightforward applicability. An attempt has been made to estimate such a scaling factor using the *Modified Exponential Decay (MED) model* [9], developed from static propagation measurements through deciduous trees in Colorado, US. The attenuation coefficient (dB/m) can be computed by the

following equation [4]:

$$\alpha \approx 0.45 f^{0.284} \quad \text{for } 0 \le d_t \le 14$$
$$\alpha \approx 1.33 f^{0.284} d_t^{-0.412} \quad \text{for } 14 \le d_t \le 400 \quad (5)$$

where f is the frequency (in GHz) and d_t is the depth of trees (in m) intercepted by the LOS signal. The scaling factor is therefore:

$$\alpha_{20GHz} \approx 2.1 \alpha_{1.5GHz} \; (dB/m). \quad (6)$$

It should be pointed out that such an estimate model is based on particular channel conditions, and that further modifications may be necessary when experimental data at Ka-band becomes available.

In the following channel modelling and LMS performance analysis at Ka-band, we use the L-band parameters with the frequency scaling technique discussed above to calculate the Ka-band channel parameters. The amplitude attenuation of the lognormally distributed LOS component at L-band equals [4]

$$A_{1.5GHz} = e^{X_{1.5}} \quad (7)$$

where $X_{1.5}$ has a Gaussian distribution with mean $\mu = \mu_{1.5}$ and variance $d_0 = \sigma_{1.5}^2$. At Ka-band with RF equal to 20 GHz, the attenuation of the received LOS signal power in dBW is 2.1 times of that at L-band (see Eq. 6), that is,

$$
\begin{aligned}
A_{20GHz}^2(dBW) &= 2.1 \, A_{1.5GHz}^2(dBW) \\
\Rightarrow A_{20GHz} &= A_{1.5GHz}^{2.1} \\
\Rightarrow e^{X_{20}} &= e^{2.1 \, X_{1.5}} \\
\Rightarrow X_{20} &= 2.1 \, X_{1.5} \\
\Rightarrow \mu_{20} &= 2.1 \, \mu_{1.5} \\
\Rightarrow \sigma_{20} &= 2.1 \, \sigma_{1.5} . \quad (8)
\end{aligned}
$$

Figure 1 is a software simulation model of the LMS channel. In our simulations, the Gaussian noise after the low-pass (LP) filter is generated by summing a large number of sine waves [6]. The bandwidth of the LP filters is B_1 for the shadowing component and B_2 for the multipath component.

Figure 2 shows the cumulative distribution of the received L-band and Ka-band signal envelopes over the fading channel with average shadowing. The analytical results are obtained from Eq. (4). In these figures, the signal amplitude level is relative to the LOS signal component without shadowing (0 dB). The Ka-band

signal loses approximately an additional 1.5 dB, 1.0 dB and 0.5 dB at the signal amplitude levels of -10 dB, -5 dB and 0 dB respectively. Figure 3 shows the cumulative distribution of the received L-band and Ka-band signal envelopes without multipath signal in the case of average shadowing. The analytic values are obtained according to Eq. (3). From this figure, one observes that the signal at Ka-band loses an additional 0 to 3.5 dB in comparison to the L-band in the weak signal range (which is the most important for fade margin calculation). Table 2 shows the amplitude level of the shadowed LOS components at the cumulative probabilities of 70%, 80% and 90%.

Table 2: Amplitude level (in dB) of shadowed LOS components at different cumulative probabilities.

Shadow-ing	RF	Pr. 70%	Pr. 80%	Pr. 90%
light	1.5 GHz	0.49	0.23	-0.10
	20 GHz	1.02	0.27	-0.63
average	1.5 GHz	-1.66	-2.07	-2.55
	20 GHz	-3.65	-4.53	-5.85
heavy	1.5 GHz	-37.4	-39.4	-41.9
	20 GHz	-77.5	-81.8	-88.3

3. Second-Order Statistics of the LMS Channel

Second-order statistics are used to describe the time-dependent fading channel performance, which include level-crossing rate (LCR) and average fading duration (AFD). In the case of Rayleigh multipath fading with lognormal shadowing, the LCR normalized with respect to the maximum Doppler frequency shift is [1]

$$LCR_n(r = R) = LCR(r = R)/F_{dm}$$
$$= \sqrt{2\pi(1-\rho^2)} \frac{b_0(b_0 + 2\rho\sqrt{b_0 d_0} + d_0)^{\frac{1}{2}}}{b_0(1-\rho^2) + 4\rho\sqrt{b_0 d_0}} p(r) \quad (9)$$

where ρ is the correlation coefficient between the envelope $r(t)$ and the envelope change rate $\dot{r}(t)$. The corresponding normalized AFD is

$$
\begin{aligned}
AFD_n(r = R) &= AFD(r = R) \cdot F_{dm} \\
&= \frac{1}{LCR_n} \int_0^R p(r) \, dr . \quad (10)
\end{aligned}
$$

The analytic values and simulation results of the second order characteristics (LCR and AFD)

for the average shadowing channel are shown in Figures 4-5, where the amplitude level of the received signal is relative to the amplitude of the LOS signal component without shadowing (0 dB). In the computer simulations, assuming a vehicle speed of 43.2 km/h as an example, the maximum Doppler frequency shifts (which is the bandwidth of the complex Gaussian noise filters used to filter the process generating the multipath fading, i.e., B_2 in Figure 1) are 60 Hz for the L-band signal and 800 Hz for the Ka-band signal. The bandwidth of the filter for the shadowing components (i.e., the B_1 of Figure 1) is taken as 1/20 of B_2, which is 3 Hz for L-band and 40 Hz for Ka-band. The signal sampling rate is 2400 Hz. Each simulation is performed over 72,000 sampled data. The results show that the maximum values of the normalized LCRs of both L-band and Ka-band are very close to 1.0, which means that the LCRs increase almost linearly with the increase of the speed of vehicle or the increase of the RF frequency. The analytic values are obtained with $\rho = 0$, i.e., no correlation between $r(t)$ and $\dot{r}(t)$. In reality, there exists some correlation between $r(t)$ and $\dot{r}(t)$ and ρ may not be a constant, which may be further confirmed by the experimental data (see Figures 2-7 of [1]). That explains the slight differences between the simulation results and the analytical results in Figures 4-5. With the channel parameters and the use of frequency scaling technique, one finds that, in the case of average shadowing, the signal level at Ka-band is slightly more attenuated than at L-band.

4. Performance Evaluation of a Coherent BPSK System

It is assumed that a carrier recovery loop can track the carrier phase jitter due to the fading channel. Therefore, only amplitude fading due to the channel is taken into account. The upper bound of the average bit error rate is [10]

$$P_e^{av} \leq \frac{1}{2} \frac{1}{\sqrt{2\pi b_0}} \cdot \frac{\sigma_N^2}{b_0 + \sigma_N^2} \cdot \\ \int_0^\infty \frac{1}{z} \cdot \exp[-\frac{(\ln z - \mu)^2}{2d_0}] \cdot \\ \exp[-\frac{z^2}{2(b_0 + \sigma_N^2)}] dz \qquad (11)$$

and if only the LOS component is considered, then

$$P_e^{av} \leq \frac{1}{2} \frac{1}{\sqrt{2\pi d_0}} \int_0^\infty \exp[-\frac{z^2}{2\sigma_N^2} - \frac{(\ln z - \mu)^2}{2d_0}] dz. \qquad (12)$$

The upper bounds (analytical values) and simulation results of bit error rate for a coherent BPSK system at L-band and Ka-band are presented in Figures 6-8. Figures 6-7 show the bit error rate due to amplitude fading of the LMS channel at L-band and Ka-band in the cases of light, average and heavy shadowing. With multipath fading and at a bit error rate of 10^{-3}, the system operating at Ka-band loses 0.75 dB, 3.5 dB and 0.6 dB as compared to L-band in the cases of light, average and heavy shadowing respectively. The LOS signal component at Ka-band suffers more additional attenuation (when compared to L-band) in average shadowing than in light shadowing, which results in more system loss at Ka-band in average shadowing (3.5 dB) than in light shadowing (0.75 dB).

In the case of heavy shadowing, the LOS component is attenuated significantly, so that the channel can be represented as a Rayleigh fading channel (with only multipath components in the received signal) at both L-band and Ka-band. The weight of the LOS component is dramatically reduced compared to the cases of both light and average shadowings. The system performance depends on the dominant multipath signal component. With the assumption that the first-order statistics are the same for the multipath fading at L and Ka bands, the additional system loss at Ka-band in the heavy shadowing condition (0.6 dB) is less than that in the average shadowing (3.5 dB), which is not the case when only the LOS component is considered. Figure 8 shows the bit error rate of the system due to average shadowing only (no multipath signal is taken into account) at L-band and Ka-band. It is shown that at a bit error rate of 10^{-3}, the Ka-band system suffers an additional loss of 3.33 dB compared to L-band system.

5. Concluding remarks

A comparison study for the land mobile satellite communication system operating at Ka-band and L-band has been performed. The modelling of LMS channel at Ka-band is based on channel experimental data at L-band and a frequency

scaling technique, because of lack of sufficient experimental data of the channel at Ka-band. Both first-order and second-order statistics of the LMS channel are analyzed. The results show that: the LOS signal component at Ka-band has 0.0 dB to 3.5 dB more attenuation in the presence of average shadowing; the channel fades have a much faster rate at Ka-band compared with that at L-band because the fading rate is approximately proportional to the RF frequency, and the normalized average fading duration (AFD) increases correspondingly at Ka-band. An upper-bound bit error rate of a coherent BPSK system in the LMS channel is derived, which is further validated by computer simulations. With multipath fading and shadowing, at a bit error rate of 10^{-3}, the system performance at Ka-band loses approximately 0.75 dB, 3.5 dB and 0.6 dB more than that at L-band; in the absence of multipath fading, the system performance at Ka-band loses approximately 3.33 dB more than that at L-band in the case of average shadowing.

References

[1] C. Loo, "A Statistical Model for a Land Mobile Satellite Link", IEEE Trans. on Vehicular Technology, vol. VT-34, pp.122-127, August 1985.

[2] J. S. Butterworth, "Propagation Measurements for Land Mobile Satellite System at 1542 MHz," Communication Research Center, Department of Communications, CRC Technical Note 723, August 1984.

[3] C. Loo, "Digital Transmission Through a Land Mobile Satellite Channel", IEEE Trans. on Communications, vol. COM-38, no.5, pp.693-697, May 1990.

[4] J. Fortuny, J. Benedicto, and M. Sforza, "Mobile Satellite Systems At Ku and Ka-Band", Proc. Second European Conference on Satellite Communications, pp.55-62, Liege, October 1991.

[5] K. Dessouky, P. Estabrook, and T.C. Jedrey, "The ACTS Mobile Terminal", JPL SATCOM Quarterly, no.2, pp.1-9, July 1991.

[6] W.C. Jakes, Microwave Mobile Communication. New York: Wiley 1974.

[7] A. Papoulis, Probability, Random Variables, and Stochastic Processes. Second Edition, McGraw-Hill International Book Company, 1984.

[8] P. Beckmann and A. Spizzichino, The Scattering of Electromagnetic Waves From Rough Surface. Artech House, 1987.

[9] M.A. Weissberger, An Initial Summary of Models for Predicting the Attenuation of Radio Waves by Trees. U.S. Dept. of Defense, Report no. ESD-TR-81-101.

[10] W. Zhuang, A. Yongaçoğlu, J.-Y. Chouinard, D. Makrakis, "Performance Analysis of EHF Land Mobile Satellite Systems," Technical Report No.1, Department of Electrical Engineering, University of Ottawa, September 1992.
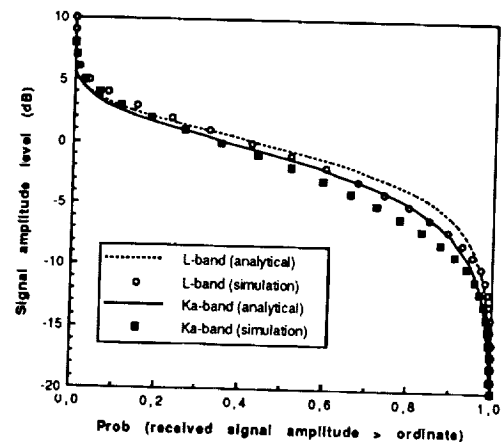
Figure 2: Received signal envelope probability distribution for average shadowing (with multipath).
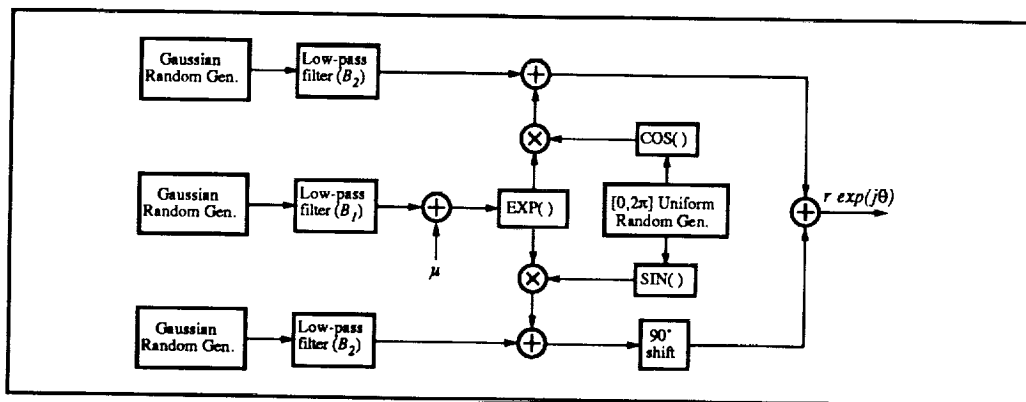
Figure 1: Land mobile satellite channel model.

503
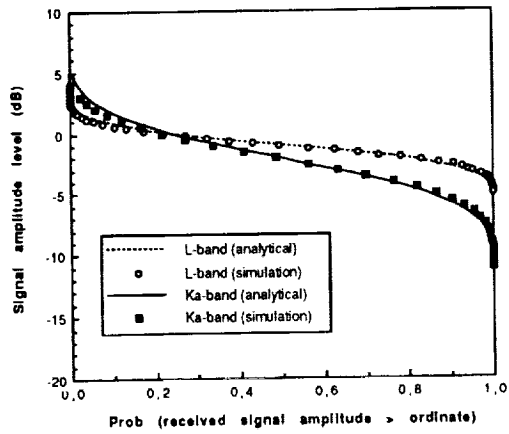
Figure 3: Received signal envelope probability distribution for average shadowing (without multipath).
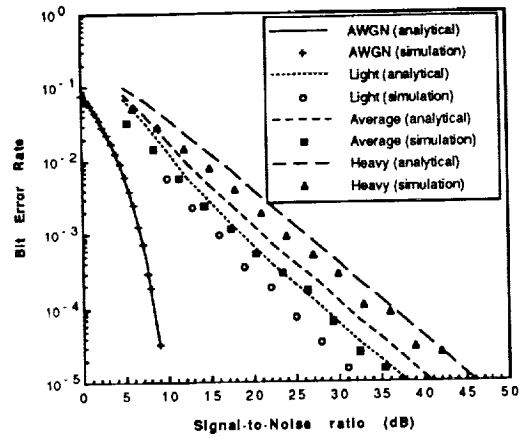
Figure 6: BER of a coherent BPSK system in a LMS channel at L-band.
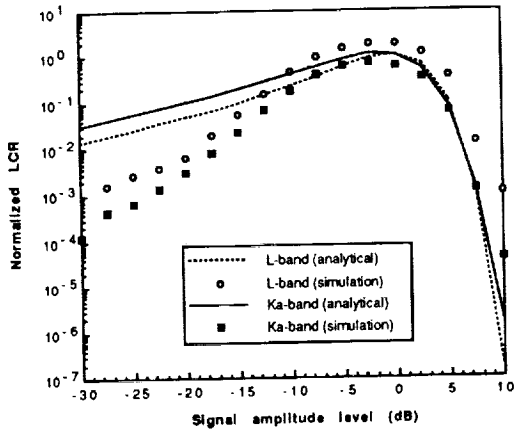
Figure 4: Normalized LCR in LMS channel at L-band and Ka-band (average shadowing).
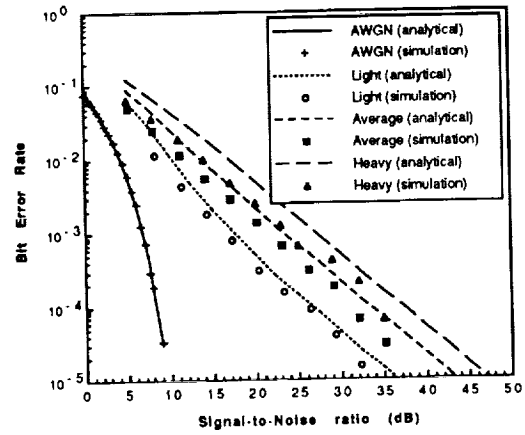
Figure 7: BER of a coherent BPSK system in a LMS channel at Ka-band.
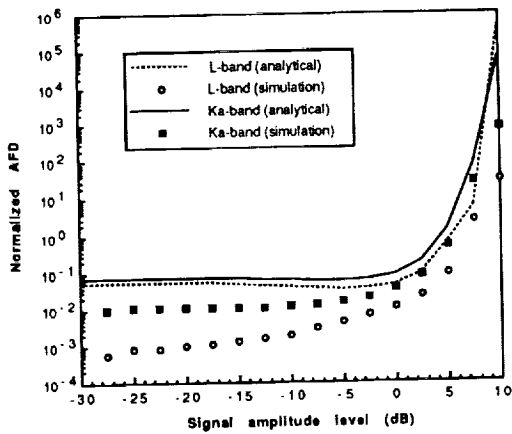
Figure 5: Normalized AFD in LMS channel at L-band and Ka-band (average shadowing).
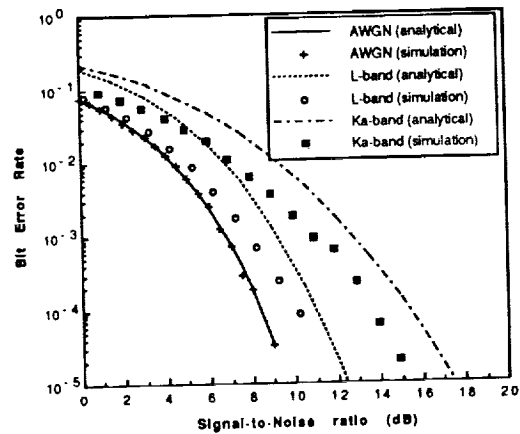
Figure 8: Performance of a coherent BPSK system over average shadowed LMS channel.

504

Adaptive Data Rate Control TDMA Systems as a Rain Attenuation Compensation Technique

Masaki Sato, Hiromitsu Wakana, Takashi Takahashi, Makoto Takeuchi, and Minoru Yamamoto
Communications Research Laboratory
Ministry of Posts and Telecommunications
893-1 Hirai, Kashima, Ibaraki 314 Japan
Tel: +81-299-84-4119
Fax: +81-299-84-4149

ABSTRACT

Rainfall attenuation has a severe effect on signal strength and impairs communication links for future mobile and personal satellite communications using Ka-band and millimeter wave frequencies. As rain attenuation compensation techniques, several methods such as uplink power control, site diversity, and adaptive control of data rate or forward error correction have been proposed. In this paper, we propose a TDMA system that can compensate rain attenuation by adaptive control of transmission rates. To evaluate the performance of this TDMA terminal, we carried out three types of experiments: experiments using a Japanese CS-3 satellite with Ka-band transponders, in-house IF loop-back experiments, and computer simulations. Experimental results show that this TDMA system has advantages over the conventional constant-rate TDMA systems, as resource sharing technique, in both bit error rate and total TDMA burst lengths required for transmitting given information.

INTRODUCTION

The Communication Research Laboratory (CRL) has been carrying out L-band mobile satellite communications experiments using the Engineering Test Satellite Five (ETS-V), which was launched in 1987. This study will be extended to advanced mobile and personal communications at Ka-band and millimeter wave frequencies using the Communications and Broadcasting Engineering Test Satellite (COMETS), which will be launched in 1997 [1]. Advantages to use such higher frequencies are much wider available frequency bandwidth and substantial system size reduction. On the other hand, we have to overcome such disadvantages as significant rain attenuation, larger Doppler shifts, higher RF component losses, larger phase jitters, etc.

At frequencies above 10 GHz, signal attenuation due to rainfall can have significant impairment on space-to-earth communication links. To compensate rain attenuation, several methods such as uplink power control[2][3], site diversity[4], and adaptive control of data rate and/or forward error correction techniques[5] have been proposed. Uplink power control and site diversity techniques are very useful for large or medium size earth stations at large networks covering different climatic regions. On the other hand, adaptive control of data rate and error correction techniques are more appropriate to small earth stations, since both small antenna size and limited RF transmit power impose a restriction over the range of the uplink power control. Moreover, these adaptive control techniques can compensate downlink attenuation as well as uplink attenuation.

In this paper, we propose a TDMA terminal with adaptive control capability of transmission rate to compensate rain attenuation. We carried out experiments using Japanese Communication Satellite-Three (CS-3) with Ka-band transponders to evaluate the performance of this terminal under rainfall conditions.

ADAPTIVE TRANSMISSION-RATE TDMA

In this Adaptive Transmission-Rate TDMA terminal, later referred to as ATR-TDMA, a receive terminal that is suffering rain attenuation requests the transmit terminal to reduce transmission rate of the TDMA burst, according to degradation in bit error rate (BER) or carrier-to-

noise density ratio (C/No). Six different transmission rates are available in this terminal. For example, a transmission rate reduction by a factor of four can compensate the degradation of 6 dB due to rain attenuation. Therefore, this system enhances the power margin by 15 dB.in all theoretically.

Figures 1 and 2 show a block diagram and a scheme of modulation and demodulation of the ATR-TDMA terminal, respectively. Data bit stream is stored in a buffer and divided into data bursts, the length of which corresponds to data bits within one TDMA frame. Data rate Rb is assigned as follows:

$$Rb = Rc\,/2^{N-2}$$
$$\text{for } N=1, 2, 3, 4, 5, \text{ and } 6 \quad (1)$$

where Rc is the reference clock rate of 4.144 Mbps in the present system, N=1 for QPSK, and N=2, 3, 4, 5, 6 for BPSK. Therefore, six possible data rates are 8288, 4144, 2072, 1036, 518, and 259 kbps.

After the baseband signal is scrambled with a pseudonoise (PN) code generated at Rc bps, a carrier is PSK modulated in burst mode. Since PSK modulator always works at the same clock rate of Rc, every TDMA bursts always occupy the same frequency bandwidth.

Receive terminal recovers clock rate from the received signal and then recovers data clock from burst timing. The present transmission rate can be known from information bits stored in the preamble of a TDMA burst. After coherently demodulated PSK signal is descrambled by the same PN code, 2^{N-2} bits are added with synchronous timing of clock rate and one information bit can be reproduced based on majority rule. This process of the synchronized sum is equivalent to reduce the transmission rate from Rc bps to $Rc/2^{N-2}$ bps. For example, a transmission rate reduction by a factor of two extends the burst length twice and BER performance can be improved by 3dB in C/No.

The TDMA frame format and data burst format are shown in Figure 3. One TDMA frame consists of a reference burst, a synchronization burst, data bursts, and initial acquisition slot. The frame period is 15 milliseconds and one control frame of 1200 millisecond period consists of 80 frames. Each data burst is divided into a preamble for receiver synchronization and data bits. This preamble consists of two parts of P1 and P2. In P1, carrier and clock recovery

patterns, and an unique word for identifying each terminal and synchronizing a burst timing are included. In P2, identification codes for transmit and receive terminals, and information bits for control of transmission rate are included. Since information bits in P1 are essential for all terminals in this TDMA network, this part is sent at the lowest transmission rate. On the other hand, since bits in P2 is necessary only for transmit and receive terminals under communication, transmission rate of P2 is the same as data rate of each TDMA burst. Moreover, using majority-rule decision of preamble information that is received over several frames, the TDMA terminal can reduce possibility of incorrect operations in the TDMA network. Transmission rates can be changed only once within one control frame.

RAIN ATTENUATION COMPENSATION EXPERIMENTS

Satellite Experiments

We carried out experiments using the CS-3 satellite to evaluate the performance of the ATR-TDMA terminal at Ka-band satellite link. Communication channels were monitored by measuring both BER and C/No with measuring equipments and a personal computer.

Since allowable BER without FEC is designed to be 10^{-3} in this system, we assigned BER of $8.0*10^{-4}$ or C/No that corresponds to BER of $8.0*10^{-4}$ as the threshold to change transmission rates. When BER or C/No is worse than the threshold for Td seconds, transmission rate is reduced half. When BER or C/No is better than the threshold for Tu seconds, transmission rate is increased twice.

Figure 4 shows the experimental result that was controlled from degradation in C/No with Td = 5 seconds and Tu = 5 seconds. Top of this figure shows rain attenuation of eighteen-hour measurement at satellite loop-back link (including both 20 GHz and 30 GHz attenuation) and 20GHz-beacon. Controlled transmission rates in kbps and measured BER are shown in middle and bottom of Figure 4, respectively. According to rain attenuation, the ATR-TDMA terminal controlled its transmission rate to keep BER better than the allowable BER with as high transmission rates as possible. This terminal can compensate rain attenuation actually up to about 15 dB (although theoretically 16dB). When

rain attenuation is larger than 15 dB or rain rate becomes faster than response time of this system, BER becomes larger than the allowable value. However, such unavailable time duration is improved and becomes considerably short.

With the lowest transmission rate at constant-rate TDMA terminals, we could keep BER better than the threshold like the ATR-TDMA terminal. However, total TDMA burst lengths required for transmitting the same information will become much larger than ATR-TDMA. Next, we study BER and total burst lengths of ATR-TDMA as a function of different Td and Tu values.

In-house Experiments

Values of parameters Td and Tu are very important for effective control of transmission rate. In the TDMA network, time duration in one TDMA frame is a common resource for every terminals. When many user terminals suffer rain attenuation, several terminals will wait to access until a vacant time slot appear and some terminals will break down due to the degradation of communication links.

In in-house experiments, the receive terminal connects with the transmit terminal through IF port and monitors BER to detect degradation in communication link. C/No is degraded by additive white Gaussian noise according to rain attenuation data that were measured and stored using satellite links. Using several values of Tu and Td, BER and total burst lengths are measured and shown in Figure 5. As Tu becomes larger, BER becomes smaller, but TDMA burst lengths, with respect to the burst length of the fastest rate, become considerably large. Both improvement in BER and increase of burst lengths is more remarkable as Td becomes smaller.

Figure 6 shows comparison of this experimental result with the result obtained by the constant-rate TDMA terminal. The lower transmission rates of N=4 and 5 can provide very good BER performance but the TDMA burst of this terminal will occupy a large part in one TDMA frame. The number of user terminals than can access this TDMA network is very restricted. The ATR-TDMA terminal has better performance in both BER and burst lengths than the conventional constant-rate TDMA.

Computer Simulation

To study the effect in BER and burst lengths under different rain conditions and different Tu, and Td, we have carried out computer simulation of the ATR-TDMA system. C/No is controlled with measured data of rain attenuation and BER is calculated from the measured BER performance of the TDMA terminal. Table 1 shows typical values of Tu and Td, which correspond to different traffic conditions in a satellite transponder. In situation of mode #3, since only a few vacant time slots remain in one TDMA fame due to high traffic condition, transmission rate cannot be reduced quickly and has to be brought back to its rate as soon as possible after the weather improves. On the other hand, mode #4 prefers to maintain the communication quality rather than to shorten used burst lengths.

Figure 7 and 8 show the probability that BER is worse than the threshold as a function of used total burst lengths using rain attenuation measured for twenty rainy days. In Figure 8, data, which are picked up from severe rain events, are normalized with the result of mode #4.

Slow reduction of transmission rates in modes #2 and #3 increases the probability that BER is worse than the threshold up to about 20% in severe rain events as shown in Figure 7. Simulation results, however, shows that ATR-TDMA is effective to compensate rain attenuation under many different rain conditions.

Figure 8 shows that values of Tu is insensitive to the probability that BER is worse than the threshold and total burst lengths decrease as Td becomes smaller. Parameter Td is more important than Tu to improve BER performance under rain attenuation.

Since the response time should be less than rain attenuation rate for successful control of transmission rate, the optimum value of Td must be as small value as possible. However, one-way propagation delay for a geostationary satellite link is on the order of 0.25 seconds, and a similar amount of time is required for receive terminals to request reduction of transmission rates to their transmit terminals. Moreover, It will take a couple of seconds for receive terminals to measure BER or C/No for measuring rain attenuation, and there are also additional system processing delays including delay due to control algorithm. Therefore, control delay of transmission rates from instantaneous rain attenuation is inevitable. In spite of such delay factors, ex-

507

perimental results showed that Td of 3 to 5 seconds are effective to compensate rain attenuation.

CONCLUSION

Adaptive transmission-rate TDMA system to compensate rain attenuation is presented. At the beginning, this system was developed for business networks consisting of different size earth stations at Ka-band frequency Therefore, transmission rates available in this system may be too fast for applications of mobile and personal satellite communications. However, the same adaptive control scheme can be applied to these systems at lower transmission rates.

To evaluate the performance, we carried out three kinds of experiments: satellite experiments, in-house experiments, and computer simulations. The ATR-TDMA system showed advantages over the the conventional constant-rate TDMA system to maintain both communication quality and capacity under rainy weather.

When we apply adaptive control of data rate to SCPC systems, the reduction of data rate will result also in a reduction of service quality. However, this TDMA scheme reduce transmission rate in RF, but does not reduce data rate at baseband. Thus service quality is not reduced except very severe rain and heavy traffic conditions. This adaptive control method is suitable to future mobile or personal satellite communication systems at higher frequencies such as Ka-band or millimeter wave for compensating rain attenuation.

REFERENCE

[1] S. Ohmori, et al. "Advanced Mobile Satellite Communication using COMETS Satellite in MM-wave and Ka-Band," *Proc. IMSC'93*, Pasadena, California, June 16-18, 1993.
[2] I. Nishiyama, R. Miura, and H. Wakana, "Closed-loop Uplink Power Control Experiments in K-band using CS-2," *Proc. ISTS*, Tokyo, Japan, 1986.
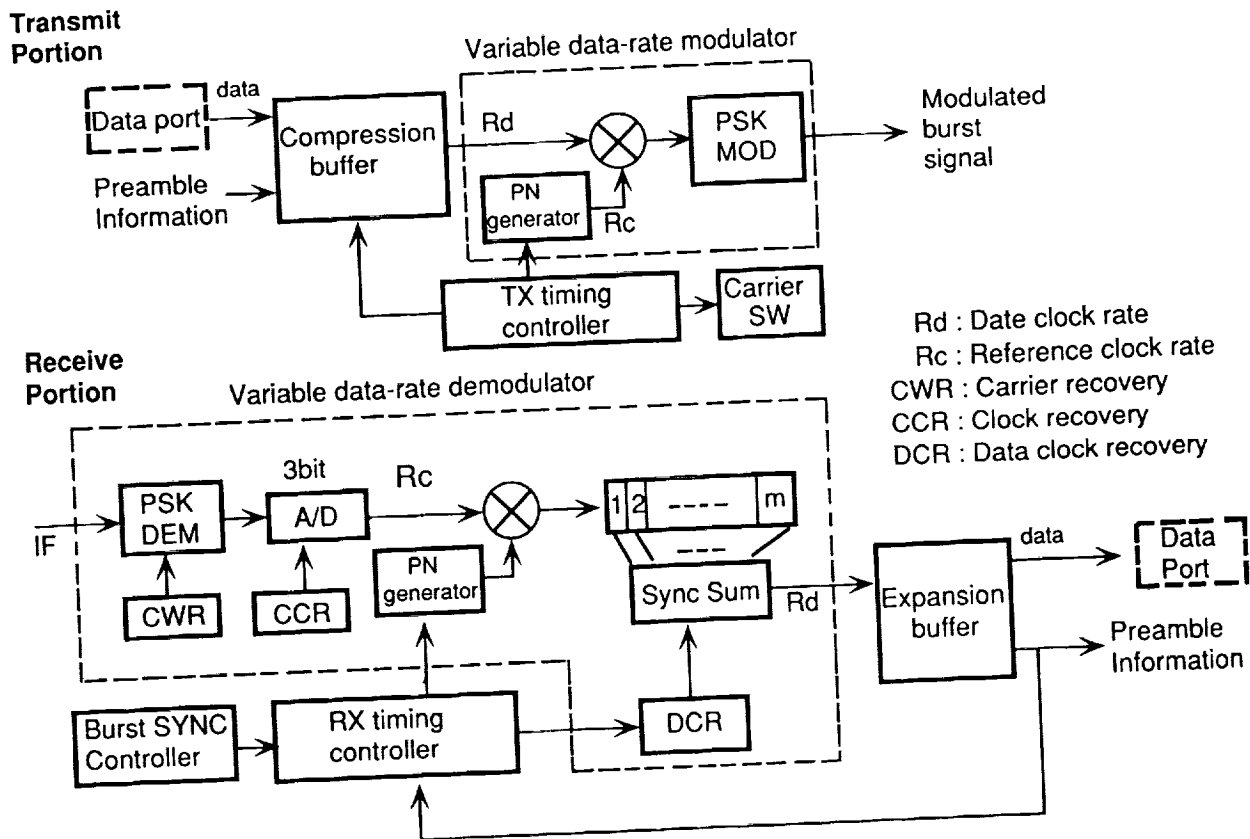
Figure 1. Block diagram of ATR-TDMA system
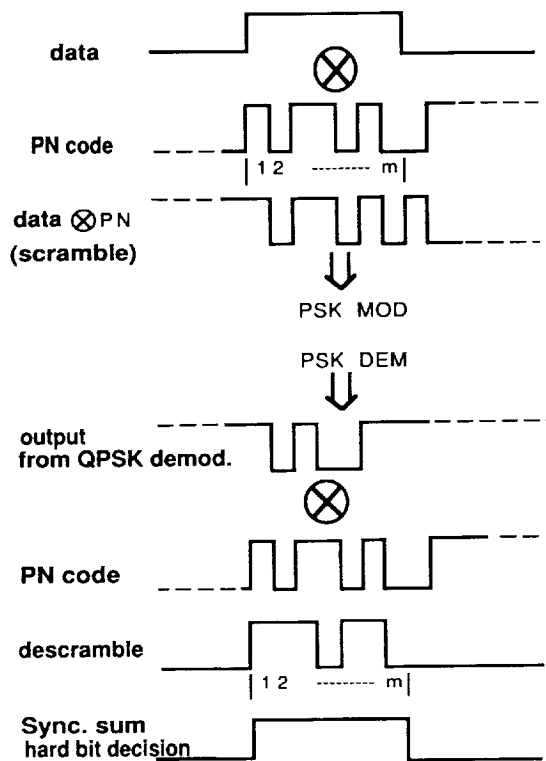
Figure 2. Scheme of ATR-TDMA

R : reference burst
A : initial acquisition slot
UW : unique word
TC : transmission-rate control bits
P1 : Preamble (all stations need to receive)
P2 : Preamble (transmit and receive stations receive)

S : synchronization burst
Dn (n=1, 2, ...) : data burst
CBTR : carrier and burst timing recovery
TX/RX ID : transmit/reseive station ID
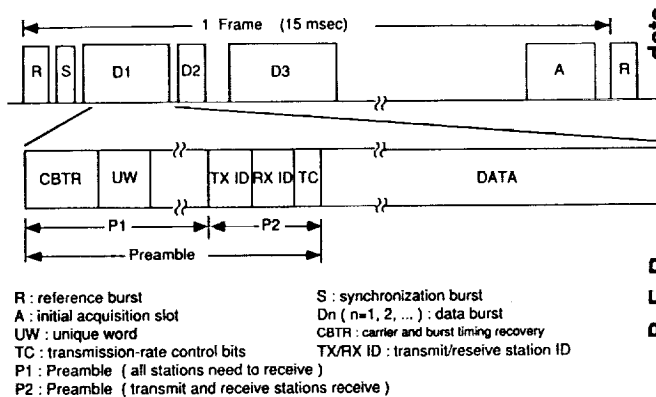
Figure 3 TDMA frame format

[3] V. O. Hentinen, "Error Performance for Adaptive Transmission on Fading Control," *IEEE Trans. Commun.*, vol. COM-22, pp. 1331-1337, 1974.

[4] CCIR Rep. 564-4, "Propagation Data and Prediction Methods required for Earth-Space Telecommunication Systems," *Recommendations and Reports of the CCIR*, vol. 5, ITU, Geneva, 1991.

[5] J. Hagenauer, "Rate Compatible Punctured Convolutional Code," *Proc. ICC'87*, pp.29.1.1-29.1.5, Seatle, USA, 1987.
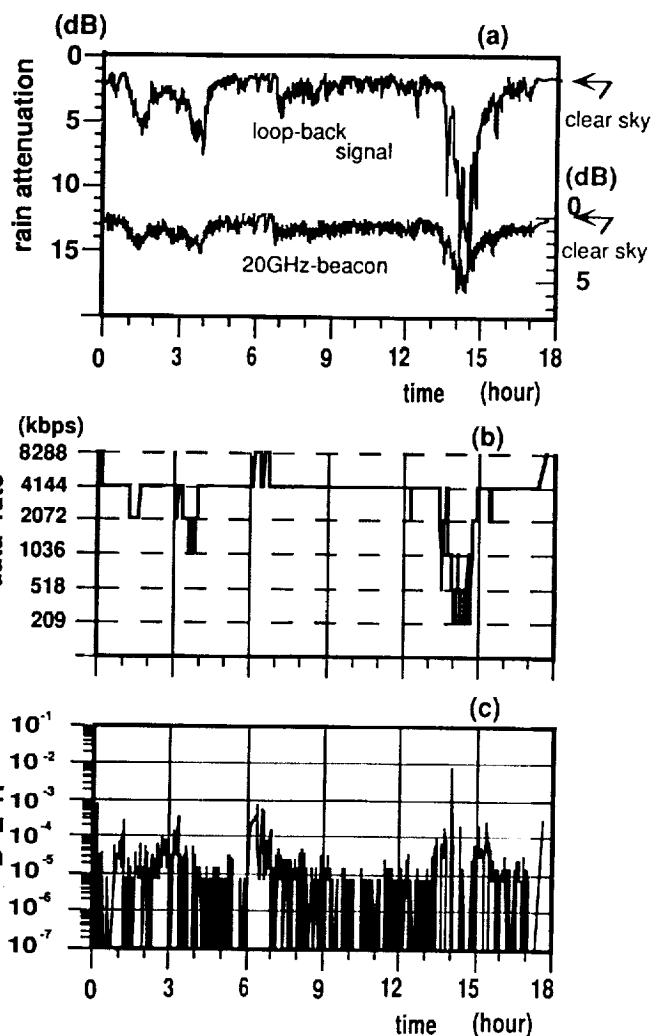
Figure 4. Experimental results using the CS-3 satellite (a) rain attenuation (b) transmission rate (c) BER
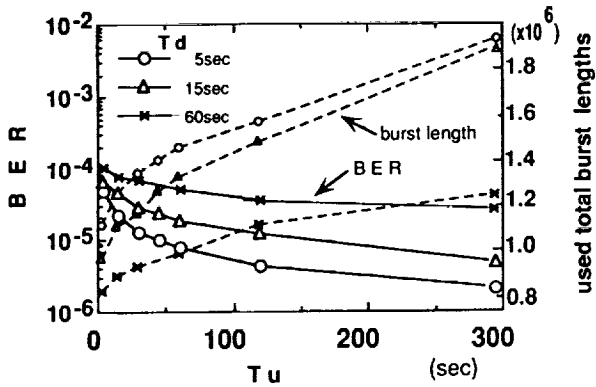
Figure 5 BER and used burst lengths as
a function of Tu and Td

Table 1. Four control modes using
different Td and Tu

Control modes	Td in sec.	Tu in sec.	Symbols
mode #1	3	3	●
mode #2	83	103	*
mode #3	83	3	△
mode #4	3	103	○
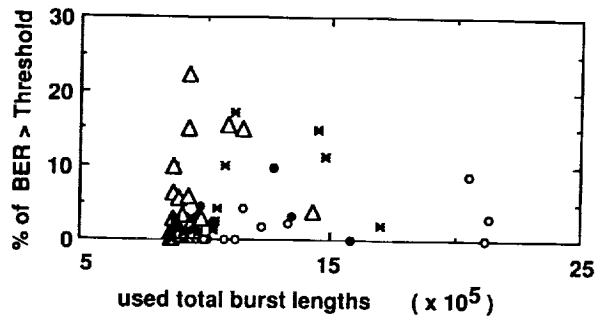
Figure 7. BER > threshold versus burst lengths

Figure 6. Comparison with constant-rate TDMA
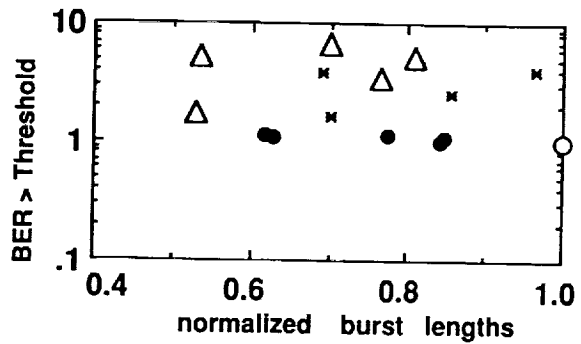
Figure 8. BER > threshold versus burst lengths
normalized with the result of mode #4

510

SATCOM Simulator Speeds MSS Deployment and Lowers Costs

Tim Carey, Roland Hassun, Dave Koberstein
Hewlett-Packard Company
1501 Page Mill Road
Palo Alto, Ca. USA
(415) 857-1501

ABSTRACT: Mobile satellite systems (MSS) are being proposed and licensed at an accellerating rate. How can the design, manufacture and performance of these systems be optimized at costs that allow a reasonable return on investment?

The answer is the use of system simulation techniques beginning early in the system design and continuing through integration, pre and post-launch and in-orbit monitoring. This paper focuses on using commercially available, validated simulation instruments to deliver accurate, repeatable and cost effective measurements throughout the life of a typical mobile satellite system.

A satellite communications test set is discussed that provides complete parametric test capability with a significant improvement in measurement speed for manufacturing, integration, pre-launch and in-orbit testing. The test set can simulate actual up and down link traffic conditions to evaluate the effects of system impairments, propagation and multipath on bit error rate (BER), channel capacity and transponder and system load balancing. Using a standard set of commercial instruments to deliver accurate, verifiable measurements anywhere in the world speeds deployment, generates measurement confidence and lowers total system cost.

THE BASIC QUESTIONS.

A mobile satellite system (MSS) consists of satellites, gateways which link the system to other fixed services, command and control earth stations, and mobile users as shown in Figure 1. Each of these elements is extensively computer modeled and simulated during system proposal and design. However, as the implementation of the system progresses through integration, launch and deployment, simulation techniques are less commonly used. Many time consuming measurements on components, sub-systems and communications links replace these simulations, often with a loss of accuracy. The basic questions to be answered remain: what level of operability exists within the system, how has performance changed over time and what is the optimal allocation of system capacity that will maximize the number of users and revenues?

To answer these questions satellite systems undergo extensive parametric testing at integration, prior to launch, after insertion into orbit and throughout operational life. The number of tests, their duration and the need to repeat them at several stages makes deployment a time consuming and costly process. Table 1 illustrates the redundancy of testing in present systems. Two alternatives are to reduce the time per test and to replace some of the testing with simulations. The satcomm test set discussed here achieves both of these improvements in a single set of test instrumentation.

Table 1. Typical Satellite System Test Matrix

	Integration	Pre-launch	DT	E/S
Effective Isotropic Radiated Power (EIRP)				
Beacon EIRP	X	X	X	X
Carrier EIRP	X	X	X	X
Modulated EIRP	X	X	X	X
EIRP Stability	X	X	X	X
Saturation Flux Density	X	X	X	
Freq Response				
Gain & Gain Flatness				
Small Signal	X	X	X	X
Saturated	X	X	X	X
Group Delay	X		X	
NPR	X		X	
Channelization	X	X	X	X
G/T	X	X	X	X
Antenna Patterns	X		X	X
Cross Polarization Isolation	X		X	X
Sidelobe Patterns	X		X	X
Telemetry Command Sens & AGC	X	X	X	
Transponder Transfer Characteristics	X	X	X	
Beacon Mod Index	X	X	X	X
Frequency Stability	X	X	X	X
E/S Receiver Sens & Characteristics				X

THE "SMART STIMULUS" CONCEPT

Traditional parametric test techniques employ relatively simple signal generators as test stimuli. These generators allow control of frequency, carrier amplitude and basic modulations. The response of the device under test is analyzed by instruments that measure power or frequency, analyze or demodulate signals to determine modulation parameters, and count data errors to evaluate transmission quality. As communications signals have increased in complexity,

the measurement instrumentation also has become more complex. Simple measurements may not completely characterize the effect the parameter under test has on system performance and comprehensive measurements are often tedious and slow.

When a satellite is placed in orbit the test environment becomes more complex. Measurement complexity is compounded by the time delay proportional to the range of the satellite from the earth station, variations in delay due to positional drift or orbit, doppler effects due to the satellite's velocity, transponder frequency translation and any reformatting of data packets in the satellite.

Many of these problems can be overcome and the measurement instrumentation simplified by using what has been termed a "smart stimulus" as a test signal source. Such a stimulus can be tailored to overcome many practical difficulties that arise in the course of making a measurement. These include the effects of frequency translation and time delays in the DUT, removal of test path amplitude and phase errors, etc. Errors caused by a time varying measurement environment can also be minimized.

The Hewlett-Packard HP 8791A Frequency Agile Signal Simulator (HP-FASS) combines direct digital synthesis technology with digital signal processing and fast transform techniques. HP-FASS is an ideal "smart stimulus" for satellite communications testing. Utilizing high clock rates, proprietary digital to analog conversion technology and a unique Waveform Generation Language, this software reconfigurable generator can modify its output signals in real time with digital precision, accuracy and repeatability. For example, HP-FASS can change its output signal to offset the effects of doppler caused by a rapidly moving low earth orbit (LEO) satellite. HP-FASS can reduce test times in repetitive measurements like gain and group delay by recalling stored sequences of frequency, amplitude and modulation and generating corrections on the fly as needed. Compared to traditional signal sources HP-FASS reduces measurement times, generates higher precision signals and measurement results, and allows the use of a simpler, lower cost test system with fewer interconnects and less complex signal routing.

Figure 2 is a block diagram of a satellite communications test set based upon the HP-FASS. This test set performs the parametric tests listed below the figure. A switching matrix is not shown since its complexity depends on the number of interconnects to the DUT. However, the use of a single HP-FASS as the stimulus and a minimum amount of measurement instrumentation greatly simplifies the signal routing.

PARAMETRIC TESTING

As discussed above many parametric tests are performed on satellites and earth stations to quantify their performance. The HP-FASS based test set significantly reduces test times for many of these tests. In addition, test accuracy and repeatability are equal or better than traditional techniques. For example, a multi-tone amplifier intermodulation test was used to establish a benchmark for comparing measurement speed. A 10 tone measurement was performed at 10 power levels on all 22 channels of each transponder.

Traditional techniques use multiple signal generators as a test stimulus. Since the intermodulation distortion is directly proportional to the peak amplitude of the input signal, the phase relationship between the various input tones is critical. Conventional signal generators do not allow control of the phase of the individual tones. This slows the measurement because the worst case phase relationship occurs only rarely as the signal sources drift in phase. The FASS-based test set performs multi-tone measurements significantly faster than traditional techniques. In the benchmark example the HP-FASS based test set completed the measurement in one-third the time of a conventional test system. HP-FASS provides complete control of both the amplitude and the phase of each individual tone. Tones may be continuous wave (CW) carriers or may have modulation imposed upon them for signal simulation.

Another type of intermodulation test is the Noise Power Ratio (NPR) test. Traditionally this test uses wideband noise sources, amplifiers, filters and attenuators to generate a white noise spectra that has a narrowband notch at the frequency of interest. While conceptually simple, in practice this test system has difficulty producing accurate results repeatably. Many hours of calibration and tuning are involved in NPR measurements on the high power amplifiers in a typical transponder. The HP-FASS test set generates a pseudo-noise spectra with a precisely controlled notch. Dynamic ranges greater than 60 dB are achieved. The HP-FASS makes this measurement fast, easy, accurate and very repeatable. Figure 3 shows the output spectra from an HP-FASS generating a NPR test signal.

Group delay is a parametric test that is performed to quantify transponder performance and as a health check during routine monitoring. Traditionally a vector network analyzer is used for benchtop component and sub-system tests that do not involve frequency translation, while a communications link

analyzer is used for transponder tests and in-orbit testing. Other techniques which require reference signals from the test stimulus eliminate their use forin-orbit measurements.

A single test set built around a HP-FASS can be used for all the group delay measurements from component level through spacecraft integration to in-orbit testing. The basic technique is similiar to that used with the communications link analyzer but is much faster. Since the HP-FASS has the advantage of digital precision in its output signals as well as 250 nano-second frequency agility, a fast frequency chirp is used to sweep a carrier across the device under test. AM or FM modulation is applied to the carrier and the modulation is recovered at the output of the DUT. AM is used for devices not in amplitude saturation while FM is used for saturated devices. The measurement technique is modified only slightly for in-orbit tests. Here where changes in range contribute errors (adding tilt to the group delay plot) and doppler shift complicates the measurement, periodicly returning to a reference frequency provides the information necessary to eliminate these errors. The digital precision and agility of the smart stimulus makes this measurement fast, easy to perform and very accurate.

Table 2 lists expected measurement times and accuracies for the HP-FASS test set when performing several typical satellite system parametric tests.

Table 2. HP-FASS Test Set Performance

Measurement	Time	Uncertainty
Gain (1 point)	2 sec	+/- 0.3 dB
Gain (500 points)	9 sec	+/- 0.3 dB
Group Delay	20 sec	+/- 1.5 nsec
AM/PM Conversion	20 sec	+/- 1 degree
Phase vs Amplitude (20 dB range)	20 sec	+/- 1 degree
Phase Noise (5Hz-100kHz)	180 sec	+/- 1.5 dB
Intermod Dist (NPR)	60 sec setup 180 sec/ten levels	+/- 0.3 dB
Spurious Search	30 sec/ 1 transp BW	+/- 2 dB
G/T	30 sec	TBD
EIRP (10 tones)	30 sec	+/- 0.5 dB
Multichannel Characterization	200 sec	+/- 0.2 dB flatness +/- 0.2 dB gain

SIGNAL and ENVIRONMENT SIMULATION

Payload designers, system planners and earth station developers need to know how the satellite system will perform with realistic traffic loading prior to launching the system into space. Once the MSS is placed in service, system operators and planners must monitor performance to optimize efficiency and minimize degradations to users. A satellite simulator based upon the HP-FASS provides fast, repeatable and cost effective evaluation and validation of systems under realistic conditions. Simulated up and down link signals can be used to evaluate payload designs, validate earth station design and optimize system monitoring.

Payload Design and Evaluation

Signal simulation is a powerful method to improve the performance and speed the development of payloads. First the design is simulated with one of the many communications simulation software packages available. Next the hardware is evaluated using test signals identical to those used in the computer simulations.

Bit error rate testing (BERT) of payloads, intermodulation testing of amplifiers and transponders, evaluation of tracking, telemetry and control (TT&C) links and payload integration and performance verification is greatly enhanced using realistic modulated signals.

Earth Station Design and Validation

Verifying that the design of earth stations meets system specifications can be a difficult and lengthy task. The HP-FASS was used to validate the design of an earth station monitoring system. Figure 4 illustrates one of the signals used in this design validation. Each channel in this multi-channel signal can have its data, data rate, modulation type, channel filter mask and amplitude individually described to replicate actual traffic loading. Having the same test signal available at all earth stations ensures consistent and precise earth station evaluation and trouble shooting.

System Monitoring

Simulated up and down link signals also can be used to determine channel capacity, to load balance transponders and to plan and evaluate system performance once a system is placed in service. Accurate evaluation of bit error rate and signal to noise ratio for different transponders and antenna beam coverages requires realistic signals. A source of precisely repeatable signals maximizes the accuracy of periodic comparisons of link performance. Accurate evaluation of link margins is critical to optimizing the utility and profitability of the system.

SYSTEM IMPAIRMENTS and PROPAGATION EFFECTS

The HP-FASS not only provides precision "ideal" signals, it can also distort them to model the effects of system impairments and propagation. Simulating these effects allows evaluation of system operating margins in a controlled environment. Transponder and earth station imperfections including transmitter and receiver gain and quadrature errors, amplitude compression, noise and end of life performance degradation can be effectively simulated. Figure 5 demonstrates two HP-FASS generated 32 QAM signals. The first has zero I/Q quadrature error, while the second has precisely 5 degrees of quadrature error.

HP-FASS can simulate doppler effects more precisely than simple signal generators. A moving platform imparts a frequency shift to the modulation components in addition to that imparted to the carrier. Simple generators usually are limited to simulating doppler shift on the carrier only.

Propagation effects can be simulated including rain attenuation and fading. Multipath simulations can be performed aross the entire 40 MHz modulation bandwidth of the HP-FASS. This allows complete multipath evaluation of an entire transponder with one simulation.

CONCLUSION

A satellite communications test set has been described that provides parametric test capability and realistic up/down link traffic simulations. Impairments and propagation effects can also be added for complete system evaluation and margin analysis. The test set uses commercially available instrumentation at the heart of which is the HP 8971A FASS "smart stimulus". The test set is easy to use and delivers faster, more repeatable and higher precision test results compared to conventional systems. The same test set can be used in all test situations from component manufacture through satellite integration to in-orbit test. The ease of generating realistic signal and environment simulations should lead to wider use of these techniques in place of some parametric tests. The use of simulations should improve the characterization of the total satellite system and lead to faster, more economical system deployment.
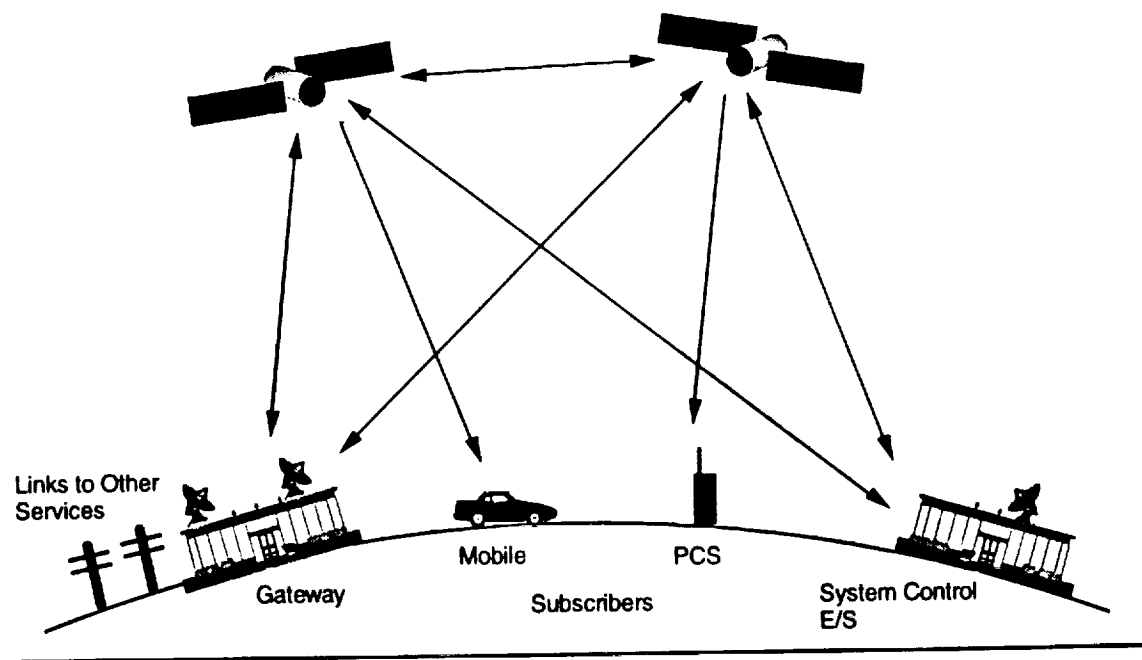
Figure 1. Elements of a typical Mobile Satellite System
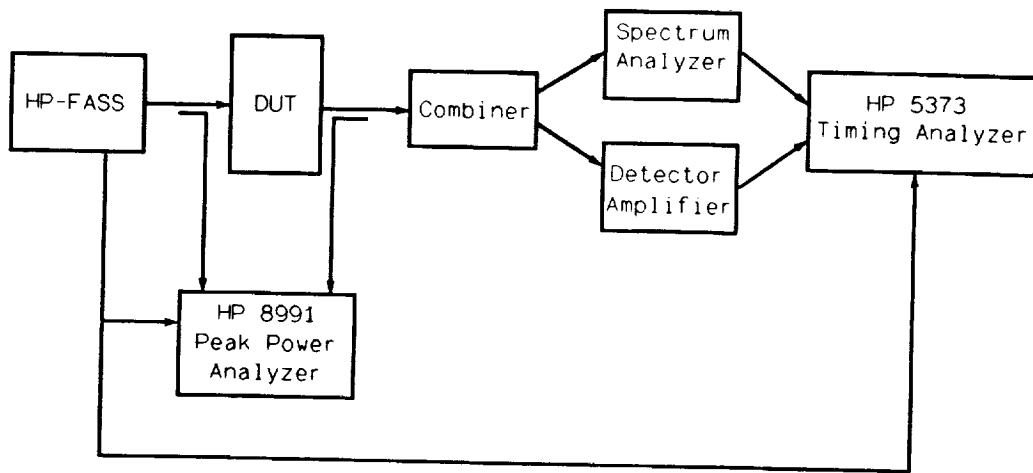
Gain   Intermod distortion   AM/PM Conversion

Gain Flatness   Spurious   Phase vs Amplitude

Gain Steps   Channel Characterization   Offset Freq Stability

                         Group Delay   Phase Noise

Figure 2. Block diagram of satellite communications test set based upon HP-FASS as a "smart stimulus".
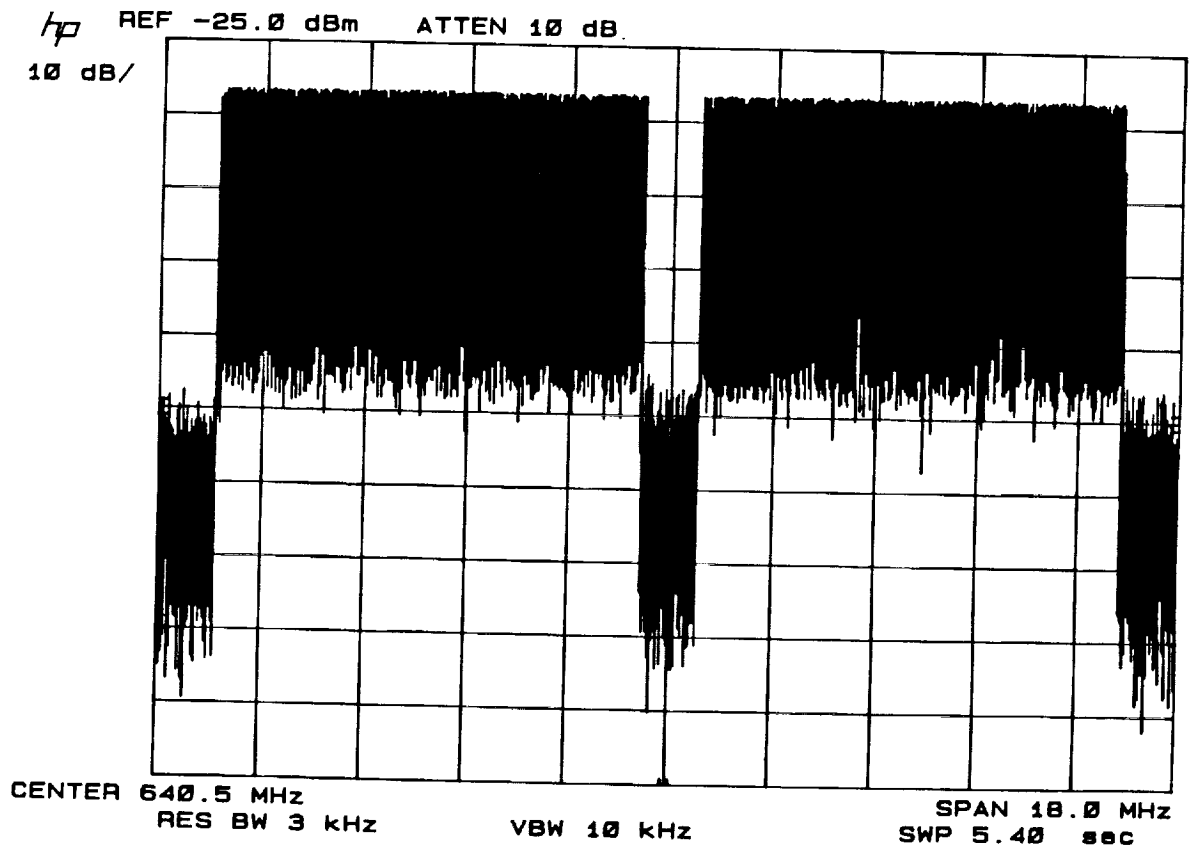
Figure 3. Noise Power Ratio measurement spectra from HP-FASS.
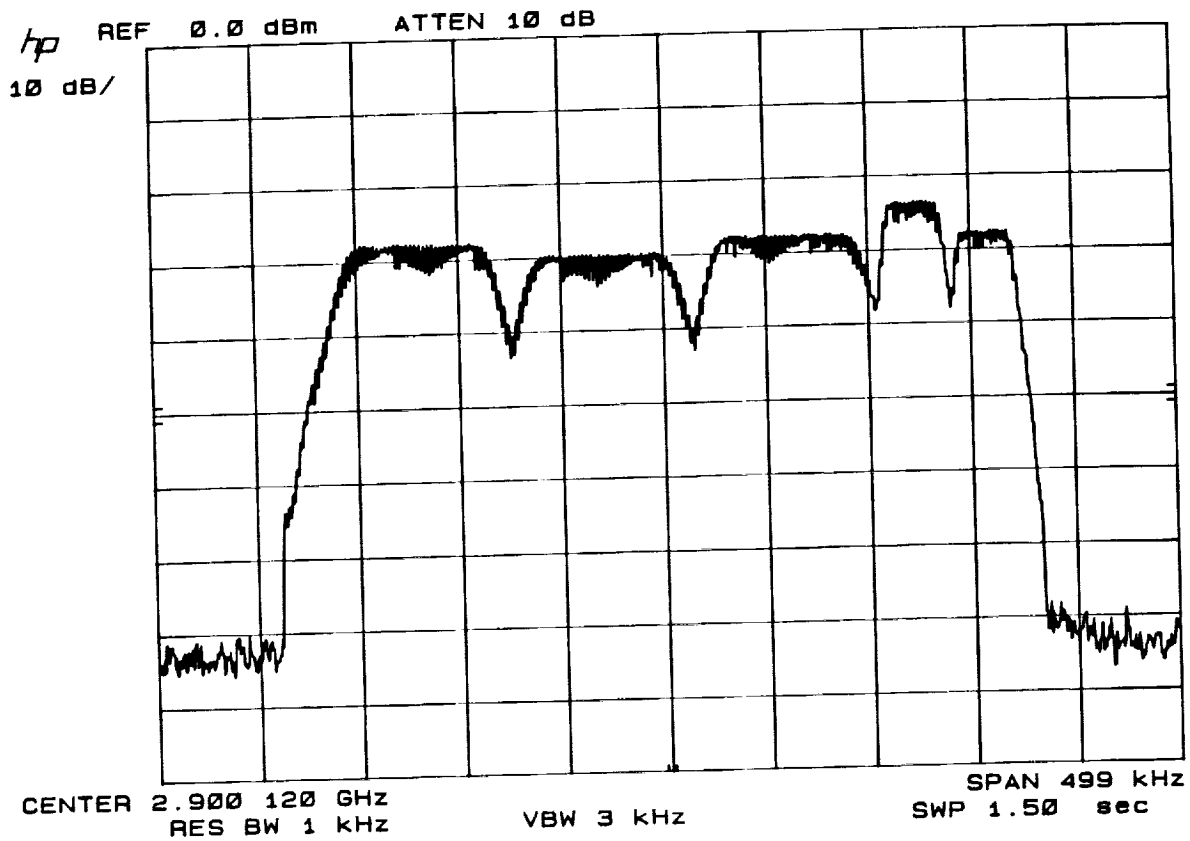
Figure 4. Multi-channel signal from HP-FASS simulating five channels with various amplitudes and data rates filtered per Intelsat masks. All channels are QPSK modulated.
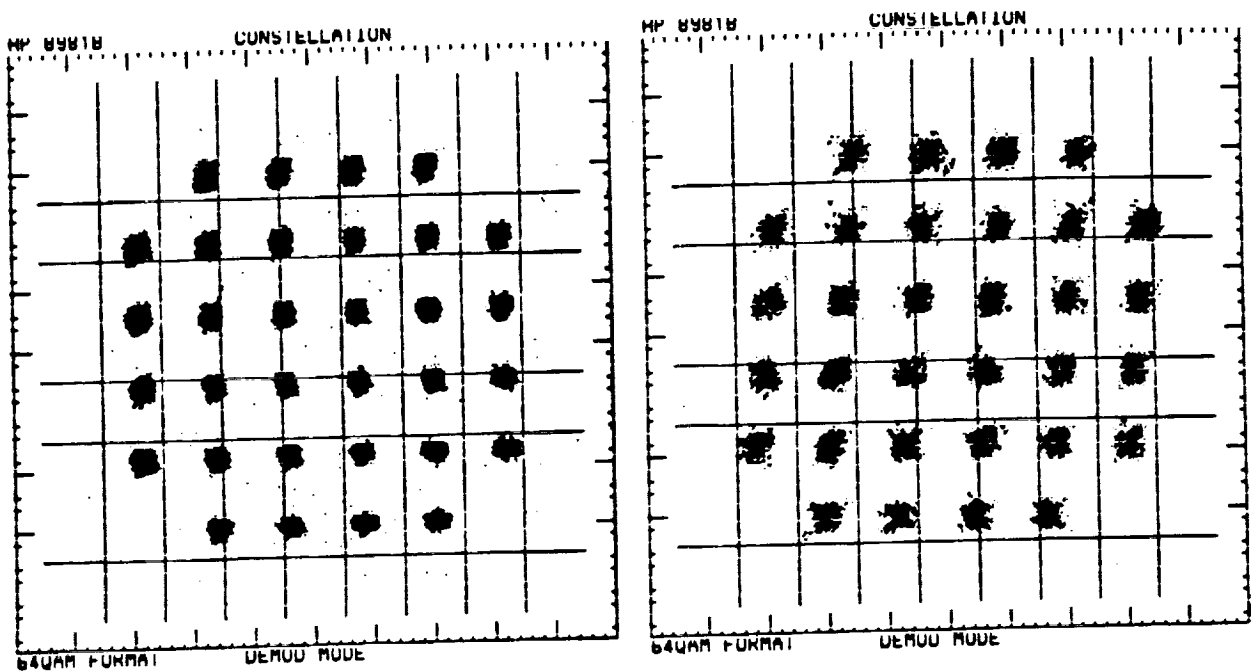
Figure 5. 32 QAM constellations generated by HP-FASS. Zero I/Q quadrature error on the left and 5 degrees quadrature error on the right.

Development of a Multilayer Interference Simulation Program for MSS Systems

Jamal S. Izadian

Loral Qualcomm Satellite Services
3825 Fabian Way MS/G54
Palo Alto, CA 94303-4604
U.S.A
Phone(415)852-5512
Fax(415)852-4148

ABSTRACT

This paper discusses the development of a multilayer interference analysis and simulation program which is used to evaluate interference between non-geostationary and geostationary satellites. In addition to evaluating interference, this program can be used in the development of sharing criteria and coordination among various Mobile Satellite Services(MSS)systems. A C++/Windows implementation of this program, called Globalstar Interference Simulation Program (GISP), has been developed and will be demonstrated in the conference.

INTRODUCTION

Since the relative position and pointing of the Geo-Stationary Orbit(GSO) and Low Earth Orbit(LEO) satellites constantly change, the parameters affecting interference also change with time and satellite positioning. With these changing parameters, the interference situation cannot be evaluated fully using conventional techniques of interference analysis. To gain better understanding of the interference situation and to develop sharing criteria, this multilayer interference analysis and simulation program was developed.

In order to help visualize the complex interference environment of MSS systems, we use the analogy of utilization of a single spectrum analyzer to view the interference signals. This spectrum analyzer can be connected to a terminal of either a victim satellite or a victim user antenna.

INTERFERENCE TO A SATELLITE

The total interference signal received by a victim satellite antenna terminal measured by the fictitious spectrum analyzer can be represented by the following summations.

$$P_{i,k}(t,f) = \sum_{j=1}^{N_s(t)} \sum_{p=1}^{N_{b_j}}$$

$$\frac{G_{i,k}(\theta_{ij}(t),\varphi_{ij}(t))G_{j,p}(\theta_{ji}(t),\varphi_{ji}(t))P_{oj,p}}{L_{i,j}(t)}$$

$$+ \sum_{j=1}^{N_u(t)} \frac{G_j(\theta_{ji}(t),\varphi_{ji}(t))G_{i,k}(\theta_{ij}(t),\varphi_{ij}(t))P_{oj}}{L_{i,j}(t)}$$

Where

- $P_{i,k}(t,f)$ is the total power spectral density at the terminal of kth antenna beam of victim satellite i, at time t and frequency f. It is measured in dBW/Hz.

- $N_s(t)$ is the number of interfering satellites visible to victim satellite i at time t.

- N_{b_j} is the number of multiple beams of interfering satellite j.

- $G_{i,k}(\theta_{ij}(t),\varphi_{ij}(t))$ is the gain of the kth antenna beam of victim satellite i at the angle $\theta_{ij}(t)$ and $\varphi_{ij}(t)$, and $\theta_{ij}(t)$ and $\varphi_{ij}(t)$ are the corresponding victim satellite i's local spherical coordinate angles towards interfering satellite j at the time instant t.

- $G_{j,p}(\theta_{ji}(t),\varphi_{ji}(t))$ is the gain of the pth antenna beam of interfering satellite j at the angle $\theta_{ji}(t)$ and $\varphi_{ji}(t)$, and $\theta_{ji}(t)$ and $\varphi_{ji}(t)$ are the corresponding interfering satellite j's local spherical coordinate angles towards victim satellite i at the time instant t.

- Po_{jp} is the power spectral density into the terminal of the pth antenna beam of interfering satellite j.

- $L_{i,j}(t)$ is the path loss between victim satellite i and interfering satellite j at time t.

In the second summation,

- $N_u(t)$ is the number of interfering mobile user units visible to victim satellite i at time t.

- $G_{i,k}(\theta_{ij}(t),\varphi_{ij}(t))$ is the gain of the kth antenna beam of victim satellite i at the angle $\theta_{ij}(t)$ and $\varphi_{ij}(t)$, and $\theta_{ij}(t)$ and $\varphi_{ij}(t)$ are the corresponding victim satellite i's local spherical coordinate angles towards interfering user unit j at the time instant t.

- $G_j(\theta_{ji}(t),\varphi_{ji}(t))$ is the gain of the antenna beam of interfering mobile user j at the angle $\theta_{ji}(t)$ and $\varphi_{ji}(t)$, and $\theta_{ji}(t)$ and $\varphi_{ji}(t)$ are the corresponding interfering user j's local spherical coordinate angles towards victim satellite i at the time instant t.

- Po_j is the power spectral density into the terminal of the antenna beam of interfering mobil unit j.

- $L_{i,j}(t)$ is the path loss between victim satellite i and interfering mobile user unit j at time t.

In the above formula, the first summation corresponds to the interference from all other satellites, whereas the second summation corresponds to interference from all ground based mobile user units.

518

INTERFERENCE TO A MOBILE UNIT

There are essentially two types of interference to a mobile user unit; the interference from all satellites who transmit in the same band as the user receiver, and other mobile users. This program currently simulates the first kind and the future plans include the implementation of second kind. To measure the total satellite interference to a mobile user unit, the fictitious spectrum analyzer is connected to terminal of antenna of the victim mobile user unit. The interference that the spectrum analyzer measures can be represented by the following formula.

$$P_j(t,f) = \sum_{i=1}^{N_s(t)} \sum_{k=1}^{N_{b_i}}$$

$$\frac{G_{i,k}(\theta_{ij}(t),\varphi_{ij}(t))G_j(\theta_{ji}(t),\varphi_{ji}(t))Po_{i,k}}{L_{i,j}(t)}$$

Where

- $P_j(t,f)$ is the total power spectral density at the terminal of antenna of victim user j at time t and frequency f. It is measured in dBW/Hz.

- $N_s(t)$ is the number of interfering satellites visible to victim mobile user unit j at time t.

- N_{b_i} is the number of multiple beams of interfering satellite i.

- $G_{i,k}(\theta_{ij}(t),\varphi_{ij}(t))$ is the gain of the kth antenna beam of interfering satellite i at the angle $\theta_{ij}(t)$ and $\varphi_{ij}(t)$, and $\theta_{ij}(t)$ and

$\varphi_{ij}(t)$ are the corresponding interfering satellites i's local spherical coordinate angles towards victim mobile user j at the time instant t.

- $G_j(\theta_{ji}(t),\varphi_{ji}(t))$ is the gain of antenna beam of victim mobile user j at the angle $\theta_{ji}(t)$ and $\varphi_{ji}(t)$, and $\theta_{ji}(t)$ and $\varphi_{ji}(t)$ are the corresponding victim mobile user j's local spherical coordinate angles towards interfering satellite i at the time instant t.

- $Po_{i,k}$ is the power spectral density into the terminal of the kth antenna beam of interfering satellite i.

- $L_{i,j}(t)$ is the path loss between victim user unit j and interfering satellite i at time t.

MULTILAYER MODELING OF INTERFERENCE

A systematic approach to partition the complex interference situation among multiple MSS satellite systems (both GSO and non-GSO) is to develop a multilayer interference model such that a computer analysis and simulation program can be developed around each layer. The formulas just presented are at the heart of GISP. In the following sections, major layers of the program are discussed.

GEOMETRIC LAYER

Since the relative position and pointing of GSO and LEO satellites constantly change, it is necessary to develop some

519

common reference systems for all satellite systems such that all satellites and user terminals can have a specific coordinate with respect to the same reference point. In this layer, the center of the earth has been identified as the center of this reference system as shown in Figure 1. Each interference source (i.e., a transmitter) and victim (i.e., a receiver) is identified by its own coordinate with respect to the center of the earth. The z-axis of the local coordinate system of a satellite or a user positioned at any point is defined as the vector from this particular point to the center of the earth. The y axis is defined in the negative direction of the normal to the plane of the orbit. A right hand coordinate system dictates that the x axis be in the plane of the satellite velocity .

The main purpose of this geometric layer is to determine whether an interference source is visible by the victim or otherwise shadowed by earth. Further processing is carried out to determine the level of interference if and only if the victim is in the line of sight of the interferer. Scattering reflection and refraction effects are considered secondary effects and are not included in the program at this stage. Major parameters to be input into this geometric layer include:satellite altitude, inclination angle, orbit phasing, orbit location or sub-satellite point (for GSO), orbit eccentricity, apogee and perigee, and others.

The computer program simulates orbits and constellations of different GSO or LEO systems, calculates the relative positions of each point (either an interference source or victim) and determines whether two points (i.e.

source and victim) are in line-of-sight or are blocked by the earth at any time of the simulation period.

ANTENNA LAYER

Once the line-of-sight between the interferer and the victim is established, the interaction between the source antenna and the victim antenna has to be modeled. Figure 2 illustrates the interaction among a single interference source and multiple victims. At this point, the local coordinate system of the satellite or user is defined and the pattern angle s θ and φ are calculated relative to these local coordinate systems. These angles are then used to determine the antenna gain levels of interferer toward the victim and the antenna gain of victim toward the interfering source. The relative distance and spatial loss between the source and victim is calculated by the geometric layer processor of the program. Thus the relative gain between the source and victim along the line-of-sight direction can be determined.

MOBILE USER UNITS

For simplicity, a uniform model of user distribution is used in this program. The earth is divided into cell regions bounded by certain latitudes and longitudes. Several mobile user units are then lumped at the center of each cell. This includes users of various MSS systems. In the uniform distribution model, it is assumed that users of different MSS systems are distributed evenly and uniformly over the same geographic area. This situation is illustrated in Figure 3.

By combining the traffic distribution profile of a MSS satellite system and the user distribution, interference between users and satellites, and between satellite and satellite can be simulated for a long period of time. To reduce the complexity of the problem, user-to-user interference is not currently considered.

PROGRAM OUTPUT

The program "measures" the total interference Power Spectral Density (PSD) at the terminal of the victim's antenna. The scope of the spectram analyzer is displayed graphically by the prgram. As the program steps in time, the location of the victim is also displayed graphically on a flat earth. The interference power information and orbital dynamics information are captured into separate files for further analysis. This information can be examined directly from the program or from any text editor.

To make the program output more comprehensive, several data reduction and statistical programs were developed. The results of the statistical analysis is also captured into a file that can be accessed from the program. The statistical and power spectral density information can be used to estimate the aggregate Io and its impact on operation of various MSS systems. $Eb/(No + Io)$ for any scenarios and any MSS system can be calculated to evaluate the system operation and link integrity and circuit capacity. Furthermore, the information provided by GISP can be used to allocate expected interference noise from different MSS systems, and thus establish a criteria for frequency sharing among various MSS systems.
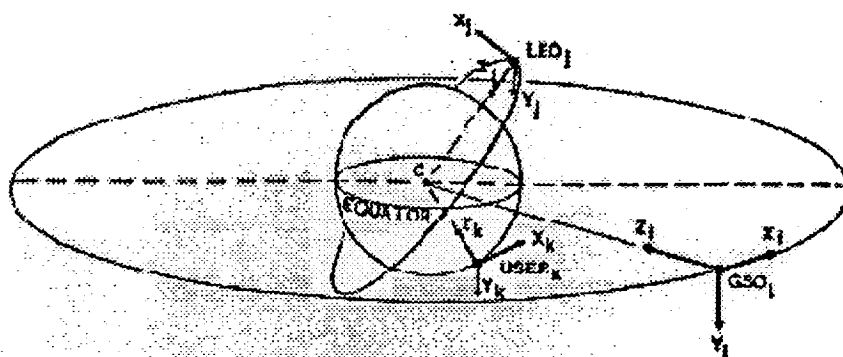
Figure 1. Illustration of various coordinate systems
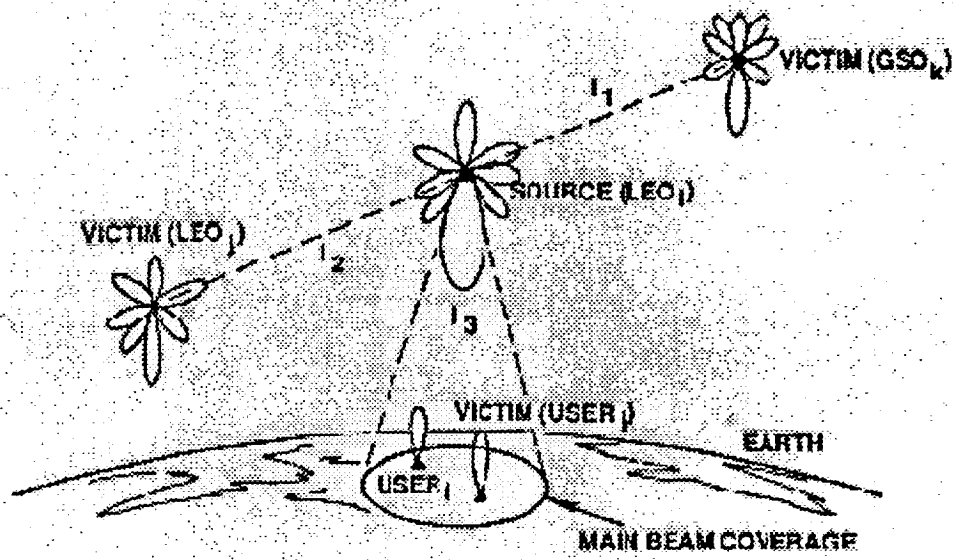
Figure 2. Interference among various satellites
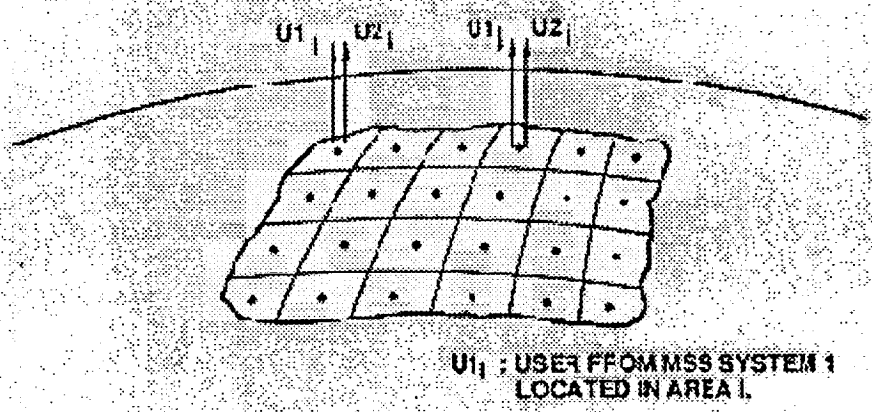
Figure 3. Illustration of user distribution cells

Handover Aspects for a Low Earth Orbit (LEO) CDMA Land Mobile Satellite (LMS) System.

P. Carter and M. A. Beach
University of Bristol
Centre for Communications Research
Queens Building, University Walk
Bristol BS8 1TR, United Kingdom
Tel: +44 272 303257,
Fax: +44 272 255265

Abstract

This paper addresses the problem of handoff in a land mobile satellite (LMS) system between adjacent satellites in a low earth orbit (LEO) constellation. In particular, emphasis is placed on the application of soft handoff in a Direct Sequence Code Division Multiple Access (DS-CDMA) LMS system. Soft handoff is explained in terms of terrestrial macroscopic diversity, in which signals transmitted via several independent fading paths are combined to enhance the link quality. This concept is then reconsidered in the context of a LEO LMS system. A two-state Markov channel model is used to simulate the effects of shadowing on the communications path from the mobile to each satellite during handoff. The results of the channel simulation form a platform for discussion regarding soft handoff, highlighting the potential merits of the scheme when applied in a LEO LMS environment.

Introduction:

The market penetration of terrestrial mobile cellular systems in Europe is ultimately limited both economically and geographically. As a result, activities within ETSI addressing UMTS (Universal Mobile Telecommunications System), concerning the design of third generation land mobile communications systems in Europe, are now looking at the possibility of a satellite-based radio interface to complement the service areas offered by terrestrial networking.

A preliminary study into the integration of LMS and terrestrial communications systems at the University of Bristol has suggested that the focus of a future LEO CDMA LMS system design will be towards that of low bit rate services (up to 9.6Kbps) enhancing a subset of the UMTS objectives [1] e.g. voice via hand held portable units.

By definition, providing continuous coverage over a specified region requires frequent handover activations between adjacent satellites in the LEO constellation ($\approx$ 10-15 min. intervals) [2]. Sectorized satellite antennas mapping cells (or sectors) onto the earths surface are key components in improving the link budget (and hence reducing mobile transmit power) and also the management of each satellite's EIRP. In contrast to terrestrial cellular systems, the cells are fixed relative to the satellite's orbit but they move rapidly across the earths surface. As a result, handover activations need to be performed at an even greater frequency (e.g. one per minute for the Iridium system [3]) between contiguous cells within a single satellite footprint.

Current research into third generation mobile terrestrial systems in Europe, more specifically the RACE CODIT [4] and LINK CDMA [5] projects, are focusing on interference limited multiple access techniques, such as DS-CDMA (Direct Sequence - Code Division Multiple Access). This spread spectrum technique transmits the signal in a bandwidth in excess of the minimum necessary to send the information. The band spread is accomplished by means of a high bit rate code which is independent of the transmitted data, and a synchronized reception with the code at the receiver is used for despreading and subsequent data recovery. DS-CDMA can support a form of signal diversity at the mobile, where signals from more than one transmitter can be combined to support a system feature known as soft handoff [6].

The requirement for a CDMA soft handoff protocol to operate in a LEO LMS environment is clear: the user must experience as little disruption as possible

during a call handoff either from sector to sector within a single satellite's footprint or from satellite to satellite.

LEO LMS System Description:

In order to study the problems of satellite handover, it is instructive to define a simplified LMS network topology. The results of any subsequent protocol simulation can be used to form a platform for further investigation and help establish the basic limitations that the handoff process places on the LMS system.

In Figure 1, a communication link between a Mobile station and an earth gateway is considered. The space segment in any communications network demands a high capital investment, and in the case of LEO LMS systems, satellites will need to be replaced after several years of operation. It is therefore logical to assume a very simple space hub design, which is limited to the function of frequency translation between the uplink and downlink. At the mobile the designer has to optimize transmit power, battery life and the size of the hand portable unit. To this end a large proportion of the network functions (e.g. routing and protocol management) are concentrated at earth gateways, which in principal will also provide the necessary interface to contemporary terrestrial systems. In addition LMS system Gateways are separated by large geographical distances and this property implies that each Gateway requires a degree of autonomy when considering the design of system operating protocols. Each earth gateway is updated with essential network information through store-and-forward techniques over the space hub.

LMS Shadowed Channel Model:

A main cause of signal level variation in the LMS environment is shadowing, in which obstructions in the radio communications path cause reduced local mean signal levels in areas tens or hundreds of metres in extent. This phenomena is particularly important in a LEO LMS system where the handover period between adjacent satellites in the constellation can last for several minutes.

Considering the slow signal variations due to shadowing, the LMS channel can be represented by a two-state channel model formulated by [7]. Areas of high received signal power correspond to line-of-sight operation and the channel state is described as *good*. Conversely, shadowed areas with low received signal powers are represented by a *bad* channel state. The switching
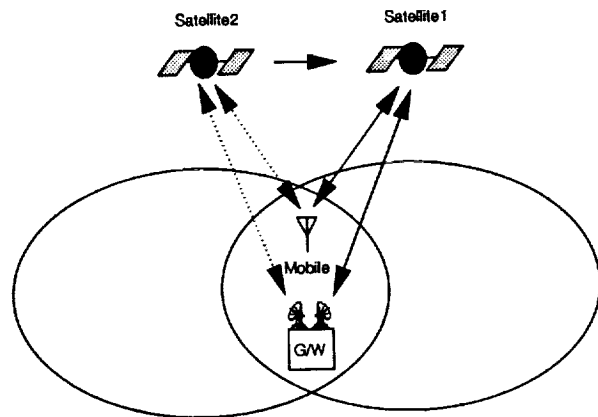
Figure 1: *Handoff between two adjacent satellites.*

process between the shadowed and unshadowed areas in which the mobile is operating can be approximated by a Markov model, see Figure 2. The durations of the good and bad channel states, t_g and t_b, are exponentially distributed.

The associated means of the channel state durations depend on the vehicle speed $v [m/s]$ and are given by,

$$\bar{t}_b = \frac{1}{P_{bg}} = \frac{D_b}{v} \tag{1}$$

and

$$\bar{t}_g = \frac{1}{P_{gb}} = \frac{D_g}{v} \tag{2}$$

where D_b and D_g are simply the average dimensions of the obstructed and unobstructed regions respectively in metres. P_{gb} and P_{bg} are the state transition probabilities and have units of $[1/s]$.

The timeshare of shadowing A is related to the durations D_b and D_g. According to [7], it is defined as

Equation (4) can be applied either to the forward (satellite to mobile) or reverse (mobile to satellite) direction, as well the corresponding anchor links between the satellite and earth gateway station.

Similarly, the short-term signal mean r_0, when the LOS path between the mobile and satellite is shadowed, can be approximated by a log-normal distribution.

$$f_{\log}(r_0) = \frac{10}{\sqrt{2\pi}\sigma \ln 10} \frac{1}{r_0} \exp[-\frac{(10\log r_0 - \mu)^2}{2\sigma^2}] \quad (5)$$

where σ^2 is the variance and μ is the mean (in dB) of $10\log r_0$.

Macroscopic Diversity:

Macroscopic diversity in terrestrial systems exploits signals received at several base stations from the same mobile transmitter in order to limit the effects of signal variations due to shadowing [8]. The signals received at each base station are used by the system to select the best communications link thus enhancing the quality of service perceived by the user. This concept can also be applied in the reverse direction with the mobile combining signal paths and these could originate from one or more base stations. For example, consider the scenario depicted in Figure 1. Macroscopic diversity therefore optimizes the overall performance of a communications link with respect to quality (for DS-CDMA systems this reduces the required signal to noise ratio to support a required error rate) and signal to co-channel interference ratio. This factor becomes very significant in interference limited systems such as CDMA.

The use of macroscopic diversity dates from the 1920's, but more recently has been considered for wireless terrestrial applications such as UMTS. More specifically, interference-limited access techniques, such as DS-CDMA can utilise both base station macroscopic and mobile path diversity to provide a system feature known as 'soft handoff'. This handoff technique is by no means confined to the realms of terrestrial communications [9]. LEO LMS systems possess similar characteristics to terrestrial mobile systems. In order to provide continuous coverage over a particular region, frequent handover activations between adjacent satellites in the LEO constellation are required. In contrast to terrestrial cellular systems, the cells, defined by each satellites antenna footprint, move through the user. See Figure 3.

Figure 2: Two-state Markov model.

$$A = \frac{D_b}{D_g + D_b} \quad (3)$$

For the present study and to provide an example for discussion, mean signal levels under LOS operation are governed by a linear path loss model or link equation given by,

$$\frac{C}{N_0} = EIRP_T + [\frac{G}{T}]_R - Lp - 10\log k \quad (4)$$

$\frac{C}{N_0}$: The ratio of the signal power to noise power spectral density after being received and amplified (dB-Hz).

$EIRP$: The effective isotropic radiated power of the transmitter (dBW).

$[\frac{G}{T}]_R$: Figure of merit of receiver (dB).

L_p: Free-space path loss (dB).

k: Boltzmann's constant expressed in decibels (-228.6 dBW-K-Hz).

In a soft handoff LMS environment, as the mobile approaches the edge of one satellite's coverage region and enters that of another, a link is established via a second satellite between the mobile and communicating Gateway (routing the call to a local PSTN). The call from the mobile is now being routed via two, or possibly more, satellites. The receivers at either end of the link can have two options available, depending on their design complexity.

1. The receivers can identify the best signals from the visible satellite and combine them. This process continues until the mobile is firmly within the antenna footprint of one particular satellite.

2. If combining is not an option, all the signal options can be continuously monitored simultaneously and after a period of evaluation the best link can be selected.

Soft handoff offers an improvement over hard handoff in a LEO LMS system by being a 'make before break' rather than a 'break before make' system. The degradation experienced in terrestrial systems in the latter case is exacerbated in LMS systems due to the longer propagation time delays ($\approx$ 14ms round trip, limiting the amount of handshaking between the mobile and Earth Gateway) and longer processing delays in acquiring signals with significant Doppler shift (up to 40kHz). By careful design of the soft handoff protocol and its signal thresholds, the 'Ping-Pong' effect (constant handing back and forth between satellite channels) common in hard-handoff terrestrial systems, can be avoided.

Model Results and Discussion:

To gain an insight into the effects of shadowing during handoff a very simple scenario describing mobile handover between two adjacent satellites, separated by 45° and at an orbital height of $1000km$, in the same plane of a polar constellation was considered. The mobile was placed at some midpoint on the earth's surface, between the two orbiting satellites. This positioning implies that both satellites are visible and that the mobile is within the overlap region of the satellite 3dB antenna footprints to validate the linear path loss model.

As an example, the set of parameters listed in Table 1 were used to simulate the LMS channel model outlined. The parameters for the two state Markov model are derived from the empirical results given by

Handover region.
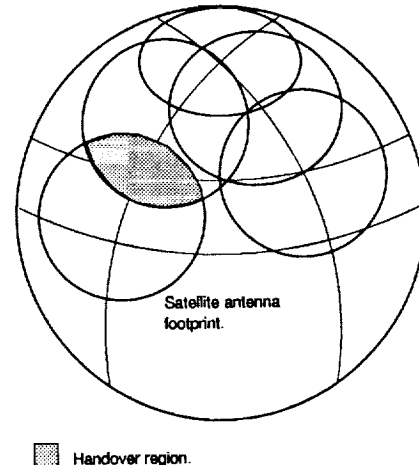
Figure 3: *A LEO polar constellation.*

[7] for a mobile to satellite elevation angle of 18° operating in a city environment. The linear path loss model is a function of the distance between the mobile and satellite and the model parameters ensure a carrier-to-noise density ratio, C/N_0, >42 dB-Hz when the mobile is in a good channel state. This minimum requirement is sufficient to provide a BER < 0.01 at 4.8kbps for QPSK modulation [10].

Figure 4 shows a 50 second time frame during the handoff period where satellite-2 is succeeding satellite-1. The two signal paths from the mobile to each satellite are shadowed, for example, by buildings. The mean Line of Sight (LOS) component is approximately constant but the additional effect of shadowing produces a variation in the signal mean by several dB. The two thresholds, T_START and T_DROP, have been arbitrarily chosen to indicate where handoff signaling in the network would start to initiate or terminate a satellite-path, as the mobile passes from one satellite footprint to another. Several potential problem areas can be identified in the use of such a window when the mobile is operating in the simulated shadowing environment.

The period of handoff in this scenario lasts for several minutes and could certainly span the duration

of a subscriber call. The thresholds T_START and T_DROP are frequently crossed and in a hard handoff system, whose protocol adheres to this set of predefined signal thresholds, handoff would be initiated repeatedly. The subsequent increase in the level of signalling within the network would reduce the satellite's battery lifetime. In addition the signaling between the mobile and gateway is limited by relatively long time delays. Under such severe operating conditions a threshold transition may exceed the timer limit of the system which could lead to a premature call termination of the mobile concerned. Clearly this situation is undesirable.

As mentioned previously, multiple access techniques such as DS-CDMA are able to support a feature known as soft handoff. The reliability of the diversity combining technique used is dependent on the amount of de-correlation between the fading statistics of each individual diversity branch, in this case the signals received from the mobile at the gateway via the two separate satellite paths. The slow fading (due to shadowing) on each satellite path illustrated by Figure 4 has a cross correlation factor of 0.0429. The low correlation factor implies that the probability that both signal paths will be in a deep fade simultaneously is also very low.

Several systems exist which capitalize on the uncorrelated fading statistics of several signal paths. Selection diversity is probably the simplest system of all where the signal with the best baseband signal-to-noise ratio is connected to the output. With respect to the simulated shadowing environment described, both signal paths would remain active during handoff. Although this type of mobile receiver would provide an improved RMS signal strength, multipath fading would still occur. However, in order to overcome short term fading effects a hybrid scheme using selection diversity and an equal gain or maximal ratio combiner could be used; the benefits of these techniques may be less significant as multipath in a LMS system is very weak when compared with mobile operation in a terrestrial urban environment. The improvement in the overall signal quality has been demonstrated for a terrestrial system by [11].

In a soft handoff system the mobile is combining signals from different satellite paths by implementing the techniques discussed. As a result both the mobile and satellite need to transmit less power to maintain the same signal strength as for a single satellite path during the handoff period. The reduction in transmitted power from the satellites and users in handoff reduces the noise within the system, and so could potentially increase the overall capacity for an interference limited system such as DS-CDMA.
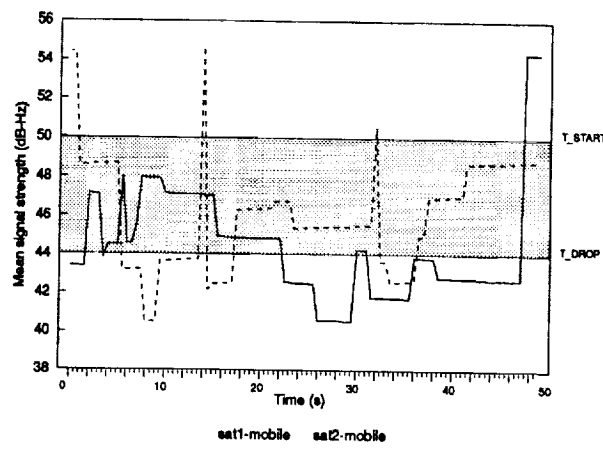
Figure 4: Short-term mean signal variation due to shadowing

PARAMETER	VALUE
EIRP/carrier	5.0 dBW
$[\frac{G}{T}]_R$	-13.0 dB-K
D_b	32.0 m
D_g	8.0 m
v	40 Km/h
A	0.80
μ	-11.8 dB
σ	4.0 dB

Table 1: Channel model parameters

527

Conclusions.

The simulation results presented have been used to illustrate some of the considerations necessary in order to assess handoff mechanisms in LEO LMS networks. In particular reference has been made to the soft handover concept which can have considerable benefits in interference limited systems such as DS-CDMA. Further, in LEO satellite systems any technique of reducing the satellite transponder transmit power will prolong the on-board battery-life. With regard to the design of the handoff protocol, careful consideration needs to be given as to the size of the handoff region and the timeout periods so as to prevent redundant signaling within the network. These parameters ultimately affect signal quality and network performance.

The future aims of the project are to devise a soft handoff protocol and evaluate its performance in various handover scenarios under a diverse range of signaling conditions.

Acknowledgements

References

[1] A. Arcidiancono. *Integration between Terrestrial-Based and Satellite-Based Land Mobile Communications Systems.* IMSC, Ottawa, 1990.

[2] G. Maral *et al. Low Earth Orbit Satellite Systems for Communications.* International Journal of Satellite Communications, Vol. 9, July 1991.

[3] J. L. Grubb. *Iridium Overview: The travellers dream come true.* IEEE Communications Magazine, November 1991.

[4] *CODIT - UMTS Code Division Test Bed.* Research and Technology Development in Advanced Communications Technologies in Europe (RACE) 1992. Annex A p.155.

[5] S. C. Swales *et al. A Comparison of CDMA Techniques for Third Generation Mobile Radio Systems.* IEEE VTC'93, New Jersey, USA, May 1993.

[6] *CDMA for Cellular and Personal Communications Networks: Theory and Achievements.* CDMA Workshop, Geneva, Switzerland. Oct 16 1991.

[7] E. Lutz *et al. The Land Mobile Satellite Communications Channel – Recording, Statistics and Channel Model.* IEEE Transactions on Vehicular Technology, Vol. 40, No.2, May 1991.

[8] R. C. Bernhardt. *Macroscopic Diversity in Frequency Reuse Radio Systems.* IEEE Journal on Selected Areas in Communications, vol. SAC-5, No. 5, pp. 227-280.

[9] P. Carter and M. A. Beach. *Handover Aspects for a Low Earth Orbit (LEO) CDMA Land Mobile Satellite (LMS) System.* COST 227 TD (093)04, Bradford, U.K., Feb. 1993.

[10] B. G. Evans. *Satellite Communications Systems. 2nd Ed.* IEE Telecommunications series 24.

[11] *CTIA Technology Forum: CDMA Field Trial.* CTIA Technology Forum, NYNEX Mobile Communications Company, 5th Dec. 1991.

Figure 1. Satellite coverages.

Figure 2. Network configuration.

Table 2. Network architectures.

	HLR	VLR
	Location / Number	Location / Number
1	One Region / 1	- / None
2	Each Region / 5	Each Region / 5
2D	Each Region / 5 (D-HLR)	- / None
3	Each LES / 25	Each LES / 25
3D	Each LES / 25 (D-HLR)	- / None

NETWORK ARCHITECTURES

In this section, five candidate network architectures, in which locations and functions of location registers differ, are presented and evaluated in terms of signaling traffic required for an outgoing call from a handheld terminal, an incoming call to a handheld terminal, and location registration by a handheld terminal.

Candidate network architecture

Five candidate network architectures are shown in Table 2. Both the number of Regions and the number of LES's per Region are assumed to be five for all architectures. The terms 'HLR' and 'VLR', which stand for a home location register and a visitor location register, respectively, are used to represent different types of database facilities or equipment in accordance with each network architecture. An HLR contains information about handheld terminals that are initially registered to that HLR, and manages these terminals when they are within the service area associated with that HLR. A

VLR is assumed to be at the same location as an HLR, and contains information about roaming terminals from service areas associated with other HLR's. A VLR manages information about roaming terminals only when they are within the service area associated with that VLR. When the VLR is informed that a roaming terminal whose information is stored in that VLR has moved outside the service area, information about that terminal is deleted.

In Type 1, only one HLR is employed in the system, which manages information about all the handheld terminals no matter where they are located. In Types 2 and 2D, one HLR is located in each Region, and in Types 3 and 3D, one HLR at each LES. In Types 2 and 3, VLR's are also employed in the system. In Types 2D and 3D, no VLR's are employed and each HLR manages information about all the terminals. To ensure correct routing, when information about a terminal is changed or updated in one HLR, information about that terminal in the other HLR's must be updated immediately. Since the information about all HLR's in Types 2D and 3D is duplicated, these HLR's are named "duplicated-HLR's (D-HLR's)".

An example of a network configuration is shown in Fig. 2. It is assumed that LES's and network control stations (NCS's) are connected through an international signaling network. One NCS is assumed to be located in each Region, which is responsible for network coordination, namely allocation of PN codes and / or frequency slots and / or time slots. The dots in Fig. 2 represent signal transfer points (STP's), which are responsible for switching of signaling messages.

530
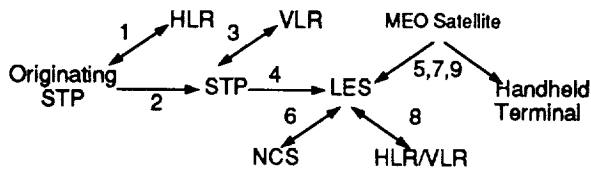
1 Location Inquiry / Notification of Location (LES or Region)
2 Initial Address Message
3 Location Inquiry / Notification of Location (LES)
4 Initial Address Message
5 Call Announcement / Response
6 Channel Assignment Request / Channel Assignment
7 Channel Assignment
8 Authentication Request / Random Number + Result
9 Random Number / Result

Figure 3. Procedure for an incoming call to a handheld terminal.

● Location of Originating STP
○ Location of Handheld Terminal

Figure 4. Twelve possible cases for an incoming call.

Evaluation of network architectures

For the evaluation of candidate network architectures, procedures for an outgoing call from a handheld terminal, an incoming call to a handheld terminal, and location registration by a handheld terminal, are defined. The defined procedure for the incoming call is shown in Fig. 3, for reference. First, location of the called terminal is requested from an HLR, and the HLR notifies the location. The call is then connected to the objective LES. In Type 2, when the terminal is roaming in another Region, the call is connected to the LES after the location of the terminal is requested from and notified by the VLR. Namely, the third and fourth steps in Fig. 3 are to be considered only in Type 2. A call announcement or paging message is then sent to the terminal, and the terminal responds to it. Next, a channel is assigned by an NCS, and an authentication procedure follows. When an authentication procedure succeeds, the call will be connected.

Signaling traffic for an averaged one event is calculated by the following method. An event here refers to an outgoing call, an incoming call and one location registration event.

First, signaling traffic, given by the product of the number of signaling bits (unit : bit) and the transmission distance (unit : kilometers), is calculated for each step in each procedure. The transmission distance at each step in each procedure differs in accordance with the

locations of the handheld terminal, the call originating point, and so on. To cover all the cases taken into account, three, twelve and fourteen cases are considered, respectively, for an outgoing call, an incoming call and location registration. Cases considered for an incoming call are shown in Fig. 4, for reference. Black dots represent locations of the STP's nearest to the call originating subscribers, and white dots locations of the called handheld terminals. An inner dashed area represents the service area of the HLR to which the terminal is initially registered. An outer hatched area represents a Region where that objective HLR is located. For example, case number 3 represents an incoming call from a subscriber located in the service area of the HLR, where the called terminal is initially registered, to the terminal roaming in a Region not covered by the service area of that HLR.

Second, the average of the signaling traffic for each event, namely for an outgoing call, an incoming call and location registration, is calculated by equally weighing all the cases considered for each event. The signaling traffic for an averaged one call is, then, calculated assuming the ratio of the number of outgoing calls to that of incoming calls is 60 % : 40 %. Finally, the signaling traffic for an averaged one event is derived assuming the ratios of the number of calls and that of location registration are 90 % : 10 % and 99 % : 1 %.

The number of signaling bits assumed is

531

categorized into the following three types :

- 400 bits, for call request, acknowledgment and location inquiry,

- 500 bits, for location information, and

- 900 bits, for information about a handheld terminal.

Transmission distances are categorized into the following three types :

- 2,000 kilometers, between an LES and the nearest STP,

- 6,500 kilometers, for transmission within the same Region,

- 13,000 kilometers, for transmission across Regions, and

- NA for transmission by the satellite links.

Transmission by satellite links is not taken into account in the evaluation, because the links and the procedures associated with them are common to all architectures.

The calculated signaling traffic is shown in Fig. 5(a), for an outgoing call, an incoming call, an averaged one call and for one location registration event. It is understood from Fig. 5(a) that signaling traffic for calls in the network types 3 and 3D is least and that in Types 2 and 2D, it is second least. With regard to location registration, signaling traffic in Types 2D and 3D are greater than that in Types 2 and 3. Especially, in Type 3D where twenty-five D-HLR's are employed in the system, signaling traffic required for one location registration event is estimated to be approximately 30×10^7 bit · kilometer, which is approximately ten times as much as that for Type 2D. This results from the assumption that the D-HLR's should be updated immediately when one of them is updated. Figure 5(b) indicates that Type 3 is the most appropriate architecture among all the architectures considered.

LOCATION DETERMINATION AND REGISTRATION

Two location determination and registration methods, named an LES-ID code detection
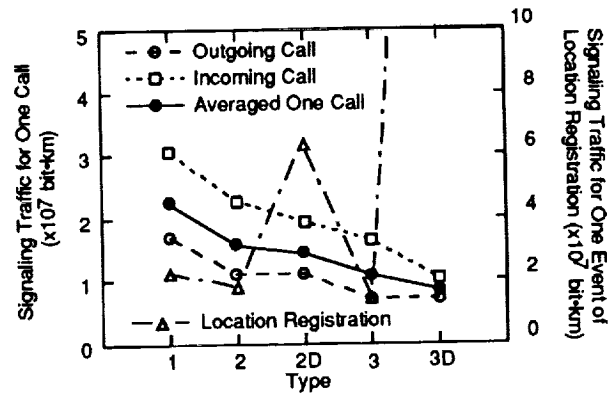
(a) For calls and location registration.
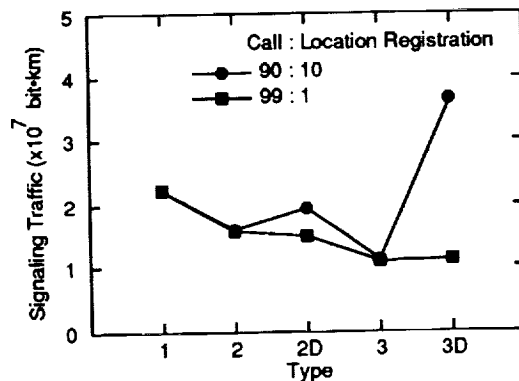
(b) For one event.

Figure 5.   Signaling traffic.

method and a location prediction method, are considered in this section. First, detailed descriptions are given for each method. Then, the number of spotbeams required for paging, or call announcement, is evaluated.

LES-ID Code Detection Method

In the LES-ID code detection method, a service area is predetermined for each LES, which should be smaller than the area that LES can cover in 100 % of time. Areas covered by an LES in 100 % of time are shown in Fig. 6. Degrees in Fig. 6 represent the latitude of LES's. These areas are calculated by assuming that a satellite and an LES are linked at a minimum elevation angle of ten degrees, and that a satellite and a handheld terminal are linked at a minimum elevation angle of 20 degrees. In the LES-ID code detection method, each LES transmits its own ID code (LES-ID code) to the

532
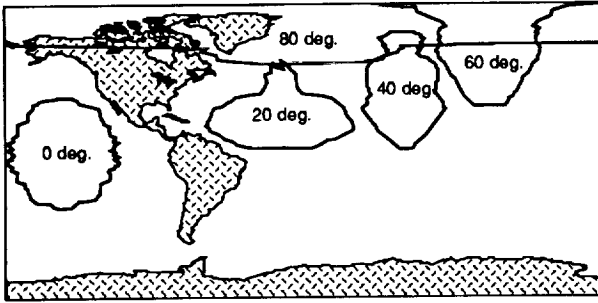
Figure 6. Example of areas covered by an LES in 100 % of time.

MEO Satellite

LES-ID

LES

Handheld Terminal

HLR/VLR

······ Mobile Link
—— Feeder Link
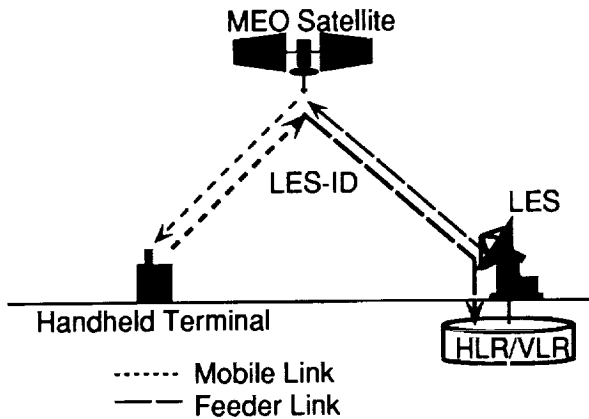
Figure 7. LES-ID code detection method.

Figure 8. Number of spotbeams required for call announcement in the LES-ID code detection method.

spotbeams required for call announcement becomes larger. The number of spotbeams required for call announcement is calculated for the areas shown in Fig. 6. Figure 8 shows the calculated results. It is seen from Fig. 8 that the mean number of spotbeams required for the call announcement is a minimum for an LES at the latitude of approximately 70 degrees.

Location Prediction Method

In the location prediction method, a handheld terminal receives a spotbeam ID code and time information, namely the time of reception, and transmits that data to an LES at a prescribed time interval. The LES routes this information to the computing facility possibly located at an NCS. The computer calculates the area the spotbeam with the received ID code illuminates at that time. For this purpose, accurate orbit parameters of all the satellites are required at the computing facility. Based on the calculated area, the computer predicts the area in which the handheld terminal is contained taking account of errors in orbit parameters and mobility of the terminal. Then, the computer sends the predicted area information to the objective location register, which is registered as the location of that terminal. With this method, the predicted area is not necessarily associated with the service area of one LES, which would be a disadvantage. Hence, two or more LES's are required for transmitting a call announcement

service area, as shown in Fig. 7, through spotbeams which illuminate the service area. For this purpose, the accurate orbit parameters of each satellite as well as computing facilities are required. A handheld terminal detects an LES-ID code by scanning all the prescribed PN codes or frequencies for receiving an LES-ID code when logging-on, at specified intervals, and when the signal quality is degraded under the predetermined threshold. The terminal registers the detected LES-ID code in an objective location register (HLR or VLR) if it does not coincide with the previously registered ID code. The location of the terminal is registered by the LES-ID code. For call announcement, spotbeams illuminating the service area of the LES with the registered ID code are identified using the orbit parameters, and a message is transmitted through these beams. As the LES service area becomes wider, location registration will be made less frequently, however, the number of

Figure 9. Location prediction method.
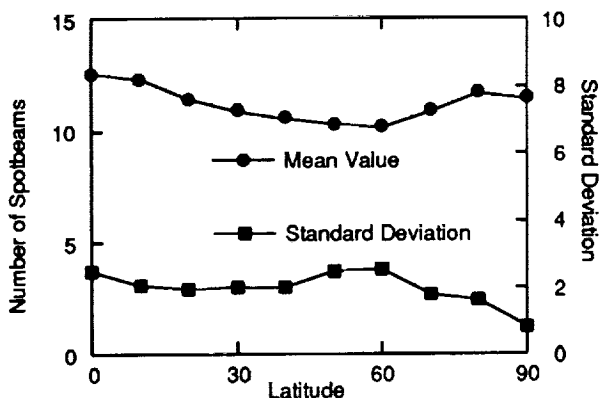
Figure 10. Number of spotbeams required for call announcement in the location prediction method.

message to a terminal. The number of spotbeams required for call announcement is calculated, and the results are shown in Fig. 10. It is assumed that the predicted area is exactly the same as the area illuminated by the spotbeam.

Discussion

Both methods for the location determination and registration considered here require accurate orbit information of all the satellites as well as computing facilities. Since a satellite at an altitude of 10,355 kilometers moves around the earth with a period of six hours, calculation of the position of all the satellites is not a heavy load for a computer. As far as the number of spotbeams required for call announcement is concerned, the location prediction method is advantageous, however, call announcement

through two or more LES's is mandatory for most of the cases. With regard to the number of location registration events made, the LES-ID code detection method is advantageous since the area covered by an LES in 100 % of time is wide, as shown in Fig. 6, and since the terminals moving in this area are not required to update their location information. To make the number of spotbeams required for call announcement with the LES-ID code detection method small, sectorization of the LES into multiple narrow service areas assigned different ID codes will be effective.

CONCLUSION

Network architectures, and location determination and registration methods for the MEO system were investigated. It was found that the network in which an HLR and a VLR are located at each LES is the most appropriate in terms of signaling traffic. With regard to the location determination and registration method, two methods, one is based on receiving an LES-ID code and the other on predicting the area in which the handheld terminal is contained, were evaluated, and advantageous and disadvantageous features of these two methods were identified.

ACKNOWLEDGMENTS

REFERENCE

[1] A. H. Ballard : "Rosette Constellations of Earth Satellites," *IEEE Trans. Aerosp. Electron. Syst.*, vol. AES-16, No.5, pp. 656-673 (Sept. 1980).

The Design and Networking of Dynamic Satellite Constellations for Global Mobile Communication Systems.

N94-22826

Cionaith J Cullen*[1], Xavier Benedicto*, Rahim Tafazolli**, Barry Evans**.

*European Space Agency, ESTEC,
Postbus 299, 2200 AG Noordwijk zh, The Netherlands.
Tel. + 1719 83922   Fax. + 1719 84596

**Center for Satellite Engineering Research (CSER),
University of Surrey, Guildford, GU25XH, England.
Tel. +483 509800   Fax. +483 34139

ABSTRACT

Various design factors for Mobile Satellite Systems, whose aim is to provide worldwide voice and data communications to users with handheld terminals, are examined. Two Network segments are identified - the Ground Segment (GS) and the Space Segment (SS) and are seen to be highly dependent on each other. The overall architecture must therefore be adapted to both of these segments, rather than each being optimised according to its own criteria. Terrestrial networks are grouped and called the Terrestrial Segment (TS). In the SS, of fundamental importance is the constellation altitude. The effect of the altitude on decisions such as constellation design choice and on Network aspects like call handover statistics are fundamental. Orbit resonance is introduced and referred to throughout. It is specifically examined for its useful properties relating to GS/SS connectivities.

INTRODUCTION

Recently there has been great interest in the provision of a mobile satellite communications service to users with handheld terminals. Low Earth Orbit (LEO) and Medium Earth Orbit (MEO) satellite constellations are expected to play a key role in such mobile satellite communication systems. These constellations are grouped together here and called Dynamic Satellite Constellations (DSCs) - due to their similar Earth visibility and Networking properties. Current DSC proposals are grouped, approximately, around either 1,000 km or 10,000 km. Earths inner radiation bands, centered around altitudes of 0.4 (electron) and 0.7 (proton) earth radii (6,378 km at the equator) are the main factors cited, however valid, when the avoidance of intervening altitudes is being justified. The futuristic scenario for world mobile communication systems are hybrid systems with fully integrated satellite and terrestrial segments[1]. More pragmatic integration scenarios are envisaged for first generation satellite systems - with interoperability with certain Public Land Mobile Networks (PLMNs), through the use of dual-mode terminals, being the early goal before further system integration is envisaged.

This paper outlines and links together important factors which need consideration for the design of these first generation DSC Networks. These mainly include SS and GS factors but some TS considerations are mentioned. Within the SS the constellation altitude is the fundamental driver. It directly effects satellite numbers and sizes and therefore launch factors. It affects the GS at a Network level in areas such as ground station distribution and call handover frequency. At a

---

[1]Mr. Cullen is currently registered as a PhD student at the University of Surrey

physical level it effects factors such as doppler shifts and link budget calculations. Aspects such as Free Space Loss (FSL) variations over the coverage area, minimum elevation angle, user terminal antenna gain and satellite antenna gain are all relevant link variables[2]. The TS is important from both an interoperability point of view and also from a GS connectivity point of view

DSC NETWORK SETUP

For this 1st generation DSC Network Architecture (NA) fully transparent satellites are assumed. Although there could be an advantage from a Network connectivity point of view, Inter-Satellite Links (ISLs) are not envisaged. There are both technical (eg. risk associated with new technologies in space) and non-technical (eg. Fixed operators fear of being by-passed) reasons why this approach is favoured. The architecture is shown in Figure 1 and its elements are now described.

A Primary Earth Station (PES) interfaces directly between the Space Segment (SS) and the Ground Segment (GS) and also between the GS and the TS. With transparent satellites each satellite needs to have a controlling PES (PES/c) in close contact with it. These are located within the satellites coverage area. Both PES types (controlling and ordinary) are involved in Network control. They are expected to be distributed around the Network at varying levels of density. Other elements, not shown but which are associated with a PES, are its Home Location Register/space (HLR/s) and its Visitor Location Register/space (VLR/s). These help with user Mobility Management (MM) and interoperability with PLMNs. For the satellite to PES link, the minimum elevation angle, e_{min}, can be lower than for the Satellite to Universal Terminal (UT) link. This is due to less variable propagation factors and results in the satellites radius of coverage for PESs being larger.

Constellation altitude directly affects the GS architecture. Each satellite in the constellation has one PES/c in its coverage area which controls the use of the satellites resources and coordinates all the UTs within the satellites UT coverage area. For LEO DSCs, high numbers of satellites are required
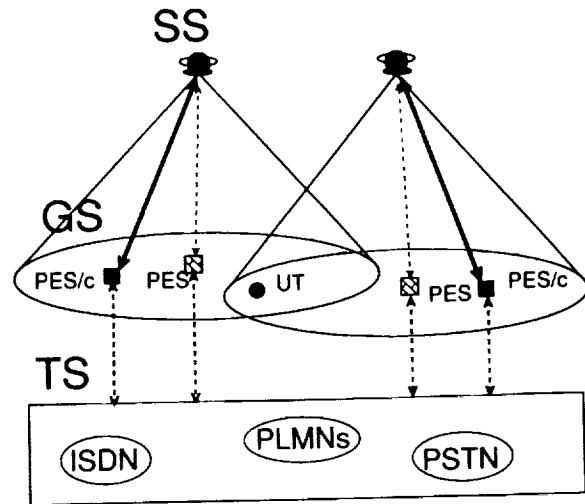
Figure 1

in order to provide even a low elevation angle coverage. This results in the Network requiring equivalently large numbers of PES/cs. For MEO DSCs, with fewer satellites, fewer PES/cs can be used. System e_{min} can also be more easily increased in MEO DSCs and this helps improve UT propagation conditions.

Satellite diversity is a very useful DSC Network property which involves the UT being in range of more than one satellite. The UT therefore has a choice of satellites available to it, through which the Network can route a call, as current traffic loadings determine. MEO DSCs, because of their greater satellite coverage overlap, generally offer the UT a higher level of satellite diversity, especially in mid-latitudes. For polar LEO constellations, satellite diversity is generally very low (eg. the Iridium constellation). The location of PES/cs could be such as to take advantage of satellite diversity, allowing lower numbers of PES/cs than satellites and thus simplifying Network control.

CONSTELLATION FACTORS

Having now introduced a baseline NA this section examines Network and link parameters which are affected by the choice

of constellation altitude. Resonant orbit altitudes, which result in very useful DSC coverage properties, are specified and explained. The Physical and Network implications of these altitudes are then reviewed.

Resonant Altitudes

The best known resonant orbit is the Geostationary Earth Orbit (GEO) at an altitude of about 36,000 km and with the satellite orbit plane having an inclination of 0 degrees. This means that the satellite remains over the same point on the equator throughout its lifetime. For other altitudes and inclinations, the satellite is always in motion relative to the earth and so a satellite ground track results. By choosing specific altitudes whose period relates to integer divisions of a sidereal day (about 23^h 56 min)., the satellites ground track can be made to repeat on a daily basis. This is called orbit resonance.

Orbit resonance is described using a ratio, commonly referred to as L:M with L and M both coprime integers. The satellite then orbits the earth L times every M days. With M set to 1, the repetition period is minimised to one day. Resonant orbits along with some of their coverage parameters for the DSC altitudes of interest, are given in table 1.

Table 1: Resonant Orbits

Orbit L:M	altitude (km)	β_{10} (deg.)	β_{30} (deg.)	ρ_{10} (km)	ρ_{30} (km)
15:1	554	15.0	7.2	1,820	1,003
14:1	880	20.1	10.5	2,518	1,511
13:1	1,248	24.6	13.6	3,225	2,071
12:1	1,666	28.7	16.6	3,925	2,652
11:1	2,146	32.5	19.6	4,648	3,302
9:1	3,367	39.9	25.5	6,378	4,848
8:1	4,163	43.4	28.4	7,350	5,790
7:1	5,144	47.0	31.4	8,565	6,942
6:1	6,391	50.5	34.4	9,993	8,339
5:1	8,041	54.2	37.5	11,886	10,147
4:1	10,354	58.0	40.7	14,439	12,583
3:1	13,892	62.0	44.2	18,222	16,332

Resonant Orbit Properties

In a resonant orbit the satellite ground track repeats itself after completing L orbits in M sidereal days, having covered 360 degrees geographical longitude. Resonant orbits therefore have the significant advantage of providing all regions of the globe with coverage patterns which repeat daily[3]. The most important advantages that this lends to the DSC Network concern satellite and frequency control. In any DSC constellation satellite ground tracks are continuously overlapping. As satellite coverage zones overlap, the Network needs to ensure that coverage zones which overlap do not result in harmful interference on DSC Network users. In resonant constellations this can be done most effectively, since, once the control procedure has been devised for one day, the same procedure can, in principle, be used throughout the constellation lifetime.

Apart form SS frequency coordination the other Network advantage provided by resonant constellations is stabilised and fully predictable visibility periods between satellites and the GS - in particular the earth stations (but, for example, it is also relevant to remote, data reporting, UTs). As a satellite passes beyond the range of its current PES/c a new PES/c must be allocated control of that satellite. With resonant orbits this passing over of satellite control can be easily defined, allowing for simple GS coordination between PES/cs. The PES/c must also know, for Resource Management (RM) purposes, which PESs are in visibility of the satellite which it controls. This is very straight forward with resonant orbits. Also, since in the initial DSC design the positioning of a satellites ascending node can be chosen, ground tracks can be optimised to some degree. More significantly, the locations of PES/cs can be made in such a way that allows them to be adapted most effectively to the satellite constellation.

Link Implications

Based on the resonant constellation altitudes of interest, link distance calculations were performed. The results are also tabulated in table 1. Various maximum slant path distances (r) are calculated according to the e_{min} value

used. Through this slant path distance, constellations can be effectively compared in terms of FSL. The significance is clarified with an example - the 4:1 altitude at 10,354 km with θ_{min} = 30 degrees has r = 12,583 km. It is 7 dB worse off in terms of FSL than the 14:1 altitude of 880 km with a worldwide θ_{min} of 10 degrees having r = 2,518 km. The size of satellite antennae and therefore their gain is related to the satellites final size and intended coverage geometry. DSC satellite numbers and launch implications are also very relevant here.

Satellite Angular Velocity, w

The satellite angular velocity, w, is a basic constellation parameter which depends directly on the constellation altitude. For circular orbits it is a constant. It affects the following: the doppler shift between the UT and the satellite and, also, the velocity of the satellites Sub-Satellite Point (SSP). Table 2 shows the maximum doppler shift (ie. at the highest frequency and at the minimum elevation angle) in the two UT frequency bands of relevance - UT Tx. 1610 - 1626.5 MHz and UT Rx. 2483.5 - 2500 MHz for the resonant altitudes of table 1. The satellites velocity and also its SSP velocity are also given. These magnitudes are important when considering call control statistics such as handover frequency - for both sat(ellite)-to-sat and cell-to-cell handover types.

DSC NETWORK FACTORS

This section mainly concerns the GS of the DSC Network. UT and call related topics are examined, with consideration mainly given to the implications of the physical parameters discussed in the previous section.

Coverage Zone Dimensions

The implications of satellite coverage radius on UT specific aspects are now related with satellite coverage aspects mentioned previously. This basically concerns approaches to user MM and to Network RM. Table 1 shows the earth centered half angle of coverage (b) for specified resonant altitudes and θ_{min} values. These figures are now related

Table 2:Satellite Motion Effects

Orbit L:M	$\omega(10^{-4})$ rads/s $\theta_{min}=10$	V_{sat} km/s	V_{ssp} km/s	Doppler Rx. kHz	Doppler Tx. kHz
15:1	10.94	7.6	7.0	57.6	37.5
14:1	10.21	7.4	6.5	53.8	35.0
13:1	9.48	7.2	6.0	50.0	32.5
12:1	8.75	7.0	5.6	46.1	30.0
11:1	8.02	6.8	5.1	42.3	27.5
9:1	6.56	6.4	4.2	34.6	22.5
8:1	5.83	6.2	3.7	30.7	20.0
7:1	5.1	5.9	3.3	26.9	17.5
6:1	4.37	5.6	2.8	23.0	15.0
5:1	3.65	5.3	2.3	19.2	12.5
4:1	2.92	4.9	1.9	15.4	10.0
3:1	2.19	4.4	1.4	11.5	7.5

to satellite coverage radii and, through different multibeam coverage geometries, to sizes of coverage zones on the earth. For cell-to-cell handovers, satellite coverage zone numbers are required.

Based on the seven cell coverage pattern, the number of coverage zones, N_t, is given by: $N_t = 1 + 3(n +1)n$, where n is the number of layers surrounding the center cell. Three different multibeam configurations are considered: 19 beams (n = 2), 37 beams (n = 3) and 61 beams (n = 4). Using these figures and satellite to UT coverage radii, important information on user Mobility Management (MM) and Network handover statistics can be obtained, which can then be used in studies on examining and optimising the Networks approach in these areas. In the following sections these sizes are considered in terms of Network MM and Network handover statistics. Table 3 lists the satellite coverage radius for different DSC altitudes and a given θ_{min} value. Coverage zone radii for some different multibeam configuratons are given in the other columns.

User MM

The most straightforward DSC Network approach to user MM is through UT beamlocation. A UT reports to the different

Table 3: Coverage Options

Orbit L:M	β_{10} (rads)	S_0(km) $(2\beta_{10}r_e)$	Beam (km) n = 2	Diam- (km) n = 3	-eter (km) n = 4
15:1	0.262	3,346	669	478	372
14:1	0.35	4,468	894	638	496
13:1	0.429	5,466	1,093	781	607
12:1	0.5	6,381	1,276	912	709
11:1	0.568	7,243	1,449	1,035	805
9:1	0.696	8,874	1,775	1,268	986
8:1	0.758	9,669	1,934	1,381	1,074
7:1	0.82	10,457	...	1,494	1,162
6:1	0.882	11,250	...	1,607	1,250
5:1	0.945	12,058	...	1,723	1,340
4:1	1.011	12,896	...	...	1,433
3:1	1.081	13,789	...	...	1,532
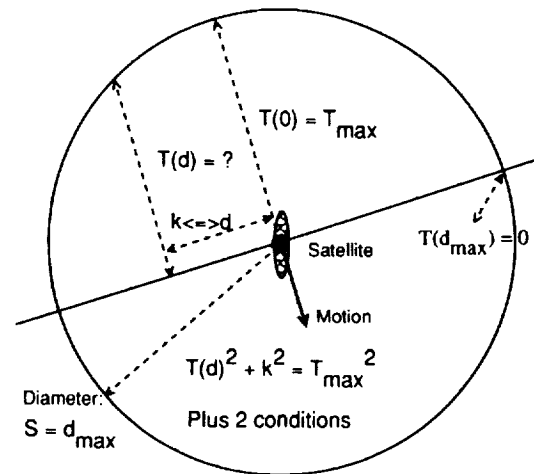
Figure 2

PES/c of the satellites in its visibility. The PES/c(s) concerned then associate the UT, through the coverage zone it used, to a set of Network-specific grid locations. Each of these is individually forwarded to the UTs HLR/s which then selects an appropriate set of grid locations and associates the UT with this set. Variations in the sizes of the satellite coverage zones have a direct bearing on the grid sizes which should be used and hence on the ultimate level of accuracy the Network has concerning the UTs location.

Call Handovers

Based on a satellites orbit period, its coverage diameter and its multibeam geometry, statistics on sat-to-sat and cell-to-cell handover frequencies can be estimated. A simple and accurate approach is now outlined. T(d) is half the visibility period between a satellite and a UT during a satellite pass, with d being the closest approach of the UT to the satellite ground track. T(0) [= T_{max}] is when the satellite passes directly above the UT and T(d_{max}) [= 0] is when the satellite passes by the UT at an elevation angle which is just below the e_{min} of the constellation. The set-up is shown in figure 2 and the problem is to find T(d) for $0 < d < d_{max}$.

From the geometry of Figure 2: T(d) = $(T_{max}^2 - k_2)^{1/2}$. Now since T(0) = T_{max} and T(d_{max}) = 0, k becomes: k = (d . T_{max}^2 / d_{max}) in which case T(d) becomes:

$$T(d) = [T_{max}^2 (1 - (d/d_{max}))]^{1/2}.$$

Using this simple equation along with a Poisson distribution of call durations, good estimates of sat-to-sat handover statistics can be obtained. Based on initial observations of MEO orbits with reasonable satellite diversity, it is likely that sat-to-sat call handovers can be avoided system through proper consideration at the call routing stage.

A simple extension of the above formula can be used in order to estimate the cell-to-cell handover statistics. The parameters only need slight alterations, depending on the multibeam coverage geometry. The same distribution for mean call duration is used.

CONCLUSION

Many important factors which affect the Networking aspects of DSCs have been reviewed. Through the use of constellation simulation software providing DSC specific data like those detailed above, the basic groundwork is laid from which more detailed DSC Networking studies can be launched.

These would mainly involve the optimisation of the systems approach to user Mobility Management and Network Resource Management. Based on these results, important Network signalling parameters can be studied allowing these channel capacities to be estimated.

REFERENCES

[1] 'Future Public Land Mobile Telecommunication Systems (FPLMTS)', *CCIR Recommendation 687*, (Question 39/8), 1990.

[2] 'Satellite Constellations for a Global Personal Communication System at L-Band", X. Benedicto et al., *European Space Agency Working Paper 1661*, ESTEC, May 1992.

[3] 'Satellite/PCN Compatibility based on resonant Sun-synchronous Orbits', Cionaith J. Cullen et al., *European Microwave Conference*, Finland, 1992.

Low Earth Orbit Satellite/Terrestrial Mobile Service Compatibility

R.E. Sheriff and J.G. Gardiner
University of Bradford
Dept. of Electrical Engineering
Bradford Road, Bradford, W. Yorkshire, England
Phone: 44 274 384053; Fax 44 274 391521

Abstract (full paper will be provided at the Conference)

Digital cellular mobile "second generation" systems are now gradually being introduced into service; one such example is GSM, which will provide a digital voice and data service throughout Europe. Total coverage is not expected to be achieved until the mid '90s, which has resulted in several proposals for the integration of GSM with a geostationary satellite service. Unfortunately, because terrestrial and space systems have been designed to optimise their performance for their particular environment, integration between a satellite and terrestrial system is unlikely to develop further than the satellite providing a back-up service. This lack of system compatibility is now being addressed by system designers of third generation systems. The next generation of mobile systems, referred to as FPLMTS (future public land mobile telecommunication systems) by CCIR and UMTS (universal mobile telecommunication system) in European research programmes, are intended to provide inexpensive, hand held terminals that can operate in either satellite, cellular or cordless environments. This poses several challenges for system designers, not least in terms of the choice of multiple access technique and power requirements.

Satellite mobile services have been dominated by the geostationary orbital type. Recently, however, a number of low earth orbit configurations have been proposed, for example Iridium. These systems are likely to be fully operational by the turn of the century, in time for the implementation of FPLMTS. The developments in LEO mobile satellite service technology were recognized at WARC-92 with the allocation of specific frequency bands for "big" LEOs, as well as a frequency allocation for FPLMTS which included a specific satellite allocation. When considering integrating a space service into the terrestrial network, LEOs certainly appear to have their attractions: they can provide global coverage, the round trip delay is of the order of tens of ms, and good visibility to the satellite is usually possible. This has resulted in their detailed investigation in the European COST 227 programme and in the work programme of the European Telecommunications Standards Institute (ETSI). This paper will consider the system implications of integrating a LEO mobile service with a terrestrial service. Results will be presented from simulation software to show how a particular orbital configuration affects the performance of the system in terms of area coverage, and visibility to a terminal for various locations and minimum elevation angle. Possible network topologies are then proposed for an integrated satellite/terrestrial network.

A Practical System for Regional Mobile Satellite Services

Randall Glein, Denis Leverson, and Dean Olmstead
Hughes Aircraft Company
Bldg. S64, MS B433
P.O. Box 80002
Los Angeles, CA 90009, USA
Telephone: (310) 364-6808
Fax: (310) 364-5545

ABSTRACT

The Regional Mobile Satellite (MSAT) concept proposes a worldwide, interconnected mobile satellite service (MSS) network in which MSAT-type satellites provide the space segment services to separate regions (i.e., one or a few countries). Using this concept, mobile communications users across entire continents can now be served by a handful of regionally controlled satellites in geostationary earth orbit (GEO). All requirements, including handheld telephone capabilities, can be cost-effectively provided using proven technologies. While other concepts of regional or global mobile communications continue to be explored, the Hughes Regional MSAT system demonstrates the near-term viability of the GEO approach.

REGIONAL MSAT—A NORTH AMERICAN EXAMPLE

Since the advent of mobile communications, users have enjoyed steadily increasing freedom from the constraints imposed by hard wire. Unfortunately, mobile communication has been limited by the height and range of radio towers. But now, high-power regional mobile satellites eliminate these restrictions.

North America, with its highly developed cellular infrastructure, has become a natural first candidate for a regional mobile satellite system. When its MSAT system is launched in 1994, the team of American Mobile Satellite Corp. (AMSC) and Telesat Mobile, Inc. (TMI) will show how entire continents can be served by the high-power spot beams of GEO satellite systems.

This network architecture consists of two MSAT satellites (Figure 1, Table 1), satellite control facilities, various earth stations, and the end users' mobile and fixed terminals. These components are common to any Regional MSAT system.

The North American system's coverage spans the entire United States, Canada, Mexico, Puerto Rico, the Virgin Islands, and the Caribbean (Figure 2). A user anywhere within this range can place a call from his or her
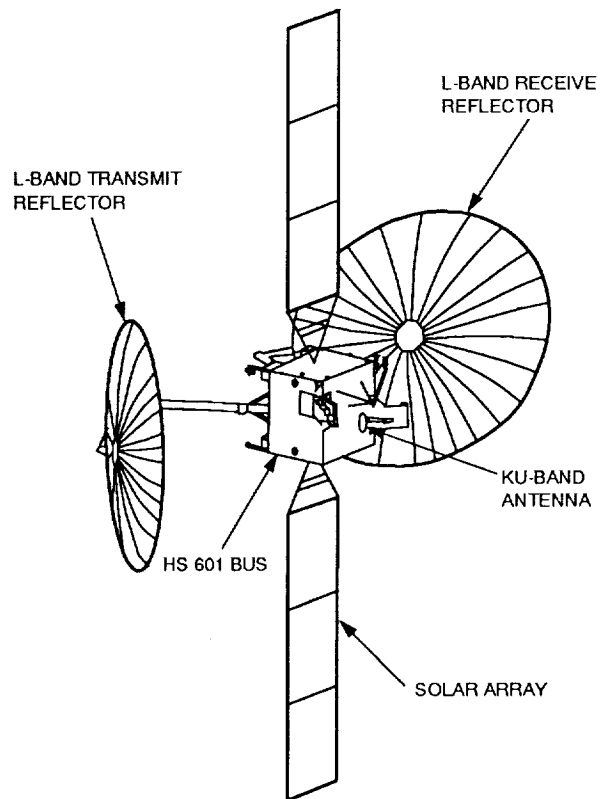
Figure 1. Regional MSAT Satellite

Table 1. Regional MSAT Space Segment Summary

Spacecraft bus	HS 601
Dry weight	2500 lb
EOL power	2880 W
L-band antennas	Two 6 x 5 m deployable mesh reflectors
Ku-band antenna	1 m shaped reflector
L-band frequencies	1530 to 1559 MHz, 1631.5 to 1660.5 MHz
L-band AEIRP	56.6 dBW at 18 dB NPR
L-band G/T	2.7 dB/K (CONUS)
Eclipse capability	85%
Service life	12 yrs
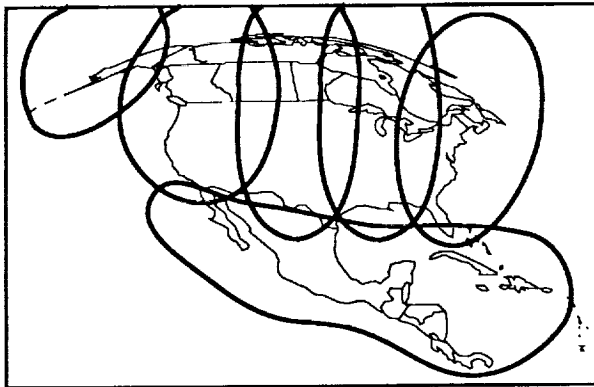
Figure 2. Approximate North American Coverage Pattern

mobile terminal. A dual-mode handset allows users who are within range of a cellular system to have their calls routed through the land-based cellular network while calls from users outside of their home cell site are automatically routed through the satellite system.

Once the call enters the satellite system, one of two Network Control Centers (NCCs) determines where and how to route the call. The NCC monitors the entire ground network [1], choosing the appropriate private or public gateway, assigning communications channels, and routing the call to achieve the most cost-effective communications link. The NCC can optimize resources and maintain service quality at the same time [2].

The system uses proven technology to accommodate a wide variety of mobile terminals. Its architecture, however, allows new technologies to be easily incorporated as they become available. New services can be implemented with no impact to the quality of the existing service. For example, advances in speech compression technology, allowing reduced channel spacing, can be incorporated as they occur with minimal impact.

This is how the technology is being put to use in the North American mobile communications market. But the advantages of this system can be applied in regional markets anywhere in the world.

ADVANTAGES OF A GEOSTATIONARY MSAT ARCHITECTURE

Mobile satellite communications is not just a novel technology application; it is a business opportunity with significant potential for profit. The financial practicality of a Regional MSAT system is one of its most attractive attributes. Though a GEO satellite may cost more per satellite than a medium earth orbit (MEO) or low earth orbit (LEO) satellite, only a single GEO satellite is required to provide complete regional coverage. This translates into system costs dramatically lower than other architectural alternatives [3].

The Regional MSAT offers inherent flexibility and modularity. Using high-power spot beams, it can be tailored to meet the needs of any specific region. This allows the GEO system to be planned and implemented independently of global developments. A Regional MSAT applied in Asia, for example, will have entirely different requirements than a system developed for South America. Yet the two systems can use compatible ground hardware and be interconnected using existing facilities.

The payload design of the Regional MSAT satellite also provides a high degree of flexibility. The design of the hybrid matrix amplification system enables power to be dynamically shared among the various beams. This allows any variation in traffic patterns to be accommodated through real-time allocation of total power among the beams. This approach provides the most efficient use of capacity based on user geography and population density over the life of the system. Additionally, the Regional MSAT provides the ability to tailor coverage by shaping the spot beams to serve only the areas that have the greatest demand. No power is wasted directing coverage beams over unpopulated or unwanted areas.

The system also efficiently uses the frequency spectrum. It employs frequency reuse between nonadjacent beams with sufficient isolation. In addition, with power-limited capacity expected to be roughly 2,000 simultaneous 4.8 kbps voice channels, the total bandwidth requirements allow multiple GEO systems to coexist within the allocated L-band MSS spectrum.

APPLICATIONS IN A REGIONAL MSAT SYSTEM

A Regional MSAT system can meet a myriad of service demands, from personal communications to industry-specific applications to infrastructure development (Figure 3). It augments existing cellular networks by providing service when users roam outside of their coverage areas and expands them by serving uncovered areas. Thus, the Regional MSAT is inherently appealing to both the cellular roamer and the unserved rural mobile user, two of the largest segments of the satellite mobile communications market. The system meets these users' need for personal, handheld communica-

tions in two distinct ways: the dual-mode handset and the pocket phone.

The handset used in the MSAT system is capable of automatically operating in two modes: As a regular cellular phone linked to the region's cellular infrastructure or as a direct link to the satellite. This dual-mode handset increases versatility and ease of user operations. When users are within a cell site, the mobile earth terminal (MET) directs the call to the cellular system. When outside of a cell, the call is routed through the L-band transceiver in the MET. This function is autonomous and transparent to the user.

One model of the dual-mode phone will also have the capability of being a handheld portable cellular phone (Figure 4). When inside a cell site, the handset for this model can be detached and used as a normal portable cellular telephone.

Now imagine that a handset can be disconnected from the MET and operated when the user is beyond the reach of a terrestrial cell site. This is the Regional MSAT pocket phone concept. With the pocket phone, satellite transmission and reception is conducted via a cordless
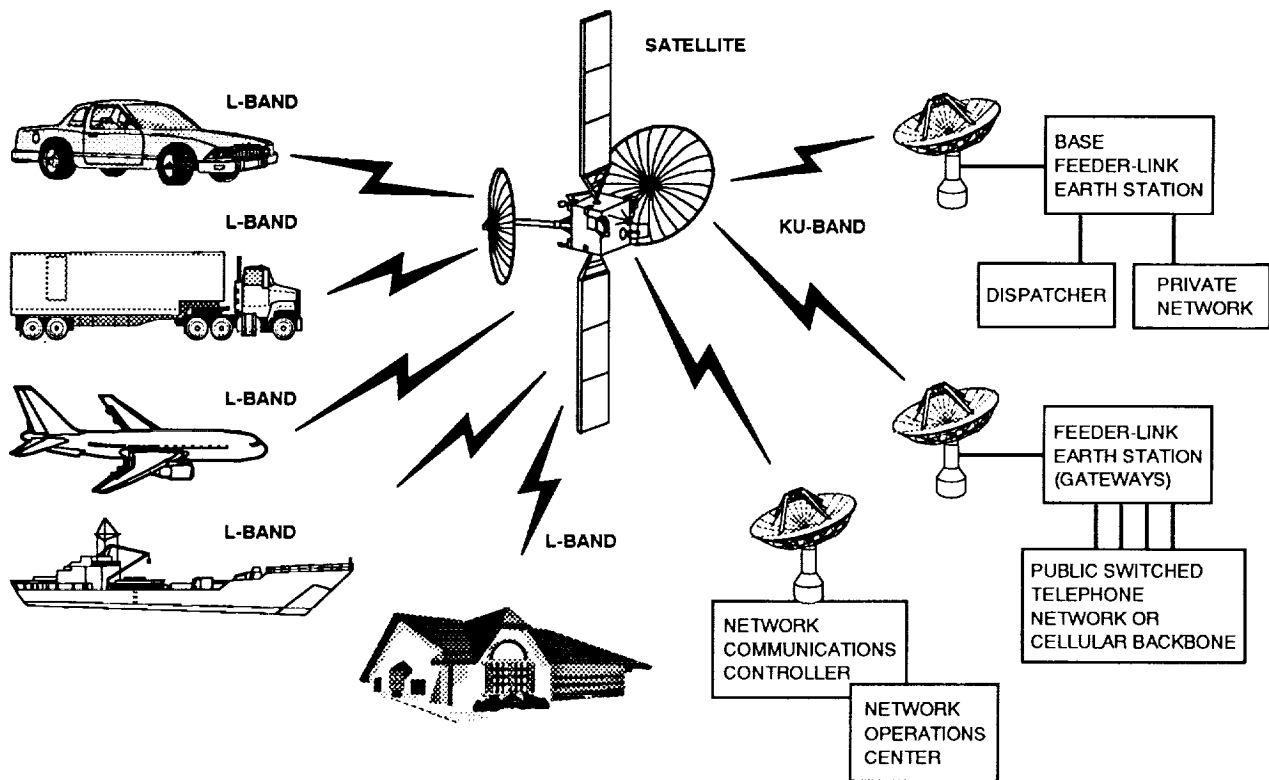
Figure 3. Regional MSAT System

EXTERNAL
MAST ANTENNA

HANDHELD PORTABLE
CELLULAR PHONE

HANDHELD PORTABLE
CELLULAR PHONE

REMOVABLE LEAD
TO EXTERNAL
ANTENNA

DOCKING CRADLE
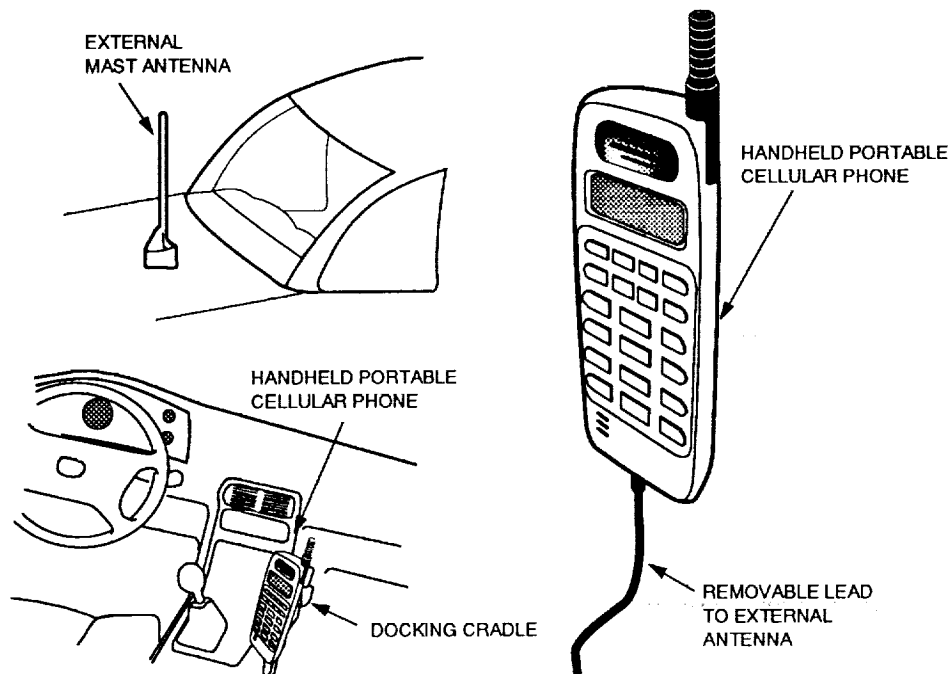
Figure 4. Multimode Phone

connection between the handset and the MET. Users need only stay within range of their MET "base station" to complete their links to the satellite, a position they are most likely to be in if they are beyond the reach of cellular communications. These capabilities give a Regional MSAT system the ability to meet the variety of personal communications needs seen in the market today, and in the foreseeable future.

Regional MSAT applications reach well beyond personal voice communications. One of the largest applications in the North American system is for the trucking industry. The MSAT system allows each vehicle to be in constant contact with a home base, customer, or destination. This is especially useful for just-in-time deliveries, in-route itinerary changes, and roadside emergencies. Mobile terminals can be equipped with Global Positioning Service (GPS) or RS-232 ports to allow voice, digital data, and positioning services to be provided. Similar applications exist for the airline and rail industries, where reliable logistical communications are essential while in route and many passenger telecommunications services are being increasingly demanded.

The system's architecture also accommodates private networks. Users can implement a virtual private network if they need that level of autonomy in their service. Users demanding a truly private network can operate their own gateway and ground station infrastructure including a dedicated link to the satellite. Both types of services are very attractive to private sector organizations that have large numbers of users, as well as government and public sector organizations such as the police, public utilities, and agencies responsible for developing a country's natural resources.

In areas where the traditional land-based communications infrastructure is still in development, a Regional MSAT system provides excellent access into rural areas that even fixed satellite services (FSS) cannot economically serve. When the cost of building an infrastructure is prohibitive, FSS-provided thin route services can be cost-effective, except when service demands are extremely low. In this case, MSS provides a cost advantage over even FSS-delivered telephone service.

REGIONAL MOBILE SATELLITE SYSTEM ECONOMICS

To assess the business viability for a regional MSS system, we must understand the economics from the perspective of both purchasing and providing service. In its initial form, the MSAT system in North America will

546

provide mobile terminals for under $2,000 each and offer voice service rates that are competitive with existing cellular roaming charges. Over time, as the subscriber base expands, these costs are likely to decrease and become affordable to more customers, thus increasing demand for mobile satellite capacity. The introduction of Regional MSAT systems around the world will expand the market for space segment, terrestrial network, and subscriber hardware, which will translate into further cost reductions to the ultimate consumers of the services.

For the service provider, the economics revolve around the start-up capital expenses, the revenues derived from subscribers, and to a lesser extent, the annual operating expenses required to run the business. From an organizational standpoint, the MSAT architecture allows various degrees of vertical integration. For example, independent service providers can provide the interface between the space segment provider and the mobile users. The space segment provider may be a wholesaler of satellite capacity, or may directly serve end users, large or small.

The following economic analysis takes the perspective of a space segment provider who provides retail services directly to mobile communicators.

Capital expenses of $400M are assumed, which includes one high-power satellite, a launch vehicle, launch insurance, and supporting ground infrastructure such as a telemetry and command facility and mobile communications network control functions. These expenses are all incurred during a three-year construction period before satellite launch.

The annual operational expenses are broken down into two categories. First is a variable expense for marketing that is based on $300 for each subscriber added to the system plus a fixed percentage (10%) of revenues that is designated for general promotion and marketing of the various mobile services. The second category is a fixed expense equal to 20% of the original capital expenses per year to account for other operating, general, and administrative expenses. These assumptions are based on, but not identical to, the cellular business model of reference [5].

Revenues are generated on an individual subscriber basis over the twelve-year satellite life,

where the average subscriber is assumed to spend $100 per month on mobile services, which could include voice, data, or a combination. This amount is assumed to include usage and monthly access fees that may be charged.

The number of subscribers is assumed to increase linearly to a maximum level of 400,000 users, based on the assumptions of 10,000 minutes per channel per month, a power-limited system capacity of 2,000 simultaneous channels, and average usage of 50 minutes per subscriber per month. This maximum level of subscribers is achieved in the fifth year of operations after launch. The analysis also includes a 2% subscriber churn rate per month, which is the monthly turnover of subscribers who drop the service. This impacts both revenues and marketing expenses.

Finally, it is also assumed that the system provider captures only 80% of the total revenues. The remaining revenue, in addition to the new subscriber marketing expenses described above, is distributed among other independent service providers for their role in signing up new subscribers and administering billing services.

The result, on a pre-tax basis, is an internal rate of return to the system provider of approximately 20%. Assuming a capital cost of 15%, this scenario results in a net present value (NPV) of roughly $135M. Financing is not included, thus the returns may be understated because potential leverage effects resulting from debt financing are not accounted for. Additionally, this scenario results in a payback period on the capital investment in just over 5 years after launch. Note also that this analysis assumes launch of only one spacecraft, which eliminates opportunity for growth after achieving system capacity, thus limiting financial returns which could be experienced by accommodating more users.

The business risk of this system is low, based on the population that can be covered from a single GEO satellite. With a capacity of 400,000 users, this type of system need be adopted only by a small percentage of the population. For instance, in a region of one billion people, a penetration rate of only 0.04% will fill the system, whereas a region with 250 million people will need to be adopted by 0.16% of the

population. These figures seem more than plausible even when the predicted availability of cellular capacity is used to limit the addressable market size.

This economic analysis is not intended to represent the only way to implement a regional mobile satellite business, but to demonstrate that a Regional MSAT system in geostationary orbit offers the potential for lucrative returns to investors. In addition, the revenue of $100 per subscriber per month can be interpreted as $50 in access fees and an average of only $1.00 per minute of usage, which is significantly below those rates expected with alternative system architectures.

CONCLUSIONS

The mobile communications market is one of the fastest growing segments of the global economy. Technology that exists today is fully capable of supporting mobile communications for entire geographic areas. Through a GEO satellite system, MSAT developers can tailor an open systems architecture to meet the unique needs of a specific region's mobile communications users. In time, as new technologies become economically viable, a Regional MSAT system can evolve, eventually providing direct-to-handheld global communications coverage. With virtually unlimited applications available today at a cost-effective rate, the Regional MSAT provides a practical—and affordable—choice for introducing mobile voice and data services to regional mobile satellite service markets around the world.

REFERENCES

[1] J. Lunsford, R. Throne, D. Gokhale, W. Garner, and G. Davies, "The AMSC/TMI Mobile Satellite Services (MSS) System Ground Segment Architecture," *A Collection of Technical Papers, Part 1; The 14th International Communication Satellite Systems Conference and Exhibit, March 22-24, 1992, Washington, DC*, pp. 405-426.
[2] L. White, A. Agarwal, B. Skerry, B. Tisdale, "North American Mobile Satellite System Signaling Architecture," *A Collection of Technical Papers, Part 1; The 14th International Communication Satellite Systems Conference and Exhibit, March 22-24, 1992, Washington, DC*, pp. 427-439.
[3] B. Elbert, P. Louie, "The Economics of Mobile Service by Satellite," *Proceedings of the Second International Mobile Satellite Conference, IMSC '90, Ottawa, Ontario, Canada, June 17-20, 1990*, pp 1875-1885.
[4] D. Whalen, G. Churan, "The American Mobile Satellite Corporation Space Segment," *A Collection of Technical Papers, Part 1; The 14th International Communication Satellite Systems Conference and Exhibit, March 22-24, 1992, Washington, DC*, pp. 394-404.
[5] E. Kwerel, J. Williams, "CHANGING CHANNELS: Voluntary Reallocation of UHF Television Spectrum," *OPP Working Paper No. 27, Office of Plans and Policy, Federal Communications Commission, November 1992.*

Advanced Mobile Satellite Communications
Using COMETS Satellite in MM-wave and Ka-band

N94-22829

Shingo Ohmori, Shunkichi Isobe,
Makoto Takeuchi, and Hideyuki Naito

Communications Research Laboratory
Ministry of Posts and Telecommunications
Koganei, Tokyo 184, Japan
Tel. +81-423-27-7504
Fax. +81-423-27-6825

ABSTRACT

Early in the 21st century, the demand for personal communications using mobile, hand-held and VSAT terminals will rapidly increase. In a future system, many different types of services should be provided with one-hop connection. The Communications Research Laboratory (CRL) has studied a future advanced mobile satellite communications system using millimeter-wave and Ka-band. In 1990, CRL started the Communications and Broadcasting Engineering Test Satellite (COMETS) project. The satellite has been developed in conjunction with NASDA and will be launched in 1997. This paper describes the COMETS payload configuration and the experimental system for the advanced mobile communications mission.

INTRODUCTION

Early in the 21st century, the need for personal communications will rapidly increase in fixed and mobile satellite services. In this environment, a mobile satellite communication system will become place, not only for use in airplanes, ships and automobiles but also in hand-held terminals and portable VSATs. Personal services offered will include many different types of transmission, from low-bit-rate data such as information of message or voice to the high-bit-rate data of still picture or band-compressed video. In to offer wide variety of services, it will be important to provide a function of one-hop connection among mobiles and VSAT terminals. It will also be necessary to develop essential techniques and devices such as beam interconnecting and hand-held terminals to realize low-cost and user-friendly systems.

The 1990's will be an era of commercial mobile satellite communications, following upon the research and development phase in the 1980's such projects as the ETS-V in Japan, PROSAT in Europe and MSAT-X in USA. In some countries, research on future mobile satellite communications systems using millimeter-wave and Ka-band has already started. For example, the ACTS program in the U.S.A. is a well-known satellite program in this category [1].

In Japan, the Communications and Broadcasting Engineering Test Satellite (COMETS) project was authorized by the government in 1990. A COMETS satellite is scheduled to be launched by an H-II rocket at the beginning of 1997. Its mission is to provide a test bed in the development of advanced technologies for the future satellite communications and broadcasting systems. One of the main purposes of COMETS is to study the feasibility of advanced mobile communications systems in millimeter-wave and Ka-band. This study will be carried out on the basis of the vast amount of research experiences of Communications Research Laboratory (CRL), such as the ETS-V and ETS-VI satellite programs [2][3].

This paper describes the COMETS payload configuration and the experimental system for the advanced mobile communications mission.

MISSON OF AN ADVANCED MOBILE SATELLITE COMMUNICATIONS

COMETS Project

The COMETS is a joint project of CRL and Japan's National Space Development Agency (NASDA). COMETS has three mission payloads. The first is an advanced mobile satellite

communications system using millimeter-wave and Ka-band, which is developed by CRL. The purpose of this mission is to develop basic technologies to realize advanced mobile satellite communications systems. The second is a 21 GHz band advanced broadcasting system developed by CRL and NASDA. The third is an inter-orbit communication system developed by NASDA using S-band and Ka-band.

Figure 1 shows a conceptual sketch of the COMETS satellite and Table 1 shows its major characteristics of COMETS. The COMETS is a three-axis stabilized geostationary satellite and has three deployable antennas and about 32 m from tip to tip along a solar arrays. Its mission life is three years and the in-orbit weight is about two tons.

Table 1   Outline of COMETS

Launch date	in Beginning of 1997
Launch vehicle	H-II rocket
Orbit position	121° E longitude
Mission life	3 years
Shape/ dimensions	Rectangular parallelepiped (approx. 2 x 3 x 3 m) Approx. 32 m length along solar arrays
Weight	for Launch : 3.8 tons for Initial geostationary position : approx. 2 tons
Power	Approx. 5.4 kW or more at end of life
Attitude stabilization Method	Three axes stabilization (feed forward compensation when the antenna is driven)
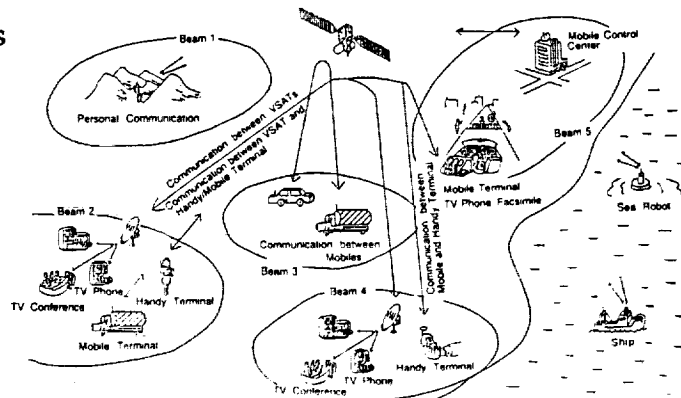
Fig.2 Service Image of Advanced Mobile Satel lite Communications System.

Fig.1 Conceptual Sketch of COMETS satellite.

Objectives of Advanced Mobile Satellite Communications Mission

Figure 2 shows a service image of an advanced mobile satellite communications system. This system has an on-board multibeam antenna, the beams of which must be connected each other. With this system, it will be possible to offer many different types of services as voice or message communications using hand-held terminals, TV phone or facsimile services using mobile terminals, and TV conference services using VSATs.

One of the objectives of the advanced mobile satellite communications mission is to develop key technologies and devices for application in the future systems. These technologies and devices are the following:

(a) One-hop connection between handy, mobile and VSAT terminals

(b) Very small millimeter-wave and Ka-band antennas for handy and mobile terminals (e.g. active phased array), and antenna tracking techniques

(c) A multi-beam interconnecting technique

(d) A link-control system for a regenerative transponder

(e) New applications for mobile satellite communications

The COMETS will develop the millimeter-wave and Ka-band frequencies for advanced mobile satellite communications. These frequencies are suitable for future mobile satellite communications because antennas of an earth terminal can be made small enough for handy terminals and they have sufficient bandwidth to provide a large capacity for a great number of terminals including personal users.

ADVANCED MOBILE SATELLITE
COMMUNICATIONS MISSON PAYLOAD

550

Outline

Table 2 shows an outline of the mission payload of advanced mobile satellite communications mission of the COMETS. The antenna has three beams; two adjacent Ka-band beams (Tokyo and Nagoya beams) and a millimeter-wave beam (Tokyo beam). As shown in Figure 3, the payload consists of the multibeam antenna, millimeter-wave and Ka-band transmitters and receivers, an IF filter bank and regenerative MODEMs which have a function of 2x2 matrix beam interconnecting.

The frequencies used in the COMETS system are 47/44 GHz bands for millimeter-wave communications and 31/21 GHz bands for Ka-band communications.

Table 2   Outline of Misson Payload

Antenna	Spot beam antenna shared with MM-wave and Ka-band (shared with feeder link antenna for inter-orbit communication) Diameter : 2 m, Circular polarization, Antenna pointing system
Beam	Two Ka-band beams (Tokyo and Nagoya beams) One MM-wave beam (Tokyo beam)

Frequency	Ka-band : 30.75-30.85 GHz (uplink)
	        20.98-21.07 GHz (downlink)
	MM-wave : 46.87-46.90 GHz (uplink)
	        43.75-43.78 GHz (downlink)

Ttransponder	Ka-band : 2 (20W and 10W SSPA) MM-wave : 1 (20W TWTA)

Operation
mode
	IF repeater :
	  2 x 2 matrix beam interconnecting by IF filter bank
	  Wide band filter (6 MHz) and narrow band filter (500 kHz)
	Regenerative transponder :
	  8 ch SCPC (uplink) / TDM (downlink)
	  Beam interconnecting by baseband switching

Multibeam Antenna

The 2-m-diameter antenna is used for both millimeter-wave and Ka-band communication. Figure 4 shows footprints of the COMETS's receiving antenna. The antenna has one spot beam in the millimeter-wave, of which the maximum gain is 55 dB. It has other two spot beams in the Ka-band, which cover Tokyo and Nagoya areas, respectively. Maximum gains of the receiving antenna are 48.3 dBi for the Tokyo beam and 45.4 dBi for the Nagoya beam. The Ka-band two beams are located close to each other for purposes of an experiment on interbeam interference. The 3 dB contour diameter of each beam is about 300 km. The antenna has an antenna pointing system which tracks a beacon signal transmitted by an earth station.

RF Section

The transponder consists of 20W and 10W Solid State Power Amplifiers (SSPAs) for Ka-band communications, a 20W TWTA for milli-
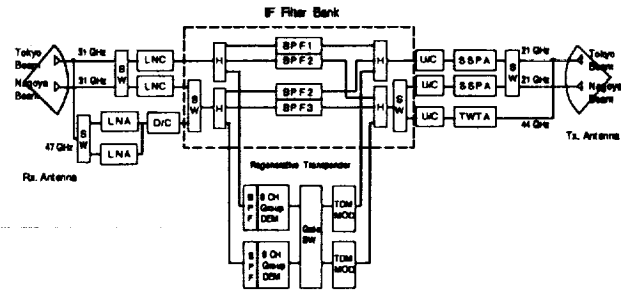
Fig.3 Block Diagram of a Transponder
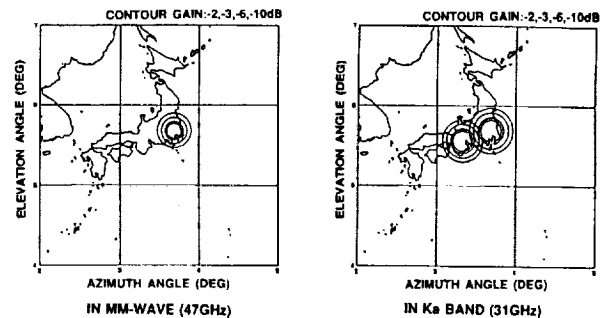
Fig. 4 Footprints of COMETS Receive Antenna.

meter-wave communications, and LNAs. An HEMT-LNA with a very low noise figure of 2.5 dB has been developed for millimeter-wave communications. The transponders for the two Ka-band beams can be switched if a malfunction occurs in either one. The frequency converters have a common local oscillator which is adopted to make it easy to compensate for frequency drift in the satellite. A frequency of the local oscillator is 14 MHz and its temperature stability is $2 \times 10\text{-}7$.

IF Filter Bank

Signals from an uplink beam are divided by the IF filter bank into three frequency sub-band, and each sub-band interconnects between Tokyo-Tokyo, Tokyo-Nagoya and Nagoya-Nagoya. Each frequency band is preassigned to each beam. With this simple and flexible method, various types of signals can be transmitted via a transparent transponder.

In using a transparent repeater, it is desirable to optimize a transponder gain and a frequency bandwidth in order to increase satellite transmitting power (EIRP) and reduce a noise power. In order to carry out communications experiments at various transmission speed,

transponders are equipped with two kinds of filters with bandwidths of 6 MHz and 500 kHz. The transponder gain can be changed within a 30 dB range.

Though the satellite has three beams, only two of them, i.e., the Tokyo beam in Ka-band, and either the Ka-band Nagoya beam or the millimeter-wave beam can be used at the same time. Then 2x2 matrix beam interconnection is achieved in the IF filter bank. Figure 5 shows the IF frequency allocation bound for the Ka-band Tokyo beam. The IF filters of each beam consist of two wide-band 6 MHz filters, and two narrow-band 500 kHz filters, and an 800 kHz filter for a regenerative MODEM. Therefore, the frequency bandwidth of each transponder is 36 MHz, including a guard band. All filters are SAW filters.

Regenerative Transponder

Table 3 shows an outline of a regenerative transponder. Eight-channel SCPC signals are received at one regenerative MODEM and a single TDM signal is transmitted. The SCPC signal transmission rate is 24 kbps or 4.8 kbps with a BPSK modulation. Eight-channel SCPC signals are demultiplexed by a digital polyphase-FFT filter and demodulated discretely. Convolutional coding with a rate 1/2 and a Viterbi decoding are used as a forward error correction (FEC).

A link control system must have such functions as channel set-up, and SCPC and TDM channel assignment. This control is achieved in the satellite by using one SCPC packet signal channel and one TDM signal time slot. The system has functions suitable for mobile satellite

Fig.5 IF Frequency Allocation for Ka-band Tokyo Beam.

communications. In order to increase link occupancy, a set-up demand from an earth terminal is stored once in a satellite buffer memory with a capacity of 20-channels and signals are assigned to a vacant channel in order. In the case of land mobile communication, a link is held for a given period of time when the link is temporarily disconnected by shadowing, or the link is disconnected automatically after a limited time when, for example, an automobile goes through a tunnel. Such a link control algorithm is under study based on the experiences of the mobile satellite communication experiments using the ETS-V satellite in 1.6/1.5 GHz.

ADVANCED MOBILE SATELLITE COMMUNICATIONS EXPERIMENTS

Example of Link Budget

The earth stations shown in Table 4 are considered to be used in the experiment. The base station will be located in the Kashima Space Research Center of the CRL.

Table 5 shows an example of a link budget. The earth terminal is located at a point where the satellite antenna gain is the maximum. In the case of an IF filter bank, a 24 kbps or 4.8 kbps signal can be transmitted between land mobile earth stations with 20-cm or 10-cm-diameter antennas in Ka-band. In the case of a regenerative transponder, the required transmitting power of an earth terminal should be enough to satisfy only the uplink C/No, because uplinks and downlinks are independent. An earth terminal with a 10-cm-diameter antenna can transmit a 24 kb/s signal at 1 W in Ka-band.

The satellite antenna gain is not so high, however, it is sufficient for experiments to verify key technologies. At the crossover point

Table 3 Outline of a Regenerative Transponder

Uplink	: SCPC
Downlink	: TDM
Number of channels	: 8 ch / beam 6 ch for continuous signals 2 ch for packet signals (including 1 ch for channel assignment)
Transmission Rate	: 24 kb/s or 4.8 kb/s
Modulation	: BPSK
Demodulation	: Polyphase-FFT filter bank and Discrete BPSK demodulation
FEC	: Rate 1/2 convolutional code Viterbi decode

552

Table 4 Earth Stations for Experiments

	Antenna Diameter	Transmitting Power	Typical Data Rate
Base Station	3~5 m	more than 20 W	
VSAT	about 30 cm	about 4 W	300 kbps
Mobile Terminal	10~20 cm	about 2 W	24 kbps
Handy Terminal	5~10 cm	about 0.5 W	4.8 kbps

Table 5 Example of Link Budget

Operation mode		IF repeater			Regen.Trans.
Frequency		Ka-bad	Ka-band	MM-band	Ka-band
Transmission rate	kb/s	24	4.8	4.8	24/192
Tx. earth station					
Tx. power	W	0.46	0.41	0.82	1.05
Tx. antenna diameter	cm	20.0	10.0	10.0	10.0
Tx. antenna gain	dB	30.2	24.2	27.8	24.2
Pass loss	dB	214.3	214.3	218.0	214.3
Rain margin	dB	5.0	5.0	7.0	5.0
S/C (receiving)					
Rx. antenna gain	dB	47.4	47.4	45.8	47.4
Rx. power	dBm	-115.1	-121.6	-122.2	-117.5
No	dBm/Hz	-169.7	-169.7	-169.7	-169.7
Uplink C/No	dB·Hz	54.6	48.1	47.5	52.2
S/C (transmitting)					
Transponder gain	dB	140.0	145.0	145.0	-
Tx. power	W	0.31	0.22	0.19	4.20
Tx. antenna gain	dB	45.0	45.0	47.8	45.0
Pass loss	dB	211.4	211.4	217.8	211.4
Rain margin	dB	2.5	2.5	4.0	2.5
Rx. earth station					
Rx. antenna gain	dB	28.4	22.3	28.7	22.3
Rx. power	dB	-115.6	-123.2	-122.4	-110.4
No	dBm/Hz	-171.5	-171.5	-171.5	-171.5
Downlink C/No	dB·Hz	55.9	48.3	49.1	62.1
Required C/No	dB·Hz	52.2	45.2	45.2	-

Location of earth station : Center of Tokyo beam
BPSK, Required Eb/No=8.4 dB (BER=10 -4)

of two Ka-band beams, the satellite receiving antenna gain lowers by about 8 dB compared to the maximum. A communication experiment on crossing beams can be conducted when a lower transmission rate is used or the experiment is conducted on a fine day free from rain attenuation. Communications experiments with a few tens of terminals at the same time is possible under restrictions such as no rain attenuation and low bit-rate communications.

Experimental Items

Items of advanced mobile satellite communications experiments using COMETS are:
(a) Various communications experiments including personal communications
(b) Experiments on a link control and an interbeam connection
(c) Propagation experiments considering shadowing and rain attenuation
(d) Evaluation of the satellite antenna and the transponders
(e) Evaluation of the land mobile earth stations

CONCLUSION

In this paper, the payload configurations of the COMETS satellite for advanced mobile satellite communication experiments and the experimental system are described. As a mission of advanced mobile satellite communications, advanced technologies are onboard the satellite such as multibeam antennas, 20 W and 10 W SSPAs in an Ka-band, a 20 W TWTA, an LNA with an excellent noise figure of 2.5 dB in a millimeter-wave, an IF filter bank, and a SCPC/TDM regenerative MODEM. The characteristics of all these on-board equipment should be proved in space for the first time in the world.

The COMETS program is now in progress and the transponders are being developed.

Further studies on the satellite and earth terminals are being carried out to establish basic technologies in advanced mobile satellite communications in millimeter-wave and Ka-band.

REFERENCES

[1] R.Richard et al., "Advanced Communications Technology Satellite (ACTS)", ICC'89, 52.1-12, 1989.
[2] N.Hamamoto et al., "Results on CRL's Mobile Satellite Communication Experiments Using ETS-V", Space Communications, No.7, pp.483-493, 1990.
[3] M.Shimada et al., "Experimental Millimeter-Wave Satellite Communications System", 17th Int. Symposium on Space Technology and Science", O-4-3, Tokyo, May 1990.
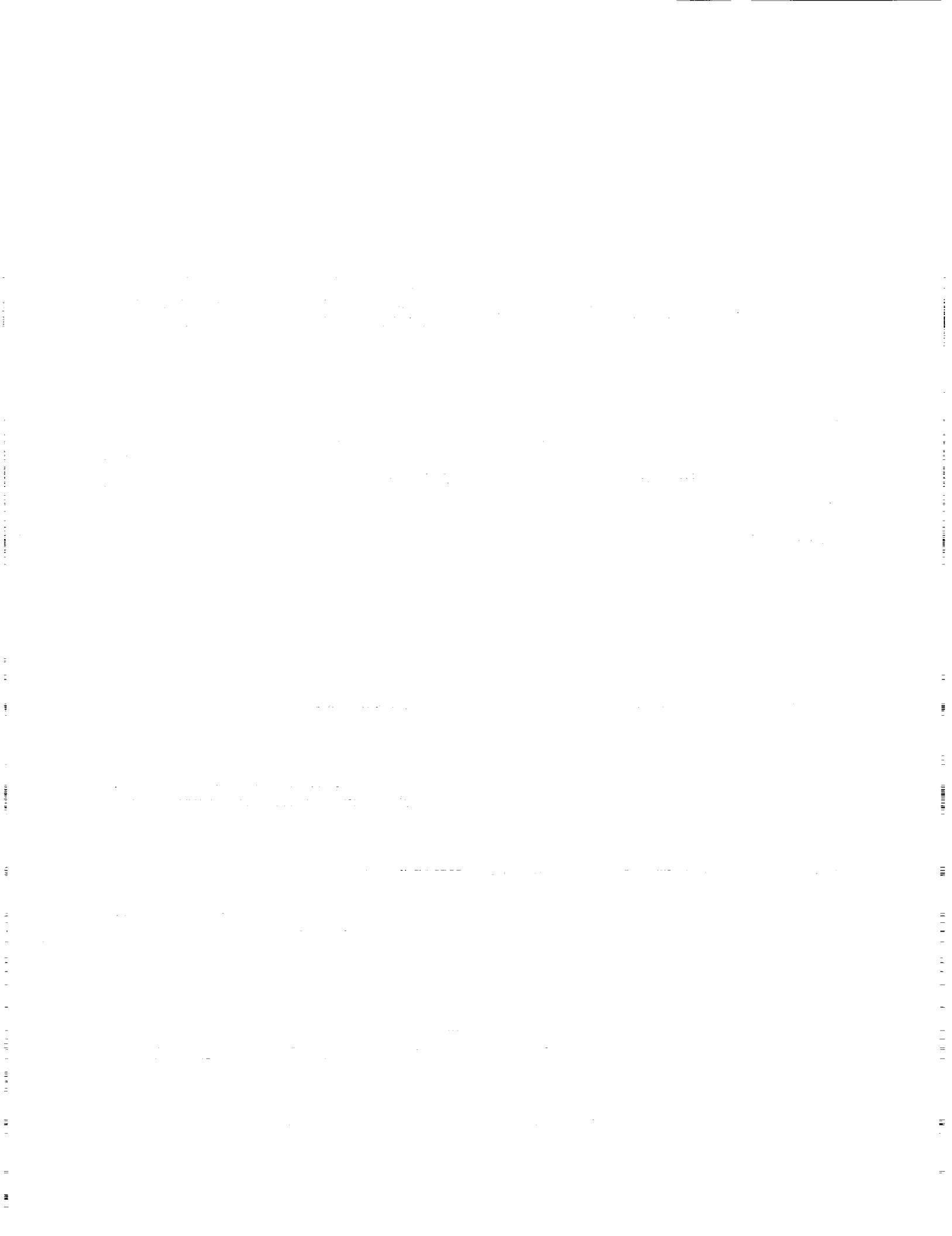
Session 12
Mobile Terminal Antennas

Session Chair—*Lot Shafai,* University of Manitoba, Canada
Session Organizer—*Martin Agan,* Jet Propulsion Laboratory, U.S.A.

Low Cost Antennas for MSAT Vehicular Applications

L. Shafai* and M. Barakat**
*Dept. Electrical and Computer Engineering, University of Manitoba
Winnipeg, Manitoba, Canada
Telephone: (204) 474-9615, FAX: (204) 261-4639
**InfoMagnetics Technologies Corporation
Winnipeg, Manitoba, Canada
Telephone: (204) 945-8811   FAX: (204) 945-1784

ABSTRACT

For Mobile MSAT applications a number of vehicular antennas have been developed that meet the program requirements. They are, however, costly to manufacture. Two antenna candidates are described here that provide adequate gain in the coverage zone and are also lower cost. One is the mast antenna that uses 3 or 4 element arrays of aquadrifilar helices. It generates omni-directional pattern in azimuth and its beam is scanned in elevation. The second unit is a planar spiral antenna and generates directional beams by a summation of the azimuthal modes. A variation of this antenna uses conical spirals to fulfill the same task. In both cases beam scanning is achieved by means of electronic switches rather than phase shifters, thus resulting in simpler configurations.

INTRODUCTION

For mobile vehicular applications several designs have already been implemented, that can be classified in three categories of arrays with electronic scanning, switched beam arrays and antennas with mechanical beam scan. For electronic scanning arrays a number of different designs and concepts have been proposed and evaluated, but, the most accepted configuration is the 19-element hexagonal array. An analysis of such arrays with microstrip circular patch elements showed the mutual coupling as the main cause for reduction of the gain in excess of element pattern role off [1]. For low elevation angles around 15-30 degrees in Canadian coverage zone, the mutual coupling affects both input impedance of the array elements and far field patterns and, consequently, decreases the array gain. Such studies also indicated that, attempts to increase the scanned gain of the array, by increasing the array size, is not successful because of enhanced mutual coupling effects with array size. The 19-element hexagonal array provides reasonable gain levels of around 10 dBic at low elevation angles and is also small in size, not to increase the cost excessively. This array configuration has therefore been selected as the most suitable candidate and implemented by a number of research groups and both microstrip circular patch and crossed-slots have been used for the array elements. The performance of these arrays are reported in literature [2-4]. For these arrays the main cost is in the beam forming electronics, that also adds to the antenna loss with subsequent reductions in G/T of the array and its power efficiency.

To remedy these problems an attempt was made to reduce the beam forming network size by utilizing dual mode array elements [5]. An array using stacked

microstrip circular patch elements was studied both analytically and experimentally. It was shown that for low elevation angles a seven-element array of stacked elements can give gain levels similar to the conventional 19-element arrays. The new array, however, required only thirteen (13) phase shifters, in lieu of eighteen (18) for the conventional arrays.

In the switched beam array category, an interesting antenna is designed and implemented using a simulated parabolic reflector antenna. The reflector surface is made by rings of monopoles that is fed by a central monopole. The reflector surface, and consequently the antenna beam, is rotated by switching monopoles preferentially open or short by a diode at their base [6]. The design is simple and does not require phase shifters for its beam scan, i.e. has lower cost and better G/T and power efficiency. However, it is linearly polarized and also not low profile, and adding a polarizer raydome further increases its height.

Because of the cost and losses associated with the beam forming network of the above arrays, mechanical scanning shows a number of attractive features, and has also been considered by a number of investigators. The most interesting design uses an array of Yagi elements made of four square microstrip patches [7]. It provides a narrow beam in azimuth that is rotated mechanically. In the elevation the beam is broad and does not require a scan. While mechanically scanned antennas offer a possible advantage in improved G/T, they naturally suffer from reliability, especially in colder regions. Electronic scanning is still the most desirable approach to consider.

Here, two new designs are introduced that have potential for low cost implementation. They provide medium gains for small size and can be used for high gain applications as well. Their advantage, however, is for medium gain antennas, where they can be fabricated at low cost.

They are based on a vertical array of helices and an array of spirals, planar or conical. Their operation principle and performance are presented briefly

Mast Antenna

The geometry of the antenna is shown in Fig. 1, and consists of a 3 or 4-element helical array. Each array element is a miniature quadrifilar helix of diameter of about 1.5 cm, and a length of one wavelength. It resembles a whip antenna that is commonly used in vehicles, and expected to have good user acceptance. Their radiation pattern is therefore omnidirectional and a beam scanning in the azimuthal direction is not necessary. However, to provide a minimum gain of 8 dBic, the array beam in the vertical direction reduces to around 15 degrees and the gain coverage is achieved by scanning in the vertical plane. A simulated gain pattern of one such array is shown in Fig. 2 and provides computed gains in excess of 9.5 dBic. The measured gain of the array element has shown that the phase error and mismatch losses reduce the gain by as much as 1 dB, within the range of the required transmit and receive bands. The expected achievable gain with a four element array is therefore around 8 dBic. This array is currently under development, and a measured pattern of the element is shown in Fig. 3. It yields a gain of 3.33 dBic and has a beam peak at 35° elevation ($\theta=55°$), ideal for beam scanning in the required range.

Planar Array

The concept of beam generation and scan using the azimuthal modes was described in earlier papers [8-9], where stacked microstrip disk antennas were used to generate the far fields of higher order TM_{n1} modes. It was shown that, selecting N-azimuthal modes, for n=1, 2, 3...N, can

558

generate a pencil beam which tilts progressively towards the plane of the array, by increasing N, the total number of azimuthal modes. Furthermore, it was shown that with circularly polarized elements the beam can be scanned readily by introducing a phase shift δ between the adjacent modes, determined by the relationship $\delta_n = n\delta_1$, where δ_1, is the phase shift of the first azimuthal mode and δ_n that of the nth mode. With such an array the number of phase shifters is limited to N-1, and the phase shift increments increase linearly with the mode order, thus resulting in progressively simpler phase shifters. The method therefore provides an array with a high scan gain at lower elevation angles simply by using higher order azimuthal modes which reduces the number of required phase shifters to a relatively small number, simplifies the phase shifter implementation and array configuration by limiting the higher order digital phase shifter to a small number.

With the above approach using phase shifters, even small number of them, between the higher order azimuthal modes still introduces phase shifter loss to the array and limits its performance. The cost associated with the phase shifter also increases the array cost. The same also applies to the Butler matrix feeds that introduce losses of similar order as the phase shifters to the array and limits its performance. An alternative approach was also proposed [9] that eliminates the phase shifter requirement, or the Butler matrices, and the array beam is scanned by a beam switching. The array loss is therefore limited only to the insertion loss of the switch, which is normally smaller than the loss of a phase shifter or the Butler matrix. Also, and for the same reason, the array cost is reduced. Here, the concept of beam forming is presented and samples of measured patterns are provided.

Basic Relationships

Assume an array consists of N antennas each radiating one of the azimuthal modes. Such an array can be implemented by N microstrip patches supporting TM_{n1} modes. Alternatively, they can be annual slots, wire loops, circular horns or any antenna with azimuthal symmetry. Here, a design using planar spirals is provided. The components of the far field radiation is therefore the summation of the far fields due to these modes and for circularly polarized antennas can be shown to be

$$\varepsilon_\theta^c = \sum_{n=1}^{N} f_n(\theta)\ e^{in\phi} \tag{1}$$

$$\varepsilon_\phi^c = \sum_{n=1}^{N} g_n(\theta)\ e^{in\phi} \tag{2}$$

where f_n and g_n are the θ-dependent parts of the field which are of the form

$$f_n(\theta) = \frac{V_n k a_n}{2}\ \frac{e^{-ikr}}{r}\ j^n[J_{n+1}(ka_n\sin\theta) - J_{n-1}(ka_n\sin\theta)] \tag{3}$$

$$g_n(\theta) = j\frac{V_n k a_n}{2}\ \frac{e^{-ikr}}{r}\ j^n[J_{n+1}(ka_n\sin\theta) + J_{n-1}(ka_n\sin\theta)] \tag{4}$$

In these equations a_n is the antenna aperture radius for radiating the nth mode and V_n is the excitation coefficient, and may be used to shape the array radiation pattern. Also, it is assumed that the excitations of different azimuthal modes are on the same azimuthal plane, such as the $\phi=0$ plane. The factor j^n in eqs (3) and (4), therefore indicates that the array beam will be directed along the $\phi=90°$ direction. Since the radiation fields are simple Fourier series, it can be shown that the beamwidth of the radiation patterns are given by $BW \simeq 2\pi/N$ and the array gain is approximately equal to $20\log_{10}(3.3\ N)$, which provides gains in

559

the range of 8, 10, 11, 12, and 13 dBic for N=2, 3, 4, 5 and 6 azimuthal modes. Since azimuthal modes radiate progressively at lower elevation angles, by increasing the number of modes the array beam gradually moves towards the array plane, i.e. the lower elevation angles. Thus, in using such a concept to design an array for vehicular applications, an appropriate number of modes are needed to form the beam in the azimuth, to increase the array gain to the desired range. The beam scanning in the azimuth provides the full coverage.

Design Examples

The concept of arrays using azimuthal modes was initially studied using stacked microstrip patch antennas, each radiating different modes. An alternative design is selected using multi-arm spiral antennas. It is a circularly polarized antenna and provides good performance over a wide frequency band. With this configuration the required azimuthal modes, i.e. n=1, 2,... N, are generated by the array symmetry, and not by different array elements. It is, thus, a suitable configuration for low cost fabrication. For this class of antennas the mode excitation and far field radiations have been studied for a large number of samples including different spiral arms, feed networks, and effects of a ground plane size. Here, the results for three examples are presented.

Fig. 4 shows the geometry for a four arm spiral, that was used in the study. A phasing network in the central region was used to excite the required azimuthal modes. Extensive numerical simulations and experimental verifications were carried out on spirals with 4 to 10 arms to evaluate the beam forming and achievable gains. Good agreements were found which indicated proper mode excitations and low loss radiation. For a 4-arm spiral two measured patterns are shown in Figs. 5a and 5b,

respectively in the azimuth and elevation planes. The measured gain over a 3 ft ground plane was about 11.0 dBic.

For a larger 6-arm spiral the corresponding measured far field patterns are shown in Figs 6a and 6b. The beamwidth in the azimuth plane is smaller at about 60°, instead of 90° for the 4-arm spiral, and consequently its gain is larger. The measured gain was about 13 dBic and its peak was found to be at $\theta=55°$, i.e. 35° elevation angle.

For some applications the antenna ground plane size introduces a physical limitation for its use, in which case an alternative design is desirable. Here, the multi-arm conical spiral is used. The cone angle is selected appropriately to shape the far field pattern. Fig. 7a and 7b show sample results for a six-arm conical spiral with a half cone angle of 30°. The measure gain for this antenna, after correcting for the input mismatch was around 12.5 dBic.

REFERENCES

[1] L. Shafai and A.K. Bhattacharyya, "Input Impedance and Radiation Characteristics of Small Microstrip Phased Arrays Including Mutual Coupling, MSAT Application", *Electromagnetics*, Vol. 6, No. 4, pp. 333-351, 1987.

[2] K.Woo, J. Huang, V. Jamnejad, D. Bell, J. Berner, P. Estabrook and A. Densmore, "Performance of a Family of Omni and Steered Antennas for Mobile Satellite Applications", Proc. Int. Mobile Satellite Conf., IMSC90, pp. 540-546, Ottawa, 1990.

[3] S. Ohmori K. Mano, K. Tanaka, M. Matsunaga and M. Tsuchiya, "A Phased Array Tracking Antenna for Vehicles", Proc. Int. Mobile Satellite Conf., IMSC90, pp. 519-522, Ottawa, 1990.

[4] K. Sato, K. Nishikawa and T. Hirako, "Field Experiments of Phased Array Antenna for Mobile Satellite Vehicle Application", Proc. Int. Symposium on Antennas & Propag., Vol. 3, pp. 653-656, Sapporo, 1992.

[5] L. Shafai, "MSAT Vehicular Antennas with Self Scanning Array Elements", Proc. Int. Mobile Satellite Conf., IMSC90, pp. 525-528, Ottawa, 1990.

[6] R. Milne, "An Adaptive Array Antenna for Mobile Satellite Communications", Proc. Int. Mobile Satellite Conf., IMSC90, pp. 529-534, Ottawa, 1990.

[7] J. Huang, A. Densmore, and D. Pozar, "Microstrip Yagi Array for MSAT Vehicle Antenna Application", Proc. Int. Mobile Satellite Conf., IMSC90, pp. 554-559, Ottawa, 1990.

[8] L. Shafai, "Scanning Properties of Circularly Polarized Microstrip Antennas", ANTEM'88, August 10-12, 1988, Winnipeg.

[9] L. Shafai, "Linear-sum Mode Arrays and Beam Forming", ANTEM'92, pp. 57-62, August 5-7, 1992, Winnipeg.

[10] D.E.N. Davies, "Circular Arrays", Chapter 12, The Handbook of Antenna Design, Vol. 2, Edit. by A.W. Rudge, K. Milne, A.D. Olver, and P. Knight. Peter Peregrinus, London, 1983.

FIGURES

Fig. 1 Configuration of a 3-element helical array.
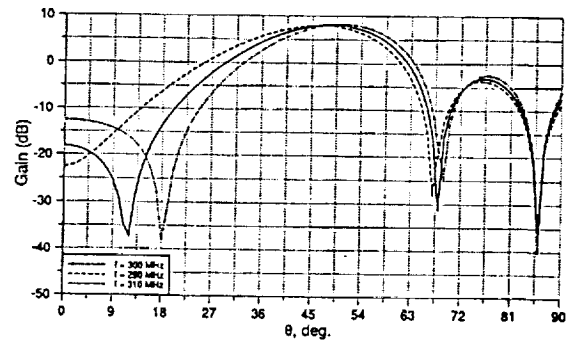
Fig. 2 Computed far field pattern of array in Fig. 1.
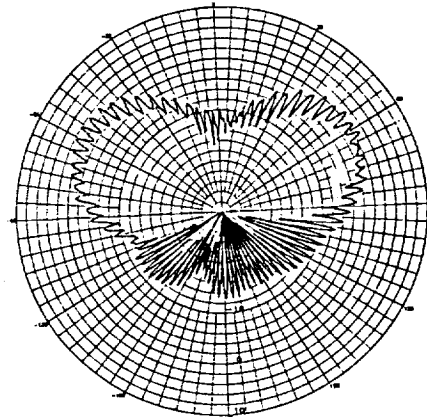
Fig. 3 Measured pattern of quadrifilar helix element, gain = 3.3 dBic.
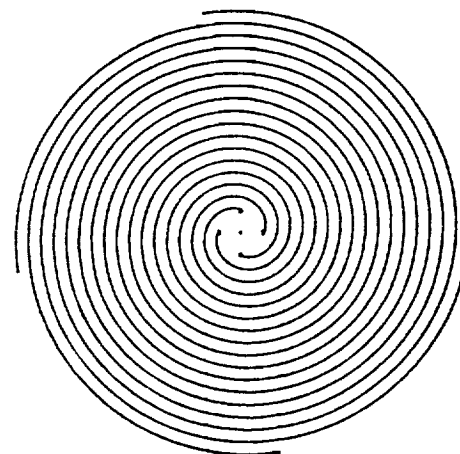
Fig. 4 Configuration of a 4-arm spiral antenna.

561
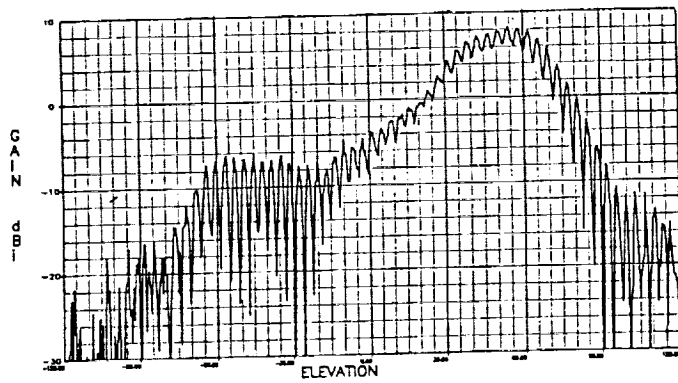
(a) elevation plane, gain = 11 dBic   (b) azimuthal plane, gain = 11 dBic

Fig. 5 Measured far field patterns of 4-arm spiral.
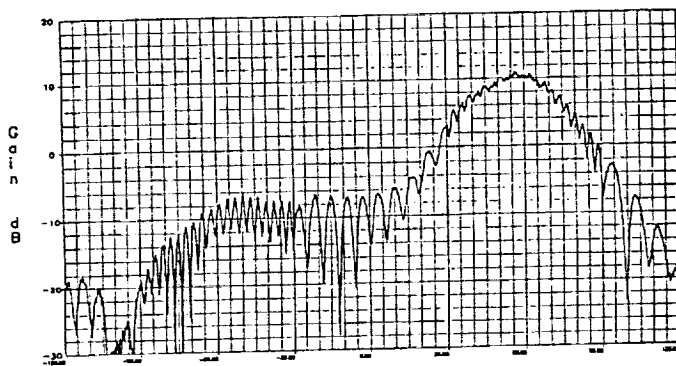
(a) elevation plane, gain = 13.4 dBic   (b) azimuthal plane, gain = 13 dBic
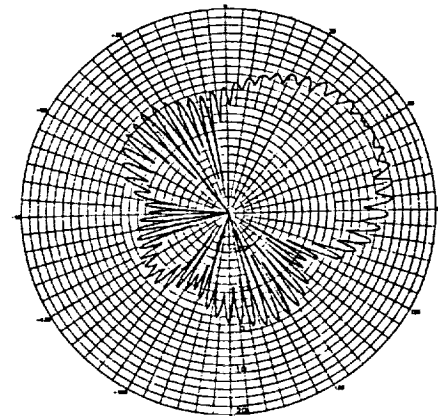
Fig. 6 Measured far field patterns of 6-arm spiral antenna.
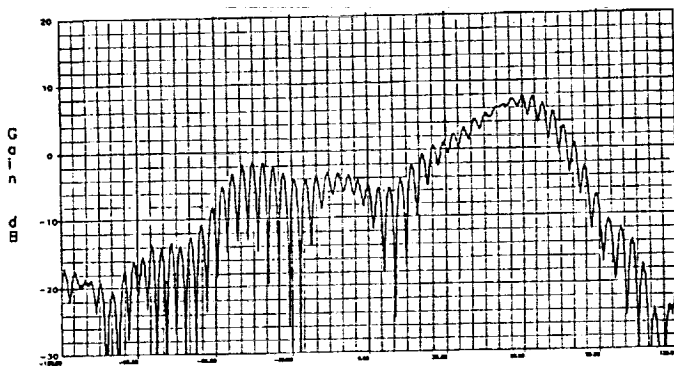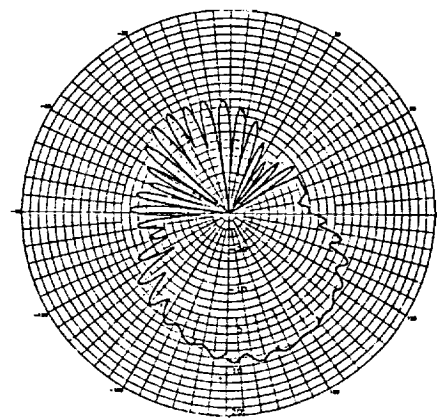
(a) elevation plane, gain = 11 dBic   (b) azimuthal plane, gain = 10.5 dBic

Fig. 7 Measured far field patterns of 6-arm conical spiral antenna.

562

K- and K_a-band Mobile-Vehicular Satellite-Tracking Reflector Antenna System for the NASA ACTS Mobile Terminal

Art Densmore, Vahraz Jamnejad, TK Wu and Ken Woo
Jet Propulsion Laboratory
California Institute of Technology
Pasadena, CA 91109
TEL (818) 354-4733
FAX (818) 393-6875

ABSTRACT

This paper describes the development of the K- and K_a-band mobile-vehicular satellite-tracking reflector antenna system for NASA's ACTS Mobile Terminal (AMT) project. ACTS is NASA's Advanced Communications Technology Satellite. The AMT project will make the first experimental use of ACTS soon after the satellite is operational, to demonstrate mobile communications via the satellite from a van on the road. The AMT antenna system consists of a mechanically steered small reflector antenna, using a shared aperture for both frequency bands and fitting under a radome of 23 cm diameter and 10 cm height, and a microprocessor-controlled antenna controller that tracks the satellite as the vehicle moves about. The RF and mechanical characteristics of the antenna and the antenna tracking control system are discussed. Measurements of the antenna performance are presented.

INTRODUCTION

The Jet Propulsion Laboratory (JPL) has developed several mobile vehicular antenna systems for satellite applications [1-10]. JPL has installed these antenna systems in vehicles equipped as mobile communications laboratories [11-12] and field-tested the equipment. The results of the field trials have been documented in the literature [13-18].

Recently a new K- and K_a-band mobile vehicle antenna system has been developed by JPL for use with NASA's Advanced Communications Technology Satellite (ACTS). The Space Shuttle will launch ACTS into its geostationary orbit in 1993 at 100 deg West longitude, above the mid-Western US. The new mobile vehicle antenna development is the AMT reflector antenna system, which will be used to demonstrate direct-dial voice, video and data communications via ACTS from a mobile vehicle while traveling in the Southern California area [19]. The reflector antenna system installs on the roof of the AMT vehicle.

ANTENNA ASSEMBLY

Figure 1 is a picture of the AMT reflector antenna shown with a transparent mock radome; the actual radome has the same hemi-ellipsoidal shape but is opaque. The external dimensions of the radome are 23 cm diameter and 10 cm peak height. The radome is a 4 mm thick "A-sandwich" and imposes insertion losses of 0.2 dB at 20 GHz (K band) and 0.4 dB at 30 GHz (Ka band). A Vellox hydrophobic coating that is nearly electromagnetically transparent keeps water from wetting the radome surface and allows the AMT to maintain communications in light rain. Figure 2 is an exploded view of the antenna assembly. All of the antenna components mount directly to the motor, which makes the assembly simple, compact and rugged. The motor is a 1.3 cm tall direct-drive two-phase

stepper motor. The reflector and feed horn mount on a disk that attaches directly to the motor (direct-drive) to accomplish azimuthal steering. Below the disk an optical encoder verifies that the motor steers the antenna to the proper angle. Figure 3 is an RF block diagram of the antenna.

The antenna incorporates an offset reflector configuration to avoid feed horn blockage. The reflector is constrained to fit with the feed horn under the radome and is relatively small, only about four by ten wavelengths at the 20 GHz band. The basically elliptical reflector shape maximizes gain while providing a relatively wide elevation beamwidth to relax the need for satellite elevation tracking. The shape of the reflector is the intersection of a paraboloid and an elliptical cylinder, with the cylinder oriented so the projection of the reflector surface is nearly a simple ellipse as viewed from both the feed horn and the satellite directions; this orientation is important to ensure good illumination of the reflector by the feed horn and a reasonably symmetrical antenna elevation pattern -- it also contours the shape of the reflector to fit well under the radome. The reflector mounts to a manually adjustable fixture that sets the nominal elevation angle of the antenna beam to potentially allow operation with ACTS in any region of the Continental United States (30-60 deg elevation).

All of the antenna RF components except the reflector and rotary joint are integrated into a single, rigid, electroformed assembly to reduce RF losses and increase mechanical integrity. Figure 4 shows the feed horn assembly, consisting of the feed horn, orthomode transducer and upper diplexer (the components above the rotary joint in figure 3). The feed horn assembly is a waveguide system that distributes both the 20 and 30 GHz signals from the rotary joint to the feed horn. The one feed horn is used for both frequency bands, with vertical polarization for the 20 GHz downlink and horizontal polarization for the 30 GHz uplink -- ACTS requires these polarizations.

Immediately behind the feed horn is the orthomode transducer. The orthomode transducer combines the two frequency bands from two different ports and channels them to the feed horn after orienting them with the proper polarizations. The upper diplexer spatially separates the two frequency bands and distributes them to the respective ports of the orthomode transducer. The diplexer makes up most of the lower portion of the assembly. The RF losses through the feed horn assembly are about 0.3 dB at 20 GHz and 0.5 dB at 30 GHz.

The rotary joint distributes the RF signals to the antenna components turned by the motor and provides the sole RF connection on the underside of the antenna. It is a single-channel coaxial unit, and as such is a relatively small unit that imposes a minimum of frictional torque. The rotary joint is only 1.3 cm in diameter and installs in the very center of the motor assembly. The choice of such a small rotary joint is a major factor in achieving the overall reduction in size of the antenna. The RF loss through the rotary joint is about 0.5 dB at both frequency bands.

SATELLITE TRACKING

Tracking the satellite requires only azimuthal steering (one-dimensional) since the antenna elevation beamwidth is wide enough to accommodate typical vehicle pitch and roll variations within any single region of operation. The satellite tracking system is a Motorola 68030 microprocessor-based hybrid feedback/feed-forward system; it steers the antenna in azimuth angle by controlling the motor in response to pointing information obtained from an inertial vehicle yaw rate sensor (feed-forward) and a mechanical dithering pointing error signal (feedback) simultaneously. The rms tracking error is only a small fraction of a degree. It is able to complete a full azimuth scan and acquire the signal in about 7 sec.

The technique used to measure antenna azimuth pointing error for tracking feedback is mechanical dithering. Mechanical dithering

involves rocking the antenna left and right sinusoidally (in azimuth angle) 1 deg in each direction at a 2 Hz rate to determine if the antenna is pointed in the direction of strongest signal. The satellite sends a special beacon for this purpose; the AMT system RF transceiver detects the beacon through the antenna and provides the detected signal to the antenna controller computer. By correlating the received signal level reported by the transceiver with the commanded dithering of the antenna angle, the antenna controller computer determines the sign and magnitude of any pointing error. Figure 5 shows the measured mechanical dithering pointing error detection function.

ANTENNA RF PERFORMANCE

Figures 6-9 present the elevation and azimuth co- and x-pol 20 and 30 GHz far-field patterns of the antenna. The patterns show the elevation coverage centered at 46 deg for operation through ACTS in southern California. Requirements for the antenna performance are made over a 12 deg range of elevation angle, centered at 46 deg -- this range accommodates +/- 6 deg typical vehicle pitch and roll variations while travelling paved roads.

Over the required elevation angle range the minimum gain at 20 GHz is 19 dBi with a maximum of 22.5 dBi, and at 30 GHz the minimum gain is 19 dBi with a maximum of 23.5 dBi. The elevation backlobes and azimuth sidelobes are more than 20 dB down from the main lobe. Peak x-pol is no greater than -15 dB. These measurements are referred to the TWTA and LNA ports of the lower diplexer, diagrammed in figure 3.

Over the required elevation angle range the receive sensitivity ratio (antenna gain over system noise temperature, or G/T) is a minimum of -6 dB/K, with a peak of -2.5 dB/K. The system noise temperature is 320 K, of which 260 K is due to the LNA and all other receiver components below it (not shown in figure 3). The remaining 60 K is due to the antenna

(everything above the LNA in figure 3), including cosmic and sky noise as well as thermal noise introduced by the dissipative losses of the antenna components (about 1 dB in all). When the antenna is pointed directly at the sun, the receive system noise temperature increases by only 0.1 dB (5 K).

The antenna handles up to 10 W transmit power applied at the lower diplexer by the TWTA. With the maximum of 10 W transmit power the maximum EIRP ranges from 30-33.5 dBW, depending on elevation angle.

Transmit-induced receiver noise (receiver desensitization) is not a problem with this antenna. There is no measurable degradation of receive sensitivity (+/- 0.05 dB) resulting from simultaneous transmission up to the maximum power level, 10 W.

CONCLUSION

JPL has successfully developed a mobile vehicle antenna system for NASA's K/K_a-band ACTS Mobile Terminal program, and initial tests show that the antenna and its satellite tracking system perform very well. It is small in size and rugged for operation in the mobile environment. It will be used for the first experimental use of the ACTS satellite soon after the satellite's launch. The AMT will demonstrate voice, video and data communication through the ACTS satellite from a mobile vehicle traveling roads in the southern California area.

ACKNOWLEDGMENT

565

REFERENCES

[1] J. Huang and A. Densmore, "Microstrip Yagi Array Antenna for Mobile Satellite Vehicle Application," *IEEE Trans. Antennas Propagat.*, Vol. AP-39, pp. 1024-1030, July 1991.

[2] V. Jamnejad , "A Mechanically Steered Monopulse Tracking Antenna for Land Mobile Satellite Applications," in *Proc. IEEE Veh. Technol. Conference,* Tampa, Florida, June 1987.

[3] D. Bell, *et al.*, "Reduced-Height, Mechanically Steered Antenna Development," *MSAT-X Quarterly*, No. 18, JPL Publication 410-13-18, January 1989.

[4] K. Woo, A. Densmore, *et al.*, "Performance of a Family of Omni and Steered Antennas for Mobile Satellite Applications," *Proc. Internat. Mobile Satellite Conf. June 1990*, JPL Publication 90-7, June 1990.

[5] J. Huang, "L-band Phased Array Antennas for Mobile Satellite Communications," in *Proc. IEEE Veh. Technol. Soc. Conference*, pp. 113-119, Tampa, Florida, June 1987.

[6] F. Colomb, *et al.*, "An ANSERLIN Array for Mobile Satellite Applications," *Proc. Internat. Mobile Satellite Conference 1990*, JPL Publication 90-7, June 1990.

[7] D. Bodnar, *et al.*, "A Novel Array Antenna for MSAT Applications," *IEEE Trans. Veh. Technol.*, Vol. VT-38, pp. 86-94, May 1989.

[8] P. Estabrook and W. Rafferty, "Mobile Satellite Vehicle Antennas: Noise Temperature and Receiver G/T," *Proc. IEEE Veh. Technol. Conference*, San Francisco, Calif., April 1989.

[9] J. Berner and R. Winkelstein, "Antenna Pointing System," *MSAT-X Quarterly*, No. 13, JPL Publication 410-13-13, January 1988.

[10] D. Bell, "Antenna Pointing Schemes Aim at High Accuracy and Robustness in a Fading Signal Environment," *MSAT-X Quarterly*, No. 3, JPL Publication 410-13-3, June 1985.

[11] R. Emerson, "Propagation Measurement Van," *MSAT-X Quarterly*, No. 13, JPL Publication 410-13-13, January 1988.

[12] J. Berner and R. Emerson, "The JPL MSAT Mobile Laboratory and the Pilot Field Experiments," *Proc. Mobile Satellite Conference 1988*, JPL Publication 88-9, May 1988.

[13] A. Densmore, "Postperformance Evaluation of the MSAT-X Antennas Used in the MSAT-X/AUSSAT Land Mobile Satellite Experiment," *MSAT-X Quarterly*, No. 24, JPL Publication 410-13-24, July 1990.

[14] K. Dessouky, *et al.*, "Field Trials of a NASA-Developed Mobile Satellite Terminal," *Proc. Internat. Mobile Satellite Conference 1990*, JPL Publication 90-7, June 1990.

[15] W. Rafferty, "Mobile Satellite Field Experiments," *MSAT-X Quarterly*, No. 11, JPL Publication 410-13-11, July 1987.

[16] J Berner, "The PiFEx Satellite-1a Experiment," *MSAT-X Quarterly*, No. 15, JPL Publication 410-13-15, June 1988.

[17] T. Jedrey, *et al.*, "The Tower-3 Experiment: An Overview," *MSAT-X Quarterly*, No. 18, JPL Publication 410-13-18, January 1989.

[18] T. Jedrey, *et al.*, "An Aeronautical-Mobile Satellite Experiment," *IEEE Veh. Technol.*, Vol. VT-40, pp. 741-749, Nov. 1991.

[19] K. Dessouky *et al.*, "The ACTS Mobile Terminal," *SATCOM Quarterly*, JPL Publication 410-33-2, July 1991.

Fig. 1 AMT Reflector Antenna

RADOME

REFLECTOR
AND FEED
ASSEMBLY

ANGULAR
OPTICAL
ENCODER

PANCAKE
STEPPER
MOTOR

ROTARY
JOINT
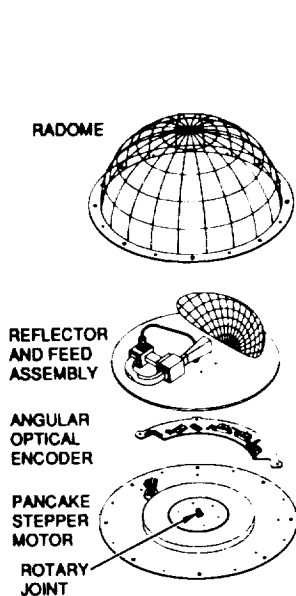
Fig. 2 Reflector Antenna
Exploded View

20 GHZ
DOWNLINK
(VERT. POL.)

30 GHZ
UPLINK
(HORIZ. POL.)

RADOME

REFLECTOR
FEED HORN

30 GHZ | ORTHOMODE
TRANSDUCER | 20 GHZ

ROTATING
PLATFORM
UNDER RADOME

DIPLEXER
(UPPER ONE)

STATIONARY
PLATFORM ON
VEHICLE ROOF

ROTARY
JOINT

ANTENNA MOTOR &
OPTICAL ENCODER

INSIDE
VEHICLE
CABIN

DIPLEXER
(LOWER ONE)

TWTA

LNA

ANTENNA
CONTROLLER
COMPUTER

30 GHZ

20 GHZ

TO/FROM RF TRANSCEIVER
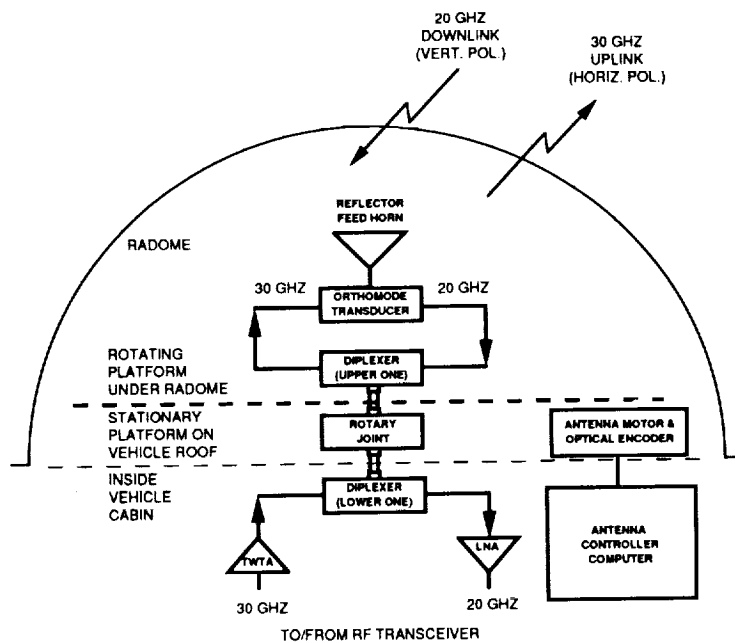
Fig. 3 Reflector Antenna Block Diagram

567

Fig. 4 Feed Horn Assembly
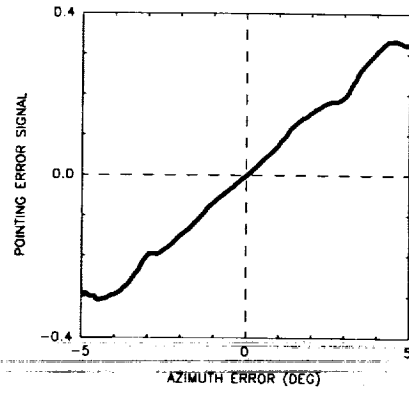
Fig. 5 Mechanical Dithering
Pointing Error Detection
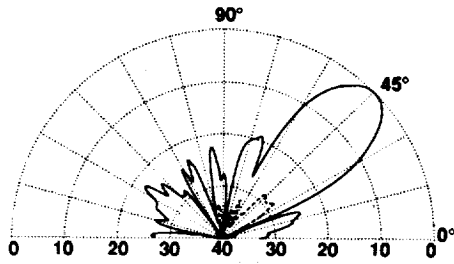
Fig. 6 Elevation Pattern, 20 GHz, Co- and X-pol.
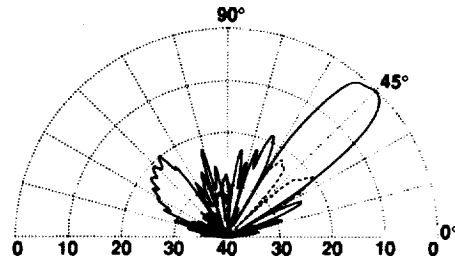
Fig. 7 Elevation Pattern, 30 GHz, Co- and X-pol.
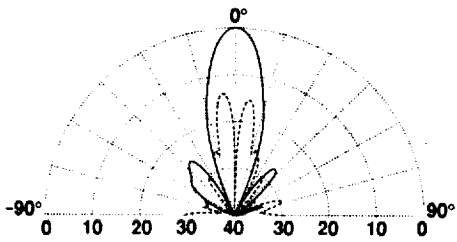
Fig. 8 Azimuth Pattern, 20 GHz, Co- and X-pol.
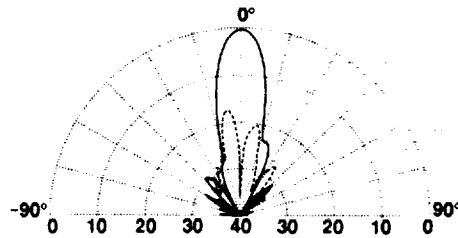
Fig. 9 Azimuth Pattern, 30 GHz, Co- and X-pol.

An Active K/K_a-Band Antenna Array for the NASA ACTS Mobile Terminal[†]

A. Tulintseff, R. Crist, A. Densmore, and L. Sukamto

Jet Propulsion Laboratory
California Institute of Technology
Pasadena, CA 91109 USA
Tel: (818) 354-7255
Fax: (818) 393-6875

ABSTRACT

An active K/K_a-band antenna array is currently under development for NASA's ACTS Mobile Terminal (AMT). The AMT task will demonstrate voice, data, and video communications to and from the AMT vehicle in Los Angeles, California, and a base station in Cleveland, Ohio, via the ACTS satellite at 30 and 20 GHz. Satellite tracking for the land-mobile vehicular antenna system involves "mechanical dithering" of the antenna, where the antenna radiates a fixed beam 46° above the horizon. The antenna is to transmit horizontal polarization and receive vertical polarization at 29.634 ± 0.15 GHz and 19.914 ± 0.15 GHz, respectively. The active array will provide a minimum of 22 dBW EIRP transmit power density and a -8 dB/K° receive sensitivity.

INTRODUCTION

The AMT active antenna array [1-3], shown in Figure 1, is a multilayered assembly in which a receive array of radiating slots and transmit array of microstrip dipoles are interleaved such that they share the same aperture to provide a compact, dual-band antenna. The slots are electro-

magnetically coupled to shielded microstrip lines connected to Monolithic Microwave Integrated Circuit (MMIC) low-noise amplifiers (LNAs) on the back side of the primary ground plane containing the slots. The dipoles reside on a dielectric sheet placed on top of the front side of the slotted ground plane, are interleaved between the slots, and are electromagnetically coupled to microstrip lines connected to MMIC high-power amplifiers (HPAs) on the front side of the primary ground plane. Inherently good isolation is expected since the receive and transmit circuitry are on opposite sides of the primary antenna ground plane.

TRANSMIT AND RECEIVE ARRAY

Printed dipole elements and their complement, linear slots, are elementary radiators that have found use in low-pofile antenna arrays. Low-profile antenna arrays, in addition to their small size and low weight characteristics, offer the potential advantage of low-cost, high-volume production with easy integration with active integrated circuit components.

Both transmit and receive arrays have peak directivities of approximately 24 dB, and will operate over a 1% and a 1.5% bandwidth, respectively. The subarrays of the AMT antenna are linear series-fed-type arrays consisting of nearly identical dipole, or slot, elements transversely electromagnetically coupled to a microstrip transmission line, a configuration selected
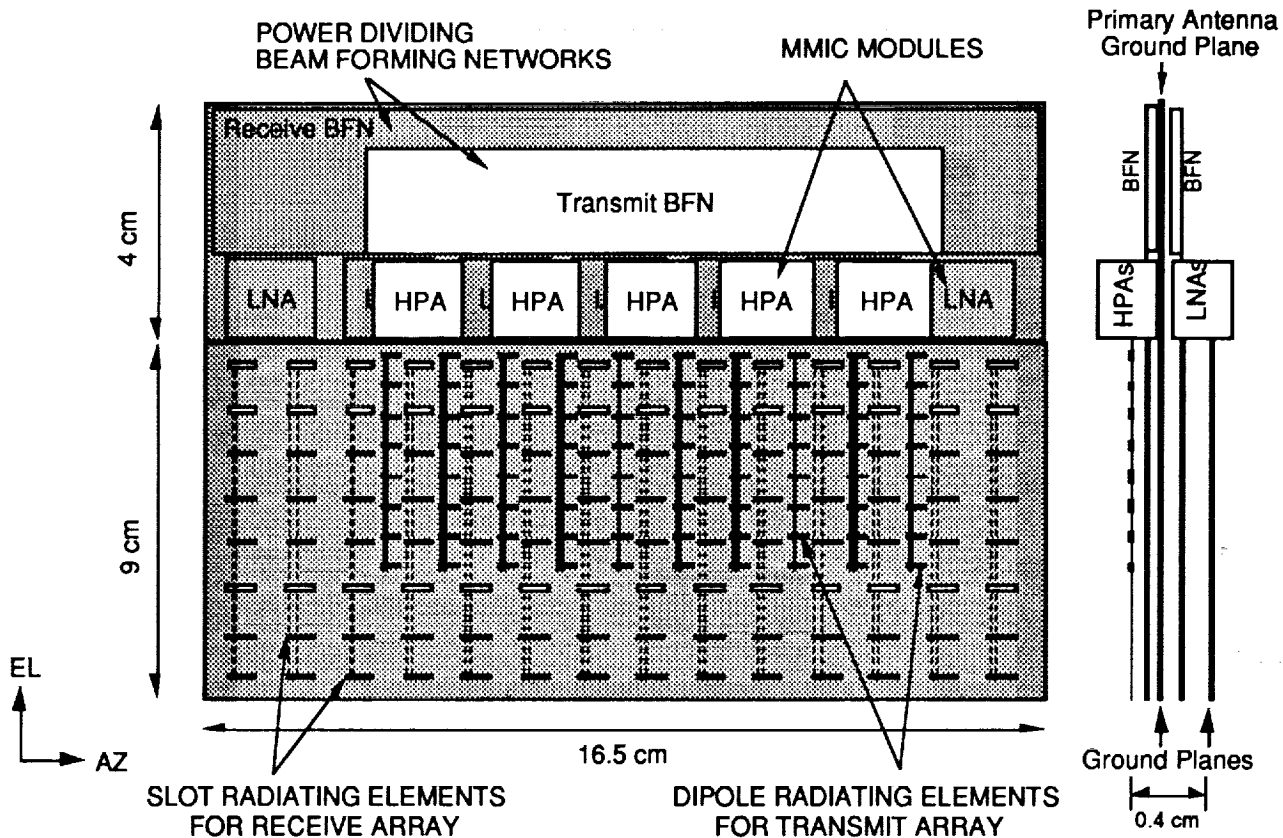
Figure 1. AMT Active Array.

to minimize losses. The transmit array consists of 10 identical linear dipole subarrays spaced $0.964\lambda_0$ apart and the receive array consists of 14 linear slot subarrays spaced $0.648\lambda_0$ apart.

The design of the linear series-fed-type arrays is achieved using transmission line theory with equivalent circuit models for the radiating elements. The element offsets and interelement line lengths are used to obtain the desired amplitude distribution and beam direction, respectively. Summarized in the following are the design and test results of both a dipole and slot series-fed-type linear array, assuming the impedance characteristics of the radiating elements are known.

Elevation Beam Direction

Consider the "symmetrically-fed" linear dipole and slot arrays shown in Figures 2 and 3, respectively, where the spacing
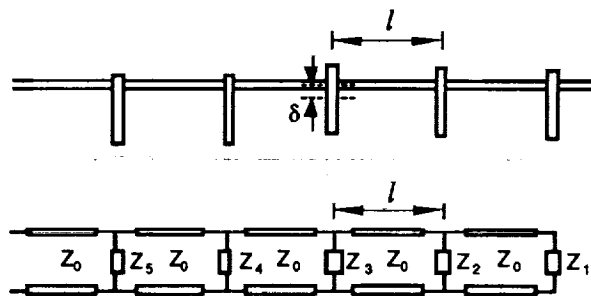
Figure 2. Linear series-fed dipole array and equivalent circuit.
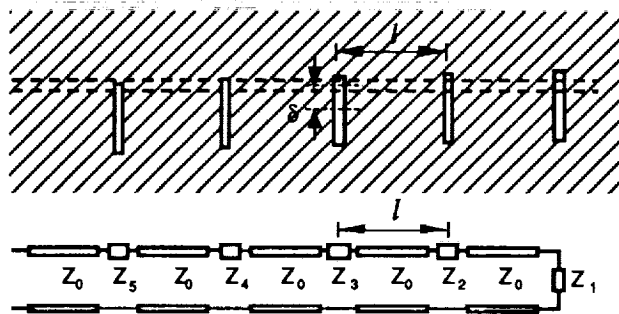
Figure 3. Linear series-fed slot array and equivalent circuit.

570

between elements is d and the length of the interconnecting transmission line is $\ell \geq d$. To direct the main beam at the proper scan angle θ_0, measured from broadside, or normal to the antenna, the following phase relationship (using $e^{j\omega t}$ time dependence) between the elements should be satisfied

$$\psi = -\beta\ell = \pm k_0 d \sin\theta_0 - m\pi$$

where m is an even integer, $\beta = k_0\sqrt{\epsilon_{r,\,\text{eff}}}$ is the propagation constant, $k_0 = 2\pi/\lambda_0$ is the free space wavenumber, λ_0 is the free space wavelength, and $\epsilon_{r,\,\text{eff}}$ is the effective dielectric constant. To minimize ℓ, i.e., minimize line loss, the above equation is solved when $\ell = d$ to obtain

$$\frac{\ell}{\lambda_0} = \frac{m/2}{\sqrt{\epsilon_{r,\,\text{eff}}} \pm \sin\theta_0}$$

Dipole Linear Array Design

In an equivalent circuit model of a linear array of N series-fed-type dipoles [4], the ith dipole represents a shunt impedance, $Z_i(\omega) = R_i(\omega) + jX_i(\omega)$, to the transmission line as shown in Figure 2, where $Z_i(\omega)$ is a function of the dipole offset, length, and width. The transmission line is characterized by its characteristic impedance Z_0 and wavenumber $k = \beta - j\alpha$, where α is the attenuation constant. Each dipole operates at resonance, such that $Z_i(\omega_0) = R_i(\omega_0)$ $(X_i(\omega_0) = 0)$, where the desired value of $R_i(\omega_0)$ is obtained by selecting the appropriate offset δ_i and length L_i.

A unit cell of the array of length ℓ, determined from above, may be defined as shown in Figure 4.
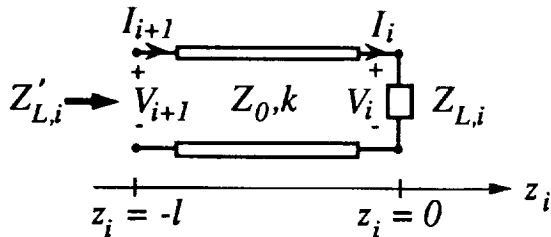
Figure 4. Linear array unit cell.

The voltage and current on the transmission line of the unit cell are given by

$$V(z_i) = V_{i+}e^{-jkz_i}\left[1 + \Gamma_{L,i}e^{j2kz_i}\right]$$
$$Z_0 I(z_i) = V_{i+}e^{-jkz_i}\left[1 - \Gamma_{L,i}e^{j2kz_i}\right]$$

where
$$\Gamma_{L,i} = \frac{Z_{L,i} - Z_0}{Z_{L,i} + Z_0}$$

$$Z_{L,i} = Z_i \parallel Z'_{L,i-1}$$

$$Z'_{L,i-1} = \frac{Z_{L,i-1} + jZ_0\tan k\ell}{jZ_{L,i-1}\tan k\ell + Z_0}Z_0$$

By taking the ratio of V_{i+1}/V_i

$$\frac{V_{i+1}}{V_i} = \frac{V(z_i = -\ell)}{V(z_i = 0)} = \frac{\left[1 + \Gamma_{L,i}e^{-j2k\ell}\right]}{\left[1 + \Gamma_{L,i}\right]}e^{jk\ell}$$

a recursive expression for the voltage at successive points along the array is obtained. The power dissipated in each dipole radiator is given by $P_i = |V_i|^2/(2R_i)$. For a given amplitude distribution, $\sqrt{P_i}$ ($i = 1, 2, \ldots, N$), and a given transmission line length $k\ell$ and R_1, the desired resonant resistances R_i are specified by the following recursive expression

$$R_i = \frac{1}{2}\frac{|V_i|^2}{P_i} = \frac{1}{2}\frac{|V_{i-1}|^2}{P_i}\frac{|1 + \Gamma_{L,i-1}e^{-j2k\ell}|^2}{|1 + \Gamma_{L,i-1}|^2}$$

When the main beam direction is broadside, or normal, to the antenna, $\theta_0 = 0$, R_1 should be specified larger than Z_0 to maintain a good input impedance match to the array. For a main beam direction off broadside, $\theta_0 \neq 0$, R_1 is set equal to Z_0 to prevent reflections that result in a second, undesired scanned beam. Note that the above equation accounts for multiple reflections on the transmission line, resulting in a progressive phase shift along the radiating elements that nearly approximates the ideal phase shift given by $\psi = \pm k_0 d \sin\theta_0 - m\pi$.

To meet the sidelobe requirement, the amplitude distribution along each linear dipole subarray must be tapered. Table 1 summarizes the required resonant resistances R_i/Z_0 given the amplitude distribution $\sqrt{P_i}$ specified in the table.
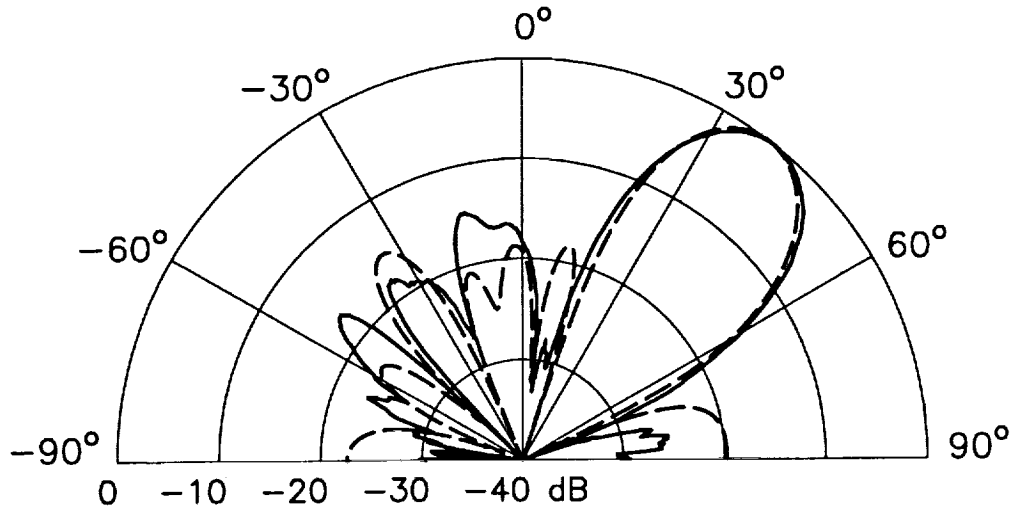
Figure 5. Elevation pattern of linear slot array.
Measured (—). Calculated (- -).

i	P_i	R_i/Z_0
1	.36	1.00
2	.49	0.75
3	.81	2.14
4	1.0	2.36
5	1.0	2.86
6	.81	6.47
7	.49	10.0
8	.36	14.5

Table 1. Linear dipole array P_i and R_i/Z_0.

Slot Linear Array Design

Similarly, in an equivalent circuit model of an array of series-fed-type slots [5], the ith slot represents a series impedance, $Z_i(\omega) = R_i(\omega) + jX_i(\omega)$, to the transmission line as shown in Figure 3. A unit cell of the array may be defined, as shown in Figure 4, similar to that of the dipole array, with the exception that

$$Z_{L,i} = Z_i + Z'_{L,i-1}$$

By taking the ratio of I_{i+1}/I_i and noting that the power dissipated in each slot radiator is $P_i = |I_i|^2 R_i/2$, a recursive expression for the slot resistances R_i is given by

$$R_i = \frac{2P_i}{|I_i|^2} = \frac{2P_i}{|I_{i-1}|^2} \frac{|1 - \Gamma_{L,i-1}|^2}{|1 - \Gamma_{L,i-1}e^{-j2k\ell}|^2}$$

when the amplitude distribution, $\sqrt{P_i}$ ($i = 1, 2, \ldots, N$), the transmission line length $k\ell$, and R_1 are specified. Similar to the transmit array, the amplitude distribution along each linear slot subarray must also be tapered to meet the sidelobe requirement. Table 2 summarizes the required resonant resistances R_i/Z_0 given the amplitude distribution $\sqrt{P_i}$ shown.

i	P_i	R_i/Z_0
1	.36	1.00
2	.49	1.33
3	.81	0.52
4	1.0	0.37
5	1.0	0.36
6	.81	0.18
7	.49	0.08
8	.36	0.07

Table 2. Linear slot array P_i and R_i/Z_0.

Experimental Results

A linear, cavity-backed slot array, consisting of 8 elements with an interelement spacing of $0.485\lambda_0$, has been fabricated and tested, operating at 20 GHz with a main beam direction approximately 40° from broadside. The slot elements were characterized both theoretically and

572

PLANAR POWER
DIVIDER

MMIC HPA

1.9 cm

16.5 cm

5.0 cm
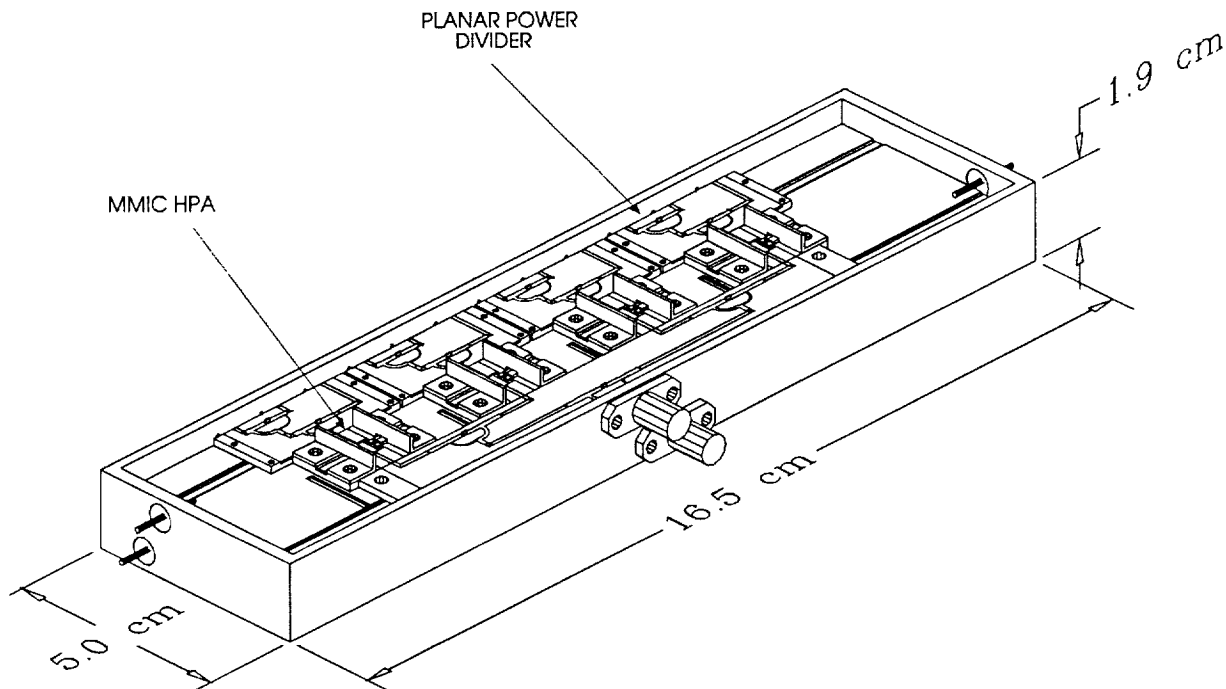
Figure 6. Transmit/Receive MMIC module.

experimentally as a function of offset, with the experimental characterization performed using the TRL calibration technique. The effective dielectric constant was taken to be approximately $\epsilon_{eff,r} = 2.1$. Due to the fact that the element resonant frequency is a function of offset, the element slot lengths are all slightly different. Shorting pins are used to suppress undesirable cavity modes. As shown in Figure 5, good agreement between predicted and measured patterns was obtained. Total loss in the slot array was measured to be approximately -1.3 dB. (Note that the attenuation of a shielded microstrip line is measured to be approximately -0.24 dB/λ_0.) Experimental results will be presented for a similar linear series-fed-type array of dipoles operating at 30 GHz.

T/R MMIC MODULE

The AMT active array antenna MMIC module contains MMIC HPAs for the transmit array and MMIC LNAs for the receive array. The MMIC circuits are connected to the transmit and receive linear subarrays: one LNA for each receive lin-

ear slot array, and one HPA for each pair of transmit linear dipole arrays. All the MMIC circuits and power dividers are assembled onto a single transmit/receive module, with the HPAs and LNAs on opposite sides of the module as illustrated in Figure 6. The T/R module is mechanically attached to the transmit and receive array structure, as shown conceptually in Figure 1, via coaxial feed-throughs.

The transmit module provides greater than 1 Watt of RF power to the dipole array at the 30 GHz transmit frequency band. Five MMIC MESFET amplifiers provide up to 0.5 W to each pair of transmit subarrays. All five MMIC HPAs are mounted on molybdenum subcarriers with a copper heat spreader beneath each device. The transmit modules are designed to maintain gate junction temperatures below 125°C. A planar five-way power dividing circuit distributes the RF signal to each amplifier subcarrier.

The receive module consists of 14 MMIC pseudomorphic HEMT (PHEMT) LNAs. Each LNA has a noise figure of approximately 3.2 dB and a gain of 9 dB at 20 GHz. Two additional MMIC LNAs are

573

located on the antenna platform to meet the G/T requirement and the DC power consumption constraint. All 14 LNAs are mounted in the receive portion of the T/R module with a 14-way planar power divider.

CONCLUSION

An active K/K_a-band antenna array is currently under development at the Jet Propulsion Laboratory for NASA's ACTS Mobile Terminal (AMT). Satellite tracking for the land-mobile vehicular antenna system involves azimuthal "mechanical dithering" of the antenna, where the antenna radiates a fixed beam 46° above the horizon. The antenna is to transmit horizontal polarization and receive vertical polarization at 29.634±0.15 GHz and 19.914±0.15 GHz, respectively, and will provide a minimum of 22 dBW EIRP transmit power density and a −8 dB/K° receive sensitivity. The AMT active antenna array is a multilayered assembly in which a receive array of radiating slots and a transmit array of microstrip dipoles are interleaved such that they share the same aperture to provide a compact, dual-band antenna. The low-profile active array design, in addition to its small size and low weight characteristics, offers the potential advantage of low-cost, high-volume production with easy integration with active integrated circuit components.

REFERENCES

[1] "AMT Active Array Antenna System Design," A. Tulintseff, R. Crist, L. Sukamto, and A. Densmore, JPL IOM AMT:336.5-91-112 (internal document), Sep. 24, 1991.

[2] "Commercial applications of the ACTS Mobile Terminal millimeter-wave antennas," A. Densmore, R. Crist, V. Jamnejad, and A. Tulintseff, *Technology 2001 Conference Proceedings*, NASA Conference Publication 3136, Vol. 1, pp. 67-71, San Jose, CA, Dec. 3-5, 1991.

[3] "Two K/K_a-band mechanically steered, land-mobile antennas for the NASA ACTS Mobile Terminal," A. Densmore, V. Jamnejad, A. Tulintseff, R. Crist, T.K. Wu, and K. Woo, *ACTS Conference '92 Proceedings*, pp. 177-188, Washington, DC, Nov. 18-19, 1992.

[4] "Analysis and design of series-fed arrays of printed-dipoles proximity-coupled to a perpendicular microstripline," N. K. Das and D. M. Pozar, *IEEE Trans. Antennas Propagat.*, Vol. 37, No. 4, pp. 435-444, Apr. 1989.

[5] "A reciprocity method of analysis for printed slot and slot-coupled microstrip antennas," D. M. Pozar, *IEEE Trans. Antennas Propagat.*, Vol. AP-34, No. 12, pp. 1439-1446, Dec. 1986.

Microstrip Monopulse Antenna for Land Mobile Communications

Q. García(*), C. Martín(*), J. C. del Valle (**), A. Jongejans(***), P. Rinous (***),
M.N. Travers(***)

(*) TeDeCe , Agrupación de empresas CSIC-IMADE-CASA; c/Serrano 144, 28006 Madrid, Spain.
Ph no. 341 5622178; Fax 341 5622156
(**) DCG Ingenieros, c/ Mendez Alvaro 34, 28045 Madrid, Spain.
(***) ESA-ESTEC, European Space Technology Center, Postbus 209, 2200 AG Noordwijk, The
Netherlands.

ABSTRACT

Low cost is one of the main requirements in
a communication system suitable for mass pro-
duction, as it is the case for satellite land mobile
communications. Microstrip technology fulfills
this requeriment which must be supported by a
low cost tracking system design. The trade off
led us to a prototype antenna composed of
microstrip patches based on electromechanical
closed-loop principle which design and the re-
sults obtained are described below.

INTRODUCTION

This paper describes an antenna and its asso-
ciated tracking system developed under contract
with the European Space Agency (ESA). This
development is part of the preparation work to
promote a European Mobile Satellite system
mainly aimed at the international road transport
industry [1].

Presently, satellite land mobile communica-
tions are offering low bit data interchange of
information, but higher bit rate and/or voice
communications are being contemplated.

Voice communication at L band requires a
medium gain antenna ($\approx$ 11dBi) which has to be
pointed to the satellite. Fixed antennas with
hemispherical coverage cannot provide this gain,
so a complete antenna system must be compo-
sed of two parts strongly related, the aerial and
the pointing subsystem [2].

The antenna specifications are similar to
those of other programs (e.g. MSAT-X or IN-
MARSAT-M). The operational frequencies at
L-band range from 1530 to 1559MHz at Rx and
from 1631.5 to 1660.5 at Tx, with a gain of aro-
und 10-12dBi in circular polarization (RHC for
testing and possibly LHC in production).

The axial ratio requirement is 3dB in the
useful beamwidth, including the effect of the car
roof, which may cause strong distortions in the
antenna pattern. Finally, in order to avoid inter-
ference caused by other satellites, a crospola-
rization isolation of 20dB was specified from
30° to 50° off antenna boresight in the azimuth
plane.

The manufacturing technique selected for
the antenna was microstrip, which provides the
lowest price when compared to other antenna
manufacturing techniques, due to the photolito-
graphic processes that this technique allows. It
must be acompanied with a careful selection of
the materials to be used, which have to perform
electrically well, while maintaining a low price.
The feed network design must follow also this
design approach, minimizing the number of
components to reduce the assembly process.

The design of the tracking system is also
involved on this low cost requirement, and this
imposes also a trade off between tracking per-
formances and price reduction techniques.

TRACKING SYSTEM

The tracking scheme selected was a closed-loop monopulse system which provides both high accuracy and real time response without requiring any additional pointing device for proper operation. The antenna information reaches, after demodulation, to a tracking receiver which commands the motor to correct the position of the antenna to the satellite direction.

A classical monopulse scheme requires two signals (called Sum -Σ- and Difference -Δ- signals) to track the satellite position. The sum signal (which also carries the information) is obtained through in-phase addition of the signals received on each radiator, and the difference signal is obtained through out-of-phase addition of the signals coming from symmetric elements in the array.

The odd characteristic of the Difference signal makes it to be null when the antenna is correctly pointed to the emitter, and the Sum channel receives a maximum in the same situation. Since both channels are independently processed in the receiver, the Sum channel is used for data handling and the Difference channel for tracking purposes, using the signal received in this channel to drive a motor controller.

Actually, the signal used for satellite tracking is not only the Δ signal, but the ratio Δ/Σ, which makes the system to be insensitive to weak fading effects. This signal is compared with a previously stored look-up table of the function values, and the antenna is pointed to the correct position from a single measurement, which makes the system to be extremely fast. Digital techniques allow this fast signal processing and decission of movement.

In a classical Monopulse scheme these two signals are downcoverted and processed through two balanced receiving chains, and an AGC is performed with the sum channel over the difference receiver, which provides the error signal. This scheme has two problems: a dual channel rotary joint and two balanced receiving chains are required.

These two drawbacks made us to consider a Modulated Monopulse scheme which had been proven to work properly in the MSAT program [3]. The block scheme is shown in the figure 1.

The sum and difference signals are generated in the RF Monopulse beamformer, and they are routed to the monopulse modulator, composed of a 180° phase shifter and a directional coupler. The difference signal goes through the shifter which is switched at a constant frequency f_c, and a signal $\Delta(t)*p(t)$ is generated at the output, where p(t) is a square wave signal. This AM modulated difference signal is added through a directional coupler to the sum signal. Since the coupling factor gives place to a path loss of $(1-C^2)^{1/2}$ in the sum channel, the output signal is:

$$V(t) = (1 - C^2)^{1/2} \Sigma(\theta,t) + C \Delta(\theta,t) p(t)$$

The modulation of the difference port frequency-multiplexes the Sum and the Difference signals. Both signals are included in V(t) independently: its spectrum has the sum signal at f_{Rx}, and the difference signal at $f_{Rx} \pm f_c$. This signal is downconverted and splitted; one of the channels is lowpass filtered and the Sum information signal is obtained, and the other branch is synchronously detected with a delayed replica of the modulating signal p(t). A ratio device provides a signal proportional to Δ/Σ used to control the antenna movements through the tracking processor.

The receiver used in this project was manufactured by SNEC(France), and it performed the detection and demodulation processes, providing two output signals which were handled by the tracking processor. The integration time of the receiver was 50ms and the output signals ranged from 0 to 3volts and from -2.5 to 2.5 volts for the sum and difference channels respectively.

The tracking processor is based in the general purpose microprocessor Z80, with three parallel I/O programmable controllers 8255 which provide a TTL-compatible interface between the data interfaces and the CPU, RAM and ROM memories for the source code and

process operations, and a minimum of additional logic.

The signals supplied by the tracking receiver are routed to two identical PMI-ADC912 Analog to Digital converters of 12 bits. The sampling frequency is 3.2 kHz, and the conversion time is 12 microseconds.

The step angle of the motor was 7.5° with a reduction ratio of 1:7. The maximum angular speed of the antenna was 40°/sec. The use of a stepper motor allows the system not to require any kind of encoder, since the microprocessor counts the number of steps to control the antenna movements.

The algorithms are stored in EPROM memory. Two 12 bits ports are inputs to the CPU which acquire the data supplied by the A/D converters. One 8 bits digital port is configured for I/O control data going to, and coming from the CPU. The data to the motor drivers is composed of the motion direction and the number of steps that the motor has to move.

The tracking receiver may also include additional pointing devices such as solid state turn rate sensors in order to maintain the link in special fading environments or when the signal coming from the satellite disappears (in a tunnel, for instance). These devices have a fast response, so they could be used as the prime tracking process, checking periodically with the open loop system in order to correct the possible drift error.

Acquisition and Tracking processes

In the initial acquisition, the processor commands the antenna to perform a 360° scan looking for the satellite. The number of steps in acquisition mode is given by the antenna beamwidth rounded to an integer number of motor steps. Then, the antenna moves in 15° steps looking for the maximum. In each step the signal level is read and averaged.

The channel used in the acquisition is the sum pattern. Once the system recognizes the maximum, the antenna is commanded to move

to the indicated position. The antenna follows the minimum path length to move to the indicated position.The value of the maximum is stored and used to calculate a threshold level which is 7dB below.

Once the antenna has been roughly pointed to the satellite direction in the initial acquisition, the system switches to the tracking algorithm to keep the antenna correctly pointed.

The signal level of the sum channel controls the system state: if its value is greater than the threshold level it remains in tracking mode, but if its value is lower than the threshold, after 5 seconds, it goes into reacquisition.

DESCRIPTION OF THE ANTENNA

In order to reduce the number of elements needed to obtain the specified gain (10-12 dBi), and to reduce also the mass and the inertia of the aerial, a low permittivity substrate ($\varepsilon \approx 1.1$) was selected, giving place to a larger size with higher gain in a single element.

Three square patches were needed to meet the gain requirement, and to comply with the intersatellite isolation specification, the lateral elements were fed with an amplitude taper of 3dB.

A substrate thickness of 5mm was taken; the initial selection of 10mm made the patch to have a quite large port to port coupling, which affected the crospolarization level. This height reduction does not affect seriously the gain of the radiator since the patch size is almost unaltered by the substrate thickness.

The VSWR bandwidth of the patch element is about 55MHz ($\approx 3\%$) with a port to port decoupling better than 30dB. Two matching networks with double-stub tuners are connected at both inputs of each radiator and to the 3dB branch coupler required for circular polarization. The circularly polarized elements are connected to the RF comparator which provides the sum and difference signals. It also provides the amplitude taper to the lateral elements in the sum pattern. Sum and difference channels

are isolated more than 35dB at Rx and about 25 at Tx. Figure 2 shows the antenna and the beam forming network layouts.

Crosstalk between sum and difference ports is an important factor in a Monopulse system since a lack of isolation gives place to errors in the difference signal, which affects the pointing error information. The isolation level obtained with our comparator ($\approx$35 dB) assured a minimum error due to coupling.

Sum and difference radiation patterns measured at midband Rx frequency are shown in the figure 3. Gain and axial ratio performances vs. frequency of the isolated antenna are shown in the figure 4.

A constraint associated to this antenna design is the broad elevation beam of the array, affected by the closely situated car roof, which acts as a ground plane. A GTD study of the ground plane effects on the antenna performances made us to select an antenna height over the ground plane of 0.5λ ($\approx$ 90 mm) to minimize the axial ratio deterioration.

The modulator which generates the difference over sum signal is used to provide the error voltage to move the antenna. It is composed of a directional coupler and a continously switched 180° phase shifter which multiplexes the sum and difference signals, providing the signal $\Sigma \pm \Delta$, routed to the receiver, where a special circuitry at IF level is used to recover the sum signal and the difference over sum signal to control the antenna.

The design of the 0-π phase modulator is based on a 180° rat race hybrid coupler. An analysis of the operation shows that the required phase shift is obtained with two diodes, oppositely biased, placed on the balanced ports of the hybrid. When one diode is biased on its forward conduction state, the other is reverse biased with the junction voltage of the first one ($\approx$ 0.85V). This operation limits the RF power handling when the system transmits. An evaluation of the power handling capability of the modulator gave 36.7dBm at Tx for the diode selected (MA/4P404).

The complete modulator network (coupler and phase shifter) is sketched in the figure 5. Sum and difference path lengths are phase balanced in order to have a correct sum ($\Sigma + \Delta$) and difference (Σ-Δ) operations. The additional length of line was included in the direct (Σ) path of the coupler, giving place to higher losses in this channel ($\approx$ 1dB). The coupling level between the difference and the input port was 10dB, and the isolation between channels was better than 20dB over the band. The rest of the RF circuitry is isolated from the DC signal with several DC blocking capacitors.

The input match of the complete outdoor unit (antenna and difference over sum modulator) measured at the rotary joint port is better than 20dB at 1550MHz and better than 13dB at 1650MHz.

MECHANICAL DESIGN

The materials used for the specific components are nylon (gears) and aluminium (supporting structures). This lowers the weight of the moving parts and reduces the required motor torque. The aluminium pieces have been thought to be press machined. The required antenna height (90mm) is included inside the radome design, which also acts as external enclosure and interface, providing installation both on a car roof or in a mast in the case of trucks.

Just two output connectors exist, one for the RF and DC line and one for the motor bias and control. This minimizes the complexity of the interfaces between the antenna and the mobile. This design allows an estimated cost in mass production of 1200US$.

The general drawing of the antenna is shown in the figure 6. The dimensions of the antenna with the radome are 27x59cm(diameter).

FUNCTIONAL TESTS

The tests done were dedicated to evaluate the tracking accuracy and the mobile to satellite link mainteinance for different environments. The antenna was mounted in a van where all

the required equipment for piloting the results had been placed. The spacecraft used for this measurements was the INMARSAT satellite, which transmits a PRODAT carrier signal at 1547.8 MHz.

Figure 7 plots one course of the mobile, where the gyrocompass reading and the antenna indication are shown. Table I shows the performances of the system in terms of signal fluctuation and pointing error, measured by comparison with the signal of a reference gyrocompass.

CONCLUSIONS

A low cost, medium gain microstrip antenna for L-band mobile communications has been shown. It is one of the first prototypes of mobile satellite antennas developed in Europe.

The operational basis of the tracking system have been presented, and the tracking and acquisition processes have been outlined. The antenna and associated RF parts have been described, and finally they have been presented relevant results on field tests.

REFERENCES

[1] A. Jongejans et al.:"EMS European Mobile System". IMSC'93
[2] "SMALL STEERABLE LAND MOBILE ANTENNA" Final Report. ref TDC-LMA-200. Dec 92. Estec contract no. 8598/89
[3] MSAT-X Quarterly. no.13 Jet Propulsion Laboratory. Jan.88
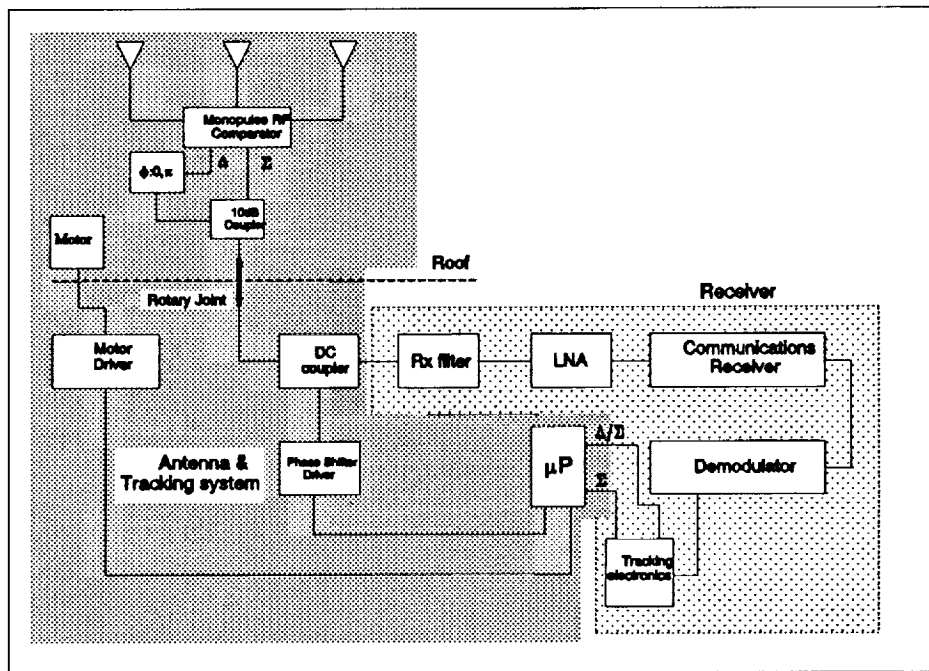
Figure 1.- Modulated monopulse schematics
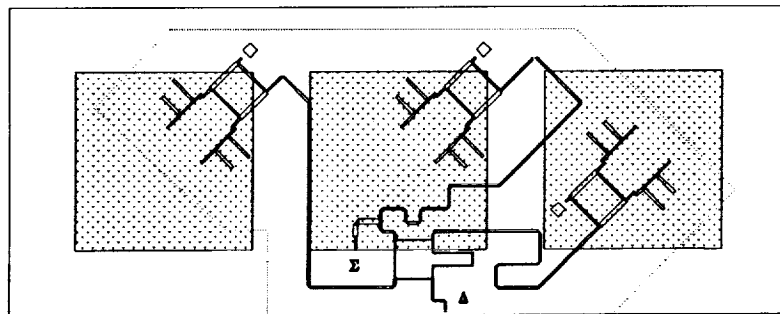
Figure 2.- Layouts of the antenna and RF components showing the dual-band matching network and the monopulse RF beamformer.
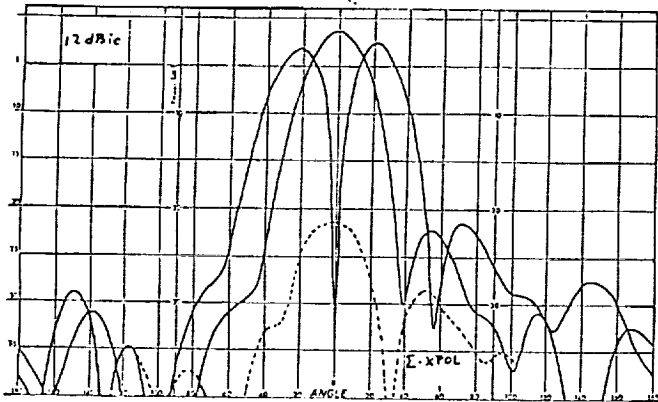
Figure 3.- Sum and Difference Radiation Patterns of the Antenna isolated from the Ground Plane. Operational Frequency: 1550MHz.
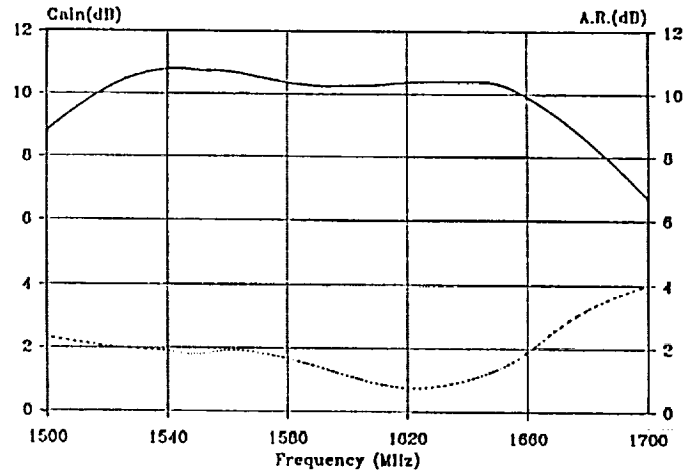
Figure 4.- Gain and Axial Ratio variation vs. frequency of the antenna, isolated from the Ground Plane.
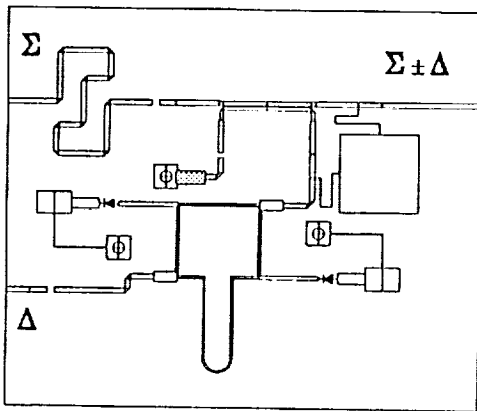
Figure 5.- Layout of the modulator component for multiplexing the difference signal over the sum channel. The antenna is isolated with DC-blocking capacitors.
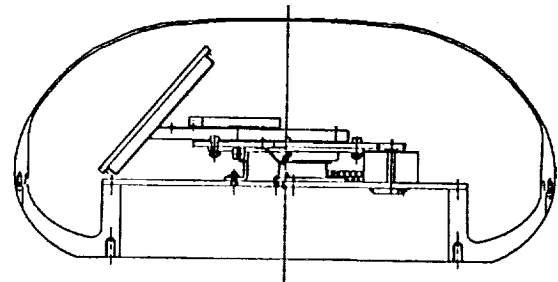
Figure 6.- Pictorial view of the antenna with the radome.
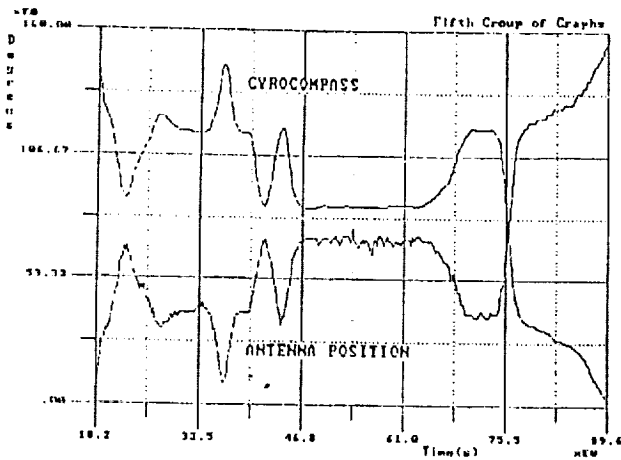
Figure 7.- Functional Test: course plot of the antenna under real conditions. Operational Frequency: 1547.8 MHz.

Table I

Course	Pointing error (degrees rms)	Signal level (dB rms)	Sample duration (sec)
Straight	0.74	-0.30	10
	1.86	-2.59	15
	1.37	-1.09	15
	3.50	-3.90	25
	1.07	-1.59	30
	1.24	-0.33	10
With turns	3.14	-0.5	42
	2.37	-1.7	30
	2.07	-1.47	30
	3.74	-1.76	20
	2.91	-1.52	45

Isolated and Coupled Superquadric Loop Antennas for Mobile Communications Applications

Michael A. Jensen and Yahya Rahmat-Samii
Department of Electrical Engineering
University of California, Los Angeles
405 Hilgard Avenue
Los Angeles, CA 90024-1594, USA
Telephone: (310) 206-3847
Fax: (310) 206-3847

ABSTRACT

This work provides an investigation of the performance of loop antennas for use in mobile communications applications. The analysis tools developed allow for high flexibility by representing the loop antenna as a superquadric curve, which includes the case of circular, elliptical, and rectangular loops. The antenna may be in an isolated environment, located above an infinite ground plane, or placed near a finite conducting plate or box. In cases where coupled loops are used, the two loops may have arbitrary relative positions and orientations. Several design examples are included to illustrate the versatility of the analysis capabilities. The performance of coupled loops arranged in a diversity scheme is also evaluated, and it is found that high diversity gain can be achieved even when the antennas are closely spaced.

INTRODUCTION

Circular and non-circular loop antennas, with shapes governed by packaging considerations, often prove to be appropriate, low-profile radiators for mobile communications devices. In some instances, new efforts to combat the effects of multipath fading without requiring increased bandwidth has motivated the use of multiple elements arranged in a diversity configuration on a single transceiver [1]. In the design of such antennas, it is important to understand the effects of loop geometry and mutual coupling on the antenna impedance, radiation characteristics, and diversity performance. This paper presents the results of two sophisticated analysis tools developed for this purpose:

(a) a Galerkin moment method algorithm for loops which are isolated or located near an infinite ground plane;

(b) a finite difference time domain (FDTD) technique for loops which are isolated or placed near finite-sized conducting objects.

ANTENNA GEOMETRY

To allow characterization of a wide variety of antenna geometries with one unified formulation, the loops are modeled as superquadric curves. This geometry is a closed loop which satisfies the equation

$$|x/a|^\nu + |y/b|^\nu = 1 \qquad (1)$$

where a and b are the semi-axes in the x and y directions respectively and ν is a "squareness parameter" which controls the variation of the loop radius of curvature. The configuration is illustrated in Fig. 1 for $\nu = 2, 3,$ and 10 and an aspect ratio of $b/a = 2$. As can be seen, variation of the values of a, b, and ν allows considerable flexibility in modeling many practical antenna
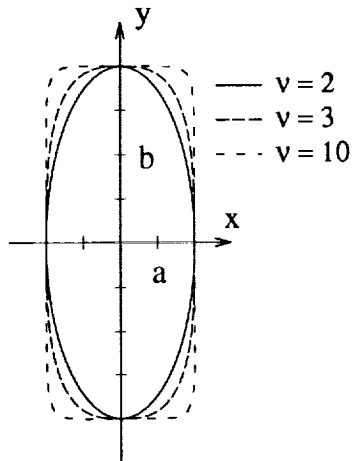
Figure 1: Superquadric geometry for $\nu = 2, 3$, and 10 with an aspect ratio of $b/a = 2$.
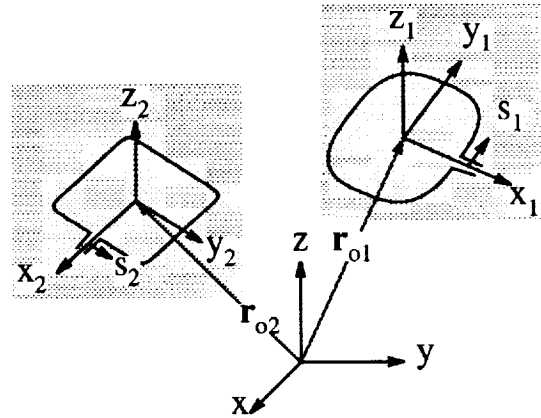
Figure 2: Geometry of two coupled loop antennas showing coordinates.

configurations. This flexibility is very important from the viewpoint of antenna packaging considerations.

For coupled loop geometries, the two superquadric antennas may have arbitrary positions and orientations and possibly different geometries, as represented in Fig. 2. Each loop is situated in its own coordinate system which may have an arbitrary position and orientation (described using Eulerian angles) with respect to the reference coordinate system.

FORMULATION

Moment Method Analysis

The moment method analysis of the coupled loop configuration makes use of a parametric expression for the superquadric curve in a coupled form of an electric field integral equation (EFIE) for thin wires. Use of this parametrization allows integration to occur on the curved loop contour rather than on the commonly-used piecewise linear representation of the curve, resulting in a more computationally efficient algorithm. Piecewise sinusoidal subsectional basis and weighting functions are used in a Galerkin form of the moment method to compute the

axial current distribution along the loop. This current is then used to compute the antenna radiation pattern, directivity, and input impedance. The formulation is extended to analyze loops placed near an infinite ground plane through modification of the Green's function in the EFIE to account for the loop image. Both delta gap and magnetic frill type source models are used as excitation schemes to allow investigation of different feeding scenarios

FDTD Analysis

In order to fully evaluate the performance of loop antennas on a small box such as might be used for a hand-held radio transceiver, the effects of this conducting case must be included in the analysis. In order to investigate this configuration, the finite-difference time-domain (FDTD) algorithm is used with Yee's cubical cells and a second order absorbing boundary condition at the outer grid truncation surface. A special subcell method is used to properly account for the finite size of wires on the antenna radiation and impedance characteristics. By using properly shaped excitation functions for the antenna feed, the antenna behavior over a wide frequency

band may be determined with this time-domain formulation. An example of a design based upon these computations is provided at the end of this paper.

DIVERSITY

One of the objectives of this work is to determine the performance of the coupled superquadric loop antennas when used in a diversity scheme for a mobile communications system. In this application, we are interested in the use of space, angle, and polarization diversity to combat the effects of short-term or Rayleigh-type fading in a multipath environment. Antenna diversity scenarios in which multiple elements are used at the receiver to reduce the effects of fading are becoming more predominant as communications systems demand increased signal quality and reliability without consuming additional use of the available frequency spectrum.

A quantitative figure of merit for the performance of an antenna diversity configuration is the envelope correlation coefficient for the signals received by two different elements. In essence, this quantity provides a measure of the "similarity" of the two signals. For cases where the incident multipath field is assumed to arrive from the horizontal plane only it can be shown [1] that the envelope correlation coefficient for two antennas may be computed from the equation

$$\rho_e = \frac{\left| \int_0^{2\pi} \vec{E}_1(\pi/2, \phi) \cdot \vec{E}_2^*(\pi/2, \phi) d\phi \right|^2}{\int_0^{2\pi} |\vec{E}_1(\pi/2, \phi)|^2 d\phi \int_0^{2\pi} |\vec{E}_2(\pi/2, \phi)|^2 d\phi} \quad (2)$$

where $\vec{E}_1$ and $\vec{E}_2$ are the vector patterns associated with each of the coupled loop antennas. Generally, a value of ρ_e less than about 0.7 provides acceptable diversity returns.
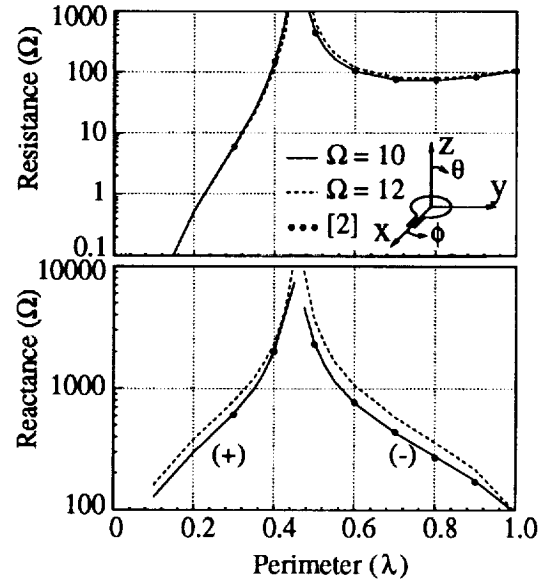
Figure 3: Input impedance versus perimeter for a single circular loop for two values of Ω. The dots are values taken from [2].

EXAMPLES

In the following examples, the parameter $\Omega = 2\ln(P/r_w)$ is used as a measure of the wire size where P is the loop perimeter and r_w is the wire radius. Fig. 3 shows the input impedance versus loop circumference for a single circular loop ($\nu = 2$, $b/a = 1$) for two values of Ω. A magnetic frill source model configured to have the dimensions of a 50Ω coaxial feeding line is used for the excitation. This plot shows that the loop antenna exhibits reasonable input impedance values for circumferences larger than about 0.7λ. The poor impedance behavior occurring for small loop circumferences can be substantially improved using proper loading techniques, thereby extending the loop to applications where the antenna size may be limited by spatial considerations. The dots in the figure correspond to data computed using a Fourier series representation for the current distribution [2]. Clearly, excellent agreement exists between the two sets of data.

An example of the use of the moment
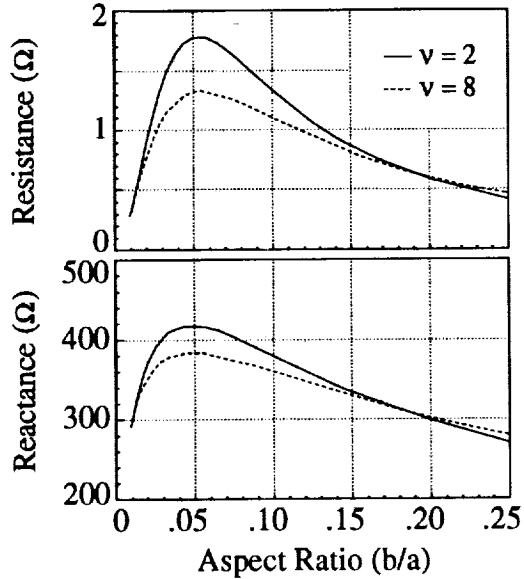
Figure 4: Input impedance versus aspect ratio b/a for a 0.25λ loop with $\Omega = 10$ for two values of ν.

Figure 5: Envelope correlation coefficient versus rotation for 0.25λ loops ($\nu = 10$, $b/a = 1$) for various separation distances.

method to determine the effects of geometry on the loop antenna performance is illustrated in Fig. 4. This plot shows the input impedance of a 0.25λ loop with $\Omega = 10$ as the aspect ratio b/a is varied. Results are shown for $\nu = 2$ and 8. From this figure, it can be seen that the input impedance varies noticeably with loop squareness. This data can be very useful in the design of loop antennas

A key feature of loop antennas is that they may be configured to achieve high diversity performance when used in a multipath fading environment. For example, Fig. 5 illustrates the variation of the envelope correlation coefficient as a function of antenna orientation for two 0.25λ loops with $b/a = 1$ and $\nu = 10$ for several values of loop separation y. In this example, one loop is held stationary while the second is rotated about its x axis as shown in the figure inset. As can be seen from Fig. 5, low correlation coefficient values can be obtained even for small antenna spacings.

The high diversity performance of crossed loops leads to the possibility of a design such as that depicted in the inset of Fig. 6. The centroid of this antenna configuration is placed 0.2λ above an infinite ground plane to represent the scenario where the antenna is mounted on a car or other vehicle. Each loop is 0.8λ in perimeter with $\nu = 5$ and $b/a = 1$. The radiation patterns for these coupled loops normalized to the antenna directivity are shown in Fig. 6 for the principal and horizontal plane cuts. The antennas are fed $90°$ out of phase which results in the symmetry in the pattern in the xy plane. If proper signal combining is used with this antenna geometry, high diversity gain can be achieved.

An example of the flexibility of the FDTD methodology to predict the performance of a strip loop placed upon a hand-held transceiver case appears in Fig. 7. The geometry of the handset/antenna system is illustrated in Fig. 7(a). Fig. 7(b) demonstrates the wideband impedance behavior for this configuration At lower frequencies, the impedance varies rapidly with frequency which results in challenging matching requirements if broadband
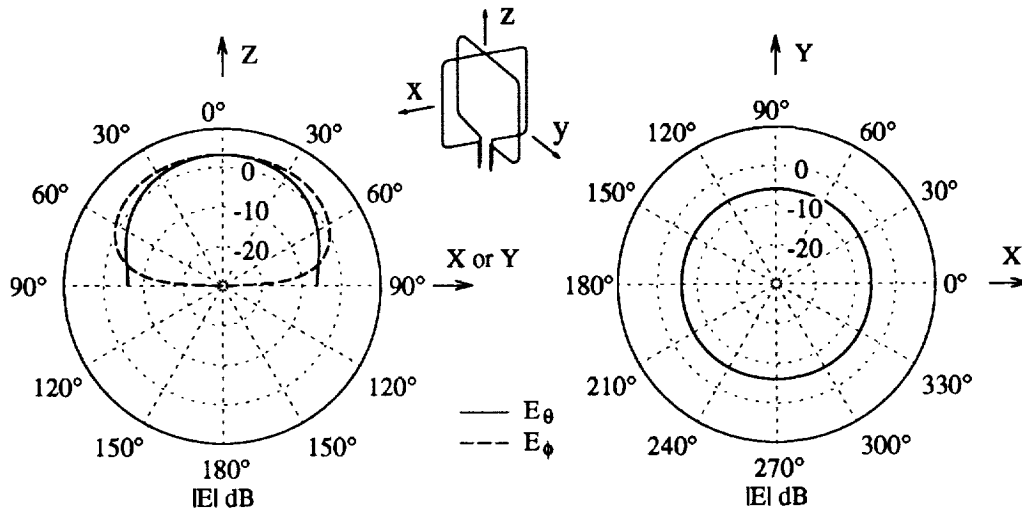
Figure 6: Directivity patterns in dB for two crossed 0.8λ superquadric loops ($\nu = 5$, $b/a = 1$) located $z_o = 0.2\lambda$ from an infinite ground plane.

performance is necessary. However, for narrowband applications, reasonable impedance values occur between the resonance peaks. For higher frequencies, the slow impedance variation with frequency allows for much wider bands of operation. The directivity patterns for the loop are provided in Fig. 7(c) for a frequency of $f = 915$MHz at which point the input impedance has a value of $53 - j246\Omega$. The asymmetries in the xz plane pattern arises from the fact that the loop is not centered on the box in the x direction to allow room for the feeding circuitry.

An example of using loading to improve the impedance characteristics of small loop antennas is provided in Fig. 8 which shows the input impedance versus frequency for a rectangular loop antenna loaded with an open circuit opposite the feed point. The loop has dimensions $a = 0.86$ cm and $b = 2.56$ cm, with a wire radius of 0.75 mm. This broadband data obtained with the FDTD methodology shows very well behaved impedance characteristics for low frequency operation, especially near 1GHz

where the loop is near $\lambda/2$ in perimeter. Such an antenna may be appropriate for hand-held transceiver applications.

CONCLUSIONS

In this paper we have demonstrated the utility of newly developed computational tools based on both moment method and FDTD algorithms in the analysis of loop antennas for mobile communications applications. The analysis has been focussed on loops described by superquadric curves to allow characterization of a large number of geometries for isolated and coupled loop configurations. The diversity performance of coupled loops has been discussed and it was shown that high diversity gain is possible even for closely spaced antennas. Several key design examples were presented to illustrate the flexibility of the simulation capabilities. Naturally, these analysis tools can be applied to the characterization of numerous other possible configurations for mobile communications antennas.

585
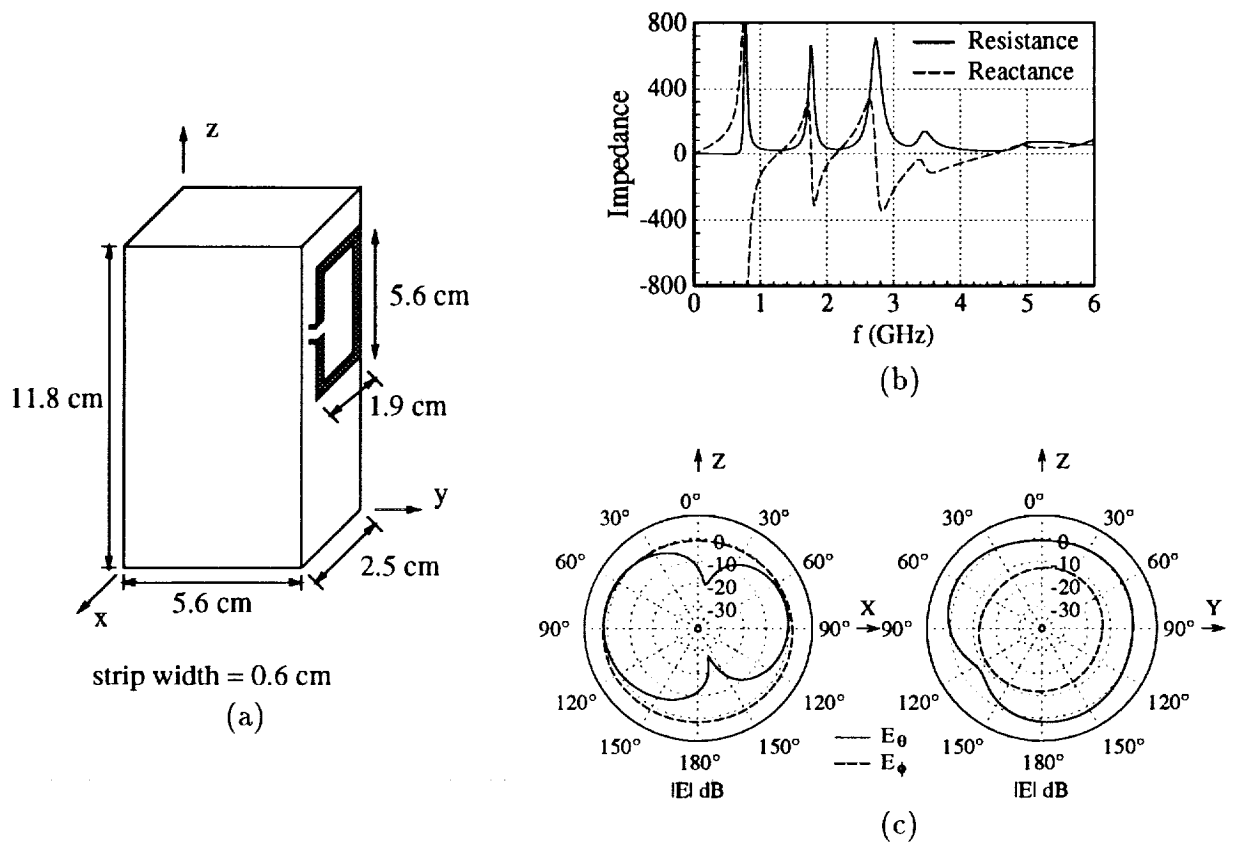
Figure 7: FDTD analysis of a strip loop on a hand-held transceiver: (a) transceiver geometry; (b) input impedance versus frequency; (c) directivity patterns at $f = 915$MHz.

REFERENCES

[1] R. Vaughan and J. Andersen, "Antenna diversity in mobile communications," *IEEE Trans. Veh. Technol.*, **VT-36**, pp. 149–172, 1987.

[2] G. Zhou and G. Smith, "An accurate theoretical model for the thin-wire circular half-loop antenna," *IEEE Trans. Antennas Propag.*, **39**, pp. 1167–1177, 1991.
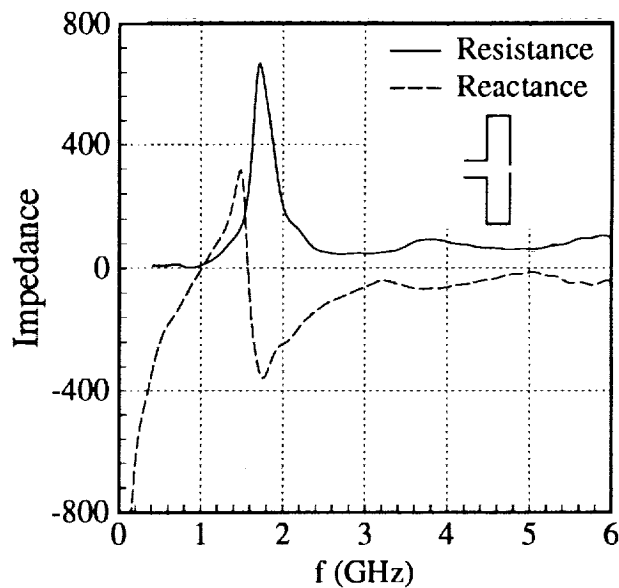
Figure 8: FDTD result of the input impedance versus frequency for a rectangular loop with $a = 0.86$ cm, $b = 2.56cm$, and $r_w = 0.75$ mm loaded with an open circuit.

L-band Mobile Terminal Antennas for Helicopters

T.K. Wu, K. Farazian, N. Golshan, D. Divsalar, S. Hinedi

Jet Propulsion Laboratory
California Institute of Technology
4800 Oak Grove Dr.
Pasadena, CA 91109
TEL (818)354-1261
FAX (818)393-6875

ABSTRACT

The feasibility of using a low gain antenna (LGA) as a mobile terminal antenna for helicopter is described in this paper. The objectives are (1) to select the lowest cost antenna system which can be easily mounted on a helicopter and capable of communicating with a satellite, and (2) to determine the best antenna position on the helicopter to mitigate the signal blockage due to rotor blades and the multipath effect from the helicopter's body. The omni-directional low gain antenna (LGA) is selected because it is simple, reliable and low cost. The helix antenna is selected among the many LGAs, because it is the most economical one and has the widest elevation beamwidth. Both 2-arm and 4-arm helices are studied experimentally to determine the antenna's performance and the scattering effects from the helicopter's body. It is found that the LGA should be located near the tail section and at least 8" above the helicopter.

INTRODUCTION

Helicopter satellite communication (H-SATCOM) is of current concern, since it has myriad applications, such as, emergency and rescue missions, off-shore drilling, fire fighting, rapid access, passenger transportation, etc. For example, the Norwegian air traffic controllers (ATCs) are monitoring helicopter trips across the North Sea to oil platforms using position data sent automatically from the helicopters to ATCs via the International Maritime Satellite (Inmarsat) [1].

Jet Propulsion Laboratory (JPL), under a contract with the Federal Aviation Administration (FAA), is conducting a study of implementing a very low-cost, small-size, light-weight, real-time communication system specifically for H-SATCOM. In this paper, the feasibility of using LGAs for H-SATCOM is studied. Here the helicopter's banking angle is assumed to be ± 60° and the satellite is the Inmarsat or American Mobile Satellite Corporation (AMSC) or the Low Earth Orbit (LEO) IRIDIUM satellite. The requirements for the helicopter antennas are (1) complying with industry standards, e.g., ARINC 741 and Inmarsat LGA's specs for aeronautical mobile terminals [2], (2) providing a 0 dBic gain in 360° azimuthal and from zenith to 40° below horizon, (3) the transmit and receive frequencies being 1.62-1.67 and 1.53-1.56 GHz, respectively, the transmit power being 19.2 watts, (4) the VSWR being 1.5:1, (5) small-size, (6) light-weight, and (7) low-cost.

There are two unique technical challenges in the determination of the best helicopter antenna location. First is the

C-8

periodic signal fading caused by the helicopter's rotor blades. Second problem is the multipath caused by the scattering from the complicated shape of the helicopter body. Thus the antenna study objectives are (1) to select the low-cost, light-weight, and small-size antenna system for H-SATCOM, and (2) to determine the best antenna position on the helicopter to minimize the signal blockage due to rotor blades and the multipath effect from the helicopter's body. The study results are summarized in the following sections.

ANTENNA SELECTION

To ensure that all the antenna options are considered, the LGAs, the steerable medium-gain antennas [3] and high gain reflector antennas [4] are all included in this exhaustive survey. Both JPL and Antenna Industry publications in this specific application were studied. The high gain ($\geq$ 20 dB) reflector antennas in L-band are usually very large in size (at least 5' in diameter and 1.25' in height) and heavy in weight. In addition, a bulky and expensive tracking system is needed to steer this reflector antenna beam to the satellite direction. Thus it is not suitable for helicopter use.

In general, the medium-gain antennas (including mechanically and electronically steered arrays [3]) are more expensive and less reliable than a low gain antenna due to the fact that an additional tracking system is required to steer the narrow antenna beam to the satellite direction. However, the omni-directional LGAs, as summarized in TABLE 1, are simple, reliable and low cost. Furthermore, the low-gain antennas are typically ten times smaller than the medium-gain antennas. This makes the mounting of the antenna on the helicopter relatively easier. Therefore, the low gain antennas are selected for the H-SATCOM.

Figure 1 shows a 4-arm helix (volute) antenna [5], which gives a cardioid pattern as depicted in Figure 2. Figure 3 shows a donut

shaped pattern of a 4-arm conical spiral antenna [6]. Note that one can change the shape, size or pitch angle of a crossed dipole or helix antenna to optimize the gain in the desired directions. The 2-arm helix and the crossed drooping dipole antennas have the widest bandwidth (covering both the transmit and receive frequencies). The 4-arm helix antenna is bandwidth limited and hence requires two antennas for uplink and downlink. But it is attractive since it only costs about $20. Since the helix antenna has the lowest cost, it is selected for the helicopter use. It is also possible to use multiple antennas or antennas in conjunction with a gyro or compass to compensate for the helicopter's maneuvers. However, due to cost and complexity it is desirable to have one or two antennas without a tracking system.

HELIX ANTENNA TEST RESULTS

Several off-the-shelf helix antennas were tested in an out-door far-field range. Figures 4 and 5 are the measured radiation pattern of a 4-arm helix antenna without and with a 23" by 23" ground plane, respectively. Figure 6 shows the severe pattern distortion as the helix antenna is placed 4" above the ground plane. Figure 7 shows the measured 2-arm helix antenna at 1.5754 GHz. From this test data, we know that this helix antenna has about 2.1 dBic peak gain, 5 dB axial ratio above horizon, and 140° half-power beamwidth. It seems that this antenna is designed to have optimized circular polarizations at 45° cone angle. The measured helix antenna performances are summarized in TABLE 2. Note that several minor discrepancies are observed as compared to TABLE 1. First, for the 4-arm helix antenna, the peak gain is about 0.8 dB lower and the half-power beamwidth (HPBW) is about 10° smaller. For the 2-arm helix antenna, the HPBW is about 20° smaller and the axial ratio is about one dB worse. These minor discrepancies may be attributed to the

measurement tolerance and uncertainty. This also implies that extra link margin should be considered for the H-SATCOM system design. The helix antenna should also be placed at least 8" away from the helicopter in order to minimize the ground plane effects.

CONCLUSION and RECOMMENDATION

The helix antenna is selected for H-SATCOM, since it is small-size, light-weight, and low-cost. Several off-the-shelf helix antennas were also tested. None of these antennas will remotely meet the H-SATCOM antenna requirements. But one can change the shape, size, or pitch angle of the helix antenna to meet the requirements. The 0 dBic elevation beamwidth of a single helix antenna is 140°. Thus two helix antennas are needed to provide a 260° coverage. Since the helix antenna's radiation pattern is very dependent on the nearby scattering objects, it is appropriate to conduct a scale model test (or full sized test) and a numerical study to precisely determine the blockage effect of the rotor blades and the helicopter body. The rationale for doing this task is that via the scale model testing we can efficiently determine the best antenna position and performance on the helicopter for SATCOM and also validate the numerical modeling software. Whenever a different helicopter or antenna is superimposed, running the computer model is the most efficient and cost-effective way to provide the SATCOM system designer the necessary and accurate antenna performance data.

ACKNOWLEDGEMENT

REFERENCES

[1] R. Riccitiello, "Satellites Modernize Air Traffic Control, Communications," *Space News*, Nov. 16-22, 1992.

[2] *Inmarsat Aeronautical System Definition Manual (SDM)*, July 1988, London, UK.

[3] K. Woo, et. al., "Performance of a Family of Omni and Steered Antennas for Mobile Satellite Applications," *Proceedings of the International Mobile Satellite Conference*, Ottawa, 1990, pp. 540-546.

[4] A.W. Rudge, et. al., *The Handbook of Antenna Design*, Chapter 3, Peter Peregrinus Ltd., London, UK. 1986.

[5] C. Kilgus, "Resonant Quadrifilar Helix," *IEEE Trans.*, vol. AP-17, no. 3, May 1969, pp. 349-351.

[6] A. Atia, "Multiple-arm Conical Log-spiral Antennas," *Ph. D. Dissertation*, UC Berkeley, 1969.
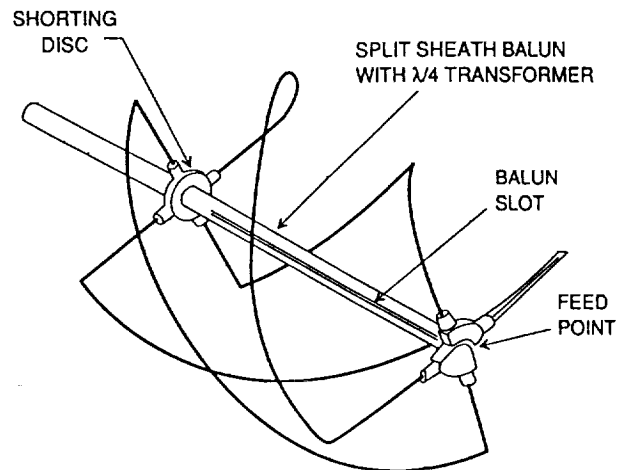
Fig. 1 4-arm helix (volute) antenna configuration

TABLE 1. L-band mobile antenna summary

Antenna Type[a]	Size (cm) HT	Size (cm) Dia.	Gain (dB)	Band-width (%)	HPBW (°)	Axial Ratio (dB)	Beam (pattern) Shape	Cost ($/unit)[b]
Mechanically Steered Array							Steered Beam in AZ	
1.Yagi Array	3.8	53	≥ 10	6.25	40	4		450
2.Tilt Array	15	51	≥ 10	6.25	40	3		600
Electronically Steered Array							Steered Beam in Both AZ and EL	
1.Ball	3.3	61	≥ 8	6.25	40	4		1600
2.Teledyne	1.8	54	≥ 8	6.25	40	4		1800
Low-Gain Omni								
1.Crossed Dipole	12	8	≥ 4	25	100	7	Cardioid/Donut	400
2.Helix (2-arm)	15.2	5.1	2	28	160	4	Cardioid/Donut	150
3.Helix (4-arm)	9	5	4.5	1.3	150	4	Cardioid/Donut	20
4.Conical Spiral (2-arm)	14	6.9	3.8	6.25	160	4	Cardioid	300
5.Conical Spiral (4-arm)	15.7	12.9	4.5	6.25	40	4.5	Donut	400
6.Cavity Backed Slot	0.8	8.3	2	6.25	120	4	Cardioid	1451

a. All the antennas are right-hand circularly polarized.
b. The cost of each antenna unit is a ROM cost based on producing 10,000 units per year over a five-year period.

TABLE 2. Summary of helix antenna's performances

Antenna Type	Frequency GHz	Axial Ratio dB	Bandwidth GHz	Peak Gain dB	HPBW degree
4-arm Helix	1.57	4	0.06	3.7	140
2-arm Helix	1.62	5	0.24	2.1	140
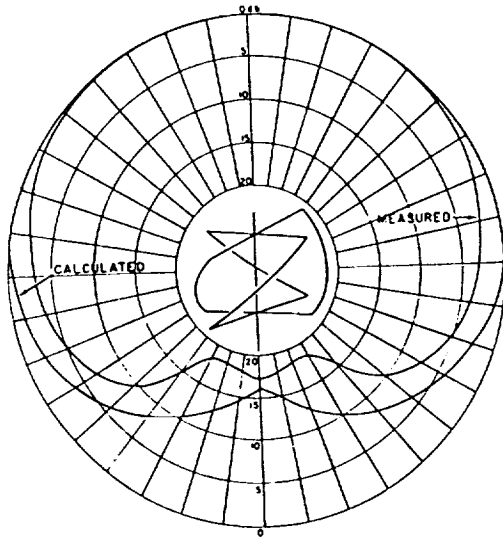
Fig.2 Typical cardioid pattern
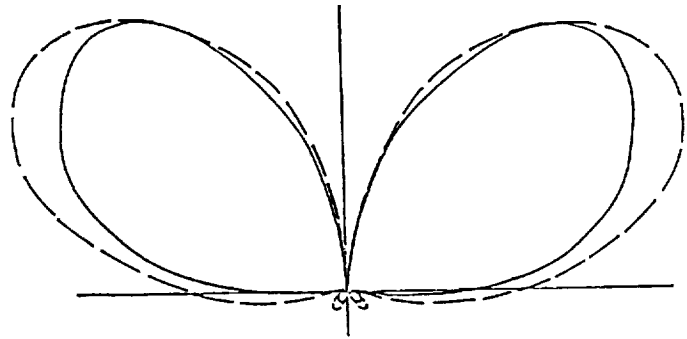
Fig. 3 Typical donut shaped pattern of conical spiral antenna
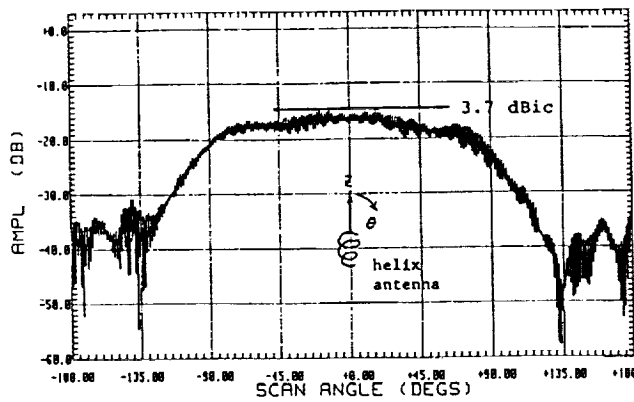
Fig.4 Measured 4-arm helix pattern
No ground plane
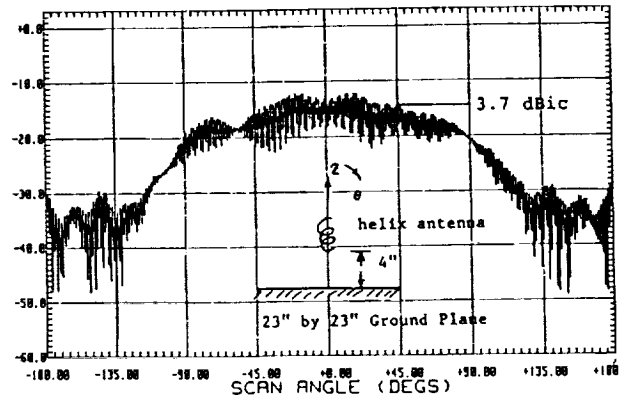
Fig.5 Measured 4-arm helix pattern
with ground plane

591
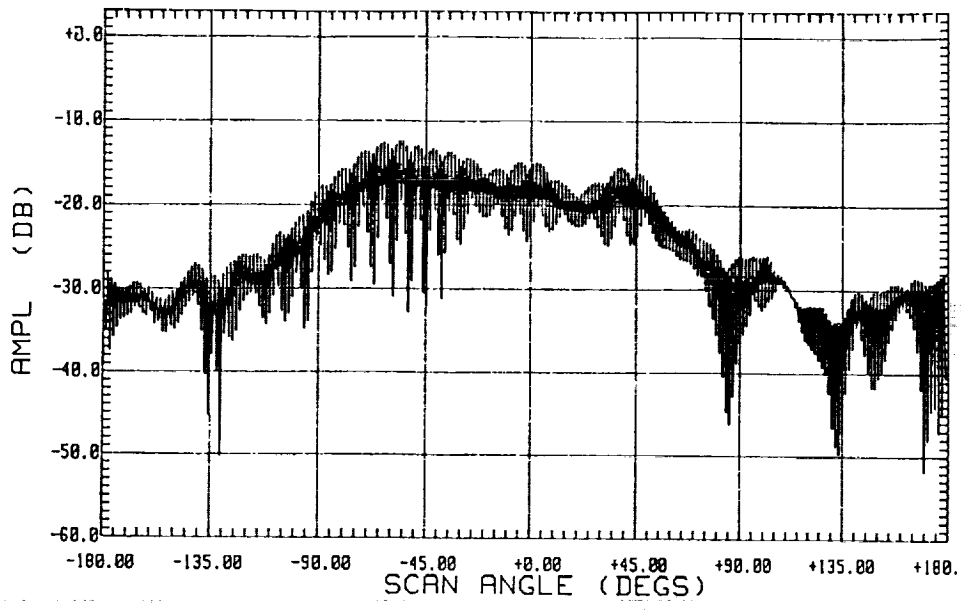
Fig. 6 Measured 4-arm helix antenna pattern at 1.575 GHz
antenna right above the finite ground plane
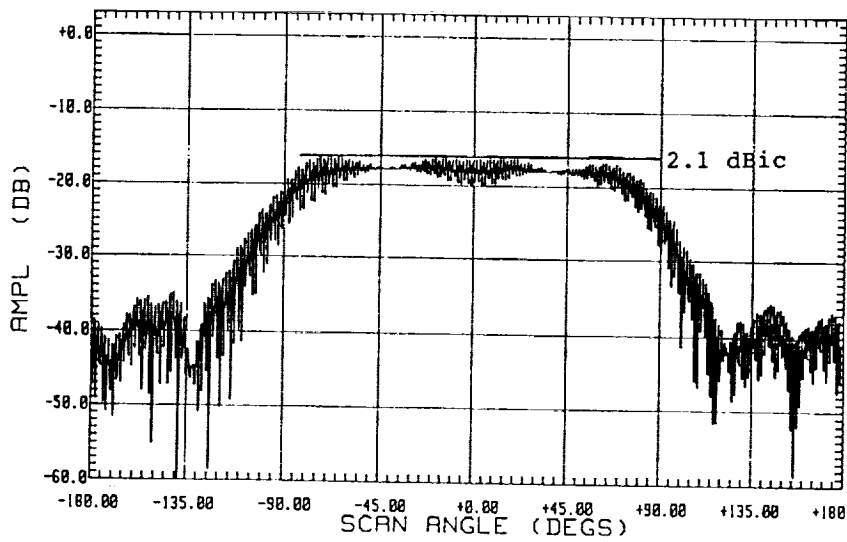
Fig. 7 Measured 2-arm helix antenna pattern

Aeronautical Satellite Antenna Steering Using Magnetic Field Sensors

John Sydor, Martial Dufour
Department of Communications
Communications Research Centre
3701 Carling Avenue
P.O. Box 11490, Station "H"
Ottawa, Ontario, Canada K2H 8S2
Telephone: (613)998-2388
Facsimile: (613)990-6339

ABSTRACT

Designers of aeronautical satellite terminals are often faced with the problem of steering a directive antenna from an airplane or helicopter. This problem is usually solved by using aircraft orientation information derived from inertial sensors on-board the aircraft in combination with satellite ephemeris information calculated from geographic coordinates. This procedure works well but relies heavily on avionics that are external to the terminal. For the majority of small aircraft and helicopters which will form the bulk of future aeronautical satcom users, such avionics either do not exist or are difficult for the satellite terminal to interface with.

At the Communications Research Centre (CRC) work has been undertaken to develop techniques that use the geomagnetic field and satellite antenna pointing vectors (both of which are stationary in a local geographical area) to track the position of a satellite relative to a moving platform such as an aircraft. The performance of this technique is examined and a mathematical steering transformation is developed within this paper. Details are given regarding the experimental program that will be undertaken to test the concepts proposed herein.

The Steering Problem

Steering an aeronautical satcom antenna using received signal strength alone is possible. However, this technique is prone to problems resulting from multipath reflections from around the aircraft, especially at the low satellite elevation angles where the wing tips, tail, and aircraft fuselage often appear within the beamwidth of the antenna.

It is believed that effective and accurate satellite antenna steering can be achieved by using the local geomagnetic field vector as a reference. By knowing the orientation of the magnetic field vector and the satellite pointing vector with respect to the aircraft's frame of reference, it is possible to maintain antenna tracking as the aircraft maneuvers.

Given that this concept works it will be possible to incorporate this electronic steering system within an aeronautical satcom terminal. This would reduce the requirement for the terminal to meet stringent avionics interface requirements and allow the use of satcom from a greater number of aircraft than currently possible. The technique has other applications, such as steering satellite antennas from ships or buoys.

The 3 Dimensional Adaptive Magnetic Sensor

Central to the magnetic field steering concept is a sensor that can resolve the instantaneous geomagnetic field in three dimensions. Such a sensor has been developed by using orthogonal adaptive magnetic field sensors.

The adaptive magnetic field sensor or compass (Ref 1) is a device which determines the angle of the magnetic field vector projected onto a

plane. This sensing plane is defined by two perpendicular magneto-resistive chip circuits. The output of these circuits is processed by a neural network which continually adapts the operation of the circuits to magnetic perturbations introduced by the aircraft. The adapted circuits give magnetic field strength readings with worst case error in the order of 2-3%. The two sensing planes are oriented orthogonally to each other to make a 3 dimensional field sensor. Currently a single board computer processes the outputs of the two sensing planes. Because of the complexity of the neural algorithms and the ancillary magneto-resistive sensor circuits, a 3 dimensional (3D) magnetic field reading is provided by the computer every 300 to 500 milliseconds. In the future the computer and supporting circuits will be integrated into several ASIC circuits which will be smaller and be capable of providing faster magnetic field readings. Currently the 3-D magnetic field sensor is housed in an aluminum box measuring 18 cm by 12 cm by 10 cm.

High Gain Antenna System

The antenna that is used in the investigation of magnetic steering (Fig.1) is an array of highly shortened helix elements (Ref. 2,3) that are wound into a conical form for better bandwidth performance. The array produces a flattened beam having gain in the order of 10-12 dBIC and a free space 3 dB beamwidth of 30 degrees azimuth by 60 degrees elevation. The antenna contains an on board diplexor/LNA and steering activation circuits and has a length of 36 inches, height of 6.5 inches and width of 13 inches.

The antenna will be used with the Ontario Air Ambulance Cessna 500 aircraft satcom terminal. The air ambulance has access to an INMARSAT channel and is used for emergency communications. Up to now the satcom terminal in the aircraft used window mounted antennas (Ref 4) which are being replaced by the new mechanically steered antenna and magnetic steering system.

Coordinate Transformations

As part of the steering algorithm it is necessary to determine a procedure for transforming changes in the pitch, roll, and heading of the aircraft to changes in the azimuth and elevation settings of the satellite antenna. Since aircraft attitude changes are sensed by the 3D sensor, the problem becomes one of accurately converting 3D sensor outputs into antenna azimuth and elevation settings (Ref 5).

The magnetic field vector β is resolved in 3D space using the two planar orthogonal magnetic field detectors (Fig. 2). One detector is set to sense the magnetic field in the heading (or azimuth) (XY) plane of the aircraft at an angle ϕ_m. The second detector is set to sense the angle of the field in the Z plane (either the pitch (XZ) plane or the roll plane (YZ)). Pitch plane readings are defined as Ω_m; roll plane readings as Ψ_m. By manipulating the projections of β into each of the three planes; it can be shown that:

$$\tan\Omega_m = \frac{\sin\theta_m \cos\phi_m}{\cos\theta_m} = \tan\theta_m \cos\phi_m \quad (1)$$

$$\tan\Psi_m = \frac{\sin\theta_m \sin\phi_m}{\cos\theta_m} = \tan\theta_m \sin\phi_m \quad (2)$$

where θ_m is the angle between β and the Z axis. Alternately;

$$\Omega_m = \tan^{-1} (\tan\theta_m \cos\phi_m) \quad (3)$$

$$\Psi_m = \tan^{-1} (\tan\theta_m \sin\phi_m) \quad (4)$$

and

$$\tan\Omega_m = \frac{\tan\Psi_m}{\tan\phi_m} \quad (5)$$

Aircraft attitude changes can be resolved as changes in heading (θ_A); pitch (θ_T) and roll (θ_B) of the aircraft (Figure 3). Now; whereas heading changes of the aircraft will result in only purely azimuthal changes in the magnetic sensor (i.e. $\Delta\theta_A = \Delta\phi_m$), pitch and/or roll changes of the aircraft will result in simultaneous changes to both ϕ_m and θ_m.

$$\Delta\theta_P = \Delta\Omega_m = \mathbf{F}_1(\Delta\phi_m, \Delta\theta_m) \quad (6)$$

$$\Delta\theta_R = \Delta\Psi_m = \mathbf{F}_2(\Delta\phi_m, \Delta\theta_m) \quad (7)$$

Equations 6 and 7 can be expressed in a differential form:

$$\begin{bmatrix} \Delta\theta_P \\ \Delta\theta_R \end{bmatrix} = \begin{bmatrix} \Delta\Omega_m \\ \Delta\Psi_m \end{bmatrix} = \begin{bmatrix} \dfrac{\partial\Omega}{\partial\theta_m} & \dfrac{\partial\Omega}{\partial\phi_m} \\ \dfrac{\partial\Psi}{\partial\theta_m} & \dfrac{\partial\Psi}{\partial\phi_m} \end{bmatrix} \begin{bmatrix} \Delta\theta_m \\ \Delta\phi_m \end{bmatrix} \quad (8)$$

After calculation of the partial derivatives of the matrix coefficients, equation (8) become:

$$\begin{bmatrix} \Delta\theta_P \\ \Delta\theta_R \end{bmatrix} = \begin{bmatrix} A_m\cos\phi_m & -B_m\sin\phi_m \\ C_m\sin\phi_m & D_m\cos\phi_m \end{bmatrix} \begin{bmatrix} \Delta\theta_m \\ \Delta\phi_m \end{bmatrix} \quad (9)$$

with the coefficients A_m, B_m, C_m and D_m defined as:

$$A_m = \frac{1}{(\cos^2\theta_m + \cos^2\phi_m\sin^2\theta_m)} \quad (10)$$

$$B_m = \frac{\sin\theta_m\cos\theta_m}{(\cos^2\theta_m + \cos^2\phi_m\sin^2\theta_m)} \quad (11)$$

$$C_m = \frac{1}{(\cos^2\theta_m + \sin^2\phi_m\sin^2\theta_m)} \quad (12)$$

$$D_m = \frac{\sin\theta_m\cos\theta_m}{(\cos^2\theta_m + \sin^2\phi_m\sin^2\theta_m)} \quad (13)$$

The equation (9) can be re-written using matrix syntax as:

$$\Delta\Theta_P = \mathbf{M}_m\,\Delta\Phi_m \quad (14)$$

where the indices p and m relate respectively to the platform (aircraft) and the magnetic sensor readings.

In equation 14 we see the relationship between a moving frame of reference (the aircraft) with respect to a fixed magnetic field. The pointing vector to the satellite (defined by the antenna azimuth and elevation angle θ_a, ϕ_a), is also with respect to this aircraft. Consequently equation (14) can be re-written to apply to antenna coordinates.

$$\Delta\Theta_P = M_a\,\Delta\Phi_a \quad (15)$$

where the indice a refers to the antenna. Combining (14) and (15) we have:

$$\Delta\Phi_a = \mathbf{M}_a^{-1}\,\mathbf{M}_m\Delta\Phi_m \quad (16)$$

which relates any change in the magnetic sensor readings to an equivalent change in the antenna position.

It can be useful to calculate the exact relation given by the equation (16). Using an equivalent equation (9) but for the antenna frame of reference, the inverse matrix $\mathbf{M}_A^{-1}$ can be expressed as:

$$M_A^{-1} = \begin{bmatrix} \dfrac{\cos\phi_a}{A_a} & \dfrac{\sin\phi_a}{C_a} \\ -\dfrac{\sin\phi_a}{B_a} & \dfrac{\cos\phi_a}{D_a} \end{bmatrix} \quad (17)$$

It follows that:

$$\begin{bmatrix} \Delta\theta_a \\ \Delta\phi_a \end{bmatrix} = \begin{bmatrix} Q_{11} & Q_{12} \\ Q_{21} & Q_{22} \end{bmatrix} \begin{bmatrix} \Delta\theta_m \\ \Delta\phi_m \end{bmatrix}$$

where

$$Q_{11} = \frac{A_m}{A_a}\cos\phi_a\cos\phi_m + \frac{C_m}{C_a}\sin\phi_a\sin\phi_m$$

595

$$Q_{12} = \frac{D_m}{C_a}\sin\phi_a\cos\phi_m - \frac{B_m}{A_a}\cos\phi_a\sin\phi_m$$

$$Q_{21} = \frac{D_m}{D_a}\cos\phi_a\cos\phi_m + \frac{B_m}{B_a}\sin\phi_a\sin\phi_m$$

$$Q_{22} = \frac{A_m}{A_a}\cos\phi_a\cos\phi_m + \frac{C_m}{C_a}\sin\phi_a\sin\phi_m$$

(18)

This relation transforms any variation in the readings of the magnetic sensor due to a pitch or roll of the aircraft, to an equivalent variation in the antenna satellite pointing angles. It is interesting to note that for the case where an axis of the aircraft's antenna frame of reference aligns with the magnetic field or satellite pointing vector, the above relationship reduces to a unit matrix. The pitch and roll variations measured by the compass will directly translate to equivalent changes for the antenna. Similarly, if the antenna is pointing opposite to magnetic north (i.e. satellite pointing vector is 180° away from magnetic north), the relation (18) transforms to a negative unit matrix resulting in steering variations being opposite to aircraft variations. Overall if the satellite pointing vector and magnetic field vector are within 30° of each other then the variation in readings of pitch or roll will closely approximate equivalent antenna variations.

Steering Ambiguity

The 3D sensor in conjunction with the aircraft possesses a number of ambiguities which can affect the accuracy of antenna steering. During instances where the magnetic field vector is parallel to any of the three coordinate axis of the magnetic sensor, it will be impossible to detect rotation of the coordinate axis about the magnetic vector. As a consequence, steering the antenna becomes ambiguous and the problem is accentuated as the antenna pointing vector becomes perpendicular to the magnetic field vector.

The ambiguity can be resolved by the steering algorithms which can detect the unique situations described above. Antenna steering under these circumstances becomes more reliant on signal strength tracking than on magnetic field tracking.

Signal Strength Sensor System

Antenna beam steering cannot be controlled solely by responses to magnetic sensor outputs. Magnetic sensor readings are produced no more than two or three times a second. Given that aircraft such as helicopters can make orientational changes of up to 45 degrees per second, an antenna steered by magnetic steering alone could be over 20 degrees off angle from the satellite before any correction attempt was made by the steering system.

Since received signal strength information can be obtained from a terminal tracking a satellite, it is advantageous to use such information to enhance and supplement the magnetic tracking. Signal strength information comes at a much faster rate than magnetic sensor information at one reading every 50 milliseconds. At high C/No (45 dBHz) the signal sensor can have a resolution of 0.35 dB. For the Ontario Air Ambulance experiments we have a choice of satellite pilot signals that can be monitored to provide signal references. In an operational system such as the Inmarsat Aeronautical system, one could monitor the P-channel signal. Figure 4 shows the magnetic and field sensor configuration for steering the antenna.

Satellite Acquisition and Beam Steering Considerations

There are a number of factors which have to be considered in the development of a suitable satellite tracking algorithm. Antenna motor response speed and beam deformation which results in variations of axial ratio, discrimination, and gain as a function of antenna to ground plane (fuselage) interaction, are factors which affect the performance of the

steering algorithm. To some degree, the fact that the antenna beam is quite broad, having less than 0.5 dB of gain variation over a 7 by 15 degree area relaxes some of the steering requirements in that changes in orientation may be detected before noticeable changes in signal strength arise.

Probably the most important event in the activation of magnetically steered antenna is satellite acquisition. This procedure will rely heavily on the detection of a pilot signal from the satellite. The antenna, under control of the steering processor, must search the sky for the host satellite. This means searching for a signalling channel at a particular frequency. Since frequency stability of the terminal may not be within some prescribed operational bounds at power up, we are faced with a three dimensional search in frequency, antenna azimuth, and antenna elevation. Such a search will be further complicated by multipath, which will be present when the aircraft is close to hangars and other metallic structures while it is on the ground.

Beam Steering Algorithms

Steering algorithms will need to monitor a number of thresholds in a tracking sequence and will need to have a variety of responses to the detected orientation changes. Very quick changes will be detected as a drop in the signal strength. The first magnetic sensor reading after a signal drop will provide important information regarding the direction of the orientation change. It will also be possible in this first instant to calculate an angular acceleration for the change and choose a response by setting antenna motor speeds. Slow changes will be handled primarily by the magnetic field steering because such changes will not result in rapid signal strength variation and will be harder to detect by signal strength sensing. Nevertheless, once a tracking search is initiated by the magnetic sensor system there will probably be a

requirement to dither the antenna to maximize the signal strength

In view of the above considerations, the steering algorithm will take on a complex form. It will have to move from the acquisition mode to the tracking mode; it will have to differentiate between slow and fast orientational changes; it will have to predict angular rates of change and directions and then actuate motors to respond to such changes. The algorithm will strive to maintain the received C/N_0 at a maximum and in essence, this will be the final objective of any algorithm.

Conclusion

With the Ontario Ambulance several types of algorithms will be tested. The experimental system is being designed in such a manner that real time performance of an algorithm can be monitored and stored for analysis. This information will be useful in determining optimal tracking strategies.

References

1 Automatic Compensation for Magnetic Field Compass, U.S. Patent 5187872 Martial Dufour, 23 February 1993.

2 Extremely Low-Profile Helix Radiating a Circularly Polarized Wave. H. Nakamo, et al., IEEE Transactions on Antennas and Propagation, Vol. 39, No. 6, June 1991.

3 Radiation Characteristics of Short Helical Antenna and its Mutual Coupling, H. Nakamo et al., Electronics letters, 1 March 1984, Vol. 20, No. 5.

4 Recent Technical Advances in General Purpose Mobile Satcom Aviation Terminals, J. Sydor, IMSC Conference '90 Proceedings., JPL Pulication 90-7, pages 579 - 586.

5 Solid Analytic Geometry, Adrian Albert, McGraw-Hill 1949, Ch. 8, Section 4.
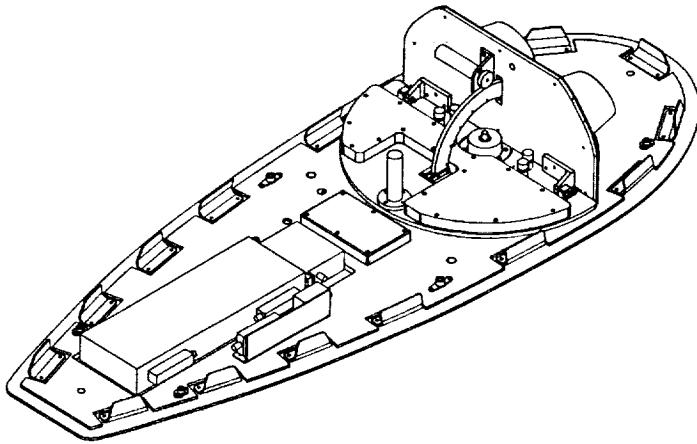
Figure 1
Mechanically Steered High Gain
Satcom Antenna
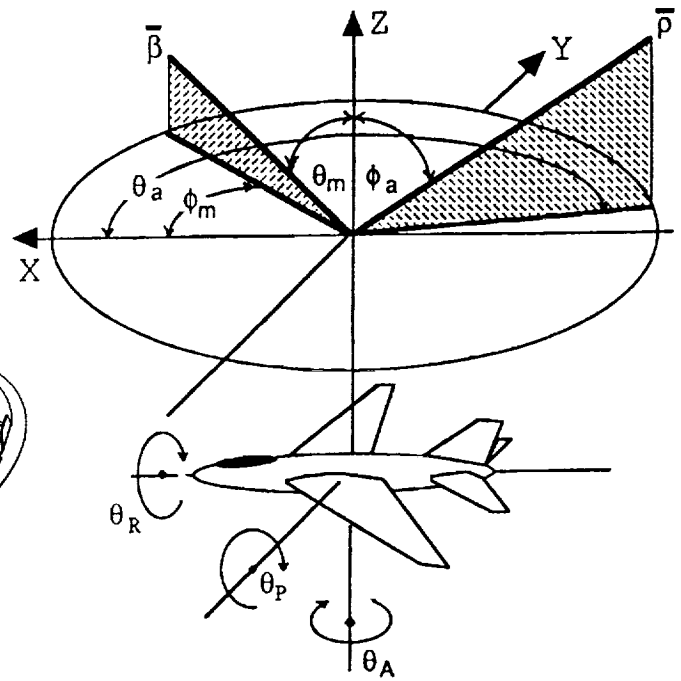
Figure 2
Magnetic Field, Antenna Pointing, and Aircraft
Orientation Coordinates
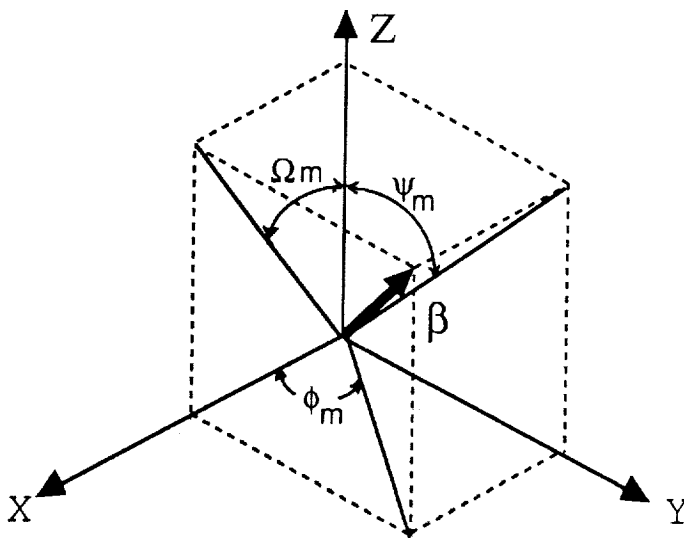
Figure 2
Resolution of the Magnetic Field Vector

Figure 4
Experimental Set Up

598

Author Index

1. Report No. 93-9	2. Government Accession No.	3. Recipient's Catalog No.

4. Title and Subtitle	5. Report Date
Proceedings of the Third International Mobile Satellite Conference IMSC'93	June 16-18, 1993
	6. Performing Organization Code

7. Author(s) R. Kwan, J. Rigley and R. Cassingham	8. Performing Organization Report No.

9. Performing Organization Name and Address	10. Work Unit No.
JET PROPULSION LABORATORY California Institute of Technology 4800 Oak Grove Drive Pasadena, California 91109	11. Contract or Grant No. NAS7-918
	13. Type of Report and Period Covered

12. Sponsoring Agency Name and Address	JPL Publication
NATIONAL AERONAUTICS AND SPACE ADMINISTRATION Washington, D.C. 20546	14. Sponsoring Agency Code RE4 BP-669-00-00-00-00

15. Supplementary Notes

16. Abstract

Satellite-based mobile communications systems provide voice and data communications to users over a vast geographic area. The users may communicate via mobile or hand-held terminals, which may also provide access to terrestrial cellular communications services. While the first and second International Mobile Satellite Conferences (Pasadena, 1988 and Ottawa, 1990) mostly concentrated on technical advances, this Third IMSC also focuses on the increasing worldwide commercial activities in Mobile Satellite Services. Because of the large service areas provided by such systems--up to and including global coverage--it is important to consider political and regulatory issues in addition to technical and user requirements issues.

The approximately 100 papers included here cover sessions in 11 areas: the direct broadcast of audio programming from satellites; spacecraft technology; regulatory and policy considerations; hybrid networks for personal and mobile applications; advanced system concepts and analysis; user requirements and applications; current and planned systems; propagation; mobile terminal technology; modulation, coding, and multiple access; and mobile antenna technology. Representatives from about 20 countries are expected to attend IMSC'93.

17. Key Words (Selected by Author(s))	18. Distribution Statement
Aircraft Communications and Navigation Communications Methods and Equipment (General) Logistics	Unclassified, unlimited

19. Security Classif. (of this report)	20. Security Classif. (of this page)	21. No. of Pages	22. Price
Unclassified	Unclassified	607	

JPL 0184 R 9/83